VOLUME 25 / NUMBER 4
FEBRUARY 23, 1987
ACC. NOS. N87-12532 TO N87-13399

NAS 1.9/4
25/4

STAR

AN ABSTRACT JOURNAL

Scientific and Technical Aerospace Reports

CHICAGO PUBLIC LIBRARY
MAR 30 1987
GOVERNMENT PUBLICATIONS

PRODUCED BY THE
SCIENTIFIC AND TECHNICAL
INFORMATION
BRANCH

NASA

NATIONAL AERONAUTICS AND SPACE ADMINISTRATION

WHAT YOU CAN DO FOR *STAR*

All users of this abstract service are urged to forward reports to be considered for announcement in *STAR*. This will aid NASA in its efforts to provide the fullest possible coverage of all scientific and technical publications that might support aeronautics and space research and development. If you have prepared relevant reports (other than those that you will transmit to NASA, DoD, or DOE through the usual contract- or grant-reporting channels), please send them for consideration to the NASA Scientific and Technical Information Facility, P.O. Box 8757, B.W.I. Airport, Maryland 21240.

Reprints of journal articles, book chapters, and conference papers are also welcome. These will be considered for announcement in *STAR's* companion journal, *International Aerospace Abstracts.*

You may specify a particular source to be included in a report announcement if you wish; otherwise the report will be placed on public sale at the National Technical Information Service. Copyrighted publications will be announced but not distributed or sold.

PURCHASE OF *STAR*

The semimonthly issues are available for sale by the Superintendent of Documents, U.S. Government Printing Office, Washington, D.C. 20402.

PUBLISHED BY:

UNITED STATES GOVERNMENT
NATIONAL AERONAUTICS AND SPACE ADMINISTRATION
SCIENTIFIC AND TECHNICAL INFORMATION BRANCH
Scientific and Technical Aerospace Reports, Volume 25, is prepared by the NASA Scientific and Technical Information Facility operated for the National Aeronautics and Space Administration by RMS Associates.

The Administrator of the National Aeronautics and Space Administration has determined that the publication of this periodical is necessary in the transaction of the public business required by law of this Agency. Use of funds for printing this periodical has been approved by the Director of the Office of Management and Budget through March 22, 1988.

US ISSN 0036-8741

INTRODUCTION

Scientific and Technical Aerospace Reports (STAR) is a major component of a comprehensive National Aeronautics and Space Administration information system covering aeronautics, space, and supporting disciplines. *STAR* is issued on the 8th and 23rd of each month and announces current publications of the following types:

- NASA, NASA contractor, and NASA grantee reports
- Reports issued by other U.S. Government Agencies, domestic and foreign institutions, universities, and private firms
- Translations in report form
- NASA-owned patents and patent applications
- Dissertations and theses

Journal, book, and conference literature, cover-to-cover journal translations, and certain foreign dissertations are announced in a companion journal, *International Aerospace Abstracts (IAA)*, available on subscription from the American Institute of Aeronautics and Astronautics, Technical Information Service, 555 West 57th Street, 12th Floor, New York, New York 10019.

SUBJECT SCOPE

Subject scope of *STAR*, and *IAA* includes all aspects of aeronautics and space research and development, supporting basic and applied research, and applications. Aerospace aspects of earth resources, energy development, conservation, oceanography, environmental protection, urban transportation, and other topics of high national priority are also covered.

OTHER NASA PUBLICATIONS

Other NASA publications and information services are described in the publication, *The NASA Scientific and Technical Information System ... and How to Use It*, available without charge from the NASA Scientific and Technical Information Facility, P.O. Box 8757, B.W.I. Airport, Maryland 21240.

HOW TO USE *STAR* SUBJECT CATEGORIES

STAR is categorized by 10 major subject divisions divided into 76 specific subject categories and one general category/division. The major subject divisions are listed in the Table of Contents, together with a note for each that defines its scope and provides any cross-references. For example:

AERONAUTICS

Includes aeronautics (general); aerodynamics; air transportation and safety; aircraft communications and navigation; aircraft design, testing and performance; aircraft instrumentation; aircraft propulsion and power; aircraft stability and control; and research and support facilities (air).

For related information see also *Astronautics*.

POSITORY
87108p

Each major division is further divided into as many as nine specific categories, which are identified by category numbers.

Abstracts in *STAR* are grouped by specific category, the categories appearing in sequential order. Category breaks in the abstract section are identified by the category number and title, and a scope note. Cross-references to other categories are provided as appropriate. For example:

02 AERODYNAMICS

Includes aerodynamics of bodies, combinations, wings, rotors, and control surfaces; and internal flow in ducts and turbomachinery.

For related information see also *34 Fluid Mechanics and Heat Transfer.*

CROSS-REFERENCES

Individual *STAR* abstracts are not ordinarily cross-referenced, except for certain conference reports or book translations that have had separate abstracts written for their component papers or chapters. Citations and abstracts of the components follow immediately after those of the parent document. When the subject content of a component differs sufficiently from the general content of the parent, a cross-reference citation also is printed at the end of the category to which it normally would have been assigned if it were independent.

DOCUMENTS ON MICROFICHE

Documents on microfiche[1] are designated by a pound sign (#) following the accession number. The pound sign is used without regard to the source or quality of the microfiche.

AVAILABILITIES

One or more sources from which a document announced in *STAR* is available to the public is given in each citation. The most commonly indicated sources and their acronyms or abbreviations are listed below. If the publication is available from a source other than those listed, the publisher and his address will be displayed on the availability line or in combination with the corporate source line.

Avail: NTIS. Sold by the National Technical Information Service. Prices for hard copy (HC) and microfiche (MF) are indicated by a price code following the letters HC or MF in the *STAR* citation. Current values for the price codes are given in the tables on page vii.

Initially distributed microfiche under the NTIS SRIM (Selected Research in Microfiche) is available at greatly reduced unit prices. For this service and for information concerning subscription to NASA printed reports, consult the NTIS Subscription Section, Springfield, Va. 22161.

NOTE ON ORDERING DOCUMENTS: When ordering NASA publications (those followed by the * symbol), use the N accession number. NASA patent applications (only the specifications are offered) should be ordered by the US-Patent-Appl-SN number. Non-NASA publications (no asterisk) should be ordered by the AD, PB, or other *report* number shown on the last line of the citation, not by the N accession number. It is also advisable to cite the title and other bibliographic identification.

Avail: SOD (or GPO). Sold by the Superintendent of Documents, U.S. Government Printing Office, in hard copy. The current price and order number are given following the availability line. (NTIS will fill microfiche requests, as indicated above, for those documents identified by a # symbol.)

(1) A microfiche is a transparent sheet of film, 105 by 148 mm in size, containing as many as 60 to 98 pages of information reduced to micro images (not to exceed 26:1 reduction).

Avail: BLL (formerly NLL): British Library Lending Division, Boston Spa, Wetherby, Yorkshire, England. Photocopies available from this organization at the price shown. (If none is given, inquiry should be addressed to the BLL.)

Avail: DOE Depository Libraries. Organizations in U.S. cities and abroad that maintain collections of Department of Energy reports, usually in microfiche form, are listed in *Energy Research Abstracts.* Services available from the DOE and its depositories are described in a booklet, *DOE Technical Information Center - Its Functions and Services* (TID-4660), which may be obtained without charge from the DOE Technical Information Center.

Avail: ESDU. Pricing information on specific data, computer programs, and details on ESDU topic categories can be obtained from ESDU International Ltd. Requesters in North America should use the Virginia address while all other requesters should use the London address, both of which are on page vi.

Avail: Fachinformationszentrum, Karlsruhe. Sold by the Fachinformationszentrum Energie, Physik, Mathematik GMBH, Eggenstein Leopoldshafen, Federal Republic of Germany, at the price shown in deutschmarks (DM).

Avail: HMSO. Publications of Her Majesty's Stationery Office are sold in the U.S. by Pendragon House, Inc. (PHI), Redwood City, California. The U.S. price (including a service and mailing charge) is given, or a conversion table may be obtained from PHI.

Avail: NASA Public Document Rooms. Documents so indicated may be examined at or purchased from the National Aeronautics and Space Administration, Public Documents Room (Room 126), 600 Independence Ave., S.W., Washington, D.C. 20546, or public document rooms located at each of the NASA research centers, the NASA Space Technology Laboratories, and the NASA Pasadena Office at the Jet Propulsion Laboratory.

Avail: Univ. Microfilms. Documents so indicated are dissertations selected from *Dissertation Abstracts* and are sold by University Microfilms as xerographic copy (HC) and microfilm. All requests should cite the author and the Order Number as they appear in the citation.

Avail: US Patent and Trademark Office. Sold by Commissioner of Patents and Trademarks, U.S. Patent and Trademark Office, at the standard price of $1.50 each, postage free. (See discussion of NASA patents and patent applications below.)

Avail: (US Sales Only). These foreign documents are available to users within the United States from the National Technical Information Service (NTIS). They are available to users outside the United States through the International Nuclear Information Service (INIS) representative in their country, or by applying directly to the issuing organization.

Avail: USGS. Originals of many reports from the U.S. Geological Survey, which may contain color illustrations, or otherwise may not have the quality of illustrations preserved in the microfiche or facsimile reproduction, may be examined by the public at the libraries of the USGS field offices whose addresses are listed in this Introduction. The libraries may be queried concerning the availability of specific documents and the possible utilization of local copying services, such as color reproduction.

Avail: Issuing Activity, or Corporate Author, or no indication of availability. Inquiries as to the availability of these documents should be addressed to the organization shown in the citation as the corporate author of the document.

NASA PATENTS AND PATENT APPLICATIONS

Patents and patent applications owned by NASA are announced in *STAR* under appropriate subject categories and are referenced in the *STAR* indexes. In the Report/Accession Number Index, patents are indexed by the NASA Case Number (which appears in lieu of the report number in other indexes), the U.S. Patent Number, the U.S. Patent Application Serial Number, and the U.S. Patent Class. Patent applications for which patents have not yet been issued are indexed by the NASA Case Number and the U.S. Patent Application Serial Number.

NASA *patent application specifications* are sold in paper copy by the National Technical Information Service at price code A02. Microfiche are sold at price code A01. The US-Patent-Appl-SN- number should be used in ordering either paper copy or microfiche from NTIS. Printed copies of *patents* (which are not microfiched) are available for purchase at $1.50 per copy from:

Commissioner of Patents and Trademarks
U.S. Patent and Trademark Office
Washington, D.C. 20231

When ordering patents, the U.S. Patent Number should be used, and payment must be remitted in advance, preferably by money order or check payable to the Commissioner of Patents and Trademarks. Prepaid purchase coupons for ordering are also available from the Patent and Trademark Office. The patents and patent applications announced in *STAR* are owned by NASA and are available for royalty-free licensing. Requests for licensing terms and further information should be addressed to:

Assistant General Counsel for Patent Matters/Code GP
National Aeronautics and Space Administration
Washington, D.C. 20546

ELIGIBILITY AND REGISTRATION FOR NASA INFORMATION PRODUCTS AND SERVICES

A variety of services is available to organizations of the following types that have registered with NASA to receive specific services or products:

1. NASA offices, research centers, contractors, subcontractors, grantees, and consultants;
2. Other U.S. Government agencies and their contractors;
3. Libraries in the United States that have arrangements with NASA to maintain collections of NASA documents for public reference;
4. Other organizations in the United States having a need for NASA documents in work related to aeronautics and space research;
5. Organizations abroad that have established reciprocal document exchange arrangements with NASA.

Only the central service points or central points of document acquisition and control within qualified organizations are eligible to register for NASA products and services. Domestic organizations that may be eligible to receive various classes of NASA publications and services should address their requests for registration or for further information to:

NASA Scientific and Technical Information Facility
ATTN: Registration Activity
P.O. Box 8757
B.W.I. Airport, Maryland 21240

Organizations abroad should direct requests to the same address, but to the attention of: International Exchange Program.

AVAILABILITY OF *STAR* ABSTRACTS ON MICROFICHE

Microfiche of the abstract sections of this issue and other issues of *STAR* are available on annual subscription from NTIS, Attn: Subscriptions, 5285 Port Royal Road, Springfield, Virginia 22161. Annual subscription rates are $70.00 North America; $140.00 foreign. Abstract sections for previous years retroactive to 1964 are available at the current rates. Microfiche for individual *STAR* issue abstract sections are not available.

PUBLIC COLLECTIONS OF NASA DOCUMENTS

DOMESTIC: NASA and NASA-sponsored documents and a large number of aerospace publications are available to the public for reference purposes at the library maintained by the American Institute of Aeronautics and Astronautics, Technical Information Service, 555 West 57th Street, 12th Floor, New York, New York 10019

EUROPEAN: An extensive collection of NASA and NASA-sponsored publications is maintained by the British Library Lending Division, Boston Spa, Wetherby, Yorkshire, England for public access. The British Library Lending Division also has available many of the non-NASA publications cited in *STAR*. European requesters may purchase facsimile copy or microfiche of NASA and NASA-sponsored documents, those identified by both the symbols # and * from ESA - Information Retrieval Service European Space Agency, 8-10 rue Mario-Nikis, 75738 Paris CEDEX 15, France.

FEDERAL DEPOSITORY LIBRARY PROGRAM

In order to provide the general public with greater access to U.S. Government publications, Congress established the Federal Depository Library Program under the Government Printing Office (GPO), with 50 regional depositories responsible for permanent retention of material, inter-library loan, and reference services. At least one copy of nearly every NASA and NASA-sponsored publication, either in printed or microfiche format, is received and retained by the 50 regional depositories. A list of the regional GPO libraries, arranged alphabetically by state, appears on the inside back cover. These libraries are *not* sales outlets. A local library can contact a Regional Depository to help locate specific reports, or direct contact may be made by an individual.

ADDRESSES OF ORGANIZATIONS

American Institute of Aeronautics and Astronautics
Technical Information Service
555 West 57th Street, 12th Floor
New York, New York 10019

British Library Lending Division,
Boston Spa, Wetherby, Yorkshire,
England

Commissioner of Patents and Trademarks
U.S. Patent and Trademark Office
Washington, D.C. 20231

Department of Energy
Technical Information Center
P.O. Box 62
Oak Ridge, Tennessee 37830

ESA-Information Retrieval Service
ESRIN
Via Galileo Galilei
00044 Frascati (Rome) Italy

ESDU International, Ltd.
1495 Chain Bridge Road
McLean, Virginia 22101

ESDU International, Ltd.
251-259 Regent Street
London, W1R 7AD, England

Fachinformationszentrum Energie, Physik, Mathematik GMBH
7514 Eggenstein Leopoldshafen
Federal Republic of Germany

Her Majesty's Stationery Office
P.O. Box 569, S.E. 1
London, England

NASA Scientific and Technical Information Facility
P.O. Box 8757
B.W.I. Airport, Maryland 21240

National Aeronautics and Space Administration
Scientific and Technical Information Branch (NTT-1)
Washington, D.C. 20546

National Technical Information Service
5285 Port Royal Road
Springfield, Virginia 22161

Pendragon House, Inc.
899 Broadway Avenue
Redwood City, California 94063

Superintendent of Documents
U.S. Government Printing Office
Washington, D.C. 20402

University Microfilms
A Xerox Company
300 North Zeeb Road
Ann Arbor, Michigan 48106

University Microfilms, Ltd.
Tylers Green
London, England

U.S. Geological Survey Library
National Center - MS 950
12201 Sunrise Valley Drive
Reston, Virginia 22092

U.S. Geological Survey Library
2255 North Gemini Drive
Flagstaff, Arizona 86001

U.S. Geological Survey
345 Middlefield Road
Menlo Park, California 94025

U.S. Geological Survey Library
Box 25046
Denver Federal Center, MS914
Denver, Colorado 80225

NTIS PRICE SCHEDULES

(Effective January 1, 1987)

Schedule A
STANDARD PRICE DOCUMENTS AND MICROFICHE

PRICE CODE	PAGE RANGE	NORTH AMERICAN PRICE	FOREIGN PRICE
A01	Microfiche	$ 6.50	$13.00
A02	001-025	9.95	19.90
A03	026-050	11.95	23.90
A04-A05	051-100	13.95	27.90
A06-A09	101-200	18.95	37.90
A10-A13	201-300	24.95	49.90
A14-A17	301-400	30.95	61.90
A18-A21	401-500	36.95	73.90
A22-A25	501-600	42.95	85.90
A99	601-up	*	*
NO1		45.00	80.00
NO2		48.00	80.00

Schedule E
EXCEPTION PRICE DOCUMENTS AND MICROFICHE

PRICE CODE	NORTH AMERICAN PRICE	FOREIGN PRICE
E01	$ 7.50	15.00
E02	10.00	20.00
E03	11.00	22.00
E04	13.50	27.00
E05	15.50	31.00
E06	18.00	36.00
E07	20.50	41.00
E08	23.00	46.00
E09	25.50	51.00
E10	28.00	56.00
E11	30.50	61.00
E12	33.00	66.00
E13	35.50	71.00
E14	38.50	77.00
E15	42.00	84.00
E16	46.00	92.00
E17	50.00	100.00
E18	54.00	108.00
E19	60.00	120.00
E20	70.00	140.00
E99	*	*

*Contact NTIS for price quote.

IMPORTANT NOTICE

NTIS Shipping and Handling Charges

U.S., Canada, Mexico — ADD $3.00 per TOTAL ORDER

All Other Countries — ADD $4.00 per TOTAL ORDER

Exceptions — Does NOT apply to:

ORDERS REQUESTING NTIS RUSH HANDLING
ORDERS FOR SUBSCRIPTION OR STANDING ORDER PRODUCTS *ONLY*

NOTE: Each additional delivery address on an order requires a separate shipping and handling charge.

VOLUME 25 NUMBER 4 / FEBRUARY 23, 1987

TABLE OF CONTENTS

AERONAUTICS

Includes aeronautics (general); aerodynamics; air transportation and safety; aircraft communications and navigation; aircraft design, testing and performance; aircraft instrumentation; aircraft propulsion and power; aircraft stability and control; and research and support facilities (air).

For related information see also *Astronautics.*

01 AERONAUTICS (GENERAL) 437

02 AERODYNAMICS 437

Includes aerodynamics of bodies, combinations, wings, rotors, and control surfaces; and internal flow in ducts and turbomachinery.

For related information see also *34 Fluid Mechanics and Heat Transfer*

03 AIR TRANSPORTATION AND SAFETY 439

Includes passenger and cargo air transport operations; and aircraft accidents.

For related information see also *16 Space Transportation* and *85 Urban Technology and Transportation.*

04 AIRCRAFT COMMUNICATIONS AND NAVIGATION 440

Includes digital and voice communication with aircraft; air navigation systems (satellite and ground based); and air traffic control.

For related information see also *17 Space Communications, Spacecraft Communications, Command and Tracking* and *32 Communications and Radar.*

05 AIRCRAFT DESIGN, TESTING AND PERFORMANCE 441

Includes aircraft simulation technology.

For related information see also *18 Spacecraft Design, Testing and Performance* and *39 Structural Mechanics.* For land transportation vehicles see *85 Urban Technology and Transportation.*

06 AIRCRAFT INSTRUMENTATION N.A.

Includes cockpit and cabin display devices; and flight instruments.

For related information see also *19 Spacecraft Instrumentation* and *35 Instrumentation and Photography.*

07 AIRCRAFT PROPULSION AND POWER 442

Includes prime propulsion systems and systems components, e.g., gas turbine engines and compressors; and onboard auxiliary power plants for aircraft.

For related information see also *20 Spacecraft Propulsion and Power, 28 Propellants and Fuels,* and *44 Energy Production and Conversion.*

08 AIRCRAFT STABILITY AND CONTROL 443

Includes aircraft handling qualities; piloting; flight controls; and autopilots.

For related information see also *05 Aircraft Design, Testing and Performance.*

09 RESEARCH AND SUPPORT FACILITIES (AIR) 444

Includes airports, hangars and runways; aircraft repair and overhaul facilities; wind tunnels; shock tubes; and aircraft engine test stands.

For related information see also *14 Ground Support Systems and Facilities (Space).*

ASTRONAUTICS

Includes astronautics (general); astrodynamics; ground support systems and facilities (space); launch vehicles and space vehicles; space transportation; space communications, spacecraft communications, command and tracking; spacecraft design, testing and performance; spacecraft instrumentation; and spacecraft propulsion and power.

For related information see also *Aeronautics*

12 ASTRONAUTICS (GENERAL) 444

For extraterrestrial exploration see *91 Lunar and Planetary Exploration.*

13 ASTRODYNAMICS 444

Includes powered and free-flight trajectories; and orbital and launching dynamics.

14 GROUND SUPPORT SYSTEMS AND FACILITIES (SPACE) 445

Includes launch complexes, research and production facilities; ground support equipment, e.g., mobile transporters; and simulators.

For related information see also *09 Research and Support Facilities (Air).*

15 LAUNCH VEHICLES AND SPACE VEHICLES 445

Includes boosters; operating problems of launch/space vehicle systems; and reusable vehicles.

For related information see also *20 Spacecraft Propulsion and Power.*

16 SPACE TRANSPORTATION 446

Includes passenger and cargo space transportation, e.g., shuttle operations; and space rescue techniques.

For related information see also *03 Air Transportation and Safety* and *18 Spacecraft Design, Testing and Performance.* For space suits see *54 Man/System Technology and Life Support.*

17 SPACE COMMUNICATIONS, SPACECRAFT COMMUNICATIONS, COMMAND AND TRACKING N.A.

Includes telemetry; space communications networks; astronavigation and guidance; and radio blackout.

For related information see also *04 Aircraft Communications and Navigation* and *32 Communications and Radar.*

18 SPACECRAFT DESIGN, TESTING AND PERFORMANCE 447

Includes satellites; space platforms; space stations; spacecraft systems and components such as thermal and environmental controls; and attitude controls.

For life support systems see *54 Man/System Technology and Life Support.* For related information see also *05 Aircraft Design, Testing and Performance, 39 Structural Mechanics,* and *16 Space Transportation.*

19 SPACECRAFT INSTRUMENTATION 449

For related information see also *06 Aircraft Instrumentation* and *35 Instrumentation and Photography.*

20 SPACECRAFT PROPULSION AND POWER 449

Includes main propulsion systems and components, e.g. rocket engines; and spacecraft auxiliary power sources.

For related information see also *07 Aircraft Propulsion and Power, 28 Propellants and Fuels, 44 Energy Production and Conversion,* and *15 Launch Vehicles and Space Vehicles.*

CHEMISTRY AND MATERIALS

Includes chemistry and materials (general); composite materials; inorganic and physical chemistry; metallic materials; nonmetallic materials; propellants and fuels; and materials processing.

23 CHEMISTRY AND MATERIALS (GENERAL) 450

24 COMPOSITE MATERIALS 451

Includes physical, chemical, and mechanical properties of laminates and other composite materials.

For ceramic materials see *27 Nonmetallic Materials.*

25 INORGANIC AND PHYSICAL CHEMISTRY 452

Includes chemical analysis, e.g., chromatography; combustion theory; electrochemistry; and photochemistry.

For related information see also *77 Thermodynamics and Statistical Physics.*

26 METALLIC MATERIALS 456

Includes physical, chemical, and mechanical properties of metals, e.g., corrosion; and metallurgy.

27 NONMETALLIC MATERIALS 462

Includes physical, chemical, and mechanical properties of plastics, elastomers, lubricants, polymers, textiles, adhesives, and ceramic materials.

For composite materials see *24 Composite Materials.*

28 PROPELLANTS AND FUELS 465

Includes rocket propellants, igniters and oxidizers; their storage and handling procedures; and aircraft fuels.

For related information see also *07 Aircraft Propulsion and Power, 20 Spacecraft Propulsion and Power,* and *44 Energy Production and Conversion.*

29 MATERIALS PROCESSING N.A.

Includes space-based development of products and processes for commercial application.

For biological materials see *55 Space Biology.*

ENGINEERING

Includes engineering (general); communications and radar; electronics and electrical engineering; fluid mechanics and heat transfer; instrumentation and photography; lasers and masers; mechanical engineering; quality assurance and reliability; and structural mechanics.

For related information see also *Physics.*

31 ENGINEERING (GENERAL) 466

Includes vacuum technology; control engineering; display engineering; cryogenics; and fire prevention.

32 COMMUNICATIONS AND RADAR 468

Includes radar; land and global communications; communications theory; and optical communications.

For related information see also *04 Aircraft Communications and Navigation* and *17 Space Communications, Spacecraft Communications, Command and Tracking.* For search and rescue see *03 Air Transportation and Safety,* and *16 Space Transportation.*

33 ELECTRONICS AND ELECTRICAL ENGINEERING 474

Includes test equipment and maintainability; components, e.g., tunnel diodes and transistors; microminiaturization; and integrated circuitry.

For related information see also *60 Computer Operations and Hardware* and *76 Solid-State Physics.*

34 FLUID MECHANICS AND HEAT TRANSFER 482

Includes boundary layers; hydrodynamics; fluidics; mass transfer and ablation cooling.

For related information see also *02 Aerodynamics* and *77 Thermodynamics and Statistical Physics.*

35 INSTRUMENTATION AND PHOTOGRAPHY 485

Includes remote sensors; measuring instruments and gages; detectors; cameras and photographic supplies; and holography.

For aerial photography see *43 Earth Resources and Remote Sensing.* For related information see also *06 Aircraft Instrumentation* and *19 Spacecraft Instrumentation.*

36 LASERS AND MASERS 488

Includes parametric amplifiers.

For related information see also *76 Solid-State Physics.*

37 MECHANICAL ENGINEERING 492

Includes auxiliary systems (nonpower); machine elements and processes; and mechanical equipment.

38 QUALITY ASSURANCE AND RELIABILITY 498

Includes product sampling procedures and techniques; and quality control.

39 STRUCTURAL MECHANICS 498

Includes structural element design and weight analysis; fatigue; and thermal stress.

For applications see *05 Aircraft Design, Testing and Performance* and *18 Spacecraft Design, Testing and Performance.*

GEOSCIENCES

Includes geosciences (general); earth resources and remote sensing; energy production and conversion; environment pollution; geophysics; meteorology and climatology; and oceanography.

For related information see also *Space Sciences.*

42 GEOSCIENCES (GENERAL) 504

43 EARTH RESOURCES AND REMOTE SENSING 506

Includes remote sensing of earth resources by aircraft and spacecraft; photogrammetry; and aerial photography.

For instrumentation see *35 Instrumentation and Photography.*

44 ENERGY PRODUCTION AND CONVERSION 512

Includes specific energy conversion systems, e.g., fuel cells; global sources of energy; geophysical conversion; and windpower.

For related information see also *07 Aircraft Propulsion and Power, 20 Spacecraft Propulsion and Power,* and *28 Propellants and Fuels.*

45 ENVIRONMENT POLLUTION 514

Includes atmospheric, noise, thermal, and water pollution.

46 GEOPHYSICS 515

Includes aeronomy; upper and lower atmosphere studies; ionospheric and magnetospheric physics; and geomagnetism.

For space radiation see *93 Space Radiation.*

47 METEOROLOGY AND CLIMATOLOGY 520

Includes weather forecasting and modification.

48 OCEANOGRAPHY 534

Includes biological, dynamic, and physical oceanography; and marine resources.

For related information see also *43 Earth Resources and Remote Sensing.*

LIFE SCIENCES

Includes life sciences (general); aerospace medicine; behavioral sciences; man/system technology and life support; and space biology.

51 LIFE SCIENCES (GENERAL) 534

52 AEROSPACE MEDICINE 535

Includes physiological factors; biological effects of radiation; and effects of weightlessness on man and animals.

53 BEHAVIORAL SCIENCES 538

Includes psychological factors; individual and group behavior; crew training and evaluation; and psychiatric research.

54 MAN/SYSTEM TECHNOLOGY AND LIFE SUPPORT 539

Includes human engineering; biotechnology; and space suits and protective clothing.

For related information see also *16 Space Transportation.*

55 SPACE BIOLOGY N.A.

Includes exobiology; planetary biology; and extraterrestrial life.

MATHEMATICAL AND COMPUTER SCIENCES

Includes mathematical and computer sciences (general); computer operations and hardware; computer programming and software; computer systems; cybernetics; numerical analysis; statistics and probability; systems analysis; and theoretical mathematics.

59 MATHEMATICAL AND COMPUTER SCIENCES (GENERAL) N.A.

60 COMPUTER OPERATIONS AND HARDWARE 543

Includes hardware for computer graphics, firmware, and data processing.

For components see *33 Electronics and Electrical Engineering.*

61 COMPUTER PROGRAMMING AND SOFTWARE 544

Includes computer programs, routines, algorithms, and specific applications, e.g., CAD/CAM.

62 COMPUTER SYSTEMS 547

Includes computer networks and special application computer systems.

63 CYBERNETICS 548

Includes feedback and control theory, artificial intelligence, robotics and expert systems.

For related information see also *54 Man/System Technology and Life Support.*

64 NUMERICAL ANALYSIS 548

Includes iteration, difference equations, and numerical approximation.

65 STATISTICS AND PROBABILITY 551

Includes data sampling and smoothing; Monte Carlo method; and stochastic processes.

66 SYSTEMS ANALYSIS 554

Includes mathematical modeling; network analysis; and operations research.

67 THEORETICAL MATHEMATICS 554

Includes topology and number theory.

PHYSICS

Includes physics (general); acoustics; atomic and molecular physics; nuclear and high-energy physics; optics; plasma physics; solid-state physics; and thermodynamics and statistical physics.

For related information see also *Engineering.*

70 PHYSICS (GENERAL) 555

For precision time and time interval (PTTI) see *35 Instrumentation and Photography;* for geophysics, astrophysics or solar physics see *46 Geophysics, 90 Astrophysics,* or *92 Solar Physics.*

71 ACOUSTICS 555
Includes sound generation, transmission, and attenuation.
For noise pollution see *45 Environment Pollution.*

72 ATOMIC AND MOLECULAR PHYSICS 556
Includes atomic structure, electron properties, and molecular spectra.

73 NUCLEAR AND HIGH-ENERGY PHYSICS 556
Includes elementary and nuclear particles; and reactor theory.
For space radiation see *93 Space Radiation.*

74 OPTICS 557
Includes light phenomena and optical devices.
For lasers see *36 Lasers and Masers.*

75 PLASMA PHYSICS 563
Includes magnetohydrodynamics and plasma fusion.
For ionospheric plasmas see *46 Geophysics.* For space plasmas see *90 Astrophysics.*

76 SOLID-STATE PHYSICS 564
Includes superconductivity.
For related information see also *33 Electronics and Electrical Engineering* and *36 Lasers and Masers.*

77 THERMODYNAMICS AND STATISTICAL PHYSICS 570
Includes quantum mechanics; theoretical physics; and Bose and Fermi statistics.
For related information see also *25 Inorganic and Physical Chemistry* and *34 Fluid Mechanics and Heat Transfer.*

SOCIAL SCIENCES

Includes social sciences (general); administration and management; documentation and information science; economics and cost analysis; law, political science, and space policy; and urban technology and transportation.

80 SOCIAL SCIENCES (GENERAL) N.A.
Includes educational matters.

81 ADMINISTRATION AND MANAGEMENT 570
Includes management planning and research.

82 DOCUMENTATION AND INFORMATION SCIENCE 570
Includes information management; information storage and retrieval technology; technical writing; graphic arts; and micrography.
For computer documentation see *61 Computer Programming and Software.*

83 ECONOMICS AND COST ANALYSIS N.A.
Includes cost effectiveness studies.

84 LAW, POLITICAL SCIENCE AND SPACE POLICY 571
Includes NASA appropriation hearings; aviation law; space law and policy; international law; international cooperation; and patent policy.

85 URBAN TECHNOLOGY AND TRANSPORTATION 571
Includes applications of space technology to urban problems; technology transfer; technology assessment; and surface and mass transportation.
For related information see *03 Air Transportation and Safety, 16 Space Transportation,* and *44 Energy Production and Conversion.*

SPACE SCIENCES

Includes space sciences (general); astronomy; astrophysics; lunar and planetary exploration; solar physics; and space radiation.
For related information see also *Geosciences.*

88 SPACE SCIENCES (GENERAL) N.A.

89 ASTRONOMY 572
Includes radio, gamma-ray, and infrared astronomy; and astrometry.

90 ASTROPHYSICS 572
Includes cosmology; celestial mechanics; space plasmas; and interstellar and interplanetary gases and dust.
For related information see also *75 Plasma Physics.*

91 LUNAR AND PLANETARY EXPLORATION 574
Includes planetology; and manned and unmanned flights.
For spacecraft design or space stations see *18 Spacecraft Design, Testing and Performance.*

92 SOLAR PHYSICS 574
Includes solar activity, solar flares, solar radiation and sunspots.
For related information see *93 Space Radiation.*

93 SPACE RADIATION 576
Includes cosmic radiation; and inner and outer earth's radiation belts.
For biological effects of radiation see *52 Aerospace Medicine.* For theory see *73 Nuclear and High-Energy Physics.*

GENERAL

Includes aeronautical, astronautical, and space science related histories, biographies, and pertinent reports too broad for categorization; histories or broad overviews of NASA programs.

99 GENERAL N.A.

Note: N.A. means that no abstracts were assigned to this category for this issue.

SUBJECT INDEX I-1
PERSONAL AUTHOR INDEX I-57
CORPORATE SOURCE INDEX I-65
CONTRACT NUMBER INDEX I-77
REPORT/ACCESSION NUMBER INDEX I-81

TYPICAL CITATION AND ABSTRACT

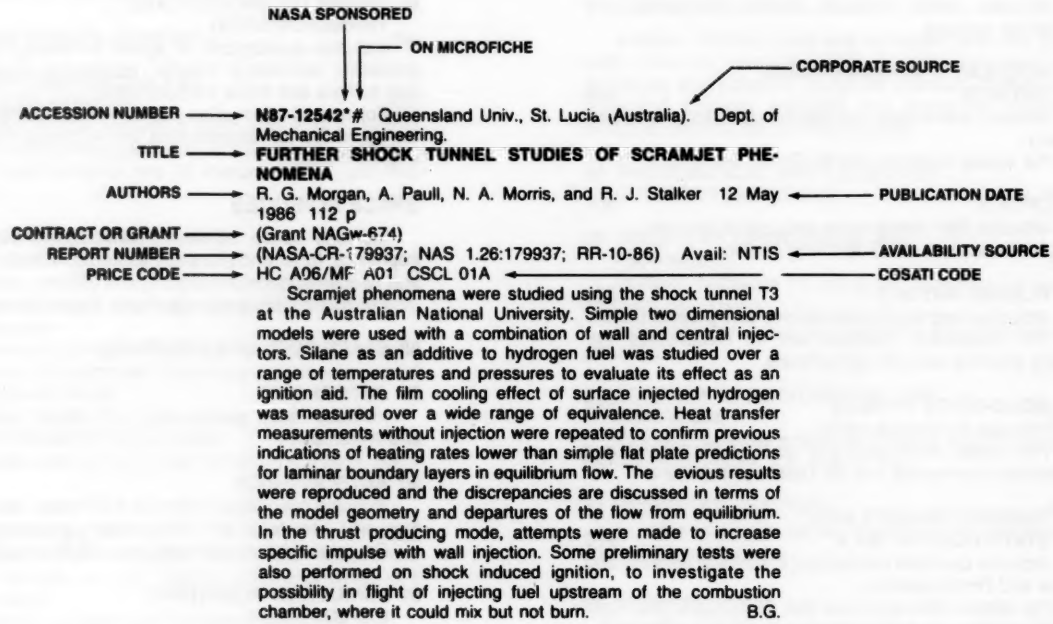
NASA SPONSORED
ON MICROFICHE
CORPORATE SOURCE
ACCESSION NUMBER
N87-12542*# Queensland Univ., St. Lucia (Australia). Dept. of Mechanical Engineering.
TITLE
FURTHER SHOCK TUNNEL STUDIES OF SCRAMJET PHENOMENA
AUTHORS
R. G. Morgan, A. Paull, N. A. Morris, and R. J. Stalker 12 May 1986 112 p
PUBLICATION DATE
CONTRACT OR GRANT
(Grant NAGw-674)
REPORT NUMBER
(NASA-CR-179937; NAS 1.26:179937; RR-10-86) Avail: NTIS
AVAILABILITY SOURCE
PRICE CODE
HC A06/MF A01 CSCL 01A
COSATI CODE
Scramjet phenomena were studied using the shock tunnel T3 at the Australian National University. Simple two dimensional models were used with a combination of wall and central injectors. Silane as an additive to hydrogen fuel was studied over a range of temperatures and pressures to evaluate its effect as an ignition aid. The film cooling effect of surface injected hydrogen was measured over a wide range of equivalence. Heat transfer measurements without injection were repeated to confirm previous indications of heating rates lower than simple flat plate predictions for laminar boundary layers in equilibrium flow. The evious results were reproduced and the discrepancies are discussed in terms of the model geometry and departures of the flow from equilibrium. In the thrust producing mode, attempts were made to increase specific impulse with wall injection. Some preliminary tests were also performed on shock induced ignition, to investigate the possibility in flight of injecting fuel upstream of the combustion chamber, where it could mix but not burn. B.G.

VOLUME 25 NUMBER 4 / FEBRUARY 23, 1987

Scientific and Technical Aerospace Reports

A Semimonthly Publication of the National Aeronautics and Space Administration

01 AERONAUTICS (GENERAL)

N87-12532* National Aeronautics and Space Administration, Washington, D.C.
AERONAUTICAL ENGINEERING: A CONTINUING BIBLIOGRAPHY WITH INDEXES
Oct. 1986 152 p
(NASA-SP-7037(205); NAS 1.21:7037(205)) Avail: NTIS HC A08 CSCL 01A

This bibliography lists 517 reports, articles and other documents introduced into the NASA scientific and technical information system in September 1986. M.G.

N87-12533# Air Force Systems Command, Wright-Patterson AFB, Ohio. Foreign Technology Div.
THE EFFECT OF A WINGLET ON THE SPATIAL VORTEX OF A SLENDER BODY AT HIGH ANGLE OF ATTACK
Wang Zixing and Wu Genxing 7 Jul. 1986 15 p Transl. into ENGLISH from Konggi Donglixue Xuebao (China), v. 3, no. 1, 1985 p 49-53
(AD-A169925; FTD-ID(RS)T-0267-86) Avail: NTIS HC A02/MF A01 CSCL 20/4

The experimental investigation of the effect of a winglet on the spatial vortex of a slender body at a high angle of attack is presented. This investigation clearly shows that the circulation of the body vortex is minimized by the winglet and the vortex position is lower than that without the winglet, so that the asymmetric problem can be solved. GRA

N87-12534# Air Force Inst. of Tech., Wright-Patterson AFB, Ohio.
THE PORTFOLIO MODEL OF TECHNOLOGICAL DEVELOPMENT IN THE AIRCRAFT INDUSTRY M.S. Thesis
David M. Snyder May 1986 56 p
(AD-A170832; AFIT/CI/NR-86-84T) Avail: NTIS HC A04/MF A01 CSCL 05/3

The aircraft industry has long been considered the quintessential high technology industry. By examining the dynamics of technological change in this industry the portfolio model of technological advancement is developed. This model may be used to describe technological advancement in large sophisticated, technology intensive systems. The rapid advancement of individual technologies as measured by improvements in specific performance parameters is evident in the aircraft industry. However, the ability of a technology to improve performance in one or more key performance parameter may lead to adverse effects in other performance parameters or may not be compatible with other technological developments that are occurring in the industry. Individual technical improvements can be characterized as either portfolio reinforcing or portfolio shifting depending on whether or not they promote shift in the way the technologies are combined into a total system or portfolio. The commercially and economically successful products appear to be those that combine technologies into an optimum bundle of performance characteristics or portfolio. Technologies that flourish are not always the technologies on the leading edge of the performance frontier, but are those technologies that product the optimum portfolio. Author (GRA)

02 AERODYNAMICS

Includes aerodynamics of bodies, combinations, wings, rotors, and control surfaces; and internal flow in ducts and turbomachinery.

For related information see also *34 Fluid Mechanics and Heat Transfer.*

N87-12535 Texas Univ., Austin.
VISCOUS-INVISCID INTERACTION IN TRANSONIC SEPARATED FLOW OVER SOLID AND POROUS AIRFOILS AND CASCADES Ph.D. Thesis
Charles Randolph Olling 1985 185 p
Avail: Univ. Microfilms Order No. DA8609621

Viscous-inviscid interaction is used to compute steady two-dimensional, transonic separated flows for cascades and isolated airfoils. The full-potential code of Dulikravich is coupled with both a laminar/transition/turbulent integral boundary-layer/tubulent wake code written by the author and the finite-difference boundary-layer code of Drela using the semi-inverse method of Carter or Wigton. The transpiration coupling concept is applied. An option for a porous airfoil with passive physical transpiration is also included. Examples are presented which demonstrate that such flows can be calculated with engineering accuracy by the present code. The equivalent transpiration velocity can be larger in cascades than for isolated airfoils. Carter's update formula gives smoother solutions for a strong shock than Wigton's update formulas, although Wigton's formulas are preferred in the early coupling cycles for cascades. The computations show that passive physical transpiration can lead to a lower drag coefficient and higher lift coefficient, a weaker shock and elimination of shock-induced separation. The extent of the porous region and permeability factor distribution of the porous region must be chosen carefully if these improvements are to be achieved. Dissert. Abstr.

N87-12536 ESDU International Ltd., London (England).
INTRODUCTION TO AERODYNAMICS DERIVITIVES, EQUATIONS OF MOTION AND STABILITY
Oct. 1986 64 p Supersedes ESDU-Aero-A.00.00.02, ESDU-Aero-A.00.00.03, ESDU-Aero-A.00.00.04, and ESDU-67039
(ESDU-86021; ISBN-0-85679-573-9; ISSN-0141-397X) Avail: ESDU

This Data Item ESDU 86021 is an addition to the Aerodynamics Sub-series. It is a comprehensive introduction to the concept and use of derivatives in determining aircraft stability. After explaining a systematic method for expressing aerodynamic forces, moments, and derivatives in dimensionless form, the equations of motion for an aircraft treated as a rigid body are developed and the linearized small-perturbation form introduced. The conditions are outlined for the separation of the equations

into a lateral and a longitudinal set, and a detailed study is made of the behavior of an aircraft disturbed with controls fixed from straight symmetric level flight. A comprehensive practical worked example illustrates the use of the techniques. A comparison is made between the ISO notation for derivatives used by ESDU, and the most widely used notation in the US, equations are given for deriving the longitudinal derivatives from the force and moment coefficients, and reference is included to all the ESDU validated data for lateral derivatives. Also included is the traditional treatment for static stability leading to the definitions of static and maneuver margins, and the relation between static stability and dynamic stability is discussed. Finally, a description is given in simple physical terms of commonly occurring lateral modes of an aircraft following a small disturbance. ESDU

N87-12537 ESDU International Ltd., London (England).
PROPELLAR/BODY INTERACTION FOR THRUST AND DRAG
Aug. 1986 20 p
(ESDU-86017; ISBN-0-85679-569-0; ISSN-0141-397X) Avail: ESDU

Available as part of the ESDU Sub-series on Aerodynamics, this document gives a simple method of estimating the thrust decrement and drag increment due to the interaction of propeller flow with a body (or nacelle) at zero incidence. It applies to smoothly contoured bodies with a tractor propeller at or near the nose or a pusher propeller at or near the tail and the propellers may be counter-rotating. It applies to Mach numbers up to 80 per cent of critical for the spinner-body combination. The method predicts the propulsive thrust in terms of the shaft thrust developed to within 2 or 3 per cent of thrust. A detailed discussion of the factors affecting the interaction effects is included. A comprehensive worked example shows how the method is used in combination with the method of ESDU 83001 for the propeller free-air thrust and of ESDU 78019 for the body drag propeller-off. ESDU

N87-12538*# National Aeronautics and Space Administration. Langley Research Center, Hampton, Va.
MACH 6 EXPERIMENTAL AND THEORETICAL STABILITY AND PERFORMANCE OF A FINNED CYLINDRICAL BODY AT ANGLES OF ATTACK UP TO 65 DEG
Edward R. Hartman and Patrick J. Johnston Sep. 1986 45 p
(NASA-TM-89050; NAS 1.15:89050) Avail: NTIS HC A03/MF A01 CSCL 01A

A theoretical and experimental investigation of the longitudinal and lateral-directional stability and control of a finned cylindrical body has been conducted at Mach 6. The angle-of-attack range extended from 20 to 65 deg. to encompass maximum lift. Stability, performance, and trim could be accurately predicted with the fins in the + arrangement but this was not the case when the fins were in the x orientation where windward fin choking occurred at angles of attack above 50 deg. reducing their effectiveness and causing pitch up. Author

N87-12539*# National Aeronautics and Space Administration. Ames Research Center, Moffett Field, Calif.
AN EXPERIMENTAL INVESTIGATION OF FREE-TIP RESPONSE TO A JET
Larry A. Young Sep. 1986 56 p
(NASA-TM-88250; A-86234; NAS 1.15:88250) Avail: NTIS HC A04/MF A01 CSCL 01A

The aerodynamic response of passively oscillating tips appended to a model helicopter rotor was investigated during a whirl test. Tip responsiveness was found to meet free-tip rotor requirements. Experimental and analytical estimates of the free-tip aerodynamic spring, mechanical spring, and aerodynamic damping were calculated and compared. The free tips were analytically demonstrated to be operating outside the tip resonant response region at full-scale tip speeds. Further, tip resonance was shown to be independent of tip speed, given the assumption that the tip forcing frequency is linearly dependent upon the rotor rotational speed. Author

N87-12540# Royal Aircraft Establishment, Farnborough (England).
AN APPROXIMATE METHOD OF ESTIMATING THE AERODYNAMIC INTERFERENCE BETWEEN TWO PARALLEL BODIES IN A SUPERSONIC FLOW (AXIAL FORCE)
Hirofumi Kondo Mar. 1985 28 p Transl. into ENGLISH from Technical Report of National Aerospace Laboratory, TR-751, 1983
(BR-100271; RAE-Trans-2131) Avail: NTIS HC A03/MF A01

An approximate method of estimating the aerodynamic interference between two parallel bodies in a supersonic flow is discussed. The formulae are derived from linearized theory. The formulae for calculating the wave drag on one body are obtained as functions of Mach number, cone semi-vertex angle, and the relative distances between bodies. Theoretical calculations are compared with wind tunnel test results, and fairly good agreement is noted. It is pointed out that the present method can easily be applied to a combination of more than two bodies. Author

N87-12541*# National Aeronautics and Space Administration. Langley Research Center, Hampton, Va.
EFFECT OF PORT CORNER GEOMETRY ON THE INTERNAL PERFORMANCE OF A ROTATING-VANE-TYPE THRUST REVERSER
Bobby L. Berrier and Francis J. Capone Dec. 1986 51 p
(NASA-TP-2624; L-16135; NAS 1.60:2624) Avail: NTIS HC A04/MF A01 CSCL 01A

An investigation has been conducted in the static-test facility of the Langley 16-Foot Transonic Tunnel to determine the effects of reverser port geometry on the internal performance of a nonaxisymmetric rotating-vane-type thrust reverser. Thrust reverser vane positions representing a spoiled-trust (partially deployed) position and a full-reverse-thrust (fully deployed) position were tested with each port geometry variable. The effects of upstream port corner radius and wall angle on internal performance were determined. In addition, the effect of the length of a simulated cooling liner (blunt-base step) near the reverser port entrance was investigated; five different lengths were tested. All tests were conducted with no external flows, and nozzle pressure ratio was varied from 1.2 to 5.0. Author

N87-12542*# Queensland Univ., St. Lucia (Australia). Dept. of Mechanical Engineering.
FURTHER SHOCK TUNNEL STUDIES OF SCRAMJET PHENOMENA
R. G. Morgan, A. Paull, N. A. Morris, and R. J. Stalker 12 May 1986 112 p
(Grant NAGw-674)
(NASA-CR-179937; NAS 1.26:179937; RR-10-86) Avail: NTIS HC A06/MF A01 CSCL 01A

Scramjet phenomena were studied using the shock tunnel T3 at the Australian National University. Simple two dimensional models were used with a combination of wall and central injectors. Silane as an additive to hydrogen fuel was studied over a range of temperatures and pressures to evaluate its effect as an ignition aid. The film cooling effect of surface injected hydrogen was measured over a wide range of equivalence. Heat transfer measurements without injection were repeated to confirm previous indications of heating rates lower than simple flat plate predictions for laminar boundary layers in equilibrium flow. The previous results were reproduced and the discrepancies are discussed in terms of the model geometry and departures of the flow from equilibrium. In the thrust producing mode, attempts were made to increase specific impulse with wall injection. Some preliminary tests were also performed on shock induced ignition, to investigate the possibility in flight of injecting fuel upstream of the combustion chamber, where it could mix but not burn. B.G.

N87-12543# Department of the Air Force, Washington, D.C.
LENGTH ADJUSTABLE STRUT LINK WITH LOW AERODYNAMIC DRAG Patent
Dudley O. Nash and James A. Crowley, inventors (to Air Force) Issued 25 Feb. 1986 8 p Supersedes AD-D011851
(AD-D012279; US-Patent-4,571,936; US-Patent-Appl-SN-753462;

US-Patent-Class-60-39.31) Avail: US Patent and Trademark Office CSCL 13/5

This invention relates to a low aerodynamic drag structural link suitable for use within the housing of a turbofan jet engine. The link includes length adjustment capability, pivotal end mounting provision, maintained airstream orientation capability, low mass and jam nut length and orientation locking. Several variations in link construction including a single ball and socket arrangement, varying link cross-section along its longitudinal length and the use of fairing nose and tail inserts are disclosed. GRA

N87-12544# JAI Associates, Mountain View, Calif.
NUMERICAL SIMULATION OF TIP VORTICES OF WINGS IN SUBSONIC AND TRANSONIC FLOWS
G. R. Srinivasan, W. J. McCroskey, J. D. Baeder, and T. A. Edwards 1986 26 p
(Contract DAAG29-85-C-0002)
(AD-A169116; ARO-21731.1-EG) Avail: NTIS HC A03/MF A01 CSCL 20/4

The formation and roll up process of the tip vortices of wings in subsonic and transonic flows is numerically simulates using a hybrid scheme of solving a zonal algorithm for thin layer Navier Stokes/Euler equations. The results are in good agreement with the available limited experimental data including the tip vortex strength. GRA

N87-12545# Analytical Methods, Inc., Redmond, Wash.
A SUMMARY OF THE DEVELOPMENT OF INTEGRAL AERODYNAMIC METHODS FOR THE COMPUTATION OF ROTOR WAKE INTERACTIONS Final Report, 1 Aug. 1981 - 30 Aug. 1984
J. M. Summa Mar. 1986 13 p
(Contract DAAG29-81-C-0032)
(AD-A169254; AMI-8605; ARO-18391.3-EG-S) Avail: NTIS HC A02/MF A01 CSCL 20/4

The purpose of the research reported here is to develop basic methodology for a generalized forward flight aerodynamic analysis method for isolated rotors. All of the work thus far has been concerned with the development of integral methods. Efforts have concentrated on analytical modeling studies and code development for fundamental vortex/blade interactions that occur in forward flight. Calculations show that vortex core deformations can be simulated but that numerical errors in the core growth should be removed in order to study such phenomena as bursting. The computed trajectory of a tip vortex passing another wing is also validated with experiment as well as the prediction of vortex induced separations. The calculation of the rotor wake in hover has been improved and the importance of secondary vortex roll ups for a modern rotor is discussed. Finally, a time stepping panel method has been formulated and verified by application to impulsively started wings. A pilot code version for unsteady rotor motions is described along with its preliminary application to a two bladed rotor. GRA

N87-12546# National Aeronautical Establishment, Ottawa (Ontario).
FORCED OSCILLATION OF A TWO-DIMENSIONAL AIRFOIL WITH NONLINEAR AERODYNAMIC LOADS
B. H. Lee and P. LeBlanc Jan. 1986 52 p
(AD-A169350; NAE-LR-617; NRC-25411) Avail: NTIS HC A04/MF A01 CSCL 20/4

Forced oscillation of a two dimensional airfoil with attached and separated flows is investigated using nonlinear unsteady aerodynamics for pitching motion derived from a time synthesization technique utilizing oscillatory loop data determined experimentally. Both one and two degree of freedom oscillations are considered. The structural dynamic equations of motion are integrated by a time marching finite difference scheme. The airfoil response is examined for different values of spring stiffness and magnitudes of externally applied moment. For two degree of freedom vibration, only small plunge amplitude is considered and the aerodynamic loads are approximated by the superposition of nonlinear terms due to pitch and linear terms due to plunge. The presence of a small amplitude plunging motion increases the pitch amplitude slightly for attached flow, while a decrease in pitch amplitude is predicted for separated flow. GRA

N87-12547 Stanford Univ., Calif.
AN ANALYSIS OF BLADE VORTEX INTERACTION AERODYNAMICS AND ACOUSTICS Ph.D. Thesis
Duck Joo Lee 1985 176 p
Avail: Univ. Microfilms Order No. DA8602500

The impulsive noise associated with helicopter flight due to blade-vortex interaction, sometimes called blade slap, is analyzed especially for the case of a close encounter of the blade-tip vortex with a following blade. Three parts of the phenomena are considered: the tip-vortex structure generated by the rotating blade, the unsteady pressure produced on the following blade during the interaction, and the acoustic radiation due to the unsteady pressure field. To simplify the problem, we confine our analysis to the situation where the vortex is aligned parallel to the blade span in which case the maximum acoustic pressure results. The 2-dimensional incompressible flow is assumed with uniform motion of the blade. The tip-vortex is modelled so that the circulation near the tip is rolled into a concentrated vortex and the extreme case of the interaction is studied when the following blade cuts through the center of this vortex core, which is turbulent and viscous. It is further assumed that during the interaction, there is no distortion of the vortex path or of the vortex itself, in other words the interaction occurs only through the boundary condition on the blade giving an unsteady pressure on the blade surface. Acoustic radiation due to the interaction is analyzed in space-fixed coordinates and in the time domain with the unsteady pressure on the blade surface as the source of chordwise compact, but spanwise noncompact radiation. Maximum acoustic pressure is related to the vortex core size and Reynolds number which are in turn functions of the blade-tip aerodynamic parameters. Finally noise reduction and performance are considered. Dissert. Abstr.

N87-12548 Texas Technological Univ., Lubbock.
A NUMERICAL MODEL FOR TWO-DIMENSIONAL UNSTEADY FLOW CALCULATIONS WITH A SURFACE PANEL METHOD Ph.D. Thesis
Bong-Jin Im 1985 132 p
Avail: Univ. Microfilms Order No. DA8607765

A numerical model for two-dimensional airfoils in unsteady motion with boundary layer separation is described. The airfoil and wake surfaces are represented by a finite set of combined source and vortex panels. The source strengths are prescribed to have the same magnitude as the normal relative velocity on the surface due to the free-stream and motion of the airfoil. The vortex strengths on the airfoil surface are determined by applying a kinematic surface tangency condition to a Green's function representation of the potential field, while simultaneously enforcing the Kutta condition. Wake shedding is governed by a dynamic free surface condition and the characteristics of the flow near any boundary layer separation points. Wake deformation is predicted by applying geometric free surface conditions. Calculation results are presented for steady motion, impulsively started rectilinear motion, harmonic pitch oscillations, and constant pitching motions. Experimental data and analytical solutions are also presented for comparison. Dissert. Abstr.

03 AIR TRANSPORTATION AND SAFETY

Includes passenger and cargo air transport operations; and aircraft accidents.

For related information see also *16 Space Transportation* and *85 Urban Technology and Transportation.*

N87-12549# National Transportation Safety Board, Washington, D. C.
AIRCRAFT ACCIDENT/INCIDENT SUMMARY REPORTS: ERIE, PENNSYLVANIA, OCTOBER 14, 1984; ALBUQUERQUE, NEW MEXICO, FEBRUARY 11, 1985

30 Sep. 1986 17 p
(PB86-910407; NTSB-AAR-86-02-Sum) Avail: NTIS HC A02/MF A01

This publication is a compilation of the reports of two separate aircraft accidents investigated by the National Transportation Safety Board. The accident locations and their dates are as follows: Erie, Pennsylvania, October 14, 1984; and Albuquerque, New Mexico, February 11, 1985. Author

N87-12550# National Transportation Safety Board, Washington, D. C. Bureau of Accident Investigation.
AIRCRAFT ACCIDENT REPORT: BAR HARBOR AIRLINES FLIGHT 1808, BEECH BE-99, N300WP, AUBURN-LEWISTON MUNICIPAL AIRPORT, AUBURN, MAINE, AUGUST 25, 1985
30 Sep. 1986 77 p
(PB86-910408; NTSB-AAR-86-06) Avail: NTIS HC A05/MF A01

About 2205 e.d.t. on August 25, 1985, Bar Harbor Airlines Flight 1818, a Beech Aircraft Corporation Model 99 crashed about 1 mile southwest of the Auburn-Lewiston Municipal Airport at Auburn, Maine, while making an instrument landing system (ILS) approach to runway 4. The weather was indefinite 300-foot ceiling, sky obscured, visibility 1 mile in light drizzle and fog. The flight was a regularly scheduled commuter flight between Boston-Logan International Airport and Bangor, Maine, with intermediate stops at Auburn, Augusta, and Waterville, Maine. All six passengers and the two flightcrew members were killed in the accident. The airplane was destroyed by impact forces and postcrash fire. The National Transportation Safety Board determined that the probable cause of the accident was the captain's continuation of an unstabilized approach which resulted in a descent below glide-scope. Contributing to the unstabilized approach was the radar controller's issuance and the captain's acceptance of a nonstandard air traffic control radar vector resulting in an excessive intercept with the localizer. Author

N87-12551# Sverdrup Technology, Inc., Arnold Air Force Station, Tenn.
ANALYSIS AND VERIFICATION OF THE ICING SCALING EQUATIONS. VOLUME 1: REVISION Final Report, 1 Aug. 1981 - 31 Mar. 1984
Gary A. Ruff Mar. 1986 80 p Prepared in cooperation with Arnold Engineering Development Center, Arnold AFS, Tenn.
(AD-A167976; AEDC-TR-85-30-Vol-1-Rev) Avail: NTIS HC A05/MF A01 CSCL 08/12

Study objectives were to evaluate the equations governing the ice-accretion process to identify proposed scaling parameters and to conduct tests to determine which, is any, of the proposed methods produced scale ice accretions. Study results include: (1) A set of equations that can be used to calculate test conditions so that scaled ice shapes are produced on geometrically similar bodies was developed and experimentally verified. (2) Posttest evaluation of the scaling parameters based on the actual test conditions was necessary for accurate evaluation of test results. (3) An icing similitude computer code, SIMICE, was developed to calculate similitude conditions using the verified scaling equations. (4) The equations were applicable over the range of meteorological conditions found in natural icing, with the possible exception of velocity. (5) Velocity is the primary limitation of the scaling equations. To maintain scaled flow fields and droplet impingement characteristics, both the model and full-scale velocities must yield a Reynolds number > or = 200,000 and < the velocity giving the critical Mach number of the body geometry. (6) At values of dynamic pressure of approximately 1.6 psia, shedding characteristics of the ice accretion were observed to affect the final ice shape. GRA

04 AIRCRAFT COMMUNICATIONS AND NAVIGATION

Includes digital and voice communication with aircraft; air navigation systems (satellite and ground based); and air traffic control.

For related information see also *17 Space Communications, Spacecraft Communications, Command and Tracking* and *32 Communications and Radar.*

N87-12552*# Douglas Aircraft Co., Inc., Long Beach, Calif.
GUIDANCE LAW SIMULATION STUDIES FOR COMPLEX APPROACHES USING THE MICROWAVE LANDING SYSTEM (MLS)
J. B. Feather Nov. 1986 80 p
(Contract NAS1-18028)
(NASA-CR-178182; NAS 1.26:178182) Avail: NTIS HC A05/MF A01 CSCL 17G

This report documents results for MLS guidance algorithm development conducted by DAC for NASA under the Advance Transport Operating Systems (ATOPS) Technology Studies program (NAS1-18028). The study consisted of evaluating guidance laws for vertical and lateral path control, as well as speed control, by simulating an MLS approach for the Washington National Airport. This work is an extension and generalization of a previous ATOPS contract (NAS1-16202) completed by DAC in 1985. The Washington river approach was simulated by six waypoints and one glideslope change and consisted of an eleven nautical mile approach path. Tracking performance was generated for 10 cases representing several different conditions, which included MLS noise, steady wind, turbulence, and windshear. Results of this simulation phase are suitable for use in future fixed-base simulator evaluations employing actual hardware (autopilot and a performance management system), as well as crew procedures and information requirements for MLS. Author

N87-12553# Air Force Systems Command, Wright-Patterson AFB, Ohio. Foreign Technology Div.
THE EFFECT OF COUPLING IN AN INERTIAL NAVIGATION PLATFORM STABILIZED SYSTEM MADE UP OF THREE SINGLE-DEGREE-OF-FREEDOM GYROSCOPES
Di Bo-Hao 13 Jun. 1986 17 p Transl. into ENGLISH from Chuanbo Gongcheng (China), no. 4, 1985 p 38-42
(AD-A169110; FTD-ID(RS)T-0283-86) Avail: NTIS HC A02/MF A01 CSCL 17/7

We shall refer to three interacting single-axis systems as a three-axis system. If the interaction between the single-axis systems is weak, the three-axis system can be studied in the single-axis approximation. This approximation could lead to great simplification in the analysis and solution of the problem. On the contrary, if the interaction between the systems is strong, the single-axis approximation is not applicable to the three-axis system. To arrive at the criteria for the applicability of the single-axis approximation, it is necessary to study the effect of coupling between the systems. One type of coupling involves the polar angle and the azimuthal angle. It depends on the geometry of the frame between the platform axes. This type of coupling can be eliminated by a coordinate transformation or an orthogonal transformation. GRA

N87-12554# Boston Univ., Mass. Dept. of Electrical Computer and Systems Engineering.
MEDIUM-FREQUENCY DATA LINK FOR DIFFERENTIAL NAVSTAR/GPS BROADCASTS Final Report, Sep. 1985 - Apr. 1986
Per K. Enge, Michael F. Ruane, and Lee Sheynblatt Jun. 1986 95 p
(Contract DTRS57-85-C-00091)
(AD-A169788; DOT-TSC-CG-86-1; DOT-CG-N-02-86) Avail: NTIS HC A05/MF A01 CSCL 17/7

Differential GPS must communicate differential corrections to civilian users of the Global Positioning System. Modulation of existing marine radiobeacons can provide the needed communica-

tion link for DGPS, provided the operation of existing radiobeacon direction finding equipment is maintained and adequate DGPS range is provided in the presence of atmospheric noise and skywave fading. Existing DF and ADF units were studied through a manufacturers' survey, and a radiobeacon modulation scheme has been proposed that maintains reliable DF and a ADF operation. MSK modulation with a frequency offset of 325 Hz is recommended, with a power offset of -3dB. This scheme limits ADF bearing errors to under 3 deg based on analysis of the modulation energy entering the effective passbands of the various ADF designs. CCir data on atmospheric noise and multipath were studies and a rate 1/2 convolutional code with constraint length 6 is recommended to provide a DGPS bit error probability of less than 0.00001. Reliable DGPS range for 10 nautical mile beacons will be 100 km, and for 30 nm beacons, 195 km. Discussion of interleaving to control atmospheric burst noise is included. GRA

N87-12555# Naval Postgraduate School, Monterey, Calif.
SOME TACTICAL ALGORITHMS FOR SPHERICAL GEOMETRY
Rex H. Shudde Mar. 1986 31 p
(AD-A170615; NPS55-86-008) Avail: NTIS HC A03/MF A01 CSCL 17/7

This report presents two great circle navigation algorithms, a closest point of approach algorithm and intercept algorithm. It also presents an implementation program for the algorithms that is written in the BASIC language for an IBM PC. Instead of using classical spherical geometry or the general spherical triangle, these algorithms incorporate rectangular coordinates and vectors on the surface of the spherical. The intent of the report is to provide algorithms for spherical Earth models that can be used for situations in which flat Earth models are not appropriate, but that do not require the sophistication of rotating Earth models. Author (GRA)

N87-13275# Strathclyde Univ., Glasgow (Scotland). Dept. of Electronic and Electrical Engineering.
FIBRE OPTIC GYROSCOPES IN INERTIAL NAVIGATION
Brian Culshaw and John D. Nuttall (Ferranti Ltd., Edinburgh (Scotland).) *In* AGARD Guided Optical Structures in the Military Environment May 1986 6 p (For primary document see N87-13273 04-74)
Avail: NTIS HC A14/MF A01

05 AIRCRAFT DESIGN, TESTING AND PERFORMANCE

Includes aircraft simulation technology.

For related information see also *18 Spacecraft Design, Testing and Performance* and *39 Structural Mechanics.* For land transportation vehicles see *85 Urban Technology and Transportation.*

N87-12556 ESDU International Ltd., London (England).
SIMPLIFIED FORMS OF PERFORMANCE EQUATIONS. ADDENDUM A: EFFECT ON AEROPLANE LEVEL SPEED OF SMALL CHANGES IN THRUST, DRAG, WEIGHT, POWER
May 1986 14 p Supersedes ESDU-EG2/1
(ESDU-86004-Add-A; ISBN-0-85679-556-9; ISSN-0141-4054) Avail: ESDU

This Data Item ESDU 86004 is an addition to the Aircraft Performance Sub-series. Equations and curves are given for a method that neglects the effects of any consequential changes in the other independent variables although, at the cost of increased complexity, a means of including such effects (in particular, compressibility effects on drag) is provided. Several worked examples show how well the simple method compares with actual operations data. This document is an Addendum to ESDU 80032, and illustrates how the equations of motion given there combined with a parabolic drag law yield valuable results. ESDU

N87-12557*# National Aeronautics and Space Administration. Ames Research Center, Moffett Field, Calif.
NASA ROTOR SYSTEMS RESEARCH AIRCRAFT: FIXED-WING CONFIGURATION FLIGHT-TEST RESULTS
R. E. Erickson, J. L. Cross, R. M. Kufeld, C. W. Acree, D. Nguyen, and R. W. Hodge (Sikorsky Aircraft, Stratford, Conn.) Feb. 1986 124 p
(NASA-TM-86789; A-85363; NAS 1.15:86789) Avail: NTIS HC A06/MF A01 CSCL 01C

The fixed-wing, airplane configuration flight-test results of the Rotor System Research Aircraft (RSRA), NASA 740, at Ames/Dryden Flight Research Center are documented. Fourteen taxi and flight tests were performed from December 1983 to October 1984. This was the first time the RSRA was flown with the main rotor removed; the tail rotor was installed. These tests confirmed that the RSRA is operable as a fixed-wing aircraft. Data were obtained for various takeoff and landing distances, control sensitivity, trim and dynamics stability characteristics, performance rotor-hub drag, and acoustics signature. Stability data were obtained with the rotor hub both installed and removed. The speed envelope was developed to 261 knots true airspeed (KTAS), 226 knots calibrated airspeed (KCAS) at 10,000 ft density altitude. The airplane was configured at 5 deg. wing incidence with 5 deg. wing flaps as a normal configuration. Level-flight data were acquired at 167 KCAS for wing incidence from 0 to 10 deg. Step inputs and doublet inputs of various magnitudes were utilized to acquire dynamic stability and control sensitivity data. Sine-wave inputs of constantly increasing frequency were used to generate parameter identification data. The maximum load factor attained was 2.34 g at 206 KCAS. Author

N87-12558*# National Aeronautics and Space Administration. Ames Research Center, Moffett Field, Calif.
THE HANDLING QUALITIES AND FLIGHT CHARACTERISTICS OF THE GRUMMAN DESIGN 698 SIMULATED TWIN-ENGINE TILT NACELLE V/STOL AIRCRAFT
Megan A. Eskey and Samuel B. Wilson, III Jun. 1986 112 p
(NASA-TM-86785; A-85361; NAS 1.15:86785) Avail: NTIS HC A06/MF A01 CSCL 01C

This paper describes three government-conducted, piloted flight simulations of the Grumman Design 698 vertical and short takeoff and landing (V/STOL) aircraft. Emphasis is placed on the aircraft's handling qualities as rated by various NASA, Navy, and Grumman Aerospace Corporating pilots with flight experience ranging from conventional takeoff and landing (CTOL) to V/STOL aircraft. Each successive simulation incorporated modifications to the aircraft in order to resolve the flight problems which were of most concern to the pilots in the previous simulation. The objective of the first simulation was to assess the basic handling qualities of the aircraft with the noncross-shafted propulsion system. The objective of the second simulation was to examine the effects of incorporating the cross-shafted propulsion system. The objective of the third simulation was to examine inoperative single-engine characteristics with and without cross-shafted engines. Author

N87-12559*# National Aeronautics and Space Administration. Lewis Research Center, Cleveland, Ohio.
A HEATER MADE FROM GRAPHITE COMPOSITE MATERIAL FOR POTENTIAL DEICING APPLICATION
Ching-cheh Hung, Michael E. Dillehay (Cleveland State Univ., Ohio), and Mark Stahl 1986 22 p Proposed for presentation at the 25th Aerospace Sciences Meeting, Reno, Nev., 12-15 Jan. 1987; sponsored by AIAA
(NASA-TM-88888; E-3298; NAS 1.15:88888) Avail: NTIS HC A02/MF A01 CSCL 01C

A surface heater was developed using a graphite fiber-epoxy composite as the heating element. This heater can be thin, highly electrically and thermally conductive, and can conform to an irregular surface. Therefore it may be used in an aircraft's thermal deicing system to quickly and uniformly heat the aircraft surface. One-ply of unidirectional graphite fiber-epoxy composite was laminated between two plies of fiber glass-epoxy composite, with nickel foil contacting the end portions of the composite and partly exposed beyond the composites for electrical contact. The model heater used brominated P-100 fibers from Amoco. The fiber's

electrical resistivity, thermal conductivity and density were 50 micro ohms per centimeter, 270 W/m-K and 2.30 gm/cubic cm, respectively. The electricity was found to penetrate through the composite in the transverse direction to make an acceptably low foil-composite contact resistance. When conducting current, the heater temperature increase reached 50 percent of the steady state value within 20 sec. There was no overheating at the ends of the heater provided there was no water corrosion. If the foil-composite bonding failed during storage, liquid water exposure was found to oxidize the foil. Such bonding failure may be avoided if perforated nickel foil is used, so that the composite plies can bond to each other through the perforated holes and therefore lock the foil in place. Author

N87-12716# Joint Publications Research Service, Arlington, Va.
POSSIBLE MILITARY APPLICATIONS OF STRATOSPHERIC AIRSHIP DISCUSSED
Junichi Kimura, Ryuichi Takeda, Yukichi Fujimatsu, and Toshiyuki Kato *In its* Japan Report: Science and Technology (JPRS-JST-86-023) 29 Aug. 1986 p 49-62 Transl. into ENGLISH from Boei Gijutsu (Tokyo, Japan), Nov. 1985 p 48-58 (For primary document see N87-12715 04-31)
Avail: NTIS HC A04/MF A01

06 AIRCRAFT INSTRUMENTATION

Includes cockpit and cabin display devices; and flight instruments.

For related information see also *19 Spacecraft Instrumentation* and *35 Instrumentation and Photography.*

No abstracts in this category.

07 AIRCRAFT PROPULSION AND POWER

Includes prime propulsion systems and systems components, e.g., gas turbine engines and compressors; and onboard auxiliary power plants for aircraft.

For related information see also *20 Spacecraft Propulsion and Power, 28 Propellants and Fuels,* and *44 Energy Production and Conversion.*

N87-12560# Cambridge Univ. (England). Dept. of Engineering.
VISUALISATION OF AXIAL TURBINE TIP CLEARANCE FLOW USING A LINEAR CASCADE
J. P. Bindon 1986 66 p
(CUED/A-Turbo/TR-122; ISSN-0309-6521) Avail: NTIS HC A04/MF A01

Gas tracer techniques were not successful in revealing anything except the very generalized movement of fluid from the mainstream into the tip clearance gap. Smoke flow visualization at low Reynolds numbers revealed much of the intricate detail of the flow structure in and around the tip clearance region. Smoke traces were injected both into the mainstream fluid via a rake and also through holes in the blade surface. At low values of clearance, there was no evidence of any separation bubble in the clearance gap and the flow was attached and well behaved as it moved from pressure to suction side. Traces injected on the pressure surface moved radially to enter the clearance gap. In passing round the pressure corner, the traces became transparent indicating an acceleration around the corner. This confirms the measurements elsewhere of extremely low values of pressure on the pressure surface corner. This local high velocity would cause a high heat transfer coefficient on the corner. A test was done to investigate the possibility of cooling the pressure corner by radially exhausting cooling air from the pressure surface near the tip. Qualitative heat transfer studies using a radiantly heated optical film appeared not to be able to resolve the small scale effects near the pressure corner but did clearly show the area of low heat transfer where the separation bubble flow stagnates and separates. Author

N87-12561# Department of the Air Force, Washington, D.C.
THRUST REVERSER-EXHAUST NOZZLE ASSEMBLY FOR A GAS TURBINE ENGINE Patent
Edward B. Thayer, inventor (to Air Force) Issued 27 May 1986 8 p Supersedes AD-D011101
(AD-D012390; US-Patent-4,591,097; US-Patent-Appl-SN-611041; US-Patent-Class-239-265.29) Avail: US Patent and Trademark Office CSCL 21/5

This patent discloses an improved thrust reverser/exhaust nozzle assembly which has a plurality of blocker devices located in the divergent section of the exhaust nozzle and a plurality of deflector devices located in the convergent section of the nozzle. The blocker and deflector devices are linked together such that they move simultaneously and maintain a substantially constant engine between forward and reverse thrust conditions. GRA

N87-12562# Allied Bendix Aerospace, Utica, N.Y. Fluid Power Div.
COMPONENT IMPROVEMENT PROGRAM TASK 83-01, 36E133 AIR TURBINE STARTER
L. Williams Feb. 1986 36 p
(Contract N00019-80-G-0607)
(AD-A169483; Rept-8720-3173U) Avail: NTIS HC A03/MF A01 CSCL 09/3

The objective of this task was to replace the mechanical cutout switch with a solid-state electronic cutout switch to improve accuracy and reliability of the automatic start cycle termination in the S-3A and F-14A aircraft. The function of the cutout switch is to terminate the start cycle at a predetermined speed. It was determined that the existing electronic circuit can be used for the 36E133/123 with only a minor resistor change to accommodate the subject unit's cutout speed. Breadboard testing was successfully completed and satisfactorily demonstrated feasibility. GRA

N87-12563# Dayton Univ., Ohio. Research Inst.
RESEARCH ON MECHANICAL PROPERTIES FOR ENGINE LIFE PREDICTION Interim Report, 1 Aug. 1984 - 31 Jul. 1985
Noel E. Ashbaugh, M. Khobaib, George A. Hartman, Tusit Weerasooriya, and A. M. Rajendran May 1986 74 p
(Contract F33615-84-C-5051)
(AD-A169570; UDR-TR-85-132; AFWAL-TR-85-4154) Avail: NTIS HC A04/MF A01 CSCL 20/11

Analytical and experimental investigations have been performed to determine crack growth behavior of metals under conditions typical of the service environments of aircraft gas turbine engines. To evaluate baseline crack growth behavior, investigations have also been conducted at elevated temperature in vacuum. The work performed can be divided into three general categories -- development of experimental and automation techniques, material characterization testing, and analytic studies. An automated laser interferometric displacement-measurement system using linear array cards has been developed. Enhancements of existing system for the measurement of crack lengths and displacements are described. A number of computer automation applications are also described. Fatigue and creep crack growth tests and creep rupture and hot corrosion tests were performed. Description of the experimental techniques and the results for these tests are included. Results of analytical investigations in both material modeling and methodology development are presented, including discussions of applications within the laboratory. GRA

N87-12564# Department of the Air Force, Washington, D.C.
TURBINE AIR SEAL WITH FULL BACKSIDE COOLING Patent Application
George Liang, inventor (to Air Force) Filed 12 May 1986 21 p
(AD-D012405; US-Patent-Appl-SN-861909) Avail: NTIS HC A02/MF A01 CSCL 11/1

This patent application relates to air seals for use in turbo-

machinery and, more particularly relates to an air seal assembly with increased cooling that is adapted to withstand elevated engine operating temperatures. The air seal comprises a full 360 degree seal ring that assemblies to the turbine by means of interlocking flanges. A two piece impingement plate which is positioned adjacent to the air seal controls and meters cooling air flow that cools ceramic seal. The backside of air seal is thereby fully cooled before heated cooling air is exhausted from the seal through holes at expansion slots and edge holes at the axial edges of the air seal. GRA

N87-12565# Sverdrup Technology, Inc., Arnold Air Force Station, Tenn.
EFFECTS OF TEST CELL RECIRCULATION ON HIGH-BYPASS TURBOFAN ENGINES DURING SIMULATED ALTITUDE TESTS Final Report, Oct. 1984 - May 1985
R. M. Dugas Aug. 1986 89 p Prepared in cooperation with AEDC, Arnold AFS, Tenn.
(AD-A171418; AEDC-TR-85-55) Avail: NTIS HC A05/MF A01 CSCL 21/5

An experimental and analytical program was conducted to determine the nature of the flow field around a subscale model of a high bypass turbofan engine installed in a representatively scaled altitude test cell. The engine model employed variable geometry and flow conditions in order to determine their effects on test cell recirculating flows, which can affect engine performance during altitude testing. Flow field data were obtained from both two axis laser Doppler velocimeters, as well as from pressure and temperature instrumentation installed on the model and test cell. Review of full and 1/10 scale test data and the results of the subscale tests indicate that test cell recirculation effects are a function of cell geometry. Measurement of test cell effects is dependent on a baseline test configuration, such as an outdoor test, where the effects are not present. GRA

08 AIRCRAFT STABILITY AND CONTROL

Includes aircraft handling qualities; piloting; flight controls; and autopilots.

For related information see also *05 Aircraft Design, Testing and Performance.*

N87-12566*# National Aeronautics and Space Administration. Langley Research Center, Hampton, Va.
EVALUATION OF A NONLINEAR PARAMETER EXTRACTION MATHEMATICAL MODEL INCLUDING THE TERM C(SUBm(SUB DELTA e SQUARED))
William T. Suit Oct. 1986 18 p
(NASA-TM-87731; NAS 1.15:87731) Avail: NTIS HC A02/MF A01 CSCL 01C

Shuttle flight test data were used to determine values for the short-period parameters. The best identified, as judged by its estimated standard deviation, was the elevon effectiveness parameter C (sub m (sub sigma e squared)). However, the scatter about the preflight prediction of C (sub m (sub sigma e squared)) was large. Other investigators have suggested that adding nonlinear terms to the mathematical model used to identify C (sub m (sub sigma e)) could reduce the scatter. The results of this investigation show that C (sub m (sub sigma e squared)) is the only identifiable nonlinear parameter applicable and that the changes in C (sub m (sub sigma e)) values when C (sub m (sub sigma e squared)) is included are in the order of ten percent for the data estimated. Author

N87-12567# Princeton Univ., N. J. Dept. of Mechanical and Aerospace Engineering.
AN APPLICATION OF A LISP BASED EXPERT SYSTEM FOR FAILURE DIAGNOSIS OF THE CH-47 FLIGHT CONTROL HYDRAULIC SYSTEM
Christopher J. Loh 2 Mar. 1986 58 p
(Contract DAAG29-84-K-0048)
(AD-A168970; ARO-20155.5-MA) Avail: NTIS HC A04/MF A01 CSCL 09/2

An investigation of the hydraulic flight control system of a Boeing CH-47 Chinook helicopter utilizing artificial intelligence techniques will be undertaken. Specifically, a knowledge based expert system will employ situation-action rules (production rules) to diagnose a failure and subsequently identify specific devices(s) which caused that failure. Moreover, because the behavior of the system is directly responsive to the goals the system is attempting to achieve, the expert system's inference engine performs a backward-chaining process via a goal-driven control strategy. The List Processing Language (LISP) is used to facilitate data processing and symbolic logic expression. GRA

N87-12568# Princeton Univ., N. J. Dept. of Mechanical and Aerospace Engineering.
A PROTOTYPE MAINTENANCE EXPERT SYSTEM FOR THE CH-47 FLIGHT CONTROL HYDRAULIC SYSTEM
Christopher J. Loh 28 Apr. 1986 182 p
(Contract DAAG29-84-K-0048)
(AD-A169019; MAE-1751; ARO-20155.8-MA) Avail: NTIS HC A09/MF A01 CSCL 14/2

An investigation of the hydraulic flight control system of a Boeing CH-47 Chinook helicopter using artificial intelligence techniques will be undertaken. Specifically, a knowledge based expert system will employ situation-action rules (production rules) to diagnose a failure and subsequently identify specific device(s) which caused that failure. Moreover, because the behavior of the system is directly responsive to the goals the system is directly attempting to achieve, the expert system's inference engine performs a backward-chaining process via a goal-driven control strategy. This strategy involves finding rules that demonstrate the hypothesis and then verifying the facts that enable the rule to work. The List Processing Language (LIPS) is used to facilitate data processing and symbolic logic expression manipulation. GRA

N87-12569# New Mexico Univ., Albuquerque.
APPLICATION OF THE AIPA (APPROXIMATE ITERATIVE PREPROCESSING ALGORITHM) TO F-106 DATA Final Report, Jul. 1984 - Jul. 1985
Sung-Won Park and J. T. Cordaro Jun. 1986 12 p
(Contract F29601-84-K-0045)
(AD-A169084; AFWL-TN-85-52) Avail: NTIS HC A02/MF A01 CSCL 20/14

This report covers the application of the AIPA numerical algorithm to measured data from the F-106 fly-by electromagnetic pulse test conducted at the AFWL in 1984. The algorithm was partially successful at reducing the data. The amplitudes of the normalized coupling coefficients for the first three poles were determined. GRA

N87-12570# Ballistic Research Labs., Aberdeen Proving Ground, Md.
BLAST GUST LOADING ON A 35 DEGREE SWEPT-BACK WING Final Report
Charles L. Fisher May 1986 141 p
(AD-A169415; BRL-MR-3519) Avail: NTIS HC A07/MF A01 CSCL 01/3

The Ballistic Research Lab (BRL) performed shock loading tests on a generic wing in the 2.44 meter shock tube. This model was previously tested on the rocked sled facility at Holloman AFB, New Mexico, and is documented in report number DNA 5211F. The purpose of the BRL test was to determine if the data gathered at Holloman AFB on gust loading of the wing could be duplicated in the shock tube. On Feb 20 and 25, 1985, tests were conducted in the BRL shock tube to obtain pressure data on a 35 degree sweptback generic wing model. These data are subsequently compared with equivalent data taken on the same model at the Holloman sled track. GRA

N87-12571# Hughes Research Labs., Malibu, Calif.
FLIGHT MODEL DISCHARGE SYSTEM Report, Nov. 1984 -

Dec. 1985
R. R. Robson, W. S. Williamson, and J. Santoru Feb. 1986 170 p
(Contract F19628-83-C-0143)
(AD-A169423; AFGL-TR-86-0036; SR-2) Avail: NTIS HC A08/MF A01 CSCL 22/1

The viability of the Flight Model Discharge System (FMDS) concept has been demonstrated by the successful fabrication and testing of a breadboard system. The FMDS is a spacecraft charge-control system designed to overcome the problem of charge buildup on a space vehicle which occurs during periods of adverse space-environmental conditions. Operational characteristics of the entire system are presented, including the electrostatic analyzers, surface potential monitors, transient pulse monitor, plasma source, and microprocessor-based controller, including its software. Results of the breadbhoard demonstration testing and the preliminary flight hardware design are also included.
Author (GRA)

09 RESEARCH AND SUPPORT FACILITIES (AIR)

Includes airports, hangars and runways; aircraft repair and overhaul facilities; wind tunnels; shock tubes; and aircraft engine test stands.

For related information see also *14 Ground Support Systems and Facilities (Space).*

N87-12572# Essex Corp., Orlando, Fla.
SIMULATOR DESIGN FEATURES FOR HELICOPTER LANDING ON SMALL SHIPS. 1: A PERFORMANCE STUDY Final Report, 1 Sep. 1981 - 26 Apr. 1985
Daniel P. Westra and Gavan Lintern 27 Sep. 1985 63 p
(Contract N61339-81-C-0105)
(AD-A169514; NAVTRASYSCEN-81-C-0105-13) Avail: NTIS HC A04/MF A01 CSCL 05/9

The Visual Technology Research Simulator (VTRS) at the Naval Training Systems Center was used to study the effects of six simulator features on performance for helicopter landings on small ships. The purpose of the experiment was to obtain information relevant to the design of simulators for skill maintenance and transition training, and to obtain information for decisions about future transfer-of-training studies. The six simulator factors were scene detail (high detail ship deck and hangar markings versus no deck and hangar markings), field of view (VTRS-wide versus reduced SH-60B operational flight trainer field of view), system visual lab (217 msec versus 117 msec), g-seat acceleration cuing (off versus on), and collective sound cuing (off versus on). These factors were tested across two levels of seastate and pilot experience. Pilots who participated in the experiment were experienced Navy H-3 rotary wing pilots. Results indicated large effects of scene detail, small to moderate effects for visual lag, small effects for field of view, and no meaningful effects for the g-seat factors and collective sound. Performance was better with the high-detail ship, the shorter visual lag, and the VTRS-wide field of view. Transfer-of-training research is recommended as the next step to further explore these findings and to obtain information directly relevant to the design of simulators for use by student pilots.
GRA

N87-12573# Essex Corp., Orlando, Fla.
SIMULATOR DESIGN AND INSTRUCTIONAL FEATURES FOR CARRIER LANDING: A FIELD TRANSFER STUDY Final Report
D. P. Westra, G. Lintern, D. J. Sheppard, K. E. Thomley, and R. Mauk 18 Jun. 1986 91 p
(Contract N61339-85-C-0044)
(AD-A169962; NAVTRASYSCEN-85-C-0044-2) Avail: NTIS HC A05/MF A01 CSCL 01/2

A transfer-of-training experiment was conducted as part of the carrier landing behavioral research program at the Visual Technology Research Simulator (VTRS). Experimental results provide information on the design and use of simulators for training the aircraft carrier landing task and also provide input on design issues for the Navy's new T-45 training system. Two visual display variables and two simulator training variables were selected for inclusion in this experiment: scene detail (day contrasted with night); field of view (wide versus narrow); approach type (circling, modified straight-in or segmented); and number of simulator trials (20, 40, or 60). 72 student pilots were trained on the VTRS prior to going through the Field Carrier Landing Practice (FCLP) phase of their pilot training program. Performance of these students at FCLP was contrasted with that of a group of 54 students who did not receive simulator training. Results show that students trained in the simulator performed better at FCLP than the control students. There was no transfer advantage for those trained with a daytime high-detail scene compared to those trained with a lower cost nighttime low-detail scene. There was also no transfer advantage for those trained with a wide FOV compared to those trained with the wide field of view compared to those trained with the lower cost narrow FOV scene.
GRA

12 ASTRONAUTICS (GENERAL)

For extraterrestrial exploration see *91 Lunar and Planetary Exploration.*

N87-12574# Committee on Science and Technology (U. S. House).
NATIONAL COMMISSION ON SPACE REPORT
1986 76 p Hearing before the Subcommittee on Space Science and Applications of the Committee on Science and Technology, 99th Congress, 2d Session, No. 129, 22 Jul. 1986
(GPO-63-143) Avail: Subcommittee on Space Science and Applications

The National Commission on Space was established by Congress in 1984 to formulate a long range agenda for U.S. civilian space activity, so long range goals, opportunities, and policy options could be identified. The process which the Commission followed to arrive at its conclusions, what those conclusions were, as well as the alternatives that were considered are discussed. The objectives and the financial projection requested to achieve them are examined.
B.G.

13 ASTRODYNAMICS

Includes powered and free-flight trajectories; and orbital and launching dynamics.

N87-12575 Colorado Univ., Boulder.
METER-LEVEL ORBIT DETERMINATION OF GEOSYNCHRONOUS SATELLITES BY AN ECONOMICAL TRACKING SYSTEM Ph.D. Thesis
TingHua Wang 1985 153 p
Avail: Univ. Microfilms Order No. DA8608651

A high-precision and low cost geosynchronous satellite tracking system was proposed. The tracking system main components are two geosynchronous satellites, four automatic ground stations and a very-long-baseline interferometry (VLBI) system. The automatic ground stations provide the doubly difference ranging measurements without precision clocks. The VLBI system consists of four one meter antennas positioned on orthogonal 6000 km baselines and uses a GPS signal for clock synchronization. A quick and simple initialization algorithm was developed to provide a reliable initial estimate. An efficient and stable two-stage Quasi-Newton-Raphson orbit determination program, in which the state perturbation transition matrix was introduced to simplify the mathematical derivation, always converges to the desired solution in five iterations. The artificial weighting matrices were carefully adjusted to desensitize the effect of the imperfection of measurements and modeling. An algorithm dependent linearized covariance method, based on batch-processing, weighted least-squares

estimation algorithm was derived and the error resulting from the process disturbances was evaluated carefully. Based on the anticipated characteristics of the 1990 era VLBI, doubly differenced ranging and dynamic model, a one meter position accuracy of geosynchronous satellites has been achieved. Dissert. Abstr.

N87-12576# Aerospace Corp., El Segundo, Calif. Electronics Research Lab.
VECTOR ANALYSIS AND SATELLITE FOOTPRINTS
R. H. Ott 20 Jun. 1986 54 p
(Contract F04701-85-C-0086)
(AD-A169832; TR-0086(6749)-1; SD-TR-86-31) Avail: NTIS HC A04/MF A01 CSCL 20/14

The use of vector analysis for deriving algorithms for generating earth coverage footprints from satellites in arbitrary orbits is presented. Extensive analysis and results are given for two examples: (1) a satellite in geosynchronous orbit, and (2) a satellite in subsynchronous orbit. The antenna beam on the satellite can be elliptic in cross section with arbitrary orientation of semi-minor and semi-major axes. GRA

N87-12577# Texas Univ., Austin.
OPTIMAL DESCENDING, HYPERSONIC TURN TO HEADING
G. R. Eisler and D. G. Hull 1986 15 p Presented at the Atmospheric Flight Mechanics Conference, Williamsburg, Va., 18 Aug. 1986
(Contract DE-AC04-76DP-00789)
(DE86-010989; SAND-86-2061C; CONF-860882-2) Avail: NTIS HC A02/MF A01

Approximations are made to the point-mass equations of motion for flight within the atmosphere. Optimal controls are formulated for a reentry vehicle to execute a maximum-terminal-velocity turn to a specified heading while executing steep, descent trajectories. A Newton scheme is used repetitively to solve a nonlinear algebraic system for two parameters in the control equations to provide the on-line guidance. Trajectory comparisons from the repetitive solution of the optimal control problem, pure numerical optimization, and simulation of sample-data guidance show good agreement, if the atmospheric model is accurate. DOE

14 GROUND SUPPORT SYSTEMS AND FACILITIES (SPACE)

Includes launch complexes, research and production facilities; ground support equipment, e.g., mobile transporters; and simulators.

For related information see also *09 Research and Support Facilities (Air).*

N87-12578# Range Commanders Council, White Sands Missile Range, N. Mex. Data Reduction and Computing Group.
DIRECTORY OF RANGE DATA CONVERSION AND PROCESSING SYSTEM, REVISION
17 Jul. 1986 556 p
(AD-A169629; DR/CG-157-84-Rev) Avail: NTIS HC A24/MF A01 CSCL 09/2

The members and associate members of the Data Reduction and Computing Group (DR&CG) of the Range Commanders Council (RCC) have exchanged information on the hardware and software systems in use at their respective ranges and agencies at regular intervals with great success. Since other range representatives found this information to be valuable, the group published a Directory of Data Conversion and Processing Systems, RCC Document 127-73, in 1973. This third edition, 157-84, contains nine chapters, with information updated since the 1980 edition. The directory covers the following topics: range data conversion, processing systems, pre/post flight computer systems, real-time computer systems, film readers, frequency and wave analysis system, data transmission system, printers and plotters, range instrumentation computer systems, telemetry front and systems, terminals and graphic displays, micrographics equipment, embedded computer. GRA

N87-12579# Range Commanders Council, White Sands Missile Range, N. Mex. Inter-Range Operations Group.
JOINT OPERATING PROCEDURE FOR INTERRANGE SCHEDULING
May 1986 11 p Supersedes report dated Jun. 1983, AD-A130680
(AD-A169636; RCC/IOG-550-86) Avail: NTIS HC A02/MF A01 CSCL 05/1

This document defines policies and procedures necessary to accomplish the orderly interrange scheduling operations support services involving two or more major ranges and test facilities. The policies and procedures described herein will be used by Department of Defense major ranges and test facilities engaged in mutual operations support and by all range users requesting support from two or more ranges. GRA

N87-12580*# National Aeronautics and Space Administration. Lyndon B. Johnson Space Center, Houston, Tex.
LUNAR LABORATORY
P. W. Keaton (Los Alamos National Lab., N. Mex.) and M. B. Duke 1986 11 p Presented at the Committee on Space Research (COSPAR), Toulouse, France, 30 Jun. 1986 Sponsored in part by NASA
(Contract W-7405-eng-36)
(NASA-TM-89209; NAS 1.15:89209; DE86-0123433; LA-UR-86-2213; CONF-8606145-1) Avail: NTIS HC A02/MF A01

An international research laboratory can be established on the Moon in the early years of the 21st Century. It can be built using the transportation system now envisioned by NASA, which includes a space station for Earth orbital logistics and orbital transfer vehicles for Earth-Moon transportation. A scientific laboratory on the Moon would permit extended surface and subsurface geological exploration; long-duration experiments defining the lunar environment and its modification by surface activity; new classes of observations in astronomy; space plasma and fundamental physics experiments; and lunar resource development. The discovery of a lunar source for propellants may reduce the cost of constructing large permanent facilities in space and enhance other space programs such as Mars exploration. DOE

15 LAUNCH VEHICLES AND SPACE VEHICLES

Includes boosters; operating problems of launch/space vehicle systems; and reusable vehicles.

For related information see also *20 Spacecraft Propulsion and Power.*

N87-12581*# National Aeronautics and Space Administration. Marshall Space Flight Center, Huntsville, Ala.
SOLAR ARRAY FLIGHT DYNAMIC EXPERIMENT
Richard W. Schock Washington May 1986 27 p
(NASA-TP-2598; NAS 1.60:2598) Avail: NTIS HC A03/MF A01 CSCL 10A

The purpose of the Solar Array Flight Dynamic Experiment (SAFDE) is to demonstrate the feasibility of on-orbit measurement and ground processing of large space structures dynamic characteristics. Test definition or verification provides the dynamic characteristic accuracy required for control systems use. An illumination/measurement system was developed to fly on space shuttle flight STS-31D. The system was designed to dynamically evaluate a large solar array called the Solar Array Flight Experiment (SAFE) that had been scheduled for this flight. The SAFDE system consisted of a set of laser diode illuminators, retroreflective targets, an intelligent star tracker receiver and the associated equipment to power, condition, and record the results. In six tests on STS-41D, data was successfully acquired from 18 retroreflector targets and ground processed, post flight, to define the solar array's dynamic

characteristic. The flight experiment proved the viability of on-orbit test definition of large space structures dynamic characteristics. Future large space structures controllability should be greatly enhanced by this capability. Author

N87-12582# Air Force Systems Command, Wright-Patterson AFB, Ohio. Foreign Technology Div.
THE CHINESE GUIDED MISSILES STRIDE TOWARD MODERNIZATION
H. Zhangnuo and Y. Mu 19 May 1986 11 p Transl. into ENGLISH from Hangkong Zhishi (China), no. 9, Sep. 1985 p 17-18
(AD-A169017; FTD-ID(RS)T-0237-86) Avail: NTIS HC A02/MF A01 CSCL 16/4

The 1985 April issue of the Japanese Aviation Intelligence magazine published an article written by Doi Hiroshi on the status of our country's guided missile technology striding toward modernization. It is solely to provide our readers with some information on what comments are being made abroad about our country's modernization of national defense. GRA

N87-12583# Texas Univ., Austin. Dept. of Aerospace Engineering and Engrg. Mech.
ADVANCED GUIDANCE ALGORITHMS FOR HOMING MISSILES WITH BEARING-ONLY MEASUREMENTS Annual Technical Report
Jason L. Speyer and David G. Hull 20 May 1986 10 p
(Grant AF-AFOSR-0371-84)
(AD-A170833; AFOSR-86-0595TR) Avail: NTIS HC A02/MF A01 CSCL 17/7

The research of this grant is directed toward the development of an advanced guidance system (navigation filter and guidance law) for a short-range air-to-air missile having a passive seeker (angle-only measurements). During this year, four subjects have been investigated. First, additional experience has been gained with the modified-gain extended Kalman filter; it is becoming apparent that it works the same as or better than the extended Kalman filter for the homing missile problem. Second, a new target-acceleration model has been developed to replace the first-order Gauss-Markov process normally used; this model allows target acceleration vector to rotate and keeps its magnitude within bounds. Third, because the homing missile problem with angle-only measurements is nonlinear, the guidance law affects the performance of the filter; a new guidance law based on maximizing a measure of the size of the information matrix has been developed and has been shown to improve filter performance. Fourth, a study of the use of new theory on fault detection has been initiated; the intent is to use this theory to detect target maneuvers (the target maneuver appears as a fault) so that the filter can be restarted. Author (GRA)

N87-12584# Ballistic Research Labs., Aberdeen Proving Ground, Md.
STABILITY OF LIQUID-FILLED PROJECTILES WITH UNUSUAL CONING FREQUENCIES Final Report
Charles H. Murphy Jul. 1986 30 p
(AD-A171460; AD-F300802; BRL-MR-3530) Avail: NTIS HC A03/MF A01 CSCL 19/1

For a liquid-filled shell, a key parameter is r, the ratio of coning frequency to spin frequency. This report considers the stability implications of r in the unusual intervals (-1,0) and (1,3). It is shown that for a low viscosity liquid treated by the Stewartson-Wedemeyer theory there is no possibility of unstable motion in these two regions. GRA

16 SPACE TRANSPORTATION

Includes passenger and cargo space transportation, e.g., shuttle operations; and space rescue techniques.

For related information see also *03 Air Transportation and Safety* and *18 Spacecraft Design, Testing and Performance.* For space suits see *54 Man/System Technology and Life Support.*

N87-12585*# National Aeronautics and Space Administration. Marshall Space Flight Center, Huntsville, Ala.
DEVELOPMENT TESTING OF LARGE VOLUME WATER SPRAYS FOR WARM FOG DISPERSAL
V. W. Keller, B. J. Anderson, R. A. Burns, G. G. Lala (New York State Univ., Albany), M. B. Meyer, and K. V. Beard (Illinois Univ., Urbana-Champaign) Washington Jun. 1986 112 p
(NASA-TP-2607; NAS 1.60:2607) Avail: NTIS HC A06/MF A01 CSCL 14B

A new brute-force method of warm fog dispersal is described. The method uses large volume recycled water sprays to create curtains of falling drops through which the fog is processed by the ambient wind and spray induced air flow. Fog droplets are removed by coalescence/rainout. The efficiency of the technique depends upon the drop size spectra in the spray, the height to which the spray can be projected, the efficiency with which fog laden air is processed through the curtain of spray, and the rate at which new fog may be formed due to temperature differences between the air and spray water. Results of a field test program, implemented to develop the data base necessary to assess the proposed method, are presented. Analytical calculations based upon the field test results indicate that this proposed method of warm fog dispersal is feasible. Even more convincingly, the technique was successfully demonstrated in the one natural fog event which occurred during the test program. Energy requirements for this technique are an order of magnitude less than those to operate a thermokinetic system. An important side benefit is the considerable emergency fire extinguishing capability it provides along the runway. Author

N87-12586# Committee on Science and Technology (U. S. Senate).
INVESTIGATION OF THE CHALLENGER ACCIDENT, VOLUME 2
1986 592 p Hearings before the Committee on Science and Technology, 99th Congress, 2d Session, No. 139, 15-26; 23-24 Jul. 1986
(GPO-64-548) Avail: Committee on Science and Technology

Testimony from three of the principal contractors responsible for developing space shuttle flight hardware is presented relative to the Challenger accident. B.G.

17 SPACE COMM., SPACECRAFT COMM., COMMAND & TRACKING

Includes telemetry; space communications networks; astronavigation and guidance; and radio blackout.

For related information see also *04 Aircraft Communications and Navigation* and *32 Communications and Radar.*

No abstracts in this category.

18 SPACECRAFT DESIGN, TESTING AND PERFORMANCE

Includes satellites; space platforms; space stations; spacecraft systems and components such as thermal and environmental controls; and attitude controls.

For life support systems see *54 Man/System Technology and Life Support.* For related information see also *05 Aircraft Design, Testing and Performance, 39 Structural Mechanics,* and *16 Space Transportation.*

N87-12587*# Martin Marietta Aerospace, New Orleans, La.
GENERAL PURPOSE AFT CARGO CARRIER STUDY, VOLUME 1 Final Technical Report
May 1985 393 p
(Contract NAS8-35564)
(NASA-CR-178905; NAS 1.26:178905) Avail: NTIS HC A17/MF A01 CSCL 22B

The Space Transportation System (STS) documents were reviewed to determine their applicability to the Aft Cargo Carrier (ACC). The ACC requirements were developed to assure that the appropriate STS requirements were met. Payload accommodations/interface was discussed. The configuration, structural details, and subsystems of the ACC design are described. Mission analysis, planning schedules, and cost are summarized. B.G.

N87-12588# Instituto de Pesquisas Espaciais, Sao Jose dos Campos (Brazil).
ATTITUDE CONTROL OF AN ARTIFICIAL SATELLITE BY EXTENDING THE LINEAR QUADRATIC REGULATOR THEORY
Luiz Carlos Gadelha deSouza and Marcelo L. deOliveira e Souza Jul. 1986 8 p In PORTUGUESE; ENGLISH summary Presented at the 6th Congresso Brasileiro de Automatica, Belo Horizonte, Brazil, 25-28 Nov. 1986
(INPE-3959-PRE/977) Avail: NTIS HC A02/MF A01

A new attitude control law for artificial satellites is presented. It is based on an extension of the theory of linear quadratic regulator to the case where the dynamics is described by a weakly nonlinear system of equations (Euler's equations) with respect to a reference system fixed to the satellite. Only the phase in which the satellite has small angles and angular velocities is considered. During it the control law is approximately linear with respect to the state. The results obtained are partial (since this is on-going research), but suggest that: (1) the nonlinear terms of the equations are relevant in the initial instants only, but they become negligible later; (2) despite those terms, the implemented control law reduces the angular velocities and angles faster than other law already simulated with success; (3) that law permits an approximate calculation of the energy expended in the process. Author

N87-12589# Instituto de Pesquisas Espaciais, Sao Jose dos Campos (Brazil).
A PROCEDURE FOR ATTITUDE DETERMINATION OF ARTIFICIAL SATELLITES UTILIZING TECHNIQUES OF STATIC AND DYNAMIC OPTIMAL ESTIMATION
Sebastiao Eduardo Corsatto Varotto, Valcir Orlando, and Roberto Vieira daFonseca Lopes Aug. 1986 7 p In PORTUGUESE; ENGLISH summary Presented at the 6th Congresso Brasileiro de Automatica, Belo Horizonte, Brazil, 25-28 Nov. 1986
(INPE-3966-PRE/981) Avail: NTIS HC A02/MF A01

This work presents an algorithm for optimal attitude estimation of artificial satellites, suitable for real time applications. The attitude estimation at each sampling time is made in two phases. In the first one a preliminary estimation is obtained by a least squares method based only on instantaneous information from noninertial attitude sensors. This is made by using the algorithm known as QUEST (Quartenion Estimator). In the second phase, the preliminary estimate, after being conveniently treated, is used as an observation to be processed by a stochastic estimator: the extended Kalman filter. The procedure is tested by means of numerical simulation in a digital computer in a problem of three-axis attitude determination of an artificial satellite. This is a gravity gradient stabilized satellite which uses attitude sensors of two types; solar and magnetic. The analysis of the results shows good performance in terms of precision, robustness and processing time compared to direct application of an extended Kalman filter estimator. Author

N87-12590# Instituto de Pesquisas Espaciais, Sao Jose dos Campos (Brazil).
PROCEDURE FOR ONE AXIS SATELLITES ATTITUDE CONTROL WITH MAGNETIC ACTUATION
Luiz Danilo Damasceno Ferreira, Valcir Orlando, and Atair Rios Neto May 1986 8 p In PORTUGUESE; ENGLISH summary Presented at the 2nd Congresso Latino Americano de Control Automatico, Argentina
(INPE-3895-PRE/937) Avail: NTIS HC A02/MF A01

The modelling and analysis phases of an attitude control system for low orbit artificial satellites using magnetic coil are presented. The function of the system is to maintain the satellite aligned with the local vertical. The control system development is considered through the application of stochastic control concepts. The satellite motion is described by the equations of motion based on Newtonian formulation. Starting from the Separation Principle, a sequential procedure is developed in which the state estimation and control problems are handled simultaneously. The state estimate is provided by Kalman filter by using the information about the positions of the satellite and of the coil parameters. The controller acts on the satellite in real time, since the coil is the only control element. Author

N87-12591# Instituto de Pesquisas Espaciais, Sao Jose dos Campos (Brazil).
RELATIVE MOTION OF THE SUN ON AN ARTIFICIAL SATELLITE [MOVIMENTO RELATIVO DO SOL SOBRE UM SATELITE ARTIFICIAL]
Valder Matos deMedeiros and Luis Carlos Gadelha deSouza Sep. 1986 18 p In PORTUGUESE; ENGLISH summary
(INPE-3985-NTE/260) Avail: NTIS HC A02/MF A01

Starting with the orbital elements of an artificial satellite, and the right ascension and declination of the Sun, one obtains by posol subroutine the spherical coordinates of the Sun with respect to a reference system fixed to the satellite, thus making possible the study of satellite movement in the laboratory. Author

N87-12592*# National Aeronautics and Space Administration. Marshall Space Flight Center, Huntsville, Ala.
VIEWPORT CONCEPT FOR SPACE STATION MODULES
Freddie Douglas, III Aug. 1986 28 p
(NASA-TM-86559; NAS 1.15:86559) Avail: NTIS HC A03/MF A01 CSCL 22B

The generic design of a 20-in. diameter viewport for the space station modules is discussed. It should possess the capabilities of meteoroid/debris protection (with no metallic cover), redundancies in its meteoroid/debris protection, and pressure sealing systems. In addition, it should provide ease of change out for maintenance or repair. The design does not take into account the bumper-shield effect of the outermost panes in the meteoroid/debris analysis. Author

N87-12593*# National Aeronautics and Space Administration, Washington, D.C.
UPPER STAGE SELECTED FOR PLANETARY MISSIONS
26 Nov. 1986 2 p
(NASA-News-Release-86-161; P86-10229) Avail: NTIS HC A02/MF A01 CSCL 22B

The National Aeronautics and Space Administration has selected the Inertial Upper Stage (IUS), a launch vehicle which fits in the cargo bay of the Space Shuttle as the baseline option to carry probes to Jupiter, Venus, and the Sun. The planetary payloads and the IUS are briefly described. B.G.

N87-12594# Instituto de Pesquisas Espaciais, Sao Jose dos Campos (Brazil).
BRIEF ANALYSIS OF NORMAL ATTITUDE ACCURACIES OF

SATELLITES WITH WHEELS OR GAS JETS [BREVE ANALISE DAS PRECISOES EM ATITUDE NORMAL DE SATELITES COM RODAS OU COM JATOS A GAS]
Marcelo LopesdeOliveiraeSouza Sep. 1986 11 p In PORTUGUESE; ENGLISH summary
(INPE-3993-NTE/262) Avail: NTIS HC A02/MF A01

The normal attitude accuracies reached by some satellites using (reaction or momentum) wheels or (cold or hot) gas jets are briefly analyzed. To do so (in the available time), the data on some successfully launched satellites are compiled in 4 tables. From their analysis it is concluded that: (1) the use of wheels is a necessary condition (NC) for reaching high accuracies (less than or equal to 1'); (2) this does not happen with gas jets, whose use is not a sufficient condition(SC) either; (3) all the analyzed remote sensing (and predecessor) satellites use wheels, besides having circular, sun-synchronous and on-phase orbits; (4) these facts are extremely relevant for redefining the characteristics of MECB's Remote Sensing Mission (unless it were changed e.g., by a ANS-like one). Author

N87-12595# Instituto de Pesquisas Espaciais, Sao Jose dos Campos (Brazil).
DENSITY AND ELECTROSTATIC POTENTIAL DISTRIBUTION AROUND A CYLINDRICAL SATELLITE [DISTRIBUICAO DE DENSIDADE E POTENCIAL ELECTROSTATIC EM TORNO DE UM SATELITE CILINDRICO]
Hans-U. Pilchowski and Isabel MdeMoraes Jul. 1986 11 p In PORTUGUESE; ENGLISH summary Presented at SBPC, Curitiba, Brazil, 9-16 Jul. 1986
(INPE-3953-NTE/258) Avail: NTIS HC A02/MF A01

The electrostatic potential distribution around a cylindrical satellite, moving with a constant speed, is presented. Magnetic field effects are neglected. The method of characteristics for solving quasi-linear partial differential equations is employed to get the approximate number density of ions and electrons. The Poisson's equation is solved by the method of finite differences, using Newton's method. The dependence of the nondimensional potential on the speed ratio, ratio of characteristic length by Deybe length, are discussed. Author

N87-12596# Instituto de Pesquisas Espaciais, Sao Jose dos Campos (Brazil).
COMPARISON OF METHODS FOR THE CALCULATION OF THERMAL CONTACT RESISTANCE OF THE FIRST BRAZILIAN SATELLITE M.S. Thesis, 6 Dec. 1985 [COMPARACAO DE METODOS PARA O CALCULO DA RESISTENCIA TERMICA DE CONTATOS DO PRIMEIRO SATELITE BRASILEIRO]
Marcia B. H. Mantelli Apr. 1986 105 p In PORTUGUESE; ENGLISH summary
(INPE-3864-TDL/217) Avail: NTIS HC A06/MF A01

A comparative study of the methods developed for the calculation of thermal contact resistance between two surfaces submitted to a perpendicular heat flux is presented. Several factors affecting this resistance are analyzed and a brief historical review of the works in this field is made, spotting the methods of interest for spacial applications. These are compared to experimental data so as to establish the most proper method for the couplings of the first Brazilian satellite. Author

N87-12597*# National Aeronautics and Space Administration. Lyndon B. Johnson Space Center, Houston, Tex.
AN APPROACH TO DESIGN KNOWLEDGE CAPTURE FOR THE SPACE STATION
D. B. Wechsler (Mitre Corp., Houston, Tex.) and K. R. Crouse 1986 14 p
(NASA-TM-89272; NAS 1.15:89272) Avail: NTIS HC A02/MF A01 CSCL 22B

The design of NASA's space station has begun. During the design cycle, and after activation of the space station, the reoccurring need will exist to access not only designs, but also deeper knowledge about the designs, which is only hinted in the design definition. Areas benefiting from this knowledge include training, fault management, and onboard automation. NASA's Artificial Intelligence Office at Johnson Space Center and The MITRE Corporation have conceptualized an approach for capture and storage of design knowledge. Author

N87-12598*# National Aeronautics and Space Administration, Washington, D.C.
MODELING THE FUNDAMENTAL CHARACTERISTICS AND PROCESSES OF THE SPACECRAFT FUNCTIONING
V. I. Bazhenov, M. I. Osin, and Yu. V. Zakharov Sep. 1986 322 p Transl. into ENGLISH of the book "Modelirovaniye Osnovnykh Kharakteristic i Protsessov Funktsionironvaniya Kosmicheskikh Apparatov" Moscow, USSR, Mashinostroenie, 1985 240 p Transl. by Kanner (Leo) Associates, Redwood City, Calif.
(Contract NASw-4005)
(NASA-TM-87999; NAS 1.15:87999) Avail: NTIS HC A14/MF A01 CSCL 22B

The fundamental aspects of modeling of spacecraft characteristics by using computing means are considered. Particular attention is devoted to the design studies, the description of physical appearance of the spacecraft, and simulated modeling of spacecraft systems. The fundamental questions of organizing the on-the-ground spacecraft testing and the methods of mathematical modeling were presented. Author

N87-12599# Defence Research Establishment, Ottawa. (Ontario).
SARSAT (SEARCH AND RESCUE SATELLITE) OPERATIONAL DATA CATEGORIZATION AND ACCURACY STUDIES
W. R. McPherson and S. Y. Slinn Sep. 1985 50 p
(AD-A169748; DREO-TN-85-26) Avail: NTIS HC A03/MF A01 CSCL 17/2

The definition of what data is transferred from the SARSAT ground tracking station to operational search and rescue users influences how well the action beacon alert data can be used. Based on an evaluation of operational search and rescue incident data collected during the SARSAT Demonstration and Evaluation, categorization and accuracy studies indicate that methods can be developed which will significantly improve the operational actioning of SARSAT generated beacon alert data. The results of these studies are presented and recommended approaches to the handling of SARSAT data are given. GRA

N87-12600# M/A-COM, Inc., Vienna, Va. Government Systems Div.
MILSTAR MODELING SURVEY Final Report, 25 Feb. 1986 - 15 Jun. 1986
26 Jun. 1986 41 p
(Contract DCA100-84-C-0009)
(AD-A169789) Avail: NTIS HC A03/MF A01 CSCL 17/2

This task was intended to aid the MILSATCOM Satellite Office (MSO) in its efforts to acquire a capability for computer modeling of the MILSTAR system. The modeling needs of the MSO were examined first, and a survey of existing MILSTAR models was then conducted. Finally, estimates were made on the level-of-effort necessary to develop a new, general purpose MIlSTAR model appropriate for the MSO. GRA

N87-12601# California Univ., Los Angeles. Dept. of Materials Science and Engineering.
NEW MATERIALS FOR SPACECRAFT STABILITY AND DAMPING: A FEASIBILITY STUDY Final Technical Report, 1 Oct. 1983 - 30 Sep. 1984
John D. Mackenzie Nov. 1985 52 p
(Grant AF-AFOSR-0221-83)
(AD-A169826; AFOSR-86-0308TR) Avail: NTIS HC A04/MF A01 CSCL 11/4

A preliminary feasibility study has been conducted on some new materials for use as structure components of spacecrafts. These included some new glasses, glass-ceramics, fibers and composites such as low expansion copper aluminosilicate glasses, hollow and oval glass fibers and hollow fiber-glass-polymer composites. The low temperature expansion coefficients, elastic moduli and damping constants were measured. Recommendations are made for further research and development of

some selected materials which appeared to be promising candidates for spacecraft structures. GRA

N87-12602# California Univ., Los Angeles. Dept. of Electrical Engineering.
A MATHEMATICAL FORMULATION OF A LARGE SPACE STRUCTURE CONTROL PROBLEM Interim Report
A. V. Balakrishnan Sep. 1985 8 p
(Grant AF-AFOSR-0318-83)
(AD-A169950; AFOSR-86-0444TR) Avail: NTIS HC A02/MF A01 CSCL 22/2

This paper presents an abstract-mathematical formulation of a Large Space Structure Control problem. The physical apparatus consists of a softly supported antenna attached to the space shuttle by a flexible beam-like truss. The control objective is to slew the antenna on command within the given accuracy and maintaining stability. The control forces and torques are applied at the shuttle end as well as the antenna end and in addition provision is made for a small number of 2-axis proof-mass actuators along the beam. The beam motion is modelled by partial differential equations. Of the variety of control problems possible we touch only on the time-optimal probable. Author (GRA)

N87-12603# Los Alamos National Lab., N. Mex.
SIMPLE DEFENSE CONSERVATIVE MODEL FOR MASS REQUIREMENTS OF HYPERVELOCITY PROJECTILE IMPACT SHIELDS FOR REENTRY VEHICLES
G. R. Spillman 1986 19 p Presented at the Hypervelocity Impact Symposium, San Antonio, Tex., 21 Oct. 1986
(Contract W-7405-eng-36)
(DE86-012407; LA-UR-86-2112; CONF-861091-1) Avail: NTIS HC A02/MF A01

Simple analytical modeling of the physics of interaction of hypervelocity (50 to 100 km/s) projectiles with a bumper shield countermeasure is given. The interaction of projectile and bumper expansion between bumper and underlying vehicle and interaction of bumper/projectile debris cloud with vehicle are examined. Projectile/bumper interactions are treated with ideal gas strong-shock and rarefaction equations. Projectile shock decay from bumper rarefaction is approximated by an impulsive shock similarity solution. A crude model for edge rarefactions is derived. Expansion of debris is treated as an expansion superimposed upon a translation with partition derived from a simple inelastic collision model. The effect of nonunity aspect ratio of compressed debris is included. Debris colliding elastically with the vehicle will impart momentum equal to twice the incident normal component. Impulse may be reduced up to a factor of 2 by stagnation radiative losses for small projectiles and large bumper/vehicle stand-off. Impulse can be enhanced by vehicle ablation from radiative coupling, shock heating (inadequate stand-off), or liquid droplet microcratering (inadequate bumper thickness). Estimates of required bumper mass are given for a specific example. DOE

19 SPACECRAFT INSTRUMENTATION

For related information see also *06 Aircraft Instrumentation* and *35 Instrumentation and Photography.*

N87-12604# Naval Research Lab., Washington, D. C.
THE SPACE STATION MILLIMETER FACILITY
K. W. Weiler, B. K. Dennison, R. M. Bevilacqua, J. H. Spencer, and K. J. Johnston 9 Jun. 1986 58 p
(AD-A168983; NRL-MP-5794) Avail: NTIS HC A04/MF A01 CSCL 22/2

A large millimeter wavelength interferometer array is proposed for construction on the planned Space Station (The Space Station Millimeter Facility--SSMF). It will have manifold applications in both basic and applied research and will be the premier instrument in the world at high radio frequencies. Earth resource mapping, middle atmospheric studies, and high frequency radio astronomy are only a few of the areas which will be significantly advanced by the availability of such an instrument. Particularly in astronomy, the ability to do observations above the disturbing and absorbing effects of the Earth's atmosphere will allow opportunities for exploration of all objects from the Sun, through the Solar System bodies, to the interstellar medium of the Milky Way and other galaxies, and out to the most distant quasars with resolution and sensitivity equalling or exceeding all existing or planned millimeter wavelength telescopes. One of the last unexplored regions of the electromagnetic spectrum, the mm-IR gap, can finally be closed. A flexible design for the SSMF is proposed, and estimate of its construction costs is made, and numerous scientific applications in a number of disciplines are discussed. GRA

N87-12605# Farran Technology Ltd., Ballincollig (Ireland).
MILLIMETER WAVE COMPONENTS Final Report
W. M. Kelly, S. U. Lidholm, B. Lyons, and G. T. Wrixon Paris ESA Nov. 1985 108 p
(Contract ESTEC-5353/83-NL-GM(SC))
(FTL-118521; ESA-CR(P)-2224; ETN-86-98103) Avail: NTIS HC A06/MF A01

Studies and component developments for the realization of low noise spaceborne radiometers between 90 and 300 GHz are summarized. The availability of local oscillator power in this frequency region via either fundamental sources or frequency multipliers is examined, as is the concept of subharmonic mixing as an alternative to fundamental mixing using a frequency doubler. A doubler from 91.5 to 183 GHz and a subharmonic mixer at 183 GHz were developed and their performance assessed. Preferred receiver designs at a number of frequencies of interest are proposed. ESA

20 SPACECRAFT PROPULSION AND POWER

Includes main propulsion systems and components, e.g., rocket engines; and spacecraft auxiliary power sources.

For related information see also *07 Aircraft Propulsion and Power, 28 Propellants and Fuels, 44 Energy Production and Conversion,* and *15 Launch Vehicles and Space Vehicles.*

N87-12606*# National Aeronautics and Space Administration. Lewis Research Center, Cleveland, Ohio.
ADVANCED SOLAR DYNAMIC SPACE POWER SYSTEMS PERSPECTIVES, REQUIREMENTS AND TECHNOLOGY NEEDS
Miles O. Dustin, Joseph M. Savino, Dovie E. Lacy, Robert P. Migra (Sverdrup Technology, Inc., Arnold Air Force Station, Tenn.), Albert J. Juhasz, and Carolyn E. Coles 1986 30 p Proposed for presentation at the Solar Energy Conference, Honolulu, Hawaii, 22-23 Mar. 1987; sponsored by ASME, JSME and JSES
(NASA-TM-88884; E-3292; NAS 1.15:88884) Avail: NTIS HC A03/MF A01 CSCL 10B

Projected NASA, Civil, Commercial, and Military missions will require space power systems of increased versatility and power levels. The Advanced Solar Dynamic (ASD) Power systems offer the potential for efficient, lightweight, survivable, relatively compact, long-lived space power systems applicable to a wide range of power levels (3 to 300 kWe), and a wide variety of orbits. The successful development of these systems could satisfy the power needs for a wide variety of these projected missions. Thus, the NASA Lewis Research Center has embarked upon an aggressive ASD reserach project under the direction of NASA's Office of Aeronautics and Space Technology (DAST). The project is being implemented through a combination of in-house and contracted efforts. Key elements of this project are missions analysis to determine the power systems requirements, systems analysis to identify the most attractive ASD power systems to meet these requirements, and to guide the technology development efforts, and technology development of key components. Author

N87-12607*# National Aeronautics and Space Administration. Marshall Space Flight Center, Huntsville, Ala.
SHIFTS IN SHUTTLE SRM PERFORMANCE BECAUSE OF AMMONIUM PERCHLORATE CRYSTAL SHAPE ON MISSIONS 51-I/J AND 61-A/B
Douglas L. Blackwell Aug. 1986 25 p
(NASA-TM-86561; NAS 1.15:86561) Avail: NTIS HC A02/MF A01 CSCL 21H

The design of the Space Shuttle vehicle configuration requires that the SRMs produce thrust within tightly-controlled limits. These limits provide assurance that Shuttle ascent performance goals will be achieved within the vehicle flight load constraints. The SRM's will perform within these limits if overall SRM reproducibility is maintained. This report will initially describe the excellent performance reproducibility of the 24 SRMs during the first 12 flights [STS-8 through STS-26 (Mission 51-F)] using the HPM SRM. Secondly, this report will describe the transient phenomena which interrupted the reproducibility in the first 20 sec of flight for four flights (Missions 51-I/J and 61-A/B). The cause of this 20 sec phenomena is postulated to be a change in the crystal shape of the ammonium perchlorate used in the propellant. This shape change coincided with the performance shift on these four flights. The ballistic effect of the crystal shape change is manifested as a change to the generic HUMP or BARF curve of the Shuttle SRM thrust/pressure-time curve. As the crystal shape change was corrected by the vendor, the performance produced by the Shuttle SRM returned to normal. Author

N87-12608*# Vibration and Acoustics, Inc., Huntsville, Ala.
SSME MAIN INJECTOR 4000 HERTZ PHENOMENON Final Report, 22 Apr. - 21 Jul. 1986
G. D. Johnston 21 Aug. 1986 8 p
(NASA Order W-85081B)
(NASA-CR-178934; NAS 1.26:178934) Avail: NTIS HC A02/MF A01 CSCL 21H

Several Space Shuttle Main Engines (SSME) have experienced very high acceleration responses measured in the main injector of the powerhead during static firings. Data from previous hot fire SSME tests relating to the 4000 hertz phenomenon were reviewed to provide a better understanding of the nature of this structural response. The objective was to technically understand the way this phenomenon works, recommend a fix and test the fix. B.G.

N87-12609*# Stanford Univ., Calif. Space, Telecommunications and Radio Science Lab.
HIGH VOLTAGE CHARACTERISTICS OF THE ELECTRODYNAMIC TETHER AND THE GENERATION OF POWER AND PROPULSION Final Report
P. Roger Williamson 23 Jan. 1986 15 p
(Contract NAS8-35502)
(NASA-CR-178949; NAS 1.26:178949) Avail: NTIS HC A02/MF A01 CSCL 10B

The Tethered Satellite System (TSS) will deploy and retrieve a satellite from the Space Shuttle orbiter with a tether of up to 100 km in length attached between the satellite and the orbiter. The characteristics of the TSS which are related to high voltages, electrical currents, energy storage, power, and the generation of plasma waves are described. A number of specific features of the tether system of importance in assessing the operational characteristics of the electrodynamic TSS are identified. B.G.

N87-12610# Princeton Univ., N. J. Dept. of Mechanical and Aerospace Engineering.
ADVANCED ELECTRIC PROPULSION MPD (MAGNETOPLASMADYNAMIC) Final Report, 15 Aug. 1979 - 31 May 1986
A. J. Kelley, W. VonJaskowsky, J. Polk, and R. G. Jahn May 1986 35 p
(Contract F04611-79-C-0039)
(AD-A169792; AFRPL-TR-86-044) Avail: NTIS HC A03/MF A01 CSCL 21/3

An in-situ method of measuring MPD (Magnetoplasmadynamic) thruster component erosion has been developed and tested on a reference multimegawatt thruster configuration. The technique involves activation of selected areas on the components to be studied by precisely controlled high energy (Me4V) ion beam bombardment. Monitoring the decrease in activity during thruster operation provides a precise (sub-micron accuracy), quantitative measure of the amount of material removed from the surface. In preliminary tests, erosion of the tungsten cathode occurred at all operating conditions, but a number of factors contributed to the lack of detectable erosion of the copper anode or the boron nitride insulator. These results tentatively indicate that cathode erosion is linearly related to the charge transfer, but scatter in the individual test sequence erosion rate data prevents a more definitive conclusion to be drawn at this time. Nevertheless, a comparison of erosion data obtained at two different pulse lengths (1 msec, 2 msec) indicates that cathode material loss is generally independent of the number of current transients. Work is continuing in a broad effort to refine the Surface Layer Activation (SLA) technique and to obtain a data base for additional thrusters. GRA

N87-12611# Argonne National Lab., Ill.
COMPUTATIONAL AND EXPERIMENTAL STUDY OF FLOW-INDUCED VIBRATION OF THE SSME MAIN INJECTOR POST
S. S. Chen, J. A. Jendrzejczyk, and M. W. Wambsganss 1986 25 p Presented at the Conference on Advanced Earth-to-Orbit: Propulsion Technology, Huntsville, Ala., 13 May 1986
(Contract W-31-109-eng-38)
(DE86-012119; CONF-8605142-1) Avail: NTIS HC A02/MF A01

The Space Shuttle Main Engine (SSME) liquid-oxygen (LOX) posts are subjected to high-velocity turbulent flow from the transfer ducts. In a preliminary assessment of the vibration problem, it was determined that the two potential excitation mechanisms for LOX post vibration are fluidelastic instability and turbulent buffeting. A fundamental study is being conducted to understand the problem and to develop techniques to avoid detrimental vibrational effects with the objective of improving engine life. This paper summarizes the results of an analytical model for fluidelastic instability and test results for turbulent buffeting of a tube array in crossflow. A general theory of fluidelastic instability for a tube array in crossflow is presented. Various techniques to obtain the motion-dependent fluid-force coefficients are discussed and the general instability characteristics are summarized. The theory is also used to evaluate the results of other mathematical models for crossflow-induced instability. The fluid excitation forces acting on a tube array are presented as a function of Reynolds number, incoming flow conditions, and tube location in an array. The experimental data show the general characteristics of flow across a tube array. As the flow passes through each row of tubes, the fluid is subjected to resistance, the effect of which is to convert some of the fluid pressure energy to turbulent energy. In the first few rows, the transformation of energy occurs in a somewhat orderly manner. As the flow reaches the interior tubes, unsteadiness of the flow increases and, usually, a randomness of the flow and its pressure fluctuation exists in the flow field. DOE

23 CHEMISTRY AND MATERIALS (GENERAL)

N87-12612# Sandia National Labs., Albuquerque, N. Mex.
POTENTIAL APPLICATIONS OF ARTIFICIALLY STRUCTURED MATERIALS FOR X-RAY MICROANALYSIS
A. D. Romig, Jr. 1986 17 p Presented at the Annual Joint Meeting of the Electron Microscopy of America and the Microbeam Analysis Society, Albuquerque, N. Mex., 10 Aug. 1986
(Contract DE-AC04-76DP-00789)
(DE86-010459; SAND-86-1032C; CONF-860829-25) Avail: NTIS HC A02/MF A01

These materials are artificially structured on the atomic scale and exhibit properties uniquely different than those found in naturally occurring or conventionally processed materials. Recent

advances in high vacuum deposition techniques have made these materials possible, since the manufacture of ASMs requires very clean environments and the capability to deposit layers with thicknesses ranging from fractions of a nm to a few nm. ASMs have been made from semiconductors, metals, metal-semiconductor combinations and metal-nonmetal combinations. The ASMs produced by layering high atomic number (Z) metals and low Z nonmetals or metals have unique X-ray interaction properties in that they can be used to produce normal incidence X-ray mirrors. It is the objective of this paper to review this new class of materials, with special emphasis on the high Z/low Z multilayer materials, describe applications for these materials currently in use for microanalysis and suggest future applications which should be considered by the X-ray microanalysis community. DOE

24 COMPOSITE MATERIALS

Includes physical, chemical, and mechanical properties of laminates and other composite materials.

For ceramic materials see *27 Nonmetallic Materials.*

N87-12613*# Washington Univ., St. Louis, Mo. Lab. for Ultrasonics.

QUANTITATIVE NON-DESTRUCTIVE EVALUATION OF COMPOSITE MATERIALS BASED ON ULTRASONIC WAVE PROPAGATION Semiannual Progress Report, 15 Mar. - 14 Sep. 1986

James G. Miller 1986 24 p

(Grant NsG-1601)

(NASA-CR-179831; NAS 1.26:179831) Avail: NTIS HC A02/MF A01 CSCL 11D

The application and interpretation of specific ultrasonic nondestructive evaluation techniques are studied. The Kramers-Kronig or generalized dispersion relationships are applied to nondestructive techniques. Progress was made on an improved determination of material properties of composites inferred from elastic constant measurements. E.R.

N87-12614*# National Aeronautics and Space Administration. Langley Research Center, Hampton, Va.

INVESTIGATION OF THE EFFECTS OF SHORT CHAIN PROCESSING ADDITIVES ON POLYMERS

Jag J. Singh, Terry L. StClair, and J. Richard Pratt Nov. 1986 10 p

(NASA-TM-89023; NAS 1.15:89023) Avail: NTIS HC A02/MF A01 CSCL 11D

The effects of low level concentrations of several short chain processing additives on the properties of the 4,4'-bis(3,4-dicarboxyphenoxy) diphenylsulfide dianhydride (BDSDA)/4,4'-diaminodiphenyl ether (ODA)/1,3'-diaminobenzene (m-phenylene diamine) (MPA) (422) copolyimide were investigated. It was noted that 5 percent MPD/phthalic anhydride (PA) is more effective than 5 percent ODA/PA and BDSDA/aniline (AN) in strengthening the host material. However, the introduction of 10 percent BDSDA/AN produces disproportionately high effects on free volume and free electron density in the host copolyimide. Author

N87-12615# MSNW, Inc., San Marcos, Calif.

PLASMA JOINING OF METAL MATRIX COMPOSITES Interim Technical Report, Dec. 1985 - Jan. 1986

G. H. Reynolds and L. Yang Feb. 1986 30 p

(Contract DAAG29-85-C-0027)

(AD-A169056; ARO-22817.2-MS-S) Avail: NTIS HC A03/MF A01 CSCL 11/4

Microstructural details of the first 1110 Al/SiC and Al(Zr)/SiC precomposited powders are described. These powders will be used for initial low pressure plasma depositions. Modeling of expected bulk and interfacial reactions and degradation mechanisms in plasma processing of the composite powder filler metals is described in detail. GRA

N87-12616# Martin Marietta Aerospace, Denver, Colo.

METALLURGICAL CHARACTERIZATION OF THE INTERFACES AND THE DAMPING MECHANISMS IN METAL MATRIX COMPOSITES Progress Report, 4 Feb. 1984 - 15 Apr. 1986

Mohan S. Misra 15 Apr. 1986 5 p

(Contract N00014-84-C-0413)

(AD-A169186; MCR-85-605-ISSUE-3) Avail: NTIS HC A02/MF A01 CSCL 11/4

Fiber reinforced metal matrix composites (MMC) are candidate structural materials for space applications because of their high specific modulus, low CTE, high electrical and thermal conductivity and high environmental resistance. Furthermore, the need for dynamic dimensional precision and weight savings in space structures suggests inherent material damping as an additional property requirement. A preliminary investigation indicates MMC exhibit improved damping with respect to conventional structural alloys of aluminum or titanium. In the present investigation, a graphite-aluminum composite (P55/6061) has been selected to study the microstructural features and mechanisms responsible for damping in MMC. The objectives for this reporting period have been as follows: establish a reliable test method and its limitations; develop reproducible damping test data at different frequencies and strain amplitude; thorough metallurgical characterizations of interfaces; suggest an operative damping mechanism in MMC; and recommendations for further investigations. GRA

N87-12617# Texas A&M Univ., College Station. Mechanics and Materials Research Center.

STRESS EFFECTS ON MOISTURE TRANSPORT IN AN EPOXY RESIN AND ITS COMPOSITE

Y. Weitsman and M. Henson Jun. 1986 11 p

(Contract N00014-82-K-0562)

(AD-A169306; MM-4762-86-15) Avail: NTIS HC A02/MF A01 CSCL 11/4

This paper presents the results of a experimental investigation of stress effects on the sorption of water vapor in an epoxy resin and its composite. Such effects were noted by several researchers in both polymers and composites, although these earlier investigations did not present a comprehensive study of the phenomenon. This paper summarizes results which were obtained recently. It is shown that in both epoxy and graphite/epoxy composites, external stresses affect the diffusion process. In the case of the resin, stresses appear to raise the moisture saturation levels while in composites stresses appear to affect the entire sorption process, accentuating the a-symmetries between absorption and desorption behavior. In both materials the moisture transport process departs both quantitatively and qualitatively from the predictions of classical, Fickean diffusion. GRA

N87-12618# Army Materials and Mechanics Research Center, Watertown, Mass. Ceramics Research Div.

MECHANICAL TESTING OF A COATED CARBON-CARBON COMPOSITE AT ELEVATED TEMPERATURES IN AIR Final Report

George D. Quinn and Jacob J. Stiglich, Jr. May 1986 24 p

(AD-A169355; MTL-TR-86-15) Avail: NTIS HC A02/MF A01 CSCL 11/4

The controlled nucleation thermochemical deposition (CNTD) process can apply a silicon carbide coating to carbon/carbon (C/C) composites. Coated C/C composite materials are potentially useful in advanced gas turbine engines particularly as static components, although rotating components are feasible. Success of such a system will require a coating that will ensure oxidation resistance and mechanical integrity. This report represents a preliminary characterization of mechanical properties of a silicon carbide coated, C/C composite at ambient and elevated temperature in air. The coating was applied by the controlled nucleation thermochemical deposition (CNTD) process. The strength, static fatigue, and oxidation results of the coated composite were favorable at temperatures up to 2372 F (1300 C) in air. GRA

N87-12619# Texas A&M Univ., College Station. Mechanics and Materials Research Center.

COUPLED DAMAGE AND MOISTURE-TRANSPORT IN FIBER-REINFORCED POLYMERIC COMPOSITES
Y. Weitsman Jan. 1986 50 p
(Contract N00014-82-K-0562)
(AD-A169379; MM-4762-86-2) Avail: NTIS HC A03/MF A01 CSCL 11/4

This paper presents a mathematical model for the coupling between moisture diffusion and damage in fiber-reinforced, polymeric composites. In these materials, moisture was observed to cause damage by a multitude of minute debondings at the fiber/matrix interfaces. The model employs concepts of continuum damage theory to describe those debondings. Formal evolutionary expressions are derived and related to the extent of damage, the stress field, moisture content and moisture gradient. The effects of damage on moisture diffusion and on reductions in moduli are aslo formulated. Qualitative comparisons with experimental results are provided. GRA

N87-12620# Southwest Research Inst., San Antonio, Tex.
MICROMECHANISMS OF CRACK GROWTH AND FRACTURE TOUGHNESS IN METAL MATRIX COMPOSITES Technical Report, 29 Apr. 1985 - 29 Apr. 1986
D. L. Davidson, J. Lankford, and G. R. Leverant Jun. 1986 47 p
(Contract N00014-85-C-0206)
(AD-A169839; SWRI-06-8602) Avail: NTIS HC A03/MF A01 CSCL 11/4

Subcritical crack growth and rapid fracture of the mechanically alloyed aluminum alloy IN-9052 reinforced with SiC particles have been investigated. Fatigue crack growth rates for the composite exceed those of the unreinforced alloy, except that the threshold stress intensity for growth is higher for the composite. Fracture toughness of the composite is about 9 square root of M cubed compared to a (reported) value of 29 square root of M cubed for the unreinforced alloy. The contributions to fracture toughness from work done within the plastic zone and in formation of the void sheet have been computed using analytical models. Fracture toughness is shown to result almost entirely from work done within the plastic zone of the growing crack. The matrix microstructure and the particulate characteristics are found to account for the elastic and fracture properties of this composite. GRA

N87-12621# Department of the Air Force, Washington, D.C.
PROCESS FOR CARBON-CARBON COMPOSITE FABRICATION Patent Application
Plotzker, inventor (to Air Force) et al Filed 16 Apr. 1986 16 p
(AD-D012413; US-Patent-Appl-SN-852597) Avail: NTIS HC A02/MF A01 CSCL 11/4

A fabrication process and apparatus are disclosed that achieve a higher density carbon-carbon article, than the prior art processes by maintaining a vertical temperature gradient in a reservoir of pitch (e.g., 550 C at the bottom to 250 C at the top) into which a carbon fiber preform is immersed. The use of the vertical temperature gradient results in a reservoir of hot fluid pitch around the upper end of the preform during pitch impregnation of the preform. This permits the fluid pitch to drain down by gravity into the interstices of the carbon fiber and the hardening pitch below. The next step of the process involves gradually increasing the pitch-hardening temperature from bottom to top to harden the pitch from bottom to top. Thereafter, the impregnated preform is carbonized at high temperature. This method takes advantage of the thermal conductivity of the carbon fibers and does not require extremely high pressures. In fact, a high pressure would be a detriment since it results in closed pores. The process of the present disclosure depends on the development of large, connected pores that can be more easily filled. This manner results in the production of suitable carbonized billets in a fraction of the time currently required and using much less energy. GRA

N87-12622# Air Force Systems Command, Wright-Patterson AFB, Ohio. Foreign Technology Div.
CARBON FIBERS
A. A. Konkin and N. F. Konnova 22 Aug. 1986 35 p Transl. into ENGLISH from Zhurnal Vsesoyuznogo Khimicheskogo Obshchestva (USSR), v. 17, no. 6, 1972 p 632-639
(AD-A171370; AD-F250645; FTD-ID(RS)T-0761-86) Avail: NTIS HC A03/MF A01 CSCL 11/2

In connection with development of missile construction, aircraft construction, mastery of space, and also other branches of technology arose acute need for high temperature (oxidation resistant) fibrous materials, reinforced plastics on basis of which were intended for exploitation at high temperatures. Common natural and synthetic fibers, including thermoresistant, could not satisfy these requirements. As a result of intensive investigations, carried out for latter by decade are developed methods of obtaining large number of high temperature (oxidation resistant) fibers different in properties, predominantly on basis of inorganic compounds. To the important of them relate carbon, boric, carbide, metallic, on the basis of oxides of the elements and some other compounds. Filamentary crystals (whisker) occupy special position in view of unique mechanical properties. This group of fibers is located on different levels of technical development. GRA

N87-12623# Argonne National Lab., Ill.
STABILITY OF MULTILAYERS AT HIGH TEMPERATURES
E. Ziegler, Y. Lepetre, I. K. Schuller, and E. Spiller (IBM Watson Research Center, Yorktown Heights, N.Y.) 1986 10 p Presented at the SPIE Technical Symposium on Applications of Artificial Intelligence, Orlando, Fla., 31 Mar. 1986 Prepared in cooperation with IBM Watson Research Center, Yorktown Heights, N.Y.
(Contract W-31-109-eng-38)
(DE86-010526; CONF-860366-7) Avail: NTIS HC A02/MF A01

The temperature stability of metal (W, WRe, Co, Cr)-carbon multilayers has been studied using X-ray diffraction (theta-2theta and Debye-Scherrer) and electron microscopy. Results show that in all cases a crystallization occurs in the temperature range 650 to 750 C. As a consequence of this crystallization, the layered structure is destroyed, the surface of the film becomes rough and the X-ray reflectivity is considerably reduced. These results imply that efficient cooling or new multilayer structures will have to be developed for use at high temperatures or under high X-ray incident flux. DOE

25 INORGANIC AND PHYSICAL CHEMISTRY

Includes chemical analysis, e.g., chromatography; combustion theory; electrochemistry; and photochemistry.

For related information see also *77 Thermodynamics and Statistical Physics.*

N87-12624 ESDU International Ltd., London (England).
VAPOUR PRESSURES AND CRITICAL POINTS OF LIQUIDS. PART 2C: ALKADIENES AND ALKYNES
Feb. 1986 60 p
(ESDU-86001-Pt-2C; ISBN-0-85679-553-4; ISSN-0141-4062) Avail: ESDU

This Data Item ESDU 86001 is an addition to the Physical Data, Chemical Engineering Sub-series. Vapor pressure data are given for 36 compounds. The data were obtained by a method described in ESDU 84021 involving a critical evaluation of experimental results in the literature, extrapolated by a recent reliable method into the low pressure region, and fitted by a Wagner equation applying over the full liquid range from the freezing to the critical point. The coefficients of the equation are given for each compound and three tables of vapor pressure are included: in SI units at 5 K intervals, in atmospheres at 5 C intervals, and in lbf/sq in at 10 F intervals. The sources of the data used are listed, and a table gives likely uncertainties in values predicted by the equation that should be allowed for in any critical situation. Critically evaluated vapor pressure data for alkanes are available in ESDU 84022, 84028, and 85002 and for alkenes in ESDU 85008 and 85016. ESDU

N87-12625 ESDU International Ltd., London (England).
VAPOUR PRESSURES AND CRITICAL POINTS OF LIQUIDS. PART 3A: C6 TO C10 ALKYLBENZENES
Jul. 1986 56 p Supersedes ESDU-73029
(ESDU-86012-Pt-3A; ISBN-0-85679-564-X; ISSN-0141-4062) Avail: ESDU

Available as part of the ESDU Sub-series on Physical Data, Chemical Engineering, this ESDU gives vapor pressure for 36 compounds. The data were obtained by a method described in ESDU 84021 involving a critical evaluation of experimental results in the literature, extrapolated by a recent reliable method into the low pressure region, and fitted by a Wagner equation applying over the full liquid range from the freezing to the critical point. The coefficients for the equation are given for each compound and three tables of vapor pressure are included: in SI units at 5 K intervals, in atmospheres at 5 C intervals, in lbf/sq in at 10 F intervals. The sources of the data used are listed, and a table gives likely uncertainties in values predicted by the equation that should be allowed for in any critical situation. ESDU

N87-12626*# Alabama Univ., Huntsville. Dept. of Chemistry.
CELLULAR SOLIDIFICATION OF TRANSPARENT MONOTECTICS Semiannual Report
William F. Kaulker Dec. 1986 12 p
(Grant NAG8-069)
(NASA-CR-177039; NAS 1.26:177039) Avail: NTIS HC A02/MF A01 CSCL 07D

Understanding how liquid phase particles are engulfed or pushed during freezing of a monotectic is addressed. The additional complication is that the solid-liquid interface is nonplanar due to constitutional undercooling. Some evidence of particle pushing where the particles are the liquid phase of the montectic was already observed. Cellular freezing of the succinonitrile-glycerol system also occurred. Only a few compositions were tested at that time. The starting materials were not especially pure so that cellular interface observed was likely due to the presence of unkown impurities, the major portion of which was water. Topics addressed include: the effort of modeling the particle pushing process using the computer, establishing an apparatus for the determination of phase diagrams, and the measurement of the temperature gradients with a specimen which will solidify on the temperature gradient microscope stage. Author

N87-12627# California Univ., Davis. Dept. of Mechanical Engineering.
COMBUSTION AND MICRO-EXPLOSION OF WATER/OIL EMULSIONS IN HIGH PRESSURE ENVIRONMENTS Final Report, 7 Dec. 1984 - 6 Dec. 1985
Chung K. Law 11 Mar. 1986 9 p
(Contract DAAG29-85-K-0010)
(AD-A168976; ARO-22486.2-EG) Avail: NTIS HC A02/MF A01 CSCL 21/2

During the reporting period we have accomplished all the objectives as stated in the proposal on gaining fundamental understanding in the combustion and micro-explosion properties of droplets of water/oil emulsions and miscible multicomponent fuel blends. Specifically, the gasification mechanisms of these multicomponent droplets have been umambiguously identified, the relative importance of the various physical and chemical factors influencing soot formation in droplet burning have been systematically assessed, and the ignition limits of fuel droplets vaporizing over a hot plate have been determined. Highlights of the specific accomplishments are separately summarized. GRA

N87-12628# Rutgers - The State Univ., New Brunswick, N. J. Dept. of Mechanical, Industrial and Aerospace Engineering.
RELATIONSHIP OF IN-CYLINDER GASEOUS AND PARTICULATE CONCENTRATION TO RADIATIVE HEAT TRANSFER IN DIRECT INJECTION-TYPE DIESEL COMBUSTION Final Report, 1 Feb. 1983 - 31 Jan. 1986
K. T. Rhee, S. L. Chang, Jeff Matonick, and Chirs Sheft 15 Apr. 1986 135 p
(Contract DAAG29-83-K-0042)
(AD-A168979; ARO-19869.13-EG) Avail: NTIS HC A07/MF A01 CSCL 21/2

The objective of the reported research was to investigate the relationship of radiation heat transfer to the in-cylinder species distribution in direct injection-type diesel engine combustion. In order to implement this objective, both the experimental and computational methods were employed during the course of the study. In the experiment, in order to obtain the in-cylinder species distribution at successive engine crank angles, a rapid sampling valve has been used on a laboratory-built single cylinder direct injection-type diesel engine. The engine for the data acquisition was constructed basically by combining a reciprocating system of an ASTM gasoline engine and a newly constructed engine cylinder head. We encountered a series of problems in the engine requiring replacement of engine components. At the end, the engine was regarded unable to meet the need of operating for an extended period of time for data gathering. Consequently, it was decided to use a new single cylinder engine. In the computational work, a radiation heat transfer model was developed to predict spectral radiation heat transfer through the engine combustion chamber wall for given in-cylinder species distributions. The discovery of a new integral function, a new exact solution of blackbody functions, a new empirical equation of adiabatic flame temperature of fuel/air systems, an analytical solution of equation of radiation functions, a parametric analysis of diesel radiation heat transfer, etc. are reported. GRA

N87-12629# Washington State Univ., Pullman.
OPTICAL SPECTROSCOPY OF DYNAMICALLY COMPRESSED LIQUIDS Final Report, 1 Apr. 1977 - 30 Jun. 1986
George E. Duvall 30 Jun. 1986 42 p
(Contract N00014-77-C-0232)
(AD-A169013; SDL-0058-FTR) Avail: NTIS HC A03/MF A01 CSCL 07/4

The objectives of this work are described in the Introduction. Accomplishments are listed and experimental approaches are described briefly. A summary is given of spectroscopy experiments in CS2 and other materials. Conclusions are: (1) there is no evidence in CS2 of an unique shock effect other than that resulting from rapid increase of pressure and temperature which accompanies compression, (2) metastable states, which can be sampled only by rapid compression, are achieved in these experiments, (3) chemical reaction rates can be measured and critical pressures and temperatures can be determined from spectral measurements in this regime, (4) changes in the UV and visible spectra of liquids studied vary from no observable effect to shifts of thousands of angstroms in absorption band edges for pressure less than 130 kbars, (5) observed spectral changes in liquid CS2 are cooperative in nature and become very small or zero at infinite dilution, (6) a combination of static high pressure and shock compression measurements is particularly valuable in unravelling the physical processes, involved, (7) shock experiments appear to represent a particularly useful adjunct to and extension of chemical processes in liquids under conditions of high temperatures and pressures. GRA

N87-12630# Lawrence Livermore National Lab., Calif.
APPLICATION OF PATTERN RECOGNITION TO METAL ION CHEMICAL IONIZATION MASS SPECTRA Interim Technical Report
R. A. Forbes, E. C. Tews, B. S. Freiser, M. B. Wise, and S. P. Perone Oct. 1985 28 p
(Contract N00014-86-F-0033)
(AD-A169061; TR-4) Avail: NTIS HC A03/MF A01 CSCL 07/4

Pattern recognition methods were used to evaluate the information content of mass spectrometry data obtained using transition metal ions as an ionization source. Data sets consisting of the chemical ionization mass spectra for Fe+ and Y+ with 72 organics (representing the six classes alkane, alkene, ketone, aldehyde, ether, and alcohol) and 24 alkanes (representing the three subclasses linear, branched, and cyclic) were subjected to pattern recognition analysis using a k-nearest neighbor approach with feature weightings. The reactivities of Fe+ and Y+ toward

the classes of compounds studied were characterized using classification accuracies as a measure of selectivity, and important chemical information was extracted from the raw data by empirical feature selection methods. A total recognition accuracy of 81% was obtained for the recognition of the six organic classes and 96% accuracy was obtained for the recognition of the three subclasses of alkanes. GRA

N87-12631# International Business Machines Corp., San Jose, Calif. Almaden Research Center.

ELECTRODE/ELECTROLYTE INTERPHASE STUDY USING POLARIZATION MODULATED FT-IR REFLECTION ABSORPTION SPECTROSCOPY

K. Kunimatsu, H. Seki, W. G. Golden, J. G. Gordon, II, and M. R. Philpott 16 May 1986 24 p

(Contract N00014-82-C-0583)

(AD-A169081; TR-9) Avail: NTIS HC A02/MF A01 CSCL 07/4

The polarization modulated Fourier transform infrared reflection-absorption spectroscopy (FT-IRRAS) is applied to the studies of adsorption and oxidation of CO on a platinum electrode in 0.5M sulfuric acid and of adsorption of cyanide on gold and silver electrodes in 0.5M sulfuric potassium sulfate. The absorption intensity of the CO on platinum electrode is ca. 4 to 5% while that of the CN(-) on silver and gold is 0.2 to 0.5%. The potential dependence of the vibrational spectra was observed for both systems. Oxidation of the linearly adsorbed CO layer proceeds by different mechanisms depending on whether CO was adsorbed at a potential in the double layer region or in the hydrogen region, i.e., at the edges of the CO islands in the former case and randomly in the latter case, in which the bridged CO species plays an important role. The vibrational frequency of the linearly adsorbed CO changes linearly with potential at a rate of 30 cm-1/volt, which is independent of anion specific adsorption. The origin of the shift is most reasonably explained by the first order Stark effect. For Ag, Au/CN(-) systems, the surface cyanide species is the linearly adsorbed CH(-). The anodic reaction products in the solution from cyanide ions and the electrode are also observed in the vibrational spectra. The bands due to surface species and those due to solution species are distinguished by measuring the spectra with s and p-polarized lights. GRA

N87-12632# International Business Machines Corp., San Jose, Calif. Almaden Research Center.

CARBON MONOXIDE ADSORPTION ON A PLATINUM ELECTRODE STUDIED BY POLARIZATION MODULATED FT-IR REFLECTION-ABSORPTION SPECTROSCOPY. 2: CO ADSORBED AT A POTENTIAL IN THE HYDROGEN REGION AND ITS OXIDATION IN ACIDS

K. Kunimatsu, H. Seki, W. G. Golden, J. G. Gordon, II, and M. R. Philpott 16 May 1986 22 p Submitted for publication

(Contract N00014-82-C-0583)

(AD-A169082; TR-10-Pt-2) Avail: NTIS HC A02/MF A01 CSCL 07/4

The carbon monoxide layer on a platinum electrode, which is adsorbed at 0.05 V relative to a normal hydrogen electrode (NHE) in 0.515 M sulfuric acid, and its oxidation to carbon dioxide at higher electrode potentials has been studied by both electrochemical and in-situ Fourier transform infrared reflection-absorption spectroscopy (FT-IRRAS). Polarization modulated FT-IRRAS was used to measured the vibrational spectra of adsorbed carbon monoxide as well as the evolved CO2 as a function of electrode potential. It is shown that the dominant surface species is linearly adsorbed CO, but that the bridge bonded species is oxidized first at about 0.20 V, giving rise to a decrease in the linear C-O stretching frequency of along with a broadening of the band. Oxidation of the linearly adsorbed CO begins at 0.35 V, producing a further, sharp decrease in the C-O stretching frequency as well as a considerable broadening of the band. It is concluded that the oxidation of the CO adlayer produced at 0.05 V occurs randomly throughout the adlayer, in contrast to oxidation at island edges, which is characteristic of CO adsorbed at 0.4 V. It is proposed that the difference in behavior of these two kinds of adsorbed CO is due to crystallographic modification of the platinum surface surface when the CO is adsorbed at 0.05 V in the hydrogen region which results in a higher density of bridge bonded CO. GRA

N87-12633# Texas Univ., Austin. Dept. of Chemistry.

ELECTROCHEMISTRY IN NEAR-CRITICAL AND SUPERCRITICAL FLUIDS. 3: STUDIES OF Br(-), I(-) AND HYDROQUINONE IN AQUEOUS SOLUTIONS

William M. Flarsheim, Yu-Min Tsou, Isaac Trachtenberg, Keith P. Johnson, and Allen J. Bard Feb. 1986 37 p

(Contract N00014-84-K-0428)

(AD-A169136; TR-3) Avail: NTIS HC A03/MF A01 CSCL 07/4

A new type of apparatus has been constructed for carrying out electrochemistry in nearcritical and supercritical aqueous solutions. The following systems have been studied at a platinum electrode: H2O/O2, I(-)/I2, Br(-)/Br2, and hydroquinone/benzoquinone. The compact, alumina flow-cell can be heated or cooled quickly, and can be recharged with fresh electrolyte solution while at high temperature and pressure. A large reduction in the potential required for the electrolysis of water was observed. Diffusivities have been measured for iodide ions and hydroquinone. General agreement with the Stokes-Einstein model was observed in the temperature range 25 C to 375 C. GRA

N87-12634# North Carolina Univ., Chapel Hill. Dept. of Chemistry.

NEW RESULTS ON LOW TEMPERATURE THERMAL OXIDATION OF SILICON Interim Report

E. A. Irene 20 Jun. 1986 36 p

(Contract N00014-83-K-0571)

(AD-A169603; TR-5) Avail: NTIS HC A03/MF A01 CSCL 07/4

The commonly accepted linear-parabolic oxidation model for the thermal oxidation of Si includes two rate processes in a steady state: reaction between Si and oxidant at the Si-SiO2 interface; and transport of oxidant through the SiO2 film. Based on available data, it is argued that the former process seems dominant for thin film growth in dry O2. A number of measured SiO2 film and Si-SiO2 interface measured properties are reported, as well as the variation of these properties with oxidation temperature and Si substrate orientation. These properties include; refractive index, density, intrinsic stress, interface fixed oxide charge and interface trapped charge. It is also observed that all of these properties display similar oxidation temperature and inert anneal behavior plus a complex orientation dependence. Through the use of a modified form for the interface reaction, a better understanding is obtained of both the origin of these measured properties, and new oxidation data taken on five Si orientations and at lower oxidation temperatures than previously reported. GRA

N87-12635# Virginia Inst. of Marine Science, Gloucester Point. Dept. of Chemical Oceanography.

INVESTIGATION OF DEVIATIONS FROM IDEALITY IN THE TWO LIQUID PHASE REGION OF SYSTEMS OF MEDIUM MOLECULAR WEIGHT HYDROCARBON MIXTURES AND WATER Final Report, 1 Jan. 1983 - 31 Dec. 1985

David R. Burris and William G. MacIntyre Feb. 1986 115 p

(Grant AF-AFOSR-0036-83)

(AD-A169752; AFOSR-86-0397TR) Avail: NTIS HC A06/MF A01 CSCL 07/4

Two-phase systems of liquid hydrocarbon mixture, containing medium molecular weight aromatic and aliphatic hydrocarbons, and water were examined in both equilibrium and kinetic experiments. Knowledge of the aqueous solution behavior of liquid hydrocarbon mixtures is important in determining the fate of hydrocarbon components of fuels and petroleum in environmental release situations. The equilibrium solute concentration for a component is given by the product of the pure compound solubility, its mole fraction in the hydrocarbon phase and its activity coefficient in the hydrocarbon phase. Hydrocarbon phase activity coefficients determined for binary hydrocarbon mixtures using static vapor pressure measurements (at 20 and 70 degs.) and those determined using water solubility results (at 20 and 70 degs.) did not differ significantly. This indicated that component aqueous phase

activity coefficients did not decrease measurably in the presence of hydrocarbon co-solutes, in contradiction to some previously published observations, and that the presence of water in the hydrocarbon phase was not significant at these temperatures. Methods for predicting multicomponent mixture solubilities were demonstrated. Aqueous solution behavior of mixtures containing a chlorinated hydrocarbon or a fatty acid surfactant was also determined. GRA

N87-12636# California Univ., Santa Barbara. Dept. of Chemistry.

ON THE INTERPLAY BETWEEN CHEMICAL REACTIONS AND PHASE TRANSITIONS FOR MOLECULES ADSORBED ON SOLID SURFACES

Mark Stiles and Horia Metiu Jul. 1986 28 p Prepared in cooperation with Cornell Univ.

(Contract N00014-82-K-0576)

(AD-A169818; TR-25) Avail: NTIS HC A03/MF A01 CSCL 07/4

There is a large body of experimental evidence suggesting that the rate of product formation in a reaction between adsorbed molecules is deeply modified when one of the reagents undergoes a phase transition or, more broadly speaking, an aggregation of some kind. Specific examples are H2 and CO oxydation; methanol transformation into a methoxy radical on O/Cu; the water reaction with oxygen to form 20H; the decomposition of N2O on Pt(111) which is affected by a phase transition in the outermost Pt layer; and the oxidation of Ni. It is suspected that similar effects might operate on supported metal catalysts. We use Monte Carlo simulations to examine the manner in which reagent aggregation affects the reaction rate between molecules adsorbed on a solid surface. We discuss the temperature and concentration dependence of the rate of product formation. GRA

N87-12637# Oak Ridge National Lab., Tenn.

IMPORTANCE OF INTERFACIAL PHENOMENA IN SEPARATION SCIENCE AND TECHNOLOGY

C. D. Scott 1986 13 p Presented at the Interfacial Phenomena in the New and Emerging Technologies, Boulder, Colo., 29 May 1986

(Contract DE-AC05-84OP-21400)

(DE86-011063; CONF-8605119-1) Avail: NTIS HC A02/MF A01

The different types of separation technologies have many common features that can be used to define a unified field. All separation processes bring about a spatial differentiation of the components of a mixture. In most cases, the separation is conducted in a heterogeneous process which requires the movement of the component of interest to, or through, an interface between phases. Thus, interfacial phenomena will frequently represent important, or even controlling, mechanisms in the separation process. There will be important needs and opportunities for interfacial research in support of advanced separation concepts. Some of these needs will be pointed out for selected areas of new or emerging technologies. DOE

N87-12638# Illinois Univ., Urbana. Dept. of Chemistry.

TRANSPORT AND RELAXATION PROCESSES IN SUPERCRITICAL FLUIDS Progress Report

J. Jonas 1986 5 p

(Contract DE-FG22-85PC-80503)

(DE86-007847; DOE/PC-80503/T1) Avail: NTIS HC A02/MF A01

We have tested our improved NMR method for determining diffusion coefficients using a sample of HO. We obtain the literature value for D to within the error of the experiment (+3%). This NMR diffusion experiment now allows us to obtain diffusion data for the naphthalene-CO system. Spin echo modulation is no longer a problem, so we may monitor the proton NMR signal from naphthalene which has the necessary sensitivity to obtain diffusion data. Diffusion measurements are now in progress. These are the first NMR diffusion measurements on a solid-supercritical fluid system. We have recently been testing the feasibility of obtaining high resolution sulfur-33 NMR spectra of solids containing sulfur dissolved in supercritical fluids. Typically sulfur linewidths in these molecules are very large (greater than 10kHz) when dissolved in liquid solution. However, the viscosity of a supercritical fluid is much less than that of a simple liquid, and thus a sulfur containing compound dissolved in a supercritical fluid should have a greatly narrowed linewidth. This would allow the characterization of sulfur containing coal liquids, for example. We have investigated the system dibenzothiophene-supercritical ethylene in this way. Unfortunately, the NMR sensitivity of ^{33}S is quite poor, and the signal to noise ratios were not sufficient to obtain the spectrum. DOE

N87-12639# Sandia National Labs., Albuquerque, N. Mex.

ELECTRON SPECTROSCOPY IN FUNDAMENTAL CATALYTIC STUDIES

D. W. Goodman and J. E. Houston 1986 12 p Presented at the Annual Joint Meeting of the Electron Microscopy of America and the Microbeam Analysis Society, Albuquerque, N. Mex., 10 Aug. 1986

(Contract DE-AC04-76DP-00789)

(DE86-008781; SAND-86-0779C; CONF-860829-11) Avail: NTIS HC A02/MF A01

A detailed understanding of the chemical nature of surface impurities and overlayers is critical to many technologically important phenomena. Modern surface spectroscopies provide us with the capability to probe many subtleties of surface/adsorbate systems and have proved to be invaluable to the development of our understanding of surface catalyzed reactions and related phenomena. This paper illustrates this point with two specific examples, the production of surface carbon in catalytic methanation over nickel and the modification of electronic properties of copper by an underlying ruthenium substrate. DOE

N87-12640# Sandia National Labs., Albuquerque, N. Mex.

ELECTRON MICROPROBE ANALYSIS: THE UPPER LIMIT OF SUBMICRON SPECTROSCOPY

P. F. Hlava and W. F. Chambers 1986 5 p Presented at the Annual Joint Meeting of the Electron Microscopy of America and the Microbeam Analysis Society, Albuquerque, N. Mex., 10 Aug. 1986

(Contract DE-AC04-76DP-00789)

(DE86-009540; SAND-86-0921C; CONF-860829-18) Avail: NTIS HC A02/MF A01

In the electron microprobe, a beam of high energy electrons is focussed to a fine point on the surface of a fairly thick specimen and the X rays produced are analyzed to determine the chemistry of the point. The spacial resolution of this instrument for chemical analysis, then, is defined by the volume of material from which the X ray signal originates. This, in turn, is related to factors such as the diameter of the electron beam, the spreading of the electron beam as it penetrates into the sample and interacts with the atoms of the sample to generate X rays, and the extent to which these primary X rays penetrate beyond the region of electron beam interaction and generate secondary X rays by the process of fluorescence. Beam voltage, current, and diameter can all be easily controlled by the analyst. Once the electrons enter the specimen, however, the analyst loses control of their density. Each individual electron follows a unique, erratic path as it passes near, passes through, or collides with parts of the atoms in the specimen. Monte Carlo calculations are a means by which many investigators have tried to model the paths of individual electrons and the interaction volume that large numbers of such electrons define. DOE

N87-12641# United Technologies Research Center, East Hartford, Conn.

OPTICAL DIAGNOSTICS FOR DIESEL ENGINE APPLICATIONS Final Technical Report

G. M. Dobbs and J. J. Sangiovanni Nov. 1985 108 p

(Contract DE-AC04-83AL-23523)

(DE86-010747; DOE/AL-23523/T1) Avail: NTIS HC A06/MF A01

Investigations have been conducted on the applicability and limitations of Coherent anti-Stokes Raman Spectroscopy (CARS) measurement of temperature and species concentration, and

laser light scattering/extinction measurement of soot number density and particle size, to diesel combustion. Experiments were conducted under simulated diesel conditions in high-pressure laminar diffusion flames and in a simulated droplet environment. Consideration was given to the effect of the presence of soot particles, fuel droplets, or fuel-rich vapor on the laser-diagnostic techniques. Problems which arise in making CARS measurements of temperature or species concentration under severely sooting conditions were studied in high-pressure flames. A new absorption interference was noted which was assigned to absorption by the C produced by ablation of soot particles by the incident laser beam. CARS conditional sampling strategies for simultaneously determining temperature and whether fuel or soot was present during a combustion event were conceived and experimentally investigated. The light scattering from fuel droplets as an interference to the measurement of accurate soot size and number density distribution parameters was studied in a droplet apparatus. A critical review of the effects of multiple scattering processes on laser light extinction/scattering in diesel combustion was conducted.
DOE

N87-12642# Johns Hopkins Univ., Baltimore, Md. Dept. of Chemical Engineering.
PHASE EQUILIBRIUM PREDICTIONS FOR POLAR AND HYDROGEN BONDING MIXTURES
M. D. Donohue, P. Vimalchand, and G. D. Ikonomou 1986 9 p
(Contract DE-AC02-81ER-10982)
(DE86-011812; DOE/ER-10982/T1) Avail: NTIS HC A02/MF A01

The Perturbed-Hard-Chain Theory (PHCT) has been generalized to treat pure compounds and mixtures with polar forces (dipoles and quadrupoles) as well as hydrogen bonding. The generalization to polar compounds is based on the perturbation expansion for anisotropic molecules by Gubbins and coworkers. The effects of hydrogen bonding are taken into account using an approach similar to that of Heidemann and Prausnitz. With these two generalizations, accurate mixture VLE and LLE predictions can be made, even for highly non-ideal systems, using pure component parameters alone.
DOE

N87-12643# Lawrence Livermore National Lab., Calif.
AXIAL DETONATOR FOR SIMULTANEOUS IGNITION OF MULTIPLE HE POINTS
D. J. Steinberg and J. P. Wade Jul. 1986 10 p Presented at the 4th International Conference on Megagauss Magnetic-Field Generation and Related Topics, Santa Fe, N. Mex., 14 Jul. 1986
(Contract W-7405-eng-48)
(DE86-011878; UCRL-93826; CONF-860703-1) Avail: NTIS HC A02/MF A01

We have designed and tested an exial detonator, 2.54 cm in diameter and constructed of 2.54-cm-long modules, that simultaneously ignites many points on the axis of a long cylinder of high explosive, which in turn uniformly expands a metal cylinder. Detonators containing up to 47 modules have been successfully tested with an RMS deviation of 0.04 to 0.05 microns.
DOE

N87-12644# Sandia National Labs., Albuquerque, N. Mex.
REAL-TIME EXPERIMENTAL MEASUREMENTS OF ISOTOPIC EXCHANGE BETWEEN GASEOUS HYDROGEN AND PALLADIUM HYDRIDE POWDER
G. W. Foltz and C. F. Melius Jun. 1986 38 p
(Contract DE-AC04-76DP-00789)
(DE86-012610; SAND-86-8225) Avail: NTIS HC A03/MF A01

A gas flow apparatus has been constructed and used to study the isotopic exchange reaction occurring between the solid and gas phases in hydrogen (deuterium) gas flows directed through packed-powder beds of beta-phase palladium dueteride (hydride). Spontaneous Raman light scattering is employed to obtain a real-time analysis of the isotopic composition of the gas (H2, D2, HD) exiting from the bed. In addition, gas pressure and flow rate measurements are made on the flow simultaneously with the composition measurements.
DOE

N87-12645# Sandia National Labs., Albuquerque, N. Mex.
DOUBLE-RESONANCE TECHNIQUES FOR HIGH-RESOLUTION RAMAN-SPECTROSCOPY
P. Esherick and A. Owyoung 1986 3 p Presented at the 10th International Conference on Raman Spectroscopy, Eugene, Ore., 31 Aug 1986
(Contract DE-AC04-76DP-00789)
(DE86-009640; SAND-86-0959C; CONF-860853-1) Avail: NTIS HC A02/MF A01

In an effort to improve the sensitivity of coherent Raman spectroscopies we have been investigating double-resonance techniques that can combine the high-resolution of stimulated Raman spectroscopy with the sensitivity of electronically resonant spectroscopies such as multiphoton ionization. One such technique that has been highly successful in our laboratory is ionization detected stimulated Raman spectroscopy (IDSRS). In IDSRS, resonant laser ionization is used to detect vibrationally excited molecules produced via stimulated Raman pumping. In a two-step process molecules are first excited to $v = 1$ levels via a driven stimulated Raman transition. Following this the rotational/vibrational distribution is probed with resonant laser ionization by a tunable UV source. Raman spectra are then obtained by scanning the frequency of one of the Raman pump sources and monitoring the ionization signal as a function of the frequency difference (Stokes shift) between this laser and the second, fixed-frequency, visible pump laser.
DOE

N87-12646# California Univ., Berkeley. Lawrence Berkeley Lab.
RAMAN SPECTROSCOPIC INVESTIGATION OF MOLECULAR HYDROGEN
K. Veirs Dec. 1985 114 p
(Contracts W-7405-eng-36; DE-AC03-76SF-00098)
(DE86-012836; LBL-20565; LA-UR-86-276) Avail: NTIS HC A06/MF A01

A state of the art gas phase Raman spectrometer was assembled at Los Alamos National Laboratory. Basic research results, both experimental and theoretical, on Raman cross sections and line positions were applied to the problem of accurate temperature determinations of molecular hydrogen at room temperature. Results are reported for Raman line positions, cross sections, and temperature determinations in gas phase hydrogen.
DOE

N87-12647# Sandia National Labs., Albuquerque, N. Mex.
COMPARATIVE THERMAL CONDUCTIVITY MEASUREMENTS AT SANDIA NATIONAL LABORATORIES
J. N. Sweet, E. P. Roth, M. Moss, G. M. Haseman, and J. A. Anaya Jun. 1986 75 p
(Contract DE-AC04-76DP-00789)
(DE86-012926; SAND-86-0840) Avail: NTIS HC A04/MF A01

A detailed examination has been made on the use of the comparative method for measuring the thermal conductivity of solid materials. Existing data analysis methods are discussed and new techniques, based on generalized linear least squares methods, are presented. An error analysis is made to determine the potential accuracy, reproducibility, and repeatability of the technique. For the case in which the reference conductivity is known to a relative accuracy of +-5%, the overall relative accuracy of the measurement is shown to be about +-6%. Experimental data are presented for the conductivities of commonly used reference materials; Pyrex 7740, Pyroceram 9606, Inconel 718, and Armco iron. Data are also given for two potential reference materials: fused silica and 304 stainless steel.
DOE

26 METALLIC MATERIALS

Includes physical, chemical, and mechanical properties of metals, e.g., corrosion; and metallurgy.

N87-12648# Missouri Univ., Rolla. Materials Research Center.
NEUTRON DIFFRACTION STUDIES OF SOME RARE EARTH-

TRANSITION METAL DEUTERIDES Final Report, 15 Nov. 1983 - 1 Dec. 1985
William J. James May 1986 92 p
(Contract DAAG29-83-K-0159)
(AD-A168995; ARO-19783.4-MS) Avail: NTIS HC A05/MF A01 CSCL 11/6

Neutron diffraction experiments were performed on Ho6Mn23. At 77K it is found to have a face-centered cubic crystal structure and a non-collinear magnetic structure, with the Ho moments tilted at an angle of 33.4 to the Mn moments. The Ho atom carries a moment of 3.8 mu sub B, while the Mn moments at the b, d, f sub 1 and f sub 2 sites are 2.1, 2.0, 2.2 and 1.9 mu sub B respectively, comparable to those found in Y6Mn23. The very low moment on the Ho atom is rationalized as resulting from the fanning of the weakly coupled rare earth moments around the net Ho moment direction, giving a low spatially averaged value. Neutron diffraction studies of three Y6(Fe1-xAlx)23 compounds (x=0.05, 0.10, 0.15) at 523K and 77K reveal substantial preferential atomic ordering of Fe and Al atoms on the four transition crystallographic sites. The Fe atoms exhibit different magnetic moments on the four sites. The ternary alloys, Y6(FexMn1-x)23, exhibit interesting magnetic behavior over a range of solid solutions of iron and manganese. The effects of the substitution of Fe by Al in the R2 (Fe1-xAlx)14B compounds (R = Y, rare earths) on their magnetic properties have been investigated. The present experimental data indicate that intermetallic compounds based on Nd2(Fe1-x-yAlxCoy) 14B have both high Curie temperatures and high coercive fields. The magnetocrystalline anisotropy of (Nd1-xSmx)2Fe14B and (Nd1-xPrx)2Fe14B has been studied by X-ray and magnetic measurements. GRA

N87-12649# State Univ. of New York, Albany. Dept. of Physics.
NUCLEAR REACTION ANALYSIS OF HYDROGEN IN METALS Final Report, Jan. 1982 - Sep. 1985
William A. Lanford 23 Mar. 1986 10 p
(Contract DAAG29-82-K-0036)
(AD-A169032; ARO-18265.20-MS) Avail: NTIS HC A02/MF A01 CSCL 07/5

Research accomplishments of a contract to utilize nuclear reaction analysis to study hydrogen in materials are summarized. These include development of new techniques (high sensitivity, non-vacuum, Doppler spectroscopy, superlattice...), the application of these techniques to study stress and electric current effects on hydrogen distribution in metals and the application of these methods to a variety of new materials. The papers prepared under this contract can be grouped under four headings: (1) Development of new techniques for study of hydrogen in materials, (2) Studies of how macroscopic variables (stress and electric currents) effect the distribution of hydrogen in metals, (3) Studies of the effects of hydrogen in various new thin film materials, and (4) Reviews. GRA

N87-12650# Colorado School of Mines, Golden. Center for Welding Research.
THE INFLUENCE OF WELDING FLUX ON THE PYROMETALLURGICAL, PHYSICAL AND MECHANICAL BEHAVIOR OF WELD METAL Final Report, 15 Feb. 1983 - 14 Feb. 1986
David L. Olson 15 May 1986 24 p
(Contract DAAG29-83-K-0046)
(AD-A169067; MT-CWR-086-017; ARO-20174.12-MS) Avail: NTIS HC A02/MF A01 CSCL 11/6

The pyrochemical behavior of submerged arc welding flux was investigated. The nature of the pyrochemical reactions are described. Mechanistic models for the pyrochemical behavior are suggested. The submerged arc welding was performed on both low carbon and high strength low alloy steels. Both thermodynamic and kinetic models are discussed. Ferrous weld metal phase transformations were investigated. The role of weld metal oxygen, weld metal inclusion and strain on the formation of acicular ferrite was characterized, analyzed and modeled. Advanced high purity - homogeneous multi-component welding fluxes were made using the sol gel process for making glass. These sol gel fluxes were used to make flux cored wires. The sol gel filled flux cored wires were used to weld microalloyed HSLA steels and were found to have excellent arc stability and low moisture content. Sol gel fluxes offer the consistency necessary for welding systems which will use in situ sensing and microprocessor control. A capacitance technique has been developed for moisture content measurements of the coating on covered electrodes. Aluminum weld metal cracking has been characterized for both binary and commercial aluminum alloys. A new model for the prediction of the susceptible and extent of hot cracking has been developed. GRA

N87-12651# Southern Univ., Baton Rouge, La. Dept. of Chemistry.
TRANSITION METAL 2: COMPLEXES OF DITHIACYCLOPHANES Final Report, 20 Sep. 1982 - 19 Sep. 1985
Earl Doomes, Thornton Rhodes, and Derald Chriss 25 Mar. 1986 16 p
(Grant DAAG29-82-G-0013)
(AD-A169107; ARO-19740.1-CH-H) Avail: NTIS HC A02/MF A01 CSCL 07/3

This investigation is related to our recent report on the synthesis and characterization of cobalt (II), copper (II), and nickel (II) complexes of the new macrocyclic ligand, 7-oxa-2,12-dithia(13) (2,6)pyridinopphane (1). The coordination chemistry of a series of structurally related macrocylclic ligands (1-8) was investigated. Macrocycles studied include oxa-, dioxa-, and thia- dithiapyridinophanes (2a, 2b, and 3a, respectively), oxa-, dioxa-, trioxa- and polymethylene-dithiaparacyclophanes (4a and 5, 4b and b) and 2,10-dithia(3.3) (2,6)pyridinophane (9). The pyridinophanes (2a, 2b, 3a and 9) formed stable crystalline complexes when treated with methanol solutions of cobalt (II), copper (II), and nickel (II) salts. However, cobalt (II) and nickel (II) salts did not form crystalline complexes when combined with the paracylcophanes (4, 5, and 6). Electronic spectra, electrolytic conductivities and magnetic susceptibilities data, and elemental analyses were utilized in the characterization of these complexes. Solution and solid state effective magnetic moments were identical for each complex derived from the oxapyridinophane 1, indicating that the same species exists in both phases. Overall, physical data support monomeric structures of general formula M(II)LX2 (where M(II) = the transition metal (II) cation, L= macrocycle, and X = halogen or thiocyanate) for all complexes studied. GRA

N87-12652# Connecticut Univ., Storrs. Dept. of Electrical Engineering and Computer Sciences.
SEMICONDUCTOR/INSULATOR FILMS FOR CORROSION PROTECTION Final Report
F. C. Jain Oct. 1985 52 p
(Contract N62269-83-M-3295)
(AD-A169119; NADC-86028-60) Avail: NTIS HC A04/MF A01 CSCL 20/12

Aluminum surfaces exhibit significantly improved corrosion protection when they are coated with suitable semiconductor/insulator thin films. These coatings, generally realized in Metal-Semiconductor (MS) or Metal-Insulator-Semiconductor (MIS) structural configurations, give rise to an interfacial electric field which acts as an effective built-in electronic barrier. This active barrier significantly impedes the transfer of electrons from the aluminum surface to foreign species which cause oxidation by accepting the electrons. Anodic polarization data on numerous samples fabricated in both MS (e.g., Al-Indium Tin Oxide (ITO)) and MIS (e.g., Al-SiO2-ITO) configurations have demonstrated the protective nature of the built-in active electronic barrier. In particular, we have observed a rest potential of -1.126 volts (1% NaCl, 2pH solution) for Al-SiO2-pITO samples in polarization tests. The electronic barrier heights have been shown to increase with: (1) the presence of a thin (20-100 A) SiO2 layer at the metal-semiconductor interface; and (2) the energy gap of ITO which depends upon the indium content. A comparison of these results with data obtained on plasma-deposited Al-Si3N4 samples is presented. GRA

N87-12653# Army Close Combat Armaments Center, Watervliet, N.Y.

EMBRITTLEMENT OF A HIGH AND A LOW STRENGTH STEEL IN LIQUID LEAD ENVIRONMENT Final Report

M. H. Kamdar Apr. 1986 28 p

(AD-A169443; ARCCB-TR-86014) Avail: NTIS HC A03/MF A01 CSCL 11/6

A study has been made of the cyclic fatigue fracture behavior of single-edge notched specimens of 4340 type high strength (yield stress 160 Ksi) and alloy steel of low strength (yield stress 100 Ksi) with and without a fatigue precrack tested in liquid lead and argon at 700 F. The high strength steel specimens were severely embrittled by liquid lead with stress intensity at fracture some two orders of magnitude lower in liquid lead than in the argon environment. The embrittlement susceptibility was the same for both the notched specimens and for the specimens that had a fatigue precrack at the root of the notch. On the other hand, identical as-notched specimens of low strength steel were immune to lead embrittlement. However, when these specimens were fatigue precracked, they were severely embrittled by liquid lead. This variation is susceptibility to embrittlement is discussed in terms of the prevalent reduction in cohesion mechanism of liquid metal embrittlement. The implications of these results in determining the embrittlement susceptibility or elimination are also discussed. GRA

N87-12654# Terra Tek, Inc., Salt Lake City, Utah.

FRACTURE TOUGHNESS OF CIP-HIP BERYLLIUM AT ELEVATED TEMPERATURES Final Report, 13 May 1980 - 13 Feb. 1981

L. M. Barker and A. H. Jones Apr. 1986 25 p

(Contract DAAG46-80-C-0038)

(AD-A169769; TR-81-50; MTL-TR-86-10) Avail: NTIS HC A02/MF A01 CSCL 11/6

The fracture toughness of CIP-HIP (Cold Isostatic Pressed-Hot Isostatic Pressed) Beryllium was determined using the short bar fracture toughness (K sub IcSB) method. The K sub IcSB value measured was 10.96 MPa x the square root of m at room temperature. This falls well within the expected range of 9 to 12 MPa x the square root of m as observed from previous fracture toughness measurements of beryllium. Toughness increased rapidly between 400 F and 500 F reaching a value of 16.7 MPa x the square root of m at 500 F. GRA

N87-12655# Battelle Memorial Inst., Columbus, Ohio.

MICROMECHANISMS AND TOUGHNESS FOR CLEAVAGE FRACTURE OF STEEL

A. R. Rosenfield and B. S. Majumdar Jun. 1986 14 p

(Contract DAAG29-85-K-0035)

(AD-A169906; ARO-21673.2-MS) Avail: NTIS HC A02/MF A01 CSCL 11/6

A complete understanding of the fracture mechanisms of steel in the ductile/brittle transition region requires analysis not only of crack initiation, but also of crack propagation. This paper reviews micrographic and fractographic experiments that give insight into both phenomena, and suggests a frame-work through which both may be related. Unstable cleavage crack initiation can occur after some blunting of the original fatigue precrack or after some stable crack growth. In either event, instability appears to be triggered by the fracture of a brittle micro-constituent ahead of the precrack. The large scatter in reported KIc values within the transition region reflects the size distribution and relative scarcity of these trigger particles. While a large number of models have attempted to correlate toughness in the ductile/brittle transition regime to events occurring ahead of the crack tip, surprisingly little attention has been paid to events occurring behind the crack front. Fractographic evidence as well as metallographic sectioning of arrested cracks show that the mechanism of rapid crack propagation by cleavage is affected strongly by partial crack-plane deflection which leaves unbroken ligaments in its wake. The tearing of these ligaments by dimple-rupture is the dominant energy-absorbing mechanism. Etch-pit experiments using an Fe-Si alloy show that the crack-tip stress intensity based on plastic zone size is extremely low. GRA

N87-12656# California Univ., Berkeley. Dept. of Materials Science and Mineral Engineering.

FATIGUE BEHAVIOR OF LONG AND SHORT CRACKS IN WROUGHT AND POWDER ALUMINUM ALLOYS Annual Report, 15 Apr. 1985 - 1 May 1986

Robert O. Ritchie and Weikang Yu 1 May 1986 127 p

(Grant AF-AFOSR-0181-82)

(AD-A169980; UCB/RP/86/A1040; AFOSR-86-0447TR) Avail: NTIS HC A07/MF A01 CSCL 11/6

The fatigue behavior of short cracks, which are small compared to the scale of the microstructure, small compared to the scale of local plasticity or simply physically small (i.e., < or = 1 mm), must be considered as one of the major factors limiting the application of defect-tolerant fatigue design for airframe and engine components. Accordingly, the current program is aimed at identifying factors which govern the growth of such short cracks (in contrast to long cracks) in a series of commercial aluminum alloys, with specific reference to behavior at near-threshold levels (below approx. .000001)mm/cycle. In this annual report, the status of the program is described in terms of (1) a description of results on the role of compression overloads in influencing fatigue crack growth in a new aluminum-lithium alloy (2090) and a comparison of behavior with results in 2124 and 7150, (2) an evaluation of the role of crack tip shielding in controlling the growth of short (50 to 400 micrometers) through-thickness cracks and small (10 to 400 micrometers) surface cracks in 2124, and (3) a general assessment of the small crack problem. It is concluded that the near-threshold behavior of long cracks and the near- and sub-threshold behavior of small cracks is strongly influenced by considerations of crack tip shielding, specifically from crack deflection and crack closure mechanisms. GRA

N87-12657# Drexel Univ., Philadelphia, Pa. Dept. of Materials Engineering.

A FUNDAMENTAL STUDY OF P/M PROCESSED ELEVATED TEMPERATURE ALUMINUM ALLOYS Annual Technical Report, 1 Oct. 1984 - 30 Sep. 1985

A. Lawley and M. J. Koczak Oct. 1985 28 p

(Grant AF-AFOSR-0010-82)

(AD-A170697; AFOSR-86-0567TR) Avail: NTIS HC A03/MF A01 CSCL 11/6

The ambient and elevated temperature strength and microstructural stability of powder processed Al-Fe-Ni alloys are being evaluated with respect to processing mode, microstructure, and microstructural stability. The overall objective is to establish a basic understanding of processing-microstructure relations in this new class of alloys in order to establish design guidelines for limiting stresses and temperatures. In the current program year, rapidly solidified prealloyed powder containing 0.19 volume fraction of FeNiAl9 dispersoid (similar to 0.18 micrometer) was mechanically alloyed (MA) and subsequently hot extruded to full density. The MA alloy is stronger than the non MA alloy at temperatures up to about 300 C. In addition, MA enhances microstructural stability at elevated temperature; for example there is no significant coarsening of the FeNiAl9 after 624 hours at 450 C. Improvements in alloy strength and stability are attributed to the presence of fine scale (similar to 30 nm) oxides and carbides introduced during MA, and which are distributed uniformly throughout the matrix, at matrix intermetallic interfaces, and on sungrain boundaries. This fine-scale dispersoid provides effective resistance to dislocation bowing (Orowan mechanism) below 300 C. At higher temperatures, dislocation climb is the controlling mechanism and the small oxides/carbides are no longer effective barriers to climb. GRA

N87-12658# Illinois Univ., Urbana. Dept. of Materials Science.

EFFECT OF HYDROGEN ON THE MECHANICAL PROPERTIES AND FRACTURE BEHAVIOR OF HIGH PURITY ALUMINUM

Felix Zeides and Howard K. Birnbaum Jul. 1986 131 p

(Contract NOOO14-83-K-0468)

(AD-A171214) Avail: NTIS HC A07/MF A01 CSCL 11/6

In this study of hydrogen effects on 99.999% pure aluminum, hydrogen was introduced by a corrosion process. Two corrosive media were used; deionized pure water was used for dynamic

hydrogen charging during mechanical tests and an alkaline solution for hydrogen precharging. Hydrogen was found to change the response of the material to plastic deformation causing softening and plastic deformation localization on the macroscale and slip line coarsening as well as an increase in their waviness on the microscale. Hydrogen did not cause an earlier onset of the macroscopic plastic instability, i.e., necking. Hydrogen modified the fracture mode from a totally ductile, chisel point type to a more brittle transgranular or intergranular fracture. Fracture started only after onset of necking. The hydrogen induced fracture modification is believed to result from the plastic deformation modification and from the effect of hydrogen on microvoid nucleation. Some fracture surfaces were covered with a film that was occasionally fragmented by a network of cracks which is believed to be a post fracture effect caused by adhesive wear between opposite fracture surfaces. Hydrogen charging resulted in formation of bulk vacancy clusters, linear dimensions shrinkage and grain growth which were interpreted as evidence for vacancy production during the corrosion reaction and for a significant hydrogen-vacancy binding enthalpy. GRA

N87-12659# Los Alamos National Lab., N. Mex.
EFFECT OF STRAIN AND STRAIN RATE ON RESIDUAL MICROSTRUCTURES IN COPPER
M. F. Stevens and P. S. Follansbee 1986 3 p Presented at the Annual Joint Meeting of the Electron Microscopy of America and the Microbeam Analysis Society, Albuquerque, N. Mex., 10 Aug. 1986
(Contract W-7405-eng-36)
(DE86-007361; LA-UR-86-797; CONF-860829-2) Avail: NTIS HC A02/MF A01

Several specimens of OFE Cu were deformed in compression to study the resulting microstructures at equivalent levels of threshold stress and strain. Equiaxed, diffuse dislocation cells are more persistent in Cu when tested at strain rates exceeding 10 sec. At quasi-static strain rates, dislocation collapse into more distinct, narrow microbands occurs at lower strain levels. DOE

N87-12660# Los Alamos National Lab., N. Mex.
EFFECT OF RESIDUAL STRAIN ON TWINNING IN SHOCK-LOADED COPPER
G. T. Gray, III 1986 3 p Presented at the Annual Joint Meeting of the Electron Microscopy of America and the Microbeam Analysis Society, Albuquerque, N. Mex., 10 Aug. 1986
(Contract W-7405-eng-36)
(DE86-007362; LA-UR-86-796; CONF-860829-1) Avail: NTIS HC A02/MF A01

Under shock-loading, twinning is observed in metals that do not twin under conventional loading conditions, for example, copper and nickel where the stacking fault energy is about 78 and 129 ergs/cm^2, respectively. Contradictions in the published data on the twinning stress in copper (from 1.6 GPa in thin films to 14.5 to 20 GPa in bulk specimens) suggest differences associated with experimental techniques. This study examines the role of residual plastic strain (epsilon sub res) on the deformation substructures, particularly twinning, in shock-loaded copper. DOE

N87-12661# Los Alamos National Lab., N. Mex.
INITIATION OF PITTING CORROSION IN MARTENSITIC STAINLESS STEELS
W. R. Cieslak, R. E. Semarge, and F. S. Bovard 1986 11 p Presented at the Annual Joint Meeting of the Electron Microscopy of America and the Microbeam Analysis Society, Albuquerque, N. Mex., 10 Aug. 1986
(Contract DE-AC04-76DP-00789)
(DE86-007627; SAND-86-0251C; CONF-860829-3) Avail: NTIS HC A02/MF A01

The form of localized corrosion known as pitting often initiates preferentially at microstructural inhomogeneities. The pit initiation resistance, therefore, is controlled by the characteristics of the initiation sites, rather than by the bulk material composition. This investigation correlates the pit initiation resistance, as measured by critical pitting potentials, with preferred pit initiation sites for 3 martensitic stainless steels. Pit initiation sites are determined by secondary electron (SE) and backscattered electron (BSE) imaging and energy dispersive and wavelength dispersive spectrometries (EDS and WDS) with a scanning electron microscope (SEM) and an electron probe microanalyzer (EPMA). DOE

N87-12662# Oak Ridge National Lab., Tenn.
APFIM STUDY OF ANTIPHASE AND GRAIN BOUNDARIES IN Ni Al
J. A. Horton and M. K. Miller 1986 5 p Presented at the Annual Joint Meeting of the Electron Microscopy of America and the Microbeam Analysis Society, Albuquerque, N. Mex., 10 Aug. 1986
(Contract DE-AC05-84OR-21400)
(DE86-008494; CONF-860829-4) Avail: NTIS HC A02/MF A01

Ni Al is an ordered intermetallic material and is potentially useful for high temperature applications. Unlike most alloys the yield stress of Ni Al actually increases with an increase in temperature. Unfortunately, pure Ni Al exhibits a brittle intergranular fracture and, consequently, low ductility. However, doping Ni Al with boron improves the mechanical properties and can result in room temperature ductilities up to 50% and a completely transgranular failure. Auger electron spectroscopy (AES) has shown that boron segregates to those boundaries which can be made to fail intergranularly and that no embrittling agents are found on fracture surfaces of pure NiAl. Atom probe field-ion microscopy (APFIM) is an excellent technique to study the structure and chemistry of good boundaries, especially for light elements such as boron. Results from this study have shown that boron segregates to both grain boundries and antiphase boundaries (APB) and that a thin phase is usually present at the grain boundaries in rapidly solidified Ni Al. DOE

N87-12663# Oak Ridge National Lab., Tenn.
APFIM STUDIES OF PHASE TRANSFORMATIONS
M. K. Miller 1986 15 p Presented at the Annual Joint Meeting of the Electron Microscopy of America and the Microbeam Analysis Society, Albuquerque, N. Mex., 10 Aug. 1986
(Contract DE-AC05-84OR-21400)
(DE86-008533; CONF-860829-8) Avail: NTIS HC A02/MF A01

The atom probe field-ion microscope (APFIM) has proven to be a very effective instrument for studying phase transformations in many metallic systems. The atom probe field-ion microscope provides a technique for direct observation and quantification of important microstructural and chemical features of the transformation such as the three-dimensional morphology of the evolving phases, the wavelength and spatial extent of the solute-rich regions, the sharpness of the interface between the phases, and the changes in composition of the coexisting phases. The atomic spatial resolution of the instrument permits the earliest stages of phase transformations to be investigated experimentally. The unrestricted mass range permits the location and quantification of all elements, including the light elements such as carbon and boron, to be determined. In this paper a summary of some of the types of information relating to phase transformations that may be obtained with the atom probe is outlined. DOE

N87-12664# Kernforschungsanlage, Juelich (West Germany).
RADIATION-INDUCED SEGREGATION TO GRAIN BOUNDARIES IN A NI-SI ALLOY
W. Kesternich, N. H. Packan (Oak Ridge National Lab., Tenn.), and H. Schroeder 1986 3 p Presented at the 11th International Congress on Electron Microscopy, Kyoto, Japan, 31 Aug. 1986
(Contract DE-AC05-84OR-21400)
(DE86-010027; CONF-860854-3) Avail: NTIS HC A02/MF A01

Solute transport by radiation-induced segregation (RIS) leads to local changes of alloy composition. RIS was studied in a binary Ni-8 at. % Si alloy by 7-MeV-proton and 28-MeV-alpha particle irradiations. Damage levels varied between 0.1 and 0.3 dpa. The irradiations were carried out at 475 C, the expected peak RIS temperature; preimplantation of helium at 700 C was carried out in some specimens. Solute segregation was studied by energy-dispersive X-ray analysis (EDX). Using very fine electron-beam

probes of 2 nm diameter from a high-brightness field-emission source, microchemical profiles across the grain boundaries were measured. Radiation-induced precipitation of Ni3Si was investigated by dark-field transmission electron microscopy (TEM). DOE

N87-12665# Lawrence Livermore National Lab., Calif.
DESIGN OF STRONG, DUCTILE, HSLA AND DUAL PHASE STEELS
G. Thomas Jan. 1986 31 p Presented at the 1st Indo/US Workshop on Iron and Technology, Ranchi, India, 6 Jan. 1986
(Contract DE-AC03-76SF-00098)
(DE86-011313; LBL-21303; CONF-860174-1) Avail: NTIS HC A03/MF A01

The alloy design programs at Berkeley which utilize the concept of two-phase steels as a means of optimizing these mutually exclusive properties are described. The idea is to design composite microstructures whereby the advantages of the second phase are optimized while the less desirable features of this phase are mitigated simultaneously by the presence of the other constituent phase. The size, distribution, shape and volume fraction of the second phase critically control the mechanical properties, especially fracture and fatigue of the dual phase systems. As a consequence, these structures offer a degree of metallurgical flexibility that is absent in single phase structures or in many precipitation strengthened systems, for attaining optimum sets of mechanical properties. Examples are presented here of martensite/austenite (approx. 2 to 5%) mixtures designed for optimum combinations of high strength, toughness, and wear properties in medium carbon steels, e.g., for mining and agricultural applications, and martensite/ferrite (approx. 80%) structure for high strength, cold formability and improved low temperature ductility in low carbon steels. Use of the latter for sheet, line pipe rods and wires is considered. DOE

N87-12666# Oak Ridge National Lab., Tenn.
BAINITE IN CHROMIUH-MOLYBDENUM STEELS
R. L. Klueh 1986 6 p Presented at the International Conference on Martensitic Transformations (ICOMAT-86), Nara, Japan, 26 Aug. 1986
(Contract DE-AC05-84OR-21400)
(DE86-011781; CONF-860879-1) Avail: NTIS HC A02/MF A01

Classically, bainite is divided into an upper and lower variety, as distinguished by microstructural differences that are related to the isothermal-transformation temperature at which the bainite is formed. Two other microstructural variations have been proposed: granular (massive) and carbide-free acicular bainite. These varieties form more readily during a continuous cool. The effect of the bainite microstructure on mechanical properties was investigated. Carbide-free acicular and granular bainite were produced by varying the cooling rate from the austenitization temperature in a 3Cr-1.5Mo steel. A cooling rate of about 100 C/min produced acicular bainite and 7 C/min produced granular bainite. After tempering to a similar ultimate tensile strength (UTS), there were marked differences in the impact behavior of the acicular and granular bainite. The tempered acicular structure developed superior Charpy V-notch impact properties: an upper shelf energy of 225 J and a ductile-brittle transition temperature of -70 C for UTS of 770 MPa. Similar impact properties for the granular bainite were obtained only after the steel was tempered to a UTS of 590 MPa. Electron microscopy studies indicated that there were differences in the precipitate and dislocation distributions in the two bainite structures, which must cause the difference in properties. DOE

N87-12667# Oak Ridge National Lab., Tenn.
USE OF ANALYTICAL ELECTRON MICROSCOPY IN EVALUATING FERRITE STABILITY IN AUSTENITIC STAINLESS STEEL WELDS
J. M. Vitek and S. A. David 1986 13 p Presented at the Annual Joint Meeting of the Electron Microscopy of America and the Microbeam Analysis Society, Albuquerque, N. Mex., 10 Aug. 1986
(Contract DE-AC05-84OR-21400)
(DE86-008537; CONF-860829-6) Avail: NTIS HC A02/MF A01

Stainless steel weld filler metals are prone to hot-cracking during welding. If the primary mode of solidification is ferrite formation rather than austenite formation, the tendency for hot-cracking is reduced. Type 308 stainless steel is such a filler metal which solidifies as primary ferrite and is relatively immune to hot-cracking problems. During further cooling, the primary ferrite transforms to austenite. When such duplex austenite plus ferrite weld microstructures are subjected to elevated temperature applications, the residual ferrite is unstable and transforms. Analytical electron microscopy has been used to study the ferrite stability. Results have provided insight into the stability of ferrite during welding and also during service at elevated temperatures. This paper considers three cases in which the use of analytical electron microscopy has led to understanding of ferrite stability in duplex type 308 stainless steel welds. DOE

N87-12668# Sandia National Labs., Albuquerque, N. Mex.
MICROSTRUCTURAL STUDY OF HIGH ENERGY DENSITY DISSIMILAR METAL WELDS
M. J. Cieslak, C. R. Hills, and T. J. Headley 1986 15 p Presented at the Annual Joint Meeting of the Electron Microscopy of America and the Microbeam Analysis Society, Albuquerque, N. Mex., 10 Aug. 1986
(Contract DE-AC04-76DP-00789)
(DE86-009284; SAND-86-0812C; CONF-860829-17) Avail: NTIS HC A02/MF A01

Electron microscopy analysis of two different CO2 laser welded dissimilar metal combinations revealed the presence of minor constituents which could be attributed to terminal solidification events. In the case of the 15-5 PH/HP 9-4-20 welds, a NbC/austenite eutectic-type constituent was identified, which accounted for the observed fusion-zone hot cracks in these welds. The identity of the interdendritic constituent first observed optically by Patterson and Milewski in 304L/625 GTA welds has been confirmed as Laves phase. It was further determined that this phase is enriched in Mo and Nb relative to the austenite matrix. DOE

N87-12669# Oak Ridge National Lab., Tenn.
SITE OCCUPATIONS IN LI SUB 2 ORDERED ALLOYS BY AXIAL ELECTRON CHANNELING MICROANALYSIS
J. Bentley 1986 3 p Presented at the Annual Joint Meeting of the Electron Microscopy of America and the Microbeam Analysis Society, Albuquerque, N. Mex., 10 Aug. 1986
(Contract DE-AC05-84OR-21400)
(DE86-009421; CONF-860829-22; CONF-860854-1) Avail: NTIS HC A02/MF A01

Experiments using analytical electron microscopes were performed on Ni3Al alloys with additions of Fe, Co, or Hf. Corrections had to be made for delocalization effects. Results agree with atom probe field-ion microscopy. DOE

N87-12670# California Univ., Berkeley. Lawrence Berkeley Lab.
ATOMIC RESOLUTION STUDY OF PRECIPITATES IN AN Al-Ge ALLOY
U. Dahmen, C. Nelson, and K. H. Westmacott Mar. 1986 5 p Presented at the Annual Joint Meeting of the Electron Microscopy of America and the Microbeam Analysis Society, Albuquerque, N. Mex., 10 Aug. 1986
(Contract DE-AC03-76SF-00098)
(DE86-011308; LBL-21287; CONF-860829-27) Avail: NTIS HC A02/MF A01

The difficulty of precipitating germanium in dilute aluminum-germanium alloys is due to a large difference in crystal structures (face-centered cubic and diamond cubic) accompanied by a substantial volume expansion of 36%. A great variety of precipitate morphologies and orientation relationships are observed. A frequently found morphology is that of <100> needles. By selected area diffraction and Moire fringes it has been established that <100> Al and <110> Ge are parallel along the needle axis. The typical aspect ratio of about 100 has made it difficult in the past to investigate the cross-sectional shape and internal structure of these needles, although some indications of internal twinning were found in plates. In the present work, the Berkeley Atomic Resolution Microscope was used to examine needles in

cross section by imaging along the <110> Ge <100> Al needle axis. DOE

N87-12671# Pacific Northwest Labs., Richland, Wash.
APPLICATION OF HYDROGEN EMBRITTLEMENT MODELS TO THE CRACK GROWTH BEHAVIOR OF FUSION REACTOR MATERIALS
R. H. Jones Mar. 1986 27 p Presented at the 2nd International Conference on Fusion Reactor Materials (ICFRM-2), Chicago, Ill., 13 Apr. 1986
(Contract DE-AC06-76RL-01830)
(DE86-011614; PNL-SA-13478; CONF-860421-51) Avail: NTIS HC A03/MF A01

Hydrogen induced crack growth rates of HT-9 have been estimated for three sources of hydrogen: the plasma, nuclear reaction and aqueous corrosion. Estimates of crack growth rates were derived using hydrogen embrittlement models which describe the temperature and hydrogen activity dependence of cracking. A crack growth rate of 10 to the -3 cm/s at a reactor operating temperature of 400 C was obtained for a steady-state hydrogen concentration of 0.5 appM resulting from (n,p) reactions, while a much slower crack growth rate was predicted for the same steady-state hydrogen concentration with an alternate model. These calculations have shown the need for further research to assess the effect of temperature on crack growth. Other sources of hydrogen give very slow hydrogen induced crack growth rates at reactor operating temperatures, while significant hydrogen induced crack growth rates are possible at lower temperatures. For instance, hydrogen from a cathodic corrosion reaction could produce a crack growth rate of 10 to the -7 cm/s at 25 C which could be significant during extended downtime. Also, a non-equilibrium hydrogen uptake from the plasma could occur from surface reaction controlled effects, and a crack growth rate of 10 to the -1 cm/s was estimated for this condition at a temperature of 75 C. DOE

N87-12672# Sandia National Labs., Albuquerque, N. Mex.
CHARACTERIZATION OF THE ATOMIC EMISSION IN INCONEL 718 ALLOY METAL VAPOR ARCS
R. L. Williamson, H. C. Peebles, L. A. Bertram, W. A. Hareland, and F. J. Zanner 1986 21 p Presented at the Vacuum Metallurgy Conference on Specialty Melting and Processing, Pittsburgh, Pa., 9 Jun. 1986
(Contract DE-AC04-76DP-00789)
(DE86-012178; SAND-86-1356C; CONF-8606148-1) Avail: NTIS HC A02/MF A01

Visible and UV emission spectroscopy was used to identify and study various atomic species in the plasma of a vacuum arc furnace during a remelt of Inconel 718. The studies were carried out at a base pressure of 10 mtorr, and with the furnace backfilled with CO to a total pressure of 100 mtorr. Various emitting species were identified, and the internal energy distributions of a number of these species were mapped out using Boltzmann plots. Internal temperatures of 6000 to 7000 K were measured for the neutral atomic species in the low pressure arc, while a value of 11,600 K was obtained for the ion temperature. In addition, the density of the highly volatile element Mn in the interelectrode region was found to be greatly enhanced compared to its relative abundance in the bulk alloy, indicating the importance of vaporization in determining the atomic composition of the arc plasma. Increasing the furnace pressure resulted in an increase in the temperature of the neutral species of 1500 to 4000 K, and an apparent suppression of the Mn vaporization rate. DOE

N87-12673# Los Alamos National Lab., N. Mex.
MECHANICS OF METAL FORMING
P. R. Dawson, G. M. Eggert, and K. K. Mathur 1986 32 p Presented at the 10th US National Congress of Applied Mechanics Conference, Austin, Tex., 16 Jun. 1986 Prepared in cooperation with Cornell Univ., Ithaca, N.Y.
(Contract W-7405-eng-36)
(DE86-012414; LA-UR-86-2065; CONF-8606132-1) Avail: NTIS HC A03/MF A01

A metal forming model is outlined for analyzing large strain bulk operations such as forging, rolling, and drawing. Plastic deformations are assumed to be viscoplastic in that the strain rate dependent flow stress depends on the strain hardening through an internal variable that evolves with the deformations. Volumetric deformations are linked to the growth of voids (porosity) using a damage model in which the porosity serves as an internal variable. Several applications are presented that demonstrate by comparison to experimental data that the model can simulate effectively the response of a workpiece under realistic forming conditions. DOE

N87-12674# Oak Ridge Y-12 Plant, Tenn.
DIAMOND-MACHINED ALUMINUM ALLOY 5083 SURFACES: CONTROLLED EXPOSURE EVALUATION
J. W. Koger, comp. Jun. 1986 10 p
(Contract DE-AC05-84OS-21400)
(DE86-012572; Y/DV-525) Avail: NTIS HC A02/MF A01

Electron spectroscopy for chemical analysis (ESCA) and scanning electron microscopy (SEM) were used to evaluate the effects of relative humidity of 0% to 85% RH and for time exposures of 1 to 100 d at room temperature on diamond-machined aluminum alloy 5083. The ESCA results showed that, in most cases, a limiting oxide thickness of approx. 12 A forms on the surface. Results showed that alloy to be slightly dependent on RH but independent of exposure time. The SEM examination revealed no observable difference in surface morphology when subjected to the controlled exposure parameters. DOE

N87-12675# Oak Ridge Y-12 Plant, Tenn.
CLEANING OF ALUMINUM ALLOY 5083
J. W. Koger, comp. Jun. 1986 6 p
(Contract DE-AC05-84OS-21400)
(DE86-012573; Y/DV-524) Avail: NTIS HC A02/MF A01

The purpose of this investigation was to evaluate several different cleaning procedures on welds with very low heat inputs. The study evaluated the Oak Ridge Y-12 Plant's chemical cleaning, another type of chemical cleaning, ion cleaning, and diamond-machined cleaning. The results showed that the diamond-machining process provides better weld joint surfaces and sound welds with minimum oxide inclusion and porosity. DOE

N87-12676# Pacific Northwest Labs., Richland, Wash.
CRACK-TIP CHEMISTRY AND FRACTURE MECHANICS-BASED MODEL OF THE CRACK GROWTH RATE/STRESS INTENSITY RELATIONSHIP FOR NI + P
R. H. Jones, M. J. Danielson, and C. A. Oster Feb. 1986 15 p Presented at the ASM Metals Congress/TMS-AIME Fall Meeting, Toronto, Ontario, Canada, 13 Oct. 1985
(Contract DE-AC06-76RL-01830)
(DE86-011106; PNL-SA-13447; CONF-8510160-18) Avail: NTIS HC A02/MF A01

A crack-tip chemistry model capable of describing the K/sub ISCC/ and stages I and II crack growth rate kinetics of Ni + P has been developed. This model incorporates the electrochemistry in the crack, IR drop effects, corrosion rate effects along the crack wall, material yield strength and plastic flow properties, and crack geometry parameters. The model predicts that cracking proceeds with a well defined threshold followed by a stage I with a rapid increase in crack growth rate and a stage II in which the crack growth rate is independent of the stress intensity; however, the threshold is underpredicted. A discussion of crack-tip shielding and critical strain effects on these calculations is presented. A critical fracture strain concept can account for the difference in the calculated and measured K/sub ISCC/. Crack growth rates in the stage II regime are underpredicted by a factor of 5. Mechanical fracture occurring simultaneously with anodic dissolution could account for this difference, but direct evidence for such a process is not available. DOE

N87-12677# Pittsburgh Univ., Pa. Dept. of Metallurgical and Materials Engineering.
MICROCHEMICAL ANALYSIS OF POLYCRYSTALLINE NI3AI AND OTHER ORDERED ALLOYS USING THE FIELD-ION MI-

CROSCOPE ATOM PROBE Progress Report
S. S. Brenner 10 Jan. 1986 11 p
(Contract DE-FG02-85ER-45213)
(DE86-013157; DOE/ER-45213/2) Avail: NTIS HC A02/MF A01

The goal of the study is to elucidate the mechanism by which boron and other solutes affect the ductility and strength of polycrystalline Ni3Al and other ordered intermetallics. The study is part of a BES-sponsored interlaboratory effort to bring various analytical and theoretical methods to bear on this question. The first discussion meeting of the members of this group was held at the Oak Ridge National Laboratory on September 20, 1985. Our initial field-ion microscopy and atom probe microanalysis results on Ni3Al were represented at that meeting. This paper summarizes the results of our study obtained during the first six months of the contract period. DOE

N87-12678# International Centre for Theoretical Physics, Trieste (Italy).
FINITE MEAN-FREE-PATHS AND THE ELECTRICAL RESISTIVITY OF LIQUID SIMPLE METALS AND BINARY ALLOYS
T. M. A. Khajil, F. Daver, and M. Tomak Aug. 1985 10 p Prepared in cooperation with Middle East Technical Univ., Ankara, Turkey
(DE86-702662; IC-85/165) Avail: NTIS (US Sales Only) HC A02/MF A01

The finite mean-free-path correction to the Ziman formalism of resistivity for liquid metals is studied. The resistivities of a series of simple liquid metals and some binary alloys are calculated using the Ferraz-March approach. DOE

27 NONMETALLIC MATERIALS

Includes physical, chemical, and mechanical properties of plastics, elastomers, lubricants, polymers, textiles, adhesives, and ceramic materials.

For composite materials see *24 Composite Materials*.

N87-12679*# National Aeronautics and Space Administration. Lewis Research Center, Cleveland, Ohio.
EFFECTS OF GRAPHITIZATION ON THE ENVIRONMENTAL STABILITY OF BROMINATED PITCH-BASED FIBERS
James R. Gaier and Melissa E. Slabe (Cleveland State Univ., Ohio) 1986 13 p Presented at the Fall Meeting of the Materials Research Society, Boston, Mass., 1-5 Dec. 1986
(NASA-TM-88899; E-3323; NAS 1.15:88899) Avail: NTIS HC A02/MF A01 CSCL 11C

The residual bromine graphite intercalation compounds of high modulus pitch-based fibers (Amoco P-55, P-75, P-100, and P-120) were formed and their resistances were monitored under a variety of environmental conditions. A threshold graphitization was observed below which the bromination reaction does not occur to an appreciable extent. The graphitization of the P-55 fibers falls below that threshold, precluding an extensive reaction. The P-75, P-100, and P-120 fibers all form bromination compounds which are stable at ambient conditions, under vacuum, and under high humidity (100 percent humidity at 60 C). The thermal stability of the resistivity increased with decreasing graphitization, with the stable temperature for P-120 being 100 C; for P-100, 200 C; and for P-75, 250 C. When cost is a consideration, bromination of pitch-based fibers is an economical way to achieve low resistivities. Author

N87-12680*# National Aeronautics and Space Administration. Langley Research Center, Hampton, Va.
INVESTIGATION OF THE EFFECTS OF COBALT IONS ON EPOXY PROPERTIES
Jag J. Singh and Diane M. Stoakley Dec. 1986 16 p
(NASA-TP-2639; L-16196; NAS 1.60:2639) Avail: NTIS HC A02/MF A01 CSCL 11G

The effects of Co(acac)sub x complexes on MY-720 epoxy properties have been investigated. It appears that Co2(+) ions form antibonding or nonbonding orbitals which increase the free volume and also reduce the cohesiveness of the host epoxy. The effects of Co2(+) ions, on the other hand, seem to result in increased Cohesiveness of the epoxy. The experimental values of magnetic moments of both types of ions in MY-720 suggest that the orbital momentum contributions of the (3d) electrons are partially conserved, though the effect is more pronounced for Co2(+) ions. The coordination environment of the cobalt ions in the host epoxy does not appear to be uniquely defined. These results indicate that the effects of metal ions on resin properties cannot be easily predicted on the basis of ligand field theory argument alone. Complex interactions between metal ions and host epoxy molecular structure suggest the desirability of parallel experimental investigations of electronic, magnetic, and mechanical properties of metal ion-containing epoxy samples for comparison with theory. Author

N87-12681*# Lehigh Univ., Bethlehem, Pa. Emulsion Polymers Inst.
ELECTROKINETIC PROPERTIES OF POLYMER COLLOIDS Final Report
F. J. Micale and D. Y. Fuenmayor Mar. 1986 14 p
(Contract NAS8-35989)
(NASA-CR-178938; NAS 1.26:178938) Avail: NTIS HC A02/MF A01 CSCL 11B

The surface of polymer colloids, especially polystyrene latexes, were modified for the purpose of controlling the electrokinetic properties of the resulting colloids. Achievement required a knowledge of electrical double layer charging mechanism, as a function of the electrolyte conditions, at the polymer/water interface. The experimental approach is to control the recipe formulation in the emulsion polymerization process so as to systematically vary the strong acid group concentration on the surface of the polymer particles. The electrophoretic mobility of these model particles will then be measured as a function of surface group concentration and as a function of electrolyte concentration and type. An effort was also made to evaluate the electrophoretic mobility of polystyrene latexes made in space and to compare the results with latexes made on the ground. Author

N87-12682# Cornell Univ., Ithaca, N.Y. Dept. of Chemistry.
FRAGMENTATION DYNAMICS OF ENERGETIC MATERIALS Final Report, 10 Jan. 1983 - 9 Jan. 1986
Edward R. Grant 13 May 1986 35 p
(Contract DAAG29-83-C-0020)
(AD-A168925) Avail: NTIS HC A03/MF A01 CSCL 07/5

A molecular beam unimolecular fragmentation mass spectrometer has been developed and applied to the study of primary dissociation processes in energetic materials. The experimental approach uses infrared multiphoton excitation to prepare isolated molecules in the beam for dissociation. Visible laser induced multiphoton ionization detects products with time-of-flight scattering angle and internal quantum state resolution. This report describes the method, spectroscopic results on CH2, CH3CHO, sym-C3N3H3 and NO2, together with experimental observations on the primary decomposition dynamics of NO2, and RCHCH2O with R = CH3, C2H5, and C6H13. GRA

N87-12683# Naval Academy, Annapolis, Md. Dept. of Physics.
IONIC CONDUCTIVITY IN SOLID, CROSSLINKED DIMETHYLSILOXANE-ETHYLENE OXIDE COPOLYMER NETWORKS CONTAINING SODIUM Interim Report
John J. Fontanella and Mary C. Wintersgill Jun. 1986 30 p
(Contract N00014-86-F-0001)
(AD-A169038; TR-21) Avail: NTIS HC A03/MF A01 CSCL 07/4

The preparation of an ion-conducting elastomeric solid based on a dimethylsiloxane-ethylene oxide copolymer complexed with a sodium salt is described. 23Na Nuclear Magnetic Resonance measurements reveal the presence of both bound and mobile sodium species throughout the temperature range -120 to 100 C. Electrical conductivity measurement over a similar temperature range are found to be consistent with the configurational entropy model for transport, with a T sub o parameter about 50 C below the central glass transition temperature T sub g. GRA

N87-12684# Boston Univ., Mass. Center for Polymer Studies.
PERCOLATION AND LOW DENSITY MATERIALS: THEORY AND APPLICATIONS Final Technical Report, 1 Oct. 1981 - 30 Sep. 1985
W. Klein, S. Redner, and H. E. Stanley May 1986 29 p
(Contract DAAG29-82-K-0003)
(AD-A169204; ARO-18263.30-PH) Avail: NTIS HC A03/MF A01 CSCL 20/11

A principal component of the contract has been the development of the renormalization group, with specific emphasis on applications to percolation and random materials. The main accomplishment is summarized in a series of several papers. One of these was identified by the Science Citation Index as being among the 100 most-cited physics papers during 1980 to 1981. This paper dealt with the problem of how the Wilson renormalization group could be applied to random systems in a fashion that yielded specific numbers that could be compared with real systems. The approach developed rests on the essential idea of percolation, that elements must connect across a macroscopic distance. This approach was extended to continuum percolation shortly thereafter, confirming that results first obtained for lattice systems also hold when there is no lattice. Other random systems, like linear and branched polymers, were found to be made tractable by the suitable modifications of our original approach. GRA

N87-12685# State Univ. of New York, Stony Brook. Dept. of Chemistry.
CHARACTERIZATION AND DYNAMICAL STUDIES OF POLYMERS IN DIPOLAR (APROTIC) LIQUIDS Final Report, 5 Jul. 1982 - 4 Jan. 1986
Ben Chu 14 Apr. 1986 7 p
(Contract DAAG29-82-K-0143)
(AD-A169243; Rept-6340A; ARO-19251.5-CH) Avail: NTIS HC A02/MF A01 CSCL 20/4

The aerodynamic breakup of liquids is an essential mechanism in many processes, e.g., fuel atomization in liquid rocket engine, turbojet afterburners and ramjets, paint spraying, aerial dissemination of insecticides, and explosive dissemination of fuels. Only limited studies have been conducted on the aerodynamic breakup of viscoelastic fluids where molecular parameters must necessarily play an important role in the control of both the magnitude of the mean mass diameter of the droplets and the droplet size distribution. The viscoelastic properties of bulk liquid can be altered by using polymer additives whose molecular weight, concentration an dcomposition control the conversion of bulk liquid into specific droplet sizes for a fixed stress and geometry. In this report, we want to summarize the experimental preparations we have made to characterize both static and dynamic properties of polymer additives in dipolar (aprotic) liquids. We have developed a generalized technique to determine the molecular weight, the molecular weight distribution, the polymer composition, the interaction parameters expressed in terms of the second virial coefficients, including both thermodynamic and hydrodynamic interactions for copolymers by means of laser light scattering. As a specific example, we characterized acryloid k-125, a quasiterpolymer used in aerodynamic breakup tests. GRA

N87-12686# Illinois Inst. of Tech., Chicago.
THE CONTROL OF POLYMER MECHANICAL BEHAVIOR BY SURFACE MODIFICATION Final Report, 1 May 1979 - 4 Jul. 1985
Lawrence J. Broutman 15 May 1986 10 p
(Contract DAAG29-79-C-0094)
(AD-A169252; ARO-16425.3-MS; ARO-19026.1-MS) Avail: NTIS HC A02/MF A01 CSCL 11/9

The effect of a brittle surface layer on the mechanical behavior of polymers has been studied. The brittle surface layer has been simulated by laminating a thin film to a polymer or by ultra violet irradiation of the surface. Fracture mechanics theories have been utilized to account for the phenomenon of surface embrittlement. A criterion has been established suggesting that embrittlement will only occur when the dynamic stress intensity factor in the brittle layer reaches a value greater than the arrest toughness of the ductile substrate. It has also been shown that the embrittlement phenomenon can be described in terms of a critical crack velocity or critical thickness. It is shown that brittle films less than .005 inches thick can cause brittle failure of polymers such as polycarbonate and ABS. It is also shown that cracks can attain velocities of up to 200 m/sec when propagating through such films. GRA

N87-12687# Department of the Air Force, Washington, D.C.
LOW TEMPERATURE FORMATION OF MULLITE Patent Application
Bulent E. Yoldas, inventor (to Air Force) Filed 28 May 1986 15 p
(AD-D012404; US-Patent-Appl-SN-867727) Avail: NTIS HC A02/MF A01 CSCL 07/1

This patent application relates to a process for preparing high purity, stoichiometric aluminum silicate (mullite). The method prepares mullite ($3Al_2O_3.2SiO_2$) by partially hydrolyzing ae dilute silicon alkoxide solution, combining an aluminum alkoxide with the partially hydrolyzed silicon alkoxide, eliminating terminal alkoxide groups and firing the material to about 985 C. GRA

N87-12688# Battelle Columbus Labs., Ohio.
HOT ISOSTATIC PRESSING OF CERAMIC POWDER COMPACTS Final Report, 1 Jun. 1984 - 31 Dec. 1985
J. K. McCoy and A. J. Markworth 15 Jan. 1986 174 p
(Grant AF-AFOSR-0238-82)
(AD-A169971; AFOSR-86-0348TR) Avail: NTIS HC A08/MF A01 CSCL 11/2

The densification of aluminum oxide in hot isostatic pressing has been studied in detail. Methods for calculating maps of densification rate as a function of temperature and applied pressure have been developed. A new mechanism, interface-reaction-controlled grain-boundary diffusion has been found which describes the densification of high-purity, fine-grained (grain radius of 0.7 micrometers) aluminum oxide powder at temperatures up to 1423 K. Theoretical models have been developed for this mechanism for both the initial and final stages of densification. Standard geometries have been used for the models; the initial stage is described in terms of impinging spherical particles, and the final stage is described in terms of isolated pores. The theoretical model is found to describe the data for fractional densities up to at least 0.9, although it breaks down for higher densities. From theoretical studies of final stage, we find indications that the discrepancy between theory and experiment is due at least in part to neglect of the effects of a distribution of pore sizes. GRA

N87-12689# Southwest Research Inst., San Antonio, Tex. Dept. of Materials Sciences.
STUDY OF HIGH TEMPERATURE FAILURE MECHANISMS IN CERAMICS Annual Report, 1 Apr. 1985 - 31 Mar. 1986
Richard A. Page and James Lankford Apr. 1986 25 p
(Contract F49620-85-C-0073)
(AD-A170001; SWRI-8578/2; AFOSR-86-0485TR) Avail: NTIS HC A02/MF A01 CSCL 11/2

This report summarizes the results of a fundamental study involving experimental characterization and analytical modeling of grain boundary cavitation and creep crack growth in structural ceramics exposed to pure tensile loading. The major experimental techniques employed in the program are the use of small-angle neutron scattering to characterize cavity nucleation and growth and stereoimaging analysis to characterize the stress and strain fields associated with growing creep cracks. In the first section of the report, the experimental progress is summarized. The design of the pure tensile creep apparatus, which is being used for the creation of bulk damage and for creep crack growth, is discussed. The progress made in the determination of surface preparation conditions that are adequate for the stereoimaging analysis is also discussed. The second section of the report describes the results of a critical review of recent experimental and theoretical studies of creep cavitation in ceramics. The results of this critical study have identified a number of stochastic aspects of cavitation. The stochastic nature of cavitation arises primarily due to the depen-

dence of both cavity nucleation and cavity growth on grain boundary sliding. A degree of randomness is also imposed by the nonuniform distribution of nucleation sites. GRA

N87-12690# Virginia Polytechnic Inst. and State Univ., Blacksburg. Center for Adhesion Science.
AN INTERDISCIPLINARY APPROACH TO PREDICTIVE MODELING OF STRUCTURAL ADHESIVE BONDING. CHARACTERIZATION OF Ti-6Al-4V OXIDES AND THE ADHESIVE/OXIDE INTERPHASE Annual Report, 18 Jun. 1984 - 18 Sep. 1985
J. A. Filbey and J. P. Wightman May 1986 70 p
(Contract N00014-82-K-0185)
(AD-A170484; CAS/CHEM-4-86; AR-86) Avail: NTIS HC A04/MF A01 CSCL 11/1

Ti-6-4, being a high strength, lightweight, corrosion resistant alloy, possesses many uses for structural adhesive bonding. Many researchers are therefore finding better pretreatments, characterizing the oxide surface and evaluating bonding performance. The work reported here will encompass both oxide characterization and evaluation of adhesive bonds. The chemical composition of oxides created by specific pretreatments was studied by XPS, AES, SIMS, contact angles, and indicator dyes. The surface topography and structure was probed by SEM, STEM, and profilometry. Following the procedures of Carre and Schultz with aluminum substrates, values for the surface energy of the Ti-6-4 oxides are obtained using an interfacial contact angle method. Because of the present interest in the use of Ti-6-4 for high temperature applications, the thermal stability of the oxide layer was investigated. Following Pike's successful use of inorganic primers as adhesion promoters on aluminum substrates, studies were begun to characterize a titanate primer. Finally, both lap shear and wedge tests have been used to evaluate the adhesive/oxide interphase. GRA

N87-12691 Department of the Navy, Washington, D. C.
RUSTY BOLT INTERMODULATION INTERFERENCE REDUCER Patent
Ramanathan Panayappan and John C. Cooper, inventors (to Navy) Issued 27 May 1986 4 p Supersedes AD-D011748
(AD-D012417; US-Patent-4,591,510; US-Patent-Appl-SN-722579; US-Patent-Class-427-125) Avail: US Patent and Trademark Office CSCL 17/2

A chemical composition formed from a chelating agent, polymeryable bonding agent, and a high dielectric solvent eliminates intermodulation interference when applied to rusty bolt junctions. Author (GRA)

N87-12692 Department of the Navy, Washington, D. C.
ADHESIVE REPAIR PATCH Patent
Leighton H. Peebles, Jr., inventor (to Navy) Issued 27 May 1986 4 p Supersedes AD-D011478
(AD-D012422; US-Patent-4,591,511; US-Patent-Appl-SN-635866; US-Patent-Class-427-142) Avail: US Patent and Trademark Office CSCL 11/1

A method for effecting repairs or the damaged component of a machinery in the field which would otherwise require high temperature treatment of the damaged components to form a metal-oxide epoxy joint in a shop. The method includes preparing a repair patch which includes a metal sheet with the metal oxide layer thereon, applying a thin high performance protective coating thereover, covering thereof with a sacrificial backing sheet and then curing the adherent-top coat backing sheet to form a highly durable bonded system which can be stored until needed. At the time of repair the backing sheet is removed by sanding or grit blasting and the adherent is applied to the structure to be repaired under ordinary temperature conditions. Author (GRA)

N87-12693# Honeywell, Inc., Bloomington, Minn. Physical Sciences Center.
SYNTHESIS OF CONJUGATED POLYMERS WITH ALTERNATING AROMATIC AND QUINONOID SEQUENCES VIA ELIMINATION ON PRECURSORS
Samson A. Jenekhe 14 Aug. 1986 15 p
(Contract N00014-84-C-0699)
(AD-A171331; TR-3) Avail: NTIS HC A02/MF A01 CSCL 07/3

An elimination reaction for the formation of conjugated polymers from polymer precursors containing alternating sp superscript 3 carbon atom and conjugated segments in the main chain is described. The resulting conjugated polymers with alternating aromatic and quinonoid sequences are inaccessible by conventional polymerization processes. The Pi-electron conjugation extension process is exemplified by reactions performed on poly(5,5',alpha-bithiophenediyl p acetoxybenzylidene) at 23 C and followed by electronic and infrared spectra. The semiconductor band gap narrowed from an initial value of 1.53 eV for the precursor polymer to about 0.83 eV for the conjugated derivative. Further evidence for the sp superscript 3 to sp superscript 2 carbon atom conversion by the elimination process is provided by infrared data. GRA

N87-12694# Sandia National Labs., Albuquerque, N. Mex.
RAMAN SPECTROSCOPY OF CARBORANES AND POLYCARBORANESILOXANES
J. A. Shelnutt 1986 15 p Presented at the Annual Joint Meeting of the Electron Microscopy of America and the Microbeam Analysis Society, Albuquerque, N. Mex., 10 Aug. 1986
(Contract DE-AC04-76DP-00789)
(DE86-009030; SAND-86-0806C; CONF-860829-15) Avail: NTIS HC A02/MF A01

Raman spectra of some m-carboranesiloxane polymers are compared with each other and with the spectrum of o-carborane and boron carbide. The comparisons and additional polarization studies allow the assignment of some vibrations to the icosahedral 1,7-dicarboranyl units, siloxy polymer connecting units, and substituent groups of the silicon atoms. The Raman investigation is directed toward understanding the interaction of carborane icosahedral units of boron-carbide semiconductor materials. DOE

N87-12695# Los Alamos National Lab., N. Mex.
PHYSICAL CHARACTERISTICS OF DIBLOCK POLYACETYLENE COPOLYMERS: PROCESSABILITY-CONDUCTIVITY CORRELATION
M. Aldissi, M. Hou, and J. Farrell 1986 7 p Presented at the International Conference on Science and Technology of Synthetic Metals, Kyoto, Japan, 1 Jun. 1986
(Contract W-7405-eng-36)
(DE86-011218; LA-UR-86-1744; CONF-8606133-3) Avail: NTIS HC A02/MF A01

The physical properties of polyacetylene diblock copolymers containing polystyrene (PS) or polyisoprene (PI) blocks of various compositions are studied using electron spin resonance, resonance Raman scattering, and room temperature conductivity measurements. This study is performed to investigate the processability-conductivity correlation in these materials and their viability as conducting systems. DOE

N87-12696# Los Alamos National Lab., N. Mex.
EFFECT OF CHAIN RIGIDITY ON CONDUCTIVITY OF CONJUGATED POLYMERS
M. Aldissi 1986 7 p Presented at the International Conference on Science and Technology of Synthetic Metals, Kyoto, Japan, 1 Jun. 1986
(Contract W-7405-eng-36)
(DE86-011263; LA-UR-86-1565; CONF-8606133-2) Avail: NTIS HC A02/MF A01

There are several ways to introduce processability to conjugated polymers, and one of them is discussed here. The basic approach involves the introduction of flexible centers in a conjugated backbone with a periodicity that allows the existence of conjugated sequences characterized by an electron mobility high enough to result in electronic conduction upon oxidation or reduction. The process consists of the use of AsF5 as a polymerization catalyst, and AsF3 as a non-conventional medium for the reaction. The Lewis acid coupling reactions, via which the polymerization occurs, result in soluble materials. Characteristics

of the materials obtained by polymerizing acetylene and some aromatic compounds are discussed. DOE

N87-12697# Los Alamos National Lab., N. Mex.
ELECTRON-ELECTRON INTERACTION EFFECTS IN QUASI-ONE-DIMENSIONAL CONDUCTING POLYMERS AND RELATED SYSTEMS
D. K. Campbell, D. Baeriswyl, and S. Mazumdar 1986 7 p Presented at the International Conference on Science and Technology of Synthetic Metals, Kyoto, Japan, 1 Jun. 1986 Prepared in cooperation with Eidgenoessische Technische Hochschule, Zurich (Switzerland) and GTE Labs, Inc., Waltham, Mass.
(Contract W-7405-eng-36)
(DE86-012434; LA-UR-86-2207; CONF-8606133-5) Avail: NTIS HC A02/MF A01

We review recent results on the role of electron-electron (e-e) interactions in quasi-one-dimensional conducting polymers and related systems. Within the Peierls-Hubbard model, the effects of both short-range (on-site U and nearest neighbor V sub 1) and long-range (V sub j/, j is greater than or equal to 2) are examined, the former using quantum Monte Carlo and the latter with exact diagonalization of finite size systems and analytic arguments. We also discuss optical absorption properties in the presence of electronic correlation, focusing on the weak and strong coupling limits. DOE

N87-12698# Oak Ridge National Lab., Tenn.
DENSIFICATION OF GRAPHITES BY IRRADIATION
C. R. Kennedy and D. Mindermann (SIGRI Electrogradhit G.m.b.H., Meitingen West Germany) 1986 7 p Presented at the Carbon Conference, Baden-Baden, West Germany, 30 Jun. 1986 Prepared in cooperation with Sigri Elektrographit G.m.b.H., Meitingen (Germany, F.R.)
(Contracts DE-AC06-76RL01857; DE-AC05-84OR-21400)
(DE86-010026; CONF-8606113-2) Avail: NTIS HC A02/MF A01

Information is presented on neutron-induced dimensional changes in the highly anisotropic hexagonal crystal structure of graphite. The sensitivity of bulk density to the densification can be confirmed to some extent by a comparison of the effect of oxidation on the dimensional changes of graphite. The oxidation irradiation results are limited, requiring assumptions that the linear increase occur isotropically for these anisotropic graphites. DOE

N87-12699# Oak Ridge National Lab., Tenn.
METALS AND CERAMICS DIVISION MATERIALS SCIENCES PROGRAM Annual Progress Report, period ending 31 Dec. 1985
J. O. Stiegler, comp. Jun. 1986 315 p
(Contract DE-AC05-84OR-21400)
(DE86-013512; ORNL/TM-10033) Avail: NTIS HC A14/MF A01

Structural characterization, high-temperature alloy research, structural ceramics, radiation effects, structure and properties of surfaces and interfaces, and collaborative research centers are discussed. DOE

N87-12700# Midwest Research Inst., Golden, Colo.
SOLID-STATE ELECTROCHROMIC SWITCHABLE WINDOW GLAZINGS Progress Report
D. K. Benson, C. E. Tracy, and M. R. Ruth Apr. 1986 71 p
(Contract DE-AC02-83CH-10093)
(DE86-004455; SERI/PR-255-2627) Avail: NTIS HC A04/MF A01

Multilayer, solid-state electrochromic coatings have been prepared and characterized. The electrochromic activity is based on hydrogen-ion insertion into a microcrystalline tungsten oxide (H sub x WO sub y) layer from a hydrated microcrystalline magnesium fluoride layer. The coatings typically consist of four layers deposited sequentially onto glass: transparent conductor (tin-doped indium oxide, ITO) 330 nm; electrochromic material (H sub x WO sub y) 500 nm; hydrated fast-ion conductor/electron current blocking layer (MgF) 100 nm; and transparent conductor (gold) 13 nm. Solar-weighted and photopic-weighted optical properties are reported for individual layers and complete multilayer coatings. The electrooptic response of complete solid-state coatings is also reported. Maximum transmittance through the four layer coatings with gold conductive layers was limited to 32% solar and 56% visible. Replacing the gold conductive layer with a tin-doped indium oxide layer increased the maximum transmittance to 59% solar and 64% visible but impaired the electrochromic response. Large area coatings were fabricated (700 cm^2) and shown to operate in the same manner as the 12 cm^2 test specimens. Preliminary analyses were made of possible production costs and possible energy savings benefits which would be derived from optimal use of such switchable window coatings. DOE

N87-12701# Midwest Research Inst., Golden, Colo. Solar Energy Research Inst.
LASER SEALED VACUUM INSULATING WINDOW Patent Application
D. K. Benson, inventor (to DOE) and C. E. Tracy, inventor (to DOE) Filed 19 Aug. 1985 27 p
(Contract DE-AC02-83CH-10093)
(DE86-013678; US-Patent-Appl-SN-767218) Avail: NTIS HC A03/MF A01

A laser sealed evacuated window panel is comprised of two glass panes held spaced apart in relation to each other by a plurality of spherical glass beads and glass welded around the edges to provide an evacuated space between the glass panes that is completely glass sealed from the exterior. The glass welded edge seal is obtained by welding the edges of the glass panes together with a laser beam while the glass panes and bead spacers are positioned in a vacuum furnace and heated to the annealing point of the glass to avoid stress fracture in the area of the glass weld. The laser welding in the furnace can be directed around the perimeter of the galss panel by a combination of rotating the glass panel and linearly translating or aiming the laser with a relay mirror. DOE

28 PROPELLANTS AND FUELS

Includes rocket propellants, igniters, and oxidizers; their storage and handling procedures; and aircraft fuels.

For related information see also *07 Aircraft Propulsion and Power, 20 Spacecraft Propulsion and Power,* and *44 Energy Production and Conversion.*

N87-12702# Weapons Systems Research Lab., Salisbury (Australia).
METHODS FOR THE SYNTHESES OF MONO-, DI-, TRI- AND TETRANITRO DERIVATIVES OF DIPHENYLAMINE
N. J. Curtis Jan. 1986 21 p
(WSRL-0436-TR; AR-004-307) Avail: NTIS HC A02/MF A01

A critical review of the methods available for the syntheses of the title compounds is presented. Concise procedures are given for the preparation of these compounds, obtained in useful yield from readily available starting materials. Author

N87-12703# Dayton Univ., Ohio.
PULSED-LASER, HIGH SPEED PHOTOGRAPHY OF ROCKET PROPELLANT SURFACE DEFLAGRATION Final Report, 1 May 1983 - 30 Sep. 1985
Roger J. Becker May 1986 104 p
(Contract F04611-83-K-0023)
(AD-A169308; UD-TR-85-147; AFRPL-TR-86-039) Avail: NTIS HC A06/MF A01 CSCL 21/9

High speed movies of solid propellant deflagration have long provided useful qualitative information on propellant behavior. Consequently, an extension of performance to include quantitative behavior of the surface, particularly the spatial relationship of particles across the surface, the temporal behavior of particles through extended periods of time, and accurate measurements of particle sizes, is highly desirable. Such measurements require the ability to take detailed movies across an extensive surface through

the propellant flame for longer periods than the residence time of a given particle. For such experiments, camera optics employing magnification are undesirable, since they severely limit both the field of view and the depth of field, and hence, the useful duration of a frame sequence. Unfortunately, high resolution without magnification pushes both the diffraction limits and the performance capabilities of standard lenses. At this limit, the modulation transfer function (MTF) of the camera optics and film will greatly affect performance. The MTF of the optics can be improved by a factor of two or more at practical spatial frequencies by the use of monochromatic light, such as the reflected light from a laser. This is especially true for off-axis rays, and important consideration when an extended field-of-view is required. The use of an intense, short-pulsed laser has the additional advantage of suppressing flame brightness and motion blur. GRA

N87-12704# Rockwell International Corp., Canoga Park, Calif. Rocketdyne Div.
PREPARATION OF ENERGETIC COMPOUNDS Final Report, 1 May 1984 - 30 Jun. 1986
M. B. Frankel, M. A. Cunningham, J. F. Weber, and L. R. Grant Jul. 1986 37 p
(Contract N00014-84-C-0234)
(AD-A170022; RI/RD86-216) Avail: NTIS HC A03/MF A01 CSCL 19/1

There is a continual quest to upgrade the performance of state-of-the-art propellants and explosives. The three principal ingredients of these systems are the oxidizer, plasticizer, and polymeric binder. Consequently, a major effort has been carried out in the past years to synthesize and characterize high-energy, high-density compounds that could be utilized for these applications. Recent research work by Dr. H. G. Adolph at the Naval Surface Weapons Center (NSWC) has revealed three attractive new propellant and/or explosive ingredients. These compounds are 1,3,3,5,7,7-hexanitrooctahydro-1,5-diazocine, a high-energy solid oxidizer candidate; 4,5-bis(fluorodinitromethyl)-1,3-dioxalane (DHFEFO), a high density liquid plasticizer candiate; and certain fluorinate polyformals, which are high density prepolymer candidates. The objective of this program was to synthesize and characterize sufficient quantities of these materials so that they could be a more fully evaluated by the technical staffs at NSWC and the Naval Weapons Center (NWC). GRA

N87-12705# Monsanto Co., Dayton, Ohio.
DETERMINATION OF THE COEFFICIENT OF THERMAL EXPANSION OF JP-4 FUELS Interim Report, Apr. 1983 - Jul. 1985
Donovan S. Duvall, Michael D. Hale, Donald J. Lewis, and Arthur D. Snyder Dec. 1985 51 p
(Contract F33615-81-C-2035)
(AD-A171495; AFWAL-TR-85-2093) Avail: NTIS HC A04/MF A01 CSCL 21/4

Precise density determinations were made on 100 JP-4 jet fuels using a Mettler/Paar Model ADS-55 density measuring system. Statistical analysis of the density measurements was performed using a computerized nonlinear regression technique; and coefficient of thermal expansion values were calculated for each fuel at 60 F. A majority of the fuels (88 out of 100) were consistent with the API published volume series correction for crude oils. GRA

N87-12706# Brookhaven National Lab., Upton, N. Y.
PRODUCTION OF A CLEAN CARBON FUEL DERIVED FROM COAL FOR USE IN STATIONARY AND MOBILE HEAT ENGINES
M. Steinberg Apr. 1986 25 p Presented at the 8th International Symposium on Coal Slurry Fuels Preparation and Utilization, Orlando, Fla., 27 May 1986
(Contract DE-AC02-76CH-00016)
(DE86-011203; BNL-38086; CONF-860548-2) Avail: NTIS HC A02/MF A01

Described is the development of a new process called HYDROCARB and the production of a new fuel product called CARBOLINE (an acronym for carbon-gasoline), which has potential world-wide economic usefulness. It is a clean carbon fuel which can be used in stationary, steam, and electrical power generating plants and for mobile transportation engines. The HYDROCARB process converts any abundantly available carbonaceous raw material such as coal, peat, tar, biomass (wood), agricultural materials and commercial and industrial wastes, into a clean carbon fuel. This fuel is produced in two forms: one is a solid particulate carbon black, which can readily be burned in a boiler, turbine, or internal combustion engine, and the other is a clean liquid carbon fuel made by mixing the solid particulate carbon black with either water, alcohol, gasoline, oils or other conventional liquid fuel to form a mix or slurry fuel CARBOLINE. Because of the vast resources of coal throughout the world, the new process will have greatest applicability in the conversion of coal to clean solid carbon fuel and to a liquid CARBOLINE mix fuel competitive with world petroleum derived fuel costs. DOE

N87-12707# Los Alamos National Lab., N. Mex.
ANVIL DETONATOR: A 300EC-STABLE, HOT-WIRE-IGNITED, NONPRIMARY-EXPLOSIVE DEVICE
R. H. Dinegar and J. O. Johnson Jul. 1986 8 p
(Contract W-7405-eng-36)
(DE86-013635; LA-10749-MS) Avail: NTIS HC A02/MF A01

The search for a combination of explosives and low-energy means of initiation that will function in the 300 C region appears to be successfully concluded. PYX, NONA, HNS-II, and KP have been employed satisfactorily as donor charges in hot-wire-ignited, flying-plate assemblies. The standard method of construction used in flying-plate detonators is unsatisfactory, however. A completely new and novel design that results in consistent initiation, employing a shock-up process has been developed. In this anvil detonator, PYX is the donor charge and NONA is the acceptor explosive. DOE

29 MATERIALS PROCESSING

Includes space-based development of products and processes for commercial applications.
For biological materials see *55 Space Biology.*

No abstracts in this category.

31 ENGINEERING (GENERAL)

Includes vacuum technology; control engineering; display engineering; cryogenics; and fire prevention.

N87-12708*# National Aeronautics and Space Administration. Lewis Research Center, Cleveland, Ohio.
PLASMA ASSISTED SURFACE COATING/MODIFICATION PROCESSES: AN EMERGING TECHNOLOGY
Talivaldis Spalvins 1986 15 p Presented at the 1st International Ion Nitriding Conference, Cleveland, Ohio, 15-17 Sep. 1985; sponsored by the American Society for Metals
(NASA-TM-88885; E-3274; NAS 1.15:88885) Avail: NTIS HC A02/MF A01 CSCL 13H

A broad understanding of the numerous ion or plasma assisted surface coating/modification processes is sought. An awareness of the principles of these processes is needed before discussing in detail the ion nitriding technology. On the basis of surface modifications arising from ion or plasma energizing and interactions, it can be broadly classified as deposition of distinct overlay coatings (sputtering-dc, radio frequency, magnetron, reactive; ion plating-diode, triode) and surface property modification without forming a discrete coating (ion implantation, ion beam mixing, laser beam irradiation, ion nitriding, ion carburizing, plasma oxidation). These techniques offer a great flexibility and are capable

in tailoring desirable chemical and structural surface properties independent of the bulk properties. Author

N87-12709# Texas Technological Univ., Lubbock. Dept. of Civil Engineering.
THE APPLICATION OF BOUNDARY-ELEMENT TECHNIQUES FOR SOME SOIL-STRUCTURE INTERACTION PROBLEMS Final Report
C. V. Vallabhan and Jayaraman Sivakumar Apr. 1986 91 p
(Contract DACW39-83-M-1805)
(AD-A168999; ATC-86-2) Avail: NTIS HC A05/MF A01 CSCL 08/13

Boundary-element technique research performed to solve soil-structure interaction problems is the basis for this report. Specifically, it was designed to answer questionable situations for long hydraulic U-Lock structures erected on elastic soil. A review of earlier research that employed the Kelvin-type element directed the decision in favor of Flamant-type boundary element. Both constant and linear elements were developed and many sample problems were dealt with to illustrate the capabilities of these elements in the problem situations of soil-structure relationships. The Flamant-type boundary element proved to be convenient, gave better results for displacement problems using the constant element, offered satisfactory behavior description of soil-structure response, required considerably fewer elements than the conventional model, provided more accuracy in stress analysis of structure, and was confirmed as very beneficial for use in input data preparation. Research was also conducted on soil-structure interaction problems with the structure modeled by the finite-element method and the soil modeled by the boundary-element method. A model problem suggested by the AEWES was selected for study and solving. The emphasis was to develop a convenient and economical technique to couple the boundary- and finite-element methods of analysis. A computer code for coupling the two methods has been developed in FORTRAN. GRA

N87-12710# Department of the Air Force, Washington, D.C.
LIGHT SOCKET REMOVAL TOOL Patent Application
Thomas E. Brokenshire, inventor (to Air Force) Filed 28 Apr. 1986 7 p
(AD-D012368; US-Patent-Appl-SN-856248) Avail: NTIS HC A02/MF A01 CSCL 13/9

This invention relates to tools for the repair and removal of light sockets having bayonet type receptacles. The invention comprises a tool for simplifying the removal of this type light socket. The tool comprises a cylindrical shaft having mating pins positioned for insertion into the bayonet type receptacle. The mating pins register with notches in the receptacle in order to firmly position the shaft within the receptacle. The tool and the light socket receptacle are then held stationary with a handle portion during removal of socket fasteners. GRA

N87-12711# Rockwell International Corp., Columbus, Ohio. North American Aircraft Operations.
FABRICATION AND TESTING OF LIGHTWEIGHT HYDRAULIC SYSTEM SIMULATOR HARDWARE Final Report, 15 May 1980 - 15 Nov. 1985
William N. Bickel and Robert K. Haning Jan. 1986 279 p
(Contract N62269-80-C-0261)
(AD-A169884; NA-85-0134; NADC-79024-60) Avail: NTIS HC A13/MF A01 CSCL 13/7

The Lightweight Hydraulic System (LHS) Advanced Development Program is a multi-phase investigation of the concept of using an 8000 psi operating pressure level to achieve smaller and lighter weight hydraulic components than those used in aircraft with conventional 3000 psi systems. This report presents the results of Phase II in which a full scale A-7E 8000 psi dual system hydraulic simulator was fabricated and tested. Tests conducted were proof pressure, system integration, baseline, dynamic performance, and 600 hours of endurance cycling. No major technological problems were encountered. Four flight control actuators accumulated over 3,000,000 cycles; one pump accumulated over 1000 hours of operation (Phase I and Phase II). Hydraulic system math models were corroborated by test data. A weight and space analysis update projected 33.1% and 36.3% savings, respectively, over an equivalent 3000 psi system. A study of simulator operating experience indicated a 23% improvement in reliability over a comparable 3000 psi system. An additional 600 hours of simulator endurance cycling are scheduled for completion in FY '86. GRA

N87-12712# Department of the Air Force, Washington, D.C.
TDD ANTENNA: FOIL FORMED, SUBSTRATE LOADED LASER WELDED ASSEMBLY Patent Application
N. L. Alfing, inventor (to Air Force) Filed 19 May 1986 9 p
(AD-D012411; US-Patent-Appl-SN-864221) Avail: NTIS HC A02/MF A01 CSCL 16/4

The antenna assembly is formed by building a shell housing by punch press operation. The housing contains the antenna features. The dielectric with load and connector is placed into the housing. Then a back is placed onto the assembly and the unit is enclosed by laser welding. This design allows the fabrication of the housing to be constructed with the antenna features built in and is simpler and less costly than prior designs. GRA

N87-12713# Hydrogen Consultants, Inc., Denver, Colo.
PHASE CHANGE THERMAL ENERGY STORAGE METHODS FOR COMBAT VEHICLES, PHASE 1 Final Report
F. E. Lynch Jun. 1986 63 p
(Contract DAAK70-85-C-0077)
(AD-A170492) Avail: NTIS HC A04/MF A01 CSCL 13/1

Three alternative cooling methods, based on latent heat absorption during phase changes, were studied for potential use in combat vehicle microclimate temperature control. Metal hydrides absorb heat as they release hydrogen gas. Plastic crystals change from one solid phase to another, absorbing heat in the process. Liquid air boils at cryogenic temperature and absorbs additional sensible heat as the cold gas mixes with the microclimate air flow. System designs were prepared for each of the three microclimate cooling concepts. These designs provide details about the three phase change materials, their containers and the auxiliary equipment needed to implement each option onboard a combat vehicle. The three concepts were compared on the basis of system mass, system volume and the energy required to regenerate them after use. Metal hydrides were found to be the lightest and smallest option by a large margin. The energy needed to regenerate a hydride thermal storage system can be extracted from the vehicle's exhaust gases. GRA

N87-12714# Los Alamos National Lab., N. Mex.
ANALYSIS OF MAGNETIC REFRIGERATION SYSTEMS WITH STAGED REGENERATORS BASED ON AN IDEALIZED MAGNETIC MATERIAL ENTROPY MODEL: 1
W. C. Overton, Jr. May 1986 78 p
(Contract W-7405-eng-36)
(DE86-013638; LA-10676-MS) Avail: NTIS HC A05/MF A01

We have performed a computer analysis of magnetic refrigerators consisting of a single magnetic-material (MM) stage (with T sub c = 70.5 K and resembling GdNi), a hot heat exchanger for rejecting heat to an LN sink, a cold heat exchanger for removing heat from a cold cryogenic load and an external regenerator having an integral number n of isolated stages with 5 less than or equal to n less than or equal to 10. We use the abbreviation REGMR for such a system. An idealized entropy-versus-temperature model is used to represent the magnetic material. The single MM stage REGMR model proves capable of producing refrigeration from 77 K down to less than 30 K. We estimate two such REGMRs in tandem could produce refrigeration to less than 15 K, depending on the cryogenic load. The numerical analysis is based on strict conservation of energy and we neglect the small hydrodynamic losses of the ^{4}He exchange-gas system and heat-transfer irreversibilities. Performance is evaluated in terms of the lowest temperature achievable, the number of cycles required to reach cyclic equilibrium, the effect of regenerator stage mass and number of stages, and the effect of cryogenic loads. A systematic comparison of the REGMR cycle with other thermodynamic cycles shows the

former is unique. The coefficient of performance is evaluated and the REGMR efficiency is determined by comparison with the ideal gas Carnot-cycle refrigerator. DOE

N87-12715# Joint Publications Research Service, Arlington, Va.
JAPAN REPORT: SCIENCE AND TECHNOLOGY
29 Aug. 1986 75 p Transl. into ENGLISH from various Japanese articles
(JPRS-JST-86-023) Avail: NTIS HC A04/MF A01

Topics addressed include: aerospace sciences, biotechnology, chemical engineering, computers, defense industry, and nuclear development. For individual titles, see N87-12716 through N87-12717.

N87-12716# Joint Publications Research Service, Arlington, Va.
POSSIBLE MILITARY APPLICATIONS OF STRATOSPHERIC AIRSHIP DISCUSSED **c05**
Junichi Kimura, Ryuichi Takeda, Yukichi Fujimatsu, and Toshiyuki Kato *In its* Japan Report: Science and Technology (JPRS-JST-86-023) 29 Aug. 1986 p 49-62 Transl. into ENGLISH from Boei Gijutsu (Tokyo, Japan), Nov. 1985 p 48-58 (For primary document see N87-12715 04-31)
Avail: NTIS HC A04/MF A01

The possibilities of a stratospheric airship of the LB (lifting body) types are studied from the aspect of operation. The meteorological conditions that most severly restrict its operation are considered. The advantages that the stratospheric airship has over other aircraft and artificial satellites are discussed. B.G.

N87-12717# Joint Publications Research Service, Arlington, Va.
STATUS OF LASER ENRICHMENT TECHNOLOGY UPDATED **c36**
Yasushi Sakabe *In its* Japan Report: Science and Technology (JPRS-JST-86-023) 29 Aug. 1986 p 63-69 Transl. into ENGLISH from Purometeusu (Tokyo, Japan), Nov. 1985 p 41-43 (For primary document see N87-12715 04-31)
Avail: NTIS HC A04/MF A01

The principles of uranium enrichment by a laser method, the technology's current status and future prospects, centered on research and development activity at the Japan Atomic Energy Research Institute and the Institute of Physical and Chemical Research are described. B.G.

32 COMMUNICATIONS AND RADAR

Includes radar; land and global communications; communications theory; and optical communications.

For related information see also *04 Aircraft Communications and Navigation* and *17 Space Communications, Spacecraft Communications, Command and Tracking.* For search and rescue see *03 Air Transportation and Safety,* and *16 Space Transportation.*

N87-12718*# National Aeronautics and Space Administration. Wallops Flight Center, Wallops Island, Va.
PULSE CODE MODULATION (PCM) DATA STORAGE AND ANALYSIS USING A MICROCOMPUTER
David E. Massey Aug. 1986 8 p
(NASA-TP-2629; Rept-822.3; NAS 1.60:2629) Avail: NTIS HC A02/MF A01 CSCL 17B

The current widespread use of microcomputers has led to the creation of some very low-cost instrumentation. A Pulse Code Modulation (PCM) storage device/data analyzer -- a peripheral plug-in board especially constructed to enable a personal computer to store and analyze data from a PCM source -- was designed and built for use on the NASA Sounding Rocket Program for PMC encoder configuration and testing. This board and custom-written software turns a computer into a snapshot PCM decommutator which will accept and store many hundreds or thousands of PCM telemetry data frames, then sift through them repeatedly. These data can be converted to any number base and displayed, examined for any bit dropouts or changes (in particular, words or frames), graphically plotted, or statistically analyzed. Author

N87-12719*# Jet Propulsion Lab., California Inst. of Tech., Pasadena.
TONE CALIBRATION TECHNIQUE: A DIGITAL SIGNALING SCHEME FOR MOBILE APPLICATIONS
Faramaz Davarian 15 Sep. 1986 72 p
(NASA-CR-179915; JPL-Pub-86-40; NAS 1.26:179915; MSAT-X-138) Avail: NTIS HC A04/MF A01 CSCL 17B

Residual carrier modulation is conventionally used in a communication link to assist the receiver with signal demodulation and detection. Although suppressed carrier modulation has a slight power advantage over the residual carrier approach in systems enjoying a high level of stability, it lacks sufficient robustness to be used in channels severely contaminated by noise, interference and propagation effects. In mobile links, in particular, the vehicle motion and multipath waveform propagation affect the received carrier in an adverse fashion. A residual carrier scheme that uses a pilot carrier to calibrate a mobile channel against multipath fading anomalies is described. The benefits of this scheme, known as tone calibration technique, are described. A brief study of the system performance in the presence of implementation anomalies is also given. B.G.

N87-12720# Instituto de Pesquisas Espaciais, Sao Jose dos Campos (Brazil).
FAULT TOLERANCE MECHANISMS FOR A NETWORK COMMUNICATION MULTIPROCESSOR [MECANISMOS DE TOLERANCIA A FALHAS PARA O MULTIPROCESSADOR DE COMUNICACAO EM REDE]
Antonio Esio Marcondes Salgado Jul. 1986 17 p In PORTUGUESE; ENGLISH summary Presented at the 1st Symposium on Computer Systems Tolerances and Faults, Sao Jose dos Compos, Brazil, Oct. 1985
(INPE-3958-PRE/876) Avail: NTIS HC A02/MF A01

The goal is to analyze the actual configuration of the Network Communication Multiprocessor (MCR) concerning the availability and reliability of the equipment. A proposal for a new configuration, including fault tolerance mechanisms is presented. Author

N87-12721*# National Aeronautics and Space Administration. Marshall Space Flight Center, Huntsville, Ala.
SPACE FLIGHT OPERATIONS COMMUNICATIONS PHRASEOLOGY AND TECHNIQUES
Steven R. Noneman Aug. 1986 16 p
(NASA-TM-86562; NAS 1.15:86562) Avail: NTIS HC A02/MF A01 CSCL 17B

Communications are a critical link in space flight operations. Specific communications phraseology and techniques have been developed to allow rapid and clear transfer of information. Communications will be clear and brief through the use of procedural words and phrases. Communications protocols standardize the required information transferred. The voicing of letters and numbers is discussed. The protocols used in air-to-ground communications are given. A glossary of communications terminology is presented in the appendix. Author

N87-12722# Massachusetts Inst. of Tech., Cambridge. Research Lab. of Electronics.
RECONSTRUCTION OF UNDERSAMPLED PERIODIC SIGNALS
Anthony J. Silva Jan. 1986 116 p
(Contract N00014-81-K-0742; Grant NSF ECS-84-07285)
(AD-A168897; TR-514) Avail: NTIS HC A06/MF A01 CSCL 09/3

Under certain conditions, a periodic signal of unknown fundamental frequency can still be recovered when sampled below the Nyquist rate, or twice the highest frequency present in the waveform. A new sampling criterion has been proposed which enumerates such conditions. It has been shown that in theory, if the signal and sampling frequencies are not integrally related, and the signal is band-limited (to a range the extent of which is known but otherwise unrestricted), then the signal waveshape can always

be recovered. If the fundamental frequency is known to lie within a range not spanning any multiple of half the sampling rate, then the temporal scaling for the reconstructed waveform can be determined uniquely, as well. Procedures have also been proposed for reducing time-scale ambiguity when the latter condition is not met. A previously presented time domain algorithm for reconstructing aliased periodic signals has been implemented and modified. A new algorithm, operating in the frequency domain, has been proposed and implemented. In the new algorithm, the signal fundamental frequency is first estimated from the discrete Fourier transform of the aliased data through an iterative procedure. This estimate is then used to sort the aliased harmonics. GRA

N87-12723# Air Force Systems Command, Wright-Patterson AFB, Ohio. Foreign Technology Div.

METRICS OF CLOSED WORLD OF FRIEDMANN, AGITATED BY ELECTRIC CHARGE (TOWARDS A THEORY ELECTROMAGNETIC FRIEDMANN'S)

M. A. Markov and V. P. Frolov 10 Jun. 1986 34 p Transl. into ENGLISH from Teoreticheskaya i Matematicheskaya Fizika (USSR), v. 3, no. 1, Apr. - Jun. 1970 p 3-17

(AD-A168981; FTD-ID(RS)T-0475-86) Avail: NTIS HC A03/MF A01 CSCL 20/10

The generalization is considered of the well known Tolman problem to the case of electrically charged dust like matter of the central symmetrical system. The first integrals of the correspondent system of the Einstein Maxwell equations are found. The problem is specificated in such a way that with the full charge of the system going to zero, the metrics of the closed Friedman world arises. Such a system is considered at the initial moment, that of maximal enlargement. With any non-vanishing but no matter how small value of the electric charge the metrics is unclosed. The metrics of the almost-Friedmanian part of the world allows the continuation through the narrow manhole (at the small charge) as the Nordstroem Reissner metrics with the parameters m sub 0 sq rt (chi) = e sub o. The expression for the electric potential in the manhole phi sub h = c-squared/sq rt chi does not depend upon the value of the electric charge. The radius of the manhole r sub h = e sub 0 sq. rt (chi)/c-squared increases with the increase of the charge. The state of the manhole as given by the classical description appears as essentially unstable from the quantum physics viewpoint. The production of various pairs in the enormous electric fields of the manhole gives rise to the polarization of the latter up to effective charge Z < 137e irrespective of the initial (no matter how great) charge of the system. GRA

N87-12724# Saint Louis Univ., Mo.

Lg WAVE EXCITATION AND PROPAGATION IN PRESENCE OF ONE-, TWO- AND THREE-DIMENSIONAL HETEROGENEITIES Scientific Report, 1 Apr. - 30 Sep. 1985

R. B. Herrmann 27 Jan. 1986 61 p

(Contract F19628-85-K-0029)

(AD-A169004; AFGL-TR-86-0025; SR-1) Avail: NTIS HC A04/MF A01 CSCL 20/14

In order to understand high frequency wave propagation, precise methods of generation of synthetic seismograms are required. This report examines the trapezoidal integration rule used by Bouchon to evaluate Hankel transforms of the Sommerfeld kernel. Numerical problems arise for integrals of some J sub 0 (kr) functions. A modification of the numerical integration technique, using a shifter mid-point rectangular rule rather than a trapezoidal rule alleviates some of the problem. For calibration of numerical integration techniques, the Haskell solution for point sources in a wholespace are extended. GRA

N87-12725# Syracuse Univ., N. Y. Dept. of Electrical and Computer Engineering.

COMPUTER PROGRAMS FOR ELECTROMAGNETIC SCATTERING FROM A SLOTTED TM CYLINDRICAL CONDUCTOR BY THE PSEUDO-IMAGE METHOD Interim Technical Report

Joseph R. Mautz and Roger F. Harrington Nov. 1985 53 p

(Contract DAAG29-84-K-0078)

(AD-A169016; SYRU/DECE/TR-85/5; TR-4; ARO-21378.5-EL) Avail: NTIS HC A04/MF A01 CSCL 20/3

Two computer programs are described and listed. Suppose that an infinitely thin perfectly conducting cylindrical surface with an infinitely long but narrow gap is illuminated by a TM plane wave. The first program uses two different methods, the methods of solution with and without pseudo-image, to calculate the tangential electric field in the gap. The second program uses the Fourier series method of solution to calculate the tangential electric field in the gap for the special case in which the surface is a nearly complete circular cylindrical shell and the TM plane were propagates perpendicular to the plane of the gap. To enable the user to verify that they are running correctly, both programs are provided with sample input and output data. GRA

N87-12726# Applied Physics, Inc., Albuquerque, N. Mex.

RADAR CROSS-SECTION OF DAMPED CYLINDERS AND DIELECTRIC STRIPS Quarterly Progress Report, Mar. - Jun. 1986

Richard Holland and Kah-Song Cho 13 Mar. 1986 53 p

(Contract N00014-85-C-0852)

(AD-A169027; API-TR-127) Avail: NTIS HC A04/MF A01 CSCL 17/9

This report presents 2D RCS (echo width) calculations for electrically and magnetically conducting circular cylinders with and without an electromagnetically damping coat. Similar calculations for dielectric cylinders and thin dielectric strips are also given. In all cases, results computed by our new TDFD code and transformed to the frequency domain are compared and overlaid with calculations performed directly in the frequency domain. Detailed preliminary documentation of the TDFD RCS code is given. GRA

N87-12727# Massachusetts Inst. of Tech., Cambridge. Research Lab. of Electronics.

BASIC AND APPLIED RESEARCH IN THE FIELD OF ELECTRONICS AND COMMUNICATIONS Final Report, 1 Nov. 1982 - 31 Oct. 1985

Jonathan Allen 19 Mar. 1986 32 p

(Contract DAAG29-83-K-0003)

(AD-A169029; ARO-19838.94-EL) Avail: NTIS HC A03/MF A01 CSCL 17/2

During this period, considerable progress was made on experimental and theoretical designs for optical waveguide switches, multiplexors, and demultiplexors that can operate at a rate of 20 gigahertz, centered around the waveguide Mach-Zehnder interferometer. Extensive investigations into device applications of coupled waveguide structures have led to the ability to inject power into one of n input waveguide ports, and deliver power from any selected port using these techniques. Basic logic gates have been formed, building the interferometer in gallium arsenide, and simple exclusive OR gates have been demonstrated. Quantum noise in phase locked laser oscillators was studied, with the goal of using light that produces noise levels less than shot noise, and hence, is in a squeezed state. Oscillations in this mode have been successfully demonstrated. During this contract, a femtosecond laser facility was built which led to the achievement of optical pulses as short as 16 femtoseconds, with a center wavelength of approximately 625 nanometers, comprised of only eight optical cycles. GRA

N87-12728# Naval Postgraduate School, Monterey, Calif.

MAXIMIZATION OF THE CAPACITY OF THE MOST SURVIVABLE CONNECTIONS IN A NETWORK M.S. Thesis

Richard V. Stockton Mar. 1986 71 p

(AD-A169065) Avail: NTIS HC A04/MF A01 CSCL 17/2

The United States is becoming increasingly dependent on telecommunications to maintain societal structure. Today, the use of communication and computer networks has attained a level which affects all lives. The loss of these networks would have a monumental effect on the everyday lives of virtually every person in the U.S. and even the world. This thesis discusses network survivability which is considered to be a function of the number of independent parallel paths between a source and destination node. A methodology is developed to determine the connectivity of a

network and then the number of independent parallel paths are determined by restricting the connectivity solution set. The capacity of the parallel paths are then maximized given that the links are not characterized by uniform capacities. GRA

N87-12729# Princeton Univ., N. J. Dept. of Mechanical and Aerospace Engineering.
A TEST ON THE RELIABILITY AND PERFORMANCE OF THE VERBEX SERIES 4000 VOICE RECOGNIZER
P. Suntharalingam Sep. 1985 21 p
(Contract DAAG29-84-K-0048)
(AD-A169066; MAE-1748; ARO-20155.6-MA) Avail: NTIS HC A02/MF A01 CSCL 17/2

Voice recognition systems are becoming increasingly widespread as forms of data entry. One such use of speech input would be as an aid to pilot communication in the cockpit. The Verbex Series 4000 Voice Recognizer (VVR) was chosen as the input channel for a forthcoming flight simulation system. The VVR is a speaker dependent unit with the ability to recognize continuous speech. An additional feature of the VVR is its use of structured grammars in defining the speech format. Tests were run to determine the VVR's reliability, and also to investigate the variations in performance for different grammar structures. Author (GRA)

N87-12730# Massachusetts Inst. of Tech., Cambridge. Research Lab. of Electronics.
KNOWLEDGE-BASED PITCH DETECTION
Webster P. Dove Jun. 1986 226 p
(Contract N00014-81-K-0742; Grant NSF ECS-84-07285)
(AD-A169069; TR-518) Avail: NTIS HC A11/MF A01 CSCL 17/2

Many problems in signal processing involve a mixture of numerical and symbolic knowledge. Examples of problems of this sort include the recognition of speech and the analysis of images. This thesis focuses on the problem of employing a mixture of symbolic and numerical knowledge within a single system, through the development of a system directed at a modified pitch detection problem. For this thesis, the conventional pitch detection problem was modified by providing a phonetic transcript and sex/age information as input to the system, in addition to the acoustic waveform. The Pitch Detector's Assistant (PDA) system that was developed is an interactive facility for evaluating ways of approaching this problem. The PDA system allows the user to interrupt processing at any point, change either input data, derived data, or problem knowledge and continue execution. Author (GRA)

N87-12731# Harry Diamond Labs., Adelphi, Md.
TRANSMISSION THROUGH FERRITE SAMPLES AT SUBMILLIMETER FREQUENCIES
Clyde A. Morrison, Barbara J. Bencivenga, and George J. Simonis May 1986 20 p
(AD-A169178; HDL-TR-2079) Avail: NTIS HC A02/MF A01 CSCL 20/14

A theoretical analysis is presented of the transmission spectra of thin magnetized ferrite slabs. The energy range chosen was 1 less than nu-bar less than 120 per cm (30 GHz less than f less than 3600 GHz). The magnetic field was assumed to lie in the plane of the ferrite slab, and the incident electromagnetic radiation was polarized parallel and perpendicular to the magnetic field. For measurements of the magnetic properties near resonance, we show that extremely stable sources are required. However, we show that meaningful measurements can be made far from magnetic resonances using a conventional Fourier transform spectrometer. GRA

N87-12732# Rome Air Development Center, Griffiss AFB, N.Y.
PHASED ARRAYS 1985 SYMPOSIUM: PROCEEDINGS
Hans P. Steyskal Aug. 1985 323 p Presented at the Phased Arrays Symposium, Bedford, Mass., 15-18 Oct. 1985; sponsored by RADC
(AD-A169316; RADC-TR-85-171) Avail: NTIS HC A14/MF A01 CSCL 09/5

The Phased Arrays '85 Symposium, sponsored by the Rome Air Development Center, the MITRE Corporation, and the University of Massachusetts, was held at the MITRE Corporation 15 to 18 October and reviewed the state-of-the-art of phased array antenna systems and of the technology for next generation systems. This report contains the full papers which were presented with clearance for unlimited distribution. GRA

N87-12733# Rome Air Development Center, Griffiss AFB, N.Y.
SURFACE CORRELATION RELATIONSHIPS IN ROUGH SURFACE SCATTERING Report, for Sep. 1984 - Sep. 1985
R. J. Papa, J. F. Lennon, and R. L. Taylor Mar. 1986 36 p
(AD-A169327; RADC-TR-86-21) Avail: NTIS HC A03/MF A01 CSCL 20/14

There are a number of approaches to the calculation of the electromagnetic scattering from rough surfaces. These techniques are important in the determination of the effects of the real environment on radar and communications systems. The models contain descriptions of the surface in terms of the statistical distribution of the heights and their degree of correlation. These features are then related to a normalized radar cross section for the terrain, sigma deg, through an electromagnetic analysis. In this report we are concerned with questions involving the application of physical optics principles to the analysis. This is important since this approach is used extensively both as a complete solution and as part of composite models. Secondly, we discussed several areas where the statistics and correlation have important roles in determining the scattering from a random rough surface. This is significant in that the usual assumption of a Gaussian distribution of heights with Gaussian correlation may not apply to all types surfaces. Power spectra results suggest that other forms would be more appropriate for some cases. In the beginning of this report, we examine statistical descriptors of a surface and establish the relationship between them and the conditions for applying a physical optics model to the scattering from that surface. We then examine the sensitivity of the distribution of scattered power to changes in the form of the surface height statistics and correlation function. GRA

N87-12734# Rome Air Development Center, Griffiss AFB, N.Y.
FOREGROUND EFFECTS ON TROPOSCATTER DIGITAL COMMUNICATION SYSTEMS Report, Nov. 1984 - Aug. 1985
Edward E. Altshuler Dec. 1985 22 p
(AD-A169380; RADC-TR-85-232) Avail: NTIS HC A02/MF A01 CSCL 17/2

Troposcatter antennas are usually pointed very close to the horizon to maximize system gain. As a result, multipath reflections from the foreground may arise. These multipath signals may have time delays that are significantly longer than direct signals, which are scattered within the common volume and thus degrade system performance. In this report, the effects of terrain-reflected multipath signals on troposcatter digital communication systems are examined. The distance that a ray travels from the transmitting antenna to a point within the common volume is calculated. The maximum differential distance that can occur for a pair of rays that intersect the common volume is than determined for a set of troposcatter geometries. The total distance that a terrain-reflected ray traverses in going from the antenna to the common volume is also calculated. It is found that, for typical troposcatter/foreground geometries, the differential distance between a direct ray and a foreground-reflected ray is small compared with the maximum differential distance that exists between direct rays within the common volume. Thus, multipath signals that would have time delays significantly longer than those scattered within the common volume must be scattered from a region outside the common volume. GRA

N87-12735# Department of the Air Force, Washington, D.C.
TRACKING SERVO COMPENSATOR WITH RATE AIDING Patent
Bill E. Burkett, inventor (to Air Force) Issued 20 May 1986 12 p Supersedes AD-D011372
(AD-D012388; US-Patent-4,590,476; US-Patent-Appl-SN-640902;

US-Patent-Class-343-7.4) Avail: US Patent and Trademark Office CSCL 17/9

A tracking servo compensator is disclosed for radar systems which steer their antenna beams using a servo-mechanism that physically moves the antenna. The disclosed tracking servo compensator permits switching between trackers (e.g., from area to point track) and from one tracked target to another without undersirable transients that could cause loss of track. Rate aiding and target range estimates are provided when tracker base motion is known. The compensator works by providing a servo signal that continually monitors the error in a servo signal that continually monitors the error in estimated track point line-of-sight angular velocity independent of which tracker is employed or the target being tracked. When base motion is known, this signal is used to update the target range estimate so that an accurate rate aiding signal is available. The servo provides smooth controlled-speed transitions between track points during mode switching, and provides an input for manual slewing of the tracker platform during offset track conditions. It also provides an estimate of platform to track point range. GRA

N87-12736# Royal Signals and Radar Establishment, Malvern (England).

A BRIEF REVIEW OF ADAPTIVE NULL STEERING TECHNIQUES

J. G. McWhirter Feb. 1986 36 p

(AD-A169548; RSRE-MEMO-3939; DRIC-BR-99244) Avail: NTIS HC A03/MF A01 CSCL 20/4

A brief theoretical review of adaptive null steering is presented. The basic theory is first outlined in the context of sidelobe cancellation systems as well as general antenna arrays. Various approaches to the practical implementation of adaptive null steering are then discussed. These fall into the two main categories of closed loop methods and direct solution methods. The closed loop methods are very cost-effective and suitable in principle, for either analog or digital processing. However, their rate of convergence is fundamentally limited and too slow for some applications. The direct solution methods do not suffer from this problem but tend to be suitable only for digital processing and are more expensive from the computational point of view. However they are well suited to parallel processing and now provide a very practical alternative due to recent advances in VLSI circuit technology. A brief discussion on the effects of multi-path propagation on adaptive null steering systems concludes this review. GRA

N87-12737# Defence Research Establishment Valcartier (Quebec).

METHOD OF RAY INTENSITY CALCULATION AS APPLIED TO ANOMALOUS PROGAGATION

D. Dion Jun. 1986 49 p

(AD-A169553; DREV-4407/86) Avail: NTIS HC A03/MF A01 CSCL 20/14

A ray tracing theory incorporating the ray intensity calculation has recently been developed at DREV. This report studies the applicability of this new ray theory to radar propagation. Using this theory, we tried to characterize the anomalous behavior of the propagation due to the refractivity of the troposphere. This report summarizes the ray theory and the validity of this approach for the study of radar propagation. A computer model has been developed to calculate ray trajectories and intensities. Considering the case of a simple surface duct, the results have shown that the intensity computation is an effective and powerful way of detecting and locating in space such singular propagation phenomena as caustics and radio holes. GRA

N87-12738# Connecticut Univ., Storrs. Dept. of Electrical Engineering and Computer Sciences.

CARRIER-SENSE STACK ALGORITHMS FOR MULTIPLE ACCESS COMMUNICATION CHANNELS

Lazaros Merakos Mar. 1986 68 p

(Contract N00014-85-K-0547)

(AD-A169774; UCT/DEECS/TR-86-3) Avail: NTIS HC A04/MF A01 CSCL 09/2

We consider the random multiple access of a collision-type, packet-switched channel, for the Poisson user model in a local area network environment, where carrier sensing techniques are possible due to small propagation delays. We propose and analyze random access algorithms that are representative of a new class of stable algorithms with limited sensing and free access characteristics. Limited sensing algorithms require that users sense the channel only while they have a packet to transmit, and, therefore, they have practical advantages over algorithms that require continuous channel sensing. The free access characteristics of the proposed algorithms simplify their implementation, since newly arrived packets are transmitted upon arrival, provided that the channel is sensed idle. Utilizing the regenerative character of the stochastic processes that are associated with the random access system, we derive lower bounds on the maximum stable throughput, and tight upper and lower bounds on the induced mean packet delay. The proposed algorithms are easy-to-implement, and they combine inherently stable operation and high performance with modest channel sensing requirements. GRA

N87-12739# Illinois Univ., Urbana. Electromagnetic Communication Lab.

DIELECTRIC ANTENNAS FOR MILLIMETER-WAVE APPLICATIONS

G. M. Wilkins and R. Mittra May 1986 38 p

(Contracts DAAG29-85-K-0183; N00014-84-C-0149)

(AD-A169885; UIEMC-86-5; UILU-ENG-86-2547; ARO-22634.3-EL) Avail: NTIS HC A03/MF A01 CSCL 09/5

A number of designs of dielectric antennas for millimeter-wave applications are presented. Included are details of the basic configuration and performance of these devices, along with discussions of modifications and their use as components in millimeter-wave integrated circuits. Specific areas of discussion include: dielectric rod antennas; periodically modulated surface-wave antennas; complex propagation constant; components for millimeter-wave integrated circuits. GRA

N87-12740# Department of the Air Force, Washington, D.C.

MULTI-ELEMENT ADAPTIVE ANTENNA ARRAY Patent Application

Kenneth R. Finken, inventor (to Air Force) Filed 3 Feb. 1986 19 p

(AD-D012410; US-Patent-Appl-SN-824994) Avail: NTIS HC A02/MF A01 CSCL 17/7

A phased array antenna is disclosed including a central reference element. This is surrounded by a plurality of sub-elements which form the adaptive elements of the array and have no feed networks. Each adaptive element is essentially an L stub, with the adaptive elements oriented such that the L top loading is circumferential around the reference element. The plurality of adaptive elements, all with different orientations of the linear top loading allows the complex weights and adaptive nulling algorithm to generate any required polarization, and form an adaptive nul to any arbitrary polarized interferring signal as required. GRA

N87-12741# California Univ., Los Angeles. Dept. of Computer Science.

ADVANCED TELEPROCESSING SYSTEMS Semiannual Technical Report, 1 Oct. 1984 - 30 Sep. 1985

Leonard Kleinrock 30 Sep. 1985 130 p

(Contracts MDA903-82-C-0064; DARPA Order 2496)

(AD-A170007) Avail: NTIS HC A07/MF A01 CSCL 09/2

Research published during this reporting period covers a broad spectrum of results in the areas of random access communications, computer networks, and distributed processing (a new and rapidly growing area of research and practical importance). In this latter area, the major works involved the behavior of distributed algorithms for election and traversal in networks, and the evaluation of the achievable and achieved parallelism in parallel processing systems. A general model of distributed processing exposed a potential areas of networks and multiaccess, our results focus on improved and innovative models. A major contribution of our

research during this reporting period is a dissertation entitled Distributed Algorithms for Election in Unidirectional and Complete Networks, by Yehuda Afek. This entire dissertation forms the body of this report. GRA

N87-12742# Naval Research Lab., Washington, D. C.
SIMULATION OF CIFF (CENTRALIZED IFF) REMOTE CONTROL DISPLAYS Memorandum Report, Feb. 1985 - Feb. 1986
Darlene L. Tucker and Lawrence M. Leibowitz 27 Jun. 1986 61 p
(AD-A170387; NRL-MR-5806) Avail: NTIS HC A04/MF A01 CSCL 17/2

This report presents the software simulation of the Remote-Control-Display (RCS) proposed to be used in the Centralized IFF (CIFF) system. A description of the simulation programs along with simulated menu formats are presented. A sample listing of the simulation programs and a brief description of the program operation are also included. Author (GRA)

N87-12743# Oregon Graduate Center for Study and Research, Beaverton. Dept. of Applied Physics and Electronic Science.
DIGEST: PROCEEDINGS OF THE INTERNATIONAL CONFERENCE ON OPTICAL AND MILLIMETER WAVE PROPAGATION AND SCATTERING IN THE ATMOSPHERE Final Report, 22 Apr. 1986 - 21 Apr. 1987
Richard A. Elliott May 1986 410 p Conference held in Florence, Italy, 27-30 May 1986
(Grant DAAL03-86-G-0088)
(AD-A170393; ARO-23498.1-EL-CF) Avail: NTIS HC A18/MF A01 CSCL 04/1

The conference was held as scheduled. Topics covered include scintillation theory, two-frequency scintillation, imaging and scintillation, coherence theory, lidar, surface scattering, nonlinear effects, transmission remote sensing, particle scattering and scintillations. Author (GRA)

N87-12744# Columbia Univ., New York. Dept. of Electrical Engineering.
PROBLEMS IN INTEGRATED DIGITAL NETWORKS Final Report, 1 Apr. 1985 - 31 Mar. 1986
Mischa Schwartz, Thomas Stern, and Aurel Lazar 13 Jun. 1986 11 p
(Contract N00014-85-K-0371)
(AD-A170442; Rept-1) Avail: NTIS HC A02/MF A01 CSCL 17/2

This final report covers work carried out under ONR Grant N00014-85-K-0371. The basic problems addressed concerned the integration of diverse traffic types--e.g., voice, data, video, facsimile, etc. into a common digital network. The work fell into three areas: (1) Hybrid Multiplexing; (2) Voice in Integrated Systems; and (3) Decentralized Optimal Flow Control. Author (GRA)

N87-12745 Department of the Navy, Washington, D. C.
TWIN APERTURE PHASED ARRAY LENS ANTENNA Patent
Theodore C. Cheston, inventor (to Navy) Issued 1 Apr. 1986 6 p Supersedes AD-D010381
(AD-D012415; US-Patent-4,580,140; US-Patent-Appl-SN-505570; US-Patent-Class-343-372) Avail: US Patent and Trademark Office CSCL 17/9

A phased array lens antenna which includes a lens having two faces disposed substantially at a right angle to each other. Transmit-receive modules which includes phase-shifter are shared between the two lens faces. Two lens antenna positioned in back-to-back relationship about a ship superstructure scan 260 deg. Author (GRA)

N87-12746# Aerospace Medical Research Labs., Wright-Patterson AFB, Ohio.
THE EFFECTS OF HIGH SUSTAINED ACCELERATION ON THE ACOUSTIC PHONETIC STRUCTURE OF SPEECH: A PRELIMINARY INVESTIGATION
Zinny S. Bond, Thomas J. Moore, and Timothy R. Anderson 21 May 1986 37 p
(AD-A170563; AAMRL-TR-86-011) Avail: NTIS HC A03/MF A01 CSCL 05/7

The acoustic-phonetic structure of speech produced under adverse circumstances such as high levels of noise, vibration, and stress, has received little investigation. The purpose of this study was to provide some preliminary data concerning speech produced under high sustained acceleration. Acoustical measurements were made of a set of words spoken by two subjects at 1 G and +6 Gz. Words produced under acceleration differed from words produced at 1 G in both spectral and durational characteristics. The formant shifts observed were similar for both speakers. The first format increased for the majority of vowels. The second format tended to be lower for the front vowels /i, epsilon/ and higher for the back vowel (u). Acceleration resulted in a raising of the first formant and a lowering of the second formant relative to the same diphthongs produced at 1 G. Author (GRA)

N87-12747# Illinois Univ., Urbana. Coordinated Science Lab.
A NEW METHOD OF SYNTHETIC APERTURE RADAR IMAGE RECONSTRUCTION USING MODIFIED CONVOLUTION BACK-PROJECTION ALGORITHM
Mita D. Desai Aug. 1986 99 p
(Contract N00014-84-C-0149)
(AD-A170652; UILU-ENG-86-2225) Avail: NTIS HC A05/MF A01 CSCL 17/9

Synthetic Aperture Radar (SAR) imager reconstruction falls into the class of inverse (deconvolution) problems. A spotlight mode SAR system obtains projections of the ground areas at various look angles. The image of the ground area is then reconstructioned from this set of projections. The Convolution Back-Projection (CBP) algorithm is widely used in Computer Aided Tomography (CAT). In this work, the CBP algorithm has been modified so that it can be applied to image reconstruction from SAR data. A quantitative evaluation using extensive computer simulation of the CBP algorithm for spotlight mode SAR is presented. Its performance is then compared with the FFT method with respect to parameters such as multiplicative noise ratio (MNR), central processing unit CPU time, and computational complexity. It has been shown that the CBP-SAR algorithm is a high quality reconstruction method that can be implemented in real-time. The parallelism inherent in the algorithm can be exploited for parallel architectures that are suitable for very large scale integration implementation. Samples from each projection can be summed into the proper pixels in the final image, as required by the back-projection operation, so that the final image is produced shortly after the final projection has arrived. Author (GRA)

N87-12748# Harry Diamond Labs., Adelphi, Md.
ELECTRIC AND MAGNETIC FIELD COUPLING THROUGH A BRAIDED-SHIELD CABLE: TRANSFER ADMITTANCE AND TRANSFER IMPEDANCE
Huey A. Roberts, Susan B. MacDonald, and Joseph Capobianco Jul. 1986 24 p
(AD-A171490; HDL-TR-2090) Avail: NTIS HC A02/MF A01 CSCL 20/14

Electric and magnetic coupling parameters are measured for a braided-shield cable. Starting with a general solution for the internal response of an externally excited cable, simple expressions which relate the coupling parameters to the internal and external currents and voltages result when the electrically short line approximation is used. These expressions are applied to experimental configurations in which the external excitation is either predominately magnetic or electric, and the internal loading is configured to exclude either the electrically or magnetically induced internal currents. The experimental results are compared with theoretical calculations appearing in the literature, and the relative importance of the electric and magnetic coupling effects is discussed. Author (GRA)

N87-12749# Texas A&M Univ., College Station. Dept. of Physics.
MEASUREMENT AND CALCULATION OF THE STOKES OR MUELLER MATRIX FOR THE SCATTERING OF ELECTROMAGNETIC RADIATION FROM IRREGULAR PARTICLES Final

Report, 1 Jul. 1983 - 31 May 1986
Edward S. Fry, George W. Kattawar, and Chia-Ren Hu 14 Sep. 1986 9 p
(Contract DAAG29-83-K-0074)
(AD-A171502; ARO-19938.7-GS) Avail: NTIS HC A02/MF A01 CSCL 20/3

This work significantly advances the understanding of electromagnetic interactions with small particles whose dimensions are of the order of a wavelength. A joint theoretical experimental approach is used so that theoretical predictions could be provided with experimental back up and vice versa. Extensive results on electromagnetic interactions with cubes and sphere multiplets have been obtained. Beautiful symmetry theorems for forward and backward scattering have been discovered. A major theoretical bonus has been the formulation of a new and very efficient method for obtaining electromagnetic scattering properties of an arbitrarily shaped particle which is built from smaller particles whose scattering has been determined. GRA

N87-12750# Lawrence Livermore National Lab., Calif.
NEW ELECTROMAGNETIC EFFECTS ASSOCIATED WITH CAVITY-BACKED APERTURES
R. W. Ziolkowski 1986 6 p Presented at the URSI International Symposium on Electromagnetic Theory in Budapest, Budapest, Hungary, 25 Aug. 1986
(Contract W-7405-eng-48)
(DE86-008768; UCRL-93482; CONF-860849-1) Avail: NTIS HC A02/MF A01

A number of canonical problems that describe coupling through apertures into enclosed regions have been solved. The scattering data generated by these cavity-backed aperture (CBA) solutions share a common property: they are dominated by resonance features closely connected to the presence of the cavity. The behavior of these CBA resonance features will be described for variations in frequencies, angles of incidence, look angles, aperture sizes, and interior object characteristics. In particular, it will be demonstrated that standard bistatic cross-sections contain information about the interior of the cavity. DOE

N87-12751# California Univ., Berkeley. Electronics Research Lab.
STABILIZING EFFECTS OF FINITE-AMPLITUDE RF WAVES ON THE INTERCHANGE INSTABILITY
N. F. Otani 28 Feb. 1986 26 p
(Contract DE-AS03-76ET-53064)
(DE86-013042; UCB/ERL-M-86/18) Avail: NTIS HC A03/MF A01

The effects of the presence of a finite-amplitude RF wave on the interchange instability are studied theoretically in a three-dimensional quasineutral Darwin two-fluid system. An exact energy conservation law is developed for the system equations. The perturbed dynamical quantities are expanded to second order in the fluid displacements and it is demonstrated that a Lagrangian exists for the system. The interchange perturbation energy is calculated and terms associated with the perturbed magnetic potential energy are analyzed. For the terms studied, it is found that no stabilization of the incompressible interchange mode occurs unless the RF wave has a parallel-propagating component, and that coupling to perpendicular-propagating sidebands does not influence the stability of perpendicularly-propagating interchange modes. The stabilizing influence of these terms also does not depend directly on the presence of RF field gradients. The analysis suggests a physical mechanism by which RF stabilization can occur - the RF wave stabilizes the interchange mode by forcing the mode to bend magnetic field lines. DOE

N87-12752# Los Alamos National Lab., N. Mex.
CIRCUIT CONSIDERATIONS FOR REPETITIVE RAILGUNS
E. M. Honih 1986 8 p Presented at the 17th Power Modulator Symposium, Seattle, Wash., 23 Jun. 1986
(Contract W-7405-eng-36)
(DE86-012369; LA-UR-86-2043; CONF-860674-9) Avail: NTIS HC A02/MF A01

Railgun electromagnetic launchers have significant military and scientific potential. They provide direct conversion of electrical energy to projectile kinetic energy, and they offer the hope of achieving projectile velocities greatly exceeding the limits of conventional guns. With over 10 km/sec already demonstrated, railguns are attracting attention for tactical and strategic weapons systems and for scientific equation-of-state research. The full utilization of railguns will require significant improvements in every aspect of system design projectile, barrel, and power source - to achieve operation on a large scale. This paper will review fundamental aspects of railguns, with emphasis on circuit considerations and repetitive operation. DOE

N87-12753# International Centre for Theoretical Physics, Trieste (Italy).
PROPAGATION OF ELECTROMAGNETIC WAVES IN SUPERLATTICES
Hang Shi and Chien-hua Tsai Aug. 1985 19 p
(DE86-702660; IC-85/163) Avail: NTIS (US Sales Only) HC A02/MF A01

The propagation characteristics of electromagnetic waves in infinite and semi-infinite superlattice media are discussed with special reference to the dispersions, attenuations and densities of states of various modes of polarization. DOE

N87-13291# Rome Univ. (Italy). Dipt. di Energetica.
BISTABILITY IN NONLINEAR WAVEGIUDES
M. Bertolotti, C. Sibilia, and I. Anselmi *In* AGARD Guided Optical Structures in the Military Environment May 1986 8 p (For primary document see N87-13273 04-74)
Avail: NTIS HC A14/MF A01

N87-13294# Communications Research Centre, Ottawa (Ontario). Optical Communications Program.
OPTOELECTRONIC BROADBAND SWITCHING FOR COMMUNICATIONS AND SIGNAL PROCESSING
R. I. MacDonald and D. K. W. Lam *In* AGARD Guided Optical Structures in the Military Environment May 1986 10 p (For primary document see N87-13273 04-74)
Avail: NTIS HC A14/MF A01

N87-12954# Joint Publications Research Service, Arlington, Va.
EFFECT OF PULSATING AURORAS ON FREQUENCY-TIME CHARACTERISTICS OF RADIO SIGNALS REFLECTED FROM AURORAL IONOSPHERE Abstract Only
A. A. Arykov, I. N. Bardeyev, A. N. Vasilyev, V. G. Korotkov, A. M. Royzen, and S. A. Rumyantsev *In its* USSR Report: Earth ScienceS (JPRS-UES-86-007) 10 Sep. 1986 1 p Transl. into ENGLISH from Geomagnetizm i Aeronomiya (Moscow, USSR), v. 26, no. 2, Mar. - Apr. 1986 p 243-246 (For primary document see N87-12946 04-42)
Avail: NTIS HC A06/MF A01

N87-12955# Joint Publications Research Service, Arlington, Va.
PHASE FLUCTUATIONS OF IONOSPHERE RADIO SIGNALS Abstract Only
V. D. Gusev and M. B. Vinogradova *In its* USSR Report: Earth Sciences (JPRS-UES-86-007) 10 Sep. 1986 2 p Transl. into ENGLISH from Geomagnetizm i Aeronomiya (Moscow, USSR), v. 26, no. 2, Mar. - Apr. 1986 p 247-252 (For primary document see N87-12946 04-42)
Avail: NTIS HC A06/MF A01

N87-12956# Joint Publications Research Service, Arlington, Va.
TRANSVERSE RESONANCES OF EARTH-IONOSPHERE WAVE GUIDE IN AURORAL REGION Abstract Only
V. S. Smirnov and A. A. Ostapenko *In its* USSR Report: Earth Sciences (JPRS-UES-86-007) 10 Sep. 1986 1 p Transl. into ENGLISH from Geomagnetizm i Aeronomiya (Moscow, USSR), v. 26, no. 2, Mar. - Apr. 1986 p 253-257 (For primary document see N87-12946 04-42)
Avail: NTIS HC A06/MF A01

N87-12957# Joint Publications Research Service, Arlington, Va.
REGULAR NOISE BACKGROUND IN VLF-RADIATION AND WORLD THUNDERSTORM CENTERS Abstract Only
G. I. Druzhin, T. V. Toropchinova, and V. I. Shapayev *In its* USSR Report: Earth Sciences (JPRS-UES-86-007) 10 Sep. 1986 1 p Transl. into ENGLISH from Geomagnetizm i Aeronomiya (Moscow, USSR), v. 26, no. 2, Mar. - Apr. 1986 p 258-264 (For primary document see N87-12946 04-42)
Avail: NTIS HC A06/MF A01

N87-12958# Joint Publications Research Service, Arlington, Va.
SPATIAL RADIO WAVE ATTENUATION DURING VERTICAL SOUNDING OF IONOSPHERE Abstract Only
P. F. Denisenko, V. I. Vodolazkin, and G. G. Vertogradov *In its* USSR Report: Earth Sciences (JPRS-UES-86-007) 10 Sep. 1986 1 p Transl. into ENGLISH from Geomagnetizm i Aeronomiya (Moscow, USSR), v. 26, no. 2, Mar. - Apr. 1986 p 322-325 (For primary document see N87-12946 04-42)
Avail: NTIS HC A06/MF A01

N87-13149# AEG-Telefunken, Ulm (West Germany). Abteilung H14E27.
OBSTACLE-WARNING RADAR FOR HELICOPTERS [DAS HINDERNISWARN-RADAR FUER HUBSCHRAUBER - EINE ANTHROPOTECHNISCHE PROBLEMSTELLUNG]
G. M. Och *In* DGLR Proceedings of a Symposium on the Evaluation of Man-Machine Systems: Methods and Problems 1985 p 25-33 In GERMAN (For primary document see N87-13146 04-54)
Avail: NTIS HC A13/MF A01

33 ELECTRONICS AND ELECTRICAL ENGINEERING

Includes test equipment and maintainability; components, e.g., tunnel diodes and transistors; microminiaturization; and integrated circuitry.

For related information see also *60 Computer Operations and Hardware* and *76 Solid-State Physics.*

N87-12754# Instituto de Pesquisas Espaciais, Sao Jose dos Campos (Brazil).
MEASUREMENT OF TIME-DEPENDENT ELECTRIC CURRENT WITH ROGOWSKI COIL [MEDIDA DE CORRENTE ELETRICA VARIAVEL NO TEMPO COM BOBINA DE ROGOWSKI]
R. S. Dallaqua and Edson DelBosco Apr. 1986 23 p In PORTUGUESE; ENGLISH summary
(INPE-3875-RPE/506) Avail: NTIS HC A02/MF A01

An apparatus to measure time-dependent electric current known as the Rogowski coil is described. The characteristic parameters which define it, the active integrator network, the calibration process of the Rogowski/integrator coil set, and the results of the experiment developed at INPE are presented. Author

N87-12755# Instituto de Pesquisas Espaciais, Sao Jose dos Campos (Brazil).
CONSTRUCTIVE AND OPERATIONAL CHARACTERISTICS OF A SYNCHRONOUS INDUCTION MOTOR [MOTOR SINCRONO DE INDUCAO: CARACTERISTICAS CONSTRUTIVAS E OPERACIONAIS]
Mario Cesar Ricci Aug. 1986 38 p In PORTUGUESE; ENGLISH summary
(INPE-3976-RPE/517) Avail: NTIS HC A03/MF A01

The constructive and operational characteristics of a Synchronous Induction Motor are described. A qualitative general torque equation is obtained and start adverse operation is analysed. Motor performance curves are presented when operated as a synchronous or stepping motor. Author

N87-12756*# National Aeronautics and Space Administration. Marshall Space Flight Center, Huntsville, Ala.
DEVELOPMENT OF LOW-TEMPERATURE TRANSISTOR MODULES TO IMPROVE THE MSFC MID-INFRARED ARRAY Final Report
C. M. Telesco, R. Decher, and P. Peters Oct. 1986 11 p
(NASA-TM-86566; NAS 1.15:86566) Avail: NTIS HC A02/MF A01 CSCL 09A

This report describes the low-temperature transistor modules designed for use with the MSFC mid-infrared array. The modules were developed in the Space Science Laboratory at Marshall Space Flight Center with Center Director's Discretionary Funds. The transistors (JFETs), which operate at a temperature of 77 K, are epoxied to a copper surface attached to a Teflon substrate. The module substrate insulates the JFETs from the 1.5K detector work surfaces and provides a convenient mounting structure for additional components such as solder pins. These modules have maintained their structural integrity during repeated temperature cycling, and they have to be convenient during maintenance and servicing of the infrared array. Author

N87-12757# Instituto de Pesquisas Espaciais, Sao Jose dos Campos (Brazil).
STABILIZATION OF VOLTAGE-CONTROLLED OSCILLATORS THROUGH RESONANT CAVITIES [ESTABILIZACAO DE OSCILADORES CONTROLADOS POR TENSAO ATRAVES DE CAVIDADES RESSONANTES]
Paulo Mello Marshall and Carlos E. Santana Jul. 1986 14 p In PORTUGUESE; ENGLISH summary
(INPE-3941-RPE/512) Avail: NTIS HC A02/MF A01

Described is a design procedure for cavity stabilization of voltage-controlled oscillators. The procedure is applied to the design of a voltage controlled oscillator, mechanically tuned in the 0.95 GHz to 1.35 GHz frequency band. Author

N87-12758# Pennsylvania State Univ., University Park. Materials Research Lab.
NEW ULTRA LOW PERMITTIVITY COMPOSITES FOR USE IN CERAMIC PACKAGING OF Ga:As INTEGRATED CIRCUITS Annual Report, 1 Aug. 1984 - 31 Jul. 1985
L. E. Cross 18 Sep. 1985 70 p
(Contract N00014-84-K-0721)
(AD-A168877) Avail: NTIS HC A04/MF A01 CSCL 09/5

This report documents work performed to develop materials systems for use in the ceramic packaging of Ga:As integrated circuits. Topics under study at Penn State are: dielectrics produced from Macro-Defect-Free (MDF) cements. Both aluminate and silicate based cements have been studied. The objectives of the first year's work have been to show that suitable test tablets can be produced which exhibit dielectric losses less than 1% into the frequency range of 2.5 GHz. Current work is focused upon lowering the permittivity level using silica microballoons dispersed in the matrix. Sol-gel preparation of both thick (25 microns) and thin (0.5 microns) SiO2 and silica:alumina films has shown that in the diphasis system, it is possible to produce crack-free monoliths with permittivities in the range 1.6 to 2.0 and loss tangents below .003. In the thin films, capping of columnar sputtered etched films has been demonstrated. For etched Schott and Vycor glass structures, permittivities in the range 2.5 to 3.0 have been measured with excellent low loss properties. Sputtered silicon films have been sucessfully etched to yield highly planar columnar structures up to 25 microns meters thick. Experiments are in progress to convert the silicon to SiO2 by an oxidation step and capping of the columnar structure using sol-gel coatings has been achieved. In a parallel program at Interamics, new families of borosilicate glass bonded alumina ceramics are being developed. GRA

N87-12759# Stanford Univ., Calif. Information Systems Lab.
SIGNAL ESTIMATION, SCATTERING THEORY AND INTERPOLATION PROBLEMS IN ONE AND TWO DIMENSIONS Final Report, 1 Jan. 1983 - 31 Dec. 1985
Thomas Kailath 28 Feb. 1986 32 p
(Contract DAAG29-83-K-0028)
(AD-A168969; ARO-19876.47-MA) Avail: NTIS HC A03/MF A01 CSCL 09/5

This document reviews research in these fields: (1) Inverse Scattering Theory; (2) VLSI and Parallel Architectures in Signal Processing; (3) Adaptive Identification and Signal Processing; and (4) Stochastic System Modeling and Realization. GRA

N87-12760# Michigan Univ., Ann Arbor. Solid-State Electronics Lab.

MILLIMETER-WAVE HETEROJUNCTION TWO-TERMINAL DEVICES Final Report, 22 Jul. 1982 - 31 May 1986

N. S. Dogan, J. R. East, M. E. Elta, and G. I. Haddad May 1986 203 p

(Contract N00014-82-K-2040)

(AD-A168985; Rept-020046-F) Avail: NTIS HC A10/MF A01 CSCL 09/1

The objective of this study is to investigate the performance of heterojunction MITATT (mixed tunnel-avalanche transit time) diodes at millimeter-wave frequencies. Along with the heterojunction MITATT diodes, GaAs double-drift IMPATT (impact ionization avalanche transit-time) diodes were also fabricated and their RF performance were evaluated. GRA

N87-12761# North Carolina Univ., Chapel Hill. Dept. of Computer Science.

A VLSI-BASED HIGH-PERFORMANCE RASTER IMAGE SYSTEM Final Report, 19 Sep. 1983 - 18 Mar. 1986

Henry Fuchs and John Poulton 8 May 1986 56 p

(Contract DAAG29-83-K-0148; Grant NSF ECS-83-00970)

(AD-A169068; ARO-21107.3-EL-A) Avail: NTIS HC A04/MF A01 CSCL 09/5

Our research objective is to create affordable, high-performance, 3-D raster display systems that harness the highly parallel computational power of custom VLSI circuits. We want to make this power available in an open system that encourages invention of new parallel algorithms for image generation and image processing. The system has many potential applications including flight and tactical displays, computer-aided mechanical design, and medical diagnosis and therapy. As in other systems, ours includes an array of memory chips forming an image buffer from which the video screen is refreshed. The novel feature of our design is that our memory chips have been custom-designed to include processing circuitry so that each pixel (dot on display) can carry out its own image-generation calculations. Calculations are distributed throughout each chip in such a way that only a very small amount of circuitry is required for each pixel. In our current chips, this processing circuitry takes up about one-third of the total area, with the remainder devoted to pixel memory. During the three years of this work, we have achieved significant experimental results. We have developed algorithms for fast image generation, including very rapid rendering of spheres and shadow-casting (our system is the only graphics machine, to our knowledge, that can render true shadows in real time). GRA

N87-12762# Texas Technological Univ., Lubbock. Pulsed Power Lab.

COORDINATED RESEARCH PROGRAM IN PULSED POWER PHYSICS Annual Report, 10 Jan. 1984 - 31 Oct. 1985

M. Kristiansen, G. Schaefer, K. Schoenbach, and H. Krompholz 20 Dec. 1985 209 p

(Grant AF-AFOSR-0032-84)

(AD-A169113; AFOSR-86-0305TR) Avail: NTIS HC A10/MF A01 CSCL 10/2

The program's, related to pulsed power research, main emphasis is on gaining a better understanding of repetitive opening and closing switch phenomena. The main effort is on diffuse discharge opening switch phenomena. The main effort is on diffuse discharge opening switches but considerable progress has also been made on understanding and describing fundamental, transient discharge phenomena. Some effort has also been given to studies of electrode erosion and insulator damage in high power closing switches. In addition several smaller studies have considered various novel ideas and concepts to determine their potential for further investigations. GRA

N87-12763# Department of the Air Force, Washington, D.C.

THE DEPARTMENT OF DEFENSE VERY HIGH SPEED INTEGRATED CIRCUIT (VHSIC) TECHNOLOGY AVAILABILITY PROGRAM PLAN FOR THE COMMITTEES ON ARMED SERVICES, UNITED STATES CONGRESS

30 Jun. 1986 81 p

(AD-A169250) Avail: NTIS HC A05/MF A01 CSCL 09/5

The House and Senate Conferees on Armed Services requested that the Secretary of Defense develop a plan to be submitted to the Committees on Armed Services of the Senate and the House of Representatives for a program to ensure that Very High Speed Integrated Circuit (VHSIC) technology is made available to weapon system developers as VHSIC components become available and mature. This report will show in summary form how all of the activities of the VHSIC program are directly aimed at making the most advanced integrated circuit technology available to weapon system developers. Author (GRA)

N87-12764# Houston Univ., Tex. Dept. of Electrical Engineering.

DEVELOPMENT OF A NUMERICAL PROCEDURE TO TREAT WIRES ATTACHED TO ARBITRARILY SHAPED CONDUCTING BODIES Final Report, 1 Sep. 1983 - 28 Feb. 1986

Donald R. Wilton and Stuart A. Long 15 Apr. 1986 84 p

(Contract DAAG29-83-K-0127)

(AD-A169384; ARO-21098.1-EL) Avail: NTIS HC A05/MF A01 CSCL 09/5

A numerical analysis procedure was developed which modeled wire radiating structures, conducting surfaces, and the junctions between them. In addition, an experimental investigation was undertaken to determine the admittance of a monopole antenna attached to a conducting box-a configuration which models several actual radiating systems. Experimental measurements and numerically predicted data were compared with good correlation noted. GRA

N87-12765# Johns Hopkins Univ., Silver Spring, Md. Applied Physics Lab.

THE 1984 IR AND D (INDEPENDENT RESEARCH AND DEVELOPMENT) ADVANCED PACKAGING STUDY

G. V. Clatterbaugh and H. C. Charles, Jr. Jun. 1986 41 p

(Contract N00024-85-C-5301)

(AD-A169388; JHU/APL/TG-1353) Avail: NTIS HC A03/MF A01 CSCL 09/1

An advanced multiyear electronic packaging project has been started. The project is a comprehensive interactive one involving theory, modeling, structure fabrication, and reliability testing. Highlights of the first year's activities are presented in this report. Important results include: the creation of integrated thermal and thermomechanical models, the prediction of lifetimes under environmental and operational stress conditions, model verification and validation by carefully controlled experimentation, development of assembly techniques, and the invention of a new method for preparing controlled solder joint height and geometry. GRA

N87-12766# Energy Research Corp., Danbury, Conn.

AIRCRAFT BATTERY STATE OF CHARGE AND CHARGE CONTROL SYSTEM Interim Report, 1 Jul. 1984 - 30 Jun. 1985

Sivaswamy Viswanathan and Allen Charkey Feb. 1986 60 p

(Contract F33615-83-C-2435)

(AD-A169411; AFWAL-TR-85-2104) Avail: NTIS HC A04/MF A01 CSCL 10/2

This Interim Report describes work done in developing an aircraft battery state of charge and charge control system. The basis for this system developed by ERC is a nickel-oxygen (NiO2) Pilot cell (0.374 Ah). This pilot cell is cycled in tandem with a nickel-cadmium battery. The oxygen pressure of the pilot cell is utilized to determine and control the state of charge of the nickel-cadmium battery. The NiO2 pilot cell baseline performance was determined during this period. The effect of using different nickel electrodes (ERC, SAFT, MARATHON) was also performed. GRA

N87-12767# Department of the Army, Washington, D. C.
TEMPERATURE AND FREQUENCY COMPENSATED ARRAY BEAM STEERING UNIT Patent Application
Kenneth D. Claborn and William C. Bailey, inventors (to Army) Filed 30 Apr. 1986 18 p
(AD-D012365; US-Patent-Appl-SN-859283) Avail: NTIS HC A02/MF A01 CSCL 09/5

Beam pointing errors and sidelobes resulting from temperature variations on the aperture and power divider of a series phased array antenna operating at a plurality of selected operating channel frequencies and having uniformly spaced elements are compensated for by placing a temperature sensor on both the aperture and power divider and converting the respective temperature outputs to digital signals which are fed to a digital beam steering unit. A pair of programmed memories are included in the beam steering unit which respond to an address or pointer corresponding to the digitized temperature values and the selected operating frequency to read out stored digitized beam steering phase gradients and feed phase correction which are combined and sequentially applied at regular intervals to symmetrically located phase shifter pairs. A uniformly compensated beam is thereafter radiated at a predetermined phase angle. GRA

N87-12768# Department of the Air Force, Washington, D.C.
CRYOGENIC WOUND ROTOR FOR LIGHTWEIGHT, HIGH VOLTAGE GENERATORS Patent Application
Charles E. Oberly, inventor (to Air Force) Filed 23 Apr. 1986 28 p
(AD-D012370; US-Patent-Appl-SN-855047) Avail: NTIS HC A03/MF A01 CSCL 10/2

Liquid hydrogen is used to completely cool all elements of the generator including bearings, stator conductor, rotor conductor, magnetic flux shield, and excitation mechanisms. By essentially immersing the generator in liquid hydrogen, cryogenic interface problems are minimized. The conductor windings will utilize pure metals such as aluminum to minimize the weight and the ohmic heat loss in the machine. Complication of liquid helium cooling for superconducting windings and quench phenomena due to thermal instabilities in the superconductors are eliminated. The use of extremely low resistance of liquid hydrogen cooled aluminum permits heat removal in the confined space of the rotor field winding at magnetic field and current density that can exceed that of superconductors. Because iron is not required in the generator, very high voltages can be generated. GRA

N87-12769# Department of the Air Force, Washington, D.C.
Ni-Co ALLOY PLAQUE FOR CATHODE OF Ni-Cd BATTERY Patent Application
John J. Lander, inventor (to Air Force) Filed 27 Mar. 1986 14 p
(AD-D012375; US-Patent-Appl-SN-844637) Avail: NTIS HC A02/MF A01 CSCL 11/6

The present invention relates generally to Ni-Cd batteries, and, in particular, relates to the plaque material attached to the cathode. Because of the wide use of nickel-cadmium batteries, the corrosion rates of nickel and nickel-cobalt alloys are of interest to nickel-cadmium battery electrochemical theory and its technology. The plaque material of the cathode consists of a Ni-Co alloy in solid solution wherein the cobalt is by weight percent one to ten percent of the alloy. Conventional methods of applying the plaque material to the nickel core may be used. It is therefore an object of the present invention to provide an improved cathode for a nickel-cadmium battery wherein the nickel corrosion is substantially lessened in the plaque material. One process of making the plaque uses a nickel powder slurry that is applied to a nickel-plated steel core. This is then sintered at a high temperature which results in a very porous structure and an welding of the nickel grains to the core. This plaque is then soaked in appropriate salts to make either a positive or a negative plate; nickel salts make a positive plate and a cadmium salts a negative plate, for example. After impregnation, the plaque is placed in an electrolyte and an electric current is passed therethrough to convert the salts to their final form. In the nickel-cadmium cell, nickel hydroxide is the active material in the positive plate. GRA

N87-12770# Department of the Air Force, Washington, D.C.
UNIQUE MECHANIZATION TO FAULT ISOLATE FAILURES OF AN ELECTRON TUBE RADIO FREQUENCY (RF) AMPLIFIER AND ITS HIGH VOLTAGE POWER SUPPLY Patent Application
Daniel G. Miller, inventor (to Air Force) Filed 4 Mar. 1986 11 p
(AD-D012376; US-Patent-Appl-SN-835923) Avail: NTIS HC A02/MF A01 CSCL 09/5

An electronics circuit for improving the fault isolation of failures between an electron tube radio frequency (RF) amplifier and its high voltage power supply is disclosed. High voltage power supplies control their output voltage by comparing a feedback voltage against a reference. This comparison is used to develop an error voltage which, in turn, drives a pulsewidth modulator that corrects the feedback voltage to the reference. The output of a digital-to-analog converter (DAC) is used as the reference voltage. The DAC is driven by a counter which would count to the correct reference voltage represented by a specific count. The final count is determined by a comparator which compares the counter output to the desired final counter and stops the counter when it is reached. GRA

N87-12771# Air Force Weapons Lab., Kirtland AFB, N. Mex.
PRELIMINARY MATERIAL TESTING OF CERAMIC AND WOOD Final Report, 1 Feb. - 1 May 1985
Raymond W. Nethers and David W. Metzger May 1986 10 p
(AD-A169557; AFWL-TN-85-47) Avail: NTIS HC A02/MF A01 CSCL 13/3

Results of preliminary tests of various construction materials subjected to high voltage electrical discharge are reported along with test conduct. Two high voltage construction materials, a wood post and a ceramic insulator, were tested. As a corollary a typical wood fastening system, similar to a TRESTLE joint, was tested. Flashing over of the ceramic insulator caused no damage, while flashing over of the wood at high overvoltages causes considerable damage. Fastening systems in sparse pattern does not appear to change the standoff voltage of the wooden beam used as an insulator. GRA

N87-12772# Massachusetts Inst. of Tech., Cambridge. Dept. of Electrical Engineering and Computer Sciences.
COMPACTION WITH AUTOMATIC JOG INTRODUCTION M.S. Thesis
F. M. Maley May 1986 37 p
(Contract N00014-80-C-0622)
(AD-A169679; VLSI-MEMO-86-316) Avail: NTIS HC A03/MF A01 CSCL 09/5

This thesis presents an algorithm for one-dimensional compaction of VLSI layouts. It differs from older methods in treating wires not as objects to be moved, but as constraints on the positions of other circuit components. These constraints are determined for each wiring layer using the theory of planar routing. Assuming that the wiring layers can be treated independently, the algorithm minimizes the width of a layout, automatically inserting as many jogs in wires as necessary. It runs in time 0(n4) on input of size n. Several heuristics are suggested for improving the algorithm's practical performance. The compaction algorithm takes as input a data structure called a sketch, which explicitly distinguishes between flexible components (wires) and rigid components (modules). The algorithm first finds constraints on the positions of modules that ensure enough space is left for wires. Next, it solves the system of constraints by a standard graph-theoretic technique, obtaining a placement for the modules. It then relies on a single-layer router to restore the wires to each circuit layer. An efficient single-layer router is already known; it is able to minimize the length of every wire, though not the number of jogs. As given, the compaction algorithm applies only to a VLSI model that requires wires to run a rectilinear grid. This restriction is needed only because the theory of planar routing (and single-layer routers) has not yet been extended to other models. GRA

N87-12773# Illinois Univ., Urbana. Computer Systems Group.
TOTALLY SELF-CHECKING CIRCUITS AND TESTABLE CMOS

CIRCUITS Ph.D. Thesis
Niraj K. Jha Jun. 1986 123 p
(Contract N00039-80-C-0556)
(AD-A169756; CSG-51; UILU-ENG-86-2217) Avail: NTIS HC A06/MF A01 CSCL 09/5

A Totally Self-Checking (TSC) circuit belongs to a class of circuits used for Concurrent Error Detection (CED) purposes. It consists of a functional circuit that has encoded inputs and outputs and a checker that monitors these outputs and gives and error indication. It is known that the traditional stuck-at fault model is not sufficient to model realistic physical failures. Techniques for implementing existing gate-level TSC circuits in CMOS, Domino-CMOS and standard CMOS technologies, so that they are TSC with respect to physical failures, are described. Design methods which reduce the transistor count, delay, and the number of tests of TSC checkers are also given. Another problem in the area of TSC circuits concerns embedded checkers whose inputs are not directly controllable. If they do not get all the required codewords to test them they cannot be guaranteed to be TSC. A new encoding technique and a design procedure to solve this problem are presented. It has been shown previously that the two-pattern tests used to test CMOS circuits can be invalidated by timing skews. A necessary and sufficient condition is derived to find out whether or not an AND-OR or and OR-AND CMOS realization exists for a given function so that a valid test set can always be found, even in the presence of arbitrary timing skews. A new Hybrid CMOS realization is introduced to take care of the cases in which this is not possible. GRA

N87-12774# Department of the Air Force, Washington, D.C.
HIGH FREQUENCY, HIGH VOLTAGE MOSFET ISOLATION AMPLIFIER Patent Application
Jones, inventor (to Air Force) et al Filed 3 Jun. 1986 24 p
(AD-D012403; US-Patent-Appl-SN-870045) Avail: NTIS HC A02/MF A01 CSCL 09/5

The present invention utilizes a high voltage isolation amplifier as the drive means for the inductor of a programmable microwave attenuator. A pair of power MOSFET devices are used to control the current flow through a magnetic yoke. The power MOSPET devices cooperate with floating operational amplifier drive circuits to act as a transconductance amplifiers and pass a load current according to command. The MOSFET isolation amplifier apparatus allows stable high frequency linear operation of MOSFET power stages and provides precise regulation of a load current through a magnetic yoke load. Variations of transfer characteristics and input parameters in the MOSFET power stages are corrected by use of a feedback signal which is generated in a current sense resistor by the load current. Such a power stage allows the implementation of isolation amplifiers which can provide high power high frequency linear regulation at elevated voltages and currents. GRA

N87-12775# Department of the Air Force, Washington, D.C.
IN-LINE DETERMINATION OF PRESENCE OF LIQUID PHASE MOISTURE IN SEALED IC PACKAGES Patent Application
N. K. Annamalai, inventor (to Air Force) Filed 19 May 1986 14 p
(AD-D012408; US-Patent-Appl-SN-864222) Avail: NTIS HC A02/MF A01 CSCL 09/3

The present invention includes an aparatus and a process for detecting moisture in sealed Integrated Circuit (IC) packages from the effect of such moisture upon the electrical characteristics of the devices. When the conductance of an IC is measured as a function of temperature across two selected pins in the absence of moisture, a decrease in conductance is seen as the temperature decreases. When moisture is present in the form of water, conductance will exhibit a sharp increase. Moisture present in the package condenses on the chip when it is called. Hence, a change in the conductance slope from positive to negative with respect to temperature, as the chip is cooled, indicates the presence of moisture in the liquid phase. Similarly, the conductance will decrease sharply when the water freezes. The presence of moisture is revealed by taking comparative measurements of conductance while cooling and heating the integrated circuit. The four sharp transitions are the following: (1) water condensing on the chip; (2) the super called water freezing into ice; (3) ice melting into water; and (4) water evaporating into the cavity. The change in conductance is quite large compared to the change in capacitance when moisture is present in the package. GRA

N87-12776# Department of the Air Force, Washington, D.C.
INTERRUPT CONTROL SWITCH INTERFACE SYSTEM Patent Application
Buddy L. Holmes, inventor (to Air Force) Filed 10 Apr. 1986 60 p
(AD-D012414; US-Patent-Appl-SN-849991) Avail: NTIS HC A04/MF A01 CSCL 09/2

Switch contacts may be monitored without pulling them. The apparatus comprises an input port module and up to eight switch reader modules, with 128 switch contacts to each. The input port module has four Z80 PIOs providing a total of eight ports for the switch reader modules, and a S-100 bus to a processor. In each switch reader module, a clock provides a four-phase cycle. An address counter cycles to address the 128 switch contacts. In a RUN mode, the operation is to address a switch contact via a multiplex unit on phase one, load the data into a latch on phase two, the output of the latch being the input of a 128-bit shift register, compare the current and previous states represented by the inputs and outputs of the shift register on phase three, advance the shift register on phase four, and advance the address counter on phase one for reading the next switch contact. During phase three, if the switch contact being addressed has changed state, the comparator generates a strobe pulse which is supplied to the port for the switch reader to initiate an interrupt to the processor. At the same time that a strobe pulse is generated, a scan inhibit command is supplied from the comparator to stop the clock. Data from the address counter and the latch output are supplied via the input port module to the processor. The processor then returns a ready signal to resume the scan. There is also a LOAD mode using 512 (4 X 128) read operations to cycle the clock and load the 128 bits of the shift register. GRA

N87-12777# Washington Univ., Seattle. Dept. of Computer Science.
DECLARATIVE DESCRIPTIONS FOR VLSI GENERATORS Interim Report
Meei-Chiueh Y. Liem Jun. 1986 115 p
(Contracts MDA903-85-K-0072; ARPA Order 4563)
(AD-A169952; TR-86-08-06-03) Avail: NTIS HC A06/MF A01 CSCL 09/5

This thesis presents a declarative generator model which can be used to guide the generation of a circuit in VLSI design. The descriptions in the model provide four equivalent representations of a circuit. They are the layout description, the mixed mode description, the schematic description, and the functional description. Each serves a unique purpose in the VLSI design process. They are correlated through corresponding components. These descriptions are declarative, abstract, robust, and structured in a hierarchical manner. The syntax and semantics of the declarative descriptions are introduced. Their applications are illustrated by examples. The declarative descriptions are shown to greatly facilitate the VLSI design process and serve as a comprehensive tool that documents the designer's ideas as well as the complexities of a circuit. Author (GRA)

N87-12778# Utah Univ., Salt Lake City. Dept. of Electrical Engineering.
EXPERIMENTAL VERIFICATION OF SOLITON THEORY USING A MICROWAVE CROSSED-FIELD AMPLIFIER Final Report, Sep. 1982 - Sep. 1985
Stephen W. Shpock Apr. 1986 71 p
(Contract F30602-82-C-0161)
(AD-A170011; RADC-TR-85-271) Avail: NTIS HC A04/MF A01 CSCL 20/3

The soliton approach of describing the operation of a microwave crossed-field amplifier (CFA) is experimentally investigated

using the Varian SFD-262 S-band CFA as the test vehicle. Theoretical predictions of voltage characteristics with corresponding observed data show close agreement over a wide range of magnetic field values. A detailed description of the experimental process is given as well as a working introduction to soliton theory. Author (GRA)

N87-12779# Aerospace Corp., El Segundo, Calif.
PICOSECOND OPTOELECTRONIC DIAGNOSTICS OF FIELD EFFECT TRANSISTORS
Donald E. Cooper and Steven C. Moss 15 Jun. 1986 15 p
(Contract F04701-85-C-0086)
(AD-A170503; TR-0086(6945-06)-3; SD-TR-86-42) Avail: NTIS HC A02/MF A01 CSCL 09/1

The frequency-dependent scattering parameters of an unpackaged GaAs field effect transistor have been measured using picosecond optoelectronic diagnostic techniques. The large bandwidth available and simple de-embedding procedures make these techniques very promising for characterization of devices operating in the millimeter-wave region. Author (GRA)

N87-12780 Department of the Navy, Washington, D. C.
ZINC/AIR CELL CATHODE Patent
John J. McEvoy, inventor (to Navy) Issued 29 Apr. 1986 5 p
(AD-D012425; US-Patent-4,585,710; US-Patent-Appl-SN-726443; US-Patent-Class-429-27) Avail: US Patent and Trademark Office CSCL 10/3

This invention relates to a cathode for an air depolarized cell in which the hydrophobic catalytic cathode contains or in integrally drophobi catalytic cathode contains or is integrally coated with, on the surface adjacent the cell separator, an absorbent material such as the gelling material used in the anode. The absorbent material, integrated with the cathode surface, adheres the separator to the cathode thereby preventing delamination and provides an electrolyte reservoir for the hydrophobic cathode. GRA

N87-12781# Purdue Univ., West Lafayette, Ind. School of Electrical Engineering.
INVESTIGATION OF A NEW CONCEPT IN SEMICONDUCTOR MICROWAVE OSCILLATORS Annual Report, 1 May 1985 - 30 Apr. 1986
James A. Cooper, Jr. 20 May 1986 32 p
(Grant AF-AFOSR-0193-85)
(AD-A170772; AFOSR-86-0527TR) Avail: NTIS HC A03/MF A01 CSCL 09/5

The goal of this research is to fabricate and characterize a new type of semiconductor device known as a contiguous-domain transferred oscillator. This device differs from existing semiconductor oscillators in several fundamental ways, and should be capable of direct electronic tuning in the range from a few gigahertz to a few hundred gigahertz. During the first year of this project, test chips were designed, masks were made, and a processing schedule was worked out. Three aspects of the processing required special attention: implant activation, resistive gate formation, and silicon nitride deposition. Uncapped flash annealing was used for implant activation, and satisfactory results were achieved. GRA

N87-12782# Purdue Univ., West Lafayette, Ind. School of Electrical Engineering.
INVESTIGATION OF A NEW CONCEPT IN SEMICONDUCTOR MICROWAVE OSCILLATORS Interim Report
James A. Cooper, Jr. 13 Nov. 1985 4 p
(Grant AF-AFOSR-0193-85)
(AD-A170831; AFOSR-86-0597TR) Avail: NTIS HC A02/MF A01 CSCL 09/5

Our project centers on the fabrication and characterization of a new type of millimeter-wave semiconductor oscillator, the so-called Contiguous-Domain Transferred-Electron Oscillator. To date, the only operational information we have about this device has been derived from computer simulation, and therefore our objective is to obtain experimental verification. The device is interesting (and potentially important) because it operates in a fundamentally different way from any existing semiconductor oscillator device, with the result that it should be capable of very high frequency oscillation (over 100 GHz) without the requirement for sub-micron drift dimensions. In addition, the oscillations are not based on a transit-time effect, and thus the frequency can be changed during operation by simply changing the rate at which carriers are admitted into the drift channel. The structure is similar to a conventional GaAs MESFET or MODFET, except that the gate is made resistive and has two contacts, one near the source and the other near the drain. We will not describe the operation of the device in detail here, but refer the reader to the original proposal and to the enclosed article. GRA

N87-12783# Columbia Univ., New York. Dept. of Electrical Engineering.
DIRECT WRITING OF MICROSTRUCTURES FOR SOLID-STATE ELECTRONICS Final Report, 1 Feb. 1984 - 31 Jan. 1986
Richard M. Osgood, Jr. 19 Apr. 1986 54 p
(Contracts F49620-84-C-0022; ARPA Order 4487; AF Proj. 2301)
(AD-A170837; AFOSR-86-0555TR) Avail: NTIS HC A04/MF A01 CSCL 09/5

This report summarizes two years of research on new laser processing techniques on opto- and microelectronics. The main results are in: (1) the demonstration of UV laser direct writing of low resistivity metal lines, and the subsequent demonstration of the usefulness of laser writing (via deposition) in the reconfiguring of an LSI circuitry; and (2) the discovery, characterization, and understanding of the techniques of light-guided etching for the fabrication of ultra-high-aspect-ratio microelectronics structures. In the case of light-guided etching, an application of the technique to optical interconnects has already been demonstrated. Author (GRA)

N87-12784# Naval Research Lab., Washington, D. C.
INPUT IMPEDANCE OF AN INFINITE LINEAR SCANNED ARRAY OF FLAT RECTANGULAR STRIPS INSIDE A DIELECTRIC LOADED PARALLEL PLATE WAVEGUIDE
S. N. Samaddar 29 Jul. 1986 58 p
(AD-A171275; NRL-MR-5830) Avail: NTIS HC A04/MF A01 CSCL 09/5

Impedance variation as a function of H-plane scan angles of an infinite linear array of flat rectangular monopoles (strips) inside a dielectric loaded parallel plate waveguide is studied both theoretically and experimentally in the S-band frequencies. In theoretical analysis simplified along the probes (monopole strips) and neglect of the effect of the gap at the junction of a probe and its coaxial feed line, were made. It is found that this simplified theory can predict qualitatively the experimental data of interest, such as input impedance. Both theory and experiments show that a dielectric slab with a relatively low dielectric constant (1.3) inserted in an appropriate manner can improve the bandwidth and impedance performance of the array. Certain experimental results show a bandwidth of about 28% with respect to the center frequency 3.5 GHz, having a VSWR <2. Another interesting result is the relation between the width W of a flat rectangular probe and the radius rho of a circular probe situated similarly inside two identical rectangular waveguides. The probe impedances or VSWR's for these situations are found to be the same, respectively, for all practical purposes when W approx. 4.882 rho, which was obtained numerically representing a correction to the electrostatic result W = 4 rho found by Wheeler. Author (GRA)

N87-12785# Naval Postgraduate School, Monterey, Calif.
TWO-DIMENSIONAL BEAMFORMING USING A FREQUENCY DOMAIN COMPLEX LEAST MEAN-SQUARES (LMS) ADAPTIVE FILTER M.S. Thesis
Francis Chan Jun. 1986 138 p
(AD-A171396) Avail: NTIS HC A07/MF A01 CSCL 09/5

The complex LMS adaptive algorithm developed by Widrow is used in the frequency domain to estimate the azimuth and elevation angles of a plane wave incident upon a planar array. The complex LMS algorithm is applied to two cases. The first case is a passive detection problem. The second case is a pulse communication problem. In both cases, complex weights are determined using

the complex LMS algorithm which cophase all of the output electrical signals from the planar array. Three versions of the complex LMS algorithm are studied and their performances are compared. Author (GRA)

N87-12786# Naval Postgraduate School, Monterey, Calif.
THE ANALYSIS OF A TRANSISTOR CAP AS A HEAT DISSIPATOR M.S. Thesis
Kathleen C. Bryant Jun. 1986 71 p
(AD-A171398) Avail: NTIS HC A04/MF A01 CSCL 09/1

This thesis develops and utilizes electro-thermal analogies to analyze the amount of heat dissipated in a typical transistor cap. A series of parametric curves are developed to illustrate the results obtained. These curves may be used by circuit designers in order to obtain a more precise estimate of the heat sink system requirements. Author (GRA)

N87-12787# Lawrence Livermore National Lab., Calif.
FABRICATION OF GATE ARRAY INTERCONNECT STRUCTURES USING DIRECT-WRITE DEPOSITION PROCESSES
F. Mitlitsky, J. C. Whitehead, A. F. Bernhardt, and B. M. McWilliams 1986 13 p Presented at the Les Houche Winter School, France, 25 Mar. 1986
(Contract W-7405-eng-48)
(DE86-010785; UCRL-94494; CONF-8603122-1) Avail: NTIS HC A02/MF A01

General principles of laser direct-write deposition processes are reviewed. Device interconnection of CMOS gate arrays by means of computer-controlled, laser-induced thermochemical surface reactions is described. Maskless, automated five-minute interconnection of 1000 gate CMOS array dies is described using discretionary laser-induced chemical vapor deposition. Eight 125-stage ring oscillators written on a single CMOS gate array die were shown to have the device-limited performance of similar patterns manufactured by a photolithographically patterned aluminum-silicon alloy. These results suggest the feasibility of using this method, Laser Pantography (LP), for rapid implementation of prototype and limited volume semi-custom VLSI circuits immediately after their design is completed. DOE

N87-12788# Science Applications International Corp., San Diego, Calif.
SODIUM-SULFUR BATTERY SYSTEMS DEVELOPMENT
K. J. Beninga and B. L. Butler May 1986 23 p Presented at the Intersociety Energy Conversion Engineering Conference, San Diego, Calif., 25 Aug. 1986
(Contract DE-AC04-76DP-00789)
(DE86-011424; SAND-86-7102C; CONF-860810-12) Avail: NTIS HC A02/MF A01

Results of Na-S battery systems analyses are presented. The performance of various network configurations for a load leveling battery in the presence of multiple cell failures was assessed with the use of a computer model. Results indicate that the life of a battery can be extended by a factor of 3 to 4 with the use of a switch to assure either open circuit or short circuit failure of each cell. Other means of extending the life of the battery are presented. Future work is outlined for the effort to design a 100 MW-h Na-S load leveling battery. DOE

N87-12789# Sandia National Labs., Albuquerque, N. Mex.
LITHIUM AMBIENT-TEMPERATURE BATTERY RELIABILITY PROGRAM, MAY 1983-APRIL 1985
C. D. Jaeger, N. H. Hall, and E. V. Thomas Jun. 1986 61 p
(Contract DE-AC04-76DP-00789)
(DE86-012247; SAND-85-1518) Avail: NTIS HC A04/MF A01

From May 1983 through April 1985 Sandia National Laboratories continued to develop and evaluate nondestructive methodology for predicting the reliability of primary lithium batteries. During this period, considerable time was spent improving the microcalorimetry data acquisition and processing software and completing the curve-fitting algorithm for the impedance data. All initial measurements were conducted, and all cells either completed the storage portion of the text matrix or remained in storage. Some statistical analyses were completed. Several nondestructive measurement variables that correlate well with remaining capacity were identified. Finally, the status of the program was evaluated and the program was tentatively extended to October 1986. DOE

N87-12790# Sandia National Labs., Albuquerque, N. Mex.
NANOSECOND SPARK GAP SWITCHING MEASUREMENTS
J. W. Ginn, D. N. Hendricks, and M. T. Buttram Jun. 1986 5 p Presented at the 17th Power Modulator Symposium, Seattle, Wash., 23 Jun. 1986
(Contract DE-AC04-76DP-00789)
(DE86-012279; SAND-86-0512C; CONF-860674-7) Avail: NTIS HC A02/MF A01

The switching time of gas and oil dielectric spark gaps was measured in the nanosecond and subnanosecond time regime. The observed switching characteristics of the two spark gaps were compared with those predicted by empirical formulas. The formulas used primarily were those developed in somewhat slower time regimes by J.C. Martin. For the given geometry, the switching times of both gaps were dominated by the resistive phase rather than by any inductive effects. The rise times observed from the output of the gas switch were consistently greater than those predicted for resistive phase duration in a gas spark. With charge times of from 50 to 60 ns to electric field values of from 170 to 350 kV/cm, 10% to 90% output rise times of from 2.8 to 8.2 ns were observed. The dielectric strength of the oil switch was consistent with the empirical prediction for oil breakdown. The oil gap was charged to electric field values of from 1.4 to 3.1 MV/cm with effective charge times of from 1.3 to 20 ns. Its output rise time was less than or equal to 400 ps. This result is not inconsistent with the empirical prediction for resistive phase duration in an oil spark. Measurement of times shorter than this were limited by the bandwidth of the available equipment. DOE

N87-12791# Varian Associates, Salt Lake City, Utah.
A 60 GHz GYROTRON DEVELOPMENT PROGRAM Final Report, Apr. 1979 - Jun. 1984
J. F. Shively, R. E. Bier, M. Caplan, M. K. Cheng, E. Choi, C. C. Conner, L. J. Craig, S. J. Evans, S. J. Evers, and K. L. Felch 1986 707 p
(Contract DE-AC05-84OR-21400)
(DE86-012488; ORNL/Sub-79-21453/21) Avail: NTIS HC A99/MF A01

The original objective of this program was to develop a microwave amplifier or oscillator capable of producing 200 kW CW power output at 110 GHz. The use of cyclotron resonance interaction was pursued, and the design phases of this effort are discussed. Later, however, the program's objective was changed to develop a family of oscillators capable of producing 200 kW of peak output power at 60 GHz. Gyrotron behavior studies were performed at 28 GHz to obtain generic design information as quickly as possible. The first experimental device at 60 GHz produced over 200 kW of peak power at a pulse duration of 20 microsec. Heating problems and mode interference were encountered. The second experimental tube incorporated an optimized gun location but also suffered from mode interference. The third experimental tube included modifications that reduced mode interference. It demonstrated 200 kW of peak output at 100 ms pulse duration. The fourth experimental tube, which used an older RF circuit design but in a CW configuration, produced 71.5 kW CW. The fifth experimental tube incorporated a thinner double-disc output window which improved window bandwidth and reduced window loss. This tube also incorporated modifications to the drift tunnel and cavity coupling, which had proven successful in the third experimental pulse tube tests. It produced 123 kW of CW output power at 60 GHz RF load coolant boiling and tube window failure terminated the tests. A new waterload was designed and constructed, and alternative window designs were explored. A secondary task of developing a 56 GHz CW tube produced in excess of 100 kW CW at this alternate frequency. Testing of the sixth experimental tube resulted in operation at CW output power in the range of 200 to 206 kW for an hour. The seventh tube was operated for about forty-five minutes with CW power output over 200 kW. DOE

N87-12792# Los Alamos National Lab., N. Mex.
EFFICIENT, MONOCHROMATIC, HIGH-POWER MICROWAVE GENERATOR
T. J. T. Kwan and C. M. Snell 1986 6 p Presented at the 6th International Conference on High Power Particle Beams, Kobe, Japan, 9 Jun. 1986
(Contract W-7405-eng-36)
(DE86-012385; LA-UR-86-1937; CONF-860665-8) Avail: NTIS HC A02/MF A01

Microwave generation by electron beams in virtual cathode configurations can achieve significant power levels. However, most designs inherently have two competing mechanisms generating microwaves; namely the oscillating virtual cathode and the reflexing electrons. These two mechanisms tend to interfere destructively with each other. Specifically, the reflexing electrons subject the electron beam to two-stream instability, causing considerable heating of the electron beam. In addition, the space-charge of the reflexing electrons can cause the diode independence to fluctuate, resulting in oscillations of the electron beam energy. We have investigated a novel idea to remove these undesirable effects and we found that high-power, narrow-band, and monochromatic microwaves could be generated with efficiency of 10 to 20%.DOE

N87-12793# California Univ., Berkeley. Lawrence Berkeley Lab.
ZINC/NICKEL OXIDE BATTERY MEMBRANE SEPARATOR STUDIES Final Report, 15 Jul. 1984 - 1 Jul. 1985
D. N. Bennion and J. S. Bradshaw Mar. 1986 19 p
(Contract DE-AC03-76SF-00098)
(DE86-012824; LBL-21261) Avail: NTIS HC A02/MF A01

Fourteen different macrocyclic compounds were synthesized for possible use in anionic exchange membranes and several polymerized with polyvinylbenzyl chloride. Two others were used in polyvinyl alcohol (PVA) membranes. Work continued to develop a suitable polymer material for the membranes. PVA could be cross-linked using a crown-ether dialdehyde as a cross-linking agent to produce a membrane with high ionic conductivity (0.02 mho/cm) and reasonable short-term stability in strong caustic solution at room temperatures. Selectivity of the membrane for hydroxide ions was essentially the same as that in the solution itself. Two new fabrication methods for polypropylene membranes were investigated and developed. Development of a two-dimensional code of a zinc-nickel oxide cell was begun. DOE

N87-12794# Sandia National Labs., Albuquerque, N. Mex.
SAW TRANSDUCTION IN ELECTROSTRICTIVE SUBSTRATES
G. R. Laguna and B. A. Auld 1986 5 p Presented at the International Symposium on Ultrasonics, Ferroelectrics and Frequency Control, Bethlehem, Pa., 9 Jun. 1986 Prepared in cooperation with Stanford Univ.
(Contract DE-AC04-76DP-00789)
(DE86-011651; SAND-86-1347C; CONF-8606121-3) Avail: NTIS HC A02/MF A01

Using electrostrictive materials for surface acoustic wave (SAW) device substrates allows for electronic control of the frequency response of the device. Centrosymmetric materials will not be piezoelectric, but by applying a static dc biasing electric field, a piezoelectric response can be induced in the substrate. If this bias field is spatially varying, then the induced piezoelectric response will also be spatially varying. In fact, since the piezoelectric response is controlled by the dc biasing electric field, changing the bias distribution will change the response of the filter. This allows for a real-time electronically programmable SAW device. The constitutive relations for pure electrostrictive materials are manipulated to show this induced piezoelectric response under an applied electric bias field. Normal mode theory is used to obtain the response of SAW devices in which a spatially varying piezoelectric response is established. The result is similar to that for standard piezoelectric theory except that the pertinent variable now becomes the spatially varying piezoelectric response. Experimental results for several spatially varying piezoelectric patterns are presented. DOE

N87-12795# Los Alamos National Lab., N. Mex.
MODELING OF HIGH-EXPLOSIVE DRIVEN PLASMA COMPRESSION OPENING SWITCHES
A. E. Greene, I. R. Lindemuth, and J. H. Goforth 1986 8 p Presented at the 4th International Conference on Megagauss Magnetic-Field Generation and Related Topics, Santa Fe, N. Mex., 14 Jul. 1986
(Contract W-7405-eng-36)
(DE86-012421; LA-UR-86-2200; CONF-860703-8) Avail: NTIS HC A02/MF A01

The initial path of the current through a plasma compression switch is through a thin (500-nm thick) metal foil. The current explodes the foil to form the seed for the conducting plasma. The behavior of the foil at this point is the same as an exploding metal fuse for which we have a simple model. We have, therefore, chosen this model as our starting point. The fuse model assumes that the foil material is homogeneous and is characterized by a single temperature and density. The thickness of the foil is assumed to be much less than the magnetic diffusion skin depth so that the magnetic field varies linearly across the foil. For the present application we assume that the side of the foil away from the channel is fixed in space while the side by the channel is untamped. The foil/plasma will, therefore, cross the channel at the expansion velocity as the foil explodes. Equations for the electrical resistance of the foil, the magnetic fields, the motion of the foil, and the kinetic and internal energies are all solved selfconsistantly. The electrical resistivity, the pressure, and the specific energy of aluminum are taken from the Los Alamos SESAME EOS library. In the case of aluminum we have created a SESAME-style table based on the theory of More and Lee which we have modified to agree with experiment where possible. DOE

N87-12796# Los Alamos National Lab., N. Mex.
TRANSFORMERS FOR EXPLOSIVE PULSED POWER COUPLING TO VARIOUS LOADS
B. L. Freeman and W. H. Bostick 1986 10 p Presented at the 4th International Conference on Megagauss Magnetic-Field Generation and Related Topics, Santa Fe, N. Mex., 14 Jul. 1986
(Contract W-7405-eng-36)
(DE86-012425; LA-UR-86-2259; CONF-860703-7) Avail: NTIS HC A02/MF A01

Tape-wound step-up transformers have been fabricated and used with magnetic flux compression generators in the past with effective coupling coefficients of approx. 0.76. We have attempted to design some units with coefficients in the range of 0.85 to 0.92 by taking advantage of newer dielectrics. The intent is to raise the voltage stress from less than or equal to 0.39 MV/cm to the range of 0.98 to 1.97 MV/cm. This has the effect of making the secondary thinner and permitting a higher coupling efficiency. Several designs for coupling the 13.2-cm-wide by 52.8-cm-long plate generator to loads in the range of 10 to 30 with an output of approx. 1 MV have been studied. These designs must take into account that the primary of the transformer is switched into the circuit as a load in parallel with the generator's ballast inductor. A final design examines the constraints imposed by attempting to transform the output of a plate generator up to 10 MV into a high impedance load. A voltage stress of 3.9 MV/cm is required in this particular design for 140 kV per turn in the secondary winding. DOE

N87-12797# Lawrence Livermore National Lab., Calif.
ELECTRONIC ENGINEERING DEPARTMENT THRUST AREA REPORT, FY 1985
J. Hymer, ed., M. Genin, ed., S. Taft, ed., J. Canada, ed., K. Gleason, ed., and D. Sapone, ed. Apr. 1986 197 p
(Contract W-7405-eng-48)
(DE86-013172; UCRL-53700-85) Avail: NTIS HC A09/MF A01

The work of the Electronics Engineering Department Thrust Area for FY-85 is described. The work includes: diagnostics and microelectronic engineering; signal and control engineering; microwave and pulsed power engineering; computer-aided engineering; modeling and simulation engineering; and systems

engineering. Discussions on each of the thrust areas have been separately indexed for inclusion in the Energy Data Base. DOE

N87-12798# California Univ., Berkeley. Lawrence Berkeley Lab.
FEASIBILITY STUDY OF A NEW ZINC-AIR BATTERY CONCEPT USING FLOWING ALKALINE ELECTROLYTE
P. N. Ross, Jr. Apr. 1986 32 p Presented at the Intersociety Energy Conversion Engineering Conference, San Diego, Calif., 25 Aug. 1986
(Contract DE-AC03-76SF-00098)
(DE86-013461; LBL-21437; CONF-860810-18) Avail: NTIS HC A03/MF A01

Proof-of-principle experiments are reported for a new concept in electrically rechargeable zinc-air batteries. The zinc electrode is a porous flow-thru type using a copper foam metal substrate with zinc deposition onto the foam metal from concentrated zincate electrolyte (as used in zinc-slurry type batteries). The bifunctional air electrode employs low-cost materials, being fabricated entirely from carbon-based precursors and small amounts of nickel and/or cobalt oxide. Corrosion measurements on the graphite materials in the air electrode indicate sufficient corrosion resistance for 8000 h life on charge. A prototype single cell was constructed having 1.5 Ah capacity producing 1.2 V discharge -2.0 charge at the three hour rate and has produced stable voltages for more than 150 cycles. Based on the 1.5 Ah prototype characteristics, design calculations for a 32 kWh battery project an energy density of about 110 Wh/kg, peak power density of 140 W/kg, electrical efficiency of 60% and an attractive materials cost of less than or equal to $20 per kWh. DOE

N87-12799# Sandia National Labs., Albuquerque, N. Mex.
VERY LOW BANDWIDTH, UNATTENDED IMAGER FOR SURVEILLANCE APPLICATIONS
P. H. Eichel and C. V. Jakowatz, Jr. 1986 7 p Presented at the 30th SPIE Technical Symposium on Optics and Optoelectronic Engineering, San Diego, Calif., 17 Aug. 1986
(Contract DE-AC04-76DP-00789)
(DE86-013570; SAND-86-0599C; CONF-860880-14) Avail: NTIS HC A02/MF A01

The need arises in certain vehicular surveillance applications for an electronic imager that can perform without human interaction and can transmit definitive images over very low bandwidth channels. The investigators have found that line scan imagers offer particular advantages toward these ends. Specifically, the use of a line scan imager facilitates the following processing steps: (1) segmentation of the vehicle from the background, (2) automatic exposure control, (3) light level equalization prior to quantization, and (4) implementation of an adaptive sampling scheme. These processing steps together with the source encoder may be implemented on a relatively low throughput processor and achieve near real time operation. The specific encoding method used here is an extended differential pulse code modulation (DPCM). A prototype system has been developed, producing medium resolution images at less than 10K bits per frame. DOE

N87-12800# Allied Bendix Corp., Kansas City, Mo.
IMAGE ENHANCEMENT EQUIPMENT CAPABILITIES Status Report
D. G. Moore Jul. 1986 22 p
(Contract DE-AC04-76DP-00613)
(DE86-013615; BDX-613-3511) Avail: NTIS HC A02/MF A01

Three inspection problems were investigated by using image enhancement techniques. This document includes descriptions of installation and development of an image enhancement system. A detailed description of the hardware and software structures is also included. Two examples portray system capabilities. The operating parameters used on the examples are included. An outline of the developed general-purpose inspection techniques used to meet further milestones is discussed briefly. DOE

N87-12801# Johnson Controls, Inc., Milwaukee, Wis.
PERFORMANCE OF ADVANCED LEAD ACID BATTERIES FOR ELECTRIC VEHICLES
B. K. Mahato, G. H. Brilmyer, and K. R. Bullock 1986 20 p Presented at the International Power Sources Symposium, Brighton, England, 8 Sep. 1986
(Contract W-31-109-eng-38)
(DE85-011476; CONF-860913-1) Avail: NTIS (US Sales Only) HC A02/MF A01

New applications for lead-acid batteries, such as electric vehicle propulsion, demand high specific energy and power and good cycle life. A research and development program at Johnson Controls, Inc., sponsored in part by the United States Department of Energy through Argonne National Laboratory, has been underway since 1978 to develop advanced electric vehicle batteries. Cell test results on and Advanced Battery design developed under this program are described. Capacity, energy and power delivered at various discharge rates are shown. Material distribution and utilization are described, and the effects of discharge rate and temperature on the material utilization of both electrodes is determined. Cycle life data at 100% depth of discharge are also presented. DOE

N87-12802# Sandia National Labs., Albuquerque, N. Mex.
LI CORROSION RESISTANT GLASSES FOR HEADERS IN AMBIENT TEMPERATURE LI BATTERIES Patent Application
E. E. Hellstrom, inventor (to DOE) and R. D. Watkins, inventor (to DOE) Filed 11 Oct. 1985 18 p
(Contract DE-AC04-76DP-00789)
(DE86-013754; US-Patent-Appl-SN-786561) Avail: NTIS HC A02/MF A01

Glass compositions containing 10 to 50 mol% CaO, 10 to 50 mol% AlO, 30 to 60 mol% BO, and 0 to 30 mol% MgO are provided. These compositions are capable of forming a stable glass-to-metal seal possessing electrical insulating properties for use in a lithium battery. Also provided are lithium cells containing a stainless steel body and molybdenum center pin electrically insulated by means of a seal produced according to the invention. DOE

N87-12803# Department of Energy, Washington, D. C.
VERY HIGH EFFICACY ELECTRODELESS HIGH INTENSITY DISCHARGE LAMPS Patent Application
P. D. Johnson, inventor (to DOE) (California Univ., Berkeley. Lawrence Berkeley Lab.) Filed 3 Oct. 1985 13 p
(Contract DE-AC03-76SF-00098)
(DE86-013760; US-Patent-Appl-SN-783730) Avail: NTIS HC A02/MF A01

An electrodeless arc lamp comprises an outer jacket hermetically sealing and thermally protecting an arc tube inside which has an upwardly convex bottom center section. The absence of chemically reactive electrode material makes it possible to use metal halides other than iodides. The tube contains chlorides, bromides or a mixture thereof of scandium and sodium in a nearly equimolar relationship in addition to mercury and an inert gas. Good color balance can be obtained at reduced reservoir temperature and with less power loss. Reduction in wall temperature makes it possible to attain longer lamp life. DOE

N87-12804# Iowa State Univ. of Science and Technology, Ames. Heat Transfer Lab.
HEAT TRANSFER CHARACTERISTICS OF SIMULATED MICROELECTRONIC CHIPS UNDER NORMAL AND ENHANCED CONDITIONS
K. A. Park and A. E. Bergles Nov. 1985 200 p Sponsored by IBM Corp., Poughkeepsie, N.Y.
(PB86-224425; ISU-ERI-AMES-86211; HTL-35) Avail: NTIS HC A09/MF A01 CSCL 09A

The heat transfer characteristics of simulated microelectronic chips were investigated with direct immersion cooling in Freon-TF (R-113). The basic heater was 4.5 mm x 4.5mm electrically heated foil. The studies of plain heaters included natural convection, nucleate boiling, and critical heat flux. Water was included as a working fluid for natural convection. Ultrasonic agitation and heat sinks were studied as enhanced cooling methods. The height effect for single flush heaters agrees qualitatively with the conventional

theory of natural convection; however, even the widest heaters have coefficients higher than predicted because of leading edge effects. The increase of the heat transfer coefficient with decreasing width is correlated. The protruding heaters have about 15% higher coefficients than the flush heaters. Data for natural convection were also obtained for in-line and staggered arrays of flush heaters with varying distances between heaters. GRA

34 FLUID MECHANICS AND HEAT TRANSFER

Includes boundary layers; hydrodynamics; fluidics; mass transfer; and ablation cooling.

For related information see also *02 Aerodynamics* and *77 Thermodynamics and Statistical Physics.*

N87-12805 ESDU International Ltd., London (England).
FLUID TRANSIENTS IN PIPES. ESTIMATION OF MAXIMUM PRESSURES AND FORCES IN STEAM LINES
Sep. 1986 73 p
(ESDU-86015; ISBN-0-85679-567-4; ISSN-0141-4011) Avail: ESDU

Available as part of the ESDU Sub-series on Fluid Mechanics (Internal Flow), this document gives a graphical method for estimating the time-dependent pressure changes and piping forces that follow from a rapid value closure in a one-pipe system of constant cross-section carrying superheated steam. The method also assumes a frictionless flow and ignores wave steepening effects. A computer program listing in FORTRAN is also included that applies to any gas that obeys the perfect gas law, and takes into account the effects of both wall friction and wave steepening. In that case sections of the pipeline can have different cross-sectional areas and that can be used to treat a pipeline with branched ends. Worked examples are included for both methods and in the case of the computer program show specimen print-out of the input data, and of the output which includes the time variation of pressure, velocity and density at three points in the pipeline chosen by the user together with values of maximum and minimum pressure at 25 points (a value that is also open to choice by the user). The example is run for a valve with a linear variation of area with time, and for one with a nonlinear characteristic. ESDU

N87-12806*# National Aeronautics and Space Administration. Langley Research Center, Hampton, Va.
TIME-DEPENDENT SOLUTION FOR AXISYMMETRIC FLOW OVER A BLUNT BODY WITH IDEAL GAS, CF4, OR EQUILIBRIUM AIR CHEMISTRY
H. Harris Hamilton, II and John R. Spall Jul. 1986 40 p
(NASA-TM-87675; NAS 1.15:87675) Avail: NTIS HC A03/MF A01 CSCL 20D

A time-asymptotic method has been used to obtain steady-flow solutions for axisymmetric inviscid flow over several blunt bodies including spheres, paraboloids, ellipsoids, and spherically blunted cones. Comparisons with experimental data and results of other computational methods have demonstrated that accurate solutions can be obtained using this approach. The method should prove useful as an analysis tool for comparing with experimental data and for making engineering calculations for blunt reentry vehicles. Author

N87-12807# Toronto Univ. (Ontario). Inst. for Aerospace Studies.
FINITE-DIFFERENCE SOLUTIONS FOR COMPRESSIBLE LAMINAR BOUNDARY-LAYER FLOWS OF A DUSTY GAS OVER A SEMI-INFINITE FLAT PLATE
B. Y. Wang and I. I. Glass Aug. 1986 121 p Sponsored in part by Natural Science and Engineering Research Council of Canada, and Defence Research Establishment, Suffield
(Contracts F-AFOSR-82-0096; DNA001-85-0368)
(UTIAS-311; ISSN-0082-5255) Avail: NTIS HC A06/MF A01

A finite difference method is used to investigate compressible, laminar boundary-layer flows of a dilute dusty gas over a semi-infinite flat plate. Details are given of the implicit finite difference schemes as well as the boundary conditions, initial conditions, and compatibility conditions for solving the gas-particle boundary layer equations. The flow profiles for both the gas and particle phases were obtained numerically along the whole length of the plate from the leading edge to far downstream of it. The finite difference solutions in the large-slip region and the small-slip region are compared with the asymptotic solutions and good agreement is achieved. The boundary-layer characteristics of interest, including the wall shear stress, the wall heat transfer rate and the displacement thickness are calculated. The alteration of the flow properties owing to the presence of particles is discussed in detail. It was found that the boundary-layer flow of a dusty gas can be divided into three distinct flow regimes which are characterized by quasi-frozen, nonequilibrium and quasi-equilibrium flows and that at a critical distance from the leading edge the particle velocity at the wall decelerates to zero and near-equilibrium is achieved between the gas and particle flows. Author

N87-12808*# Stanford Univ., Calif.
TRANSITION AND MIXING IN AXISYMMETRIC JETS AND VORTEX RINGS
Gary A. Allen, Jr. and Brian J. Cantwell Washington NASA Oct. 1986 246 p
(Grants NsG2-392; NAG2-21)
(NASA-CR-3893; NAS 1.26:3893) Avail: NTIS HC A11/MF A01 CSCL 20D

A class of impulsively started, axisymmetric, laminar jets produced by a time dependent joint source of momentum are considered. These jets are different flows, each initially at rest in an unbounded fluid. The study is conducted at three levels of detail. First, a generalized set of analytic creeping flow solutions are derived with a method of flow classification. Second, from this set, three specific creeping flow solutions are studied in detail: the vortex ring, the round jet, and the ramp jet. This study involves derivation of vorticity, stream function, entrainment diagrams, and evolution of time lines through computer animation. From entrainment diagrams, critical points are derived and analyzed. The flow geometry is dictated by the properties and location of critical points which undergo bifurcation and topological transformation (a form of transition) with changing Reynolds number. Transition Reynolds numbers were calculated. A state space trajectory was derived describing the topological behavior of these critical points. This state space derivation yielded three states of motion which are universal for all axisymmetric jets. Third, the axisymmetric round jet is solved numerically using the unsteady laminar Navier Stokes equations. These equations were shown to be self similar for the round jet. Numerical calculations were performed up to a Reynolds number of 30 for a 60x60 point mesh. Animations generated from numerical solution showed each of the three states of motion for the round jet, including the Re = 30 case. Author

N87-12809# Instituto de Pesquisas Espaciais, Sao Jose dos Campos (Brazil).
MODULATION TRANSFER FUNCTION (MTF) OF THE GEOMETRICAL IMAGE RESOLUTION OF THE THERMAL INFRARED BAND M.S. Thesis [FUNCAO DE TRANSFERENCIA DE MODULACAO (MTF) NA RESOLUCAO GEOMETRICA DE IMAGENS NA FAIXA DO INFRAVERMELHO TERMAL]
Hiromiti Yoshioka Jul. 1986 94 p In PORTUGUESE; ENGLISH summary
(INPE-3964-TDL/231) Avail: NTIS HC A05/MF A01

The modulation transfer function (MTF) of an imaging system is composed by the MTF's of its subsystems. The MTF of the system contributes to the formation of the EIFOV (Effective Instantaneous Field of View). In this work the MTF of an imaging system operating in a thermal infrared band was calculated. In this way, it was possible to theoretically establish the EIFOV of the equipment. Then, several experiments consisting of flights over targets with well-known temperature and dimensions were made. The images were analyzed using a microdensitometer and the

resultant curves compared to those estimated in theory. Degradations in the EIFOV due to roll movements of the airborne platform were observed. A stabilized platform can solve this problem.
Author

N87-12810# Royal Aircraft Establishment, Farnborough (England).
THE CALCULATION OF SEPARATED FLOWS OF LOW-VISCOSITY LIQUIDS USING THE BATCHELOR MODEL
S. I. Chernyshenko Apr. 1985 13 p Transl. into ENGLISH from Mekhanika Zhidkosti i Gaza, v. 2, 1984 p 40-45
(BR-100272; RAE-Trans-2133) Avail: NTIS HC A02/MF A01

Conditions of applicability and examples of application of the Batchelor Model (BM) are considered. The application of the BM to flow near a plate mounted perpendicularly to a wall at the stagnation point is examined, and a method for solving the corresponding eddy-potential problem is described. The application of a precise form of the condition for determining vorticity is also examined. It is shown that eddy-potential flow cannot be the limit (at Re approaching infinity) of laminar flow behind a step; arguments in favor of an analogous conclusion with regard to flow past blunt bodies are presented.
Author

N87-12811# Virginia Polytechnic Inst. and State Univ., Blacksburg. Dept. of Engineering Science and Mechanics.
ANALYSIS OF THE NONLINEAR STABILITY OF CIRCULAR COUETTE FLOW Final Report, 16 Jun. 1982 - 15 Dec. 1985
Thorwald Herbert Jun. 1986 78 p
(Contract DAAG29-82-K-0129)
(AD-A168951; ARO-18744.15-MA) Avail: NTIS HC A05/MF A01 CSCL 20/4

The work under this contract aimed at three major goals: (1) Reveal the origin of the despin moment that may cause severe flight instability of spin-stabilized artillery shells with liquid payloads; (2) Explore the potential of high-order perturbation methods for describing nonlinear properties of single modes and mode interactions in hydrodynamic stability; and (3) Analyze the mechanism of state selection in unstable circular Taylor-Couette flow.
GRA

N87-12812# Army Engineer Waterways Experiment Station, Vicksburg, Miss. Hydraulics Lab.
PRESSURE CALCULATION FOR TWO-DIMENSIONAL FLOW INSIDE HYDRAULIC STRUCTURES Final Report
Robert S. Bernard Apr. 1986 36 p
(AD-A169039; WES/MP/HL-86-2) Avail: NTIS HC A03/MF A01 CSCL 20/4

When static pressure inside a hydraulic structure falls below some critical value, voids containing water vapor form therein. The voids then collapse with great force, pitting and eroding the internal surfaces of the structure. The formation/collapse of these voids is called cavitation, and the prevention thereof is a prime concern in structural design. The VORTEX code has been used to calculate pressure distributions for three distinct flow conditions in the outlet works for Taylorsville Lake, Salt River, Kentucky. A method has been developed for computing the two-dimensional pressure distributions inside hydraulic structures. Velocities are first obtained by finite difference solution of the Navier-Stokes equations in stream-function/vorticity form. Pressure is then calculated by numerical integration of the momentum equation. The method was incorporated for arbitrary geometry in the VORTEX computer code, which uses boundary-fitted grids generated by the WESCOR code. Computed results compare well with piezometric data from physical-model tests for the Taylorsville outlet works, indicating that the VORTEX code may be useful in identifying and eliminating flow conditions that promote cavitation.
GRA

N87-12813# York Univ. (Ontario). Dept. of Earth and Atmospheric Science.
LOW Q SPIN-UP FROM REST Final Report, 15 May 1982 - 15 Dec. 1985
Keith D. Aldridge May 1986 35 p
(Contract DAAG29-82-K-0113)
(AD-A169106; ARO-18784.3-EG) Avail: NTIS HC A03/MF A01 CSCL 19/4

Eigenfrequencies and decay rates of inertial waves have been measured for both Newtonian and non-Newtonian fluids contained in a cylindrical cavity while the fluid spins up from rest. The waves were excited by precessing the lid of the container until resonance was reached and detected by measuring disturbance pressure differences while the waves decayed freely. Measurements extend from 0.5 spin up times to steady state and over a range of Reynolds numbers 100-45,000 for the Newtonian fluids with precession amplitudes in the range 0.006-0.0328 radians. Measured eigenfrequencies agree to within a few percent with those previously calculated. Decay rates compare less favorably because they are more difficult to measure experimentally and to calculate theoretically. New methods of analysis were developed to recover the eigenfrequencies and decay rates. Previously used iterative techniques were modified to allow for the removal of the effects of recording filters and also automate the procedures used made possible with improved estimates of errors. New results for non Newtonian fluids which show shear thickening are presented. These fluids have anomalous behavior in the dependence of eigenfrequency and decay rate on time since the container's rotation began compared to that of a Newtonian fluid.
GRA

N87-12814# Stanford Univ., Calif. Center for Large Scale Scientific Computation.
ADAPTIVE GRID TECHNIQUES FOR ELLIPTIC FLUID-FLOW PROBLEMS
S. C. Caruso, J. H. Ferziger, and J. Oliger Dec. 1985 205 p
(Contract N00014-82-K-0335)
(AD-A169471; CLASSIC-85-10) Avail: NTIS HC A10/MF A01 CSCL 20/4

The adaptive grid techniques are described for elliptic fluid flow problems. The method is an extension of a local refinement technique developed by Berger for systems of hyperbolic equations. Local refined grids are overlaid on a coarser base grid. Recursive use of this technique allows an arbitrary degree of grid refinement. Two classes of elliptic flows are identified; they are characterized as having strong or weak viscous inviscid interactions. Adaptive solution strategies, active and passive, respectively, are developed for each class. The simpler method is used to solve the steady, laminar, incompressible Navier Stokes equations. Central differencing of the convective terms is implemented with the defect-correction method to stabilize the solution method for all cell Reynolds numbers. Uniform grid calculations are performed for the laminar backstep flow. Richardson estimated solution and truncation errors are compared to accurate estimates of the same quantities for the backstep flow. The solution error is well predicted. The truncation error estimates are less accurate, but they reliably indicate where grid refinement is required. Active adaptive calculations of the backstep are made, using boundary aligned refinement.
GRA

N87-12815# Naval Postgraduate School, Monterey, Calif.
IN-LINE AND TRANSVERSE FORCES ON SMOOTH AND ROUGH CYLINDERS IN OSCILLATORY FLOW AT HIGH REYNOLDS NUMBERS Interim Report, Jul. 1985 - Jul. 1986
Turgut Sarpkaya 4 Jul. 1986 176 p
(Grant NSF CEE-82-10264)
(AD-A169562; NPS69-86-003) Avail: NTIS HC A09/MF A01 CSCL 20/4

This report presents the results of an extensive experimental investigation of the in line and transverse forces acting on smooth, sand roughened, and marine roughened circular cylinders (k/D = 1/50) of identical length to diameter ratio (L/D = 2) placed in a sinusoidally oscillating flow. The drag, inertia, and the maximum force coefficients have been determined through the use of the Fourier analysis. The transverse force (lift) has been analyzed in terms of its root mean square value. In addition, the amplitude of the first ten harmonics have been determined. The results are presented in both graphical and tabulated form in terms of the Reynolds number, Keulegan Carpenter number, relative roughness and the frequency parameter beta (= Re/K).
GRA

N87-12816# Dayton Univ., Ohio. Research Inst.
COMPUTATIONAL FLUID DYNAMIC STUDIES OF CERTAIN DUCTED BLUFF-BODY FLOWFIELDS RELEVANT TO TURBOJET COMBUSTORS. VOLUME 1: TIME-DEPENDENT CALCULATIONS WITH THE k-EPSILON TURBULENCE MODEL FOR AN EXISTING CENTERBODY COMBUSTOR Final Report, 16 Aug. 1984 - 30 Sep. 1985
M. S. Raju and L. Krishnamurthy Jul. 1986 53 p
(Contract F22615-84-C-2411)
(AD-A171434; UDR-TR-85-82-Vol-1; AFWAL-TR-86-2004-Vol-1) Avail: NTIS HC A04/MF A01 CSCL 21/2

A numerical investigation of the near-wake region in a ducted bluff-body combustor by finite-difference computations is reported. The numerical predictions are based upon the time-dependent, compressible Navier-Stokes equations and the k-epsilon turbulence model. The standard k-epsilon turbulence model was modified to account for the nonstationary terms. The time-dependent calculations predictions addressed the nonreacting near-wake flow field of the centerbody combustor with only the annular air stream present. Flowfield predictions for a combustor inlet mass flow of 2 kg/s with the time-dependent formulation incorporating the k-epsilon turbulence model show the attainment of a steady-state recirculating flow in the near wake. The slow axial migration of the recirculation vortex towards the exit boundary which was noticed in the earlier time-dependent calculations without a turbulence model is not longer present. Present results have thus eliminated the appearance of reverse flow at the exit boundary with the consequent incompatibility of the boundary conditions, and thereby the spu rious shedding-like behavior observed previously. The steady-state results in the present study demonstrate internal consistency with the time-averaged measurements and predictions for the locations of the vortex center and the centerline rear stagnation point. GRA

N87-12817# Colorado State Univ., Fort Collins. Dept. of Mechanical Engineering.
NATURAL CONVECTION IN AN ENCLOSURE WITH DISCRETE ROUGHNESS ELEMENTS ON A VERTICAL HEATED WALL
S. Shakerin, M. S. Bohn (Midwest Research Inst., Golden, Colo.), and R. I. Loehrke Feb. 1986 9 p Presented at the International Heat Transfer Conference, San Francisco, Calif., 17 Aug. 1986 Prepared in cooperation with Solar Energy Research Inst., Golden, Colo.
(Contract DE-AC02-83CH-10093)
(DE86-004424; SERI/TP-252-2812; CONF-860805-7) Avail: NTIS HC A02/MF A01

Natural convection flow next to a heated wall with single and repeated, two-dimensional, rectangular roughness elements is studied numerically and experimentally. The objective is to determine how these roughness elements influence heat transfer rates from the wall. Each roughness element consists of a thermally conducting, horizontal cylinder of rectangular cross section attached to the heated, isothermal wall of an enclosure. The height of roughness is on the order of the boundary layer thickness. Dye flow visualization in water confirms the numerical prediction that the steady flow over these elements does not separate. Only at high Rayleigh numbers, when the boundary layer below the roughness is unsteady, is local instantaneous flow reversal observed. Although steady flow reversals near the wall are not predicted or observed, nearly stagnant regions are formed, particularly between closely spaced cylinders. The surface heat flux in these stagnant regions is relatively low, so the total heat transfer rate may be nearly the same as for a smooth wall in spite of the increased surface area. DOE

N87-12818# Sandia National Labs., Albuquerque, N. Mex.
APPLICATION OF FLUX-CORRECTED TRANSPORT (FCT) TO HIGH RAYLEIGH NUMBER NATURAL CONVECTION IN A POROUS MEDIUM
R. J. Gross, M. R. Baer, and C. E. Hickox 1986 29 p Presented at the International Heat Transfer Conference, San Francisco, Calif., 17 Aug. 1986
(Contract DE-AC04-76DP-00789)
(DE86-004603; SAND-85-1552C; CONF-860805-4) Avail: NTIS HC A03/MF A01

A numerical technique designed to solve a wide class of convectively dominated flow problems is applied to natural convective flow in a porous medium at large Rayleigh number. The technique is a finite difference method based on flux-corrected transport (FCT) and possesses four desirable numerical properties: stability, accuracy, monotonicity, and conservation. Steady natural convection is investigated for Rayleigh numbers as large as 10,000. An efficient methodology for obtaining steady state solutions is illustrated. A simulation is performed for transient thermal convection at a Rayleigh number of 2500. Transient natural convection involving both heat and mass transfer is illustrated for a Rayleigh number of 2500, Lewis number of 2, and buoyancy ratio of 0.1. All simulations are performed in a square cavity with heated vertical side walls. DOE

N87-12819# Sandia National Labs., Albuquerque, N. Mex.
DETONATION CELLULAR STRUCTURE AND IMAGE PROCESSING
J. E. Shepherd and S. R. Tieszen 1986 31 p Presented at the 21st International Symposium on Combustion, Munich, West Germany, 3 Aug. 1986
(Contract DE-AC04-76DP-00789)
(DE86-006467; SAND-86-0033; CONF-860804-8) Avail: NTIS HC A03/MF A01

Gaseous detonations universally exhibit an instability that is manifested as cellular patterns on witness plates (sooted foils) or open shutter photographs. The characteristic dimension or cell width lambda of the periodic cellular pattern has previously been shown to correlate with failure diameter, critical diffraction aperture dimension and direct initiation energy requirements. Due to the importance of predicting these parameters in assessing detonability hazards, a quantitative method for cell size mesurement is urgently needed. We discuss a technique based on digital image processing of sooted foil records and illustrate the results with data from experiments performed in the Heated Detonation Tube facility at Sandia. We demonstrate that image processing can be used to eliminate some of the uncertainty now present in cell size measurements. The possibility of quantifying cellular irregularity is also explored. DOE

N87-12820# Pacific Northwest Labs., Richland, Wash.
GENERALIZATION OF ONE-DIMENSIONAL SOLUTE TRANSPORT: A STOCHASTIC-CONVECTIVE FLOW CONCEPTUALIZATION
C. S. Simmons Apr. 1986 14 p Presented at the 6th Annual AGU Front Range Branch Hydrology Days, Fort Collins, Colo., 16 Apr. 1986
(Contract DE-AC06-76RL-01830)
(DE86-011117; PNL-SA-13861; CONF-8604214-1) Avail: NTIS HC A02/MF A01

A stochastic-convective representation of one-dimensional solute transport is derived. It is shown to conceptually encompass solutions of the conventional convection-dispersion equation. This stochastic approach, however, does not rely on the assumption that dispersive flux satisfies Fick's diffusion law. Observable values of solute concentration and flux, which together satisfy a conservation equation, are expressed as expectations over a flow velocity ensemble, representing the inherent random processess that govern dispersion. Solute concentration is determined by a Lagrangian pdf for random spatial displacements, while flux is determined by an equivalent Eulerian pdf for random travel times. A condition for such equivalence is derived for steady nonuniform flow, and it is proven that both Lagrangian and Eulerian pdfs are required to account for specified initial and boundary conditions on a global scale. Furthermore, simplified modeling of transport is justified by proving that an ensemble of effectively constant velocities always exists that constitutes an equivalent representation. An example of how a two-dimensional transport problem can be reduced to a single-dimensional stochastic viewpoint is also presented to further clarify concepts. DOE

N87-12821# Sandia National Labs., Albuquerque, N. Mex.
STUDY OF NUMERICAL SOLUTION METHODS FOR TWO-PHASE FLOWS
R. J. Gross and M. R. Baer Apr. 1986 50 p
(Contract DE-AC04-76DP-00789)
(DE86-012265; SAND-84-1633) Avail: NTIS HC A03/MF A01

A time-splitting numerical technique is developed to solve systems of highly coupled, hyperbolic partial differential equations. The method is illustrated by solving two different model two-phase flow problems. Results obtained by the technique are compared to results obtained from three established numerical methods: upwind differencing, the method of lines and flux-corrected transport, and to known exact solutions. To demonstrate the ability of the time splitting technique in solving a complex two-phase flow with transportive and phase interaction exhibiting greatly disparate timescales, the problem of deflagration-to-detonation transition in a granular explosive is solved numerically. The results show that the time-splitting method offers increased accuracy, but that in one dimension the method is 20% to 500% computationally more costly. However, in multidimensional calculations, time-splitting should offer an economy of computer cost and storage. DOE

N87-12822# Los Alamos National Lab., N. Mex.
FREE-LAGRANGIAN HYDRODYNAMICS USING MASSLESS TRACER POINTS
R. A. Clark 1986 6 p Presented at the Numerical Methods in Fluid Dynamics, Beijing, China, 23 Jun. 1986
(Contract W-7405-eng-36)
(DE86-012406; LA-UR-86-2118; CONF-8606136-1) Avail: NTIS HC A02/MF A01

The partial differential equations (PDEs) describing the time evolution of compressible fluid flow in two and three dimensions are usually solved numerically in the Eulerian frame of reference as opposed to the Lagrangian frame. This is especially true of flows involving large distortions. Lagrangian codes based upon Lagrangian cells do not run very long when the cells become distorted. In order to avoid the problem of cell distortion we have developed a Lagrangian code named HOBO based upon massless tracer points. These tracer points can be thought of as being embedded in, and moving with the fluid. The PDEs which we are trying to solve at each of the points are four equations which represent conservation of mass, momentum and energy, and an equation of state. DOE

N87-12823# City Coll. of the City Univ. of New York. Inst. of Applied Chemical Physics.
THEORY OF DEVELOPED HYDRODYNAMICAL TURBULENCE
B. Levich 1986 6 p
(Contract DE-AC02-80ER-10559)
(DE86-012796; DOE/ER-10559/T2) Avail: NTIS HC A02/MF A01

Several topics are briefly discussed in this progress report. The concept of turbulence based on a theory of helical fluctuations is discussed. The fluid mechanics of three phase bubble motion in a capillary tube is discussed. The influence of surfactants on droplet translation and mass transfer in a continuous phase is presented. DOE

N87-12824# Los Alamos National Lab., N. Mex.
APPARATUS FOR DOWNWARD TRANSPORT OF HEAT Patent Application
D. A. Neeper, inventor (to DOE) and J. C. Hedstrom, inventor (to DOE) Filed Aug. 1985 24 p
(Contract W-7405-eng-36)
(DE86-013700; US-Patent-Appl-SN-762367) Avail: NTIS HC A02/MF A01

An apparatus for the downward transport of heat by vaporization of a working fluid, usually from a collector which can be powered by the Sun to a condenser which drains the condensed working fluid to a lower reservoir, is controlled by a control valve which is operationally dependent upon the level of working fluid in either the lower reservoir or an upper reservoir which feeds the collector. Condensed working fluid is driven from the lower to the upper reservoir by vaporized working fluid whose flow is controlled by the control valve. The upper reservoir is in constant communication with the condenser which prevents a buildup in temperature/pressure as the apparatus goes through successive pumping cycles. DOE

N87-12825# International Centre for Theoretical Physics, Trieste (Italy).
PERIODIC HEAT TRANSFER THROUGH AN INHOMOGENEOUS MEDIUM
M. Y. Balla Oct. 1985 10 p
(DE86-702988; IC-85/220) Avail: NTIS (US Sales Only) HC A02/MF A01

One dimensional heat conduction equation has been investigated for periodic heat transfer in an inhomogeneous bounded medium. Exact analytical solutions for some typical thermal conductivity profiles have been obtained. Also an approximate solution has been attempted for the first time for heat conduction problems which is applicable for any arbitrary variation of thermal conductivity. Numerical appreciation for a parabolic thermal conductivity profile shows that results from approximate approach are in excellent agreement with those obtained by the exact analytical approach. DOE

N87-12826# Iowa State Univ. of Science and Technology, Ames.
ANALYSIS OF LAMINAR FLOW HEAT TRANSFER IN UNIFORM TEMPERATURE CIRCULAR TUBES WITH TAPE INSERTS
R. M. Manglik and A. E. Bergles May 1986 148 p Sponsored by Brown Fintube Co., Houston, Tex.
(PB86-224763; ISU-ERI-AMES-86290; HTL-39) Avail: NTIS HC A07/MF A01 CSCL 20M

Constant property, laminar flow heat transfer in a semicircular tube with uniform wall temperature has been analyzed to define the lower bound of heat transfer augmentation in circular tubes with twisted-tape inserts. Two thermal boundary conditions, which correspond to the two extremes of the fin effect of twisted tapes encountered in practical applications, are considered. Numerical solutions, employing finite-difference formulations for the governing momentum and energy equations were carried out for the thermal entrance region and for fully developed flow. GRA

35 INSTRUMENTATION AND PHOTOGRAPHY

Includes remote sensors; measuring instruments and gages; detectors; cameras and photographic supplies; and holography.

For aerial photography see *43 Earth Resources and Remote Sensing*. For related information see also *06 Aircraft Instrumentation*, and *19 Spacecraft Instrumentation*.

N87-12827# Instituto de Pesquisas Espaciais, Sao Jose dos Campos (Brazil).
A VARIATIONAL PRINCIPLE FOR THE PLASMA CENTRIFUGE
Gerson Otto Ludwig Sep. 1986 13 p Presented at the 15th International Symposium on Rarified Gas Dynamics, Grado, Italy, Jun. 1986
(INPE-3989-PRE/992) Avail: NTIS HC A02/MF A01

A variational principle is derived which describes the stationary state of the plasma column in a plasma centrifuge. Starting with the fluid equations in a rotating frame the theory is developed using the method of irreversible thermodynamics. This formulation easily leads to an expression for the density distribution of the l-species at sedimentation equilibrium, taking into account the effect of the electric and magnetic forces. Assuming stationary boundary conditions and rigid rotation nonequilibrium states the condition for thermodynamic stability integrated over the volume of the system reduces, under certain restrictions, to the principle of minimum entropy production in the stationary state. This principle yields a variational problem which is equivalent to the original

problem posed by the stationary fluid equations. The variational method is useful in achieving approximate solutions that give the electric potential and current distributions in the rotating plasma column consistent with an assumed plasma density profile.
Author

N87-12828*# National Aeronautics and Space Administration. Marshall Space Flight Center, Huntsville, Ala.
THE MULTISPECTRAL ATMOSPHERIC MAPPING SENSOR (MAMS): INSTRUMENT DESCRIPTION, CALIBRATION AND DATA QUALITY
Gary J. Jedlovec, W. Paul Menzel, Robert Atkinson, Gregory S. Wilson, and John Arvesen Aug. 1986 42 p
(NASA-TM-86565; NAS 1.15:86565) Avail: NTIS HC A03/MF A01 CSCL 14B

A new instrument has been developed to produce high resolution imagery in eight visible and three infared spectral bands from an aircraft platform. An analysis of the data and calibration procedures has shown that useful data can be obtained at up to 50 m resolution with a 2.5 milliradian aperture. Single sample standard errors for the measurements are 0.5, 0.2, and 0.9 K for the 6.5, 11.1, and 12.3 micron spectral bands, respectively. These errors are halved when a 5.0 milliradian aperture is used to obtain 100 m resolution data. Intercomparisons with VAS and AVHRR measurements show good relative calibration. MAMS development is part of a larger program to develop multispectral Earth imaging capabilities from space platforms during the 1990s. Author

N87-12829*# General Electric Co., Schenectady, N. Y. Corporate Research and Development Dept.
ADVANCED OPTICAL SMOKE METERS FOR JET ENGINE EXHAUST MEASUREMENT Final Report
Robert W. Pitz Sep. 1986 43 p
(Contract NAS3-24084)
(NASA-CR-179459; NAS 1.26:179459) Avail: NTIS HC A03/MF A01 CSCL 14B

Smoke meters with increased sensitivity, improved accuracy, and rapid response are needed to measure the smoke levels emitted by modern jet engines. The standard soiled tape meter in current use is based on filtering, which yields long term averages and is insensitive to low smoke levels. Two new optical smoke meter techniques that promise to overcome these difficulties have been experimentally evaluated: modulated transmission (MODTRAN) and photothermal deflection spectroscopy (PDS). Both techniques are based on light absorption by smoke, which is closely related to smoke density. They are variations on direct transmission measurements which produce a modulated signal that can be easily measured with phase sensitive detection. The MODTRAN and PDS techniques were tested on low levels of smoke and diluted samples of NO2 in nitrogen, simulating light adsorption due to smoke. The results are evaluated against a set of ideal smoke meter criteria that include a desired smoke measurement range of 0.1 to 12 mg cu.m. (smoke numbers of 1 to 50) and a frequency response of 1 per second. The MODTRAN instrument is found to be inaccurate for smoke levels below 3 mg/cu.m. and is able to make a only about once every 20 seconds because of its large sample cell. The PDS instrument meets nearly all the characteristics of an ideal smoke meter: it has excellent sensitivity over a range of smoke levels from 0.1 to 20 mg/cu.m. (smoke numbers of 1 to 60) and good frequency response (1 per second). Author

N87-12830*# National Aeronautics and Space Administration. Ames Research Center, Moffett Field, Calif.
SUPPLEMENTARY CALIBRATION TEST OF THE TIP-AERODYNAMICS- AND ACOUSTICS-TEST PRESSURE TRANSDUCERS
Michael E. Watts Jul. 1986 44 p
(NASA-TM-88312; A-86273; NAS 1.15:88312) Avail: NTIS HC A03/MF A01 CSCL 14B

A calibration test is described that was performed to supplement the normal calibration of the 188 pressure transducers used in the Tip Aerodynamics and Acoustics Test. This calibration led to the identification of 15 transducers which had a slope change of greater than 7% from the initial calibration. The calibration procedure is described and the results presented. The effect of the slope changes on the pressure distributions are described, followed by a method to compensate for these changes. Author

N87-12831*# National Aeronautics and Space Administration. Ames Research Center, Moffett Field, Calif.
DEVELOPMENT OF BURIED WIRE GAGES FOR MEASUREMENT OF WALL SHEAR STRESS IN BLASTANE EXPERIMENTS Interim Report, Oct. 1986
Sreedhara V. Murthy (University of the Pacific, Stockton, Calif.) and Frank W. Steinle Sep. 1986 38 p
(Contract NCC2-357)
(NASA-TM-89212; NAS 1.15:89212) Avail: NTIS HC A03/MF A01 CSCL 14B

Buried Wire Gages operated from a Constant Temperature Anemometer System are among the special types of instrumentation to be used in the Boundary Layer Apparatus for Subsonic and Transonic flow Affected by Noise Environment (BLASTANE). These Gages are of a new type and need to be adapted for specific applications. Methods were developed to fabricate Gage inserts and mount those in the BLASTANE Instrumentation Plugs. A large number of Gages were prepared and operated from a Constant Temperature Anemometer System to derive some of the calibration constants for application to fluid-flow wall shear-stress measurements. The final stage of the calibration was defined, but could not be accomplished because of non-availability of a suitable flow simulating apparatus. This report provides a description of the Buried Wire Gage technique, an explanation of the method evolved for making proper Gages and the calibration constants, namely Temperature Coefficient of Resistance and Conduction Loss Factor. Author

N87-12832# Department of the Air Force, Washington, D.C.
METAL THICKNESS MEASUREMENTS USING RADIOGRAPHY Patent Application
P. M. Achrekar, inventor (to Air Force) Filed 16 Apr. 1986 11 p
(AD-D012373; US-Patent-Appl-SN-852683) Avail: NTIS HC A02/MF A01 CSCL 11/6

The present invention relates broadly to a radiographic inspection technique, and in particular to a metal thickness measurement method using radiography. The localized areas wherein the effective metal thickness is less than the minimum that is required for radiation shielding and which can render a shielding enclosure functionless, is readily determined. The invention comprises a process for assuring metal thickness in small regions. The actual metal thickness of small regions can be verified by comparing the optical densities of sections of the metal i.e., stepwedge. A comparator microphotometer, which compares optical densities of spectrum lines from spectrophotometers, compares the optical density of spectrum lines on an exposed spectrum plate (metal under test) with a standard plate (stepwedge). GRA

N87-12833# Department of the Air Force, Washington, D.C.
HIGH RESOLUTION OPTICAL FIBER PRINT HEAD Patent
Michael J. Meier, inventor (to Air Force) Issued 20 May 1986 4 p Supersedes AD-D010348
(AD-D012384; US-Patent-4,590,492; US-Patent-Appl-SN-502028; US-Patent-Class-346-107R) Avail: US Patent and Trademark Office CSCL 14/5

A high resolution printing head for a line printer using photographic recording medium has a plurality of modules connected to form a two dimensional printing array. Each module has three fiber optic ribbons bonded together to form a staggered array of fibers. An apertured mask is photolithographically attached to the two dimensional array so that there is one aperture positioned over each fiber. The aperture has a cross-section less than the fiber so there is no overlapping of output light from each fiber and the apertures are also staggered so that a three fold increase in line density is achieved over conventional single ribbon arrays. GRA

N87-12834# Army Missile Command, Redstone Arsenal, Ala. Guidance and Control Directorate.
EVALUATION OF THE COLLINS/ROCKWELL TWO AXIS GYRO/ACCELEROMETER SENSOR CLUSTER (PHASE 3 UNIT)
Chris Roberts and Aubrey Rodgers Oct. 1985 40 p
(AD-A169810; AD-E950849; AMSMI/TR-RD-GC-86-2) Avail: NTIS HC A03/MF A01 CSCL 17/7

The Phase 3 Two-Axis Gyro/Accelerometer (TAGA) cluster is a strapdown IMU (Inertial Measurement Unit) with prelaunch self-calibration capabilities. The self-calibration mechanism allows for computer directed self tests which measure eight major performance parameters prior to launch. The purpose of this evaluation is to confirm performance stability of these eight parameters. The performance stability will decide the method of thermal compensation. Author (GRA)

N87-12835# Army Missile Command, Redstone Arsenal, Ala. Guidance and Control Directorate.
EVALUATION OF THE MULTIFUNCTION SENSOR ACCELERATION SENSITIVE TERMS MU SUB A AND MU SUB B
Chris Roberts and Aubrey Rodgers Oct. 1985 26 p
(AD-A169811; AD-E950850; AMSMI/TR-RD-GC-86-1) Avail: NTIS HC A03/MF A01 CSCL 17/7

Collins makes the assumption that g-sensitive terms MUA2 and MUB2 are small and therefore negligible. The purpose of this study is to determine if this assumption is valid. Laboratory tests were carefully performed to confirm the magnitudes of these terms. The results clearly show a significant gyro error when the terms are assumed small, stable, and negligible. Author (GRA)

N87-12836 Department of the Navy, Washington, D. C.
FIBER-OPTIC MAGNETIC GRADIOMETER WITH VARIABLE MAGNETIC BIASING FIELDS Patent
Kee P. Koo and George H. Sigel, Jr., inventors (to Navy) Issued 27 May 1986 10 p
(AD-D012423; US-Patent-4,591,786; US-Patent-Appl-SN-641656; US-Patent-Class-324-244) Avail: US Patent and Trademark Office CSCL 17/6

This patent discloses a fiber optic magnetic gradiometer for measuring both ac and dc magnetic field gradient. The gradiometer utilizes an optical interferometer with magnetostrictive magnetic field sensing elements in each of the interferometer arms. Ac and dc magnetic field biasing is achieved by disposing each of the magnetic field sensing elements within its own magnetic field coil and utilizing a variable dc current source for applying dc current to each magnetic coil. An ac current source at frequency w sub o connected across the circuits of the dc current sources is used in conjuction with a variable attenuator to control the ac bias to the respective magnetic coils. The detected output from the interferometer is processed either by bandpass filters or a spectrum analyzer to obtain the signal component w sub o, which is proportional to the external dc gradient magnetifc field, and at w sub o + w sub s, (where w sub s is external ac magnetic field frequency), which is proportional to the external ac magnetic field gradient. GRA

N87-12837# Air Force Weapons Lab., Kirtland AFB, N. Mex.
HOLOGRAPHIC STORAGE IN ION-IMPLANTED, FERROELECTRIC-PHASE PLZT CERAMICS
J. A. Bullington, S. Mancha, R. Carter, R. Heimlich, and C. E. Land (Sandia National Labs., Albuquerque, N. Mex.) 1986 15 p Presented at the International Symposium on Ultrasonics, Ferroelectrics and Frequency Control, Bethlehem, Pa., 9 Jun. 1986 Prepared in cooperation with Sandia National Labs., Albuquerque, N. Mex.
(Contract DE-AC04-76DP-00789)
(DE86-010475; SAND-86-0990C; CONF-8606121-1) Avail: NTIS HC A02/MF A01

Holographic storage has been achieved in thin, optically polished plates of Ni + Ne implanted, ferroelectric-phase PLZT 7/65/35 ceramics using a photoferroelectric storage process first reported in 1976. Exposure energies used for the present experiments were 6 to 7 mJ/cm(2) at 514 nm wavelength which represents an improvement of three orders of magnitude over the photosensitivity of the transverse-field assisted photoinduced change of refractive index in unmodified ferroelectric-phase PLZT reported by Micheron et al. in 1972. DOE

N87-12838# Sandia National Labs., Albuquerque, N. Mex.
DEVELOPMENT OF A LARGE-APERTURE PLZT SHUTTER WITH ENHANCED OPERATIONAL/ENVIRONMENTAL CAPABILITIES
J. O. Harris, Jr., R. P. Cutler, and G. R. Dulleck 1986 6 p Presented at the International Symposium on Ultrasonics, Ferroelectrics and Frequency Control, Bethlehem, Pa., 9 Jun. 1986
(Contract DE-AC04-76DP-00789)
(DE86-011643; SAND-85-2748C; CONF-8606121-2) Avail: NTIS HC A02/MF A01

PLZT thermal/flash protective shutters ranging in size from 25mm to 101mm in diameter have been developed by Sandia National Laboratories for industrial and military applications. A larger diameter shutter, 147mm, with enhanced environmental and operational capabilities was required for window ports. This paper describes a production PLZT shutter which provides these characteristics via the incorporation of new lens sealing techniques, packaging design, polarizers, and electronic subsystems. DOE

N87-12839# Lawrence Livermore National Lab., Calif.
SLITLESS, INTENSIFIED READOUT, GATED SPECTROMETER: WAVELENGTH AND EFFICIENCY CALIBRATION, TIME RESPONSE CHARACTERIZATION
M. Gerassimenko and M. C. Fowler Jun. 1986 9 p Presented at the 30th SPIE Technical Symposium on Optics and Optoelectronic Engineering, San Diego, Calif., 17 Aug. 1986
(Contract W-7405-eng-48)
(DE86-012349; UCRL-94098; CONF-860880-10) Avail: NTIS HC A02/MF A01

A spectrometer has been developed specifically for the X-ray laser effort at Lawrence Livermore National Laboratory (LLNL). The instrument takes advantage of the small divergence and size of the lasing source by positioning all three components - the source, a custom-ruled grating, and a microchannel plate (MCP) detector - on the Rowland circle. The sum of incident and diffracted angles is kept constant. Illuminating a pinhole at the source location with a z-pinch produces wavelength calibration at several energy ranges in the 65- to 200-eV interval. The same source used in conjunction with the MCP camera and Kodak 101 film yields the absolute detector efficiency. Ion bombardment of a beryllium target at the source location produces the X-rays necessary to determine the absolute efficiency of the grating-detector combination at 107 eV. Grating efficiency is then deduced from the MCP efficiency at that energy. Three 25- stripline structures on the MCP allow sub-nanosecond gating of the spectrometer, which improves the signal-to-background ratio. The rise time response of the entire MCP detector-cable assembly is about 200 ps. We also measured the transmission of the filters that are used in suppressing ultraviolet backgrounds. DOE

N87-12840# Sandia National Labs., Albuquerque, N. Mex.
TIME PROJECTION COMPTON SPECTROMETER (TPCS)
G. T. Baldwin and J. R. Lee 1986 24 p Presented at the 23rd Annual Conference on Nuclear and Space Radiation Effects, Providence, R.I., 20 Jul. 1986
(Contract DE-AC04-76DP-00789)
(DE86-012950; SAND-86-0357C; CONF-860706-13) Avail: NTIS HC A02/MF A01

We present a new technique for measuring the energy spectrum of X-rays emitted by high-intensity, medium-voltage flash X-ray sources. The method sorts Compton electrons by drift velocity time-of-flight in a non-uniform magnetic field. We explain the conceptual design of the spectrometer, show how we have modeled it using Monte Carlo methods, and discuss the procedure for unfolding X-ray spectrum information from electron time-of-flight data. The technique appears promising, especially for short-pulse X-ray sources. DOE

N87-12841# Massachusetts Inst. of Tech., Cambridge.
DEVELOPMENT OF AN INEXPENSIVE, HIGH RESOLUTION POSITRON MULTIWIRE PROPORTIONAL COUNTER Progress Report, 1985
1986 13 p
(Contract DE-AC02-78EV-04969)
(DE86-011576; DOE/EV-04969/T5) Avail: NTIS HC A02/MF A01

The 10cm chamber had been used in conjunction with the new reconstruction algorithm. Ongoing investigations are testing system performance, including three-dimensional resolution and contrast ratio for various objects. The chambers have experienced reliability problems, even with the 90% argon-10% ethane mixture. This new gas has helped stability somewhat, but we must still compromise sensitivity by running at less than desired anode voltages. This results in two effects: loss of anode events, and a reduced number of valid cathode events. This translates into a reduced coincidence event rate. Some electronic problems have also developed, resulting in the loss of one anode amplifier in chamber 1 and a non-uniform cathode sensitivity in chamber 2. DOE

N87-12842# Sandia National Labs., Albuquerque, N. Mex.
DOUBLE-ENDED TUNING FORK QUARTZ ACCELEROMETER
W. J. Kass and G. S. Snow 1986 22 p Presented at the 40th Annual Symposium on Frequency Control, Philadelphia, Pa., 28 May 1986
(Contract DE-AC04-76DP-00789)
(DE86-012277; SAND-86-0219C; CONF-8605156-1) Avail: NTIS HC A02/MF A01

Quartz accelerometers with frequency output have been designed and built using etched double-ended tuning fork technology. These devices consist of two tuning forks connected in a cantilever beam configuration with beryllium-copper spacers which serves as a proof mass and inboard spacer. The frequency outputs of each tuning fork resonant circuit are mixed to yield an output frequency of approximately 1kHz at zero acceleration. The sensitivity of the devices is approximately 1Hz/G. The fundamental vibration frequency of the cantilever beam is 2200Hz in this undamped device. Shock testing up to 1500G has indicated good survivability characteristics. Individual fork measurements compared with assembled cantilevers tested in a +- 1G field in the temperature range of -55C to +85C indicate that residual stresses associated with assembly contributes to the temperature sensitivity of the bias frequency. Centrifuge testing has been conducted over the range of 0-120G with an indicated non-linearity of less than 2mG. DOE

N87-12969*# Jet Propulsion Lab., California Inst. of Tech., Pasadena.
RADIOMETRIC CALIBRATION OF THE AIRBORNE IMAGING SPECTROMETER
Deanne Tucker and Gregg Vane *In its* Proceedings of the Second Airborne Imaging Spectrometer Data Analysis Workshop 15 Aug. 1986 p 17-20 (For primary document see N87-12968 04-43)
Avail: NTIS HC A10/MF A01 CSCL 14B

N87-12970*# Stanford Telecommunications, Inc., Sunnyvale, Calif.
COMPARISON OF VARIOUS TECHNIQUES FOR CALIBRATION OF AIS DATA
Dar A. Roberts, Yasushi Yamaguchi (Geological Survey of Japan, Kawasaki.), and Ronald J. P. Lyon *In* JPL Proceedings of the Second Airborn Imaging Spectrometer Data Analysis Workshop 15 Aug. 1986 p 21-30 (For primary document see N87-12968 04-43)
Avail: NTIS HC A10/MF A01 CSCL 14B

36 LASERS AND MASERS

Includes parametric amplifiers.
For related information see also *76 Solid-State Physics.*

N87-12843# Instituto de Pesquisas Espaciais, Sao Jose dos Campos (Brazil).
INFLUENCE OF A STRONG LASER FIELD ON THE STOPPING POWER FOR CHARGED TEST PARTICLES IN FUSION PLASMAS
N. R. Arista, R. M. O. Galvao, and L. C. M. Miranda Aug. 1986 26 p Submitted for publication
(INPE-3977-PRE/988) Avail: NTIS HC A03/MF A01

The influence of a high-intensity electromagnetic wave on the classical energy loss rate of the ion in nondegenerate plasmas is calculated. It is shown that the laser field decreases the plasma stopping power and makes it anisotropic with respect to the polarization of the wave electric field. Author

N87-12844# California Inst. of Tech., Pasadena. Dept. of Applied Physics.
HIGH POWER SEMICONDUCTOR LASER SOURCES Annual Report, 12 Mar. 1985 - 11 Mar. 1986
R. Lang, J. Salzman, and Amnon Yariv 10 Jun. 1986 14 p
(Contract N00014-85-K-0211)
(AD-A168900) Avail: NTIS HC A02/MF A01 CSCL 20/12

Unstable semiconductor lasers have been fabricated and their potential as high power laser sources has been analyzed. GRA

N87-12845# TRW Electronics and Defense Sector, Redondo Beach, Calif.
APPLICATION OF NONLINEAR OPTICS TO FREE ELECTRON LASER SYSTEMS Final Report, Dec. 1984 - May 1986
C. Shih, G. Neil, J. Menders, and T. Yang 6 Jun. 1986 149 p
(Contract N00014-84-C-0668)
(AD-A168950) Avail: NTIS HC A07/MF A01 CSCL 20/5

Novel free electron laser (FEL) resonator concepts employing nonlinear optics techniques were developed in support of advanced FEL technologies. Among these concepts, three major schemes were studied for details as to their potential applications to the ground-based FEL systems: phase conjugate cavity and phase conjugate outcoupling for RF linac FEL resonators, and phase conjugate beam conversion for induction linac FEL devices. These schemes involve the utilization of some novel nonlinear optics techniques that have received very little attention before: multiple pulse stimulated Brillouin scattering, short-pulse four wave mixing, and four wave stimulated Brillouin scattering. Theoretical studies, modeling and proof of principle experiments have been performed to explore these phenomena. The analytical theory and numerical simulation showed the feasibility of these techniques to meet the system requirements and also determined parametrically the operational conditions. The experiments for short-pulse four wave mixing and four wave stimulated Brillouin scattering were conducted in carbon disulfide and acetone media, respectively. The results verified the scaling relations and demonstrated high conjugate reflectivities (about 1000) for a weak signal. GRA

N87-12846# Naval Research Lab., Washington, D. C.
HIGH GAIN FREE ELECTRON LASER OSCILLATORS
W. P. Marable, P. Sprangle, and Cha-Mei Tang 6 Jun. 1986 21 p
(AD-A169002; NRL-MR-5679) Avail: NTIS HC A02/MF A01 CSCL 20/5

We have carried out a fully relativistic, nonlinear analysis of the spatial and temporal evolution of multiple modes within a free electron laser oscillator. The analysis is both analytical and numerical, and is conducted self-consistently with the framework of the Vlasov-Maxwell system of equations, including the collective effects produced by the longitudinal space-charge wave potential. The analytic calculation of the small signal gain yields a dispersion relation for the moderate to high gain (Gamma L $>$ 1) operation of the free electron laser. The numerical simulations verify the analytic results for the linear gain regime and predicts high efficiencies for the nonlinear saturated state of the radiation fields. GRA

N87-12847# District of Columbia Univ., Washington, D. C.
FEASIBILITY OF INVESTIGATING SMITH-PURCELL FREE-ELECTRON LASER CONFIGURATIONS BY ELECTRON ENERGY LOSS STUDIES Final Report, Sep. 1980 - Dec. 1985
Leslie C. Speller and Arthur N. Thorpe (Howard Univ., Washington, D. C.) 9 Jun. 1986 11 p
(Grant DAAG29-80-G-0013)
(AD-A169059; ARO-17852.1-PH-H) Avail: NTIS HC A02/MF A01 CSCL 20/5

An electron beam of energies 20 - 25 KeV was passed over an optical metallic grating (600 lines/mm) and the energy loss spectrum was obtained. The loss peak values, determined to be between approx. (1.8 - 1.9eV), were in fair agreement with the predicted values. However, these results could not be reproduced. GRA

N87-12848# Air Force Academy, Colo.
OPTICAL ROTATION SENSORS Final Report, Oct. 1980 - Nov. 1985
James R. Rotge, Bill J. Simmons, G. Thomas Kroncke, and Daniel J. Stech May 1986 44 p
(AD-A169357; FJSRL-TR-86-0002) Avail: NTIS HC A03/MF A01 CSCL 17/7

Research efforts were concentrated on passive ring laser rotation sensor technology. Initial efforts were performed on supportive projects, e.g., laser stabilization, followed by a 0.62 sq m passive resonant ring laser gyro (PRRLG), leading to the development of a 60 sq m system mounted on the pneumatically supported isolation test platform (Iso-Pad) at FJSRL. Numerous sub-system tasks and a feasibility 0.62 sq m PRRLG were completed, supporting projections of very high resolution performance by a large 60 sq m PRRLG. The expected performance of the large PRRLG, on the order of 10 to the minus 10th power ERU (earth rate units), would provide an accurate error model applicable to Air Force operational ring laser gyros, a new source of geophysical data, e.g., earth wobble and variations in earth rotation, a proven design concept applicable to Air Force sensor needs as reference to MX instruments tests, and relativity experiments. This report documents the many accomplishments leading to, and the status of the large PRRLG at the date of the PRRLG stop order, November 1985. GRA

N87-12849# Boeing Aerospace Co., Seattle, Wash.
FEL (FREE ELECTRON LASER) OPTICS COATING TEST PROGRAM (DESIGN PHASE OF SAMPLE INTRODUCTION CHAMBER) Final Report
John L. Adamski and David A. G. Deacon Feb. 1986 76 p
(Contracts N00014-85-C-0039; ARPA Order 9031)
(AD-A169474) Avail: NTIS HC A05/MF A01 CSCL 20/5

The performance of the free electron laser for the directed energy weapons application depends critically on only three technologies: the high brightness accelerator, the FEL amplifier, and the cavity optics. The goal of this program is to examine the performance of the optical elements under the combined loading of the fundamental and the harmonic emissions of the FEL amplifier. The performance of both the RF linac based FEL and the induction linac based FEL may be subject to significant limitations due to UV-induced absorption in the early optical elements following the FEL amplifier. These limitations are expected to appear suddenly at a certain fluence level, with little warning. Our central objective in this program is to measure the rate of the UV induced absorption, and to identify the scaling parameters so that we can predict with some confidence the performance limitations of the optics. When these limits are reached in the experimental programs, a knowledge of the scaling relations and possible countermeasures will be invaluable in planning an appropriate response to the problem. GRA

N87-12850# Department of the Army, Washington, D. C.
CYLINDRICAL LASER WELDER Patent Application
Thomas E. Honeycutt and Thomas G. Roberts, inventors (to Army) Filed 15 May 1986 7 p
(AD-D012398; US-Patent-Appl-SN-864638) Avail: NTIS HC A02/MF A01 CSCL 13/9

Brass retainer rings are currently fastened to artillery shells by spinning each shell at a high rate and then jamming the ring on it so that it is fastened or welded by friction between the two objects. This is an energy-inefficient process which heats and weakens more material than is desirable. The shell spinning at a high rate is also potentially dangerous. A laser welder is provided that generates output energy focused on a circular or cylindrical shape for simultaneously welding around a 360 degs circumference without unnecessarily heating large amounts of material. The welder may be used to fasten cylindrical shaped objects, gears and shafts together, which is difficult to do by conventional means. The welder may also be used to fasten one cylinder to another. To accomplish the welding, a laser has an unstable optical cavity arranged with its feedback mirror centered to generate a circular output beam having an obscuration in the center. A circularly-symmetric, off-axis concave mirror focuses the output beam onto the objects being fastened and away from the center line or axis of the circular beam. GRA

N87-12851# Rochester Univ., N. Y. Dept. of Chemistry.
HETEROGENEOUS CATALYSIS WITH LASERS Final Report, 1 Jun. 1980 - 31 Aug. 1986
Thomas F. George Jun. 1986 14 p
(Contract N00014-80-C-0472)
(AD-A169601; UROCHESTER/DC/85/TR-72) Avail: NTIS HC A02/MF A01 CSCL 07/5

Theoretical techniques have been developed to describe a variety of laser-induced molecular rate processes occurring at solid surfaces which are involved in heterogeneous catalysis. Such processes include adsorption, migration, chemical reactions and desorption. The role of surface phonons in laser-selective processes and laser heating has been analyzed. The importance of electronic degrees of freedom has been considered for semiconductor and metal substrates, with special emphasis on the laser excitation of surface states. Surface-modified photochemistry has also been investigated, where the effect of a metal surface on the resonance fluorescence spectrum of a laser-driven atom/molecule has been assessed by means of surface-dressed optical Bloch equations. It is seen that the spectrum can be significantly different from the gas-phase case. Two related gas-surface collision processes have also been studied. First, the feasibility of the formation of the electron-hole pairs in a semiconductor by vibrationally excited molecules has been explored. Second, charge transfer in ion-surface collisions has been examined for both one-electron and two-electron transfer processes. Work has been initiated on microstructures and rough structures, including clusters and surface gratings. GRA

N87-12852# Rockwell International Science Center, Thousand Oaks, Calif.
IODINE MONOFLUORIDE ENERGY TRANSFER STUDIES Final Report, 13 Jun. 1983 - 31 Oct. 1984
A. T. Pritt Jun. 1986 77 p
(Contract F29601-83-C-0048)
(AD-A169781; SC5366.51FR; AFWL-TR-85-04) Avail: NTIS HC A05/MF A01 CSCL 20/5

Electronic-to-electronic (E-E) energy transfer from NF(b superscript 1 sigma +) to IF(X superscript 1 sigma +), producing IF(B superscript 3 Pi(O+)), was investigated using both spatially resolved data from a chemiluminescence flow tube apparatus and temporarily resolved data following pulsed excitation in a flow tube. The b superscript 1 sigma + state of NF was generated by the F-HN3 reaction under steady-state flow tube conditions and by the NF(a superscript 1 delta)+I* pooling reaction for the temporally resolved studies. Results of this study show that the source of IF(B superscript 3 Pi(O+)) in these chemiluminescence reactions stems from E-E energy transfer, that the rate of the transfer reaction depends strongly on the vibrational distribution in the ground state of IF, that the rate is independent of the vibrational distribution in the NF(b superscript 1 sigma +), and that the efficiency of the transfer rate is greater than 20%. The rate constant for the E-E energy transfer was measured to be 1.5 + or - 0.2 x 10 to the

-11 power cc/molecule/s for an IF(x superscript 1 sigma +) vibrational distribution corresponding to 800 K. These results are explained in terms of an energy transfer mechanism requiring that the individual state-to-state rates are proportional to the probabilities associated with vertical transitions. GRA

N87-12853# California Univ., Los Angeles.
HIGH REPETITION RATE ELECTRON BEAM RF-ACCELERATION AND SUB-MILLIMETER WAVE GENERATION VIA A FREE ELECTRON LASER Report, 15 Aug. 1985 - 14 Feb. 1986
N. C. Luhmann, Jr. and D. B. McDermott 14 Feb. 1986 6 p
(Contract N00014-84-K-0569)
(AD-A169846; AD-E750914) Avail: NTIS HC A02/MF A01 CSCL 20/5

We investigate through numerical simulation the advantages of a multicavity linac for improving the quality of the electron beam due to the technique of phase synchronism. This will also increase the shunt resistance of the accelerator which is desirous if very high energy is the goal. However, if a particular energy is required, then the shunt resistance must be held constant. Fortunately, a cavity's quality factor, Q, is approximately inversely proportional to its length if its aspect ratio is much less than one. Therefore, the shunt resistance can be controlled by varying the length of the cavities. GRA

N87-12854# Department of the Army, Washington, D. C.
DOPPLER EFFECT LASER VELOCITY MEASURING SYSTEM Patent
George R. Edlin, inventor (to Army) Issued 17 Jun. 1986 8 p
(AD-D012401; US-Patent-4,595,287; US-Patent-Appl-SN-571766; US-Patent-Class-356-28.5) Avail: US Patent and Trademark Office CSCL 20/6

The frequency shift of reflected laser beam from a target is transformed into an angular measurement which is proportional to the velocity of the target relative to the measurement platform. The system uses the refraction angle of the reflected beam from a movable optical grating to produce the angular measurement. GRA

N87-12855# Toronto Univ. (Ontario). Chemical Labs.
STUDY IN MOLECULAR LASERS Final Report, 1 Jun. 1984 - 31 May 1985
George Burns Aug. 1985 7 p
(Grant AF-AFOSR-0127-84)
(AD-A169933; AFOSR-86-0422TR) Avail: NTIS HC A02/MF A01 CSCL 07/4

Principal progress was achieved in the field classical studies of diatom dissociation. 3-D trajectory calculations of dissociating bromine and fluorine were conducted over a range of temperatures, and using several significantly different potential energy surfaces. A library consisting over a two million trajectories was accummulated. These trajectories were used to test the strong collision assumption, important in several theories of unimolecular reactions and in some theories of thermal diatom dissociation. The assumption was shown to be not valid for the case of dissociating bromine and fluorine. Properties of the steady state of dissociating diatoms were investigated. Papers, now in preparation, involve study of nonequilibrium energy and angular momentum distribution functions; accumulation, interpretation and classification of data on inelastic and reactive collisions; and study of scaling factors and vibrational-rotational coupling in dissociating diatoms. Experiments, still in progress, aimed at measuring recombination rates of fluorine atoms. Time delayed photoelectric effect was explained in terms of a release of trapped electrons at the surface of photocathode. GRA

N87-12856# Illinois Univ., Urbana. Charged Particle Research Lab.
OPTICAL PUMPING OF HIGH POWER LASERS WITH AN ARRAY OF PLASMA PINCHES Final Report, 1 Nov. 1981 - 31 Oct. 1984
Kyekyoon K. Kim 1 Apr. 1986 31 p
(Grant AF-AFOSR-0017-82)
(AD-A169960; AFOSR-86-0479TR) Avail: NTIS HC A03/MF A01 CSCL 20/5

Two dense plasma focus systems, the hypocycloidal pinch and the Mather type were investigated as the potential excitation light sources for high energy, short wavelength lasers. Using the hypocycloidal pinch (HCP), extensive lasing experiments were successfully performed, for the first time, on organic dyes producing results indicative of the capabilities and limitations the HCP system as an optical pump. A proof of principle lasing experiment was also performed for the first time using the Mather type dense plasma focus (MDPF) sucsessfully. Results thus far indicate that both HCP and MDPF are excellent high energy, short wavelength optical pumps and that as an optical pump, the MDPF system is more versatile, efficient, and powerful than the HCP system, especially in the short wavelength spectral region. GRA

N87-12857 Department of the Navy, Washington, D. C.
RESONANT PHOTON PUMPING MECHANISMS FOR A PLASMA X-RAY LASER Patent
Raymond C. Elton, inventor (to Navy) Issued 27 May 1986 7 p
Supersedes AD-D010901
(AD-D012416; US-Patent-4,592,056; US-Patent-Appl-SN-569686; US-Patent-Class-372-5) Avail: US Patent and Trademark Office CSCL 20/5

This patent discloses a lasing system for lasing at X-ray wavelengths. In one embodiment, a neon-like sulfur ion S(6+) plasma is caused to radiate on its 3d to 2 p transition to pump a lithium like neon Ne(7+) plasma to obtain X-ray lasing. In a second embodiment, a lithium-like silicon Si(11+) ion plasma is caused to radiate on the 3d to 2p transition to pump lithium like magnesium Mg(9+) plasma to obtain X-ray lasing. GRA

N87-12858# Battelle Columbus Labs., Ohio.
LASER PRODUCED X-RAY FOR HIGH RESOLUTION LITHOGRAPHY AND A PHOTOIONIZATION LASER Final Report
Harold Epstein, Dave Applebaum, and Bernerd Campbell 14 Feb. 1986 83 p
(Grant AF-AFOSR-0066-82)
(AD-A170782; AFOSR-86-0553TR) Avail: NTIS HC A05/MF A01 CSCL 20/6

The majority of the project was spent investigating laser produced X rays for high resolution lithography. This work involved measurements over an extensive parameter matrix. Specifically, efficiency of conversions to X rays was qualified as a function of: (1) laser pulse energy, (2) laser pulse width, (3) plasma profile, (4) laser wavelength, (5) target atomic number, (6) initial focal area, and (7) focal ratio of the lens. Experimental research was performed on a photoionization X ray laser concept. Specifically, a thin polyethylene, oxidicarbonate film was vaporized. Fifteen nanoseconds into its expansion, the vapor was illuminated by a 200 psec Fe spectrum X ray pulse. Photoionization of the inner K shell of oxygen was then observed. The potential efficiency of this type of laser was found to be comparatively low. GRA

N87-12859# Yale Univ., New Haven, Conn.
POPULATION INVERSIONS IN LASER-INITIATED VACUUM ARCS Final Report, 1 Feb. 1981 - 31 Jan. 1986
Mahadevan Krishnan and Gary L. Haller 17 Jun. 1986 77 p
(Grant AF-AFOSR-0077-81)
(AD-A170811; AFOSR-86-0522TR) Avail: NTIS HC A05/MF A01 CSCL 20/3

Population inversions were studied in laser initiated vacuum arcs. Inversion mechanisms include three body recombination pumping in expanding, laser produced plasmas, and resonant photoexcitation using line radiation. Significant gain was measured on the Balmer lines H sub alpha and H sub beta in expanding, laser produced plasmas of carbon/polyethylene. Research then focused on resonant photoexcitation of one ion by line radiation from another ion. Fluorescence was measured at UV wavelengths in CII pumped by Al III. A new class of photoexcited lasers was identified, in Be like ions, with wavelengths from 2177A in C III pumped by Mn VI, to 200 A in Mg IX pumped by Al XI. Fluorescence

and small signal gain were measured in C III pumped by Mn VI. Finally, laser oscillation was demonstrated in C III at 2177 and 2163A. These are the first UV lasers to be pumped by resonant photoexcitation. By isoelectronic scaling, it should be possible to produce soft X-ray lasers using the principles elucidated by this research. Photopumped lasers could prove to be the most efficient soft X-ray lasers in the future. GRA

N87-12860# Sandia National Labs., Albuquerque, N. Mex.
KINETIC AND THERMODYNAMIC STUDIES OF PULSED LASER IRRADIATION
P. S. Peercy and M. O. Thompson 1986 10 p Presented at the Society of Photo-Optical Instrumentation Engineers International Symposium: Topics in Optical and Optoelectronic Applied Sciences and Engineering, Quebec City, Canada, 2 Jun. 1986 Prepared in cooperation with Cornell Univ., Ithaca, N.Y.
(Contract DE-AC04-76DP-00789)
(DE86-012175; SAND-85-2830C; CONF-860620-8) Avail: NTIS HC A02/MF A01

Simultaneous measurements of the transient conductance, to determine the molten layer thickness versus time, and the time-dependent surface reflectance, to determine the melt duration at the surface during pulsed laser irradiation, are reviewed. These real-time measurements have been applied in a variety of studies of Si and Si-based alloys. In crystalline Si, melt initiates at the surface and propagates to some depth, whereupon the motion of the liquid/solid interface reverses and the material solidifies. In amorphous Si, these measurements were used to determine the melting temperature of the amorphous phase and the mechanism by which explosive crystallization occurs. In Si implanted with impurities, combined transient conductance and reflectance measurements reveal the occurrence of such novel melt and solidification scenarios as internal nucleation of melt and surface nucleation of solid on molten Si. Internal melts, which were previously unexpected, appear to be quite common and explain unusual microstructures observed by TEM. DOE

N87-12861# Sandia National Labs., Albuquerque, N. Mex.
REACTOR-PUMPED LASER EXPERIMENTS IN THE SANDIA SPR-3 FACILITY
D. A. McArthur, G. N. Hays, D. R. Neal, P. S. Pickard, and J. K. Rice 1986 15 p Presented at the Fast Burst Reactor Workshop, Albuquerque, N. Mex., 8 Apr. 1986
(Contract DE-AC04-76DP-00789)
(DE86-012163; SAND-86-1011C; CONF-860420-4) Avail: NTIS HC A02/MF A01

Experiments on the excitation of short-wavelength gas lasers have recently been performed in the central cavity of the Sandia fast burst reactor SPR-III. Small-signal gain coefficients approx. 0.7%/cm were measured in XeF laser mixtures excited with either the He-3 (n,p)T reaction or with fission fragments emitted from the wall of the laser cell. Specialized apparatus helpful in performing these measurements is described. Preliminary experiments included measurement of radiation effects on cell window materials and laser mirrors, and measurement of energy deposition in the laser gas as a function of time for various cell geometries and polyethylene moderator thicknesses. The optical distortion of the laser medium by the energy deposition process was much more severe for fission fragment excitation. Fluorescence spectra were also measured for XeF laser mixtures with an optical multichannel analyzer, and these spectra were consistent with the XeF gain measurements. DOE

N87-12862# Naval Research Lab., Washington, D. C.
COMPARISON OF RAYLEIGH-TAYLOR GROWTH WITH 1.0 M AND 0.25 M LASERS
M. H. Emery, J. H. Gardner, and S. E. Bodner 29 May 1986 13 p
(DE86-012217; NRL-MR-5796) Avail: NTIS HC A02/MF A01

It is shown through numerical simulation that the Rayleigh-Taylor growth rate in laser-ablatively accelerated targets is reduced below the classical value (kg)(sup 1/2), by factors of 3 to 4 with 0.25 micron laser light. The simulation results are supported by an analytical expression for the growth rates. These results provide further evidence for the viability of high-aspect ratio shells in direct-drive laser fusion. DOE

N87-12863# Los Alamos National Lab., N. Mex.
CO SUB 2 LASER SUSTAINED CW DISCHARGE ATOMIC BEAM SOURCE
J. B. Cross, D. A. Cremers, L. H. Spangler, M. A. Hoffbauer, and F. A. Archuleta 1986 11 p Presented at the 15th International Symposium on Rarefied Gas Dynamics, Grado, Italy, 16 Jun. 1986
(Contract W-7405-eng-36)
(DE86-012383; LA-UR-86-1943; CONF-860636-3) Avail: NTIS HC A02/MF A01

A high pressure, supersonic, laser sustained plasma nozzle beam source was developed for the production of intense (greater than 10 to the 19th power particles/s/sr) beams of atomic and/or radical species having kinetic energies in the range of 1 to 10 eV. A high plasma temperature (10 to 30,000 K) is produced in the throat of a hydrodynamic expansion nozzle by sustaining a CW optical discharge in a gas using a high power CW CO2 laser. Gas mixtures are expanded through the nozzle/discharge region creating energetic atoms and molecules. An oxygen atom beam was produced with a kinetic energy of 2 to 3 eV and an intensity of approximately 10 to the 18th power O-atoms/s/sr. O-atom collisions (1 eV) from an uncharacterized nickel surface shows strong specular scattering with approximately 50% energy loss to the surface. Argon beams having kinetic energies between 5 to 10 eV with intensities of greater than 10 to the 19th power atoms/s/sr were also produced. DOE

N87-12864# Los Alamos National Lab., N. Mex.
THEORY AND SIMULATION OF HIGH-BRIGHTNESS ELECTRON BEAM PRODUCTION FROM LASER-IRRADIATED PHOTOCATHODES IN THE PRESENCE OF dc AND RF ELECTRIC FIELDS
M. E. Jones and W. Peter 1986 14 p Presented at the 6th International Conference on High Power Particle Beams, Kobe, Japan, 9 Jun. 1986
(Contract W-7405-eng-36)
(DE86-012384; LA-UR-86-1941; CONF-860665-7) Avail: NTIS HC A02/MF A01

To take advantage of properties of laser-controlled photodiodes to produce electron beams, a new set of diode design criteria are needed. An analytical and numerical study of the geometrical and temporal factors that affect the design of high-brightness electron beams is presented. This study extends our previous work on this concept to include the effects of laser pulse shape, and emittance effects in the presence of RF fields. In general, the diode will not be space-charge limited. Therefore, the conventional Pierce electrode shapes are not appropriate. Furthermore, the finite temporal profile of the electron beams introduces a time-dependent space charge into the design problem. The approach taken here to minimize the emittance growth from the temporal profile of the space charge is to operate at low perveance. To obtain high currents, large electric fields are required. We exploit the fact that the electron emission is controlled by the laser and is independent of the voltage on the diode. The diode can then be driven by an rf field. In principle, operating at higher frequency al lows higher breakdown limits, so the perveance can be made very small. However, operating at too high an RF frequency introduces other detrimental effects. DOE

N87-12865# California Univ., Berkeley. Lawrence Berkeley Lab.
HIGH-GAIN FREE ELECTRON LASERS AS GENERATORS OF SHORT WAVELENGTH COHERENT RADIATION
K. J. Kim and C. Pellegrini (Brookhaven National Lab., Upton, N. Y.) May 1986 10 p Presented at the Topical Meeting on Short Wavelength Coherent Radiation: Generation and Application, Monterey, Calif., 24 Apr. 1986 Prepared in cooperation with Brookhaven National Lab., Upton, N.Y.
(Contract DE-AC03-76SF-00098)
(DE86-012500; LBL-21562; CONF-8604220-1) Avail: NTIS

HC A02/MF A01

The development of coherent radiation in high-gain free electron lasers, either from initial noise or from low-power input radiation, is analyzed in terms of three-dimensional Maxwell-Klimontovich equations. Exponential growth and saturation, transverse radiation profiles, transverse coherence and spectral features are discussed. Two possible systems of high-gain free electron lasers, one based on a storage ring and by-pass, another based on a linac and damping rings, are considered for the generation of 400 A radiation. DOE

N87-12866# Los Alamos National Lab., N. Mex.
MOESSBAUER-BORRMANN SUPERRADIANCE
G. C. Baldwin, M. S. Feld, J. P. Hannon, J. T. Hutton, and G. T. Trammell 1986 12 p Presented at the International Colloquium on X-ray Lasers, Aussois, France, 14 Apr. 1986 Prepared in cooperation with Massachusetts Inst. of Tech. and Rice Univ.
(Contract W-7405-eng-36)
(DE86-012373; LA-UR-86-2010; CONF-8604224-2) Avail: NTIS HC A02/MF A01

The kinetic behavior of a gamma-ray laser is comprised of an array of isomeric nuclei located at regular lattice sites in a perfect single crystal of dimensions and structure so chosen as to favor anomalous emission into that Borrmann mode having the maximum possible number of component Bragg-reflected beams, which greatly reduces the excitation requirements. The analysis of several hypothetical systems shows that superradiance, rather than amplified spontaneous emission, will then be the preferred mode of deexcitation, provided the nuclei can be pumped rapidly to a short-lived Moessbauer level while preserving crystal integrity. This warrants a search for solutions to the major problems: candidate nuclides, preparation of a storage isomer, and interlevel transfer from storage to lasing state. DOE

N87-13286# Plessey Co. Ltd., Romsey (England).
A STUDY OF METHODS OF PHASE NOISE REDUCTION OF SEMICONDUCTOR LASERS FOR SENSOR APPLICATIONS
J. P. Dakin and P. B. Withers *In* AGARD Guided Optical Structures in the Military Environment May 1986 7 p (For primary document see N87-13273 04-74)
Avail: NTIS HC A14/MF A01

N87-12717# Joint Publications Research Service, Arlington, Va.
STATUS OF LASER ENRICHMENT TECHNOLOGY UPDATED
Yasushi Sakabe *In its* Japan Report: Science and Technology (JPRS-JST-86-023) 29 Aug. 1986 p 63-69 Transl. into ENGLISH from Purometeusu (Tokyo, Japan), Nov. 1985 p 41-43 (For primary document see N87-12715 04-31)
Avail: NTIS HC A04/MF A01

37 MECHANICAL ENGINEERING

Includes auxiliary systems (nonpower); machine elements and processes; and mechanical equipment.

N87-12867 California Univ., Los Angeles.
ON THE DEXTERITY OF ROBOTIC MANIPULATORS Ph.D. Thesis
ZoneChang Jim Lai 1986 195 p
Avail: Univ. Microfilms Order No. DA8606465

The dissertation deals with the dexterity of 6R manipulators. It consists of four parts. In the first part, the characteristics of a robot's service angle to a given point are studied by introducing the concepts of service sphere and free service region. It is shown that the entire service angle can be categorized into a number of free service regions. The relationship between the service angle and service regions is subsequently formulated into a set of theorems and criteria. In the second part, the singularity problem of six-link robots is investigated. This problem is studied by introducing the concepts of singular state with finite internal degree-of-freedom and singular state with infinitesimal internal degree-of-freedom. A set of theorems and corollaries about a robot's singular states are presented. The third part investigates the motion characteristics of a six-link robot when its hand is considered to be attached to a given point with a ball-and-socket joint. The characteristics of the locus of joint six in the neighborhood of some interesting points is studied. The fourth part studies the dexterity of various wrist structures. In this part, a general wrist, with its last link having common normal and twist angle equal zero, is first investigated. Later, both Euler-Angle and Roll-Pitch-Yaw wrists are studied in detail. Conditions which govern the superiority between these two wrist structures over each other are derived. Dissert. Abstr.

N87-12868 ESDU International Ltd., London (England).
FRICTIONAL AND RETARDING FORCES ON AIRCRAFT TYRES. PART 4: ESTIMATION OF EFFECTS OF YAW
Sep. 1986 29 p
(ESDU-86016-Pt-4; ISBN-0-85679-568-2; ISSN-0141-4054) Avail: ESDU

Available as part of the ESDU Sub-series on Aircraft Performance, this ESDU gives expressions and data for calculating the forces and moments acting on the tire-ground contact area during unbraked and braked yawed rolling. The methods have been verified against experimental data drawn from a wide range of sources in the literature for speeds up to 100 knots, for a wide range of tire sizes, inflation pressures, vertical loads and runway surface conditions. Applications include estimation of minimum control speed on the ground and investigation of stopping performance with asymmetric reverse thrust and/or asymmetric braking and/or cross winds and/or low friction surface. ESDU

N87-12869*# National Aeronautics and Space Administration. Ames Research Center, Moffett Field, Calif.
THE EVALUATION OF A NUMBER OF PROTOTYPES FOR THE FREE-TIP ROTOR CONSTANT-MOMENT CONTROLLER
Larry A. Young Feb. 1986 76 p
(NASA-TM-86664; A-85059; NAS 1.15:86664) Avail: NTIS HC A05/MF A01 CSCL 01C

The development of several prototypes of a constant moment controller, a critical component of the free-tip rotor (FTR) concept, is described. Also presented are the experimental results of a whirl test designed to select a final controller configuration to be included in a future wind-tunnel test of this innovative rotor system. A brief explanation of the FTR concept and its history are included. The paper documents the controller design constraints, each prototype's operating principle, the evaluation test, and the individual prototype test results. A recommended design is identified, along with the selection rationale. Author

N87-12870# Wisconsin Univ., Madison. Engine Combustion Lab.
DIESEL CYLINDER GAS-SIDE HEAT FLUX TO A CERAMIC SURFACE Final Report, 18 May 1981 - 30 Jun. 1985
Gary L. Borman and Jeffrey C. Huang 1 Jun. 1986 42 p
(Contract DAAG29-81-K-0082)
(AD-A168948; ARO-18188.3-EG) Avail: NTIS HC A03/MF A01 CSCL 21/7

Results of four research projects each dealing with instantaneous heat flux to the cylinder head of reciprocating engine are given. The projects are: heat flux measurements in a diesel engine with variations in injection pressure, nozzle tips and swirl; development of instrumentation for radiation measurements in a diesel cylinder; heat flux measurements to various surfaces on the head of diesel engine including a normaly cooled metal surface, an insulated metal surface and a zirconia surface; and initial attempts to simultaneously measure the fluid motion and heat flux in a motored engine boundary layer. The variation of injection pressure nozzle tips and swirl in a direct injection diesel showed strong coupling between combustion and heat flux. An instrument for radiation measurement which uses a wall jet to reduce convection is described. Compression of the jet by the combustion heat release prevents zeroing of the convection. The major portion of the research was devoted to heat flux measurements to the surface of an instrumentation plug in the head of a single

TACOM-LABECO diesel. Comparisons made between data for insulated and uninsulated surfaces show that the hot metal surface gave reduced time averaged heat transfer, but gave a higher peak heat flux than a normally cooled surface. Data for zirconia plate surface showed a reduction in peak flux which was larger than predicted from the rise in surface temperature alone. GRA

N87-12871# Office of Naval Research, London (England).
WELDING RESEARCH IN SCANDINAVIA: AN ASSESSMENT
Kenneth D. Challenger 11 Jun. 1986 8 p
(AD-A169036; ONRL-R-2-86) Avail: NTIS HC A02/MF A01 CSCL 11/6

This report briefly describes the contributions that the Scandinavian countries--Denmark, Finland, Norway, and Sweden--are making. Topics which should be closely followed by US researchers are: hyperbaric welding, computer aided design/computer aided manufacturing, applications to welding, mathematical modeling of the weld process, and hydrogen assisted cracking of steel welds. GRA

N87-12872# National Aeronautical Establishment, Ottawa (Ontario).
LITERATURE REVIEW ON THE DESIGN OF COMPOSITE MECHANICALLY FASTENED JOINTS
C. Poon Feb. 1986 71 p
(AD-A169112; NAE-AN-37; NRC-25442) Avail: NTIS HC A04/MF A01 CSCL 13/5

This report presents a literature review of the state-of-the-art analytical and experimental methodologies adopted in the aerospace industry for the design of mechanically fastened joints in composite structures. Results and conclusions obtained from the published literature relating to the effects of critical parameters, which include composite material system, fastener configuration and joint geometry, on the mechanical behavior and failure modes of composite mechanically fastened joints are discussed. Further research required to improve the design of composite mechanically fastened joints is identified as a result of this review. GRA

N87-12873# Office of Naval Research, London (England).
WELDING SCIENCE AND TECHNOLOGY IN EUROPE: A SURVEY AND ASSESSMENT
Kenneth D. Challenger 20 Jun. 1986 12 p
(AD-A169279; ONRL-R-3-86) Avail: NTIS HC A02/MF A01 CSCL 13/8

Welding research is organized and coordinated differently within each country, but the International Institute of Welding, serves to coordinate the results on an international scale. The UK, West Germany, and Scandinavia are leading the technological progress in Western Europe, but Eastern Europe places more emphasis on welding research than does the West. In all of Europe the research tends to be applied rather than basic. This report includes a list of key people. GRA

N87-12874# Department of the Air Force, Washington, D.C.
SUPER GRIPPER VARIABLE VANE ARM Patent Application
G. E. Ludwick, inventor (to Air Force) Filed 27 Mar. 1986 12 p
(AD-D012364; US-Patent-Appl-SN-844636) Avail: NTIS HC A02/MF A01 CSCL 13/5

This patent application discloses a variable vane assembly which entails a vane arm which integrally engages with a vane stem without the use of threaded fasteners. The vane stem has a tip with parallel slots on opposite sides which are spaced below the end of the tip. At the end of the tip is an end slot which is perpendicular to the parallel slots. The tip of the vane stem has a ramped side parallel with the end slot. The vane arm is a flat wide metal strip that serves as the vane blade and integrally connects with the end slot. The vane arm is a flat wide metal strip that serves as the vane blade and integrally connects with the vane stem using two ears, which are turned inwards to engage with the parallel slots in the vane stem. Additionally, a central leaf exists between the two ears which turns downwards to fit in the end slot in the tip of the vane stem. The central leaf thereby acts as an axial retainer and allows the vane arm to be rotated with the rotation of the vane stem. GRA

N87-12875# Department of the Air Force, Washington, D.C.
SLIDING DUCT SEAL Patent Application
Andrew MacGee, inventor (to Air Force) Filed 24 Apr. 1986 14 p
(AD-D012369; US-Patent-Appl-SN-855243) Avail: NTIS HC A02/MF A01 CSCL 11/1

A seal assembly for forming an air seal around conduits or accessories crossing aircraft engine bypass ducts is discussed. The seal assembly comprises a seal retainer plate, a seal plate and a seal ring. The seal ring has two opposingly spring legs which seat and form air seals at the duct wall and the seal plate. GRA

N87-12876# Department of the Air Force, Washington, D.C.
MULTI USE GRIPPER FOR INDUSTRIAL ROBOT Patent Application
Steven P. Jones, inventor (to Air Force) Filed 21 Apr. 1986 17 p
(AD-D012371; US-Patent-Appl-SN-854234) Avail: NTIS HC A02/MF A01 CSCL 13/9

This document describes a robot gripping device for holding and gripping a variety of electronic components. The robot gripping device comprises a guide frame, a drive motor and gripping blocks having fingers. One finger has three prongs on a fingertip. Another finger has two prongs on a fingertip. The fingertips accommodate axial resistor-type components at v-grooves and radial capacitor-type components are accommodated by fingertip portions. Cylindrical can shaped components are accommodated by a slight beveling at fingertip portions as well as a set back of portion on prong. The fingers are capable of controlled movements to various centered positions by means of motor. When the fingers are brought together they interlock. Author (GRA)

N87-12877# Department of the Air Force, Washington, D.C.
SHOCK ABSORBING DEVICE WITH INTEGRAL PRESSURE RELIEF VALVE Patent Application
Robert L. Franzen, inventor (to Air Force) Filed 25 Nov. 1985 22 p
(AD-D012379; US-Patent-Appl-SN-801341) Avail: NTIS HC A02/MF A01 CSCL 13/7

This patent application discloses a liquid spring shock absorbing device, comprising an hydraulic piston with an integral surge valve. The hydraulic piston is positioned within a fluid filled piston housing and is made up of a piston body, a spring reaction plate and a piston head. A large belleville spring and a small belleville spring are positioned adjacent to the spring reaction plate. Short duration shocks are transmitted by the fluid to cause rotation of the small belleville spring which opens relief valve port. Long duration, high intensity shocks cause compression of both belleville springs, opening of relief valve port and movement of hydraulic piston. GRA

N87-12878# Department of the Air Force, Washington, D.C.
OVER-CENTER TOGGLE LATCH Patent
Farley T. Hinds, inventor (to Air Force) Issued 13 May 1986 4 p Supersedes AD-D011753
(AD-D012393; US-Patent-4,588,216; US-Patent-Appl-SN-640623; US-Patent-Class-292-113) Avail: US Patent and Trademark Office CSCL 13/5

An improved low profile over-center toggle latch having a latch arm with an internally threaded latch barrel nut for adjustable cooperation with a threated latch draw bolt is presented. The bolt is pivotally coupled to a latch handle assembly. The latter comprises projecting sidewalls and a grip end. The latch handle assembly is mounted by means of integral flanges cooperating with journals defined in a mounting stirrup, the latter being mounted on the container body. GRA

N87-12879# Department of the Air Force, Washington, D.C.
MULTIPLE RATE SHOCK ISOLATOR DAMPING VALVE Patent

Robert M. Foster, inventor (to Air Force) 13 May 1986 8 p Supersedes AD-D011429
(AD-D012394; US-Patent-4,588,053; US-Patent-Appl-SN-651961; US-Patent-Class-188-275) Avail: US Patent and Trademark Office CSCL 13/7

In this patent a hydraulic shock isolator damping valve exhibiting variable damping on degree of valve extension is described which comprises a hydraulic cylinder defining closed fluid reservoirs at each end, a piston within the cylinder and interconnecting the structural members between which relative movement is damped, the piston having first and second axially spaced portions sized for slidably engaging the inner surface of the cylinder and including an intermediate third axial portion of reduced outer diametric size, the first and second portions including a predetermined number of axial holes sized for displacement of fluid through the piston in response to movement of the piston through the piston in response to movement of the piston through the fluid, and an annular member of outer diameter smaller than the first and second portions slidable on the third portion between confronting surfaces of the first and second portions, the annular member including a pair of peripheral flanges, each including axial holes smaller in size and corresponding in number to and registering with axial holes is the first and second portions. GRA

N87-12880# Department of the Air Force, Washington, D.C.
SELF-LOCKING OUTER AIR SEAL WITH FULL BACKSIDE COOLING Patent Application
George Liang, inventor (to Air Force) Filed 12 May 1986 14 p
(AD-D012406; US-Patent-Appl-SN-861908) Avail: NTIS HC A02/MF A01 CSCL 11/1

This patent application describes an air seal assembly for a gas turbine engine comprising a full ring cover plate and seal segment attached to impingement boxes. The impingement boxes have counter mounted hooks that interlock with a turbine flange and cover plate to secure the seal assembly. Holes in the impingement boxes direct cooling air to the entire backs the of seal. Seals are mounted to the impingement boxes by pedestals are positioned to enhance seal flexibility since axial edges are unrestrained. GRA

N87-12881# Department of the Air Force, Washington, D.C.
IMPROVED VANE PLATFORM SEALING AND RETENTION MEANS Patent Application
George A. Bonner, inventor (to Air Force) Filed 12 May 1986 16 p
(AD-D012407; US-Patent-Appl-SN-861905) Avail: NTIS HC A02/MF A01 CSCL 11/1

This patent application describes improved vane platform feather seal is disclosed for use in turbine engines. This feather seal contains a flat, thin feather seal, which is attached by adhesive to ease assembly to an L-shaped retainer plate to result in a combined thickness of 0.032 inches. This new seal may be used to replace the inner vane platform seals which are currently used in F-100 turbine engines, which have a history of not bending easily to conform to seal slots. The new seal provides improved platform sealing without loss of platform retention in the event of vane burn through. GRA

N87-12882# Rensselaer Polytechnic Inst., Troy, N.Y. Dept. of Mechanical Engineering, Aeronautical Engineering and Mechanics.
FUNDAMENTAL RESEARCH ON TRIBOLOGY Final Report, Mar. 1983 - May 1986
Frederick F. Ling Jul. 1986 38 p
(Contract DAAG29-83-K-0058)
(AD-A169974; ARO-19879.25-EG) Avail: NTIS HC A03/MF A01 CSCL 11/8

Tribology, the science and technology of friction-lubrication-wear, is vital to the design, manufacture and utilization of virtually every system with moving parts. Its purpose is to optimize the energy efficiency, product durability and reliability of machines and systems. Topics investigated by an interdisciplinary team were: surface mechanics; studies of microscopic surface phenomena prior to microscopic changes; surface reaction kinetic studies related to wear processes; physicochemical processes in the contact line region; thermal control of friction; fundamental study of solid lubrication in the SEM; lubricated sliding studies in the SEM; friction reduction in an I.C. engine; start-stop evaluation of gas bearing materials; continuous wear measurement by on-line Ferrography; and wear of copper-based brake material. GRA

N87-12883# Illinois Univ., Urbana. Dept. of Mechanical and Industrial Engineering.
EFFECT OF CONVECTION ON WELD POOL SHAPE AND MICROSTRUCTURE Progress Report, 15 Apr. 1984 - 14 Apr. 1986
J. Mazumder, M. M. Chen, C. L. Chan, and R. Zehr Jul. 1986 146 p
(Contract N00014-84-K-0315)
(AD-A170488) Avail: NTIS HC A07/MF A01 CSCL 11/6

The role of convection in weld pools is of great interest due to its effect on weld pool shapes and weld defects. A quantitative understanding of convection in the weld pool is being developed. In this part of the effort major emphasis has been to model surface tension driven flow. The Lorentz force effect is incorporated towards the end of the two year effort. The significant achievements of the program are: (1) Stagnation flow analysis for center of the weldpool which provided algebraic expressions for temperature and velocity. This solution clarifies the scaling problems; (2) Three dimensional axisymmetric model for surface tension driven flow with flat surface assumption which predicted the pool shape for stationary heat source such as in the case of spot welds; (3) Three dimensional perturbation model for surface tension driven flow with flat surface which predict velocity field, temperature field, effect of trace elements and self-consistent prediction of the pool shape and cooling rate; (d) Three dimensional model with flat and free surface which predicted same as above with more realistic boundary condition. This model can also predict effect of Lorentz Force. A series of controlled experiments has been carried out to verify pool shape and liquid velocity. This verified the trend predicted by the model. GRA

N87-12884# Air Force Inst. of Tech., Wright-Patterson AFB, Ohio.
INTEGRATING COMPUTER VISION WITH A ROBOT ARM SYSTEM M.S. Thesis
James E. Wingate 1986 51 p
(AD-A171278; AFIT/CI/NR-86-127T) Avail: NTIS HC A04/MF A01 CSCL 17/8

The goal of this project is to interface an image processing system to a robot arm system. Computer vision is used to compute the location and orientation of a block in the work space so that the block may be grasped and manipulated by a robot arm. A detailed explanation of how information flows from the image processor to the robot arm system is given. This flow can be broken down into three different steps. In the first step, a gradient map from a digitized image of the work space is transferred, one line at a time, from the Grinnell image processor to its host, a VAX 11/750. As each line of the gradient map is uploaded, the coordinates of pixels on the edges of a block (edge pixels) are stored in an array. Storing the coordinates of only the edge pixels results in significant image compression. The second step involves processing the edge pixel coordinate array to extract relevant features. The location of the corners of a block is all that is needed to compute the location of the centroid and the orientation of the block in the work space. In step three, the centroid and roll ang le information is sent from the VAX to the robot arm system host, a DUAL microcomputer. One of the robot arms is selected and appropriate commands are sent to that arm to grasp and manipulate the block. GRA

N87-12885# Oak Ridge Y-12 Plant, Tenn.
HEAT MEASUREMENTS IN INERTIA WELDING OF ALUMINUM TO STEEL
R. J. Reagan Jun. 1986 21 p
(Contract DE-AC05-84OR-21400)

(DE86-012463; Y/DW-627) Avail: NTIS HC A02/MF A01
Measurements of the total heat generated at the interface during inertia welding of 316 stainless steel to aluminum-1100 (99.5% pure) at the Oak Ridge Y-12 Plant are presented. Transient temperature measurements of the weld are also given. A full treatment of calorimetric methods is included in the discussion. In measuring the heat generated during the weld, it was found that the conversion efficiency of kinetic energy in the flywheel to frictional heat energy at the interface is greater than 85%. DOE

N87-12886# Oak Ridge National Lab., Tenn.
WELDING PROCEDURE SPECIFICATION. MANUAL GAS TUNGSTEN ARC AND SEMIAUTOMATIC GAS METAL ARC WELDING OF CHROMIUM-NICKEL STEEL. SUPPLEMENT 1: RECORDS OF PROCEDURE QUALIFICATION TESTS
C. H. Wodtke, D. R. Frizzell, and W. A. Plunkett Jun. 1986 15 p
(Contract DE-AC05-84OR-21400)
(DE86-012521; ORNL/M-15/S1) Avail: NTIS HC A02/MF A01
Procedure WPS-306-ASME-6 is qualified under Section IX of the ASME Boiler and Pressure Vessel Code for manual gas tungsten arc and semiautomatic gas metal arc welding of 300 Series Cr-Ni steels (P-8-1), in thickness range 0.375 to 2.0 inch; filler metal is ER3XX (F-6, A-8); shielding gases are argon (GTAW) and 98-2 argon-oxygen. DOE

N87-12887# Oak Ridge National Lab., Tenn.
MACHINE GAS METAL ARC WELDING OF CARBON STEEL. WELDING PROCEDURE SPECIFICATION. SUPPLEMENT 1: RECORDS OF PROCEDURE QUALIFICATION TESTS
C. H. Wodtke and D. R. Frizzell Jun. 1986 12 p
(Contract DE-AC05-84OR-21400)
(DE86-012530; ORNL/M-6/S1) Avail: NTIS HC A02/MF A01
Procedure WPS-110-ASME-1 is qualified under Section IX of the ASME Boiler and Pressure Vessel Code for machine gas metal arc welding of carbon steels (P-1-1), in thickness range 0.280 to 0.75 inch; filler metal is E70S-3 (F-6, A-1); shielding gas is 95-5 argon-oxygen. DOE

N87-12888# Oak Ridge National Lab., Tenn.
WELDING PROCEDURE SPECIFICATION. SEMIAUTOMATIC GAS METAL ARC WELDING OF CARBON STEELS. SUPPLEMENT 1: RECORDS OF PROCEDURE QUALIFICATION TESTS
C. H. Wodtke, D. R. Frizzell, and W. A. Plunkett Jun. 1986 10 p
(Contract DE-AC05-84OR-21400)
(DE86-012531; ORNL/M-5/S1) Avail: NTIS HC A02/MF A01
Procedure WPS-109-ASME-2 is qualified under Section IX of the ASME Boiler and Vessel Code for semiautomatic gas metal arc welding of carbon steel (P-1-1), in thickness range 0.187 to 2.0 inch; filler metal is ER70S-3 (F-6, A-1); shielding gas is 95-5 argon-oxygen. DOE

N87-12889# Oak Ridge National Lab., Tenn.
WELDING PROCEDURE SPECIFICATION. MANUAL GAS TUNGSTEN ARC AND SEMIAUTOMATIC GAS METAL ARC WELDING OF CARBON STEEL. SUPPLEMENT 1: RECORDS OF PROCEDURE QUALIFICATION TESTS
C. H. Wodtke, D. R. Frizzell, and W. A. Plunkett Jun. 1986 14 p
(Contract DE-AC05-84OR-21400)
(DE86-012532; ORNL/M-4/S1) Avail: NTIS HC A02/MF A01
Procedure WPS-107-ASME-1 is qualified under Section IX of the ASME Boiler and Vessel Code for manual gas tungsten arc and semiautomatic gas metal arc welding of carbon steel (P-1-1), in thickness range of 0.237 to 2.0 inch; filler metal is ER70S-3 (F-6d, A-1); shielding gas for GTAW is argon and for GMAW is 95-5 argon-oxygen. DOE

N87-12890# Oak Ridge National Lab., Tenn.
GAS TUNGSTEN ARC AND SHIELDED METAL ARC WELDING OF CARBON STEEL. WELDING PROCEDURE SPECIFICATION. SUPPLEMENT 1: RECORDS OF PROCEDURE QUALIFICATION TESTS
C. H. Wodtke, D. R. Frizzell, and W. A. Plunkett Jun. 1986 13 p
(Contract DE-AC05-84OR-21400)
(DE86-012533; ORNL/M-3/S1) Avail: NTIS HC A02/MF A01
Procedure WPS-104-ASME-2 is qualified under Section IX of the ASME Boiler and Pressure Vessel Code for gas tungsten arc and shielded metal arc welding of carbon steels (P-1-1), in thickness range 0.25 to 1.0 inch; filler metals are E70S-3 (F-6, A-1) (GTAW) and E6010 (F-3, A-1) (SMAW): shielding gas is argon (GTAW). DOE

N87-12891# Oak Ridge National Lab., Tenn.
WELDING PROCEDURE SPECIFICATION. SUPPLEMENT 1: RECORDS OF PROCEDURE QUALIFICATION TESTS. SHIELDED METAL ARC WELDING OF CARBON STEEL
C. H. Wodtke, D. R. Frizzell, and J. H. Mitchell Jun. 1986 14 p
(Contract DE-AC05-84OR-21400)
(DE86-012535; ORNL/M-1/S1) Avail: NTIS HC A02/MF A01
Procedure WPS-101-ASME-2 is qualified under Section IX of the ASME Boiler and Pressure Vessel Code for shielded metal arc welding of carbon steels (P-1-1), in thickness range 0.125 to 0.75 inch; filler metal is E6010 (F-3, A-1). DOE

N87-12892# Oak Ridge National Lab., Tenn.
WELDING PROCEDURE SPECIFICATION. GAS TUNGSTEN ARC WELDING OF CHROMIUM-NICKEL STEEL TO CHROMIUM-MOLYBDENUM STEEL. SUPPLEMENT 1: RECORDS OF PROCEDURE QUALIFICATION TESTS
C. H. Wodtke, D. R. Frizzell, and W. A. Plunkett Jun. 1986 11 p
(Contract DE-AC05-84OR-21400)
(DE86-012536; ORNL/M-36/S1) Avail: NTIS HC A02/MF A01
Procedure WPS--2104-ASME-1 is qualified under Section IX of the ASME Boiler and Pressure Vessel Code for gas tungsten arc welding of 300 series Cr-Ni steels (P-8-1) to 2 1/4-1Mo steels (P-5-1), in thickness range 0.187 to 1.0 inch; filler metal is ERNiCr-3 (F-43); shielding gas is argon. DOE

N87-12893# Oak Ridge National Lab., Tenn.
GAS TUNGSTEN ARC WELDING OF ALUMINUM ALLOYS 6XXX. WELDING PROCEDURE SPECIFICATION. SUPPLEMENT 1: RECORDS OF PROCEDURE QUALIFICATION TESTS
C. H. Wodtke, D. R. Frizzell, and W. A. Plunkett Jun. 1986 23 p
(Contract DE-AC05-84OR-21400)
(DE86-012548; ORNL/M-24/S1) Avail: NTIS HC A02/MF A01
Procedure WPS-1003 is qualified under Section IX of the ASME Boiler and Pressure Vessel Code for gas tungsten arc welding of aluminum alloys 6061 and 6063 (P-23), in thickness range 0.035 to 0.516 inch; filler metal is ER4043 (F-23) or ER5356 (F-22); shielding gas is argon. DOE

N87-12894# Oak Ridge National Lab., Tenn.
GAS TUNGSTEN ARC WELDING OF CARBON STEEL TO NICKEL-CHROMIUM-IRON. WELDING PROCEDURE SPECIFICATION. SUPPLEMENT 1: RECORDS OF PROCEDURE QUALIFICATION TESTS
C. H. Wodtke and D. R. Frizzell Jun. 1986 15 p
(Contract DE-AC05-84OR-21400)
(DE86-012549; ORNL/M-51/S1) Avail: NTIS HC A02/MF A01
Procedure WPS-2651-ASME-1 is qualified under Section IX of the ASME Boiler and Pressure Vessel Code for gas tungsten arc welding of carbon steel (P-1-1) to nickel-chromium-iron (P-43), in thickness range 0.125 to 0.432 inch; filler metal is ERNiCr-3 (F-43); shielding gas is argon. DOE

N87-12895# Oak Ridge National Lab., Tenn.
GAS TUNGSTEN ARC WELDING OF CHROMIUM-NICKEL STEEL TO NICKEL-MOLYBDENUM-CHROMIUM-IRON. WELDING PROCEDURE SPECIFICATION. SUPPLEMENT 1: RECORDS OF PROCEDURE QUALIFICATION TESTS
C. H. Wodtke, D. R. Frizzell, and W. A. Plunkett Jun. 1986 17 p
(Contract DE-AC05-84OR-21400)
(DE86-012550; ORNL/M-50/S1) Avail: NTIS HC A02/MF A01
Procedure WPS-2604-ASME-5 is qualified under Section IX of the ASME Boiler and Pressure Vessel Code for gas tungsten arc welding of 300 series Cr-Ni steels (P-8-1) to nickel-molybdenum-

chromium-iron (P-44), in thickness range 0.035 to 0.5 inch; filler metal is ERNiCr-3 (F-43); shielding gas is argon. DOE

N87-12896# Oak Ridge National Lab., Tenn.
WELDING PROCEDURE SPECIFICATION: GAS TUNGSTEN ARC WELDING OF NICKEL TO NICKEL-CHROMIUM-IRON. SUPPLEMENT 1: RECORDS OF PROCEDURE QUALIFICATION TESTS
C. H. Wodtke, D. R. Frizzell, and W. A. Plunkett Jun. 1986 19 p
(Contract DE-AC05-84OR-21400)
(DE86-012557; ORNL/M-43/S1) Avail: NTIS HC A02/MF A01

Procedure WPS-2302-ASME-3 is qualified under Section IX of the ASME Boiler and Pressure Vessel Code for gas tungsten arc welding of nickel N02200 or N02201 (P-41) to nickel-chromium-iron N06600 (P-43), in thickness range 0.035 to 0.432 inch; filler metal is ERNiCrFe-5 (F-43); shielding gas is argon. DOE

N87-12897# Oak Ridge National Lab., Tenn.
GAS TUNGSTEN ARC WELDING OF ALUMINUM ALLOYS 3004, 5052 AND 5X54 TO 6XXX. WELDING PROCEDURE SPECIFICATION. SUPPLEMENT 1: RECORDS OF PROCEDURE QUALIFICATION TESTS
C. H. Wodtke, D. R. Frizzell, and W. A. Plunkett Jun. 1986 10 p
(Contract DE-AC05-84OR-21400)
(DE86-012561; ORNL/M-39/S1) Avail: NTIS HC A02/MF A01

Procedure WPS-2203 is qualified under Section IX of the ASME Boiler and Pressure Vessel Code for gas tungsten arc welding of aluminum alloys 3004, 5052, 5154, and 5454 (P-22) to 6061 and 6063 (P-23), in thickness range 0.062 to 0.5 inch; filler metal is ER4043 (F-23); shielding gas is argon. DOE

N87-12898# Lawrence Livermore National Lab., Calif.
BUFFERED EXPLOSIONS IN STEEL PRESSURE VESSELS
L. A. Glenn 1986 12 p Presented at the 9th International Conference on High Energy Rate Fabrication, Novosibirsk, USSR, 18 Aug. 1986
(Contract W-7405-eng-48)
(DE86-008763; UCRL-94255; CONF-860844-1) Avail: NTIS HC A02/MF A01

The impulse delivered to the walls of a vessel containing an explosion will increase if material is placed between the walls and the charge. If the impulse application time is small in comparison with the eigenperiod of the vessel, the wall stress will increase in direct proportion to the impulse. Conversely, if the application period can be extended beyond half the eigenperiod, the peak stress will be proportional to the ratio of the impulse to the delivery period. With powder or granular buffers, it is possible for the delivery period to increase faster than the impulse as the buffer mass is increased. This is the reason why certain powders, or porous materials, can provide stress reduction even below that observed by evacuating the space between the walls and the explosive. If the buffer material is to serve as an effective mitigator, it must collapse on shock loading to a final density that depends only weakly on pressure; the criterion is that the wave speed in the material that impacts the wall must be small compared with the impact (particle) speed. This behavior apparently occurs with salt, at least for modest values of the charge parameter, but to a lesser extent with snow under the same conditions. The vermiculite data are comparable to the salt in the charge parameter region where the two overlap; with increasing explosive, however, the vermiculite appears to behave like the snow and its effectiveness as a mitigator rapidly diminishes. It is also clear that once the wave speed criterion is seriously violated, the use of a powder buffer will result in a higher wall stress than if only air filled the space between walls and charge. DOE

N87-12899# Lawrence Livermore National Lab., Calif.
SHOWER AND HIGH-PRESSURE OIL TEMPERATURE CONTROL
D. B. DeBra (Stanford Univ., Calif.), R. A. Victor, and J. B. Bryan Mar. 1986 20 p Presented at the 36th International Institution for Production Engineering Research General Assembly, Jerusalem, Israel, 16 Aug. 1986 Prepared in cooperation with Lawrence Livermore National Lab., Calif.
(Contract W-7405-eng-48)
(DE86-009398; UCRL-94273; CONF-860839-2) Avail: NTIS HC A02/MF A01

Oil showering for temperature control of precision tools is an effective way of achieving close temperature stability and isolation from variations in room air temperature. The oil must be controlled to temperature variations less than tolerances specified for machine and parts. Principal disturbances come from heat transfer into the plumbing between the heat exchanger and the tool and from variations in the chill water in the heat exchanger. We describe the successful employment of measuring techniques, isolation from disturbances, and the use of integral control with proportional and commercially available temperature controllers. Commercially available heat exchangers are low-pressure devices. For high-pressure oil applications a pump follows the heat exchanger, and, because of the high velocities and large surface area, the oil passing the pump is sensitive to heat from its motor and from room air. Combinations of feedback from different locations in the system are discussed. Compromises with regard to measuring at the functional point versus minimizing time delay, and the importance of measuring near the site of disturbing heat sources lead to multiple sensors in some cases. Each measurement may be used through integral feedback to provide the best performance. The introduction of integral control to commercial a-c bridge controllers can be awkward. Six approaches are compared, and the millidegree performance of our current designs is presented. DOE

N87-12900# Oak Ridge National Lab., Tenn.
LOCALIZED ION MILLING OF METALLIC AND CERAMIC TEM SPECIMENS
A. T. Fisher and J. Bentley 1986 3 p Presented at the Annual Joint Meeting of the Electron Microscopy of America and the Microbeam Analysis Society, Albuquerque, N. Mex., 10 Aug. 1986
(Contract DE-AC05-84OR-21400)
(DE86-009538; CONF-860829-23) Avail: NTIS HC A02/MF A01

The utility of localized ion milling in the preparation of metallic and ceramic specimens for TEM and AEM is being evaluated from the standpoint of optimizing procedures and identifying limitations and milling characteristics. The equipment used was a Gatan model 645 precision ion milling system (PIMS). This device is a scanning ion beam instrument with which selected areas of a sample can be imaged by either secondary electron or secondary ion signals and selectively ion milled in a small region within the imaged area. The 1 to 10 keV ion beam can be focussed to a 2 micron spot. Specimens are thinned without removing them from the electron microscope specimen holder. DOE

N87-12901# SKF Industries, Inc., King of Prussia, Pa.
MECHANICAL INTERACTIONS OF ROUGH SURFACES Quarterly Progress Report, Apr. 1 - 30 Jun. 1986
J. I. McCool Jun. 1986 7 p
(Contract DE-AC02-84ER-13163)
(DE86-010886; DOE/ER-13163/11) Avail: NTIS HC A02/MF A01

Simulation studies have been performed to yield the complete distribution of asperity contact area, load and pressure as a function of the separation of rough surfaces. Microcontact models ordinarily yield just the average value of these quantities with no measure of the scatter about the average. The low sliding speed microcontact flash temperature distribution is shown to be computable as a by product of the determination of the microcontact area distribution. A Coulomb friction model for traction in the mixed film regime is tested against published data. The required Coulomb friction coefficient is found to be unreasonably large. A suggested explanation is that only contacts larger than some critical minimum can cause loss of electrical insulation between sliding disks. Preliminary ceramic microfracture experiments have resulted in plastic deformation rather than fracture at asperity tips. DOE

N87-12902# Los Alamos National Lab., N. Mex.
LIQUID METAL THERMOACOUSTIC ENGINE
G. W. Swift, A. Migliori, and J. C. Wheatley 1986 7 p Presented

at the Intersociety Energy Conversion Engineering Conference, San Diego, Calif., 25 Aug., 1986
(Contract W-7405-eng-36)
(DE86-011264; LA-UR-86-1548; CONF-860810-6) Avail: NTIS HC A02/MF A01

We are studying a liquid metal thermoacoustic engine both theoretically and experimentally. This type of engine promises to produce large quantities of electrical energy from heat at modest efficiency with no moving parts. A sound wave is usually thought of as consisting of pressure oscillations, but always attendant to the pressure oscillation are temperature oscillations. The combination produces a rich variety of thermoacoustic effects. These effects are usually so small that they are never noticed in everyday life; nevertheless under the right circumstances they can be harnessed to produce powerful heat engines, heat pumps, and refrigerators. In our liquid metal thermoacoustic engine, heat flow from a high temperature source to a low temperature sink generates a high-amplitude standing acoustic wave in liquid sodium. This acoustic power is converted to electric power by a simple magnetohydrodynamic effect at the acoustic oscillation frequency. We have developed a detailed thermoacoustic theory applicable to this engine, and find that a reasonably designed liquid sodium engine operating between 700 C and 100 C should generate about 60 W/cm(2) of acoustic power at about 1/3 of Carnot's efficiency. Construction of a 3000 W-thermal laboratory model engine has just been completed, and we have exciting preliminary experimental results as of the time of preparation of this manuscript showing, basically, that the engine works. We have also designed and built a 1 kHz liquid sodium magnetohydrodynamic generator and have extensive measurements on it. It is now very well characterized both experimentally and theoretically. The first generator of its kind, it already converts acoustic power to electric power with 40% efficiency. DOE

N87-12903# Oak Ridge National Lab., Tenn.
LINEAR HARMONIC ANALYSIS OF FREE-PISTON STIRLING ENGINES
N. C. J. Chen and F. P. Griffin Jun. 1986 104 p
(Contract DE-AC05-84OR-21400)
(DE86-012451; ORNL/CON-172) Avail: NTIS HC A06/MF A01

The equations that govern the behavior of free-piston Stirling engines are nonlinear differential equations. Traditional solution methods have been time-stepping integrations that can be plagued by numerical instabilities and can use large amounts of computer time. Closed-form analytical solutions are possible if the working gas behaves isothermally or if the nonlinear terms in the governing equations are replaced with accurate approximations. An almost closed-form solution method, called the linear harmonic analysis (LHA), has been developed for free-piston Stirling engine applications by representing all of the periodic variables with harmonic functions. The solution method accounts for the important thermodynamic losses that are coupled together in free-piston engines, yet it is efficient enough for optimization studies. The LHA method was compared with a standard numerical integration method to verify its mathematical accuracy. The LHA and numerical predictions for a sample free-piston Stirling engine configuration differed by less than 5% for all important parameters. Sensitivity studies using the LHA method have also shown that the thermodynamic loss assumptions used in an analysis can have a significant impact on the predicted dynamic behavior of a free-piston Stirling engine. DOE

N87-12904# Sandia National Labs., Albuquerque, N. Mex.
EFFECTS OF INERTIA WELD PARAMETERS AND CONTAMINATION ON WELD FLASH SHAPE AND ON JOINT STRENGTH: AN IMPROVED STUDY
M. W. Mote Jun. 1986 41 p
(Contract DE-AC04-76DP-00789)
(DE86-013074; SAND-85-8239) Avail: NTIS HC A03/MF A01

Inertia welds of four dissimilar metal pairs in three configurations were made with extensive variations in energy and force to discover limits for the weld process and assure that process monitoring of welds provides quality assessment. In a related study of the effect of surface contamination, using one set of welding parameters, we showed that in two cases wherein only one of the metals in the pair deforms, contamination can preclude welding without altering weld configuration or upset. However, contamination had no effect on all-steel welds. DOE

N87-12905# Auburn Univ., Ala.
SENSOR CONTROLLED ROBOTIC WELDING FOR NUCLEAR APPLICATIONS Annual Progress Report
B. A. Chin, N. H. Madsen, and J. S. Goodling 30 May 1986 18 p
(Contract DE-FG05-85NE-37949)
(DE86-013110; DOE/NE-37949/1) Avail: NTIS HC A02/MF A01

Significant accomplishments towards the development of an adaptive robotic welding system have been made during the first eight months of the project. The project is currently within budget and on schedule. Accomplishments were both scientific and programmatic in form. A list of the scientific accomplishments follows: demonstrated that the thermal profiles generated for intentionally induced defects during the welding process are similar in steel, aluminum and stainless steel. The conclusion is therefore that infrared sensing is applicable to the welding of over 90% of all materials used in the energy industry. Completed design and testing of a first generation communication system used to transfer information from the infrared camera to the computer in a near real time form. This demonstrates that information can be obtained, sorted, transferred and received in a time frame consistent with on-line process control. Demonstrated rudimentary seam tracking using infrared sensing and closed loop logic routines. A linear relationship exists between measured peak surface temperature and depth of penetration. Similarily, a linear relationship exists between measured infrared width and weld bead width. These relations suggest that penetration parameters may be controlled using surface measurements as obtained by infrared thermography. DOE

N87-12906# Allied Bendix Corp., Kansas City, Mo.
RESISTANCE SEAM WELDING
R. G. Thatcher Jul. 1986 16 p
(Contract DE-AC04-76DP-00613)
(DE86-013288; BDX-613-3557) Avail: NTIS HC A02/MF A01

Work was conducted to develop the capability to produce miniature resistance seam welds at the Bendix Kansas City Division (BKC) of Allied Corporation. This effort was initiated to weld aluminum foil to polyimide-backed copper foil on a flat cable. A parallel gap resistance welding head capable of accessing material from one side only was designed and fabricated for this purpose. Welds were made between aluminum and copper foils using the parallel gap resistance seam welding head. Bonds were made proving the welding head design was feasible. Aluminum to copper weld joints were analyzed by cross sectioning, electron beam microprobe analysis, and environmental testing. As expected with this material combination, testing indicated the presence of brittle, crack sensitive intermetallics in the weld zone. Work was expanded to develop a general resistance seam welding process capable of welding metal foils where there was access to both sides of the material. An opposed electrode welding head was designed and fabricated for this purpose. DOE

N87-12907# Allied Bendix Corp., Kansas City, Mo.
REVIEW OF ROBOTIC COMPONENT INSERTION SYSTEM FOR PRINTED WIRING ASSEMBLIES
K. J. Groot Jul. 1986 12 p
(Contract DE-AC04-76DP-00613)
(DE86-013510; BDX-613-3512) Avail: NTIS HC A02/MF A01

Robotic insertion systems for printed wiring assemblies are currently in use in industry. These systems can be interfaced with current BKC processing to increase efficiency, decrease cost, and improve quality. The requirements for a system which would satisfy BKC requirements are outlined. DOE

N87-12908# Edgerton, Germeshausen and Grier, Inc., Idaho Falls, Idaho.

CONCURRENT ULTRASONIC WELD EVALUATION SYSTEM Patent Application
D. W. Hood, inventor (to DOE), J. A. Johnson, inventor (to DOE), and H. B. Smartt, inventor (to DOE) Filed Sep. 1985 22 p
(Contract DE-AC07-76ID-01570)
(DE86-013772; US-Patent-Appl-SN-772527) Avail: NTIS HC A02/MF A01

A system for concurrent, non-destructive evaluation of partially completed welds for use in conjunction with an automated welder is described. The system utilizes real time, automated ultrasonic inspection of a welding operation as the welds are being made by providing a transducer which follows a short distance behind the welding head. Reflected ultrasonic signals are analyzed utilizing computer based digital pattern recognition techniques to discriminate between good and flawed welds on a pass by pass basis. The system also distinguishes between types of weld flaws. DOE

38 QUALITY ASSURANCE AND RELIABILITY

Includes product sampling procedures and techniques; and quality control.

N87-12909# Committee on Science and Technology (U. S. House).
NASA'S QUALITY ASSURANCE PROGRAM
1986 163 p Hearing before the Subcommittee on Space Science and Applications of the Committee on Science and Technology, 99th Congress, 2d Session, No. 126, 21 May 1986
(GPO-63-142) Avail: Subcommittee on Space Science and Applications

The number of quality assurance personnel have declined dramatically since the Apollo Program. The facts and implications of the decline were examined. A system of checks and balances to accomplish quality control were also discussed. A panel of well-known experts described how an ideal quality assurance program should work. B.G.

N87-12910*# National Aeronautics and Space Administration. Lewis Research Center, Cleveland, Ohio.
NDE RELIABILITY AND PROCESS CONTROL FOR STRUCTURAL CERAMICS
George Y. Baaklini 1986 17 p Proposed for presentation at the 32nd International Gas Turbine Conference and Exhibition, Anaheim, Calif., 31 May - 4 Jun. 1987; sponsored by ASME
(NASA-TM-88870; E-3276; NAS 1.15:88870) Avail: NTIS HC A02/MF A01 CSCL 14D

The reliability of microfocus x-radiography and scanning laser acoustic microscopy for detecting microvoids in silicon nitride and silicon carbide was statistically evaluated. Materials- and process-related parameters that influenced the statistical findings in research samples are discussed. The use of conventional x-radiography in controlling and optimizing the processing and sintering of an Si3N4-Si02-Y203 composition designated NASA 6Y is described. Radiographic evaluation and guidance helped develop uniform high-density Si3N4 modulus-of-rupture bars with improved four-point flexural strength (857, 544, and 462 MPa at room temperature, 1200 C, and 1370 C, respectively) and reduced strength scatter. Author

N87-12911# Army Belvoir Research and Development Center, Fort Belvoir, Va.
RELIABILITY PREDICTION MODELS FOR MECHANICAL EQUIPMENT Interim Report, Oct. 1985 - Oct. 1986
James D. Raze Oct. 1985 66 p
(AD-A169775; Rept-2425) Avail: NTIS HC A04/MF A01 CSCL 13/9

The purpose of this report is to present a proposed methodology for predicting the reliability of mechanical equipment and solicit comments as to the potential utility of a complete handbook of reliability prediction procedures. The prediction methodology being developed considers the critical failure modes of a mechanical component, its material strengths, and the operating stresses at the component level. This method of analysis permits a prediction of the failure rate for each component of a mechanical system based upon the operating environment. GRA

N87-12912# Naval Personnel Research and Development Center, San Diego, Calif. Human Factors and Organizational Systems Lab.
QUALITY MANAGEMENT: AN ANNOTATED BIBLIOGRAPHY
Marilyn Monda, Pattie J. Thrapp, and Edith L. Goldberg Jun. 1986 92 p
(AD-A169816; HFOSL-TN-72-86-07) Avail: NTIS HC A05/MF A01 CSCL 05/1

As America strives to compete in the international marketplace, many U.S. businesses have adopted a new way of managing and measuring quality and productivity. The quality management methods focus on the systematic measurement and control of work processes. Successful quality management programs are credited with increases in profit, reduction of waste, and improved management-worker relations. This annotated bibliography is oriented toward those persons who are new to or only recently acquainted with the concept of quality management. The main body of journal articles, books, videotapes, and magazines selected from academia and industry focus on the introduction of the concepts, the terminology, and the personalities associated with the quality management movement. Citations include information about the author, date, title, and source, as well as a set of terms that summarize the key concepts of the citation and a brief abstract. Several articles are identified and recommended as an orientation to the field of total quality management. GRA

39 STRUCTURAL MECHANICS

Includes structural element design and weight analysis; fatigue; and thermal stress.

For applications see *05 Aircraft Design, Testing and Performance* and *18 Spacecraft Design, Testing and Performance.*

N87-12913 Maryland Univ., College Park.
A NEW AND EFFICIENT FORMULATION FOR FINITE ELEMENT ANALYSIS OF THIN SHELL STRUCTURES UNDERGOING SMALL AND LARGE DEFLECTION Ph.D. Thesis
Jeong-Joo Rhiu 1985 238 p
Avail: Univ. Microfilms Order No. DA8608851

New finite element formulations are developed based on the Hellinger-Reissner principle with independent strain. By dividing assumed strain fields into the lower order part and the higher order part, the new formulations can be made much more efficient than the standard mixed formulations. Moreover, the present approach provides a rational way of introducing stabilization matrix to suppress undesirable spurious kinematic modes in finite element formulations. A nine node degenerate solid shell element based on the new formulation has been developed and tested for linear thin plate and shell problems. The numerical results indicate that this element is free of locking and successful in suppressing undesirable spurious kinematic modes. This nine node element is also extended to the analysis of thin shells undergoing large deflection in conjunction with the total Lagrangian scheme. A proper choice of integration strategy leads to a much simplified and less expensive formulation for geometrically nonlinear thin shells. Dissert. Abstr.

N87-12914 ESDU International Ltd., London (England).
GUIDE TO THE USE OF DATA ITEMS ON THE FATIGUE STRENGTH OF WELDED JOINTS IN STEELS
Jul. 1986 23 p
(ESDU-86013; ISBN-0-85679-565-8; ISSN-0141-4089; ISSN-0144-2805) Avail: ESDU

Available as part of the ESDU Sub-series on Stress and Strength and on Engineering Structures, this ESDU discusses

factors that affect the fatigue strength of a welded joint and, in particular, from fracture mechanics arguments shows that the strength is independent of the strength properties of the parent material. Similar arguments show the likely effect of size is to reduce the fatigue strength over that found in smaller joints (such as laboratory specimens on which many of the fatigue data available depend). The influence of residual stresses, and in turn their effect on the way mean stress is experienced, is discussed, and the use of thermal stress relieving is considered. Various design options for joints are indicated, together with likely crack initiation sites in each case. A complete directory of some 30 possible types of welded joints for which fatigue data are included in other ESDU documents (75016, 76007, 76032, 77011, 78016, 78023 and 81007) are listed together with their equivalent type and class of weld as defined in BS 5400. ESDU

N87-12915*# Case Western Reserve Univ., Cleveland, Ohio. Dept. of Civil Engineering.
ANALYSIS OF MIXED-MODE CRACK PROPAGATION USING THE BOUNDARY INTEGRAL METHOD Final Report
Alexander Mendelson and Louis J. Ghosn Sep. 1986 194 p
(Grant NAG3-396)
(NASA-CR-179518; NAS 1.26:179518) Avail: NTIS HC A09/MF A01 CSCL 20K

Crack propagation in a rotating inner raceway of a high speed roller bearing is analyzed using the boundary integral equation method. The method consists of an edge crack in a plate under tension, upon which varying Hertzian stress fields are superimposed. A computer program for the boundary integral equation method was written using quadratic elements to determine the stress and displacement fields for discrete roller positions. Mode I and Mode II stress intensity factors and crack extension forces G sub 00 (energy release rate due to tensile opening mode) and G sub r0 (energy release rate due to shear displacement mode) were computed. These calculations permit determination of that crack growth angle for which the change in the crack extension forces is maximum. The crack driving force was found to be the alternating mixed-mode loading that occurs with each passage of the most heavily loaded roller. The crack is predicted to propagate in a step-like fashion alternating between radial and inclined segments, and this pattern was observed experimentally. The maximum changes DeltaG sub 00 and DeltaG sub r0 of the crack extension forces are found to be good measures of the crack propagation rate and direction. Author

N87-12916# Ecole Polytechnique, Montreal (Quebec). Dept. of Mechanical Engineering.
DYNAMIC ANALYSIS OF ANISOTROPIC CONICAL SHELLS
Aouni A. Lakis and Hamid Ouriche Oct. 1986 128 p
(EPM/RT-86-36) Avail: NTIS HC A07/MF A01

An analysis is presented of the static and dynamic equilibrium of thin anisotropic and non-uniform conical shells, subjected to different boundary conditions. The procedure used was a hybrid one, based on Sander's shell theory and on the finite element method as applied to thin shells having variable thickness and anisotropic elastic properties, but limited to cases of linear elasticity. The displacement functions were derived from Sander's equations. The stiffness and mass matrices were derived by exact analysis integration. The free vibration problem of conical shells was reduced to an eigenvalues and eigenvectors problem. The convergence of the method proved to be satisfactory and the frequencies and displacements were compared with existing results. Author

N87-12917# Ecole Polytechnique, Montreal (Quebec). Dept. of Mechanical Engineering.
NON-LINEAR ANALYSIS OF CYLINDRICAL SHELLS
Aouni A. Lakis and Alberto Toledano Sep. 1986 103 p
(EPM/RT-86-37) Avail: NTIS HC A06/MF A01

A theory to predict the influence of geometric nonlinearities on the natural frequencies of an empty anisotropic cylindrical shell was presented. It was a hybrid of finite element and classical thin shell theories. Sanders-Koiter's nonlinear and strain-displacement relations were used. Displacement functions were evaluated using linearized equations of motion. Modal coefficients were then obtained for these displacement functions. Expressions for the mass, linear and nonlinear stiffness matrices were derived through the finite element method. The uncoupled equations were solved with the help of elliptic functions. The period and frequency variations were first determined as a function of shell amplitudes and then compared with the results in the literature. Author

N87-12918# Ecole Polytechnique, Montreal (Quebec). Dept. of Mechanical Engineering.
ANALYSIS OF ANISOTROPIC THIN CONICAL SHELLS
Aouni A. Lakis and Patrick Boisnaud 1986 146 p
(EPM/RT-86-38) Avail: NTIS HC A07/MF A01

A theory is presented for the static and dynamic analysis of thin conical anisotropic shells with bending resistance subject to an arbitrary distribution of loads. Sander's basic equilibrium equations were reduced to three differential equations of motion. Displacement, deformation, and stress relative to arbitrary boundary loadings and arbitrary distributed load were determined as a function of the shell characteristics. All boundary condition cases were derived in terms of eight constants. This theory was developed for thin shells where thickness is a function of the longitudinal direction generator to give homogeneous equations of motion. The numerical analysis is devoted to solving the characteristic equations for isotropic shells. The results are presented in the form of tables and graphs. The graphs are given in terms of the thickness-to-length ratio. Author

N87-12919# Ecole Polytechnique, Montreal (Quebec). Dept. of Mechanical Engineering.
DYNAMIC ANALYSIS OF A TIMOSHENKO BEAM USING A FINITE ELEMENT APPROACH
Aouni A. Lakis and N. D. Trinh 1986 179 p
(EPM/RT-86-34) Avail: NTIS HC A09/MF A01

The finite element method was used in this investigation in order to determine the static and dynamic behavior of non-uniform Timoshenko beams subjected to various boundary conditions. When using this approach, the general displacement functions are based on the cubic polynomial expansion of the three principal quantities as degrees of freedom: transverse displacement, rotation of the cross section and shear deformation. The stiffness and mass matrices, however, are derived from expressions of the strain and kinetic energy which are based on the assumptions of curved, slightly curved and straight beams. In addition, a formula was obtained from the general equation for a slightly curved beam and as a result, frequency equations for a straight beam were obtained for ten common types, taking into account all the forced and natural boundary conditions. Good agreement was achieved by comparing the results of these models with exact solutions, as well as with other numerical methods for straight and tapered beams. In order to test the rate of convergence, the natural frequencies of typical cases were calculated as a function of the number of elements. Results showed that the model converged rapidly and required only a small number of elements to achieve good results. Finally, the present analysis demonstrated the reliability of the model chosen by including the transverse shear and rotary inertia effects at the higher modes. Author

N87-12920# École Polytechnique, Montreal (Quebec). Dept. of Mechanical Engineering.
FREE VIBRATION OF AXISYMMETRIC AND BEAM-LIKE CYLINDRICAL SHELLS, PARTIALLY FILLED WITH LIQUID
Aouni A. Lakis and Marwan Sinno 1986 142 p
(EPM/RT-86-35) Avail: NTIS HC A07/MF A01

A theory is presented for the determination of free vibration characteristics of anisotropic thin cylindrical shells, partially or completely filled with liquid for two circumferential wave numbers, n = 0 breathing and n = 1 beam-like. The method used was a hybrid one, based on the finite element method and supported by classical shell theories. The shell was subdivided into cylindrical finite elements and the displacement functions were obtained using

the shell's equations. Expressions for the mass and stiffness matrices for a finite element and for the whole structure were obtained. Similarly, a finite element was developed for the liquid in cases of potential flow. The natural frequencies of the shell in vacuo and partially filled were obtained and compared with existing experiments and other theories. Author

N87-12921*# National Aeronautics and Space Administration. Marshall Space Flight Center, Huntsville, Ala.
EFFECTS OF VARIABLES UPON PYROTECHNICALLY INDUCED SHOCK RESPONSE SPECTRA
James Lee Smith May 1986 61 p
(NASA-TP-2603; NAS 1.60:2603) Avail: NTIS HC A04/MF A01 CSCL 20K

Throughout the aerospace industry, large variations of 50 percent (6 dB) or more are continually noted for linear shaped charge (LSC) generated shock response spectra (SRS) from flight data (from the exact same location on different flights) and from plate tests (side by side measurements on the same test). A research program was developed to investigate causes of these large SRS variations. A series of ball drop calibration tests to verify calibration of accelerometers and a series of plate tests to investigate charge and assembly variables were performed. The resulting data were analyzed to determine if and to what degree manufacturing and assembly variables, distance from the shock source, data acquisition instrumentation, and shock energy propagation affect the SRS. LSC variables consisted of coreload, standoff, and apex angle. The assembly variable was the torque on the LSC holder. Other variables were distance from source of accelerometers, accelerometer mounting methods, and joint effects. Results indicated that LSC variables did not affect SRS as long as the plate was severed. Accelerometers mounted on mounting blocks showed significantly lower levels above 5000 Hz. Lap joints did not affect SRS levels. The test plate was mounted in an almost free-free state; therefore, distance from the source did not affect the SRS. Several varieties and brands of accelerometers were used, and all but one demonstrated very large variations in SRS. Author

N87-12922*# National Aeronautics and Space Administration. Langley Research Center, Hampton, Va.
FACTORS INFLUENCING ELASTIC STRESSES IN DOUBLE CANTILEVER BEAM SPECIMENS
J. H. Crews, Jr., K. N. Shivakumar (Analytical Services and Materials, Inc., Hampton, Va.), and I. S. Raju Nov. 1986 34 p
(NASA-TM-89033; NAS 1.15:89033) Avail: NTIS HC A03/MF A01 CSCL 20K

An elastic stress analysis was conducted for a double cantilever beam (DCB) specimen using finite-element methods. The purpose of this study was to identify the important parameters that influence stresses ahead of the delamination front. The study focused on an aluminum DCB specimen, typical of adhesively-bonded joints, and on a graphite/epoxy specimen representing a cocured composite. Opening mode sigma sub y stresses ahead of the crack tip were calculated and compared with those for a monolithic reference specimen. Beyond the singularity-dominated region very near the crack tip, the sigma sub y distribution was elevated compared to the monolithic case. Both the adhesive thickness and the adherend transverse (thickness-direction) stiffness were found to influence the elevation of sigma sub y. In contrast, adherend thickness and longitudinal stiffness has very little effect on this stress distribution. Estimates for adhesive yielding beyond the aluminum DCB crack tip showed that both the area and height of the plastic zone increased to a peak value for increasing adhesive thicknesses. Results from this study would provide insight for comparing data from different DCB specimens and for designing new DCB specimens. Author

N87-12923*# Pratt and Whitney Aircraft, East Hartford, Conn.
ON 3-D INELASTIC ANALYSIS METHODS FOR HOT SECTION COMPONENTS (BASE PROGRAM) Annual Status Report
R. B. Wilson, M. J. Bak, S. Nakazawa, and P. K. Banerjee Feb. 1986 206 p
(Contract NAS3-23697)
(NASA-CR-175060; NAS 1.26:175060; ASR-2; PWA-5940-36) Avail: NTIS HC A10/MF A01 CSCL 29K

A 3-D Inelastic Analysis Method program is described. This program consists of a series of new computer codes embodying a progression of mathematical models (mechanics of materials, special finite element, boundary element) for streamlined analysis of: (1) combustor liners, (2) turbine blades, and (3) turbine vanes. These models address the effects of high temperatures and thermal/mechanical loadings on the local (stress/strain)and global (dynamics, buckling) structural behavior of the three selected components. Three computer codes, referred to as MOMM (Mechanics of Materials Model), MHOST (Marc-Hot Section Technology), and BEST (Boundary Element Stress Technology), have been developed and are briefly described in this report. Author

N87-12924*# National Aeronautics and Space Administration. Lewis Research Center, Cleveland, Ohio.
A CONSTITUTIVE LAW FOR FINITE ELEMENT CONTACT PROBLEMS WITH UNCLASSICAL FRICTION
Michael E. Plesha and Bruce M. Steinetz Nov. 1986 19 p
(NASA-TM-88838; E-3181; NAS 1.15:88838; ICOMP-86-1) Avail: NTIS HC A02/MF A01 CSCL 20K

Techniques for modeling complex, unclassical contact-friction problems arising in solid and structural mechanics are discussed. A constitutive modeling concept is employed whereby analytic relations between increments of contact surface stress (i.e., traction) and contact surface deformation (i.e., relative displacement) are developed. Because of the incremental form of these relations, they are valid for arbitrary load-deformation histories. The motivation for the development of such a constitutive law is that more realistic friction idealizations can be implemented in finite element analysis software in a consistent, straightforward manner. Of particular interest is modeling of two-body (i.e., unlubricated) metal-metal, ceramic-ceramic, and metal-ceramic contact. Interfaces involving ceramics are of engineering importance and are being considered for advanced turbine engines in which higher temperature materials offer potential for higher engine fuel efficiency. Author

N87-12925# Washington Univ., Seattle. Dept. of Mechanical Engineering.
A STUDY OF THE MECHANISM OF DYNAMIC DUCTILE FRACTURE OF TWO-PHASE MATERIALS Final Report, 1982 - 1985
Minoru Taya, Ian W. Hall, and H. S. Yoon 30 May 1986 35 p
(Contract DAAG29-82-K-0144)
(AD-A168966; ARO-18325.7-EG) Avail: NTIS HC A03/MF A01 CSCL 20/11

Dynamic ductile fracture of two phase material have been investigated in two stages. The first stage is a model study where an idealized two phase material, single crystal Cu-SiO2 was used to study the initiation and growth of voids, the dislocation morphology and the other microscopic behavior that took place in the as-impacted specimen. Important findings are voids were nucleated from only a fraction of secondary particles SiO2, the larger strain has induced the higher void density, and the dislocation cell structures were formed with the average cell size being constant for the range of strain rates investigated. Analytical models were constructed with the aim of simulating the void growth in a two phase material subjected to high strain rate deformation, static void growth model and dynamic void growth model. A comparison of the void density indicated the static void growth model can predict the experimental results reasonably well for the smaller strain, but it fails to predict for the larger strain, while the dynamic void growth model can simulate the void growth well for the entire range of strain and strain rates. The second stage conducts a series of experiments on more realistic two phase materials, Al-Si alloy and SiC(w) or SiC(p)/Al composite. The mode of the initiation and growth of voids was observed in the specimens that were impacted by Split Hopkinson bar test. The void density was also measured along the specimen axis and its values were compared

with the analytical results by the static void growth model, resulting in a reasonably good agreement. GRA

N87-12926# Brown Univ., Providence, R. I. Div. of Engineering.
AN ANALYSIS OF SHEAR BAND DEVELOPMENT INCORPORATING HEAT CONDUCTION
J. LeMonds and A. Needleman May 1986 37 p
(Contract DAAG29-85-K-0003)
(AD-A168972; ARO-22306.5-EG) Avail: NTIS HC A03/MF A01 CSCL 20/13

We incorporate the effects of material temperature sensitivity and heat conduction into an infinite band type analysis of shear localization. Full account is taken of finite geometry changes, but inertial effects are neglected. An energy balance is written between homogeneously deforming bands in a manner that models conditions in our recent finite element study of shear band development from internal inhomogeneities in a solid subject to plane strain compression. The band analysis requires specification of an imperfection amplitude and a length scale over which heat conduction effects are significant. These are chosen to match results of a finite element analysis. The predictions of the simple band analysis and the results of full finite element calculations are then compared for a wide range of material properties for both isotropic and kinematic hardening characterizations of the flow potential surface. The predicted dependence of the onset of localization on material properties such as strain hardening and strain rate sensitivity is the same for both types of analysis. GRA

N87-12927# Brown Univ., Providence, R. I. Div. of Engineering.
FINITE ELEMENT ANALYSES OF SHEAR LOCALIZATION IN RATE AND TEMPERATURE DEPENDENT SOLIDS
J. LeMonds and A. Needleman May 1986 59 p
(Contract DAAG29-85-K-0003)
(AD-A169057; ARO-22306.6-EG) Avail: NTIS HC A04/MF A01 CSCL 20/11

The effects of strain hardening, strain rate sensitivity, thermal softening, heat conduction and the imposed strain rate on the shear localizaton process in plane strain compression are examined. Deformation, stress and temperature fields are computed in an infinite solid which contains a periodic rectangular array of inhomogeneities. The inhomogeneities give rise to non-uniform deformation fields which, under certain conditions, may localize in the form of a shear band. Boundary conditions are prescribed such that the resulting fields possess periodicity with respect to the inhomogeneity distribution. In this manner, attention may be confined to a rectangular region of the solid which surrounds a single inhomogeneity. Full two-dimensional analyses are performed within the context of a viscoplasticity theory which, in the rate independent limit, corresponds to flow theory with combined isotropic and kinematic hardening. Full account is taken of finite strain and rotation effects, but attention is confined to quasi-static loading. The initiation and propagation of shear bands is examined for the bounding theories of isotropic and kinematic hardening. The predicted response depends significantly on the multi-axial hardening characterization of the solid. GRA

N87-12928# Brown Univ., Providence, R. I.
FEASIBILITY STUDY OF TEST PROBLEMS FOR FINITE ELEMENT/FINITE DIFFERENCE PROGRAMS FOR STRUCTURAL DYNAMICS Final Technical Report, 1 Aug. 1985 - 31 Jan. 1986
P. S. Symonds and H. Kolsky 12 Mar. 1986 12 p
(Contract DAAG29-85-K-0201)
(AD-A169058; ARO-23225.1-EG) Avail: NTIS HC A02/MF A01 CSCL 13/13

This research has resulted in additional calculations which will provide essential guides to future work. Using the Shanley model as a cheap and effective tool, calculated results show the influence of the geometrical parameter eta (= thickness of sandwich beam/half span) and of damping. It is seen that the anomalous behavior occurs only in a small range of thickness. Damping changes the response behavior fundamentally: counter-intuitive behavior still occurs but in a much more irregular manner, suggestive of chaotic behavior. Calculations using ABAQUS for the pinned uniform beam of standard dimensions and for a test specimen of slightly different dimensions show the characteristic diagrams for the two cases. It is surprising that qualitatively different shapes are obtained for the critical range of loads. The anomalous behavior being studied is evidently sensitive to parameters in unexpected ways. GRA

N87-12929# California Univ., Berkeley.
INTERNATIONAL CONFERENCE/WORKSHOP ON SMALL FATIGUE CRACKS (2ND) HELD IN SANTA BARBARA, CALIFORNIA ON 5-10 JANUARY 1986 Final Report
Robert O. Ritchie and James Lankford 31 Mar. 1986 31 p
Conference held in Santa Barbara, 5-10 Jan. 1986
(Grant DAAG29-85-G-0110)
(AD-A169060; ARO-23038.1-MS-CF) Avail: NTIS HC A03/MF A01 CSCL 11/6

This document provides a description and technical summary of the Second International Engineering Foundation Conference/ Workshop on Small Fatigue Cracks, held in Santa Barbara, California, 5 to 10 January, 1986. It provides a current assessment of the pertinent issues with respect to definition, differences in behavior compared to long cracks, environmental effects, driving forces for small crack extension, intrinsic thresholds, and the application of small crack methodology to life prediction and alloy design. A listing of the conference participants and the technical program are appended to the report. GRA

N87-12930# Brown Univ., Providence, R. I. Div. of Engineering.
A FINITE ELEMENT METHOD FOR LOCALIZED FAILURE ANALYSIS
Michael Ortiz, Yves Leroy, and Alan Needleman 15 Apr. 1986 43 p
(Contract N00014-85-K-0720; Grant NSF NSM-84-19338)
(AD-A169117) Avail: NTIS HC A03/MF A01 CSCL 12/1

A method is proposed which aims at enhancing the performance of general classes of elements in problems involving strain localization. The method exploits information concerning the process of localization which is readily available at the element level. A bifurcation analysis is used to determine the geometry of the localized deformation modes. When the onset of localization is detected, suitably defined shape functions are added to the element interpolation which closely reproduce the localized modes. The extra degrees of freedom representing the amplitudes of these modes are eliminated by static condensation. The proposed methodology can be applied to 2D and 3D problems involving arbitrary rate-independent material behavior. Numerical examples demonstrate the ability of the method to resolve the geometry of localized failure modes to the highest resolution allowed by the mesh. Author (GRA)

N87-12931# Naval Research Lab., Washington, D. C.
INFLUENCE OF SHEAR MODULUS ON THE BEHAVIOR OF ACOUSTICALLY TRANSPARENT MATERIALS Interim Report, 9 Jan. 1984 - 12 Jan. 1985
Pieter S. Dubbelday 30 Apr. 1986 16 p
(AD-A169289; NRL-MR-5745) Avail: NTIS HC A02/MF A01 CSCL 17/1

Materials are under construction that match the density, rho and dilatational sound speed, c as closely as possible to the values of seawater, while maintaining sufficient rigidity to serve for structural purposes. The demand for rigidity implies a larger shear modulus than is typical for the usual rho-c elastomers. Matching of density and sound speed results in transparency for fluids only; the finite shear modulus in a solid admits the presence of a shear wave, which causes deviation from ideal rho-c behavior. In this report the effect is analyzed of a finite shear modulus on the reflection of plane waves by an infinite plate of the rho-c material. Examples are given of the reflection coefficient as a function of incidence angle for various combinations of density and sound speed close to ideal, and various ratios of plate thickness to dilatational wavelength. The effect of a finite loss factor in the shear modulus is known. GRA

N87-12932# Texas A&M Univ., College Station. Mechanics and Materials Center.

STRESS ASSISTED DIFFUSION IN ELASTIC AND VISCOELASTIC MATERIALS

Y. Weitsman Nov. 1985 37 p

(Contract N00014-82-K-0562)

(AD-A169296; MM-4762-85-19) Avail: NTIS HC A03/MF A01 CSCL 11/9

The governing field equations and boundary conditions for stress assisted diffusion are derived from basic principles of continuum mechanics and irreversible thermodynamics. Attention is confined to elastic and viscoelastic material response, with emphasis on isotropy and the case of small strains. It is shown that both the diffusion process and the saturation levels are stress dependent. In viscoelastic materials the time-dependence of the moisture boundary condition causes the saturation level to drift with time. In addition, the diffusion process becomes nonlinear in stress, in spite of the linearity of the mechanical behavior. GRA

N87-12933# Dayton Univ., Ohio.

MAGNA (MATERIALLY AND GEOMETRICALLY NONLINEAR ANALYSIS). ADDENDUM 1, PARTS 1-4 Final Report, Sep. 1982 - Mar. 1984

R. A. Brockman May 1986 191 p

(Contract F33615-82-K-3402)

(AD-A169383; AFWAL-TR-82-3098-ADD-1) Avail: NTIS HC A09/MF A01 CSCL 20/11

The finite element program MAGNA (Materially And Geometrically Nonlinear Analysis), has been developed for nonlinear static and dynamic analysis of complex three dimensional structures. This program is applicable to large structural response problems involving bars, membranes, beams, plates, shells, and three dimensional solids, experiencing large displacements, finite strains, large rotations, and plastic deformation. This revision package reflects a number of additions and modifications to the MAGNA software. These include the migration of CDC program versions from NOS/BE to the NOS operating system, conversion of source code to FORTRAN-77 (ANSI X3.9-1978), elimination of file naming and numbering conflicts among different program options, usage of CRAY COS V1.11 lk which is compatible with both CRAY-1 and CRAY-X/MP computers, conversion to IBM computers under the OS/VS2 MVS operating system, modification of VAX/VMS and CRAY restart options, addition of a cyclic symmetry feature in natural frequency analysis with an option for static condensation. GRA

N87-12934# Army Close Combat Armaments Center, Watervliet, N.Y.

LINEAR ELASTIC FRACTURE TESTING: CURRENT STATUS WITHIN ASTM COMMITTEE E-24 ON FRACTURE

John H. Underwood Apr. 1986 20 p

(AD-A169442; ARCCB-TR-86015) Avail: NTIS HC A02/MF A01 CSCL 20/11

The current status of elastic-stress-controlled fracture testing within ASTM is summarized, including example test results from high-strength steel forgings used for cannon. Plane-strain fracture toughness test methods were emphasized. Areas for future work were also discussed, including rapid crack growth tests, correlative tests, and tests for composite materials. GRA

N87-12935# North Carolina Univ., Chapel Hill. Dept. of Chemistry.

INTRINSIC SiO2 FILM STRESS MEASUREMENTS ON THERMALLY OXIDIZED Si Interim Report

E. Kobeda and E. A. Irene 20 Jun. 1986 28 p

(Contract N00014-83-K-0571)

(AD-A169602; TR-7) Avail: NTIS HC A03/MF A01 CSCL 07/4

We have investigated the effects of varying Si oxidation conditions on intrinsic film stress for SiO2 films formed on Si. This study includes stress measurements on four Si orientations: (100), (110), (111), and (311); at oxidation temperatures ranging from 700 to 1100 C; wet (H2O) vs. dry (O2) oxidations for (100) and (111) surfaces; and the effects of post-oxidation annealing on stress. We find an orientation dependence for intrinsic stress which scales in the following manner: (110) > (311) > (100) > (111); a reduction in stress for wet vs. dry studies; and an even larger reduction for post-oxidation anneals. A recently proposed step model seems to account for the differences in stress with Si orientation. A number of Si oxidation models based on intrinsic stress are compared in their ability to describe the observed behavior, and we conclude that within the Deal-Grove oxidation model, the linear rate constant is strongly influenced by stress in the initial regime while stress is also likely to be important for thicker films. GRA

N87-12936# Washington Univ., St. Louis, Mo. Center for Computational Mechanics.

COMPUTATION OF THE AMPLITUDE OF STRESS SINGULAR TERMS FOR CRACKS AND REENTRANT CORNERS Final Report

Barna A. Szabo and Ivo Babuska Feb. 1986 35 p

(Contract N00014-85-K-0169; Grant AF-AFOSR-0315-82)

(AD-A169796; AD-E900585; WU/CCM-86/1) Avail: NTIS HC A03/MF A01 CSCL 20/11

The theoretical basis and performance characteristics of two new methods for the computation of the coefficients of the terms of asymptotic expansions at reentrant corners from finite element solutions are presented. The methods, called the contour integral method and the cutoff function method, are very efficient: The coefficients converge to their true values as fast as the strain energy, or faster. In order to make the presentation as simple as possible, we assume that the elastic body is homogeneous and isotropic, is loaded by boundary tractions only and, in the neighborhood of the reentrant corner, its boundaries are stress free. The methods described herein can be adapted to cases without such restrictions. GRA

N87-12937# Army Close Combat Armaments Center, Watervliet, N.Y.

COMPUTATION OF RESIDUAL STRESSES DUE TO PHASE TRANSFORMATIONS DURING QUENCHING OF HOLLOW CYLINDERS Final Report

J. D. Vasilakis Jul. 1986 39 p

(AD-A170493; ARCCB-TR-86024) Avail: NTIS HC A03/MF A01 CSCL 20/11

A previous paper described a method for computing the stresses due to the combined effects of transient temperatures and material phase transformations. The general purpose finite element program ADINAT/ADINA was used to compute both the transient temperatures and the associated stresses. The problem considered was that of an axisymmetric hollow cylinder undergoing a water-spray quench. The present work considers a similar model, but is better able to describe the residual stress state because of the availability of a more accurate set of properties for the material expansion due to the phase transformation. Effects on the transient and residual stresses due to modifications of the material expansion and varying quench rates are discussed. It was found that the stresses due to the transformation are more severe than those due to the transient temperatures alone. Inelastic behavior is found to occur in all the cases considered and high residual stresses can exist on the inner and outer surfaces. While dependent on actual material composition, these residual stresses can lead to quench cracking. The model describes the rapid quenching of steel gun tubes for the purpose of developing a martensitic grain structure and desired physical properties in the tube. GRA

N87-12938# Army Close Combat Armaments Center, Watervliet, N.Y.

UNLOADING-COMPLIANCE AND LOAD-DROP ANALYSIS OF J(Ic) TEST OF IRRADIATED 348 STAINLESS STEEL Final Technical Report

J. H. Underwood, F. M. Haggag, and W. G. Reuter Jun. 1986 31 p

(AD-A170494; ARCCB-TR-86021) Avail: NTIS HC A03/MF A01 CSCL 11/6

Procedures for determining J integral fracture toughness were applied to load versus load-line displacement data from a series of three point bend specimens of irradiated 348 stainless steel tested at 23 C and 427 C. ASTM Method E813 for J sub Ic was emphasized, using both unloading-compliance and load-drop measures of crack growth. An effective modulus procedure was included in the unloading compliance method using recently published load line displacement results. Two procedures were used for calculating J sub Ic from the J versus unloading compliance crack growth plots: the linear fit procedure from E813 and a power law fit with a 0.2 mm offset value of J sub Ic. Based on the results of these various procedures, conclusions were reached regarding the most consistent measures of fracture toughness from these data. Suggestions were given regarding the use of effective modulus with unloading compliance measurement of crack growth and the limitations of the load drop method for measuring crack growth. GRA

N87-12939# Fairchild Republic Co., Farmingdale, N.Y.
ASSESSMENT OF DAMAGE TOLERANCE REQUIREMENTS AND ANALYSES: A USER'S MANUAL FOR CRACK GROWTH AND CRACK INITIATION ANALYSIS: DAMGRO Final Report, Sep. 1982 - May 1986
Mier Levy and Albert Kuo 31 May 1986 142 p
(Contract F33615-82-C-3215)
(AD-A171209; AFWAL-TR-86-3028) Avail: NTIS HC A07/MF A01 CSCL 01/3

A structural test program of typical aircraft structural configurations was conducted to assess the current Air Force damage tolerance design requirements defined in MIL-A-83444. The specimens, made of 2024-T3XX and 7075-T6XX, were subjected to randomized flight-by-flight spectra, representative of fighter/trainer and bomber/cargo type loading spectra, respectively, and to a constant amplitude loading spectrum. A total of two-hundred fifty-six specimens were tested. The test results were correlated with analytical predictions using crack growth and crack initiation methods. As a result of this study, recommendation is provided to the validity of MIL-A-83444, to develop guidelines for selection of critical crack locations, and to assess the state-of-the art analytical capabilities in predicting crack growth and crack initiation time. This report presents the user's manual of the computer program DAMGRO. This program has been developed in conjunction with this contract, and used to predict the crack growth and crack initiation of the structural test specimens. Author (GRA)

N87-12940# Oak Ridge National Lab., Tenn.
INFLUENCE OF EXPERIMENTAL SCATTER ON THE ANALYSIS AND EXTRAPOLATION OF STRESS-RUPTURE DATA
M. K. Booker 1986 24 p Presented at the ASME Pressure Vessel and Piping Conference and Exhibit, Chicago, Ill., 20 Jul. 1986
(Contract DE-AC05-84OR-21400)
(DE86-009510; CONF-860722-10; CONF-860727-3) Avail: NTIS HC A02/MF A01

A great deal of research has been performed in the area of analysis and extrapolation of stress rupture data for more than three decades. Most of this work has concentrated on development of clever model forms for describing behavior in a simple mathematical way. However, little direct consideration has been given to the importance of inherent data scatter for such analyses. This paper presents a direct discussion of that topic, including an illustration of the impact of data scatter for several computer simulated data sets for which true behavior and the true amount of scatter are known by definition. The results clearly indicate that less attention should be paid to development of clever model forms for fitting data, and more should be paid to the use of sound, valid statistical techniques for the fitting of whatever models are used. DOE

N87-12941# Sandia National Labs., Albuquerque, N. Mex.
SHOCK-INDUCED SOLID STATE CHEMISTRY: THEORETICAL BACKGROUND
Y. Hori Jun. 1986 63 p
(Contract DE-AC04-76DP-00789)
(DE86-012741; SAND-86-0922) Avail: NTIS HC A04/MF A01

This report is a survey of the theoretical background of solid state chemistry relevant to high pressure shock wave loading. It is intended to be a study of selected theoretical concepts which are important for laying a foundation to make quantitative predictions concerning shock-induced chemical processes in nonenergetic solids. Since solid state reactions are often quite complex even under static conditions, the report is not intended to offer quick solutions to the very complex, and sometimes ill defined problems, but is to build a perspective to gain theoretical insight into some of them. The plan of the report is as follows: In Section 2, we collected a few relationships about chemical reactions from classical thermodynamics. In Section 3, we reviewed the nonequilibrium solid states created under shock wave loading with special focus on defects and heat and mass transport. Section 4 deals with selected concepts that may be useful to cope with reactions that result from the highly defective nonequilibrium states. Section 5 discusses several approaches for integrating microscopic mechanisms into continuum framework. Section 6 contains some recommendations for future research. DOE

N87-12942# Brookhaven National Lab., Upton, N. Y.
MOLECULAR DYNAMIC STUDIES OF CRACK PROPAGATION. THE ROLE OF THE INTERATOMIC POTENTIAL
G. J. Dienes 1986 6 p Presented at the Role of Hungarians in the Scientific and Technological Progress of the World, Budapest, Hungary, 4 Aug. 1986
(Contract DE-AC02-76CH-00016)
(DE86-009942; BNL-37960; CONF-860852-1) Avail: NTIS HC A02/MF A01

We have used the molecular dynamic simulation technique in studying a variety of solid state problems, ranging from equation-of-state and shock wave propagation to epitaxy and various aspects of crack propagation. In these simulations, which are classical, Newton's equations-of-motion are solved for each particle at every step to yield positions, velocities, forces and energies. An important limitation of the technique is that one has to put an interatomic potential into the calculation. Within these restrictions the technique is exact and is very powerful in automatically incorporating many body and anharmonic effects into the calculation. For complicated processes, such as crack propagation, there is a practical limitation to two dimensions, simply by the availability of computing capabilities, if a large enough sample, representative of bulk processes is to be used. DOE

N87-12943# Ames Lab., Iowa.
CRACK PROPAGATION IN HIGH STRAIN REGIONS OF A STEEL CONTAINMENT
F. Fanous and L. Greimann 1986 15 p Presented at the 3rd Workshop on Integrity of Containments for Nuclear Power Plants, Washington, D.C., 21 May 1986
(Contract W-7405-eng-82)
(DE86-011437; IS-M-578; CONF-860507-8) Avail: NTIS HC A02/MF A01

During a severe accident, a containment may develop a controlled relatively small leak before the pressure reaches the point where general rupture of the shell occurs. Another hypothesis states that an overall failure will occur with total release of the vessel contents. This work represents a preliminary study to predict crack propagation from an initially small defect in a high strain location in a typical steel containment. The J integral approach is used. A virtual crack extension method for calculating J is developed for use with general finite element programs. Two through cracks with different lengths were found to be unstable at the pressure which caused a surface crack to propagate through the containment thickness. In other words, the resulting through crack will not be stable and general failure will occur with the almost instantaneous release of the vessel contents. DOE

N87-12944# Oak Ridge National Lab., Tenn.
DATA REQUIREMENTS TO MODEL CREEP IN 9Cr-1Mo-V STEEL

R. W. Swindeman 1986 7 p Presented at the 3rd Symposium on Nonlinear Constitutive Relations for High Temperature Applications, Cleveland, Ohio, 11 Jun. 1986
(Contract DE-AC05-84OR-21400)
(DE86-011754; CONF-8606138-2) Avail: NTIS HC A02/MF A01

Models for creep behavior are helpful in predicting response of components experiencing stress redistributions due to cyclic loads, and often the analyst would like information that correlates strain rate with history assuming simple hardening rules such as those based on time or strain. On the other hand, much progress has been made in the development of unified constitutive equations that include both hardening and softening through tha introduction of state variables whose evolutions are history dependent. Although it is difficult to estimate specific data requirements for general application, there are several simple measurements that can be made in the course of creep testing and results reported in data bases. The issue is whether or not such data could be helpful in developing unified equations, and, if so, how should such data be reported. Data produced on a martensitic 9Cr-1Mo-V-Nb steel were examined with these issues in mind. DOE

N87-12945# Sandia National Labs., Albuquerque, N. Mex.
USING COMBINED EXPERIMENT/ANALYSIS TO GENERATE DYNAMIC CRITICAL STRESS INTENSITY DATA
D. V. Swenson and A. R. Ingraffea 1986 34 p Presented at the 19th National Symposium on Fracture Mechanics (ASTM), San Antonio, Tex., 30 Jun. 1986 Prepared in cooperation with Cornell Univ.
(Contract DE-AC04-76DP-00789)
(DE86-013578; SAND-86-1337C; CONF-860675-3) Avail: NTIS HC A03/MF A01

In this paper, we give a short description of a finite element model of mixed-mode dynamic crack propagation. We then discuss the use of combined experiment/analysis procedures to generate critical stress intensity data as a function of crack velocity. Because of the sensitivity of the analysis to boundary conditions and specified crack velocity, it is difficult to generate reliable K sub ID (v) data using this approach. This is due to uncertainties in both the analysis and measured crack position. Suggestions are made for alternate test methods to reduce some of these uncertainties. DOE

42 GEOSCIENCES (GENERAL)

N87-12946# Joint Publications Research Service, Arlington, Va.
USSR REPORT: EARTH SCIENCES
10 Sep. 1986 112 p Transl. into ENGLISH from various Russian articles
(JPRS-UES-86-007) Avail: NTIS HC A06/MF A01

Articles from various Russian publications on the Earth Sciences are translated. Major subject headings are Meteorology, Oceanography, Terrestrial Geophysics, Physics of the Atmosphere, and Arctic and Anarctic Research. Representative titles might be: Meteorological Effects of Geotectonic Phenomena Hypothesized; Two Layer Structure of Magnetically Active Layer of Oceanic Lithosphere; Fossil Finds by Siberian Paleontologists Add to Understanding of Life Development Chronology; Evaluating Nonlinear Effects in Propagation of Acoustic Pulse in Atmospheric Surface Layer in Inversions; and Proposals for Advancement of Year Round Arctic Shipping. For individual titles, see N87-12947 through N87-12958.

N87-12947# Joint Publications Research Service, Arlington, Va.
METEOROLOGICAL EFFECTS OF GEOTECTONIC PHENOMENA HYPOTHESIZED Abstract Only **c47**
G. Afanasyev *In its* USSR Report: Earth Sciences (JPRS-UES-86-007) 10 Sep. 1986 2 p Transl. into ENGLISH from Sovetskaya Litva (Riga, USSR), 27 Apr. 1986 p 2 (For primary document see N87-12946 04-42)
Avail: NTIS HC A06/MF A01

When meteorological data for several years in succession are carefully analyzed: heightened or lowered atmospheric pressures are observed more frequently over certain regions of the planet than others, at which cyclones and anticyclones originate. The natural conclusion, is that the source of the weather is located in the depths of the planet, in its mantle. This hypothesis was advanced at a conference on geotectonics which took place in the USSR. When the mantle interacts with the earth's core, so-called mantle channels form. They are fluctuating columns of matter 25 to 30 kilometers in diameter and 2,900 kilometers tall. This leads to the appearance of gravitational anomalies which are too weak to affect molecules of air directly, but they are quite sufficient to alter, by 1,000 times or more, the concentration of aerosols-droplets of water about 0.2 micrometer in diameter which are suspended in the air. These aerosols are condensation centers for water vapors, and their concentration directly affects the weather, as meteorologists demonstrated long ago. If the concentration changed in a certain place, the heatbalance of the atmosphere also changed there; areas heightened or lowered pressure occurred, and a cyclone or anticyclone was formed. E.R.

N87-12948# Joint Publications Research Service, Arlington, Va.
THIRD INTERNATIONAL SYMPOSIUM ON TROPICAL METEOROLOGY Abstract Only **c47**
V. N. Ivanov *In its* USSR Report: Earth Sciences (JPRS-UES-86-007) 10 Sep. 1986 1 p Transl. into ENGLISH from Izvestiya Akademii Nauk SSSR: Fiziki Atmosfery i Okeana (Moscow, USSR), v. 22, no. 2, Feb. 1986 p 221-223 Symposium held in Yalta, 24-31 Mar. 1985 (For primary document see N87-12946 04-42)
Avail: NTIS HC A06/MF A01

The Third International Symposium on Tropical Meteorology was held at Yalta. The 100 specialists present represented scientific institutes in the USSR, Cuba and Vietnam. Twelve special reports and 18 other communications were presented on the subject of tropical meteorology and hurricane research. The subjects dealt with included prediction of the trajectories of tropical cyclones, generation and development of tropical cyclones, numerical and laboratory modeling of tropical cyclones, structure and energetics of tropical cyclones, clouds and artificial inducement of precipitation. Three types of prognostic models (hydrodynamic, statistical and semiempirical) were discussed. Author

N87-12949# Joint Publications Research Service, Arlington, Va.
AVAILABLE POTENTIAL ENERGY IN UPPER LAYER OF WORLD OCEAN Abstract Only **c46**
V. S. Arsenyev and V. A. Burkov *In its* USSR Report: Earth Sciences (JPRS-UES-86-007) 10 Sep. 1986 1 p Transl. into ENGLISH from Doklady Akademii Nauk SSSR (Moscow, USSR), v. 287, no. 4, Apr. 1986 p 986-989 (For primary document see N87-12946 04-42)
Avail: NTIS HC A06/MF A01

The available potential energy (APE) is calculated for large scale motion in the entire world ocean (with the exception of the Arctic Ocean) to a depth of 1500 m. The highest values of APE are found to occur in the regions of Antarctic divergence (more than 55 x 10 to the 5th J/sq m), subpolar divergence in the Atlantic (more than 35 x 10 to the 5th J/sq m), and northern subtropical convergence in the Pacific south of Japan (more than 30 x 10 to the 5th J/sq m). E.R.

N87-12950# Joint Publications Research Service, Arlington, Va.
DESERTIFICATION: GLOBAL ECOLOGICAL PROBLEM Abstract Only **c46**
N. S. Orlovskiy *In its* USSR Report: Earth Sciences (JPRS-UES-86-007) 10 Sep. 1986 2 p Transl. into ENGLISH from Voprosy Filisofii (Moscow, USSR), no. 2, Feb. 1986 p 113-123 (For primary document see N87-12946 04-42)
Avail: NTIS HC A06/MF A01

It is suggested that western practices and analyses of desertification fail to take social factors into account, and do not promote progressive technology that would preserve the environment while bringing progress. It is claimed that Soviet practices

have minimized ecological damage by use of a different socioeconomic structure and by planning. In Central Asia, efforts since the 1930's have focused on controlling shifting sands with both dry grass and brush, as well as physicochemical means. In Turkmenistan sand dune damage to irrigated fields is completely controlled, although some local areas of desertification have been noted near well sites and in industrialized desert areas. Prevention of land damage in irrigated areas has required careful drainage system construction to avoid mineral deposits while making maximum use of ground water reserves. Technological backwardness is noted in some irrigated areas of Central Asia, and the extent of saline soils of various types is of concern. Disposal of irrigation water after its use is another problem still being resolved in Central Asia. Irrigation and water disposal in the basins of Syrdarya, Amudarya and Ili Rivers have caused a decline in the level of the Aral Sea. In addition, lands in the deltas of the Syrdarya and Amudarya have suffered desertification. Author

N87-12951# Joint Publications Research Service, Arlington, Va.
EVALUATING NONLINEAR EFFECTS IN PROPAGATION OF ACOUSTIC PULSE IN ATMOSPHERIC SURFACE LAYER IN INVERSIONS Abstract Only **c71**
I. P. Chunchuzov *In its* USSR Report: Earth Sciences (JPRS-UES-86-007) 10 Sep. 1986 2 p Transl. into ENGLISH from Izvestiya Akademii Nauk SSSR: Fizika Atmosfery i Okeana (Moscow, USSR), v. 22, no. 2, Feb. 1986 p 151-159 (For primary document see N87-12946 04-42)
Avail: NTIS HC A06/MF A01

The general features of propagation of powerful acoustic disturbances in the atmospheric surface layer were analyzed. They can be generated by natural sources, such as volcanic eruptions, earthquakes and thunderstorms or by such artificial sources as powerful exlosions. An attempt was made to clarify the contribution made by nonlinear effects to the process of propagation of powerful acoustic disturbances in a surface waveguide. It is shown that in some cases such a nonlinear process of waveguide propagation of sound can be described by a nonlinear equation which is a nonlinear analogue of the well-known parabolic equation. Proceeding on this basis, it is shown that in the case of a point source nonlinear effects and waveguide dispersion can result in the appearance of cylindrical solitons at great distances which attenuate with distance far more slowly than a linearly propagated pulse. An equation is derived whose solution describes low change of the initially plane soliton in the course of propagation. Author

N87-12952# Joint Publications Research Service, Arlington, Va.
EXPERIMENTAL RESEARCH ON TURBULENCE IN UPPER-LEVEL TROPOSPHERIC CLOUDS Abstract Only **c46**
V. K. Dmitriyev, T. P. Kapitanova, V. D. Litvinova, N. Z. Pinus, G. A. Potertikova, and G. N. Shur *In its* USSR Report: Earth Sciences (JPRS-UES-86-007) 10 Sep. 1986 1 p Transl. into ENGLISH from Izvestiya Akademii Nauk SSSR: Fizika Atmosfery i Okeana (Moscow, USSR), v. 22, no. 2, Feb. 1986 p 143-150 (For primary document see N87-12946 04-42)
Avail: NTIS HC A06/MF A01

Flight studies of turbulence in cirrus clouds were made in late 1981 and early 1982. The experiments were carried out with a wide array of scientific instrumentation for measuring mean temperature, humidity, wind velocity and direction, fluctuations of temperature and the horizontal and vertical components of the wind vector. Parameters were measured in two ranges of spatial scales of disturbance (from hundreds of meters to 2 to 3 km and from 5 to 6 to 30 to 40 km). The two ranges correspond to micro- and mesoscale pulsations. Horizontal flights with a length up to 500 km were made at 5 to 6 levels. Nineteen multilever flight experiments were made. Flights were made in cirrostratus clouds and in the clear sky. The collected data were used in constructing vertical atmospheric sections and in tabulating the results of synchronous measurements of the vertical and horizontal fluctuations of velocity and temperature fluctuations, rate of dissipation of turbulent energy into heat, rate of evening-out of temperature inhomogeneities and structural characteristic of the fluctuating temperature field. This made it possible to define the distinguishing characteristics of turbulence in cirrostratus clouds and in jet streams. Author

N87-12953# Joint Publications Research Service, Arlington, Va.
SOLAR CONTROL OF GEOPHYSICAL PHENOMENA Abstract Only **c46**
V. F. Loginov and G. V. Fedorovich *In its* USSR Report: Earth Sciences (JPRS-UES-86-007) 10 Sep. 1986 1 p Transl. into ENGLISH from Zemlya i Vselennaya (Moscow, USSR), no. 1, Jan. - Feb. 1986 p 58-61 (For primary document see N87-12946 04-42)
Avail: NTIS HC A06/MF A01

An all-union conference on Interrelationship of Meteorological Phenomena and Processes in Circumterrestrial Space was held in Moscow. The purpose was a review of progress in study of different mechanisms of interrelationships of geophysical and meteorological processes and phenomena in the upper atmosphere and in space. The change in the influx of solar radiation to the Earth during the last century was studied. On the basis of data on parameters of the Earth's orbit and brightness of the solar disk they concluded that the influx of solar radiation is decreasing not only due to a change in the brightness of the solar disk, but also due to a change in the parameters of the Earth's orbit with a duration from several years to several decades. Changes in composition and temperature of the ozone layer under the influence of UV radiation and cosmic rays was discussed. Although ozone for the most part is found in the lower and middle stratosphere and solar flares have little effect on its total content, there is good basis for assuming that the ozone mechanism plays a definite role in changes in weather and climate. The role was also studied of the Earth's electrical field in solar-terrestrial relationships, which plays an important role in the propagation of disturbances in the circumterrestrial medium and must be taken into account in studying the process of preparation of earthquakes. Author

N87-12954# Joint Publications Research Service, Arlington, Va.
EFFECT OF PULSATING AURORAS ON FREQUENCY-TIME CHARACTERISTICS OF RADIO SIGNALS REFLECTED FROM AURORAL IONOSPHERE Abstract Only **c32**
A. A. Arykov, I. N. Bardeyev, A. N. Vasilyev, V. G. Korotkov, A. M. Royzen, and S. A. Rumyantsev *In its* USSR Report: Earth ScienceS (JPRS-UES-86-007) 10 Sep. 1986 1 p Transl. into ENGLISH from Geomagnetizm i Aeronomiya (Moscow, USSR), v. 26, no. 2, Mar. - Apr. 1986 p 243-246 (For primary document see N87-12946 04-42)
Avail: NTIS HC A06/MF A01

The spectrum of constant wave radio signals reflected and dissipated by the ionosphere can provide much information about processes in the ionosphere. Experimental study of dynamics of spectral variations of radio signals reflected from the auroral ionosphere during periods of pulsating auroras is reported. The experiments were conducted on a 60 km path at a geomagnetic latitude averaging 63 deg. A constant signal with plane polarization was sent at 3.3 MHz. Analysis of experimental data show that the undisturbed signal, in a band of several Hz around the working frequency, was expanded noticeably in amplitude by the aurora disturbances. Optical pulsations and spectral variations support the explanation of spectral variations as a result of Doppler frequency shifts and changes in electron concentration profiles. Auroras with an interval of about 10 seconds were accompanied by specific variations in SW radio signals reflected in the E region of the auroral ionosphere. Spectral variations are explained by the Doppler shift of signal frequency during changes in ionization density created by rapidly changing currents of precipitating electrons during pulsating auroras. Author

N87-12955# Joint Publications Research Service, Arlington, Va.
PHASE FLUCTUATIONS OF IONOSPHERE RADIO SIGNALS Abstract Only **c32**
V. D. Gusev and M. B. Vinogradova *In its* USSR Report: Earth Sciences (JPRS-UES-86-007) 10 Sep. 1986 2 p Transl. into ENGLISH from Geomagnetizm i Aeronomiya (Moscow, USSR),

v. 26, no. 2, Mar. - Apr. 1986 p 247-252 (For primary document see N87-12946 04-42)
Avail: NTIS HC A06/MF A01

Phase fluctuations were observed in reflections of radio signals in regions of the ionosphere containing various inhomogeneities. While these fluctuations affect operations of radio systems, they also offer new information about the structure and dimensions of scattering inhomogeneities. Geometric optics are used for correct expression of wave phase reflections from the ionosphere during oblique propagation. Calculations take account of dielectric permeability and beam trajectories. A second series of calculations related to determination of phase fluctuations of waves during propagation in a fixed-thickness layer with slant incidence relative to the boundary. Fluctuations of horizontal beam shift at the output from the distributive layer are also treated mathematically. Results indicate that ionosphere inhomogeneities can be used to determine dielectric properties of materials. Author

N87-12956# Joint Publications Research Service, Arlington, Va.
TRANSVERSE RESONANCES OF EARTH-IONOSPHERE WAVE GUIDE IN AURORAL REGION Abstract Only c32
V. S. Smirnov and A. A. Ostapenko *In its* USSR Report: Earth Sciences (JPRS-UES-86-007) 10 Sep. 1986 1 p Transl. into ENGLISH from Geomagnetizm i Aeronomiya (Moscow, USSR), v. 26, no. 2, Mar. - Apr. 1986 p 253-257 (For primary document see N87-12946 04-42)
Avail: NTIS HC A06/MF A01

Contemporary studies of low freqeuncy radiation have defined the precise structure of such signals in the auroral region. A study is reported of spectral and polarized features of transverse resonances and the relationship to ionospheric parameters. So-called Schumann resonances were studied with frequencies from a few to tens of Hz. Strong attenuation in that range virtually excludes wave interference and makes it difficult to generate global resonances in the kiloherz frequency range. Thus, modulations in those frequencies are local in nature. They make it possible to use a plane model of the earth-ionosphere wave guide and allow direct determination of the wave equation, which is discussed. Results show that at high latitude degeneration effects are manifested in periods of leakage of hard particles when the ionosphere is at low altitudes; soft particles are found when the ionosphere limits are at higher altitudes. A stepped mathematical model gave a rough approximation of actual ionization. Ordinary and extraordinary modes were found to correspond to waves of left and right polarization, respectively, with relatively low values for particle disintegration. Theoretical values correlated well with experimental data on low-frequency radiation wave. Author

N87-12957# Joint Publications Research Service, Arlington, Va.
REGULAR NOISE BACKGROUND IN VLF-RADIATION AND WORLD THUNDERSTORM CENTERS Abstract Only c32
G. I. Druzhin, T. V. Toropchinova, and V. I. Shapayev *In its* USSR Report: Earth Sciences (JPRS-UES-86-007) 10 Sep. 1986 1 p Transl. into ENGLISH from Geomagnetizm i Aeronomiya (Moscow, USSR), v. 26, no. 2, Mar. - Apr. 1986 p 258-264 (For primary document see N87-12946 04-42)
Avail: NTIS HC A06/MF A01

Regular noise emissions (RNE) in VLF radiations are typified by their constant nature. Attempts to develop qualitative analysis procedures for defining various sources in the RNE amplitude by observing the day-long course of intensity at several recording stations are reported. Signal azimuth findings were made using a magnetic dipole antenna. A preliminary hypothesis held that only two sources, discrete and isotropic points, contributed to RNE amplitude. Actually, it was found that two or more sources could be involved simultaneously. Errors for three factors are discussed: the RNE source with extreme limits, several simultaneous discrete sources and measurement error parameters. Varying evening and nighttime readings were recorded, with minor morning changes as well. They were found at all recording stations. Quasi-constant azimuths of radiation during definite periods indicate that localized RNE sources should exist during these periods. During fall and winter periods, world thunderstorm cells were found to play a key role in RNE formation, but further research is needed to determine whether thunderstorm activity alone accounts for RNE generation. Author

N87-12958# Joint Publications Research Service, Arlington, Va.
SPATIAL RADIO WAVE ATTENUATION DURING VERTICAL SOUNDING OF IONOSPHERE Abstract Only c32
P. F. Denisenko, V. I. Vodolazkin, and G. G. Vertogradov *In its* USSR Report: Earth Sciences (JPRS-UES-86-007) 10 Sep. 1986 1 p Transl. into ENGLISH from Geomagnetizm i Aeronomiya (Moscow, USSR), v. 26, no. 2, Mar. - Apr. 1986 p 322-325 (For primary document see N87-12946 04-42)
Avail: NTIS HC A06/MF A01

Radio wave attenuation due to energy losses in the ionosphere was studied. The field is expressed by the equation: E = A exp(-L sub e/r sub eff). It concentrates on determining the effective distance in the actual ionosphere in relation to an illuminated area of the earth's surface. The vector of the inverse geomagnetic field strength effect is also included in the mathematical model. It is noted that the results are reliable for all but the longitudinal propagation of regular radio waves. Corrections are suggested. The method has a correctable level of error. Author

43 EARTH RESOURCES AND REMOTE SENSING

Includes remote sensing of earth resources by aircraft and spacecraft; photogrammetry; and aerial photography.

For instrumentation see *35 Instrumentation and Photography.*

N87-12959# Instituto de Pesquisas Espaciais, Sao Jose dos Campos (Brazil).
GEOLOGIC REMOTE SENSING AT INPE: AN OVERVIEW
Chan Chiang Liu, Jose Eduardo Rodrigues, and Paulo Roberto Martini Aug. 1986 18 p Presented at the Seminar on Geologic Applications of Remote Sensing, Sao Jose dos Campos, Brazil, Dec. 1985
(INPE-3975-PRE/987) Avail: NTIS HC A02/MF A01

In Brazil, LANDSAT imagery has been used for regional geological and mineral resources mapping. The launching of the first LANDSAT is a milestone in the history of geological surveys by remote sensing techniques in this country. Because LANDSAT images give a bird's eye view of the earth's surface, this regional geological mapping has been carried out first, and then followed by structural and geotectonic studies. On the other hand, because LANDSAT data in digital format on Computer Compatible Tapes (CCT) are available to be analyzed by computer-processing techniques, research for mineral deposits and rock formation identification have been possible especially in recent years. Author

N87-12960# Instituto de Pesquisas Espaciais, Sao Jose dos Campos (Brazil).
EVALUATION OF REMOTE SENSING TECHNIQUES TO THE DETECTION OF CHANGES IN A FLUVIAL SYSTEM DUE TO HUMAN INFLUENCE: THE EXAMPLE OF CANAS RIVER BASIN (SAO PAULO STATE, BRAZIL)
Evlyn M. L. M. Novo and Adilson Avansi deAbreu (Sao Paulo Univ. (Brazil).) Aug. 1986 36 p Submitted for publication
(INPE-3970-PRE/983) Avail: NTIS HC A03/MF A01

The main objective of this study is to exemplify the use of remote sensing data to evaluate human interference in fluvial systems. River Canas Basin was selected as a test site since it belongs to the Paraiba River basin where human action has disrupted natural equilibrium. Multitemporal aerial photography was analyzed so as to detect changes in fluvial morphology. The rate of environmental change was checked against remote sensing data available by using field work information. Results permitted identification river channel changes over time as well as local factors which explain the variability of change rates. Author

N87-12961# Instituto de Pesquisas Espaciais, Sao Jose dos Campos (Brazil).
CROP YIELD MODELING FOR CLIMATE IMPACT STUDIES. PART 1: REASONING AND RESULTS
Fausto Carlos deAlmeida Aug. 1986 12 p Presented at the IIASA Meeting on Assessment of Climate Impact on Agriculture in Semiarid and High Altitude Regions, Laxenburg, Austria, 8-12 Oct. 1984
(INPE-3967-PRE/982-Pt-1) Avail: NTIS HC A02/MF A01

The use of regression crop yield models (RCY) for Climate Impact Assessment Studies requires some basic features sometimes not encountered in most RCY models. Many of the RCY models developed have a different aim, i.e., to give a reasonable estimate of the yield of a given crop, for a given location, based on a historical technological trend and suitably chosen meteorological variables. In general they offer good prediction efficacy, i.e., occuracy and lead time, but should be carefully analyzed when used for other purposes, such as in Climate Impact Assessment Studies. Depending on what kind of climate scenario we are dealing with, the RCY model chosen has to be able to assimilate the impact of the respective meteorological variables on yield. For this, the model should be representative, i.e., should not depend on the historical time series period we chose to work with. Its regression coefficients should be stable with no change in sign and present a very small (combined) variance, otherwise the climate impact, represented by changes of the meteorological variables being tested, can be masked by its (the regression coefficients) variance. Author

N87-12962# Instituto de Pesquisas Espaciais, Sao Jose dos Campos (Brazil).
ENERGY RECEIPT PARTITIONING OVER THE AMAZON FOREST
Leonardo DeanedeAbreuSa, Yelisetty Viswanadham, and Antonio Ocimar Manzi Aug. 1986 46 p Submitted for publication
(INPE-3980-PRE/990) Avail: NTIS HC A03/MF A01

The present study involved determination of the experimental energy receipt partitioning over the tropical Amazon forest. Diurnal variation of net radiation (Q*), sensible heat flux (Q sub H) and latent heat flux (Q sub E) is presented. The daytime Q sub E is in phase with Q* and it is always an important term in the energy balance. The daily averaged Q sub E is 59 to 100% of the daily Q* whereas Q sub H is 5 to 28% at the Amazon forest site (2 deg. 57 deg. S; 59 deg. 57 deg W) for the sample periods. The results present evidence that Q sub E over the Amazon forest is greater than Q* in the afternoon hours. The role of sensible heat advection in maintaining large Q sub E over the forest surface is discussed. Hourly Bowen ratio (beta) values for two compaigns are presented. During daylight hours, the differences in beta are not significant, and exhibit a systematic pattern. The only time that the variation in Bowen ratio increased significantly was a sunrise and sunset when the thermal structure of the air was changing from a strong inversion to lapse and vice versa. The diurnal beta values changed from -3.50 to 0.85. The mean hourly beta calculated from values from 0700 to 1600h, varied from 0.05 to 0.85. Author

N87-12963# Instituto de Pesquisas Espaciais, Sao Jose dos Campos (Brazil).
REPORT OF THE AD-HOC COMMISSION ON REMOTE SENSING [RELATORIO DA COMISSAO AD-HOC EM SENSORIAMENTO REMOTO]
Aug. 1986 31 p In PORTUGUESE; ENGLISH summary
(INPE-3981-NTE/259) Avail: NTIS HC A03/MF A01

The results of the Commission for the Remote Sensing Areas, following INPE's Director request is presented. Author

N87-12964# Instituto de Pesquisas Espaciais, Sao Jose dos Campos (Brazil).
A PARTITION OF SENSIBLE AND LATENT HEAT FLUXES ABOVE THE TERRA FIRMA AREA IN THE AMAZON FOREST (GRADIENT METHOD) [PARTICAO DE FLUXOS DE CALOR SENSIVEL E DE CALOR LATENTE ACIMA DA FLORESTA AMAZONICA DE TERRA FIRME (METODO DOS GRADIENTES)]
Leonardo DeanedeAbreuSa, Antonio Ocimar Manzi, and Yelisetty Viswanadham Aug. 1986 18 p In PORTUGUESE; ENGLISH summary Presented at the 30th Reuaniao Anual da S.B.P.C., Curitiba, Brazil, 9-16 Jul., 1986
(INPE-3972-PRE/985) Avail: NTIS HC A02/MF A01

A partition of net radiation to sensible and latent heat fluxes above the Amazon Forest canopy is studied. The observational site (2 degrees 57 minutes S, 59 degrees W) of the Terra firma area in the Amazon forest is near Manaus, AM. The Bowen ratio values for distinct layers above the canopy are calculated using the profile method. Diurnal variation of these values are presented. The results show that the daytime Bowen ratios obtained during nonprecipiatation days for higher layer are greater than for lower layer. This may be attributed to the influence of this transpiration from adjacnt air layers above the canopy. This process reduces the temperature of the adjacent air layers above the canopy and increases the specific humidity in those layers. The data obtained for the period July 1984 to April 1985 were utilized in the analysis. Author

N87-12965*# Jet Propulsion Lab., California Inst. of Tech., Pasadena.
ERS-1 SAR DATA PROCESSING
Kon Leung, Thomas Bicknell, and Kenneth Vines 1 Sep. 1986 34 p
(NASA-CR-179913; JPL-Pub-86-33; NAS 1.26:179913) Avail: NTIS HC A03/MF A01 CSCL 05B

To take full advantage of the synthetic aperature radar (SAR) to be flown on board the European Space Agency's Remote Sensing Satellite (ERS-1) (1989) and the Canadian Radarsat (1990), the implementation of a receiving station in Alaska is being studied to gather and process SAR data pertaining in particular to regions within the station's range of reception. The current SAR data processing requirement is estimated to be on the order of 5 minutes per day. The Interim Digital Sar Processor (IDP) which was under continual development through Seasat (1978) and SIR-B (1984) can process slightly more than 2 minutes of ERS-1 data per day. On the other hand, the Advanced Digital SAR Processore (ADSP), currently under development for the Shuttle Imaging Radar C (SIR-C, 1988) and the Venus Radar Mapper, (VMR, 1988), is capable of processing ERS-1 SAR data at a real time rate. To better suit the anticipated ERS-1 SAR data processing requirement, both a modified IDP and an ADSP derivative are being examined. For the modified IDP, a pipelined architecture is proposed for the mini-computer plus array processor arrangement to improve throughout. For the ADSP derivative, a simplified version is proposed to enhance ease of implementation and maintainability while maintaing real time throughput rates. These processing systems are discussed and evaluated. Author

N87-12966# Instituto de Pesquisas Espaciais, Sao Jose dos Campos (Brazil).
PHOTOGRAPHIC SENSORS: BASIC CONCEPTS [SENSORES FOTOGRAFICOS: CONCEITOS BASICOS]
Chan Chang Liu and Jose Eduardo Rodrigues Sep. 1986 43 p In PORTUGUESE; ENGLISH summary
(INPE-3990-MD/031) Avail: NTIS HC A03/MF A01

This paper of photographic systems is prepared for the Postgraduate course on Remote Sensing of the Instituto de Pesquisas Espaciais (INPE) and is suitable both as teaching material or as reference. It provides almost all aspects of photography, taking and processing photographs, physical factors affecting their quality, type of camera, films, filters and so on. This work is not exhaustive but is a summary of subjects extensively covered in the literature. Therefore, readers should be quickly able to understand and apply the photographic remote sensing techniques to their disciplines. Author

N87-12967*# National Aeronautics and Space Administration. Ames Research Center, Moffett Field, Calif.
A COMPUTATIONAL METHOD TO MODEL RADAR RETURN

RANGE IN A POLYGONALLY BASED, COMPUTER-GENERATED-IMAGERY SIMULATION

F. J. Moran and J. D. Phillips Jul. 1986 22 p
(NASA-TM-88324; A-86313; NAS 1.15:88324) Avail: NTIS HC A02/MF A01 CSCL 08B

Described is a method for modeling a ground-mapping radar system for use in simulations where the terrain is in a polygonal form commonly used with computer generated imagery (CGI). The method employs a unique approach for rapidly rejecting polygons not visible to the radar to facilitate the real-time simulation of the radar return. This rapid rejection of the nonvisible polygons requires the precalculation and storage of a set of parameters that do not vary during the simulation. The calculation of a radar range as a function of the radar forward-looking angle to the CGI terrain is carried out only for the visible polygons. This method was used as part of a simulation for terrain-following helicopter operations on the vertical motion simulator at the NASA Ames Research Center. It proved to be an efficient means for returning real-time simulated radar range data. Author

N87-12968*# Jet Propulsion Lab., California Inst. of Tech., Pasadena.

PROCEEDINGS OF THE SECOND AIRBORNE IMAGING SPECTROMETER DATA ANALYSIS WORKSHOP

Gregg Vane, ed. and Alexander F. H. Goetz, ed. 15 Aug. 1986 218 p Workshop held in Pasadena, Calif., 6-8 May 1986 Sponsored by NASA
(NASA-CR-179924; JPL-Pub-86-35; NAS 1.26:179924) Avail: NTIS HC A10/MF A01 CSCL 05B

Topics addressed include: calibration, the atmosphere, data problems and techniques, geological research, and botanical and geobotanical research. For individual titles, see N87-12969 through N87-12987.

N87-12969*# Jet Propulsion Lab., California Inst. of Tech., Pasadena.

RADIOMETRIC CALIBRATION OF THE AIRBORNE IMAGING SPECTROMETER **c35**

Deanne Tucker and Gregg Vane *In its* Proceedings of the Second Airborne Imaging Spectrometer Data Analysis Workshop 15 Aug. 1986 p 17-20 (For primary document see N87-12968 04-43)
Avail: NTIS HC A10/MF A01 CSCL 14B

Several laboratory calibration tests were developed for the Airborne Imaging Spectrometer (AIS). The goals of these tests are to adjust the physical alignment of the detector within the optical system and set the spectral endpoints, and produce a calibration file of multipliers which equalizes the relative responses of each of the detector elements in the entire two-dimensional array. Tests are also performed as part of an ongoing effort to provide absolute radiometric calibration. The tests are described and the merits and limitations of each are discussed. Author

N87-12970*# Stanford Telecommunications, Inc., Sunnyvale, Calif.

COMPARISON OF VARIOUS TECHNIQUES FOR CALIBRATION OF AIS DATA **c35**

Dar A. Roberts, Yasushi Yamaguchi (Geological Survey of Japan, Kawasaki.), and Ronald J. P. Lyon *In* JPL Proceedings of the Second Airborn Imaging Spectrometer Data Analysis Workshop 15 Aug. 1986 p 21-30 (For primary document see N87-12968 04-43)
Avail: NTIS HC A10/MF A01 CSCL 14B

The Airborne Imaging Spectrometer (AIS) samples a region which is strongly influenced by decreasing solar irradiance at longer wavelengths and strong atmospheric absorptions. Four techniques, the Log Residual, the Least Upper Bound Residual, the Flat Field Correction and calibration using field reflectance measurements were investigated as a means for removing these two features. Of the four techniques field reflectance calibration proved to be superior in terms of noise and normalization. Of the other three techniques, the Log Residual was superior when applied to areas which did not contain one dominant cover type. In heavily vegetated areas, the Log Residual proved to be ineffective. After removing anomalously bright data values, the Least Upper Bound Residual proved to be almost as effective as the Log Residual in sparsely vegetated areas and much more effective in heavily vegetated areas. Of all the techniques, the Flat Field Correction was the noisiest. Author

N87-12971*# Jet Propulsion Lab., California Inst. of Tech., Pasadena.

ANALYSIS OF AIS RADIOMETRY WITH EMPHASIS ON DETERMINATION OF ATMOSPHERIC PROPERTIES AND SURFACE REFLECTANCE

J. E. Conel, S. Adams, R. E. Alley, G. Hoover, and S. Schultz *In its* Proceedings of the Second Airborne Imaging Spectrometer Data Analysis Workshop 15 Aug. 1986 p 31-51 (For primary document see N87-12968 04-43)
Avail: NTIS HC A10/MF A01 CSCL 05B

Airborne Imaging Spectrometer data from Mono Lake, California, were studied in order to establish spectral radiance of test areas under solar illumination. The objective is to provide a method of atmospheric correction for major absorbers from the spectrometer data themselves. Crucial to the analysis is radiometric calibration of the instrument. Good agreement is found between calculated and measured radiances for uniform surface targets (beaches), but simulations of atmospheric properties with LOWTRAN lead to unreasonably low values of atmospheric precipitable water. Absorptions from carbon dioxide are not detected in the AIS data, but are strongly present in the LOWTRAN model. The apparent low contrast of all atmospheric absorption bands leads to a study of contamination from overlapping spectral orders in the AIS data. The suspected contamination is shown unambiguously to be present beyond approximately 1500 nm and consists of an extra radiance term including atmospheric bands from the delta/2 wavelength interval. A rigorous removal of the unwanted spectral contamination does not seem possible for any data taken in the rock mode. Rough estimates for tree-mode observations might be pieced together is a suitable after-the-fact radiometric calibration of the instrument can be formulated. Author

N87-12972*# Commonwealth Scientific and Industrial Research Organization, Ryde (Australia). Div. of Mineral Physics and Mineralogy.

AIRBORNE SPECTRORADIOMETRY: THE APPLICATION OF AIS DATA TO DETECTING SUBTLE MINERAL ABSORPTION FEATURES

Terry D. Cocks and Andy A. Green *In* JPL Proceedings of the Second Airborne Imaging Spectrometer Data Analysis Workshop 15 Aug. 1986 p 52-62 (For primary document see N87-12968 04-43)
Avail: NTIS HC A10/MF A01 CSCL 05B

Analysis of Airborne Imaging Spectrometer (AIS) data acquired in Australia has revealed a number of operational problems. Horizontal striping in AIS imagery and spectral distortions due to order overlap were investigated. Horizontal striping, caused by grating position errors can be removed with little or no effect on spectral details. Order overlap remains a problem that seriously compromises identification of subtle mineral absorption features within AIS spectra. A spectrometric model of the AIS was developed to assist in identifying spurious spectral features, and will be used in efforts to restore the spectral integrity of the data. Author

N87-12973*# Geological Survey, Lakewood, Colo. Geologic Div.

ATMOSPHERIC-WATER ABSORPTION FEATURES NEAR 2.2 MICROMETERS AND THEIR IMPORTANCE IN HIGH SPECTRAL RESOLUTION REMOTE SENSING

Fred A. Kruse and Roger N. Clark *In* JPL Proceedings of the Second Airborne Imaging Spectrometer Data Analysis Workshop 15 Aug. 1986 p 63-73 (For primary document see N87-12968 04-43)
Avail: NTIS HC A10/MF A01 CSCL 05B

Selective absorption of electromagnetic radiation by atmospheric gases and water vapor is an accepted fact in terrestrial remote sensing. Until recently, only a general knowledge of atmospheric effects was required for analysis of remote sensing

data; however, with the advent of high spectral resolution imaging devices, detailed knowledge of atmospheric absorption bands has become increasingly important for accurate analysis. Detailed study of high spectral resolution aircraft data at the U.S. Geological Survey has disclosed narrow absorption features centered at approximately 2.17 and 2.20 micrometers not caused by surface mineralogy. Published atmospheric transmission spectra and atmospheric spectra derived using the LOWTRAN-5 computer model indicate that these absorption features are probably water vapor. Spectral modeling indicates that the effects of atmospheric absorption in this region are most pronounced in spectrally flat materials with only weak absorption bands. Without correction and detailed knowledge of the atmospheric effects, accurate mapping of surface mineralogy (particularly at low mineral concentrations) is not possible. Author

N87-12974*# National Aeronautics and Space Administration. Ames Research Center, Moffett Field, Calif.

DESTRIPING AIS DATA USING FOURIER FILTERING TECHNIQUES

Chris Hlavka *In* JPL Proceedings of the Second Airborne Imaging Spectrometer Data Analysis Workshop 15 Aug. 1986 p 74-80 (For primary document see N87-12968 04-43)

Avail: NTIS HC A10/MF A01 CSCL 05B

Airborne Imaging Spectrometers (AIS) data collected in 1984 and 1985 showed pronounced striping in the vertical and horizontal directions. This striping reduced the signal to noise ratio so that features of the spectra of forest canopies were obscured or altered by noise. This noise was removed by application of a notch filter to the Fourier transform of the imagery in each waveband. Author

N87-12975*# Brown Univ., Providence, R. I. Dept. of Geological Sciences.

ABUNDANCE AND DISTRIBUTION OF MINERAL COMPONENTS ASSOCIATED WITH MOSES ROCK (KIMBERLITE) DIATREME

John F. Mustard and Carle M. Pieters *In* JPL Proceedings of the Second Airborne Imaging Spectrometer Data Analysis Workshop 15 Aug. 1986 p 81-85 (For primary document see N87-12968 04-43)

Avail: NTIS HC A10/MF A01 CSCL 05B

The surface mineralogy in and around Moses Rock diatreme, a kimberlite-bearing dike in SW Utah, was examined using internally calibrated Airborne Imaging Spectrometer (AIS) data. Distinct near-infrared absorption characteristics of clays, gypsum, and serpentine (a key marker for kinberlite concentration) allowed the surface units containing these components to be identified spatially and the relative abundance of each component measured. Within the dike itself, channels and dispersed components of kimberlite and blocks of country rocks were accurately determined. Author

N87-12976*# Stanford Telecommunications, Inc., Sunnyvale, Calif. Dept. of Applied Earth Sciences.

COMPARISON OF THE 1984 AND 1985 AIS DATA OVER THE SINGATSE RANGE (YERINGTON), NEVADA

R. J. P. Lyon *In* JPL Proceedings of the Second Airborne Imaging Spectrometer Data Analysis Workshop 15 Aug. 1986 p 86-95 (For primary document see N87-12968 04-43)

Avail: NTIS HC A10/MF A01 CSCL 05B

The Singatse Range is composed of a series of 53 types of volcanic, plutonic, metamorphic, and sedimentary rocks. In addition the Jurassic plutonic rocks are also of economic interest for their copper mineralization which is contained in a porphyry dike swarm. The 1984 and 1985 flight results from the Airborne Imaging Spectrometer (AIS) instrument flown in the NASA/JPL C-130 aircraft are contrasted and compared. The 1984 data are less noisy than the 1985, in which many sets of vertical stripings from bad detectors can be seen. Significantly however, enough of the hydrothermal alteration patterns can be seen in each line at the mutual crossing points that one can say that the specific targets were detected in both year's flights. The spectra of both years are corrupted by the second-order effect from the grating, but 0-H bond absorption at essentially correct wavelengths for sericite and/or kaolinite can be seen. Author

N87-12977*# Nevada Univ., Reno. School of Mines.

IDENTIFICATION OF HYDROTHERMAL ALTERATION ASSEMBLAGES USING AIRBORNE IMAGING SPECTROMETER DATA

Sandra C. Feldman and James V. Taranik *In* JPL Proceedings of the Second Airborne Imaging Spectrometer Data Analysis Workshop 15 Aug. 1986 p 96-101 (For primary document see N87-12968 04-43)

Avail: NTIS HC A10/MF A01 CSCL 05B

Airborne Imaging Spectrometer (AIS) data, field and laboratory spectra and samples for X-ray diffraction analysis were collected in argillically altered Tertiary volcanic rocks in the Hot Creek Range, Nevada. From laboratory and field spectral measurements in the 2.0 to 2.4 micron range and using a spectroradiometer with a 4 nm sampling interval, the absorption band centers for kaolinite were loacted at 2.172 and 2.215 microns, for montmorillonite at 2.214 micron and for illite at 2.205. Based on these values and the criteria for resolution and separtion of spectral features, a spectral sampling interval of less than 4 nm is necessary to separate the clays. With an AIS spectral sampling interval of 9.3 nm, a spectral matching algorithm is more effective for separating kaolinite, montmorillonite, ad illite in Hot Creek Range than using the location of absorption minima alone. Author

N87-12978*# Nevada Univ., Reno. School of Mines.

DETECTION OF HYDROTHERMAL ALTERATION AT VIRGINIA CITY, NEVADA USING AIRBORNE IMAGING SPECTROMETRY (AIS)

Amy Hutsinpiller and James V. Taranik *In* JPL Proceedings of the Second Airborne Imaging Spectrometer Data Analysis Workshop 15 Aug. 1986 102-108 (For primary document see N87-12968 04-43)

Avail: NTIS HC A10/MF A01 CSCL 05B

Airborne Imaging Spectrometer (AIS) data were collected over Virginia City, Nevada; an area of gold and silver mineralization with extensive surface exposures of altered volcanic rocks. The data were corrected for atmospheric effects by a flat-field method, and compared to library spectra of various alteration minerals using a spectral analysis program SPAM. Areas of strong clay alteration were identified on the AIS images that were mapped as kaolinitic, illitic, and sericitic alterations zones. Kaolinitic alteration is distinguishable in the 2.1 to 2.4 and 1.2 to 1.5 micrometer wavelength regions. Montmorillonite, illite, and sericite have absorption features similar to each other at 2.2 micrometer wavelength. Montnorillonite and illite also may be present in varying proportions within one Ground Instantaneous Field of View (GIFOV). In general AIS data is useful in identifying alteration zones that are associated with or lie above precious metal mineralization at Virginia City. Author

N87-12979*# Commonwealth Scientific and Industrial Research Organization, Ryde (Australia). Div. of Mineral Physics and Mineralogy.

PRELIMINARY GEOLOGICAL INVESTIGATION OF AIS DATA AT MARY KATHLEEN, QUEENSLAND, AUSTRALIA

Jon F. Huntington, Andy A. Green, Maurice D. Craig, and Terry D. Cocks *In* JPL Proceedings of the Second Airborne Imaging Spectrometer Data Analysis Workshop 15 Aug. 1986 p 109-131 (For primary document see N87-12968 04-43)

Avail: NTIS HC A10/MF A01 CSCL 05B

The Airborne Imaging Spectrometer (AIS) was flown over granitic, volcanic, and calc-silicate terrain around the Mary Kathleen Uranium Mine in Queensland, in a test of its mineralocial mapping capabilities. An analysis strategy and restoration and enhancement techniques were developed to process the 128 band AIS data. A preliminary analysis of one of three AIS flight lines shows that the data contains considerable spectral variation but that it is also contaminated by second-order leakage of radiation from the near-infrared region. This makes the recognition of expected spectral absorption shapes very difficult. The effect appears worst in terrains containing considerable vegetation. Techniques that try

to predict this supplementary radiation coupled with the log residual analytical technique show that expected mineral absorption spectra can be derived. The techniques suggest that with additional refinement correction procedures, the Australian AIS data may be revised. Application of the log residual analysis method has proved very successful on the cuprite, Nevada data set, and for highlighting the alunite, linite, and SiOH mineralogy. Author

N87-12980*# Geological Survey, Denver, Colo. Geologic Div.
USE OF DIGITAL MUNSELL COLOR SPACE TO ASSIST INTERPRETATION OF IMAGING SPECTROMETER DATA: GEOLOGIC EXAMPLES FROM THE NORTHERN GRAPEVINE MOUNTAINS, CALIFORNIA AND NEVADA
Fred A. Kruse, Daniel H. Knepper, Jr., and Roger N. Clark *In* JPL Proceedings of the Second Airborne Imaging Spectrometer Data Analysis Workshop 15 Aug. 1986 p 132-138 (For primary document see N87-12968 04-43)
Avail: NTIS HC A10/MF A01 CSCL 05B

Techniques using Munsell color transformations were developed for reducing 128 channels (or less) of Airborne Imaging Spectrometer (AIS) data to a single color-composite-image suitable for both visual interpretation and digital analysis. Using AIS data acquired in 1984 and 1985, limestone and dolomite roof pendants and sericite-illite and other clay minerals related to alteration were mapped in a quartz monzonite stock in the northern Grapevine Mountains of California and Nevada. Field studies and laboratory spectral measurements verify the mineralogical distributions mapped from the AIS data. Author

N87-12981*# Geological Survey, Reston, Va.
NEAR-INFRARED DETECTION OF AMMONIUM MINERALS AT IVANHOE HOT SPRINGS, NEVADA
M. Dennis Krohn *In* JPL Proceedings of the Second Airborne Imaging Spectrometer Data Analysis Workshop 15 Aug. 1986 p 138-144 (For primary document see N87-12968 04-43)
Avail: NTIS HC A10/MF A01 CSCL 05B

Airborne Imaging Spectrometer (AIS) data were collected over the fossil hot spring deposit at Ivanhoe, Nevada in order to determine the surface distribution of NH4-bearing minerals. Laboratory studies show that NH4-bearing minerals have characteristic absorption features in the near-infrared (NIR). Ammonium-bearing feldspars and alunites were observed at the surface of Ivanhoe using a hand-held radiometer. However, first look analysis of the AIS images showed that the line was about 500 m east of its intended mark, and the vegetation cover was sufficiently dense to inhibit preliminary attempts at making relative reflectance images for detection of ammonium minerals. Author

N87-12982*# National Aeronautics and Space Administration. Ames Research Center, Moffett Field, Calif.
ANALYSIS OF AIS DATA OF THE BONANZA CREEK EXPERIMENTAL FOREST, ALASKA
Michael A. Spanner and David L. Peterson *In* JPL Proceedings of the Second Airborne Imaging Spectrometer Data Analysis Workshop 15 Aug. 1986 p 144-152 (For primary document see N87-12968 04-43)
Avail: NTIS HC A10/MF A01 CSCL 05B

Airborne Imaging Spectrometer (AIS) data were acquired in 1985 over the Bonanza Creek Experimental Forest, Alaska for the analysis of canopy characteristics including biochemistry. Concurrent with AIS overflights, foliage from fifteen coniferous and deciduous forest stands were analyzed for a variety of biochemical constituents including nitrogen, lignin, protein, and chlorophyll. Preliminary analysis of AIS spectra indicates that the wavelength region between 1450 to 1800 nanometers (nm) displays distinct differences in spectral response for some of the forest stands. A flat field subtraction (forest stand spectra - flat field spectra) of the AIS spectra assisted in the interpretation of features of the spectra that are related to biology. Author

N87-12983*# Washington Univ., St. Louis, Mo. Center for the Space Sciences.
SOIL TYPES AND FOREST CANOPY STRUCTURES IN SOUTHERN MISSOURI: A FIRST LOOK WITH AIS DATA
Glen M. Green and Raymond E. Arvidson *In* JPL Proceedings of the Second Airborne Imaging Spectrometer Data Analysis Workshop 15 Aug. 1986 p 153-161 (For primary document see N87-12968 04-43)
Avail: NTIS HC A10/MF A01 CSCL 05B

Spectral reflectance properties of deciduous oak-hickory forests covering the eastern half of the Rolla Quadrangle were examined using Thematic Mapper (TM) data acquired in August and December, 1982 and Airborne Imaging Spectrometer (AIS) data acquired in August, 1985. For the TM data distinctly high relative reflectance values (greater than 0.3) in the near infrared (Band 4, 0.73 to 0.94 micrometers) correspond to regions characterized by xeric (dry) forests that overlie soils with low water retention capacities. These soils are derived primarily from rhyolites. More mesic forests characterized by lower TM band 4 relative reflectances are associated with soils of higher retention capacities derived predominately from non-cherty carbonates. The major factors affecting canopy reflectance appear to be the leaf area index (LAI) and leaf optical properties. The Suits canopy reflectance model predicts the relative reflectance values for the xeric canopies. The mesic canopy reflectance is less well matched and incorporation of canopy shadowing caused by the irregular nature of the mesic canopy may be necessary. Preliminary examination of high spectral resolution AIS data acquired in August of 1985 reveals no more information than found in the broad band TM data. Author

N87-12984*# Geological Survey, Reston, Va.
GEOBOTANICAL STUDIES AT PILOT MOUNTAIN, NORTH CAROLINA USING THE AIRBORNE IMAGING SPECTROMETER
N. M. Milton, P. A. Walsh, and T. L. Purdy *In* JPL Proceedings of the Second Airborne Imaging Spectrometer Data Analysis Workshop 15 Aug. 1986 p 162-170 (For primary document see N87-12968 04-43)
Avail: NTIS HC A10/MF A01 CSCL 05B

Airborne Imaging Spectrometer (AIS) data were acquired for several vegetation types within the humid temperate eastern United States. The spectral region covered, 0.9 to 2.1 microns, was little used in vegetation studies. A preliminary analysis of spectral curves suggests that variations between vegetation spectra may be useful for discriminating plant communities. Calibration and normalization procedures must be refined to compensate for cloud cover, detector and other system noise, and possible second-order effects. Author

N87-12985*# National Aeronautics and Space Administration. Ames Research Center, Moffett Field, Calif.
TRACE ELEMENT-INDUCED STRESS IN FRESHWATER WETLAND VEGETATION: PRELIMINARY RESULTS
Byron L. Wood and Louisa H. Beck (California Univ., Berkeley.) *In* JPL Proceedings of the Second Airborne Imaging Spectrometer Data Analysis Workshop 15 Aug. 1986 p 171-179 (For primary document see N87-12968 04-43)
Avail: NTIS HC A10/MF A01 CSCL 05B

Airborne Imaging Spectrometer (AIS) data were acquired over an area of freshwater wetlands in Central California on September 23, 1985. Plant samples were subsequently collected along the flight line with the goal of relating plant tissue chemistry to spectral reflectance in the near-infrared region. It was determined that a consistent relationship existed between spectral response and plant tissue chemistry. This was especially evident in the 1500 to 1700 nm region. Author

N87-12986*# Jet Propulsion Lab., California Inst. of Tech., Pasadena.
PATTERNS OF VEGETATION IN THE OWENS VALLEY, CALIFORNIA
Susan L. Ustin (California Univ., Berkeley.), Barrett N. Rock, and Roy A. Woodward *In its* Proceedings of the Second Airborne Imaging Spectrometer Data Analysis Workshop 15 Aug. 1986 p 180-186 (For primary document see N87-12968 04-43)
Avail: NTIS HC A10/MF A01 CSCL 05B

Spectral characteristics of semi-arid shrub communities were examined using Airborne Imaging Spectrometer (AIS) data collected in the tree mode on 23 May 1985. Mesic sites with relatively high vegetation density and distinct zonation patterns exhibited greater spectral signature variations than sites with more xeric shrub communities. Spectral signature patterns were not directly related to vegetation density or physiognomy, although spatial maps derived from an 8-channel maximum likelihood classification were supported by photo-interpreted surface features. In AIS data, the principal detected effect of shrub vegetation on the alluvial fans is to lower reflectance across the spectrum. These results are similar to those reported during a period of minimal physiological activity in autumn, indicating that shadows cast by vegetation canopies are an important element of soil-vegetation interaction under conditions of relatively low canopy cover. Author

N87-12987*# Oregon State Univ., Corvallis. Environmental Remote Sensing Lab.

AIS SPECTRA OF DESERT SHRUB CANOPIES

Rjay Murray, Dennis L. Isaacson, Barry J. Schrumpf, William J. Ripple, and Anthony J. Lewis *In* JPL Proceedings of the Second Airborne Imaging Spectrometer Data Analysis Workshop 15 Aug. 1986 p 187-193 (For primary document see N87-12968 04-43) Avail: NTIS HC A10/MF A01 CSCL 05B

Airborne Imaging Spectrometer (AIS) data were collected 30 August 1985 from a desert shrub community in central Oregon. Spectra from artificial targets placed on the test site and from bare soil, big sagebrush (Artemesia tridentata wyomingensis), silver sagebrush (Artemesia cana bolander), and exposed volcanic rocks were studied. Spectral data from grating position 3 (tree mode) were selected from 25 ground positions for analysis by Principal Factor Analysis (PFA). In this grating position, as many as six factors were identified as significant in contributing to spectral structure. Channels 74 through 84 (tree mode) best characterized between-class differences. Other channels were identified as nondiscriminating and as associated with such errors as excessive atmospheric absorption and grating positin changes. The test site was relatively simple with the two species (A. tridentata and A. cana) representing nearly 95% of biomass and with only two mineral backgrounds, a montmorillonitic soil and volcanic rocks. If, as in this study, six factors of spectral structure can be extracted from a single grating position from data acquired over a simple vegetation community, then AIS data must be considered rich in information-gathering potential. Author

N87-12988# Instituto de Pesquisas Espaciais, Sao Jose dos Campos (Brazil).

IN RETROSPECT: THE IMPACT OF RESEARCH PRODUCTION IN THE AREA OF REMOTE SENSING [EM RETROSPECTIVE: O IMPACTO DA PRODUCAO CIENTIFICA NA AREA DE SENSORIAMENTO REMOTO]

Evlyn Marcia LeaodeMoraesNovo Sep. 1986 48 p In PORTUGUESE; ENGLISH summary

(INPE-3987-NTE/261) Avail: NTIS HC A03/MF A01

Research in the area of remote sensing and its impact on the Brazilian scientific community is analyzed. A historical approach was adopted establishing a relationship among the main development phases of remote sensing in Brazil and the main research lines adopted by the Remote Sensing Department. It was concluded that the Remote Sensing Project had its main objectives changed along with its history. The lack of human resources prepared to deal with this new subject can be considered the main reason for low scientific production. While in other areas of INPE, people were sent to receive special training in developed countries, in the Remote Sensing area it did not happen. Author

N87-12989# Instituto de Pesquisas Espaciais, Sao Jose dos Campos (Brazil).

REPORT ON THE ACTIVITIES OF THE IRRIGATED CROP SURVEY IN SAO PAULO STATE FROM REMOTE SENSING PRODUCTS, PHASE 2 [RELATORIO DE ATIVIDADES DO PROJETO CADASTRAMENTO DE AREAS IRRIGADAS NO ESTADO DE SAO PAULO ATRAVES DE DADOS DE SENSORIAMENTO REMOTO, FASE 2]

Sergio dosAnjosFerreiraPinto, Evlyn Marcia LeaodeMoraesNovo, Mario Valerio Filho, Sherry Chou Chen, and Roberto Rosa Jul. 1986 63 p In PORTUGUESE; ENGLISH summary Original document contains color illustrations

(INPE-3950-RPE/513) Avail: NTIS HC A04/MF A01

The methodology used in the project Irrigated Crop Survey in Sao Paulo State and its main results are presented. The project developed through a joint agreement between INPE/MCT and DAEE/S.P. The Itatiba/Braganca Paulista (SP) test site was selected. Sequential TM/LANDSAT data were applied with the objective of evaluating the total irrigated area. Field data were collected which permitted comparison between two methods for irrigated area estimation: direct expansion model using only field data collected in sample segments, regression model combining ground information extracted from remote sensing products. The performance of TM composites TM 2 (BLUE); TM 3 (GREEN) and TM 4 (RED); TM 5 (BLUE); TM 3 (GREEN) and TM 4 (RED) were compared to identify the best mix to detect irrigated crops. The results demonstrated that a reduction of 94.02% in the estimated variance was obtained by using the regression model. The comparison of the increase of date-to-date irrigated area from May to October showed that the 3 first overpasses were sufficient to map some 90% of the total irrigated area. The performance of the TM compositions were not significantly different in relation to its potential for detecting irrigated crops. Author

N87-12990# Instituto de Pesquisas Espaciais, Sao Jose dos Campos (Brazil).

GENERATION OF IMAGES WITH RECORDED AUXILLARY DATA FOR THE LANDSAT THEMATIC MAPPER (TM) IMAGERY M. S. Thesis, Mar. 1985 [GERACAO DE IMAGENS COM DADOS AUXILIARES REGISTRADOS A IMAGENS TM—LANDSAT]

Jose Borges Escada, Jr. Sep. 1986 66 p In PORTUGUESE; ENGLISH summary

(INPE-3982-TDL/234) Avail: NTIS HC A04/MF A01

A system for storing and recovering auxiliary data is implemented so that the latter can be correlated with a given Thematic Mapper scene in a way that these auxiliary data can be treated as a Thematic Mapper image. The resources available at the Processing Subsystem of the Image Generation Department of INPE (Instituto de Pesquisas Espaciais - Institute for Space Research) for generating photographic or digital images will then allow the generation of geocoded artificial images with the same characteristics of a Thematic Mapper scene. The gray levels associated with each geocoded image pixel will represent not the terrain radiometry, but the corresponding auxiliary data. Author

N87-12991# Atmospheric and Environmental Research, Inc., Cambridge, Mass.

INTERCOMPARISON OF DMSP OLS, NOAA AVHRR, GOES VISSR (DEFENSE METEOROLOGICAL SATELLITE PROGRAM OPERATIONAL LINESCAN SYSTEM, NATIONAL OCEANOGRAPHIC AND ATMOSPHERIC ADMINISTRATION ADVANCED VERY HIGH RESOLUTION RADIOMETER, GOES VISIBLE INFRARED SPIN-SCAN RADIOMETER) AND LANDSAT MSS IMAGERY FOR CLOUD PR OPERTY DETERMINATION: RECOMMENDATIONS FOR DIGITAL DATA ANALYSIS Final Report, 18 Jun. - 18 Dec. 1985

R. G. Isaacs, J. C. Barnes, L. D. Petro, and R. D. Worsham 18 Jan. 1986 144 p

(Contract F19628-85-C-0102)

(AD-A169285; P142F; AFGL-TR-86-0012) Avail: NTIS HC A07/MF A01 CSCL 04/2

Concurrent visible and infrared cloud imagery from four satellite sensors (DMSP OLS, NOAA AVHRR, GOES VISSR, LANDSAT MSS) have been intercompared. Inherent differences in cloud field analyses are noted due to sensor characteristics such as spatial and spectral resolution and scene/sensor geometry. Digital data were manipulated to simulate one sensor's data from that of another. Recommendations for further analysis of the collected data sets are provided. GRA

N87-12992# Pacific Northwest Labs., Richland, Wash.
REMOTE SENSING TO DETECT ECOLOGICAL IMPACTS ASSOCIATED WITH ACID DEPOSITION Final Report
P. VanVoris and G. E. Wukelic May 1986 67 p
(Contract DE-AC06-76RL-01830)
(DE86-011649; EPRI-EA-4607) Avail: NTIS HC A04/MF A01

A planning study was conducted to determine the potential applications of remote sensing for detecting ecological impacts that have been reportedly caused by acid deposition. The project was divided into two phases: a technology assessment phase (Phase I) and a prototype demonstration (Phase II). The emphasis of the project was on detecting ecological change, not on determining the cause of that change. The latter is the role of ground-based research. Phase I consisted of an assessment of terrestrial and aquatic components that are indicative of sensitivity to acid deposition. The assessment identified remote sensing as the optimal cost-effective method for measuring the rate of change of land use, crop type, and forest canopy health over large geographic areas. In Phase II, spectral reflectance in the near-infrared region of the spectrum from forest canopies of Camel's Hump State Forest from two Landsat scenes from the summers of 1976 and 1983 were compared. Significant increases in spectral reflectance from the forest were detected when the pixels were compared, and it is hypothesized that this increase is indicative of a decline in forest growth and canopy closure. However, because of project limitations, no ground-truth data were collected by Battelle-Northwest scientists to verify the findings of the remote sensing analyses. A comprehensive research program is recommended to further investigate the use of remote sensing to detect ecological damage and its relationship to possible causative agents. Future research should also focus on the use of remote sensing for identifying ecosystems that may be sensitive to perturbations like acid deposition and improving our ability to model ecological processes. Priority should be given to detecting, monitoring, and modeling changes in forested watersheds. DOE

N87-12993# Butler Univ., Indianapolis, Ind.
COMPARISON OF TROPICAL FOREST SURVEYS
J. Molofsky, C. A.S. Hall (Cornell Univ., Ithaca, N.Y.), and N. Myers Jun. 1986 70 p Prepared in cooperation with Cornell Univ., Ithaca, NY.; Myers (Norman), Oxford (UK).
(Contract DE-AC05-84OR-21400)
(DE86-011699; DOE/NBB-0078) Avail: NTIS HC A04/MF A01

This report examines the two most recent studies of tropical forest areas and rates of forest loss: Norman Myers' conversion of Tropical Moist Forests (1980), and the FAO/UNEP Tropical Forest Resources Assessment Project in order to identify and clarify discrepancies between them. The apparent discrepancy between their respective estimates of deforestation rates has been the basis of a continuing controversy. Myers' report was concerned principally with the conversion of virgin forests to other land use and the resulting extinction of tropical species. The FAO/UNEP report emphasized the availability of forest resources to meet the future fuelwood, housing, and economic needs of UN member states. The present paper attempts to identify more precisely the differences between the two studies in order to integrate the large tropical forest data base from these two sources into a cohesive whole. Specifically, we identify those countries covered in both surveys where the largest differences occur. The study was not designed to assess all discrepancies between Myers and FAO but only the discrepancies for those countries where both investigators have given specific numbers. DOE

N87-12994# Computer Applied Techniques Ltd., Malahide (Ireland).
STUDY OF SATELLITE SYSTEMS TO MONITOR EARTH'S RADIATION BUDGET Final Report
E. OMongain, S. Daultry, and J. G. Campbell Paris ESA Jan. 1986 158 p
(Contract ESA-5716/83-NL-MS)
(CAP-420-071; ESA-CR(P)-2230; ETN-86-98111) Avail: NTIS HC A08/MF A01

The problems of designing a system to simulate the end-to-end process of satellite based Earth Radiation Budget (ERB) measurements were investigated. Such a system would be used to simulate and determine the accuracy achievable in ERB studies with different orbit and instrument scenarios. A practical system to simulate the process is outlined. Effective modeling of error sources, in the measurement and inversion process, is important. Key elements of the system are an Earth radiation model, a measurement system model, and a data processing model; this latter element includes the simulation of calibration and inversion processes. ESA

N87-12995# Executive Office of the President, Washington, D. C. Office of Science and Technology Policy.
EARTH SCIENCES RESEARCH IN THE CIVIL SPACE PROGRAM
Oct. 1985 42 p
(PB86-232014) Avail: NTIS HC A03/MF A01 CSCL 22A

The report has been prepared in response to the President's National Space Strategy Directive to the Office of Science and Technology Policy to review and define the goals and missions of the various agencies in the area of Earth Science research. GRA

44 ENERGY PRODUCTION AND CONVERSION

Includes specific energy conversion systems, e.g., fuel cells; global sources of energy; geophysical conversion; and windpower.

For related information see also *07 Aircraft Propulsion and Power, 20 Spacecraft Propulsion and Power,* and *28 Propellants and Fuels.*

N87-12996# Minnesota Univ., Minneapolis. Dept. of Chemistry.
A STUDY OF ENERGY CONVERSION DEVICES USING PHOTOACTIVE ORGANOMETALLIC ELECTROCATALYSTS Final Report, Feb. 1982 - Jun. 1985
John F. Evans and Kent R. Mann 23 May 1986 32 p
(Contract DAAG29-82-K-0063)
(AD-A169096; ARO-18767.9-CH) Avail: NTIS HC A03/MF A01 CSCL 10/2

The purpose of this project was to examine the feasibility of the use of transition metal hexakis arylisocyanide complexes confined to polymeric thin films in solar energy conversion systems. The chemical systems of interest were chromium, molybdenum and tungsten arylisocyanide complexes which had been previously examined in terms of their solution spectroscopy and photochemistry and had been found to have rather long excited state lifetimes. Since we had shown that charge transfer complexes in thin polymer films supported on electrode surfaces were viable routes to solar energy conversion composites, we chose to extend our studies to include these more promising complexes. The goals of the project then became threefold: 1) examine the thermodynamics and kinetics of charge transfer in the systems in which we had shown feasibility (polymeric ferrocenes) so as to understand the physical phenomena which were liable to control the overall efficiency and turnover numbers for the polymer bound photoelectrocatalysts, 2) further characterize the electrochemistry and physical inorganic chemistry of the more promising Cr, Mo and W hexakis arylisocyanide photoelectrocatalysts, and 3) examine ways by which these MLCT complexes could be entrapped in various polymer matrices. GRA

N87-12997# Midwest Research Inst., Golden, Colo.
STATUS AND FUTURE OF GOVERNMENT-SUPPORTED AMORPHOUS SILICON RESEARCH IN THE US
W. L. Wallace and E. S. Sabisky Jun. 1986 6 p Presented at the 2nd International Photovoltaic Science and Engineering Conference, Beijing, China, 1 Aug. 1986
(Contract DE-AC02-83CH-10093)
(DE86-010702; SERI/TP-211-2960; CONF-860874-2) Avail: NTIS HC A02/MF A01

The Amorphous Silicon Research Project (ASRP) was estab-

lished at the Solar Energy Research Institute in 1983 and is responsible for all US Department of Energy government supported research activities in the field of amorphous silicon photovoltaics. The objectives and research directions of the project have been established by a Five-Year Research Plan, which was developed at SERI in cooperation with the Department of Energy in 1984 and is divided into research on single-junction and multi-junction solar cells. DOE/SERI has recently initiated a new three year program to be performed in collaboration with US industry to perform work on high efficiency amorphous silicon solar cells and submodules. The objectives of this initiative are: (1) to achieve 18% efficiencies for small area multi-junction amorphous silicon cells, and (2) to achieve amorphous silicon submodule efficiencies in the 10 to 13% range for single-junction and multi-junction submodule configurations over areas of at least 1000 cm^2. DOE

N87-12998# Oak Ridge National Lab., Tenn.
DEVELOPMENT OF REGENERABLE ENERGY STORAGE FOR SPACE MULTIMEGAWATT APPLICATIONS
M. Olszewski 1986 5 p Presented at the Intersociety Energy Conversion Engineering Conference, San Diego, Calif., 25 Aug., 1986
(Contract DE-AC05-84OR-21400)
(DE86-011070; CONF-860810-9) Avail: NTIS HC A02/MF A01

A program has recently been initiated as a part of the national Strategic Defense Initiative (SDI) to develop energy storage technology for space power applications. This program is jointly conducted by the Department of Energy and the Department of Defense. It is focused on the development of advanced technologies in regenerable energy storage that will be required for generation of multimegawatt levels of sprint power for SDI space missions. Energy storage technology considered in the program relate to devices that have a high specific capacity for energy storage, which can provide high levels of electric power on demand, and which may be recharged with electric power. The devices of principal interest are electrochemical batteries, chemical fuel cells, and electromechanical flywheels (the latter includes the motors and generators used to provide the electrical to mechanical coupling). The intent of the program is to resolve technical feasibility issues associated with an electrically regenerable energy storage system satisfying SDI needs. Specifically, energy storage technology will be developed through the proof-of-concept stage within the next six years that provides a specific power greater than 2.5 kW/kg with an energy storage density of at least 450 kJ/kg. DOE

N87-12999# Los Alamos National Lab., N. Mex.
INTEGRATED HEAT PIPE-THERMAL STORAGE DESIGN FOR A SOLAR RECEIVER
E. S. Keddy, J. T. Sena, K. Woloshun, M. A. Merrigan, and G. Heidenreich (Sundstrand Corp., Rockford, Ill.) 1986 8 p Presented at the Intersociety Energy Conversion Engineering Conference, San Diego, Calif., 25 Aug., 1986
(Contract W-7405-eng-36)
(DE86-011235; LA-UR-86-1840; CONF-860810-5) Avail: NTIS HC A02/MF A01

Light-weight heat pipe wall elements that incorporate a thermal storage subassembly within the vapor space are being developed as part of the Organic Rankine Cycle Solar Dynamic Power Systems (ORC-SDPS) receiver for the space station application. The operating temperature of heat pipe elements is in the 770 to 810°K range with a design power throughput of 4.8 kW per pipe. The total heat pipe length is 1.9 M. The Rankine cycle boiler heat transfer surfaces are positioned within the heat pipe vapor space, providing a relatively constant temperature input to the vaporizer. The heat pipe design employs axial arteries and distribution wicked thermal storage units with potassium as the working fluid. Stainless steel is used as the containment tube and screen material. Performance predictions for this configuration have been conducted and the design characterized as a function of artery geometry, distribution wick thickness, porosity, pore size, and permeability. Details of the analysis and of fabrication and assembly procedures are presented. DOE

N87-13000# Nevada Univ., Boulder City.
DUAL TEMPERATURE THERMAL STORAGE WITH COMPLEX COMPOUNDS
U. Rockenfeller and J. F. Martin (Oak Ridge National Lab., Tenn.) 1986 6 p Presented at the Intersociety Energy Conversion Engineering Conference, San Diego, Calif., 25 Aug., 1986 Prepared in cooperation with Oak Ridge National Lab., TN.
(Contract DE-AC05-84OR-21400)
(DE86-011511; CONF-860810-11) Avail: NTIS HC A02/MF A01

Storage of thermal energy through the formation or dissociation of complex compounds is described. A solid-vapor reaction of an absorbant, a metal inorganic salt, and an absorbate, the ligand of the complex provides energy storage for a heat pump cycle. One system is capable of dual temperature storage; that is, storage of cool for air conditioning and storage of heat for heating. Laboratory experiments which define the material and reaction characteristics of a sodium bromide/ammonia system were performed. The reaction rates, storage density and other operating parameters are described in functional form. The performance of a heat pump storage system is projected from these experimentally determined properties. The resulting system compares favorably with existing cool storage systems and with proposed heat or cool storage systems. DOE

N87-13001# California Polytechnic State Univ., San Luis Obispo.
PROOF OF FEASIBILITY OF A NOVEL INVERTER FOR PHOTOVOLTAIC POWER CONDITIONING
A. Dickerson Apr. 1986 78 p
(Contract DE-AC04-76DP-00789)
(DE86-012729; SAND-86-7031) Avail: NTIS HC A05/MF A01

The Dickerson inverter concept obtains a sinewave current from an array that is segmented into a number of subarrays. These subarrays are switched among the ac phases so that the current from a given subarray is continuous and each phase is connected at all times to one or more subarrays. The control scheme assures a unity power factor current with real-time adjustment to power-system disturbances. A proof-of-concept inverter has been operated into a three-phase power system, with the dc supplied from a motor-generator set plus regulators that closely simulated the current-voltage characteristics of a photovoltaic array. The performance for the inverter has been projected for a 480V, three-phase system at the 50 kVA level. Computer simulations showed 98% utilization of array power was possible with efficiency better than 98% and harmonic content of 18% without filtering. An analysis of filtering costs indicates that reduction to 5% can be achieved at under $0.003 per watt for typical central-station applications. A more complex configuration was also analyzed with results of 99% utilization, 8% harmonic content, and the same efficiency. The intended power range for these inverters is 50 to 250 kVA per unit. The cost to produce the inverter at the 50 kVA level in quantities of 1000 units is estimated to be $0.05 per watt. DOE

N87-13002# Sandia National Labs., Albuquerque, N. Mex.
PROCEEDINGS OF THE SOLAR THERMAL TECHNOLOGY CONFERENCE
R. B. Diver, ed. Jun. 1986 345 p Presented at the Solar Thermal Central Receiver and Distributed Receiver Annual Conference, Albuquerque, N. Mex. 17 Jun. 1986
(Contract DE-AC04-76DP-00789)
(DE86-011703; SAND-86-0536; CONF-860619) Avail: NTIS HC A15/MF A01

The Solar Thermal Technology Conference was held on June 17 to 19, 1986 at the Marriott Hotel, Albuquerque, New Mexico. The meeting was sponsored by the United States Department of Energy and Sandia National Laboratories. Topics covered during the conference included a status summary of the Sandia Solar Thermal Development Project, perspectives on central and distributed receiver technology including energy collection and conversion technologies, systems analyses and applications

experiments. The proceedings contain summaries (abstracts plus principal visual aids) of the presentations made at the conference. DOE

N87-13003# Delaware Univ., Newark. Inst. of Energy Conversion.
STABLE, HIGH-EFFICIENCY, CuInSe2-BASED POLYCRYSTALLINE THIN-FILM TANDEM SOLAR CELLS Semiannual Subcontract Report, 16 Mar. 1985 - 15 Sep. 1985
R. W. Birkmire, J. E. Phillips, and J. D. Meakin May 1986 116 p
(Contract DE-AC02-83CH-10093)
(DE86-010705; SERI/STR-211-2951) Avail: NTIS HC A06/MF A01

The major obstacle to developing a high-efficiency CdTe/CdS cell has been the lack of reproducibility. A number of process modifications have been made to overcome this. Some progress was made with a cell in which the CdTe is deposited onto a transparent ohmic contact; however, difficulties continued to be encountered in controlling the CdTe conductivity. Effort has been redirected to a cell in which the CdTe is deposited onto the CdS, leaving an exposed CdTe surface to which ohmic contact can be made. Research on the CuInSe/CdS cell has established that high efficiency can be achieved over a broad CuInSe composition range and a wide substrate temperature range. DOE

N87-13004# Midwest Research Inst., Golden, Colo. Solar Energy Research Inst.
SOLID STATE PHOTOVOLTAIC RESEARCH BRANCH ANNUAL REPORT, FY 1985
May 1986 214 p
(Contract DE-AC02-83CH-10093)
(DE86-010708; SERI/PR-212-2877) Avail: NTIS HC A10/MF A01

This report summarizes the progress of the Solid State Photovoltaics Research Branch of the Solar Energy Research Institute from 1 October 1984 through 30 September 1985. The five technical sections of the report cover these main areas of SERI's in-house research: Semiconductor Crystal Growth, Amorphous Silicon Research, Polycrystalline Thin Films, III-V High-Efficiency Photovoltaic Cells, and Solid State Theory. The task in each section was to explain the purpose and major accomplishments of the work in the context of the US Department of Energy's Photovoltaic Research Program plans. Lists of current, relevant publications are also included. DOE

N87-13005# New Mexico State Univ., Las Cruces. Physical Science Lab.
EXPERIMENTAL INVESTIGATION OF THERMOCHEMICAL TRANSPORT FOR SOLAR APPLICATIONS USING SULFUR TRIOXIDE
J. H. McCrary, G. E. McCrary, and J. I. Martinez May 1986 102 p Prepared in cooperation with Sandia National Labs.
(Contract DE-AC04-76DP-00789)
(DE86-011762; SAND-86-7028) Avail: NTIS HC A06/MF A01

The high temperature catalytic dissociation of sulfur trioxide and the synthesis of its products in a closed-loop system presents an attractive prospect for converting, transporting and recovering solar energy. A laboratory scale, closed-loop, sulfur-oxide based experimental system was assembled and operated on the NMSU campus to demonstrate technical feasibility and to study the engineering problems associated with this chemical cycle. The system, which operated at a nominal 500 watts of energy conversion, contained most of the elements of a large scale power plant. Twelve separate experiments were performed with the system in a study of system stability during start-up and shut-down procedures and dissociator temperature variations. Descriptions of the laboratory closed-loop and the chemical reactors are given along with the experimental procedure, conditions, and results for each of the tests. Extensive discussion is given on the solar implications that the results from these experiments may have, and recommendations are made for follow-on experiments that may assist in resolving potential problems for thermochemical transport in a solar-powered plant. DOE

N87-13006# Sandia National Labs., Albuquerque, N. Mex.
PHOTOVOLTAIC CONCENTRATOR TECHNOLOGY PROJECT, FOURTEENTH PROJECT INTEGRATION MEETING, JUNE 10-11, 1986
May 1986 263 p Proceedings of the 14th Concentrator Photovoltaic Integration Meeting, Albuquerque, N. Mex., 10 Jun. 1986
(Contract DE-AC04-76DP-00789)
(DE86-012051; SAND-86-0058/1; CONF-8606123-Pt-1-Summ)
Avail: NTIS HC A12/MF A01

The meeting reported on covered research on photovoltaic concentrators and their components, including concentrator cells, cell assemblies, Fresnel lenses and concentrator modules, tracking structures and control systems, and complete concentrator arrays. This report contains abstracts of presentations made at the meeting and status summaries for current research contracts. DOE

N87-13007# Oak Ridge National Lab., Tenn.
STEFAN-TYPE PROBLEM WITH VOID FORMATION AND ITS EXPLICIT SOLUTION
A. D. Solomon and D. G. Wilson Jun. 1986 26 p
(Contract DE-AC05-84OR-21400)
(DE86-013521; ORNL-6277) Avail: NTIS HC A03/MF A01

The density of most materials changes under melting and freezing. For certain materials being considered as potential latent heat storage materials for use in a space station, this density change may be large. A density change induces a change of volume of the material occupying a given container and this creates vapor bubbles or voids. We have formulated a problem that models a phase change process with such a void and that has an explicit solution. We examine the solution to gain a further understanding of the thermal and phase change performance of a material in which such voids form. We also look at the related problem of melting a material in which a void is initially present. Examples are given of the performance of a lithium fluoride phase change material subject to melting and freezing. DOE

45 ENVIRONMENT POLLUTION

Includes atmospheric, noise, thermal, and water pollution.

N87-13008# Instituto de Pesquisas Espaciais, Sao Jose dos Campos (Brazil).
A PARTITION OF SENSIBLE AND LATENT HEAT FLUXES ABOVE THE TERRA FIRMA AREA IN THE AMAZON FOREST [UMA PARTICAO DE FLUXOS DE CALOR SENSIVEL E DE CALOR LATENTE ACIMA DA FLORESTA AMAZONICA DE TERRA FIRME]
Leonardo DeanedeAbreuSa, Antonio Ocimar Mansi, and Yelisetty Viswanadham Jul. 1986 27 p In PORTUGUESE; ENGLISH summary Presented at a Workshop on GTE/ABLE-2A at INPE, 3-7 Feb. 1986
(INPE-3949-PRE/970) Avail: NTIS HC A03/MF A01

The partition of net radiation to sensible and latent fluxes above the Amazonian forest is studied. The Bowen ratio daily variability is discussed and its values are compared when calculated by different methods and distinct height above canopy. The variation of potential temperature gradient above forest canopy as a function of net radiation is also studied. Small values of potential temperature gradients and large values of net radiation obtained during daytime indicate that there was a strong convective activity in the Amazonian region. These results agreed very well with other forest observational results. The data utilized were collected from 21 to 24, August, 1984, related to the third field campaign of the Micrometeorological Experiment in the Amazon Basin. Author

N87-13009# Oak Ridge National Lab., Tenn.
EVALUATING ECOSYSTEM RESPONSE TO TOXICANT STRESS: A STATE SPACE APPROACH
A. R. Johnson 1986 30 p Presented at the 10th Symposium on Aquatic Toxicology and Hazard Assessment, New Orleans, La., 4 May, 1986

(Contract DE-AC05-84OR-21400)
(DE86-011777; CONF-8605137-3) Avail: NTIS HC A03/MF A01

Ecosystems can be regarded as complex biogeochemical systems maintained in a state of thermodynamic nonequilibrium by the flow of materials and energy. The state of such a system at any given time is generally assumed to be characterized by a finite set of variables. If these variables are taken to be the components of a vector, the instantaneous state of an ecosystem can be represented by a single point in an abstract multidimensional space. As an ecosystem undergoes changes in state, changes in the position of the corresponding vector will result, tracing out a state trajectory over time. Within the state space approach formulated above, the response of an ecosystem to a perturbation, such as the introduction of a toxicant, can be viewed as a displacement of the state vector away from its unperturbed trajectory. Such an approach was used to analyze data from a study of the response of experimental ponds and microcosms to chronic additions of a coal-derived synthetic oil. Ecosystem-level response surfaces and dose-response curves were derived based on the average separation (distance of displacement) of exposed ecosystems relative to controls. The results exhibited patterns analogous to those observed in classical toxicology based on organismal response, and could be used to define acceptable exposure conditions. The state space approach described here provides a coherent and objective framework for summarizing a large multivariate data set, and it should be of general use in providing both qualitative and quantitative descriptions of the behavior of perturbed ecosystems. DOE

N87-13010# California Univ., Berkeley. Lawrence Berkeley Lab.
CHARACTERIZATION OF INFORMATION REQUIREMENTS FOR STUDIES OF CO2 EFFECTS: WATER RESOURCES, AGRICULTURE, FISHERIES, FORESTS AND HUMAN HEALTH
M. R. White, ed. Dec. 1985 244 p
(Contract DE-AC03-76SF-00098)
(DE86-012477; DOE/ER-0236) Avail: NTIS HC A11/MF A01

The report discusses how climate change and vegetative response will affect selected areas of our way of life as a result of increased carbon dioxide concentrations. Needs for future research are identified. Separate abstracts have been prepared for individual chapters. DOE

N87-13011# National Bureau of Standards, Washington, D.C. Gas and Particulate Science Div.
HIGH ACCURACY STANDARDS AND REFERENCE METHODOLOGY FOR CARBON DIOXIDE IN AIR
W. L. Zielinski, Jr., E. E. Hughes, I. L. Barnes, J. W. Elkins, and H. L. Rook Jun. 1986 100 p
(Contract DE-AI01-76PR-06010)
(DE86-012643; DOE/PR-06010/31) Avail: NTIS HC A05/MF A01

This report summarizes the activities and accomplishments of a three-year NBS program for the development of standards and reference methodology for carbon dioxide (CO) in air that was designed to: (1) develop defined Standard Reference Materials (SRM's) for CO in air at atmospheric concentrations having a total uncertainty (95% confidence level) not exceeding 0.1% relative; (2) assess the equivalency of absolute gravimetry employed by the National Bureau of Standards (NBS) and absolute manometry employed by the Scripps Institution of Oceanography (SIO) for the development of accurate standards for CO in air at atmospheric concentrations; and (3) develop a state-of-the-art isotope dilution mass spectrometer (ID-MS) system and associated methodology to serve as an NBS-based reference method for absolute independent confirmation of CO concentrations in CO in air standards. DOE

N87-13012# Oak Ridge National Lab., Tenn.
DIRECT EFFECTS OF ATMOSPHERIC CO2 ENRICHMENT ON PLANTS AND ECOSYSTEMS: A BIBLIOGRAPHY WITH ABSTRACTS
B. R. Strain and J. D. Cure Jun. 1986 197 p
(Contract DE-AC05-84OR-21400)
(DE86-013525; ORNL/CDIC-13) Avail: NTIS HC A09/MF A01

This bibliography contains 1032 references, with author abstracts or summaries where possible, on the subject of direct effects of atmospheric CO enrichment on plants and ecosystems. The references are indexed by keywords, which appear in the title or abstract of the reference or describe the subject of the paper. The bibliography is preceded by an introduction, which summarizes the possible global consequences of increased atmospheric concentrations of carbon dioxide with emphasis on the direct effects on plants and their responses. DOE

N87-13013# Sonoma Technology, Inc., Santa Rosa, Calif.
SOUTHERN CALIFORNIA AIR QUALITY STUDY (SCAQS) SUGGESTED PROGRAM PLAN Final Report
D. Blumenthal, J. Watson, and D. Lawson Jun. 1986 187 p
(Contract ARB-A4-114-32)
(PB86-223427; ARB-R-86/278) Avail: NTIS HC A09/MF A01 CSCL 04A

The program plan outlines a suggested measurement and management approach and reviews the technical background for the Southern California Air Quality Study(SCAQS). SCAQS will be a multi-year, integrated, cooperative study which will be funded by government agencies, industry groups, and individual corporate sponsors. The goal of SCAQS is to develop a comprehensive air quality and meteorological data base for the South Coast Air Basin that can be used to test, evaluate, and improve elements of air quality simulation models for oxidants, PM-10, fine particles, toxic air contaminants, and acidic species. In addition, SCAQS will address specific technical questions regarding the emission, transport, transformation, and deposition of pollutants. The study is planned to take place in 1987 during six weeks in early summer and four weeks in late fall. Extensive routine air quality, aerosol, and meteorological measurements and additional special studies will take place on about 19 days during the study. GRA

N87-13014# Battelle Pacific Northwest Labs., Richland, Wash.
STUDY OF THE FORMATION AND TRANSPORT OF ACIDIC SPECIES BY NON-PRECIPITATING CUMULUS CLOUDS DURING VENTEX-84
A. J. Alkezweeny Jul. 1986 41 p Sponsored by EPA
(PB86-220357; EPA/600/3-86/039) Avail: NTIS HC A03/MF A01 CSCL 04A

The report is the second in a series that describes the VENTEX field studies conducted near Lexington, K.Y. The first one was published by Alkezweeny (1984). In the report, description of the experiment conducted during the summer of 1984 (VENTEX-84), from July 8 to August 18, are presented, and samples of the data collected are given. Possible uses of the data and example of data manipulation are illustrated. The principal objectives of the program are as follows: to determine the production of sulfate and nitrate aerosol particles by non-precipitating cumulus clouds; and to investigate the vertical transport of pollutants caused by cumulus convection. GRA

46 GEOPHYSICS

Includes aeronomy; upper and lower atmosphere studies; ionospheric and magnetospheric physics; and geomagnetism.

For space radiation see *93 Space Radiation.*

N87-13015*# International Council of Scientific Unions, Urbana, Ill.
MIDDLE ATMOSPHERE PROGRAM. HANDBOOK FOR MAP, VOLUME 21
C. F. Sechrist, Jr., ed. Jul. 1986 117 p Sponsored by NASA and UNESCO
(NASA-CR-179893; NAS 1.26:179893; MAP-HANDBOOK-21)
Avail: SCOSTEP Secretariat, Illinois Univ., 1406 West Green Street, Urbana, Ill. 61801 CSCL 04A

Topics covered include: minutes of the Middle Atmospheric

Program (MAP) Steering Committee; workshops on atmospheric tides; national reports on MAP activities; and dynamics project report. For individual titles, see N87-13016 through N87-13019.

N87-13016*# International Council of Scientific Unions, Urbana, Ill.

ATMOSPHERIC TIDES MIDDLE ATMOSPHERE PROGRAM (ATMAP): REPORT OF THE WORKSHOP, KYOTO, JAPAN, DECEMBER 5-6, 1984

Jeffrey M. Forbes, ed., T. Aso, S. Avery, S. Bowhill, L. Coy, J. Forbes, G. Fraser, S. Fukao, S. Kato, D. Kurshner et al *In its* Middle Atmosphere Program. Handbook for Map, volume 21 Jul. 1986 p 12-55 (For primary document see N87-13015 04-46)

Avail: SCOSTEP Secretariat, Illinois Univ., 1406 West Green Street, Urbana, Ill. 61801 CSCL 04A

Experimentalists, data analysts, and theoreticians were brought together to study and interpret the results of four solstice campaigns conducted prior to the symposium. Emphasis was placed on campaigns III and V. Topics discussed included: review of the data and evaluation of the consistency with available theoretical models; interpretation of the data; recommendations on how the Atmospheric Tides Middle Atmosphere Program (ATMAP) results should reach the open literature such that the advancement of middle atmosphere science and the proprietary rights of the individual experimenters are best served; and recommendations concerning future campaigns and the future emphasis of ATMAP. B.G.

N87-13017*# Boston Univ., Mass.

PROCEEDINGS OF THE WORKSHOP ON ATMOSPHERIC TIDES, PRAGUE, CZECHOSLOVAKIA, AUGUST 14, 1985

Jeffrey M. Forbes *In* International Council of Scientific Unions Middle Atmosphere Program. Handbook for MAP, volume 21 Jul. 1986 p 56-64 (For primary document see N87-13015 04-46)

Avail: SCOSTEP Secretariat, Illinois Univ., 1406 West Green Street, Urbana, Ill. 61801 CSCL 04A

The pros and cons of various methods of extracting tidal fields from radar data were discussed. B.G.

N87-13018*# International Council of Scientific Unions, Urbana, Ill.

MINUTES OF MAP/WINE EXPERIMENTERS MEETING, PRAGUE, CZECHOSLOVAKIA, AUGUST 13, 1985

U. vonZahn *In its* Middle Atmosphere Program. Handbook for MAP, volume 21 Jul. 1986 p 65-69 (For primary document see N87-13015 04-46)

Avail: SCOSTEP Secretariat, Illinois Univ., 1406 West Green Street, Urbana, Ill. 61801 CSCL 04A

Topics addressed include: methods of tidal analysis; tidal climatologies for the month of December and June; guidelines for construction of monthly climatologies; and future plans. B.G.

N87-13019*# National Aeronautics and Space Administration. Langley Research Center, Hampton, Va.

COORDINATED STUDY OF THE BEHAVIOR OF THE MIDDLE ATMOSPHERE IN WINTER: MONTHLY MEAN COMPARISONS OF SATELLITE AND RADIOSONDE DATA AND DERIVED QUANTITIES

William L. Grose, ed. and Clive D. Rodgers, ed. (Oxford Univ. (England).) *In* International Council of Scientific Unions Middle Atmosphere Program. Handbook for MAP, volume 21 Jul. 1986 p 79-110 (For primary document see N87-13015 04-46)

Avail: SCOSTEP Secretariat, Illinois Univ., 1406 West Green Street, Urbana, Ill. 61801 CSCL 04A

A series of workshops were conducted for intercomparison of middle atmosphere data from a variety of sounding systems. The purposes were several: intercomparison of temperature data from various sources: characterization of any observed differences with an attempt to understand those differences, and to provide guidance to users of the data as to the validity of derived quantitites. B.G.

N87-13020# Instituto de Pesquisas Espaciais, Sao Jose dos Campos (Brazil).

STRATOSPHERIC BALLOON EXPERIMENTS Final Report

U. B. Jayanthi, J. Braga, C. D. Pritsopoulo, F. S. Blanco, and R. V. Correa Sep. 1986 35 p

(INPE-3995-RPE/519) Avail: NTIS HC A03/MF A01

Three stratospheric balloon-borne experiments were conducted at the Tenente Rodolfo Marsh and Comandante Ferraz Stations in the Antarctic region to study the x-ray and gamma ray atmospheric background. The first experiment was flown in January 1984 to measure gamma ray flux and spectrum in the 0.2 to 4.8 MeV range at different altitudes. Experiments more sophisticated with similar objectives for x-rays (28.5 to 185 KeV) and for gamma rays (0.2 to 4.8 KeV) and for gamma rays (0.2 to 4.8 MeV) were conducted in two balloon flights in Jan/Feb. 1985 at Cmte. Ferraz base. The altitude spectral data is required to construct source functions at these latitude ranges. It was also desireable to use ceiling float data for the detection of enhanced line emissions and charge particle precipitation events. The gamma ray experiment provided ground radioactivity obtaining at the Cmte. Ferraz base and gamma ray spectra at lower stratospheric altitudes. The x-ray data near ceiling altitudes have been utilized to evaluate atmospheric build-up effects. Author

N87-13021*# Maryland Univ., College Park. Dept. of Physics and Astronomy.

DEVELOPMENT OF A SENSITIVE SUPERCONDUCTING GRAVITY GRADIOMETER FOR GEOLOGICAL AND NAVIGATIONAL APPLICATIONS Final Report, Jul. 1980 - Jul. 1985

H. J. Paik and J.-P. Richard Washington NASA Sep. 1986 217 p

(Contract NAS8-33822)

(NASA-CR-4011; NAS 1.26:4011) Avail: NTIS HC A10/MF A01 CSCL 08G

A sensitive and stable gravity gradiometer would provide high resolution gravity measurements from space. The instrument could also provide precision tests of fundamental laws of physics and be applied to inertial guidance systems of the future. This report describes research on the superconducting gravity gradiometer program at the University of Maryland from July 1980 to July 1985. The report describes the theoretical and experimental work on a prototype superconducting gravity gradiometer. The design of an advanced three-axis superconducting gravity gradiometer is also discussed. Author

N87-13022*# National Aeronautics and Space Administration. Langley Research Center, Hampton, Va.

DESCRIPTION OF DATA ON THE NIMBUS 7 LIMS MAP ARCHIVE TAPE: OZONE AND NITRIC ACID

Ellis E. Remsberg, Robert J. Kurzeja, Kenneth V. Haggard, James M. Russell, III, and Larry L. Gordley Dec. 1986 73 p

(NASA-TP-2625; L-16136; NAS 1.60:2625) Avail: NTIS HC A04/MF A01 CSCL 04A

The Nimbus 7 Limb Infrared Monitor of the Stratosphere (LIMS) data set has been processed into a Fourier coefficient representation with a Kalman filter algorithm applied to profile data at individual latitudes and pressure levels. The algorithm produces synoptic data at noon Greenwich Mean Time (GMT) from the asynoptic orbital profiles. This form of the data set is easy to use and is appropriate for time series analysis and further data manipulation and display. Ozone and nitric acid results are grouped together in this report because the LIMS vertical field of views (FOV's) and analysis characteristics for these species are similar. A comparison of the orbital input data with mixing ratios derived from Kalman filter coefficients indicates errors in mixing ratio of generally less than 5 percent, with 15 percent being a maximum error. The high quality of the mapped data was indicated by coherence of both the phases and the amplitudes of waves with latitude and pressure. Examples of the mapped fields are presented, and details are given concerning the importance of diurnal variations, the removal of polar stratospheric cloud signatures, and the interpretation of bias effects in the data near the tops of profiles. Author

N87-13023*# Johns Hopkins Univ., Baltimore, Md. Dept. of Earth and Planetary Sciences.
MIDDLE ATMOSPHERE MODELING Final Report
Darrell F. Strobel Jun. 1985 23 p
(Grant NAG5-489)
(NASA-CR-179934; NAS 1.26:179934) Avail: NTIS HC A02/MF A01 CSCL 04A

Breaking gravity waves generate and maintain a background level of turbulence which is capable of producing substantial cooling and/or heating in the upper mesosphere and lower thermosphere. The net thermodynamic effect of breaking gravity waves is critically dependent on the eddy Prandt number (P sub t) applicable to mesospheric turbulence. When P sub t is approximately 1, the calculations of the heat budget for the mesopause region imply that the globally averaged eddy or turbulent diffusion coefficient cannot exceed .000001 sq cm/s. This upper limit on turbulant diffusion applies to both potential temperature transport and chemically inert tracer transport when radiative damping is neglible. For chemically active species larger diffusion coefficients are permitted, because the effective eddy diffusion coefficient is increased by an additive term L/2 gamma (sup 2), where L is the chemical loss rate and gamma is the vertical wavenumber. For P sub t is approximately 4 to 6, the turbulent diffusion of momentum (D sub M) is sufficiently greater than the turbulent diffusion of heat (D sub H) that the conversion of gravity wave energy to heat with high efficiency nearly balances the divergence of the downward eddy heat flux in the wave breaking zone. Therefore the heat budget of the mesopause region would no longer provide a powerful and useful constraint on D sub H. If P sub t exceeds 6 with high efficiency for energy conversion to heat, gravity waves would heat the mesosphere throughout the wave breaking region. Author

N87-13024*# Science and Technology Corp., Hampton, Va.
SAGE 2 SATELLITE DATA SET VALIDATION Final Report
Geoffrey S. Kent and Pi-Huan Wang Nov. 1986 131 p
(Contract NAS1-17959)
(NASA-CR-178189; NAS 1.26:178189; STC-TR-2108) Avail: NTIS HC A07/MF A01 CSCL 04A

The results of a validation study of data obtained by the Stratospheric Aerosol and Gas Experiment 2 satellite experiment (SAGE 2) are given. Preliminary SAGE 2 data have been available for the period October, 1984 to May, 1985. In addition, the results of two correlative experimental measurement series have been studied in detail, as well as climatological data obtained by other techniques, including ground-based and airborne lidar. The study shows the SAGE 2 data to be of great potential value to studies of the microphyiscs of stratospheric aerosols, the chemistry of trace gases and stratospheric dynamics. A small number of unidentified errors in the current preliminary data set are described. These will be removed from the next version of the data set which is anticipated to be of archival quality. Author

N87-13025# Air Force Geophysics Lab., Hanscom AFB, Mass.
A SEMI-EMPIRICAL LOW-LATITUDE IONOSPHERIC MODEL Environmental Research Papers
David N. Anderson, Michael Mendillo, and Bruce Herniter 10 Oct. 1985 108 p
(AD-A168899; AFGL-TR-85-0254; AFGL-ERP-933) Avail: NTIS HC A06/MF A01 CSCL 04/1

Since current empirical models specifying low-latitude electron density profiles severely underestimate the daytime plasma density scale-height and total electron content (TEC), a Semi-empirical, Low-latitude, Ionospheric Model (SLIM) was developed which is not only more realistic but is also computationally fast. Electron density profiles (180 to 1800 km) are theoretically calculated as a function of latitude (every 2 deg between 24 N and 24 S dip latitude) and local time (every half-hour over 24 hours LT) by solving the time-dependent plasma continuity equation. Assuming a Chapman-like profile, sets of coefficients are then generated which reproduce these individual profiles. The coefficients themselves are easily stored, quickly retrieved and form the basis for a fast, portable, semi-empirical computer code. This report describes briefly the input parameters used to theoretically calculate profiles and the procedures used to generate the coefficients. The SLIM profiles are compared with the Chiu and Bent empirical models for Equinox, solar maximum conditions. Finally electron densities, the coefficients, TEC and 6300 A airglow intensities are listed in tabular form for three seasons (Equinox, June solstice, and December solstice) and two solar cycle periods (solar maximum and solar minimum). Author (GRA)

N87-13026# North Carolina State Univ., Raleigh. Dept. of Marine, Earth and Atmospheric Science.
THEORETICAL STUDY ON THE CORRELATION BETWEEN WIDEBAND ELECTROMAGNETIC SPECTRA AND GEOLOGICAL STRUCTURES Final Report, 1 Sep. 1983 - 28 Feb. 1986
I. J. Won Apr. 1986 56 p
(Contract DAAG29-83-K-0152)
(AD-A168971; ARO-20065.2-GS) Avail: NTIS HC A04/MF A01 CSCL 08/7

A theoretical study has been performed to establish a mathematical means to compute the electromagnetic response of an earth having continuous and arbitrary conductivity variations, and to formulate a transfer function that can convert a wideband frequency-domain response to a continuous conductivity-depth function. The study was based upon past experiences in both theoretical and experimental aspects of frequency-domain electromagnetic method. A new formal integral representation was formulated for Maxwell's equations for a medium having an arbitrary conductivity function. It was shown that the representation is suitable for forward problems and, through a proper integral transform, the inverse may possibly exist. An attempt is being made to derive a transfer conductivity-depth profile. Author (GRA)

N87-13027# Southwest Research Inst., San Antonio, Tex.
MAGNETOSPHERIC PLASMA STUDIES USING DATA FROM THE DYNAMICS EXPLORER HIGH AND LOW ALTITUDE PLASMA INSTRUMENTS Final Report, 15 Apr. 1982 - 31 Dec. 1985
J. N. Barfield Feb. 1986 83 p
(Contract F19628-82-K-0024)
(AD-A169010; AFGL-TR-86-0034) Avail: NTIS HC A05/MF A01 CSCL 04/1

The reported research focused primarily upon plasma processes in and near the plasma cusp. The following areas were studied: plasma injection and transport in the mid-altitude polar cusp; observations of counterstreaming electrons at high altitudes; observations of upward electron beams and their relationship to region 1 Birkeland currents; observations of the electron population responsible for the 6300A SAR arc emission, polar rain observations; polar wind observations; and observations of ion and electron acceleration events produced by parallel electric fields. The primary observing platform for the research reported here was Dynamic Explorer 1 (DE-1). The DE-1 High Altitude Plasma Instrument (HAPI) consists of five electrostatic analyzers mounted in a fan-shaped angular array at angles of 45, 78, 90, 102, and 135 deg. with respect to the spacecraft spin axis. Each analyzer makes differential measurements of electrons and positive ions over an energy/charge range of 5 eV/e to 32 keV/e. Energy stepping proceeds at commandable rates of up to 64 sec, providing three-dimensional plasma distribution functions at the six second spin rate or DE-1. GRA

N87-13028# Iowa Univ., Iowa City. Dept. of Physics and Astronomy.
THE CURRENT-VOLTAGE RELATIONSHIP IN AURORAL CURRENT SHEETS Progress Report, 1986
D. R. Weimer, D. A. Gurnett, C. K. Goertz, J. D. Menietti, and J. L. Burch Mar. 1986 38 p
(Contract N00014-85-K-0404)
(AD-A169074; U-OF-IOWA-86-21) Avail: NTIS HC A03/MF A01 CSCL 04/1

The current-voltage relation within narrow auroral current sheets is examined through the use of high-resolution data from the high altitude Dynamics Explorer 1 satellite. The north-south per-

pendicular electric field and the east-west magnetic field are shown for three cases in which there are large amplitude, oppositely directed paired electric fields and narrow current sheets. These data are shown to indicate that there is a linear Ohm's law relationship between the current density and the parallel potential drop within the narrow current sheets. This linear relationship had previously been verified for large-scale auroral formations greater than 20 km wide at the ionosphere. The evidence shown here extends our knowledge down to the scale size of discrete auroral arcs. Author (GRA)

N87-13029# Oklahoma State Univ., Stillwater. Electronics Lab.
INSTRUMENTATION RESEARCH AND SUPPORT SERVICES Final Report, 13 Feb. 1981 - 30 Jun. 1985
R. F. Buck 30 Sep. 1985 109 p
(Contract F19628-81-C-0079)
(AD-A169278; AFGL-TR-85-0255) Avail: NTIS HC A06/MF A01 CSCL 14/2

This report summarizes upper air research support services supplied to the Air Force Geophysics Laboratory. These services include design and construction of both air-borne and ground based equipment, as well as the supply of personnel and related equipment at a number of remote sites. Both analog and digital systems are described. Related activities have included studies and research activities directed toward anticipated future requirements for support. Author (GRA)

N87-13030# Saint Louis Univ., Mo.
Lg WAVE EXCITATION AND PROPAGATION IN PRESENCE OF ONE-, TWO-, AND THREE-DIMENSIONAL HETEROGENEITIES Scientific Report, 1 Oct. 1985 - 31 Mar. 1986
R. B. Herrmann 1 Feb. 1986 26 p
(Contract F19628-85-K-0029)
(AD-A169325; AFGL-TR-86-0026; SR-2) Avail: NTIS HC A03/MF A01 CSCL 08/11

A detailed study of Lg wave excitation and propagation from a sequence of earthquakes in New Brunswick is performed. Primary conclusions are that Lg Q increases with frequency. Perhaps more importantly for regional source studies is the observation of significant high frequency Pn and Sn arrivals at 1000 km which are much greater than the Lg arrival. Source estimates based on the Lg provide reasonable estimates of seismic moment, but corner frequencies differ from short distance measurements. GRA

N87-13031# SRI International Corp., Menlo Park, Calif.
COORDINATED RADAR AND SATELLITE STUDIES OF IONOSPHERIC CURRENTS IN THE AURORAL ZONE AND POLAR CAP Final Report, 1 Sep. 1982 - 31 Dec. 1985
Roland T. Tsunoda, Anne Q. Smith, John D. Kelly, and Robert M. Robinson Dec. 1985 39 p
(Contract F19628-82-K-0045)
(AD-A169466; AFGL-TR-86-0022) Avail: NTIS HC A03/MF A01 CSCL 04/1

The objective is to provide real time surveillance of short term predictions in the electrodynamic state of the ionosphere and magnetosphere. The desired approach is to obtain all necessary environmental information by remote sensing or by in situ sampling from satellites; the parameters include electric fields, field-aligned currents, and ionospheric conductivities. Recently, a DMSP (Defense Meteorological Satellite Program) satellite has been launched (Flight 7) equipped with a triaxial fluxgate magnetometer. To qualify this type of instrument for participation in the above objective, an investigation was made of field aligned currents estimated from two different approaches: using magnetometer measurements made by the DMSP-F7 satellite and using ionospheric measurements made by the Sondrestrom incoherent scatter radar. Three events are analyzed when near simultaneous measurements were made by both instruments during satellite passes over the radar. Varying degrees of correlation were found in the derived field aligned currents. In all three cases, the gross features measured by the two methods were similar. The differences are discussed in terms of measurement error, analysis approximation, and geophysical uncertainties. GRA

N87-13032# Air Force Geophysics Lab., Hanscom AFB, Mass.
COLLECTION OF IONS IN THE STRATOSPHERE Interim Report, Sep. 1984 - Sep. 1985
Christopher Sherman 9 Dec. 1985 41 p
(AD-A169905; AFGL-TR-85-0317; AFGL-ERP-944) Avail: NTIS HC A03/MF A01 CSCL 04/1

The processes involved in sampling of ions in the stratosphere have been examined and ranked in order of importance. Several typical calculations related to collection of ions in the stratosphere have been made. In this procedure, difficulties that may arise in solving such problems have been pointed out. The overall program, if continued, would be strengthened by further theoretical support along the lines initiated here. GRA

N87-13033# Air Force Geophysics Lab., Hanscom AFB, Mass.
BALLOON-BORNE, HIGH ALTITUDE GRAVIMETRY: THE FLIGHT OF DUCKY 1a (11 OCTOBER 1983) Interim Scientific Report, Nov. 1982 - Dec. 1985
Andrew R. Lazarewicz, Brenda J. Schilinski, Ralph J. Cowie, Catherine L. Rice, Peter Moss, and Leonard N. Carter (Bedford Research Associates, Mass.) 31 Dec. 1985 86 p
(AF Proj. 7600)
(AD-A169942; AFGL-TR-85-0342; AFGL-ERP-943) Avail: NTIS HC A05/MF A01 CSCL 08/5

Gravity measurements from a high-altitude balloon were made in late September to verify global and upward-continued gravity models. The first flight was intended to provide balloon motion and environment data with a preliminary estimate of the quality of measured gravity values. A balloon operates in a dynamic, largely unpredictable environment; thus, the gravimeter senses accelerations due to balloon motions as well as gravitational acceleration. Independent measurements of balloon motions from an intertial navigation package (three accelerometers, three rate gyros, three-axis magnetometer and two tiltmeters) combined with ground tracking (X, Y and Z position and velocity) will allow for separation of balloon-induced accelerations from gravitational acceleration to 1 mGal, using tracking data to an accuracy of about 5 cm/sec in velocity for Eotvos corrections, and position to 1 m. This first engineering flight was planned to coincide with the lowest seasonal wind velocities over Holloman AFB, where AFGL has its permanent balloon launch facility. Mild wind velocities are desired to provide the most benign environment possible during the testing phase, and to keep the balloon within tracking range. The experiment design, launch, and flight operations, and a first look at the data are presented. GRA

N87-13034# Massachusetts Inst. of Tech., Cambridge. Earth Resources Lab.
DEVELOPMENT OF ULTRASONIC MODELLING TECHNIQUES FOR THE STUDY OF SEISMIC WAVE SCATTERING DUE TO CRUSTAL INHOMOGENEITIES Final Report, 13 Apr. 1983 - 30 Sep. 1985
M. N. Toksoz, Anton M. Dainty, and Edmond E. Charrette, III Mar. 1986 86 p
(Contract F19628-83-K-0027)
(AD-A170017; AFGL-TR-86-0087) Avail: NTIS HC A05/MF A01 CSCL 08/11

Scattering of Rayleigh waves from surface features was investigated using three-dimensional ultrasonic models at frequencies near 1 MHz and two dimensional finite difference calculations. Models were constructed of aluminum blocks and an aluminum powder-epoxy composite of lower density and seismic velocity. The aluminum has similar seismic velocities and density to igneous and metamorphic rocks while the composite is similar to sedimentary materials. Kilometers in the earth are scaled to millimeters in the models which makes 1 MHz in the models equivalent to 1 Hz in the earth, typical of the frequencies observed in regional seismograms. Relief on the models which was a few millimeters, the order of a wavelength, was restricted to an isolated circular mesa of composite on a metal block and an isolated circular

depression both unfilled and filled with composite. Calculations were made for similar situations by the finite difference method; comparisons indicated a general similarity in the seismograms, allowing us to use the finite difference calculations to gain physical insight into the scattering process. Topography alone produces attenuation due to scattering into reflected surface waves and body waves. Adding low velocity composite to the model considerably changes this picture. GRA

N87-13035# Denver Univ., Colo. Dept. of Physics.
MEASUREMENT OF ATMOSPHERIC EMISSION SPECTRA AT HIGH ALTITUDES Final Report, 8 Nov. 1982 - 8 Nov. 1985
F. H. Murcray, F. J. Murcray, D. G. Murcray, and A. Goldman 22 Nov. 1985 14 p
(Contract F19628-83-K-0006)
(AD-A170143; AFGL-TR-86-0061) Avail: NTIS HC A02/MF A01 CSCL 04/1

The objective of this contract has been to obtain high spectral resolution atmospheric emission data at altitudes up to 40 km. In order to accomplish this cryogenically cooled moving mirror Michelson interferometer system was constructed that is capable of operating independently while being carried aloft by a large balloon. Interpretation of the atmospheric emission spectra obtained under this contract requires a computer program that can calculate theoretical atmospheric emission spectra on a line by line basis. All such programs rely on an accurate list of line parameters of molecules of atmospheric interest. GRA

N87-13036# Air Force Geophysics Lab., Hanscom AFB, Mass.
IMPROVING foF2 PREDICTION FOR THE SUNRISE TRANSITION PERIOD Final Report, Oct. 1984 - Sep. 1985
B. S. Dandekar and J. Buchau 29 Jan. 1986 65 p
(AD-A170457; AFGL-TR-86-0028; AFGL-ERP-946) Avail: NTIS HC A04/MF A01 CSCL 04/1

During the 2- to 3-hr sunrise transition period, the relative change in foF2 is 20 to 60 percent per hour and is independent of solar activity. The change is largest in winter and smallest in summer. To prevent the skip distance from changing by more than 250 km, that is, to maintain continuous illumination of at least 50 percent of the barrier (nominal width 500 km), requires that the operating frequency be changed for every 6 percent change in foF2. Thus, in the case of an OTH system, the operating frequency has to be adjusted during the sunrise period every 6 to 20 min (seasonal dependence) for satisfactory performance. To accommodate such rapid changes, an empirical algorithm has been tested for improved foF2 predictions during sunrise. The prediction scheme is based on the availability of relevant (under the oblique raypath) real time ionospheric data. GRA

N87-13037# Ohio State Univ., Columbus. Dept. of Civil Engineering.
AN ANALYSIS OF THE ACOUSTIC CHARACTERISTICS OF ABSS (ACOUSTIC BACKSCATTER SYSTEM) AND ITS DEPLOYMENTS Report, 1 Oct. 1982 - 31 Mar. 1986
Keith W. Bedford and Charles M. Libicki Jul. 1986 110 p
(Contract N00014-83-K-0003)
(AD-A170487) Avail: NTIS HC A06/MF A01 CSCL 17/1

The benthic boundary layer is the interface between the world ocean and the earth beneath. Extending from the top of the Ekman layer, where bottom drag begins to exert its influence on the general oceanic circulation, down to a few centimeters below the sediment surface, it is the site of exchange of momentum, heat, solutes and suspended load. To aid in investigating these zones the ABSS (Acoustic Backscatter System) a combination 5 MHz - 1 MHz system is deployed by the High Energy Benthic Boundary Layer Experiment (HEBBLE) team on the Nova Scotian Rise at a depth of 4800m. This device can, without entering the observed flow, sense suspended sediment simultaneously in over 100 1-cm range bins, as frequently as one hundred times per second, while the low frequency transducer of ABSS looks upward through the Ekman layer, using the same measurement principle, but in 20 cm range bins. Inasfar as their sampling density in space and time for turbulent fluid mechanical data, these devices are quite unprecedented. GRA

N87-13038# Air Force Inst. of Tech., Wright-Patterson AFB, Ohio.
A SIMPLE SOLAR, SPECTRAL MODEL FOR STUDYING THE EFFECTS OF CLOUD COVER AND SURFACE ALBEDO ON THE INCOMING SOLAR RADIATION Ph.D. Thesis
Alfred M. Powell, Jr. 1986 131 p
(AD-A171284; AFIT/CI/NR-86-123D) Avail: NTIS HC A07/MF A01 CSCL 04/1

The effect of cloud cover and surface albedo on the solar insolation at the surface of the Earth was investigated. The model uses Bird's (1984) clear sky model for direct normal and diffuse horizontal irradiance as its basis. Bird's model was modified to include inclined surfaces and cloud cover. The clouds were modelled using parameterizations developed by Welch, Cox and Davis (1980) and a weighting technique to account for cloud shape using plane parallel calculations. The radiative transfer in the cloud was modelled by a two stream approximation known as the Shuster Schwarzchild method. The model results were compared with clear sky broadband and spectral observations, and cloudy broadband observations. The effects of cloud amount, cloud thickness, cloud type, and surface albedo are demonstrated. Cloud amount and cloud thickness are the predominant cloud factors affecting insolation. High surface albedos tend to slow the decrease in insolation due to increasing cloud cover; while low surface albedos cause greater variation in insolation under the same circumstances. GRA

N87-13039# Lawrence Livermore National Lab., Calif.
ATMOSPHERIC ILLUMINATION AND SHADOWS, REVISION 1
N. L. Max 15 Jan. 1986 8 p Presented at SIGGRAPH '86, Dallas, Tex., 18 Aug., 1986
(Contract W-7405-eng-48)
(DE86-010971; UCRL-93965-Rev-1; CONF-860875-1-Rev-1) Avail: NTIS HC A02/MF A01

The shadow volume algorithm of Frank Crow was reorganized to provide information on the regions of illuminated space in front of each visible surface. This information is used to calculate the extra intensity due to atmospheric scattering, so when the atmosphere is partly in shadow, columns of scattered light will be visible. For efficiency in sorting the shadow edges, the image is computed in polar coordinates. DOE

N87-13040# Lawrence Livermore National Lab., Calif.
PARAMETERIZED NUMERICAL FIT TO TOTAL COLUMN OZONE CHANGES CALCULATED BY THE LLNL 1-D MODEL OF THE TROPOSPHERE AND STRATOSPHERE
P. S. Connell May 1986 24 p
(Contract W-7405-eng-48)
(DE86-011008; UCID-20782) Avail: NTIS HC A02/MF A01

In this note we present a numerical parameterization of the results of the LLNL one-dimensional model for total column ozone change in terms of surface emissions or abundances of the various source species. The LLNL model was used in an earlier study to evaluate a significant number of time-dependent scenarios of future trends in the emissions or atmospheric abundances of CFC-11, CFC-12, CFC-22, CFC-113, CCl, CHCCl, CO, CH, NO, Halon-1301 and Halon-1211. This parameterization produces calculated ozone changes within about 2% (column ozone change relative to the 1985 model atmosphere) of the actual complete model calculation for a wide range of scenarios and ozone changes. It therefore can approximately represent the actual 1-D model for the purposes of economic analysis of regulatory strategies. It is, however, crucial to note that the 1-D model results, and consequently this parameterization, are subject to substantial uncertainties. Future improvements in our knowledge of atmospheric photochemical kinetics and transport in the troposphere and stratosphere should be expected to modify these current results. DOE

N87-13041 Drexel Univ., Philadelphia, Pa.
CONVECTIVE SURFACE LAYERS: INFLUENCE OF THE BOUND-

ARY LAYER DEPTH Ph.D. Thesis
Kurt Tyler Loveland 1985 256 p
Avail: Univ. Microfilms Order No. DA8605423

Two methods, one semi-empirical and the other theoretical, are employed to develop a new theory for predicting the behavior of turbulence characteristics in convective surface layers. This theory is based on three length scales; the height above the ground, the Monin-Obukhov length, and the boundary layer depth (h). The chief advantages are its relative simplicity, its ability to predict the height dependence of the mean gradients and second moments in a manner consistent with their observed behavior in the atmosphere and in large-eddy simulations, and it is consistent with the theoretical requirements of free convection similarity. The semi-empirical method is based on nonlinear least squares fits to a generalized Businger-Dyer formulation with up to four unknown parameters. Using data obtained primarily from the Kansas and Minnesota field experiments, this method is applied to the universal functions for the wind and temperature gradients, the standard deviation of the horizontal wind velocity, the variances of vertical velocity and temperature, the streamwise heat flux, and the turbulence dissipation. Dissert. Abstr.

N87-13045*# Colorado Univ., Boulder. Dept. of Astrophysics, Planetary and Atmospheric
THEORETICAL AND EXPERIMENTAL STUDIES IN SUPPORT OF THE GEOPHYSICAL FLUID FLOW EXPERIMENT
John Hart and Juri Toomre *In* NASA. Marshall Space Flight Center NASA/MSFC FY-85 Atmospheric Processes Research Review Oct. 1985 3 p (For primary document see N87-13043 04-47)
Avail: NTIS HC A07/MF A01 CSCL 04B

N87-13046*# National Aeronautics and Space Administration. Marshall Space Flight Center, Huntsville, Ala.
THEORETICAL AND EXPERIMENTAL DESIGN STUDIES FOR THE ATMOSPHERIC GENERAL CIRCULATION EXPERIMENT
William W. Fowlis, David H. Hathaway, Timothy L. Miller, Glyn O. Roberts (Roberts Associates, Inc., Vienna, Va.), and Kenneth J. Kopecky (Drake Univ., Des Moines, Iowa.) *In its* NASA/MSFC FY-85 Atmospheric Processes Research Review Oct. 1985 2 p (For primary document see N87-13043 04-47)
Avail: NTIS HC A07/MF A01 CSCL 04A

N87-13049*# Pennsylvania State Univ., University Park. Dept. of Meteorology.
THE USE OF SATELLITE DATA IN UNDERSTANDING AND PREDICTING CONVECTIVE AND LARGE-SCALE DYNAMICAL PROCESSES
John A. Dutton, John H. E. Clark, and Hampton N. Shirer *In* NASA. Marshall Space Flight Center NASA/MSFC FY-85 Atmospheric Processes Research Review Oct. 1985 2 p (For primary document see N87-13043 04-47)
Avail: NTIS HC A07/MF A01 CSCL 04A

N87-12949# Joint Publications Research Service, Arlington, Va.
AVAILABLE POTENTIAL ENERGY IN UPPER LAYER OF WORLD OCEAN Abstract Only
V. S. Arsenyev and V. A. Burkov *In its* USSR Report: Earth Sciences (JPRS-UES-86-007) 10 Sep. 1986 1 p Transl. into ENGLISH from Doklady Akademii Nauk SSSR (Moscow, USSR), v. 287, no. 4, Apr. 1986 p 986-989 (For primary document see N87-12946 04-42)
Avail: NTIS HC A06/MF A01

N87-12950# Joint Publications Research Service, Arlington, Va.
DESERTIFICATION: GLOBAL ECOLOGICAL PROBLEM Abstract Only
N. S. Orlovskiy *In its* USSR Report: Earth Sciences (JPRS-UES-86-007) 10 Sep. 1986 2 p Transl. into ENGLISH from Voprosy Filisofii (Moscow, USSR), no. 2, Feb. 1986 p 113-123 (For primary document see N87-12946 04-42)
Avail: NTIS HC A06/MF A01

N87-12952# Joint Publications Research Service, Arlington, Va.
EXPERIMENTAL RESEARCH ON TURBULENCE IN UPPER-LEVEL TROPOSPHERIC CLOUDS Abstract Only
V. K. Dmitriyev, T. P. Kapitanova, V. D. Litvinova, N. Z. Pinus, G. A. Potertikova, and G. N. Shur *In its* USSR Report: Earth Sciences (JPRS-UES-86-007) 10 Sep. 1986 1 p Transl. into ENGLISH from Izvestiya Akademii Nauk SSSR: Fizika Atmosfery i Okeana (Moscow, USSR), v. 22, no. 2, Feb. 1986 p 143-150 (For primary document see N87-12946 04-42)
Avail: NTIS HC A06/MF A01

N87-12953# Joint Publications Research Service, Arlington, Va.
SOLAR CONTROL OF GEOPHYSICAL PHENOMENA Abstract Only
V. F. Loginov and G. V. Fedorovich *In its* USSR Report: Earth Sciences (JPRS-UES-86-007) 10 Sep. 1986 1 p Transl. into ENGLISH from Zemlya i Vselennaya (Moscow, USSR), no. 1, Jan. - Feb. 1986 p 58-61 (For primary document see N87-12946 04-42)
Avail: NTIS HC A06/MF A01

47 METEOROLOGY AND CLIMATOLOGY

Includes weather forecasting and modification.

N87-13042 ESDU International Ltd., London (England).
CHARACTERISTICS OF ATMOSPHERIC TURBULENCE NEAR THE GROUND. PART 3: VARIATIONS IN SPACE AND TIME FOR STRONG WINDS (NEUTRAL ATMOSPHERE)
Oct. 1986 39 p Supersedes ESDU-75001
(ESDU-86010-Pt-3; ISBN-0-85679-562-3; ISSN-0143-2702) Avail: ESDU

This Data Item ESDU 86010 is an addition to the Wind Engineering Sub-series. It is the third in a group providing comprehensive atmospheric turbulence characteristics, and deals with the relationship between values measured at two points in space of the three turbulence velocity components. It covers joint-probability, cross-correlations, coherence and phase angle (giving cross-spectral densities) and integral length scales of all turbulence components in any direction. The data apply throughout the atmospheric boundary layer and for different types of terrain. Since the length scales are all related to that for the along-wind component in the along-wind direction, effects of roughness changes on all of them can be accounted for through their effect on that length scale predicted using ESDU 85020. The data were derived from the von Karman equations modified to take acount of the distorting (anisotropic) effects near the ground. The theoretical basis allows rational extrapolation from measurements made at moderate wind speeds to much higher design speed case when, in particular, much longer length scales are obtained. ESDU

N87-13043*# National Aeronautics and Space Administration. Marshall Space Flight Center, Huntsville, Ala.
NASA/MSFC FY-85 ATMOSPHERIC PROCESSES RESEARCH REVIEW
William W. Vaughan, comp. and Fay Porter, comp. Oct. 1985 143 p Review held in Huntsville, Ala. 7-9 May 1985 and in Columbia, Md., 8-12 Jul. 1985
(NASA-CP-2402; M-503; NAS 1.55:2402) Avail: NTIS HC A07/MF A01 CSCL 04B

The two main areas of focus for the research program are global scale processes and mesoscale processes. Geophysical fluid processes, satellite doppler lidar, satellite data analysis, atmospheric electricity, doppler lidar wind research, and mesoscale modeling are among the topics covered. For individual titles, see N87-13044 through N87-13096.

N87-13044*# National Aeronautics and Space Administration. Marshall Space Flight Center, Huntsville, Ala.
THEORETICAL AND EXPERIMENTAL STUDIES OF BAROCLINIC PROCESSES
Tim Miller, Fred Leslie, Dan Fitzjarrald, and Nathaniel Reynolds *In its* NASA/MSFC FY-85 Atmospheric Processes Research

Review Oct. 1985 2 p (For primary document see N87-13043 04-47)
Avail: NTIS HC A07/MF A01 CSCL 04B

An experimental study in a baroclinic annulus with heating and cooling on the upper and lower horizontal surfaces was completed. Four basic regimes of flow were observed: (1) axisymmetric flow, (2) cellular (deep) convection, (3) convective rolls (boundary layer), and (4) baroclinic instability. There was no symmetric (or nearly symmetric) baroclinic instability observed, although it was determined by numerical calculations that we transversed regions in parameter space where the symmetric instability was present. The non-symmetric baroclinic instability (Eady type) was observed instead. Although the vertical depth was rather small and hence viscous damping was strong, large-amplitude baroclinic waves were made possible by imposing a very weak static stability. Author

N87-13045*# Colorado Univ., Boulder. Dept. of Astrophysics, Planetary and Atmospheric
THEORETICAL AND EXPERIMENTAL STUDIES IN SUPPORT OF THE GEOPHYSICAL FLUID FLOW EXPERIMENT c46
John Hart and Juri Toomre *In* NASA. Marshall Space Flight Center NASA/MSFC FY-85 Atmospheric Processes Research Review Oct. 1985 3 p (For primary document see N87-13043 04-47)
Avail: NTIS HC A07/MF A01 CSCL 04B

Meteorologists and astrophysicists interested in large scale planetary and solar circulations have come to recognize the importance of rotation and stratification in determining the character of these flows. In particular, the effect of latitude-dependent Coriolis force on nonlinear convection is thought to play a crucial role in such phenomena as differential rotation on the Sun, cloud band orientation on Jupiter, and the generation of magnetic fields in thermally driven dynamos. The continuous low-gravity environment of the orbiting space shuttle offers a unique opportunity to make laboratory studies of such large-scale thermally driven flows under the constraint imposed by rotation and sphericity. This is possible because polarization forces in a dielectric liquid, which are linearly dependent on fluid temperature, give rise to an effectively radial buoyancy force when a radial electrostatic field is imposed. The Geophysical Fluid Flow Cell (GFFC) is an implementation of this ideal in which fluid is contained between two rotating hemispheres that are differentially heated and stressed with a large a-c voltage. The experiment, to be flown on Spacelab III (currently set for launch April 29, 1985), will explore non-linear mode selection and high Rayleigh number turbulence in a rotating convecting spherical shell of liquid. Experiments will be carried out in a low driving parameter range where some limited numerical experimentation is currently feasible, as well as in a parameter range significantly beyond numerical computation for many years. Author

N87-13046*# National Aeronautics and Space Administration. Marshall Space Flight Center, Huntsville, Ala.
THEORETICAL AND EXPERIMENTAL DESIGN STUDIES FOR THE ATMOSPHERIC GENERAL CIRCULATION EXPERIMENT c46
William W. Fowlis, David H. Hathaway, Timothy L. Miller, Glyn O. Roberts (Roberts Associates, Inc., Vienna, Va.), and Kenneth J. Kopecky (Drake Univ., Des Moines, Iowa.) *In its* NASA/MSFC FY-85 Atmospheric Processes Research Review Oct. 1985 2 p (For primary document see N87-13043 04-47)
Avail: NTIS HC A07/MF A01 CSCL 04A

The major criterion for the Atmospheric General Circulation Experiment (AGCE) design is that it be possible to realize strong baroclinic instability in the spherical configuration chosen. A configuration was selected in which a hemispherical shell of fluid is subjected to latitudinal temperature gradients on its spherical boundaries and the latitudinal boundaries are insulators. Work in the laboratory with a cylindrical version of this configuration revealed more instabilities than baroclinic instability. Since researchers fully expect these additional instabilities to appear in the spherical configuration also, they decided to continue the laboratory cylindrical annulus studies. Four flow regimes were identified: an axisymmetric Hadley circulation, boundary layer convection, baroclinic waves and deep thermal convection. Regime diagrams were prepared. Author

N87-13047*# Simpson Weather Associates, Inc., Charlottesville, Va.
MULTISCALE MODELING TO EVALUATE PROPOSED SPACE-BASED DOPPLER LIDAR SAMPLING STRATEGIES
G. D. Emmitt *In* NASA. Marshall Space Flight Center NASA/MSFC FY-85 Atmospheric Processes Research Review Oct. 1985 2 p (For primary document see N87-13043 04-47)
Avail: NTIS HC A07/MF A01 CSCL 04B

A proposal has been made to place a pulsed Doppler lidar on a space platform (Huffaker, et al., 1980; Emmitt, 1982) in a low earth orbit (200 to 800 km) to measure the atmospheric winds with a spatial resolution commensurate with the current continental rawinsonde network density - i.e., 300 to 500 km resolution. In the case of the space-based doppler lidar, the full range of space scales applies. Single shot pulses with dimensions of 10 x 1000 meters are used to sample areas 100,000 x 100,000 meters to resolved mass flow structure with wavelength of 1 million meters. Simulation studies, therefore, require an equally broad range of atmospheric models. A general circulation model is appropriate to answer questions regarding the impact of a global wind measuring system upon synoptic forecasts. Since the nominal resolution of the spacebased system is expected to be a few 100's of kilometers, then a numerical model with mesoscale dynamics is required. The meaning of an average Doppler shift within a laser pulse volume must be evaluated with models of turbulent/convective scale motions and aerosol gradients. Examples of how models on all these scales have been applied in an ongoing simulation study are presented. In particular, the uncertainties in a mesoscale wind estimate are separated into those arising from pulse scale variances and those due to sample distribution within a prescribed resolution volume. Trade-offs between accuracy and representativeness are discussed in terms of the model results. Author

N87-13048*# National Aeronautics and Space Administration. Marshall Space Flight Center, Huntsville, Ala.
ESTIMATION OF PRECIPITATION FROM GOES IR IMAGERY DURING FGGE: APPLICATION TO DIAGNOSTIC STUDIES
Franklin R. Robertson *In its* NASA/MSFC FY-85 Atmospheric Processes Research Review Oct. 1985 5 p (For primary document see N87-13043 04-47)
Avail: NTIS HC A07/MF A01 CSCL 04B

The objectives were to (1) develop a method of estimating open-ocean rainfall and associated latent heat release via GOES IR satellite imagery; (2) to use remote precipitation estimates to investigate the role of diabatic forcing in the maintenance of the South Pacific Convergence Zone (SPCZ) during FGGE SOP-1/; and (3) to assess the significance of non-quasigeostrophic transports of energy in several cyclogenetic events preceding the development of a North Atlantic blocking episode during FGGE SOP-1. The bulk of the early FY-85 work was directed toward development of the single pixel indexing technique (SPI) which assigns a rain rate to GOES IR black-body temperatures, T sub b, via a non-linear statistical relationship developed with raingauge measurements. The method was tested against radar-derived rainfall during GATE raingauge measurements over coastal North Carolina and island stations in the South Pacific Ocean. Skill was found comparable to Arkin's method (1979 MWR) in convective situations. The results suggest that transferring a rain algorithm from one oceanic regime to another may not require substantial modification of coefficients or tunable parameters. Twelve H mean rainfall amounts were produced for the region bounded by 10 deg. N, 50 deg. S, 120 deg W and 170 deg. E during the period January 10 to 16, 1979. These estimates constitute a basic input to diagnostic calculations of diabatic heating over the SPCZ region. ECMWF level III-b data analyses was used to compute several components of the APE balance in the South Pacific during the period January 10 to 18, 1979. Author

N87-13049*# Pennsylvania State Univ., University Park. Dept. of Meteorology.

THE USE OF SATELLITE DATA IN UNDERSTANDING AND PREDICTING CONVECTIVE AND LARGE-SCALE DYNAMICAL PROCESSES c46

John A. Dutton, John H. E. Clark, and Hampton N. Shirer *In* NASA. Marshall Space Flight Center NASA/MSFC FY-85 Atmospheric Processes Research Review Oct. 1985 2 p (For primary document see N87-13043 04-47)

Avail: NTIS HC A07/MF A01 CSCL 04A

A two-layer truncated baroclinic spectral model was developed to study the long-term evolution of disturbances to a baroclinically unstable mean flow. Topography and crudely-parameterized radiative processes were accounted for. As a result of Robert Schlaak's discovery of the underlying barotropic nature of the index oscillation as well as reviewers suggestions about the original manuscript, the model has been revised to allow for barotropic as well as baroclinic wave-mean flow interactions. The form-drag exerted by the topography on the barotropic part of the mean flow is larger than on the baroclinic part and thus researchers anticipate significant changes from the original calculations on the index oscillation when it is strongly modulated by topography. Researchers believe that since the index oscillation accounts for a significant portion of atmospheric temporal variance, the long term predictability could be improved if reliable forecasts of the index oscillation were available. Two spectral models of the index oscillation, one barotropic and the other baroclinic, have been developed. The latter allows for moisture, radiation, land-sea temperature contrasts, and energy exchanges with the underlying surface. Author

N87-13050*# Illinois State Water Survey, Champaign.

VARIATION OBJECTIVE ANALYSES FOR CYCLONE STUDIES

Gary L. Achtemeier, Stanley Q. Kidder, and Harry T. Ochs *In* NASA. Marshall Space Flight Center NASA/MSFC FY-85 Atmospheric Processes Research Review Oct. 1985 4 p (For primary document see N87-13043 04-47)

Avail: NTIS HC A07/MF A01 CSCL 04B

The objectives were to: (1) develop an objective analysis technique that will maximize the information content of data available from diverse sources, with particular emphasis on the incorporation of observations from satellites with those from more traditional immersion techniques; and (2) to develop a diagnosis of the state of the synoptic scale atmosphere on a much finer scale over a much broader region than is presently possible to permit studies of the interactions and energy transfers between global, synoptic and regional scale atmospheric processes. The variational objective analysis model consists of the two horizontal momentum equations, the hydrostatic equation, and the integrated continuity equation for a dry hydrostatic atmosphere. Preliminary tests of the model with the SESMAE I data set are underway for 12 GMT 10 April 1979. At this stage of purpose of the analysis is not the diagnosis of atmospheric structures but rather the validation of the model. Model runs for rawinsonde data and with the precision modulus weights set to force most of the adjustment of the wind field to the mass field have produced 90 to 95 percent reductions in the imbalance of the initial data after only 4-cycles through the Euler-Lagrange equations. Sensitivity tests for linear stability of the 11 Euler-Lagrange equations that make up the VASP Model 1 indicate that there will be a lower limit to the scales of motion that can be resolved by this method. Linear stability criteria are violated where there is large horizontal wind shear near the upper tropospheric jet. Author

N87-13051*# Purdue Univ., West Lafayette, Ind. Dept. of Geosciences.

UTILIZATION OF SATELLITE CLOUD INFORMATION TO DIAGNOSE THE ENERGY STATE AND TRANSFORMATIONS IN EXTRATROPICAL CYCLONES

Phillip J. Smith *In* NASA. Marshall Space Flight Center NASA/MSFC FY-85 Atmospheric Processes Research Review Oct. 1985 2 p (For primary document see N87-13043 04-47)

Avail: NTIS HC A07/MF A01 CSCL 04B

An important component of the research was a continuing investigation of the impact of latent release on extratropical cyclone development. Previous efforts to accomplish this task have focused on the energy balance and the vertical motion field of an intense winter extratropical cyclone over the United States. During this fiscal year researchers turned their attention to a more fundamental diagnostic variable, the height tendency. Central to this effort is the use of a modified form of the quasi-geostrophic height tendency equation, in which geostrophic wind components have been replaced by observed winds and a latent heat release term has been added. This methodology was adopted to produce a simple diagnostic model which retains the essential mechanisms of quasi-geostrophic theory but more faithfully describes observed wave development when the Rossby Number approaches and exceeds 0.5. Results to date indicate that the new model yields height tendencies that are superior to those obtained from the quasi-geostrophic formulation and are sufficiently close to the observed tendencies to be a useful tool for diagnosing the principle large-scale forcing mechanisms in th e700-300 mb layer. Of the three forcing terms included in the new model, vortity advection is in general dominant. The most persistent challenge to this dominance is made by the thermal advection. On the whole, latent heat release plays a secondary role. Finally, during the rapid intensification observed for this cyclone, all three processes complement each other in forcing height falls. Author

N87-13052*# Purdue Univ., West Lafayette, Ind. Dept. of Geosciences.

DYNAMICS AND ENERGETICS OF THE SOUTH PACIFIC CONVERGENCE ZONE DURING FGGE SOP-1

Dayton G. Vincent *In* NASA. Marshall Space Flight Center NASA/MSFC FY-85 Atmospheric Processes Research Review Oct. 1985 3 p (For primary document see N87-13043 04-47)

Avail: NTIS HC A07/MF A01 CSCL 04B

The major research objectives are to diagnose the physical processes responsible for the maintenance of the South Pacific Convergence Zone (SPCZ) and to examine the role of the SPCZ in the large-scale circulation patterns of the Southern Hemisphere. To accomplish these objectives researchers used several data sources which include: a modified set of Level III-b upper air analyses, originally produced by ECMWF (Vincent, 1982); subjectively analyzed surface analyses for the South Pacific based on island station reports (Vincent, 1985); outgoing longwave radiation values supplied to us by NOAA/NESDIS; and equivalent black body temperatures and precipitation rates derived by Robertson. In the past year researchers found that wave number four plays an inportant role in the Southern Hemisphere tropics during the 15-day period when the sPCZ was a dominant feature, particularly with regard to the baroclinic conversion of potential to kinetic energy (Huang and Vincent, 1985). The convectively-active SPCZ area was found to make a significant contribution to this conversion process; thus, it appears that baroclinic effects and latent heating are important in maintaining the SPCZ. Recently efforts concentrated on two research tasks, an examination of cyclone activity within the SPCZ (Kann, 1985; Vincent, 1985; Vincent and Kann, 1985) and a study of the heat and moisture budgets in the South Pacific (Miller, et al., 1985). It was found that cyclonic disturbances occurred with regularity in the Zone from 10 to 17 January. Author

N87-13053*# Texas A&M Univ., College Station. Dept. of Meteorology.

APPLICATION OF SATELLITE DATA TO TROPIC/SUBTROPIC MOISTURE COUPLING

James P. McGuirk and Aylmer H. Thompson *In* NASA. Marshall Space Flight Center NASA/MSFC FY-85 Atmospheric Processes Research Review Oct. 1985 3 p (For primary document see N87-13043 04-47)

Avail: NTIS HC A07/MF A01 CSCL 04B

The objective is to develop analysis tools for use of satellite data to interpret synoptic-scale systems in data-void regions. Interim goals are to: (1) quantify the synoptic information content of satellite data; and (2) utilize these data in the diagnosis of moisture bursts

in the eastern tropical Pacific Ocean. Researchers developed and implemented a statistical procedure for using TIROS N microwave data to infer infrared channel data for overcast conditions; they used the same procedure for deducing full TIROS N channel radiance profiles from NOAA 5 VTPR channel data over regions where the TIROS N data are missing. An empirical orthogonal function analysis of twice-daily channel radiance fields over the tropical eastern Pacific was completed. The vertically oriented eigenfunctions were interpreted in terms of typical meteorological events. The horizontal distribution of the eigenfunction amplitudes relates these meteorological signals to moisture bursts. A pair of moisture burst climatologies is complete: one of four years using infrared imagery (including the highly anomalous 1982 to 83 cold season); the other implementing 850 to 200 mb wind analyses in conjunction with GOES imagery. A number of different evaluations of the synoptic evolution of moisture fields (enhanced infrared imagery, moisture channel data, FGGE humidity analysis, and in situ station and sounding observations) are compared. All have limitations; all can be utilized together; all together are still less than adequate in the tropical Pacific. Author

N87-13054*# National Aeronautics and Space Administration. Marshall Space Flight Center, Huntsville, Ala. Dept. of Geology and Geophysics.

OBSERVATIONAL AND THEORETICAL STUDIES OF THE EVOLVING STRUCTURE OF BAROCLINIC WAVES: ATTRACTOR DYNAMICS OF GLOBAL WEATHER SYSTEMS

Barry Saltzman, Anthony R. Hansen, Richard N. Nagle, and Chung-Muh Tang (Universities Space Research Association, Columbia, Md.) *In its* NASA/MSFC FY-85 Atmospheric Processes Research Review Oct. 1985 2 p (For primary document see N87-13043 04-47)

Avail: NTIS HC A07/MF A01 CSCL 04B

Significant progress was made in developing a six-component dry model of mid-latitude baroclinic wave evolution, and a ten-component moist model. These models include representations of airflow over mountians and non-adiabatic processes. As a first step, the properties of a reduced, three component, baroclinic system are studied. The classical baroclinic stability criteria emerge as the properties of one of the three equilibria admitted, with the remaining two equilibria forming the attractor region for the observed weather activity. Passive tracer evolution in a baroclinic wave was studied. A model in which only constituents trapped within low atmospheric levels are considered, has been extended to include the possibility for fluxes into the upper levels of the atmosphere. The reported results for the lower levels achieved previously are shown to be qualitatively similar to those obtained by these new calculations in which the vertical flux constraint is removed. An extensive study of an 8-year record of global outgoing longwave radiation for the Northern Hemisphere reveals that blocking events exhibit only a weak signature of blocking highs, as measured by relatively low values of the ratio of the standard deviation to the mean value of the observed long wave outgoing radiation. Though present in many cases, the signature is not a strongly distinctive feature of the blocking episodes. Author

N87-13055*# National Aeronautics and Space Administration. Marshall Space Flight Center, Huntsville, Ala.

DEEP CONVECTION IN MESOSCALE CONVECTIVE SYSTEMS

Steven J. Goodman *In its* NASA/MSFC FY-85 Atmospheric Processes Research Review Oct. 1985 1 p (For primary document see N87-13043 04-47)

Avail: NTIS HC A07/MF A01 CSCL 04B

A study was undertaken to examine the evolution of radar echoes and lightning attending the convective storms in mesoscale convective systems (MCS) and the relationships between the spatial and temporal evolution of deep convection and the storm environment, precipitation, severe weather, and lightning. The total number of ground discharges ranges from 10,000 to 30,000 over the life cycle of the MCS with peak sustained rates (for up to 10 consecutive hours) in excess of 2000 per hour. The peak lightning activity occurs from 5 to 20 hours after the first storms and anywhere from 7 hours prior to 7 hours after the time of the maximum areal extent of the MCS for very similar synoptic environments. Thus, it appears that mesoscale and sub-synoptic scale mechanisms are responsible for these large temporal variation in lightning activity. In addition, we have found that the lightning rates in MCS's are not related to either the size or the duration of the MCS. Preliminary results suggest that the MCA's with embedded squall lines produce the greatest flash rates. Author

N87-13056*# National Oceanic and Atmospheric Administration, Norman, Okla.

SEVERE STORM ELECTRICITY

W. David Rust and Donald R. MacGorman *In* NASA. Marshall Space Flight Center NASA/MSFC FY-85 Atmospheric Processes Research Review Oct. 1985 5 p (For primary document see N87-13043 04-47)

Avail: NTIS HC A07/MF A01 CSCL 04B

During FY-85, Researchers conducted a field program and analyzed data. The field program incorporated coordinated measurements made with a NASA U2. Results include the following: (1) ground truth measurements of lightning for comparison with those obtained by the U2; (2) analysis of dual-Doppler radar and dual-VHF lightning mapping data from a supercell storm; (3) analysis of synoptic conditions during three simultaneous storm systems on 13 May 1983 when unusually large numbers of positive cloud-to-ground (+CG) flashes occurred; (4) analysis of extremely low frequency (ELF) wave forms; and (5) an assessment of a cloud -ground strike location system using a combination of mobile laboratory and fixed-base TV video data. Author

N87-13057*# National Aeronautics and Space Administration. Marshall Space Flight Center, Huntsville, Ala.

STORM SEVERITY DETECTION (RF)

R. L. Johnson (Southwest Research Inst., San Antonio, Tex.) and S. J. Goodman *In its* NASA/MSFC FY-85 Atmospheric Processes Research Review Oct. 1985 2 p (For primary document see N87-13043 04-47)

Avail: NTIS HC A07/MF A01 CSCL 04B

Atmospheric electrical emissions occurring in association with Hurricane Alicia were observed by two crossed baseline phase linear interferometers. The sensors were located in San Antonio, Texas, and at Marshall Space Flight Center (MSFC), Huntsville, Alabama. An analysis of the data has indicated that the direction finding (DF) performance of the San Antonio site was extremely good while the DF performance at the MSFC site evidenced erratic behavior. A check of the data acquisition hardware revealed an intermitted problem in one of the radio receiver channels. Since the system has experienced several lightning strikes during the early spring of 1984, it was necessary to ship the entire rack of equipment back to SwRI for refurbishment. Analysis of the DF data from the interferometer site at San Antonio is being done. A limited subset of the MSFC data acquired during Hurricane Alicia has been found to be valid. These were data which satisfied the phase linearity criteria. Approximately 2,000 location estimates have been produced on the valid data. The results of the DF analysis and the location data are being correlated with the McIDAS data base at Marshall Space Flight Center, and with the radar summary data provided by the Hurricane Research Division using the National weather Service radar Facility at Galveston, Texas. Author

N87-13058*# Wisconsin Univ., Madison. Space Science and Engineering Center.

STUDIES OF LIGHTNING DATA IN CONJUNCTION WITH GEOSTATIONARY SATELLITE DATA

Brian Auvine and David Martin *In* NASA. Marshall Space Flight Center NASA/MSFC FY-85 Atmospheric Processes Research Review Oct. 1985 2 p (For primary document see N87-13043 04-47)

Avail: NTIS HC A07/MF A01 CSCL 04B

Since January, work has been proceeding on the first phase of this project: the creation of an extensive real-time lightning data base accessible via the Space Science and Engineering

Center Mcidas system. The purpose of this endeavor is two-fold: to enhance the availability and ease of access to lightning data among the various networks, governmental and research agencies; and to test the feasiblity and desirability of such efforts in succeeding years. The final steps in the creation of the necessary communications links, hardware, and software are in the process of being completed. Operations ground rules for access among the various users have been discussed and are being refined. While the research planned for the last year of the project will rely for the most part on archived, quality-controlled data from the various networks, the real-time data will provide a valuable first-look at potentially interesting case studies. For this purpose, tools are being developed on Mcidas for display and analysis of the data as they become available. In conjunction with concurrent GOES real-time imagery, strike locations can be plotted, gridded and contoured, or displayed in various statistical formats including frequency distributions, histograms, and scatter plots. The user may also perform these functions in relation to arbitrarily defined areas on the satellite image. By mid-May these preparations for the access and analysis of real-time lightning data are expected to be complete. Author

N87-13059*# National Aeronautics and Space Administration. Marshall Space Flight Center, Huntsville, Ala.
LIGHTNING MAPPER AND THE FUTURE
Hugh J. Christian *In its* NASA/MSFC FY-85 Atmospheric Processes Research Review Oct. 1985 2 p (For primary document see N87-13043 04-47)
Avail: NTIS HC A07/MF A01 CSCL 04B

A trade-off analysis was completed that reveals how the lightning mapper detection efficiency will change as a function of interference filter bandwidth, pixel field of view, and telescope aperture. It is shown that the critical parameter on which we have minimum flexibility is filter band-width. The problem is that too narrow a filter bandwidth is incompatible with wide areal coverage. The trade-off analysis demonstrates that an 80 percent lightning detection efficiency will technically be relatively straight-forward, while a 90 percent detection efficiency will apparently be difficult to achieve. Three focal plane designs are currently under consideration. One would use a single large, solid state silicon integrating array with multiple output channels and off-the-focal-plane analog, time domain, background removing fibers. A second design would use the same technology, but the sensor would consist of up to four virtually independent focal plane arrays. This design reduces the areal coverage of each detector. Thus narrower interference filters could be utilized. Superior performance would be realized at a probable increase in cost. The final design would use a three-dimensional focal plane in order to perform background removal at the focal plane. Superior performance would be achieved along with reduced weight and power requirements. Unfortunately, this focal plane technology is still under development. Author

N87-13060*# National Aeronautics and Space Administration. Marshall Space Flight Center, Huntsville, Ala.
SPACE SHUTTLE/MESOSCALE LIGHTNING EXPERIMENT
Otha H. Vaughan, Jr., B. Vonnegut (State Univ. of New York, Binghamton.), and Marx Brook (New Mexico Inst. of Mining and Technology, Socorro.) *In its* NASA/MSFC FY-85 Atmospheric Processes Research Review Oct. 1985 1 p (For primary document see N87-13043 04-47)
Avail: NTIS HC A07/MF A01 CSCL 04B

A payload integration plan (PIP) is now being developed with Johnson Space Center integration personnel which covers management, structural thermal, electrical power/avionics, training, ground operations, safety requirements, etc., in support of this experiment. If a Shuttle flight can be identified, researchers hope to conduct the experiment in the late summer or fall of 1985. Some preliminary TV lightning data has been collected by Shuttle crews on 41D and 51D and researchers are doing an analysis of it. Additional flights will be conducted to obtain data on Mesoscale Lightning Observations. Researchers will continue to study how to improve the data collection using the onboard TV cameras. By more interaction with the crews who have used the TV camera to obtain TV of lightning, they are planning to optimize the crew time and have better TV camera operations management to produce more useful data. As the crews are better trained in the use of the gain control settings and/or camera iris operations, the quality of the TV data will be improved. Author

N87-13061*# National Aeronautics and Space Administration. Marshall Space Flight Center, Huntsville, Ala.
OPTICAL CHARACTERISTICS OF LIGHTNING AND THUNDERSTORM CURRENTS
E. Philip Krider (Arizona Univ., Tucson.) and Richard J. Blakeslee *In its* NASA/MSFC FY-85 Atmospheric Processes Research Review Oct. 1985 1 p (For primary document see N87-13043 04-47)
Avail: NTIS HC A07/MF A01 CSCL 04B

Researchers determined that lightning can be used to determine the diurnal variations of thunderstorms, i.e., storms that produce audible thunder, and that these variations are also in good agreement with diurnal variations in rainfall and convective activity. Measurements of the Maxwell current density, J sub m, under active thunderstorms show that this physical quantity is quasi-steady between lightning discharges and that lightning does not produce large changes in J sub m. Maps of J sub m show contours of iso-current density that are consistent with the locations of radar echos and the locations of where lightning has altered the cloud charge distribution. Author

N87-13062*# National Aeronautics and Space Administration. Marshall Space Flight Center, Huntsville, Ala.
OPTICAL CHARACTERISTICS OF LIGHTNING
Steven J. Goodman *In its* NASA/MSFC FY-85 Atmospheric Processes Research Review Oct. 1985 3 p (For primary document see N87-13043 04-47)
Avail: NTIS HC A07/MF A01 CSCL 04B

A study of the optical characteristics of cloud-to-ground dischargers and how they compare with intracloud flashes was completed. Time resolved optical (7774A) and electric field-change waveforms were measured above clouds from a U2 airplane coincident with ground-based measurements of lightning. The optical pulse trains are studied for within and between flash variability. Specifically, for each flash researchers examine the 10, 50 (full width half maximum), and 90 percent pulse widths; the 10-10, 10-50, 10-90, and 10-peak percent amplitude rise times; the radiances (optical power densities); radiant energy densities; and pulse intervals. The optical pulse characteristics of first strokes, subsequent strokes, the intracloud components of cloud-to-ground flashes and intracloud flashes as viewed from above cloud are shown to exhibit very similar waveshapes, radiances and radiant energy densities. Descriptive statistics on these pulse categories were tabulated for 25 visually confirmed cloud-to-ground flashes (229 optical pulses) and 232 intracloud flashes (3126 optical pulses). A companion study of lightning observations above and below cloud in storms, storm complexes, and mesoscale convective systems has also been completed. Researchers compared the mapping of total lightning activity from above clouds with ground-based measurements and storm evolution. Although the total (IC + CG) lightning activity is the more representative indication of thunderstorm growth and decay, the ground strike data can be used to locate, diagnose, and track storm evolution in a number of instances. Author

N87-13063*# National Aeronautics and Space Administration. Marshall Space Flight Center, Huntsville, Ala.
AIRBORNE ATMOSPHERIC ELECTRICITY EXPERIMENTS
Richard J. Blakeslee *In its* NASA/MSFC FY-85 Atmospheric Processes Research Review Oct. 1985 2 p (For primary document see N87-13043 04-47)
Avail: NTIS HC A07/MF A01 CSCL 04B

During the 1984 U2 spring flight program, lightning spectra were measured in the wavelengths from 380 nm to 900 nm with a temporal resolution of 5 ms. With this capability, researchers simultaneously acquired both visible near-infrared lightning spectra

on a pulse to pulse basis, so that the spectral variability within a flash, as well as flash to flash variations, can be studied. Preliminary results suggest that important variations do occur, particularly in the strengths of the hydrogen and singly ionized nitrogen emission lines. Also, the results have revealed significant differences in the integrated energy distributions between the lightning spectra measured above clouds and the spectral measurements of cloud-to-ground lightning made at the ground. In particular, the ratio of the energy in the near-IR to that in the visible is around 1 to 2 for cloud top spectra versus about 1/3 for surface observations. Detailed analyses of the 1984 lightning spectral data is being conducted. This data should provide improved understanding about the optical transmission properties of thunderclouds and the physics of the lightning discharge process. Efforts continue on developing and testing background signal removal algorithms using U2 spectometer and optical array sensor day-flight data sets. The goal of this research is to develop an algorithm satisfying Lightning Mapper Sensor requirements. Author

N87-13064*# Mississippi Univ., University.
MOBILE INTERCEPT OF STORMS
Roy T. Arnold *In* NASA. Marshall Space Flight Center NASA/MSFC FY-85 Atmospheric Processes Research Review Oct. 1985 2 p (For primary document see N87-13043 04-47)
Avail: NTIS HC A07/MF A01 CSCL 04B

The primary goal was to acquire lightning data to serve as ground truth for U2 overflights. Researchers were successful in instrumenting the Univ. of Mississippi/National Severe Storms Lab. (UM/NSSL) mobile laboratory and in coordinating storm intercept through communication to the U2 provided by airplane guidance at NSSL and through direct communication with the U2 pilot from a portable transceiver in the mobile lab. A demonstration showed that a mobile laboratory can be directed within a large geographical area and used to collect ground truth data for comparison with airborne data on a routine basis with proper utilization of forecasts, nowcasts, and communication among all participants. After the U2 flights, researchers turned their attention solely to intercepting severe storms within the area of Oklahoma with good Doppler radar coverage. They incorporated a second vehicle, which followed the mobile lab and from which they released instrumented balloons. This project utilized a standard meteorological rawinsonde and a balloon-borne electric field meter. They were successful in flying, tracking, and receiving data from mobily launched balloons on several days. Researchers believe that they have demonstrated the ability to obtain meteorological and electrical data in severe storms using instrumented balloons. This also includes the capability to launch into the mesocyclone region and for multiple launches in the same storm. Author

N87-13065*# State Univ. of New York, Albany. Dept. of Atmospheric Science.
REMOTE OBSERVATIONS OF SEVERE STORMS
Richard E. Orville *In* NASA. Marshall Space Flight Center NASA/MSFC FY-85 Atmospheric Processes Research Review Oct. 1985 2 p (For primary document see N87-13043 04-47)
Avail: NTIS HC A07/MF A01 CSCL 04B

The focus of current research activities is on: (1) analyzing spectra from cloud-to-ground lightning and intracloud lightning; (2) site error analyses and sensitivity tests for direction finders in the East Coast network; (3) integration of lightning location data with satellite images on the Wisconsin McIDAS system; and (4) fundamental studies of the relation between meteorological parameters and characteristics of lightning determined by the SUNYA Lightning Detection Network. Author

N87-13066*# California Univ., Davis. Dept. of Land, Air and Water Resources.
AIRBORNE DOPPLER MEASUREMENTS OF THE CENTRAL CALIFORNIA EXTENDED SEA BREEZE
John J. Carroll *In* NASA. Marshall Space Flight Center NASA/MSFC FY-85 Atmospheric Processes Research Review Oct. 1985 2 p (For primary document see N87-13043 04-47)
Avail: NTIS HC A07/MF A01 CSCL 04B

One data acquisition flight was executed in the late summer of 1984. The flight paths were designed to obtain measurements of the extended sea breeze penetration into the central valley of California over several hours. Data from this flight are being processed at Marshall Space Flight Center prior to release for analysis. Author

N87-13067*# National Aeronautics and Space Administration. Marshall Space Flight Center, Huntsville, Ala.
ANALYSIS OF DOPPLER LIDAR DATA
Jeffry Rothermel *In its* NASA/MSFC FY-85 Atmospheric Processes Research Review Oct. 1985 2 p (For primary document see N87-13043 04-47)
Avail: NTIS HC A07/MF A01 CSCL 04B

Dual Doppler lidar analyses of data taken by pulsed lidars demonstrated feasibility of deriving wind fields from coordinated lidar scans. Limited case histories of thunderstorm outflows were obtained. Co-located comparison between Marshall Space Flight Center lidar and NCAR 5.5 cm radar demonstrated desirability of lidar in cases of marginal radar reflectivity in clear air and low-elevation scans. Analysis continued on backscattered intensity and velocity measurements made from April 1983 to February 1984. A slant path method was used to calculate vertical profiles of volumetric backscatter and adsorption in the lower troposphere. High-quality VAD scans were identified as candidates for investigating feasibility of calculating horizontal motion fields using single Doppler lidar. Activities during FY-85 also included participation in Fall 1984 airborne Doppler lidar flight experiments. Preliminary data review was begun using McIdas system. Analysis of backscatter and absorpiton profiles continues. Focus is on understanding spatial and temporal variations, as well as frequency distribution, of backscatter at several tropospheric levels. Results from this study provide input to evaluation of clean/dirty airmass hypothesis of aerosol distribution. Assistance is being given to preparation of a comprehensive, global backscatter measurement plan. Analysis of data from Fall 1984 flight experiments is just beginning. Work has begun on preprocessing data to minimize errors due to electro-optic modulator malfunction during flights. Author

N87-13068*# National Aeronautics and Space Administration. Marshall Space Flight Center, Huntsville, Ala.
AIRBORNE DOPPLER LIDAR ACTIVITIES
D. R. Fitzjarrald and J. W. Bilbro *In its* NASA/MSFC FY-85 Atmospheric Processes Research Review Oct. 1985 2 p (For primary document see N87-13043 04-47)
Avail: NTIS HC A07/MF A01 CSCL 04B

During August and September 1984, 20 research flights were conducted by the CV990 with airborne doppler lidar installed. Nine of these flights were dedicated to the Lidar project. Excellent data were obtained in the Carquenez Strait downwind of San Francisco Bay, showing the divergence of the flow as it passes into the Central Valley. The data clearly show the horizontal and vertical structure of the wind flow in the pass region and adjoining parts of the Central Valley. Data were also obtained in the vicinity of Mount Shasta in northern California, showing the flow in the lee of the isolated mountain. Preliminary analyses of these flights using the McIdas interactive graphics system have been accomplished, and procurements have been initiated for detailed scientific analyses. A partial failure of a crucial optical component resulted in contamination of a portion of the wind data that were obtained in the Mount Shasta and subsequent flights. Analyses are underway to attempt reconstruction of the data to minimize the effects of the failure. Data were obtained in conjunction with a microwave wind profiler at Penn State University. It is expected that data reconstruction will be of use in this case. Procurement has been initiated for scientific analyses of these results. The improved airborne Lidar system performed well. In most of the research flights a large number of different scan angles were used to obtain the vertical structure of the wind fields being investigated. Author

N87-13069*# National Aeronautics and Space Administration. Marshall Space Flight Center, Huntsville, Ala.
RESPONSE OF THE MESOSCALE ATMOSPHERE TO DIABATIC

HEATING

Franklin R. Robertson *In its* NASA/MSFC FY-85 Atmospheric Processes Research Review Oct. 1985 2 p (For primary document see N87-13043 04-47)

Avail: NTIS HC A07/MF A01 CSCL 04B

A study was initiated to determine the influence of convective latent heat release/diabatic heating on the production of kinetic energy during AVE/SESAME I. The primary focus has been on the relative importance of thermally forced modification of the wind field through thickness and height gradient changes versus inertial-advective effects via the diabatic component of vertical motion. Preliminary results have shown that because of the strong vertical shear over the convective region, ageostrophic response is primarily caused by the latter process. The diagnostic parameterization of convective heating has been extended for use in conjunction with satellite precipitation estimates in data-poor oceanic regions. An initial application was made to a mesoscale convective system embedded in the South Pacific convergence zone. Comparison to the heating field diagnosed as a residual in the thermodynamic equation using the ECMWF III-b analyses showed that the methodology will be useful in explaining the observed heating fields and determining the relative contribution of moist processes to the total diabatic heating. Research activities are now concentrated in the following areas: (1) Determining the sensitivity of vertical heating profiles to partitioning of gridscale versus convective precipitation; (2) assessing the possible effects of incorrect analyzed gridscale vertical motions on residuals in the heat budgets computed with the ECMWF III-b data sets.

Author

N87-13070*# Wisconsin Univ., Madison. Space Science and Engineering Center.

MESOSCALE AGEOSTROPHIC CIRCULATIONS ASSOCIATED WITH BAROCLINIC JET STREAKS

Donald R. Johnson *In* NASA. Marshall Space Flight Center NASA/MSFC FY-85 Atmospheric Processes Research Review Oct. 1985 1 p (For primary document see N87-13043 04-47)

Avail: NTIS HC A07/MF A01 CSCL 04B

In regard to research completed, a complete list of publications and theses sponsored through the support of the NASA Severe Storms Research Project under NASA contract NAS8-33222 is given.

Author

N87-13071*# Chicago Univ., Ill.

ANALYSIS OF SATELLITE DATA FOR SENSOR IMPROVEMENT (DETECTION OF SEVERE STORMS FROM SPACE

T. Theodore Fujita *In* NASA. Marshall Space Flight Center NASA/MSFC FY-85 Atmospheric PRocesses Research Review Oct. 1985 1 p (For primary document see N87-13043 04-47)

Avail: NTIS HC A07/MF A01 CSCL 04B

A climatological study of downbursts in Arkansas, Louisiana, Tennessee, Mississippi, Alabama, and Georgia was carried out, as well as studies of the Huntsville area microbursts on July 7, 1984, and a Decatur microburst on August 1984.

Author

N87-13072*# National Aeronautics and Space Administration. Marshall Space Flight Center, Huntsville, Ala.

SEVERE STORM DETECTION WITH PASSIVE 37 GHz OBSERVATIONS

Roy W. Spencer, Michael R. Howland (Wisconsin Univ., Madison.), and David W. Martin *In its* NASA/MSFC FY-85 Atmospheric Processes Research Review Oct. 1985 2 p (For primary document see N87-13043 04-47)

Avail: NTIS HC A07/MF A01 CSCL 04B

The research objective was to determine the information content of satellite passive 37 GHz brightness temperatures on the severity of thunderstorms through the measurement of the attenuation (scattering) signature of precipitation. The severe storm detection potential of satellite-observed passive 37 GHz radiances was evaluated by comparing Nimbus-7 Scanning Multi-channel Microwave Radiometer (SMMR) data to reports of severe weather contained in the NSSFC severe weather log for calendar years 1979 and 1980 over the United States east of the Rocky Mountains. Heavy thunderstorms have a characteristic signature in the form of localized very low 37 GHz T sub B from scattering by precipitation-size ice particles (thick cirrus being transparent at this frequency). The local noon and midnight snapshots taken by the SMMR on alternating days (with incomplete areal coverage of the U.S. on any given day) were scanned to find cases of strong scattering by precipitation, revealed by large differences between the 18 and 37 GHz brightness temperatures, the 37 GHz T sub B being at least 20 C lower than the 18 GHz T sub B. The value of the 37 GHz T sub b was then compared to severe weather reports within one hour of the SMMR observation time, in the vicinity of the SMMR-observed storm. It was found that the degree to which the T sub B were lowered was a fairly good indicator of the probability that the storm was severe. Of 263 storms observed by the SMMR during 1979 and 1980, 54 percent had severe weather associated with them for a T sub b below 203 K, while 8 percent of those above this threshold were severe.

Author

N87-13073*# National Aeronautics and Space Administration. Marshall Space Flight Center, Huntsville, Ala.

AUTOMATED MESOSCALE WINDS DERIVED FROM GOES MULTISPECTRAL IMAGERY

Gregory S. Wilson and Robert J. Atkinson (General Electric Co., Huntsville, Ala.) *In its* NASA/MSFC FY-85 Atmospheric Processes Research Review Oct. 1985 2 p (For primary document see N87-13043 04-47)

Avail: NTIS HC A07/MF A01 CSCL 04B

An automated technique for extracting mesoscale winds from sequences of GOES visible infrared spin scan radiatiometer (VISSR) image pairs has been developed, tested extensively, and configured for quasi-real time research applications on the Atmospheric Sciences Division's research computing sytem. The entire system of computer codes was successfully vectorized for execution on an array processor resulting in job turnaround in less than 1 hour. An objective quality control system provides much greater than 99 percent accuracy in eliminating questionable wind estimates. Dynamical analysis of cloud wind divergence has revealed temporally consistent convergence centers on the meso-beta scale that are highly correlated with ongoing and future developing convective storms.

Author

N87-13074*# National Aeronautics and Space Administration. Marshall Space Flight Center, Huntsville, Ala.

SATELLITE PASSIVE MICROWAVE RAIN MEASUREMENT TECHNIQUES FOR LAND AND OCEAN

Roy W. Spencer *In its* NASA/MSFC FY-85 Atmospheric Processes Research Review Oct. 1985 3 p (For primary document see N87-13043 04-47)

Avail: NTIS HC A07/MF A01 CSCL 04B

Multiseasonal rainfall was found to be measurable over land with satellite passive microwave data, based upon comparisons between Nimbus 7 Scanning Multichannel Microwave Radiometer (SMME) brightness temperatures (T sub B) and operational WSR-57 radar rain rates. All of the SMMR channels (bipolarized 37, 21, 18, 10.7, and 6.6. GHz T sub B) were compared to radar reflectivities for 25 SMMR passes and 234 radar scans over the U.S. during the spring, summer, and fall of 1979. It was found that the radar rain rates were closely related to the difference between 37 and 21 GHz T sub B. This result is due to the volume scattering effects of precipitation which cause emissivity decreases with frequency, as opposed to emissive surfaces (e.g., water) whose emissivities increase with frequency. Two frequencies also act to reduce the effects of thermometric temperature variations on T sub B to a miminum. During summer and fall, multiple correlation coefficients of 0.80 and 0.75 were obtained. These approach the limit of correlation that can be expected to exist between two very different data sources, especially in light of the errors attributable to manual digitization of PPI photographs of variable quality from various operational weather radar not calibrated for research purposes. During the spring, a significantly lower (0.63) correlation was found. This poorer performance was traced to cases of wet, unvegetated soil being sensed at the

lower frequencies through light rain, partly negating the rain scattering signal. Author

N87-13075*# National Aeronautics and Space Administration. Marshall Space Flight Center, Huntsville, Ala.
REMOTE SENSING OF SEVERE CONVECTIVE STORMS
R. J. Hung (Alabama Univ., Huntsville.), R. E. Smith, and G. S. West *In its* NASA/MSFC FY-85 Atmospheric Processes Research Review Oct. 1985 3 p (For primary document see N87-13043 04-47)
Avail: NTIS HC A07/MF A01 CSCL 04B

The Tibet Plateau significantly affects the initiation and development of heavy rainfall and severe storms in China, just as the Rocky Mountains influence local severe storms in the United States. The study shows that the heavy rainfall in the Plateau area is usually preceded by a high growth rate of the convective clouds, followed by a rapid collapse of the cloud top. The study also shows that the tops of the convective clouds associated with heavy rainfall over the Plateau usually lie between the altitude of the two tropopauses which exist over the Plateau. There is good agreement between the collapsing of the cloud as observed from the satellite imagery, and the beginning of the rainfall observed by the ground stations and also between the dissipation of the cloud observed from the satellite infrared imagery, and the ending of the rainfall, observed by the ground stations. Comparison of the volumetric dissipation of clouds per unit area over the location of the ground station with the rainfall recorded at that station shows a linear relationship for rainfall mounts exceeding 8 mm. The ratio of observed rainfall at the ground station over the satellite observed cloud volume dissipation per unit area was also computed. The result shows that the ratio is almost constant with the value of 9.55 mm/(pixel . km/pixel) for rainfall amounts exceeding 15 mm; and the variation is less then 10 percent for rainfall mounts between 8 and 15 mm. Needless to say, further investigation is required to verify this ratio. Author

N87-13076*# Drexel Univ., Philadelphia, Pa. Dept. of Physics and Atmospheric Science.
LAMPS SOFTWARE AND MESOSCALE PREDICTION STUDIES
D. J. Perkey *In* NASA. Marshall Space Flight Center NASA/MSFC FY-85 Atmospheric Processes Research Review Oct. 1985 1 p (For primary document see N87-13043 04-47)
Avail: NTIS HC A07/MF A01 CSCL 04B

The full-physics version of the LAMPS model has been implemented on the Perkin-Elmer computer. In Addition, LAMPS graphics processors have been rewritten to the run on the Perkin-Elmer and they are currently undergoing final testing. Numerical experiments investigating the impact of convective parameterized latent heat release on the evolution of a precipitating storm have been performed and the results are currently being evaluated. Curent efforts include the continued evaluation of the impact of initial conditions on LAMPS model results. This work will help define measurement requirements for future research field projects as well as for observations in support of operational forecasts. Also, the impact of parameterized latent heat on the evolution of precipitating systems is continuing. This research is in support of NASA's proposed Earth Observation Mission (EOM).

N87-13077*# South Dakota School of Mines and Technology, Rapid City.
MESOSCALE-CLOUD SCALE SIMULATION OF CONVECTIVE RESPONSE
Fred J. Kopp and Richard T. McNider (Alabama Univ., Huntsville.) *In* NASA. Marshall Space Flight Center NASA/MSFC FY-85 Atmospheric Processes Research Review Oct. 1985 3 p (For primary document see N87-13043 04-47)
Avail: NTIS HC A07/MF A01 CSCL 04B

The importance of mesoscale moisture information in the forecasting of weather events is being studied. A test is being prepared with the March 6, 1982 Vertical Atmospheric Sounder/Atmospheric Variability Experiment (VAS/AVE) case study to be run on the sub-synoptic scale model (SSM). Intracomparison of three carefully designed simulations should isolate the role of mesoscale information in the initial conditions for both moisture and vertical motion. Three simulations will be made for the period 1200Z 6 March to 0000Z 7 March starting with the regular synoptic time data of 1200Z. The distinction between the three cases arises from data manipulation at 1800Z midway through the forecast period. Comparison of results for the 1800Z to 0000Z time period will give the information desired. Author

N87-13078*# Universities Space Research Association, Huntsville, Ala.
MESOSCALE RESEARCH ACTIVITIES WITH THE LAMPS MODEL
Michael W. Kalb *In* NASA. Marshall Space Flight Center NASA/MSFC FY-85 Atmospheric Processes Research Review Oct. 1985 2 p (For primary document see N87-13043 04-47)
Avail: NTIS HC A07/MF A01 CSCL 04B

Researchers achieved full implementation of the LAMPS mesoscale model on the Atmospheric Sciences Division computer and derived balanced and real wind initial states for three case studies: March 6, April 24, April 26, 1982. Numerical simulations were performed for three separate studies: (1) a satellite moisture data impact study using Vertical Atmospheric Sounder (VAS) precipitable water as a constraint on model initial state moisture analyses; (2) an evaluation of mesoscale model precipitation simulation accuracy with and without convective parameterization; and (3) the sensitivity of model precipitation to mesoscale detail of moisture and vertical motion in an initial state. Author

N87-13079*# Wisconsin Univ., Madison. Dept. of Meteorology.
COOPERATIVE VAS PROGRAM WITH NASA MARSHALL SPACE FLIGHT CENTER
David D. Houghton *In* NASA. Marshall Space Flight Center NASA/MSFC FY-85 Atmospheric Processes Research Review Oct. 1985 2 p (For primary document see N87-13043 04-47)
Avail: NTIS HC A07/MF A01 CSCL 04B

The importance of mesoscale moisture information in the forecasting of weather events is discussed. A test is being prepared with the March 6, 1982 Vertical Atmospheric Sounder/Atmospheric Variability Experiment (VAS/AVE) case study to be run on the sub-synoptic scale model (SSM). Model intracomparison of three carefully designed simulations should isolate the role of mesoscale information in the initial conditions for both moisture and vertical motion. Three simulations will be made for the period 1200Z 6 March to 0000Z 7 March starting with the regular synoptic time data of 1200Z. The distinction between the three cases arises from data manipulation at 1800Z midway through the forecast period: (1) Control Case: no alterations at 1800Z. (2) Moisture Information Suppression: at 1800Z the model simulation field for water vapor, which by this time contains considerable mesoscale structure, is replaced by a smoothed version from which the mesoscale structure has been eliminated. No other variables are structure altered. (3) Vertical Motion Information Suppression: at 1800Z the model is subjected to a dead start procedure which primarily imposes a nondivergent constraint of the horizontal motion field field suppressing vertical motion. The main effect is to eliminate the mesoscale component. Comparison of results for the 1800Z to 0000Z time period will give the information desired. Author

N87-13080*# Wisconsin Univ., Madison. Space Science and Engineering Center.
THE ASSIMILATION OF SATELLITE SOUNDINGS, WINDS AND SATELLITE PRODUCTS IN A MESOSCALE ANALYSIS/FORECAST SYSTEM
George R. Diak and William L. Smith *In* NASA. Marshall Space Flight Center NASA/MSFC FY-85 Atmospheric Processes Research Review Oct. 1985 2 p (For primary document see N87-13043 04-47)
Avail: NTIS HC A07/MF A01 CSCL 04B

Investigations in FY-85 were centered on three case study days in 1982. Two of these, March 6 and April 24, were Atmospheric Variability Experiment/Verical Atmospheric Sounder (AVE/VAS) days for which high spatial and temporal resolution RAOB and

Vertical Atmospheric Sounder (VAS) data sets were available. The third investigation day, April 26, was a day of interesting severe weather. In the last part of FY-84 and early FY-85 we were able to demonstrate most importantly the complimentary nature of satellite soundings and winds in a forecast/analysis system. In our variational analysis scheme, cloud drift and water vapor winds enter into the height field as gradient information. The cloud drift winds especially, have the character of supplying information in cloudy areas where satellite soundings are not possible. In the April 26 experiments, analyses and forecasts using the combination satellite winds and soundings were superior to those using only soundings. Good consistency was shown between independent satellite forecasts from different initialization times run to the same verification time. A significant accomplishment in FY-85 was expanding experiments on April 26 to include quasi-continuous initialization inserting satellite soundings and winds from several different times into an analysis/forecast. Contrary to the first set of experiments on April 26, here forecast initialization fields were not independent, but contained satellite information from two data times. Author

N87-13081*# National Aeronautics and Space Administration. Marshall Space Flight Center, Huntsville, Ala.

NUMERICAL SIMULATION OF CONVECTIVE RESPONSE TO MESOSCALE FORCING

Richard T. McNider (Alabama Univ., Huntsville.), Fred J. Kopp (South Dakota School of Mines and Technology, Rapid City.), Michael W. Kalb (Universities Space Research Association, Huntsville, Ala.), and Gregory Wilson, S. *In its* NASA/MSFC FY-85 Atmospheric Processes Research Review Oct. 1985 2 p (For primary document see N87-13043 04-47)

Avail: NTIS HC A07/MF A01 CSCL 04B

A two-dimensional mesoscale model was used to initialize a two-dimensional cloud model with both mesoscale thermodynamic and dynamic information utilized in the initialization. The Mesoscale-cloud mdoel linkage was used to examine differential convective response due to mesoscale variations for the April 24, 1982 Atmospheric Variability Experiment-Vertical Atmospheric Sounder (AVE-VAS), Case 4. On this day both data analyses and mesoscale model simulations indicated strong variations in thermodynamic and dynamic structure across the panhandle of Texas where a moderately strong convective line formed. Using the cloud model, the current research has shown a preferred area for strong convection to occur due to concomitant mesoscale convergence and mesoscale destabilization of the atmosphere. Author

N87-13082*# Saint Louis Univ., Mo. Dept. of Earth and Atmospheric Sciences.

A SUMMARY OF RESEARCH ON MESOSCALE ENERGETICS OF SEVERE STORM ENVIRONMENTS

Henry E. Fuelberg *In* NASA. Marshall Space Flight Center NASA/MSFC FY-85 Atmospheric Processes Research Review Oct. 1985 3 p (For primary document see N87-13043 04-47)

Avail: NTIS HC A07/MF A01 CSCL 04B

The goals of this research were to better understand interactions between areas of intense convection and their surrounding mesoscale environments by using diagnostic budgets of kinetic (KE) and available potential energy (APE). Three cases of intense convection were examined in detail. 1) Atmospheric Variability Experiments (AVE) carried out on 24 to 25 April 1975 were studied. Synoptic scale data at 3 to 6 hour intervals, contained two mesoscale convective complexes (MCCs). Analyses included total KE budgets and budgets of divergent and rotational components of KE. 2) AVE-Severe Environmental Storms and Mesoscale Experiments (SESAME)-4 carried out on 10 to 11 April 1979 were studied. Synotpic and meso alpha-scale data (250 km spacing, 3 hour intervals), contained the Red River Valley tornado outbreak. Analyses included total KE budgets (separate synoptic and mesoscale version), budgets for the divergent and rotational components, and the generation of APE by diabatic processes. 3) AVE-SESAME 5 studies were carried out on 20 to 31 May 1979. Synoptic and meso beta-scale data (75 km spacing, 1 1/2 to 3 hour intervals), contained a small MCC. Analyses include separate KE budgets for the synotic and meso beta-scales and a water vapor budget. Major findings of these investigations are: (1) The synoptic scale storm environment contains energy conversions and transports that are comparable to those of mature midlatitude cyclones. (2) Energetic in the mesoscale storm environment are often an order of magnitude larger than those in an undisturbed region. (3) Mesoscale wind maxima form in the upper troposphere on the poleward sides of convective areas, whereas speeds decrease south of storm regions. Author

N87-13083*# Wisconsin Univ., Madison. Space Science and Engineering Center.

TIME COMPOSITE SOUNDING

Christopher Hayden *In* NASA. Marshall Space Flight Center NASA/MSFC FY-85 Atmospheric Processes Research Review Oct. 1985 1 p (For primary document see N87-13043 04-47)

Avail: NTIS HC A07/MF A01 CSCL 04B

In the time composite sounding mode, the Vertical Atmospheric Sounder (VAS) data is collected in a series of images of one spin each rather than in the dwell sound mode where single lines are repeatedly scanned. A drawback of the time composite method is temporal smearing of the data, but to compensate this there is also the chance that shifting cloud patterns will permit better spatial coverage. Time composite sounding was performed for a single case study, June 14, 1984. Four, ten minute single spin swaths were processed. The principal conclusion was that the time composite results were at least equivalent to the conventional dwell sounding results, despite the fact that compositing was done in a less than optimum way because of software limitations. Author

N87-13084*# Colorado State Univ., Fort Collins.

INVESTIGATIONS OF SEVERE/TORNADIC THUNDERSTORM DEVELOPMENT AND EVOLUTION BASED ON SATELLITE AND AVE/SESAME/VAS DATA

Thomas H. VonderHaar and James F. W. Purdom *In* NASA. Marshall Space Flight Center NASA/MSFC FY-85 Atmospheric Processes Research Review Oct. 1985 4 p (For primary document see N87-13043 04-47)

Avail: NTIS HC A07/MF A01 CSCL 04B

Development of cloud relative tracking for severe thunderstorm identification and the beginning of the development of mesoscale airmass characteristics based on vertical atmospheric sounding data were accomplished. Author

N87-13085*# Wisconsin Univ., Madison. Dept. of Meteorology.

DETECTION OF ROTATING THUNDERSTORMS USING SATELLITE IMAGERY

C. E. Anderson and Robert Schlesinger *In* NASA. Marshall Space Flight Center NASA/MSFC FY-85 Atmospheric Processes Research Review Oct. 1985 2 p (For primary document see N87-13043 04-47)

Avail: NTIS HC A07/MF A01 CSCL 04B

In the case of the Carolina tornadoes, researchers prepared visible and IR GOES imagery covering the period 2000 Z when the storm entered South Carolina from Georgia until it exited North Carolina at 0200 Z into Virginia. The GOES IR imagery clearly demonstrated that this storm was imbedded in a continuously propagating mesolow with a well defined cold dome. The ground damage track paralleled exactly with the cold dome throughout the storm's life across the Carolinas. There were no advanced very high resolution radiometer (AVHRR) data during the period to allow researchers to inspect the cloud top for warm temperature anomalies. The Carolina storm did exhibit rightward deviating outflow which was oriented about 60 degrees to the 300 mb streamlines. The tornadoes of April 27, 1984 were part of a tornado producing cold front which stretched from Oklahoma to Minnesota. As the front moved eastward it touched off numerous tornadoes in eastern Wisconsin. GOES imagery for this data was prepared and it was strikingly clear that all along the North-South oriented squall line, the individual tunderstorms had cirrus plumes which had remarkable right deviation to the upper air flow. Unlike the Carolina long track supercell cell-mesolow system, these storms

were isolated individual thunderstorms which touched off at least 16 tornadoes in eastern Wisconsin stretching from the Milwaukee area on the south to Vilas County in the north. The monster tornado of June 8, 1984 which leveled 90 percent of the village of Barneveld, Wisconsin and killed 9 persons is also discussed.
Author

N87-13086*# Saint Louis Univ., Mo. Dept. of Earth and Atmospheric Sciences.
STATISTICAL ANALYSIS AND USE OF VAS RADIANCE DATA
Henry E. Fuelberg *In* NASA. Marshall Space Flight Center NASA/MSFC FY-85 Atmospheric Processes Research Review Oct. 1985 3 p (For primary document see N87-13043 04-47)
Avail: NTIS HC A07/MF A01 CSCL 04B

Researchers goals are to describe the information content of Vertical Atmospheric Sounder (VAS) radiance data, especially the 6.7 micrometers water vapor channel, to better interpret the atmosphere's water vapor structure from 6.7 micrometers imagery, and to investigate new analysis and forecasting techniques utilizing retrieved VAS soundings. Researchers made major progress toward these goals during FY-85. They are investigating 6.7 micrometer imagery on 6 to 7 March 1982, a day when special mesoscale ground truth data were collected during the 1982 atmospheric variability experiment/vertical amospheric sounder (AVE/VAS) field experiment. A dark (dry) image streak having mesoscale details was located over the special data region, and it provides the major focus of the case study. Mesoscale radiosonde-derived humidity data are found to verify fine scale features of the image that are not evident from the standard National Weather Service network. Thus, VAS imagery is a reliable detector of mesoscale moisture structure during this case. To investigate causes for the image streak, researchers are calculating water vapor budgets. Subsidence is found to be a factor in the current case as well; however, patterns of descent are not related to the jet streak according to traditional conceptual models. Thus, it appears that more research into jet stream dynamics is needed in order to better interpret 6.7 micrometer imagery.
Author

N87-13087*# National Aeronautics and Space Administration. Marshall Space Flight Center, Huntsville, Ala.
IMPROVED SATELLITE RETRIEVALS AND MESOSCALE MOISTURE VARIABILITY
Gary J. Jedlovec *In its* NASA/MSFC FY-85 Atmospheric Processes Research Review Oct. 1985 3 p (For primary document see N87-13043 04-47)
Avail: NTIS HC A07/MF A01 CSCL 04B

The investigations over the past year have led to the finalization of results from the study of mesoscale atmospheric parameters derived from the visible infrared spin scan radiometer (VISSR) atmospheric sounder (VAS). Soundings from several retrieval techniques for the 6 to 7 March 1982 special observation period were evaluated for mesoscale accuracy. Specific results and comparisons between data from a regression and two physical retrieval schemes are forthcoming in the Journal of Atmospheric and Oceanic Technology (JTech) this year. A generalization of these results is outlined. Large temperature and moisture biases existed in the VAS derived profiles, particularly in layers near inversions. Standard errors ranged from 1 to 3 C and 3 to 6 C for temperature and dewpoint, respectively. Parameters derived from VAS soundings (geopotential height, thickness, and precipitable water) often reflected the temperature and moisture profile biases. VAS derived mesoscale gradients were often weaker than those from corresponding rawinsonde data. Little improvement was made in defining the vertical structure of the atmosphere over the first guess information. VAS soundings were able to improve in the horizontal structure due to the high spatial resolution of the radiance data.
Author

N87-13088*# National Aeronautics and Space Administration. Marshall Space Flight Center, Huntsville, Ala.
STUDIES OF HUMID CONTINENTAL HAZE DURING SPACE
David A. Bowdle and William A. Greene *In its* NASA/MSFC FY-85 Atmospheric Processes Research Review Oct. 1985 2 p (For primary document see N87-13043 04-47)
Avail: NTIS HC A07/MF A01 CSCL 04B

A concept for a solar radiometer network to provide supporting data during the Satellite Preciptiation and Cloud Experiment (SPACE) was developed. Each of the 9 prime and 10 supplementary SPACE ground sites will be equipped with an upward pointing global solar pyranometer. About half of the sites will also be equipped with upward pointing diffuse (shade ring) solar pyranometers, and a downward pointing global albedo pyranometer. These radiometers will be used to monitor the spatial and temporal variability of solar insolation and haze optical depth. The insolation data will ultimately be input to numerical models of the pre-storm and near-storm boundary layer. The optical depth data will be compared with simultaneous measurements from airborne and satellite-based passive visible radiometers and airborne lidars.
Author

N87-13089*# Alabama Univ., Huntsville. Environmental and Energy Center.
PRELIMINARY PLANNING FOR THE SATELLITE PRECIPITATION AND CLOUD EXPERIMENT (SPACE) FIELD PROGRAM
Steven F. Williams and Richard T. McNider *In* NASA. Marshall Space Flight Center NASA/MSFC FY-85 Atmospheric Processes Research Review Oct. 1985 2 p (For primary document see N87-13043 04-47)
Avail: NTIS HC A07/MF A01 CSCL 04B

Preliminary planning has been performed to support NASA/Marshall Space Flight Center (MSFC) in the coordination of the field experiment to be conducted in Central Tennessee, Northern Alabama, and Mississippi during the Spring/Summer of 1986. The goal of Satellite Precipitation and Cloud Experiments (SPACE) is to investigate mesoscale cloud/precipitation systems and development of associated satellite remote sensing technology. The field program will incorporate remote sensing observations from aircraft, satellite imagery, radar observations, ground based lightning measurements, rawinsonde observations, and various surface meteorological observations. The coordination of existing and special observation networks will provide a data base for analysis of precipitation events and provide ground truth comparisons for remote sensing capabilities. Existing surface-based observational networks include National Weather Service Meso/Alpha Scale Rawinsonde, radar, and surface measurements; the Tennessee Valley Authority automated and manual precpitation recording stations; and NASA/MSFC lightning measurement stations. Special observational features to be implemented include a meso/beta scale rawinsonde network, a special surface observational network within the rawinsonde network, and the installation of a RADAP II/ICRAD data processing unit on the National Weather Service radar at Nashville, TN. Initial coordination of these observational requirements to accomplish the goals of SPACE have been performed.
Author

N87-13090*# New Technology, Inc., Huntsville, Ala.
ATMOSPHERIC MODELING AND SENSOR SIMULATION (AMASS) STUDY
Karen G. Parker *In* NASA. Marshall Space Flight Center NASA/MSFC FY-85 Atmospheric Processes Research Review Oct. 1985 3 p (For primary document see N87-13043 04-47)
Avail: NTIS HC A07/MF A01 CSCL 04B

A 4800 band synchronous communications link was established between the Perkin-Elmer (P-E) 3250 Atmospheric Modeling and Sensor Simulation (AMASS) system and the Cyber 205 located at the Goddard Space Flight Center. An extension study of off-the-shelf array processors offering standard interface to the Perkin-Elmer was conducted to determine which would meet computational requirements of the division. A Floating Point Systems AP-120B was borrowed from another Marshall Space Flight Center laboratory for evaluation. It was determined that available array processors did not offer significantly more capabilities than the borrowed unit, although at least three other vendors indicated that standard Perkin-Elmer interfaces would be marketed in the future. Therefore, the recommendation was made to continue

to utilize the 120B ad to keep monitoring the AP market. Hardware necessary to support requirements of the ASD as well as to enhance system performance was specified and procured. Filters were implemented on the Harris/McIDAS system including two-dimensional lowpass, gradient, Laplacian, and bicubic interpolation routines.

N87-13091*# Wisconsin Univ., Madison. Space Science and Engineering Center.
THE METEOROLOGICAL INTERACTIVE DATA DISPLAY SYSTEM
Verner E. Suomi and J. T. Young *In* NASA. Marshall Space Flight Center NASA/MSFC FY-85 Atmospheric Processes Research Review Oct. 1985 1 p (For primary document see N87-13043 04-47)
Avail: NTIS HC A07/MF A01 CSCL 04B

During FY-85 the data gathering process was completed. This gave researchers a reasonably complete picture of the Shuttle's operational weather support units and requirements. They expanded on the site visits of FY-84 with telephone follow-up. They finalized recommendations and wrote the final report. The final report was accepted by NASA and has been published as NASA Contractor Report CR-171418. Author

N87-13092*# Wisconsin Univ., Madison. Space Science and Engineering Center.
A DESIGN STUDY FOR A THREE-DIMENSIONAL DISPLAY COMPUTER TERMINAL FOR METEOROLOGICAL INFORMATION
Verner E. Suomi, Robert J. Krauss, Bill Hibbard, and J. T. Young *In* NASA. Marshall Space Flight Center NASA/MSFC FY-85 Atmospheric Processes Research Review Oct. 1985 1 p (For primary document see N87-13043 04-47)
Avail: NTIS HC A07/MF A01 CSCL 04B

The software developed on this project in FY-84 was put into final form and documented for McIDAS user access. The various users have been asked to utilize the techniques and to provide feedback to the developers. Researchers have received limited feedback to date, but nearly all has been helpful and generally favorable. The stereo display has been used by most of the operational users of McIDAS or its progenies. Specifically, the National Hurricane Center, the National Severe Storm Forecast Center, the National Meteorological Center, and the Cape Canaveral Forecast Facility have all made use of the 4-D display techniques to help evaluate meteorological situations on various occasions. Author

N87-13093*# National Aeronautics and Space Administration. Marshall Space Flight Center, Huntsville, Ala.
INTERACTIVE INFORMATION PROCESSING FOR NASA'S MESOSCALE ANALYSIS AND SPACE SENSOR PROGRAM
Karen G. Parker (New Technology, Inc., Huntsville, Ala.), Laura MacLean, Norman Reavis, Gregory Wilson, John S. Hickey (Atsuko Computing International, Huntsville, Ala.), Michael Dickerson, Shogo Karitani, and David Keller (Universities Space Research Association, Huntsville, Ala.) *In its* NASA/MSFC FY-85 Atmospheric Processes Research Review Oct. 1985 14 p (For primary document see N87-13043 04-47)
Avail: NTIS HC A07/MF A01 CSCL 04B

The Atmospheric Sciences Division (ASD) of the Systems Dynamics Laboratory at NASA's Marshall Space Flight Center (MSFC) is currently involved in interactive information processing for the Mesoscale Analysis and Space Sensor (MASS) program. Specifically, the ASD is engaged in the development and implementation of new space-borne remote sensing technology to observe and measure mesoscale atmospheric processes. These space measurements and conventional observational data are being processed together to gain an improved understanding of the mesoscale structure and the dynamical evolution of the atmosphere relative to cloud development and precipitation processes. To satisfy its vast data processing requirements, the ASD has developed a Researcher Computer System consiting of three primary computer systems which provides over 20 scientists with a wide range of capabilities for processing and displaying a large volumes of remote sensing data. Each of the computers performs a specific function according to its unique capabilities. Author

N87-13094*# National Aeronautics and Space Administration. Marshall Space Flight Center, Huntsville, Ala.
DOPPLER WIND PROFILE EXPERIMENT
James E. Arnold *In its* NASA/MSFC FY-85 Atmospheric Processes Research Review Oct. 1985 1 p (For primary document see N87-13043 04-47)
Avail: NTIS HC A07/MF A01 CSCL 04B

The data collection phase of a Doppler wind measurement experiment supported by high-resolution Jimsphere/FPS-16 wind data and Windsonde data was carried out at the Kennedy Space Center in February, March and early April of 1985. The Doppler wind measurements were made using a hybrid doppler profiler put in place by the Johnson Space Center and a SOUSY profiler operated by Radian Corporation. Both systems operated at 50 Mhz. Although the doppler profiler systems were located 10 km apart to enable concurrent operation of the systems for data comparison, little concurrent data were obtained due to set-up delays with the SOUSY system, and system problems with the WPL system during the last month of the test. During the test period, special serial Jimsphere soundings were taken at two-hour intervals on six days in March and April in addition to balloon soundings taken in support of the Shuttle launch operations. In addition, there is temperature, moisture and wind information available from the daily morning Radiosonde sounding taken at the Kennedy site. The balloon release point was at the same location as the SOUSY profiler. Vertical resolution of the SOUSY profiler was 150 M to approximately 20 km. The vertical resolution of the WPL profiler was 290 M to 10 km and 870 M to 17 km. Winds determined form the Jimsphere balloon have a vertical resolution of 30 M. Author

N87-13095*# National Aeronautics and Space Administration. Marshall Space Flight Center, Huntsville, Ala.
MULTISPECTRAL ATMOSPHERIC MAPPING SENSOR OF MESOSCALE WATER VAPOR FEATURES
Paul Menzel (Wisconsin Univ., Madison.), Gary Jedlovec, Greg Wilson, Robert Atkinson, and William Smith, w4560409 *In its* NASA/MSFC FY-85 Atmospheric Processes Research Review Oct. 1985 4 p (For primary document see N87-13043 04-47)
Avail: NTIS HC A07/MF A01 CSCL 04B

The Multispectral atmospheric mapping sensor was checked out for specified spectral response and detector noise performance in the eight visible and three infrared (6.7, 11.2, 12.7 micron) spectral bands. A calibration algorithm was implemented for the infrared detectors. Engineering checkout flights on board the ER-2 produced imagery at 50 m resolution in which water vapor features in the 6.7 micron spectral band are most striking. These images were analyzed on the Man computer Interactive Data Access System (McIDAS). Ground truth and ancillary data was accessed to verify the calibration. Author

N87-13096*# National Aeronautics and Space Administration. Marshall Space Flight Center, Huntsville, Ala.
FIRST MEETING OF THE WORKING GROUP ON THE SHUTTLE MICROWAVE PRECIPITATION RADIOMETER (SMPR)
In its NASA/MSFC FY-85 Atmospheric Processes Research Review Oct. 1985 2 p (For primary document see N87-13043 04-47)
Avail: NTIS HC A07/MF A01 CSCL 04B

The working group agreed that the first (primary) objective should be the determination of methods for the accurate measurement of total rain water and total cloud water with passive microwave methods. There was no argument on the points concerning nonlinear relationships between T sub B and rain rate (R) over the range of important rain rates (half of oceanic rainfall occurs at rates greater than 15 mm h-1), such that variations in rain rate within a footprint lead to an incorrect measurement of the average rate for that footprint, and one cannot determine the characteristics of the sensed rain area. This is especially true

near 18 GHz, where the dynamic range above 15 mm h-1 is very small because this frequency does not clearly fall in either a scattering regime or emissive regime at these wavelengths. It is also not clear whether very low frequency (emissive) techniques will be the best at measuring rain processes, or high frequency (scattering) techniques, where precipitation-size ice plays a major role in the signal attenuation. It is still not known what signal of rain is at certain rates on an observational basis because of the many different conditions that can exist within a single satellite observed footprint. Author

N87-13097# Colorado State Univ., Fort Collins. Dept. of Atmospheric Science.
SUMMARY OF 1986 ATLANTIC TROPICAL CYCLONE ACTIVITY AND VERIFICATION OF AUTHOR'S SEASONAL FORECAST
William M. Gray 24 Nov. 1986 22 p Sponsored by NSF
Avail: NTIS HC A02/MF A01

Tropical cyclone activity which occurred in the Atlantic in 1986 and which verified the seasonal forecast of this activity that was issued in late May and updated in late July was summarized. This forecast was based on previous research which relates seasonal Atlantic hurricane activity to: the El Nino (EN); the Quasi-Biennial Oscillation (QBO) of equatorial 30 mb strateospheric wind; the Carribbean Basin-Gulf of Mexico Sea-Level Pressure Anomaly (SLPA) in spring and eary summer; and lower latitude Caribbean Basin 200 mb zonal wind anomaly in June and July. Author

N87-13098*# National Aeronautics and Space Administration. Goddard Space Flight Center, Greenbelt, Md.
RADIATION FLUX TABLES FOR ICRCCM USING THE GLA GCM RADIATION CODES
Harshvardhan Jun. 1986 97 p
(NASA-TM-89270; NAS 1.15:89270) Avail: NTIS HC A05/MF A01 CSCL 04B

Tabulated values of longwave and shortwave radiation fluxes and also cooling and heating rates in the atmosphere for standard atmospheric profiles are presented. The radiation codes used in the Goddard general circulation model were employed for the computations. These results were obtained for an international intercomparison projected called Intercomparison of Radiation Codes in Climate Models (ICRCCM). Author

N87-13099# Federal Aviation Administration, Atlantic City, N.J. Technical Center.
THE SITING, INSTALLATION AND OPERATIONAL SUITABILITY OF THE AUTOMATED WEATHER OBSERVING SYSTEM (AWOS) AT HELIPORTS Final Report, Feb. 1985- Apr. 1986
Rene A. Matos, John R. Sackett, Philip M. Shuster, and Rosanne M. Weiss Aug. 1986 70 p
(DOT/FAA/PM-86/30; DOT/FAA/CT-85/9) Avail: NTIS HC A04/MF A01

The Federal Aviation Administration (FAA) Technical Center was tasked to site, install, and evaluate an Automated Weather Observing System (AWOS) at a heliport. The conclusions of the evaluation of the AWOS at the Technical Center's Interim Concept Development Heliport are given. By using the AWOS equipment installed at the Interim Concept Development Heliport, in conjunction with literature research, the following test objectives were addressed: (1) locations in the vicinity of the heliport in which helicopter operations could influence the environment causing transient AWOS sensor performance were identified; (2) areas for sensor location near the heliport that provided the most beneficial information to the pilot were identified; (3) optimal sensor location in relationship to predominant approach and departure paths was determined; (4) siting criteria and recommendations for AWOS equipment installation at heliports were developed; (5) the operational suitability of the AWOS equipment for heliport installations was determined; and (6) additional maintenance requirements for the AWOS as the result of heliport installation were identified.

N87-13100# Air Force Environmental Technical Applications Center, Scott AFB, Ill.
STATION CLIMATIC SUMMARIES, EUROPE Data Summary Report
Apr. 1986 436 p Supersedes USAFETAC/DS-84/019
(AD-A167888; USAFETAC/DS-86/033; USAFETAC/DS-84/019) Avail: NTIS HC A19/MF A01 CSCL 04/2

This report contains a collection of summarized monthly and annual climatic data for specific locations in Europe. Summarized climatological elements are: percent frequency of occurrence of ceiling and visibility; means, extremes and number of days with specified values of temperature, precipitation, and snowfall; means of relative humidity, vapor pressure, dew point, pressure altitude, and cloud cover; prevailing wind direction, with mean and extreme speeds; and number of days with thunderstorms and fog. GRA

N87-13101# Air Force Geophysics Lab., Hanscom AFB, Mass.
SENSITIVITY TESTS OF A SURFACE-LAYER WINDFLOW MODEL TO EFFECTS OF STABILITY AND VEGETATION
John M. Lanicci 25 Oct. 1985 54 p
(AD-A169136; AFGL-TR-85-0265; AFGL-ERP-934) Avail: NTIS HC A04/MF A01 CSCL 04/2

This study examines the sensitivity of surface-layer windflow over gently rolling terrain to different stability conditions, both with and without the effects of vegetation used to modify terrain heights and determine surface roughness. The numerical model used produces simulations of surface-layer windflow by using Gauss's Principle of Least Constraints to allow an initially uniform windfield to adjust to topography and buoyancy forces while conserving mass. The model experiments used simulated meteorological data (at only one observation point) and detailed terrain and vegetation data (on a 51-by-51 grid with 100 m spacing) for an area covering 5 by 5 km over the Fort Polk Military Reservation in Louisiana. Results show that the model simulates topographically induced flows such as cold air drainage and upslope flow, despite the simple physics employed. We also show that the presence of tall vegetation over the area (mainly coniferous and deciduous trees) alters the flow patterns under various stability conditions. These effects are shown to be caused primarily by changes in the area of chemical transport and diffusion, because they mean that even gently rolling terrain influences the surface windflow, and that tall vegetation has a considerable influence as well. GRA

N87-13102# South Dakota School of Mines and Technology, Rapid City. Inst. of Atmospheric Sciences.
A DETAILED ANALYSIS OF THE INFLUENCE OF EDDY EXCHANGE PROCESSES UPON THE DEVELOPMENT OF RADIATION FOG Final Report, 19 Sep. 1983 - 18 Mar. 1986
Ronald M. Welch Apr. 1986 41 p
(Contract DAAG29-83-K-0165)
(AD-A169233; SDSMT/IAS/R-86/03; ARO-20576.3-GS) Avail: NTIS HC A03/MF A01 CSCL 04/1

After decades of theoretical development, fog models have evolved to the point of qualitative agreement with observations. Current models are capable of simulating observed quasi-periodic oscillations in fog variables as well as the various stages of fog growth. It is now anticipated that continued efforts towards greater model sophistication will lead to at least limited quantitative agreement with observations and improved predictive capability. Application of very high resolution Landsat digital data to fog episodes has revealed the stratocumulus nature of fog. That other satellite imagery has shown little hint of this cellular structure is due to the fact that the fog elements are generally smaller than the spatial resolution available on these satellite platforms. The ratio of wavelength between cells and the height of the boundary layer is in agreement with values obtained for Benard cells and longitudinal rolls in cloud systems. The processes occurring in fogs are similar, but on a smaller scale, to those responsible for these boundary layer cloud systems. Therefore, further studies of fog processes are expected to provide quantitative information concerning the processes responsible for Benard cells, longitudinal rolls and cloud top entrainment instability. GRA

N87-13103# North Carolina Univ., Raleigh.
MICROMETEOROLOGICAL TRANSITIONS IN THE MORNING

BOUNDARY LAYER OVER ROLLING TERRAIN Final Report, 1982 - 1985
Allen J. Riordan and Jerry M. Davis 20 Mar. 1986 34 p
(Contract DAAG29-82-K-0183)
(AD-A169237; ARO-19649.3-GS) Avail: NTIS HC A03/MF A01 CSCL 04/2

Six years of temperature and wind data from two 60m micrometeorological towers in the piedmont of the Carolinas were analyzed. One tower was near a large lake, the other in mostly-forested terrain. Statistics of the basic tower measurements were generated and their time evolution was described for the morning transition period near sunrise. A stepwise regression model was developed and tested to predict the daily transition time at each site based on tower variables. To determine large-scale influences on the local inversion and its morning transition, the local tower data from each site were then related to the synoptic-scale pressure field over the eastern one-third of the United States. To accomplish the comparison, an objective typing scheme was developed in which the gridded daily sea-level pressure field was expressed in terms of eigenvector types. Results document the average morning transition sequence in terms of systematic changes in radiation, wind and temperatures. The regression models are quite similar at both sites and predict transition time with a least-squared regression of 0.76 for clear mornings at the forested site. The eigenvector analysis successfully categorized each day's pressure field into ten types. These showed very close association with the local inversion intensity at sunrise, but had very little relation to morning transition time at each site. Author (GRA)

N87-13104# Atmospheric and Environmental Research, Inc., Cambridge, Mass.
IMPROVING NUMERICAL WEATHER PREDICTION BY MAXIMIZING THE USE OF ASSIMILATED SATELLITE DATA Final Report, 1 Jan. 1983 - 31 Dec. 1985
L. D. Kaplan, J. F. Louis, R. N. Hoffman, R. G. Isaacs, and W. J. Gutowski 20 Dec. 1985 169 p
(Contract F19628-83-C-0027)
(AD-A169295; P79-FINAL; AFGL-TR-85-0298) Avail: NTIS HC A08/MF A01 CSCL 04/2

An extensive literature review showed a disparity between the large amount of satellite data currently or potentially available for meteorological parameters and the relatively small amount that is actually utilized. The review also documented the various existing data retrieval techniques. Algorithms were developed and modified to retrieve temperature and moisture profiles from satellite infrared and millimeter/microwave radiances. Tools were developed, based on existing Air Force computer codes, to include and test the effect of satellite data in numerical weather prediction. The use of the logarithm of specific humidity as a forecast variable was investigated. The FGGE level II and III data sets existing at AFGL were completed to include all of the special observing periods and to form the basis of data assimilation tests. Finally, an attempt was made to optimize a cloudiness parameterization scheme on the basis of satellite retrievals. A number of recommendations are made for further work in satellite data retrieval, data assimilation and numerical weather prediction. They include the continuation of some of the items presented here, as well as suggestions for new avenues of research. GRA

N87-13105# Air Force Environmental Technical Applications Center, Scott AFB, Ill.
REVISED UNIFORM SUMMARY OF SURFACE WEATHER OBSERVATIONS (RUSSWO). PARTS A-F ELLINGTON ANGB, TEXAS Data Summary Report, Jul. 1941 - Feb. 1986
21 May 1986 298 p
(AD-A169389; USAFETAC/DS-86/024) Avail: NTIS HC A13/MF A01 CSCL 04/2

A six-part statistical data summary of surface weather observations for: Ellington ANGB FL. Summary consists of: PART A, Weather Conditions and Atmospheric Phenomena; PART B, Precipitation; PART C, Surface Winds; PART D, Ceiling and Visibility; PART E, Psychrometric Summaries; PART F, Pressure Summaries. See USAFETAC/TN-83/001 (AD-A132186), An Aid for Using the Revised Uniform Summary of Surface Weather Observations (RUSSWOs) for complete descriptions of contents and instructions for use. Author (GRA)

N87-13106# Air Force Environmental Technical Applications Center, Scott AFB, Ill.
REVISED UNIFORM SUMMARY OF SURFACE WEATHER OBSERVATIONS (RUSSWO). PARTS A-F, FORT RICHARDSON, ALASKA Data Summary Report, Feb. 1977 - Feb. 1986
16 Jun. 1986 292 p
(AD-A169390; USAFETAC/DS-86/025) Avail: NTIS HC A13/MF A01 CSCL 04/2

A six-part statistical data summary of surface weather observations for: FT Richardson AK. Summary consists of: PART A, Weather Conditions and Atmospheric Phenomena; PART B, Precipitation; PART C, Surface Winds; PART D, Ceiling and Visibility; PART E, Psychrometric Summaries; PART F, Pressure Summaries. See USAFETAC/TN-83/001 (AD-A123186), An Aid for Using the Revised Uniform Summary of Surface Weather Observations (RUSSWOs) for complete descriptions of contents and instructions for use. Author (GRA)

N87-13107# Air Force Environmental Technical Applications Center, Scott AFB, Ill.
WHEELER AFB, HAWAII LIMITED SURFACE OBSERVATIONS CLIMATIC SUMMARY (LISOCS), PARTS 1-5 Data Summary Report, Jun. 1974 - May 1984
17 Jun. 1986 231 p
(AD-A169391; USAFETAC/DS-86/026) Avail: NTIS HC A11/MF A01 CSCL 04/2

A statistical data summary is given of surface weather observation climatology for Wheeler AFB, HI. This summary is similar to the Revised Uniform Summary of Surface Weather Observations (RUSSWO), but is based on data collected from limited-duty weather observing stations; i.e., those that take weather observations less than 24 hours a day, 7 days a week. The summary is in five parts: Part 1, Weather Conditions and Atmospheric Phenomena; Part 2, Surface winds; Part 3, Ceiling and Visibility; Part 4, Psychrometric summaries; and Part 5 Pressure Summaries. Note that Precipitation, is omitted. See USAFETAC/TN-83/001 9AD-A132186), An aid for Using the Revised Uniform Summary of Surface Weather Observations (RUSSWOs), for complete descriptions of contents and instructions for use. Author (GRA)

N87-13108# Research and Data Systems, Inc., Lanham, Md.
CONVERSION OF THE NOLAPS (NAVY OPERATIONAL LOCAL ATMOSPHERIC PREDICTION SYSTEM) MODEL TO THE HP9845 Final Report, 1-11 Apr. 1985
Phillip Ardanuy Feb. 1986 40 p
(Contract N00228-84-D-3155; F59-551)
(AD-A169538; NEPRF-CR-86-03) Avail: NTIS HC A03/MF A01 CSCL 04/2

As a first effort in developing an atmospheric predictive capability for the Tactical Environment Support System (TESS), the model used for the Navy Operational Local Atmospheric Prediction System (NOLAPS) is converted to the HP9845B, Option 275. Three primary steps are involved in this conversion. First, the model is converted from FORTRAN to BASIC code, made to duplicate exisiting model results, and benchmarked for time purpose. The converted model in renamed NOWLAPS (Navy Over-Water Local Atmospheric Prediction System). Second, a user-interactive capability is developed for this desk-top system. And third, an interactive graphics package is developed to display the model results. GRA

N87-13109# Ophir Corp., Lakewood, Colo.
A SENSITIVITY STUDY OF A ONE-DIMENSIONAL TIME-DEPENDENT WARM CUMULUS CLOUD MODEL Scientific Report, No. 2, 1 Jan. - 31 Aug. 1985
Raina J. Eckhardt Sep. 1985 16 p
(Contract F19628-83-C-0130)
(AD-A170141; AFGL-TR-85-0331) Avail: NTIS HC A02/MF A01 CSCL 04/1

A one-dimensional time-dependent computer cloud model was initiated with a composite of two soundings from day 226 of the GATE project. The soundings were recorded on August 14, 1974 at 1200 Z, off the west coast of Africa from two ships, the Dallas (USA) and Vise (USSR). The model simulates the life cycle of a cylindrical shaped warm cumulus cloud which is in hydrostatic equilibrium. Although it is formulated in one-dimension, it includes effects from the surrounding environment by turbulent and dynamic entrainment. A series of model runs were executed in which several parameters were varied in order to observe their effects on the evolution of the model cloud. These parameters were: cloud radius, heat pulse duration, cloud condensation nuclei, and model time step duration. GRA

N87-13110# Air Force Inst. of Tech., Wright-Patterson AFB, Ohio.
A REVIEW OF MICROBURSTS AND THEIR ANALYSIS AND DETECTION WITH DOPPLER RADAR M.S. Thesis
Gerald L. Freeman 1986 75 p
(AD-A170458; AFIT/CI/NR-86-98T) Avail: NTIS HC A04/MF A01 CSCL 04/2

Microbursts are small downbursts, less than 4km in outflow size, with peak winds lasting only 2 to 5 minutes. They can be classified as either midair or surface microbursts and also either wet or dry microbursts. All microbursts are characterized by a vertical downrush of air with a divergent outflow at its base. The parent clouds associated with microbursts are: Cumulonimbus; Towering Cumulus; and Anvil Cirrus. Most origin theories credit thermodynamic factors with microburst creation. Wolfson (1983) contends that microbursts result from dynamically induced vertical pressure gradients that are intrinsic characteristics of strong mesocyclone circulation. Doppler radar is the primary tool for detecting and observing microbursts. Wind field mapping is accomplished by either a single, dual or triple radar configuration. Single radar analysis methods require the most external assumptions but are the least expensive. Multiple radar techniques provide more accuracy but are more costly. Wilson and Roberts (1983) propose a number of alternatives for realtime operational detection of microbursts in an airport environment. Of these alternatives they chose a single radar, on airport configuration as the optimum choice when considering economic feasibility as well as technical performance. Author (GRA)

N87-13111# Air Force Inst. of Tech., Wright-Patterson AFB, Ohio.
EXTRATERRESTRIAL FORCING, ATMOSPHERIC ELECTRICITY AND THE OCCURRENCE OF THUNDERSTORMS M.S. Thesis
Angelo M. Nuzzo Aug. 1986 91 p
(AD-A170463; AFIT/CI/NR-86-99T) Avail: NTIS HC A05/MF A01 CSCL 04/2

It is generally accepted by many scientists that a cause-effect relationship exists between solar activity and weather. Statistical evidence is provided to support this concept; atmospheric electricity and stratospheric-tropospheric exchange are highlighted. Although many accept the idea, there are those who are skeptical about such a relationship because no definite physical mechanism exists between the two. This is a topic of much discussion and debate. It is believed that the shielding of the Earth from galactic cosmic rays during increased periods of solar activity plays a key role in the process. Several of the mechanisms discussed rely on this concept. The emphasis will be on the attention in this area. On the topic of the atmospheric electrical mechanism, two hypotheses are presented: those of Markson and Hale. Finally, the stratospheric-tropospheric exchange mechanism is introduced. This mechanism is similar to the atmospheric electrical mechanism in that it also depends on the possible modulation of the thunderstorm generator by solar activity. Tropopause folding events are presented as a vital link in the stratospheric-tropospheric exchange mechanism. Author (GRA)

N87-13112# Naval Air Systems Command, Washington, D. C.
US NAVY CLIMATIC STUDY OF THE CARIBBEAN SEA AND GULF OF MEXICO. VOLUME 2: EAST CARIBBEAN SEA
Mar. 1986 221 p
(AD-A171487; NAVAIR-50-1C-544-Vol-2) Avail: NTIS HC A10/MF A01 CSCL 04/2

Charts for: clouds; precipitation; visibility tables; ceiling-visibility (mid range); ceiling-visibility (low range); wind-visibility-cloudiness; scalar mean wind speed; wind speed less than 11 and greater than or = to 34 knots; wind speed 11-21 and 22-33 knots; surface wind roses; air and sea temperature; wave height isopleths; wave height tables; surface currents (seasonal). GRA

N87-13113# Sandia National Labs., Albuquerque, N. Mex.
METEOROLOGICAL TOWER DATA, YUCCA RIDGE (YR) SITE, JANUARY-JUNE 1983. NEVADA NUCLEAR WASTE STORAGE INVESTIGATIONS PROJECT
H. W. Church, D. L. Freeman, K. Boro, and R. T. Egami Jun. 1986 50 p Prepared in cooperation with Nevada Univ., Reno (Contract DE-AC04-76DP-00789)
(DE86-012732; SAND-85-1053) Avail: NTIS HC A03/MF A01

The purpose of the NNWSI meteorological data collection program is to support environmental evaluations of site suitability for a nuclear waste repository. This is the first in a series of data summaries for the Yucca Ridge Site in southern Nevada and covers the 6-month period of January to June, 1983. DOE

N87-13114# National Oceanic and Atmospheric Administration, Silver Spring, Md. Air Resources Lab.
METEOROLOGICAL SUMMARY OF WATOX (WESTERN ATLANTIC OCEAN EXPERIMENT) 1985 RESEARCH INTENSIVE, FEBRUARY-APRIL
R. S. Artz, U. Dayan, and S. G. Sheridan May 1986 79 p
(PB86-226792; NOAA-TM-ERL-ARL-143) Avail: NTIS HC A05/MF A01 CSCL 04B

Flow along the mid-Atlantic Coast and over Bermuda was studied using the NOAA King Air Aircraft and two ground sampling stations. The period studied was mid-February through mid-April 1985. The report presents the surface synoptic charts and the air parcel forecast trajectories associated with these events along with a climatology indicating what types of events were sought and how many could be expected between February and April of a typical year. Finally, the meteorological tools available for each forecast are discussed and examples are given. GRA

N87-13115# National Weather Service, Kansas City, Mo.
SOME PROPOSALS FOR MODIFYING THE PROBABILITY OF PRECIPITATION PROGRAM OF THE NATIONAL WEATHER SERVICE
W. E. Sangster and M. D. Manker Jul. 1986 38 p
(PB86-226636; NOAA-TM-NWS-CR-82) Avail: NTIS HC A03/MF A01 CSCL 04B

The technical memorandum proposes reducing the number of probability classes from 12 (or 13) to six in order to allow a new kind of verification display. Also, some new scores designed to put more emphasis on catching the larger amounts with high PoP's will be presented. The possibilities of changing the thresholds for the probability event from the present .01 inch to three thresholds of Trace, .04 inch will be explored. GRA

N87-13116# National Oceanic and Atmospheric Administration, Boulder, Colo. Environmental Sciences Group.
CALIBRATION AND ACCURACY OF THE NOAA/ERL GUST PROBE SYSTEM AND INTERCOMPARISON WITH OTHER SYSTEMS
G. G. Greenhut and R. O. Gilmer Oct. 1985 36 p
(PB86-221736; NOAA-TM-ERL-ESG-22) Avail: NTIS HC A03/MF A01 CSCL 04B

The calibration techniques for the National Oceanic and Atmospheric Administration/Environmental Research Laboratories (NOAA/ERL) gust probe system are reviewed and the instrumental errors associated with the measurement of the fluxes of latent and sensible heat and momentum are calculated. Power spectra and cospectra of the fluctuating meteorological variables are displayed and comparisons of the eddy fluxes from the gust probe system with bulk aerodynamic calculations are reviewed. GRA

N87-13117# National Oceanic and Atmospheric Administration, Boulder, Colo. Environment Sciences Group.
EFFECTS OF REDUCED SPATIAL RESOLUTION ON THE NEXRAD STORM SEQUENCE ALGORITHMS
C. McAdie May 1986 61 p
(PB86-221728; NOAA-TM-ERL-ESG-21) Avail: NTIS HC A04/MF A01 CSCL 04B

The spatial resolution of radar reflectivities obtained from NCAR's CP-2 Doppler radar on 4 June 1983, 2130-2230 G.m.t., is reduced by averaging and skipping range gates, and skipping entire rays. The number of storms identified by the NEXRAD Storm Sequence algorithms increases as the averaging of skipping interval is lengthened. Causes of the increase are ground clutter effects, multiple identification of storms, and enhanced detection of small storms. Large isolated thunderstorms are consistently identified at all spatial resolutions tested. GRA

N87-12947# Joint Publications Research Service, Arlington, Va.
METEOROLOGICAL EFFECTS OF GEOTECTONIC PHENOMENA HYPOTHESIZED Abstract Only
G. Afanasyev *In its* USSR Report: Earth Sciences (JPRS-UES-86-007) 10 Sep. 1986 2 p Transl. into ENGLISH from Sovetskaya Litva (Riga, USSR), 27 Apr. 1986 p 2 (For primary document see N87-12946 04-42)
Avail: NTIS HC A06/MF A01

N87-12948# Joint Publications Research Service, Arlington, Va.
THIRD INTERNATIONAL SYMPOSIUM ON TROPICAL METEOROLOGY Abstract Only
V. N. Ivanov *In its* USSR Report: Earth Sciences (JPRS-UES-86-007) 10 Sep. 1986 1 p Transl. into ENGLISH from Izvestiya Akademii Nauk SSSR: Fiziki Atmosfery i Okeana (Moscow, USSR), v. 22, no. 2, Feb. 1986 p 221-223 Symposium held in Yalta, 24-31 Mar. 1985 (For primary document see N87-12946 04-42)
Avail: NTIS HC A06/MF A01

48 OCEANOGRAPHY

Includes biological, dynamic, and physical oceanography; and marine resources.

For related information see also *43 Earth Resources and Remote Sensing.*

N87-13118# Instituto de Pesquisas Espaciais, Sao Jose dos Campos (Brazil).
ON THE WALKER CIRCULATION OF 1983-84
Mary Toshie Kayano, V. Brahmananda Rao, and Antonio Divino Moura Jul. 1986 16 p Submitted for publication
(INPE-3952-PRE/971) Avail: NTIS HC A02/MF A01

The El Nino - Southern Oscillation (ENSO) event of 1983 was extraordinary in many ways. First indication of positive sea surface temperature (SST) anomalies appeared in Central Pacific during the southern winter rather than near the coast of South America during the southern summer as happened in other events. By the beginning of 1983, the Southern Oscillation Index (SOI) reached a value of 3.5 standard deviations below normal, the lowest on record since 1935. Several recent papers have documented the onset phase of this event. What is not adequately discussed is the collapse phase of this ENSO event and the return to normal atmospheric conditions. Further, an overlooked aspect of this ENSO event is the associated Walker circulation and its vertical structure. In this note we show that the return to normal conditions was associated with a spectacular reversal of several atmospheric characteristics. Our calculations showed significant correlation between the SOI and one important atmospheric property, hitherto not well examined, namely, water vapor. Our results also show an awesome interconnection between such properties of the atmosphere as vertical velocity, water vapor, rainfall and thermodynamic structure to the phase of ENSO.
Author

N87-13119# Army Cold Regions Research and Engineering Lab., Hanover, N. H.
MIZEX: A PROGRAM FOR MESOSCALE AIR-ICE-OCEAN INTERACTION EXPERIMENTS IN ARCTIC MARGINAL ICE ZONES. 8: A SCIENCE PLAN FOR A WINTER MARGINAL ICE ZONE EXPERIMENT IN THE FRAM STRAIT/GREENLAND SEA, 1987/89
Kenneth Davidson, Ira Dyer, Dean Horn, Ola Johannessen, and Peter Mikhalevsky Apr. 1986 58 p
(AD-A169070; CRREL-SR-86-9) Avail: NTIS HC A04/MF A01 CSCL 20/1

The present plan is motivated by the need to improve our understanding of the fundamentals of acoustic propagation, noise, and electromagnetic remote sensing in the winter marginal ice zone (MIZ). The plan strongly emphasizes oceanography, ice dynamics, and meteorology. In fact, the latter disciplines must be deeply enough researched to resolve fundamental questions entailing air/ice/ocean interaction, heat and mass exchanges and balances, growth and decay of ice-edge eddies, etc. Detailed scientific objectives are examined for oceanography, meteorology, ice physics, remote sensing, and acoustics together with detailed experimental plans, and a discussion of logistics for these experiments. GRA

N87-13120# Environmental Research Inst. of Michigan, Ann Arbor. Radar Div.
NONLINEAR INTERACTIONS IN THE MICROWAVE SENSING OF OCEANIC INTERNAL WAVES
David R. Lyzenga 15 Feb. 1986 47 p Sponsored by Navy
(AD-A169776; ERIM-155900-37-R) Avail: NTIS HC A03/MF A01 CSCL 08/3

Theories for the interaction of surface waves with internal wave-induced surface currents are reviewed, and applied to the problem of microwave sensing of internal waves. Several types of nonlinearities are discussed, including those associated with the wave-current interaction process (within the context of infinitesimal-amplitude wave theory), those associated with nonlinear surface wave dynamics, and those associated with electromagnetic scattering from nonlinear surface waves. Results of a numerical integration of the wave equation are presented and compared with linearized perturbation solutions in order to illustrate some of these nonlinearities. GRA

N87-13121# Rhode Island Univ., Kingston. Graduate School of Oceanography.
THE GULF STREAM DYNAMICS EXPERIMENT. INVERTED ECHO SOUNDER DATA REPORT FOR THE JUNE 1984 TO MAY 1985 DEPLOYMENT PERIOD Summary Report, Jun. 1984 - May 1985
Karen L. Tracey, Meghan Cronin, and D. Randolph Watts Dec. 1985 185 p
(Contract N00014-81-C-0062; Grant NSF OCE-82-01222)
(AD-A170758; URI/GSO-TR-85-3) Avail: NTIS HC A09/MF A01 CSCL 08/10

The Gulf Stream Dynamics Experiment was conducted in the region just northeast of Cape Hatteras from April 1983 to May 1985 to study the propagation and growth characteristics of Gulf Stream meanders. Data collected as part of the field experiment included inverted echo sounders, current meter moorings, and AXBT survey flights. This report documents the inverted echo sounder data collected from June 1984 to May 1985. Time series plots of the half-hourly travel time and low-pass filtered thermocline depth measurements are presented for eighteen instruments. Bottom pressure and temperature, measured at four of the sites, are also plotted. Basic statistics are given for all the data records shown. Maps of the thermocline depth field in a 240 km by 460 km region are presented at daily intervals. Author (GRA)

51 LIFE SCIENCES (GENERAL)

N87-13122*# National Aeronautics and Space Administration. Ames Research Center, Moffett Field, Calif.

CREW FACTORS IN FLIGHT OPERATIONS. PART 3: THE OPERATIONAL SIGNIFICANCE OF EXPOSURE TO SHORT-HAUL AIR TRANSPORT OPERATIONS
H. Clayton Foushee, John K. Lauber, Michael M. Baetge (Informatics General Corp., Palo Alto, Calif.), and Dorothea B. Acomb (San Jose State Univ., Calif.) Aug. 1986 67 p
(NASA-TM-88322; A-86338; NAS 1.15:88322) Avail: NTIS HC A04/MF A01 CSCL 06S

Excessive flightcrew fatigue has potentially serious safety consequences. Laboratory studies have implicated fatigue as a causal factor associated with varying levels of performance deterioration depending on the amount of fatigue and the type of measure utilized in assessing performance. These studies have been of limited utility because of the difficulty of relating laboratory task performance to the demands associated with the operation of a complex aircraft. The performance of 20 volunteer twin-jet transport crews is examined in a full-mission simulator scenario that included most aspects of an actual line operation. The scenario included both routine flight operations and an unexpected mechanical abnormality which resulted in a high level of crew workload. Half of the crews flew the simulation within two to three hours after completing a three-day, high-density, short-haul duty cycle (Post-Duty condition). The other half flew the scenario after a minimum of three days off duty (Pre-Duty) condition). The results revealed that, not surprisingly, Post-Duty crews were significantly more fatigued than Pre-Duty crews. However, a somewhat counter-intuitive pattern of results emerged on the crew performancemeasures. In general, the performance of Post-Duty crews was significantly better than that of Pre-Duty crews, as rated by an expert observer on a number of dimensions relevant to flight safety. Analyses of the flightcrew communication patterns revealed that Post-Duty crews communicated significantly more overall, suggesting, as has previous research, that communication is a good predictor of overall crew performance. Author

N87-13123# State Univ. of New York, Buffalo. Dept. of Biophisical Sciences.
MECHANICAL TRANSDUCTION: UNIFICATION
Frederick Sachs Jun. 1986 4 p Repr. from NIPS, v. 1, Jun. 1986 p 98-100
(Contract DAAG29-85-K-0135)
(AD-A171191; ARO-22560.1-LS) Avail: NTIS HC A02/MF A01 CSCL 06/3

The transduction mechanical stimuli into electrical responses is essential for audition, kinesthesis, proprioception, and autonomic sensation of pressure and volume. The primary event in transduction is the opening of an ion channel whose linkage to the cytoskeleton provides high sensitivity. When linked to adapting mechanical structures, this scheme can account for the presently known properties of various mechanical transducers.Author (GRA)

N87-13124# Brookhaven National Lab., Upton, N. Y.
X-RAY FLUORESCENCE WITH SYNCHROTRON RADIATION
K. W. Jones, B. M. Gordon, A. L. Hanson, J. G. Pounds, and G. Schidlovsky Mar. 1986 10 p Presented at the Annual Joint Meeting of the Electron Microscopy of America and the Microbeam Analysis Society, Albuquerque, N. Mex., 10 Aug. 1986
(Contract DE-AC02-76CH-00016)
(DE86-010543; BNL-38006; CONF-860829-26) Avail: NTIS HC A02/MF A01

X-ray fluorescence (XRF) has long been used to make measurements of trace element concentrations in biological materials with very high sensitivity. It has not been previously possible to work with micrometer spatial resolutions because of the relatively low brightness of X-ray tubes. This situation is much improved by using synchrotron storage ring X-ray sources since the brightness of the synchrotron source is many orders of magnitude higher than is obtained with the most intense tube sources. These intense sources open the possibility of using the XRF technique for measurements with resolutions of approximately cellular dimensions. A description of a current research project at Brookhaven which uses synchrotron radiation induced X-ray emission (SRIXE) is presented to illustrate a specific application of the method in biology. DOE

52 AEROSPACE MEDICINE

Includes physiological factors; biological effects of radiation; and effects of weightlessness on man and animals.

N87-13125* National Aeronautics and Space Administration, Washington, D.C.
AEROSPACE MEDICINE AND BIOLOGY: A CONTINUING BIBLIOGRAPHY WITH INDEXES
Nov. 1986 53 p
(NASA-SP-7011(290); NAS 1.21:7011(290)) Avail: NTIS HC A04 CSCL 06E

This bibliography lists 125 reports, articles and other documents introduced into the NASA scientific and technical information system in October 1986. M.G.

N87-13126# Anco Engineers, Inc., Culver City, Calif.
RADIOGRAPHIC DETERMINATION OF MASS AND INERTIAL TENSOR OF ANATOMICAL SEGMENTS Final Report
May 1986 43 p
(Contract N00014-85-C-0594)
(AD-A169122; ANCO-1663.15) Avail: NTIS HC A03/MF A01 CSCL 06/19

The Naval Medical Research and Development Command desires to nondestructively measure the inertial properties of nonhuman primate bodies and limbs, with possible extension to humans. The results can be used in building accurate body dynamics models for crash and seat ejection studies. ANCO has investigated the use of multi-axis radiographs (X-ray photographs) of anatomical segments with high energy photons, which allows the determination of total mass, center of gravity, and the inertia tensor. This technique does not require any knowledge of the nature of the tissues studied (or their absorption coefficient) and does not require expensive CT-scan equipment. It was concluded that by using relatively inexpensive and simple equipment, the inertial properties could be determined with an accuracy of 5% to 10%, except for the off-diagonal terms of the inertia tensor where the errors could be larger. This larger error, however, is of limited concern in body dynamic studies. GRA

N87-13127# Army Research Inst. of Environmental Medicine, Natick, Mass.
HYPOTHERMIC EFFECTS ON VASCULAR CONTRACTILITY AND REACTIVITY
N. R. Bandick and D. E. Roberts 1 Jan. 1986 23 p
(AD-A169142) Avail: NTIS HC A02/MF A01 CSCL 06/19

This study compared the reactive and contractile properties of helical strips of femoral arteries taken from normothermic rabbits and rabbits that were anesthetized with pentobarbitol and cooled to 25 C at a rate of 7 C per hour. The purpose of this comparison was to see if intrinsic factors would alter the sensitivity and/or contractility of this vascular muscle to norepinephrine during whole body hypothermia. We found that, after two hours of in-vivo hypothermia, the hypothermic derived tissue was from 10 to 100X more sensitive to norepinephrine than the normothermic derived tissue. This augmented sensitivity continued while the tissue was in-vitro for at least twelve hours. The dose-response curves of the hypothermic derived arteries were shifted to the left of the normothermic arteries resulting in a greater contractility at lower levels of agonist. Moreover, the normothermic tissue contracted slower than the hypothermic. The maximal tension developed by the strips was equivalent. This study has identified prolonged alternations of receptor sensitivities and contractility properties attributable to in-vivo influences than can, in part, explain the disruptions of blood pressure during and following whole body hypothermia. GRA

N87-13128# Army Research Inst. of Environmental Medicine, Natick, Mass.

QUANTIFICATION OF RESPIRATORY MUSCLE PERFORMANCE

Stephen R. Muza Jun. 1986 17 p

(AD-A169208; USARIEM-M38/86) Avail: NTIS HC A02/MF A01 CSCL 06/16

Quantification of respiratory muscle force, velocity and length are usually indirect measurements assessed from pressure, air flow and volume, respectively. Pressure produced by the respiratory muscles is measured at sites within the airways, rib cage and abdomen. Quantification of diaphragmatic tension is obtained by measurement of transdiaphragmatic pressure (P sub di) (gastric minus esophageal pressures). The strength of the inspiratory muscles working in concert is the voluntary static maximum inspiratory pressure measured at the mouth, briefly sustained near functional residual capacity (FRC). The inspiratory muscles' velocity of shortening is quantified by measuring the inspiratory flow rate (V sub I). Since the V sub I varies over the duration of inspiration (T sub I), the mean inspiratory flow rate (V sub I/T sub I) is typically used. Finally, changes in the respiratory muscles' length are inferred from measurements of volume. The duration of sustained voluntary hyperpnea is inversely related to the time-pressure integral of the diaphragm (T sub I/T sub T.P sub di/P sub di max) and the mean V sub I. Thus, measurements of pressure, flow and volume yield quantitative indices of respiratory muscle performance. GRA

N87-13129# Michigan Univ., Ann Arbor. Transportation Research Inst.

ANALYSIS OF HEAD AND NECK DYNAMIC RESPONSE OF THE US ADULT MILITARY POPULATION Final Annual Technical Report, 1 Oct. 1984 - 1 Feb. 1986

A. C. Bosio and B. M. Bowman 15 Apr. 1986 135 p

(Contract N00014-81-K-0603)

(AD-A169563; UMTRI-86-14; FATR-3) Avail: NTIS HC A07/MF A01 CSCL 06/19

Mechanisms of head/neck dynamic response were investigated for NBDL volunteer data in -Gx and +Gy acceleration vectors with the MVMA 2-D and VOM 3-D Crash Victim Simulation models. Computer simulation of human subject response yielded mechanical constants pertinent to the design of a Biofidelic Manikin (BFM). Improved biofidelity for a two-joint neck model was achieved by relocating the lower neck pivot point inferior and posterior to anatomic T1. In -Gx, the magnitude and duration for condyles extension, in particular, was improved while satisfactory acceleration response was maintained. Exercising the neck model at -6Gx and -15Gx showed that it was necessary to use nonlinear stiffnesses for the lower neck joint in flexion. Two modes of extension motion at the occipital condyles were seen in the volunteer subjects. The first mode was extension with rebound (some subjects demonstrating flexion). The second mode was peak extension followed by further increase in the extension motion. The two modes of condyles extension appear to depend on some pre-test condition - probably muscle tensing since the short duration of the head and neck motion in a test (300 ms) should not allow muscular reaction beginning after the onset of the test to be a factor. Simulations with a model that has passive neck elements give only the extension with rebound response, i.e., mode one response. Thus, on the basis of simulations, it can probably be said that mode one response results for subjects who are not pretensed and mode two response results for pretensed subjects. GRA

N87-13130# Technion - Israel Inst. of Tech., Haifa. Faculty of Medicine.

SLEEPABILITY AND WAKEABILITY FOLLOWING SLEEP DEPRIVATION Final Report, period ending Aug. 1982

Peretz Lavie May 1986 30 p

(Contracts DAJA37-81-C-0237; DA Proj. 2Q1-61102-B-74-D)

(AD-A169578; ARI-RN-86-64) Avail: NTIS HC A03/MF A01 CSCL 06/19

This research note discusses experiments investigating the infrastructure of arousal during the habitual waking day following one night of total sleep deprivation. Based on the data collected during the experiment, it can be concluded that wakeability, the ability to remain awake, and sleepability, the ability to fall asleep, following sleep deprivation, are not complimentary processes, but are probably governed by different mechanisms. The practical implications of these results to the scheduling of replacement naps are discussed. GRA

N87-13131# Army Research Inst. of Environmental Medicine, Natick, Mass.

HUMAN THERMOREGULATORY MODEL FOR IMMERSION IN COLD WATER

Peter Tikuisis, Richard R. Gonzalez, and Kent B. Pandolf Jun. 1986 35 p

(AD-A169779; USARIEM-M-39/86) Avail: NTIS HC A03/MF A01 CSCL 06/19

A mathematical model of thermoregulation has been developed to simulate human physiological responses to cold-water immersion. Data were obtained from experiments where thirteen healthy male volunteers were totally immersed under resting and nude conditions for 1 h in water temperatures of 20 and 28 C. Mean measured rectal temperature (T sub re) fell by about 0.9 and 0.5 C in 20 and 28 C water for all subjects, yet mean measured metabolic rate (M) rose by about 275 and 90 W for the lean mass group (n=7) and 195 and 45 W for the normal mass group (n=6). To predict the observed T sub re and M values, the present model differed from its predecessors by (a)determining a thermally neutral body temperature profile such that the measured and predicted initial values of T sub re and M were matched, (b)including thermal inputs for shivering from the skin independent of their inclusion with the central temperature to account for the observed initial rapid rise in M, (c)confining the initial shivering to the trunk region to avoid an overly large predicted initial rate of rectal cooling, and (d) calculating the steady state of convective heat loss by assuming a zero rate of heat storage in the skin compartment. GRA

N87-13132# National Maritime Research Center, Kings Point, N. Y. Computer Aided Operations Research Facility.

APPLICATION OF HEART RATE MEASUREMENTS TO MARITIME RESEARCH SIMULATOR

Elliot Wald Mar. 1986 68 p

(AD-A169988; CAORF-60-7805-01) Avail: NTIS HC A04/MF A01 CSCL 06/16

An experiment was performed on the Ship Simulator of the Computer Aided Operations Research Facility (CAORF) to determine the feasibility of relating the instantaneous heart rates of test subjects with the nature of their on-bridge activity at the time of measurement. It was found that experienced mariners confronted with potential collision situations on the simulator or with difficult maneuvering problems in restricted waters generally experienced elevated heart rates indicative of increased cognitive and emotional arousal. It was also found that variability of heart rate appears to be useful in differentiatng workload demands imposed on the mariner by different navigation conditions. The fact that physiological reactions were observed to occur on the simulator in situations which would be expected to be emotionally arousing indicates, first, that the simulator is recreating, to a degree, the real-world atmosphere, and second, that heart rate measurements can be usefully applied in future research to detect emotional and or cognitive levels of arousal. GRA

N87-13133# Beth Israel Hospital, Boston, Mass.

FRACTURE AND VISCOELASTIC CHARACTERISTICS OF THE HUMAN CERVICAL SPINE

W. T. Edwards, W. C. Hayes, Y. F. Kou, M. S. Coffee, and A. A. White, III 1986 221 p

(Contract F49620-81-K-0010)

(AD-A170002; AFOSR-86-0453TR) Avail: NTIS HC A10/MF A01 CSCL 06/16

Cervical spine segments were tested both nondestructively and destructively to determine the load-displacement relationships and

vertebral strength. For this study, a servo-hydraulic multi-degree of freedom material testing machine was designed and constructed. This new system, called the Planar Testing Apparatus (PTA), was used to generate motions needed to characterize the sagittal response of spine segments. A study of the viscoelastic properties of two vertebrae lumbar spine segments was conducted following the completion of the PTA to check and demonstrate the test system. The results from seven lumbar specimens were also included in this report. The cervical spine segments consisted of three vertebrae and their interconnecting soft tissue, discs, and ligaments. A noninvasive electro-mechanical displacement measuring apparatus was constructed to monitor the six degree of freedom motion of the middle vertebral body as it moved relative to the two adjacent vertebrae during the mechanical tests. Results for cervical spine specimens indicated that a low displacement rates (less than 5 mm/sec or 5 deg/sec) there was no dependence of spinal segment stiffness on displacement rate. Curves for load vs. displacement (both axila and shear) and moment vs. sagittal bending displayed large regions of small load and low slope as displacements increased. GRA

N87-13134# Army Research Inst. of Environmental Medicine, Natick, Mass.
SELF-PACED HEAT ACCLIMATION PROCEDURES
Lawrence E. Armstrong, Roger W. Hubbard, Jane P. DeLuca, and Elaine L. Christensen Mar. 1986 39 p
(AD-A170533; USARIEM-T-8/86) Avail: NTIS HC A03/MF A01 CSCL 06/19

The purpose of this investigation was to evaluate the effectiveness of self-paced heat acclimation (SPHA) procedures. Fourteen males performed 100 nmin of intermittent exercise during 9 SPHA work-rest cycles, on eight days. Exercise consisted of 8.279 P or - 0.527 to 9.799 + or - 0.433 km of treadmill running per day. SPHA trials were effective in improving heat tolerance in that significant ($p < .05$) reductions were observed (day 1 vs day 8) in final heart rate (HR), Delta HR, final rectal temperatures (Tre), Delta Tre, final mean weighted skin temperature (Tsk), and Delta Tsk. Resting plasma volume expanded significantly ($p <. 05$) from day 1 to day 4, but sweat rate was unchanged. Group mean exercise intensities and ratings of perceived exertion were not statistically different from days 2 7, let the number of trials terminate because subjects exceeded HR and Tre safety limits (22 out of 112 trials) declined during heat acclimation (days 1-4 = 16, days 5-8 = 6). Symptoms of heat illness (piloerection, chills, dizziness, vomiting) were observed in 16.1% of all trials; 11 out of 14 subjects (78.6%) experienced one or more or these symptoms during SPHA trials. GRA

N87-13135# Yale Univ., New Haven, Conn. Dept. of Ophthalmology and Visual Science.
LIMITS OF PATTERN DISCRIMINATION IN HUMAN VISION Final Report, Jan. 1983 - Dec. 1985
Joy Hirsch 3 Feb. 1986 30 p
(Contract F49620-83-C-0026)
(AD-A170756; AFOSR-86-0569TR) Avail: NTIS HC A03/MF A01 CSCL 05/10

This investigation was focused on identification of various limits of human spatial discrimination, two-dimensional sampling properties of the retinal photoreceptor lattice, and the consequences for spatial vision. Highlights from this study are briefly listed: (1) Foveal Spatial Discriminations are hyperacuity tasks; (2) The spatial-frequency discrimination function (delta f/f vs f) is segmented; (3) The discrimination segments can be related to retinal sampling; (4) Scaling mechanisms apply to low resolution tasks; (5) The photoreceptor lattice is a highly ordered hexagonal array; (6) A hexagonal component exists in spatial discrimination; and (7) A new metric model of spatial vision is based on visual sampling. GRA

N87-13136# Michigan Univ., Ann Arbor.
HIGH-RESOLUTION ANALYSIS OF EYE MOVEMENTS Final Report, 15 Jun. 1983 - 15 Nov. 1984
John Jonides 15 Apr. 1986 12 p
(Grant AF-AFOSR-0269-83)
(AD-A170779; AFOSR-86-0512TR) Avail: NTIS HC A02/MF A01 CSCL 06/16

A computerized laboratory was constructed to monitor eye movements, to present visual stimuli, and to collect and record the performance of human subjects in information processing tasks. Author (GRA)

N87-13137# Harvard Medical School, Boston, Mass. Dept. of Physiology and Biophysics.
PHARMACOLOGICAL RESETTING OF THE CIRCADIAN SLEEP-WAKE CYCLE Final Technical Report, 1 Apr. 1983 - 31 Mar. 1986
Martin C. Moore-Ede 30 May 1986 27 p
(Grant AF-AFOSR-0194-83)
(AD-A170804; AFOSR-86-0545TR) Avail: NTIS HC A03/MF A01 CSCL 06/16

This research program developed strategies to reset the timing of the circadian (approximately 24-hour) sleep-wake cycle so that individuals could be maintained fully awake in any predetermined time in the 24-hour day. This capability would be of direct benefit in minimizing the deleterious effects of jet-lag and could promote alertness in facilities which must be staffed 24 hours a day. The studies utilized a diurnal primate primate, the squirrel monkey (Saimiri sciureus), with a well defined circadian neurophysiology and sleep-wake physiology. This animal has a consolidated sleep-wake cycle that is comparable to that in humans. During the three-year period of funding, the circadian sleep-wake organization in squirrel monkeys was characterized, and the rate of resynchronization after phase shifts of environmental light-dark cycles was determined. GRA

N87-13138# Sloan-Kettering Inst. for Cancer Research, New York. Biophysics Lab.
BIOLOGICAL AND CLINICAL DOSIMETRY, JULY 1, 1964 TO DECEMBER 31, 1984 Final Report
J. S. Laughlin and L. Zeitz 1986 191 p
(Contract DE-AC02-76EV-03522)
(DE86-006947; DOE/EV-03522/T4) Avail: NTIS HC A09/MF A01

Systems for the determination of absorbed dose in biological research and clinical applications are developed. The primary method under study is the local absorbed dose calorimeter. In addition, secondary dosimetric systems such as ionization chambers, chemical dosimeters and thermoluminescent dosimeters (TLD) are being developed and applied to provide an absolute basis for the evaluation and comparison of experiments, treatments and other procedures using radiation. In keeping with these objectives this project has accomplished significant advances in the following areas: (1) local absorbed dose calorimetry; (2) neutron dosimetry; (3) dosimetry of ultra-high intensity radiation sources; (4) solid state detector and germanium gamma camera program; (5) dosimetry for brachytherapy; and (6) non-isolated sensor calorimeters. DOE

N87-13139# Pacific Northwest Labs., Richland, Wash.
PHYSICAL INTERACTION OF 1-Hz TO 100 kHz ELECTRIC AND MAGNETIC FIELDS WITH LIVING ORGANISMS
W. T. Kaune Apr. 1986 45 p Presented at the 22nd Annual Meeting of the National Council on Radiation Protection and Measurements, Washington, D.C., 2 Apr. 1986
(Contract DE-AC06-76RL-01830)
(DE86-012323; PNL-SA-13962; CONF-860451-1) Avail: NTIS HC A03/MF A01

The paper discusses, from a physical point of view, interactions between biological systems and electric and/or magnetic fields characterized by frequencies extending from 1 Hz to 100 kHz. DOE

N87-13155# Ludwig-Maximilians-Universitaet, Munich (West Germany). Orthopaedische Klinik und Poliklinik.
INVESTIGATION OF VIBRATIONS OF THE SPINAL COLUMN OF HEALTHY SUBJECTS [SCHWINGUNGSUNTERSUCHUNGEN

DER WIRBELSAEULE GESUNDER PROBANDEN]
J. Piehler, F.-W. Hagena, C. J. Wirth, F. Huettig (Messerschmitt-Boelkow-Blohm G.m.b.H., Ottobrunn (West Germany).), and K. Sauer (Hochschule der Bundeswehr, Munich (West Germany).) *In* DGLR Proceedings of a Symposium on the Evaluation of Man-Machine Systems: Methods and Problems 1985 p 114-126 In GERMAN (For primary document see N87-13146 04-54)
Avail: NTIS HC A13/MF A01

53 BEHAVIORAL SCIENCES

Includes psychological factors; individual and group behavior; crew training and evaluation; and psychiatric research.

N87-13140*# New Mexico Inst. of Mining and Technology, Socorro.
NOSL EXPERIMENT SUPPORT Final Report, 1 Jan. 1980 - 31 Jul. 1986
Marx Brook 2 Oct. 1986 4 p
(Contract NAS8-33817)
(NASA-CR-178947; NAS 1.26:178947) Avail: NTIS HC A02/MF A01 CSCL 05I

An optical lightning detector was constructed and flown, along with Vinton cameras and a Fairchild Line Scan Spectrometer, on a U-2 during the summer of 1979. The U-2 lightning data was obtained in daylight, and was supplemented with ground truth taken at Langmuir Laboratory. Simulations were prepared as required to establish experiment operating procedures and science training for the astronauts who would operate the Night/Day Optical Survey of Thunderstorm Lightning (NOSL) equipment during the STS-2 NOSL experiment on the Space Shuttle. Data was analyzed and papers were prepared for publication. B.G.

N87-13141*# National Aeronautics and Space Administration. Ames Research Center, Moffett Field, Calif.
CREW COMMUNICATION AS A FACTOR IN AVIATION ACCIDENTS
Joseph Goguen, Charlotte Linde, and Miles Murphy Aug. 1986 29 p
(NASA-TM-88254; A-86254; NAS 1.15:88254) Avail: NTIS HC A03/MF A01 CSCL 05I

The crew communication process is analyzed. Planning and explanation are shown to be well-structured discourse types, described by formal rules. These formal rules are integrated with those describing the other most important discourse type within the cockpit: the command-and-control speech act chain. The latter is described as a sequence of speech acts for making requests (including orders and suggestions), for making reports, for supporting or challenging statements, and for acknowledging previous speech acts. Mitigation level, a linguistic indication of indirectness and tentativeness in speech, was an important variable in several hypotheses, i.e., the speech of subordinates is more mitigated than the speech of superiors, the speech of all crewmembers is less mitigated when they know that they are in either a problem or emergency situation, and mitigation is a factor in failures of crewmembers to initiate discussion of new topics or have suggestions ratified by the captain. Test results also show that planning and explanation are more frequently performed by captains, are done more during crew- recognized problems, and are done less during crew-recognized emergencies. The test results also indicated that planning and explanation are more frequently performed by captains than by other crewmembers, are done more during crew-recognized problems, and are done less during-recognized emergencies.

N87-13142# New York Univ., New York.
PERCEPTUAL FACTORS IN WORKLOAD: A NEUROMAGNETIC STUDY Annual Report, 1 Jan. - 31 Dec. 1985
Lloyd Kaufman and Samuel J. Williamson 28 Feb. 1986 55 p
(Contract F49620-85-K-0004)
(AD-A169934; AFOSR-86-0417TR; AR-1) Avail: NTIS HC A04/MF A01 CSCL 05/10

A background section describes the neuromagnetic method and its history. There were an elevation of N1 and P2 (using a quasi-steady state stimulus). The fields associated with these sources increased in intensity during attention. This is not due to the activity of sources recruited during attention, but to Modulated activity of neurons in or near primary auditory cortex. This is consistent with a Triesman like filter theory of attention. Also, physical parameters of stimulation, e.q., loudness, have little or no effects. However, the effect is sharply diminished when both stimuli are presented to both ears with equal loudness. A collaboration with other investigators is planned to compare our results with results obtained in a more conventional manner. A new method for obtaining graded levels of attention is described. A visual experiment is underway, and is giving us similar results. A single-position method for determining the location, orientation and strength of the dipole source is described. This method will be applied to a P300 study, which will follow-up an odd-ball study just completed. The latter gave results similar to those obtained previously, but the method is sufficiently insensitive to determine if changing P300 latency is due to a change in source. The planned experiment should make this possible. GRA

N87-13143# Essex Corp., Orlando, Fla.
EYE MOVEMENTS AS AN INDEX OF MENTAL WORKLOAD Final Report, 15 Jul. 1985 - 14 Mar. 1986
James G. May, Robert S. Kennedy, Mary C. Williams, William P. Dunlap, and Julie R. Brannan 17 Mar. 1986 20 p
(Contract F49620-85-C-0121)
(AD-A169941; AFOSR-86-0416TR) Avail: NTIS HC A02/MF A01 CSCL 06/5

Two investigations were carried out to assess the feasibility of using eye movement measures as nonintrusive indicants of mental workload. In the first experiment, measures of saccadic latency and eye movement velocity were obtained during alternating eye movement scans while subjects were differentially task loaded by simple, moderate, and complex auditory tone counting. The latency and eye movement velocity measures changed but did not differ reliably as tone counting complexity (workload) was increased. In the second experiment, the spatial extent of spontaneous saccades was measured under three levels of tone counting complexity. The results indicated that the extent of such eye movements varied inversely (p less than .0151) as tone counting complexity increased. This index appears to hold promise for the development of an objective indicator of mental workload. Author (GRA)

N87-13144# Illinois Univ., Champaign. Cognitive Psychophysiology Lab.
THE EVENT RELATED BRAIN POTENTIAL AS AN INDEX OF INFORMATION PROCESSING AND COGNITIVE ACTIVITY. A PROGRAM OF BASIC RESEARCH. SUPPLEMENT A: NEUROMAGNETIC STUDIES Annual Progress Report, 20 Apr. 1984 - 31 Dec. 198
Lloyd Kaufman and Emanuel Donchin 31 Mar. 1986 23 p
(Contract F49620-85-C-0041)
(AD-A169978; CPL-86-1A; AFOSR-86-0451TR-Suppl-A) Avail: NTIS HC A02/MF A01 CSCL 05/10

A study was conducted to evaluate the feasibility of obtaining concurrent measures of event-related potentials (ERPs), and event-related magnetic fields (ERFs). Subjects participated in an oddball task while simultaneous ERPs and ERFs were recorded. Isocontour field maps generated for the P300 component are consistent with the suggestion that the P300 may be generated in, or near, the hippocampal formation. GRA

N87-13145# Federal Aviation Administration, Washington, D.C. Office of Aviation Medicine.
THE FLIGHT SERVICE STATION TRAINING PROGRAM: 1981-1985 Final Report
John J. Convey Jun. 1986 18 p
(AD-A171485; DOT/FAA/AM/86-6) Avail: NTIS HC A02/MF A01 CSCL 05/9

This report describes the performance of the ATC classes in the Flight Service Station Training Program 1981 to 1985 on the skills tests and laboratory exercises in Preflight (pilot briefing), inflight, and Emergency Services. Over 80% of the final grade for the program is based on these measures. The average scores of the classes on the skills tests, especially on Inflight, have increased from 1981 to 1985. The different forms of both the Preflight test and the Emergency Services test appear to be equivalent as intended; however, Form G and Form H of the Inflight test are easier than Form D and Form E. The average scores of the classes on the laboratory tests were constant from 1981 to 1985; however, the averages on the Inflight laboratory exercises have declined steadily. Overall, these classes have performed better on the skills tests and laboratory exercises, except for Inflight, than did the reference classes of 1978 and 1979. GRA

N87-13153# Deutsche Gesellschaft fuer Luft- und Raumfahrt, Bonn (West Germany).
THE MEASUREMENT OF THE PSYCHOLOGICAL WORKLOAD DURING TASK-RELATED ACTIVITIES, INCLUDING CAR DRIVING, BY COMPETING TIME INTERVAL ESTIMATION [DIE MESSUNG DER PSYCHISCHEN BEANSPRUCHUNG WAEHREND AUFGANENBEZOGENER TAETIGKEITEN EINSCHLIESSLICH FAHRZEUGFUEHRUNG DURCH KONKURRIERENDE ZEITINTERVALLSCHAETZUNGEN]
Dieter Wiegand *In its* Proceedings of a Symposium on the Evaluation of Man-Machine Systems: Methods and Problems 1985 p 84-93 In GERMAN (For primary document see N87-13146 04-54)
Avail: NTIS HC A13/MF A01

54 MAN/SYSTEM TECHNOLOGY AND LIFE SUPPORT

Includes human engineering; biotechnology; and space suits and protective clothing.

For related information see also *16 Space Transportation.*

N87-13146# Deutsche Gesellschaft fuer Luft- und Raumfahrt, Bonn (West Germany).
PROCEEDINGS OF A SYMPOSIUM ON THE EVALUATION OF MAN-MACHINE SYSTEMS: METHODS AND PROBLEMS [BEWERTUNG VON MENSCH-MASCHINE-SYSTEMEN. METHODEN UND PROBLEMATIK]
1985 277 p Partly in GERMAN and ENGLISH Symposium held in Cologne, West Germany, 14-15 Nov. 1985
(DGLR-85-04; ISBN-3-922010-30-X; ETN-86-98080) Avail: NTIS HC A13/MF A01

Anthropometric handicaps in helicopter cockpits; an obstacle-warning radar for helicopters; the workload and stress of a cockpit crew; and the simulation of human service reliability in the manual control of aircraft were studied. The system-ergonomic workload in highly automated process control tasks; and psychological workload during task-related activities were analyzed. A research method to determine the quality of task mastering by navigators in ship guidance; and the vibrations of the spinal column were tested. Human factors engineering in nuclear power plant control; and the ergonomic requirements for the design of control rooms were investigated. The possibilities of the eye-mark investigation as an anthropotechnical method to study man machine systems; measures, basic conceptions and inquiry techniques for the evaluation of man machine systems were studied. The empirical determination of the acceptable user surface in automated air conditioning systems was investigated. For individual titles, see N87-13147 through N87-13165. ESA

N87-13147# Forschungsinstitut fuer Anthropotechnik, Wachtberg (West Germany).
EVALUATION OF MAN MACHINE SYSTEMS: INTRODUCTION AND OVERVIEW [BEWERTUNG VON MENSCH-MASCHINE-SYSTEMEN, EINFUEHRUNG UND UEBERSICHT]
K.-P. Gaertner and W. Stein *In* DGLR Proceedings of a Symposium on the Evaluation of Man-Machine Systems: Methods and Problems 1985 p 2-9 In GERMAN (For primary document see N87-13146 04-54)
Avail: NTIS HC A13/MF A01

The organization, evaluation, and study of man-machine systems are discussed. Decisions to be made during each of these tasks are specified. Emprirical and model-based methods of studying man-machine systems are briefly addressed. Problems to be overcome in reconciling the various goals involved in optimizing man-machine systems are considered. ESA

N87-13148# Institute of Aviation Medicine, Manching (West Germany).
ANTHROPOMETRIC HANDICAPS IN THE CONSTRUCTION OF A HELICOPTER COCKPIT [ANTHROPOMETRISCHE VORGABEN FUER DIE KONSTRUKTION EINES HUBSCHRAUBER-COCKPITS]
G. Kroh *In* DGLR Proceedings of a Symposium on the Evaluation of Man-Machine Systems: Methods and Problems 1985 p 10-24 In GERMAN (For primary document see N87-13146 04-54)
Avail: NTIS HC A13/MF A01

Helicopter pilots were used to test the dummy cockpit of a helicopter now under dwevelopment in order to develop a data base for the seating and the steering organs. Seated tests showed that the postures assumed by the pilots during flights generally did not agree with those envisioned in the construction specifications. This was due to the relatively large discrepancy in arm length between the 5th and the 99th percentile. To prevent their arms from getting tired, the pilots pushed the seat back farther than expected by the designer. Suggestions are also briefly made for the location of the stick and pedals. ESA

N87-13149# AEG-Telefunken, Ulm (West Germany). Abteilung H14E27.
OBSTACLE-WARNING RADAR FOR HELICOPTERS [DAS HINDERNISWARN-RADAR FUER HUBSCHRAUBER - EINE ANTHROPOTECHNISCHE PROBLEMSTELLUNG] c32
G. M. Och *In* DGLR Proceedings of a Symposium on the Evaluation of Man-Machine Systems: Methods and Problems 1985 p 25-33 In GERMAN (For primary document see N87-13146 04-54)
Avail: NTIS HC A13/MF A01

An obstacle warning radar concept for helicopters is described in both the test and operational phases. A radar sonde is mounted on the front of the helicopter under a radome and senses the atmosphere forward over a range of 180 deg azimuth and 32 deg elevation. The ray is directed by a fast-rotating mirror, resulting in an image-renewal rate of two per second. Obstacles can be detected to a distance of 800 m. depending on atmospheric conditions and obstacle size. ESA

N87-13150# Technische Univ., Berlin (West Germany). Inst. fuer Luft- und Raumfahrt.
DETERMINATION OF THE LOAD AND STRESS OF A COCKPIT CREW DURING AIRCRAFT PILOTING USING TASK NETWORKS AND THE SIMULATION LANGUAGE SAINT [ERMITTLUNG VON PILOTENBELASTUNG BZW. -BEANSPRUCHUNG BEI DER FLUGZEUGFUEHRUNG MIT HELFE VON AUFGABEN-NETZWERKEN UND SAINT]
M. Fricke, U. Kopp, and D. Niemeyer *In* DGLR Proceedings of a Symposium on the Evaluation of Man-Machine Systems: Methods and Problems 1985 p 34-45 In GERMAN (For primary document see N87-13146 04-54)
Avail: NTIS HC A13/MF A01

The load/stress on a cockpit crew of a B 727 during an ILS CAT I flight was investigated by digital simulation of more than 20 flights. A model describing the complex working process of the flight crew and its interaction with the environment is developed. The simulation flights are described, and the various tasks engaged in by the crew during the flights are specified and discussed. ESA

N87-13151# Messerschmitt-Boelkow-Blohm G.m.b.H., Ottobrunn (West Germany). Hubschrauber und FLugzeuge.

APPLICATION OF THE TASK TAXONOMY METHOD TO THE SIMULATION OF HUMAN SERVICE RELIABILITY IN THE MANUAL CONTROL OF AIRCRAFT [ANWENDUNG DER METHODE DER AUFGABENTAXONOMIE ZUR SIMULATION MENSCHLICHEN BEDIENZUVERLAESSIGKEIT BEI DER MANUELLEN STEUERUNG VON FLUGZEUGEN]

K. Brauser *In* DGLR Proceedings of a Symposium on the Evaluation of Man-Machine Systems: Methods and Problems 1985 p 46-61 In GERMAN (For primary document see N87-13146 04-54) (MBB/LKE-301/S/PUB/216) Avail: NTIS HC A13/MF A01

The method of problem taxonomy, based on data on human reliability and aimed at obtaining improved surveying and evaluation of such data, is described. The simulation of the problem of manual steering of an aircraft pitching axis during landing approach using this method together with the simulation program SAINT is discussed. The human error probability for various steering errors obtained using the method is reported. ESA

N87-13152# Forschungsinstitut fuer Anthropotechnik, Wachtberg (West Germany).

SYSTEM-ERGONOMIC WORKLOAD ANALYSIS FOR HIGHLY AUTOMATED PROCESS CONTROL TASKS [SYSTEMERGONOMISCHE BELASTUNGSANALYSEN BEI HOCHAUTOMATISIERTEN PROZESSFUEHRUNGSAUFGABEN]

B. Doering *In* DGLR Proceedings of a Symposium on the Evaluation of Man-Machine Systems: Methods and Problems 1985 p 62-83 In GERMAN (For primary document see N87-13146 04-54) Avail: NTIS HC A13/MF A01

A method to evaluate the ergonomic design of the interface operator-process guiding center in a highly automated shipbuilding industry was developed. The method determines task difficulty due to this intersection, on the basis of load factors the value of which are subjectively evaluated. The acquired information can be a basis for an improved interface design. A simulation model which reproduces the work process of the operator and the technical processes including perturbation, and which allows a comparative evaluation of different work situations was developed. The difficulties of the single tasks of the work process are classified by the model. The result of the simulation is information about the duration of the single work difficulties, as well as an integrative workload index which allows a comparative evaluation of the effects of different perturbations on the work situations. ESA

N87-13153# Deutsche Gesellschaft fuer Luft- und Raumfahrt, Bonn (West Germany).

THE MEASUREMENT OF THE PSYCHOLOGICAL WORKLOAD DURING TASK-RELATED ACTIVITIES, INCLUDING CAR DRIVING, BY COMPETING TIME INTERVAL ESTIMATION [DIE MESSUNG DER PSYCHISCHEN BEANSPRUCHUNG WAEHREND AUFGANENBEZOGENER TAETIGKEITEN EINSCHLIESSLICH FAHRZEUGFUEHRUNG DURCH KONKURRIERENDE ZEITINTERVALLSCHAETZUNGEN] **c53**

Dieter Wiegand *In its* Proceedings of a Symposium on the Evaluation of Man-Machine Systems: Methods and Problems 1985 p 84-93 In GERMAN (For primary document see N87-13146 04-54)

Avail: NTIS HC A13/MF A01

Time interval estimations were performed on subjects to determine psychological workloads of car drivers. Active time interval estimates were given by 101 subjects at rest and during activity. The estimates concerned tests related to driving and driver's choice, and a trip with a 5T truck. Distinction was made between traffic-free and traffic-loaded driving, as well as between experienced and inexperienced drivers. The results show that the dispersion of the time estimate distributions makes a highly significant distinction between the different reference loads; this is also valid for the subdivisions in the driving tests. The tests show that the measuring method is also suited for field conditions. ESA

N87-13154# Fachhochschule, Hamburg (West Germany). Fachbereich Seefahrt.

DEVELOPMENT OF A RESEARCH METHOD TO DETERMINE THE QUALITY OF TASK MASTERING BY NAVIGATORS IN SHIP GUIDANCE [ENTWICKLUNG EINES UNTERSUCHUNGSVERFAHRENS ZUR ERMITTLUNG DER QUALITAET DER AUFGABENBEWAELTIGUNG VON NAUTIKERN BEI DER SCHIFFSFUEHRUNG]

Jens Froese, Anita Damico (Merchant Marine Research Center, New York, N.Y.), Ulrich Pedersen (Hapag-Lloyd A.G., Hamburg (West Germany).), and Nadine Sablowski (Hamburg Univ. (West Germany).) *In* DGLR Proceedings of a Symposium on Evaluation of Man-Machine Systems: Methods and Problems 1985 p 94-113 In GERMAN (For primary document see N87-13146 04-54)

Avail: NTIS HC A13/MF A01

An evaluation method for the effects of ship bridge occupation and installation on the quality of navigation was developed using the ship navigation and simulation program SUSAN. Preliminary results show that the method is suitable for research purposes. ESA

N87-13155# Ludwig-Maximilians-Universitaet, Munich (West Germany). Orthopaedische Klinik und Poliklinik.

INVESTIGATION OF VIBRATIONS OF THE SPINAL COLUMN OF HEALTHY SUBJECTS [SCHWINGUNGSUNTERSUCHUNGEN DER WIRBELSAEULE GESUNDER PROBANDEN] **c52**

J. Piehler, F.-W. Hagena, C. J. Wirth, F. Huettig (Messerschmitt-Boelkow-Blohm G.m.b.H., Ottobrunn (West Germany).), and K. Sauer (Hochschule der Bundeswehr, Munich (West Germany).) *In* DGLR Proceedings of a Symposium on the Evaluation of Man-Machine Systems: Methods and Problems 1985 p 114-126 In GERMAN (For primary document see N87-13146 04-54)

Avail: NTIS HC A13/MF A01

Kinetics tests were conducted to determine the magnitude of the deforming forces on the human spinal column. The vibration test setup including a digital vibration control system is described. Results reveal complex spinal column characteristics: in each plane of the spine a specific transmission behavior is observed. The supposition that the transmission behavior of all other spinal column sections can be deduced from one single position is questioned. ESA

N87-13156# Technischer Uerberwachungs-Verein Rheinland, e.V., Cologne (West Germany). Inst. fuer Unfallforschung und Ergonomie.

REVIEW OF THE METHODS APPLIED IN THE FEDERAL REPUBLIC OF GERMANY TO INVESTIGATE HUMAN FACTORS IN NUCLEAR POWER PLANT CONTROL [UEBERLICK UEBER IN DER BRD ANGEWANDTE METHODEN ZUR UNTERSUCHUNG MENSCHLICHER FAKTOREN IN KERNKRALTWERKSWARTEN]

D. B. Thomas *In* DGLR Proceedings of a Symposium on the Evaluation of Man-Machine Systems: Methods and Problems 1985 p 127-136 In GERMAN (For primary document see N87-13146 04-54)

Avail: NTIS HC A13/MF A01

Human factors evaluation methods for nuclear power plants are presented. Field studies provide primary information, but laboratory studies in which the variables can be manipulated without the contaminating influence of external factors, are required for predictions but are missing for German nuclear power plants and cannot simply be taken from other countries because the operational parameters are different. ESA

N87-13157# Technischer Uerberwachungs-Verein Rheinland, e.V., Cologne (West Germany). Inst. fuer Unfallforschung und Ergonomie.

SIMULATION OF DISTURBANCES ON THE NUCLEAR POWER PLANT SIMULATOR. THE PROBLEM OF THE INTERPRETATION OF OPERATOR ACTIONS AND THEIR COGNITIVE BACKGROUNDS AS A BASIS FOR DESIGN RECOMMENDATIONS [STOERUNGSSIMULATION AM KRAFTWERKSIMULATOR - ZUM PROBLEM DER INTERPRETATION VON OPERATEURHANDLUNGEN UND DEREN KOGNITIVER HINTERGRUENDE ALS BASIS FUER GESTALTUNGSEMPFEHLUNGEN]

Gerhard Becker *In* DGLR Proceedings of a Symposium on the Evaluation of Man-Machine Systems: Methods and Problems 1985

p 137-154 In GERMAN (For primary document see N87-13146 04-54)
Avail: NTIS HC A13/MF A01

Parameters which influence the correctness of the mental model representation of unusual process evolutions were studied on a simulator in order to improve the understanding of operators in nuclear power plants. The operator's position and complex technical connections are described. Power control, steam barrier supply, and turbine condenser in a power plant are described. The simulated disturbance situation and the behavior of the operators are discussed. The results show that, even in the case of simple disturbances, error management is a very complex and diversified task. Knowledge-based, rule-based, and skill-based operator's behavior are discussed. ESA

N87-13158# Kraftwerk Union A.G. Reaktortechnik, Erlangen (West Germany).
ERGONOMIC REQUIREMENTS FOR THE DESIGN OF CONTROL ROOMS. EVALUATION METHOD [ERGONOMISCHE ANFORDERUNGEN AN DIE WARTENGESTALTUNG -BEWERTUNGSMETHODE]
W. Hinz *In* DGLR Proceedings of a Symposium on the Evaluation of Man-Machine Systems: Methods and Problems 1985 p 155-164 In GERMAN (For primary document see N87-13146 04-54)
Avail: NTIS HC A13/MF A01

A method for the ergonomic qualitative evaluation of control rooms (command post, control stand) is presented. The aim was to develop design standards in order to secure suitable working conditions. Each operational situation is classified with respect to the action which the operators have to take in order to evaluate and influence the process. The method provides a starting point for a more objective evaluation, but requires expert designers because a number of evaluation criteria are lacking. ESA

N87-13159# Dornier-Werke G.m.b.H., Friedrichshafen (West Germany).
A METHOD FOR THE OPTIMUM DESIGN OF THE MAN MACHINE INTERFACE [EIN VERFAHREN ZUR OPTIMALEN GESTALTUNG DER MENSCH-MASCHINE-SCHNITTSTELLE]
V. Behrendt, H.-D. Hartfiel (Kraftwerk Union A.G. Reaktortechnik, Erlangen (West Germany).), H.-R. Mannhaupt (Technische Univ., Munich (West Germany).), W. Preuss (Cologne Univ. (West Germany).), and D.-B. Thomas *In* DGLR Proceedings of a Symposium on the Evaluation of Man-Machine Systems: Methods and Problems 1985 p 165-186 In GERMAN (For primary document see N87-13146 04-54)
Avail: NTIS HC A13/MF A01

A task-related, ergonomic method for the optimization of man machine systems was developed and applied to nuclear power plants. The operator's tasks and the man machine interface are analyzed. A catalog of ergonomic design recommendations is given. The relations between these recommendations and the operations are explained. The applicability of the method is demonstrated in principle, but a number of open questions still remains. ESA

N87-13160# Deutsche Forschungs- und Versuchsanstalt fuer Luft- und Raumfahrt, Brunswick (West Germany). Inst. fuer Flugfuehrung.
THE EYE-MARK INVESTIGATION AS AN ANTHROPOTECHNICAL METHOD TO STUDY MAN MACHINE SYSTEMS [DIE BLICKZIELUNTERSUCHUNG ALS ANTHROPOTECHNISCHE UNTERSUCHUNGSMETHODE IM MENSCH-MASCHINE-SYSTEM]
Rainer Uckermann *In* DGLR Proceedings of a Symposium on the Evaluation of Man-Machine Systems: Methods and Problems 1985 p 187-199 In GERMAN (For primary document see N87-13146 04-54)
Avail: NTIS HC A13/MF A01

Methods and instrumentation used in research on the sequence of eye fixations performed by an aircraft pilot as he guides an aircraft are discussed. The oculogram method, the cornea-reflex method, and the motionless method used in the DEBIC apparatus are summarized, and the apparatus used by the DFVLR are described. Research results obtained using these methods and apparatus are briefly discussed. ESA

N87-13161# Technische Univ., Brunswick (West Germany). Fachgebeit Arbeitswissenschaft.
BASIC CONCEPTIONS FOR THE EVALUATION OF MAN MACHINE SYSTEMS [GRUNDKONZEPT FUER DIE BEWERTUNG VON MENSCH-MASCHINE-SYSTEMEN]
J.-H. Kirchner *In* DGLR Proceedings of a Symposium on the Evaluation of Man-Machine Systems: Methods and Problems 1985 p 200-212 In GERMAN (For primary document see N87-13146 04-54)
Avail: NTIS HC A13/MF A01

The requirements for evaluating man-machine systems are given, and evaluation procedures are discussed in detail. Direct and indirect evaluation of man-machine systems is addressed. A concept for such evaluation is developed, stressing its ergonomic aspects. ESA

N87-13162# Dortmund Univ. (West Germany). Inst. fuer Arbeitsphysiologie.
INQUIRY TECHNIQUES FOR THE EVALUATION OF MAN MACHINE SYSTEMS [BEFRAGUNGSTECHNIKEN BEI DER BEWERTUNG VON MENSCH-MASCHINE-SYSTEMEN]
Martin Schuette *In* DGLR Proceedings of a Symposium on the Evaluation of Man-Machine Systems: Methods and Problems 1985 p 213-228 In GERMAN (For primary document see N87-13146 04-54)
Avail: NTIS HC A13/MF A01

The study of loads imposed on a person and the resulting psychophysical consequences for that person in the context of a man-machine interaction is discussed. Both environmentally caused and task-based loads are considered. Two approaches to investigating these aspects of man-machine systems are examined, an older one-dimensional approach and a more recent multidimensional one. The resulting evaluation of loads in either absolute or relative terms is discussed. ESA

N87-13163# Standard Elektrik Lorenz A.G., Stuttgart (West Germany). Forchungszentrum.
A MEASURE OF USABILITY
W. Flohrer *In* DGLR Proceedings of a Symposium on the Evaluation of Man-Machine Systems: Methods and Problems 1985 p 229-238 (For primary document see N87-13146 04-54)
Avail: NTIS HC A13/MF A01

In order to evaluate the usability of technical equipment not only the time of operation and the error rate have to be considered but also the learning process, i.e., the function time of operation versus number of repeated test trials. The analysis of data (test results), collected over many years, has shown, that the learning curve can be approximated by a simple mathematical formula; the parameters of which differ from one system, device or equipment to another but can easily be calculated. The parameters found can be used to evaluate technical equipment with respect to its usability. Such a measure of usability could enable the engineer or manager to compare technical equipment not only by technical viewpoints or costs but also by one criterion of human factors engineering. ESA

N87-13164# Muenster Univ. (West Germany). Psychologisches Inst. 2.
EVALUATION OF THE BEARING AND KNOWLEDGE REQUIREMENTS OF MAN MACHINE SYSTEMS [DIE BEWERTUNG DER LERN- UND WISSENSANFORDERUNGEN VON MENSCH-MASCHINE-SYSTEMEN]
Tom Boesser *In* DGLR Proceedings of a Symposium on the Evaluation of Man-Machine Systems: Methods and Problems 1985 p 239-248 In GERMAN (For primary document see N87-13146 04-54)
Avail: NTIS HC A13/MF A01

The division of the learning process into an acquisition and an exercise phase is outlined. Examples of learning processes

are given. The theoretical and methodological fundamentals of the evaluation method are explained. The method was tested on a number of simple examples and proves to be usable. Problems encountered in the practical application of the method are presented. The implementation of improvements is planned. ESA

N87-13165# Siemens A.G., Karlsruhe (West Germany). Systemtechnische Entwicklung.
EMPIRICAL DETERMINATION AMONG SUPERINTENDENTS OF THE ACCEPTABLE USER SURFACE IN DIGITALLY AUTOMATED HEATING-VENTILATION AIR CONDITIONING SYSTEMS [EMPIRISCHE ERMITTLUNG DER FUER HAUSMEISTER AKZEPTABLEN BENUTZEROBERFLAECHE BEI DIGITAL AUTOMATISIERTEN HEIZUNGS-LUEFTUNGS-KLIMA-ANLAGEN]
H. J. Charwat *In* DGLR Proceedings of a Symposium on the Evaluation of Man-Machine Systems: Methods and Problems 1985 p 249-269 In GERMAN (For primary document see N87-13146 04-54)
Avail: NTIS HC A13/MF A01

Inquiries were conducted among superintendents of heating-ventilation air (HVA) conditioning systems in order to provide information for an acceptable and successful design of such systems. The user surface is only correct if it is accordance with the knowledge, the comprehension, the expectations, and the practical behavior of the potential user. The superintendents' tasks were divided into six groups. A set of increasingly concrete questions was asked for each group (method of stepwise concretization) in order to exclude any suggestive effect. Verbal understanding problems were overcome by visualization. A design of a control system based on the results of these inquiries is presented. ESA

N87-13166*# National Aeronautics and Space Administration. Marshall Space Flight Center, Huntsville, Ala.
THE ECOLOGY OF MICROORGANISMS IN A SMALL CLOSED SYSTEM: POTENTIAL BENEFITS AND PROBLEMS FOR SPACE STATION
Elizabeth B. Rodgers Oct. 1986 61 p
(NASA-TM-86563; NAS 1.15:86563) Avail: NTIS HC A04/MF A01 CSCL 06K

The inevitble presence on the space station of microorganisms associated with crew members and their environment will have the potential for both benefits and a range of problems including illness and corrosion of materials. This report reviews the literature presenting information about microorganisms pertinent to Environmental Control and Life Support (ECLS) on the space station. The perspective of the report is ecological, viewing the space station as an ecosystem in which biological relationships are affected by factors such as zero gravity and by closure of a small volume of space. Potential sites and activities of microorganisms on the space station and their environmental limits, microbial standards for the space station, monitoring and control methods, effects of space factors on microorganisms, and extraterrestrial contamination are discussed. Author

N87-13167*# McDonnell-Douglas Astronautics Co., Houston, Tex.
ADVANCED EVA SYSTEM DESIGN REQUIREMENTS STUDY Final Technical Report
Jan. 1986 248 p
(Contract NAS9-17299)
(NASA-CR-171942; NAS 1.26:171942; MDC-W0072) Avail: NTIS HC A11/MF A01 CSCL 05H

Design requirements and criteria for the Space Station Advanced Extravehicular Activity System (EVAS) including crew enclosures, portable life support systems, maneuvering propulsion systems, and related extravehicular activity (EVA) support equipment were defined and established. The EVA mission requirements, environments, and medical and physiological requirements, as well as opertional, procedures, and training issues were considered. B.G.

N87-13168# Olis Engineering, Sedalia, Colo.
CONCEPT STUDY - VEHICLE WASTE DISPOSAL SYSTEM Final Report, 1 Aug. 1985 - 28 Jan. 1986
Carter K. Lord 28 Jan. 1986 30 p
(Contract DAAE07-85-C-R089)
(AD-A169045; TACOM-TR-13155) Avail: NTIS HC A03/MF A01 CSCL 13/6

This concept study was initiated to investigate the feasibility of developing a waste disposal system to process and dispose of human waste generated in combat vehicles operating in a nuclear, biological, and chemical (NBC) contaminated environment. GRA

N87-13169# Naval Biodynamics Lab., New Orleans, La.
GUIDELINES FOR SAFE HUMAN EXPERIMENTAL EXPOSURE TO IMPACT ACCELERATION
Marc S. Weiss and Leonard S. Lustick 1986 33 p
(AD-A169347; NBDL-86R006) Avail: NTIS HC A03/MF A01 CSCL 06/19

The objective of the human volunteer impact experiments at the Naval Biodynamics Laboratory (NBDL) is to provide a quality data base for modeling human dynamic and phsyiological responses to impact, and for establishing the relationship between dynamic response parameters and injury. To achieve this objective, the human volunteer impact experiments must be conducted at levels of impact that may produce discomfort but are safe in as much as the experiments have an acceptably low probability of producing any permanent or irreversible injury. These safe levels of impact are derived from one or more of the following sources: (1) exposures employed in previous NBDL research with human subjects; (2) human exposure data from other research sources; (3) exposures using human surrogates/human cadavers; and, (4) mathematical modeling techniques. Based on a review of these sources, limits suggested to the Committee for the Protection of Human Subjects as safe guidelines are included. These are recommended limits for torso-restrained NBDL volunteers, where the freely moving head and neck are the anatomical segments most at risk. GRA

N87-13170# Department of the Air Force, Washington, D.C.
RAPID ACTING ELECTRO-PNEUMATIC ANTI-G SUIT CONTROL VALVE Patent Application
Robert E. VanPatten, inventor (to Air Force) Filed 24 Feb. 1986 23 p
(AD-D012377; US-Patent-Appl-SN-831901) Avail: NTIS HC A02/MF A01 CSCL 13/7

This patent application discloses a novel anti-G suit valve system which provides very rapid response to imminent high acceleration. The disclosed embodiments of the new valve system can be retrofitted to existing mechanical and anti-G valves to create a hybrid valve system capable of achieving the desired qualities of fast triggering of the valve in response to imminent acceleration and maximum rate inflation of the anti-G suit. The new valve system measures acceleration and, by differentiation, the rate of change of acceleration. When both acceleration and rate of change of acceleration exceed preselected values, a solenoid mounted in place of the press-to-test button on a mechanical anti-G valve is energized for a preselected period of time to fully depress the valve spindle, providing maximum rate delivery of pressurized air. The hybrid valve reverts to normal operation at the end of the preselected period of time. Another embodiment monitors an aircraft computer control system digital data bus and adds the requirement of detecting preselected signal values from the data bus to trigger the delivery of pressurized air. A modification of this embodiment requires only the detection of the preselected data bus signal values to initiate maximum rate delivery of pressurized air for the preselected period of time. The anti-G suit valve system may also be operated by manually determining the imminent likelihood of high acceleration and manually actuating the maximum rate delivery. GRA

N87-13171# Department of the Air Force, Washington, D.C.
IMPROVED ANTI-G SUIT Patent Application
Thomas J. Jennings, inventor (to Air Force) Filed 24 Feb. 1986 14 p
(AD-D012378; US-Patent-Appl-SN-831886) Avail: NTIS HC A02/MF A01 CSCL 15/5

This patent application discloses an improved anti-G suit which incorporates stiffening inserts sized and shaped to cover each inflatable air bladder and inserted between the bladders and the anti-G suit fabric. The stiffeners may be made of polypropylene, neoprene rubber, or a composite structure of Kevlar fabric and polyethylene. A butt strap covers the buttocks of an aircrew member and is secured by belts extending across the abdominal and the high bladders of the anti-G suit. Inflation of the air bladders pulls the strap butt to compress the butt strap tightly against the aircrew member's buttocks. GRA

N87-13172# Computer Technology Associates, Inc., McLean, Va.
HUMAN PERFORMANCE ASPECTS OF SMALL SCREEN DISPLAYS: A LITERATURE REVIEW REVEALING THE LACK OF SPECIFIC RESEARCH Final Report
Rebecca L. Shannon and Lisa J. Stewart May 1986 59 p
(Contract DAAK11-84-D-0008)
(AD-A170660; HEL-TN-5-86) Avail: NTIS HC A04/MF A01 CSCL 05/10

Literature from diverse disciplines pertinent to the human performance aspects of small screen displays was examined. In particular, four subtopics were focused on. They include: display size, defined as number of characters per number of lines; protocols, defined as ways users interact with a system to achieve their goals; abbreviations; and vocabulary. The results indicate the lack of specific research on small screen displays but also indicate a trend in current research interest and towards interest in the near future. The report points out other research trends and voids and contains an annotated bibliography of more than 100 source documents. Author (GRA)

55 SPACE BIOLOGY

Includes exobiology; planetary biology; and extraterrestrial life.

No abstracts in this category.

59 MATHEMATICAL AND COMPUTER SCIENCES (GENERAL)

No abstracts in this category.

60 COMPUTER OPERATIONS AND HARDWARE

Includes hardware for computer graphics, firmware, and data processing.

For components see *33 Electronics and Electrical Engineering.*

N87-13173# Instituto de Pesquisas Espaciais, Sao Jose dos Campos (Brazil).
UTILIZATION OF IMPACT DOT MATRIX PRINTERS [UTILITARIOS PARA IMPRESSORAS MATRICIAIS EM PROCESSAMENTO DIGITAL DE IMAGENS]
Adriana Abrahao, Moacir Godoy, Jr., and Joao Argemiro deCarvalho Paiva Sep. 1986 64 p In PORTUGUESE; ENGLISH summary
(INPE-3991-RPE/518) Avail: NTIS HC A04/MF A01

Instructions for using a graphic output system adapted to an impact dot matrix printer are presented. This system represents an improvement on conventional printing systems developed for alphanumeric printers. Author

N87-13174# Massachusetts Univ., Amherst. Dept. of Electrical and Computer Engineering.
YIELD AND PERFORMANCE ENHANCEMENT THROUGH REDUNDANCY IN VLSI AND WSI MULTI-PRECESSOR SYSTEMS
Israel Koren and Dhiraj K. Pradhan 1986 52 p
(Grant AF-AFOSR-0052-84)
(AD-A169930; AFOSR-86-0389TR) Avail: NTIS HC A04/MF A01 CSCL 09/2

New challenges have been brought to fault-tolerant computing and processor architecture research because of developments in IC technology. One emergent area is development of architectures, built by interconnecting a large number of processing elements on a single chip or wafer. Two important areas, related to such VLSI processor arrays, are the focus of this paper; they are fault-tolerance, and yield improvement techniques. Fault-tolerance in these VLSI processor arrays is of real practical significance; it provides for much-needed reliability improvement. Therefore, we first describe the underlying concepts of fault-tolerance at work in these multi-processor systems. These precepts are useful to then present certain techniques that will incorporate fault-tolerance integrally into the design. In the second part of the paper we discuss models that evaluate how yield enhancement and reliability improvement may be achieved by certain fault-tolerant techniques. Author (GRA)

N87-13175# Sandia National Labs., Albuquerque, N. Mex.
RELIABILITY STUDY OF RETENTION AND MEMORY GATE INTEGRITY IN A 1K MNOS RAM
R. D. Nasby, W. M. Miller, and R. L. White 1986 6 p Presented at the 8th IEEE Non-Volatile Semiconductor Memory Workshop, Vail, Colo., 18 Aug. 1986
(Contract DE-AC04-76DP-00789)
(DE86-010483; SAND-86-2079C; CONF-860872-1) Avail: NTIS HC A02/MF A01

The reliability of a 1K MNOS RAM with regards to retention and nitride gate integrity has been demonstrated. Over 400 devices were screened and life tested to demonstrate 0.999 reliability during device life. The device was a 1K MNOS memory used in a RAM application with an erase/write cycle of 32 microseconds and a life specification of 1E7 cycles. DOE

N87-13176# Sandia National Labs., Albuquerque, N. Mex.
SPRINT 3: SERIAL-PARALLEL REMOTE INTERFACE SYSTEM DEVELOPMENT REPORT
J. S. Rathbun Mar. 1986 55 p
(Contract DE-AC04-76DP-00789)
(DE86-010590; SAND-84-2273) Avail: NTIS HC A04/MF A01

This development report/reference manual describes a high-speed digital Serial/Parallel Remote Interface System (SPRINT), which was developed to function as a primary data interface in the Remote Digitizing/High-Density Digital Recording system currently under development to interface the Remote Complex Wave Vibration Test Facility (Bldg. 6610) with the Central Vibration Test Control Facility (Bldg. 6650) at SNLA/AIII. The SPRINT system described in this report provides serial transmission of high-speed parallel data originating in Bldg. 6610 via synchronous fiber-optic links to Bldg. 6650, where the incoming serial data is converted back to parallel form and transferred to disc media for subsequent processing/reduction. From an input/output standpoint, the SPRINT system is electrically transparent, capable of providing parallel data through rates of up to 1 megaword/sec for 22-bit parallel input data while maintaining a serial bit-error rate of less than 10^{-15} with virtual immunity to EMI/RFI associated noise. This report will discuss the electrical characteristics and operation of the SPRINT system from both system and component-level viewpoints. DOE

61 COMPUTER PROGRAMMING AND SOFTWARE

Includes computer programs, routines, algorithms, and specific applications, e.g., CAD/CAM.

N87-13177# Instituto de Pesquisas Espaciais, Sao Jose dos Campos (Brazil).
A PROCEDURE FOR AUTOMATIC TREATMENT OF DYNAMIC SYSTEMS STATE OBSERVATION BIAS ERRORS
Valcir Orlando and Atair Rios Neto May 1986 8 p In PORTUGUESE; ENGLISH summary
(INPE-3908-PRE/918) Avail: NTIS HC A02/MF A01

Bias type errors are generally present in measurements either due to the equipment or to external phonomena. In this work a procedure to directly treat biased observations in the Kalman filter state estimation process, with no need of a priori bias correction, is presented. To do this a dynamic compensation process is used by modelling the observation bias as a first-order Gauss Markov dynamic process. The resulting bias dynamic equations are then incorporated into the dynamic system equations. The procedure was tested by computerized simulation of a low altitude artificial satellite orbit estimation, using range and range rate simulated tracking data considering atmospheric refraction bias errors.
Author

N87-13178*# Jet Propulsion Lab., California Inst. of Tech., Pasadena.
OBSERVATION MODEL AND PARAMETER PARTIALS FOR THE JPL VLBI PARAMETER ESTIMATION SOFTWARE MASTERFIT-1986
O. J. Sovers and J. L. Fanselow 1 Aug. 1986 68 p
(NASA-CR-179919; JPL-Pub-83-39-Rev-2; NAS 1.26:179919) Avail: NTIS HC A04/MF A01 CSCL 09B

In applications of radio interferometry to geodynamics and astrometry, observed values of delay and delay rate obtained from observations of many different radio sources must be passed simultaneously through a multiparameter estimation routine to extract the significant model parameters. As the accuracy of radio interferometry has improved, increasingly complete models for the delay and delay rate observables have been developed. The current status of the delay model used in the Jet Propulsion Laboratory multiparameter estimation program MASTERFIT is described. It is assumed that the reader has at least a cursory knowledge of the principles of very long baseline interferometery. The delay model is the sum of four major model components: geometry, clock, troposphere, and ionosphere. Current models for these components, as well as their partial derivatives with respect to parameters that are to be adjusted by multiparameter fits to the data are presented. The geometric delay is discussed. The technique used to obtain the delay rate model from the delay model is described. The values of physical constants used in MASTERFIT are given. Model improvements that may be required by more accurate data in the future are outlined. Author

N87-13179# Instituto de Pesquisas Espaciais, Sao Jose dos Campos (Brazil).
TOOL TO DEVELOP REAL TIME SIMULATION SYSTEMS M.S. Thesis [FERRAMENTA PARA DESENVOLVIMENTO DE SISTEMAS DE SIMULACAO EM TEMPO REAL]
Carmen Lucia RuybaldosSantos Aug. 1986 196 p In PORTUGUESE; ENGLISH summary
(INPE-3979-TDL/233) Avail: NTIS HC A09/MF A01

The development of a tool for testing and documenting the constituent subsystems of a real time simulation system, written in FORTRAN language, is described. This tool can be seen as an environment to simulate the operation of all subsystems of the simulated system, except one: the subsystem under test. The documentation of each subsystem is attached to it. Simulation results are presented by means of tables and curves. The tool was used in perfecting the flight simulator for the Empresa Brasileira de Aeronautica (EMBRAER) T-27 airplane, developed at the Centro tecnico Aeroespacial - CTA (IPD-PEA). Accompanying the report are printouts regarding the results of a simulation and documentation for the atmosphere subsystem which is part of the simulator described above. Author

N87-13180# Stanford Univ., Calif. Systems Optimization Lab.
USER'S GUIDE FOR NPSOL (VERSION 4.0): A FORTRAN PACKAGE FOR NONLINEAR PROGRAMMING
Philip E. Gill, Walter Murray, Michael A. Saunders, and Margaret H. Wright Jan. 1986 60 p
(Contracts N00014-85-K-0343; DAAG29-84-K-0156)
(AD-A169115; SOL-86-2; ARO-21592.8-MA) Avail: NTIS HC A04/MF A01 CSCL 09/2

This report forms the user's guide for Version 4.0 of NPSOL, a set of Fortran subroutines designed to minimize a smooth function subject to constraints, which may include simple bounds on the variables, linear constraints and smooth nonlinear constraints. (NPSOL may also be used for unconstrained, bound-constrained and linearly constrained optimization.) The user must provide subroutines that define the objective and constraint functions and (optionally) their gradients. All matrices are treated as dense, and hence NPSOL is not intended for large sparse problems. NPSOL uses a sequential quadratic programming (SQP) algorithm, in which the search directions is the solution of a quadratic programming (QP) subproblem. The algorithm treats bounds, linear constraints and nonlinear constraints separately. The Hessian of each QP subproblem is a positive-definite quasi-Newton approximation to the Hessian of the Lagrangian function. The steplength at each iteration is required to produce a sufficient decrease an augmented Lagrangian merit function. Each QP subproblem is solved using a quadratic programming package with several features that improve the efficiency of an SPQ algorithm. Author (GRA)

N87-13181# Army Military Personnel Center, Alexandria, Va.
SPECIAL ASSOCIATIVE PREPROCESSING STRUCTURES FOR QUALITATIVE FEATURE EXTRACTION Final Report
Michael C. Bibby 11 Jun. 1986 173 p
(AD-A169147) Avail: NTIS HC A08/MF A01 CSCL 09/2

Existing pattern recognition and classification algorithms in computer vision require vast amounts of computations on input data. As a result, memory access time is a critical parameter in system performance. Tremendous parallelism in structure and algorithm is required for the system to operate in real-time. A preprocessing structure for qualitative feature extraction which meets these system requirements is presented. In general, the structural architecture consists of a cellular array of pixel-processors each containing an inherently parallel associative memory element. As such, memory access time is minimal and parallelism is maximized. By varying this basic structure with regard to interconnection and additional logic, specific structures result which are capable of extracting measures of specific qualitative features. In this thesis two specific structures are described which extract, respectively, the qualitative features of texture regularity and line trend. Applications of these structures are presented. Low-level simulation and performance estimates indicate these applications are viable and amenable to real-time operation. Suggestions for the development of structures which extract other features or multiple features are described. GRA

N87-13182# Stanford Univ., Calif. Systems Optimization Lab.
AN IMPLICIT ENUMERATION ALGORITHM WITH BINARY-VALUED CONSTRAINTS
Yieh-Hwang Wan Mar. 1986 113 p
(Contract N00014-85-K-0343)
(AD-A169256; SU-SOL-86-5) Avail: NTIS HC A06/MF A01 CSCL 09/2

In many capital budgeting problems, the basic decisions simply are whether to approve or reject various capital investment proposals. This naturally gives rise to binary decision variables and an integer programming formulation of the problem. In fact, this type of problem is one of the most important areas of application of integer programming. General-purpose algorithms for binary integer programming frequently are applied to capital

budgeting problems. However, such problems generally have a great deal of special structure, including contraints for mutually exclusive alternatives, contingent alternatives, and other interdependencies. (A project which can be undertaken at different discrete levels is a good exampie for mutually exclusive alternatives and a simple kind of contingent alternative concerns two-stage projects, where the second stage can be undertaken only if its first stage couterpart has been undertaken already. A similar relationship also can exist between two groups of mutually exclusive alternatives.) Many group contingent constraints, which are common in capital budgeting problems and scheduling problems, are binary valued. A capital budgeting model is presented. GRA

N87-13183# Naval Postgraduate School, Monterey, Calif.
A SOFTWARE IMPLEMENTATION OF AN INTERACTIVE GRAPHICS SYSTEM FOR THREE DIMENSIONAL MODELING AND LAYOUT M.S. Thesis
Surasak Mungsing Mar. 1986 52 p
(AD-A169264) Avail: NTIS HC A04/MF A01 CSCL 05/8

This thesis examines interactive techniques for viewing a 3-D building model in a walkthrough fashion and for placing 3-D piping into a 3-D building model. The focus of research is software implementation using the C programming language and the IRIS Graphics Library on the Silicon Graphics Inc. IRIS Turbo 2400 interactive graphics system. The first part of the research is concerned with drawing, viewing a 3-D building model, and examining interactive techniques required for building walkthrough mechanisms. The second part is concerned with the development of techniques necessary to allow the placement of 3-D piping into a 3-D building model using 2-D graphics display and a mouse device. The algorithms and implementation of these techniques are presented. GRA

N87-13184# California Univ., Irvine. Dept. of Information and Computer Science.
LANGUAGE ACQUISITION AND MACHINE LEARNING Interim Report, Jun. - Dec. 1985
Pat Langley and Jamie G. Carbonell 1 Feb. 1986 40 p
(Contract N00014-84-K-0345)
(AD-A169581; UCI-ICS-TR-86-12; TR-4) Avail: NTIS HC A03/MF A01 CSCL 09/2

Recent progress in the field of machine learning is reviewed and implications for computational models of language acquisition examined. As a framework for understanding this research, the authors propose four component tasks involved in learning from experience-aggregation, clustering, characterization, and storage. They then consider four common problems studied by machine learning researchers, i.e., learning from examples, heuristics learning, conceptual clustering, and learning macro-operators, describing each in terms of the framework. After this, they turn to the problem of grammar acquisition, relating this problem to other learning tasks and reviewing four AI systems that have addressed the problem. Finally, they note some limitations of the earlier work and propose an alternative approach to modeling the mechanisms underlying language acquisition. Author (GRA)

N87-13185# George Washington Univ., Washington, D.C. Inst. for Management Science and Engineering.
THE CONTINUOUS PROJECTIVE SUMT METHOD FOR CONVEX PROGRAMMING
Garth P. McCormick 4 Jun. 1986 24 p
(AD-A169847; AD-E750914; GWU/IMSE/SERIAL-T-507/86) Avail: NTIS HC A02/MF A01 CSCL 12/1

An algorithm for solving convex programming problems is derived from the differential equations characterizing the trajectory of unconstrained minimizers of the classical logarithmic barrier function method. Convergence of this continuous Projective SUMT (sequential unconstrained minimization techniques) method to a global solution of a convex programming problem is proved under minimal assumptions. Extension of the algorithm to a form which handles linear equality constraints produces a differential equation analogue of Karmarkar's projective method for linear programming. The concluding discussion includes a discrete form of the algorithm. GRA

N87-13186# IIT Research Inst., Rome, N.Y.
CATALOG OF RESOURCES FOR EDUCATION IN ADA (TRADE NAME) AND SOFTWARE ENGINEERING (CREASE), VERSION 4.0
May 1986 312 p
(Contract MDA903-83-C-0306)
(AD-A169892) Avail: NTIS HC A14/MF A01 CSCL 09/2

Over the last twenty-five years software technology has made enormous strides. The Ada program serves as a focal point for the consolidation of state-of-the-art thinking about this technology. Proper use of the technology can contribute significantly to controlling the cost and improving the quality of software. However, this is a sophisticated technology, and its proper use depends upon sophisticated education and training for the people applying it. The effectiveness of the Ada programming language will be determined by the degree to which people are able to use it to implement software engineering practices in applications programming. A carefully planned education and training program, which teaches both fundamental software engineering concepts and the effective use of the Ada language, is therefore essential. This publication is intended to serve as a source of information about resources available to those who are planning such programs, with the hope that will not only serve as a ready reference, but will also increase awareness of the many aspects of education in Ada and Software Engineering. Author (GRA)

N87-13187# Wisconsin Univ., Madison. Dept. of Computer Sciences.
SOR (SUCCESSIVE OVER-RELAXATION) MGR (MULTIGRID ALGORITHM)(nu) EXPERIMENTS ON THE CRYSTAL MULTICOMPUTER
David Kamowitz Jan. 1986 49 p
(Grants NSF MCS-81-05904; AF-AFOSR-0275-82)
(AD-A169929; AFOSR-86-0411TR) Avail: NTIS HC A03/MF A01 CSCL 09/2

This report describes distributed implementations of the red/black SOR algorithm and of the MGR(nu) multigrid algorithm on the Crystal multicomputer. Rates of convergence and observed effciencies for both algorithms are compared. GRA

N87-13188# Texas Univ., Austin. Dept. of Computer Sciences.
HIGH PERFORMANCE PARALLEL COMPUTING Final Report, 1 Feb. 1984 - 31 Jan. 1985
J. C. Browne and G. J. Lipovski 22 Jan. 1986 23 p
(Contract F49620-84-C-0020)
(AD-A169981; AFOSR-86-0457TR) Avail: NTIS HC A02/MF A01 CSCL 09/2

The 1984/85 accomplishments of the research project High Performance Parallel Computing included bringing the prototype of the Texas Reconfigurable Array Computer (TRAC) to a configuration and to a state of stability where it could support execution of simple assembly language programs, initial development of a unified model of parallel computation which is a basis for a programming environment uniting process and data flow models of parallel computation, bringing to operational status on an alternative host one of the two parallel programming languages (the Computation Structures Language, CSL) originally intended for use on TRAC, exploration of the expressive capabilities of this programming language, initiation of development of a graphical programming language based on the unified model of parallel computation mentioned preceding, major progress on a graphically interfaced Petri Net-based performance modeling system for parallel computations and development of algorithms for scheduling of circuits to realize configurations in configurable banyan network based computer architectures. GRA

N87-13189# Georgia Inst. of Tech., Atlanta. Production and Distribution Research Center.
AN IMPLICIT ENUMERATION PROCEDURE FOR THE GENERAL LINEAR COMPLEMENTARITY PROBLEM

Faiz A. Al-Khayyal Jun. 1986 41 p
(Contract N00014-86-K-0173)
(AD-A170397; PDRC-86-05) Avail: NTIS HC A03/MF A01 CSCL 12/1

An algorithm is presented for solving a quadratic programming formulation of the linear complementarity problem. No assumptions on the problem data are required. The algorithm is designed to solve the problem by implicitly enumerating the 2 superscript n complementary cones. Geometrically, the procedure amounts to searching the extreme points of a sequence of faces of the constraint polyhedron of decreasing dimension. An extension to the procedure for finding all solutions of an arbitrary complementarity problem is also discussed. The procedure has been implemented and tested on forty randomly generated problems (up to fifty dimensional) having dense indefinite defining matrices. The results of these tests demonstrate the superiority of this approach over two competing methods. GRA

N87-13190# Clarkson Univ., Potsdam, N.Y. Dept. of Electrical and Computer Engineering.
A RULE-BASED PATTERN MATCHING SYSTEM FOR THE RECOGNITION OF THREE-DIMENSIONAL LINE DRAWN OBJECTS: A FOUNDATION FOR VIDEO TRACKING
Y. S. Fong 1986 83 p
(Contract N00014-85-C-2421)
(AD-A170701) Avail: NTIS HC A05/MF A01 CSCL 09/2

Object recognition is an important subtask in image understanding, moving object tracking, and scene analysis. When identifying an object in a scene, it is essential that the same object is recognized from different view angles. Also, in cases where the object is occluded or the image is noisy, the recognition is expected to function under the existence of uncertainty. A system for object recognition, with emphasis on view angle independence, is studied. The system uses simple line drawn objects as the input image. An algorithm to extract important information from the image is developed. A rule-based pattern matching scheme is used to recognize the object in the image. In each decision made, a confidence factor is associated to indicate the system's certainty in making this decision. This study shows that the rule-based pattern matching system is a useful and flexible framework for object recognition and scene analysis. Author (GRA)

N87-13191# Massachusetts Inst. of Tech., Cambridge. Lab. for Computer Science.
INTRODUCTION TO THE THEORY OF NESTED TRANSACTIONS
Nancy Lynch and Michael Merritt Jul. 1986 65 p Prepared in cooperation with Bell Telephone Labs., Murray Hill, N.J.
(Contracts N00014-85-K-0168; N00014-83-K-0125; DAAG29-84-K-0058; Grant NSF DCR-83-02391)
(AD-A171428; MIT/LCS/TR-367) Avail: NTIS HC A04/MF A01 CSCL 09/2

This paper develops the foundation for a general theory of nested transactions. We present a simple formal model for studying concurrency and resiliency in a nested environment. This model has distinct advantages over the many alternatives, the greatest of which is the unification of a subject replete with formalisms, correctness conditions and proof techniques. The authors are presently engaged in an ambitious project to recast the substantial amount of work in nested transactions within this single intuitive framework. These pages contain the preliminary results of that project - a description of the model, and its use in stating and proving correctness conditions for two variations of a well-known algorithm. GRA

N87-13192# Institute for Defense Analyses, Alexandria, Va.
PROCEEDINGS OF THE IDA WORKSHOP ON FORMAL SPECIFICATION AND VERIFICATION OF ADA (TRADE NAME) (1ST) HELD IN ALEXANDRIA, VIRGINIA ON 18-20 MARCH 1985
Clyde G. Roby Dec. 1985 389 p Workshop held in Alexandria, Va., 18-20 Mar. 1985
(Contract MDA903-84-C-0031)
(AD-A171507; AD-E500793; IDA-M-146; IDA/HQ-85-30658) Avail: NTIS HC A17/MF A01 CSCL 09/2

The first IDA Workshop identified current issues in Ada verification: the uses of formal verification; what verification techniques and verification systems are available; what practical experience is there in the use of these approaches and who has this experience; what impact does Ada have on verification (both before and during coding activities); what are the major problems in the verification field; and what needs to be done to overcome these problems. Slides presented at the two-and-half day workshop are included. GRA

N87-13193# Oak Ridge National Lab., Tenn.
MATRIX FACTORIZATION ON A HYPERCUBE MULTIPROCESSOR
G. A. Geist and M. T. Heath Aug. 1985 21 p Presented at the Conference on Hypercube Multiprocessors, Knoxville, Tenn., 26 Aug. 1985
(Contract DE-AC05-84OR-21400)
(DE86-011775; CONF-8508178-1) Avail: NTIS HC A02/MF A01

This paper is concerned with parallel algorithms for matrix factorization on distributed-memory, message-passing multiprocessors, with special emphasis on the hypercube. Both Cholesky factorization of symmetric positive definite matrices and LU factorization of nonsymmetric matrices using partial pivoting are considered. The use of the resulting triangular factors to solve systems of linear equations by forward and back substitutions is also considered. Efficiencies of various parallel computational approaches are compared in terms of empirical results obtained on an Intel iPSC hypercube. DOE

N87-13194# Stanford Univ., Calif. Dept. of Operations Research.
SINGLE-PHASE METHOD FOR QUADRATIC PROGRAMMING
S. C. Hoyle Apr. 1986 69 p
(Contract DE-AS03-76ER-72018)
(DE86-012156; SOL-86-9) Avail: NTIS HC A04/MF A01

This report describes a single-phase quadratic programming (QP) method. A need for such a method is apparent when solving a sequence of closely-related QPs. One example of this is in the area of nonlinear programming, which uses sequential quadratic programming. Another example is sensitivity analysis involving the constraints. In both of these examples, if the quadratic problems are large-scale and the initial point is infeasible, the single-phase method of this report may be particularly useful. If the Hessian is indefinite, the method will find a local minimum when solving a dense QP, and a constrained stationary point when solving a large-scale QP. If the Hessian is positive definite, it will find the global minimum. The single-phase method of this report is an active-set method which solves a sequence of equality-constraint quadratic programs (EQP). It differs from other active-set methods in that the current iterate may violate constraints in the working set (the prediction of thhe active set). Special care has been taken to avoid rank deficiency in the working set. An efficient means of solving the successive EQPs of a large-scale problem is included. Finally, an implementation of the method for dense QPs is described. DOE

N87-13195# Lawrence Livermore National Lab., Calif.
USING 3-DIMENSIONAL GRAPHICS TO VISUALIZE MULTIVARIATE SCIENTIFIC DATA
S. L. Grotch Apr. 1986 15 p Presented at the Symposium on Measurement of Toxic Air Pollutants, Raleigh, N.C., 27 Apr. 1986
(Contract W-7405-eng-48)
(DE86-010788; UCRL-93658; CONF-860426-2) Avail: NTIS HC A02/MF A01

The two dimensional plot is unquestionably the most commonplace graphics tool of the scientist. Yet in dealing with problems often involving high dimensionality, more sophisticated representations (such as 3D) are only infrequently used. In the work reported here, several real-world examples are used to illustrate the wide variety and the resultant interpretive potential possible through the use of three dimensional graphics. These examples are a study of climate data and of air pollution monitoring. Among the

variety of 3D plots presented are discrete point plots; mesh-like surface plots showing either theoretical or empirical model behavior; and combinations of points and surfaces. Some of the many techniques available to enhance the utility of such graphics are shown. DOE

N87-13196# Virginia Polytechnic Inst. and State Univ., Blacksburg. Dept. of Computer Science.
HOMPACK: A SUITE OF CODES FOR GLOBALLY CONVERGENT HOMOTOPY ALGORITHMS
L. T. Watson, S. C. Billups (Sandia National Labs., Albuquerque, N. Mex.), and A. P. Morgan (General Motors Research Labs., Warren, Mich.) 11 Nov. 1985 26 p Presented at the SIAM National Meeting, Boston, MA., 21 Jul. 1986 Prepared in cooperation with Sandia National Labs., Albuquerque, NM.; General Motors Research Labs., Warren, MI.
(Contract DE-AC04-76DP-00789)
(DE86-011644; SAND-86-1328C; CONF-860744-1; TR-85-34) Avail: NTIS HC A03/MF A01

There are algorithms for finding zeros or fixed points of nonlinear systems of equations that are globally convergent for almost all starting points, i.e., with probability one. The essence of all such algorithms is the construction of an appropriate homotopy map and then tracking some smooth curve in the zero set of this homotopy map. HOMPACK provides three qualitatively different algorithms for tracking the homotopy zero curve: ordinary differential equation based, normal flow, and augmented Jacobian matrix. Separate routines are also provided for dense and sparse Jacobian matrices. A high level driver is included for the special case of polynomial systems. DOE

N87-13197# Sandia National Labs., Albuquerque, N. Mex. Scientific Operating Systems Div.
INTERPRETIVE MODEL FOR A CONCURRENCY METHOD
C. L. Carter Jun. 1986 24 p
(Contract DE-AC04-76DP-00789)
(DE86-012743; SAND-86-0586) Avail: NTIS HC A02/MF A01

A Concurrency Method is a language embodying the data flow characteristics of data-drive and single-assignment. The interpreter for A Concurrency Method models a physical machine with an architecture directed toward this language. The interpreter is a complete system with scheduler, editor, load balancer and message handler. This model embraces some architectural features in other data flow machines and models and combines these features in a manner most conductive to this language. DOE

N87-13198# Oak Ridge National Lab., Tenn.
SURVEY OF THE CHARACTERISTICS OF VERY HIGH LEVEL LANGUAGES
R. S. Loffman 1986 5 p Presented at the 17th International Rochester Conference, Rochester, N.Y., 2 Jun. 1986
(Contract DE-AC05-84OR-21400)
(DE86-012240; CONF-8606152-1) Avail: NTIS HC A02/MF A01

Although there is no consensus on the characteristics of very high level languages (VHLLs), ample evidence exists that users of such languages have several expectations. As a result of an extensive survey of the literature and communications with researchers, it was concluded that six characteristics of VHLLs are desired. These are that the language: (1) be nonprocedural, (2) allow implicit referencing, (3) provide a good interface between user and computer, (4) allow for verification, (5) be extensible, and (6) provide the means for better data representation. It was also concluded that no existing language has all six characteristics. DOE

N87-13199# Oak Ridge National Lab., Tenn.
SOLVING SCIENTIFIC PROBLEMS ON HYPERCUBE PARALLEL COMPUTERS
R. C. Ward 15 May 1986 5 p Presented at the Supercomputing Decision for Scientific Computing Conference, Fairfax, Va., 15 May 1986
(Contract DE-AC05-84OR-21400)
(DE86-012622; CONF-8605160-1) Avail: NTIS HC A02/MF A01

The presentation discusses the research activities on hypercube parallel computers at Oak Ridge National Laboratory and assesses the potential of hypercubes for solving large scale scientific computational problems. Items discussed are the reasons ORNL purchased two hypercube computers, the results of basic research on matrix computations, the status of the seven applications projects being converted to run on the hypercube, the suggested steps for programming parallel computers, and the advantages and problem areas of the hypercube architecture for solving today's scientific problems. DOE

62 COMPUTER SYSTEMS

Includes computer networks and special application computer systems.

N87-13200# Sparta, Inc., McLean, Va.
DEPARTMENT OF DEFENSE GATEWAY ARCHITECTURE AND FUNCTIONAL REQUIREMENTS Final Report
11 Dec. 1985 64 p
(Contract DCA100-84-C-0085)
(AD-A169086; URW-5-DCA-043) Avail: NTIS HC A04/MF A01 CSCL 17/2

This document presents the functional requirements for DoD Internetwork gateways. The requirements themselves are highlighted in Sections 3 and 5 through 7. In addition, Section 1 discusses the motivations for these requirements in terms of Gateway's role the DoD Internetwork; Section 2 discusses successful gateway designs. Section 4 illuminates several gateway design tradeoff areas, where design options can be used to match specific operational and performance requirements. GRA

N87-13201# California Univ., Berkeley.
DISTRIBUTED NAME SERVERS: NAMING AND CACHING IN LARGE DISTRIBUTED COMPUTING ENVIRONMENTS
Douglas B. Terry Dec. 1985 133 p
(Contracts N00039-84-C-0089; ARPA Order 4871)
(AD-A169225) Avail: NTIS HC A07/MF A01 CSCL 09/2

Name services facilitate sharing in distributed environments by allowing objects to be named unambiguously and maintaining a set of application-defined attributes for each named object. Existing distributed name services, which manage names based on their syntactic structure, may lack the flexibility needed by large, diverse, and evolving computing communities. A new approach, structure-free name management, separates three activities; choosing names, selecting the storage sites for object attributes, and resolving an object's name to its attributes. Administrative entities apportion the responsibility for managing various names, while the name service's information needed to locate an object's attributes can be independently reconfigured to improve performance or meet changing demands. An analytical performance model for distributed name services provides assessments of the effect of various design and configuration choices on the cost of name service operations. Measurements of Xerox's Grapevine registration service are used as inputs to the model to demonstrate the benefits of replicating an object's attributes to coincide with sizeable localities of interest. Additional performance benefits result from client's acquiring local caches of name service data treated as hints. A cache management strategy that maintains a minimum leval of cache accuracy is shown to be more effective than the usual technique of maximizing the hit ratio. Author (GRA)

N87-13202# California Univ., Berkeley.
AVAILABILITY AND CONSISTENCY OF GLOBAL INFORMATION IN COMPUTER NETWORKS Final Report, 1 Sep. 1983 - 31 Oct. 1985
C. V. Ramamoorthy May 1986 212 p
(Contract DAAG29-83-K-0086)
(AD-A169247; ARO-19159.3-EL) Avail: NTIS HC A10/MF A01 CSCL 09/2

A principal feature of computer networks is the ability of the

various sites of the network to access and update shared information. At the application level, the global information takes the form of shared file systems, databases, etc., and at lower levels, it takes the form of status information used in controlling the network. This research focused techniques for maintaining the availability of global information in the face of various kinds of failures and the consistency of global information in the presence of concurrency. Two failure models were considered: the crash model, in which failures are instantly detected, and the malfunction model, in which an indefinite period of time may lapse before failures are detected. A network status maintenance scheme based on a global clock facility was designed for the crash model. For the malfunction model, an approach to maintaining the correctness of global information and preventing error propagation was developed. Centralized and distributed deadlock detection algorithms were developed for distributed databases. Author (GRA)

63 CYBERNETICS

Includes feedback and control theory, artificial intelligence, robotics and expert systems.

For related information see also *54 Man/System Technology and Life Support.*

N87-13203*# Martin Marietta Aerospace, Denver, Colo.
EVALUATION OF AUTOMATED DECISIONMAKING METHODOLOGIES AND DEVELOPMENT OF AN INTEGRATED ROBOTIC SYSTEM SIMULATION. APPENDIX B: ROBSIM PROGRAMMER'S GUIDE
D. C. Haley, B. J. Almand, M. M. Thomas, L. D. Krauze, K. D. Gremban, J. C. Sanborn, J. H. Kelly, T. M. Depkovich, W. J. Wolfe, and T. Nguyen Mar. 1986 318 p
(Contract NAS1-16759)
(NASA-CR-178052; NAS 1.26:178052; MCR-85-665-App-B) Avail: NTIS HC A14/MF A01 CSCL 09B

The purpose of the Robotic Simulation (ROBSIM) program is to provide a broad range of computer capabilities to assist in the design, verification, simulation, and study of robotic systems. ROBSIM is programmed in FORTRAM 77 and implemented on a VAX 11/750 computer using the VMS operating system. The programmer's guide describes the ROBSIM implementation and program logic flow, and the functions and structures of the different subroutines. With the manual and the in-code documentation, an experienced programmer can incorporate additional routines and modify existing ones to add desired capabilities. E.R.

N87-13204# Xerox Corp., Palo Alto, Calif. Intelligent Systems Lab.
SOAR USER'S MANUAL Report, 1 Jan. 1982 - 15 Jun. 1985
John E. Laird 31 Jan. 1986 118 p
(Contracts N00014-82-C-0067; F33615-81-K-1539)
(AD-A169005; ISL-15) Avail: NTIS HC A06/MF A01 CSCL 05/10

Soar is an architecture for general intelligence that has been applied to a variety of tasks: many of the classic artificial intelligence (AI) toy tasks such as the Tower of Hanoi, and the Blocks World; tasks that appear to involve complex, non-search reasoning, such as syllogisms, the three wise men puzzle, and sequence extrapolation; and large tasks requiring expert-level knowledge, such as the R1 computer-configuration task. This chapter provides a brief overview of the Soar architecture. In Soar, every task or problem is formulated as heuristic search in a problem space to achieve a goal. A problem space consists of a set of states and a set of operators that transform one state into another. Problem solving is the process of moving from a given initial state in the problem space through immediate states generated by operators until a desired state is reached that is recognized as attaining the goal. For each goal, there is always a single current problem space, state, and operator. The current problem space, state and operator, together with the goal, form a context. Goals (and their contexts) can have subgoals (and associated contexts), which form a strict goal-subgoal hierarchy. Soar is an architecture for problem solving and learning, based on heuristic search and chunking. GRA

64 NUMERICAL ANALYSIS

Includes iteration, difference equations, and numerical approximation.

N87-13205# Instituto de Pesquisas Espaciais, Sao Jose dos Campos (Brazil).
A GENERALIZED PROJECTION METHOD FOR THE SOLUTION OF ALGEBRAIC LINEAR SYSTEMS
Ricardo L. U. deFreitasPinto and Atair Rios Neto Apr. 1986 21 p Sponsored by Instituto de Pesquisas Espaciais, Sao Jose dos Compos (Brazil) Submitted for publication
(INPE-3874-PRE/930) Avail: NTIS HC A02/MF A01

A sequential procedure for the solution of systems of algebraic linear equations with the number of equations less than or equal to the number of unknowns is presented. Following a strategy based on properties of matrices that can be considered as a generalization of the concept of a projection matrix, an algorithm is developed with a structure inspired in the linear estimation Kalman filter. Associated properties are presented and explored in terms of practical applications, together with numerical examples. The applications include pseudoinversion, optimization of quadratic objective functions with linear constraints, and iterative techniques for the solution of ill-conditioned linear systems. Author

N87-13206# Instituto de Pesquisas Espaciais, Sao Jose dos Campos (Brazil).
PERFORMANCE ANALYSIS OF SOME NUMERICAL ALGORITHMS IN THE RESOLUTION OF ODES ARTIFICIAL SATELLITE PROBLEMS [ANALISE DE DESEMPENHO DE ALGUNS ALGORITMOS NUMERICOS NA RESOLUCAO DE EDOS EM PROBLEMAS DE SATELITES ARTIFICIAIS]
Kondapalli Rama Rao Sep. 1986 16 p In PORTUGUESE; ENGLISH summary Presented at the 7th Congresso Latino-Americano sobre Metodos Computacionais para Engenharia, Sao Carlos, Brazil, 4-7 December 1986
(INPE-3996-PRE/995) Avail: NTIS HC A02/MF A01

A preliminary analysis of performance of some numerical algorithms (three Runge-Kutta algorithms of different orders, one multistep algorithm, and two extrapolation algorithms) for the resolution of ordinary differential equations (ODEs) of artificial satellite problems, is performed. Choosing a set of test problems, the analysis is done comparing these algorithms in terms of number of derivative function evaluations, accuracy obtained, overhead, and total processing time. The preliminary results and some useful conclusions concerning these algorithms are presented. Author

N87-13207# Clarkson Univ., Potsdam, N.Y. Dept. of Mathematics and Computer Science.
NONLINEAR WAVES Final Report, 1 Jun. 1976 - 31 May 1986
Mark J. Ablowitz and Athanssisos S. Fokas 27 May 1986 144 p
(Contract N00014-76-C-0867)
(AD-A168934) Avail: NTIS HC A07/MF A01 CSCL 12/1

The central theme involved in this work is the continuing study of certain fundamental features associated with the nonlinear wave propagation arising in and motivated by physical problems. The usefulness of the work is attested to by the varied applications, and wide areas of interest in physics, engineering and mathematics. The work accomplished involves wave propagation in a number of areas including fluid mechanics, plasma physics, theoretical physics, statistical mechanics, nonlinear optics, multidimensional solitons, multidimensional inverse problems, Painleve equations, direct linearization of certain nonlinear wave equations, DBAR problems, Riemann Hilbert boundary value problems, algebraic methods and symmetry analysis of multidimensional systems, differential geometry, etc. Of particular interest to the Navy is the recent discovery that many of the equations describing ship

hydrodynamics in channels of finite depth obey nonlinear equations which have been studied extensively. GRA

N87-13208# Chicago Univ., Ill.
SOME INVESTIGATIONS INTO VARIABLE MESHES FOR NUMERICAL SOLUTION OF PARTIAL DIFFERENTIAL EQUATIONS Final Report, Jul. 1982 - Jul. 1985
Todd F. Dupont 22 May 1986 9 p
(Contract DAAG29-82-K-0157)
(AD-A168977; ARO-19524.1-MA) Avail: NTIS HC A02/MF A01 CSCL 12/1

This study involved investigation of numerical methods for the approximate solution of partial differential equations. Specifically, the following two topics were investigated: Spatial meshes that change with time; and Space-time finite elements. The work involved both theoretical investigations and computational experiments. GRA

N87-13209# Rice Univ., Houston, Tex. Dept. of Mathematical Sciences.
ITERATIVE METHODS FOR LARGE LINEAR AND NONLINEAR LEAST SQUARES PROBLEMS Final Report, 1 Feb. 1983 - 31 Jan. 1986
John E. Dennis 31 Mar. 1986 6 p
(Contract DAAG29-83-K-0035)
(AD-A169028; ARO-19428.4-MA) Avail: NTIS HC A02/MF A01 CSCL 12/1

Under a grant to 8 graduate students the most exciting research accomplishment is a new trust region approach to global convergence for nonlinear programming problems. Testing has also begun on a variable metric variant of the Kamarkar linear programming algorithm that could be of great practical significance if very preliminary tests are any indication. Other interesting work has been a unified convergence analysis for the many variants of the conjugate gradient method, a convergence analysis of the popular Nelder-Mead algorithm, a novel use of interactive computer graphics to obtain user preferences in multi-objective optimization, a convergence analysis of the EM algorithm for mixture density estimation, and a survey of all the work done by researchers in various fields on nonlinear programming problems in which some subset of the variables always appear linearly. GRA

N87-13210# Stanford Univ., Calif. Dept of Operations Research.
THE OPTIMAL LINEAR COMBINATION OF CONTROL VARIATES IN THE PRESENCE OF BIAS
Peter W. Glynn and Donald L. Iglehart Mar. 1986 23 p
(Contract DAAG29-84-K-0030; Grant NSF ECS-84-04809)
(AD-A169111; TR-12; ARO-20927.12-MA) Avail: NTIS HC A02/MF A01 CSCL 12/1

The method of control variates has been extensively studied as a technique for obtaining variance reductions for complex simulations. The method basically requires that the practitioner be able to identify processes for which the asymptotic mean is known; the knowledge of those asymptotic means is then used to obtain a variance reduction. The authors' goal is to study a specific aspect of the small-sample theory for control variates. Their particular interest focuses on the loss of efficiency incurred when only the asymptotic mean is known, as opposed to the true (small-sample) mean. The results obtained have implications for the application of control variates to the steady-state estimation problem. Specifically, in many steady-state simulations, only the asymptotic means of the control variates are known. The results obtained here complement other small-sample studies on control variates in which the focus is on the degradation in performance caused by estimation of the optimal control coefficients. Our methods can also be used to study small-sample properties of the method of multiple estimates. GRA

N87-13211# California Univ., Berkeley.
AN INTUITIVE APPROACH TO GEOMETRIC CONTINUITY FOR PARAMETRIC CURVES AND SURFACES
Tony D. DeRose and Brian A. Barsky 1986 11 p
(Contracts N00039-84-C-0089; ARPA Order 4871)
(AD-A169654) Avail: NTIS HC A02/MF A01 CSCL 12/1

This report defines the nth order geometric continuity for parametric curves and surfaces, and derived the Beta constraints that are necessary and sufficient for it. Derivation of the Beta constraints is based on a simple principle of reparametrisation in conjunction with the univariate chain rule for curves, and the bivariate chain rule for surfaces. This approach uncovers the connection between geometric continuity for curves and geometric continuity for surfaces, provides new insight into the nature of geometric continuity in general, and allows the determination of the Beta constraints with less effort than previously required. Use of the Beta constraints for G to the nth power continuity allows the introduction of n shape parameters for curves, and $n(n+3)$ shape functions for surfaces. The shape parameters and shape functions may be used to modify the shape of a geometrically continuous curve or surface, respectively. However, geometric continuity is only appropriate for applications where rate aspects of the parametrisations are unimportant since discontinuities in rate are allowed. GRA

N87-13212# Maryland Univ., College Park. Inst. for Physical Science and Technology.
REGULARITY OF THE SOLUTION OF ELLIPTIC PROBLEMS WITH PIECEWISE ANALYTIC DATA. PART 1: BOUNDARY VALUE PROBLEMS FOR LINEAR ELLILPTIC EQUATION OF SECOND ORDER Final Report
I. Babuska and B. Guo May 1986 73 p
(Contract N00014-85-K-0169)
(AD-A169771; BN-1047-Pt-1) Avail: NTIS HC A04/MF A01 CSCL 12/1

This paper is the first in a series devoted to the analysis of the regularity of the solution of elliptic partial differential equations with piecewise analytic data. The present paper analyzes the case of linear, second order partial differential of elliptic type. These results are essential for the design and the analysis of the h-p version of the finite element method for solving the elliptic differential equations of structural engineering. GRA

N87-13213# Maryland Univ., College Park. Inst. for Physical Science and Technology.
ASYMPTOTICALLY EXACT A-POSTERIORI ERROR ESTIMATOR FOR BIQUADRATIC ELEMENTS Final Report
Ivo Babuska and Dehao Yu (Academia Sinica, Beijing (China).) Jun. 1986 35 p
(Contract N00014-85-K-0169; Grant NSF DMS-83-15216)
(AD-A169798; AD-E900585; BN-1050) Avail: NTIS HC A03/MF A01 CSCL 12/1

The paper addresses the finite element method with a-posterioria error estimation for elements of degree p=1 and p=2. It gives the formulae for the error indicators and error estimators. Basic mathematical characterization of the estimators are given and it is shown that the estimators for $p = 1$ and $p = 2$ have different structures. Numerical examples show the effectivity of the approach and the high quality of the estimator. GRA

N87-13214# Maryland Univ., College Park. Inst. for Physical Science and Technology.
AN EXPERT-SYSTEM-LIKE FEEDBACK APPROACH IN THE HP-VERSION OF THE FINITE ELEMENT METHOD Final Report
I. Babuska and Ernst Rank May 1986 53 p
(Contract N00014-85-K-0169)
(AD-A169855; AD-E750914; BN-1048) Avail: NTIS HC A04/MF A01 CSCL 12/1

It has been theoretically shown that exponential rate of convergence in the energy norm can be obtained by a proper combination of the h- and p- extension of the finite element method for essentially all engineering problems in plane elasticity, including those with singularities in the exact solution. In this paper we present an expert system frame, which guides the user to an optimal selection of the mesh and degree distribution. After a crude preliminary computation the expert system predicts the

performance of various mesh and degree combinations and provides the analyst with rational support for his decisions about the mesh design, numerical examples show that the suggested approach gives superior results with minimum effort in human data preparation and computer time. GRA

N87-13215# Maryland Univ., College Park. Dept. of Management Sciences and Statistics.
NOTE ON A CHARACTERIZATION OF EXPONENTIAL DISTRIBUTIONS Technical Report, Sep. 1985 - Aug. 1986
Samuel Kota and F. W. Steutel Jul. 1986 5 p
(Contract N00014-84-K-0301)
(AD-A169896; UM/MSS-86/4) Avail: NTIS HC A02/MF A01 CSCL 12/1

Let U be uniformly distributed on (0,1) and let Y and Y' =(d) Y be random vectors with nonnegative components, U, Y and Y' independent. It is shown that the relation Y =(d) U(Y + Y') is satisfied if and only if the components of Y are multiples of a single exponentially distributed random variable. M.G.

N87-13216# Colorado Univ., Boulder. Dept. of Computer Science.
SOLVING SYSTEMS OF NONLINEAR EQUATIONS BY TENSOR METHODS
Robert B. Schnabel and Paul D. Frank Jun. 1986 32 p
(Contract DAAG29-84-K-0140; NSF DCR-84-03483)
(AD-A169927; CU-CS-334-86; ARO-21453.3-MA) Avail: NTIS HC A03/MF A01 CSCL 12/1

Tensor methods are a class of general purpose methods for solving systems of nonlinear equations. They are especially intended to efficiently solve problems where the Jacobian matrix at the solution is singular or ill-conditioned, while remaining at least as efficient as standard methods on nonsingular problems. Their distinguishing feature is that they base each iteration on a quadratic model of the nonlinear function. The model has a simple second order term that allows it to interpolate more information about the nonlinear function than standard, linear model based methods, without significantly increasing the cost of forming, storing, or solving the model. This paper summarizes two types of tensor methods, derivative tensor methods that calculate an analytic or finite difference Jacobian at each iteration, and secant tensor methods that avoid Jacobian evaluations. Both are shown to require no more function or derivative information per iteration, and hardly more storage or arithmetic operations per iteration, than standard linear model based methods. Computational results are presented that indicate that both tensor methods are consistently at least as reliable as the corresponding linear model based methods, and are significantly more efficient, both on nonsingular and on singular test problems. Author (GRA)

N87-13217# Pittsburgh Univ., Pa. Center for Multivariate Analysis.
VALIDITY OF EDGEWORTH EXPANSIONS OF MINIMUM CONTRAST ESTIMATORS FOR GAUSSIAN ARMA PROCESSES
Masanobu Taniguchi Dec. 1985 45 p
(Contract F49620-85-C-0008)
(AD-A169931; TR-85-49; AFOSR-86-0398TR) Avail: NTIS HC A03/MF A01 CSCL 12/1

Let (X sub t) be a Gaussian Autoregression Multivariant Analysis (ARMA) process with spectral density f sub p (lambda), where p is an unknown parameter. To estimate multivarant analysis we propose a minimum contrast estimation method which includes the maximum likelihood method and the quasi-maximum likelihood method as special cases. Let p-bar sub T be the minimum contrast estimator of p. Then we derive the Edgeworth expansion of the distribution of p-bar sub T up to third order, and provide its validity. By this Edgeworth expansion we can see that this minimum contrast estimator is always second-order asymptotically efficient in the class of second-order asymptotically median unbiased estimators. Also the third-order asymptotic comparisons among minimum contrast estimators will be discussed. GRA

N87-13218# Maryland Univ., College Park. Dept. of Mathematics.
ZERO-CROSSINGS ANALYSIS
Benjamin Kedem Jan. 1986 73 p
(Grant AF-AFOSR-0187-82)
(AD-A169937; AFOSR-86-0413TR) Avail: NTIS HC A04/MF A01 CSCL 12/1

A coherent development of zero crossing based methods and theory appropriate for fast signal analysis are advanced. Quite a few ideas pertaining to zero crossing counts found in the literature can be expressed and interpreted with the help of this more general setup. A central issue addressed in some detail, is the fruitful connection which exists between zero crossing counts and linear filtering. This connection is explored and interpreted with the help of a certain zero crossing spectral representation, is then applied in spectral analysis, detection and discrimination. Zero crossing counts in filtered time series are called higher order crossings. The theme of the work is that higher order crossings analysis provides a useful descriptive as well as analytical tool that can in many respects match spectral analysis. To a great extent these two types of analysis are in fact equivalent, but each emphasizes a different point of view. Advantages offered by higher order crossings are great simplicity and a drastic data reduction. GRA

N87-13219# Arizona Univ., Tucson.
INEQUALITIES FOR PROBABILITY CONTENTS OF CONVEX SETS VIA GEOMETRIC AVERAGE
Moshe Shaked and Y. L. Tong Nov. 1985 19 p Prepared in cooperation with Georgia Inst. of Tech.
(Grants NSF MCS-82-00096; AF-AFOSR-0205-84)
(AD-A169938; AFOSR-86-0399TR) Avail: NTIS HC A02/MF A01 CSCL 12/1

This paper derives an inequality for a large class of density functions and a large class fo convex sets. The most general results are given for the bivariate case. An extention to the n-dimensional case appears to be difficult except for some special cases such as the case of independent identically distributed random variables or when the underlying joint density is spherically symmetric. The class of convex sets considered includes D sub infinity and D sub 2 as special cases and special applications are given for elliptically contoured distributions and scale parameters families. In al! these cases, universal upper bounds on the probability contents can be given by substituting the values of the a sub i's by their geometric mean. GRA

N87-13220# Massachusetts Inst. of Tech., Cambridge. Lab. for Information and Decision Systems.
LONG TIME ESTIMATES FOR THE HEAT KERNEL ASSOCIATED WITH A UNIFORMLY SUBELLIPIC SYMMETRIC SECOND ORDER OPERATOR
S. Kusuoka (Tokyo Univ. (Japan).) and D. Stroock Jun. 1986 39 p
(Contract DAAG29-84-K-0005; Grant NSF DMS-84-15211)
(AD-A169949; LIDS-P-1568; ARO-20980.54-MA) Avail: NTIS HC A03/MF A01 CSCL 12/1

Second order subelliptic operators have been the subject of a considerable amount of research in recent years. Starting with the paper Rothschild and Stein, in which the sharp form of Hormander's famous subellipticity theorem is proved, and continuing through the work of Fefferman and Phong and Sanchez-Calle, it has become increasingly clear that precise regularity estimates for these operators depend intimately on the geometry associated with the operator under consideration. The main purpose of this article is to obtain bounds, from above and below, on p(t,x,y), t epsilon (1, infinity), in terms of standard heat kernels. GRA

N87-13221# Massachusetts Inst. of Tech., Cambridge. Lab. for Information and Decision Systems.
UPPER BOUNDS FOR SYMMETRIC MARKOV TRANSITION FUNCTIONS
E. A. Carlen, S. Kusuoka (Tokyo Univ. (Japan).), and D. W. Stroock Jun. 1986 52 p
(Contract DAAG29-84-K-0005; Grant NSF DMS-84-15211)

(AD-A170010; LIDS-P-1569; ARO-20980.53-MA) Avail: NTIS HC A04/MF A01 CSCL 12/1

A large number of properties which are peculiar to symmetric Markov semigroups stem from the fact that such semigroups can be analyzed simultaneously by Hilbert space techniques as well as techniques coming from maximum principle considerations. The feature of symmetric Markov semigroups in which this fact is most dramatically manifested is the central role played by the Dirichlet form. In particular, the Dirichlet form is a remarkably powerful tool with which to compare symmetric Markov semigroups. The present paper consists of a number of examples which illustrate this point. There exist tight relationships between uniform decay estimates on the semigroup and certain Sobolev like inequalities involving the Dirichlet form. GRA

N87-13222# Maryland Univ., Baltimore. Dept. of Mathematics.
THE h-p VERSION OF THE FINITE ELEMENT METHOD WITH QUASIUNIFORM MESHES Summary Report
Ivo Babuska and Manil Suri 1 May 1986 64 p
(Grants NSF DMS-83-15216; AF-AFOSR-0322-85)
(AD-A170144; MRR-86-1; AFOSR-86-0362TR) Avail: NTIS HC A04/MF A01 CSCL 12/1

The h-p version is analyzed with a quasiuniform mesh and uniform p to get an error estimate which is simultaneously optimal in both p and h. Estimates are also proven for the h-p version when the solution has singularities in the corners of the domain and in the case when essential (Dirichlet) conditions are prescribed but are not in the subspace of finite elements. Finally, a numerical example is presented which illustrates the applicability of the developed (asymptotic) theory in a range of h and p used in practice. B.G.

N87-13223# Clarkson Univ., Potsdam, N.Y.
EIGENVECTORS OF GRAPHS Annual Report, 1 Jul. 1985 - 1960 Jun. 1986
David L. Powers 26 Jun. 1986 11 p
(Contract N00014-85-K-0497)
(AD-A170562) Avail: NTIS HC A02/MF A01 CSCL 12/1

Let z be an eigenvector of the adjacency matrix A of a connected graph G. Say a vertix is positive, nonnegative, zero, etc. if the same is true of the corresponding element of z. If z is an eigenvector for the second largest eigenvalue of A, it is known that the nonnegative vertices of G form a connected subgraph. This separation of vertices according to sign provides the basis for studying the structure of G as revealed by its eigenvectors, inequalities on the number of edges joining positive and negative vertices, bounds on the number of zero vertices, bounds on multiplicities and some description of the variability of the elements of z. The rows of an eigenmatrix provide a mapping of the vertices of G into m-dimensional euclidean space. Some graphs thus draw themselves. This phenomenon is especially interesting if the graph is the skeleton of a polytope. GRA

N87-13224# North Carolina Univ., Chapel Hill. Center for Stochastic Processes.
SEMIGROUPS AND POISSON-APPROXIMATION Technical Report, Sep. 1985 - Aug. 1986
P. Deheuvels and D. Pfeifer Dec. 1985 13 p
(Contract F49620-85-C-0144)
(AD-A170944; AFOSR-86-0339TR; TR-132) Avail: NTIS HC A02/MF A01 CSCL 12/1

This paper extends previous work of the authors on Poisson approximation for (general) independent Bernoulli summands with respect to the total variation distance, without imposing any conditions on the underlying parameters. This enables one to study also the case of unbounded means, without asymptotic uniform smallness of the individual summands, provided that the variance increases with the same rate as the mean. An important practical situation in which such an asymptotic behavior occurs is described by Ross's Markov chain model for the Simplex Algorithm in linear programming, which will be discussed as an example of possible application. Author (GRA)

N87-13225# Stanford Univ., Calif. Dept. of Operations Research.
ALGORITHM FOR POSITIVE DEFINITE LEAST SQUARE ESTIMATION OF PARAMETERS
Hui Hu May 1986 17 p
(Contract DE-AS03-76ER-72018)
(DE86-012159; SOL-86-12) Avail: NTIS HC A02/MF A01

An algorithm for positive definite least square estimation of parameters is presented. This estimation problem arises from the PILOT dynamic macro-economic model and is equivalent to an infinite convex quadratic program. It differs from ordinary least square estimations in that the fitting matrix is required to be positive definite. The algorithm solves the infinite convex quadratic program by generating and solving a sequence of ordinary convex quadratic programs. By specifying a constant, the algorithm will find an approximate optimal solution after finitely many interations, or will tend to an optimal solution in the limit. The algorithm is generalized to solve a class of infinite convex programs. DOE

N87-13226# Oak Ridge National Lab., Tenn.
QUANTITATIVE ASSESSMENT OF THE EFFECT OF PARTIAL PIVOTING IN SPARSE ORDINARY DIFFERENTIAL EQUATION SOLVERS
S. Thompson May 1986 29 p
(Contract DE-AC05-84OR-21400)
(DE86-012592; ORNL-6207) Avail: NTIS HC A03/MF A01

The effect of partial pivoting in automatic ordinary differential equation solvers which utilize sparse matrix techniques is discussed. Two solvers are considered, the well-known LSODES solver and a derivate LSOD28. LSODES uses the Yale Sparse Matrix Package which does not perform partial pivoting. LSOD28 uses the Harwell MA28 Sparse Matrix Package which does perform partial pivoting. Results are presented for a benchmark problem which contains several features typically present in realistic problems. The results demonstrate that both solvers perform satisfactorily. At the same time, they demonstrate the relative effects of partial pivoting for the benchmark problem. In particular, they suggest that partial pivoting substantially improves neither the efficiency nor the reliability of LSODES for such problems. They support the argument that partial pivoting is not necessarily required in adaptive solvers to solve complex problems accurately and efficiently. DOE

N87-13227*# National Aeronautics and Space Administration. Langley Research Center, Hampton, Va.
QUALITY ASSESSMENT AND CONTROL OF FINITE ELEMENT SOLUTIONS Final Report
I. Babuska (Maryland Univ., College Park.) and Ahmed K. Noor May 1986 50 p Prepared in cooperation with George Washington Uni
(Grant NGR-09-010-078; Contract N00014-85-K-0169)
(NASA-TM-89208; NAS 1.15:89208; AD-A169773; BN-1049) Avail: NTIS HC A03/MF A01 CSCL 12/1

Status and some recent developments in the techniques for assessing the reliability of finite element solutions are summarized. Discussion focuses on a number of aspects including: the major types of errors in the finite element solutions; techniques used for a posteriori error estimation and the reliability of these estimators; the feedback and adaptive strategies for improving the finite element solutions; and postprocessing approaches used for improving the accuracy of stresses and other important engineering data. Also, future directions for research needed to make error estimation and adaptive movement practical are identified. Author (GRA)

65 STATISTICS AND PROBABILITY

Includes data sampling and smoothing; Monte Carlo method; and stochastic processes.

N87-13228# Princeton Univ., N. J.
DESIGN AND ANALYSIS OF EXPERIMENTS AND MORE REAL-

ISTIC TECHNIQUES FOR DATA ANALYSIS Final Report, 30 Jun. 1976 - 31 Jan. 1986
John W. Tukey Mar. 1986 51 p
(Contract DAAG29-79-C-0205; Grant DAAG29-76-G-0298)
(AD-A168921; ARO-19442.26-MA; ARO-14244.15-MA; ARO-16669.28-MA) Avail: NTIS HC A04/MF A01 CSCL 12/1

The research has focused on on data analysis techniques. Some of the more innovative contributions include: graphical analysis of variance, configural polysampling, so far the only direct approach to robustness in actual finite-sized samples, compromise MLEs as a more flexible, often closely approximate approach to robustness, calculations for many explicit randomizations as the trustworthy and stringent analysis for the randomized experiment, simple devices for presenting motion using an overhead projector, work on pushback techniques and related ideas, effective confidence intervals based on only 2 of the observed values in a sample, new insight into multiple comparisons, fits with many exact-zero residuals sharing other good properties, and a deeper insight into, and robust procedures for, analysis of variance. GRA

N87-13229# Illinois Univ., Chicago. Dept. of Information and Decision.
STATISTICAL MODELS AND METHODS FOR CLUSTER ANALYSIS AND IMAGE SEGMENTATION Final Report, 15 Jun. 1982 - 15 Jun. 1985
Stanley L. Sclove 15 Mar. 1986 18 p
(Contract DAAG29-82-K-0155)
(AD-A169145; U1C/DQM/ARO-85-2; ARO-19085.12-MA) Avail: NTIS HC A02/MF A01 CSCL 17/8

Clustering of individuals, segmentation of time series and segmentation of numerical images can all be considered as labeling problems, for each can be described in terms of pairs (x sub t, g sub t), t = 1,2,...,n, where x sub t is the observation at instance t and g sub t is the unobservable label of instance t. The labels are to be estimated, along with any unspecified distributional parameters. In cluster analysis the values of t are the individuals (cases) observed and the x's are independent. In time series the values of t are time instants and there is temporal correlation. In numerical image segmentation the values of t denote picture elements (pixels) and spatial correlation between neighboring pixels can be utilized. The idea in segmentation is that signals and time series often are not homogeneous but rather are generated by mechanisms or processes with various phases. Similarly, images are not homogeneous but contain various objects. Segmentation is a process of attempting to recover automatically the phases or objects. Author (GRA)

N87-13230# Florida State Univ., Tallahassee. Dept. of Statistics.
ASYMPTOTIC THEORY FOR SIEVE ESTIMATORS IN SEMI-MARTINGALE REGRESSION MODELS
Ian W. McKeague Mar. 1986 35 p
(Contract DAAG29-82-K-0168)
(AD-A169207; FSU-STATISTICS-M722; TR-D-86-ARO; ARO-19367.35-MA) Avail: NTIS HC A03/MF A01 CSCL 12/1

This paper studies the estimation of functions alpha sub 1, ..., alpha sub p describing the temporal influence of p covariate processes in a regression model for semi-martingales. McKeague (1986) introduced sieve estimators for alpha sub 1, ..., alpha sub p and established consistency in sq l-norm. In this paper the asymptotic distribution theory for the integrated sieve estimators is developed. Smoothed sieve estimators are shown to be pointwise consistent and rates of convergence are provided. Author (GRA)

N87-13231# Stanford Univ., Calif. Dept. of Operations Research.
RECURSIVE MOMENT FORMULAS FOR SEMI-MARKOV PROCESSES
Chia-Hon Chien Apr. 1986 30 p
(Contract DAAG29-84-K-0030; Grant NSF MCS-82-03483)
(AD-A169253; ARO-20927.13-MA; SU-TR-13) Avail: NTIS HC A03/MF A01 CSCL 12/1

Let X = (X(t):t > or = 0) be an irreducible semi-markov process (SMP) on countable state space E. For fixed Z an element of E, let T(z) =inf(t > or = 0:X(t-)not =z, X(t)=z) and set Y(f) = integral from 0 to T sub z of f(X(t))dt, where f: E approaches R is an arbitrary function. Our objective is to study the mixed moments of the form E pi from i = 1 to r of Y(f sub i), when f sub i: E approaches R is an arbitrary function, for i = 1,2,...r, and r is a positive integer. This quantity is especially relevant to the regenerative simulation. Also, several useful variations and generalizations are introduced and studied. GRA

N87-13232# Florida State Univ., Tallahassee. Dept. of Statistics.
A REVERSAL ARGUMENT FOR STORAGE MODELS DEFINED ON SEMI-MARKOV PROCESSES
Eric S. Tollar Feb. 1986 39 p
(Contract DAAG29-82-K-0168)
(AD-A169262; FSU-TR-M721; TR-D-85-ARO; ARO-19367.36-MA) Avail: NTIS HC A03/MF A01 CSCL 12/1

For many storage models defined on some semi-Markov process X(t), the asymptotic distribution of the imbedded discrete time process can often be determined by exploiting the properties of the dual of the underlying Markov chain X sub n, which effectively reverses the process. If this is the case, a technique is given which under certain regularity conditions shows the asymptotic distribution of the entire continuous time process can be obtained, and is equal to an altered version of the reversed discrete time process. It is shown this method not only can be applied to models where the asymptotic distribution was previously unknown, but can also improve upon characterizing many of the results for models in which the asymptotic behavior is obtained by a renewal argument. Author (GRA)

N87-13233# Stanford Univ., Calif. Dept. of Statistics.
A UNIFIED APPROACH TO CONSTRUCTING NONPARAMETRIC RANK TESTS
Douglas E. Critchlow 6 Jul. 1986 66 p
(Contract N00014-86-K-0156)
(AD-A169815; TR-376) Avail: NTIS HC A04/MF A01 CSCL 12/1

One shortcoming of the present theory of rank tests is that such tests have usually been constructed on a case by case basis, in a quite ad hoc (albeit clever) manner. This paper attempts to provide the basis for a more unified approach to rank tests. It investigates a general, yet simple construction, which simultaneously generates many rank test statistics, for a multitude of hypothesis testing situations. The proposed construction uses metrics on the permutation group in a novel way: the proposed test statistic is the distance between two sets of permutations. This new construction is applied systematically to the two-sample and multi-sample location problems, the two-way layout problem, the one-sample location problem, the two-sample dispersion problem with equal medians, and the problem of testing for trend. It is shown that the construction works in a variety of testing situations; gives rise to many familiar rank test statistics; produces several other test statistics which are less familiar, yet equally plausible; and enables one to extend rank tests to other hypothesis testing situations. Some connections with the existing nonparametric theory are discussed. GRA

N87-13234# Georgia Inst. of Tech., Atlanta.
HEREDITY OF STATIONARY AND REVERSIBLE STOCHASTIC PROCESSES
Richard F. Serfozo 25 Mar. 1986 6 p
(Grant AF-AFOSR-0367-84)
(AD-A169926; AFOSR-86-0381TR) Avail: NTIS HC A02/MF A01 CSCL 12/1

When a stochastic process (a random measure, set, field, etc. on a group) is stationary, ergodic, or reversible, then certain functions of this process inherit these properties. This document presents sufficient conditions for this inheritance. Author (GRA)

N87-13235# Georgia Inst. of Tech., Atlanta.
EXTREME VALUES OF BIRTH AND DEATH PROCESSES AND QUEUES
Richard F. Serfozo 25 Mar. 1986 28 p
(Grant AF-AFOSR-0367-84)
(AD-A169932; AFOSR-86-0384TR) Avail: NTIS HC A03/MF A01 CSCL 12/1

This document studies the asymptotic behavior of maximum values of birth and death processes over large time intervals. In most cases, the distributions of these maxima, under standard linear normalizations, either do not converge or they converge to a degenerate distribution. However, by allowing the birth and death rates to vary in a certain manner as the time interval increases, we show that the maxima do indeed have three possible limit distributions. Two of these are classical extreme value distributions and the third one is a new distribution. This third distribution is the best one for practical applications. Our results are for transient as well as recurrent birth and death processes and related queues. For transient processes, the focus is on the maxima conditioned that they are finite. Author (GRA)

N87-13236# South Carolina Univ., Columbia. Dept. of Statistics.
SMOOTH NONPARAMETRIC QUANTILE ESTIMATION UNDER CENSORING: SIMULATIONS AND BOOTSTRAP METHODS
W. J. Padgett and L. A. Thombs May 1986 29 p
(Contract MIPR-ARO-139-85; Grant AF-AFOSR-0156-84)
(AD-A169935; TR-116; Rept-62N05-17; AFOSR-86-0431TR) Avail: NTIS HC A03/MF A01 CSCL 12/1

The objectives of this paper are two-fold. One is to report results of extensive Monte Carlo simulations which demonstrate the behavior of the mean squared error of the kernel estimator with respect to bandwidth. These simulations provide a method of choosing an optimal bandwidth when the form of the lifetime and censoring distributions are known. Also, they compare the kernel-type estimator with the product-limit qauntile estimator. Five commonly used parametric lifetime distributions, two censoring mechanisms, and four different kernel functions are considered in this study, which is an extension of the brief simulations for exponential distributions reported by Padgett (1986). The second objective is to present a nonparametric method for bandwidth selection based on the bootstrap for right-censored data. This data-based procedure used the bootstrap to estimate mean squared error, and is both an extension and modification of the methods proposed by Padgett. Bandwidth selection using the bootstrap is important for small and moderately large samples since no exact expressions exist for the mean squared error of the kernel-type quantile estimator. GRA

N87-13237# North Carolina Univ., Chapel Hill. Chapel Hill Center for Stochastic Processes.
EXTREMAL PROCESSES, RECORD TIMES AND STRONG APPROXIMATION
Dietmar Pfeifer Dec. 1985 15 p
(Contract F49620-85-C-0144)
(AD-A169972; TR-131; AFOSR-86-0340TR) Avail: NTIS HC A02/MF A01 CSCL 12/1

Given an i.i.d. sequence of random variables (r.v.'s) with continuous cumulative distribution function (CDF) F, the author presents a simple construction for the jump times of an extremal process on the same probability space which interpolate the given record times. This gives another approach to the strong approximation of extremal processes as developed by Deheuvels (1981, 1982, 1983), and allows for a more detailed investigation of the relationship between the record times of the given sequence and the jump times of the extremal process. In particular, it is shown that the number S of surplus jump time points in (1, infinity) over the record times is approximately Poisson distributed with an exact mean of E(S) = 1 - C, C denoting Euler's constant.
Author (GRA)

N87-13238# Pittsburgh Univ., Pa. Center for Multivariate Analysis.
ON REDUCTION OF DIMENSIONALITY UNDER MULTIVARIATE REGRESSION AND CANONICAL CORRELATION MODELS
P. R. Krishnaiah Apr. 1986 53 p
(Contract F49620-85-C-0008)
(AD-A170025; TR-86-10; AFOSR-86-0343TR) Avail: NTIS HC A04/MF A01 CSCL 12/1

In this paper, the author gives a review of the literature on various techniques for determination of the ranks of regression matrix and canonical correlation matrix. Also, methods of selection of important original variables under multivariate regression and canonical correlation models are reviewed. The methods reviewed involve not only tests of hypotheses but also model selection methods based upon information theoretic criteria. Author (GRA)

N87-13239# Pittsburgh Univ., Pa. Dept. of Mathematics and Statistics.
A MULTIVARIATE EXTENSION OF HOEFFDING'S LEMMA
Henry W. Block and Zhaoben Fang Nov. 1985 24 p
(Contract N00014-84-K-0084; Grant AF-AFOSR-0113-84)
(AD-A170170; TR-85-10; AFOSR-86-0410TR) Avail: NTIS HC A02/MF A01 CSCL 12/1

Hoeffding's Lemma gives an integral representation of the covariance of two random variables in terms of difference between their joint and marginal probability functions. This identity has been found to be a useful tool in studying the dependence structure of various random vectors. A generalization of this result for more than two random variables is given. This involves an integral representation of the multivariate joint cumulant. Applications of this result include characterizations of independence. Relationships with various types of dependence are also given.
Author (GRA)

N87-13240# Arizona Univ., Tucson.
A BAYESIAN APPROACH TO QUANTILE AND RESPONSE PROBABILITY ESTIMATION WITH APPLICATIONS IN RELIABILITY
Moshe Shaked and Nozer D. Singpurwalla (George Washington Univ., Washington, D.C.) Aug. 1985 24 p Prepared in cooperation with George Washington Univ.
(Grant AF-AFOSR-0205-84)
(AD-A170455; AFOSR-86-0352TR) Avail: NTIS HC A02/MF A01 CSCL 12/1

This paper studies a Bayesian approach for the estimation of potency curve which is assumed to be nondecreasing and cocave. This is done by assigning a Dirichlet prior to transformations of some unknown parameters. The choice is made of the prior and investigate several aspects of the problem, such as the properties of the posterior distribution as well as a numerical implementation of the suggested procedure. A procedure for estimating the quantiles is also given. Applications in reliability theory are described. The procedure is illustrated numerically via an example from a government laboratory. GRA

N87-13241# Pittsburgh Univ., Pa. Center for Multivariate Analysis.
PATTERN RECOGNITION BASED ON SCALE INVARIANT DISCRIMINANT FUNCTIONS
Tarmo M. Pukkila and C. R. Rao Apr. 1986 18 p
(Contract F49620-85-C-0008)
(AD-A170809; TR-86-09; AFOSR-86-0575TR) Avail: NTIS HC A02/MF A01 CSCL 12/1

Some probability models for classifying individuals as belonging to one of two or more populations using scale invariant discriminant functions are considered. The investigation is motivated by practical situations where the observed data on an individual are in the form of ratios of some basic measurements or measurements scaled by an unknown non-negative number. The probability models are obtained by considering a p-vector random variable X with a known distribution and deriving the distribution of the random vector Y = G(X) .1 X, where G(X) is a non-negative measure of size such that G(lambda X) = Lambda G(X) for lambda > 0. Explicit expressions are obtained for the densities of what are called

Angular Gaussian, Compositional Gaussian, Type 1 and Compositional Gaussian, Type 2 distributions. Author (GRA)

N87-13242# California Univ., Berkeley. Lawrence Berkeley Lab.
TWO ISSUES CONCERNING THE ANALYSIS OF GROUPED DATA
S. Selvin Feb. 1986 15 p Presented at the Conference of the Society for Epidemiologic Research, Pittsburg, Pa., 11 Jun. 1986
(Contract DE-AC03-76SF-00098)
(DE86-008401; LBL-20963; CONF-860694-1) Avail: NTIS HC A02/MF A01

Simple statistical models are used to illustrate two important issues arising in the analysis of grouped data. The consequences are explored of grouping continuous data and analyzing the resulting contingency table. Specifically, an expression for the loss of power is derived when an odds ratio is used to assess risk measured by a continuous variable. Also explored are the consequences of employing correlation and regression coefficients to analyze summary variables derived from grouped data (ecologic data). An expression is given that demonstrates the magnitude of a bias (ecologic fallacy) resulting from analyzing a specific type of grouped data. DOE

66 SYSTEMS ANALYSIS

Includes mathematical modeling; network analysis; and operations research.

N87-13243*# Massachusetts Inst. of Tech., Cambridge. Lab. for Information and Decision Systems.
FEEDBACK SYSTEM DESIGN WITH AN UNCERTAIN PLANT
D. Milich, L. Valavani, and M. Athans Oct. 1986 6 p
(Grant NAG2-297; Contract NOOO14-82-K-0582; Grant NSF ECS-82-10960; NR Proj. 606-003)
(NASA-CR-176887; NAS 1.26:176887; LIDS-P-1614) Avail: NTIS HC A02/MF A01 CSCL 12B

A method is developed to design a fixed-parameter compensator for a linear, time-invariant, SISO (single-input single-output) plant model characterized by significant structured, as well as unstructured, uncertainty. The controller minimizes the H(infinity) norm of the worst-case sensitivity function over the operating band and the resulting feedback system exhibits robust stability and robust performance. It is conjectured that such a robust nonadaptive control design technique can be used on-line in an adaptive control system. Author

N87-13244# Instituto de Pesquisas Espaciais, Sao Jose dos Campos (Brazil).
APPLICATION OF A NETWORK ASSOCIATIVE SCENE ANALYSIS MODEL [EMPREGO DE UM MODELO DE REDE ASSOCIATIVA NA ANALISE DE CENAS]
Paulo Ouvera Simoni and Celso de Renna e Souza Jul. 1986 16 p In PORTUGUESE; ENGLISH summary Presented at the 2nd Portuguese Meeting of Artifical Intelligence, Lisbon, Portugal, 9-11 Oct. 1986
(INPE-3945-PRE/967) Avail: NTIS HC A01/MF A01

A knowledge representation associative network model is described, based in concept structuring and use of formulae and decision rules for relating concepts, plus part and predicate relations. The general decision rule format is such that quantified expressions may occur in the premise and in the conclusion. An inference procedure for the part relation is presented allowing a representation compression, and the problem of conflicts brought about by this procedure is discussed. For the use of the knowledge stored in the network, relative to a given application, a control mechanism is defined, with associated structures that store alterations, in the form of concept and predicate instances, that must be propagated, as well as problems for which solutions are sought. It is shown that these control structures permit forward and backward rule chaining. Characteristics of various scene analysis models are discussed, and it is shown how the control mechanism, associated to a mixed initiative process for obtaining measures, permits a generalization of these models. Author

N87-13245# Institute for Defense Analyses, Alexandria, Va.
DUEL BETWEEN AN ASAT (ANTI-SATELLITE) WITH MULTIPLE KILL VEHICLES AND A SPACE-BASED WEAPONS PLATFORM WITH KINETIC ENERGY WEAPONS Final Report, Oct. 1984 - Dec. 1985
Pythagoras Cutchis Jan. 1986 38 p
(Contract MDA903-84-C-0031)
(AD-A168946; AD-E500768; IDA-M-144; IDA/HQ-86-30858) Avail: NTIS HC A03/MF A01 CSCL 15/3

A mathematical model is described for a duel between a ground-based anti-satellite (ASAT) and a space-based weapons platform defending itself with kinetic energy weapons. The ASAT carries one to six kill vehicles and the space platform may first attack the ASAT booster with one to three defense missiles. If the ASAT kill vehicles collectively survive the boost phase, they are each subject to a post-boost phase attack consisting of one to three defense missiles. A formula for the probability of killing the space platform with a single ASAT launch is derived as a function of the vehicle reliabilities, target detection probabilities, kill probabilities, and number of participating vehicles. Formulas are also given for the probability of kill if the space platform defends itself with a high-energy laser or with both high-energy laser and defense missiles. Illustrative examples are calculated for the case in which the space platform is defended by defense missiles only. It is assumed that all offense and defense reliabilities, detection probabilities, and kill probabilities are equal to 0.90. A sensitivity analysis illustrates the effect of a variation in any one of the assumed parameters on the probability of killing the space platform when all other parameters are held equal to 0.90. GRA

N87-13246# Army Research Office, Research Triangle Park, N. C.
PROCEEDINGS OF THE CONFERENCE ON THE DESIGN OF EXPERIMENTS IN ARMY RESEARCH DEVELOPMENT AND TESTING (31ST) HELD AT THE MADISON, WISCONSIN ON 23-25 OCTOBER 1986 Interim Technical Report
Jun. 1986 292 p
(AD-A169473; ARO-86-2) Avail: NTIS HC A13/MF A01 CSCL 12/1

Partial Contents are approaches to statistical validation of simulation models; Distribution under dependence of nonparametric two-sample tests; statistical models and methods for cluster analysis and segmentation; A comparison of methods for factor analysis of visibility; Small composite design; Considerations in small sample quantal response testing; Human factors affecting subjective judgments; Use of expert opinion in the reliability assessment of the M-1 Abrams tank; Application of hypothesis testing to performance appraisal; Models for contingency table data; On a class of probability density functions; Plotting mathematical functions on a standard line printer; Statistical comparison of the ability of camouflage colors to blend with terrain background under high and low sun angles; Weibull tail modeling for estimating confidence on quantiles from censored samples; The Lindstrom-Madden method for series systems with repeated components; How to display data badly; and Accelerated life test: an overview and some recent advances. GRA

67 THEORETICAL MATHEMATICS

Includes topology and number theory.

N87-13247# California Univ., Santa Barbara. Dept. of Mathematics.
MATRIX THEORY Annual Report, 1 Jul. 1985 - 30 Jun. 1986
Henry K. Minc 20 Jun. 1986 6 p
(Contract N00014-85-K-0489)
(AD-A169139) Avail: NTIS HC A02/MF A01 CSCL 12/1

Research activity during the past year concerned permanents

of (0,1) circulants. A method for constructing a recurrence formula for expressing the permanent of any (0,1)-circulant is developed in terms of permanents of (0,1) circulants of the same type of lower orders. GRA

N87-13248# Stanford Univ., Calif. Systems Optimization Lab.
MAINTAINING LU FACTORS OF A GENERAL SPARSE MATRIX
Philip E. Gill, Walter Murray, Michael A. Saunders, and Margaret H. Wright May 1986 33 p
(Contracts N00014-85-K-0343; DAAG29-84-K-0156; DE-AA03-76SF-00326; DE-AS03-76ER-72018; Grants NSF DCR-84-13211; NSF ECS-83-12142)
(AD-A169255; SU-SOL-86-6) Avail: NTIS HC A03/MF A01 CSCL 12/1

The authors describe a set of procedures for computing and updating an LU factorization of a sparse matrix A, where A may be square (possibly singular) or rectangular. The procedures include a Markowitz factorization and a Bartels-Golub update, similar to those of Reid (1976, 1982). The updates provided are addition, deletion or replacement of a row or column of A, and rank-one modification. (Previously, column replacement has been the only update available). Various design features of the implementation (LUSOL) are described, and computational comparisons are made with the LA05 and MA28 packages of Reid (1976) and Duff (1977). GRA

70 PHYSICS (GENERAL)

For precision time and time interval (PTTI) see *35 Instrumentation and Photography;* for geophysics, astrophysics or solar physics see *46 Geophysics, 90 Astrophysics,* or *92 Solar Physics.*

N87-13249# Department of the Army, Washington, D. C.
PARAMETRIC LINEAR VARIATION OF A LEAKAGE FREE PERMANENT MAGNET FIELD SOURCE Patent Application
Herbert Leupold, Ernest Potenziani, II, and John Clarke, inventors (to Army) Filed 30 May 1986 18 p
(AD-D012359) Avail: NTIS HC A02/MF A01 CSCL 20/3

This patent application discloses a magnetic circuit with a remanence varying cylindrical magnet having a bore and a remanence varying cladding magnet circumscribing the cylindrical magnet creating a longitudinally increasing axial magnetic field within the bore. The cladding magnet has a radial magnetization transverse to the axial magnetization of the cylindrical magnet resulting in a constant magnetic potential along the outer exterior surface of the magnetic circuit. GRA

N87-13250# Crucible Materials Corp., Pittsburgh, Pa. Crucible Research Center.
TEMPERATURE COMPENSATION IN THE 2:17 TYPE MAGNETS Final Report, Jan. 1983 - Dec. 1985
K. S. Narasimhan, F. E. Camp, Bao-Min Ma, and C. J. Willman Mar. 1986 18 p
(Contract DAAG29-83-C-0007)
(AD-A169487; ARO-19511.3-MS) Avail: NTIS HC A02/MF A01 CSCL 20/3

Development of temperature compensated magnets was undertaken in both '2:17' and NdFeB type of alloys. A number of alloys has been identified that can produce energy product in excess of 40 MGOe in the uncompensated material. Computer programs were developed for identifying key compositions that were then processed successfully into temperature compensated magnets. Current materials can produce temperature compensated magnets with an energy product not exceeding 22 MGOe. Further work is necessary to develop temperature compensated magnets with an energy product exceeding 30 MGOe. GRA

71 ACOUSTICS

Includes sound generation, transmission and attenuation. For noise pollution see *45 Environment Pollution.*

N87-13251 ESDU International Ltd., London (England).
COMPUTER-BASED ESTIMATION PROCEDURE FOR COAXIAL JET NOISE. INCLUDING FAR-FIELD SUBSONIC JET MIXING NOISE DATABASE FOR STATIONARY, COPLANAR CONICAL NOZZLES
Sep. 1986 108 p Supersedes ESDU-85043
(ESDU-86019; ISBN-0-85679-571-2; ISSN-0307-0115) Avail: ESDU

This Data Item ESDU 86019 is an addition to the Noise Sub-series. A program listing is provided for interpolating within or extrapolating a data base. The variables considered make it particularly applicable to estimating noise from co-axial jets. A comprehensive data base is provided for jet mixing noise of static engines with conical nozzles, but the user may provide an alternative data base that could include installation and flight effects as well as other noise components (such as combustion and shock noise) or may supplement the provided data base with additinal data. The interpolation/extrapolation routine uses a least-squares fitting procedure in which two or three independent variables may be involved. Two of the variables are the primary jet velocity and the velocity ratio of the two streams but the third may be chosen by the user. Appropriate weighting of the data is included. The program is listed in both BASIC and FORTRAN and is available as appropriate media (magnetic tape or punched cards) as ESDUpac 1055. ESDU 85018 deals with the case of the single-stream jet. ESDU

N87-13252*# National Aeronautics and Space Administration. Lewis Research Center, Cleveland, Ohio.
CRUISE NOISE OF COUNTERROTATION PROPELLER AT ANGLE OF ATTACK IN WIND TUNNEL
James H. Dittmar Oct. 1986 35 p
(NASA-TM-88869; E-3275; NAS 1.15:88869) Avail: NTIS HC A03/MF A01 CSCL 20A

The noise of a counterrotation propeller at angle of attack was measured in the NASA Lewis 8- by 6-Foot Supersonic Wind Tunnel at cruise conditions. Noise increases of as much as 4 dB were measured at positive angles of attack on the tunnel side wall, which represented an airplane fuselage. These noise increases could be minimized or eliminated by operating the counterrotation propeller with the front propeller turning up-inboard. This would require oppositely rotating propellers on opposite sides of the airplane. Noise analyses at different bandwidths enabled the separate front- and rear-propeller tones, as well as the total noise, at each harmonic to be determined. A simplified noise model was explored to show how the observed circumferential noise patterns of the separate propeller tones might have occurred. The total noise pattern, which represented the sum of the front- and rear-propeller tones at a particular harmonic, showed trends that would be hard to interpret without the separate-tone results. Therefore it is important that counterrotation angle-of-attack noise data be taken in such a manner that the front- and rear-propeller tones can be separated. Author

N87-13253# Department of the Air Force, Washington, D.C.
MULTICHANNEL PHASE NOISE MEASUREMENT SYSTEM Patent Application
Stephen P. Caldwell, inventor (to Air Force) Filed 21 Apr. 1986 16 p
(AD-D012372; US-Patent-Appl-SN-853827) Avail: NTIS HC A02/MF A01 CSCL 14/2

A multichannel phase noise measuring system is disclosed which is capable of measuring the phase noise of two signal sources operating between 100 MHz and 24 GHz. This system has two input channels and a mixer which produces a difference frequency betweeen the signals received in the input channels. The difference frequency containing the phase noise is frequency multiplied and amplified to raise the phase noise level 12 dB. The

multiplied and amplified difference signal is phase locked to a commercially available frequency synthesizer with inferior noise characteristics to the units being tested. By amplifying the phase noise of the original signls above the phase noise levels of the commericially available frequency synthesizer, they become measurable. GRA

N87-12951# Joint Publications Research Service, Arlington, Va.
EVALUATING NONLINEAR EFFECTS IN PROPAGATION OF ACOUSTIC PULSE IN ATMOSPHERIC SURFACE LAYER IN INVERSIONS Abstract Only
I. P. Chunchuzov *In its* USSR Report: Earth Sciences (JPRS-UES-86-007) 10 Sep. 1986 2 p Transl. into ENGLISH from Izvestiya Akademii Nauk SSSR: Fizika Atmosfery i Okeana (Moscow, USSR), v. 22, no. 2, Feb. 1986 p 151-159 (For primary document see N87-12946 04-42)
Avail: NTIS HC A06/MF A01

72 ATOMIC AND MOLECULAR PHYSICS

Includes atomic structure, electron properties, and molecular spectra.

N87-13254# Cornell Univ., Ithaca, N.Y. Lab. of Atomic and Solid State Physics.
CALCULATED VERSUS EXPERIMENTAL CHARGE DENSITY DISTRIBUTION OF Be METAL
A. J. Pindor, S. H. Vosko, and C. J. Unrigar Jun. 1986 21 p
(Contract N00014-82-K-0576)
(AD-A168924; TR-23) Avail: NTIS HC A02/MF A01 CSCL 20/8

We have performed self-consistent Linearized Augmented Plane Wave calculations of the charge density of metallic beryllium, with and without warping of the interstitial potential, using the Local Density Approximation for the exchange and correlation energy functional. Overall agreement with the newest x-ray form factors is good, and it is argued that the remaining discrepancies have their source in the inadequacy of the local Density Approximation and, for some reflections, in neglecting the non-sphericity of the core charge density. GRA

N87-13255# Argonne National Lab., Ill.
BAND DESCRIPTION OF MATERIALS WITH LOCALIZING ORBITALS
D. D. Koelling Mar. 1986 31 p Presented at the Special Sanibel Symposium, St. Augustine, Fla., 8 Mar. 1986
(Contract W-31-109-eng-38)
(DE86-010529; CONF-8603121-2) Avail: NTIS HC A03/MF A01

Density functional theory is a form of many-body theory which maps the problem onto an equivalent single particle-like system by limiting to the ground state (or some limited ensemble). So it should be surprising that this ground state theory could have relevance to the excitation properties of a material , and yet it does when used carefully. However, the most interesting materials involve active orbitals which are at least partially localized in space and this has profound effects both on the ground state and the excitation spectrum. A long term interest is in Ce and actinide compounds such that the popular concerns are mixed valence, heavy fermions, and the various forms of magnetic transitions. Band structure calculations can give a great deal of information concerning the mechanisms and degree of the localization as shown by examples using the Ce and U L12 structured materials and the Ce cubic Laves phase materials. There are some difficulties due to an incomplete knowledge of the functionals involved which causes an underestimate of the local character. This is illustrated and discussed. DOE

N87-13256# Oak Ridge National Lab., Tenn.
PHOTOEMISSION FROM OBLATE SILVER SPHEROIDS WITH POLARIZED VACUUM UV EXCITATION
E. T. Arakawa, J. P. Goudonnet, and T. Inagaki 1986 4 p Presented at the 8th International Conference on Vacuum Ultraviolet Radiation Physics, Lund, Sweden, 4 Aug. 1986
(Contract DE-AC05-84OR-21400)
(DE86-008896; CONF-860845-1) Avail: NTIS HC A02/MF A01

A 3 nm thick silver film was evaporated on a quartz slide and then heated for 60 s at 400 C. The resulting spheroids were 60 nm in diameter with average center-to-center distance of 110 nm. These particles were flattened out along the substrate normal with a typical ratio of minor axis length to major axis length being 0.2. Photoemission measurements were made using a Seya-Namioka monochromator with an air discharge lamp. The dependence of the photo yield on the polarization of the incident light was determined with a VUV transmission polarizer made of cleaved LiF plates. DOE

N87-13257# Brookhaven National Lab., Upton, N. Y.
POLARIZED H(-) SOURCE DEVELOPMENT AT BNL
J. G. Alessi, A. Hershcovitch, A. Kponou, T. Niinikoski, and T. Sluyters 1986 4 p Presented at the Linear Accelerator Conference, Stanford, Calif., 2 Jun. 1986
(Contract DE-AC02-76CH-00016)
(DE86-012704; BNL-38233; CONF-860629-16) Avail: NTIS HC A02/MF A01

The AGS polarized H source (PONI-1) now produces currents of 25-40 A, and has operated reliably during polarized physics runs. A new polarized source, having as its goal mA's of H-vector, is now under development. An atomic hydrogen beam has been cooled to about 20 K with a forward flux of approx. 10 atoms/s/sr. A superconducting solenoid having a calculated acceptance angle of 0.1 sr for the cold H beam, is now being built. An ionizer for the resulting polarized H beam based on resonant charge exchange of H with D, is being tested. 500 A of H have been produced by ionizing an unpolarized H beam using this ionizer. DOE

73 NUCLEAR AND HIGH-ENERGY PHYSICS

Includes elementary and nuclear particles; and reactor theory.

For space radiation see *93 Space Radiation.*

N87-13258# Westinghouse Research and Development Center, Pittsburgh, Pa.
MODELS AND RADIATION OF RAILGUN PLASMA ARMATURES WITH NON-IDEAL PLASMA PROPERTIES Final Report, 1 Oct. 1983 - 30 Sep. 1985
Y. C. Thio and L. S. Frost 30 May 1986 52 p
(Contract DAAG29-83-C-0030)
(AD-A169349; ARO-20115.2-EG) Avail: NTIS HC A04/MF A01 CSCL 20/7

A theoretical framework for modeling the characteristics of railgun plasma armatures is developed taking into account non ideal transport properties and equation of state. The electrical resistivity of the plasma is calculated as a sum of contributions from electron ion and electron neutral collisions. Non ideal correction to the ionization potential and pressure in Saha's equation and the equation of state is included. A steady-state magneto-gasdynamic model improved over earlier works is developed. In this model, the net Lorentz force exerted on the plasma armature is exactly accounted for. The model studies the radiation emanating from the plasma armature. It is found, on the one hand, that the radiation from the plasma armature under the conditions of most railgun experiments conducted in the past is sufficiently high to cause ablation. On the other hand, the modelling results also indicate that there indeed exist domains of operating parameters in which radiative ablation of the wall materials can be completely eliminated. Whether these favorable domains of operating parameters can be realized in practice remains a development of the future, though preliminary experiments conducted in a companion program sponsored by DoE and experiments in other institutions based upon the theoretical

recommendations developed here have produced significant reduction of ablation of the rails. GRA

N87-13259# Columbia Univ., New York. Dept. of Physics.
THEORETICAL HIGH ENERGY PHYSICS Progress Report, 1 May 1985 - 30 Apr. 1986
T. D. Lee May 1986 23 p
(Contract DE-AC02-76ER-02271)
(DE86-012669; DOE/ER-02271/109; COO-2271-109) Avail: NTIS HC A02/MF A01

Activities are reported in these areas: lattice QCD numerical studies; U(1)-vector current in the presence of arbitrary left and right chiral gauge fields and an arbitrary Higgs field; spectrum degeneracy of non-relativistic spin 1/2 particles in the field of a dyon; multiloop amplitudes of the closed bosonic and fermionic Polyakov strings in their critical dimensions; second order Coulomb scattering of an electron by a system with near degeneracy between states of opposite parity; production and annihilation of heavy neutrinos in the early universe; the effect of retardation on the energy levels of Rydberg helium atoms; Hawking radiation from black holes; the Eden model of cluster growth; and the quantum Hall effect. DOE

N87-13260# Los Alamos National Lab., N. Mex.
COMPACT REACTOR/ORC POWER SOURCE
K. L. Meier, W. L. Kirchner, and G. J. Willcutt 1986 7 p Presented at the Intersociety Energy Conversion Engineering Conference, San Diego, Calif., 25 Aug., 1986
(Contract W-7405-eng-36)
(DE86-011252; LA-UR-86-1643; CONF-860810-7) Avail: NTIS HC A02/MF A01

A compact power source that combines an organic Rankine Cycle (ORC) electric generator with a nuclear reactor heat source is being designed and fabricated. Incorporating existing ORC technology with proven reactor technology, the compact reactor/ORC power source offers high reliability while minimizing the need for component development. Thermal power at 125 kWt is removed from the coated particle fueled, graphite moderated reactor by heat pipes operating at 500 C. Outside the reactor vessel and connected to the heat pipes are vaporizers in which the toluene ORC working fluid is heated to 370 C. In the turbine-alternator-pump (TAP) combined-rotating unit, the thermal energy of the toluene is converted to 25 kWe of electric power. Lumped parameter systems analyses combined with a finite element thermal analysis have aided in the power source design. The analyses have provided assurance of reliable multiyear normal operation as well as full power operation with upset conditions, such as failed heat pipes and inoperative ORC vaporizers. Because of inherent high reliability, long life, and insensitivity to upset conditions, this power source is especially suited for use in remote, inaccessible locations where fuel delivery and maintenance costs are high. DOE

N87-13261# Los Alamos National Lab., N. Mex.
SPACE NUCLEAR SAFETY PROGRAM Progress Report, Oct. - Dec. 1984
T. G. George, comp. May 1986 55 p
(Contract W-7405-eng-36)
(DE86-012767; LA-10673-PR) Avail: NTIS HC A04/MF A01

This quarterly report covers studies related to the use of (Pu-238)O2 in radioisotope power systems carried out for the Office of Special Nuclear Projects of the US Department of Energy by Los Alamos National Laboratory. Most of the studies discussed are ongoing; the results and conclusions described may change as the work progresses. DOE

N87-13262# Los Alamos National Lab., N. Mex.
NEUTRONIC DESIGN STUDIES FOR AN UNATTENDED, LOW POWER REACTOR
R. G. Palmer and J. W. Durkee, Jr. 1986 23 p Presented at the Advances in Reactor Physics and Safety Meeting, Saratoga Springs, N.Y., 17 Sep., 1986
(Contract W-7405-eng-36)
(DE86-011228; LA-UR-86-1879; CONF-860906-13) Avail: NTIS HC A02/MF A01

The Los Alamos National Laboratory is involved in the design and demonstrations of a small, long-lived nuclear heat and electric power source for potential applications at remote sites where alternate fossil energy systems would not be cost effective. This paper describes the neutronic design analysis that was performed to arrive at two conceptual designs, one using thermoelectric conversion, the other using an organic Rankine cycle. To meet the design objectives and constraints a number of scoping and optimization studies were carried out. The results of calculations of control worths, temperature coefficients of reactivity and fuel depletion effects are reported. DOE

N87-13263# Rensselaer Polytechnic Inst., Troy, N.Y. Div. of Nuclear Engineering.
COMPACT REACTOR STUDIES Technical Progress Report, 1 Dec. 1985 - 30 Nov. 1986
D. Steiner Jun. 1986 11 p
(Contract DE-FG02-85ER-52118)
(DE86-013247; DOE/ER-52118/T2) Avail: NTIS HC A02/MF A01

This is a status report on technical progress relative to the tasks identified for the first year of this activity (1 December 1985 - 30 November 1986). The continuation of this proposal in this submission describes plans for the second year of the project. It is noted that a new task is proposed as part of the effort for next year. The new task is in the area of blanket design for the Engineering Test Reactor (ETR). The ETR activity is a new effort within the Office of Fusion Energy and planning. The RPI Fusion Engineering Program has been conducting research on a novel blanket concept which we believe may be of substantial benefit to the ETR activity. Thus, we are requesting additional support to participate in the ETR activity. DOE

74 OPTICS

N87-13264*# National Aeronautics and Space Administration. Langley Research Center, Hampton, Va.
THEORY FOR COMPUTING THE FIELD SCATTERED FROM A SMOOTH INFLECTED SURFACE
Raymond L. Barger and Allen K. Dominek 1986 23 p
(NASA-TP-2632; L-16157; NAS 1.60:2632) Avail: NTIS HC A01/MF A01 CSCL 20F

A theory is described for computing the reflected or scattered field from a smooth body with inflection points. These inflections occur in certain directions at each surface point for which the total (Gaussian) curvature is zero or negative. For surface illumination in one of these critical directions, the usual reflection formulas obtained by the high-frequency approximation are inapplicable, and a shadow zone exists in the reflected field. Scattering into the shadow zone is treated, as well as specular reflection. This theory should have a variety of applications such as for certain optics problems, computer graphics modeling of three-dimensional shapes, and the design and analysis of specialized microwave reflector antennas. Author

N87-13265# California Inst. of Tech., Pasadena. Dept. of Applied Research.
PHASE CONJUGATE OPTICS AND PICOSECOND OPTOELECTRONICS Final Report, 14 Feb. 1983 - 28 Feb. 1986
S. K. Kwong, G. Rakuljic, J. Paslaski, and A. Yariv 8 May 1986 13 p
(Contract DAAG29-83-K-0048)
(AD-A169180; ARO-19881.26-PH) Avail: NTIS HC A02/MF A01 CSCL 20/6

Large Coupling coefficient (>10/cm) photorefractive crystals have been developed. The infrared response and the temperature dependence of these crystals have been studied. The applications of these crystals such as image subtraction, wavefront

conversion and bistable oscillations have been developed. The ultimate bandwidth limitations of the self-pumped phase conjugate mirror have been investigated. High speed detectors for use at the 1.3 micrometers region have been developed. During this reporting period we have been conducting research on properties of photorefractive crystals and their applications, and the phase conjugation of picosecond light pulses. GRA

N87-13266# Department of the Air Force, Washington, D.C.
METHOD OF FABRICATING HIGH EFFICIENCY BINARY PLANAR OPTICAL ELEMENTS Patent Application
Wilfrid Veldkamp, inventor (to Air Force) Filed 16 Apr. 1986 43 p
(AD-D012374; US-Patent-Appl-SN-852587) Avail: NTIS HC A03/MF A01 CSCL 20/6

The high diffraction efficiency regime of binary gratings occurs at periodicities on the order of a wavelength in order to produce grating which diffract radiation with efficiencies of greater than 90%, a fabrication procedure is disclosed which uses holographic and very large scale integration techniques which allow fine control over the periodicity and depth parameters to produce binary planar optical elements having a ratio of lambda/T greater than one (where lambda equals the wavelength of an illuminating wavefront, and T equals the grating periodicity). Additionally, the disclosed process produces high optical quality diffractive elements with phase precision of as high as lambda/100. These diffractive elements include laser beam multiplexers, beam profile shapers, and binary lenses which are lossless optical transfer functions. GRA

N87-13267# Department of the Air Force, Washington, D.C.
THREE DIMENSIONAL OPTICAL RECEIVER HAVING PROGRAMMABLE GAIN SENSOR STAGES Patent
Nathan Bluzer, inventor (to Air Force) Issued 20 May 1986 12 p Supersedes AD-D010970
(AD-D012389; US-Patent-4,590,505; US-Patent-Appl-SN-569639; US-Patent-Class-337-24) Avail: US Patent and Trademark Office CSCL 17/8

A three dimensional optical image receiver having sensor stages with a programmable gain capability is presented. Operation of the receiver occurs entirely in the charge domain upon the charge initially generated by the optical signal. GRA

N87-13268# Department of the Army, Washington, D. C.
BEAM STEERING MIRROR CONSTRUCTION Patent Application
Frederick G. Eitel, inventor (to Army) Filed 28 Apr. 1986 9 p
(AD-D012399; US-Patent-Appl-SN-856263) Avail: NTIS HC A02/MF A01 CSCL 20/6

A beam steering mirror is trunnion mounted about a primary axis relative to a ring structure. The ring structure is trunnion mounted on a secondary axis 90 deg from the primary axis of the beam steering mirror and in the same plane. The ring structure is trunnion mounted about its secondary axis relative to a stationary support structure. The ring structure and the beam steering mirror each have electric torque actuators for adjusting the beam steering mirror and the ring structure relative to the stationary support structure. GRA

N87-13269# Dayton Univ., Ohio. Research Inst.
OPTICAL PROCESSING Interim Report, 1 Jun. - 31 Dec. 1985
Steven C. Gustafson 31 Dec. 1985 522 p
(Contract N00014-85-K-0479)
(AD-A169882; UDR-TR-85-148) Avail: NTIS HC A22/MF A01 CSCL 09/2

The technical contributions were as follows: (1) Optical parallel 2-D neighborhood processor and optical processor assessment technique; (2) High accuracy with moderately accurate components and optical fredkin gate architectures; (3) Integrated optical threshold computing, pipelined polynomial processor, and all optical analog/digital converter; (4) Adaptive optical associative memory model with attention; (5) Effectiveness of parallelism and connectivity in optical computers; (6) Optical systolic array processing using an integrated acoustooptic module; (7) Optical threshold elements and networks, holographic threshold processors, adaptive matched spatial filtering, and coherence theory in optical computing; (8) Time-varying optical processing for sub-pixel targets, optical Kalman filtering, and adaptive matched filtering; (9) Optical degrees of freedom, ultra short optical pulses, number representations, content-addressable-memory processors, and integrated optical Givens rotation devices; (10) Optical J-K flip flop analysis and interfacing for optical computers; (11) Matrix multiplication algorithms and limits of incoherent optical computers; (12) Architecture for machine vision with sensor fusion, pattern recognition functions, and neural net implementations; (13) Optical computing algorithms, architectures, and components; and (14) Dynamic optical interconnections, advantages and architectures. GRA

N87-13270# Department of the Air Force, Washington, D.C.
METHOD AND APPARATUS FOR RAPID OPTICAL PHASING Patent Application
Mark G. Baciak, inventor (to Air Force) Filed 30 Apr. 1986 18 p
(AD-D012412; US-Patent-Appl-SN-857621) Avail: NTIS HC A02/MF A01 CSCL 20/6

This document discloses a method and apparatus for rapid optical phasing of optical devices utilizing white light interference fringe finding. The apparatus comprises a white light source, a beam splitter, a scanning mirror and a stationary reflective surface. The scanning mirror is moved in piston while reflected light is observed by an electro optic sensor at a receiver. A nulled pattern has been previously established at the receiver. An electrical signal from the electro optic sensor is mounted at amplification and recording means to identify variations in reflected light intensity that are caused by white light fringes. White light fringes only occur at zero optical difference, i.e., when the scanning mirror and stationary reflective surface are in phase. GRA

N87-13271# Galileo Electro-Optics Corp., Sturbridge, Mass.
FEASIBILITY OF MAKING COHERENT FIBER-OPTIC ARRAYS FROM FUSED SILICA Final Report
J. E. Rourke, Dean J. Geraci, and Mark L. DeLong Jul. 1986 24 p
(Contract DAAA15-85-C-0111)
(AD-A170873; BRL-CR-558) Avail: NTIS HC A02/MF A01 CSCL 20/6

Coherent fiber-optic bundles offer opportunities for application of state-of-the-art electro-optic imaging techniques to the sighting and fire-control problem. However, conventional fiber-optics are limited in this application by their high attenuation coefficients (up to 2000 dB/km). Fused silica fiber with its low attenuation (1-50 dB/km), offers substantial improvement. GRA

N87-13272# California Univ., Berkeley. Lawrence Berkeley Lab.
X-RAY DATA BOOKLET, REVISION
D. Vaughan, ed. Apr. 1986 154 p
(Contract DE-AC03-76SF-00098)
(DE86-012650; LBL-PUB-490-Rev.) Avail: NTIS HC A08/MF A01

A compilation of data is presented. Included are properties of the elements, electron binding energies, characteristic x-ray energies, fluorescence yields for K and L shells, Auger energies, energy levels for hydrogen-, helium-, and neonlike ions, scattering factors and mass absorption coefficients, and transmission bands of selected filters. Also included are selected reprints on scattering processes, x-ray sources, optics, x-ray detectors, and synchrotron radiation facilities. DOE

N87-13273# Advisory Group for Aerospace Research and Development, Neuilly-Sur-Seine (France). Electromagnetic Wave Propulsion Panel.
GUIDED OPTICAL STRUCTURES IN THE MILITARY ENVIRONMENT
H. Hodara, ed. and P. Crosignani, ed. Loughton, England May 1986 310 p Meeting held in Istanbul, Turkey, 23-27 Sep. 1985
(AGARD-CP-383; ISBN-92-835-0391-0) Avail: NTIS HC A14/MF A01

A new technology has arisen and is expanding quickly; single

mode structures in the form of optical fibers and planar waveguides operating at long wavelength, 1.3 micron and beyond, with minimum attenuation and dispersion. Fibers with attenuation below 0.5 dB/km, and bandwidths in the hundreds of GHz-Km have opened up long distance, repeaterless transmission on land and underwater. In addition, the single mode structure has bred a new class of passive devices: sensors capable of detecting sound, magnetic field, motion, temperature, humidity and many other characteristics, all of them approaching the theoretical detection limit. New active components are developing: single mode, high efficiency, long life chips operating at room temperature, electro-optic switches and components capable of generating new frequencies through Raman scattering and other nonlinear phenomena. For individual titles, see N87-13274 through N87-13306.

N87-13274# Naval Research Lab., Washington, D. C.
PROGRESS IN OPTICAL FIBER SENSORS
T. G. Giallorenzi *In* AGARD Guided Optical Structures in the Military Environment May 1986 13 p (For primary document see N87-13273 04-74)
Avail: NTIS HC A14/MF A01

A review of the status of Optical Fiber Sensor Technology is presented and the effects of laser noise and demodulation techniques on performance are reviewed. Recent work on the development of fiber telemetry scheme for use with optical fiber sensors is also detailed. Author

N87-13275# Strathclyde Univ., Glasgow (Scotland). Dept. of Electronic and Electrical Engineering.
FIBRE OPTIC GYROSCOPES IN INERTIAL NAVIGATION c04
Brian Culshaw and John D. Nuttall (Ferranti Ltd., Edinburgh (Scotland).) *In* AGARD Guided Optical Structures in the Military Environment May 1986 6 p (For primary document see N87-13273 04-74)
Avail: NTIS HC A14/MF A01

The potential application of fiber optic gyroscopes (FOG) in interial navigation (IN) systems is discussed. The requirements for IN are briefly reviewed and compared to the reported performance of experimental FOG's. This leads to the identification of areas in which further work is necessary, in both physical understanding and technological developments. Author

N87-13276# McDonnell-Douglas Astronautics Co., Huntington Beach, Calif.
COMPARISON OF RING LASER AND FIBER-OPTIC GYRO TECHNOLOGY
E. Udd, S. F. Watanabe, and R. F. Cahill *In* AGARD Guided Optical Structures in the Military Environment May 1986 14 p (For primary document see N87-13273 04-74)
Avail: NTIS HC A14/MF A01

Substantial progress has been made in recent years toward the development of producible fiber-optic rotation sensors. These devices have the potential of being the solid-state replacement for many applications currently using mechanical gyro technology. Ring laser gyro technology which has been under development for approximately 23 years is now being introduced into commercial and military aircraft for inertial navigation. The fundamentals of the usage of Sagnac interferometry for rotation sensing is reviewed as well as the differences between fiber-optic gyro and ring laser gyro technology. Examples are given of applications where fiber-optic gyro or ring laser gyro technology is particularly suitable. Distinctions are made between analog fiber-optic gyros which offer the lowest possible cost but are limited in performance capability and digital fiber-optic gyros which offer the wide dynamic range and accurate scale factor correction required for more stringent applications. Author

N87-13277# Litton Systems (Canada) Ltd., Rexdale, (Ontario). Advanced Optical Systems Group.
CLOSED LOOP FIBER OPTIC GYRO
D. H. Lewis, B. Bednarz, J. A. Dankowych, K. Jew, G. Joslin, and W. A. Young *In* AGARD Guided Optical Structures in the Military Environment May 1986 10 p (For primary document see N87-13273 04-74)
Avail: NTIS HC A14/MF A01

A breadboard closed loop gyroscope using ordinary single mode fiber and a multi-mode diode laser is described. Closed loop rotation rate bias stability data are presented for both short term and long term. The performance of the gyro is displayed in the frequency domain as well as in the time domain. The performance achieved was a rotation rate noise of 5 deg/hr for 1 sec. integration, 0.55 deg/hr for 100 second integration and an extrapolated drift of 0.09 deg/hr. The long term (6 hours) bias stability was 1 deg/hr. Author

N87-13278# Plessey Co. Ltd., Romsey (England).
PROGRESS WITH MULTIPLEXED SENSOR ARRAYS BASED ON REFLECTION AT SPLICED JOINTS BETWEEN SENSORS
J. P. Dakin, C. A. Wade, and P. B. Withers *In* AGARD Guided Optical Structures in the Military Environment May 1986 6 p (For primary document see N87-13273 04-74)
Avail: NTIS HC A14/MF A01

Recent progress made in developing a time-division-multiplexed, fiber optic hydrophone array using optical time domain reflectometry (OTDR) techniques is reported. Recently, improvements have been made in four main areas: (1) development of partially reflecting splices; (2) development of a high power single mode gas laser for use in the present system; (3) development of a balanced-optical-path arrangement to allow shorter coherence length sources to be used in future systems; and (4) development of an all-fiber frequency shifter, with the ultimate aim of producing a complete all-fiber system. E.R.

N87-13279# Plessey Co. Ltd., Romsey (England).
MAGNETIC AND PRESSURE SENSORS USING THE COMPENSATED POLARIMETRIC SENSOR CONFIGURATION
J. P. Dakin, C. R. Batchellor, and J. A. Rex *In* AGARD Guided Opitcal Structures in the Military Environment May 1986 7 p (For primary document see N87-13273 04-74)
Avail: NTIS HC A14/MF A01

The identical lengths of high birefringence fiber spliced together with a 90 deg axial rotation to couple their orthogonal birefringent axes form the basis of a compensated polarimetric optical fiber sensor. This can be used to detect differential strains in the two fiber lengths caused by such phenomena as hydrostatic pressure or magnetic fields (the strain being introduced by magnetostrictive material bonded to the fiber). Magnetic and pressure sensors were constructed using this principle and show good sensitivity yet better stability then Mach-Zehnder arrangements. Author

N87-13280# Consiglio Nazionale delle Ricerche, Florence (Italy). Istituto de Ricerca sulle Onde Elettromagnetiche.
FIBER OPTIC DEVICE FOR TEMPERATURE REMOTE SENSING
A. M. Scheggi, M. Brenci, G. Conforti, F. Cosi, R. Falciai, and A. G. Mignani *In* AGARD Guided Optical Structures in the Military Environment May 1986 5 p (For primary document see N87-13273 04-74)
Avail: NTIS HC A14/MF A01

An optical-fiber temperature sensor is presented which is based on light amplitude modulation induced by a thermosensitive cladding applied on the distal end of the fiber. The experimental set-up for detecting and processing the signal is described, and the measured characteristics of the thermometer are reported. Author

N87-13281# National Bureau of Standards, Boulder, Colo.
OPTICAL FIBER SENSORS FOR THE MEASUREMENT OF PULSED ELECTRIC CURRENTS
G. W. Day, J. D. O. McFadden, L. R. Veeser (Los Alamos National Lab., N. Mex.), G. I. Chandler, and R. W. Cernosek (Sandia National Labs., Albuquerque, N. Mex.) *In* AGARD Guided Optical Structures in the Military Environment May 1986 9 p (For primary document see N87-13273 04-74)
Avail: NTIS HC A14/MF A01

Recent progress in the design of fiber sensors for pulsed electric currents is reviewed. Several of the most useful sensor configurations are described and compared. Models are used to predict the transfer function of these sensors, their sensitivity to non-ideal fiber properties, particularly linear birefringence, and methods for overcoming these problems. Other recent research is examined to suggest the prospect for sensors with improved sensitivity and stability. Author

N87-13282# Fondazione Ugo Bordoni, Rome (Italy). Istituo Superiore P. T.

NONLINEAR ELLIPSE ROTATION IN A LOW-BIREFRINGENCE OPTICAL FIBER

B. Crosignani, S. Trillo, P. DiPorto, and S. Wabnitz *In* AGARD Guided Optical Structures in the Military Environment May 1986 3 p Prepared in cooperation with Rome Univ., Italy (For primary document see N87-13273 04-74)

Avail: NTIS HC A14/MF A01

The rotation of the polarization ellipse taking place in a low-birefringence single mode optical fiber and associated with the nonlinear optical Kerr effect is theoretically investigated. A detailed description of a proposed experiment for measuring the nonlinear refractive index through the ellipse rotation is also furnished. Author

N87-13283# Thomson-CSF, Orsay (France). Lab. Central de Recherches.

PROGRESS IN OPTICAL FIBER GYROSCOPES USING INTEGRATED OPTICS

H. C. Lefevre, J. P. Bettini, S. Vatoux, and M. Papuchon *In* AGARD Guided Optical Structures in the Military Environment May 1986 13 p (For primary document see N87-13273 04-74)

Avail: NTIS HC A14/MF A01

A quarter of a liter brass-board of a fibergyro using a multifunction integrated optic circuit (splitter, polarizer and phase modulator), a superluminescent diode and 250 meters of polarization holding fiber is described. The photon noise limited random walk performance is 0.004 deg/sq. rt. H. A simple model to evaluate birefringence induced non-reciprocities, and an original method of signal processing, the digital phase ramp, to solve the problem of scale factor linearity and accuracy are also presented. Author

N87-13284# Bell Telephone Labs., Inc., Murray Hill, N. J.

WAVELENGTH DIVISION MULTIPLEXING AT 1.5 MICRONS FOR HIGH CAPACITY OPTICAL TRANSMISSION

J. Hegarty, N. A. Olsson, and R. A. Logan *In* AGARD Guided Optical Structures in the Military Environment May 1986 8 p (For primary document see N87-13273 04-74)

Avail: NTIS HC A14/MF A01

A method is described for multiplexing several channels of information, closely spaced in wavelength, together in one single-mode fiber. The results are reported of a recent 10-channel experiment at 1.5 micrometers in which 10 distributed feedback lasers, modulated at 2 Gbits/s, were multiplexed together and transmitted over 68.3 km of fiber giving a system capacity of 1.37 terabit-km/s. The channel spacing was 1.35 nm and the multiplexer insertion loss was 3 db. Crosstalk, including Raman crosstalk, was found to be negligible. Author

N87-13285# Consiglio Nazionale delle Ricerche, Florence (Italy). Istituto di Recerca sulle Onde Elettromagnetiche.

A SPHERICAL WAVEGUIDE MULTIPLEXER-DEMULTIPLEXER

V. Russo, S. Sottini, G. C. Righini, and S. Trigari *In* AGARD Guided Optical Structures in the Military Environment May 1986 8 p (For primary document see N87-13273 04-74)

Avail: NTIS HC A14/MF A01

A wavelength multiplexer-demultiplexer (MUX - DEMUX) which can work also a tapping element was suggested and tested. This device is based on the imaging properties of a hemispheric geodesic lens. The aberrations of this lens were evaluated and some examples of the potential performance of the device are given: in particular the MUX - DEMUX seems to be quite interesting in the case of monomode fibers, showing a diffraction limited performance. Experimental tests are in progress, utilizing a spherical waveguide fabricated by ion exchange on a glass substrate, and gratings with 540 or 1200 grooves/mm. The results already available are quite encouraging and confirm the expected advantages of this approach with respect to previous devices. Author

N87-13286# Plessey Co. Ltd., Romsey (England).

A STUDY OF METHODS OF PHASE NOISE REDUCTION OF SEMICONDUCTOR LASERS FOR SENSOR APPLICATIONS c36

J. P. Dakin and P. B. Withers *In* AGARD Guided Optical Structures in the Military Environment May 1986 7 p (For primary document see N87-13273 04-74)

Avail: NTIS HC A14/MF A01

Many optical sensors based on fiber interferometry have been proposed. The majority of these use interferometers of the Mach-Zehnder or Michelson type, in which the optical path lengths of the two arms are often unequal. Under these conditions, a highly coherent light source is necessary to avoid signal/noise degradation due to fluctuations in the phase or frequency of the source. Single mode gas lasers are sufficiently coherent, but their large size, critical alignment requirements, and cost, limit their appeal as light sources for optical sensors. Semiconductor lasers, however, are compact, rugged and potentially low-priced devices, but the magnitude of the phase noise is such that, to obtain microradian sensitivity in interferometric sensors, only path differences less than one millimetre between the signal and reference arms can be tolerated. This imbalance may be increased if the magnitude of the laser phase noise can be reduced using either passive optical feedback or active control of the laser drive current. Both approaches are described. Described first are proposed experiments to examine the feasibility of using an array of suitably spaced mirrors to provide passive optical feedback. Secondly, experiments to measure phase noise reduction produced by active control of the laser drive current are reported together with their results. Author

N87-13287# McDonnell-Douglas Astronautics Co., Huntington Beach, Calif.

OPTICAL QUADRATURE DEMODULATOR FOR COHERENT DETECTION AND SENSOR APPLICATIONS

S. F. Watanabe, A. A. Joseph, H. B. Turner, S. A. Holmes, and J. T. Freidah *In* AGARD Guided Optical Structures in the Military Environment May 1986 6 p (For primary document see N87-13273 04-74)

Avail: NTIS HC A14/MF A01

A new device was designed, built and demonstrated which provides exceptional performance in a very small, potentially very low cost unit. Balanced quadrature detection for homodyne or heterodyne detection of phase or frequency encoded signal information is accomplished with microradian phase sensitivities over a broad range of environments and for a broad dynamic range of signal levels and frequencies. Results of current development testing are presented along with brief discussions of potential applications to coherent detection for interferometers, sensors, and communications. Author

N87-13288# Siemens A.G., Munich (West Germany). Research Labs.

EFFECTS OF OPTICAL FEEDBACK ON THE PERFORMANCE OF HIGH DATA RATE SINGLE-MODE FIBER SYSTEMS

R. Keil, K. Mathyssek, and E. Hoermann *In* AGARD Guided Optical Structures in the Military Environment May 1986 15 p (For primary document see N87-13273 04-74)

Avail: NTIS HC A14/MF A01

Performance measurements data accomplished on a 678 Mbit/s single-mode fiber optic transmission system for various laser diode structures and more importantly under different near- and far-end optical feedback conditions are presented. Specifically, for two integral coupling schemes i.e., the drawn fiber taper with a lens and hemispherically ended graded index fiber lens (GRINFLENS) the near-end optical feedback are modelled and

simple method for its experimental assessment are given. Feedback induced variations of lasing spectra and of mode partition noise and their influences on bit error rate (BER) data are experimentally determined for a dispersive single-mode fiber transmission link with the two coupling arrangements. Comparative measurements were done with a butt-coupled fiber and with a non-dispersive fiber system. Furthermore, far-end reflections from a connector joint and their quantitative influence on BER data were investigated. Author

N87-13289# Barr and Stroud Ltd., Glasgow (Scotland).
PERFORMANCE OF INTEGRATED OPTICAL FREQUENCY SHIFTERS PIGTAILED TO HIGH BIREFRINGENCE FIBRES USING ION-MILLED GROOVES
I. Andonovic, W. Johnstone, D. N. Macfadyen, A. McDonach, M. S. Ner, and S. Beaumont *In* AGARD Guided Optical Structures in the Military Environment May 1986 8 p Prepared in cooperation with Glasgow Univ., Scotland (For primary document see N87-13273 04-74)
Avail: NTIS HC A14/MF A01

The practical application of lithium niobate integrated optical devices in the severe military environments that will be experienced by the fiber optic gyroscope, requires the development of a cheap, efficient and robust means of interconnecting optical fibers and integrated optical chips. One technique for fiber to chip coupling is the use of ion-milled alignment grooves in the Lithium Niobate substrate to accurately locate the fiber end with the end of the waveguide. This technique uses a photolithographic process for the most precise alignment stages and is therefore amenable to mass production and automation. Efficient coupling of light was observed between optical fibers chemically etched to a diameter of about ten microns and waveguides formed by the indiffusion of titanium. The use of chemically etched optical fibers and ion-milled grooves allows a high packing density of chip/fiber connections, offereing space saving in terms of device lengths as well as lateral separation. Results are presented for the coupling of light to integrated optical waveguides from high birefringence optical fibers using ion-milled alignment grooves, and the degree of polarisation preservation achieved is related to the performance of integrated optical phase modulators. Author

N87-13290# Arizona Univ., Tucson. Optical Sciences Center.
NONLINEAR PLANAR GUIDED WAVE INTERACTIONS AND DEVICES
G. I. Stegeman, C. T. Seaton, and H. G. Winful (GTE Labs., Inc., Waltham, Mass.) *In* AGARD Guided Optical Structures in the Military Environment May 1986 9 p (For primary document see N87-13273 04-74)
Avail: NTIS HC A14/MF A01

A variety of applications of third-order nonlinear integrated optics to optical signal processing are discussed. These include guided wave devices based on an intensity-dependent refractive index such as upper and lower threshold devices, all-optical switching devices, all-optical modulation devices, optical logic, and optical bistability. Multiple waveforms mixing with degenerate four-wave mixing to produce signal convolution and time inversion on a picosecond time scale are also discussed. Author

N87-13291# Rome Univ. (Italy). Dipt. di Energetica.
BISTABILITY IN NONLINEAR WAVEGIUDES c32
M. Bertolotti, C. Sibilia, and I. Anselmi *In* AGARD Guided Optical Structures in the Military Environment May 1986 8 p (For primary document see N87-13273 04-74)
Avail: NTIS HC A14/MF A01

The propagation of electromagnetic waves in a nonlinear waveguide is studied. For simplicity a three layer structure is considered with the two external media of semi-infinite extent. The mode dispersion equation is derived together with the power carried by the single mode in the structure, showing that bistability can occur in some case. Author

N87-13292# Arizona Univ., Tucson. Optical Sciences Center.
INTEGRATED OPTICS OPTICAL LIMITERS
C. T. Seaton, J. D. Valera, and G. I. Stegeman *In* AGARD Guided Optical Structures in the Military Environment May 1986 7 p (For primary document see N87-13273 04-74)
Avail: NTIS HC A14/MF A01

Two novel, low-power, guided-wave optical limiters were demonstrated. Both are based on intensity-dependent refractive indices and involve phenomena unique to optical waveguides. The first utilizes newly discovered nonlinear guided waves that exhibit optical-limiting action for a film bounded by a nonlinear medium. The second relies on an intensity-dependent reduction in coupling efficiency when waveguide modes are excited by prism or grating couplers. In both cases, preliminary experiments have demonstrated optical limiting action. Author

N87-13293# ANT Nachrichtentechnik, Backnang (West Germany).
PIN-FET PREAMPLIFIER FOR HIGH-SPEED OPTICAL TRANSMISSION SYSTEMS
B. Schwaderer *In* AGARD Guided Optical Structures in the Military Environment May 1986 6 p (For primary document see N87-13273 04-74)
Avail: NTIS HC A14/MF A01

The design of a hybrid integrated PIN-FET transimpedance preamplifier is given for long-haul optical transmission systems at 1.3 micrometers wavelength with bit rates of 140 Mbit/s and 565 Mbit/s. The preamplifier uses a GaInAs/InP PIN-photodiode with a dark current of less than 10 nA, a high spectral responsivity of greater than 0.7 A/W at 5V bias supply and a GaAs-MESFET with 45 mS transconductance and about 0.7 pF input capacitance. Using transimpedance-resistors of 50 kilo-ohm and 25 kilo-ohm the design goals of receiver sensitivities are -43 dBm for the 140 Mbit/s system and -36.7 dBm for the 565 Mbit/s system respectively for BER equal to or less than 10(-9). The measured values of - 42.8 dBm and - 35.8 dBm including connector losses are within the predicted ranges. Author

N87-13294# Communications Research Centre, Ottawa (Ontario). Optical Communications Program.
OPTOELECTRONIC BROADBAND SWITCHING FOR COMMUNICATIONS AND SIGNAL PROCESSING c32
R. I. MacDonald and D. K. W. Lam *In* AGARD Guided Optical Structures in the Military Environment May 1986 10 p (For primary document see N87-13273 04-74)
Avail: NTIS HC A14/MF A01

By employing a hybrid technology using electronic and optical integration, optical isolation levels can be attained in a switch matrix without the need to switch light. Bandwidths of several GHz, subnanosecond switching time and crosstalk below 50 dB were demonstated in monolithically integrated optoelectronic switch matrices. These devices show high promise as central switches in star configuration communication systems where very high bandwidth or very large array size is required. Advantages over foreseeable alternative technologies include size and power consumption as well as performance. In addition, optoelectronic switch matrices have unique properties that suggest their application in a number of signal processing situations where precise broadband signal delays are required, such as in the phasing of arrays, or the production of tunable filters. Recent work in these areas are described. Author

N87-13295# Siemens A.G., Munich (West Germany). Research Labs.
ACOUSTOOPTIC SPECTRUM ANALYZER USING A PLANAR BRAGG-CELL
M. Stockmann and P. Clemens *In* AGARD Guided Optical Structures in the Military Environment May 1986 5 p (For primary document see N87-13273 04-74)
Avail: NTIS HC A14/MF A01

The design principles and the performance characteristics of a miniaturized acoustooptic RF-spectrum analyzer are presented. The device yields a time-band-width-product of more than 300. Using a planar Bragg-cell fabricated on a LiNbO3 substrate and air between Bragg-cell and detector array the time-bandwidth-product was doubled compared to the minibulk as well as the

integrated optic spectrum analyzer for the same device length. The time resolution of the spectrum analyzer is 33 usec and its linear dynamic range 28 dB. Author

N87-13296# Naval Research Lab., Washington, D. C. Optical Sciences Div.
PREPARATION AND PROPERTIES OF INFRARED TRANSMITTING HEAVY METAL FLUORIDE GLASS OPTICAL FIBERS
Danh C. Tran *In* AGARD Guided Optical Structures in the Military Environment May 1986 6 p (For primary document see N87-13273 04-74)
Avail: NTIS HC A14/MF A01

In present silica fiber technology, optical attenuation at the intrinsic minimum level of about 0.15 dB/km at 1.6 micrometer has been attained. Non-oxide glasses based on heavy metal fluorides potentially can offer intrinsic minimum losses several orders of magnitude lower than that of silica, owing to a lower Rayleigh scattering loss contribution and an extended infrared absorption edge. As a result, heavy metal fluoride glasses are most promising for long distance repeaterless optical communication heavy metal fluoride glasses are most promising for long distance repeaterless optical comunication systems. The published literature on fluoride glasses and fiber is studied to provide a complete review of the present state-of-the-art in the field. Candidate fluoride glasses for fiberization are evaluated on the basis of their infrared transparency as well as their glass forming ability. The synthesis of high optical quality bulk fluoride glasses by conventional casting and the fabrication of fibers using both preform and crucible techniques are discussed. The optical properties of the fluoride glass fiber are evaluated based on the absorption loss contribution associated with hydroxyl groups and transition metal/rare-earth impurities, and on the scattering loss component arising from both Rayleigh scattering and processing induced defects such as microcrystallization, phase separation and particle inclusions. Author

N87-13297# Standard Telecommunication Labs. Ltd., Harlow (England).
GLASS FIBRES FOR TRANSMISSION IN THE 8-12 MICROMETERS WAVEBAND
N. J. Pitt and M. G. Scott *In* AGARD Guided Optical Structures in the Military Environment May 1986 8 p (For primary document see N87-13273 04-74)
Avail: NTIS HC A14/MF A01

Chalcogenide glasses, crystalline halides and hollow waveguides were assessed for transmission in the 8 to 12 micrometer waveband. Of these, chalcogenide glasses were selected for development of fiber optic materials. The bulk properties of a range of glasses were studied and compositions chosen to optimize transmission and thermal stability. The role of major impurities and the procedures used to minimise them are described. Selected compositions were drawn into long lengths of polymer coated fiber with diameters controlled accurately up to 500 micrometers. Current fibers transmit at CO2 laser wavelengths with losses of 5 to 10 dB/m but potential for substantial improvement still exists. Mechanical testing has shown that with suitable coatings chalcogenide fibers are flexible enough to sustain a bend radius of the order of 1 cm. Author

N87-13298# Stanford Univ., Calif. Crystal Science Div.
SINGLE CRYSTAL FIBERS
Robert S. Feigelson *In* AGARD Guided Optical Structures in the Military Environment May 1986 9 p (For primary document see N87-13273 04-74)
Avail: NTIS HC A14/MF A01

Single crystal fibers are just now emerging as a new frontier in both materials science and device technology. Various methods have already been developed for the preparation of single crystal fibers of a wide range of materials with useful properties. Along with discussions of fiber growth methods and potential applications for single crystal fibers, current research on the growth of laser, nonlinear optic, and IR transmitting single crystal fibers are also discussed. Author

N87-13299# Rennes Univ. (France). Lab. de Chimie Minerale D.
FLUORIDE GLASSES FOR INFRARED WAVEGUIDES [VERRES FLUORES POUR GUIDES D'ONDE INFRA ROUGE]
J. Lucas *In* AGARD Guided Optical Structures in the Military Environment May 1986 7 p In FRENCH (For primary document see N87-13273 04-74)
Avail: NTIS HC A14/MF A01

The realization of optical waveguides is more promising beginning with materials in the glassy state than to begin with polycrystalline or monocrystalline materials. At the present time, the glasses which correspond to the best compromise between the bandwidth of transmission, the ultra-transparence potential, low diffusion loss, and fiber preparation techniques are the fluoride glasses. The tetrafluoride glasses with a zirconium base permits transmission through fiber of up to 4 microns, those with a base of the heavy metals (thorium, indium, rare earths, etc.) up to 5 microns. The potential applications in long distance telecommunications (considering very low theoretical losses, 10(-3) dB/km) are discussed as well as short distance applications involving collection technologies and energy transport. Author

N87-13300# British Telecom Research Labs., Ipswich (England).
WIDE BANDWIDTH, LONG DISTANCE FIBRE-OPTIC COMMUNICATION SYSTEMS
S. D. Walker, L. C. Blank, and L. Bickers *In* AGARD Guided Optical Structures in the Military Environment May 1986 9 p (For primary document see N87-13273 04-74)
Avail: NTIS HC A14/MF A01

Recent advances in laser, fiber and receiver technology have allowed a series of unrepeated optical transmission system experiments to be carried out. These spans ranged from 90 km to 250 km at line-rates from 34 Mbit/s to 2 Gbit/s. At data-rates of 34 Mbit/s and 140 Mbit/s, a single-line 1.525 micrometers distributed feedback laser was used in conjunction with step-index monomode fiber spans up to 251.6 km. In a second set of experiments, a 1.55 micron multi-longitudinal-mode laser gave error-free transmission over lengths of dispersion-shifted fiber up to 233 km. For gigabit transmission experiments, a 1.535 micron single-line laser and dispersion-shifted fiber provided a further systen option which resulted in a recent fully-regenerated 2 Gbit/s, 90 km trial featuring commercially-available GaAs logic components. The various system configurations implemented are described and the technical options for further long-span, unrepeatered optical transmission experiments using current and developmental direct-detection technology in the 1.5 micron wavelength region are reviewed. Author

N87-13301# TRW, Inc., Redondo Beach, Calif. Fiber Optic Communications.
PERFORMANCE OF RF FIBER OPTIC LINKS
Thomas R. Joseph and William E. Stephens *In* AGARD Guided Optical Structures in the Military Environment May 1986 12 p (For primary document see N87-13273 04-74)
Avail: NTIS HC A14/MF A01

RF fiber optic links have numerous applications to microwave systems. To fully exploit their usefulness, the RF system designer must understand their properties in terms of the performance parameters that are used to describe the terminal properties of other RF components such as loss, signal to noise, linearity, and dynamics. The performance of direct and external modulation fiber optic links in terms of those parameters are explained. Specific examples of a 4.1 to 4.7 GHz direct modulation link and a 2.0 to 12.0 GHz external modulation link are used. Author

N87-13302# Shape Technical Center, The Hague (Netherlands).
FIBER OPTICS: A SURVIVABLE AND COST-EFFECTIVE TRANSMISSION MEDIUM FOR TERRESTRIAL NETWORKS
M. Aslam *In* AGARD Guided Optical Structures in the Military Environment May 1986 10 p (For primary document see N87-13273 04-74)
Avail: NTIS HC A14/MF A01

The performance of a fiber-optic transmission system is

affected by nuclear radiation. The nuclear scenario is discussed vis the terrestrial network, the essential characteristics are identified, and on this basis the principles for the design of a strategic communication fiber-optic cable system are derived. The details of a cost analysis applicable to various scenarios are also given; the costs of each scenario are compared with those of a microwave line-of-site system of approximately the same capacity. Author

N87-13303# Messerschmitt-Boelkow-Blohm G.m.b.H., Munich (West Germany). Dynamics Div.
SINGLE-MODE-FIBERS FOR FIBEROPTIC-GUIDED MISSILES: A COMPARISON WITH GRADED-INDEX MULTIMODE FIBERS
K. H. Niederhofer and W. D. Schuck *In* AGARD Guided Optical Structures in the Military Environment May 1986 8 p (For primary document see N87-13273 04-74)
Avail: NTIS HC A14/MF A01

For a few years there have been activities in the application of optical fibers as a broadband, secure transmission medium between a ground-station and tactical missiles for ranges of about 10 km. The idea is to put the gunner's eye, i.e., a suitable imaging device, into the missile to provide a lock-on-after-launch capability together with a man-in-the-loop option. A key problem is the rapid payout of the fiber from the missile during flight. Several successful flight test campaigns have been carried out, where Kevlar-reinforced graded-index multimode fibers have been used for transmission of command- and TV-signals. The affects of additional attenuation resulting from the reinforcement, the bobbin-technology and payout process are well controlled. For the first development of fiberoptic guidance systems single-mode transmission was not taken into account, since the suitable components were expensive, sensible and not readily available. Today the single-mode technology is quite advanced and offers some benefits compared with multimode transmission. The most important points are the higher bandwidth and the lower attenuation. As long as the missile range is below 10 km, this is no decisive advantage, but it encourages the extension of the missile range to much more than 10 km. The comparison of costs gives no clear-cut statement, but the production costs for single-mode fibers tend to be below that of multimode fibers. If the hardness against nuclear radiation is compared, single-mode fibers give the better results. Author

N87-13304# Hughes Research Labs., Malibu, Calif.
LIGHTWAVE TECHNOLOGY IN FUTURE RADAR EQUIPMENT DESIGNS
C. M. Gee, A. E. Popa, and H. W. Yen *In* AGARD Guided Optical Structures in the Military Environment May 1986 8 p (For primary document see N87-13273 04-74)
Avail: NTIS HC A14/MF A01

Lightwave device technology can be implemented in future active aperture radar arrays. Transmitter and receiver components for a fiber optic antenna feed manifold in which the transceiver modules are connected to a central computer are reviewed. Present link signal to noise iimitations imposed by the performance of these components are analyzed, and promising trends in component development are discussed. Author

N87-13305# Army Communications-Electronics Command, Fort Monmouth, N.J.
TACTICAL FIBER OPTIC ASSEMBLY REQUIREMENTS
Vasilios E. Kalomiris *In* AGARD Guided Optical Structures in the military Environment May 1986 9 p (For primary document see N87-13273 04-74)
Avail: NTIS HC A14/MF A01

The unique features of militarized fiber optic assemblies are outlined. The stringent requirements that make tactical deployment a challenge to the fiber optic industry are summarized. The requirements are broken down to the component level: fiber, cable and connector. These demands on components are necessary to assure successful system operation. The compilation of specifications is presented in tabular form to serve as a reference for those interested in satisfying a host of ground systems needs. The significance of the performance of the cable assembly in the performance of the optical subsystem is also described. In addition, the requirements that the transceivers have to meet are reported and a comparison of the tactical and fixed plant is presented. E.R.

N87-13306# Bell Communications Research, Inc., Morristown, N.J. Exchange Network Research Div.
A HYBRID TRANSMISSION SCHEME ON SINGLE MODE FIBERS FOR TACTICAL COMMUNICATIONS
Steven S. Cheng *In* AGARD Guided Optical Structures in the Military Environment May 1986 6 p (For primary document see N87-13273 04-74)
Avail: NTIS HC A14/MF A01

The availability of single-mode fibers and long wavelength devices enables the system designers to consider new link design with much improved performance not presently available in either the multimode fiber or the traditional metallic conductor systems. A hybrid transmission scheme is proposed on single-mode fibers in a star configuration. At the command post, a primary laser and its standby laser running at the cw mode are followed by an optical splitter. Each output port is then externally modulated for downstream transmission. At each remote site, a dedicated LED is used for upstream transmission where the bandwidth requirement and therefore the dispersion penalty is generally lower. The cost, reliability and flexibility of this hybrid transmission scheme are examined. The use of bidirectional WDM devices and remote external modulators with polarization control is described as two potential variations to enhance this basic hybrid scheme. The deployment of such a system will provide cost effective transmission links in a tactical environment suitable for high bandwidth analog and digital transmission. Author

75 PLASMA PHYSICS

Includes magnetohydrodynamics and plasma fusion.
For ionospheric plasmas see *46 Geophysics*. For space plasmas see *90 Astrophysics*.

N87-13307*# Alabama Univ., Huntsville. School of Science.
SPACE PLASMA RESEARCH Final Report, Aug. 1980 - Aug. 1986
Richard H. Comfort and James L. Horwitz Sep. 1986 26 p
(Contract NAS8-33982)
(NASA-CR-178965; NAS 1.26:178965) Avail: NTIS HC A03/MF A01 CSCL 20I

Four basic areas were covered: development of analysis techniques and software and numerical simulations; data analysis and interpretation; spacecraft sheath studies; and laboratory studies. The important details were documented in terms of either appropriate software documentation or publication in referred publication, conference proceeding and technical reports. The major accomplishments are summarized, followed by a chronological listing of the publications and presentations which resulted from the research. B.G.

N87-13308# Puerto Rico Univ., Rio Piedras. Dept. of Physics.
FLUIDS IN CONTACT WITH A HARD SURFACE: UNIVERSITY OF THE BRIDGE FUNCTIONS FOR THE DENSITY PROFILE
Y. Rosenfeld and L. Blum 27 May 1986 32 p
(Contract N00014-81-C-0776)
(AD-A168945; AD-E500768; TR-22) Avail: NTIS HC A03/MF A01 CSCL 20/9

The modified hypernetted chain theory (MHNC) for density profiles of fluids in contact with a hard, smooth surface is found to possess a remarkably simple and interesting property: The accuracy of the MHNC and the universality of the bridge functions for the density profiles can be tested without resort to any detailed solution of the integral equations. It is given by the degree of universality of the bulk bridge parameter when expressed in terms of the second partial derivative of the free energy with respect to a certain density equation. This function (F) as obtained from MHNC calculations for bulk simple fluids is found to be remarkably

independent of the pair potential. As an example for the accuracy of the resulting method, the one component plasma near a hard wall is discussed. Author (GRA)

N87-13309# Air Force Geophysics Lab., Hanscom AFB, Mass.
MEDIUM- AND LONG-WAVELENGTH INFRARED EMISSION FROM A LASER-PRODUCED OXYGEN PLASMA
Jonathan B. Lurie and James C. Baird 31 Dec. 1985 29 p
(AD-A169475; AFGL-TR-0341; AFGL-ERP-942) Avail: NTIS HC A03/MF A01 CSCL 20/9

Experiments on a laser-produced oxygen plasma were observed by medium wavelength (MWIR) and long wavelength (LWIR) infrared emission. This research is part of a continuing series of LINUS (Laser Induced Nuclear Simulation) experiments starting in the short wavelength infrared (SWIR) and extended to longer wavelengths to continue studies on highly excited oxygen atom states produced by three-body recombination in a highly ionized, laser-produced plasma. The first observations of emission in the 5 to 8 micron region from a recombining oxygen plasma are reported, including the first experimental observation of 6h sup 3,5H yields 5g sup 3,5G sup 0 and 6g sup 3,5G sup 0 yields 5f sup 3,5 F calculated to be at 7.450 microns and 7.426 microns, respectively. The observed linewidths of these MWIR emissions are discussed using a Stark lineshape analysis. GRA

N87-13310# Physical Sciences, Inc., Andover, Mass.
IONIZATION PHENOMENA ABOUT THE SPACE SHUTTLE Final Report, 15 Jul. 1985 - 15 Jan. 1986
George E. Caledonia, James C. Person, and D. Hastings Jan. 1986 75 p
(Contract F19628-85-C-0098)
(AD-A170542; PSI-098/TR-555; AFGL-TR-86-0045) Avail: NTIS HC A04/MF A01 CSCL 20/9

The available information on observations of neutral and ionic species and plasma properties around the Space Shuttle has been reviewed. Possible Shuttle environment electron/ion generation mechanisms have been evaluated. In particular, ion observations have been successfully interpreted within the framework of a kinetic analysis which incorporates Shuttle cloud/ambient interactions, flow, and electromagnetic effects. GRA

N87-13311# Massachusetts Inst. of Tech., Cambridge. Plasma Fusion Center.
TARA VACUUM SYSTEM
R. S. Post, P. Brindza, P. Goodrich, and M. P. Gaudreau Nov. 1985 8 p Presented at the 32nd AVS National Vacuum Symposium and Topical Conference, Houston, Tex., 19 Nov. 1985
(Contract DE-AC02-78ET-51013)
(DE86-011873; DOE/ET-51013/171; PFC/CP-86-4; CONF-851174-42) Avail: NTIS HC A02/MF A01

The Tara tandem mirror experiment vacuum system will be discussed including system design, specifications, and performance required for plug thermal barrier operation. A detailed description of the major pumping systems, reflux control, plasma pumping, measurement and control, fast gas handling and quality control procedures will be presented. Data from the two 5 month periods of operation will be presented. DOE

N87-13312# Los Alamos National Lab., N. Mex.
TWO-DIMENSIONAL DYNAMICS OF THE PLASMA WAKEFIELD ACCELERATOR
R. Keinigs, M. E. Jones, and J. J. Su (California Univ., Los Angeles.) 1986 12 p Presented at the 6th International Conference on High Power Particle Beams, Kobe, Japan, 9 Jun. 1986 Prepared in cooperation with California Univ., Los Angeles.
(Contract W-7405-eng-36)
(DE86-012382; LA-UR-86-1952; CONF-860665-6) Avail: NTIS HC A02/MF A01

The plasma wakefield accelerator (PWFA) is an accelerator concept based on utilizing a large amplitude plasma wave to accelerate relativistic electrons to ultra-high energy. The plasma wave represents the wave produced by a relativistic beam as it passes through a cold plasma. As the beam enters the plasma its space charge polarizes the background. When the beam tail passes the plasma is left with a large oscillating induced charge. The wakefields are derived assuming that the charge and current profiles of the driving bunch remain fixed. An estimate is made of the condition necessary for maintaining the profile of the driving bunch. The current required to result in an accelerating field approaching the wavebreaking limit is estimated. The beam dynamics for a small beam are simulated based on these estimates. The results of the studies reported indicate that the self-consistent transverse motion of the driving bunch makes pulse tailoring impossible to maintain. DOE

76 SOLID-STATE PHYSICS

Includes superconductivity.

For related information, see also *33 Electronics and Electrical Engineering* and *36 Lasers and Masers.*

N87-13313*# National Aeronautics and Space Administration. Pasadena Office, Calif.
FET CHARGE SENSOR AND VOLTAGE PROBE Patent
Paul A. Robinson, Jr. Issued 12 Aug. 1986 7 p
(NASA-Case-NPO-16045-1; US-Patent-4,605,946; US-Patent-Appl-SN-641146; US-Patent-Class-357-23.1; US-Patent-Class-357-23.12; US-Patent-Class-357-29; US-Patent-Class-357-52; US-Patent-Class-357-30; US-Patent-Class-250-338; US-Patent-Class-250-370) Avail: US Patent and Trademark Office CSCL 20L

A MOSFET structure having a biased gate covered with an insulator is described. The insulator is of such a thickness as to render the structure capable of giving a measure of accumulated charge. The structure is also capable of being used in a stacked structure as a particle spectrometer. E.R.

N87-13314# Aerospace Corp., El Segundo, Calif. Space Sciences Lab.
COMPARISON OF 2D MEMORY SEU TRANSPORT SIMULATION WITH EXPERIMENTS
R. Koga and W. A. Kolasinski 1 Sep. 1986 27 p
(ATR-86(8139)-2) Avail: NTIS HC A03/MF A01

Single event upset (SEU) simulations in SRAM were performed, and the results are compared to experimental data on 16K bit memories. The simulations consisted of simultaneous calculations of charge transport and transient circuit response for four cross-coupled CMOS transistors following the introduction of a slab of excess carries into the off p-channel drain. The experiments collected upset rates produced in the memories by 163 MeV argon ions directed normally to the chip surface. Agreement between experiment and calculation was achieved when the p-channel transistors were integrated into a single block of silicon as in the memory cell layout and scaling was done on the Auger coefficients to compensate for an inherent 2D effect. Author

N87-13315# Department of the Air Force, Washington, D.C.
QUARTZ GROWTH ON X-SEEDS Patent
Alton F. Armington and John J. Larkin, inventors (to Air Force) Issued 18 Mar. 1986 5 p Supersedes AD-D011031
(AD-D012269; US-Patent-4,576,808; US-Patent-Appl-SN-566130; US-Patent-Class-423-335) Avail: NTIS Avail: US Patent and Trademark Office CSCL 20/2

According to the present invention, dislocation-free quartz crystal boules, which are especially valuable for use in frequency and timing device applications, can be produced by utilizing a seed crystal cut or sliced from the X-plus region of a synthetically grown quartz boule. The seed crystal takes the form of a rectangular prism shaped slab or plate with its length directed along the crystallographic Y-axis orientation, its width directed along the X-axis orientation, its width directed along the X-axis orientation, and its thickness in the Z-axis orientation. Accordingly, the primary object of this invention is to provide synthetic quartz seed crystals for use in growing substantially dislocation-free quartz crystal boules

for use in timing and frequency devices. Another object of this invention is to greatly reduce the number of dislocations and other defects in synthetic quartz grown for oscillator applications. Still another object of this invention is to provide Z-faced quartz seed crystals cut or sliced from the X-plus growing region of a quartx crystal boule. GRA

N87-13316# California Univ., Berkeley. Dept. of Chemical Engineering.
PLASMA-ENHANCED DEPOSITION AND PROCESSING OF TRANSITION METALS AND TRANSITION METAL SILICIDES FOR VLSI Final Report, 1 Feb. 1983 - 31 Jan. 1986
Dennis W. Hess 20 May 1986 16 p
(Contract DAAG29-83-K-0039)
(AD-A168963; ARO-19996.9-MS) Avail: NTIS HC A02/MF A01 CSCL 20/12

Radiofrequency (rf) discharges have been used to deposit films of tungsten, molybdenum and titanium silicide. As-deposited tungsten films, from tungsten hexafluoride and hydrogen source gases, were metastable (beta W), with significant (>1 atomic percent) fluorine incorporation. Film resistivities were 40-55 micro ohm - cm due to the beta W, but dropped to about 8 micro ohm cm after a short heat treatment at 700 C which resulted in a phase transition to alpha W (bcc form). The high resistivity (>10,000 micro ohm) associated with molybdenum films deposited from molybdenum hexafluoride and hydrogen appeared to be a result of the formation of molybdenum trifluoride in the deposited material. Titanium silicide films formed from a discharge of titanium tetrachloride, silane, and hydrogen, displayed resistivities of about 150 micro ohm cm, due to small amounts of oxygen and chlorine incorporated during deposition. Plasma etching studies of tungsten films with fluorine containing gases suggest that the etchant species for tungsten in these discharges are fluorine atoms. GRA

N87-13317# Texas Instruments, Inc., Dallas.
INCREMENTAL QUENCH RESEARCH
L. Colombo and A. J. Syllaios 30 May 1986 50 p
(Contract DAAG29-85-C-0005)
(AD-A168980; TI-U1-134375-F; ARO-22602.1-MS-A) Avail: NTIS HC A03/MF A01 CSCL 20/2

The growth of large homogeneous (Hg,Cd)Te single crystals by the incremental quenching process/traveling heater method was investigated. The method is based on the sequential freezing of shallow melts that have large surface-to-volume ratios onto a large diameter growing ingot. The resulting polycrystalline (Hg,Dd) Te ingot has a bimodal microstructure with small grains on the outer surface and dendrides at the center of the ingot. Subsequent annealing of the ingots at a temperature below the solidus promotes grain growth on the order of 25 mm in diameter. Growth of large area crystals by the traveling heater method has been successfully demonstrated where 22- by 40-mm crystals have been grown without a seed. The crystals show very low subgrain boundary structures with dislocation densities ranging from 50,000 per sq cm to 300,000 per sq cm as measured by the etch pit method. The electrical characteristics of smaller crystals (20 mm in diameter) grown by the traveling heater method have shown purification during growth. GRA

N87-13318# Colorado State Univ., Fort Collins. Dept. of Physics.
MICROWAVE LOSS PROPERTIES OF HEXAGONAL FERRITES FOR MILLIMETER WAVE APPLICATIONS Final Report, 15 Aug. 1984 - 14 Feb. 1986
Carl E. Patton 15 Mar. 1986 13 p
(Contract DAAG29-84-K-0172)
(AD-A168982; ARO-21210.2-MS) Avail: NTIS HC A02/MF A01 CSCL 20/2

This short term post LRCP contract was designed to explore the application of the off-resonance effective linewidth technique to hexagonal ferrite materials at X-band frequencies. This objective has been accomplished. It has been demonstrated that the technique works quite well for both uniaxial and planar ferrite materials. The key result for millimeter wave applications is that a significant part of the microwave losses in these materials appears to be related to inhomogeneities. The effective losses which would determine insertion loss parameters for off-resonance device applications would appear to be much lower than one would infer from a direct ferromagnetic resonance linewidth determination. It was also possible to use the technique to measure the off-resonance loss properties in uniaxial materials at X-band, even though the large anisotropy fields precluded the observation of the FMR peak. The application of the technique to planar samples has also led to a new approach to the analysis of fundamental microwave relaxation processes in ferrite materials. GRA

N87-13319# Cornell Univ., Ithaca, N.Y. Lab. of Atomic and Solid State Physics.
SEARCH FOR FAR INFRARED RADIATION FROM OPTICALLY AND ACOUSTICALLY PUMPED DEFECT MODES Final Report, 14 Feb. 1983 - 13 Feb. 1986
A. J. Sievers 15 Apr. 1986 54 p
(Contract DAAG29-83-K-0044)
(AD-A169159; ARO-19793.4-PH) Avail: NTIS HC A04/MF A01 CSCL 20/5

More than one elastic ground state configuration has been found for both monatomic and polyatomic defects matrix isolated in alkali halide crystals. Multiple ground states give rise to persistent changes in the vibrational absorption spectrum of molecules when the internal vibrational modes of the defect are excited with a high resolution but tunable IR laser. The end result is that spectral holes with a width characteristic of the dephasing time of the vibrational mode can be created in the inhomogeneously strain broadened spectrum. The technique has been used to identify CN-:Na+, a new kind of vibrational defect which hole burns and also shows vibrational fluorescence in the IR. The discovery of the first solid state IR vibrational laser was a direct consequence of these kinds of measurements. The observations of transient and persistent hole burning, of vibrational fluorescence and of vibrational laser radiation demonstrate that diatomic molecules are more weakly coupled to the lattice than are polyatomics. GRA

N87-13320# Ceres Corp., Waltham, Mass.
STUDY TO DETERMINE THE FEASIBILITY OF UTILIZING SKULL-MELTING TECHNIQUES FOR THE GROWTH OF SINGLE CRYSTALS OF YTTRIUM VANADATE Final Report, 15 Sep. 1982 - 14 Sep. 1984
Joseph F. Wenckus and Wilson P. Menashi 1 Apr. 1986 32 p
(Contract DAAG29-81-C-0035)
(AD-A169249; ARO-18492.1-PH-S) Avail: NTIS HC A03/MF A01 CSCL 20/2

The goal of this program is to explore the feasibility of utilizing RF induction heated skull-melting techniques for the growth of optical quality crystals of yttrium vanadate (YVO4). In a parallel effort, experiments were also carried out to explore the fusion and recrystallization of yttrium aluminum garnet (YAG) in a cold crucible. Yttrium vanadate melts were achieved in cold crucibles up to 157 mm in diameter operating at an RF frequency of 3 MHz. However, attempts to Czochralski crystal growth were not successful due to poor thermal geometry and dissociation of the skull-contained melt. Experiments suggest that oxygen overpressures in excess of 2 atmos. may be useful in suppressing the dissociation rate of YVO4 melts. Skull-melting of YAG was achieved using an RF frequency of 3 MHz (no melting was observed at lower frequencies). However, the melts tended to slowly de-couple and freeze spontaneously; stable melts could not be maintained for periods beyond 2-3 hours. GRA

N87-13321# Arizona State Univ., Tempe. Center for Solid State Electronics Research.
DEGENERACY IN THE ENSEMBLE MONTE CARLO METHOD FOR HIGH FIELD TRANSPORT IN SEMICONDUCTORS
P. Lugli and D. K. Ferry 1 Jul. 1986 8 p
(Contracts N0014-84-K-0053; RRO210301; NR Proj. 619003)
(AD-A169456; N86.3) Avail: NTIS HC A02/MF A01 CSCL 20/12

An algorithm to include the Pauli exclusion principle in the Ensemble Monte Carlo method is presented. The results indicate that significant changes in the transport properties of GaAs have to be expected when degenerate conditions are reached. Important repercussions should be found in the modeling of microwave devices, where one often deals with highly doped regions. GRA

N87-13322# Department of the Air Force, Washington, D.C.
RAPID SYNTHESIS OF INDIUM PHOSPHIDE Patent Application
J. A. Adamski, inventor (to Air Force) Filed 25 Nov. 1985 23 p (AD-D012362; US-Patent-Appl-SN-801348) Avail: NTIS HC A02/MF A01 CSCL 20/12

This invention relates to an improved method for fabricating a highly pure, crystalline semiconductor material having stoichiometric proportions. More particularly, this invention concerns itself with an improved method for producing highly pure, stoichiometric indium phosphide crystalline materials (which are especially useful as substrates for epitaxy procedures) in a rapid manner as compared with past procedures. Indium phosphide, a group III-V semiconductor compound, has been found to be especially useful in two areas of technical interest. Its large band gap (1.35 eV) and high electron mobility make it useful as a semiconductor material, especially when employed in its highly pure form, and as a crystalline substrate for device fabrication by epitaxial deposition techniques. This abstract discloses a process for the high pressure synthesis of InP using an independent temperature control of a three zone furnace incorporating a heat pipe provides a stable temperature profile throughout the synthesis cycle. Internal/external pressure control of the quartz ampoule is maintained by use of a water cooled baffle and a temperature/pressure balancing program. Complete synthesis is achieved in less than five hours. GRA

N87-13323# Cornell Univ., Ithaca, N.Y. Lab. of Atomic and Solid State Physics.
SPHERICAL CLUSTERS OF SIMPLE METALS: MADELUNG ENERGIES AND STRUCTURE
M. Manninen Jun. 1986 14 p
(Contract N00014-82-K-0576)
(AD-A169560; TR-24) Avail: NTIS HC A02/MF A01 CSCL 20/12

Recent experiments on the magic numbers of small sodium clusters suggest that variation of the binding energy of clusters as a function of their size is dominated by the filling of energy levels of electrons moving in a spherical potential. For large clusters it is expected that the electron density distribution starts to be more and more spherical as the cluster increases. The purpose of this communication is to show that if the electron density distribution is assumed to be spherically symmetric, the resulting ionic configuration is determined mainly due to a classical Madelung energy. Furthermore it is shown that the ground state structures of the clusters are generally not small pieces of simple lattices (bcc, fcc, or hcp), but take always a more spherical shape (e.g., icosahedral in the case of a 13 atom cluster). The variation of the structural energy as a function of the cluster size is found to be somewhat smaller than the variation arising from the filling of single electron energy shells giving support to the idea that the dominant magic numbers are determined by the electronic shell structure of a square well potential. GRA

N87-13324# Johns Hopkins Univ., Baltimore, Md.
QUANTUM CHEMICAL INVESTIGATIONS OF THE MECHANISM OF CATIONIC POLYMERIZATION AND THEORETICAL PREDICTION OF CRYSTAL DENSITIES AND DECOMPOSITION PATHWAYS OF ENERGETIC MOLECULES Annual Summary Report, 1 Oct. 1984 - 30 Sep. 1985
Joyce J. Kaufman 15 Nov. 1985 56 p
(Contract N00014-80-C-0003)
(AD-A169805; AD-E900585; TR-6) Avail: NTIS HC A04/MF A01 CSCL 07/4

Contents of this report include Conversion of Our Programs to CRAY Vector Supercomputers; Calculations for Cationic Polymerization of Energetic Monomers; MRD-CI Calculations on Decomposition Pathways of Energetic Nitrocompounds; POLY-CRYST; Ab-Initio Atom Class - Atom Class Potential Functions and Prediction of Crystal Densities. In anticipation of significant access to the NRL CRAY XMP-12 supercomputer we devoted major attention this past year to converting our programs to that computer, which runs under a COS operating systems. As a preliminary to carrying out MRD-CI calculations on the attack of oxetane on protonated oxetane in the propagation step of cationic polymerization, we initiated MRD-CI calculations on opening the oxetane ring and the protonated oxetane ring. We carried out MRD-CI calculations for the dissociation of the >C-NO2 bond in nitrobenzene. We continued testing of our POLY-CRYST program for ab-initio calculations in crystals and polymers. We also implemented further additions to the INTER-MOLASYS program including the capability of calculating the dispersion energy contributions by a variation-perturbation procedure. We have also calculated further ab-initio atom class-atom class potential functions. GRA

N87-13325# California Univ., Los Angeles. Dept. of Chemistry and Biochemistry.
DONOR-ACCEPTOR ONE STEP ENERGY TRANSFER VIA EXCHANGE COUPLING ON A FRACTAL LATTICE Interim Technical Report
C. L. Yang and M. A. El-Sayed 7 Jul. 1986 29 p
(Contract N00014-83-K-0341)
(AD-A169843; TR-48) Avail: NTIS HC A03/MF A01 CSCL 20/12

Temporal behavior of donor intensity, I sub D (t), resulting from one step donor-acceptor electronic excitation energy transfer process via exchange mechanism is calculated on fractal lattices, with discrete dilation symmetry, of Euclidean dimension, d = 2, and fractal dimension, D, ranging from 1.99 to 1.0. I sub D (t) is fitted to the approximate equation of Klafter-Blumen (K-B) which is useful in fitting experimental results to determine fractal dimension from the slope of the expected straight line obtained by plotting in(-in I sub d (t)), vs. in 1 sub D t). The result for fractal lattice with D = 1.99 indicates that the approximation is appropriate for the time range used in our calculations. The results for different fractal lattices also show that the K-B equation indeed gives a straight line for structure when D/d is not much smaller than unity. As this ratio decreases, deviation from the expected straight line results and an oscillatory behavior is observed. From the latter structural information (i.e., fractal dimensionality, and geometrical parameters characterizing the fractal lattices) as well as the molecular interaction parameter gamma, the distance dependence of the exchange interaction can be determined. GRA

N87-13326# Geoscience, Ltd., Solana Beach, Calif.
THERMOPHYSICAL PROPERTIES MEASUREMENTS OF GALLIUM ARSENIDE AND CADMIUM TELLURIDE Final Report, 1 Nov. 1984 - 31 Aug. 1986
H. F. Poppendiek, C. M. Sabin, D. J. Connelly, P. M. Peuron, and R. J. Whaley Jun. 1986 19 p
(Contract DAAG29-85-C-0003)
(AD-A169901; GLR-254; ARO-22600.1-MS-A) Avail: NTIS HC A02/MF A01 CSCL 20/12

Geoscience is under contract to the U.S. Army to measure thermophysical properties of two semiconductor materials, cadmium telluride and gallium arsenides. The specific properties to be determined are coefficient of linear thermal expansion, specific heat, grey body emissivity, and thermal conductivity. During this study, Geoscience developed a new method of making infrared emissivity measurements at higher temperatures with no particular limitations. This final report summarizes the results of emissivity and coefficient of thermal expansion measurements made for both cadmium telluride and gallium arsenide. GRA

N87-13327# Brown Univ., Providence, R. I. Div. of Engineering.
PICOSECOND NONLINEAR RESONANT INTERACTIONS IN SEMICONDUCTORS Final Report, 1 Jan. 1982 - 30 Sep. 1985
Arto V. Nurmikko 15 Mar. 1986 60 p

(Contract F49620-82-C-0044)
(AD-A169992; AFOSR-86-0448TR) Avail: NTIS HC A04/MF A01 CSCL 09/1

This research was aimed at advancing understanding and utilization of selected optical properties of semiconductors containing magnetic elements. Emphasis was placed on the interaction of such materials with ultrashort pulses of laser radiation in order to study coupled electronic and magnetic excitations under selected nonequilibrium conditions. We hoped to generate novel results through experimental research for applications to fast optoelectronic devices. The mixed crystal semiconductors (Cd, Mn)Se and (Cd, Mn)Te were used. The contract work has generated a number of firsts, e.g., we measured the formation of local, microscopic magnetically oriented domains through real-time spectroscopy with picosecond laser pulses. Author (GRA)

N87-13328# Rockwell International Corp., Thousand Oaks, Calif. Science Center.
GROWTH OF FERRO-ELECTRIC TUNGSTEN BRONZE EPITAXIAL THIN FILMS FOR ELECTRO-OPTIC DEVICE APPLICATIONS Final Report, 30 Sep. 1982 - 30 Nov. 1985
R. R. Neurgaonkar and J. R. Oliver Jun. 1986 65 p
(Contract N00014-82-C-2466; DARPA Order 4540)
(AD-A170783; SC5340.13FR) Avail: NTIS HC A04/MF A01 CSCL 22/2

Strontium Barium Biobates:60 doped with Ce and Fe crystals have now been grown with improved optical quality using the Czochralski technique. The liquid phase epitaxial (LPE) growth of SBN:46 on SBN:60 substrate has also been successfully demonstrated, with particularly good results for (100) and (110) film orientations. The recent photorefractive measurements on Ce doped SBN:60 crystals show that the Tungsten Bronze, SBN:60 crystals are superior in many respects to BaTi03 because of enhanced two beam coupling coefficients, sensitivity and the overall flexibility of tungsten bronze crystals. La3+-doped SBN:50 single crystals have also been grown for pyroelectric detector studies and it was found that the growth of doped crystals is possible. Crystals as large as 1 to 1.5 cm in diameter have been grown successfully. Current measurements show that this composition exhibits excellent pyroelectric and dielectric properties to use in longitudinal configuration; hence, work is in progress to use this composition for pyroelectric detector applications. The role of other cations such as calcium and yttrium has also been studied and they appear to be promising for the proposed device applications. GRA

N87-13329# Optical Society of America, Washington, D. C.
PROCEEDINGS OF THE TOPICAL MEETING ON THE MICROPHYSICS OF SURFACES, BEAMS AND ADSORBATES HELD IN SANTA FE, NEW MEXICO ON 4-6 FEBRUARY 1985 Final Report, 1 Nov. 1984 - 18 Dec. 1985
Jarus W. Quinn 18 Dec. 1985 208 p Meeting held in Santa Fe, N. Mex., 4-6 Feb. 1985
(Grant AF-AFOSR-0018-85)
(AD-A170797; AFOSR-86-0469TR) Avail: NTIS HC A10/MF A01 CSCL 07/4

The Topical Meeting on Microphysics of Surfaces, Beams, and Adsorbates was organized within the interdisciplinary area of molecule/surface interactions induced, or studied, by laser and ion beam techniques. Especially emphasized was the molecular physics and electromagnetism of beam activated chemical reactions for applications in fabrication of semiconductor devices, in photocatalysis, and in optical recording. Emphasis was on the laser spectroscopy of molecular collision and reaction processes on surfaces, new sensitive or high resolution spectroscopies for studies of adsorbates, and optical methods applied to surface characterization. GRA

N87-13330# Brown Univ., Providence, R. I. Div. of Engineering.
PICOSECOND NONLINEAR RESONANT INTERACTIONS IN SEMICONDUCTORS Annual Report, 1 Jan. - 31 Dec. 1984
Arto V. Nurmikko Mar. 1986 15 p
(Contract F49620-82-C-0044)
(AD-A170813; AFOSR-86-0525TR; AR-3) Avail: NTIS HC A02/MF A01 CSCL 20/12

This research was aimed at advancing understanding and utilization of selected optical properties of semiconductors containing magnetic elements. Emphasis was placed on the interaction of such materials with ultrashort pulses of laser radiation in order to study coupled electronic and magnetic excitations under selected nonequilibrium conditions. We hoped to generate novel results through experimental research for applications to fast optoelectronic devices. The mixed crystal semiconductors (Cd, Mn)Se and (Cd, Mn)Te were used. The contract work has generated a number of firsts, e.g., we measured the formation of local, microscopic magnetically oriented domains through real-time spectroscopy with picosecond laser pulses. Author (GRA)

N87-13331# Hughes Research Labs., Malibu, Calif.
KINETICS AND MECHANISMS ON THE MOLECULAR BEAM ETCHING OF SEMICONDUCTORS Final Report, 15 Aug. 1982 - 15 Feb. 1986
H. P. Gillis Jul. 1986 58 p
(Contract DAAG29-82-C-0020)
(AD-A171360; ARO-19068.1-EL) Avail: NTIS HC A04/MF A01 CSCL 13/8

The main issue addressed was the role of the ion beam in control of anisotropy and selectivity in the ion-beam assisted etching (IBAE) of layered samples of Si and SiO2, as are used in CMOS gate applications. The results on patterned samples were correlated directly with the geometrical relationship of the incident beams and the sample. Rate data were obtained which suggest that the reaction proceeds by facilitated attack of reactant species at defect sites created by the ion beam. It was demonstrated that ion beam energy greater than 500 eV caused inadequate selectivity between Si and SiO2. It was shown that inadequate selectivity is the main problem holding back implementation of IBAE as a practical process. It is suggested that additional work in the direction of low energy IBAE (50-500 eV) be pursued. GRA

N87-13332# Minnesota Univ., Minneapolis. Dept. of Electrical Engineering.
QUANTUM 1/F NOISE IN SOLID STATE DOUBLE DEVICES, IN PARTICULAR Hg(1-x)CdxTe DIODES Final Report, 16 Sep. 1985 - 15 Mar. 1986
A. vanderZiel 22 May 1986 33 p
(Contract DAAG29-85-K-0235)
(AD-A171438; ARO-22874.1-EL) Avail: NTIS HC A03/MF A01 CSCL 20/10

It is shown how one can discriminate between two modes of diffusion 1/f noise fluctuations in p-n diodes: (1) all minority carriers contribute to the noise; (2) only the excess minority carriers contribute to the noise. The n(+)-p Hg(1-x)Cd(x)Te diodes seem to follow case (1) at back bias. For forward biased diodes S sub I(f)/I-sq is independent of bias, as expected for surface recombination in the p-region. P+-i-n Si diodes seem to follow case (2) at first sight, but this would be an erroneous conclusion, since in these diodes the noise is caused by recombination in the space charge region. The experiments give Si(f)/(abs. vol. I) = constant, as expected for recombination 1/f noise. In Hg1-xCdxTe the carrier lifetime has not yet been established, and hence the alpha sub H/tau data cannot be used to evaluate alpha sub H. It seems reasonable, however, that for x = 0.30 the estimated value of alpha sub H lies between the coherent state value .0046 and the incoherent state value .00005 depending on the value of tau. More accurate determination of tau (both theoretical and experimental) are being planned. GRA

N87-13333# Case Western Reserve Univ., Cleveland, Ohio.
EPITAXIAL CRYSTALLIZATION AND EPITAXIAL POLYMERIZATION AS TOOLS FOR MOLECULAR ENGINEERING Final Report, 1 Sep. 1983 - 31 Aug. 1986
Jerome B. Lando and Scott E. Rickert 30 Jul. 1986 15 p
(Contract DAAG29-83-K-0130)
(AD-A171506; ARO-20280.1-CH) Avail: NTIS HC A02/MF A01 CSCL 20/12

A study has been made of the use of epitaxial crystallization of polymers, epitaxial polymerization and combinations of surface interactions and reactions to produce polymer epilayers with unique structures, morphologies, and properties. Classically, epitaxial crystallization of polymers is the oriented crystallization of polymers during interaction with a crystalline substrate. Epitaxial polymerization involves the crystallization of a monomer on a crystalline substrate and subsequent polymerization initiated thermally by ionizing radiation or by chemical doping. In addition, a technique termed graphoepitaxy has been utilized which results from crystallization along deliberate deformities or topologies such as grooves in the substrate surface, and not necessarily crystallographic interactions. GRA

N87-13334# State Univ. of New York, Stony Brook. Dept. of Materials Science and Engineering.

ENERGETICS OF DISLOCATION RELAXATION ASSOCIATED WITH CLEAVAGE IN Cd-DOPED ZINC CRYSTALS AS PROBED BY SYCHROTRON TOPOGRAPHY

H. A. Schmitz, J. C. Bilello, and Z. Rek (Stanford Univ., Calif.) 1986 38 p Presented at the International Conference on Low-Energy Dislocation Structures, Charlottesville, Va., 10 Aug. 1986 Prepared in cooperation with Stanford Univ., CA.

(Contract DE-FG02-84ER-45098)

(DE86-002968; DOE/ER-45098/11; CONF-860809-1) Avail: NTIS HC A03/MF A01

An almost ten-fold increase in the cleavage energy of 0.1% Cd-doped zinc crystals has been previously reported in the literature and attributed to an increase in the intrinsic surface energy. The energetics of the cleavage process as a function of dopant concentration over the range 0.01, 0.03, 0.06 and 0.13% Cd has been systematically measured and correlated with the observed dislocation microstructure induced by crack initiation and growth. The dislocation relaxation zones were determined by nondestructive observations using synchrotron radiation topography. Since the primary cleavage and slip systems are co-planar, previous workers have ignored plastic relaxation and assumed fracture had to proceed in a purely brittle fashion. Synchrotron topography results indicated extensive plastic relaxation at the crack tip and also downstream during crack propagation. Based on these observations a modified Griffith analysis could be used to determine the relative contributions to the cleavage energy due to the intrinsic surface and dislocation relaxation processes. It was concluded that the latter process is the dominant factor in controlling the fracture toughness of these alloys. DOE

N87-13335# Oak Ridge National Lab., Tenn.

RECRYSTALLIZATION BEHAVIOR OF ION BEAM MODIFIED ALPHA-Al SUB 2 O SUB 3

P. S. Sklad 1986 5 p Presented at the Annual Joint Meeting of the Electron Microscopy of America and the Microbeam Analysis Society, Albuquerque, N. Mex., 10 Aug. 1986

(Contract DE-AC05-84OR-21400)

(DE86-009353; CONF-860829-21) Avail: NTIS HC A02/MF A01

Transmission electron microscopy was used to study amorphized implanted O-Al O. The response of the as-implanted amorphous layer to thermal aging varied with annealing temperature and time. The recrystallization is total and epitaxial at 1190°C. DOE

N87-13336# Sandia National Labs., Albuquerque, N. Mex.

ELECTRON DIFFRACTION ANALYSIS OF THE PENTAGONAL ARRANGEMENT OF GRAINS FOUND IN CVD PURE Ni FILMS

A. N. Campbell, M. J. Carr, and J. B. VanderSande (Massachusetts Inst. of Tech., Cambridge.) 1986 3 p Presented at the Annual Joint Meeting of the Electron Microscopy of America and the Microbeam Analysis Society, Albuquerque, N. Mex., 10 Aug. 1986 Prepared in cooperation with Massachusetts Inst. of Tech., Cambridge.

(Contract DE-AC04-76DP-00789)

(DE86-009023; SAND-86-0567C; CONF-860829-16) Avail: NTIS HC A02/MF A01

The structure of each crystal in the pentagon is fcc, as verified by diffraction patterns from individual grains. It is suggested that the large pentagonal regions observed were nucleated by small decahedral clusters of Ni atoms during the early stages of the deposition. However, for grains as large as those shown the body centered orthorhombic structure is not stable; at some point during the growth process the crystal structure reverted to the energetically preferred fcc. The relative orientation between the individual crystals, having been established by the decahedral nucleus, was preserved during growth. The 7.5 deg. mismatch was taken up evenly around the pentagon by the formation of dislocations and/or secondary twins at the boundaries. DOE

N87-13337# Ames Lab., Iowa.

IN-SITU INTERDIFFUSION MEASUREMENTS IN HgTe-CdTe SUPERLATTICES

J. L. Staudenmann, R. D. Horning, R. D. Knox, J. Reno, I. K. Sou, J. P. Faurie, and D. K. Arch 1986 17 p Presented at the Northeast Regional Meeting on Semiconductor-based Heterostructure Interfacial Structure and Stability, Murray Hill, N.J., 1 May 1986

(Contract W-7405-eng-82)

(DE86-011429; IS-M-576; CONF-8605111-2) Avail: NTIS HC A02/MF A01

HgTe-CdTe superlattices have been proposed as a tunable narrow bandgap semiconductor (E sub g approx. 0.1 to 0.16 eV) having potential applications in the long wavelength infrared region. The usefulness of such narrow band gap optical material relies on the stability of the constitutent Hg, Cd, and Te atoms across the heterointerfaces of the superlattice structure (interdiffusion). Temperature dependent in-situ x-ray diffraction measurements have been carried out on several HgTe-CdTe samples to determine the extent of interdiffusion of the Hg, Cd, and Te atoms in the superlattice region. The estimated interdiffusion constants D(T) are based on the analysis of the x-ray satellite intensities as a function of time for given temperatures T. The results show that the diffused (1,1,1) HgTe-CdTe superlattices are intrinsically more stable than Hg(1-x)Cd(x)Te alloys: the superlattice diffusion constants are considerably lower than those for alloys. The results further show that, even at room temperature, the lifetime of such a HgTe-CdTe superlattice device is probably limited and that it also seems to depend upon the environment. DOE

N87-13338# Southern Univ., Baton Rouge, La. Dept. of Physics.

EXPERIMENTAL THIN FILM DEPOSITION AND SURFACE ANALYSIS TECHNIQUES

W. E. Collins and B. Rambabu 1986 14 p Presented at the International Workshop on Ionic Batteries, Singapore, Singapore, 2 Jun. 1986

(Contract W-7405-eng-36)

(DE86-011222; LA-UR-86-1781; CONF-8606159-1) Avail: NTIS HC A02/MF A01

An attempt has been made to present some of the thin-film deposition and surface analysis techniques which may be useful in growing superionic conducting materials. Emphasis is made on the importance of being careful in selecting process parameters and materials in order to produce films with properties outlined in this article. Also, special care should be given to proper consideration of grain boundary effects. DOE

N87-13339# Sandia National Labs., Albuquerque, N. Mex.

STRUCTURAL FEATURES AT THE Si-SiO2 INTERFACE

K. L. Brower Jul. 1986 30 p Presented at the 4th International Symposium on Magnetic Resonance in Colloid and Interface Science, Munster, West Germany, 21 Jul. 1986

(Contract DE-AC04-76DP-00789)

(DE86-012947; SAND-86-0787C; CONF-860748-1) Avail: NTIS HC A03/MF A01

Electron paramagnetic resonance studies of defects at the Si-SiO2 interface are presented which deal with the hyperfine interactions, strain effects, and spin-spin interactions. Our hyperfine studies include studies of the O-17 and Si-29 hyperfine interactions associated with dangling bonds localized on Si atoms at the (001)

and (111) Si-SiO2 interfaces. These studies indicate that oxygen is not an immediate part of the defect structure. Strain is manifested in the EPR spectra by Zeeman and hyperfine broadening effects from which we deduce that the rms deviation in the vertical position of the defect Si atoms is approximately 0.02 A. A computational model for calculating the dipolar contribution to the linewidth due to unpaired spins at the interface is presented. The contribution to the total linewidth of the P/sub b/ Zeeman resonance, which is 2.1 G (fwhm), is calculated to be 0.35 G for the case in which the applied magnetic field is perpendicular to the (111) Si-SiO2 interface. DOE

N87-13340# International Centre for Theoretical Physics, Trieste (Italy).
POSSIBILITY OF USING DC CONDUCTIVITY FOR INVESTIGATING PHASE TRANSITION IN AMORPHOUS SEMICONDUCTORS
M. K. El-Mously and N. K. Mina Jul. 1985 16 p Prepared in cooperation with Ain Shams Univ., Cairo (Egypt)
(DE86-702646; IC-85/119) Avail: NTIS (US Sales Only) HC A02/MF A01

Different formulas were applied to deduce the effective or the generalized electrical conductivity of double phase systems. These formulas were revised and fitted to the experimental data of the binary systems amorphous-crystal (a-c) and liquid-crystal (l-c) for pure elementary selenium and selenium doped by other elements. Both connected medium and statistical mixture theories can be applied depending on the nature of the system under investigation. DOE

N87-13341# International Centre for Theoretical Physics, Trieste (Italy).
SURFACE GREEN FUNCTION MATCHING FOR A THREE-DIMENSIONAL NON-LOCAL CONTINUUM
J. O. A. Idiodi Jul. 1985 21 p
(DE86-702647; IC-85/125) Avail: NTIS (US Sales Only) HC A02/MF A01

With a view toward helping to bridge the gap, from the continuum side, between discrete and continuum models of crystalline, elastic solids, explicit results are presented for nonlocal stress tensors that describe exactly some lattice dynamical models that have been widley used in the literature for cubic lattices. The Surface Green Function Matching (SGFM) method, which has been used successfully for a variety of surface problems, is then extended, within a continuum approach, to a nonlocal continuum that models a three-dimensional discrete lattice. The practical use of the method is demonstrated by performing a fairly complete analytical study of the vibrational surface modes of the SSC semi-infinite medium. Some results are presented for the (100) direction of the (001) surface of the SCC lattice. DOE

N87-13342# International Centre for Theoretical Physics, Trieste (Italy).
SURFACE AND ADSORPTION-LIKE STATES WITHIN THE NEARLY FREE ELECTRON APPROXIMATION
L. Jurczyszyn Jul. 1985 11 p
(DE86-702651; IC-85/136) Avail: NTIS (US Sales Only) HC A02/MF A01

The energy properties of surface and absorption-like states were considered. In comparison with quasi-three-dimensional model which was presented earlier, the model described in this paper has pure three-dimensional character. Electronic states in fcc crystals were described using two-band model of the nearly free electron approximation. Absorbed atoms, treated as scattering centers were described by the small radium potential approximation. DOE

N87-13343# International Centre for Theoretical Physics, Trieste (Italy).
THEORY OF FRACTIONAL QUANTUM HALL EFFECT
I. Z. Kostadinov Aug. 1985 27 p
(DE86-702652; IC-85/141) Avail: NTIS (US Sales Only) HC A03/MF A01

A theory of the Fractional Quantum Hall Effect is constructed based on magnetic flux fractionization, which lead to instability of the system against selfcompression. A theorem is proved stating that arbitrary potentials fail to lift a specific degeneracy of the Landau level. For the case of 1/3 fractional filling a model 3-particles interaction is constructed breaking the symmetry. The rigid 3-particles wave function plays the role of order parameter. In a BCS type of theory the gap in the single particles spectrum is produced by the 3-particles interaction. The mean field critical behavior and critical parameters are determined as well as the Ginsburg-Landau equation coefficients. The Hall conductivity is calculated from the first principles and its temperature dependence is found. The simultaneous tunnelling of 3,5,7 etc. electrons and quantum interference effects are predicted. DOE

N87-13344# International Centre for Theoretical Physics, Trieste (Italy).
USE OF WANNIER FUNCTION IN THE CALCULATIONS OF BAND STRUCTURE OF COVALENT CRYSTALS
Dong Lu and Guang Yang Oct. 1985 14 p Prepared in cooperation with Fudan Univ., Shanghai, China
(DE86-702668; IC-85/191) Avail: NTIS (US Sales Only) HC A02/MF A01

A variational procedure has been used to build up Wannier functions to study the energy bands of diamond, silicon and O-tin. For the case of silicon the Wannier function, density of charge and band structure are calculated self-consistently and a simple method in a non-self-consistent way has been used to compute the band structure of diamond, silicon and O-tin. The method seems to be effective to describe the electronic properties of covalent crystals. DOE

N87-13345# International Centre for Theoretical Physics, Trieste (Italy).
TUNNELING EFFECT IN SUPERCONDUCTORS WITH MAGNETIC IMPURITIES
M. Ahmed Jul. 1985 14 p
(DE86-702723; IC-85/109) Avail: NTIS (US Sales Only) HC A02/MF A01

We investigate the influence of transition metal impurities on the amplitude of the Josephson tunneling current. We consider a junction made up of two identical superconductors containing transition metal impurities and define a parameter K which is the normalized difference of the derivative of Josephson currents for superconductin pairs with and without magnetic impurities. We find K=0 for U/Pi Gamma is greater than 1 and K=0.129 for U/PI Gamma is much greater than 1 in the Abrikosov-Gorkov theory, as well as large deviations of K from this value for 1 is greater than U/Pi Gamma is greater than 3, where U/Pi Gamma is the parameter of the Anderson theory. DOE

N87-13346# International Centre for Theoretical Physics, Trieste (Italy).
FLUX SPIRAL INSTABILITY IN A TRANSPORT CURRENT CARRYING TYPE 2 SUPERCONDUCTOR
L. N. Shehata and A. G. Saif Aug. 1985 18 p
(DE86-702724; IC-85/153) Avail: NTIS (US Sales Only) HC A02/MF A01

The nucleation of vortex flux lines on a surface of a transport current carrying type 2 superconductor in the presence of an external magnetic field H (sub e) occurs at H (sub e) is approximately = H (sub c1), the first critical field. A spiral flux line in a long cylinder and in a long thin ellipsoid is investigated. In the latter case the force-free magnetic fields are also considered. DOE

77 THERMODYNAMICS AND STATISTICAL PHYSICS

Includes quantum mechanics; theoretical physics; and Bose and Fermi statistics.

For related information see also *25 Inorganic and Physical Chemistry* and *34 Fluid Mechanics and Heat Transfer.*

N87-13347# Air Force Systems Command, Wright-Patterson AFB, Ohio. Foreign Technology Div.
JOURNAL OF ENGINEERING THERMOPHYSICS (SELECTED ARTICLES)
Lianfeng Duan, Baochang Dong, Zhaolong Wang, Yaolin Gao, and Keming Li 24 Jun. 1986 51 p Transl. into ENGLISH from Gongcheng Rewuli Xuebao China), v. 3, no. 2, May 1982 p 123-130, 135-137, 183-189
(AD-A169452; FTD-ID(RS)T-0312-86) Avail: NTIS HC A04/MF A01 CSCL 13/7

The Journal of Engineering Thermophysics, vol.3, no.2, May 1982, contains articles on the following topics: Effect of Part Span Shroud on Performance of a Single Stage Compressor; Effect of the Rear Stage Casing Treatment on the Overall Performance of a Multistage Axial Flow Compressor; Investigations on Performance of Swept Wing aircraft; Cascade of Axial Flow Compressor; and Thermal Performance of Turbine Vane with Ceramic Coatings with Enhanced Cooling. GRA

N87-13348# International Centre for Theoretical Physics, Trieste (Italy).
INDUCED QUANTUM TORSION
G. Denardo and E. Spallucci Jul. 1985 14 p Prepared in cooperation with Istituto Nazionale di Fisica Nucleare, Trieste (Italy)
(DE86-702616; IC-85/111) Avail: NTIS (US Sales Only) HC A02/MF A01

We study pregeometry in the framework of a Poincare gauge theory. The Rieman-Cartan space-time is shown to be an effective geometry for this model in the low energy limit. By using Heat Kernal techniques we find the induced action for curvature and torsion. We obtain in this way the usual Einstein-Hilbert action plus an axial Maxwell term describing the propagation of a massless, axial vector torsion field. DOE

N87-13349# International Centre for Theoretical Physics, Trieste (Italy).
SUPERCONFORMAL TENSOR CALCULUS AND MATTER COUPLINGS IN SIX DIMENSIONS
E. Bergshoeff, E. Sezgin, and A. van Proeyen Jul. 1985 59 p Prepared in cooperation with Louvain Univ. (Belgium)
(DE86-702617; IC-85/112) Avail: NTIS (US Sales Only) HC A04/MF A01

Using superconformal tensor calculus we constructed general interactions of N=2, d=6 supergravity with a tensor multiplet and a number of scalar, vector, and linear multiplets. We start from the superconformal algebra which we realize on a 40 + 40 Weyl multiplet and on several matter multiplets. A special role is played by the tensor multiplet, which cannot be treated as an ordinary matter multiplet, but leads to a second 40 + 40 version of the Weyl multiplet. We also obtain a 48 + 48 off-shell formulation of Poincare supergravity coupled to a tensor multiplet. DOE

80 SOCIAL SCIENCES (GENERAL)

Includes educational matters.

No abstracts in this category.

81 ADMINISTRATION AND MANAGEMENT

Includes management planning and research.

N87-13350# Naval Postgraduate School, Monterey, Calif.
REGRESSION MODELS OF QUARTERLY OVERHEAD COSTS FOR SIX GOVERNMENT AEROSPACE CONTRACTORS M.S. Thesis
David J. Jerabek Mar. 1986 94 p
(AD-A169185) Avail: NTIS HC A05/MF A01 CSCL 14/1

Since overhead costs constitute a large percentage of total cost for aerospace contractors, it is important to be able to predict them accurately. The research performed in this thesis takes six government aerospace contractors and obtains regression models of their overhead costs that can be utilized for forecasting purposes. This method is preferable to some of the more commonly used methods because it estimates overhead costs directly, eliminating reliance upon predicted overhead rates. After the data were transformed to eliminate the effects of autocorrelation, excellent structural results were obtained for five of the six aerospace contractors. A Monte Carlo simulation was performed to compare various estimators of the autocorrelation. Two of the estimators were found to be superior. These two estimators are both two-stage estimators that are calculated utilizing Wallis's test statistic for fourth-order autocorrelation. Author (GRA)

82 DOCUMENTATION AND INFORMATION SCIENCE

Includes information management; information storage and retrieval technology; technical writing; graphic arts; and micrography.

For computer documentation see *61 Computer Programming and Software.*

N87-13351# Army Field Artillery School, Fort Sill, Okla. Library Div.
GOVERNMENT LIBRARIES. A PERIODICALS BIBLIOGRAPHY, TOGETHER WITH LIST OF BIBLIOGRAPHIES AND INDEXES Final Report
Lester L. Miller, Jr. 4 Jul. 1986 21 p
(AD-A169422; USAFAS/MSTLD/SB116) Avail: NTIS HC A02/MF A01 CSCL 05/2

This two part number presents research on government libraries, here and aboard. The second portion consists of a bio-bibliography on bibliographies and indexes compiled by the Morris Swett Technical Library staff. GRA

N87-13352# Orlando Technology, Inc., Shalimar, Fla.
TSAR (THEATER SIMULATION OF AIRBASE RESOURCES) DATABASE DICTIONARY F-4E Final Report, 1 Aug. 1985 - 31 Jul. 1986
Dale Robinson and Cliff Gornto 28 Mar. 1986 257 p
(AD-A169575) Avail: NTIS HC A12/MF A01 CSCL 05/2

A significant problem for analysts and simulation model users is the availability of complete documentation of input databases. The Theater Simulation of Airbase Resources (TSAR) model is no exception. This TSAR dictionary documents the F-4E database by translating the database codes to their English equivalents, presents graphic network models for the decision logic networks for aircraft repair tasks, and a cross-reference index to facilitate its use by modelers and analysts. GRA

N87-13353# Naval Postgraduate School, Monterey, Calif.
FEDERAL INFORMATION SYSTEMS MANAGEMENT: PROBLEMS, SOLUTIONS AND MORE PROBLEMS Final Report
Dan C. Boger, Carl R. Jones, and Norman R. Lyons Jul. 1986 28 p
(AD-A171366; AD-F250645; NPS-54-86-006) Avail: NTIS

HC A03/MF A01 CSCL 05/1

Although there are numerous problems associated with the management of Federal information systems, the usual solutions proposed for these problems have had and will have little, if any, effects. This paper examines the characteristics of Federal information systems and shows that most proposed solutions are directed at symptoms of the problems and not at their underlying causes. These solutions do not reflect the public sector nature of Federal information systems and hence, are either unrealistic or ineffectual. The authors do not propose another panacea. GRA

N87-13354# Sandia National Labs., Albuquerque, N. Mex.
ELECTRONIC FORMS. HOW CLOSE TO VALUE-ADDED PROCESSING
J. R. Schofield, Jr. Apr. 1986 49 p Presented at the USDOE/ Contracts Automated Office Support Systems (AOSS) Conference, Pittsburgh, Pa., 14 May 1986
(Contract DE-AC04-76DP-00789)
(DE86-010484; SAND-86-1072C; CONF-8605126-1) Avail: NTIS HC A03/MF A01

The number of automated applications developed to support administrative activities continues to grow. While electronic mail and word processing are familiar office automation activities, other areas are under development consideration. One of the newer areas is electronic forms. The features that electronic forms need to employ, the challenges to electronic forms implementation and the integration with organizational data processing strategy are the subject of this paper. Purpose of this paper is to identify related issues for the reader. An electronic form is used in this paper to describe a system that captures, edits, routes, processes, tracks, secures and archives data electronically. The term form is used synonomously with electronic form. Paper forms are so identified. DOE

N87-13355# Martin Marietta Energy Systems, Inc., Oak Ridge, Tenn.
DATA TAGGING IN THE ENERGY DATA BASE
A. E. Ekkebus 1986 6 p Presented at the 14th Consultative Meeting of the INIS Liaison Officers, Washington, D.C., 5 May 1986
(Contract DE-AC05-84OR-21400)
(DE86-010621; CONF-8605125-1) Avail: NTIS HC A02/MF A01

The purpose of this study was to survey the use of data tagging in the Energy Data Base. INIS records are a subset of the Energy Data Base. The survey audience consisted of twelve heavy users of the Energy Data Base; primarily they are in the libraries of the national laboratories supported by the US Department of Energy. The libraries were contacted and told of this study. They were given an explanation of data tagging in late January and were requested to be aware of potential uses of data tagging during the study period that would extend until mid-March. At the end of the period, the libraries were contracted for their opinions about various aspects of data tagging. DOE

N87-13356# California Univ., Berkeley. Lawrence Berkeley Lab.
FURTHER RESULTS ON INTERPOLATION SEARCHING OF DATABASES
Z. J. Li and H. K.T. Wong Feb. 1986 25 p
(Contract DE-AC03-76SF-00098)
(DE86-012822; LBL-20708) Avail: NTIS HC A02/MF A01

Known results of the Interpolation Search Algorithm on ordered tables are extended in three ways. First, the effect of batching the search queries is examined. Second, the basically main-memory algorithm is applied to a more typical database environment, i.e., a blocked secondary memory. Third, a hybrid algorithm is examined to remedy the worst case behavior of the pure Interpolation Search in the event of non-uniform distribution of the ordered file while retaining the average complexity. Algorithms, analytic expressions and experiment results of these extensions are given and described. Analytic expressions of these algorithms are validated by the experiments. DOE

83 ECONOMICS AND COST ANALYSIS

Includes cost effectiveness studies.

No abstracts in this category.

84 LAW, POLITICAL SCIENCE AND SPACE POLICY

Includes NASA appropriation hearings; aviation law; space law and policy; international law; international cooperation; and patent policy.

N87-13357# Committee on Appropriations (U. S. House).
DEPARTMENT OF HOUSING AND URBAN DEVELOPMENT-INDEPENDENT AGENCIES APPROPRIATIONS FOR 1987, PART 7
1986 257 p Hearings before the Subcommittee on HUD and Independent Agencies of the Committee on Appropriations, 99th Congress, 2d Session, 13 May 1986
(GPO-61-970) Avail: Subcommittee on HUD and Independent Agencies

Appropriations for the 1987 Fiscal Year for National Aeronautics and Space Administration programs are discussed. B.G.

85 URBAN TECHNOLOGY AND TRANSPORTATION

Includes applications of space technology to urban problems; technology transfer; technology assessment; and surface and mass transportation.

For related information see also *03 Air Transportation and Safety, 16 Space Transportation,* and *44 Energy Production and Conversion.*

N87-13358*# Denver Univ., Colo.
THE UNCOUNTED BENEFITS: FEDERAL EFFORTS IN DOMESTIC TECHNOLOGY TRANSFER
Richard L. Chapman and Kathryn Hirst Jul. 1986 366 p
(Contract NASw-3466)
(NASA-CR-177044; NAS 1.26:177044) Avail: NTIS HC A16/MF A01 CSCL 05A

Organized technology transfer activities conducted by the agencies of the U.S. government are described. The focus is upon agency or departmental level activity rather than the laboratory level. None of the programs on which information was collected has been assessed or evaluated individually. However, the aggregate programs of the government have been judged in terms of obvious gaps and opportunities for future improvement. An overview, descriptions of the various agency or department programs of technology transfer, a list of persons interviewed or consulted during the survey, and a bibliography of publications, reports and other material made available to the study staff are given. An extensive appendix of illustrative material collected from the various programs is also given. Author

N87-13359*# National Aeronautics and Space Administration. Lewis Research Center, Cleveland, Ohio.
PROGRESS OF STIRLING CYCLE ANALYSIS AND LOSS MECHANISM CHARACTERIZATION Final Report
Roy C. Tew, Jr. 1986 19 p Presented at the 24th Automotive Technology Development Meeting, Dearborn, Mich., 27-30 Oct. 1986; sponsored by Society of Automotive Engineers
(NASA-TM-88891; DOE/NASA-50112/67; E-3302; NAS 1.15:88891) Avail: NTIS HC A01/MF A01 CSCL 10B

An assessment of Stirling engine thermodynamic modeling

and design codes shows a general deficiency; this deficiency is due to poor understanding of the fluid flow and heat transfer phenomena that occur in the oscillating flow and pressure level environment within the engines. Stirling engine thermodynamic loss mechanisms are listed. Several experimental and computational research efforts now underway to characterize various loss mechanisms are reviewed. The need for additional experimental rigs and rig upgrades is discussed. Recent developments and current efforts in Stirling engine thermodynamic modeling are also reviewed. Author

N87-13360# Naval Postgraduate School, Monterey, Calif.
AN EXAMINATION OF TECHNOLOGY TRANSFER AS A TOOL FOR MANAGEMENT M.S. Thesis
Don B. McCorkendale Mar. 1986 58 p
(AD-A169184) Avail: NTIS HC A04/MF A01 CSCL 05/1

An examination of the technology transfer process as it relates to contemporary management practice is made. The objective is to acquaint the reader with the concept of technology transfer and the mechanism of information flow within business organizations. Included is an in-depth analysis of the predictive model of technology transfer with an amphasis on the interrelationship between management and the factors affecting information flow. Author (GRA)

N87-13361# Pacific Northwest Labs., Richland, Wash.
TECHNOLOGY TRANSFER AT PACIFIC NORTHWEST LABORATORY Annual Report, FY 1985
M. Clement, J. M. Rusin, K. Drumheller, I. D. Hays, L. C. Schmid, and S. K. Edler Jan. 1986 54 p
(Contract DE-AC06-76RL-01830)
(DE86-012333; PNL-SA-13717) Avail: NTIS HC A04/MF A01

Technology transfer activities at Pacific Northwest Laboratory (PNL) for FY 1985 are summarized in this report. Objectives of these activities are as follows: Transfer federally funded and PNL-developed technology to state and local governments and the private sector; encourage and develop strong relationships between the region's educational institutions (elementary through college levels) to aid technology development and application; and assist in the transfer of federally funded technology that is developed elsewhere. DOE

88 SPACE SCIENCES (GENERAL)

No abstracts in this category.

89 ASTRONOMY

Includes radio, gamma-ray, and infrared astronomy, and astrometry.

N87-13362*# Smithsonian Astrophysical Observatory, Cambridge, Mass.
SPACE INFRARED TELESCOPE FACILITY WIDE FIELD AND DIFFRACTION LIMITED ARRAY CAMERA (IRAC) Semiannual Status Report, 1 Mar. - 31 Aug. 1986
Giovanni G. Fazio Oct. 1986 69 p
(Grant NAG2-316)
(NASA-CR-177041; NAS 1.26:177041; SASR-4) Avail: NTIS HC A04/MF A01 CSCL 03A

IRAC focal plane detector technology was developed and studies of alternate focal plane configurations were supported. While any of the alternate focal planes under consideration would have a major impact on the Infrared Array Camera, it was possible to proceed with detector development and optical analysis research based on the proposed design since, to a large degree, the studies undertaken are generic to any SIRTF imaging instrument. Development of the proposed instrument was also important in a situation in which none of the alternate configurations has received the approval of the Science Working Group. E.R.

N87-13363*# National Aeronautics and Space Administration. Ames Research Center, Moffett Field, Calif.
INFRARED REFLECTION NEBULAE IN ORION MOLECULAR CLOUD 2
Yvonne Pendleton, M. W. Werner, R. Capps (Hawaii Univ., Honolulu.), and D. Lester (Texas Univ., Austin.) Jun. 1986 46 p
(NASA-TM-88259; A-86276; NAS 1.15:88259) Avail: NTIS HC A03/MF A01 CSCL 03A

New obervations of Orion Molecular Cloud-2 have been made from 1-100 microns using the NASA Infrared Telescope Facility and the Kuiper Airborne Observatory. An extensive program of polarimetry, photometry and spectrophotometry has shown that the extended emission regions associated with two of the previously known near infrared sources, IRS1 and IRS4, are infrared reflection nebulae, and that the compact sources IRS1 and IRS4 are the main luminosity sources in the cloud. The constraints from the far infrared observations and an analysis of the scattered light from the IRS1 nebula show that OMC-2/IRS1 can be characterized by L less than or equal to 500 Solar luminosities and T approx. 1000 K. The near infrared (1-5) micron albedo of the grains in the IRS1 nebula is greater than 0.08. Author

N87-13364 Arizona Univ., Tucson.
INVESTIGATIONS OF LONG-PERIOD DQ HERCULIS STAR Ph.D. Thesis
William Roy Penning 1986 190 p
Avail: Univ. Microfilms Order No. DA8613445

The magnetic rotator model has long been the favored explanation for coherent photometric modulations in the DQ Herculis class of cataclysmic variables. However, to date, all evidence supporting this model has been of the indirect variety. Unlike their synchronously rotating cousins, the AM Herculis objects, DQ Herculis stars have not yet been discovered to emit polarized radiation. Therefore, in light of this crucial lack, the evidence used to place these objects in the magnetic cataclysmic variable category has been strictly circumstantial, based primarily on the coherence of the photometric periodicities. For this work, time-resolved spectroscopy of four long-period DQ Herculis stars was performed. In addition, two of the same objects were observed with a new, sensitive circular polarimeter. Coherent variations in the wavelength of emission lines were found with the spectroscopic observations. A model is put forth, explaining this phenomenon as being due to varying illumination from a bright spot on the primary. This adds strength to the magnetic rotator model. Circular polarization was definitely found in one object studied, and possibly in a second. In a later chapter of the thesis, the model of the rotating bright spot illuminating the disk is explored in further detail, including modeling with a minicomputer. Afterward, a problem brought out by the low polarization coupled with large amplitude photometric variations and a cool spectrum is investigated, namely, whether it is possible to produce large amounts of cyclotron radiation without producing large amounts of circular polarization. Dissert. Abstr.

90 ASTROPHYSICS

Includes cosmology; celestial mechanics; space plasmas; and interstellar and interplanetary gases and dust.
For related information see also *75 Plasma Physics.*

N87-13365*# Michigan Univ., Ann Arbor. Dept. of Astronomy.
OBSERVATIONAL STUDY OF ION-ELECTRON EQUILIBRATION AND OF CLOUD EVAPORATION IN SUPERNOVA REMNANTS UNDER THE HEAO-2 GUEST INVESTIGATOR PROGRAM Final Project Report, 1 Jun. 1985 - 30 Sep. 1986

Richard G. Teske 30 Sep. 1986 11 p
(Grant NAG8-535)
(NASA-CR-179922; NAS 1.26:179922) Avail: NTIS HC A02/MF A01 CSCL 03B

Observations of three selected supernovae remnants (Cygnus Loop, IC 443, and Puppis A) were made in the forbidden coronal iron lines (Fe X) lambda 6374 and (Fe XIV) lambda 5303. The resulting data was compared quantitatively with Einstein images of the same objects, and an attempt was made to determine (a) the process by which ion and electron energies are equilibrated behind the shock front in the ISM and (b) whether cloud evaporation occurs within the hot remnant interiors. Spatially-resolved X ray emission were modeled for Sedov-Taylor blast wave models of supernovae remnants (SNR) under conditions of non-equlibrium ionization. The computations are intended to provide results that can be directly compared with Einstein high resolution image (HRI) and imaging proportional counter (IPS) data. The computer program for predicting the spatial distribution of HRI and IPS counting rates was completed, and final testing of it had begun. E.R.

N87-13366*# National Aeronautics and Space Administration. Goddard Space Flight Center, Greenbelt, Md.
HIGH ENERGY NEUTRINO ABSORPTION AND ITS EFFECTS ON STARS IN CLOSE X-RAY BINARIES
T. K. Gaisser and F. W. Stecker Jul. 1986 21 p Submitted for publication
(NASA-TM-89269; NAS 1.15:89269) Avail: NTIS HC A02/MF A01 CSCL 03B

The physics and astrophysics of high energy neutrino production and interactions in close X-ray binary systems are studied. These studies were stimulated by recent observations of ultrahigh energy gamma-rays and possibly other ultrahigh energy particles coming from the directions of Cygnus X-3 and other binary systems and possessing the periodicity characteristics of these systems. Systems in which a compact object, such as a neutron star, is a strong source of high energy particles which, in turn, produce photons, neutronos and other secondary particles by interactions in the atmosphere of the companion star were considered. The highest energy neutrinos are absorbed deep in the companion and the associated energy deposition may be large enough to effect its structure or lead to its ultimate disruption. This neutrino heating was evaluated, starting with a detailed numerical calculation of the hadronic cascade induced in the atmosphere of the companion star. For some theoretical models, the resulting energy deposition from neutrino absorption may be so great as to disrupt the companion star over an astronomically small timescale of the order of 10,000 years. Even if the energy deposition is smaller, it may still be high enough to alter the system substantially, perhaps leading to quenching of high energy signals from the source. Given the cosmic ray luminosities required to produce the observed gamma rays from cygnus X-3 and LMX X-4, such a situation may occur in these sources. E.R.

N87-13367*# National Aeronautics and Space Administration. Goddard Space Flight Center, Greenbelt, Md.
ON THE TWO STATES OF CYG X-1 AND RELATED SOURCES
Demosthenes Kazanas Jul. 1986 15 p Submitted for publication
(NASA-TM-89265; NAS 1.15:89265) Avail: NTIS HC A02/MF A01 CSCL 03B

A model for active galactic nuclei (AGN), employing quasi-spherical accretion onto a black hole, when scaled down to solar mass objects, provides a straightforward account of the bimodal spectral behavior of Cyg X-1 and the other galactic black hole candidates. It is argued that the change in the spectrum is due to the drastic increase of the source compactness (L/R) with the accretion rate m and the subsequent conversion of most of the energy released by accretion into e(+)e(-) pairs. It is also argued that similar changes may be observed in active galactic nuclei.
Author

N87-13368*# Pennsylvania State Univ., University Park. Dept. of Astronomy
CONTINUUM RADIATION FROM ACTIVE GALACTIC NUCLEI: A STATISTICAL STUDY
Takashi Isobe, Eric D. Feigelson (National Science Foundation, Washington, D.C.), Kulinder P. Singh (Danish Space Research Inst., Lyngby.), and Ajit Kembhavi (Tata Inst. of Fundamental Research, Bombay (India).) 1986 81 p
(Grant NAG8-555)
(NASA-CR-179925; NAS 1.26:179925) Avail: NTIS HC A05/MF A01 CSCL 03B

The physics of the continuum spectrum of active galactic nuclei (AGNs) was examined using a large data set and rigorous statistical methods. A data base was constructed for 469 objects which include radio selected quasars, optically selected quasars, X-ray selected AGNs, BL Lac objects, and optically unidentified compact radio sources. Each object has measurements of its radio, optical, X-ray core continuum luminosity, though many of them are upper limits. Since many radio sources have extended components, the core component were carefully selected out from the total radio luminosity. With survival analysis statistical methods, which can treat upper limits correctly, these data can yield better statistical results than those previously obtained. A variety of statistical tests are performed, such as the comparison of the luminosity functions in different subsamples, and linear regressions of luminosities in different bands. Interpretation of the results leads to the following tentative conclusions: the main emission mechanism of optically selected quasars and X-ray selected AGNs is thermal, while that of BL Lac objects is synchrotron; radio selected quasars may have two different emission mechanisms in the X-ray band; BL Lac objects appear to be special cases of the radio selected quasars; some compact radio sources show the possibility of synchrotron self-Compton (SSC) in the optical band; and the spectral index between the optical and the X-ray bands depends on the optical luminosity. Author

N87-13369# Naval Postgraduate School, Monterey, Calif.
CLASSIFICATION OF N-TYPE CARBON STARS M.S. Thesis
William V. Bollwerk Jun. 1986 75 p
(AD-A171399) Avail: NTIS HC A04/MF A01 CSCL 03/2

Carbon stars are in an advanced state of evolution and are of interest for understanding the rapid evolutionary processes during late stages of stellar evolution. They are cool ($T < 4000K$) stars with an atmospheric carbon to oxygen ratio (C/O) greater than one. Most other classes of stars exhibit atmospheric $C/O < 1$. Low resolution spectrophotometry has been used to examine the relationship between spectral class and effective temperatures in a sample of eleven cool carbon stars. Using effective temperatures from lunar occultation observations of Tsuji and Ridgeway et al, CN and C2 features have been examined for their utility as classification criteria. It is found that C2 strength is not a reliable temperature classification parameter, while CN should be useful. Comparison of the carbon star classification systems of Keenan and Morgan and that of Richer with recent derived temperatures and the results of this study indicates that the Richer classification system more accurately reflects the temperatures of cool carbon stars. GRA

N87-13370# Paraiba Univ., Joao Pessoa (Brazil). Dept. de Fisica.
SUPERGRAVITY
V. deOliveiraRivelles 1985 53 p In PORTUGUESE
(DE86-701481; INIS-BR-426) Avail: NTIS (US Sales Only) HC A04/MF A01

The main aspects of the supergravity are presented. Several implications are discussed when the global symmetry is transformated in a local one. The super symmetric Higgs mechanism as well as the Kaluza-Klein theory are also discussed. DOE

N87-13371# Los Alamos National Lab., N. Mex.
LOS ALAMOS SCIENCE, NUMBER 13, SPRING 1986
N. G. Cooper 1986 75 p
(Contract W-7405-eng-36)

(DE86-012864; LA-UR-86-730) Avail: NTIS HC A04/MF A01

A review of the advances that have been made in the field of X-ray astrophysics is presented. A discussion of the information which can be gleaned from the spectra is also presented. The internal dynamics of neutron stars is discussed. Models of neutron star structure are discussed. A cooperative experiment which measured the spectra of Cygnus X-3 (10^9 to 10^{18} hertz) is discussed. The role of angular momentum in the cosmology of the universe is discussed. DOE

N87-13372# International Centre for Theoretical Physics, Trieste (Italy).

CANONICAL QUANTIZATION OF GRAVITY

T. Christodoulakis and J. Zanelli Jul. 1985 15 p Prepared in cooperation with Chile Univ., Santiago

(DE86-702615; IC-85/102) Avail: NTIS (US Sales Only) HC A02/MF A01

We present a scheme for carrying out in part the program of quantization of gravity in canonical form. The idea is to exploit the covariance of any Lagrangian theory under changes in the generalized coordinates, to select a particular ordering for the operator constraints of quantum gravity. A modified form of the canonical commutation relations (CRSs) is used which maintains full covariance under diffeomorphisms in three-space. The resulting commutator algebra of these operators is found to close, as required by consistency. Some remarks are made about the possible renormalizability and unitarity of the resulting theory, as well as the possible vanishing of the renormalized cosmological constant. DOE

N87-13373# International Centre for Theoretical Physics, Trieste (Italy).

ASTRO-PARTICLE-PHYSICS

A. Salam Sep. 1985 6 p

(DE86-702946; IC-85/227) Avail: NTIS (US Sales Only) HC A02/MF A01

Opening remarks at the Fourth Marcel Grossman Meeting, 17 to 21 June 1985, in Rome, Italy, are reported. The meeting was concerned with the symbiosis of cosmology and particle physics. Numerous connections between work in particle physics and cosmology, in both experimental and theoretical areas, are pointed out. DOE

N87-13374 Washington Univ., Seattle.

PLANE-PARALLEL AND BOW SHOCK MODELS OF HERBIG-HARO OBJECTS Ph.D. Thesis

Alejandro Christian Raga 1985 154 p

Avail: Univ. Microfilms Order No. DA8613204

It is now generally accepted that the emission line spectrum of Herbig-Haro objects is formed in the recombination region behind a shock wave. Plane-parallel shock wave models have been quite successful at reproducing many of the observed characteristics of these spectra, but in order to be able to predict line profiles and the spatial distribution of the emission, at least two-dimensional models are needed. In this thesis, a model for a bow shock formed around a bullet (which moves supersonically with respect to the surrounding medium) is developed, and is then used to predict position-velocity diagrams (i.e., long-slit spectra) and two-dimensional intensity contour maps for several emission lines. The thesis is divided into two parts: (1) A calculation of stationary, plane parallel shock wave models, in which a full treatment of the pre-shock region is included. The emission line spectra of both the pre- and the post-shock regions are predicted. (2) The development of a bow shock model (for a gas with an important radiative energy loss), from which the spatially resolved line spectrum is predicted. A qualitative comparison of the predictions from the bow shock models with recent observations of Herbig-Haro objects HH 1 and HH 32 shows that, at least for these two objects, a good agreement between the observations and the theory of a radiating bow shock is obtained. This seems to indicate that the emission line spectra of these two Herbig-Haro objects are formed in the recombination region behind a bow shock. Dissert. Abstr.

91 LUNAR AND PLANETARY EXPLORATION

Includes planetology; and manned and unmanned flights.

For spacecraft design or space stations see *18 Spacecraft Design, Testing and Performance.*

N87-13375*# National Aeronautics and Space Administration, Washington, D.C.

THE UPPER ATMOSPHERE OF VENUS: A TENTATIVE EXPLANATION OF ITS ROTATION

C. Boyer Sep. 1986 13 p Transl. into ENGLISH from L'Astronomie (France), v. 100, Feb. 1986 p 77-83 Transl. by Kanner (Leo) Associates, Redwood City, Calif.

(Contract NASw-4005)

(NASA-TM-88505; NAS 1.15:88505) Avail: NTIS HC A02/MF A01 CSCL 03B

The upper atmosphere of Venus seems to revolve every 4 days, while the planet rotates in 243 days. Mariner 10 UV data on the changing positions of dark spots in the upper Venusian clouds have supported estimations of speeds ranging from 120-240 m/s. High rates of acceleration and deceleration occur on the night side, the former between -110 to -90 deg and the latter continuing to -50 deg. Arch and Y formations have been seen repeatedly between -110 to -70 deg. The highest are seen at about -90 deg and the lowest at about -30 deg. The temperature of the cloud layer at 60 km altitude is about 20 C, the pressure is nearly one earth atmosphere, and complex molecules, including O, C, H, N and S and combinations of these are present in abundance. Author

N87-13376*# National Aeronautics and Space Administration, Washington, D.C.

RELIEF AND GEOLOGY OF THE NORTH POLAR REGION OF THE PLANET VENUS

R. O. Kuzmin, G. A. Burba, V. P. Shashkina, A. F. Bogomolov, N. V. Zherikhin, G. I. Skrypnik, L. V. Kudrin, M. Yu. Bergman, O. N. Rzhiga, A. I. Sidorenko et al Sep. 1986 25 p Transl. into ENGLISH from Astronomicheskiy Vestnik (Moscow, USSR), v. 20, no. 3, 1986 p 177-196 Transl. by Kanner (Leo) Associates, Redwood City, Calif.

(Contract NASw-4005)

(NASA-TM-88498; NAS 1.15:88498) Avail: NTIS HC A02/MF A01 CSCL 03B

Description of topographic features is given for the North polar region of the planet Venus. Principal geomorphic types of terrain are characterized as well as their geologic relations. Relative ages of geologic units in Venus North polar region are discussed. Author

92 SOLAR PHYSICS

Includes solar activity, solar flares, solar radiation and sunspots.

For related information see *93 Space Radiation.*

N87-13377# Instituto de Pesquisas Espaciais, Sao Jose dos Campos (Brazil).

SOLAR FLUX AND GEOMAGNETIC ACTIVITY PREDICTION

Roberto VieriradaFonsecaLopez, Helio Koiti Kuga, and Valdemir Carrara May 1986 6 p Presented at TELECON, Rio De Janeiro, Brazil, 10-13 Oct. 1985

(INPE-3884-PRE/934) Avail: NTIS HC A02/MF A01

The main concern is the establishment of prediction models for the solar activity which greatly influences the behavior of the upper atmosphere constituent elements. Such models are aimed at applications in orbit computations of close earth satellites (< 1000 km) which, within this altitude range, are affected by atmospheric drag. Author

N87-13378# Instituto de Pesquisas Espaciais, Sao Jose dos Campos (Brazil).
REPETITION RATES OF FAST PULSES IN MM-WAVES/X-RAY SOLAR BURSTS
E. Correia and P. Kaufmann Aug. 1986 29 p Presented at the 2nd CESRA Workshop, Aubigny, France, Jun. 1986 Sponsored in part by FINEP
(INPE-3974-PRE/986) Avail: NTIS HC A03/MF A01

The solar burst of 21 May, 1984, 1326 UT, presented radio spectral emission with turnover frequency above 90 GHz, well correlated in time with hard X-ray emission. It consisted of seven major time structures (1-3 seconds in duration), and each structure consisted of various fast pulses (30-60 ms rise times). The spectral indices between 30-90 GHz, and the power-law indices at hard X-ray exhibited sudden changes for each major time structure. The subsecond pulses are nearly in phase at 30 and 90 GHz, but the relative amplitude of the pulses at 90 GHz (approx. = 50%) were considerably larger than at 30 GHz (less than 5%). It was found that the 90 GHz and the 100 keV X-rays fluxes are proportional to the repetition rates of the subsecond pulses, and that the hard X-rays power law indices harden for higher repetition rates. Author

N87-13379*# National Aeronautics and Space Administration. Goddard Space Flight Center, Greenbelt, Md.
MAX '91: AN ADVANCED PAYLOAD FOR THE EXPLORATION OF HIGH ENERGY PROCESSES ON THE ACTIVE SUN
Jun. 1986 62 p
(NASA-TM-89271; NAS 1.15:89271) Avail: NTIS HC A04/MF A01

The results of a NASA science working group established to study a follow-on to the Solar Maximum Mission are given. A complement of instruments is suggested, with the primary objective of studying the physics of energetic processes in cosmic plasmas by observing high-energy phenomena in solar flares. High-quality flare observations will be possible with these instruments during the next peak in solar activity expected to last from 1990 through at least 1995. The primary objective of MAX '91 is to study energetic processes in cosmic plasmas by observing high-energy phenomena in solar flares. These processes, which are of general astrophysical importance, include energy release, particle acceleration, and energy transport. Results from comprehensive observing programs conducted during the last solar cycle have demonstrated the great scientific potential of high-energy emissions for addressing these central physical processes. Consequently, a payload optimized for observations of high-energy solar flare phenomena is suggested for MAX '91. It consists of the following four specific instruments: (1) a Fourier-transform X-ray and gamma-ray imager covering the energy range from a few keV to 1 MeV with arcsecond spatial resolution; (2) a cooled germanium X-ray and gamma-ray spectrometer with keV spectral resolution covering the energy range from 10 keV to 50 MeV; (3) Bragg spectrometers with high spectral resolution at wavelengths between 1 and 9 angstrons; and (4) a soft X-ray, EUV, or UV imaging instrument with arcsecond spatial resolution. Author

N87-13380# Alaska Univ., Fairbanks. Geophysical Inst.
A STUDY OF THE RELATIONSHIP BETWEEN SOLAR ACTIVITY AND INTERPLANETARY FIELD VARIATIONS Final Report, 14 May - 30 Sep. 1985
S. I. Akasofu and L. C. Lee Feb. 1986 25 p
(Contract F19628-85-K-0045)
(AD-A169983; AFGL-TR-86-0032) Avail: NTIS HC A02/MF A01 CSCL 03/2

The origin of large values of the interplanetary magnetic field Bz component, the nature of the so-caled driver gas, the origin of the high speed solar wind streams are the three major issues in solar-terrestrial physics. Several initial attempts are made to study them and find new steps toward a better understanding. GRA

N87-13381# Louisiana State Univ., Baton Rouge. Dept. of Physics and Astronomy.
SOLAR FLARES AND MAGNETOSPHERIC PARTICLES: INVESTIGATIONS BASED UPON THE ONR-60 EXPERIMENTS AND ONR-604 EXPERIMENTS Annual Letter Report, 1 May 1985 - 30 Jun. 1986
John P. Wefel 27 Jun. 1986 16 p
(Contract N00014-83-K-0365)
(AD-A170620) Avail: NTIS HC A02/MF A01 CSCL 04/1

The project involves analysis of the data returned from the ONR-602 (Phoenix-1) experiment on the S81-1 in mission in 1982, correlation of the Phoenix-1 dataset with other measurements and scientific planning for the launch and operation of a sister experiment, ONR-604, on the CRES mission. During the past year significant progress was made in understanding the ONR-602 instrument performance and the dataset, in analyzing the low energy protons observed in the equatorial belt, in summarizing solar energetic particle observations, and in working with the CRRES/SPACERAD Science Team. GRA

N87-13382# Los Alamos National Lab., N. Mex.
MAGNETIC FIELD RE-ARRANGEMENT AFTER PROMINENCE ERUPTION
R. A. Kopp and G. Poletto 1986 6 p Presented at the NASA Workshop on Coronal and Prominence Plasmas, Berkeley Springs, W. Va., 8 Apr. 1986 Prepared in cooperation with Osservatorio Astrofisico di Arcetri, Florence (Italy).
(Contract W-7405-eng-36)
(DE86-012393; LA-UR-86-1906; CONF-8604219-1) Avail: NTIS HC A02/MF A01

It has long been known that magnetic reconnection plays a fundamental role in a variety of solar events. Although mainly invoked in flare problems, large-scale loops interconnecting active regions, evolving coronal hole boundaries, the solar magnetic cycle itself, provide different evidence of phenomena which involve magnetic reconnection. A further example might be given by the magnetic field rearrangement which occurs after the eruption of a prominence. Since most often a prominence reforms after its disappearance and may be observed at about the same position it occupied before erupting, the magnetic field has to undergo a temporary disruption to relax back, via reconnection, to a configuration similar to the previous one. The above sequence of events is best observable in the case of two-ribbon (2-R) flares but most probably is associated with all filament eruptions. Even if the explanation of the magnetic field rearrangement after 2-R flares in terms of reconnection is generally accepted, the lack of a three-dimensional model capable of describing the field reconfiguration, has prevented, up to now, a thorough analysis of its topology as traced by Hℓ/x-ray loops. The purpose of the present work is to present a numerical technique which enables one to predict and visualize the reconnected configuration, at any time, and therefore allows one to make a significant comparison of observations and model predictions throughout the whole process. DOE

N87-13383# Los Alamos National Lab., N. Mex.
LARGE-SCALE ELECTRIC FIELDS RESULTING FROM MAGNETIC RECONNECTION IN THE CORONA
R. A. Kopp and G. Poletto 1986 6 p Presented at the NASA Workshop on Coronal and Prominence Plasmas, Berkeley Springs, W. Va., 8 Apr. 1986 Prepared in cooperation with Osservatorio Astrofisico di Arcetri
(Contract W-7405-eng-36)
(DE86-012391; LA-UR-86-1907; CONF-8604219-2) Avail: NTIS HC A02/MF A01

The method of Forbes and Priest (2-D model) is applied to the large two-ribbon flare of July 29, 1973, for which both detailed Hℓ observations and magnetic data are available. For this flare the ribbons were long, nearly straight, and parallel to each other, and the 2-D model for the coronal field geometry may be adequate. The temporal profile E(t) is calculated and indicates that reconnection sets in at the beginning of the decay phase. From this time the electric field grows rapidly to a maximum value of about 2 V/cm within just a few minutes. Thereafter it decreases monotonically with time. DOE

N87-13384# International Centre for Theoretical Physics, Trieste (Italy).
EQUILIBRIUM CONFIGURATION OF CORONAL LOOPS
V. Krishan Aug. 1985 10 p
(DE86-702711; IC-85/96) Avail: NTIS (US Sales Only) HC A02/MF A01

The steady-state pressure structure of a solar coronal loop is describable by a superposition of Chandrasekhar-Kendall functions. Each Chandrasekhar-Kendall function represents a force-free state. We extend this work to study the dynamical evolution of the loop as it moves outwards in the external medium while constantly maintaining its minimal energy configuration. This enables one to calculate the rate of energy dissipation as the loop moves outwards remaining in the minimal energy state under the invariance of the magnetic helicity and the magnetic fluxes. It is found that the nonaxisymmetric state becomes more favorable when the external pressure falls below a critical value. DOE

N87-13385 Georgia Inst. of Tech., Atlanta.
MODEL STUDIES OF SOLAR SPECTRAL IRRADIANCE AT THE BOTTOM AND TOP OF A CLOUDY ATMOSPHERE Ph.D. Thesis
Mark Vaughan Paris 1985 146 p
Avail: Univ. Microfilms Order No. DA8604013

The development and testing of a spectral model for transmission of solar radiation through a cloudy atmosphere are described. Clear-sky effects include absorption by ozone, water vapor, the uniformly-mixed gases and aerosols; and scattering by air molecules (Rayleigh scattering) and aerosols. These optical effects are treated with a Beer's Law relationship using extinction coefficients for each of 145 spectral intervals from 0.29 to 3.0 microns. Cloud optical effects are treated with the delta-Eddington approximation. The model calculates spectral irradiances at the surface and the top of the atmosphere. The model is tested against 221 hours of broad-band and spectral (greater than 630 nm) irradiances measured at the Georgia Tech Solar Energy Meteorological Research and Training Site. Upward irradiances at the top of the atmosphere are converted into directional radiances through empirical bidirectional reflectance factors and the resulting radiances are compared against radiances for 168 hours measured by satellite at the same time and at the same hours measured by satellite at the same time and at the same location. The model reproduces measured surface irradiances with a root-mean-square error of 11.7% of the model mean. The directional reflectances have an rms error of 16.4% of the model mean; when nine outlying points are removed from the data, the remaining data have an rms error of 12.5% of the mean. Testing of the model indicates that it has sufficient accuracy for such purposes as calibration of satellite sensors in the visible spectrum. Dissert. Abstr.

N87-13386 California Univ., Los Angeles.
THE CARBON TWELVE TO CARBON THIRTEEN ISOTOPE RATIO OF THE INTERSTELLAR MEDIUM IN THE NEIGHBORHOOD OF THE SUN Ph.D. Thesis
Isabel Hawkins 1986 293 p
Avail: Univ. Microfilms Order No. DA8614091

The C-12/C-13 ratio in the interstellar medium (ISM) was obtained from optical observations of interstellar CH+ toward five stars in the solar neighborhood. This isotope ratio is a probe of nucleosynthesis and imposes stringent constraints on galactic chemical evolutionary models. As a result of this work, we have found that the local interstellar medium C-12/C-13 abundance ratios toward four different lines of sight are uniform within 14%. We thus provide concrete evidence in favor of the existence of a homogeneous ISM in a small scale. The similarity among the C-12/C-13 ratios determined in four interstellar clouds possessing different physical conditions, precludes the possibility that fractionation or selective photodissociation of CH+ are taking place in these regions. We can then safety state that the (12)CH+/(13) CH+ isotope ratios we have observed are representative of the C-12/C-13 ratios in the gas. We have thus calculated a weighted mean ratio of 43 +/- 4 from the measured values toward our program stars. From our observations we have been able to assess the amount of processing of material by nucleosynthesis in stars that has occurred since the formation of the Sun. Since our derived ISM ratios are a factor of two smaller than the value of 89 in the solar system, we concluded that the ISM has evolved chemically since the formation of the Sun, in accordance with the predictions put forth by the majority of the galactic chemical evolutionary models. Dissert. Abstr.

N87-13387*# Stanford Univ., Calif. Center for Space Science and Astrophysics.
RAPID FLUCTUATIONS IN SOLAR FLARES
P. A. Sturrock Apr. 1986 31 p
(Contracts N00014-85-K-0111; NGL-05-020-272)
(NASA-CR-179894; NAS 1.26:179894; AD-A169586; AD-E500769; CSSA-ASTRO-86-29) Avail: NTIS HC A03/MF A01 CSCL 03/2

Study of rapid fluctuations in the emission of radiation from solar flares provides a promising approach for probing the magnetoplasma structure and plasma processes that are responsible for a flare. It is proposed that elementary flare bursts in X ray and microwave emission may be attributed to fine structure of the coronal magnetic field, related to the aggregation of photospheric magnetic field into magnetic knots. Fluctuations that occur on a sub-second time scale may be due to magnetic islands that develop in current sheets during magnetic reconnection. The impulsive phase may sometimes--or possibly always--represent the superposition of a large number of the elementary energy release processes responsible for elementary flare bursts. If so, one faces the challenge of trying to explain the properties of the impulsive phase in terms of the properties of the elementary processes. For instance, if the impulsive phase produces a power law energy distribution of energetic particles, this may be due to scaling laws governing the elementary processes rather than to power-law accelerations in each elementary event. GRA

93 SPACE RADIATION

Includes cosmic radiation; and inner and outer earth's radiation belts.

For biological effects of radiation see *52 Aerospace Medicine*. For theory see *73 Nuclear and High-Energy Physics*.

N87-13388# Instituto de Pesquisas Espaciais, Sao Jose dos Campos (Brazil).
A SURVEY OF HARD-X-RAYS AT BALLOON ALTITUDES OF THE EARTH'S ATMOSPHERE
O. Pinto, Jr., W. D. Gonzalez, and J. M. daCosta Jul. 1986 9 p Sponsored in part by Fundo Nacional de Desenvolvimento Cientifico e Tecnologico Submitted for publication
(INPE-3954-PRE/972) Avail: NTIS HC A02/MF A01

A brief discussion of hard X-ray measurements in the Earth's atmosphere is presented. In this context, recent measurements using balloon-borne detectors in the South Atlantic Magnetic Anomaly (SAMA) have provided the first evidence of the presence of hard X-rays produced by natural electron precipitation in this region. These hard X-rays are compared to those due to other sources. Author

N87-13389# Aerospace Corp., El Segundo, Calif. Space Sciences Lab.
CONTRIBUTIONS TO THE 18TH INTERNATIONAL COSMIC RAY CONFERENCE
J. Bernard Blake, J. F. Fennell, R. Koga, N. Katz, D. S. P. Dearborn (Arizona Univ., Tucson.), and Steven H. Margolis (Washington Univ., St. Louis, Mo.) 10 Mar. 1986 20 p Conference held in Bangalore, India
(ATR-86(9558)-11) Avail: NTIS HC A02/MF A01

Four papers presented at the 18th International Cosmic Ray Conference are compiled. Topic areas include: ultraheavy cosmic rays, secondary production of gamma rays in the Jovian magnetosphere, the stellar upper mass limit in an OB association, and a

data processing unit for satellite- borne composition instrumentation. For individual titles, see N87-13390 through N87-13393.

N87-13390# Washington Univ., St. Louis, Mo. Center for the Space Sciences.

THE ULTRAHEAVY COSMIC RAYS: PROPAGATION AND SELECTIVE ACCELERATION

Steven H. Margolis and J. Bernard Blake (Aerospace Corp., El Segundo, Calif.) *In* Aerospace Corp. Contributions to the 18th International Cosmic Ray Conference 10 Mar. 1986 p 1-4 Previously announced in IAA as A85-23003 (For primary document see N87-13389 04-93)

Avail: NTIS HC A02/MF A01

Results of calculations of ultraheavy cosmic ray propagation are examined in the light of recent observations and theoretical advances with the objective of distinguishing the effects of propagation from nucleosynthesis and preferential acceleration. The results presented here have been calculated by the method described in Margolis (1983), with elements from iron (Z = 26) to uranium (Z = 92) combined in a single calculation. The source abundances of Anders and Ebihara (1982) have been used as a reference composition. It is shown, in particular, that the relative abundances of Sr and Ba are substantially increased by using the modified ionization potential dependence (MIPD) compared with solar abundance and the first ionization potential dependence (FIPD) models. In contrast, Pb shows similar enhancements in both FIPD and MIPD models. IAA

N87-13391# Aerospace Corp., El Segundo, Calif. Space Sciences Lab.

THE SECONDARY PRODUCTION OF GAMMA RAYS IN THE JOVIAN MAGNETOSPHERE

J. Bernard Blake and Steven H. Margolis (Washington Univ., St. Louis, Mo.) *In its* Contributions to the 18th International Cosmic Ray Conference 10 Mar. 1986 p 5-8 Previously announced as A85-22972 (For primary document see N87-13389 04-93)

Avail: NTIS HC A02/MF A01

Photons in the MeV and above energy range resulting from interactions of energetic protons and electrons in the Jovian magnetosphere with the Jovian satellite Amalthea are studied. The photon flux as a function of Jovian radii is found to be 0.2/sq R(J) per sq cm/sec, a relatively low value. If the magnetospheric configuration at Jupiter is similar to that of the Earth, a nearly radiation-free region may exist below the trapped particles, but sufficiently high for an observing satellite to orbit with a reasonable drag lifetime. IAA

N87-13392# Aerospace Corp., El Segundo, Calif. Space Sciences Lab.

THE STELLAR UPPER MASS LIMIT IN AN OB ASSOCIATION AND IMPLICATIONS FOR COSMIC RAYS AND COSMIC ABUNDANCES

J. Bernard Blake and D. S. P. Dearborn (Arizona Univ., Tucson.) *In its* Contributions to the 18th International Cosmic Ray Conference 10 Mar. 1986 p 9-12 (For primary document see N87-13389 04-93)

Avail: NTIS HC A02/MF A01

Some implications are considered of the possibility that the collapse of the solar nebula was induced by the supernova of an extremely massive star or, at least, such a star was in the vicinity of the protosolar nebula prior to its collapse to form the solar system. A very large star in the vicinity of the protosolar nebula can contribute to the protosolar nebula in several ways which differ from a smaller (but still large) star: (1) the high mass-loss rate of a very large star implies the dispersion into the nearby interstellar medium of many solar masses of freshly synthesized material (a substantial dilution can occur before its contribution is masked); (2) a significant amount of Al-26 is synthesized and dispersed well before the subsequent supernova; (3) energy is available in the stellar wind for accelerating cosmic rays in sufficient quantities to heavily irradiate nearby material; (4) the absence of freshly synthesized Pu-244 (no resetting of the plutonium clock) can be understood in a natural way; and (5) a significant amount of Pd-107 can be dispersed into the interstellar medium during a WC stage. Author

N87-13393# Aerospace Corp., El Segundo, Calif. Space Sciences Lab.

A VERSATILE DATA PROCESSING UNIT (DPU) FOR SATELLITE-BORNE COMPOSITION INSTRUMENTATION

J. Bernard Blake, J. F. Fennell, R. Koga, and N. Katz *In its* Contributions to the 18th International Cosmic Ray Conference 10 Mar. 1986 p 13-16 Previously announced in IAA as A85-22970 (For primary document see N87-13389 04-93)

Avail: NTIS HC A02/MF A01

A data processing unit (DPU) for use with a charge-composition experiment to be flown aboard the VIKING auroral research satellite is described. The design of this DPU is such that it can be readily adapted to a variety of cosmic-ray composition experiments. IAA

N87-13394*# New Hampshire Univ., Durham. Gamma-Ray Astronomy Group.

THE GAMMA-RAY SPECTROMETER EXPERIMENT ON THE SOLAR MAXIMUM MISSION SATELLITE Final Report, 16 Oct. 1984 - 15 Apr. 1986

E. L. Chupp 15 Apr. 1986 67 p

(Contracts NAS5-28609; NAS5-23761)

(NASA-Cr-177877; NAS 1.26:177877) Avail: NTIS HC A04/MF A01 CSCL 03B

Observations by the Gamma-Ray Spectrometer (GRS) on the Solar Maximum Mission (SMM) are examined. This detector system is sensitive to high-energy X-rays, gamma-rays, and energetic neutrons. These neutral quanta provide a probe of the highest energy processes in a flare. The GRS has recorded over 150 flares since launch. In addition to the solar discoveries, the SMM GRS has made important discoveries about cosmic gamma-ray sources. These discoveries are summarized. B.G.

N87-13395*# National Aeronautics and Space Administration. Goddard Space Flight Center, Greenbelt, Md.

NEUTRON AND ANTINEUTRON PRODUCTION IN ACCRETION ONTO COMPACT OBJECTS

Charles D. Dermer and Reuven Ramaty Jul. 1986 16 p Submitted for publication

(NASA-TM-89264; NAS 1.15:89264) Avail: NTIS HC A02/MF A01 CSCL 03B

Nuclear reactions in the hot accretion plasma surrounding a collapsed star are a source of neutrons, primarily through spallation and pion-producing reactions, and antineutrons, principally through the reaction p+p yields p+p+n+anti-n. We calculate spectra of neutrons and antineutrons produced by a variety of nonthermal energetic particle distributions in which the target particles are either at rest or in motion. If only neutral particles are free to escape the interaction site, a component of the proton and antiproton fluxes in the cosmic radiation results from the neutrons and antineutrons which leave the accretion plasma and subsequently decay in the interstellar medium. This additional antiproton component could account for the enhanced flux of antiprotons in the cosmic radiation, compared to values expected from the standard leaky-box model of cosmic-ray propagation and confinement. Moreover, the low-energy antiproton flux measured by Buffington et al. (1981) could result from target-particle motion in the accretion plasma. This model for the origin of antiprotons predicts a narrow 2.223 MeV line which could be observable. Author

N87-13396# Ames Lab., Iowa.

VERY HIGH ENERGY GAMMA RAY ASTROPHYSICS

R. C. Lamb and D. A. Lewis 25 Mar. 1986 14 p

(Contract DE-AC02-80ER-10774)

(DE86-013319; DOE/ER-10774/6) Avail: NTIS HC A02/MF A01

The Whipple Observatory's atmospheric Cerenkov camera has detected TeV radiation from four galactic sources: the Crab Nebula, Cygnus X-3, Hercules X-1, and 4U0115+63. Recent simulations encourage the view that unwanted cosmic-ray background showers may be suppressed by a large factor. Emphasis

in the coming year will be on determining optimum selection criteria for enhancing gamma-ray signals and in developing a prototype camera with finer angular resolution as a first step towards implementation of the HERCULES concept. DOE

N87-13397# Edgerton, Germeshausen and Grier, Inc., Idaho Falls, Idaho.
CHARACTERIZATION OF THE GAMMA RADIATION IN SPACE AND IN THE ATMOSPHERE
M. A. Lee May 1986 53 p
(Contract DE-AC07-76ID-01570)
(DE86-013445; EGG-PHY-7272) Avail: NTIS HC A04/MF A01

A characterization of the gamma-ray fields found in space and in the atmosphere is given. Included are values for the energies and intensities of gamma rays as observed in several experiments and reported in the open literature. Characteristics of the diffuse gamma-ray continuum are presented along with a brief discussion of the sources of this radiation. Also given are discrete gamma-ray line energies and intensities which have been observed in space and in the atmosphere. DOE

N87-13398 Virginia Univ., Charlottesville.
X-RAY EMISSION FROM SUPERNOVA REMNANTS Ph.D. Thesis
Andrew James SackvilleHamilton 1984 327 p
Avail: Univ. Microfilms Order No. DA8517472

This thesis deals with the x-ray spectra of supernova remnants (SNRs), and in particular the x-ray spectra of the two young Type 1 SNRs SN1006 and Tycho. Firstly an extensive grid of nonequilibrium model spectra of SNRs in the adiabatic blast stage of evolution is computed, and numerous diagnostics of the state and composition of the blast wave plasma are plotted over parameter space. It is demonstrated that the spectrum of an adiabatic blast wave is a good approximation to several other model SNR structures in which emission is dominated by gas undergoing quasi steady state ionization near a shock front. None of these structures appears able to account for the observed spectra of SN1006 or Tycho. A new similarity solution for the early time evolution of uniform ejecta moving into an external medium is presented. It is argued that the x-ray spectra of SN1006 and Tycho are consistent with emission mainly from a reverse shock into 1.4 M(solar) of initially uniform density SN ejecta consisting of pure heavy elements, moving into a uniform medium. Satisfactory fits to the observed spectra are obtained with a two layer structure of ejecta, an outer layer of unprocessed material, and an inner layer of mixed processed heavy elements. The structure of ejecta inferred is similar for both SN1006 and Tycho, the marked difference between the two spectra being attributed largely to the lower density of the ambient medium around SN1006. The results are consistent with the theory of Type 1 SNe as exploded white dwarfs, and resolve the apparent problems of too little iron, and too much total mass, deduced by other authors from earlier analyses of the x-ray emission of SN1006 and Tycho. Dissert. Abstr.

N87-13399 Stanford Univ., Calif.
OBSERVATIONS ON THE STANFORD 4800 KG GRAVITY WAVE DETECTOR WITH A COSMIC RAY MONITOR Ph.D. Thesis
Bruce Evan Moskowitz 1986 120 p
Avail: Univ. Microfilms Order No. DA8612771

The group at Stanford University has constructed a 4800 kg cryogenic detector which is the most sensitive detector for gravitational radiation successfully operated to date. In this dissertation data are presented from the 1985 run of 36.8 days aggregate collection time. Over the full bandwidth of approximately 13 Hz, the optimum detector noise temperature was found to be 8 mK when the system was operated at 4.3 K. An actual filter was implemented over a 5 Hz bandwidth which yielded the filtered noise temperature of 15 mK. Filtering over the entire bandwidth and operation of a dilution refrigerator at 1 K should lower the noise temperature to below 3 mK. The rate of events whose signal temperature exceeded 0.6 K was found to be higher than that for a similar run in 1981, partly due to greater general activity in the laboratory. A preliminary coincidence experiment was conducted between the Stanford detector and a room temperature detector in Guangzhou, China. In a total of 9.38 days of simultaneous data collection the number of coincidences observed was entirely consistent with random statistics. In the second half of this dissertation, the effect of cosmic rays on a gravity wave bar detector is considered. A one-dimensional thermoacoustic model is used to predict the size of the signal. Measurable effects are restricted to rarer events which may easily be vetoed as gravity wave candidates. Dissert. Abstr.

99 GENERAL

No abstracts in this category.

Typical Subject Index Listing

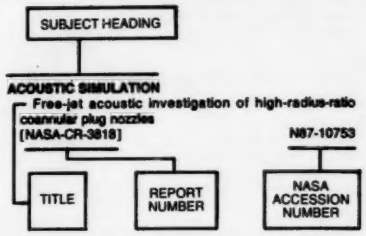

The subject heading is the key to the subject content of the document. Titles, report numbers, and accession numbers of pertinent documents are provided under each subject heading. When the title is insufficiently descriptive of the document content, a title extension has been added, separated from the title by three hyphens. The report number helps to indicate the type of document cited (e.g., NASA report, NASA translation, NASA contractor report). The NASA accession number is the number by which the document abstracts are arranged in this journal and by which the document is sold or requested. The titles, with title extensions if present, are arranged under each subject heading in ascending accession number order. The subject headings have been selected from the latest revision of the *NASA Thesaurus* (NASA SP-7053).

A

ABSORPTION SPECTRA
Electrode/electrolyte interphase study using polarization modulated FT-IR reflection absorption spectroscopy
[AD-A169081] N87-12631
ABSORPTION SPECTROSCOPY
Optical spectroscopy of dynamically compressed liquids
[AD-A169013] N87-12629
Electrode/electrolyte interphase study using polarization modulated FT-IR reflection absorption spectroscopy
[AD-A169081] N87-12631
ABSORPTIVITY
X-ray data booklet, revision
[DE86-012650] N87-13272
ACCELERATED LIFE TESTS
A Bayesian approach to quantile and response probability estimation with applications in reliability
[AD-A170455] N87-13240
Proceedings of the conference on the design of experiments in army research development and testing (31st) held at the Madison, Wisconsin on 23-25 October 1986
[AD-A169473] N87-13246
ACCELERATION (PHYSICS)
SSME main injector 4000 Hertz phenomenon
[NASA-CR-178934] N87-12608
Balloon-borne, high altitude gravimetry: The flight of DUCKY 1a (11 October 1983)
[AD-A169942] N87-13033
ACCELERATION TOLERANCE
Analysis of head and neck dynamic response of the US adult military population
[AD-A169563] N87-13129
ACCELEROMETERS
Evaluation of the Collins/Rockwell two axis gyro/accelerometer sensor cluster (phase 3 unit)
[AD-A169810] N87-12834
Evaluation of the multifunction sensor acceleration sensitive terms MU sub A and MU sub B
[AD-A169611] N87-12835
Double-ended tuning fork quartz accelerometer
[DE86-012277] N87-12842
Development of a sensitive superconducting gravity gradiometer for geological and navigational applications
[NASA-CR-4011] N87-13021
ACCEPTOR MATERIALS
Donor-acceptor one step energy transfer via exchange coupling on a fractal lattice
[AD-A169643] N87-13325
ACCESS CONTROL
Carrier-sense stack algorithms for multiple access communication channels
[AD-A169774] N87-12738
ACCIDENT PREVENTION
Obstacle-warning radar for helicopters N87-13149
ACCIDENTS
Investigation of the Challenger accident, volume 2
[GPO-64-548] N87-12586
NASA's quality assurance program
[GPO-63-142] N87-12909
ACCRETION DISKS
On the two states of CYG X-1 and related sources
[NASA-TM-89265] N87-13367
ACID RAIN
Remote sensing to detect ecological impacts associated with acid deposition
[DE86-011649] N87-12992
Study of the formation and transport of acidic species by non-precipitating cumulus clouds during VENTEX-84
[PB86-220357] N87-13014
ACOUSTIC FREQUENCIES
Knowledge-based pitch detection
[AD-A169069] N87-12730
ACOUSTIC MEASUREMENT
Supplementary calibration test of the tip-aerodynamics-and acoustics-test pressure transducers
[NASA-TM-88312] N87-12830
An analysis of the acoustic characteristics of ABSS (acoustic backscatter system) and its deployments
[AD-A170487] N87-13037
ACOUSTIC PROPAGATION
USSR report: Earth sciences
[JPRS-UES-86-007] N87-12946
Evaluating nonlinear effects in propagation of acoustic pulse in atmospheric surface layer in inversions N87-12951
ACOUSTIC PROPERTIES
The effects of high sustained acceleration on the acoustic phonetic structure of speech: A preliminary investigation
[AD-A170563] N87-12746
ACOUSTIC SCATTERING
An analysis of the acoustic characteristics of ABSS (acoustic backscatter system) and its deployments
[AD-A170487] N87-13037
ACOUSTIC VELOCITY
Influence of shear modulus on the behavior of acoustically transparent materials
[AD-A169299] N87-12931
ACOUSTO-OPTICS
Optical processing
[AD-A169682] N87-13269
Acoustooptic spectrum analyzer using a planar Bragg-cell N87-13295
ACQUISITION
Language acquisition and machine learning
[AD-A169581] N87-13184
ACTUATORS
Fabrication and testing of lightweight hydraulic system simulator hardware
[AD-A169684] N87-12711
ADA (PROGRAMMING LANGUAGE)
Catalog of Resources for Education in Ada (Trade name) and Software Engineering (CREASE), version 4.0
[AD-A169692] N87-13186
Proceedings of the IDA Workshop on Formal Specification and Verification of Ada (trade name) (1st) held in Alexandria, Virginia on 18-20 March 1985
[AD-A171507] N87-13192
ADAPTIVE CONTROL
A brief review of adaptive null steering techniques
[AD-A169548] N87-12736
Sensor controlled robotic welding for nuclear applications
[DE86-013110] N87-12905
Feedback system design with an uncertain plant
[NASA-CR-176887] N87-13243
ADAPTIVE FILTERS
Two-dimensional beamforming using a frequency domain complex Least Mean-Squares (LMS) adaptive filter
[AD-A171396] N87-12785
ADHESION
Zinc/air cell cathode
[AD-D012425] N87-12780
ADHESIVE BONDING
An interdisciplinary approach to predictive modeling of structural adhesive bonding. Characterization of Ti-6Al-4V oxides and the adhesive/oxide interphase
[AD-A170484] N87-12690
Adhesive repair patch
[AD-D012422] N87-12692
ADSORPTION
Electrode/electrolyte interphase study using polarization modulated FT-IR reflection absorption spectroscopy
[AD-A169081] N87-12631
Carbon monoxide adsorption on a platinum electrode studied by polarization modulated FT-IR reflection-absorption spectroscopy. 2: CO adsorbed at a potential in the hydrogen region and its oxidation in acids
[AD-A169082] N87-12632
On the interplay between chemical reactions and phase transitions for molecules adsorbed on solid surfaces
[AD-A169818] N87-12636
Proceedings of the Topical Meeting on the Microphysics of Surfaces, Beams and Adsorbates held in Santa Fe, New Mexico on 4-6 February 1985
[AD-A170797] N87-13329
Surface and adsorption-like states within the nearly free electron approximation
[DE86-702651] N87-13342
AEROACOUSTICS
An analysis of blade vortex interaction aerodynamics and acoustics N87-12547
AERODYNAMIC CHARACTERISTICS
NASA rotor systems research aircraft: Fixed-wing configuration flight-test results
[NASA-TM-86789] N87-12557
The handling qualities and flight characteristics of the Grumman design 698 simulated twin-engine tilt Nacelle V/STOL aircraft
[NASA-TM-86785] N87-12558
AERODYNAMIC COEFFICIENTS
Supplementary calibration test of the tip-aerodynamics-and acoustics-test pressure transducers
[NASA-TM-88312] N87-12830
AERODYNAMIC CONFIGURATIONS
Assessment of damage tolerance requirements and analyses: A user's manual for crack growth and crack initiation analysis: DAMGRO
[AD-A171209] N87-12939
AERODYNAMIC DRAG
Propeller/body interaction for thrust and drag
[ESDU-86017] N87-12537
Length adjustable strut link with low aerodynamic drag
[AD-D012279] N87-12543
AERODYNAMIC FORCES
The effect of a winglet on the spatial vortex of a slender body at high angle of attack
[AD-A169925] N87-12533
A summary of the development of integral aerodynamic methods for the computation of rotor wake interactions
[AD-A169254] N87-12545
AERODYNAMIC INTERFERENCE
An approximate method of estimating the aerodynamic interference between two parallel bodies in a supersonic flow (axial force)
[BR-100271] N87-12540

AERODYNAMIC LOADS
Introduction to aerodynamics derivitives, equations of motion and stability
[ESDU-86021] N87-12536
Forced oscillation of a two-dimensional airfoil with nonlinear aerodynamic loads
[AD-A169350] N87-12546
AERODYNAMIC STABILITY
Analysis of the nonlinear stability of circular Couette flow
[AD-A168951] N87-12811
AERODYNAMICS
Aeronautical Engineering: A continuing bibliography with indexes
[NASA-SP-7037(206)] N87-12532
Analysis and verification of the icing scaling equations. Volume 1: Revision
[AD-A167976] N87-12551
Characterization and dynamical studies of polymers in dipolar (aprotic) liquids
[AD-A169243] N87-12685
AERONAUTICAL ENGINEERING
Aeronautical Engineering: A continuing bibliography with indexes
[NASA-SP-7037(205)] N87-12532
AEROSOLS
Measurement and calculation of the Stokes or Mueller matrix for the scattering of electromagnetic radiation from irregular particles
[AD-A171502] N87-12749
SAGE 2 satellite data set validation
[NASA-CR-178189] N87-13024
AEROSPACE ENGINEERING
The portfolio model of technological development in the aircraft industry
[AD-A170832] N87-12534
Japan report: Science and Technology
[JPRS-JST-86-023] N87-12715
AEROSPACE ENVIRONMENTS
Ionization phenomena about the space shuttle
[AD-A170542] N87-13310
AEROSPACE INDUSTRY
Literature review on the design of composite mechanically fastened joints
[AD-A169112] N87-12872
AEROSPACE MEDICINE
Aerospace Medicine and Biology: A continuing bibliography with indexes
[NASA-SP-7011(290)] N87-13125
AEROSPACE SYSTEMS
Regression models of quarterly overhead costs for six government aerospace contractors
[AD-A169185] N87-13350
AIR CONDITIONING EQUIPMENT
Empirical determination among superintendents of the acceptable user surface in digitally automated heating-ventilation air conditioning systems N87-13165
AIR COOLING
Self-locking outer air seal with full backside cooling
[AD-D012406] N87-12880
AIR DUCTS
Sliding duct seal
[AD-D012369] N87-12875
AIR FLOW
Sensitivity tests of a surface-layer windflow model to effects of stability and vegetation
[AD-A169136] N87-13101
Meteorological summary of WATOX (western Atlantic Ocean experiment) 1985 research intensive, February-April
[PB86-226792] N87-13114
AIR LOCKS
Self-locking outer air seal with full backside cooling
[AD-D012406] N87-12880
AIR QUALITY
Southern California Air Quality Study (SCAQS) suggested program plan
[PB86-223427] N87-13013
AIR SEA ICE INTERACTIONS
MIZEX: A program for mesoscale air-ice-ocean interaction experiments in arctic marginal ice zones. 8: A science plan for a winter marginal ice zone experiment in the Fram Strait/Greenland Sea, 1987/89
[AD-A169070] N87-13119
AIR TRAFFIC CONTROL
Aircraft accident report: Bar Harbor Airlines Flight 1808, Beech BE-99, N300WP, Auburn-Lewiston Municipal Airport, Auburn, Maine, August 25, 1985
[PB86-910408] N87-12550
AIRBORNE EQUIPMENT
The Multispectral Atmospheric Mapping Sensor (MAMS): Instrument description, calibration and data quality
[NASA-TM-86565] N87-12828
Radiometric calibration of the airborne imaging spectrometer N87-12969
Comparison of various techniques for calibration of AIS data N87-12970
Analysis of AIS radiometry with emphasis on determination of atmospheric properties and surface reflectance N87-12971
Airborne spectroradiometry: The application of AIS data to detecting subtle mineral absorption features N87-12972
Destriping AIS data using Fourier filtering techniques N87-12974
Abundance and distribution of mineral components associated with Moses Rock (kimberlite) diatreme N87-12975
Comparison of the 1984 and 1985 AIS data over the Singatse Range (Yerington), Nevada N87-12976
Identification of hydrothermal alteration assemblages using airborne imaging spectrometer data N87-12977
Detection of hydrothermal alteration at Virginia City, Nevada using Airborne Imaging Spectrometry (AIS) N87-12978
Preliminary geological investigation of AIS data at Mary Kathleen, Queensland, Australia N87-12979
Use of digital Munsell color space to assist interretation of imaging spectrometer data: Geologic examples from the northern Grapevine Mountains, California and Nevada N87-12980
Near-infrared detection of ammonium minerals at Ivanhoe Hot Springs, Nevada N87-12981
Analysis of AIS data of the Bonanza Creek Experimental Forest, Alaska N87-12982
Soil types and forest canopy structures in southern Missouri: A first look with AIS data N87-12983
Geobotanical studies at Pilot Mountain, North Carolina using the airborne imaging spectrometer N87-12984
Trace element-induced stress in freshwater wetland vegetation: Preliminary results N87-12985
Patterns of vegetation in the Owens Valley, California N87-12986
AIS spectra of desert shrub canopies N87-12987
Instrumentation research and support services
[AD-A169278] N87-13029
Airborne atmospheric electricity experiments N87-13063
Mobile intercept of storms N87-13064
Airborne Doppler measurements of the central California extended sea breeze N87-13066
AIRBORNE/SPACEBORNE COMPUTERS
MAGNA (Materially And Geometrically Nonlinear Analysis). Addendum 1, parts 1-4
[AD-A169383] N87-12933
A versatile Data Processing Unit (DPU) for satellite-borne composition instrumentation N87-13393
AIRCRAFT ACCIDENT INVESTIGATION
Aircraft accident/incident summary reports: Erie, Pennsylvania, October 14, 1984; Albuquerque, New Mexico, February 11, 1985
[PB86-910407] N87-12549
Aircraft accident report: Bar Harbor Airlines Flight 1808, Beech BE-99, N300WP, Auburn-Lewiston Municipal Airport, Auburn, Maine, August 25, 1985
[PB86-910408] N87-12550
AIRCRAFT ACCIDENTS
Crew communication as a factor in aviation accidents
[NASA-TM-88254] N87-13141
AIRCRAFT CARRIERS
Simulator design and instructional features for carrier landing: A field transfer study
[AD-A169962] N87-12573
AIRCRAFT COMMUNICATION
Crew communication as a factor in aviation accidents
[NASA-TM-88254] N87-13141
AIRCRAFT CONFIGURATIONS
NASA rotor systems research aircraft: Fixed-wing configuration flight-test results
[NASA-TM-86789] N87-12557
AIRCRAFT CONTROL
Determination of the load and stress of a cockpit crew during aircraft piloting using task networks and the simulation language SAINT N87-13150
Application of the task taxonomy method to the simulation of human service reliability in the manual control of aircraft
[MBB/LKE-301/S/PUB/216] N87-13151
AIRCRAFT ENGINES
Research on mechanical properties for engine life prediction
[AD-A169570] N87-12563
Analysis of mixed-mode crack propagation using the boundary integral method
[NASA-CR-179518] N87-12915
AIRCRAFT EQUIPMENT
A heater made from graphite composite material for potential deicing application
[NASA-TM-88888] N87-12559
Fabrication and testing of lightweight hydraulic system simulator hardware
[AD-A169684] N87-12711
Aircraft battery state of charge and charge control system
[AD-A169411] N87-12766
TSAR (Theater Simulation of Airbase Resources) database dictionary F-4E
[AD-A169575] N87-13352
AIRCRAFT HYDRAULIC SYSTEMS
Fabrication and testing of lightweight hydraulic system simulator hardware
[AD-A169684] N87-12711
AIRCRAFT INDUSTRY
The portfolio model of technological development in the aircraft industry
[AD-A170832] N87-12534
AIRCRAFT LANDING
Simulator design features for helicopter landing on small ships. 1: A performance study
[AD-A169514] N87-12572
Simulator design and instructional features for carrier landing: A field transfer study
[AD-A169962] N87-12573
Frictional and retarding forces on aircraft tyres. Part 4: Estimation of effects of yaw
[ESDU-86016-PT-4] N87-12868
AIRCRAFT MAINTENANCE
TSAR (Theater Simulation of Airbase Resources) database dictionary F-4E
[AD-A169575] N87-13352
AIRCRAFT NOISE
An analysis of blade vortex interaction aerodynamics and acoustics N87-12547
Cruise noise of counterrotation propeller at angle of attack in wind tunnel
[NASA-TM-88869] N87-13252
AIRCRAFT PERFORMANCE
Simplified forms of performance equations. Addendum A: Effect on aeroplane level speed of small changes in thrust, drag, weight, power
[ESDU-86004-ADD-A] N87-12556
NASA rotor systems research aircraft: Fixed-wing configuration flight-test results
[NASA-TM-86789] N87-12557
AIRCRAFT SAFETY
Crew factors in flight operations. Part 3: The operational significance of exposure to short-haul air transport operations
[NASA-TM-88322] N87-13122
AIRCRAFT STABILITY
Introduction to aerodynamics derivitives, equations of motion and stability
[ESDU-86021] N87-12536
NASA rotor systems research aircraft: Fixed-wing configuration flight-test results
[NASA-TM-86789] N87-12557
AIRCRAFT STRUCTURES
Carbon fibers
[AD-A171370] N87-12622
AIRCRAFT TIRES
Frictional and retarding forces on aircraft tyres. Part 4: Estimation of effects of yaw
[ESDU-86016-PT-4] N87-12868
AIRFOILS
Viscous-inviscid interaction in transonic separated flow over solid and porous airfoils and cascades N87-12535
Forced oscillation of a two-dimensional airfoil with nonlinear aerodynamic loads
[AD-A169350] N87-12546
AIRFRAMES
Assessment of damage tolerance requirements and analyses: A user's manual for crack growth and crack initiation analysis: DAMGRO
[AD-A171209] N87-12939
AIRGLOW
Measurement of atmospheric emission spectra at high altitudes
[AD-A170143] N87-13035
Atmospheric illumination and shadows, revision 1
[DE86-010971] N87-13039
AIRPORTS
A review of microbursts and their analysis and detection with Doppler radar
[AD-A170458] N87-13110
TSAR (Theater Simulation of Airbase Resources) database dictionary F-4E
[AD-A169575] N87-13352
AIRSHIPS
Possible military applications of stratospheric airship discussed N87-12716
AIRSPEED
Simplified forms of performance equations. Addendum A: Effect on aeroplane level speed of small changes in thrust, drag, weight, power
[ESDU-86004-ADD-A] N87-12556

ALASKA
Analysis of AIS data of the Bonanza Creek Experimental Forest, Alaska N87-12982
Revised Uniform Summary of Surface Weather Observations (RUSSWO). Parts A-F, Fort Richardson, Alaska
[AD-A169390] N87-13106
ALBEDO
A simple solar, spectral model for studying the effects of cloud cover and surface albedo on the incoming solar radiation
[AD-A171284] N87-13038
ALERTNESS
Sleepability and wakeability following sleep deprivation
[AD-A169578] N87-13130
ALGEBRA
Canonical quantization of gravity
[DE86-702615] N87-13372
ALGORITHMS
Guidance law simulation studies for complex approaches using the Microwave Landing System (MLS)
[NASA-CR-178182] N87-12552
Some tactical algorithms for spherical geometry
[AD-A170615] N87-12555
Application of the AIPA (Approximate Iterative Preprocessing Algorithm) to F-106 data
[AD-A169084] N87-12569
Advanced guidance algorithms for homing missiles with bearing-only measurements
[AD-A170833] N87-12583
On the interplay between chemical reactions and phase transitions for molecules adsorbed on solid surfaces
[AD-A169818] N87-12636
Carrier-sense stack algorithms for multiple access communication channels
[AD-A169774] N87-12738
Multi-element adaptive antenna array
[AD-D012410] N87-12740
A new method of synthetic aperture radar image reconstruction using modified convolution back-projection algorithm
[AD-A170652] N87-12747
A VLSI-based high-performance raster image system
[AD-A169068] N87-12761
Compaction with automatic jog introduction
[AD-A169679] N87-12772
Two-dimensional beamforming using a frequency domain complex Least Mean-Squares (LMS) adaptive filter
[AD-A171396] N87-12785
Development of an inexpensive, high resolution positron multiwire proportional counter
[DE86-011576] N87-12841
Atmospheric illumination and shadows, revision 1
[DE86-010971] N87-13039
Airborne atmospheric electricity experiments N87-13063
An implicit enumeration algorithm with binary-valued constraints
[AD-A169256] N87-13182
A software implementation of an interactive graphics system for three dimensional modeling and layout
[AD-A169264] N87-13183
The continuous projective sumt method for convex programming — sequential unconstrained minimization techniques
[AD-A169847] N87-13185
SOR (Successive Over-Relaxation) MGR (multigrid algorithm)(nu) experiments on the crystal multicomputer
[AD-A169929] N87-13187
An implicit enumeration procedure for the general linear complementarity problem
[AD-A170397] N87-13189
Matrix factorization on a hypercube multiprocessor
[DE86-011775] N87-13193
HOMPACK: A suite of codes for globally convergent homotopy algorithms
[DE86-011644] N87-13196
A generalized projection method for the solution of algebraic linear systems
[INPE-3874-PRE/930] N87-13205
Performance analysis of some numerical algorithms in the resolution of ODEs artificial satellite problems
[INPE-3996-PRE/995] N87-13206
Algorithm for positive definite least square estimation of parameters
[DE86-012159] N87-13225
Maintaining LU factors of a general sparse matrix
[AD-A169255] N87-13248
Degeneracy in the ensemble Monte Carlo method for high field transport in semiconductors
[AD-A160456] N87-13321
ALKALI HALIDES
Search for far infrared radiation from optically and acoustically pumped defect modes
[AD-A169159] N87-13319
ALKYL COMPOUNDS
Vapour pressures and critical points of liquids. Part 3A: C8 to C10 alkylbenzenes
[ESDU-86012-PT-3A] N87-12625
ALKYNES
Vapour pressures and critical points of liquids. Part 2C: Alkadienes and alkynes
[ESDU-86001-PT-2C] N87-12624
ALLOYS
Characterization of the atomic emission in Inconel 718 alloy metal vapor arcs
[DE86-012178] N87-12672
Metals and Ceramics Division Materials Sciences Program
[DE86-013512] N87-12699
International Conference/Workshop on Small Fatigue Cracks (2nd) held in Santa Barbara, California on 5-10 January 1986
[AD-A169060] N87-12929
ALTITUDE SIMULATION
Effects of test cell recirculation on high-bypass turbofan engines during simulated altitude tests
[AD-A171418] N87-12565
ALUMINUM
Effect of hydrogen on the mechanical properties and fracture behavior of high purity aluminum
[AD-A171214] N87-12658
Heat measurements in inertia welding of aluminum to steel
[DE86-012463] N87-12885
Factors influencing elastic stresses in double cantilever beam specimens
[NASA-TM-89033] N87-12922
ALUMINUM ALLOYS
Metallurgical characterization of the interfaces and the damping mechanisms in metal matrix composites
[AD-A169186] N87-12616
Micromechanisms of crack growth and fracture toughness in metal matrix composites
[AD-A169639] N87-12620
Fatigue behavior of long and short cracks in wrought and powder aluminum alloys
[AD-A169960] N87-12656
A fundamental study of P/M processed elevated temperature aluminum alloys
[AD-A170697] N87-12657
APFIM study of antiphase and grain boundaries in Ni Al
[DE86-008494] N87-12662
Atomic resolution study of precipitates in an Al-Ge alloy
[DE86-011308] N87-12670
Diamond-machined aluminum alloy 5083 surfaces: Controlled exposure evaluation
[DE86-012572] N87-12674
Cleaning of aluminum alloy 5083
[DE86-012573] N87-12675
Gas tungsten arc welding of aluminum alloys 6XXX. Welding procedure specification. Supplement 1: Records of procedure qualification tests
[DE86-012548] N87-12893
Gas tungsten arc welding of aluminum alloys 3004, 5052 and 5x54 to 6xxx. Welding procedure specification. Supplement 1: Records of procedure qualification tests
[DE86-012561] N87-12897
ALUMINUM OXIDES
Hot isostatic pressing of ceramic powder compacts
[AD-A169971] N87-12688
ALUMINUM SILICATES
Low temperature formation of mullite
[AD-D012404] N87-12687
AMAZON REGION (SOUTH AMERICA)
Energy receipt partitioning over the Amazon forest
[INPE-3980-PRE/990] N87-12962
A partition of sensible and latent heat fluxes above the terra firma area in the Amazon Forest (gradient method)
[INPE-3972-PRE/985] N87-12964
A partition of sensible and latent heat fluxes above the terra firma area in the Amazon forest
[INPE-3949-PRE/970] N87-13008
AMINES
Methods for the syntheses of mono-, di-, tri- and tetranitro derivatives of diphenylamine
[WSRL-0436-TR] N87-12702
AMMONIUM COMPOUNDS
Near-infrared detection of ammonium minerals at Ivanhoe Hot Springs, Nevada N87-12961
AMMONIUM PERCHLORATES
Shifts in shuttle SRM performance because of ammonium perchlorate crystal shape on missions 51-I/J and 61-A/B
[NASA-TM-86561] N87-12607
AMMUNITION
Stability of liquid-filled projectiles with unusual coning frequencies
[AD-A171460] N87-12584
AMORPHOUS MATERIALS
Status and future of government-supported amorphous silicon research in the US
[DE86-010702] N87-12997
AMPLIFIERS
Unique mechanization to fault isolate failures of an electron tube Radio Frequency (RF) amplifier and its high voltage power supply
[AD-D012376] N87-12770
AMPLITUDE MODULATION
Fiber optic device for temperature remote sensing N87-13280
AMPLITUDES
Metallurgical characterization of the interfaces and the damping mechanisms in metal matrix composites
[AD-A169186] N87-12616
ANALYSIS (MATHEMATICS)
The application of boundary-element techniques for some soil-structure interaction problems
[AD-A168999] N87-12709
ANGLE OF ATTACK
The effect of a winglet on the spatial vortex of a slender body at high angle of attack
[AD-A169925] N87-12533
Mach 6 experimental and theoretical stability and performance of a finned cylindrical body at angles of attack up to 65 deg
[NASA-TM-89050] N87-12538
Cruise noise of counterrotation propeller at angle of attack in wind tunnel
[NASA-TM-88869] N87-13252
ANGULAR MOMENTUM
Los Alamos Science, number 13, spring 1986
[DE86-012864] N87-13371
ANISOTROPIC SHELLS
Dynamic analysis of anisotropic conical shells
[EPM/RT-86-36] N87-12916
ANISOTROPY
Kinetics and mechanisms on the molecular beam etching of semiconductors
[AD-A171360] N87-13331
ANNEALING
Recrystallization behavior of ion beam modified Alpha-Al sub 2 O sub 3
[DE86-009353] N87-13335
ANNIHILATION REACTIONS
The gamma-ray spectrometer experiment on the solar maximum mission satellite
[NASA-CR-177877] N87-13394
ANNUAL VARIATIONS
US Navy climatic study of the Caribbean Sea and Gulf of Mexico. Volume 2: East Caribbean Sea
[AD-A171487] N87-13112
The Gulf Stream dynamics experiment. Inverted echo sounder data report for the June 1984 to May 1985 deployment period
[AD-A170758] N87-13121
ANNULAR FLOW
Computational fluid dynamic studies of certain ducted bluff-body flowfields relevant to turbojet combustors. Volume 1: Time-dependent calculations with the k-epsilon turbulence model for an existing centerbody combustor
[AD-A171434] N87-12616
ANODES
Advanced electric propulsion MPD (magnetoplasmadynamic)
[AD-A169792] N87-12610
ANOMALIES
Tone calibration technique: A digital signaling scheme for mobile applications
[NASA-CR-179915] N87-12719
Low Q spin-up from rest
[AD-A169106] N87-12813
Summary of 1986 Atlantic tropical cyclone activity and verification of author's seasonal forecast N87-13097
ANTARCTIC REGIONS
Stratospheric balloon experiments
[INPE-3995-RPE/519] N87-13020
ANTENNA ARRAYS
Phased arrays 1985 symposium: Proceedings
[AD-A169316] N87-12732
A brief review of adaptive null steering techniques
[AD-A169548] N87-12736
Multi-element adaptive antenna array
[AD-D012410] N87-12740
Twin aperture phased array lens antenna
[AD-D012415] N87-12745
Input impedance of an infinite linear scanned array of flat rectangular strips inside a dielectric loaded parallel plate waveguide
[AD-A171275] N87-12784
ANTENNA DESIGN
Dielectric antennas for millimeter-wave applications
[AD-A169885] N87-12739

Development of a numerical procedure to treat wires attached to arbitrarily shaped conducting bodies
[AD-A169364] N87-12764

ANTENNA RADIATION PATTERNS
Vector analysis and satellite footprints
[AD-A169832] N87-12576

ANTENNAS
A mathematical formulation of a large space structure control problem
[AD-A169950] N87-12602
Foreground effects on tropocatter digital communication systems
[AD-A169380] N87-12734

ANTHROPOMETRY
Proceedings of a Symposium on the Evaluation of Man-Machine Systems: Methods and Problems
[DGLR-85-04] N87-13146
Anthropometric handicaps in the construction of a helicopter cockpit — seats N87-13148

ANTINUCLEONS
Neutron and antineutron production in accretion onto compact objects
[NASA-TM-89264] N87-13395

ANTIREFLECTION COATINGS
Solid-state electrochromic switchable window glazings
[DE86-004455] N87-12700

APERTURES
New electromagnetic effects associated with cavity-backed apertures
[DE86-008768] N87-12750
Development of a large-aperture PLZT shutter with enhanced operational/environmental capabilities
[DE86-011643] N87-12838

APPLICATIONS PROGRAMS (COMPUTERS)
Fluid transients in pipes. Estimation of maximum pressures and forces in steam lines
[ESDU-86015] N87-12805
MAGNA (Materially And Geometrically Nonlinear Analysis). Addendum 1, parts 1-4
[AD-A169383] N87-12933
Conversion of the NOLAPS (Navy Operational Local Atmospheric Prediction System) model to the HP9845
[AD-A169536] N87-13108

APPROACH
Guidance law simulation studies for complex approaches using the Microwave Landing System (MLS)
[NASA-CR-178182] N87-12552
Simulator design and instructional features for carrier landing: A field transfer study
[AD-A169962] N87-12573

APPROPRIATIONS
Department of Housing and Urban Development-independent agencies appropriations for 1987, part 7
[GPO-61-970] N87-13357

APPROXIMATION
An approximate method of estimating the aerodynamic interference between two parallel bodies in a supersonic flow (axial force)
[BR-100271] N87-12540
Semigroups and Poisson-approximation
[AD-A170944] N87-13224
Extremal processes, record times and strong approximation
[AD-A169972] N87-13237
Surface and adsorption-like states within the nearly free electron approximation
[DE86-702651] N87-13342

ARC LAMPS
Very high efficacy electrodeless high intensity discharge lamps
[DE86-013760] N87-12803

ARC WELDING
The influence of welding flux on the pyrometallurgical, physical and mechanical behavior of weld metal
[AD-A169067] N87-12650
Welding procedure specification. Manual gas tungsten arc and semiautomatic gas metal arc welding of chromium-nickel steel. Supplement 1: Records of procedure qualification tests
[DE86-012521] N87-12886
Machine gas metal arc welding of carbon steel. Welding procedure specification. Supplement 1: Records of procedure qualification tests
[DE86-012530] N87-12887
Welding procedure specification. Semiautomatic gas metal arc welding of carbon steels. Supplement 1: Records of procedure qualification tests
[DE86-012531] N87-12888
Welding procedure specification. Manual gas tungsten arc and semiautomatic gas metal arc welding of carbon steel. Supplement 1: Records of procedure qualification tests
[DE86-012532] N87-12889
Gas tungsten arc and shielded metal arc welding of carbon steel. Welding procedure specification. Supplement 1: Records of procedure qualification tests
[DE86-012533] N87-12890
Welding procedure specification. Supplement 1: Records of procedure qualification tests. Shielded metal arc welding of carbon steel
[DE86-012535] N87-12891
Welding procedure specification. Gas tungsten arc welding of chromium-nickel steel to chromium-molybdenum steel. Supplement 1: Records of procedure qualification tests
[DE86-012536] N87-12892

ARCHITECTURE (COMPUTERS)
Tone calibration technique: A digital signaling scheme for mobile applications
[NASA-CR-179915] N87-12719
Fault tolerance mechanisms for a network communication multiprocessor
[INPE-3958-PRE/876] N87-12720
Signal estimation, scattering theory and interpolation problems in one and two dimensions
[AD-A168969] N87-12759
ERS-1 SAR data processing
[NASA-CR-179913] N87-12965
Special associative preprocessing structures for qualitative feature extraction
[AD-A169147] N87-13181
High performance parallel computing
[AD-A169981] N87-13188
Interpretive model for a concurrency method
[DE86-012743] N87-13197
Solving scientific problems on hypercube parallel computers
[DE86-012622] N87-13199
Department of Defense gateway architecture and functional requirements
[AD-A169086] N87-13200
SOAR user's manual
[AD-A169005] N87-13204

ARCTIC REGIONS
MIZEX: A program for mesoscale air-ice-ocean interaction experiments in arctic marginal ice zones. 8: A science plan for a winter marginal ice zone experiment in the Fram Strait/Greenland Sea, 1987/89
[AD-A169070] N87-13119

ARMATURES
Models and radiation of railgun plasma armatures with non-ideal plasma properties
[AD-A169349] N87-13256

ARMED FORCES (UNITED STATES)
Revised Uniform Summary of Surface Weather Observations (RUSSWO). Parts A-F Ellington ANGB, Texas
[AD-A169389] N87-13105
Proceedings of the conference on the design of experiments in army research development and testing (31st) held at the Madison, Wisconsin on 23-25 October 1986
[AD-A169473] N87-13246

ARRAYS
Development of low-temperature transistor modules to improve the MSFC mid-infrared array
[NASA-TM-86566] N87-12756
Fabrication of gate array interconnect structures using direct-write deposition processes
[DE86-010785] N87-12787

ARTIFICIAL INTELLIGENCE
An application of a LISP based expert system for failure diagnosis of the CH-47 flight control hydraulic system
[AD-A168970] N87-12567
A prototype maintenance expert system for the CH-47 flight control hydraulic system
[AD-A169019] N87-12568
Application of pattern recognition to metal ion chemical ionization mass spectra
[AD-A169061] N87-12630
Language acquisition and machine learning
[AD-A169581] N87-13184
Survey of the characteristics of very high level languages
[DE86-012240] N87-13198
SOAR user's manual
[AD-A169005] N87-13204
Application of a network associative scene analysis model
[INPE-3945-PRE/967] N87-13244

ARTIFICIAL SATELLITES
Vector analysis and satellite footprints
[AD-A169832] N87-12576
Attitude control of an artificial satellite by extending the linear quadratic regulator theory
[INPE-3959-PRE/977] N87-12588
A procedure for attitude determination of artificial satellites utilizing techniques of static and dynamic optimal estimation
[INPE-3966-PRE/981] N87-12589
Procedure for one axis satellites attitude control with magnetic actuation
[INPE-3895-PRE/937] N87-12590
Performance analysis of some numerical algorithms in the resolution of ODEs artificial satellite problems
[INPE-3998-PRE/995] N87-13206

ASPECT RATIO
Comparison of Rayleigh-Taylor growth with 1.0 m and 0.25 m lasers
[DE86-012217] N87-12862

ASSEMBLIES
Super gripper variable vane arm
[AD-D012364] N87-12874

ASSEMBLY LANGUAGE
High performance parallel computing
[AD-A169981] N87-13188

ASSOCIATIVE PROCESSING (COMPUTERS)
Special associative preprocessing structures for qualitative feature extraction
[AD-A169147] N87-13181

ASTROMETRY
Observation model and parameter partials for the JPL VLBI parameter estimation software MASTERFIT-1986
[NASA-CR-179919] N87-13178

ASTRONAUT TRAINING
NOSL experiment support
[NASA-CR-178947] N87-13140

ASTRONOMICAL MODELS
On the two states of CYG X-1 and related sources
[NASA-TM-89265] N87-13367
X-ray emission from supernova remnants N87-13396

ASTRONOMICAL OBSERVATORIES
Very high energy gamma ray astrophysics
[DE86-013319] N87-13396

ASTRONOMICAL SPECTROSCOPY
Investigations of long-period DQ Herculis star N87-13364

ASTRONOMICAL TELESCOPES
The space station millimeter facility
[AD-A168983] N87-12604

ASTROPHYSICS
Continuum radiation from active galactic nuclei: A statistical study
[NASA-CR-179925] N87-13368
Very high energy gamma ray astrophysics
[DE86-013319] N87-13396

ASYMPTOTIC METHODS
The optimal linear combination of control variates in the presence of bias
[AD-A169111] N87-13210
Semigroups and Poisson-approximation
[AD-A170944] N87-13224
Extreme values of birth and death processes and queues
[AD-A169932] N87-13235
Smooth nonparametric quantile estimation under censoring: Simulations and bootstrap methods
[AD-A169935] N87-13236

ASYMPTOTIC SERIES
Validity of Edgeworth expansions of minimum contrast estimators for Gaussian ARMA processes
[AD-A169931] N87-13217
Asymptotic theory for sieve estimators in semimartingale regression models
[AD-A169207] N87-13230
A reversal argument for storage models defined on semi-Markov processes
[AD-A169262] N87-13232

ATLANTIC OCEAN
Summary of 1986 Atlantic tropical cyclone activity and verification of author's seasonal forecast N87-13097
Meteorological summary of WATOX (western Atlantic Ocean experiment) 1985 research intensive, February-April
[PB86-226792] N87-13114
A survey of hard-X-rays at balloon altitudes of the Earth's atmosphere
[INPE-3954-PRE/972] N87-13388

ATMOSPHERIC BOUNDARY LAYER
Studies of humid continental haze during SPACE N87-13088

ATMOSPHERIC CHEMISTRY
SAGE 2 satellite data set validation
[NASA-CR-178189] N87-13024

ATMOSPHERIC CIRCULATION
Convective surface layers: Influence of the boundary layer depth N87-13041
Theoretical and experimental studies of barocinic processes N87-13044
Theoretical and experimental design studies for the Atmospheric General Circulation Experiment N87-13046

Multiscale modeling to evaluate proposed space-based Doppler lidar sampling strategies N87-13047
Variation objective analyses for cyclone studies N87-13050
Utilization of satellite cloud information to diagnose the energy state and transformations in extratropical cyclones N87-13051
Dynamics and energetics of the South Pacific Convergence Zone during FGGE SOP-1 N87-13052
Observational and theoretical studies of the evolving structure of baroclinic waves: Attractor dynamics of global weather systems N87-13054
Response of the mesoscale atmosphere to diabatic heating N87-13069
Analysis of satellite data for sensor improvement (detection of severe storms from space N87-13071
Numerical simulation of convective response to mesoscale forcing N87-13081
Radiation flux tables for ICRCCM using the GLA GCM radiation codes
[NASA-TM-89270] N87-13098
On the Walker circulation of 1983-84
[INPE-3952-PRE/371] N87-13118
The upper atmosphere of Venus: A tentative explanation of its rotation
[NASA-TM-88505] N87-13375

ATMOSPHERIC COMPOSITION
Characterization of information requirements for studies of CO2 effects: Water resources, agriculture, fisheries, forests and human health
[DE86-012477] N87-13010
High accuracy standards and reference methodology for carbon dioxide in air
[DE86-012643] N87-13011
SAGE 2 satellite data set validation
[NASA-CR-178189] N87-13024
Parameterized numerical fit to total column ozone changes calculated by the LLNL 1-D model of the troposphere and stratosphere
[DE86-011008] N87-13040

ATMOSPHERIC CORRECTION
Atmospheric-water absorption features near 2.2 micrometers and their importance in high spectral resolution remote sensing N87-12973
Identification of hydrothermal alteration assemblages using airborne imaging spectrometer data N87-12977
Preliminary geological investigation of AIS data at Mary Kathleen, Queensland, Australia N87-12979

ATMOSPHERIC EFFECTS
Comparison of various techniques for calibration of AIS data N87-12970
Analysis of AIS radiometry with emphasis on determination of atmospheric properties and surface reflectance N87-12971

ATMOSPHERIC ELECTRICITY
NASA/MSFC FY-85 Atmospheric Processes Research Review
[NASA-CP-2402] N87-13043
Storm severity detection (RF) N87-13057
Airborne atmospheric electricity experiments N87-13063
Extraterrestrial forcing, atmospheric electricity and the occurrence of thunderstorms
[AD-A170483] N87-13111

ATMOSPHERIC GENERAL CIRCULATION EXPERIMENT
Theoretical and experimental design studies for the Atmospheric General Circulation Experiment N87-13046

ATMOSPHERIC HEATING
Response of the mesoscale atmosphere to diabatic heating N87-13069

ATMOSPHERIC MODELS
Middle atmosphere modeling
[NASA-CR-179934] N87-13023
SAGE 2 satellite data set validation
[NASA-CR-178189] N87-13024
A semi-empirical low-latitude ionospheric model
[AD-A166899] N87-13025
Improving foF2 prediction for the sunrise transition period
[AD-A170457] N87-13036
Parameterized numerical fit to total column ozone changes calculated by the LLNL 1-D model of the troposphere and stratosphere
[DE86-011008] N87-13040
Multiscale modeling to evaluate proposed space-based Doppler lidar sampling strategies N87-13047
The use of satellite data in understanding and predicting convective and large-scale dynamical processes N87-13049
Variation objective analyses for cyclone studies N87-13050
Observational and theoretical studies of the evolving structure of baroclinic waves: Attractor dynamics of global weather systems N87-13054
Mesoscale research activities with the LAMPS model N87-13078
Cooperative VAS program with NASA Marshall Space Flight Center N87-13079
Atmospheric Modeling And Sensor Simulation (AMASS) study N87-13090
Radiation flux tables for ICRCCM using the GLA GCM radiation codes
[NASA-TM-89270] N87-13098
A detailed analysis of the influence of eddy exchange processes upon the development of radiation fog
[AD-A169233] N87-13102
Conversion of the NOLAPS (Navy Operational Local Atmospheric Prediction System) model to the HP9845
[AD-A169538] N87-13108
A sensitivity study of a one-dimensional time-dependent warm cumulus cloud model
[AD-A170141] N87-13109
Model studies of solar spectral irradiance at the bottom and top of a cloudy atmosphere N87-13385

ATMOSPHERIC MOISTURE
Application of satellite data to tropic/subtropic moisture coupling N87-13053
Observational and theoretical studies of the evolving structure of baroclinic waves: Attractor dynamics of global weather systems N87-13054
Cooperative VAS program with NASA Marshall Space Flight Center N87-13079
Statistical analysis and use of VAS radiance data N87-13086
Improved satellite retrievals and mesoscale moisture variability N87-13087
Studies of humid continental haze during SPACE N87-13088

ATMOSPHERIC PHYSICS
Instrumentation research and support services
[AD-A169278] N87-13029
Measurement of atmospheric emission spectra at high altitudes
[AD-A170143] N87-13035
Airborne atmospheric electricity experiments N87-13063

ATMOSPHERIC PRESSURE
Meteorological effects of geotectonic phenomena hypothesized N87-12947
Station climatic summaries, Europe
[AD-A167888] N87-13100
Micrometeorological transitions in the morning boundary layer over rolling terrain
[AD-A169237] N87-13103
Revised Uniform Summary of Surface Weather Observations (RUSSWO). Parts A-F, Fort Richardson, Alaska
[AD-A169390] N87-13106

ATMOSPHERIC RADIATION
Regular noise background in VLF-radiation and world thunderstorm centers N87-12957
Stratospheric balloon experiments
[INPE-3995-RPE/519] N87-13020
A detailed analysis of the influence of eddy exchange processes upon the development of radiation fog
[AD-A169233] N87-13102

ATMOSPHERIC SCATTERING
Digest: Proceedings of the International Conference on Optical and Millimeter Wave Propagation and Scattering in the Atmosphere
[AD-A170393] N87-12743
Model studies of solar spectral irradiance at the bottom and top of a cloudy atmosphere N87-13385

ATMOSPHERIC SOUNDING
Spatial radio wave attenuation during vertical sounding of ionosphere N87-12958
NASA/MSFC FY-85 Atmospheric Processes Research Review
[NASA-CP-2402] N87-13043
Mesoscale-cloud scale simulation of convective response N87-13077
Mesoscale research activities with the LAMPS model N87-13078
Cooperative VAS program with NASA Marshall Space Flight Center N87-13079
The assimilation of satellite soundings, winds and satellite products in a mesoscale analysis/forecast system N87-13080
Numerical simulation of convective response to mesoscale forcing N87-13081
Time composite sounding N87-13083
Investigations of severe/tornadic thunderstorm development and evolution based on satellite and AVE/SESAME/VAS data N87-13084
Statistical analysis and use of VAS radiance data N87-13086
Improved satellite retrievals and mesoscale moisture variability N87-13087
Multispectral atmospheric mapping sensor of mesoscale water vapor features N87-13095
A sensitivity study of a one-dimensional time-dependent warm cumulus cloud model
[AD-A170141] N87-13109

ATMOSPHERIC TEMPERATURE
Station climatic summaries, Europe
[AD-A167888] N87-13100
Micrometeorological transitions in the morning boundary layer over rolling terrain
[AD-A169237] N87-13103

ATMOSPHERIC TIDES
Middle Atmosphere Program. Handbook for MAP, volume 21
[NASA-CR-179893] N87-13015
Atmospheric Tides Middle Atmosphere Program (ATMAP): Report of the workshop, Kyoto, Japan, December 5-6, 1984 N87-13016
Proceedings of the Workshop on Atmospheric Tides, Prague, Czechoslovakia, August 14, 1985 N87-13017
Minutes of MAP/WINE experimenters meeting, Prague, Czechoslovakia, August 13, 1985 N87-13018

ATMOSPHERIC TURBULENCE
Evaluating nonlinear effects in propagation of acoustic pulse in atmospheric surface layer in inversions N87-12951
Experimental research on turbulence in upper-level tropospheric clouds N87-12952
Solar control of geophysical phenomena N87-12953
Characteristics of atmospheric turbulence near the ground. Part 3: Variations in space and time for strong winds (neutral atmosphere)
[ESDU-86010-PT-3] N87-13042
A review of microbursts and their analysis and detection with Doppler radar
[AD-A170458] N87-13110

ATOMIC BEAMS
CO sub 2 laser sustained CW discharge atomic beam source
[DE86-012383] N87-12563
Polarized H(-) source development at BNL
[DE86-012704] N87-13257

ATOMIC ENERGY LEVELS
Synthesis of conjugated polymers with alternating aromatic and quinonoid sequences via elimination on precursors
[AD-A171331] N87-12693

ATOMIC SPECTRA
Characterization of the atomic emission in Inconel 718 alloy metal vapor arcs
[DE86-012178] N87-12672

ATOMIC STRUCTURE
Semiconductor/insulator films for corrosion protection
[AD-A169119] N87-12652

ATOMS
Synthesis of conjugated polymers with alternating aromatic and quinonoid sequences via elimination on precursors
[AD-A171331] N87-12693

ATTENTION
Perceptual factors in workload: A neuromagnetic study
[AD-A169934] N87-13142

ATTITUDE (INCLINATION)
The handling qualities and flight characteristics of the Grumman design 698 simulated twin-engine tilt Nacelle V/STOL aircraft
[NASA-TM-86785] N87-12558

ATTITUDE CONTROL
Attitude control of an artificial satellite by extending the linear quadratic regulator theory
[INPE-3959-PRE/977] N87-12588
A procedure for attitude determination of artificial satellites utilizing techniques of static and dynamic optimal estimation
[INPE-3966-PRE/981] N87-12589
Procedure for one axis satellites attitude control with magnetic actuation
[INPE-3895-PRE/937] N87-12590
Brief analysis of normal attitude accuracies of satellites with wheels or gas jets
[INPE-3993-NTE/262] N87-12594

ATTITUDE STABILITY
Brief analysis of normal attitude accuracies of satellites with wheels or gas jets
[INPE-3993-NTE/262] N87-12594

AUDITORY PERCEPTION
Perceptual factors in workload: A neuromagnetic study
[AD-A169934] N87-13142

AUGER SPECTROSCOPY
Electron spectroscopy in fundamental catalytic studies
[DE86-006781] N87-12639

AURORAL ABSORPTION
Transverse resonances of Earth-ionosphere wave guide in auroral region N87-12956

AURORAL IRRADIATION
Effect of pulsating aurorae on frequency-time characteristics of radio signals reflected from auroral ionosphere N87-12954

AURORAL ZONES
Coordinated radar and satellite studies of ionospheric currents in the auroral zone and polar cap
[AD-A169466] N87-13031
AURORAS
The current-voltage relationship in auroral current sheets
[AD-A169074] N87-13028
AUSTENITE
Design of strong, ductile, HSLA and dual phase steels
[DE86-011313] N87-12665
AUSTENITIC STAINLESS STEELS
Use of analytical electron microscopy in evaluating ferrite stability in austenitic stainless steel welds
[DE86-008537] N87-12667
AUSTRALIA
Airborne spectroradiometry: The application of AIS data to detecting subtle mineral absorption features
N87-12972
Preliminary geological investigation of AIS data at Mary Kathleen, Queensland, Australia N87-12979
AUTOMATIC CONTROL
Evaluation of the Collins/Rockwell two axis gyro/accelerometer sensor cluster (phase 3 unit)
[AD-A169810] N87-12834
Evaluation of the multifunction sensor acceleration sensitive terms MU sub A and MU sub B
[AD-A169811] N87-12835
The siting, installation and operational suitability of the Automated Weather Observing System (AWOS) at heliports
[DOT/FAA/PM-86/30] N87-13099
System-ergonomic workload analysis for highly automated process control tasks N87-13152
Empirical determination among superintendents of the acceptable user surface in digitally automated heating-ventilation air conditioning systems N87-13165
Evaluation of automated decisionmaking methodologies and development of an integrated robotic system simulation. Appendix B: ROBSIM programmer's guide
[NASA-CR-176052] N87-13203
Electronic forms. How close to value-added processing
[DE86-010484] N87-13354
AUTOMOBILES
The measurement of the psychological workload during task-related activities, including car driving, by competing time interval estimation N87-13153
AVAILABILITY
The Department of Defense Very High Speed Integrated Circuit (VHSIC) Technology Availability Program plan for the Committees on Armed Services, United States Congress
[AD-A169250] N87-12763
AVALANCHE DIODES
Millimeter-wave heterojunction two-terminal devices
[AD-A169985] N87-12760
AXIAL FLOW
Journal of engineering thermophysics (selected articles)
[AD-A169452] N87-13347
AXIAL FLOW TURBINES
Visualisation of axial turbine tip clearance flow using a linear cascade
[CUED/A-TURBO/TR-122] N87-12560
AXISYMMETRIC FLOW
Time-dependent solution for axisymmetric flow over a blunt body with ideal gas, CF4, or equilibrium air chemistry
[NASA-TM-87675] N87-12806
Transition and mixing in axisymmetric jets and vortex rings
[NASA-CR-3893] N87-12808
AZIMUTH
Some tactical algorithms for spherical geometry
[AD-A170615] N87-12555
Two-dimensional beamforming using a frequency domain complex Least Mean-Squares (LMS) adaptive filter
[AD-A171396] N87-12785

B

BACKSCATTERING
An analysis of the acoustic characteristics of ABSS (acoustic backscatter system) and its deployments
[AD-A170487] N87-13037
Analysis of Doppler lidar data N87-13067
BACKWARD DIFFERENCING
Quantitative assessment of the effect of partial pivoting in sparse ordinary differential equation solvers
[DE86-012592] N87-13226
BAINITE
Bainite in chromium-molybdenum steels
[DE86-011781] N87-12666
BALLISTICS
Low Q spin-up from rest
[AD-A169106] N87-12813
BALLOON-BORNE INSTRUMENTS
Collection of ions in the stratosphere
[AD-A169905] N87-13032
Mobile intercept of storms N87-13064
Doppler wind profile experiment N87-13094
BAND STRUCTURE OF SOLIDS
Band description of materials with localizing orbitals
[DE86-010529] N87-13255
BANDPASS FILTERS
Fiber-optic magnetic gradiometer with variable magnetic biasing fields
[AD-D012423] N87-12836
BANDWIDTH
Very low bandwidth, unattended imager for surveillance applications
[DE86-013570] N87-12799
Smooth nonparametric quantile estimation under censoring: Simulations and bootstrap methods
[AD-A169935] N87-13236
BAROCLINIC INSTABILITY
Theoretical and experimental studies of baroclinic processes N87-13044
Theoretical and experimental design studies for the Atmospheric General Circulation Experiment
N87-13046
BAROCLINIC WAVES
Theoretical and experimental studies of baroclinic processes N87-13044
Theoretical and experimental design studies for the Atmospheric General Circulation Experiment
N87-13046
The use of satellite data in understanding and predicting convective and large-scale dynamical processes
N87-13049
Dynamics and energetics of the South Pacific Convergence Zone during FGGE SOP-1 N87-13052
Observational and theoretical studies of the evolving structure of baroclinic waves: Attractor dynamics of global weather systems N87-13054
BAROTROPIC FLOW
The use of satellite data in understanding and predicting convective and large-scale dynamical processes
N87-13049
BATTERY CHARGERS
Aircraft battery state of charge and charge control system
[AD-A169411] N87-12766
BAYES THEOREM
A Bayesian approach to quantile and response probability estimation with applications in reliability
[AD-A170455] N87-13240
BEAM WAVEGUIDES
Transverse resonances of Earth-ionosphere wave guide in auroral region N87-12956
BEAMS (RADIATION)
Method and apparatus for rapid optical phasing
[AD-D012412] N87-13270
BEAMS (SUPPORTS)
Feasibility study of test problems for finite element/finite difference programs for structural dynamics
[AD-A169058] N87-12926
BEND TESTS
Unloading-compliance and load-drop analysis of J(Ic) test of irradiated 348 stainless steel
[AD-A170494] N87-12938
BENDING
Analysis of anisotropic thin conical shells
[EPM/RT-86-38] N87-12918
BENZENE
Vapour pressures and critical points of liquids. Part 3A: C6 to C10 alkylbenzenes
[ESDU-86012-PT-3A] N87-12625
BERMUDA
Meteorological summary of WATOX (western Atlantic Ocean experiment) 1985 research intensive, February-April
[PB86-226792] N87-13114
BERNOULLI THEOREM
Semigroups and Poisson-approximation
[AD-A170944] N87-13224
BERYLLIUM
Fracture toughness of CIP-HIP beryllium at elevated temperatures
[AD-A169789] N87-12654
Calculated versus experimental charge density distribution of Be metal
[AD-A168924] N87-13254
BIAS
Fiber-optic magnetic gradiometer with variable magnetic biasing fields
[AD-D012423] N87-12836
A procedure for automatic treatment of dynamic systems state observation bias errors
[INPE-3906-PRE/918] N87-13177
BIBLIOGRAPHIES
Aeronautical Engineering: A continuing bibliography with indexes
[NASA-SP-7037(205)] N87-12532
Quality management: An annotated bibliography
[AD-A169616] N87-12912
Direct effects of atmospheric CO2 enrichment on plants and ecosystems: A bibliography with abstracts
[DE86-013525] N87-13012
Mesoscale ageostrophic circulations associated with baroclinic jet streaks N87-13070
Aerospace Medicine and Biology: A continuing bibliography with indexes
[NASA-SP-7011(290)] N87-13125
Human performance aspects of small screen displays: A literature review revealing the lack of specific research
[AD-A170660] N87-13172
Government libraries. A periodicals bibliography, together with list of bibliographies and indexes
[AD-A169422] N87-13351
BILLETS
Process for carbon-carbon composite fabrication
[AD-D012413] N87-12621
BINARY ALLOYS
Finite mean-free-paths and the electrical resistivity of liquid simple metals and binary alloys
[DE86-702662] N87-12678
BINARY DATA
Method of fabricating high efficiency binary planar optical elements
[AD-D012374] N87-13266
BINARY STARS
Investigations of long-period DQ Herculis star
N87-13364
Los Alamos Science, number 13, spring 1986
[DE86-012864] N87-13371
BINARY SYSTEMS (MATERIALS)
Investigation of deviations from ideality in the two liquid phase region of systems of medium molecular weight hydrocarbon mixtures and water
[AD-A169752] N87-12635
A study of the mechanism of dynamic ductile fracture of two-phase materials
[AD-A168966] N87-12925
Possibility of using dc conductivity for investigating phase transition in amorphous semiconductors
[DE86-702648] N87-13340
BIOASTRONAUTICS
Aerospace Medicine and Biology: A continuing bibliography with indexes
[NASA-SP-7011(290)] N87-13125
BIOCHEMISTRY
Analysis of AIS data of the Bonanza Creek Experimental Forest, Alaska N87-12962
Trace element-induced stress in freshwater wetland vegetation: Preliminary results N87-12965
BIODYNAMICS
Radiographic determination of mass and inertial tensor of anatomical segments
[AD-A169122] N87-13126
Fracture and viscoelastic characteristics of the human cervical spine
[AD-A170002] N87-13133
Guidelines for safe human experimental exposure to impact acceleration
[AD-A169347] N87-13169
BIOLOGICAL EFFECTS
Aerospace Medicine and Biology: A continuing bibliography with indexes
[NASA-SP-7011(290)] N87-13125
Physical interaction of 1-Hz to 100 kHz electric and magnetic fields with living organisms
[DE86-012323] N87-13139
BIOLOGY
Biological and clinical dosimetry, July 1, 1964 to December 31, 1984
[DE86-006947] N87-13138
BIOPHYSICS
Mechanical transduction: Unification
[AD-A171191] N87-13123
Physical interaction of 1-Hz to 100 kHz electric and magnetic fields with living organisms
[DE86-012323] N87-13139
BIOTECHNOLOGY
Japan report: Science and Technology
[JPRS-JST-86-023] N87-12715
BIOTITE
Abundance and distribution of mineral components associated with Moses Rock (kimberlite) diatreme
N87-12975
BIREFRINGENCE
Nonlinear ellipse rotation in a low-birefringence optical fiber N87-13262

BISTABLE CIRCUITS
Phase conjugate optics and picosecond optoelectronics
[AD-A169180] N87-13265
BIVARIATE ANALYSIS
Inequalities for probability contents of convex sets via geometric average
[AD-A169938] N87-13219
BL LACERTAE OBJECTS
Continuum radiation from active galactic nuclei: A statistical study
[NASA-CR-179925] N87-13368
BLACK HOLES (ASTRONOMY)
On the two states of CYG X-1 and related sources
[NASA-TM-89265] N87-13367
BLADE SLAP NOISE
An analysis of blade vortex interaction aerodynamics and acoustics N87-12547
BLADE TIPS
An analysis of blade vortex interaction aerodynamics and acoustics N87-12547
The evaluation of a number of prototypes for the free-tip rotor constant-moment controller
[NASA-TM-86664] N87-12869
BLANKETS (FUSION REACTORS)
Compact reactor studies
[DE86-013247] N87-13263
BLAST LOADS
Blast gust loading on a 35 degree swept-back wing
[AD-A169415] N87-12570
BLUNT BODIES
Time-dependent solution for axisymmetric flow over a blunt body with ideal gas, CF4, or equilibrium air chemistry
[NASA-TM-87675] N87-12806
Computational fluid dynamic studies of certain ducted bluff-body flowfields relevant to turbojet combustors. Volume 1: Time-dependent calculations with the k-epsilon turbulence model for an existing centerbody combustor
[AD-A171434] N87-12816
BODIES OF REVOLUTION
Theory for computing the field scattered from a smooth inflected surface
[NASA-TP-2632] N87-13264
BOILERS
Welding procedure specification. Manual gas tungsten arc and semiautomatic gas metal arc welding of chromium-nickel steel. Supplement 1: Records of procedure qualification tests
[DE86-012521] N87-12886
Welding procedure specification. Manual gas tungsten arc and semiautomatic gas metal arc welding of carbon steel. Supplement 1: Records of procedure qualification tests
[DE86-012532] N87-12889
Welding procedure specification. Gas tungsten arc welding of chromium-nickel steel to chromium-molybdenum steel. Supplement 1: Records of procedure qualification tests
[DE86-012536] N87-12892
BOLTS
Over-center toggle latch
[AD-D012393] N87-12878
BONDING
Phase equilibrium predictions for polar and hydrogen bonding mixtures
[DE86-011812] N87-12642
BONES
Fracture and viscoelastic characteristics of the human cervical spine
[AD-A170002] N87-13133
BORON CARBIDES
Raman spectroscopy of carboranes and polycarboranesiloxanes
[DE86-009030] N87-12894
BORON OXIDES
Li corrosion resistant glasses for headers in ambient temperature Li batteries
[DE86-013754] N87-12902
BOSONS
Supergravity
[DE86-701481] N87-13370
BOTANY
Proceedings of the Second Airborne Imaging Spectrometer Data Analysis Workshop
[NASA-CR-179924] N87-12968
BOUNDARY ELEMENT METHOD
The application of boundary-element techniques for some soil-structure interaction problems
[AD-A168999] N87-12709
BOUNDARY LAYER SEPARATION
A summary of the development of integral aerodynamic methods for the computation of rotor wake interactions
[AD-A169254] N87-12545
BOUNDARY LAYERS
An analysis of the acoustic characteristics of ABSS (acoustic backscatter system) and its deployments
[AD-A170487] N87-13037
Convective surface layers: Influence of the boundary layer depth N87-13041
BOUNDARY VALUE PROBLEMS
Analysis of mixed-mode crack propagation using the boundary integral method
[NASA-CR-179518] N87-12915
Regularity of the solution of elliptic problems with piecewise analytic data. Part 1: Boundary value problems for linear elliptic equation of second order
[AD-A169771] N87-13212
Comparison of 2D memory SEU transport simulation with experiments
[ATR-86(8139)-2] N87-13314
Large-scale electric fields resulting from magnetic reconnection in the corona
[DE86-012391] N87-13383
BOW WAVES
Plane-parallel and bow shock models of Herbig-Haro objects N87-13374
BRAIN
X-ray fluorescence with synchrotron radiation
[DE86-010543] N87-13124
The event related brain potential as an index of information processing and cognitive activity. A program of basic research. Supplement A: Neuromagnetic studies
[AD-A169978] N87-13144
BRAZIL
Geologic remote sensing at INPE: An overview
[INPE-3975-PRE/987] N87-12959
In retrospect: The impact of research production in the area of remote sensing
[INPE-3987-NTE/261] N87-12988
BREMSSTRAHLUNG
Continuum radiation from active galactic nuclei: A statistical study
[NASA-CR-179925] N87-13368
BRIGHTNESS
FEL (Free Electron Laser) optics coating test program (design phase of sample introduction chamber)
[AD-A169474] N87-12849
BRILLOUIN ZONES
Use of Wannier function in the calculations of band structure of covalent crystals
[DE86-702668] N87-13344
BRITTLENESS
The control of polymer mechanical behavior by surface modification
[AD-A169252] N87-12886
BROADBAND
Theoretical study on the correlation between wideband electromagnetic spectra and geological structures
[AD-A168971] N87-13026
BROADCASTING
Medium-frequency data link for differential NAVSTAR/GPS broadcasts
[AD-A169788] N87-12554
BROMINATION
Effects of graphitization on the environmental stability of brominated pitch-based fibers
[NASA-TM-88899] N87-12679
BROMINE
Electrochemistry in near-critical and supercritical fluids. 3: Studies of Br(-), I(-) and hydroquinone in aqueous solutions
[AD-A169138] N87-12633
BRONZES
Growth of ferro-electric tungsten bronze epitaxial thin films for electro-optic device applications
[AD-A170783] N87-13328
BUBBLES
Theory of developed hydrodynamical turbulence
[DE86-012796] N87-12823
Stefan-type problem with void formation and its explicit solution
[DE86-013521] N87-13007
BUDGETING
An implicit enumeration algorithm with binary-valued constraints
[AD-A169256] N87-13182
BUTT JOINTS
Guide to the use of data items on the fatigue strength of welded joints in steels
[ESDU-86013] N87-12914

C

CADMIUM SULFIDES
Stable, high-efficiency, CuInSe2-based polycrystalline thin-film tandem solar cells
[DE86-010705] N87-13003
CADMIUM TELLURIDES
Stable, high-efficiency, CuInSe2-based polycrystalline thin-film tandem solar cells
[DE86-010705] N87-13003
Thermophysical properties measurements of gallium arsenide and cadmium telluride
[AD-A169901] N87-13326
In-situ interdiffusion measurements in HgTe-CdTe superlattices
[DE86-011429] N87-13337
CALCIUM OXIDES
Li corrosion resistant glasses for headers in ambient temperature Li batteries
[DE86-013754] N87-12902
CALCULUS
Superconformal tensor calculus and matter couplings in six dimensions
[DE86-702617] N87-13349
CALIBRATING
Measurement of time-dependent electric current with Rogowski coil
[INPE-3875-RPE/506] N87-12754
The Multispectral Atmospheric Mapping Sensor (MAMS): Instrument description, calibration and data quality
[NASA-TM-86565] N87-12828
Supplementary calibration test of the tip-aerodynamics-and acoustics-test pressure transducers
[NASA-TM-88312] N87-12830
Development of buried wire gages for measurement of wall shear stress in Blastane experiments
[NASA-TM-89212] N87-12831
Radiometric calibration of the airborne imaging spectrometer N87-12969
Analysis of AIS radiometry with emphasis on determination of atmospheric properties and surface reflectance N87-12971
Abundance and distribution of mineral components associated with Moses Rock (kimberlite) diatreme N87-12975
Calibration and accuracy of the NOAA/ERL gust probe system and intercomparison with other systems
[PB86-221736] N87-13116
CALIFORNIA
Analysis of AIS radiometry with emphasis on determination of atmospheric properties and surface reflectance N87-12971
Use of digital Munsell color space to assist interpretation of imaging spectrometer data: Geologic examples from the northern Grapevine Mountains, California and Nevada N87-12980
Trace element-induced stress in freshwater wetland vegetation: Preliminary results N87-12985
Patterns of vegetation in the Owens Valley, California N87-12986
Southern California Air Quality Study (SCAQS) suggested program plan
[PB86-223427] N87-13013
CAMERA SHUTTERS
Development of a large-aperture PLZT shutter with enhanced operational/environmental capabilities
[DE86-011643] N87-12838
CAMERAS
Very high energy gamma ray astrophysics
[DE86-013319] N87-13396
CANCELLATION CIRCUITS
A brief review of adaptive null steering techniques
[AD-A169548] N87-12736
CANONICAL FORMS
Canonical quantization of gravity
[DE86-702615] N87-13372
CANOPIES (VEGETATION)
A partition of sensible and latent heat fluxes above the terra firma area in the Amazon Forest (gradient method)
[INPE-3972-PRE/985] N87-12964
Destriping AIS data using Fourier filtering techniques N87-12974
Analysis of AIS data of the Bonanza Creek Experimental Forest, Alaska N87-12982
Soil types and forest canopy structures in southern Missouri: A first look with AIS data N87-12983
Geobotanical studies at Pilot Mountain, North Carolina using the airborne imaging spectrometer N87-12984
Patterns of vegetation in the Owens Valley, California N87-12986
AIS spectra of desert shrub canopies N87-12987
CANTILEVER BEAMS
Factors influencing elastic stresses in double cantilever beam specimens
[NASA-TM-89033] N87-12922
CAPILLARY TUBES
Theory of developed hydrodynamical turbulence
[DE86-012796] N87-12823

CARBON
Synthesis of conjugated polymers with alternating aromatic and quinonoid sequences via elimination on precursors
[AD-A171331] N87-12693
Production of a clean carbon fuel derived from coal for use in stationary and mobile heat engines
[DE86-011203] N87-12706

CARBON DIOXIDE CONCENTRATION
Characterization of information requirements for studies of CO2 effects: Water resources, agriculture, fisheries, forests and human health
[DE86-012477] N87-13010
High accuracy standards and reference methodology for carbon dioxide in air
[DE86-012643] N87-13011
Direct effects of atmospheric CO2 enrichment on plants and ecosystems: A bibliography with abstracts
[DE86-013525] N87-13012

CARBON DIOXIDE LASERS
CO sub 2 laser sustained CW discharge atomic beam source
[DE86-012383] N87-12683

CARBON FIBERS
Carbon fibers
[AD-A171370] N87-12822
Effects of graphitization on the environmental stability of brominated pitch-based fibers
[NASA-TM-88699] N87-12679

CARBON MONOXIDE
Carbon monoxide adsorption on a platinum electrode studied by polarization modulated FT-IR reflection-absorption spectroscopy. 2: CO adsorbed at a potential in the hydrogen region and its oxidation in acids
[AD-A169082] N87-12632

CARBON STARS
Classification of N-type carbon stars
[AD-A171399] N87-13369

CARBON STEELS
Design of strong, ductile, HSLA and dual phase steels
[DE86-011313] N87-12665
Machine gas metal arc welding of carbon steel. Welding procedure specification. Supplement 1: Records of procedure qualification tests
[DE86-012530] N87-12687
Welding procedure specification. Semiautomatic gas metal arc welding of carbon steels. Supplement 1: Records of procedure qualification tests
[DE86-012531] N87-12688
Welding procedure specification. Manual gas tungsten arc and semiautomatic gas metal arc welding of carbon steel. Supplement 1: Records of procedure qualification tests
[DE86-012532] N87-12689
Gas tungsten arc and shielded metal arc welding of carbon steel. Welding procedure specification. Supplement 1: Records of procedure qualification tests
[DE86-012533] N87-12690
Welding procedure specification. Supplement 1: Records of procedure qualification tests. Shielded metal arc welding of carbon steel
[DE86-012535] N87-12691
Gas tungsten arc welding of carbon steel to nickel-chromium-iron. Welding procedure specification. Supplement 1: Records of procedure qualification tests
[DE86-012549] N87-12694

CARBON 12
The carbon twelve to carbon thirteen isotope ratio of the interstellar medium in the neighborhood of the sun
N87-13366

CARBON 13
The carbon twelve to carbon thirteen isotope ratio of the interstellar medium in the neighborhood of the sun
N87-13366

CARBON-CARBON COMPOSITES
Mechanical testing of a coated carbon-carbon composite at elevated temperatures in air
[AD-A169355] N87-12618
Process for carbon-carbon composite fabrication
[AD-D012413] N87-12621

CARBORANE
Raman spectroscopy of carboranes and polycarboranesiloxanes
[DE86-009030] N87-12694

CARDIOVASCULAR SYSTEM
Hypothermic effects on vascular contractility and reactivity
[AD-A169142] N87-13127

CARIBBEAN SEA
US Navy climatic study of the Caribbean Sea and Gulf of Mexico. Volume 2: East Caribbean Sea
[AD-A171487] N87-13112

CASCADE FLOW
Viscous-inviscid interaction in transonic separated flow over solid and porous airfoils and cascades N87-12535

CATACLYSMIC VARIABLES
Investigations of long-period DQ Herculis star
N87-13364

CATALYSIS
Electron spectroscopy in fundamental catalytic studies
[DE86-006781] N87-12639
Heterogeneous catalysis with lasers
[AD-A169601] N87-12851

CATALYSTS
On the interplay between chemical reactions and phase transitions for molecules adsorbed on solid surfaces
[AD-A169618] N87-12636
Effect of chain rigidity on conductivity of conjugated polymers
[DE86-011263] N87-12696

CATHODES
Efficient, monochromatic, high-power microwave generator
[DE86-012365] N87-12792

CATIONS
Application of pattern recognition to metal ion chemical ionization mass spectra
[AD-A169061] N87-12630

CAVITATION FLOW
Study of high temperature failure mechanisms in ceramics
[AD-A170001] N87-12689
Pressure calculation for two-dimensional flow inside hydraulic structures
[AD-A169039] N87-12812

CAVITIES
FEL (Free Electron Laser) optics coating test program (design phase of sample introduction chamber)
[AD-A169474] N87-12849

CAVITY RESONATORS
New electromagnetic effects associated with cavity-backed apertures
[DE86-008766] N87-12750
Stabilization of voltage-controlled oscillators through resonant cavities
[INPE-3941-RPE/512] N87-12757
Application of nonlinear optics to free electron laser systems
[AD-A168950] N87-12845

CELESTIAL REFERENCE SYSTEMS
Relative motion of the Sun on an artificial satellite
[INPE-3985-NTE/260] N87-12591

CELL CATHODES
Ni-Co alloy plaque for cathode of Ni-Cd battery
[AD-D012375] N87-12769
Zinc/air cell cathode
[AD-D012425] N87-12780

CEMENTS
New ultra low permittivity composites for use in ceramic packaging of Ga:As integrated circuits
[AD-A168877] N87-12758

CENTRIFUGES
A variational principle for the plasma centrifuge
[INPE-3969-PRE/992] N87-12827

CERAMIC COATINGS
Mechanical testing of a coated carbon-carbon composite at elevated temperatures in air
[AD-A169355] N87-12618
Journal of engineering thermophysics (selected articles)
[AD-A169452] N87-13347

CERAMICS
Comparative thermal conductivity measurements at Sandia National Laboratories
[DE86-012926] N87-12647
Hot isostatic pressing of ceramic powder compacts
[AD-A169971] N87-12686
Study of high temperature failure mechanisms in ceramics
[AD-A170001] N87-12689
Metals and Ceramics Division Materials Sciences Program
[DE86-013612] N87-12699
New ultra low permittivity composites for use in ceramic packaging of Ga:As integrated circuits
[AD-A168877] N87-12758
Preliminary material testing of ceramic and wood
[AD-A169557] N87-12771
Holographic storage in ion-implanted, ferroelectric-phase PLZT ceramics
[DE86-010475] N87-12837
Diesel cylinder gas-side heat flux to a ceramic surface
[AD-A168948] N87-12870
NDE reliability and process control for structural ceramics
[NASA-TM-88870] N87-12910
A constitutive law for finite element contact problems with unclassical friction
[NASA-TM-88838] N87-12924

CH-47 HELICOPTER
An application of a LISP based expert system for failure diagnosis of the CH-47 flight control hydraulic system
[AD-A169970] N87-12567
A prototype maintenance expert system for the CH-47 flight control hydraulic system
[AD-A169019] N87-12588

CHALCOGENIDES
Glass fibres for transmission in the 8-12 micrometers waveband N87-13297

CHALLENGER (ORBITER)
Investigation of the Challenger accident, volume 2
[GPO-84-548] N87-12586

CHANNEL NOISE
Multichannel phase noise measurement system
[AD-D012372] N87-13253

CHARGE DISTRIBUTION
Optical characteristics of lightning and thunderstorm currents N87-13061

CHARGED PARTICLES
Fragmentation dynamics of energetic materials
[AD-A169925] N87-12662
Influence of a strong laser field on the stopping power for charged test particles in fusion plasmas
[INPE-3977-PRE/988] N87-12843

CHARTS
US Navy climatic study of the Caribbean Sea and Gulf of Mexico. Volume 2: East Caribbean Sea
[AD-A171487] N87-13112

CHEMICAL ANALYSIS
Electron microprobe analysis: The upper limit of submicron spectroscopy
[DE86-009540] N87-12640
An interdisciplinary approach to predictive modeling of structural adhesive bonding. Characterization of Ti-6Al-4V oxides and the adhesive/oxide interphase
[AD-A170484] N87-12690
Experimental thin film deposition and surface analysis techniques
[DE86-011222] N87-13338

CHEMICAL BONDS
Investigation of the effects of short chain processing additives on polymers
[NASA-TM-89023] N87-12614
Carbon monoxide adsorption on a platinum electrode studied by polarization modulated FT-IR reflection-absorption spectroscopy. 2: CO adsorbed at a potential in the hydrogen region and its oxidation in acids
[AD-A169082] N87-12632
Rusty bolt intermodulation interference reducer
[AD-D012417] N87-12691
Quantum chemical investigations of the mechanism of cationic polymerization and theoretical prediction of crystal densities and decomposition pathways of energetic molecules
[AD-A169805] N87-13324

CHEMICAL COMPOSITION
Investigation of deviations from ideality in the two liquid phase region of systems of medium molecular weight hydrocarbon mixtures and water
[AD-A169752] N87-12635
Microchemical analysis of polycrystalline Ni3Al and other ordered alloys using the field-ion microscope atom probe
[DE86-013157] N87-12677
An interdisciplinary approach to predictive modeling of structural adhesive bonding. Characterization of Ti-6Al-4V oxides and the adhesive/oxide interphase
[AD-A170484] N87-12690

CHEMICAL ENGINEERING
Vapour pressures and critical points of liquids. Part 2C: Alkadienes and alkynes
[ESDU-86001-PT-2C] N87-12624
Japan report: Science and Technology
[JPRS-JST-86-023] N87-12715

CHEMICAL EQUILIBRIUM
Investigation of deviations from ideality in the two liquid phase region of systems of medium molecular weight hydrocarbon mixtures and water
[AD-A169752] N87-12635

CHEMICAL FUELS
Combustion and micro-explosion of water/oil emulsions in high pressure environments
[AD-A169976] N87-12627

CHEMICAL LASERS
Iodine monofluoride energy transfer studies
[AD-A169781] N87-12852

CHEMICAL PROPERTIES
Combustion and micro-explosion of water/oil emulsions in high pressure environments
[AD-A169976] N87-12627
Application of pattern recognition to metal ion chemical ionization mass spectra
[AD-A169061] N87-12630

Plasma assisted surface coating/modification processes: An emerging technology
[NASA-TM-88885] N87-12708

CHEMICAL REACTIONS
Synthesis of conjugated polymers with alternating aromatic and quinonoid sequences via elimination on precursors
[AD-A171331] N87-12693
Shock-induced solid state chemistry: Theoretical background
[DE86-012741] N87-12941

CHEMICAL REACTORS
Experimental investigation of thermochemical transport for solar applications using sulfur trioxide
[DE86-011762] N87-13005

CHEMILUMINESCENCE
Iodine monofluoride energy transfer studies
[AD-A169781] N87-12852

CHINA
The Chinese guided missiles stride toward modernization
[AD-A169017] N87-12582

CHIPS (ELECTRONICS)
Compaction with automatic jog introduction
[AD-A169679] N87-12772
Investigation of a new concept in semiconductor microwave oscillators
[AD-A170772] N87-12781
Heat transfer characteristics of simulated microelectronic chips under normal and enhanced conditions
[PB86-224425] N87-12804
Comparison of 2D memory SEU transport simulation with experiments
[ATR-86(8139)-2] N87-13314

CHIPS (MEMORY DEVICES)
A VLSI-based high-performance raster image system
[AD-A169068] N87-12761
Reliability study of retention and memory gate integrity in a 1K MNOS RAM
[DE86-010483] N87-13175

CHROMIUM ALLOYS
Bainite in chromium-molybdenum steels
[DE86-011781] N87-12666
Gas tungsten arc welding of carbon steel to nickel-chromium-iron. Welding procedure specification. Supplement 1: Records of procedure qualification tests
[DE86-012549] N87-12894

CHROMIUM STEELS
Welding procedure specification. Manual gas tungsten arc and semiautomatic gas metal arc welding of chromium-nickel steel. Supplement 1: Records of procedure qualification tests
[DE86-012521] N87-12886
Gas tungsten arc welding of chromium-nickel steel to nickel-molybdenum-chromium-iron. Welding procedure specification. Supplement 1: Records of procedure qualification tests
[DE86-012550] N87-12895

CIRCADIAN RHYTHMS
Sleepability and wakeability following sleep deprivation
[AD-A169578] N87-13130
Pharmacological resetting of the circadian sleep-wake cycle
[AD-A170804] N87-13137

CIRCUIT RELIABILITY
Reliability study of retention and memory gate integrity in a 1K MNOS RAM
[DE86-010483] N87-13175

CIRCUITS
Experimental verification of soliton theory using a microwave crossed-field amplifier
[AD-A170011] N87-12778

CIRCULAR CYLINDERS
Radar cross-section of damped cylinders and dielectric strips
[AD-A169027] N87-12726
In-line and transverse forces on smooth and rough cylinders in oscillatory flow at high Reynolds numbers
[AD-A169562] N87-12815
Cylindrical laser welder
[AD-D012398] N87-12850

CIRCULAR POLARIZATION
Investigations of long-period DQ Herculis star
N87-13364

CIRCULAR TUBES
Analysis of laminar flow heat transfer in uniform temperature circular tubes with tape inserts
[PB86-224763] N87-12826

CIRCULAR WAVEGUIDES
A spherical waveguide multiplexer-demultiplexer
N87-13285

CIRRUS CLOUDS
Experimental research on turbulence in upper-level tropospheric clouds N87-12952

CLADDING
Parametric linear variation of a leakage free permanent magnet field source
[AD-D012359] N87-13249

CLASSIFICATIONS
Application of pattern recognition to metal ion chemical ionization mass spectra
[AD-A169061] N87-12630
Special associative preprocessing structures for qualitative feature extraction
[AD-A169147] N87-13181
Classification of N-type carbon stars
[AD-A171399] N87-13369

CLAYS
Detection of hydrothermal alteration at Virginia City, Nevada using Airborne Imaging Spectrometry (AIS)
N87-12978
Use of digital Munsell color space to assist interpretation of imaging spectrometer data: Geologic examples from the northern Grapevine Mountains, California and Nevada N87-12980

CLEAN FUELS
Production of a clean carbon fuel derived from coal for use in stationary and mobile heat engines
[DE86-011203] N87-12706

CLEANING
Cleaning of aluminum alloy 5083
[DE86-012573] N87-12675

CLEAR AIR TURBULENCE
Analysis of satellite data for sensor improvement (detection of severe storms from space N87-13071

CLEAVAGE
Micromechanisms and toughness for cleavage fracture of steel
[AD-A169906] N87-12655
Energetics of dislocation relaxation associated with cleavage in Cd-doped zinc crystals as probed by sychrotron topography
[DE86-002968] N87-13334

CLIMATE
Characterization of information requirements for studies of CO2 effects: Water resources, agriculture, fisheries, forests and human health
[DE86-012477] N87-13010
SAGE 2 satellite data set validation
[NASA-CR-178189] N87-13024
US Navy climatic study of the Caribbean Sea and Gulf of Mexico. Volume 2: East Caribbean Sea
[AD-A171487] N87-13112

CLIMATOLOGY
Wheeler AFB, Hawaii Limited Surface Observations Climatic Summary (LISOCS), parts 1-5
[AD-A169391] N87-13107

CLINICAL MEDICINE
Biological and clinical dosimetry, July 1, 1984 to December 31, 1984
[DE86-006947] N87-13136

CLOSED ECOLOGICAL SYSTEMS
The ecology of microorganisms in a small closed system: Potential benefits and problems for space station
[NASA-TM-86563] N87-13166

CLOUD COVER
Third International Symposium on Tropical Meteorology N87-12948
Geobotanical studies at Pilot Mountain, North Carolina using the airborne imaging spectrometer N87-12984
A simple solar, spectral model for studying the effects of cloud cover and surface albedo on the incoming solar radiation
[AD-A171284] N87-13038

CLOUD PHYSICS
A detailed analysis of the influence of eddy exchange processes upon the development of radiation fog
[AD-A169233] N87-13102
A sensitivity study of a one-dimensional time-dependent warm cumulus cloud model
[AD-A170141] N87-13109

CLOUDS
Intercomparison of DMSP OLS, NOAA AVHRR, GOES VISSR (Defense Meteorological Satellite Program Operational Linescan System, National Oceanographic and Atmospheric Administration Advanced Very High Resolution Radiometer, GOES Visible Infrared Spin-Scan Radiometer) and Landsat MSS imagery for cloud property determination: Recommendations for digital data analysis
[AD-A169285] N87-12991

CLOUDS (METEOROLOGY)
Utilization of satellite cloud information to diagnose the energy state and transformations in extratropical cyclones N87-13051
Analysis of satellite data for sensor improvement (detection of severe storms from space N87-13071
Time composite sounding N87-13083
Detection of rotating thunderstorms using satellite imagery N87-13085
Studies of humid continental haze during SPACE N87-13088
Preliminary planning for the Satellite Precipitation And Cloud Experiment (SPACE) Field Program N87-13089
Interactive information processing for NASA's mesoscale analysis and space sensor program N87-13093
First meeting of the Working Group on the Shuttle Microwave Precipitation Radiometer (SMPR) N87-13096
Model studies of solar spectral irradiance at the bottom and top of a cloudy atmosphere N87-13365

CLUMPS
Spherical clusters of simple metals: Madelung energies and structure
[AD-A169560] N87-13323

CLUSTER ANALYSIS
Statistical models and methods for cluster analysis and image segmentation
[AD-A169145] N87-13229

CMOS
Totally self-checking circuits and testable CMOS circuits
[AD-A169756] N87-12773
Kinetics and mechanisms on the molecular beam etching of semiconductors
[AD-A171360] N87-13331

COAL
Production of a clean carbon fuel derived from coal for use in stationary and mobile heat engines
[DE86-011203] N87-12706

COALESCING
Development testing of large volume water sprays for warm fog dispersal
[NASA-TP-2607] N87-12585

COASTS
Meteorological summary of WATOX (western Atlantic Ocean experiment) 1985 research intensive, February-April
[PB86-226792] N87-13114

COAXIAL CABLES
Electric and magnetic field coupling through a braided-shield cable: Transfer admittance and transfer impedance
[AD-A171490] N87-12748

COBALT
Investigation of the effects of cobalt ions on epoxy properties
[NASA-TP-2639] N87-12680

COBALT ALLOYS
Ni-Co alloy plaque for cathode of Ni-Cd battery
[AD-D012375] N87-12769

COCKPITS
A test on the reliability and performance of the verbex series 4000 voice recognizer
[AD-A169066] N87-12729
Anthropometric handicaps in the construction of a helicopter cockpit — seats N87-13148

CODING
On 3-D inelastic analysis methods for hot section components (base program)
[NASA-CR-175060] N87-12923
MAGNA (Materially And Geometrically Nonlinear Analysis). Addendum 1, parts 1-4
[AD-A169383] N87-12933

COEFFICIENT OF FRICTION
Frictional and retarding forces on aircraft tyres. Part 4: Estimation of effects of yaw
[ESDU-86016-PT-4] N87-12868

COGNITION
The event related brain potential as an index of information processing and cognitive activity. A program of basic research. Supplement A: Neuromagnetic studies
[AD-A169978] N87-13144

COGNITIVE PSYCHOLOGY
Simulation of disturbances on the nuclear power plant simulator. The problem of the interpretation of operator actions and their cognitive backgrounds as a basis for design recommendations N87-13157

COHERENT RADIATION
High-gain free electron lasers as generators of short wavelength coherent radiation
[DE86-012500] N87-12865

COLD WATER
Human thermoregulatory model for immersion in cold water
[AD-A169779] N87-13131

COLLISION AVOIDANCE
Obstacle-warning radar for helicopters N87-13149

COLLISIONAL PLASMAS
Models and radiation of railgun plasma armatures with non-ideal plasma properties
[AD-A169349] N87-13258

COLLISIONS
Study in molecular lasers
[AD-A169933] N87-12855

COLLOIDS
Electrokinetic properties of polymer colloids
[NASA-CR-178936] N87-12681
COMBINED STRESS
Using combined experiment/analysis to generate dynamic critical stress intensity data
[DE86-013578] N87-12945
COMBUSTION
Optical diagnostics for diesel engine applications
[DE86-010747] N87-12641
COMBUSTION CHAMBERS
Relationship of in-cylinder gaseous and particulate concentration to radiative heat transfer in direct injection-type diesel combustion
[AD-A168979] N87-12628
Computational fluid dynamic studies of certain ducted bluff-body flowfields relevant to turbojet combustors. Volume 1: Time-dependent calculations with the k-epsilon turbulence model for an existing centerbody combustor
[AD-A171434] N87-12816
COMBUSTION PHYSICS
Further shock tunnel studies of scramjet phenomena
[NASA-CR-179937] N87-12542
COMMAND GUIDANCE
Single-mode-fibers for fiberoptic-guided missiles: A comparison with graded-index multimode fibers
N87-13303
COMMERCE
Quality management: An annotated bibliography
[AD-A168816] N87-12912
COMMUNICATION CABLES
Fiber optics: A survivable and cost-effective transmission medium for terrestrial networks N87-13302
COMMUNICATION EQUIPMENT
Department of Defense gateway architecture and functional requirements
[AD-A169086] N87-13200
COMMUNICATION NETWORKS
Fault tolerance mechanisms for a network communication multiprocessor
[INPE-3958-PRE/876] N87-12720
Advanced teleprocessing systems
[AD-A170007] N87-12741
Department of Defense gateway architecture and functional requirements
[AD-A169086] N87-13200
Fiber optics: A survivable and cost-effective transmission medium for terrestrial networks N87-13302
COMMUNICATION SATELLITES
MILSTAR modeling survey
[AD-A169789] N87-12600
COMMUTATORS
Canonical quantization of gravity
[DE86-702615] N87-13372
COMPACTING
Hot isostatic pressing of ceramic powder compacts
[AD-A169971] N87-12688
COMPARISON
Comparison of methods for the calculation of thermal contact resistance of the first Brazilian satellite
[INPE-3864-TDL/217] N87-12596
Comparison of tropical forest surveys
[DE86-011699] N87-12993
COMPENSATORS
Tracking servo compensator with rate aiding
[AD-D012388] N87-12735
COMPLEX COMPOUNDS
Dual temperature thermal storage with complex compounds
[DE86-011511] N87-13000
COMPONENT RELIABILITY
Investigation of the Challenger accident, volume 2
[GPO-64-548] N87-12586
COMPOSITE MATERIALS
Metallurgical characterization of the interfaces and the damping mechanisms in metal matrix composites
[AD-A169186] N87-12616
Stress effects on moisture transport in an epoxy resin and its composite
[AD-A169306] N87-12617
Quartz growth on X-seeds
[AD-D012269] N87-13315
COMPOSITE STRUCTURES
Metallurgical characterization of the interfaces and the damping mechanisms in metal matrix composites
[AD-A169186] N87-12616
Literature review on the design of composite mechanically fastened joints
[AD-A169112] N87-12872
Improved anti-G suit
[AD-D012378] N87-13171
COMPRESSED AIR
Rapid acting electro-pneumatic anti-G suit control valve
[AD-D012377] N87-13170
COMPRESSIBLE FLOW
Finite-difference solutions for compressible laminar boundary-layer flows of a dusty gas over a semi-infinite flat plate
[UTIAS-311] N87-12807
Free-Lagrangian hydrodynamics using massless tracer points
[DE86-012406] N87-12822
COMPRESSIBLE FLUIDS
Optical spectroscopy of dynamically compressed liquids
[AD-A169013] N87-12629
COMPRESSING
Optical spectroscopy of dynamically compressed liquids
[AD-A169013] N87-12629
COMPUTATION
Comparison of methods for the calculation of thermal contact resistance of the first Brazilian satellite
[INPE-3864-TDL/217] N87-12596
Method of ray intensity calculation as applied to anomalous propagation
[AD-A169553] N87-12737
A computational method to model radar return range in a polygonally based, computer-generated-imagery simulation
[NASA-TM-86324] N87-12967
SOR (Successive Over-Relaxation) MGR (multigrid algorithm)(nu) experiments on the crystal multicomputer
[AD-A169929] N87-13187
Quantitative assessment of the effect of partial pivoting in sparse ordinary differential equation solvers
[DE86-012592] N87-13226
COMPUTATIONAL FLUID DYNAMICS
Transition and mixing in axisymmetric jets and vortex rings
[NASA-CR-3893] N87-12808
Adaptive grid techniques for elliptic fluid-flow problems
[AD-A169471] N87-12814
Computational fluid dynamic studies of certain ducted bluff-body flowfields relevant to turbojet combustors. Volume 1: Time-dependent calculations with the k-epsilon turbulence model for an existing centerbody combustor
[AD-A171434] N87-12816
Study of numerical solution methods for two-phase flows
[DE86-012265] N87-12821
COMPUTATIONAL GRIDS
Adaptive grid techniques for elliptic fluid-flow problems
[AD-A169471] N87-12814
SOR (Successive Over-Relaxation) MGR (multigrid algorithm)(nu) experiments on the crystal multicomputer
[AD-A169929] N87-13187
Some investigations into variable meshes for numerical solution of partial differential equations
[AD-A169977] N87-13208
An expert-system-like feedback approach in the hp-version of the finite element method
[AD-A169855] N87-13214
COMPUTER AIDED DESIGN
A VLSI-based high-performance raster image system
[AD-A169068] N87-12761
Compaction with automatic jog introduction
[AD-A169679] N87-12772
Declarative descriptions for VLSI generators
[AD-A169952] N87-12777
Electronic Engineering Department Thrust Area report, FY 1985
[DE86-013172] N87-12797
Welding research in Scandinavia: An assessment
[AD-A169036] N87-12871
A software implementation of an interactive graphics system for three dimensional modeling and layout
[AD-A169264] N87-13183
An expert-system-like feedback approach in the hp-version of the finite element method
[AD-A169855] N87-13214
COMPUTER AIDED MANUFACTURING
Welding research in Scandinavia: An assessment
[AD-A169036] N87-12871
COMPUTER ASSISTED INSTRUCTION
Catalog of Resources for Education in Ada (Trade name) and Software Engineering (CREASE), version 4.0
[AD-A169892] N87-13186
COMPUTER DESIGN
A versatile Data Processing Unit (DPU) for satellite-borne composition instrumentation N87-13393
COMPUTER GRAPHICS
A computational method to model radar return range in a polygonally based, computer-generated-imagery simulation
[NASA-TM-86324] N87-12967
Conversion of the NOLAPS (Navy Operational Local Atmospheric Prediction System) model to the HP9845
[AD-A169538] N87-13108
Utilization of impact dot matrix printers
[INPE-3991-RPE/518] N87-13173
Special associative preprocessing structures for qualitative feature extraction
[AD-A169147] N87-13181
A software implementation of an interactive graphics system for three dimensional modeling and layout
[AD-A169264] N87-13183
Using 3-dimensional graphics to visualize multivariate scientific data
[DE86-010788] N87-13195
Iterative methods for large linear and nonlinear least squares problems
[AD-A169028] N87-13209
COMPUTER INFORMATION SECURITY
Proceedings of the IDA Workshop on Formal Specification and Verification of Ada (trade name) (1st) held in Alexandria, Virginia on 18-20 March 1985
[AD-A171507] N87-13192
COMPUTER NETWORKS
Maximization of the capacity of the most survivable connections in a network
[AD-A169065] N87-12726
Atmospheric Modeling And Sensor Simulation (AMASS) study N87-13090
Interactive information processing for NASA's mesoscale analysis and space sensor program
N87-13093
Availability and consistency of global information in computer networks
[AD-A169247] N87-13202
COMPUTER PROGRAMMING
High frequency, high voltage MOSFET isolation amplifier
[AD-D012403] N87-12774
Catalog of Resources for Education in Ada (Trade name) and Software Engineering (CREASE), version 4.0
[AD-A169892] N87-13186
Proceedings of the IDA Workshop on Formal Specification and Verification of Ada (trade name) (1st) held in Alexandria, Virginia on 18-20 March 1985
[AD-A171507] N87-13192
Iterative methods for large linear and nonlinear least squares problems
[AD-A169028] N87-13209
COMPUTER PROGRAMS
Computer programs for electromagnetic scattering from a slotted TM cylindrical conductor by the pseudo-image method
[AD-A169016] N87-12725
On 3-D inelastic analysis methods for hot section components (base program)
[NASA-CR-175060] N87-12923
Detection of hydrothermal alteration at Virginia City, Nevada using Airborne Imaging Spectrometry (AIS)
N87-12978
LAMPS software and mesoscale prediction studies
N87-13076
Observation model and parameter partials for the JPL VLBI parameter estimation software MASTERFIT-1986
[NASA-CR-179919] N87-13178
Maintaining LU factors of a general sparse matrix
[AD-A169255] N87-13248
Temperature compensation in the 2:17 type magnet s
[AD-A169487] N87-13250
COMPUTER STORAGE DEVICES
Special associative preprocessing structures for qualitative feature extraction
[AD-A169147] N87-13181
Distributed name servers: Naming and caching in large distributed computing environments
[AD-A169225] N87-13201
COMPUTER SYSTEMS DESIGN
Interpretive model for a concurrency method
[DE86-012743] N87-13197
COMPUTER TECHNIQUES
A new method of synthetic aperture radar image reconstruction using modified convolution back-projection algorithm
[AD-A170852] N87-12747
Evaluation of the Collins/Rockwell two axis gyro/accelerometer sensor cluster (phase 3 unit)
[AD-A169810] N87-12834
Integrating computer vision with a robot arm system
[AD-A171278] N87-12884
High-resolution analysis of eye movements
[AD-A170779] N87-13136
Yield and performance enhancement through redundancy in VLSI and WSI multi-precessor systems
[AD-A169930] N87-13174
Single-phase method for quadratic programming
[DE86-012156] N87-13194
COMPUTER VISION
Integrating computer vision with a robot arm system
[AD-A171278] N87-12884

COMPUTERIZED SIMULATION
Modeling the fundamental characteristics and processes of the spacecraft functioning
[NASA-TM-87999] N87-12598
MILSTAR modeling survey
[AD-A169789] N87-12600
Method of ray intensity calculation as applied to anomalous propagation
[AD-A169553] N87-12737
Electronic Engineering Department Thrust Area report, FY 1985
[DE86-013172] N87-12797
Transition and mixing in axisymmetric jets and vortex rings
[NASA-CR-3893] N87-12808
Pressure calculation for two-dimensional flow inside hydraulic structures
[AD-A169039] N87-12812
Development of an inexpensive, high resolution positron multiwire proportional counter
[DE86-011576] N87-12841
Mechanical interactions of rough surfaces
[DE86-010886] N87-12901
Linear harmonic analysis of free-piston Stirling engines
[DE86-012451] N87-12903
A computational method to model radar return range in a polygonally based, computer-generated-imagery simulation
[NASA-TM-86324] N87-12967
Atmospheric-water absorption features near 2.2 micrometers and their importance in high spectral resolution remote sensing N87-12973
Photovoltaic Concentrator Technology Project, Fourteenth Project Integration Meeting, June 10-11, 1986
[DE86-012051] N87-13006
Atmospheric illumination and shadows, revision 1
[DE86-010971] N87-13039
Numerical simulation of convective response to mesoscale forcing N87-13081
Atmospheric Modeling And Sensor Simulation (AMASS) study N87-13090
Analysis of head and neck dynamic response of the US adult military population
[AD-A169563] N87-13129
Tool to develop real time simulation systems
[INPE-3979-TDL/233] N87-13179
Evaluation of automated decisionmaking methodologies and development of an integrated robotic system simulation. Appendix B: ROBSIM programmer's guide
[NASA-CR-178052] N87-13203
Two-dimensional dynamics of the plasma Wakefield accelerator
[DE86-012362] N87-13312

COMPUTERS
Directory of range data conversion and processing system, revision
[AD-A169629] N87-12578
Japan report: Science and Technology
[JPRS-JST-86-023] N87-12715

CONCURRENT PROCESSING
Interpretive model for a concurrency method
[DE86-012743] N87-13197

CONDUCTIVE HEAT TRANSFER
An analysis of shear band development incorporating heat conduction
[AD-A169972] N87-12926

CONFERENCES
Digest: Proceedings of the International Conference on Optical and Millimeter Wave Propagation and Scattering in the Atmosphere
[AD-A170393] N87-12743
International Conference/Workshop on Small Fatigue Cracks (2nd) held in Santa Barbara, California on 5-10 January 1986
[AD-A169060] N87-12929
Proceedings of the Second Airborne Imaging Spectrometer Data Analysis Workshop
[NASA-CR-179924] N87-12968
Proceedings of the Solar Thermal Technology Conference
[DE86-011703] N87-13002
Middle Atmosphere Program. Handbook for MAP, volume 21
[NASA-CR-179883] N87-13015
Atmospheric Tides Middle Atmosphere Program (ATMAP): Report of the workshop, Kyoto, Japan, December 5-6, 1984 N87-13016
Proceedings of the Workshop on Atmospheric Tides, Prague, Czechoslovakia, August 14, 1985 N87-13017
Minutes of MAP/WINE experimenters meeting, Prague, Czechoslovakia, August 13, 1985 N87-13018
Proceedings of a Symposium on the Evaluation of Man-Machine Systems: Methods and Problems
[DGLR-85-04] N87-13146
Proceedings of the IDA Workshop on Formal Specification and Verification of Ada (trade name) (1st) held in Alexandria, Virginia on 18-20 March 1985
[AD-A171507] N87-13192
Proceedings of the conference on the design of experiments in army research development and testing (31st) held at the Madison, Wisconsin on 23-25 October 1986
[AD-A169473] N87-13246
Contributions to the 18th International Cosmic Ray Conference
[ATR-86(9558)-11] N87-13389

CONFIDENCE LIMITS
Smooth nonparametric quantile estimation under censoring: Simulations and bootstrap methods
[AD-A169935] N87-13236

CONFINEMENT
Tara vacuum system
[DE86-011673] N87-13311

CONGRESSIONAL REPORTS
National Commission on Space report
[GPO-63-143] N87-12574
Investigation of the Challenger accident, volume 2
[GPO-64-548] N87-12586
NASA's quality assurance program
[GPO-63-142] N87-12909
Department of Housing and Urban Development-independent agencies appropriations for 1987, part 7
[GPO-61-970] N87-13357

CONICAL SHELLS
Dynamic analysis of anisotropic conical shells
[EPM/RT-86-36] N87-12916
Analysis of anisotropic thin conical shells
[EPM/RT-86-38] N87-12918

CONJUGATION
Synthesis of conjugated polymers with alternating aromatic and quinonoid sequences via elimination on precursors
[AD-A171331] N87-12693
Effect of chain rigidity on conductivity of conjugated polymers
[DE86-011263] N87-12696

CONNECTORS
Light socket removal tool
[AD-D012368] N87-12710

CONSTITUTIVE EQUATIONS
Coupled damage and moisture-transport in fiber-reinforced polymeric composites
[AD-A169379] N87-12619
Data requirements to model creep in 9Cr-1Mo-V steel
[DE86-011754] N87-12944

CONSTRUCTION
Beam steering mirror construction
[AD-D012399] N87-13268

CONSTRUCTION MATERIALS
Periodic heat transfer through an inhomogeneous medium
[DE86-702966] N87-12825

CONTACT RESISTANCE
Comparison of methods for the calculation of thermal contact resistance of the first Brazilian satellite
[INPE-3664-TDL/217] N87-12596

CONTAINMENT
Crack propagation in high strain regions of a steel containment
[DE86-011437] N87-12943

CONTAMINATION
Effects of inertia weld parameters and contamination on weld flash shape and on joint strength: An improved study
[DE86-013074] N87-12904

CONTINUITY
An intuitive approach to geometric continuity for parametric curves and surfaces
[AD-A169654] N87-13211

CONTINUUM MECHANICS
Percolation and low density materials: Theory and applications
[AD-A169204] N87-12684
Surface green function matching for a three-dimensional non-local continuum
[DE86-702647] N87-13341
Continuum radiation from active galactic nuclei: A statistical study
[NASA-CR-179925] N87-13368

CONTRACTORS
Investigation of the Challenger accident, volume 2
[GPO-64-548] N87-12586
Regression models of quarterly overhead costs for six government aerospace contractors
[AD-A169185] N87-13350

CONTRAROTATING PROPELLERS
Cruise noise of counterrotation propeller at angle of attack in wind tunnel
[NASA-TM-88869] N87-13252

CONTROL BOARDS
Ergonomic requirements for the design of control rooms. Evaluation method N87-13158

CONTROL SIMULATION
Application of the task taxonomy method to the simulation of human service reliability in the manual control of aircraft
[MBB/LKE-301/S/PUB/216] N87-13151

CONTROL STABILITY
Feedback system design with an uncertain plant
[NASA-CR-176867] N87-13243

CONTROL SYSTEMS DESIGN
Empirical determination among superintendents of the acceptable user surface in digitally automated heating-ventilation air conditioning systems N87-13165
Feedback system design with an uncertain plant
[NASA-CR-176867] N87-13243

CONTROL VALVES
Rapid acting electro-pneumatic anti-G suit control valve
[AD-D012377] N87-13170

CONTROLLERS
Flight model discharge system
[AD-A169423] N87-12571
Problems in integrated digital networks
[AD-A170442] N87-12744
Aircraft battery state of charge and charge control system
[AD-A169411] N87-12766
Electronic Engineering Department Thrust Area report, FY 1985
[DE86-013172] N87-12797
The evaluation of a number of prototypes for the free-tip rotor constant-moment controller
[NASA-TM-86664] N87-12969
Feedback system design with an uncertain plant
[NASA-CR-176867] N87-13243

CONVECTION
Application of flux-corrected transport (FCT) to high Rayleigh number natural convection in a porous medium
[DE86-004603] N87-12818
Theoretical and experimental studies of baroclinic processes N87-13044
The use of satellite data in understanding and predicting convective and large-scale dynamical processes N87-13049
Optical characteristics of lightning and thunderstorm currents N87-13061
Response of the mesoscale atmosphere to diabatic heating N87-13069
Automated mesoscale winds derived from GOES multispectral imagery N87-13073
LAMPS software and mesoscale prediction studies N87-13076
Mesoscale research activities with the LAMPS model N87-13078
Numerical simulation of convective response to mesoscale forcing N87-13081
A summary of research on mesoscale energetics of severe storm environments N87-13082

CONVECTION CLOUDS
Study of the formation and transport of acidic species by non-precipitating cumulus clouds during VENTEX-84
[PB86-220357] N87-13014
Remote sensing of severe convective storms N87-13075

CONVECTION CURRENTS
Coordinated radar and satellite studies of ionospheric currents in the auroral zone and polar cap
[AD-A169488] N87-13031

CONVECTIVE FLOW
Adaptive grid techniques for elliptic fluid-flow problems
[AD-A169471] N87-12814
Natural convection in an enclosure with discrete roughness elements on a vertical heated wall
[DE86-004424] N87-12817
Convective surface layers: Influence of the boundary layer depth N87-13041

CONVECTIVE HEAT TRANSFER
Natural convection in an enclosure with discrete roughness elements on a vertical heated wall
[DE86-004424] N87-12817
Effect of convection on weld pool shape and microstructure
[AD-A170488] N87-12883

CONVERGENCE
HOMPACK: A suite of codes for globally convergent homotopy algorithms
[DE86-011644] N87-13196
The h-p version of the finite element method with quasiuniform meshes
[AD-A170144] N87-13222
Asymptotic theory for sieve estimators in semimartingale regression models
[AD-A169207] N87-13230

Extreme values of birth and death processes and queues
[AD-A169932] N87-13235

COOLING
The analysis of a transistor cap as a heat dissipator
[AD-A171398] N87-12786

COORDINATE TRANSFORMATIONS
The effect of coupling in an inertial navigation platform stabilized system made up of three single-degree-of-freedom gyroscopes
[AD-A169110] N87-12553

COORDINATES
Some tactical algorithms for spherical geometry
[AD-A170615] N87-12555

COPOLYMERS
Investigation of the effects of short chain processing additives on polymers
[NASA-TM-89023] N87-12614
Physical characteristics of diblock polyacetylene copolymers: Processability-conductivity correlation
[DE86-011218] N87-12695

COPPER
Effect of strain and strain rate on residual microstructures in copper
[DE86-007361] N87-12659
Effect of residual strain on twinning in shock-loaded copper
[DE86-007362] N87-12660

CORIOLIS EFFECT
Theoretical and experimental studies in support of the geophysical fluid flow experiment N87-13045

CORNER FLOW
Effect of port corner geometry on the internal performance of a rotating-vane-type thrust reverser
[NASA-TP-2624] N87-12541

CORONAL HOLES
Magnetic field re-arrangement after prominence eruption
[DE86-012393] N87-13382

CORONAL LOOPS
Equilibrium configuration of coronal loops
[DE86-702711] N87-13384

CORRELATION
Theoretical study on the correlation between wideband electromagnetic spectra and geological structures
[AD-A168971] N87-13026
Deep convection in mesoscale convective systems N87-13055
On reduction of dimensionality under multivariate regression and canonical correlation models
[AD-A170025] N87-13238

CORROSION
Initiation of pitting corrosion in martensitic stainless steels
[DE86-007827] N87-12661

CORROSION PREVENTION
Semiconductor/insulator films for corrosion protection
[AD-A169119] N87-12652
Zinc/air cell cathode
[AD-D012425] N87-12780

CORROSION RESISTANCE
Initiation of pitting corrosion in martensitic stainless steels
[DE86-007827] N87-12661
Li corrosion resistant glasses for headers in ambient temperature Li batteries
[DE86-013754] N87-12802

COSMIC RAY SHOWERS
Very high energy gamma ray astrophysics
[DE86-013319] N87-13396

COSMIC RAYS
Contributions to the 18th International Cosmic Ray Conference
[ATR-86(9558)-11] N87-13389
The ultraheavy cosmic rays: Propagation and selective acceleration N87-13390
The stellar upper mass limit in an OB association and implications for cosmic rays and cosmic abundances N87-13392
Neutron and antineutron production in accretion onto compact objects
[NASA-TM-89264] N87-13395
Observations on the Stanford 4800 KG gravity wave detector with a cosmic ray monitor N87-13399

COSMOLOGY
Los Alamos Science, number 13, spring 1986
[DE86-012864] N87-13371
Astro-particle-physics
[DE86-702948] N87-13373

COST ANALYSIS
Regression models of quarterly overhead costs for six government aerospace contractors
[AD-A169185] N87-13350

COST ESTIMATES
Regression models of quarterly overhead costs for six government aerospace contractors
[AD-A169185] N87-13350

COSTS
General purpose aft cargo carrier study, volume 1
[NASA-CR-178905] N87-12587

COUETTE FLOW
Analysis of the nonlinear stability of circular Couette flow
[AD-A168951] N87-12811

COUNTING
The event related brain potential as an index of information processing and cognitive activity. A program of basic research. Supplement A: Neuromagnetic studies
[AD-A169978] N87-13144

COUNTING CIRCUITS
Totally self-checking circuits and testable CMOS circuits
[AD-A169756] N87-12773

COUPLING
The effect of coupling in an inertial navigation platform stabilized system made up of three single-degree-of-freedom gyroscopes
[AD-A169110] N87-12553
Electric and magnetic field coupling through a braided-shield cable: Transfer admittance and transfer impedance
[AD-A171490] N87-12748
Transformers for explosive pulsed power coupling to various loads
[DE86-012425] N87-12796
Donor-acceptor one step energy transfer via exchange coupling on a fractal lattice
[AD-A169843] N87-13325

COUPLING COEFFICIENTS
Application of the AIPA (Approximate Iterative Preprocessing Algorithm) to F-106 data
[AD-A169084] N87-12569

COVARIANCE
A multivariate extension of Hoeffding's lemma
[AD-A170170] N87-13239

CRAB NEBULA
Very high energy gamma ray astrophysics
[DE86-013319] N87-13396

CRACK PROPAGATION
Research on mechanical properties for engine life prediction
[AD-A169570] N87-12563
Micromechanisms of crack growth and fracture toughness in metal matrix composites
[AD-A169839] N87-12620
Micromechanisms and toughness for cleavage fracture of steel
[AD-A169906] N87-12655
Fatigue behavior of long and short cracks in wrought and powder aluminum alloys
[AD-A169960] N87-12656
Effect of hydrogen on the mechanical properties and fracture behavior of high purity aluminum
[AD-A171214] N87-12658
Application of hydrogen embrittlement models to the crack growth behavior of fusion reactor materials
[DE86-011614] N87-12671
Crack-tip chemistry and fracture mechanics-based model of the crack growth rate/stress intensity relationship for Ni + P
[DE86-011106] N87-12676
The control of polymer mechanical behavior by surface modification
[AD-A169252] N87-12686
Study of high temperature failure mechanisms in ceramics
[AD-A170001] N87-12689
Analysis of mixed-mode crack propagation using the boundary integral method
[NASA-CR-179518] N87-12915
International Conference/Workshop on Small Fatigue Cracks (2nd) held in Santa Barbara, California on 5-10 January 1986
[AD-A169060] N87-12929
Linear elastic fracture testing: Current status within ASTM committee E-24 on fracture
[AD-A169442] N87-12934
Assessment of damage tolerance requirements and analyses: A user's manual for crack growth and crack initiation analysis: DAMGRO
[AD-A171209] N87-12939
Molecular dynamic studies of crack propagation. The role of the interatomic potential
[DE86-009942] N87-12942
Crack propagation in high strain regions of a steel containment
[DE86-011437] N87-12943
Using combined experiment/analysis to generate dynamic critical stress intensity data
[DE86-013578] N87-12945
Energetics of dislocation relaxation associated with cleavage in Cd-doped zinc crystals as probed by sychrotron topography
[DE86-002968] N87-13334

CRACKING (FRACTURING)
Linear elastic fracture testing: Current status within ASTM committee E-24 on fracture
[AD-A169442] N87-12934

CRACKS
The influence of welding flux on the pyrometallurgical, physical and mechanical behavior of weld metal
[AD-A169067] N87-12650
Fatigue behavior of long and short cracks in wrought and powder aluminum alloys
[AD-A169960] N87-12656
International Conference/Workshop on Small Fatigue Cracks (2nd) held in Santa Barbara, California on 5-10 January 1986
[AD-A169060] N87-12929
Computation of the amplitude of stress singular terms for cracks and reentrant corners
[AD-A169796] N87-12936

CRASH INJURIES
Analysis of head and neck dynamic response of the US adult military population
[AD-A169563] N87-13129

CRASH LANDING
Aircraft accident/incident summary reports: Erie, Pennsylvania, October 14, 1984; Albuquerque, New Mexico, February 11, 1985
[PB86-910407] N87-12549
Aircraft accident report: Bar Harbor Airlines Flight 1808, Beech BE-99, N300WP, Auburn-Lewiston Municipal Airport, Auburn, Maine, August 25, 1985
[PB86-910406] N87-12550

CREEP PROPERTIES
Study of high temperature failure mechanisms in ceramics
[AD-A170001] N87-12689
Data requirements to model creep in 9Cr-1Mo-V steel
[DE86-011754] N87-12944

CREEP TESTS
Research on mechanical properties for engine life prediction
[AD-A169570] N87-12563

CRITERIA
Basic conceptions for the evaluation of man machine systems N87-13161

CRITICAL POINT
Vapour pressures and critical points of liquids. Part 3A: C8 to C10 alkylbenzenes
[ESDU-86012-PT-3A] N87-12625

CROP INVENTORIES
Crop yield modeling for climate impact studies. Part 1: Reasoning and results
[INPE-3967-PRE/982-PT-1] N87-12961

CROSS FLOW
Computational and experimental study of flow-induced vibration of the SSME main injector post
[DE86-012119] N87-12611

CROSSED FIELDS
Experimental verification of soliton theory using a microwave crossed-field amplifier
[AD-A170011] N87-12778

CROSSLINKING
Ionic conductivity in solid, crosslinked dimethylsiloxane-ethylene oxide copolymer networks containing sodium
[AD-A169038] N87-12683

CRUISING FLIGHT
Cruise noise of counterrotation propeller at angle of attack in wind tunnel
[NASA-TM-88869] N87-13252

CRYOGENIC COOLING
Cryogenic wound rotor for lightweight, high voltage generators
[AD-D012370] N87-12768

CRYOGENIC EQUIPMENT
Observations on the Stanford 4800 KG gravity wave detector with a cosmic ray monitor N87-13399

CRYOGENICS
Analysis of magnetic refrigeration systems with staged regenerators based on an idealized magnetic material entropy model: 1
[DE86-013638] N87-12714
Development of low-temperature transistor modules to improve the MSFC mid-infrared array
[NASA-TM-86566] N87-12756

CRYSTAL DEFECTS
Shock-induced solid state chemistry: Theoretical background
[DE86-012741] N87-12941

Search for far infrared radiation from optically and acoustically pumped defect modes
[AD-A169159] N87-13319
Structural features at the Si-SiO2 interface
[DE86-012947] N87-13339

CRYSTAL DISLOCATIONS
Quartz growth on X-seeds
[AD-D012269] N87-13315
Energetics of dislocation relaxation associated with cleavage in Cd-doped zinc crystals as probed by sychrotron topography
[DE86-002968] N87-13334

CRYSTAL GROWTH
New results on low temperature thermal oxidation of silicon
[AD-A169603] N87-12634
Solid State Photovoltaic Research Branch annual report, FY 1985
[DE86-010708] N87-13004
Quartz growth on X-seeds
[AD-D012269] N87-13315
Incremental quench research
[AD-A168960] N87-13317

CRYSTAL LATTICES
Moessbauer-Bormann superradiance
[DE86-012373] N87-12866
Surface green function matching for a three-dimensional non-local continuum
[DE86-702647] N87-13341

CRYSTAL OPTICS
Phase conjugate optics and picosecond optoelectronics
[AD-A169160] N87-13265

CRYSTAL STRUCTURE
Shifts in shuttle SRM performance because of ammonium perchlorate crystal shape on missions 51-I/J and 61-A/B
[NASA-TM-86561] N87-12607
Neutron diffraction studies of some rare earth-transition metal deuterides
[AD-A168995] N87-12648
Fatigue behavior of long and short cracks in wrought and powder aluminum alloys
[AD-A169960] N87-12656
Densification of graphites by irradiation
[DE86-010026] N87-12698
Spherical clusters of simple metals: Madelung energies and structure
[AD-A169560] N87-13323
Epitaxial crystallization and epitaxial polymerization as tools for molecular engineering
[AD-A171508] N87-13333
Electron diffraction analysis of the pentagonal arrangement of grains found in CVD pure Ni films
[DE86-009023] N87-13336
Surface and adsorption-like states within the nearly free electron approximation
[DE86-702651] N87-13342

CRYSTAL SURFACES
Carbon monoxide adsorption on a platinum electrode studied by polarization modulated FT-IR reflection-absorption spectroscopy. 2: CO adsorbed at a potential in the hydrogen region and its oxidation in acids
[AD-A169062] N87-12632

CRYSTALLIZATION
Epitaxial crystallization and epitaxial polymerization as tools for molecular engineering
[AD-A171508] N87-13333
Possibility of using dc conductivity for investigating phase transition in amorphous semiconductors
[DE86-702646] N87-13340

CRYSTALS
Quantum chemical investigations of the mechanism of cationic polymerization and theoretical prediction of crystal densities and decomposition pathways of energetic molecules
[AD-A169805] N87-13324
Use of Wannier function in the calculations of band structure of covalent crystals
[DE86-702668] N87-13344

CUMULUS CLOUDS
Study of the formation and transport of acidic species by non-precipitating cumulus clouds during VENTEX-84
[PB86-220357] N87-13014
A sensitivity study of a one-dimensional time-dependent warm cumulus cloud model
[AD-A170141] N87-13109

CURRENT SHEETS
The current-voltage relationship in auroral current sheets
[AD-A169074] N87-13026

CURVES (GEOMETRY)
HOMPACK: A suite of codes for globally convergent homotopy algorithms
[DE86-011644] N87-13196
An intuitive approach to geometric continuity for parametric curves and surfaces
[AD-A169654] N87-13211

CYCLONES
Meteorological effects of geotectonic phenomena hypothesized N87-12947
Summary of 1986 Atlantic tropical cyclone activity and verification of author's seasonal forecast N87-13097

CYCLOTRON RESONANCE DEVICES
A 60 GHz gyrotron development program
[DE86-012486] N87-12791

CYLINDRICAL BODIES
Mach 6 experimental and theoretical stability and performance of a finned cylindrical body at angles of attack up to 65 deg
[NASA-TM-89050] N87-12538
Density and electrostatic potential distribution around a cylindrical satellite
[INPE-3953-NTE/258] N87-12595
Axial detonator for simultaneous ignition of multiple HE points
[DE86-011878] N87-12643
Computer programs for electromagnetic scattering from a slotted TM cylindrical conductor by the pseudo-image method
[AD-A169016] N87-12725
Low Q spin-up from rest
[AD-A169106] N87-12813
Parametric linear variation of a leakage free permanent magnet field source
[AD-D012359] N87-13249

CYLINDRICAL SHELLS
Cylindrical laser welder
[AD-D012398] N87-12850
Non-linear analysis of cylindrical shells
[EPM/RT-86-37] N87-12917
Free vibration of axisymmetric and beam-like cylindrical shells, partially filled with liquid
[EPM/RT-86-35] N87-12920

CZOCHRALSKI METHOD
Study to determine the feasibility of utilizing skull-melting techniques for the growth of single crystals of yttrium vanadate
[AD-A169249] N87-13320

D

DAMAGE ASSESSMENT
Coupled damage and moisture-transport in fiber-reinforced polymeric composites
[AD-A169379] N87-12619
Study of high temperature failure mechanisms in ceramics
[AD-A170001] N87-12689
Assessment of damage tolerance requirements and analyses: A user's manual for crack growth and crack initiation analysis: DAMGRO
[AD-A171209] N87-12939

DAMPERS (VALVES)
Multiple rate shock isolator damping valve
[AD-D012394] N87-12879

DAMPING
A mathematical formulation of a large space structure control problem
[AD-A169950] N87-12602
Radar cross-section of damped cylinders and dielectric strips
[AD-A169027] N87-12726

DAMPING TESTS
Metallurgical characterization of the interfaces and the damping mechanisms in metal matrix composites
[AD-A169186] N87-12616

DATA ACQUISITION
An approach to design knowledge capture for the space station
[NASA-TM-89272] N87-12597
Influence of experimental scatter on the analysis and extrapolation of stress-rupture data
[DE86-009510] N87-12940
Report of the Ad-Hoc Commission on remote sensing
[INPE-3981-NTE/259] N87-12963
Generation of images with recorded auxiliary data for the LANDSAT Thematic Mapper (TM) imagery
[INPE-3982-TDL/234] N87-12990
The meteorological interactive data display system N87-13091

DATA BASE MANAGEMENT SYSTEMS
Data tagging in the Energy Data Base
[DE86-010621] N87-13355

DATA BASES
Introduction to the theory of nested transactions
[AD-A171428] N87-13191
Availability and consistency of global information in computer networks
[AD-A169247] N87-13202
Computer-based estimation procedure for coaxial jet noise. Including far-field subsonic jet mixing noise database for stationary, coplanar conical nozzles
[ESDU-86019] N87-13251
Further results on interpolation searching of databases
[DE86-012822] N87-13356

DATA COMPRESSION
A versatile Data Processing Unit (DPU) for satellite-borne composition instrumentation N87-13393

DATA CORRELATION
Comparison of the 1984 and 1985 AIS data over the Singatse Range (Yerington), Nevada N87-12976
Coordinated study of the behavior of the middle atmosphere in winter: Monthly mean comparisons of satellite and radiosonde data and derived quantities N87-13019
SAGE 2 satellite data set validation
[NASA-CR-178189] N87-13024

DATA LINKS
Medium-frequency data link for differential NAVSTAR/GPS broadcasts
[AD-A169788] N87-12554
Performance of RF fiber optic links N87-13301
A hybrid transmission scheme on single mode fibers for tactical communications N87-13306

DATA MANAGEMENT
Federal information systems management: Problems, solutions and more problems
[AD-A171366] N87-13353

DATA PROCESSING
Evaluation of a nonlinear parameter extraction mathematical model including the term C(subm(sub delta e squared))
[NASA-TM-87731] N87-12566
A prototype maintenance expert system for the CH-47 flight control hydraulic system
[AD-A169019] N87-12568
SARSAT (Search and Rescue Satellite) operational data categorization and accuracy studies
[AD-A169748] N87-12599
Pulse Code Modulation (PCM) data storage and analysis using a microcomputer
[NASA-TP-2629] N87-12718
Report of the Ad-Hoc Commission on remote sensing
[INPE-3981-NTE/259] N87-12963
ERS-1 SAR data processing
[NASA-CR-179913] N87-12965
Airborne spectroradiometry: The application of AIS data to detecting subtle mineral absorption features N87-12972
Atmospheric-water absorption features near 2.2 micrometers and their importance in high spectral resolution remote sensing N87-12973
NASA/MSFC FY-85 Atmospheric Processes Research Review
[NASA-CP-2402] N87-13043
Interactive information processing for NASA's mesoscale analysis and space sensor program N87-13093
NOSL experiment support
[NASA-CR-178947] N87-13140
Tool to develop real time simulation systems
[INPE-3979-TDL/233] N87-13179
Design and analysis of experiments and more realistic techniques for data analysis
[AD-A168921] N87-13228
Two issues concerning the analysis of grouped data
[DE86-006401] N87-13242
Space plasma research
[NASA-CR-178965] N87-13307
Electronic forms. How close to value-added processing
[DE86-010484] N87-13354

DATA PROCESSING EQUIPMENT
Directory of range data conversion and processing system, revision
[AD-A169629] N87-12578

DATA REDUCTION
Directory of range data conversion and processing system, revision
[AD-A169629] N87-12578
Pulse Code Modulation (PCM) data storage and analysis using a microcomputer
[NASA-TP-2629] N87-12718
Adaptive grid techniques for elliptic fluid-flow problems
[AD-A169471] N87-12814
Zero-crossings analysis
[AD-A169937] N87-13218
Design and analysis of experiments and more realistic techniques for data analysis
[AD-A168921] N87-13228

DATA RETRIEVAL
Improved satellite retrievals and mesoscale moisture variability N87-13087

Further results on interpolation searching of databases
[DE86-012822] N87-13356

DATA STORAGE
An approach to design knowledge capture for the space station
[NASA-TM-89272] N87-12597
Pulse Code Modulation (PCM) data storage and analysis using a microcomputer
[NASA-TP-2629] N87-12718
Generation of images with recorded auxiliary data for the LANDSAT Thematic Mapper (TM) imagery
[INPE-3982-TDL/234] N87-12990

DATA STRUCTURES
Survey of the characteristics of very high level languages
[DE86-012240] N87-13198

DATA TRANSMISSION
SPRINT 3: Serial-Parallel Remote Interface System development report
[DE86-010590] N87-13176

DEBRIS
Simple defense conservative model for mass requirements of hypervelocity projectile impact shields for reentry vehicles
[DE86-012407] N87-12603

DECISION MAKING
An implicit enumeration algorithm with binary-valued constraints
[AD-A169256] N87-13182
Evaluation of automated decisionmaking methodologies and development of an integrated robotic system simulation. Appendix B: ROBSIM programmer's guide
[NASA-CR-178052] N87-13203
Application of a network associative scene analysis model
[INPE-3945-PRE/967] N87-13244

DEFECTS
Effect of convection on weld pool shape and microstructure
[AD-A170488] N87-12883

DEFENSE INDUSTRY
Japan report: Science and Technology
[JPRS-JST-86-023] N87-12715

DEFENSE PROGRAM
Possible military applications of stratospheric airship discussed N87-12716
The Department of Defense Very High Speed Integrated Circuit (VHSIC) Technology Availability Program plan for the Committees on Armed Services, United States Congress
[AD-A169250] N87-12763
Department of Defense gateway architecture and functional requirements
[AD-A169086] N87-13200

DEFLAGRATION
Pulsed-laser, high speed photography of rocket propellant surface deflagration
[AD-A169308] N87-12703

DEFLECTION
A new and efficient formulation for finite element analysis of thin shell structures undergoing small and large deflection N87-12913

DEFORESTATION
Comparison of tropical forest surveys
[DE86-011699] N87-12993

DEFORMATION
Effect of strain and strain rate on residual microstructures in copper
[DE86-007361] N87-12659
Mechanics of metal forming
[DE86-012414] N87-12673
Study of high temperature failure mechanisms in ceramics
[AD-A170001] N87-12689
A study of the mechanism of dynamic ductile fracture of two-phase materials
[AD-A168966] N87-12925

DEGREES OF FREEDOM
The effect of coupling in an inertial navigation platform stabilized system made up of three single-degree-of-freedom gyroscopes
[AD-A169110] N87-12553
A finite element method for localized failure analysis
[AD-A169117] N87-12930

DEICING
A heater made from graphite composite material for potential deicing application
[NASA-TM-88688] N87-12559

DELAY
Observation model and parameter partials for the JPL VLBI parameter estimation software MASTERFIT-1986
[NASA-CR-179919] N87-13178

DEMODULATION
Tone calibration technique: A digital signaling scheme for mobile applications
[NASA-CR-179915] N87-12719
Progress in optical fiber sensors N87-13274

DEMULTIPLEXING
A spherical waveguide multiplexer-demultiplexer N87-13285

DENDRITIC CRYSTALS
Incremental quench research
[AD-A168960] N87-13317

DENSIFICATION
Densification of graphites by irradiation
[DE86-010026] N87-12898

DENSITY (NUMBER/VOLUME)
Calculated versus experimental charge density distribution of Be metal
[AD-A168924] N87-13254

DENSITY DISTRIBUTION
Calculated versus experimental charge density distribution of Be metal
[AD-A168924] N87-13254

DENSITY MEASUREMENT
Metal thickness measurements using radiography
[AD-D012373] N87-12832

DEPOSITION
Plasma joining of metal matrix composites
[AD-A169058] N87-12615
Mechanical testing of a coated carbon-carbon composite at elevated temperatures in air
[AD-A169355] N87-12618
Plasma-enhanced deposition and processing of transition metals and transition metal silicides for VLSI
[AD-A168963] N87-13316

DESERTIFICATION
USSR report: Earth sciences
[JPRS-UES-86-007] N87-12946
Desertification: Global ecological problem N87-12950

DESERTS
AIS spectra of desert shrub canopies N87-12987

DESIGN ANALYSIS
Viewport concept for space station modules
[NASA-TM-88559] N87-12592
An approach to design knowledge capture for the space station
[NASA-TM-89272] N87-12597
Ergonomic requirements for the design of control rooms. Evaluation method N87-13158
Design and analysis of experiments and more realistic techniques for data analysis
[AD-A168921] N87-13228

DETECTION
Remote sensing to detect ecological impacts associated with acid deposition
[DE86-011649] N87-12992
Severe storm electricity N87-13056
Storm severity detection (RF) N87-13057
Lightning mapper and the future N87-13059
Remote observations of severe storms N87-13065
Investigations of severe/tornadic thunderstorm development and evolution based on satellite and AVE/SESAME/VAS data N87-13084
Detection of rotating thunderstorms using satellite imagery N87-13085
A rule-based pattern matching system for the recognition of three-dimensional line drawn objects: A foundation for video tracking
[AD-A170701] N87-13190
Observations on the Stanford 4800 KG gravity wave detector with a cosmic ray monitor N87-13399

DETONATION
Detonation cellular structure and image proces
[DE86-006487] N87-12819
Study of numerical solution methods for two-phase flows
[DE86-012285] N87-12821

DETONATORS
Axial detonator for simultaneous ignition of multiple HE points
[DE86-011878] N87-12643
Anvil detonator: A 300EC-stable, hot-wire-ignited, nonprimary-explosive device
[DE86-013635] N87-12707

DEUTERIDES
Real-time experimental measurements of isotopic exchange between gaseous hydrogen and palladium hydride powder
[DE86-012610] N87-12644
Neutron diffraction studies of some rare earth-transition metal deuterides
[AD-A168995] N87-12648

DEUTERIUM
Real-time experimental measurements of isotopic exchange between gaseous hydrogen and palladium hydride powder
[DE86-012610] N87-12644

DIAGNOSIS
An application of a LISP based expert system for failure diagnosis of the CH-47 flight control hydraulic system
[AD-A168970] N87-12567

DIAMONDS
Use of Wannier function in the calculations of band structure of covalent crystals
[DE86-702668] N87-13344

DIATOMIC MOLECULES
Study in molecular lasers
[AD-A169933] N87-12855

DICTIONARIES
TSAR (Theater Simulation of Airbase Resources) database dictionary F-4E
[AD-A169575] N87-13352

DIELECTRIC PROPERTIES
New ultra low permittivity composites for use in ceramic packaging of Ga:As integrated circuits
[AD-A168877] N87-12758

DIELECTRICS
Radar cross-section of damped cylinders and dielectric strips
[AD-A169027] N87-12726
Dielectric antennas for millimeter-wave applications
[AD-A169885] N87-12739
Input impedance of an infinite linear scanned array of flat rectangular strips inside a dielectric loaded parallel plate waveguide
[AD-A171275] N87-12784
Theoretical and experimental studies in support of the geophysical fluid flow experiment N87-13045

DIENES
Vapour pressures and critical points of liquids. Part 2C: Alkadienes and alkynes
[ESDU-86001-PT-2C] N87-12624

DIESEL ENGINES
Relationship of in-cylinder gaseous and particulate concentration to radiative heat transfer in direct injection-type diesel combustion
[AD-A168979] N87-12628
Optical diagnostics for diesel engine applications
[DE86-010747] N87-12641
Diesel cylinder gas-side heat flux to a ceramic surface
[AD-A168948] N87-12870

DIESEL FUELS
Optical diagnostics for diesel engine applications
[DE86-010747] N87-12641

DIFFERENTIAL EQUATIONS
The continuous projective sumt method for convex programming --- sequential unconstrained minimization techniques
[AD-A169847] N87-13185
Performance analysis of some numerical algorithms in the resolution of ODEs artificial satellite problems
[INPE-3996-PRE/995] N87-13206
Solving systems of nonlinear equations by tensor methods
[AD-A169927] N87-13216

DIFFRACTION LIMITED CAMERAS
Pulsed-laser, high speed photography of rocket propellant surface deflagration
[AD-A169308] N87-12703
Space infrared telescope facility wide field and diffraction limited array camera (IRAC)
[NASA-CR-177041] N87-13362

DIFFUSION
Transport and relaxation processes in supercritical fluids
[DE86-007847] N87-12638
Hot isostatic pressing of ceramic powder compacts
[AD-A169971] N87-12688
Generalization of one-dimensional solute transport: A stochastic-convective flow conceptualization
[DE86-011117] N87-12820
Stress assisted diffusion in elastic and viscoelastic materials
[AD-A169296] N87-12932
In-situ interdiffusion measurements in HgTe-CdTe superlattices
[DE86-011429] N87-13337

DIFFUSION ELECTRODES
Coordinated research program in pulsed power physics
[AD-A169113] N87-12762

DIGITAL COMPUTERS
Atmospheric Modeling And Sensor Simulation (AMASS) study N87-13090

DIGITAL DATA
SPRINT 3: Serial-Parallel Remote Interface System development report
[DE86-010590] N87-13176

DIGITAL SIMULATION
Determination of the load and stress of a cockpit crew during aircraft piloting using task networks and the simulation language SAINT N87-13150
DIGITAL SYSTEMS
Phased arrays 1985 symposium: Proceedings [AD-A169316] N87-12732
Problems in integrated digital networks [AD-A170442] N87-12744
DIGITAL TECHNIQUES
Tone calibration technique: A digital signaling scheme for mobile applications [NASA-CR-179915] N87-12719
DIGITAL TO ANALOG CONVERTERS
Unique mechanization to fault isolate failures of an electron tube Radio Frequency (RF) amplifier and its high voltage power supply [AD-D012376] N87-12770
DIPHENYL COMPOUNDS
Methods for the syntheses of mono-, di-, tri- and tetranitro derivatives of diphenylamine [WSRL-0436-TR] N87-12702
DIRECTION FINDING
Medium-frequency data link for differential NAVSTAR/GPS broadcasts [AD-A169788] N87-12554
DIRECTORIES
Directory of range data conversion and processing system, revision [AD-A169629] N87-12578
DIRICHLET PROBLEM
The h-p version of the finite element method with quasiuniform meshes [AD-A170144] N87-13222
DISCRIMINANT ANALYSIS (STATISTICS)
Pattern recognition based on scale invariant discriminant functions [AD-A170809] N87-13241
DISCRIMINATION
Limits of pattern discrimination in human vision [AD-A170756] N87-13135
DISPLACEMENT
Non-linear analysis of cylindrical shells [EPM/RT-86-37] N87-12917
DISPLAY DEVICES
Simulator design and instructional features for carrier landing: A field transfer study [AD-A169962] N87-12573
Simulation of CIFF (Centralized IFF) remote control displays [AD-A170387] N87-12742
A new method of synthetic aperture radar image reconstruction using modified convolution back-projection algorithm [AD-A170652] N87-12747
A VLSI-based high-performance raster image system [AD-A169068] N87-12761
The meteorological interactive data display system N87-13091
A design study for a three-dimensional display computer terminal for meteorological information N87-13092
Human performance aspects of small screen displays: A literature review revealing the lack of specific research [AD-A170660] N87-13172
Utilization of impact dot matrix printers [INPE-3991-RPE/518] N87-13173
DISSOCIATION
Study in molecular lasers [AD-A169933] N87-12855
Quantum chemical investigations of the mechanism of cationic polymerization and theoretical prediction of crystal densities and decomposition pathways of energetic molecules [AD-A169805] N87-13324
DISTRIBUTED PROCESSING
Advanced teleprocessing systems [AD-A170007] N87-12741
Distributed name servers: Naming and caching in large distributed computing environments [AD-A169225] N87-13201
Availability and consistency of global information in computer networks [AD-A169247] N87-13202
DISTRIBUTION (PROPERTY)
First meeting of the Working Group on the Shuttle Microwave Precipitation Radiometer (SMPR) N87-13096
DISTRIBUTION FUNCTIONS
Note on a characterization of exponential distributions [AD-A169896] N87-13215
A multivariate extension of Hoeffding's lemma [AD-A170170] N87-13239
DIURNAL VARIATIONS
A partition of sensible and latent heat fluxes above the terra firma area in the Amazon Forest (gradient method) [INPE-3972-PRE/985] N87-12964
DMSP SATELLITES
Intercomparison of DMSP OLS, NOAA AVHRR, GOES VISSR (Defense Meteorological Satellite Program Operational Linescan System, National Oceanographic and Atmospheric Administration Advanced Very High Resolution Radiometer, GOES Visible Infrared Spin-Scan Radiometer) and Landsat MSS imagery for cloud property determination: Recommendations for digital data analysis [AD-A169285] N87-12991
DOCUMENTS
Electronic forms. How close to value-added processing [DE86-010484] N87-13354
DONOR MATERIALS
Donor-acceptor one step energy transfer via exchange coupling on a fractal lattice [AD-A169843] N87-13325
DOPED CRYSTALS
Energetics of dislocation relaxation associated with cleavage in Cd-doped zinc crystals as probed by sychrotron topography [DE86-002968] N87-13334
DOPPLER EFFECT
Doppler effect laser velocity measuring system [AD-D012401] N87-12854
DOPPLER RADAR
NASA/MSFC FY-85 Atmospheric Processes Research Review [NASA-CP-2402] N87-13043
Multiscale modeling to evaluate proposed space-based Doppler lidar sampling strategies N87-13047
Mobile intercept of storms N87-13064
Airborne Doppler measurements of the central California extended sea breeze N87-13066
Analysis of Doppler lidar data N87-13067
Airborne Doppler lidar activities N87-13068
Doppler wind profile experiment N87-13094
A review of microbursts and their analysis and detection with Doppler radar [AD-A170458] N87-13110
DOSIMETERS
Biological and clinical dosimetry, July 1, 1964 to December 31, 1984 [DE86-006947] N87-13138
DRAG
Simplified forms of performance equations. Addendum A: Effect on aeroplane level speed of small changes in thrust, drag, weight, power [ESDU-86004-ADD-A] N87-12556
DRAG REDUCTION
Length adjustable strut link with low aerodynamic drag [AD-D012279] N87-12543
DRIFT RATE
Closed loop fiber optic gyro N87-13277
DROP TESTS
Unloading-compliance and load-drop analysis of J(Ic) test of irradiated 348 stainless steel [AD-A170494] N87-12938
DROPS (LIQUIDS)
Theory of developed hydrodynamical turbulence [DE86-012796] N87-12823
DUCTED BODIES
Computational fluid dynamic studies of certain ducted bluff-body flowfields relevant to turbojet combustors. Volume 1: Time-dependent calculations with the k-epsilon turbulence model for an existing centerbody combustor [AD-A171434] N87-12816
DUCTILITY
A study of the mechanism of dynamic ductile fracture of two-phase materials [AD-A168966] N87-12925
DUMMIES
Analysis of head and neck dynamic response of the US adult military population [AD-A169563] N87-13129
DUST
Finite-difference solutions for compressible laminar boundary-layer flows of a dusty gas over a semi-infinite flat plate [UTIAS-311] N87-12807
DYNAMIC CHARACTERISTICS
Fragmentation dynamics of energetic materials [AD-A168925] N87-12682
Characterization and dynamical studies of polymers in dipolar (aprotic) liquids [AD-A169243] N87-12685
The control of polymer mechanical behavior by surface modification [AD-A169252] N87-12686
MIZEX: A program for mesoscale air-ice-ocean interaction experiments in arctic marginal ice zones. 8: A science plan for a winter marginal ice zone experiment in the Fram Strait/Greenland Sea, 1987/89 [AD-A169070] N87-13119
DYNAMIC LOADS
Unloading-compliance and load-drop analysis of J(Ic) test of irradiated 348 stainless steel [AD-A170494] N87-12938
DYNAMIC RESPONSE
Feasibility study of test problems for finite element/finite difference programs for structural dynamics [AD-A169058] N87-12928
MAGNA (Materially And Geometrically Nonlinear Analysis). Addendum 1, parts 1-4 [AD-A169383] N87-12933
Analysis of head and neck dynamic response of the US adult military population [AD-A169563] N87-13129
DYNAMIC STABILITY
NASA rotor systems research aircraft: Fixed-wing configuration flight-test results [NASA-TM-86789] N87-12557
DYNAMIC STRUCTURAL ANALYSIS
Feasibility study of test problems for finite element/finite difference programs for structural dynamics [AD-A169058] N87-12928
DYNAMICAL SYSTEMS
A procedure for attitude determination of artificial satellites utilizing techniques of static and dynamic optimal estimation [INPE-3966-PRE/961] N87-12589
Constructive and operational characteristics of a synchronous induction motor [INPE-3976-RPE/517] N87-12755

E

E REGION
Effect of pulsating auroras on frequency-time characteristics of radio signals reflected from auroral ionosphere N87-12954
EARTH ATMOSPHERE
The space station millimeter facility [AD-A168963] N87-12604
High accuracy standards and reference methodology for carbon dioxide in air [DE86-012643] N87-13011
Atmospheric illumination and shadows, revision 1 [DE86-010971] N87-13039
Characterization of the gamma radiation in space and in the atmosphere [DE86-013445] N87-13397
EARTH CRUST
Development of ultrasonic modelling techniques for the study of seismic wave scattering due to crustal inhomogeneities [AD-A170017] N87-13034
EARTH IONOSPHERE
Transverse resonances of Earth-ionosphere wave guide in auroral region N87-12956
The current-voltage relationship in auroral current sheets [AD-A169074] N87-13028
Coordinated radar and satellite studies of ionospheric currents in the auroral zone and polar cap [AD-A169466] N87-13031
EARTH MANTLE
USSR report: Earth sciences [JPRS-UES-86-007] N87-12946
Meteorological effects of geotectonic phenomena hypothesized N87-12947
EARTH OBSERVATIONS (FROM SPACE)
Study of satellite systems to monitor Earth's radiation budget [CAP-420-071] N87-12994
Remote observations of severe storms N87-13065
Analysis of satellite data for sensor improvement (detection of severe storms from space N87-13071
EARTH ORBITS
Vector analysis and satellite footprints [AD-A169832] N87-12576
Procedure for one axis satellites attitude control with magnetic actuation [INPE-3895-PRE/937] N87-12590
EARTH PLANETARY STRUCTURE
Some tactical algorithms for spherical geometry [AD-A170615] N87-12555
Earth sciences research in the Civil Space Program [PB86-232014] N87-12995
Theoretical study on the correlation between wideband electromagnetic spectra and geological structures [AD-A168971] N87-13026
Balloon-borne, high altitude gravimetry: The flight of DUCKY 1a (11 October 1983) [AD-A169942] N87-13033
Development of ultrasonic modelling techniques for the study of seismic wave scattering due to crustal inhomogeneities [AD-A170017] N87-13034

EARTHQUAKES
Lg wave excitation and propagation in presence of one-, two-, and three-dimensional heterogeneities
[AD-A169325] N87-13030
ECHO SOUNDING
The Gulf Stream dynamics experiment. Inverted echo sounder data report for the June 1984 to May 1985 deployment period
[AD-A170758] N87-13121
ECOLOGY
Patterns of vegetation in the Owens Valley, California N87-12986
ECONOMETRICS
On reduction of dimensionality under multivariate regression and canonical correlation models
[AD-A170025] N87-13238
ECOSYSTEMS
Evaluating ecosystem response to toxicant stress: a state space approach
[DE86-011777] N87-13009
Direct effects of atmospheric CO2 enrichment on plants and ecosystems: A bibliography with abstracts
[DE86-013525] N87-13012
EDUCATION
In retrospect: The impact of research production in the area of remote sensing
[INPE-3987-NTE/261] N87-12986
Technology transfer at Pacific Northwest Laboratory
[DE86-012333] N87-13361
EFFICIENCY
Two issues concerning the analysis of grouped data
[DE86-006401] N87-13242
Method of fabricating high efficiency binary planar optical elements
[AD-D012374] N87-13266
EIGENVALUES
Low Q spin-up from rest
[AD-A169106] N87-12813
EIGENVECTORS
Eigenvectors of graphs
[AD-A170562] N87-13223
EJECTA
X-ray emission from supernova remnants N87-13396
EJECTION
Radiographic determination of mass and inertial tensor of anatomical segments
[AD-A169122] N87-13126
EL NINO
On the Walker circulation of 1983-84
[INPE-3952-PRE/971] N87-13118
ELASTIC BODIES
Computation of the amplitude of stress singular terms for cracks and reentrant corners
[AD-A169796] N87-12936
ELASTIC CYLINDERS
Computation of residual stresses due to phase transformations during quenching of hollow cylinders
[AD-A170493] N87-12937
ELASTIC PROPERTIES
Quantitative non-destructive evaluation of composite materials based on ultrasonic wave propagation
[NASA-CR-179831] N87-12613
Micromechanisms of crack growth and fracture toughness in metal matrix composites
[AD-A169839] N87-12620
Factors influencing elastic stresses in double cantilever beam specimens
[NASA-TM-89033] N87-12922
Stress assisted diffusion in elastic and viscoelastic materials
[AD-A169296] N87-12932
Linear elastic fracture testing: Current status within ASTM committee E-24 on fracture
[AD-A169442] N87-12934
An expert-system-like feedback approach in the hp-version of the finite element method
[AD-A169855] N87-13214
ELASTOMERS
Ionic conductivity in solid, crosslinked dimethylsiloxane-ethylene oxide copolymer networks containing sodium
[AD-A169038] N87-12683
ELECTRIC ARCS
Population inversions in laser-initiated vacuum arcs
[AD-A170611] N87-12859
ELECTRIC BATTERIES
Zinc/air cell cathode
[AD-D012425] N87-12780
Sodium-sulfur battery systems development
[DE86-011424] N87-12788
Zinc/nickel oxide battery membrane separator studies
[DE86-012824] N87-12793
Feasibility study of a new zinc-air battery concept using flowing alkaline electrolyte
[DE86-013461] N87-12798
Li corrosion resistant glasses for headers in ambient temperature Li batteries
[DE86-013754] N87-12802
Development of regenerable energy storage for space multimegawatt applications
[DE86-011070] N87-12996
ELECTRIC CHARGE
Metrics of closed world of Friedmann, agitated by electric charge (towards a theory electromagnetic Friedmann's)
[AD-A168961] N87-12723
Calculated versus experimental charge density distribution of Be metal
[AD-A168924] N87-13254
FET charge sensor and voltage probe
[NASA-CASE-NPO-16045-1] N87-13313
ELECTRIC COILS
Measurement of time-dependent electric current with Rogowski coil
[INPE-3875-RPE/506] N87-12754
ELECTRIC CONDUCTORS
Development of a numerical procedure to treat wires attached to arbitrarily shaped conducting bodies
[AD-A169384] N87-12764
ELECTRIC CURRENT
A heater made from graphite composite material for potential deicing application
[NASA-TM-88888] N87-12559
Nuclear reaction analysis of hydrogen in metals
[AD-A169032] N87-12649
Measurement of time-dependent electric current with Rogowski coil
[INPE-3875-RPE/506] N87-12754
High frequency, high voltage MOSFET isolation amplifier
[AD-D012403] N87-12774
Transformers for explosive pulsed power coupling to various loads
[DE86-012425] N87-12796
Optical fiber sensors for the measurement of pulsed electric currents N87-13281
ELECTRIC DISCHARGES
Coordinated research program in pulsed power physics
[AD-A169113] N87-12762
Preliminary material testing of ceramic and wood
[AD-A169557] N87-12771
ELECTRIC FIELDS
Influence of a strong laser field on the stopping power for charged test particles in fusion plasmas
[INPE-3977-PRE/988] N87-12843
Theory and simulation of high-brightness electron beam production from laser-irradiated photocathodes in the presence of dc and RF electric fields
[DE86-012384] N87-12864
Solar control of geophysical phenomena N87-12953
The current-voltage relationship in auroral current sheets
[AD-A169074] N87-13028
Two-dimensional dynamics of the plasma Wakefield accelerator
[DE86-012382] N87-13312
Large-scale electric fields resulting from magnetic reconnection in the corona
[DE86-012391] N87-13383
ELECTRIC GENERATORS
Compact reactor/ORC power source
[DE86-011252] N87-13260
ELECTRIC MOTOR VEHICLES
Performance of advanced lead acid batteries for electric vehicles
[DE85-011476] N87-12801
ELECTRIC POTENTIAL
FET charge sensor and voltage probe
[NASA-CASE-NPO-16045-1] N87-13313
ELECTRIC PULSES
Nanosecond spark gap switching measurements
[DE86-012279] N87-12790
Optical fiber sensors for the measurement of pulsed electric currents N87-13281
ELECTRIC SWITCHES
Coordinated research program in pulsed power physics
[AD-A169113] N87-12762
Interrupt control switch interface system
[AD-D012414] N87-12776
ELECTRICAL ENGINEERING
Electronic Engineering Department Thrust Area report, FY 1985
[DE86-013172] N87-12797
ELECTRICAL IMPEDANCE
Electric and magnetic field coupling through a braided-shield cable: Transfer admittance and transfer impedance
[AD-A171490] N87-12748
Development of a numerical procedure to treat wires attached to arbitrarily shaped conducting bodies
[AD-A169384] N87-12764
Lithium Ambient-Temperature Battery Reliability Program, May 1983-April 1985
[DE86-012247] N87-12789
Quantum 1/F noise in solid state double devices, in particular Hg(1-x)CdxTe diodes
[AD-A171436] N87-13332
ELECTRICAL INSULATION
Preliminary material testing of ceramic and wood
[AD-A169557] N87-12771
ELECTRICAL MEASUREMENT
Measurement of time-dependent electric current with Rogowski coil
[INPE-3875-RPE/506] N87-12754
ELECTRICAL PROPERTIES
Ionic conductivity in solid, crosslinked dimethylsiloxane-ethylene oxide copolymer networks containing sodium
[AD-A169038] N87-12683
ELECTRICAL RESISTIVITY
Metallurgical characterization of the interfaces and the damping mechanisms in metal matrix composites
[AD-A169186] N87-12616
Finite mean-free-paths and the electrical resistivity of liquid simple metals and binary alloys
[DE86-702662] N87-12678
Physical characteristics of diblock polyacetylene copolymers: Processability-conductivity correlation
[DE86-011218] N87-12695
Effect of chain rigidity on conductivity of conjugated polymers
[DE86-011263] N87-12696
In-line determination of presence of liquid phase moisture in sealed IC packages
[AD-D012408] N87-12775
Possibility of using dc conductivity for investigating phase transition in amorphous semiconductors
[DE86-702648] N87-13340
ELECTRO-OPTICS
Picosecond optoelectronic diagnostics of field effect transistors
[AD-A170503] N87-12779
Direct writing of microstructures for solid-state electronics
[AD-A170637] N87-12783
High power semiconductor laser sources
[AD-A168900] N87-12844
Phase conjugate optics and picosecond optoelectronics
[AD-A169180] N87-13265
Optical processing
[AD-A169882] N87-13269
Method and apparatus for rapid optical phasing
[AD-D012412] N87-13270
Feasibility of making coherent fiber-optic arrays from fused silica
[AD-A170873] N87-13271
Optoelectronic broadband switching for communications and signal processing N87-13294
Picosecond nonlinear resonant interactions in semiconductors
[AD-A169992] N87-13327
Growth of ferro-electric tungsten bronze epitaxial thin films for electro-optic device applications
[AD-A170783] N87-13328
ELECTROCATALYSTS
A study of energy conversion devices using photoactive organometallic electrocatalysts
[AD-A169096] N87-12996
ELECTROCHEMICAL CORROSION
Ni-Co alloy plaque for cathode of Ni-Cd battery
[AD-D012375] N87-12769
ELECTROCHEMICAL OXIDATION
Carbon monoxide adsorption on a platinum electrode studied by polarization modulated FT-IR reflection-absorption spectroscopy. 2: CO adsorbed at a potential in the hydrogen region and its oxidation in acids
[AD-A169082] N87-12632
ELECTROCHEMISTRY
Electrochemistry in near-critical and supercritical fluids. 3: Studies of Br(-), I(-) and hydroquinone in aqueous solutions
[AD-A169138] N87-12633
Fluids in contact with a hard surface: University of the bridge functions for the density profile
[AD-A168945] N87-13308
ELECTRODELESS DISCHARGES
Very high efficacy electrodeless high intensity discharge lamps
[DE86-013760] N87-12803

ELECTRODES
Electrode/electrolyte interphase study using polarization modulated FT-IR reflection absorption spectroscopy
[AD-A169081] N87-12631
Electrochemistry in near-critical and supercritical fluids. 3: Studies of Br(-), I(-) and hydroquinone in aqueous solutions
[AD-A169138] N87-12633
Aircraft battery state of charge and charge control system
[AD-A169411] N87-12766
Feasibility study of a new zinc-air battery concept using flowing alkaline electrolyte
[DE86-013461] N87-12798
ELECTRODYNAMICS
High voltage characteristics of the electrodynamic tether and the generation of power and propulsion
[NASA-CR-178949] N87-12809
Coordinated radar and satellite studies of ionospheric currents in the auroral zone and polar cap
[AD-A169466] N87-13031
ELECTROENCEPHALOGRAPHY
The event related brain potential as an index of information processing and cognitive activity. A program of basic research. Supplement A: Neuromagnetic studies
[AD-A169978] N87-13144
ELECTROKINETICS
Electrokinetic properties of polymer colloids
[NASA-CR-178938] N87-12681
ELECTROLYSIS
Electrochemistry in near-critical and supercritical fluids. 3: Studies of Br(-), I(-) and hydroquinone in aqueous solutions
[AD-A169138] N87-12633
ELECTROLYTES
Electrode/electrolyte interphase study using polarization modulated FT-IR reflection absorption spectroscopy
[AD-A169081] N87-12631
Electrochemistry in near-critical and supercritical fluids. 3: Studies of Br(-), I(-) and hydroquinone in aqueous solutions
[AD-A169138] N87-12633
Electrokinetic properties of polymer colloids
[NASA-CR-178938] N87-12681
Zinc/air cell cathode
[AD-D012425] N87-12780
Feasibility study of a new zinc-air battery concept using flowing alkaline electrolyte
[DE86-013461] N87-12798
ELECTROMAGNETIC ABSORPTION
Model studies of solar spectral irradiance at the bottom and top of a cloudy atmosphere N87-13385
ELECTROMAGNETIC FIELDS
Physical interaction of 1-Hz to 100 kHz electric and magnetic fields with living organisms
[DE86-012323] N87-13139
ELECTROMAGNETIC INTERFERENCE
Optical fiber sensors for the measurement of pulsed electric currents N87-13281
ELECTROMAGNETIC NOISE
Regular noise background in VLF-radiation and world thunderstorm centers N87-12957
A study of methods of phase noise reduction of semiconductor lasers for sensor applications N87-13286
ELECTROMAGNETIC PROPERTIES
Potential applications of artificially structured materials for X-ray microanalysis
[DE86-010459] N87-12612
New electromagnetic effects associated with cavity-backed apertures
[DE86-008768] N87-12750
Microwave loss properties of hexagonal ferrites for millimeter wave applications
[AD-A168982] N87-13318
ELECTROMAGNETIC PULSES
Application of the AIPA (Approximate Iterative Preprocessing Algorithm) to F-106 data
[AD-A169084] N87-12569
Basic and applied research in the field of electronics and communications
[AD-A169029] N87-12727
ELECTROMAGNETIC RADIATION
Transmission through ferrite samples at submillimeter frequencies
[AD-A169178] N87-12731
Theory for computing the field scattered from a smooth inflected surface
[NASA-TP-2632] N87-13264
ELECTROMAGNETIC SCATTERING
Computer programs for electromagnetic scattering from a slotted TM cylindrical conductor by the pseudo-image method
[AD-A169016] N87-12725
Nonlinear interactions in the microwave sensing of oceanic internal waves
[AD-A169776] N87-13120
ELECTROMAGNETIC SHIELDING
Parametric linear variation of a leakage free permanent magnet field source
[AD-D012359] N87-13249
ELECTROMAGNETIC SPECTRA
Theoretical study on the correlation between wideband electromagnetic spectra and geological structures
[AD-A168971] N87-13026
ELECTROMAGNETIC WAVE TRANSMISSION
Method of ray intensity calculation as applied to anomalous propagation
[AD-A169553] N87-12737
Digest: Proceedings of the International Conference on Optical and Millimeter Wave Propagation and Scattering in the Atmosphere
[AD-A170393] N87-12743
ELECTROMAGNETISM
Proceedings of the Topical Meeting on the Microphysics of Surfaces, Beams and Adsorbates held in Santa Fe, New Mexico on 4-6 February 1985
[AD-A170797] N87-13329
ELECTROMAGNETS
Experimental verification of soliton theory using a microwave crossed-field amplifier
[AD-A170011] N87-12778
Temperature compensation in the 2:17 type magnet s
[AD-A169487] N87-13250
ELECTRON ACCELERATORS
FEL (Free Electron Laser) optics coating test program (design phase of sample introduction chamber)
[AD-A169474] N87-12849
Two-dimensional dynamics of the plasma Wakefield accelerator
[DE86-012382] N87-13312
ELECTRON BEAMS
Efficient, monochromatic, high-power microwave generator
[DE86-012385] N87-12792
Feasibility of investigating Smith-Purcell free-electron laser configurations by electron energy loss studies
[AD-A169059] N87-12847
High repetition rate electron beam RF-Acceleration and sub-millimeter wave generation via a free electron laser
[AD-A169646] N87-12853
Theory and simulation of high-brightness electron beam production from laser-irradiated photocathodes in the presence of dc and RF electric fields
[DE86-012384] N87-12864
Magnetospheric plasma studies using data from the dynamics explorer high and low altitude plasma instruments
[AD-A169010] N87-13027
ELECTRON DENSITY (CONCENTRATION)
Density and electrostatic potential distribution around a cylindrical satellite
[INPE-3953-NTE/258] N87-12595
Calculated versus experimental charge density distribution of Be metal
[AD-A168924] N87-13254
Spherical clusters of simple metals: Madelung energies and structure
[AD-A169560] N87-13323
ELECTRON DENSITY PROFILES
A semi-empirical low-latitude ionospheric model
[AD-A168899] N87-13025
ELECTRON DIFFRACTION
Electron diffraction analysis of the pentagonal arrangement of grains found in CVD pure Ni films
[DE86-009023] N87-13336
ELECTRON DISTRIBUTION
Calculated versus experimental charge density distribution of Be metal
[AD-A168924] N87-13254
Spherical clusters of simple metals: Madelung energies and structure
[AD-A169560] N87-13323
ELECTRON ENERGY
Feasibility of investigating Smith-Purcell free-electron laser configurations by electron energy loss studies
[AD-A169059] N87-12847
Observational study of ion-electron equilibration and of cloud evaporation in supernova remnants under the HEAO-2 guest investigator program
[NASA-CR-179922] N87-13365
ELECTRON FLUX DENSITY
The secondary production of gamma rays in the Jovian magnetosphere N87-13391
ELECTRON MICROSCOPY
Use of analytical electron microscopy in evaluating ferrite stability in austenitic stainless steel welds
[DE86-008537] N87-12667
Site occupations in Li sub 2 ordered alloys by axial electron channeling microanalysis
[DE86-009421] N87-12669
Localized ion milling of metallic and ceramic TEM specimens
[DE86-009538] N87-12900
ELECTRON OPTICS
FEL (Free Electron Laser) optics coating test program (design phase of sample introduction chamber)
[AD-A169474] N87-12849
ELECTRON OSCILLATIONS
High gain free electron laser oscillators
[AD-A169002] N87-12846
ELECTRON PARAMAGNETIC RESONANCE
Structural features at the Si-SiO2 interface
[DE86-012947] N87-13339
ELECTRON PROBES
Electron microprobe analysis: The upper limit of submicron spectroscopy
[DE86-009540] N87-12840
ELECTRON SPECTROSCOPY
Electron spectroscopy in fundamental catalytic studies
[DE86-008781] N87-12839
ELECTRON STATES
X-ray data booklet, revision
[DE86-012650] N87-13272
ELECTRON TRANSFER
Investigation of a new concept in semiconductor microwave oscillators
[AD-A170831] N87-12762
Heterogeneous catalysis with lasers
[AD-A169601] N87-12851
Study in molecular lasers
[AD-A169933] N87-12855
ELECTRON TUBES
Unique mechanization to fault isolate failures of an electron tube Radio Frequency (RF) amplifier and its high voltage power supply
[AD-D012378] N87-12770
ELECTRON TUNNELING
Theory of Fractional Quantum Hall Effect
[DE86-702652] N87-13343
Tunneling effect in superconductors with magnetic impurities
[DE86-702723] N87-13345
ELECTRON-ION RECOMBINATION
Ionization phenomena about the space shuttle
[AD-A170542] N87-13310
ELECTRONIC EQUIPMENT
Fault tolerance mechanisms for a network communication multiprocessor
[INPE-3958-PRE/876] N87-12720
Multi use gripper for industrial robot
[AD-D012371] N87-12876
ELECTRONIC EQUIPMENT TESTS
Totally self-checking circuits and testable CMOS circuits
[AD-A169756] N87-12773
Reliability study of retention and memory gate integrity in a 1K MNOS RAM
[DE86-010483] N87-13175
ELECTRONIC PACKAGING
The 1984 IR and D (Independent Research and Development) advanced packaging study
[AD-A169388] N87-12765
ELECTRONIC RECORDING SYSTEMS
Electronic forms. How close to value-added processing
[DE86-010484] N87-13354
ELECTRONS
Synthesis of conjugated polymers with alternating aromatic and quinonoid sequences via elimination on precursors
[AD-A171331] N87-12693
Electron-electron interaction effects in quasi-one-dimensional conducting polymers and related systems
[DE86-012434] N87-12697
X-ray data booklet, revision
[DE86-012650] N87-13272
ELECTROPHYSIOLOGY
The event related brain potential as an index of information processing and cognitive activity. A program of basic research. Supplement A: Neuromagnetic studies
[AD-A169978] N87-13144
ELECTROSTATIC CHARGE
Density and electrostatic potential distribution around a cylindrical satellite
[INPE-3953-NTE/258] N87-12595
ELECTROSTATIC PROBES
Flight model discharge system
[AD-A169423] N87-12571
ELECTROSTRICTION
SAW transduction in electrostrictive substrates
[DE86-011651] N87-12794

ELEVATION ANGLE
Two-dimensional beamforming using a frequency domain complex Least Mean-Squares (LMS) adaptive filter
[AD-A171396] N87-12785
ELLIPSES
Adaptive grid techniques for elliptic fluid-flow problems
[AD-A169471] N87-12814
ELLIPTIC DIFFERENTIAL EQUATIONS
Regularity of the solution of elliptic problems with piecewise analytic data. Part 1: Boundary value problems for linear elliptic equation of second order
[AD-A169771] N87-13212
Long time estimates for the heat kernel associated with a uniformly subelliptic symmetric second order operator
[AD-A169949] N87-13220
EMBRITTLEMENT
Embrittlement of a high and a low strength steel in liquid lead environment
[AD-A169443] N87-12653
APFIM study of antiphase and grain boundaries in Ni Al
[DE86-008494] N87-12662
EMERGENCIES
The Flight Service Station Training Program: 1981-1985
[AD-A171485] N87-13145
EMISSION SPECTRA
Characterization of the atomic emission in Inconel 718 alloy metal vapor arcs
[DE86-012178] N87-12672
Measurement of atmospheric emission spectra at high altitudes
[AD-A170143] N87-13035
Airborne atmospheric electricity experiments N87-13063
Medium- and long-wavelength infrared emission from a laser-produced oxygen plasma
[AD-A169475] N87-13309
Observational study of ion-electron equilibration and of cloud evaporation in supernova remnants under the HEAO-2 guest investigator program
[NASA-CR-179922] N87-13365
Plane-parallel and bow shock models of Herbig-Haro objects N87-13374
EMISSIVITY
Thermophysical properties measurements of gallium arsenide and cadmium telluride
[AD-A169901] N87-13326
EMULSIONS
Combustion and micro-explosion of water/oil emulsions in high pressure environments
[AD-A168976] N87-12627
END EFFECTORS
On the dexterity of robotic manipulators N87-12867
ENERGY ABSORPTION
Buffered explosions in steel pressure vessels
[DE86-008783] N87-12898
ENERGY BUDGETS
USSR report: Earth sciences
[JPRS-UES-86-007] N87-12948
Available potential energy in upper layer of world ocean N87-12949
Energy receipt partitioning over the Amazon forest
[INPE-3980-PRE/990] N87-12962
Study of satellite systems to monitor Earth's radiation budget
[CAP-420-071] N87-12994
ENERGY CONVERSION
Combustion and micro-explosion of water/oil emulsions in high pressure environments
[AD-A168976] N87-12627
Liquid metal thermoacoustic engine
[DE86-011264] N87-12902
Proceedings of the Solar Thermal Technology Conference
[DE86-011703] N87-13002
ENERGY CONVERSION EFFICIENCY
Status and future of government-supported amorphous silicon research in the US
[DE86-010702] N87-12997
Proof of feasibility of a novel inverter for photovoltaic power conditioning
[DE86-012729] N87-13001
Middle atmosphere modeling
[NASA-CR-179934] N87-13023
ENERGY DISSIPATION
Feasibility of investigating Smith-Purcell free-electron laser configurations by electron energy loss studies
[AD-A169059] N87-12847
Equilibrium configuration of coronal loops
[DE86-702711] N87-13384
ENERGY DISTRIBUTION
A partition of sensible and latent heat fluxes above the terra firma area in the Amazon forest
[INPE-3949-PRE/970] N87-13008
ENERGY LEVELS
Surface and adsorption-like states within the nearly free electron approximation
[DE86-702651] N87-13342
Theory of Fractional Quantum Hall Effect
[DE86-702652] N87-13343
ENERGY POLICY
Data tagging in the Energy Data Base
[DE86-010621] N87-13355
ENERGY STORAGE
Development of regenerable energy storage for space multimegawatt applications
[DE86-011070] N87-12998
ENERGY TRANSFER
Heterogeneous catalysis with lasers
[AD-A169601] N87-12851
Iodine monofluoride energy transfer studies
[AD-A169781] N87-12852
Experimental investigation of thermochemical transport for solar applications using sulfur trioxide
[DE86-011762] N87-13005
Donor-acceptor one step energy transfer via exchange coupling on a fractal lattice
[AD-A169643] N87-13325
Rapid fluctuations in solar flares
[NASA-CR-179894] N87-13387
ENGINE PARTS
Component improvement program task 83-01, 36E133 air turbine starter
[AD-A169483] N87-12562
Relationship of in-cylinder gaseous and particulate concentration to radiative heat transfer in direct injection-type diesel combustion
[AD-A168979] N87-12628
ENGINE STARTERS
Component improvement program task 83-01, 36E133 air turbine starter
[AD-A169483] N87-12562
ENGINES
Liquid metal thermoacoustic engine
[DE86-011264] N87-12902
ENRICHMENT
Status of laser enrichment technology updated N87-12717
ENUMERATION
An implicit enumeration procedure for the general linear complementarity problem
[AD-A170397] N87-13189
ENVIRONMENT EFFECTS
Evaluation of remote sensing techniques to the detection of changes in a fluvial system due to human influence: The example of Canas River Basin (Sao Paulo State, Brazil)
[INPE-3970-PRE/983] N87-12960
Direct effects of atmospheric CO2 enrichment on plants and ecosystems: A bibliography with abstracts
[DE86-013525] N87-13012
ENVIRONMENT MODELS
Surface correlation relationships in rough surface scattering
[AD-A169327] N87-12733
Conversion of the NOLAPS (Navy Operational Local Atmospheric Prediction System) model to the HP9845
[AD-A169538] N87-13108
ENVIRONMENTAL CONTROL
The ecology of microorganisms in a small closed system: Potential benefits and problems for space station
[NASA-TM-86563] N87-13166
ENVIRONMENTAL MONITORING
Effects of graphitization on the environmental stability of brominated pitch-based fibers
[NASA-TM-88899] N87-12679
ENVIRONMENTAL SURVEYS
International Conference/Workshop on Small Fatigue Cracks (2nd) held in Santa Barbara, California on 5-10 January 1986
[AD-A169060] N87-12929
ENVIRONMENTAL TESTS
Diamond-machined aluminum alloy 5083 surfaces: Controlled exposure evaluation
[DE86-012572] N87-12674
Evaluation of the multifunction sensor acceleration sensitive terms MU sub A and MU sub B
[AD-A169611] N87-12835
EPITAXY
Rapid synthesis of indium phosphide
[AD-D012362] N87-13322
Epitaxial crystallization and epitaxial polymerization as tools for molecular engineering
[AD-A171506] N87-13333
EPOXY RESINS
Stress effects on moisture transport in an epoxy resin and its composite
[AD-A169306] N87-12617
Investigation of the effects of cobalt ions on epoxy properties
[NASA-TP-2639] N87-12680
EQUATIONS OF MOTION
Introduction to aerodynamics derivatives, equations of motion and stability
[ESDU-86021] N87-12536
Simplified forms of performance equations. Addendum A: Effect on aeroplane level speed of small changes in thrust, drag, weight, power
[ESDU-86004-ADD-A] N87-12556
A mathematical formulation of a large space structure control problem
[AD-A169950] N87-12602
Dynamic analysis of anisotropic conical shells
[EPM/RT-86-36] N87-12916
Analysis of anisotropic thin conical shells
[EPM/RT-86-38] N87-12918
Dynamic analysis of a Timoshenko beam using a finite element approach
[EPM/RT-86-34] N87-12919
Free vibration of axisymmetric and beam-like cylindrical shells, partially filled with liquid
[EPM/RT-86-35] N87-12920
EQUATIONS OF STATE
Phase equilibrium predictions for polar and hydrogen bonding mixtures
[DE86-011812] N87-12642
Models and radiation of railgun plasma armatures with non-ideal plasma properties
[AD-A169349] N87-13258
EQUILIBRIUM EQUATIONS
Dynamic analysis of anisotropic conical shells
[EPM/RT-86-36] N87-12916
EQUIPARTITION THEOREM
A partition of sensible and latent heat fluxes above the terra firma area in the Amazon forest
[INPE-3949-PRE/970] N87-13008
EQUIPMENT SPECIFICATIONS
Circuit considerations for repetitive railguns
[DE86-012369] N87-12752
Development of an inexpensive, high resolution positron multiwire proportional counter
[DE86-011576] N87-12841
Double-ended tuning fork quartz accelerometer
[DE86-012277] N87-12842
EQUIVALENT CIRCUITS
The analysis of a transistor cap as a heat dissipator
[AD-A171398] N87-12786
ERGODIC PROCESS
Heredity of stationary and reversible stochastic processes
[AD-A169926] N87-13234
EROSION
Advanced electric propulsion MPD (magnetoplasmadynamic)
[AD-A169792] N87-12610
ERROR ANALYSIS
Comparative thermal conductivity measurements at Sandia National Laboratories
[DE86-012926] N87-12647
A procedure for automatic treatment of dynamic systems state observation bias errors
[INPE-3908-PRE/918] N87-13177
The optimal linear combination of control variates in the presence of bias
[AD-A169111] N87-13210
Asymptotically exact a-posteriori error estimator for biquadratic elements
[AD-A169798] N87-13213
The h-p version of the finite element method with quasiuniform meshes
[AD-A170144] N87-13222
ERROR DETECTION CODES
Totally self-checking circuits and testable CMOS circuits
[AD-A169756] N87-12773
ERRORS
Unique mechanization to fault isolate failures of an electron tube Radio Frequency (RF) amplifier and its high voltage power supply
[AD-D012376] N87-12770
Evaluation of the multifunction sensor acceleration sensitive terms MU sub A and MU sub B
[AD-A169811] N87-12835
Airborne spectroradiometry: The application of AIS data to detecting subtle mineral absorption features N87-12972
Availability and consistency of global information in computer networks
[AD-A169247] N87-13202
Quality assessment and control of finite element solutions
[NASA-TM-89208] N87-13227

ESOPHAGUS
Quantification of respiratory muscle performance
[AD-A169208] N87-13128

ESTIMATES
The measurement of the psychological workload during task-related activities, including car driving, by competing time interval estimation N87-13153
Asymptotically exact a-posteriori error estimator for biquadratic elements
[AD-A169798] N87-13213
Algorithm for positive definite least square estimation of parameters
[DE86-012159] N87-13225

ESTIMATING
An approximate method of estimating the aerodynamic interference between two parallel bodies in a supersonic flow (axial force)
[BR-100271] N87-12540
Asymptotic theory for sieve estimators in semimartingale regression models
[AD-A169207] N87-13230

ETCHING
New ultra low permittivity composites for use in ceramic packaging of Ga:As integrated circuits
[AD-A168877] N87-12758
Investigation of a new concept in semiconductor microwave oscillators
[AD-A170772] N87-12781
Fabrication of gate array interconnect structures using direct-write deposition processes
[DE86-010785] N87-12787
Plasma-enhanced deposition and processing of transition metals and transition metal silicides for VLSI
[AD-A168963] N87-13316
Kinetics and mechanisms on the molecular beam etching of semiconductors
[AD-A171360] N87-13331

ETHYLENE OXIDE
Ionic conductivity in solid, crosslinked dimethylsiloxane-ethylene oxide copolymer networks containing sodium
[AD-A169038] N87-12683

EULER EQUATIONS OF MOTION
Numerical simulation of tip vortices of wings in subsonic and transonic flows
[AD-A169116] N87-12544

EUROPE
Welding science and technology in Europe: A survey and assessment
[AD-A169279] N87-12873
Minutes of MAP/WINE experimenters meeting, Prague, Czechoslovakia, August 13, 1985 N87-13018
Station climatic summaries, Europe
[AD-A167888] N87-13100

EVALUATION
Evaluating ecosystem response to toxicant stress: a state space approach
[DE86-011777] N87-13009
Evaluation of man machine systems: Introduction and overview N87-13147
Ergonomic requirements for the design of control rooms. Evaluation method N87-13158
Basic conceptions for the evaluation of man machine systems N87-13161
A measure of usability — man machine systems N87-13163
Evaluation of the bearing and knowledge requirements of man machine systems N87-13164

EVAPOTRANSPIRATION
A partition of sensible and latent heat fluxes above the terra firma area in the Amazon Forest (gradient method)
[INPE-3972-PRE/985] N87-12964

EVOKED RESPONSE (PSYCHOPHYSIOLOGY)
Application of heart rate measurements to maritime research simulator
[AD-A169988] N87-13132

EXAMINATION
An examination of technology transfer as a tool for management
[AD-A169184] N87-13360

EXCHANGING
Donor-acceptor one step energy transfer via exchange coupling on a fractal lattice
[AD-A169843] N87-13325

EXCITATION
Reactor-pumped laser experiments in the Sandia SPR-3 Facility
[DE86-012163] N87-12861
Band description of materials with localizing orbitals
[DE86-010529] N87-13255
Picosecond nonlinear resonant interactions in semiconductors
[AD-A169992] N87-13327

EXCITONS
Picosecond nonlinear resonant interactions in semiconductors
[AD-A170813] N87-13330

EXHAUST NOZZLES
Thrust reverser-exhaust nozzle assembly for a gas turbine engine
[AD-D012390] N87-12561
Effects of test cell recirculation on high-bypass turbofan engines during simulated altitude tests
[AD-A171418] N87-12565

EXOBIOLOGY
Aerospace Medicine and Biology: A continuing bibliography with indexes
[NASA-SP-7011(290)] N87-13125

EXPANSION
New materials for spacecraft stability and damping: A feasibility study
[AD-A169826] N87-12601

EXPERT SYSTEMS
An application of a LISP based expert system for failure diagnosis of the CH-47 flight control hydraulic system
[AD-A168970] N87-12567
A prototype maintenance expert system for the CH-47 flight control hydraulic system
[AD-A169019] N87-12568
Knowledge-based pitch detection
[AD-A169069] N87-12730
An expert-system-like feedback approach in the hp-version of the finite element method
[AD-A169855] N87-13214
Application of a network associative scene analysis model
[INPE-3945-PRE/967] N87-13244

EXPLOSIONS
Buffered explosions in steel pressure vessels
[DE86-008763] N87-12898

EXPLOSIVES
Axial detonator for simultaneous ignition of multiple HE points
[DE86-011878] N87-12643
Preparation of energetic compounds
[AD-A170022] N87-12704
Modeling of high-explosive driven plasma compression opening switches
[DE86-012421] N87-12795
Transformers for explosive pulsed power coupling to various loads
[DE86-012425] N87-12796
Study of numerical solution methods for two-phase flows
[DE86-012265] N87-12821

EXPONENTIAL FUNCTIONS
Note on a characterization of exponential distributions
[AD-A169896] N87-13215

EXTERNAL SURFACE CURRENTS
Density and electrostatic potential distribution around a cylindrical satellite
[INPE-3953-NTE/258] N87-12595

EXTRAPOLATION
Computer-based estimation procedure for coaxial jet noise. Including far-field subsonic jet mixing noise database for stationary, coplanar conical nozzles
[ESDU-86019] N87-13251

EXTRAVEHICULAR ACTIVITY
Advanced EVA system design requirements study
[NASA-CR-171942] N87-13167

EXTREMUM VALUES
Extremal processes, record times and strong approximation
[AD-A169972] N87-13237

EYE MOVEMENTS
High-resolution analysis of eye movements
[AD-A170779] N87-13136
Eye movements as an index of mental workload
[AD-A169941] N87-13143
The eye-mark investigation as an anthropotechnical method to study man machine systems N87-13160

F

F REGION
Improving foF2 prediction for the sunrise transition period
[AD-A170457] N87-13036

F-4 AIRCRAFT
TSAR (Theater Simulation of Airbase Resources) database dictionary F-4E
[AD-A169575] N87-13352

F-106 AIRCRAFT
Application of the AIPA (Approximate Iterative Preprocessing Algorithm) to F-106 data
[AD-A169084] N87-12569

FABRICATION
The 1984 IR and D (Independent Research and Development) advanced packaging study
[AD-A169388] N87-12765
Fabrication of gate array interconnect structures using direct-write deposition processes
[DE86-010785] N87-12787
Method of fabricating high efficiency binary planar optical elements
[AD-D012374] N87-13268
Plasma-enhanced deposition and processing of transition metals and transition metal silicides for VLSI
[AD-A168963] N87-13316

FABRICS
Improved anti-G suit
[AD-D012378] N87-13171

FACTOR ANALYSIS
AIS spectra of desert shrub canopies N87-12987

FACTORIZATION
Matrix factorization on a hypercube multiprocessor
[DE86-011775] N87-13193
Maintaining LU factors of a general sparse matrix
[AD-A169255] N87-13248

FAILURE
Study of high temperature failure mechanisms in ceramics
[AD-A170001] N87-12689

FAILURE ANALYSIS
The control of polymer mechanical behavior by surface modification
[AD-A169252] N87-12686
Literature review on the design of composite mechanically fastened joints
[AD-A169112] N87-12872
Reliability prediction models for mechanical equipment
[AD-A169775] N87-12911
A finite element method for localized failure analysis
[AD-A169117] N87-12930
Availability and consistency of global information in computer networks
[AD-A169247] N87-13202

FAIRINGS
Length adjustable strut link with low aerodynamic drag
[AD-D012279] N87-12543

FAR INFRARED RADIATION
Medium- and long-wavelength infrared emission from a laser-produced oxygen plasma
[AD-A169475] N87-13309
Search for far infrared radiation from optically and acoustically pumped defect modes
[AD-A169159] N87-13319

FARADAY EFFECT
Optical fiber sensors for the measurement of pulsed electric currents N87-13281

FARM CROPS
Report on the activities of the irrigated crop survey in Sao Paulo State from remote sensing products, phase 2
[INPE-3950-RPE/513] N87-12989

FAST NUCLEAR REACTORS
Reactor-pumped laser experiments in the Sandia SPR-3 Facility
[DE86-012163] N87-12861

FASTENERS
Light socket removal tool
[AD-D012368] N87-12710
Literature review on the design of composite mechanically fastened joints
[AD-A169112] N87-12872
Super gripper variable vane arm
[AD-D012364] N87-12874

FATIGUE (BIOLOGY)
Crew factors in flight operations. Part 3: The operational significance of exposure to short-haul air transport operations
[NASA-TM-88322] N87-13122

FATIGUE (MATERIALS)
Embrittlement of a high and a low strength steel in liquid lead environment
[AD-A169443] N87-12653
Micromechanisms and toughness for cleavage fracture of steel
[AD-A169906] N87-12655
Fatigue behavior of long and short cracks in wrought and powder aluminum alloys
[AD-A169980] N87-12656
International Conference/Workshop on Small Fatigue Cracks (2nd) held in Santa Barbara, California on 5-10 January 1986
[AD-A169060] N87-12929

FATIGUE LIFE
Fatigue behavior of long and short cracks in wrought and powder aluminum alloys
[AD-A169980] N87-12656
Fundamental research on tribology
[AD-A169974] N87-12982

FATIGUE TESTS
Research on mechanical properties for engine life prediction
[AD-A169570] N87-12563
Linear elastic fracture testing: Current status within ASTM committee E-24 on fracture
[AD-A169442] N87-12934
FAULT TOLERANCE
Fault tolerance mechanisms for a network communication multiprocessor
[INPE-3958-PRE/876] N87-12720
Yield and performance enhancement through redundancy in VLSI and WSI multi-processor systems
[AD-A169930] N87-13174
FEASIBILITY ANALYSIS
New materials for spacecraft stability and damping: A feasibility study
[AD-A169826] N87-12601
Proof of feasibility of a novel inverter for photovoltaic power conditioning
[DE86-012729] N87-13001
FEDERAL BUDGETS
National Commission on Space report
[GPO-63-143] N87-12574
Department of Housing and Urban Development-independent agencies appropriations for 1987, part 7
[GPO-61-970] N87-13357
FEEDBACK
Unique mechanization to fault isolate failures of an electron tube Radio Frequency (RF) amplifier and its high voltage power supply
[AD-D012376] N87-12770
FEEDBACK CONTROL
Experimental investigation of thermochemical transport for solar applications using sulfur trioxide
[DE86-011762] N87-13005
Feedback system design with an uncertain plant
[NASA-CR-176887] N87-13243
Closed loop fiber optic gyro N87-13277
Wide bandwidth, long distance fibre-optic communication systems N87-13300
FERRITES
Use of analytical electron microscopy in evaluating ferrite stability in austenitic stainless steel welds
[DE86-008537] N87-12667
Transmission through ferrite samples at submillimeter frequencies
[AD-A169178] N87-12731
Microwave loss properties of hexagonal ferrites for millimeter wave applications
[AD-A168982] N87-13318
FERROELECTRICITY
Holographic storage in ion-implanted, ferroelectric-phase PLZT ceramics
[DE86-010475] N87-12837
Growth of ferro-electric tungsten bronze epitaxial thin films for electro-optic device applications
[AD-A170783] N87-13328
FIBER COMPOSITES
A heater made from graphite composite material for potential deicing application
[NASA-TM-88888] N87-12559
FIBER OPTICS
Carrier-sense stack algorithms for multiple access communication channels
[AD-A169774] N87-12738
High resolution optical fiber print head
[AD-D012384] N87-12833
Fiber-optic magnetic gradiometer with variable magnetic biasing fields
[AD-D012423] N87-12836
SPRINT 3: Serial-Parallel Remote Interface System development report
[DE86-010590] N87-13176
Feasibility of making coherent fiber-optic arrays from fused silica
[AD-A170873] N87-13271
Guided Optical Structures in the Military Environment
[AGARD-CP-383] N87-13273
Progress in optical fiber sensors N87-13274
Fibre optic gyroscopes in inertial navigation N87-13275
Comparison of ring laser and fiber-optic gyro technology N87-13276
Closed loop fiber optic gyro N87-13277
Progress with multiplexed sensor arrays based on reflection at spliced joints between sensors N87-13278
Magnetic and pressure sensors using the compensated polarimetric sensor configuration N87-13279
Fiber optic device for temperature remote sensing N87-13280
Optical fiber sensors for the measurement of pulsed electric currents N87-13281
Nonlinear ellipse rotation in a low-birefringence optical fiber N87-13282
Progress in optical fiber gyroscopes using integrated optics N87-13283
Wavelength division multiplexing at 1.5 microns for high capacity optical transmission N87-13284
A spherical waveguide multiplexer-demultiplexer N87-13285
A study of methods of phase noise reduction of semiconductor lasers for sensor applications N87-13286
Effects of optical feedback on the performance of high data rate single-mode fiber systems N87-13288
Performance of integrated optical frequency shifters pigtailed to high birefringence fibres using ion-milled grooves N87-13289
Nonlinear planar guided wave interactions and devices N87-13290
Optoelectronic broadband switching for communications and signal processing N87-13294
Preparation and properties of infrared transmitting heavy metal fluoride glass optical fibers N87-13296
Glass fibres for transmission in the 8-12 micrometers waveband N87-13297
Fluoride glasses for infrared waveguides N87-13299
Wide bandwidth, long distance fibre-optic communication systems N87-13300
Performance of RF fiber optic links N87-13301
Fiber optics: A survivable and cost-effective transmission medium for terrestrial networks N87-13302
Single-mode-fibers for fiberoptic-guided missiles: A comparison with graded-index multimode fibers N87-13303
Lightwave technology in future radar equipment designs N87-13304
Tactical fiber optic assembly requirements N87-13305
A hybrid transmission scheme on single mode fibers for tactical communications N87-13306
FIBER REINFORCED COMPOSITES
Coupled damage and moisture-transport in fiber-reinforced polymeric composites
[AD-A169379] N87-12619
FIELD EFFECT TRANSISTORS
Development of low-temperature transistor modules to improve the MSFC mid-infrared array
[NASA-TM-86566] N87-12756
High frequency, high voltage MOSFET isolation amplifier
[AD-D012403] N87-12774
Picosecond optoelectronic diagnostics of field effect transistors
[AD-A170503] N87-12779
PIN-FET preamplifier for high-speed optical transmission systems N87-13293
FET charge sensor and voltage probe
[NASA-CASE-NPO-16045-1] N87-13313
FIELD THEORY (PHYSICS)
Metrics of closed world of Friedmann, agitated by electric charge (towards a theory electromagnetic Friedmann's)
[AD-A168981] N87-12723
FIGHTER AIRCRAFT
TSAR (Theater Simulation of Airbase Resources) database dictionary F-4E
[AD-A169575] N87-13352
FILM COOLING
Further shock tunnel studies of scramjet phenomena
[NASA-CR-179937] N87-12542
FINITE DIFFERENCE THEORY
Finite-difference solutions for compressible laminar boundary-layer flows of a dusty gas over a semi-infinite flat plate
[UTIAS-311] N87-12807
Computational fluid dynamic studies of certain ducted bluff-body flowfields relevant to turbojet combustors. Volume 1: Time-dependent calculations with the k-epsilon turbulence model for an existing centerbody combustor
[AD-A171434] N87-12816
Application of flux-corrected transport (FCT) to high Rayleigh number natural convection in a porous medium
[DE86-004603] N87-12818
Study of numerical solution methods for two-phase flows
[DE86-012265] N87-12821
Feasibility study of test problems for finite element/finite difference programs for structural dynamics
[AD-A169058] N87-12928
Development of ultrasonic modelling techniques for the study of seismic wave scattering due to crustal inhomogeneities
[AD-A170017] N87-13034
FINITE ELEMENT METHOD
The 1984 IR and D (Independent Research and Development) advanced packaging study
[AD-A169388] N87-12765
Adaptive grid techniques for elliptic fluid-flow problems
[AD-A169471] N87-12814
A new and efficient formulation for finite element analysis of thin shell structures undergoing small and large deflection N87-12913
Dynamic analysis of anisotropic conical shells
[EPM/RT-86-36] N87-12916
Non-linear analysis of cylindrical shells
[EPM/RT-86-37] N87-12917
Dynamic analysis of a Timoshenko beam using a finite element approach
[EPM/RT-86-34] N87-12919
Free vibration of axisymmetric and beam-like cylindrical shells, partially filled with liquid
[EPM/RT-86-35] N87-12920
A constitutive law for finite element contact problems with unclassical friction
[NASA-TM-88838] N87-12924
Finite element analyses of shear localization in rate and temperature dependent solids
[AD-A169057] N87-12927
Feasibility study of test problems for finite element/finite difference programs for structural dynamics
[AD-A169058] N87-12928
A finite element method for localized failure analysis
[AD-A169117] N87-12930
MAGNA (Materially And Geometrically Nonlinear Analysis). Addendum 1, parts 1-4
[AD-A169363] N87-12933
Computation of the amplitude of stress singular terms for cracks and reentrant corners
[AD-A169796] N87-12936
Computation of residual stresses due to phase transformations during quenching of hollow cylinders
[AD-A170493] N87-12937
Some investigations into variable meshes for numerical solution of partial differential equations
[AD-A168977] N87-13206
Regularity of the solution of elliptic problems with piecewise analytic data. Part 1: Boundary value problems for linear elliptic equation of second order
[AD-A169771] N87-13212
Asymptotically exact a-posteriori error estimator for biquadratic elements
[AD-A169798] N87-13213
An expert-system-like feedback approach in the hp-version of the finite element method
[AD-A169855] N87-13214
The h-p version of the finite element method with quasiuniform meshes
[AD-A170144] N87-13222
Quality assessment and control of finite element solutions
[NASA-TM-89208] N87-13227
FINNED BODIES
Mach 6 experimental and theoretical stability and performance of a finned cylindrical body at angles of attack up to 65 deg
[NASA-TM-89050] N87-12538
FIXED WINGS
NASA rotor systems research aircraft: Fixed-wing configuration flight-test results
[NASA-TM-86789] N87-12557
FLANGES
Over-center toggle latch
[AD-D012393] N87-12878
FLAT PLATES
Finite-difference solutions for compressible laminar boundary-layer flows of a dusty gas over a semi-infinite flat plate
[UTIAS-311] N87-12807
FLIGHT CHARACTERISTICS
NASA rotor systems research aircraft: Fixed-wing configuration flight-test results
[NASA-TM-86789] N87-12557
FLIGHT CONTROL
Introduction to aerodynamics derivitives, equations of motion and stability
[ESDU-86021] N87-12536
An application of a LISP based expert system for failure diagnosis of the CH-47 flight control hydraulic system
[AD-A168970] N87-12567
A prototype maintenance expert system for the CH-47 flight control hydraulic system
[AD-A169019] N87-12568
Flight model discharge system
[AD-A169423] N87-12571
Simulator design features for helicopter landing on small ships. 1: A performance study
[AD-A169514] N87-12572
Fabrication and testing of lightweight hydraulic system simulator hardware
[AD-A169884] N87-12711
FLIGHT CREWS
Crew factors in flight operations. Part 3: The operational significance of exposure to short-haul air transport operations
[NASA-TM-88322] N87-13122

Crew communication as a factor in aviation accidents
[NASA-TM-88254] N87-13141
Determination of the load and stress of a cockpit crew during aircraft piloting using task networks and the simulation language SAINT N87-13150
Improved anti-G suit
[AD-D012378] N87-13171

FLIGHT OPTIMIZATION
Optimal descending, hypersonic turn to heading
[DE86-010989] N87-12577

FLIGHT SIMULATION
The handling qualities and flight characteristics of the Grumman design 698 simulated twin-engine tilt Nacelle V/STOL aircraft
[NASA-TM-86785] N87-12558
A test on the reliability and performance of the verbex series 4000 voice recognizer
[AD-A169066] N87-12729

FLIGHT SIMULATORS
Simulator design features for helicopter landing on small ships. 1: A performance study
[AD-A169514] N87-12572
Simulator design and instructional features for carrier landing: A field transfer study
[AD-A169962] N87-12573

FLIGHT STABILITY TESTS
The handling qualities and flight characteristics of the Grumman design 698 simulated twin-engine tilt Nacelle V/STOL aircraft
[NASA-TM-86785] N87-12558

FLIGHT TESTS
NASA rotor systems research aircraft: Fixed-wing configuration flight-test results
[NASA-TM-86789] N87-12557
Evaluation of a nonlinear parameter extraction mathematical model including the term C(subm(sub delta e squared))
[NASA-TM-87731] N87-12566

FLIGHT TRAINING
The Flight Service Station Training Program: 1981-1985
[AD-A171485] N87-13145

FLOW CHARACTERISTICS
Fluid transients in pipes. Estimation of maximum pressures and forces in steam lines
[ESDU-86015] N87-12805
Transition and mixing in axisymmetric jets and vortex rings
[NASA-CR-3893] N87-12808

FLOW DISTRIBUTION
Viscous-inviscid interaction in transonic separated flow over solid and porous airfoils and cascades N87-12535
Analysis and verification of the icing scaling equations. Volume 1: Revision
[AD-A167976] N87-12551
Effects of test cell recirculation on high-bypass turbofan engines during simulated altitude tests
[AD-A171418] N87-12565
Time-dependent solution for axisymmetric flow over a blunt body with ideal gas, CF4, or equilibrium air chemistry
[NASA-TM-87675] N87-12806
Computational fluid dynamic studies of certain ducted bluff-body flowfields relevant to turbojet combustors. Volume 1: Time-dependent calculations with the k-epsilon turbulence model for an existing centerbody combustor
[AD-A171434] N87-12816

FLOW EQUATIONS
Transition and mixing in axisymmetric jets and vortex rings
[NASA-CR-3893] N87-12808
Pressure calculation for two-dimensional flow inside hydraulic structures
[AD-A169039] N87-12812
Study of numerical solution methods for two-phase flows
[DE86-012265] N87-12821
Quantitative assessment of the effect of partial pivoting in sparse ordinary differential equation solvers
[DE86-012592] N87-13226

FLOW MEASUREMENT
Development of buried wire gages for measurement of wall shear stress in Blastane experiments
[NASA-TM-89212] N87-12831

FLOW THEORY
The calculation of separated flows of low-viscosity liquids using the Batchelor Model
[BR-100272] N87-12810

FLOW VELOCITY
Thrust reverser-exhaust nozzle assembly for a gas turbine engine
[AD-D012390] N87-12561
Characteristics of atmospheric turbulence near the ground. Part 3: Variations in space and time for strong winds (neutral atmosphere)
[ESDU-86010-PT-3] N87-13042

FLOW VISUALIZATION
Visualisation of axial turbine tip clearance flow using a linear cascade
[CUED/A-TURBO/TR-122] N87-12560

FLUID DYNAMICS
Characterization and dynamical studies of polymers in dipolar (aprotic) liquids
[AD-A169243] N87-12685

FLUID FILLED SHELLS
Theoretical and experimental studies in support of the geophysical fluid flow experiment N87-13045

FLUID FLOW
Adaptive grid techniques for elliptic fluid-flow problems
[AD-A169471] N87-12814
Theoretical and experimental studies in support of the geophysical fluid flow experiment N87-13045
Theoretical and experimental design studies for the Atmospheric General Circulation Experiment N87-13046
Progress of Stirling cycle analysis and loss mechanism characterization
[NASA-TM-88891] N87-13359

FLUID MECHANICS
Nonlinear waves
[AD-A168934] N87-13207

FLUID PRESSURE
Fluid transients in pipes. Estimation of maximum pressures and forces in steam lines
[ESDU-86015] N87-12805

FLUID-SOLID INTERACTIONS
Fluids in contact with a hard surface: University of the bridge functions for the density profile
[AD-A168945] N87-13308

FLUORESCENCE
X-ray data booklet, revision
[DE86-012650] N87-13272

FLUX DENSITY
Microstructural study of high energy density dissimilar metal welds
[DE86-009284] N87-12668

FLYWHEELS
Brief analysis of normal attitude accuracies of satellites with wheels or gas jets
[INPE-3993-NTE/262] N87-12594

FOG
A detailed analysis of the influence of eddy exchange processes upon the development of radiation fog
[AD-A169233] N87-13102

FOG DISPERSAL
Development testing of large volume water sprays for warm fog dispersal
[NASA-TP-2607] N87-12585

FOOTPRINTS
Vector analysis and satellite footprints
[AD-A169832] N87-12576

FORCED VIBRATION
Forced oscillation of a two-dimensional airfoil with nonlinear aerodynamic loads
[AD-A169350] N87-12546

FORECASTING
National Commission on Space report
[GPO-63-143] N87-12574

FOREST MANAGEMENT
Comparison of tropical forest surveys
[DE86-011699] N87-12993

FORESTS
A partition of sensible and latent heat fluxes above the terra firme area in the Amazon Forest (gradient method)
[INPE-3972-PRE/985] N87-12964
Destriping AIS data using Fourier filtering techniques N87-12974
Analysis of AIS data of the Bonanza Creek Experimental Forest, Alaska N87-12982
Soil types and forest canopy structures in southern Missouri: A first look with AIS data N87-12983
Characterization of information requirements for studies of CO2 effects: Water resources, agriculture, fisheries, forests and human health
[DE86-012477] N87-13010

FORGING
Linear elastic fracture testing: Current status within ASTM committee E-24 on fracture
[AD-A169442] N87-12934

FORMAT
A test on the reliability and performance of the verbex series 4000 voice recognizer
[AD-A169066] N87-12729

FORMING TECHNIQUES
Mechanics of metal forming
[DE86-012414] N87-12673

FORMULAS (MATHEMATICS)
Matrix theory
[AD-A169139] N87-13247

FORTRAN
Maintaining LU factors of a general sparse matrix
[AD-A169255] N87-13248

FOURIER ANALYSIS
Atmospheric Tides Middle Atmosphere Program (ATMAP): Report of the workshop, Kyoto, Japan, December 5-8, 1984 N87-13016

FOURIER SERIES
Computer programs for electromagnetic scattering from a slotted TM cylindrical conductor by the pseudo-image method
[AD-A169016] N87-12725
Analysis of anisotropic thin conical shells
[EPM/RT-86-38] N87-12918

FOURIER TRANSFORMATION
Electrode/electrolyte interphase study using polarization modulated FT-IR reflection absorption spectroscopy
[AD-A169081] N87-12631
Destriping AIS data using Fourier filtering techniques N87-12974

FOVEA
Limits of pattern discrimination in human vision
[AD-A170758] N87-13135

FRACTURE MECHANICS
Fracture toughness of CIP-HIP beryllium at elevated temperatures
[AD-A169769] N87-12654
Micromechanisms and toughness for cleavage fracture of steel
[AD-A169906] N87-12655
Effect of hydrogen on the mechanical properties and fracture behavior of high purity aluminum
[AD-A171214] N87-12658
Crack-tip chemistry and fracture mechanics-based model of the crack growth rate/stress intensity relationship for Ni + P
[DE86-011106] N87-12678
The control of polymer mechanical behavior by surface modification
[AD-A169252] N87-12686
Guide to the use of data items on the fatigue strength of welded joints in steels
[ESDU-86013] N87-12914
Analysis of mixed-mode crack propagation using the boundary integral method
[NASA-CR-179518] N87-12915
Computation of the amplitude of stress singular terms for cracks and reentrant corners
[AD-A169796] N87-12936
Influence of experimental scatter on the analysis and extrapolation of stress-rupture data
[DE86-009510] N87-12940
Using combined experiment/analysis to generate dynamic critical stress intensity data
[DE86-013578] N87-12945

FRACTURE STRENGTH
Micromechanisms of crack growth and fracture toughness in metal matrix composites
[AD-A169839] N87-12620
Fracture toughness of CIP-HIP beryllium at elevated temperatures
[AD-A169769] N87-12654
Guide to the use of data items on the fatigue strength of welded joints in steels
[ESDU-86013] N87-12914
Unloading-compliance and load-drop analysis of J(Ic) test of irradiated 348 stainless steel
[AD-A170494] N87-12938
Energetics of dislocation relaxation associated with cleavage in Cd-doped zinc crystals as probed by synchrotron topography
[DE86-002968] N87-13334

FRACTURES (MATERIALS)
A study of the mechanism of dynamic ductile fracture of two-phase materials
[AD-A169866] N87-12925

FRACTURING
Linear elastic fracture testing: Current status within ASTM committee E-24 on fracture
[AD-A169442] N87-12934
Fracture and viscoelastic characteristics of the human cervical spine
[AD-A170002] N87-13133

FRAGMENTATION
Fragmentation dynamics of energetic materials
[AD-A169925] N87-12682

FREE CONVECTION
Natural convection in an enclosure with discrete roughness elements on a vertical heated wall
[DE86-004424] N87-12617

FREE ELECTRON LASERS
Application of nonlinear optics to free electron laser systems
[AD-A169950] N87-12645
High gain free electron laser oscillators
[AD-A169002] N87-12646
Feasibility of investigating Smith-Purcell free-electron laser configurations by electron energy loss studies
[AD-A169059] N87-12647

FEL (Free Electron Laser) optics coating test program (design phase of sample introduction chamber)
[AD-A169474] N87-12849
High repetition rate electron beam RF-Acceleration and sub-millimeter wave generation via a free electron laser
[AD-A169646] N87-12853
High-gain free electron lasers as generators of short wavelength coherent radiation
[DE86-012500] N87-12865
FREE VIBRATION
Free vibration of axisymmetric and beam-like cylindrical shells, partially filled with liquid
[EPM/RT-86-35] N87-12920
FREEZING
Incremental quench research
[AD-A169980] N87-13317
FREQUENCY ANALYZERS
Acoustooptic spectrum analyzer using a planar Bragg-cell N87-13295
FREQUENCY DIVIDERS
Temperature and frequency compensated array beam steering unit
[AD-D012365] N87-12767
FREQUENCY MODULATION
Performance of RF fiber optic links N87-13301
FREQUENCY SHIFT
Doppler effect laser velocity measuring system
[AD-D012401] N87-12854
Performance of integrated optical frequency shifters pigtailed to high birefringence fibres using ion-milled grooves N87-13289
FRESNEL LENSES
Photovoltaic Concentrator Technology Project, Fourteenth Project Integration Meeting, June 10-11, 1986
[DE86-012051] N87-13006
FRICTION
Fundamental research on tribology
[AD-A169974] N87-12882
A constitutive law for finite element contact problems with unclassical friction
[NASA-TM-88838] N87-12924
FUEL CELLS
Development of regenerable energy storage for space multimegawatt applications
[DE86-011070] N87-12996
FUEL COMBUSTION
Combustion and micro-explosion of water/oil emulsions in high pressure environments
[AD-A169976] N87-12627
FUEL SYSTEMS
Relationship of in-cylinder gaseous and particulate concentration to radiative heat transfer in direct injection-type diesel combustion
[AD-A169979] N87-12628
FUNCTIONAL ANALYSIS
Statistical analysis and use of VAS radiance data N87-13086
FUNCTIONAL DESIGN SPECIFICATIONS
A method for the optimum design of the man machine interface N87-13159
Department of Defense gateway architecture and functional requirements
[AD-A169066] N87-13200
FUSES (ORDNANCE)
New ultra low permittivity composites for use in ceramic packaging of Ga:As integrated circuits
[AD-A168877] N87-12758
FUSION REACTORS
Application of hydrogen embrittlement models to the crack growth behavior of fusion reactor materials
[DE86-011614] N87-12671
Tara vacuum system
[DE86-011873] N87-13311

G

GALACTIC NUCLEI
On the two states of CYG X-1 and related sources
[NASA-TM-89265] N87-13367
Continuum radiation from active galactic nuclei: A statistical study
[NASA-CR-179925] N87-13368
GALAXIES
The space station millimeter facility
[AD-A169963] N87-12604
GALLIUM ARSENIDES
Basic and applied research in the field of electronics and communications
[AD-A169029] N87-12727
New ultra low permittivity composites for use in ceramic packaging of Ga:As integrated circuits
[AD-A168877] N87-12758
Picosecond optoelectronic diagnostics of field effect transistors
[AD-A170503] N87-12779
Thermophysical properties measurements of gallium arsenide and cadmium telluride
[AD-A169901] N87-13326
GAMMA RAY BURSTS
Stratospheric balloon experiments
[INPE-3995-RPE/519] N87-13020
GAMMA RAY LASERS
Moessbauer-Borrmann superradiance
[DE86-012373] N87-12866
GAMMA RAY SPECTROMETERS
MAX '91: An advanced payload for the exploration of high energy processes on the active sun
[NASA-TM-89271] N87-13379
The gamma-ray spectrometer experiment on the solar maximum mission satellite
[NASA-CR-177877] N87-13394
GAMMA RAYS
Contributions to the 18th International Cosmic Ray Conference
[ATR-86(9558)-11] N87-13389
The secondary production of gamma rays in the Jovian magnetosphere N87-13391
The gamma-ray spectrometer experiment on the solar maximum mission satellite
[NASA-CR-177877] N87-13394
Characterization of the gamma radiation in space and in the atmosphere
[DE86-013445] N87-13397
GAS DYNAMICS
Further shock tunnel studies of scramjet phenomena
[NASA-CR-179937] N87-12542
Models and radiation of railgun plasma armatures with non-ideal plasma properties
[AD-A169349] N87-13258
GAS EXCHANGE
Real-time experimental measurements of isotopic exchange between gaseous hydrogen and palladium hydride powder
[DE86-012610] N87-12644
GAS FLOW
Finite-difference solutions for compressible laminar boundary-layer flows of a dusty gas over a semi-infinite flat plate
[UTIAS-311] N87-12807
GAS IONIZATION
Ionization phenomena about the space shuttle
[AD-A170542] N87-13310
GAS JETS
Brief analysis of normal attitude accuracies of satellites with wheels or gas jets
[INPE-3993-NTE/262] N87-12594
GAS LASERS
Optical rotation sensors
[AD-A169357] N87-12848
Reactor-pumped laser experiments in the Sandia SPR-3 Facility
[DE86-012163] N87-12861
GAS TUNGSTEN ARC WELDING
Gas tungsten arc and shielded metal arc welding of carbon steel. Welding procedure specification. Supplement 1: Records of procedure qualification tests
[DE86-012533] N87-12890
Welding procedure specification. Supplement 1: Records of procedure qualification tests. Shielded metal arc welding of carbon steel
[DE86-012535] N87-12891
Welding procedure specification. Gas tungsten arc welding of chromium-nickel steel to chromium-molybdenum steel. Supplement 1: Records of procedure qualification tests
[DE86-012536] N87-12892
Gas tungsten arc welding of aluminum alloys 6XXX. Welding procedure specification. Supplement 1: Records of procedure qualification tests
[DE86-012548] N87-12893
Gas tungsten arc welding of carbon steel to nickel-chromium-iron. Welding procedure specification. Supplement 1: Records of procedure qualification tests
[DE86-012549] N87-12894
Gas tungsten arc welding of chromium-nickel steel to nickel-molybdenum-chromium-iron. Welding procedure specification. Supplement 1: Records of procedure qualification tests
[DE86-012550] N87-12895
Welding procedure specification: Gas tungsten arc welding of nickel to nickel-chromium-iron. Supplement 1: Records of procedure qualification tests
[DE86-012557] N87-12896
Gas tungsten arc welding of aluminum alloys 3004, 5052 and 5x54 to 8xxx. Welding procedure specification. Supplement 1: Records of procedure qualification tests
[DE86-012561] N87-12897
GAS TURBINE ENGINES
Thrust reverser-exhaust nozzle assembly for a gas turbine engine
[AD-D012390] N87-12561
GAS TURBINES
Research on mechanical properties for engine life prediction
[AD-A169570] N87-12563
Mechanical testing of a coated carbon-carbon composite at elevated temperatures in air
[AD-A169355] N87-12618
Production of a clean carbon fuel derived from coal for use in stationary and mobile heat engines
[DE86-011203] N87-12706
Self-locking outer air seal with full backside cooling
[AD-D012406] N87-12880
GAS WELDING
Welding procedure specification. Manual gas tungsten arc and semiautomatic gas metal arc welding of chromium-nickel steel. Supplement 1: Records of procedure qualification tests
[DE86-012521] N87-12886
Machine gas metal arc welding of carbon steel. Welding procedure specification. Supplement 1: Records of procedure qualification tests
[DE86-012530] N87-12887
Welding procedure specification. Semiautomatic gas metal arc welding of carbon steels. Supplement 1: Records of procedure qualification tests
[DE86-012531] N87-12888
Welding procedure specification. Manual gas tungsten arc and semiautomatic gas metal arc welding of carbon steel. Supplement 1: Records of procedure qualification tests
[DE86-012532] N87-12889
GAS-SOLID INTERACTIONS
Real-time experimental measurements of isotopic exchange between gaseous hydrogen and palladium hydride powder
[DE86-012610] N87-12644
GASES
Double-resonance techniques for high-resolution Raman-spectroscopy
[DE86-009640] N87-12645
Modeling of high-explosive driven plasma compression opening switches
[DE86-012421] N87-12795
Detonation cellular structure and image proces
[DE86-006467] N87-12819
GATES (CIRCUITS)
Basic and applied research in the field of electronics and communications
[AD-A169029] N87-12727
Declarative descriptions for VLSI generators
[AD-A169952] N87-12777
Fabrication of gate array interconnect structures using direct-write deposition processes
[DE86-010785] N87-12787
FET charge sensor and voltage probe
[NASA-CASE-NPO-16045-1] N87-13313
GAUGE THEORY
Theoretical high energy physics
[DE86-012669] N87-13259
GEOBOTANY
Proceedings of the Second Airborne Imaging Spectrometer Data Analysis Workshop
[NASA-CR-179924] N87-12968
Analysis of AIS radiometry with emphasis on determination of atmospheric properties and surface reflectance N87-12971
Geobotanical studies at Pilot Mountain, North Carolina using the airborne imaging spectrometer N87-12984
GEODYNAMICS
Observation model and parameter partials for the JPL VLBI parameter estimation software MASTERFIT-1986
[NASA-CR-179919] N87-13178
GEOLOGICAL SURVEYS
Geologic remote sensing at INPE: An overview
[INPE-3975-PRE/987] N87-12959
Relief and geology of the north polar region of the planet Venus
[NASA-TM-88498] N87-13376
GEOLOGY
Proceedings of the Second Airborne Imaging Spectrometer Data Analysis Workshop
[NASA-CR-179924] N87-12968
GEOMAGNETISM
Solar flux and geomagnetic activity prediction
[INPE-3884-PRE/934] N87-13377
GEOMETRIC RECTIFICATION (IMAGERY)
Modulation Transfer Function (MTF) of the geometrical image resolution of the thermal infrared band
[INPE-3964-TDL/231] N87-12809
GEOMETRY
Some tactical algorithms for spherical geometry
[AD-A170615] N87-12555

GEOPHYSICS
USSR report: Earth sciences
[JPRS-UES-86-007] N87-12946
Meteorological effects of geotectonic phenomena hypothesized N87-12947
Solar control of geophysical phenomena N87-12953
Earth sciences research in the Civil Space Program
[PB86-232014] N87-12995
NASA/MSFC FY-85 Atmospheric Processes Research Review
[NASA-CP-2402] N87-13043
Theoretical and experimental studies in support of the geophysical fluid flow experiment N87-13045

GEOSTROPHIC WIND
Utilization of satellite cloud information to diagnose the energy state and transformations in extratropical cyclones N87-13051
Observational and theoretical studies of the evolving structure of baroclinic waves: Attractor dynamics of global weather systems N87-13054

GEOSYNCHRONOUS ORBITS
Meter-level orbit determination of geosynchronous satellites by an economical tracking system N87-12575

GERMANIUM ALLOYS
Atomic resolution study of precipitates in an Al-Ge alloy
[DE86-011306] N87-12670

GLASS
Ionic conductivity in solid, crosslinked dimethylsiloxane-ethylene oxide copolymer networks containing sodium
[AD-A169038] N87-12683
Laser sealed vacuum insulating window
[DE86-013678] N87-12701
New ultra low permittivity composites for use in ceramic packaging of Ga:As integrated circuits
[AD-A168877] N87-12758
Li corrosion resistant glasses for headers in ambient temperature Li batteries
[DE86-013754] N87-12802

GLASS FIBERS
Glass fibres for transmission in the 8-12 micrometers waveband N87-13297
Single crystal fibers N87-13298
Fluoride glasses for infrared waveguides N87-13299

GLIDE PATHS
Guidance law simulation studies for complex approaches using the Microwave Landing System (MLS)
[NASA-CR-178182] N87-12552

GLOBAL POSITIONING SYSTEM
Medium-frequency data link for differential NAVSTAR/GPS broadcasts
[AD-A169788] N87-12554
Multi-element adaptive antenna array
[AD-D012410] N87-12740

GOALS
National Commission on Space report
[GPO-63-143] N87-12574

GOES SATELLITES
Intercomparison of DMSP OLS, NOAA AVHRR, GOES VISSR (Defense Meteorological Satellite Program Operational Linescan System, National Oceanographic and Atmospheric Administration Advanced Very High Resolution Radiometer, GOES Visible Infrared Spin-Scan Radiometer) and Landsat MSS imagery for cloud pr operty determination: Recommendations for digital data analysis
[AD-A169285] N87-12991
Estimation of precipitation from GOES IR imagery during FGGE: Application to diagnostic studies N87-13048
Studies of lightning data in conjunction with geostationary satellite data N87-13058
Automated mesoscale winds derived from GOES multispectral imagery N87-13073
Detection of rotating thunderstorms using satellite imagery N87-13085

GOVERNMENTS
Government libraries. A periodicals bibliography, together with list of bibliographies and indexes
[AD-A169422] N87-13351
The uncounted benefits: Federal efforts in domestic technology transfer
[NASA-CR-177044] N87-13358
Technology transfer at Pacific Northwest Laboratory
[DE86-012333] N87-13361

GRAIN BOUNDARIES
APFIM study of antiphase and grain boundaries in Ni Al
[DE86-008494] N87-12662
Radiation-induced segregation to grain boundaries in a Ni-Si alloy
[DE86-010027] N87-12664
Hot isostatic pressing of ceramic powder compacts
[AD-A169971] N87-12688
Study of high temperature failure mechanisms in ceramics
[AD-A170001] N87-12689
Experimental thin film deposition and surface analysis techniques
[DE86-011222] N87-13338

GRAIN SIZE
Electron diffraction analysis of the pentagonal arrangement of grains found in CVD pure Ni films
[DE86-009023] N87-13336

GRAMMARS
A test on the reliability and performance of the verbex series 4000 voice recognizer
[AD-A169066] N87-12729

GRAPHITE
Densification of graphites by irradiation
[DE86-010026] N87-12698

GRAPHITE-EPOXY COMPOSITES
A heater made from graphite composite material for potential deicing application
[NASA-TM-88888] N87-12559

GRAPHITIZATION
Effects of graphitization on the environmental stability of brominated pitch-based fibers
[NASA-TM-88899] N87-12679

GRAPHS (CHARTS)
Eigenvectors of graphs
[AD-A170582] N87-13223

GRATINGS (SPECTRA)
Method of fabricating high efficiency binary planar optical elements
[AD-D012374] N87-13266

GRAVIMETRY
High accuracy standards and reference methodology for carbon dioxide in air
[DE86-012643] N87-13011
Balloon-borne, high altitude gravimetry: The flight of DUCKY 1a (11 October 1983)
[AD-A169942] N87-13033

GRAVITATION
Balloon-borne, high altitude gravimetry: The flight of DUCKY 1a (11 October 1983)
[AD-A169942] N87-13033
Canonical quantization of gravity
[DE86-702615] N87-13372

GRAVITATIONAL WAVES
Observations on the Stanford 4800 KG gravity wave detector with a cosmic ray monitor N87-13399

GRAVITY GRADIOMETERS
Development of a sensitive superconducting gravity gradiometer for geological and navigational applications
[NASA-CR-4011] N87-13021

GRAVITY WAVES
Middle atmosphere modeling
[NASA-CR-179934] N87-13023

GREEN'S FUNCTIONS
Surface green function matching for a three-dimensional non-local continuum
[DE86-702647] N87-13341

GROUND STATIONS
SARSAT (Search and Rescue Satellite) operational data categorization and accuracy studies
[AD-A169748] N87-12599

GROUND SUPPORT EQUIPMENT
Instrumentation research and support services
[AD-A169278] N87-13029

GROUND WIND
Sensitivity tests of a surface-layer windflow model to effects of stability and vegetation
[AD-A169136] N87-13101
Wheeler AFB, Hawaii Limited Surface Observations Climatic Summary (LISOCS), parts 1-5
[AD-A169391] N87-13107
Calibration and accuracy of the NOAA/ERL gust probe system and intercomparison with other systems
[PB86-221736] N87-13116

GROUP THEORY
Upper bounds for symmetric Markov transition functions
[AD-A170010] N87-13221
A unified approach to constructing nonparametric rank tests
[AD-A169815] N87-13233
Two issues concerning the analysis of grouped data
[DE86-008401] N87-13242

GROWTH
Comparison of Rayleigh-Taylor growth with 1.0 m and 0.25 m lasers
[DE86-012217] N87-12662

GUIDANCE (MOTION)
Advanced guidance algorithms for homing missiles with bearing-only measurements
[AD-A170833] N87-12583

GULF STREAM
The Gulf Stream dynamics experiment. Inverted echo sounder data report for the June 1984 to May 1985 deployment period
[AD-A170758] N87-13121

GUST LOADS
Blast gust loading on a 35 degree swept-back wing
[AD-A169415] N87-12570

GUSTS
Calibration and accuracy of the NOAA/ERL gust probe system and intercomparison with other systems
[PB86-221736] N87-13116

GYROSCOPES
The effect of coupling in an inertial navigation platform stabilized system made up of three single-degree-of-freedom gyroscopes
[AD-A169110] N87-12563

GYROSCOPIC STABILITY
Evaluation of the Collins/Rockwell two axis gyro/accelerometer sensor cluster (phase 3 unit)
[AD-A169810] N87-12834
Evaluation of the multifunction sensor acceleration sensitive terms MU sub A and MU sub B
[AD-A169811] N87-12835

H

HALL EFFECT
Theory of Fractional Quantum Hall Effect
[DE86-702652] N87-13343

HARDENING (MATERIALS)
An analysis of shear band development incorporating heat conduction
[AD-A168972] N87-12926

HARDNESS
Fluids in contact with a hard surface: University of the bridge functions for the density profile
[AD-A168945] N87-13308

HARMONIC ANALYSIS
Linear harmonic analysis of free-piston Stirling engines
[DE86-012451] N87-12903

HARMONICS
Cruise noise of counterrotation propeller at angle of attack in wind tunnel
[NASA-TM-88860] N87-13252

HAWAII
Wheeler AFB, Hawaii Limited Surface Observations Climatic Summary (LISOCS), parts 1-5
[AD-A169391] N87-13107

HAZE
Studies of humid continental haze during SPACE N87-13088

HEAD (ANATOMY)
Guidelines for safe human experimental exposure to impact acceleration
[AD-A169347] N87-13169

HEART RATE
Application of heart rate measurements to maritime research simulator
[AD-A169968] N87-13132
Self-paced heat acclimation procedures
[AD-A170533] N87-13134

HEAT ACCLIMATIZATION
Self-paced heat acclimation procedures
[AD-A170533] N87-13134

HEAT BUDGET
Study of satellite systems to monitor Earth's radiation budget
[CAP-420-071] N87-12994

HEAT EXCHANGERS
Phase change thermal energy storage methods for combat vehicles, phase 1
[AD-A170492] N87-12713
Analysis of magnetic refrigeration systems with staged regenerators based on an idealized magnetic material entropy model: 1
[DE86-013638] N87-12714

HEAT FLUX
Comparison of methods for the calculation of thermal contact resistance of the first Brazilian satellite
[INPE-3864-TDL/217] N87-12598
Application of flux-corrected transport (FCT) to high Rayleigh number natural convection in a porous medium
[DE86-004603] N87-12818
Diesel cylinder gas-side heat flux to a ceramic surface
[AD-A168948] N87-12870
A partition of sensible and latent heat fluxes above the terra firma area in the Amazon Forest (gradient method)
[INPE-3972-PRE/985] N87-12964

HEAT MEASUREMENT
Lithium Ambient-Temperature Battery Reliability Program, May 1983-April 1985
[DE86-012247] N87-12789

HEAT OF COMBUSTION
Diesel cylinder gas-side heat flux to a ceramic surface
[AD-A166948] N87-12670
HEAT PIPES
Integrated heat pipe-thermal storage design for a solar receiver
[DE86-011235] N87-12999
Compact reactor/ORC power source
[DE86-011252] N87-13260
Neutronic design studies for an unattended, low power reactor
[DE86-011228] N87-13262
HEAT PUMPS
Dual temperature thermal storage with complex compounds
[DE86-011511] N87-13000
HEAT RESISTANT ALLOYS
The influence of welding flux on the pyrometallurgical, physical and mechanical behavior of weld metal
[AD-A169067] N87-12650
HEAT SINKS
The analysis of a transistor cap as a heat dissipator
[AD-A171398] N87-12786
HEAT STORAGE
Phase change thermal energy storage methods for combat vehicles, phase 1
[AD-A170492] N87-12713
Integrated heat pipe-thermal storage design for a solar receiver
[DE86-011235] N87-12999
Dual temperature thermal storage with complex compounds
[DE86-011511] N87-13000
Stefan-type problem with void formation and its explicit solution
[DE86-013521] N87-13007
HEAT TOLERANCE
Self-paced heat acclimation procedures
[AD-A170533] N87-13134
HEAT TRANSFER
Further shock tunnel studies of scramjet phenomena
[NASA-CR-179937] N87-12542
Visualisation of axial turbine tip clearance flow using a linear cascade
[CUED/A-TURBO/TR-122] N87-12560
Analysis of magnetic refrigeration systems with staged regenerators based on an idealized magnetic material entropy model: 1
[DE86-013638] N87-12714
The analysis of a transistor cap as a heat dissipator
[AD-A171398] N87-12786
Application of flux-corrected transport (FCT) to high Rayleigh number natural convection in a porous medium
[DE86-004603] N87-12818
Apparatus for downward transport of heat
[DE86-013700] N87-12824
Periodic heat transfer through an inhomogeneous medium
[DE86-702966] N87-12825
Analysis of laminar flow heat transfer in uniform temperature circular tubes with tape inserts
[PB86-224763] N87-12826
Diesel cylinder gas-side heat flux to a ceramic surface
[AD-A166948] N87-12670
Heat measurements in inertia welding of aluminum to steel
[DE86-012463] N87-12685
Integrated heat pipe-thermal storage design for a solar receiver
[DE86-011235] N87-12999
MIZEX: A program for mesoscale air-ice-ocean interaction experiments in arctic marginal ice zones. 8: A science plan for a winter marginal ice zone experiment in the Fram Strait/Greenland Sea, 1987/89
[AD-A169070] N87-13119
Progress of Stirling cycle analysis and loss mechanism characterization
[NASA-TM-88901] N87-13359
HEAT TRANSFER COEFFICIENTS
Heat transfer characteristics of simulated microelectronic chips under normal and enhanced conditions
[PB86-224425] N87-12804
HEATERS
A heater made from graphite composite material for potential deicing application
[NASA-TM-88868] N87-12559
Incremental quench research
[AD-A168980] N87-13317
HEATING
Heat measurements in inertia welding of aluminum to steel
[DE86-012463] N87-12685
HEAVY IONS
Resonant photon pumping mechanisms for a plasma X-ray laser
[AD-D012416] N87-12857
HEAVY NUCLEI
The ultraheavy cosmic rays: Propagation and selective acceleration N87-13390
HELICOPTER CONTROL
Obstacle-warning radar for helicopters N87-13149
HELICOPTER DESIGN
Anthropometric handicaps in the construction of a helicopter cockpit — seats N87-13148
HELICOPTERS
Simulator design features for helicopter landing on small ships. 1: A performance study
[AD-A169514] N87-12572
The siting, installation and operational suitability of the Automated Weather Observing System (AWOS) at heliports
[DOT/FAA/PM-86/30] N87-13099
HELIOSTATS
Proceedings of the Solar Thermal Technology Conference
[DE86-011703] N87-13002
HELIPORTS
The siting, installation and operational suitability of the Automated Weather Observing System (AWOS) at heliports
[DOT/FAA/PM-86/30] N87-13099
HERBIG-HARO OBJECTS
Plane-parallel and bow shock models of Herbig-Haro objects N87-13374
HETEROJUNCTION DEVICES
Millimeter-wave heterojunction two-terminal devices
[AD-A168985] N87-12760
HETEROJUNCTIONS
Millimeter-wave heterojunction two-terminal devices
[AD-A168985] N87-12760
In-situ interdiffusion measurements in HgTe-CdTe superlattices
[DE86-011429] N87-13337
HEURISTIC METHODS
An implicit enumeration procedure for the general linear complementarity problem
[AD-A170397] N87-13189
SOAR user's manual
[AD-A169005] N87-13204
HIGH ACCELERATION
The effects of high sustained acceleration on the acoustic phonetic structure of speech: A preliminary investigation
[AD-A170563] N87-12746
Rapid acting electro-pneumatic anti-G suit control valve
[AD-D012377] N87-13170
HIGH ALTITUDE BALLOONS
Balloon-borne, high altitude gravimetry: The flight of DUCKY 1a (11 October 1983)
[AD-A169942] N87-13033
HIGH ENERGY INTERACTIONS
Duel between an ASAT (anti-satellite) with multiple kill vehicles and a space-based weapons platform with kinetic energy weapons
[AD-A168946] N87-13245
Theoretical high energy physics
[DE86-012669] N87-13259
Astro-particle-physics
[DE86-702946] N87-13373
The gamma-ray spectrometer experiment on the solar maximum mission satellite
[NASA-CR-177877] N87-13394
HIGH ENERGY PROPELLANTS
Preparation of energetic compounds
[AD-A170022] N87-12704
HIGH GAIN
High-gain free electron lasers as generators of short wavelength coherent radiation
[DE86-012500] N87-12865
HIGH LEVEL LANGUAGES
Catalog of Resources for Education in Ada (Trade name) and Software Engineering (CREASE), version 4.0
[AD-A169892] N87-13186
Proceedings of the IDA Workshop on Formal Specification and Verification of Ada (trade name) (1st) held in Alexandria, Virginia on 18-20 March 1985
[AD-A171507] N87-13192
Survey of the characteristics of very high level languages
[DE86-012240] N87-13196
HIGH POWER LASERS
High power semiconductor laser sources
[AD-A168900] N87-12844
Optical pumping of high power lasers with an array of plasma pinches
[AD-A169960] N87-12856
HIGH PRESSURE
Combustion and micro-explosion of water/oil emulsions in high pressure environments
[AD-A168976] N87-12627
Shower and high-pressure oil temperature control
[DE86-009396] N87-12899
HIGH RESOLUTION
Pulsed-laser, high speed photography of rocket propellant surface deflagration
[AD-A169308] N87-12703
HIGH SPEED PHOTOGRAPHY
Pulsed-laser, high speed photography of rocket propellant surface deflagration
[AD-A169308] N87-12703
HIGH STRENGTH STEELS
Embrittlement of a high and a low strength steel in liquid lead environment
[AD-A169443] N87-12653
Micromechanisms and toughness for cleavage fracture of steel
[AD-A169906] N87-12655
HIGH TEMPERATURE
Stability of multilayers at high temperatures
[DE86-010526] N87-12623
Anvil detonator: A 300EC-stable, hot-wire-ignited, nonprimary-explosive device
[DE86-013635] N87-12707
On 3-D inelastic analysis methods for hot section components (base program)
[NASA-CR-175060] N87-12923
Compact reactor/ORC power source
[DE86-011252] N87-13260
HIGH TEMPERATURE FLUIDS
Electrochemistry in near-critical and supercritical fluids. 3: Studies of Br(-), I(-) and hydroquinone in aqueous solutions
[AD-A169138] N87-12633
HIGH TEMPERATURE PLASMAS
CO sub 2 laser sustained CW discharge atomic beam source
[DE86-012383] N87-12663
HIGH VOLTAGES
Unique mechanization to fault isolate failures of an electron tube Radio Frequency (RF) amplifier and its high voltage power supply
[AD-D012376] N87-12770
Preliminary material testing of ceramic and wood
[AD-A169557] N87-12771
HILBERT SPACE
Upper bounds for symmetric Markov transition functions
[AD-A170010] N87-13221
HIPPOCAMPUS
The event related brain potential as an index of information processing and cognitive activity. A program of basic research. Supplement A: Neuromagnetic studies
[AD-A169978] N87-13144
HOLDERS
Multi use gripper for industrial robot
[AD-D012371] N87-12876
HOLOGRAPHY
Holographic storage in ion-implanted, ferroelectric-phase PLZT ceramics
[DE86-010475] N87-12837
Development of a large-aperture PLZT shutter with enhanced operational/environmental capabilities
[DE86-011643] N87-12838
HOMING
Advanced guidance algorithms for homing missiles with bearing-only measurements
[AD-A170833] N87-12583
HOMODYNE RECEPTION
Optical quadrature demodulator for coherent detection and sensor applications N87-13287
HOMOGENEITY
The influence of welding flux on the pyrometallurgical, physical and mechanical behavior of weld metal
[AD-A169067] N87-12650
HOMOTOPY THEORY
HOMPACK: A suite of codes for globally convergent homotopy algorithms
[DE86-011644] N87-13196
HOT ISOSTATIC PRESSING
Hot isostatic pressing of ceramic powder compacts
[AD-A169971] N87-12685
HOUSINGS
TDD antenna: Foil formed, substrate loaded laser welded assembly
[AD-D012411] N87-12712
HUBBLE SPACE TELESCOPE
Space infrared telescope facility wide field and diffraction limited array camera (IRAC)
[NASA-CR-177041] N87-13362

HUMAN BEHAVIOR
Evaluation of remote sensing techniques to the detection of changes in a fluvial system due to human influence: The example of Canas River Basin (Sao Paulo State, Brazil)
[INPE-3970-PRE/983] N87-12960
Application of heart rate measurements to maritime research simulator
[AD-A169988] N87-13132
HUMAN BEINGS
Analysis of head and neck dynamic response of the US adult military population
[AD-A169563] N87-13129
Guidelines for safe human experimental exposure to impact acceleration
[AD-A169347] N87-13169
HUMAN BODY
Radiographic determination of mass and inertial tensor of anatomical segments
[AD-A169122] N87-13126
Physical interaction of 1-Hz to 100 kHz electric and magnetic fields with living organisms
[DE86-012323] N87-13139
Concept study - vehicle waste disposal system
[AD-A169045] N87-13168
Guidelines for safe human experimental exposure to impact acceleration
[AD-A169347] N87-13169
HUMAN FACTORS ENGINEERING
Crew communication as a factor in aviation accidents
[NASA-TM-88254] N87-13141
Proceedings of a Symposium on the Evaluation of Man-Machine Systems: Methods and Problems
[DGLR-85-04] N87-13146
Evaluation of man machine systems: Introduction and overview N87-13147
System-ergonomic workload analysis for highly automated process control tasks N87-13152
Investigation of vibrations of the spinal column of healthy subjects N87-13155
Review of the methods applied in the Federal Republic of Germany to investigate human factors in nuclear power plant control N87-13156
Ergonomic requirements for the design of control rooms. Evaluation method N87-13158
A method for the optimum design of the man machine interface N87-13159
Inquiry techniques for the evaluation of man machine systems N87-13162
A measure of usability — man machine systems N87-13163
Advanced EVA system design requirements study
[NASA-CR-171942] N87-13167
Proceedings of the conference on the design of experiments in army research development and testing (31st) held at the Madison, Wisconsin on 23-25 October 1986
[AD-A169473] N87-13246
HUMAN PERFORMANCE
Quantification of respiratory muscle performance
[AD-A169208] N87-13128
Human performance aspects of small screen displays: A literature review revealing the lack of specific research
[AD-A170660] N87-13172
HUMAN REACTIONS
Application of heart rate measurements to maritime research simulator
[AD-A169988] N87-13132
HUMIDITY
Diamond-machined aluminum alloy 5083 surfaces: Controlled exposure evaluation
[DE86-012572] N87-12674
Studies of humid continental haze during SPACE N87-13088
HURRICANES
Third International Symposium on Tropical Meteorology N87-12948
Variation objective analyses for cyclone studies N87-13050
Utilization of satellite cloud information to diagnose the energy state and transformations in extratropical cyclones N87-13051
Dynamics and energetics of the South Pacific Convergence Zone during FGGE SOP-1 N87-13052
Deep convection in mesoscale convective systems N87-13055
Storm severity detection (RF) N87-13057
Summary of 1986 Atlantic tropical cyclone activity and verification of author's seasonal forecast N87-13097
HYDRAULIC EQUIPMENT
Pressure calculation for two-dimensional flow inside hydraulic structures
[AD-A169039] N87-12812
Shock absorbing device with integral pressure relief valve
[AD-D012379] N87-12877
Reliability prediction models for mechanical equipment
[AD-A169775] N87-12911
HYDRAULIC SHOCK
Multiple rate shock isolator damping valve
[AD-D012394] N87-12879
HYDRIDES
Real-time experimental measurements of isotopic exchange between gaseous hydrogen and palladium hydride powder
[DE86-012610] N87-12644
HYDROCARBONS
Investigation of deviations from ideality in the two liquid phase region of systems of medium molecular weight hydrocarbon mixtures and water
[AD-A169752] N87-12635
HYDRODYNAMIC EQUATIONS
Nonlinear waves
[AD-A168934] N87-13207
HYDRODYNAMICS
Characterization and dynamical studies of polymers in dipolar (aprotic) liquids
[AD-A169243] N87-12685
Free-Lagrangian hydrodynamics using massless tracer points
[DE86-012406] N87-12822
Theory of developed hydrodynamical turbulence
[DE86-012796] N87-12823
HYDROGEN
Real-time experimental measurements of isotopic exchange between gaseous hydrogen and palladium hydride powder
[DE86-012610] N87-12644
Raman spectroscopic investigation of molecular hydrogen
[DE86-012836] N87-12648
Nuclear reaction analysis of hydrogen in metals
[AD-A169032] N87-12649
HYDROGEN BONDS
Phase equilibrium predictions for polar and hydrogen bonding mixtures
[DE86-011812] N87-12642
HYDROGEN EMBRITTLEMENT
Effect of hydrogen on the mechanical properties and fracture behavior of high purity aluminum
[AD-A171214] N87-12658
Application of hydrogen embrittlement models to the crack growth behavior of fusion reactor materials
[DE86-011614] N87-12671
HYDROGEN FUELS
Production of a clean carbon fuel derived from coal for use in stationary and mobile heat engines
[DE86-011203] N87-12706
HYDROGEN IONS
Polarized H(-) source development at BNL
[DE86-012704] N87-13257
HYDROLOGY
Generalization of one-dimensional solute transport: A stochastic-convective flow conceptualization
[DE86-011117] N87-12820
Report of the Ad-Hoc Commission on remote sensing
[INPE-3981-NTE/259] N87-12963
HYDROPHONES
Progress with multiplexed sensor arrays based on reflection at spliced joints between sensors N87-13278
HYDROSTATICS
Variation objective analyses for cyclone studies N87-13050
HYPERBOLIC DIFFERENTIAL EQUATIONS
Study of numerical solution methods for two-phase flows
[DE86-012265] N87-12821
HYPERFINE STRUCTURE
Structural features at the Si-SiO2 interface
[DE86-012947] N87-13339
HYPERSONIC FLIGHT
Optimal descending, hypersonic turn to heading
[DE86-010989] N87-12577
HYPERSPACES
Matrix factorization on a hypercube multiprocessor
[DE86-011775] N87-13193
HYPERVELOCITY GUNS
Models and radiation of railgun plasma armatures with non-ideal plasma properties
[AD-A169349] N87-13258
HYPERVELOCITY PROJECTILES
Simple defense conservative model for mass requirements of hypervelocity projectile impact shields for reentry vehicles
[DE86-012407] N87-12603
HYPERVENTILATION
Quantification of respiratory muscle performance
[AD-A169208] N87-13128
HYPOTHERMIA
Hypothermic effects on vascular contractility and reactivity
[AD-A169142] N87-13127

I

ICE
Analysis and verification of the icing scaling equations. Volume 1: Revision
[AD-A167976] N87-12551
First meeting of the Working Group on the Shuttle Microwave Precipitation Radiometer (SMPR) N87-13096
ICE ENVIRONMENTS
MIZEX: A program for mesoscale air-ice-ocean interaction experiments in arctic marginal ice zones. 8: A science plan for a winter marginal ice zone experiment in the Fram Strait/Greenland Sea, 1987/89
[AD-A169070] N87-13119
ICE FORMATION
Analysis and verification of the icing scaling equations. Volume 1: Revision
[AD-A167976] N87-12551
IFF SYSTEMS (IDENTIFICATION)
Simulation of CIFF (Centralized IFF) remote control displays
[AD-A170387] N87-12742
IGNITION
Axial detonator for simultaneous ignition of multiple HE points
[DE86-011878] N87-12643
Anvil detonator: A 300EC-stable, hot-wire-ignited, nonprimary-explosive device
[DE86-013635] N87-12707
IGNITION LIMITS
Combustion and micro-explosion of water/oil emulsions in high pressure environments
[AD-A168976] N87-12627
IMAGE ANALYSIS
Knowledge-based pitch detection
[AD-A169069] N87-12730
Generation of images with recorded auxiliary data for the LANDSAT Thematic Mapper (TM) imagery
[INPE-3982-TDL/234] N87-12990
Multispectral atmospheric mapping sensor of mesoscale water vapor features N87-13095
Application of a network associative scene analysis model
[INPE-3945-PRE/967] N87-13244
IMAGE ENHANCEMENT
Image enhancement equipment capabilities
[DE86-013615] N87-12800
IMAGE PROCESSING
A VLSI-based high-performance raster image system
[AD-A169068] N87-12781
Very low bandwidth, unattended imager for surveillance applications
[DE86-013570] N87-12799
Detonation cellular structure and image proces
[DE86-006467] N87-12819
Integrating computer vision with a robot arm system
[AD-A171278] N87-12884
Automated mesoscale winds derived from GOES multispectral imagery N87-13073
Statistical models and methods for cluster analysis and image segmentation
[AD-A169145] N87-13229
IMAGE RECONSTRUCTION
A new method of synthetic aperture radar image reconstruction using modified convolution back-projection algorithm
[AD-A170652] N87-12747
IMAGES
A rule-based pattern matching system for the recognition of three-dimensional line drawn objects: A foundation for video tracking
[AD-A170701] N87-13190
IMAGING SPECTROMETERS
Radiometric calibration of the airborne imaging spectrometer N87-12969
Comparison of various techniques for calibration of AIS data N87-12970
Analysis of AIS radiometry with emphasis on determination of atmospheric properties and surface reflectance N87-12971
Airborne spectroradiometry: The application of AIS data to detecting subtle mineral absorption features N87-12972
Destriping AIS data using Fourier filtering techniques N87-12974
Abundance and distribution of mineral components associated with Moses Rock (kimberlite) diatreme N87-12975
Comparison of the 1984 and 1985 AIS data over the Singatse Range (Yerington), Nevada N87-12976
Identification of hydrothermal alteration assemblages using airborne imaging spectrometer data N87-12977

Detection of hydrothermal alteration at Virginia City, Nevada using Airborne Imaging Spectrometry (AIS) N87-12978

Preliminary geological investigation of AIS data at Mary Kathleen, Queensland, Australia N87-12979

Use of digital Munsell color space to assist interretation of imaging spectrometer data: Geologic examples from the northern Grapevine Mountains, California and Nevada N87-12980

Near-Infrared detection of ammonium minerals at Ivanhoe Hot Springs, Nevada N87-12981

Analysis of AIS data of the Bonanza Creek Experimental Forest, Alaska N87-12982

Soil types and forest canopy structures in southern Missouri: A first look with AIS data N87-12983

Geobotanical studies at Pilot Mountain, North Carolina using the airborne imaging spectrometer N87-12984

Trace element-induced stress in freshwater wetland vegetation: Preliminary results N87-12985

Patterns of vegetation in the Owens Valley, California N87-12986

AIS spectra of desert shrub canopies N87-12987

IMAGING TECHNIQUES

Digest: Proceedings of the International Conference on Optical and Millimeter Wave Propagation and Scattering in the Atmosphere
[AD-A170393] N87-12743

The Multispectral Atmospheric Mapping Sensor (MAMS): Instrument description, calibration and data quality
[NASA-TM-86565] N87-12828

Proceedings of the Second Airborne Imaging Spectrometer Data Analysis Workshop
[NASA-CR-179924] N87-12968

Comparison of various techniques for calibration of AIS data N87-12970

Airborne spectroradiometry: The application of AIS data to detecting subtle mineral absorption features N87-12972

Atmospheric-water absorption features near 2.2 micrometers and their importance in high spectral resolution remote sensing N87-12973

Destriping AIS data using Fourier filtering techniques N87-12974

Use of digital Munsell color space to assist interretation of imaging spectrometer data: Geologic examples from the northern Grapevine Mountains, California and Nevada N87-12980

IMPACT

Remote sensing to detect ecological impacts associated with acid deposition
[DE86-011649] N87-12992

IMPACT ACCELERATION

Analysis of head and neck dynamic response of the US adult military population
[AD-A169563] N87-13129

Guidelines for safe human experimental exposure to impact acceleration
[AD-A169347] N87-13169

IMPACT TESTS

Guidelines for safe human experimental exposure to impact acceleration
[AD-A169347] N87-13169

Space nuclear safety program
[DE86-012767] N87-13261

IMPEDANCE MATCHING

Input impedance of an infinite linear scanned array of flat rectangular strips inside a dielectric loaded parallel plate waveguide
[AD-A171275] N87-12784

IMPEDANCE MEASUREMENT

Lithium Ambient-Temperature Battery Reliability Program, May 1983-April 1985
[DE86-012247] N87-12789

IMPURITIES

Effects of inertia weld parameters and contamination on weld flash shape and on joint strength: An improved study
[DE86-013074] N87-12904

Tunneling effect in superconductors with magnetic impurities
[DE86-702723] N87-13345

INCOHERENT SCATTER RADAR

Coordinated radar and satellite studies of ionospheric currents in the auroral zone and polar cap
[AD-A169466] N87-13031

INCONEL (TRADEMARK)

Comparative thermal conductivity measurements at Sandia National Laboratories
[DE86-012926] N87-12647

Characterization of the atomic emission in Inconel 718 alloy metal vapor arcs
[DE86-012178] N87-12672

INDEXES (DOCUMENTATION)

Government libraries. A periodicals bibliography, together with list of bibliographies and indexes
[AD-A169422] N87-13351

INDIUM PHOSPHIDES

Rapid synthesis of indium phosphide
[AD-D012362] N87-13322

INDUCTION MOTORS

Constructive and operational characteristics of a synchronous induction motor
[INPE-3976-RPE/517] N87-12755

INDUSTRIAL MANAGEMENT

Quality management: An annotated bibliography
[AD-A169816] N87-12912

INELASTIC STRESS

On 3-D inelastic analysis methods for hot section components (base program)
[NASA-CR-175060] N87-12923

INEQUALITIES

Inequalities for probability contents of convex sets via geometric average
[AD-A169938] N87-13219

INERTIA

Radiographic determination of mass and inertial tensor of anatomical segments
[AD-A169122] N87-13126

INERTIAL NAVIGATION

The effect of coupling in an inertial navigation platform stabilized system made up of three single-degree-of-freedom gyroscopes
[AD-A169110] N87-12553

Fibre optic gyroscopes in inertial navigation N87-13275

Comparison of ring laser and fiber-optic gyro technology N87-13276

INERTIAL PLATFORMS

Evaluation of the Collins/Rockwell two axis gyro/accelerometer sensor cluster (phase 3 unit)
[AD-A169810] N87-12834

Evaluation of the multifunction sensor acceleration sensitive terms MU sub A and MU sub B
[AD-A169811] N87-12835

INERTIAL UPPER STAGE

Upper stage selected for planetary missions
[NASA-NEWS-RELEASE-86-161] N87-12593

INFLATABLE STRUCTURES

Improved anti-G suit
[AD-D012378] N87-13171

INFORMATION DISSEMINATION

The uncounted benefits: Federal efforts in domestic technology transfer
[NASA-CR-177044] N87-13358

INFORMATION RETRIEVAL

Improving numerical weather prediction by maximizing the use of assimilated satellite data
[AD-A169295] N87-13104

INFORMATION SYSTEMS

Space flight operations communications phraseology and techniques
[NASA-TM-86562] N87-12721

Federal information systems management: Problems, solutions and more problems
[AD-A171366] N87-13353

INFORMATION TRANSFER

Survey of the characteristics of very high level languages
[DE86-012240] N87-13198

INFRARED ABSORPTION

Preparation and properties of infrared transmitting heavy metal fluoride glass optical fibers N87-13296

Single crystal fibers N87-13298

Fluoride glasses for infrared waveguides N87-13299

INFRARED ASTRONOMY

Infrared reflection nebulae in Orion molecular cloud 2
[NASA-TM-88253] N87-13363

INFRARED DETECTORS

Development of low-temperature transistor modules to improve the MSFC mid-infrared array
[NASA-TM-86566] N87-12756

Modulation Transfer Function (MTF) of the geometrical image resolution of the thermal infrared band
[INPE-3964-TDL/231] N87-12809

Description of data on the Nimbus 7 LIMS map archive tape: Ozone and nitric acid
[NASA-TP-2625] N87-13022

Multispectral atmospheric mapping sensor of mesoscale water vapor features N87-13095

INFRARED IMAGERY

Modulation Transfer Function (MTF) of the geometrical image resolution of the thermal infrared band
[INPE-3964-TDL/231] N87-12809

Intercomparison of DMSP OLS, NOAA AVHRR, GOES VISSR (Defense Meteorological Satellite Program Operational Linescan System, National Oceanographic and Atmospheric Administration Advanced Very High Resolution Radiometer, GOES Visible Infrared Spin-Scan Radiometer) and Landsat MSS imagery for cloud pr operty determination: Recommendations for digital data analysis
[AD-A169285] N87-12991

Remote sensing of severe convective storms N87-13075

INFRARED LASERS

Search for far infrared radiation from optically and acoustically pumped defect modes
[AD-A169159] N87-13319

INFRARED PHOTOGRAPHY

Intercomparison of DMSP OLS, NOAA AVHRR, GOES VISSR (Defense Meteorological Satellite Program Operational Linescan System, National Oceanographic and Atmospheric Administration Advanced Very High Resolution Radiometer, GOES Visible Infrared Spin-Scan Radiometer) and Landsat MSS imagery for cloud pr operty determination: Recommendations for digital data analysis
[AD-A169285] N87-12991

Space infrared telescope facility wide field and diffraction limited array camera (IRAC)
[NASA-CR-177041] N87-13362

INFRARED RADIATION

Intercomparison of DMSP OLS, NOAA AVHRR, GOES VISSR (Defense Meteorological Satellite Program Operational Linescan System, National Oceanographic and Atmospheric Administration Advanced Very High Resolution Radiometer, GOES Visible Infrared Spin-Scan Radiometer) and Landsat MSS imagery for cloud pr operty determination: Recommendations for digital data analysis
[AD-A169285] N87-12991

Estimation of precipitation from GOES IR imagery during FGGE: Application to diagnostic studies N87-13048

Phase conjugate optics and picosecond optoelectronics
[AD-A169180] N87-13265

Medium- and long-wavelength infrared emission from a laser-produced oxygen plasma
[AD-A169475] N87-13309

INFRARED SCANNERS

The Multispectral Atmospheric Mapping Sensor (MAMS): Instrument description, calibration and data quality
[NASA-TM-86565] N87-12828

INFRARED SPECTRA

Measurement of atmospheric emission spectra at high altitudes
[AD-A170143] N87-13035

INFRARED SPECTROSCOPY

Electrode/electrolyte interphase study using polarization modulated FT-IR reflection absorption spectroscopy
[AD-A169081] N87-12631

INFRARED TRACKING

Eye movements as an index of mental workload
[AD-A169941] N87-13143

INJECTION LASERS

High power semiconductor laser sources
[AD-A168900] N87-12844

INJURIES

Guidelines for safe human experimental exposure to impact acceleration
[AD-A169347] N87-13169

INORGANIC CHEMISTRY

A study of energy conversion devices using photoactive organometallic electrocatalysts
[AD-A169096] N87-12996

INSERTION

Review of robotic component insertion system for printed wiring assemblies
[DE86-013510] N87-12907

INSERTION LOSS

Microwave loss properties of hexagonal ferrites for millimeter wave applications
[AD-A168982] N87-13318

INSERTS

Analysis of laminar flow heat transfer in uniform temperature circular tubes with tape inserts
[PB86-224763] N87-12826

Improved anti-G suit
[AD-D012378] N87-13171

INSOLATION

Studies of humid continental haze during SPACE N87-13068

INSPECTION

Image enhancement equipment capabilities
[DE86-013615] N87-12800

Concurrent ultrasonic weld evaluation system
[DE86-013772] N87-12908

INSTRUMENT LANDING SYSTEMS
Aircraft accident/incident summary reports: Erie, Pennsylvania, October 14, 1984; Albuquerque, New Mexico, February 11, 1985
[PB86-910407] N87-12549
INTAKE SYSTEMS
Journal of engineering thermophysics (selected articles)
[AD-A169452] N87-13347
INTEGRATED CIRCUITS
Phased arrays 1985 symposium: Proceedings
[AD-A169316] N87-12732
New ultra low permittivity composites for use in ceramic packaging of Ga:As integrated circuits
[AD-A168877] N87-12758
A VLSI-based high-performance raster image system
[AD-A169068] N87-12761
The Department of Defense Very High Speed Integrated Circuit (VHSIC) Technology Availability Program plan for the Committees on Armed Services, United States Congress
[AD-A169250] N87-12763
The 1984 IR and D (Independent Research and Development) advanced packaging study
[AD-A169388] N87-12765
Compaction with automatic jog introduction
[AD-A169679] N87-12772
Totally self-checking circuits and testable CMOS circuits
[AD-A169756] N87-12773
In-line determination of presence of liquid phase moisture in sealed IC packages
[AD-D012408] N87-12775
Image enhancement equipment capabilities
[DE86-013615] N87-12800
Progress in optical fiber gyroscopes using integrated optics N87-13283
Plasma-enhanced deposition and processing of transition metals and transition metal silicides for VLSI
[AD-A168963] N87-13316
INTEGRATED OPTICS
Optical processing
[AD-A169882] N87-13289
Progress in optical fiber gyroscopes using integrated optics N87-13283
Performance of integrated optical frequency shifters pigtailed to high birefringence fibres using ion-milled grooves N87-13289
Nonlinear planar guided wave interactions and devices N87-13290
Integrated optics optical limiters N87-13292
Acoustooptic spectrum analyzer using a planar Bragg-cell N87-13295
INTEGRATORS
Measurement of time-dependent electric current with Rogowski coil
[INPE-3875-RPE/506] N87-12754
INTERACTIONAL AERODYNAMICS
Propeller/body interaction for thrust and drag
[ESDU-86017] N87-12537
INTERATOMIC FORCES
Molecular dynamic studies of crack propagation. The role of the interatomic potential
[DE86-009942] N87-12942
INTERFACES
Metallurgical characterization of the interfaces and the damping mechanisms in metal matrix composites
[AD-A169186] N87-12616
Importance of interfacial phenomena in separation science and technology
[DE86-011063] N87-12637
INTERFACIAL TENSION
An interdisciplinary approach to predictive modeling of structural adhesive bonding. Characterization of Ti-6Al-4V oxides and the adhesive/oxide interphase
[AD-A170484] N87-12690
Fluids in contact with a hard surface: University of the bridge functions for the density profile
[AD-A168945] N87-13308
INTERFEROMETERS
Basic and applied research in the field of electronics and communications
[AD-A169029] N87-12727
Storm severity detection (RF) N87-13057
INTERIOR BALLISTICS
Circuit considerations for repetitive railguns
[DE86-012369] N87-12752
INTERMETALLICS
APFIM study of antiphase and grain boundaries in Ni Al
[DE86-006494] N87-12662
Microchemical analysis of polycrystalline Ni3Al and other ordered alloys using the field-ion microscope atom probe
[DE86-013157] N87-12677
INTERMODULATION
Rusty bolt intermodulation interference reducer
[AD-D012417] N87-12691
INTERNAL COMBUSTION ENGINES
Combustion and micro-explosion of water/oil emulsions in high pressure environments
[AD-A168976] N87-12627
Production of a clean carbon fuel derived from coal for use in stationary and mobile heat engines
[DE86-011203] N87-12706
INTERNAL WAVES
Nonlinear interactions in the microwave sensing of oceanic internal waves
[AD-A169776] N87-13120
INTERNATIONAL COOPERATION
Welding science and technology in Europe: A survey and assessment
[AD-A169279] N87-12873
INTERPLANETARY MAGNETIC FIELDS
A study of the relationship between solar activity and interplanetary field variations
[AD-A169963] N87-13380
INTERPOLATION
Solving systems of nonlinear equations by tensor methods
[AD-A169927] N87-13216
Computer-based estimation procedure for coaxial jet noise. Including far-field subsonic jet mixing noise database for stationary, coplanar conical nozzles
[ESDU-86019] N87-13251
Further results on interpolation searching of databases
[DE86-012822] N87-13356
INTERPROCESSOR COMMUNICATION
Advanced teleprocessing systems
[AD-A170007] N87-12741
Availability and consistency of global information in computer networks
[AD-A169247] N87-13202
INTERSTELLAR CHEMISTRY
The carbon twelve to carbon thirteen isotope ratio of the interstellar medium in the neighborhood of the sun N87-13386
INTERSTELLAR MATTER
The carbon twelve to carbon thirteen isotope ratio of the interstellar medium in the neighborhood of the sun N87-13386
INVERSE SCATTERING
Signal estimation, scattering theory and interpolation problems in one and two dimensions
[AD-A168969] N87-12759
INVERTED CONVERTERS (DC TO AC)
Proof of feasibility of a novel inverter for photovoltaic power conditioning
[DE86-012729] N87-13001
INVESTIGATION
Investigation of the effects of cobalt ions on epoxy properties
[NASA-TP-2639] N87-12680
INVESTMENTS
An implicit enumeration algorithm with binary-valued constraints
[AD-A169256] N87-13182
INVISCID FLOW
Viscous-inviscid interaction in transonic separated flow over solid and porous airfoils and cascades N87-12535
Time-dependent solution for axisymmetric flow over a blunt body with ideal gas, CF4, or equilibrium air chemistry
[NASA-TM-87675] N87-12806
The calculation of separated flows of low-viscosity liquids using the Batchelor Model
[BR-100272] N87-12810
IODINE
Electrochemistry in near-critical and supercritical fluids. 3: Studies of Br(-), I(-) and hydroquinone in aqueous solutions
[AD-A169138] N87-12633
IODINE COMPOUNDS
Iodine monofluoride energy transfer studies
[AD-A169781] N87-12852
ION BEAMS
Localized ion milling of metallic and ceramic TEM specimens
[DE86-009538] N87-12900
Kinetics and mechanisms on the molecular beam etching of semiconductors
[AD-A171360] N87-13331
Recrystallization behavior of ion beam modified Alpha-Al sub 2 O sub 3
[DE86-009353] N87-13335
ION CURRENTS
Ionic conductivity in solid, crosslinked dimethylsiloxane-ethylene oxide copolymer networks containing sodium
[AD-A169038] N87-12683
ION DENSITY (CONCENTRATION)
Collection of ions in the stratosphere
[AD-A169905] N87-13032
ION EMISSION
Influence of a strong laser field on the stopping power for charged test particles in fusion plasmas
[INPE-3977-PRE/988] N87-12843
ION EXCHANGE MEMBRANE ELECTROLYTES
Zinc/nickel oxide battery membrane separator studies
[DE86-012824] N87-12793
ION IMPLANTATION
Investigation of a new concept in semiconductor microwave oscillators
[AD-A170772] N87-12781
Holographic storage in ion-implanted, ferroelectric-phase PLZT ceramics
[DE86-010475] N87-12837
Recrystallization behavior of ion beam modified Alpha-Al sub 2 O sub 3
[DE86-009353] N87-13335
ION INJECTION
Magnetospheric plasma studies using data from the dynamics explorer high and low altitude plasma instruments
[AD-A169010] N87-13027
ION IRRADIATION
Advanced electric propulsion MPD (magnetoplasmadynamic)
[AD-A169792] N87-12810
ION MICROSCOPES
APFIM studies of phase transformations
[DE86-006533] N87-12663
Microchemical analysis of polycrystalline Ni3Al and other ordered alloys using the field-ion microscope atom probe
[DE86-013157] N87-12677
ION SOURCES
Polarized H(-) source development at BNL
[DE86-012704] N87-13257
IONIZATION
Application of pattern recognition to metal ion chemical ionization mass spectra
[AD-A169061] N87-12630
Double-resonance techniques for high-resolution Raman-spectroscopy
[DE86-009640] N87-12645
IONOSPHERIC CURRENTS
Coordinated radar and satellite studies of ionospheric currents in the auroral zone and polar cap
[AD-A169466] N87-13031
IONOSPHERIC DISTURBANCES
Effect of pulsating auroras on frequency-time characteristics of radio signals reflected from auroral ionosphere N87-12954
IONOSPHERIC ELECTRON DENSITY
A semi-empirical low-latitude ionospheric model
[AD-A168899] N87-13025
IONOSPHERIC PROPAGATION
Phase fluctuations of ionosphere radio signals N87-12955
Transverse resonances of Earth-ionosphere wave guide in auroral region N87-12956
Improving foF2 prediction for the sunrise transition period
[AD-A170457] N87-13036
IONOSPHERIC SOUNDING
Spatial radio wave attenuation during vertical sounding of ionosphere N87-12958
IONS
Investigation of the effects of cobalt ions on epoxy properties
[NASA-TP-2639] N87-12680
Space plasma research
[NASA-CR-178965] N87-13307
IRON ALLOYS
A fundamental study of P/M processed elevated temperature aluminum alloys
[AD-A170697] N87-12657
IRRADIANCE
Moessbauer-Borrmann superradiance
[DE86-012373] N87-12666
Model studies of solar spectral irradiance at the bottom and top of a cloudy atmosphere N87-13385
IRRADIATION
Radiation-induced segregation to grain boundaries in a Ni-Si alloy
[DE86-010027] N87-12664
The control of polymer mechanical behavior by surface modification
[AD-A169252] N87-12686
Densification of graphites by irradiation
[DE86-010026] N87-12698
Kinetic and thermodynamic studies of pulsed laser irradiation
[DE86-012175] N87-12660

IRRIGATION
Report on the activities of the irrigated crop survey in Sao Paulo State from remote sensing products, phase 2
[INPE-3950-RPE/513] N87-12989
ISOLATORS
Multiple rate shock isolator damping valve
[AD-D012394] N87-12679
ISOSTATIC PRESSURE
Fracture toughness of CIP-HIP beryllium at elevated temperatures
[AD-A169769] N87-12654
Hot isostatic pressing of ceramic powder compacts
[AD-A169971] N87-12688
ITERATIVE SOLUTION
SOR (Successive Over-Relaxation) MGR (multigrid algorithm)(nu) experiments on the crystal multicomputer
[AD-A169929] N87-13187
A generalized projection method for the solution of algebraic linear systems
[INPE-3874-PRE/930] N87-13205
Solving systems of nonlinear equations by tensor methods
[AD-A169927] N87-13216
Quantitative assessment of the effect of partial pivoting in sparse ordinary differential equation solvers
[DE86-012592] N87-13226

J

J INTEGRAL
Unloading-compliance and load-drop analysis of J(Ic) test of irradiated 348 stainless steel
[AD-A170484] N87-12938
JAPAN
Possible military applications of stratospheric airship discussed N87-12716
JET AIRCRAFT
TSAR (Theater Simulation of Airbase Resources) database dictionary F-4E
[AD-A169575] N87-13352
JET EXHAUST
Advanced optical smoke meters for jet engine exhaust measurement
[NASA-CR-179459] N87-12829
JET FLOW
Transition and mixing in axisymmetric jets and vortex rings
[NASA-CR-3893] N87-12808
JET LAG
Pharmacological resetting of the circadian sleep-wake cycle
[AD-A170804] N87-13137
JET MIXING FLOW
Transition and mixing in axisymmetric jets and vortex rings
[NASA-CR-3893] N87-12808
Computer-based estimation procedure for coaxial jet noise. Including far-field subsonic jet mixing noise database for stationary, coplanar conical nozzles
[ESDU-86019] N87-13251
JET STREAMS (METEOROLOGY)
Statistical analysis and use of VAS radiance data N87-13066
JOINTS (JUNCTIONS)
Literature review on the design of composite mechanically fastened joints
[AD-A169112] N87-12872
JP-4 JET FUEL
Determination of the coefficient of thermal expansion of JP-4 fuels
[AD-A171495] N87-12705
JUPITER ATMOSPHERE
The secondary production of gamma rays in the Jovian magnetosphere N87-13391

K

KALMAN FILTERS
Advanced guidance algorithms for homing missiles with bearing-only measurements
[AD-A170833] N87-12583
SARSAT (Search and Rescue Satellite) operational data categorization and accuracy studies
[AD-A169748] N87-12599
Description of data on the Nimbus 7 LIMS map archive tape: Ozone and nitric acid
[NASA-TP-2825] N87-13022
A procedure for automatic treatment of dynamic systems state observation bias errors
[INPE-3908-PRE/918] N87-13177
A generalized projection method for the solution of algebraic linear systems
[INPE-3874-PRE/930] N87-13205
Optical processing
[AD-A169682] N87-13269
Solar flux and geomagnetic activity prediction
[INPE-3884-PRE/934] N87-13377
KERNEL FUNCTIONS
Lg wave excitation and propagation in presence of one-, two- and three-dimensional heterogeneities
[AD-A169004] N87-12724
Long time estimates for the heat kernel associated with a uniformly subelliptic symmetric second order operator
[AD-A169949] N87-13220
Smooth nonparametric quantile estimation under censoring: Simulations and bootstrap methods
[AD-A169935] N87-13236
Induced quantum torsion
[DE86-702616] N87-13348
KERR ELECTROOPTICAL EFFECT
Nonlinear ellipse rotation in a low-birefringence optical fiber N87-13282
KINEMATICS
Introduction to aerodynamics derivatives, equations of motion and stability
[ESDU-86021] N87-12536
KINETIC ENERGY
Circuit considerations for repetitive railguns
[DE86-012369] N87-12752
Response of the mesoscale atmosphere to diabatic heating N87-13069
Duel between an ASAT (anti-satellite) with multiple kill vehicles and a space-based weapons platform with kinetic energy weapons
[AD-A169946] N87-13245
KINETIC FRICTION
Frictional and retarding forces on aircraft tyres. Part 4: Estimation of effects of yaw
[ESDU-86016-PT-4] N87-12868
KINETICS
The influence of welding flux on the pyrometallurgical, physical and mechanical behavior of weld metal
[AD-A169057] N87-12650
A study of energy conversion devices using photoactive organometallic electrocatalysts
[AD-A169096] N87-12996
KITS
Adhesive repair patch
[AD-D012422] N87-12692
KNOWLEDGE
Evaluation of the bearing and knowledge requirements of man machine systems N87-13164
KRAMERS-KRONIG FORMULA
Quantitative non-destructive evaluation of composite materials based on ultrasonic wave propagation
[NASA-CR-179631] N87-12613

L

LAGRANGE MULTIPLIERS
User's guide for NPSOL (version 4.0): A Fortran package for nonlinear programming
[AD-A169115] N87-13180
LAMINAR BOUNDARY LAYER
Finite-difference solutions for compressible laminar boundary-layer flows of a dusty gas over a semi-infinite flat plate
[UTIAS-311] N87-12807
LAMINAR FLOW
Transition and mixing in axisymmetric jets and vortex rings
[NASA-CR-3893] N87-12808
Analysis of laminar flow heat transfer in uniform temperature circular tubes with tape inserts
[PB86-224763] N87-12826
LAMINATES
Stability of multilayers at high temperatures
[DE86-010526] N87-12623
The control of polymer mechanical behavior by surface modification
[AD-A169252] N87-12686
LANDAU-GINZBURG EQUATIONS
Theory of Fractional Quantum Hall Effect
[DE86-702652] N87-13343
LANDING
Guidance law simulation studies for complex approaches using the Microwave Landing System (MLS)
[NASA-CR-178182] N87-12552
LANDING SIMULATION
Guidance law simulation studies for complex approaches using the Microwave Landing System (MLS)
[NASA-CR-178182] N87-12552
LANDSAT SATELLITES
Geologic remote sensing at INPE: An overview
[INPE-3975-PRE/967] N87-12959
Report on the activities of the irrigated crop survey in Sao Paulo State from remote sensing products, phase 2
[INPE-3950-RPE/513] N87-12989
Generation of images with recorded auxiliary data for the LANDSAT Thematic Mapper (TM) imagery
[INPE-3982-TDL/234] N87-12990
Intercomparison of DMSP OLS, NOAA AVHRR, GOES VISSR (Defense Meteorological Satellite Program Operational Linescan System, National Oceanographic and Atmospheric Administration Advanced Very High Resolution Radiometer, GOES Visible Infrared Spin-Scan Radiometer) and Landsat MSS imagery for cloud property determination: Recommendations for digital data analysis
[AD-A169285] N87-12991
LANGUAGES
Language acquisition and machine learning
[AD-A169581] N87-13184
LARGE SCALE INTEGRATION
Direct writing of microstructures for solid-state electronics
[AD-A170837] N87-12783
LARGE SPACE STRUCTURES
Solar array flight dynamic experiment
[NASA-TP-2598] N87-12581
A mathematical formulation of a large space structure control problem
[AD-A169950] N87-12602
LASER APPLICATIONS
Solar array flight dynamic experiment
[NASA-TP-2598] N87-12581
Pulsed-laser, high speed photography of rocket propellant surface deflagration
[AD-A169308] N87-12703
Japan report: Science and Technology
[JPRS-JST-86-023] N87-12715
Status of laser enrichment technology updated N87-12717
Coordinated research program in pulsed power physics
[AD-A169113] N87-12762
Advanced optical smoke meters for jet engine exhaust measurement
[NASA-CR-179459] N87-12829
Slitless, intensified readout, gated spectrometer: Wavelength and efficiency calibration, time response characterization
[DE86-012349] N87-12839
Heterogeneous catalysis with lasers
[AD-A169601] N87-12851
Theory and simulation of high-brightness electron beam production from laser-irradiated photocathodes in the presence of dc and RF electric fields
[DE86-012384] N87-12864
Guided Optical Structures in the Military Environment
[AGARD-CP-383] N87-13273
Progress in optical fiber sensors N87-13274
Wavelength division multiplexing at 1.5 microns for high capacity optical transmission N87-13284
A hybrid transmission scheme on single mode fibers for tactical communications N87-13306
Medium- and long-wavelength infrared emission from a laser-produced oxygen plasma
[AD-A169475] N87-13309
LASER FUSION
Influence of a strong laser field on the stopping power for charged test particles in fusion plasmas
[INPE-3977-PRE/968] N87-12843
Comparison of Rayleigh-Taylor growth with 1.0 m and 0.25 m lasers
[DE86-012217] N87-12862
LASER HEATING
Kinetic and thermodynamic studies of pulsed laser irradiation
[DE86-012175] N87-12860
LASER INDUCED FLUORESCENCE
Population inversions in laser-initiated vacuum arcs
[AD-A170811] N87-12859
LASER INTERFEROMETRY
Research on mechanical properties for engine life prediction
[AD-A169570] N87-12563
A study of methods of phase noise reduction of semiconductor lasers for sensor applications N87-13286
LASER MODE LOCKING
Optical rotation sensors
[AD-A169357] N87-12848
LASER OUTPUTS
High power semiconductor laser sources
[AD-A168900] N87-12844
Doppler effect laser velocity measuring system
[AD-D012401] N87-12854
CO sub 2 laser sustained CW discharge atomic beam source
[DE86-012383] N87-12863
Method of fabricating high efficiency binary planar optical elements
[AD-D012374] N87-13266

LASER PLASMAS
Influence of a strong laser field on the stopping power for charged test particles in fusion plasmas
[INPE-3977-PRE/986] N87-12843
Population inversions in laser-initiated vacuum arcs
[AD-A170811] N87-12859
LASER PUMPING
Fragmentation dynamics of energetic materials
[AD-A169925] N87-12682
Resonant photon pumping mechanisms for a plasma X-ray laser
[AD-D012416] N87-12857
Laser produced X-ray for high resolution lithography and a photoionization laser
[AD-A170782] N87-12858
Population inversions in laser-initiated vacuum arcs
[AD-A170811] N87-12859
LASER SPECTROSCOPY
Wide bandwidth, long distance fibre-optic communication systems N87-13300
LASER WEAPONS
FEL (Free Electron Laser) optics coating test program (design phase of sample introduction chamber)
[AD-A169474] N87-12849
Duel between an ASAT (anti-satellite) with multiple kill vehicles and a space-based weapons platform with kinetic energy weapons
[AD-A169946] N87-13245
LASER WELDING
Microstructural study of high energy density dissimilar metal welds
[DE86-009264] N87-12668
Laser sealed vacuum insulating window
[DE86-013678] N87-12701
TDD antenna: Foil formed, substrate loaded laser welded assembly
[AD-D012411] N87-12712
Cylindrical laser welder
[AD-D012396] N87-12850
LASER WINDOWS
Laser sealed vacuum insulating window
[DE86-013678] N87-12701
LASERS
Study in molecular lasers
[AD-A169933] N87-12855
LASING
Mossebauer-Borrmann superradiance
[DE86-012373] N87-12666
LATCHES
Over-center toggle latch
[AD-D012393] N87-12878
LATENT HEAT
A partition of sensible and latent heat fluxes above the terra firma area in the Amazon Forest (gradient method)
[INPE-3972-PRE/965] N87-12964
LAMPS software and mesoscale prediction studies N87-13076
LATEX
Electrokinetic properties of polymer colloids
[NASA-CR-178936] N87-12681
LATTICE VIBRATIONS
Percolation and low density materials: Theory and applications
[AD-A169204] N87-12684
Search for far infrared radiation from optically and acoustically pumped defect modes
[AD-A169159] N87-13319
LAYOUTS
Compaction with automatic jog introduction
[AD-A169579] N87-12772
LEAD (METAL)
Embrittlement of a high and a low strength steel in liquid lead environment
[AD-A169443] N87-12653
LEAD ACID BATTERIES
Performance of advanced lead acid batteries for electric vehicles
[DE85-011476] N87-12801
LEAD ZIRCONATE TITANATES
Holographic storage in ion-implanted, ferroelectric-phase PLZT ceramics
[DE86-010475] N87-12837
LEARNING
Evaluation of the bearing and knowledge requirements of man machine systems N87-13164
LEARNING MACHINES
Language acquisition and machine learning
[AD-A169581] N87-13184
LEAST SQUARES METHOD
Iterative methods for large linear and nonlinear least squares problems
[AD-A169028] N87-13209
Algorithm for positive definite least square estimation of parameters
[DE86-012159] N87-13225
LENNARD-JONES POTENTIAL
Molecular dynamic studies of crack propagation. The role of the interatomic potential
[DE86-009942] N87-12942
LENS ANTENNAS
Twin aperture phased array lens antenna
[AD-D012415] N87-12745
LENS DESIGN
A spherical waveguide multiplexer-demultiplexer N87-13285
LENSES
Pulsed-laser, high speed photography of rocket propellant surface deflagration
[AD-A169308] N87-12703
Method of fabricating high efficiency binary planar optical elements
[AD-D012374] N87-13286
LIBRARIES
Government libraries. A periodicals bibliography, together with list of bibliographies and indexes
[AD-A169422] N87-13351
LIFE (DURABILITY)
Research on mechanical properties for engine life prediction
[AD-A169570] N87-12563
Performance of advanced lead acid batteries for electric vehicles
[DE85-011476] N87-12801
International Conference/Workshop on Small Fatigue Cracks (2nd) held in Santa Barbara, California on 5-10 January 1986
[AD-A169060] N87-12929
Compact reactor/ORC power source
[DE86-011252] N87-13260
LIFE SUPPORT SYSTEMS
Advanced EVA system design requirements study
[NASA-CR-171942] N87-13167
LIGHT (VISIBLE RADIATION)
Basic and applied research in the field of electronics and communications
[AD-A169029] N87-12727
Lightwave technology in future radar equipment designs N87-13304
LIGHT AMPLIFIERS
High gain free electron laser oscillators
[AD-A169002] N87-12846
FEL (Free Electron Laser) optics coating test program (design phase of sample introduction chamber)
[AD-A169474] N87-12849
LIGHT EMITTING DIODES
Progress in optical fiber gyroscopes using integrated optics N87-13283
LIGHT MODULATION
Fiber optic device for temperature remote sensing N87-13280
Acoustooptic spectrum analyzer using a planar Bragg-cell N87-13295
LIGHT TRANSMISSION
PIN-FET preamplifier for high-speed optical transmission systems N87-13293
LIGHTNING
Deep convection in mesoscale convective systems N87-13055
Severe storm electricity N87-13056
Storm severity detection (RF) N87-13057
Studies of lightning data in conjunction with geostationary satellite data N87-13058
Lightning mapper and the future N87-13059
Space shuttle/mesoscale lightning experiment N87-13060
Optical characteristics of lightning and thunderstorm currents N87-13061
Optical characteristics of lightning N87-13062
Airborne atmospheric electricity experiments N87-13063
Remote observations of severe storms N87-13065
NOSL experiment support
[NASA-CR-178947] N87-13140
LIMITER CIRCUITS
Integrated optics optical limiters N87-13292
LIMITS (MATHEMATICS)
Upper bounds for symmetric Markov transition functions
[AD-A170010] N87-13221
LINE OF SIGHT
Pulsed-laser, high speed photography of rocket propellant surface deflagration
[AD-A169308] N87-12703
LINE SPECTRA
Airborne atmospheric electricity experiments N87-13063
Plane-parallel and bow shock models of Herbig-Haro objects N87-13374
LINEAR ACCELERATORS
FEL (Free Electron Laser) optics coating test program (design phase of sample introduction chamber)
[AD-A169474] N87-12849
High repetition rate electron beam RF-Acceleration and sub-millimeter wave generation via a free electron laser
[AD-A169646] N87-12853
High-gain free electron lasers as generators of short wavelength coherent radiation
[DE86-012500] N87-12865
LINEAR EQUATIONS
An implicit enumeration procedure for the general linear complementarity problem
[AD-A170397] N87-13189
A generalized projection method for the solution of algebraic linear systems
[INPE-3874-PRE/930] N87-13205
LINEAR FILTERS
Zero-crossings analysis
[AD-A169937] N87-13218
LINEAR PROGRAMMING
Iterative methods for large linear and nonlinear least squares problems
[AD-A169028] N87-13209
Semigroups and Poisson-approximation
[AD-A170944] N87-13224
LINEAR SYSTEMS
Input impedance of an infinite linear scanned array of flat rectangular strips inside a dielectric loaded parallel plate waveguide
[AD-A171275] N87-12784
LINEARITY
Nonlinear waves
[AD-A169834] N87-13207
Parametric linear variation of a leakage free permanent magnet field source
[AD-D012359] N87-13249
LIQUID ATOMIZATION
Characterization and dynamical studies of polymers in dipolar (aprotic) liquids
[AD-A169243] N87-12685
LIQUID CRYSTALS
Possibility of using dc conductivity for investigating phase transition in amorphous semiconductors
[DE86-702646] N87-13340
LIQUID FILLED SHELLS
Stability of liquid-filled projectiles with unusual coning frequencies
[AD-A171480] N87-12584
Free vibration of axisymmetric and beam-like cylindrical shells, partially filled with liquid
[EPM/RT-86-35] N87-12920
LIQUID METALS
Embrittlement of a high and a low strength steel in liquid lead environment
[AD-A169443] N87-12653
Finite mean-free-paths and the electrical resistivity of liquid simple metals and binary alloys
[DE86-702662] N87-12679
Liquid metal thermoacoustic engine
[DE86-011264] N87-12902
LIQUID PHASE EPITAXY
Growth of ferro-electric tungsten bronze epitaxial thin films for electro-optic device applications
[AD-A170783] N87-13328
LIQUID PHASES
Investigation of deviations from ideality in the two liquid phase region of systems of medium molecular weight hydrocarbon mixtures and water
[AD-A169752] N87-12635
LIQUID-SOLID INTERFACES
Cellular solidification of transparent monotectics
[NASA-CR-177039] N87-12626
LITHIUM
Lithium Ambient-Temperature Battery Reliability Program, May 1983-April 1985
[DE86-012247] N87-12789
LITHIUM ALLOYS
Site occupations in Li sub 2 ordered alloys by axial electron channeling microanalysis
[DE86-009421] N87-12659
LOAD DISTRIBUTION (FORCES)
Fracture and viscoelastic characteristics of the human cervical spine
[AD-A170002] N87-13133
LOADS (FORCES)
Transformers for explosive pulsed power coupling to various loads
[DE86-012425] N87-12796
Analysis of mixed-mode crack propagation using the boundary integral method
[NASA-CR-179518] N87-12915
Analysis of anisotropic thin conical shells
[EPM/RT-86-36] N87-12918

LOGARITHMS
Improving numerical weather prediction by maximizing the use of assimilated satellite data
[AD-A169295] N87-13104
LOGIC CIRCUITS
Declarative descriptions for VLSI generators
[AD-A169952] N87-12777
Fabrication of gate array interconnect structures using direct-write deposition processes
[DE86-010785] N87-12787
LOW DENSITY MATERIALS
Percolation and low density materials: Theory and applications
[AD-A169204] N87-12684
LOW NOISE
Millimeter wave components — spaceborne microwave radiometers
[FTL-118521] N87-12605
LOW PASS FILTERS
Atmospheric Modeling And Sensor Simulation (AMASS) study N87-13090
LUBRICATION
Fundamental research on tribology
[AD-A169974] N87-12682
LUMINAIRES
Light socket removal tool
[AD-D012368] N87-12710
LUNAR BASES
Lunar laboratory
[NASA-TM-89209] N87-12580
LUNAR EXPLORATION
Lunar laboratory
[NASA-TM-89209] N87-12580
LUNAR SPACECRAFT
Lunar laboratory
[NASA-TM-89209] N87-12580
LUNAR SURFACE
Lunar laboratory
[NASA-TM-89209] N87-12580

M

MACH NUMBER
Mach 6 experimental and theoretical stability and performance of a finned cylindrical body at angles of attack up to 65 deg
[NASA-TM-89050] N87-12538
MACHINE TOOLS
Shower and high-pressure oil temperature control
[DE86-009396] N87-12699
MACHINING
Cleaning of aluminum alloy 5083
[DE86-012573] N87-12675
MAGNETIC ANOMALIES
A survey of hard-X-rays at balloon altitudes of the Earth's atmosphere
[INPE-3954-PRE/972] N87-13388
MAGNETIC CIRCUITS
Parametric linear variation of a leakage free permanent magnet field source
[AD-D012359] N87-13249
MAGNETIC COILS
Procedure for one axis satellites attitude control with magnetic actuation
[INPE-3895-PRE/937] N87-12590
MAGNETIC COOLING
Analysis of magnetic refrigeration systems with staged regenerators based on an idealized magnetic material entropy model: 1
[DE86-013638] N87-12714
MAGNETIC DOMAINS
Picosecond nonlinear resonant interactions in semiconductors
[AD-A170813] N87-13330
MAGNETIC FIELDS
Coordinated radar and satellite studies of ionospheric currents in the auroral zone and polar cap
[AD-A169466] N87-13031
Magnetic and pressure sensors using the compensated polarimetric sensor configuration N87-13279
Two-dimensional dynamics of the plasma Wakefield accelerator
[DE86-012362] N87-13312
Flux spiral instability in a transport current carrying type 2 superconductor
[DE86-702724] N87-13346
Rapid fluctuations in solar flares
[NASA-CR-179894] N87-13387
MAGNETIC FLUX
Equilibrium configuration of coronal loops
[DE86-702711] N87-13384
MAGNETIC INDUCTION
Theoretical study on the correlation between wideband electromagnetic spectra and geological structures
[AD-A169971] N87-13026
MAGNETIC MATERIALS
Picosecond nonlinear resonant interactions in semiconductors
[AD-A169992] N87-13327
MAGNETIC MIRRORS
Stabilizing effects of finite-amplitude RF waves on the interchange instability
[DE86-013042] N87-12751
MAGNETIC MOMENTS
Transition metal. 2: Complexes of dithiacycloph anes
[AD-A169107] N87-12651
MAGNETIC PERMEABILITY
Transition metal. 2: Complexes of dithiacycloph anes
[AD-A169107] N87-12651
MAGNETIC PROPERTIES
Transmission through ferrite samples at submillimeter frequencies
[AD-A169178] N87-12731
MAGNETIC PUMPING
High repetition rate electron beam RF-Acceleration and sub-millimeter wave generation via a free electron laser
[AD-A169846] N87-12653
MAGNETIC RESONANCE
Transmission through ferrite samples at submillimeter frequencies
[AD-A169178] N87-12731
Transverse resonances of Earth-ionosphere wave guide in auroral region N87-12956
Perceptual factors in workload: A neuromagnetic study
[AD-A169934] N87-13142
MAGNETIC STARS
Investigations of long-period DQ Herculis star N87-13364
MAGNETIC STORMS
Magnetospheric plasma studies using data from the dynamics explorer high and low altitude plasma instruments
[AD-A169010] N87-13027
MAGNETIZATION
Temperature compensation in the 2:17 type magnet a
[AD-A169487] N87-13250
MAGNETOHYDRODYNAMICS
Liquid metal thermoacoustic engine
[DE86-011264] N87-12902
Large-scale electric fields resulting from magnetic reconnection in the corona
[DE86-012391] N87-13383
MAGNETOMETERS
Fiber-optic magnetic gradiometer with variable magnetic biasing fields
[AD-D012423] N87-12836
Magnetic and pressure sensors using the compensated polarimetric sensor configuration N87-13279
MAGNETOPLASMADYNAMICS
Advanced electric propulsion MPD (magnetoplasmadynamic)
[AD-A169792] N87-12610
MAGNETOSPHERE
Magnetospheric plasma studies using data from the dynamics explorer high and low altitude plasma instruments
[AD-A169010] N87-13027
Solar flares and magnetospheric particles: Investigations based upon the ONR-60 experiments and ONR-604 experiments
[AD-A170620] N87-13381
The secondary production of gamma rays in the Jovian magnetosphere N87-13391
MAGNETOSPHERIC ELECTRON DENSITY
Magnetospheric plasma studies using data from the dynamics explorer high and low altitude plasma instruments
[AD-A169010] N87-13027
MAGNETOSTRICTION
Fiber-optic magnetic gradiometer with variable magnetic biasing fields
[AD-D012423] N87-12836
MAGNETRONS
Polarized H(-) source development at BNL
[DE86-012704] N87-13257
MAGNIFICATION
Pulsed-laser, high speed photography of rocket propellant surface deflagration
[AD-A169308] N87-12703
MAINTENANCE
Adhesive repair patch
[AD-D012422] N87-12692
MAN ENVIRONMENT INTERACTIONS
Desertification: Global ecological problem N87-12950
MAN MACHINE SYSTEMS
Proceedings of a Symposium on the Evaluation of Man-Machine Systems: Methods and Problems
[DGLR-85-04] N87-13146
Evaluation of man machine systems: Introduction and overview N87-13147
A method for the optimum design of the man machine interface N87-13159
The eye-mark investigation as an anthropotechnical method to study man machine systems N87-13160
Basic conceptions for the evaluation of man machine systems N87-13161
Inquiry techniques for the evaluation of man machine systems N87-13162
A measure of usability — man machine systems N87-13163
Evaluation of the bearing and knowledge requirements of man machine systems N87-13164
MAN-COMPUTER INTERFACE
A test on the reliability and performance of the verbex series 4000 voice recognizer
[AD-A169066] N87-12729
Survey of the characteristics of very high level languages
[DE86-012240] N87-13196
MANAGEMENT METHODS
An examination of technology transfer as a tool for management
[AD-A169184] N87-13360
MANAGEMENT PLANNING
Joint operating procedure for interrange scheduling
[AD-A169636] N87-12579
MANEUVERS
Advanced EVA system design requirements study
[NASA-CR-171942] N87-13167
MANIPULATORS
On the dexterity of robotic manipulators N87-12867
Multi use gripper for industrial robot
[AD-D012371] N87-12876
Integrating computer vision with a robot arm system
[AD-A171276] N87-12884
MANUAL CONTROL
Application of the task taxonomy method to the simulation of human service reliability in the manual control of aircraft
[MBB/LKE-301/S/PUB/216] N87-13151
MANY ELECTRON EFFECTS
Band description of materials with localizing orbitals
[DE86-010529] N87-13255
MAPPING
The space station millimeter facility
[AD-A168983] N87-12604
A new method of synthetic aperture radar image reconstruction using modified convolution back-projection algorithm
[AD-A170652] N87-12747
Report of the Ad-Hoc Commission on remote sensing
[INPE-3981-NTE/259] N87-12983
Comparison of the 1984 and 1985 AIS data over the Singatse Range (Yerington), Nevada N87-12976
Lightning mapper and the future N87-13059
Airborne atmospheric electricity experiments N87-13063
Multispectral atmospheric mapping sensor of mesoscale water vapor features N87-13095
A review of microbursts and their analysis and detection with Doppler radar
[AD-A170458] N87-13110
Relief and geology of the north polar region of the planet Venus
[NASA-TM-88498] N87-13376
MARKET RESEARCH
Quality management: An annotated bibliography
[AD-A169616] N87-12912
MARKING
Distributed name servers: Naming and caching in large distributed computing environments
[AD-A169225] N87-13201
Data tagging in the Energy Data Base
[DE86-010621] N87-13355
MARKOV PROCESSES
Upper bounds for symmetric Markov transition functions
[AD-A170010] N87-13221
Recursive moment formulas for semi-Markov processes
[AD-A169253] N87-13231
A reversal argument for storage models defined on semi-Markov processes
[AD-A169262] N87-13232
MARTENSITE
Design of strong, ductile, HSLA and dual phase steels
[DE86-011313] N87-12665
MARTENSITIC STAINLESS STEELS
Initiation of pitting corrosion in martensitic stainless steels
[DE86-007627] N87-12661
Data requirements to model creep in 9Cr-1Mo-V steel
[DE86-011754] N87-12944

MASS
Simple defense conservative model for mass requirements of hypervelocity projectile impact shields for reentry vehicles
[DE86-012407] N87-12603
MASS DISTRIBUTION
Characterization and dynamical studies of polymers in dipolar (aprotic) liquids
[AD-A169243] N87-12685
MASS FLOW
Computational fluid dynamic studies of certain ducted bluff-body flowfields relevant to turbojet combustors. Volume 1: Time-dependent calculations with the k-epsilon turbulence model for an existing centerbody combustor
[AD-A171434] N87-12816
MASS SPECTROMETERS
Fragmentation dynamics of energetic materials
[AD-A168925] N87-12682
Collection of ions in the stratosphere
[AD-A169905] N87-13032
MASS SPECTROSCOPY
Application of pattern recognition to metal ion chemical ionization mass spectra
[AD-A169061] N87-12630
High accuracy standards and reference methodology for carbon dioxide in air
[DE86-012643] N87-13011
MASS TRANSFER
Application of flux-corrected transport (FCT) to high Rayleigh number natural convection in a porous medium
[DE86-004603] N87-12618
Theory of developed hydrodynamical turbulence
[DE86-012796] N87-12623
MATCHED FILTERS
Optical processing
[AD-A169882] N87-13269
MATCHING
A rule-based pattern matching system for the recognition of three-dimensional line drawn objects: A foundation for video tracking
[AD-A170701] N87-13190
MATERIALS HANDLING
Concept study - vehicle waste disposal system
[AD-A169045] N87-13168
MATERIALS RECOVERY
Importance of interfacial phenomena in separation science and technology
[DE86-011063] N87-12637
MATHEMATICAL MODELS
Numerical simulation of tip vortices of wings in subsonic and transonic flows
[AD-A169116] N87-12544
A summary of the development of integral aerodynamic methods for the computation of rotor wake interactions
[AD-A169254] N87-12545
A numerical model for two-dimensional unsteady flow calculations with a surface panel method N87-12548
Analysis and verification of the icing scaling equations. Volume 1: Revision
[AD-A167976] N87-12551
Simplified forms of performance equations. Addendum A: Effect on aeroplane level speed of small changes in thrust, drag, weight, power
[ESDU-86004-ADD-A] N87-12556
Evaluation of a nonlinear parameter extraction mathematical model including the term C(subm(sub delta e squared))
[NASA-TM-87731] N87-12566
Modeling the fundamental characteristics and processes of the spacecraft functioning
[NASA-TM-87999] N87-12596
Simple defense conservative model for mass requirements of hypervelocity projectile impact shields for reentry vehicles
[DE86-012407] N87-12603
Computational and experimental study of flow-induced vibration of the SSME main injector post
[DE86-012119] N87-12611
Coupled damage and moisture-transport in fiber-reinforced polymeric composites
[AD-A169379] N87-12619
Micromechanisms of crack growth and fracture toughness in metal matrix composites
[AD-A169639] N87-12620
Signal estimation, scattering theory and interpolation problems in one and two dimensions
[AD-A168969] N87-12759
The 1984 IR and D (Independent Research and Development) advanced packaging study
[AD-A169388] N87-12765
SAW transduction in electrostrictive substrates
[DE86-011651] N87-12794
Generalization of one-dimensional solute transport: A stochastic-convective flow conceptualization
[DE86-011117] N87-12820
Double-ended tuning fork quartz accelerometer
[DE86-012277] N87-12842
Comparison of Rayleigh-Taylor growth with 1.0 m and 0.25 m lasers
[DE86-012217] N87-12862
Welding research in Scandinavia: An assessment
[AD-A169036] N87-12871
Linear harmonic analysis of free-piston Stirling engines
[DE86-012451] N87-12903
On 3-D inelastic analysis methods for hot section components (base program)
[NASA-CR-175060] N87-12923
Influence of experimental scatter on the analysis and extrapolation of stress-rupture data
[DE86-009510] N87-12940
Molecular dynamic studies of crack propagation. The role of the interatomic potential
[DE86-009942] N87-12942
Crop yield modeling for climate impact studies. Part 1: Reasoning and results
[INPE-3967-PRE/982-PT-1] N87-12961
Sensitivity tests of a surface-layer windflow model to effects of stability and vegetation
[AD-A169136] N87-13101
Micrometeorological transitions in the morning boundary layer over rolling terrain
[AD-A169237] N87-13103
Introduction to the theory of nested transactions
[AD-A171428] N87-13191
Statistical models and methods for cluster analysis and image segmentation
[AD-A169145] N87-13229
Asymptotic theory for sieve estimators in semimartingale regression models
[AD-A169207] N87-13230
Pattern recognition based on scale invariant discriminant functions
[AD-A170809] N87-13241
Proceedings of the conference on the design of experiments in army research development and testing (31st) held at the Madison, Wisconsin on 23-25 October 1986
[AD-A169473] N87-13246
MATHEMATICAL PROGRAMMING
An implicit enumeration algorithm with binary-valued constraints
[AD-A169256] N87-13182
Maintaining LU factors of a general sparse matrix
[AD-A169255] N87-13248
MATRICES (MATHEMATICS)
Matrix factorization on a hypercube multiprocessor
[DE86-011775] N87-13193
A generalized projection method for the solution of algebraic linear systems
[INPE-3874-PRE/930] N87-13205
Eigenvectors of graphs
[AD-A170562] N87-13223
On reduction of dimensionality under multivariate regression and canonical correlation models
[AD-A170025] N87-13238
Maintaining LU factors of a general sparse matrix
[AD-A169255] N87-13248
MATRIX THEORY
Matrix theory
[AD-A169139] N87-13247
MAXIMUM LIKELIHOOD ESTIMATES
Validity of Edgeworth expansions of minimum contrast estimators for Gaussian ARMA processes
[AD-A169931] N87-13217
MAXWELL EQUATION
High-gain free electron lasers as generators of short wavelength coherent radiation
[DE86-012500] N87-12865
MEAN FREE PATH
Finite mean-free-paths and the electrical resistivity of liquid simple metals and binary alloys
[DE86-702662] N87-12678
MEASURING INSTRUMENTS
Advanced optical smoke meters for jet engine exhaust measurement
[NASA-CR-179459] N87-12829
Development of buried wire gages for measurement of wall shear stress in Blastane experiments
[NASA-TM-89212] N87-12831
A procedure for automatic treatment of dynamic systems state observation bias errors
[INPE-3908-PRE/918] N87-13177
MECHANICAL DEVICES
Rapid acting electro-pneumatic anti-G suit control valve
[AD-D012377] N87-13170
MECHANICAL PROPERTIES
The influence of welding flux on the pyrometallurgical, physical and mechanical behavior of weld metal
[AD-A169067] N87-12650
Embrittlement of a high and a low strength steel in liquid lead environment
[AD-A169443] N87-12653
Effect of hydrogen on the mechanical properties and fracture behavior of high purity aluminum
[AD-A171214] N87-12658
Investigation of the effects of cobalt ions on epoxy properties
[NASA-TP-2639] N87-12680
Maximization of the capacity of the most survivable connections in a network
[AD-A169065] N87-12728
Adaptive grid techniques for elliptic fluid-flow problems
[AD-A169471] N87-12814
Mechanical transduction: Unification
[AD-A171191] N87-13123
MELTING
Kinetic and thermodynamic studies of pulsed laser irradiation
[DE86-012175] N87-12960
Stefan-type problem with void formation and its explicit solution
[DE86-013521] N87-13007
MELTS (CRYSTAL GROWTH)
Incremental quench research
[AD-A168980] N87-13317
Study to determine the feasibility of utilizing skull-melting techniques for the growth of single crystals of yttrium vanadate
[AD-A169249] N87-13320
MEMORY (COMPUTERS)
Comparison of 2D memory SEU transport simulation with experiments
[ATR-86(8139)-2] N87-13314
MENTAL PERFORMANCE
Eye movements as an index of mental workload
[AD-A169941] N87-13143
MERCURY CADMIUM TELLURIDES
Incremental quench research
[AD-A168980] N87-13317
Quantum 1/F noise in solid state double devices, in particular Hg(1-x)CdxTe diodes
[AD-A171436] N87-13332
MERCURY TELLURIDES
In-situ interdiffusion measurements in HgTe-CdTe superlattices
[DE86-011429] N87-13337
MESON-MESON INTERACTIONS
Neutron and antineutron production in accretion onto compact objects
[NASA-TM-89264] N87-13395
MESOSCALE PHENOMENA
NASA/MSFC FY-85 Atmospheric Processes Research Review
[NASA-CP-2402] N87-13043
Deep convection in mesoscale convective systems N87-13055
Space shuttle/mesoscale lightning experiment N87-13060
Optical characteristics of lightning N87-13062
Airborne Doppler measurements of the central California extended sea breeze N87-13066
Response of the mesoscale atmosphere to diabatic heating N87-13069
Automated mesoscale winds derived from GOES multispectral imagery N87-13073
LAMPS software and mesoscale prediction studies N87-13076
Mesoscale-cloud scale simulation of convective response N87-13077
Mesoscale research activities with the LAMPS model N87-13078
Cooperative VAS program with NASA Marshall Space Flight Center N87-13079
The assimilation of satellite soundings, winds and satellite products in a mesoscale analysis/forecast system N87-13080
Numerical simulation of convective response to mesoscale forcing N87-13081
A summary of research on mesoscale energetics of severe storm environments N87-13082
Investigations of severe/tornadic thunderstorm development and evolution based on satellite and AVE/SESAME/VAS data N87-13084
Statistical analysis and use of VAS radiance data N87-13086
Improved satellite retrievals and mesoscale moisture variability N87-13087
Preliminary planning for the Satellite Precipitation And Cloud Experiment (SPACE) Field Program N87-13089
Interactive information processing for NASA's mesoscale analysis and space sensor program N87-13093
Multispectral atmospheric mapping sensor of mesoscale water vapor features N87-13095

METAL COATINGS
Solid-state electrochromic switchable window glazings
[DE86-004455] N87-12700
METAL CRYSTALS
Energetics of dislocation relaxation associated with cleavage in Cd-doped zinc crystals as probed by synchrotron topography
[DE86-002966] N87-13334
METAL FATIGUE
Guide to the use of data items on the fatigue strength of welded joints in steels
[ESDU-86013] N87-12914
METAL FILMS
Plasma-enhanced deposition and processing of transition metals and transition metal silicides for VLSI
[AD-A169963] N87-13316
METAL FLUORIDES
Preparation and properties of infrared transmitting heavy metal fluoride glass optical fibers N87-13296
Fluoride glasses for infrared waveguides N87-13299
METAL FOILS
A heater made from graphite composite material for potential deicing application
[NASA-TM-88886] N87-12559
Modeling of high-explosive driven plasma compression opening switches
[DE86-012421] N87-12795
Resistance seam welding
[DE86-013288] N87-12906
METAL HYDRIDES
Phase change thermal energy storage methods for combat vehicles, phase 1
[AD-A170492] N87-12713
METAL IONS
Application of pattern recognition to metal ion chemical ionization mass spectra
[AD-A169061] N87-12630
METAL JOINTS
Rusty bolt intermodulation interference reducer
[AD-D012417] N87-12661
METAL MATRIX COMPOSITES
Plasma joining of metal matrix composites
[AD-A169056] N87-12615
Metallurgical characterization of the interfaces and the damping mechanisms in metal matrix composites
[AD-A169186] N87-12616
Micromechanisms of crack growth and fracture toughness in metal matrix composites
[AD-A169639] N87-12620
METAL PLATES
Metal thickness measurements using radiography
[AD-D012373] N87-12632
METAL SHEETS
Adhesive repair patch
[AD-D012422] N87-12692
METAL SURFACES
On the interplay between chemical reactions and phase transitions for molecules adsorbed on solid surfaces
[AD-A169618] N87-12636
Semiconductor/insulator films for corrosion protection
[AD-A169119] N87-12652
Diamond-machined aluminum alloy 5083 surfaces: Controlled exposure evaluation
[DE86-012572] N87-12674
Cleaning of aluminum alloy 5083
[DE86-012573] N87-12675
Metals and Ceramics Division Materials Sciences Program
[DE86-013512] N87-12699
A constitutive law for finite element contact problems with unclassical friction
[NASA-TM-88838] N87-12924
METAL VAPORS
Characterization of the atomic emission in Inconel 718 alloy metal vapor arcs
[DE86-012178] N87-12672
METAL WORKING
Mechanics of metal forming
[DE86-012414] N87-12673
METAL-NITRIDE-OXIDE-SILICON
Reliability study of retention and memory gate integrity in a 1K MNOS RAM
[DE86-010483] N87-13175
METALLIC GLASSES
Preparation and properties of infrared transmitting heavy metal fluoride glass optical fibers N87-13296
METALS
Potential applications of artificially structured materials for X-ray microanalysis
[DE86-010459] N87-12612
Nuclear reaction analysis of hydrogen in metals
[AD-A169032] N87-12649
APFIM studies of phase transformations
[DE86-008533] N87-12663
Microstructural study of high energy density dissimilar metal welds
[DE86-009284] N87-12668
Mechanics of metal forming
[DE86-012414] N87-12673
Calculated versus experimental charge density distribution of Be metal
[AD-A169924] N87-13254
Spherical clusters of simple metals: Madelung energies and structure
[AD-A169560] N87-13323
METASTABLE STATE
Percolation and low density materials: Theory and applications
[AD-A169204] N87-12684
METEOROLOGICAL FLIGHT
Experimental research on turbulence in upper-level tropospheric clouds N87-12952
Meteorological summary of WATOX (western Atlantic Ocean experiment) 1985 research intensive, February-April
[PB86-226792] N87-13114
METEOROLOGICAL PARAMETERS
Possible military applications of stratospheric airship discussed N87-12716
Remote observations of severe storms N87-13065
Improving numerical weather prediction by maximizing the use of assimilated satellite data
[AD-A169295] N87-13104
Revised Uniform Summary of Surface Weather Observations (RUSSWO). Parts A-F Ellington ANGB, Texas
[AD-A169389] N87-13105
Revised Uniform Summary of Surface Weather Observations (RUSSWO). Parts A-F, Fort Richardson, Alaska
[AD-A169390] N87-13106
Wheeler AFB, Hawaii Limited Surface Observations Climatic Summary (LISOCS), parts 1-5
[AD-A169391] N87-13107
Meteorological tower data, Yucca Ridge (YR) site, January-June 1983. Nevada Nuclear Waste Storage Investigations Project
[DE86-012732] N87-13113
METEOROLOGICAL RADAR
Satellite passive microwave rain measurement techniques for land and ocean N87-13074
Preliminary planning for the Satellite Precipitation And Cloud Experiment (SPACE) Field Program N87-13089
A review of microbursts and their analysis and detection with Doppler radar
[AD-A170458] N87-13110
Effects of reduced spatial resolution on the NEXRAD storm sequence algorithms
[PB86-221728] N87-13117
METEOROLOGICAL SATELLITES
Coordinated radar and satellite studies of ionospheric currents in the auroral zone and polar cap
[AD-A169466] N87-13031
Analysis of satellite data for sensor improvement (detection of severe storms from space N87-13071
The assimilation of satellite soundings, winds and satellite products in a mesoscale analysis/forecast system N87-13080
Time composite sounding N87-13083
Improved satellite retrievals and mesoscale moisture variability N87-13087
Preliminary planning for the Satellite Precipitation And Cloud Experiment (SPACE) Field Program N87-13089
Improving numerical weather prediction by maximizing the use of assimilated satellite data
[AD-A169295] N87-13104
METEOROLOGY
Analysis and verification of the icing scaling equations. Volume 1: Revision
[AD-A167976] N87-12551
Meteorological effects of geotectonic phenomena hypothesized N87-12947
SAGE 2 satellite data set validation
[NASA-CR-178169] N87-13024
Lightning mapper and the future N87-13059
Mesoscale ageostrophic circulations associated with baroclinic jet streaks N87-13070
The meteorological interactive data display system N87-13091
A design study for a three-dimensional display computer terminal for meteorological information N87-13092
MIZEX: A program for mesoscale air-ice-ocean interaction experiments in arctic marginal ice zones. 6: A science plan for a winter marginal ice zone experiment in the Fram Strait/Greenland Sea, 1987/89
[AD-A169070] N87-13119
METHYL COMPOUNDS
Ionic conductivity in solid, crosslinked dimethylsiloxane-ethylene oxide copolymer networks containing sodium
[AD-A169038] N87-12663
MICHELSON INTERFEROMETERS
Measurement of atmospheric emission spectra at high altitudes
[AD-A170143] N87-13035
MICROANALYSIS
Potential applications of artificially structured materials for X-ray microanalysis
[DE86-010459] N87-12612
Site occupations in Li sub 2 ordered alloys by axial electron channeling microanalysis
[DE86-009421] N87-12669
MICROCOMPUTERS
Pulse Code Modulation (PCM) data storage and analysis using a microcomputer
[NASA-TP-2529] N87-12716
MICROELECTRONICS
Direct writing of microstructures for solid-state electronics
[AD-A170837] N87-12783
Electronic Engineering Department Thrust Area report, FY 1985
[DE86-013172] N87-12797
Heat transfer characteristics of simulated microelectronic chips under normal and enhanced conditions
[PB86-224425] N87-12804
High power semiconductor laser sources
[AD-A169900] N87-12844
MICROMECHANICS
Micromechanisms of crack growth and fracture toughness in metal matrix composites
[AD-A169639] N87-12620
Molecular dynamic studies of crack propagation. The role of the interatomic potential
[DE86-009942] N87-12942
MICROMETEOROLOGY
Micrometeorological transitions in the morning boundary layer over rolling terrain
[AD-A169237] N87-13103
MICROORGANISMS
The ecology of microorganisms in a small closed system: Potential benefits and problems for space station
[NASA-TM-88563] N87-13166
MICROPROCESSORS
Flight model discharge system
[AD-A169423] N87-12571
MICROSTRUCTURE
Plasma joining of metal matrix composites
[AD-A169056] N87-12615
Micromechanisms of crack growth and fracture toughness in metal matrix composites
[AD-A169639] N87-12620
Fatigue behavior of long and short cracks in wrought and powder aluminum alloys
[AD-A169960] N87-12656
A fundamental study of P/M processed elevated temperature aluminum alloys
[AD-A170697] N87-12657
Effect of strain and strain rate on residual microstructures in copper
[DE86-007361] N87-12659
Effect of residual strain on twinning in shock-loaded copper
[DE86-007362] N87-12660
APFIM studies of phase transformations
[DE86-008533] N87-12663
Bainite in chromium-molybdenum steels
[DE86-011781] N87-12666
Microstructural study of high energy density dissimilar metal welds
[DE86-009284] N87-12668
Atomic resolution study of precipitates in an Al-Ge alloy
[DE86-011306] N87-12670
Direct writing of microstructures for solid-state electronics
[AD-A170837] N87-12783
Kinetic and thermodynamic studies of pulsed laser irradiation
[DE86-012175] N87-12880
Effect of convection on weld pool shape and microstructure
[AD-A170488] N87-12883
Localized ion milling of metallic and ceramic TEM specimens
[DE86-009536] N87-12900
Incremental quench research
[AD-A168980] N87-13317
Surface green function matching for a three-dimensional non-local continuum
[DE86-702547] N87-13341

MICROWAVE AMPLIFIERS
Experimental verification of soliton theory using a microwave crossed-field amplifier
[AD-A170011] N87-12776
A 60 GHz gyrotron development program
[DE86-012488] N87-12791
MICROWAVE ANTENNAS
Dielectric antennas for millimeter-wave applications
[AD-A169685] N87-12739
MICROWAVE EMISSION
Rapid fluctuations in solar flares
[NASA-CR-179694] N87-13387
MICROWAVE EQUIPMENT
Degeneracy in the ensemble Monte Carlo method for high field transport in semiconductors
[AD-A169456] N87-13321
MICROWAVE LANDING SYSTEMS
Guidance law simulation studies for complex approaches using the Microwave Landing System (MLS)
[NASA-CR-178182] N87-12552
MICROWAVE OSCILLATORS
Millimeter wave components — spaceborne microwave radiometers
[FTL-118521] N87-12605
Investigation of a new concept in semiconductor microwave oscillators
[AD-A170772] N87-12781
Investigation of a new concept in semiconductor microwave oscillators
[AD-A170831] N87-12782
MICROWAVE RADIOMETERS
Millimeter wave components — spaceborne microwave radiometers
[FTL-118521] N87-12605
Severe storm detection with passive 37 GHz observations N87-13072
Satellite passive microwave rain measurement techniques for land and ocean N87-13074
First meeting of the Working Group on the Shuttle Microwave Precipitation Radiometer (SMPR) N87-13096
MICROWAVE TRANSMISSION
Digest: Proceedings of the International Conference on Optical and Millimeter Wave Propagation and Scattering in the Atmosphere
[AD-A170393] N87-12743
Performance of RF fiber optic links N87-13301
MICROWAVES
Efficient, monochromatic, high-power microwave generator
[DE86-012385] N87-12792
Satellite passive microwave rain measurement techniques for land and ocean N87-13074
Theory for computing the field scattered from a smooth inflected surface
[NASA-TP-2632] N87-13264
Microwave loss properties of hexagonal ferrites for millimeter wave applications
[AD-A168982] N87-13318
MIDDLE ATMOSPHERE
Middle Atmosphere Program. Handbook for MAP, volume 21
[NASA-CR-179693] N87-13015
Atmospheric Tides Middle Atmosphere Program (ATMAP): Report of the workshop, Kyoto, Japan, December 5-6, 1984 N87-13016
Proceedings of the Workshop on Atmospheric Tides, Prague, Czechoslovakia, August 14, 1985 N87-13017
Minutes of MAP/WINE experimenters meeting, Prague, Czechoslovakia, August 13, 1985 N87-13018
Coordinated study of the behavior of the middle atmosphere in winter: Monthly mean comparisons of satellite and radiosonde data and derived quantities N87-13019
Middle atmosphere modeling
[NASA-CR-179934] N87-13023
MIE SCATTERING
Measurement and calculation of the Stokes or Mueller matrix for the scattering of electromagnetic radiation from irregular particles
[AD-A171502] N87-12749
MILITARY AIR FACILITIES
Revised Uniform Summary of Surface Weather Observations (RUSSWO). Parts A-F Ellington ANGB, Texas
[AD-A169389] N87-13105
MILITARY SPACECRAFT
MILSTAR modeling survey
[AD-A169789] N87-12600
MILITARY TECHNOLOGY
Tactical fiber optic assembly requirements N87-13305
MILITARY VEHICLES
Concept study - vehicle waste disposal system
[AD-A169045] N87-13168
MILLIMETER WAVES
Dielectric antennas for millimeter-wave applications
[AD-A169685] N87-12739
Picosecond optoelectronic diagnostics of field effect transistors
[AD-A170503] N87-12779
Microwave loss properties of hexagonal ferrites for millimeter wave applications
[AD-A168982] N87-13318
Repetition rates of fast pulses in MM-waves/X-ray solar bursts
[INPE-3974-PRE/986] N87-13378
MINERAL EXPLORATION
Report of the Ad-Hoc Commission on remote sensing
[INPE-3981-NTE/259] N87-12983
MINERALOGY
Abundance and distribution of mineral components associated with Moses Rock (kimberlite) diatreme N87-12975
Comparison of the 1984 and 1985 AIS data over the Singatse Range (Yerington), Nevada N87-12976
Identification of hydrothermal alteration assemblages using airborne imaging spectrometer data N87-12977
Preliminary geological investigation of AIS data at Mary Kathleen, Queensland, Australia N87-12979
MINERALS
Detection of hydrothermal alteration at Virginia City, Nevada using Airborne Imaging Spectrometry (AIS) N87-12978
Near-infrared detection of ammonium minerals at Ivanhoe Hot Springs, Nevada N87-12981
MIRROR FUSION
Tara vacuum system
[DE86-011873] N87-13311
MIRRORS
Potential applications of artificially structured materials for X-ray microanalysis
[DE86-010459] N87-12612
Beam steering mirror construction
[AD-D012399] N87-13268
MIS (SEMICONDUCTORS)
Semiconductor/insulator films for corrosion protection
[AD-A169119] N87-12652
MISSILE ANTENNAS
TDD antenna: Foil formed, substrate loaded laser welded assembly
[AD-D012411] N87-12712
MISSILE COMPONENTS
Carbon fibers
[AD-A171370] N87-12622
Optical rotation sensors
[AD-A169357] N87-12848
MISSILE CONTROL
Fibre optic gyroscopes in inertial navigation N87-13275
Single-mode-fibers for fiberoptic-guided missiles: A comparison with graded-index multimode fibers N87-13303
MISSILE DESIGN
The Chinese guided missiles stride toward modernization
[AD-A169017] N87-12582
MISSILES
The Chinese guided missiles stride toward modernization
[AD-A169017] N87-12582
MISSION PLANNING
General purpose aft cargo carrier study, volume 1
[NASA-CR-178905] N87-12587
Advanced solar dynamic space power systems perspectives, requirements and technology needs
[NASA-TM-88884] N87-12606
MISSOURI
Soil types and forest canopy structures in southern Missouri: A first look with AIS data N87-12983
MIXING
Recursive moment formulas for semi-Markov processes
[AD-A169253] N87-13231
MIXTURES
Investigation of deviations from ideality in the two liquid phase region of systems of medium molecular weight hydrocarbon mixtures and water
[AD-A169752] N87-12635
MOBILE COMMUNICATION SYSTEMS
Tone calibration technique: A digital signaling scheme for mobile applications
[NASA-CR-179915] N87-12719
MODELS
Procedure for one axis satellites attitude control with magnetic actuation
[INPE-3895-PRE/937] N87-12590
MILSTAR modeling survey
[AD-A169789] N87-12600
Ionic conductivity in solid, crosslinked dimethylsiloxane-ethylene oxide copolymer networks containing sodium
[AD-A169036] N87-12683
An implicit enumeration algorithm with binary-valued constraints
[AD-A169256] N87-13182
A reversal argument for storage models defined on semi-Markov processes
[AD-A169262] N87-13232
TSAR (Theater Simulation of Airbase Resources) database dictionary F-4E
[AD-A169575] N87-13352
Progress of Stirling cycle analysis and loss mechanism characterization
[NASA-TM-88891] N87-13359
MODULATION TRANSFER FUNCTION
Modulation Transfer Function (MTF) of the geometrical image resolution of the thermal infrared band
[INPE-3964-TDL/231] N87-12809
MODULES
Development of low-temperature transistor modules to improve the MSFC mid-infrared array
[NASA-TM-86566] N87-12756
MOISTURE
Stress effects on moisture transport in an epoxy resin and its composite
[AD-A169306] N87-12617
MOISTURE CONTENT
Coupled damage and moisture-transport in fiber-reinforced polymeric composites
[AD-A169379] N87-12619
MOISTURE METERS
In-line determination of presence of liquid phase moisture in sealed IC packages
[AD-D012406] N87-12775
MOLECULAR BEAM EPITAXY
Proceedings of the Topical Meeting on the Microphysics of Surfaces, Beams and Adsorbates held in Santa Fe, New Mexico on 4-6 February 1985
[AD-A170797] N87-13329
MOLECULAR BEAMS
Fragmentation dynamics of energetic materials
[AD-A168925] N87-12682
Kinetics and mechanisms on the molecular beam etching of semiconductors
[AD-A171360] N87-13331
MOLECULAR CHAINS
Effect of chain rigidity on conductivity of conjugated polymers
[DE86-011263] N87-12698
MOLECULAR CLOUDS
Infrared reflection nebulae in Orion molecular cloud 2
[NASA-TM-86259] N87-13363
MOLECULAR ELECTRONICS
Epitaxial crystallization and epitaxial polymerization as tools for molecular engineering
[AD-A171506] N87-13333
MOLECULAR EXCITATION
Fragmentation dynamics of energetic materials
[AD-A168925] N87-12682
Picosecond nonlinear resonant interactions in semiconductors
[AD-A170813] N87-13330
MOLECULAR INTERACTIONS
On the interplay between chemical reactions and phase transitions for molecules adsorbed on solid surfaces
[AD-A169818] N87-12636
Characterization and dynamical studies of polymers in dipolar (aprotic) liquids
[AD-A169243] N87-12685
Quantum chemical investigations of the mechanism of cationic polymerization and theoretical prediction of crystal densities and decomposition pathways of energetic molecules
[AD-A169805] N87-13324
Proceedings of the Topical Meeting on the Microphysics of Surfaces, Beams and Adsorbates held in Santa Fe, New Mexico on 4-6 February 1985
[AD-A170797] N87-13329
MOLECULAR OSCILLATIONS
Study in molecular lasers
[AD-A169933] N87-12655
MOLECULAR OSCILLATORS
High gain free electron laser oscillators
[AD-A169002] N87-12646
MOLECULAR ROTATION
Study in molecular lasers
[AD-A169933] N87-12655
MOLECULAR STRUCTURE
Investigation of the effects of short chain processing additives on polymers
[NASA-TM-89023] N87-12614
Application of pattern recognition to metal ion chemical ionization mass spectra
[AD-A169061] N87-12630

MOLYBDENUM
Bainite in chromium-molybdenum steels
[DE86-011781] N87-12606
MOMENTS
Recursive moment formulas for semi-Markov processes
[AD-A169253] N87-13231
MONOPOLE ANTENNAS
Development of a numerical procedure to treat wires attached to arbitrarily shaped conducting bodies
[AD-A169384] N87-12764
Input impedance of an infinite linear scanned array of flat rectangular strips inside a dielectric loaded parallel plate waveguide
[AD-A171275] N87-12784
MONOTECTIC ALLOYS
Cellular solidification of transparent monotectics
[NASA-CR-177039] N87-12626
MONTE CARLO METHOD
On the interplay between chemical reactions and phase transitions for molecules adsorbed on solid surfaces
[AD-A169818] N87-12636
Electron microprobe analysis: The upper limit of submicron spectroscopy
[DE86-009540] N87-12640
Smooth nonparametric quantile estimation under censoring: Simulations and bootstrap methods
[AD-A169935] N87-13236
Degeneracy in the ensemble Monte Carlo method for high field transport in semiconductors
[AD-A169456] N87-13321
MOON
Lunar laboratory
[NASA-TM-89209] N87-12580
MORPHOLOGY
A study of the mechanism of dynamic ductile fracture of two-phase materials
[AD-A169668] N87-12925
MOSSBAUER EFFECT
Mossbauer-Borrmann superradiance
[DE86-012373] N87-12666
MOUNTAINS
Use of digital Munsell color space to assist interretation of imaging spectrometer data: Geologic examples from the northern Grapevine Mountains, California and Nevada N87-12980
MOUTH
Quantification of respiratory muscle performance
[AD-A169208] N87-13128
MULLITES
Low temperature formation of mullite
[AD-D012404] N87-12687
MULTICHANNEL COMMUNICATION
Multichannel phase noise measurement system
[AD-D012372] N87-13253
MULTIPATH TRANSMISSION
Foreground effects on troposcatter digital communication systems
[AD-A169380] N87-12734
Single-mode-fibers for fiberoptic-guided missiles: A comparison with graded-index multimode fibers N87-13303
MULTIPLE ACCESS
Carrier-sense stack algorithms for multiple access communication channels
[AD-A169774] N87-12738
Advanced teleprocessing systems
[AD-A170007] N87-12741
Wavelength division multiplexing at 1.5 microns for high capacity optical transmission N87-13284
MULTIPLEXING
Basic and applied research in the field of electronics and communications
[AD-A169029] N87-12727
Interrupt control switch interface system
[AD-D012414] N87-12776
MULTIPROCESSING (COMPUTERS)
Fault tolerance mechanisms for a network communication multiprocessor
[INPE-3958-PRE/876] N87-12720
Atmospheric Modeling And Sensor Simulation (AMASS) study N87-13090
Yield and performance enhancement through redundancy in VLSI and WSI multi-processor systems
[AD-A169930] N87-13174
MULTISENSOR APPLICATIONS
Evaluation of the Collins/Rockwell two axis gyro/accelerometer sensor cluster (phase 3 unit)
[AD-A169810] N87-12834
MULTISPECTRAL BAND SCANNERS
The Multispectral Atmospheric Mapping Sensor (MAMS): Instrument description, calibration and data quality
[NASA-TM-86565] N87-12828
Multispectral atmospheric mapping sensor of mesoscale water vapor features N87-13095
MULTISPECTRAL LINEAR ARRAYS
Progress with multiplexed sensor arrays based on reflection at spliced joints between sensors N87-13278
MULTISPECTRAL RADAR
Automated mesoscale winds derived from GOES multispectral imagery N87-13073
MULTIVARIATE STATISTICAL ANALYSIS
On reduction of dimensionality under multivariate regression and canonical correlation models
[AD-A170025] N87-13238
A multivariate extension of Hoeffding's lemma
[AD-A170170] N87-13239
MUSCLES
Quantification of respiratory muscle performance
[AD-A169208] N87-13128
MUSCULAR STRENGTH
Quantification of respiratory muscle performance
[AD-A169208] N87-13128

N

NACELLES
The handling qualities and flight characteristics of the Grumman design 698 simulated twin-engine tilt Nacelle V/STOL aircraft
[NASA-TM-86785] N87-12558
NAMING
Distributed name servers: Naming and caching in large distributed computing environments
[AD-A169225] N87-13201
NASA PROGRAMS
NASA's quality assurance program
[GPO-63-142] N87-12909
Department of Housing and Urban Development-independent agencies appropriations for 1987, part 7
[GPO-61-970] N87-13357
NASA SPACE PROGRAMS
Earth sciences research in the Civil Space Program
[PB86-232014] N87-12995
NAVIER-STOKES EQUATION
Numerical simulation of tip vortices of wings in subsonic and transonic flows
[AD-A169116] N87-12544
Adaptive grid techniques for elliptic fluid-flow problems
[AD-A169471] N87-12814
NAVIGATION
Some tactical algorithms for spherical geometry
[AD-A170615] N87-12555
Development of a research method to determine the quality of task mastering by navigators in ship guidance N87-13154
NAVIGATORS
Development of a research method to determine the quality of task mastering by navigators in ship guidance N87-13154
NEBULAE
The stellar upper mass limit in an OB association and implications for cosmic rays and cosmic abundances N87-13392
NECK (ANATOMY)
Guidelines for safe human experimental exposure to impact acceleration
[AD-A169347] N87-13169
NETWORK ANALYSIS
Availability and consistency of global information in computer networks
[AD-A169247] N87-13202
NETWORK CONTROL
MILSTAR modeling survey
[AD-A169789] N87-12800
NEUROPHYSIOLOGY
Perceptual factors in workload: A neuromagnetic study
[AD-A169934] N87-13142
NEUTRINOS
High energy neutrino absorption and its effects on stars in close X-ray binaries
[NASA-TM-89269] N87-13366
NEUTRON DIFFRACTION
Neutron diffraction studies of some rare earth-transition metal deuterides
[AD-A169995] N87-12648
NEUTRON SPECTRA
Neutron and antineutron production in accretion onto compact objects
[NASA-TM-89264] N87-13395
NEUTRON STARS
Los Alamos Science, number 13, spring 1986
[DE86-012864] N87-13371
NEUTRONS
Neutron and antineutron production in accretion onto compact objects
[NASA-TM-89264] N87-13395
NEVADA
Comparison of the 1984 and 1985 AIS data over the Singatse Range (Yerington), Nevada N87-12976
Identification of hydrothermal alteration assemblages using airborne imaging spectrometer data N87-12977
Detection of hydrothermal alteration at Virginia City, Nevada using Airborne Imaging Spectrometry (AIS) N87-12978
Use of digital Munsell color space to assist interretation of imaging spectrometer data: Geologic examples from the northern Grapevine Mountains, California and Nevada N87-12980
Near-infrared detection of ammonium minerals at Ivanhoe Hot Springs, Nevada N87-12981
Meteorological tower data, Yucca Ridge (YR) site, January-June 1983. Nevada Nuclear Waste Storage Investigations Project
[DE86-012732] N87-13113
NEW BRUNSWICK
Lg wave excitation and propagation in presence of one-, two-, and three-dimensional heterogeneities
[AD-A169325] N87-13030
NEW MEXICO
Balloon-borne, high altitude gravimetry: The flight of DUCKY 1a (11 October 1983)
[AD-A169942] N87-13033
NICKEL
Radiation-induced segregation to grain boundaries in a Ni-Si alloy
[DE86-010027] N87-12664
Crack-tip chemistry and fracture mechanics-based model of the crack growth rate/stress intensity relationship for Ni + P
[DE86-011106] N87-12676
Welding procedure specification. Manual gas tungsten arc and semiautomatic gas metal arc welding of chromium-nickel steel. Supplement 1: Records of procedure qualification tests
[DE86-012521] N87-12686
Welding procedure specification: Gas tungsten arc welding of nickel to nickel-chromium-iron. Supplement 1: Records of procedure qualification tests
[DE86-012557] N87-12696
Electron diffraction analysis of the pentagonal arrangement of grains found in CVD pure Ni films
[DE86-009023] N87-13336
NICKEL ALLOYS
A fundamental study of P/M processed elevated temperature aluminum alloys
[AD-A170697] N87-12657
APFIM study of antiphase and grain boundaries in Ni Al
[DE86-008494] N87-12662
Ni-Co alloy plaque for cathode of Ni-Cd battery
[AD-D012375] N87-12769
NICKEL CADMIUM BATTERIES
Aircraft battery state of charge and charge control system
[AD-A169411] N87-12766
Ni-Co alloy plaque for cathode of Ni-Cd battery
[AD-D012375] N87-12769
NICKEL STEELS
Gas tungsten arc welding of chromium-nickel steel to nickel-molybdenum-chromium-iron. Welding procedure specification. Supplement 1: Records of procedure qualification tests
[DE86-012550] N87-12695
NICKEL ZINC BATTERIES
Zinc/nickel oxide battery membrane separator studies
[DE86-012824] N87-12793
NIMBUS 7 SATELLITE
Description of data on the Nimbus 7 LIMS map archive tape: Ozone and nitric acid
[NASA-TP-2625] N87-13022
Severe storm detection with passive 37 GHz observations N87-13072
Satellite passive microwave rain measurement techniques for land and ocean N87-13074
NITRIC ACID
Description of data on the Nimbus 7 LIMS map archive tape: Ozone and nitric acid
[NASA-TP-2625] N87-13022
NITRO COMPOUNDS
Methods for the syntheses of mono-, di-, tri- and tetranitro derivatives of diphenylamine
[WSRL-0436-TR] N87-12702
NITROGEN FLUORIDES
Iodine monofluoride energy transfer studies
[AD-A169781] N87-12952
NITROGEN OXIDES
Remote sensing to detect ecological impacts associated with acid deposition
[DE86-011649] N87-12992

NOAA SATELLITES
Intercomparison of DMSP OLS, NOAA AVHRR, GOES VISSR (Defense Meteorological Satellite Program Operational Linescan System, National Oceanographic and Atmospheric Administration Advanced Very High Resolution Radiometer, GOES Visible Infrared Spin-Scan Radiometer) and Landsat MSS imagery for cloud pr operty determination: Recommendations for digital data analysis
[AD-A169285] N87-12991
Application of satellite data to tropic/subtropic moisture coupling N87-13053
NOISE INTENSITY
Basic and applied research in the field of electronics and communications
[AD-A169029] N87-12727
NOISE MEASUREMENT
Multichannel phase noise measurement system
[AD-D012372] N87-13253
NOISE PREDICTION (AIRCRAFT)
Computer-based estimation procedure for coaxial jet noise. Including far-field subsonic jet mixing noise database for stationary, coplanar conical nozzles
[ESDU-86019] N87-13251
NOISE REDUCTION
Application of the AIPA (Approximate Iterative Preprocessing Algorithm) to F-106 data
[AD-A169084] N87-12569
Cruise noise of counterrotation propeller at angle of attack in wind tunnel
[NASA-TM-88869] N87-13252
A study of methods of phase noise reduction of semiconductor lasers for sensor applications N87-13286
NOISE SPECTRA
Geobotanical studies at Pilot Mountain, North Carolina using the airborne imaging spectrometer N87-12984
Closed loop fiber optic gyro N87-13277
Effects of optical feedback on the performance of high data rate single-mode fiber systems N87-13288
NONDESTRUCTIVE TESTS
Quantitative non-destructive evaluation of composite materials based on ultrasonic wave propagation
[NASA-CR-179831] N87-12613
Lithium Ambient-Temperature Battery Reliability Program, May 1983-April 1985
[DE86-012247] N87-12789
Metal thickness measurements using radiography
[AD-D012373] N87-12832
Concurrent ultrasonic weld evaluation system
[DE86-013772] N87-12908
NONEQUILIBRIUM IONIZATION
Observational study of ion-electron equilibration and of cloud evaporation in supernova remnants under the HEAO-2 guest investigator program
[NASA-CR-179922] N87-13365
NONLINEAR EQUATIONS
Non-linear analysis of cylindrical shells
[EPM/RT-86-37] N87-12917
Evaluating nonlinear effects in propagation of acoustic pulse in atmospheric surface layer in inversions N87-12951
Nonlinear waves
[AD-A168934] N87-13207
Solving systems of nonlinear equations by tensor methods
[AD-A169927] N87-13216
NONLINEAR OPTICS
Application of nonlinear optics to free electron laser systems
[AD-A168950] N87-12845
Nonlinear waves
[AD-A168934] N87-13207
Bistability in nonlinear waveguides N87-13291
Integrated optics optical limiters N87-13292
NONLINEAR PROGRAMMING
User's guide for NPSOL (version 4.0): A Fortran package for nonlinear programming
[AD-A169115] N87-13180
The continuous projective sumt method for convex programming — sequential unconstrained minimization techniques
[AD-A169847] N87-13185
Single-phase method for quadratic programming
[DE86-012156] N87-13194
Iterative methods for large linear and nonlinear least squares problems
[AD-A169028] N87-13209
NONLINEAR SYSTEMS
Forced oscillation of a two-dimensional airfoil with nonlinear aerodynamic loads
[AD-A169350] N87-12546
NONLINEARITY
Forced oscillation of a two-dimensional airfoil with nonlinear aerodynamic loads
[AD-A169350] N87-12546
Evaluation of a nonlinear parameter extraction mathematical model including the term C(subm(sub delta squared))
[NASA-TM-87731] N87-12566
Nonlinear waves
[AD-A168934] N87-13207
NONPARAMETRIC STATISTICS
A unified approach to constructing nonparametric rank tests
[AD-A169815] N87-13233
Smooth nonparametric quantile estimation under censoring: Simulations and bootstrap methods
[AD-A169935] N87-13236
NORMALITY
Extreme values of birth and death processes and queues
[AD-A169932] N87-13235
Smooth nonparametric quantile estimation under censoring: Simulations and bootstrap methods
[AD-A169935] N87-13236
NORTH CAROLINA
Geobotanical studies at Pilot Mountain, North Carolina using the airborne imaging spectrometer N87-12984
Micrometeorological transitions in the morning boundary layer over rolling terrain
[AD-A169237] N87-13103
NOZZLE DESIGN
CO sub 2 laser sustained CW discharge atomic beam source
[DE86-012383] N87-12663
Computer-based estimation procedure for coaxial jet noise. Including far-field subsonic jet mixing noise database for stationary, coplanar conical nozzles
[ESDU-86019] N87-13251
NOZZLE FLOW
Effects of test cell recirculation on high-bypass turbofan engines during simulated altitude tests
[AD-A171418] N87-12565
NOZZLE GEOMETRY
Effect of port corner geometry on the internal performance of a rotating-vane-type thrust reverser
[NASA-TP-2624] N87-12541
NUCLEAR BINDING ENERGY
Spherical clusters of simple metals: Madelung energies and structure
[AD-A169560] N87-13323
NUCLEAR FUSION
Compact reactor studies
[DE86-013247] N87-13263
NUCLEAR MAGNETIC RESONANCE
Transport and relaxation processes in supercritical fluids
[DE86-007847] N87-12638
Ionic conductivity in solid, crosslinked dimethylsiloxane-ethylene oxide copolymer networks containing sodium
[AD-A169038] N87-12683
NUCLEAR POWER PLANTS
Crack propagation in high strain regions of a steel containment
[DE86-011437] N87-12943
Review of the methods applied in the Federal Republic of Germany to investigate human factors in nuclear power plant control N87-13156
Simulation of disturbances on the nuclear power plant simulator. The problem of the interpretation of operator actions and their cognitive backgrounds as a basis for design recommendations N87-13157
A method for the optimum design of the man machine interface N87-13159
Compact reactor/ORC power source
[DE86-011252] N87-13260
NUCLEAR POWER REACTORS
Neutronic design studies for an unattended, low power reactor
[DE86-011228] N87-13262
NUCLEAR PUMPING
Reactor-pumped laser experiments in the Sandia SPR-3 Facility
[DE86-012163] N87-12861
NUCLEAR RADIATION
Fiber optics: A survivable and cost-effective transmission medium for terrestrial networks N87-13302
NUCLEAR REACTIONS
Nuclear reaction analysis of hydrogen in metals
[AD-A169032] N87-12649
NUCLEATION
Mechanical testing of a coated carbon-carbon composite at elevated temperatures in air
[AD-A169355] N87-12618
Percolation and low density materials: Theory and applications
[AD-A169204] N87-12684
Study of high temperature failure mechanisms in ceramics
[AD-A170001] N87-12689
Shock-induced solid state chemistry: Theoretical background
[DE86-012741] N87-12941
Flux spiral instability in a transport current carrying type 2 superconductor
[DE86-702724] N87-13348
NULL ZONES
A brief review of adaptive null steering techniques
[AD-A169548] N87-12736
Method and apparatus for rapid optical phasing
[AD-D012412] N87-13270
NUMERICAL ANALYSIS
Numerical simulation of tip vortices of wings in subsonic and transonic flows
[AD-A169116] N87-12544
A summary of the development of integral aerodynamic methods for the computation of rotor wake interactions
[AD-A169254] N87-12545
Application of the AIPA (Approximate Iterative Preprocessing Algorithm) to F-106 data
[AD-A169084] N87-12569
Relationship of in-cylinder gaseous and particulate concentration to radiative heat transfer in direct injection-type diesel combustion
[AD-A168979] N87-12828
Study of numerical solution methods for two-phase flows
[DE86-012265] N87-12821
Collection of ions in the stratosphere
[AD-A169905] N87-13032
Some investigations into variable meshes for numerical solution of partial differential equations
[AD-A168977] N87-13208
Space plasma research
[NASA-CR-178965] N87-13307
NUMERICAL INTEGRATION
Lg wave excitation and propagation in presence of one-, two- and three-dimensional heterogeneities
[AD-A169004] N87-12724
NUMERICAL WEATHER FORECASTING
Improving numerical weather prediction by maximizing the use of assimilated satellite data
[AD-A168295] N87-13104

O

OCCULTATION
Measurement and calculation of the Stokes or Mueller matrix for the scattering of electromagnetic radiation from irregular particles
[AD-A171502] N87-12749
OCCUPATION
Site occupations in Li sub 2 ordered alloys by axial electron channeling microanalysis
[DE86-009421] N87-12669
OCEAN CURRENTS
Nonlinear interactions in the microwave sensing of oceanic internal waves
[AD-A169776] N87-13120
OCEAN DYNAMICS
Available potential energy in upper layer of world ocean N87-12949
OCEAN MODELS
An analysis of the acoustic characteristics of ABSS (acoustic backscatter system) and its deployments
[AD-A170487] N87-13037
OCEAN SURFACE
Available potential energy in upper layer of world ocean N87-12949
OCEANOGRAPHIC PARAMETERS
US Navy climatic study of the Caribbean Sea and Gulf of Mexico. Volume 2: East Caribbean Sea
[AD-A171487] N87-13112
OCEANOGRAPHY
Intercomparison of DMSP OLS, NOAA AVHRR, GOES VISSR (Defense Meteorological Satellite Program Operational Linescan System, National Oceanographic and Atmospheric Administration Advanced Very High Resolution Radiometer, GOES Visible Infrared Spin-Scan Radiometer) and Landsat MSS imagery for cloud pr operty determination: Recommendations for digital data analysis
[AD-A169285] N87-12991
MIZEX: A program for mesoscale air-ice-ocean interaction experiments in arctic marginal ice zones. 6: A science plan for a winter marginal ice zone experiment in the Fram Strait/Greenland Sea, 1987/89
[AD-A169070] N87-13119
OCEANS
Satellite passive microwave rain measurement techniques for land and ocean N87-13074
OILS
Combustion and micro-explosion of water/oil emulsions in high pressure environments
[AD-A168976] N87-12627

Shower and high-pressure oil temperature control
[DE86-009398] N87-12899
ONBOARD DATA PROCESSING
A versatile Data Processing Unit (DPU) for satellite-borne composition instrumentation N87-13393
OPERATORS (MATHEMATICS)
Long time estimates for the heat kernel associated with a uniformly subelliptic symmetric second order operator
[AD-A169949] N87-13220
OPERATORS (PERSONNEL)
Simulation of disturbances on the nuclear power plant simulator. The problem of the interpretation of operator actions and their cognitive backgrounds as a basis for design recommendations N87-13157
OPTICAL BISTABILITY
Bistability in nonlinear waveguides N87-13291
OPTICAL COMMUNICATION
Three dimensional optical receiver having programmable gain sensor stages
[AD-D012389] N87-13267
Single crystal fibers N87-13298
OPTICAL COMPUTERS
Optical processing
[AD-A169682] N87-13269
OPTICAL COUPLING
Basic and applied research in the field of electronics and communications
[AD-A169029] N87-12727
Performance of integrated optical frequency shifters pigtailed to high birefringence fibres using ion-milled grooves N87-13289
Integrated optics optical limiters N87-13292
OPTICAL DATA PROCESSING
Optical processing
[AD-A169682] N87-13269
OPTICAL EQUIPMENT
Development of a large-aperture PLZT shutter with enhanced operational/environmental capabilities
[DE86-011643] N87-12838
FEL (Free Electron Laser) optics coating test program (design phase of sample introduction chamber)
[AD-A169474] N87-12849
Method and apparatus for rapid optical phasing
[AD-D012412] N87-13270
Guided Optical Structures in the Military Environment
[AGARD-CP-383] N87-13273
OPTICAL FILTERS
Development of a large-aperture PLZT shutter with enhanced operational/environmental capabilities
[DE86-011643] N87-12838
OPTICAL GYROSCOPES
Fibre optic gyroscopes in inertial navigation N87-13275
Comparison of ring laser and fiber-optic gyro technology N87-13276
Closed loop fiber optic gyro N87-13277
Progress in optical fiber gyroscopes using integrated optics N87-13283
OPTICAL HETERODYNING
Optical quadrature demodulator for coherent detection and sensor applications N87-13287
OPTICAL MEASUREMENT
Advanced optical smoke meters for jet engine exhaust measurement
[NASA-CR-179459] N87-12829
OPTICAL MEASURING INSTRUMENTS
The Multispectral Atmospheric Mapping Sensor (MAMS): Instrument description, calibration and data quality
[NASA-TM-86565] N87-12828
Optical rotation sensors
[AD-A169357] N87-12848
Three dimensional optical receiver having programmable gain sensor stages
[AD-D012389] N87-13267
OPTICAL POLARIZATION
Nonlinear ellipse rotation in a low-birefringence optical fiber N87-13282
OPTICAL PROPERTIES
Digest: Proceedings of the International Conference on Optical and Millimeter Wave Propagation and Scattering in the Atmosphere
[AD-A170393] N87-12743
Optical characteristics of lightning and thunderstorm currents N87-13061
Optical characteristics of lightning N87-13062
Analysis of Doppler lidar data N87-13067
Three dimensional optical receiver having programmable gain sensor stages
[AD-D012389] N87-13267
Study to determine the feasibility of utilizing skull-melting techniques for the growth of single crystals of yttrium vanadate
[AD-A169249] N87-13320
Picosecond nonlinear resonant interactions in semiconductors
[AD-A169992] N87-13327
OPTICAL PUMPING
Iodine monofluoride energy transfer studies
[AD-A169781] N87-12852
Optical pumping of high power lasers with an array of plasma pinches
[AD-A169980] N87-12856
OPTICAL RADAR
Digest: Proceedings of the International Conference on Optical and Millimeter Wave Propagation and Scattering in the Atmosphere
[AD-A170393] N87-12743
NASA/MSFC FY-85 Atmospheric Processes Research Review
[NASA-CP-2402] N87-13043
Multiscale modeling to evaluate proposed space-based Doppler lidar sampling strategies N87-13047
Airborne Doppler measurements of the central California oceanbed sea breeze N87-13066
Analysis of Doppler lidar data N87-13067
Airborne Doppler lidar activities N87-13068
OPTICAL RESONATORS
Application of nonlinear optics to free electron laser systems
[AD-A168950] N87-12845
OPTICAL SWITCHING
Optoelectronic broadband switching for communications and signal processing N87-13294
OPTICAL TRANSFER FUNCTION
Method of fabricating high efficiency binary planar optical elements
[AD-D012374] N87-13266
OPTICAL WAVEGUIDES
Basic and applied research in the field of electronics and communications
[AD-A169029] N87-12727
Guided Optical Structures in the Military Environment
[AGARD-CP-383] N87-13273
Nonlinear planar guided wave interactions and devices N87-13290
Bistability in nonlinear waveguides N87-13291
Integrated optics optical limiters N87-13292
PIN-FET preamplifier for high-speed optical transmission systems N87-13293
Glass fibres for transmission in the 8-12 micrometers waveband N87-13297
Fluoride glasses for infrared waveguides N87-13299
Wide bandwidth, long distance fibre-optic communication systems N87-13300
Tactical fiber optic assembly requirements N87-13305
A hybrid transmission scheme on single mode fibers for tactical communications N87-13306
OPTIMAL CONTROL
Optimal descending, hypersonic turn to heading
[DE86-010969] N87-12577
Attitude control of an artificial satellite by extending the linear quadratic regulator theory
[INPE-3959-PRE/977] N87-12588
The optimal linear combination of control variates in the presence of bias
[AD-A169111] N87-13210
OPTIMIZATION
A procedure for attitude determination of artificial satellites utilizing techniques of static and dynamic optimal estimation
[INPE-3966-PRE/981] N87-12589
Design of strong, ductile, HSLA and dual phase steels
[DE86-011313] N87-12665
The continuous projective sumt method for convex programming — sequential unconstrained minimization techniques
[AD-A169847] N87-13185
Algorithm for positive definite least square estimation of parameters
[DE86-012159] N87-13225
ORBIT CALCULATION
Meter-level orbit determination of geosynchronous satellites by an economical tracking system N87-12575
ORBITAL ELEMENTS
Relative motion of the Sun on an artificial satellite
[INPE-3985-NTE/260] N87-12591
ORBITAL MECHANICS
Solar flux and geomagnetic activity prediction
[INPE-3864-PRE/934] N87-13377
ORBITAL POSITION ESTIMATION
Meter-level orbit determination of geosynchronous satellites by an economical tracking system N87-12575
ORBITAL SPACE STATIONS
The space station millimeter facility
[AD-A168983] N87-12604
Advanced EVA system design requirements study
[NASA-CR-171942] N87-13167
ORBITALS
Band description of materials with localizing orbitals
[DE86-010529] N87-13255
OREGON
AIS spectra of desert shrub canopies N87-12987
ORGANIC COMPOUNDS
Application of pattern recognition to metal ion chemical ionization mass spectra
[AD-A169061] N87-12630
ORGANIZATIONS
An examination of technology transfer as a tool for management
[AD-A169184] N87-13360
ORGANOMETALLIC COMPOUNDS
Transition metal. 2: Complexes of dithiacycloph anes
[AD-A169107] N87-12851
ORION NEBULA
Infrared reflection nebulae in Orion molecular cloud 2
[NASA-TM-88259] N87-13363
ORTHOGONALITY
The effect of coupling in an inertial navigation platform stabilized system made up of three single-degree-of-freedom gyroscopes
[AD-A169110] N87-12553
OSCILLATING CYLINDERS
In-line and transverse forces on smooth and rough cylinders in oscillatory flow at high Reynolds numbers
[AD-A169562] N87-12815
OSCILLATING FLOW
Forced oscillation of a two-dimensional airfoil with nonlinear aerodynamic loads
[AD-A169350] N87-12546
In-line and transverse forces on smooth and rough cylinders in oscillatory flow at high Reynolds numbers
[AD-A169562] N87-12815
OSCILLATIONS
An experimental investigation of free-tip response to a jet
[NASA-TM-88250] N87-12539
A detailed analysis of the influence of eddy exchange processes upon the development of radiation fog
[AD-A169233] N87-13102
OSCILLATORS
A 60 GHz gyrotron development program
[DE86-012488] N87-12791
OUTGASSING
Ionization phenomena about the space shuttle
[AD-A170542] N87-13310
OUTLIERS (STATISTICS)
Two issues concerning the analysis of grouped data
[DE86-008401] N87-13242
OXIDATION
New results on low temperature thermal oxidation of silicon
[AD-A169603] N87-12634
Diamond-machined aluminum alloy 5083 surfaces: Controlled exposure evaluation
[DE86-012572] N87-12674
Intrinsic SiO2 film stress measurements on thermally oxidized Si
[AD-A169602] N87-12935
OXIDATION RESISTANCE
Mechanical testing of a coated carbon-carbon composite at elevated temperatures in air
[AD-A169355] N87-12618
OXYGEN PLASMA
Medium- and long-wavelength infrared emission from a laser-produced oxygen plasma
[AD-A169475] N87-13309
Ionization phenomena about the space shuttle
[AD-A170542] N87-13310
OXYGEN PRODUCTION
CO sub 2 laser sustained CW discharge atomic beam source
[DE86-012383] N87-12863
OZONE
Description of data on the Nimbus 7 LIMS map archive tape: Ozone and nitric acid
[NASA-TP-2625] N87-13022
Parameterized numerical fit to total column ozone changes calculated by the LLNL 1-D model of the troposphere and stratosphere
[DE86-011006] N87-13040
Radiation flux tables for ICRCCM using the GLA GCM radiation codes
[NASA-TM-89270] N87-13098
OZONOSPHERE
Solar control of geophysical phenomena N87-12953

P

PACIFIC OCEAN
Dynamics and energetics of the South Pacific Convergence Zone during FGGE SOP-1 N87-13052

Application of satellite data to tropic/subtropic moisture coupling N87-13053
On the Walker circulation of 1983-84
[INPE-3952-PRE/971] N87-13118
PACKET SWITCHING
Carrier-sense stack algorithms for multiple access communication channels
[AD-A169774] N87-12738
PAIR PRODUCTION
Neutron and antineutron production in accretion onto compact objects
[NASA-TM-89264] N87-13395
PALLADIUM COMPOUNDS
Real-time experimental measurements of isotopic exchange between gaseous hydrogen and palladium hydride powder
[DE86-012610] N87-12644
PANEL METHOD (FLUID DYNAMICS)
A numerical model for two-dimensional unsteady flow calculations with a surface panel method N87-12548
PANELS
Carbon fibers
[AD-A171370] N87-12622
PARALLEL COMPUTERS
Solving scientific problems on hypercube parallel computers
[DE86-012622] N87-13199
PARALLEL FLOW
An approximate method of estimating the aerodynamic interference between two parallel bodies in a supersonic flow (axial force)
[BR-100271] N87-12540
PARALLEL PLATES
Input impedance of an infinite linear scanned array of flat rectangular strips inside a dielectric loaded parallel plate waveguide
[AD-A171275] N87-12784
PARALLEL PROCESSING (COMPUTERS)
Advanced teleprocessing systems
[AD-A170007] N87-12741
A VLSI-based high-performance raster image system
[AD-A169068] N87-12761
High performance parallel computing
[AD-A169961] N87-13188
Matrix factorization on a hypercube multiprocessor
[DE86-011775] N87-13193
Solving scientific problems on hypercube parallel computers
[DE86-012622] N87-13199
PARAMETER IDENTIFICATION
Evaluation of a nonlinear parameter extraction mathematical model including the term C(subm(sub delta e squared))
[NASA-TM-87731] N87-12566
PARAMETERIZATION
Parametric linear variation of a leakage free permanent magnet field source
[AD-D012359] N87-13249
PARTIAL DIFFERENTIAL EQUATIONS
Study of numerical solution methods for two-phase flows
[DE86-012265] N87-12821
Free-Lagrangian hydrodynamics using massless tracer points
[DE86-012406] N87-12822
SOR (Successive Over-Relaxation) MGR (multigrid algorithm)(nu) experiments on the crystal multicomputer
[AD-A169929] N87-13187
Some investigations into variable meshes for numerical solution of partial differential equations
[AD-A169977] N87-13206
Quantitative assessment of the effect of partial pivoting in sparse ordinary differential equation solvers
[DE86-012592] N87-13226
PARTICLE ACCELERATION
The ultraheavy cosmic rays: Propagation and selective acceleration N87-13390
The gamma-ray spectrometer experiment on the solar maximum mission satellite
[NASA-CR-177877] N87-13394
PARTICLE INTERACTIONS
Electron-electron interaction effects in quasi-one-dimensional conducting polymers and related systems
[DE86-012434] N87-12697
High energy neutrino absorption and its effects on stars in close X-ray binaries
[NASA-TM-89269] N87-13366
PARTICLE PRODUCTION
High energy neutrino absorption and its effects on stars in close X-ray binaries
[NASA-TM-89269] N87-13366
PARTICLE TELESCOPES
A versatile Data Processing Unit (DPU) for satellite-borne composition instrumentation N87-13393
PARTICLE THEORY
Theoretical high energy physics
[DE86-012669] N87-13259
PARTICLES
Solar flares and magnetospheric particles: Investigations based upon the ONR-60 experiments and ONR-604 experiments
[AD-A170620] N87-13381
PARTITIONS (STRUCTURES)
Detonation cellular structure and image proces
[DE86-006467] N87-12819
PATENT APPLICATIONS
Laser sealed vacuum insulating window
[DE86-013678] N87-12701
Li corrosion resistant glasses for headers in ambient temperature Li batteries
[DE86-013754] N87-12802
Very high efficacy electrodeless high intensity discharge lamps
[DE86-013760] N87-12803
PATTERN RECOGNITION
Application of pattern recognition to metal ion chemical ionization mass spectra
[AD-A169061] N87-12830
Concurrent ultrasonic weld evaluation system
[DE86-013772] N87-12906
Limits of pattern discrimination in human vision
[AD-A170756] N87-13135
Special associative preprocessing structures for qualitative feature extraction
[AD-A169147] N87-13181
A rule-based pattern matching system for the recognition of three-dimensional line drawn objects: A foundation for video tracking
[AD-A170701] N87-13190
On reduction of dimensionality under multivariate regression and canonical correlation models
[AD-A170025] N87-13238
Pattern recognition based on scale invariant discriminant functions
[AD-A170809] N87-13241
PAYLOAD RETRIEVAL (STS)
High voltage characteristics of the electrodynamic tether and the generation of power and propulsion
[NASA-CR-178949] N87-12809
PERCOLATION
Percolation and low density materials: Theory and applications
[AD-A169204] N87-12684
PERFORMANCE PREDICTION
Proof of feasibility of a novel inverter for photovoltaic power conditioning
[DE86-012729] N87-13001
PERFORMANCE TESTS
Modeling the fundamental characteristics and processes of the spacecraft functioning
[NASA-TM-87999] N87-12596
Fabrication and testing of lightweight hydraulic system simulator hardware
[AD-A169884] N87-12711
Fault tolerance mechanisms for a network communication multiprocessor
[INPE-3958-PRE/876] N87-12720
Lithium Ambient-Temperature Battery Reliability Program, May 1983-April 1985
[DE86-012247] N87-12789
Development of an inexpensive, high resolution positron multiwire proportional counter
[DE86-011576] N87-12841
PERIDOTITE
Abundance and distribution of mineral components associated with Moses Rock (kimberlite) diatreme N87-12975
PERIODIC VARIATIONS
On the Walker circulation of 1983-84
[INPE-3952-PRE/971] N87-13118
PERMANENT MAGNETS
Parametric linear variation of a leakage free permanent magnet field source
[AD-D012359] N87-13249
PERMUTATIONS
A unified approach to constructing nonparametric rank tests
[AD-A169815] N87-13233
PERSONAL COMPUTERS
Simulation of CIFF (Centralized IFF) remote control displays
[AD-A170387] N87-12742
PERSONNEL
Instrumentation research and support services
[AD-A169278] N87-13029
PERTURBATION
Introduction to aerodynamics derivatives, equations of motion and stability
[ESDU-86021] N87-12536
PHARMACOLOGY
Pharmacological resetting of the circadian sleep-wake cycle
[AD-A170804] N87-13137
PHASE CHANGE MATERIALS
Phase change thermal energy storage methods for combat vehicles, phase 1
[AD-A170492] N87-12713
Stefan-type problem with void formation and its explicit solution
[DE86-013521] N87-13007
PHASE COHERENCE
Optical quadrature demodulator for coherent detection and sensor applications N87-13267
PHASE CONJUGATION
Application of nonlinear optics to free electron laser systems
[AD-A168660] N87-12845
PHASE CONTROL
Method and apparatus for rapid optical phasing
[AD-D012412] N87-13270
PHASE DEMODULATORS
Optical quadrature demodulator for coherent detection and sensor applications N87-13267
PHASE DETECTORS
Optical quadrature demodulator for coherent detection and sensor applications N87-13267
PHASE DIAGRAMS
Cellular solidification of transparent monotectics
[NASA-CR-177039] N87-12626
Phase equilibrium predictions for polar and hydrogen bonding mixtures
[DE86-011812] N87-12642
Stefan-type problem with void formation and its explicit solution
[DE86-013521] N87-13007
PHASE SHIFT
Phase fluctuations of ionosphere radio signals N87-12955
PHASE TRANSFORMATIONS
On the interplay between chemical reactions and phase transitions for molecules adsorbed on solid surfaces
[AD-A169818] N87-12636
The influence of welding flux on the pyrometallurgical, physical and mechanical behavior of weld metal
[AD-A169067] N87-12650
APFIM studies of phase transformations
[DE86-006533] N87-12663
Computation of residual stresses due to phase transformations during quenching of hollow cylinders
[AD-A170493] N87-12937
Stefan-type problem with void formation and its explicit solution
[DE86-013521] N87-13007
Plasma-enhanced deposition and processing of transition metals and transition metal silicides for VLSI
[AD-A168963] N87-13316
Possibility of using dc conductivity for investigating phase transition in amorphous semiconductors
[DE86-702646] N87-13340
Astro-particle-physics
[DE86-702946] N87-13373
PHASED ARRAYS
Phased arrays 1985 symposium: Proceedings
[AD-A169316] N87-12732
Multi-element adaptive antenna array
[AD-D012410] N87-12740
Twin aperture phased array lens antenna
[AD-D012415] N87-12745
Temperature and frequency compensated array beam steering unit
[AD-D012365] N87-12767
PHONETICS
The effects of high sustained acceleration on the acoustic phonetic structure of speech: A preliminary investigation
[AD-A170563] N87-12746
PHOSPHORUS
Crack-tip chemistry and fracture mechanics-based model of the crack growth rate/stress intensity relationship for Ni + P
[DE86-011106] N87-12576
PHOTOABSORPTION
Electron-electron interaction effects in quasi-one-dimensional conducting polymers and related systems
[DE86-012434] N87-12697
PHOTOCATHODES
Theory and simulation of high-brightness electron beam production from laser-irradiated photocathodes in the presence of dc and RF electric fields
[DE86-012384] N87-12664
PHOTOCHEMICAL REACTIONS
Heterogeneous catalysis with lasers
[AD-A169601] N87-12851

Parameterized numerical fit to total column ozone changes calculated by the LLNL 1-D model of the troposphere and stratosphere
[DE86-011006] N87-13040

PHOTODECOMPOSITION
Fragmentation dynamics of energetic materials
[AD-A168925] N87-12682

PHOTODIODES
Theory and simulation of high-brightness electron beam production from laser-irradiated photocathodes in the presence of dc and RF electric fields
[DE86-012364] N87-12664
PIN-FET preamplifier for high-speed optical transmission systems N87-13293

PHOTOELECTRIC EFFECT
Study in molecular lasers
[AD-A169933] N87-12655

PHOTOELECTRIC EMISSION
Photoemission from oblate silver spheroids with polarized vacuum UV excitation
[DE86-008696] N87-13256

PHOTOELECTROCHEMISTRY
A study of energy conversion devices using photoactive organometallic electrocatalysts
[AD-A169096] N87-12996

PHOTOGRAPHIC EQUIPMENT
Photographic sensors: Basic concepts
[INPE-3990-MD/031] N87-12966

PHOTOGRAPHY
Detonation cellular structure and image proces
[DE86-008467] N87-12819

PHOTOINTERPRETATION
Patterns of vegetation in the Owens Valley, California N87-12966

PHOTOIONIZATION
Laser produced X-ray for high resolution lithography and a photoionization laser
[AD-A170782] N87-12658

PHOTOLITHOGRAPHY
High resolution optical fiber print head
[AD-D012384] N87-12633
Laser produced X-ray for high resolution lithography and a photoionization laser
[AD-A170782] N87-12658
Performance of integrated optical frequency shifters pigtailed to high birefringence fibres using ion-milled grooves N87-13289

PHOTONS
Fragmentation dynamics of energetic materials
[AD-A168925] N87-12682
Resonant photon pumping mechanisms for a plasma X-ray laser
[AD-D012416] N87-12657
The secondary production of gamma rays in the Jovian magnetosphere N87-13391

PHOTORECEPTORS
Limits of pattern discrimination in human vision
[AD-A170756] N87-13135

PHOTOSPHERE
Rapid fluctuations in solar flares
[NASA-CR-179894] N87-13387

PHOTOVOLTAIC CELLS
Solid State Photovoltaic Research Branch annual report, FY 1985
[DE86-010706] N87-13004
Photovoltaic Concentrator Technology Project, Fourteenth Project Integration Meeting, June 10-11, 1986
[DE86-012051] N87-13006

PHOTOVOLTAIC CONVERSION
Proof of feasibility of a novel inverter for photovoltaic power conditioning
[DE86-012729] N87-13001

PHOTOVOLTAIC EFFECT
Status and future of government-supported amorphous silicon research in the US
[DE86-010702] N87-12997

PHYSICAL FITNESS
Self-paced heat acclimation procedures
[AD-A170533] N87-13134

PHYSIOLOGICAL EFFECTS
Crew factors in flight operations. Part 3: The operational significance of exposure to short-haul air transport operations
[NASA-TM-88322] N87-13122
Mechanical transduction: Unification
[AD-A171191] N87-13123
Application of heart rate measurements to maritime research simulator
[AD-A169988] N87-13132

PHYSIOLOGICAL RESPONSES
Analysis of head and neck dynamic response of the US adult military population
[AD-A169563] N87-13129
Human thermoregulatory model for immersion in cold water
[AD-A169779] N87-13131

PHYSIOLOGY
Advanced EVA system design requirements study
[NASA-CR-171942] N87-13167

PICOSECOND PULSES
Picosecond optoelectronic diagnostics of field effect transistors
[AD-A170503] N87-12779

PIEZOELECTRICITY
SAW transduction in electrostrictive substrates
[DE86-011651] N87-12794

PILOT ERROR
Aircraft accident report: Bar Harbor Airlines Flight 1808, Beech BE-99, N300WP, Auburn-Lewiston Municipal Airport, Auburn, Maine, August 25, 1985
[PB86-910406] N87-12550

PILOT PERFORMANCE
Simulator design and instructional features for carrier landing: A field transfer study
[AD-A169962] N87-12573
The Flight Service Station Training Program: 1981-1985
[AD-A171485] N87-13145
Application of the task taxonomy method to the simulation of human service reliability in the manual control of aircraft
[MBB/LKE-301/S/PUB/216] N87-13151

PILOT TRAINING
Simulator design features for helicopter landing on small ships. 1: A performance study
[AD-A169514] N87-12572
Simulator design and instructional features for carrier landing: A field transfer study
[AD-A169962] N87-12573
The Flight Service Station Training Program: 1981-1985
[AD-A171485] N87-13145

PIPE FLOW
Fluid transients in pipes. Estimation of maximum pressures and forces in steam lines
[ESDU-86015] N87-12805

PIPELINING (COMPUTERS)
ERS-1 SAR data processing
[NASA-CR-179913] N87-12965

PIPES (TUBES)
Pressure calculation for two-dimensional flow inside hydraulic structures
[AD-A169039] N87-12812
Gas tungsten arc welding of chromium-nickel steel to nickel-molybdenum-chromium-iron. Welding procedure specification. Supplement 1: Records of procedure qualification tests
[DE86-012550] N87-12895
Welding procedure specification: Gas tungsten arc welding of nickel to nickel-chromium-iron. Supplement 1: Records of procedure qualification tests
[DE86-012557] N87-12896
Gas tungsten arc welding of aluminum alloys 3004, 5052 and 5x54 to 6xxx. Welding procedure specification. Supplement 1: Records of procedure qualification tests
[DE86-012561] N87-12897

PISTON ENGINES
Diesel cylinder gas-side heat flux to a ceramic surface
[AD-A168948] N87-12870
Linear harmonic analysis of free-piston Stirling engines
[DE86-012451] N87-12903

PITCH (MATERIAL)
Process for carbon-carbon composite fabrication
[AD-D012413] N87-12621
Effects of graphitization on the environmental stability of brominated pitch-based fibers
[NASA-TM-88899] N87-12679

PITCHING MOMENTS
Forced oscillation of a two-dimensional airfoil with nonlinear aerodynamic loads
[AD-A169350] N87-12546

PITTING
Initiation of pitting corrosion in martensitic stainless steels
[DE86-007627] N87-12661

PLANE WAVES
Computer programs for electromagnetic scattering from a slotted TM cylindrical conductor by the pseudo-image method
[AD-A169016] N87-12725
Two-dimensional beamforming using a frequency domain complex Least Mean-Squares (LMS) adaptive filter
[AD-A171396] N87-12785
Influence of shear modulus on the behavior of acoustically transparent materials
[AD-A169289] N87-12931

PLANTS (BOTANY)
Trace element-induced stress in freshwater wetland vegetation: Preliminary results N87-12985
Characterization of information requirements for studies of CO2 effects: Water resources, agriculture, fisheries, forests and human health
[DE86-012477] N87-13010
Direct effects of atmospheric CO2 enrichment on plants and ecosystems: A bibliography with abstracts
[DE86-013525] N87-13012

PLASMA CLOUDS
Ionization phenomena about the space shuttle
[AD-A170542] N87-13310

PLASMA COMPRESSION
Modeling of high-explosive driven plasma compression opening switches
[DE86-012421] N87-12795

PLASMA CONTROL
Tara vacuum system
[DE86-011873] N87-13311

PLASMA DENSITY
Optical pumping of high power lasers with an array of plasma pinches
[AD-A169960] N87-12656

PLASMA DIAGNOSTICS
MAX '91: An advanced payload for the exploration of high energy processes on the active sun
[NASA-TM-89271] N87-13379

PLASMA DYNAMICS
Magnetospheric plasma studies using data from the dynamics explorer high and low altitude plasma instruments
[AD-A169010] N87-13027

PLASMA FOCUS
Optical pumping of high power lasers with an array of plasma pinches
[AD-A169960] N87-12656

PLASMA INTERACTIONS
Ionization phenomena about the space shuttle
[AD-A170542] N87-13310

PLASMA JETS
Plasma-enhanced deposition and processing of transition metals and transition metal silicides for VLSI
[AD-A168963] N87-13316

PLASMA PHYSICS
Space plasma research
[NASA-CR-178985] N87-13307

PLASMA PINCH
Optical pumping of high power lasers with an array of plasma pinches
[AD-A169960] N87-12656

PLASMA PUMPING
Tara vacuum system
[DE86-011873] N87-13311

PLASMA RADIATION
Models and radiation of railgun plasma armatures with non-ideal plasma properties
[AD-A169349] N87-13258
Rapid fluctuations in solar flares
[NASA-CR-179894] N87-13387

PLASMA WAVES
Two-dimensional dynamics of the plasma Wakefield accelerator
[DE86-012382] N87-13312

PLASMAS (PHYSICS)
Plasma assisted surface coating/modification processes: An emerging technology
[NASA-TM-88885] N87-12708
A variational principle for the plasma centrifuge
[INPE-3989-PRE/992] N87-12827
Two-dimensional dynamics of the plasma Wakefield accelerator
[DE86-012382] N87-13312
Large-scale electric fields resulting from magnetic reconnection in the corona
[DE86-012391] N87-13383

PLASMASPHERE
Magnetospheric plasma studies using data from the dynamics explorer high and low altitude plasma instruments
[AD-A169010] N87-13027

PLASTIC DEFORMATION
Effect of hydrogen on the mechanical properties and fracture behavior of high purity aluminum
[AD-A171214] N87-12658

PLASTIC FLOW
Feasibility study of test problems for finite element/finite difference programs for structural dynamics
[AD-A169058] N87-12928

PLASTIC PROPERTIES
MAGNA (Materially And Geometrically Nonlinear Analysis). Addendum 1, parts 1-4
[AD-A169383] N87-12933

PLASTICIZERS
Preparation of energetic compounds
[AD-A170022] N87-12704

PLASTICS
Carbon fibers
[AD-A171370] N87-12622
PLATEAUS
Remote sensing of severe convective storms N87-13075
PLATINUM
Electrochemistry in near-critical and supercritical fluids. 3: Studies of Br(-), I(-) and hydroquinone in aqueous solutions
[AD-A169138] N87-12633
PLOTTERS
Using 3-dimensional graphics to visualize multivariate scientific data
[DE86-010788] N87-13195
PLOTTING
Using 3-dimensional graphics to visualize multivariate scientific data
[DE86-010788] N87-13195
PNEUMATIC CONTROL
Rapid acting electro-pneumatic anti-G suit control valve
[AD-D012377] N87-13170
POISSON DENSITY FUNCTIONS
Extremal processes, record times and strong approximation
[AD-A169972] N87-13237
POLAR CAPS
Coordinated radar and satellite studies of ionospheric currents in the auroral zone and polar cap
[AD-A169466] N87-13031
POLAR REGIONS
Coordinated radar and satellite studies of ionospheric currents in the auroral zone and polar cap
[AD-A169466] N87-13031
Relief and geology of the north polar region of the planet Venus
[NASA-TM-88498] N87-13378
POLARIMETERS
Magnetic and pressure sensors using the compensated polarimetric sensor configuration N87-13279
POLARIZATION (CHARGE SEPARATION)
Semiconductor/insulator films for corrosion protection
[AD-A169119] N87-12652
POLARIZATION (WAVES)
Electrode/electrolyte interphase study using polarization modulated FT-IR reflection absorption spectroscopy
[AD-A169081] N87-12631
Photoemission from oblate silver spheroids with polarized vacuum UV excitation
[DE86-008896] N87-13256
POLARIZED ELECTROMAGNETIC RADIATION
Propagation of electromagnetic waves in superlattices
[DE86-702660] N87-12753
Investigations of long-period DQ Herculis star N87-13364
POLICIES
Report of the Ad-Hoc Commission on remote sensing
[INPE-3981-NTE/259] N87-12963
Technology transfer at Pacific Northwest Laboratory
[DE86-012333] N87-13361
POLLUTION CONTROL
Southern California Air Quality Study (SCAQS) suggested program plan
[PB86-223427] N87-13013
POLLUTION TRANSPORT
Study of the formation and transport of acidic species by non-precipitating cumulus clouds during VENTEX-84
[PB86-220357] N87-13014
POLYACETYLENE
Physical characteristics of diblock polyacetylene copolymers: Processability-conductivity correlation
[DE86-011218] N87-12695
Effect of chain rigidity on conductivity of conjugated polymers
[DE86-011263] N87-12696
POLYCRYSTALS
Microchemical analysis of polycrystalline Ni3Al and other ordered alloys using the field-ion microscope atom probe
[DE86-013157] N87-12677
Stable, high-efficiency, CuInSe2-based polycrystalline thin-film tandem solar cells
[DE86-010705] N87-13003
POLYGONS
A computational method to model radar return range in a polygonally based, computer-generated-imagery simulation
[NASA-TM-88324] N87-12967
POLYIMIDES
Investigation of the effects of short chain processing additives on polymers
[NASA-TM-89023] N87-12614
POLYMER CHEMISTRY
Coupled damage and moisture-transport in fiber-reinforced polymeric composites
[AD-A169379] N87-12619
A study of energy conversion devices using photoactive organometallic electrocatalysts
[AD-A169096] N87-12996
POLYMERIC FILMS
A study of energy conversion devices using photoactive organometallic electrocatalysts
[AD-A169096] N87-12996
POLYMERIZATION
Electrokinetic properties of polymer colloids
[NASA-CR-178938] N87-12681
Effect of chain rigidity on conductivity of conjugated polymers
[DE86-011263] N87-12696
Epitaxial crystallization and epitaxial polymerization as tools for molecular engineering
[AD-A171506] N87-13333
POLYMERS
Electron-electron interaction effects in quasi-one-dimensional conducting polymers and related systems
[DE86-012434] N87-12697
POLYNOMIALS
Matrix theory
[AD-A169139] N87-13247
POLYPROPYLENE
Zinc/nickel oxide battery membrane separator studies
[DE86-012824] N87-12793
POLYSTYRENE
Electrokinetic properties of polymer colloids
[NASA-CR-178938] N87-12681
Physical characteristics of diblock polyacetylene copolymers: Processability-conductivity correlation
[DE86-011218] N87-12695
POPULATION INVERSION
Population inversions in laser-initiated vacuum arcs
[AD-A170811] N87-12859
POROSITY
Viscous-inviscid interaction in transonic separated flow over solid and porous airfoils and cascades N87-12535
POROUS MATERIALS
Process for carbon-carbon composite fabrication
[AD-D012413] N87-12621
Application of flux-corrected transport (FCT) to high Rayleigh number natural convection in a porous medium
[DE86-004603] N87-12818
PORTS (OPENINGS)
Effect of port corner geometry on the internal performance of a rotating-vane-type thrust reverser
[NASA-TP-2624] N87-12541
Viewport concept for space station modules
[NASA-TM-86559] N87-12592
POSITION (LOCATION)
Severe storm electricity N87-13056
Storm severity detection (RF) N87-13057
Lightning mapper and the future N87-13059
Detection of rotating thunderstorms using satellite imagery N87-13065
POTENTIAL ENERGY
Circuit considerations for repetitive railguns
[DE86-012369] N87-12752
Molecular dynamic studies of crack propagation. The role of the interatomic potential
[DE86-009942] N87-12942
Available potential energy in upper layer of world ocean N87-12949
POWDER (PARTICLES)
Real-time experimental measurements of isotopic exchange between gaseous hydrogen and palladium hydride powder
[DE86-012610] N87-12644
Hot isostatic pressing of ceramic powder compacts
[AD-A169971] N87-12688
POWDER METALLURGY
A fundamental study of P/M processed elevated temperature aluminum alloys
[AD-A170697] N87-12657
POWDERED ALUMINUM
Plasma joining of metal matrix composites
[AD-A169056] N87-12615
Fatigue behavior of long and short cracks in wrought and powder aluminum alloys
[AD-A169980] N87-12656
POWER CONDITIONING
Proof of feasibility of a novel inverter for photovoltaic power conditioning
[DE86-012729] N87-13001
PREAMPLIFIERS
PIN-FET preamplifier for high-speed optical transmission systems N87-13293
PRECESSION
Low Q spin-up from rest
[AD-A169106] N87-12813
PRECIPITATION
Severe storm detection with passive 37 GHz observations N87-13072
LAMPS software and mesoscale prediction studies N87-13076
Preliminary planning for the Satellite Precipitation And Cloud Experiment (SPACE) Field Program N87-13089
PRECIPITATION (METEOROLOGY)
Station climatic summaries, Europe
[AD-A167888] N87-13100
Improving numerical weather prediction by maximizing the use of assimilated satellite data
[AD-A169295] N87-13104
Revised Uniform Summary of Surface Weather Observations (RUSSWO). Parts A-F, Fort Richardson, Alaska
[AD-A169390] N87-13106
Some proposals for modifying the Probability of Precipitation Program of the National Weather Service
[PB86-226636] N87-13115
PREDICTION ANALYSIS TECHNIQUES
Crack-tip chemistry and fracture mechanics-based model of the crack growth rate/stress intensity relationship for Ni + P
[DE86-011106] N87-12676
Reliability prediction models for mechanical equipment
[AD-A169775] N87-12911
Conversion of the NOLAPS (Navy Operational Local Atmospheric Prediction System) model to the HP9845
[AD-A169536] N87-13108
Computer-based estimation procedure for coaxial jet noise. Including far-field subsonic jet mixing noise database for stationary, coplanar conical nozzles
[ESDU-86019] N87-13251
Quantum chemical investigations of the mechanism of cationic polymerization and theoretical prediction of crystal densities and decomposition pathways of energetic molecules
[AD-A169805] N87-13324
Regression models of quarterly overhead costs for six government aerospace contractors
[AD-A169185] N87-13350
Solar flux and geomagnetic activity prediction
[INPE-3864-PRE/934] N87-13377
PREDICTIONS
Research on mechanical properties for engine life prediction
[AD-A169570] N87-12563
Advanced solar dynamic space power systems perspectives, requirements and technology needs
[NASA-TM-88884] N87-12606
Some proposals for modifying the Probability of Precipitation Program of the National Weather Service
[PB86-226636] N87-13115
Effects of reduced spatial resolution on the NEXRAD storm sequence algorithms
[PB86-221728] N87-13117
PREPROCESSING
Special associative preprocessing structures for qualitative feature extraction
[AD-A169147] N87-13181
PRESSES
TDD antenna: Foil formed, substrate loaded laser welded assembly
[AD-D012411] N87-12712
PRESSURE DISTRIBUTION
Pressure calculation for two-dimensional flow inside hydraulic structures
[AD-A169039] N87-12612
PRESSURE EFFECTS
Optical spectroscopy of dynamically compressed liquids
[AD-A169013] N87-12629
PRESSURE MEASUREMENT
High accuracy standards and reference methodology for carbon dioxide in air
[DE86-012643] N87-13011
PRESSURE OSCILLATIONS
Fluid transients in pipes. Estimation of maximum pressures and forces in steam lines
[ESDU-86015] N87-12605
PRESSURE SENSORS
Supplementary calibration test of the tip-aerodynamics-and acoustics-test pressure transducers
[NASA-TM-88312] N87-12630
Magnetic and pressure sensors using the compensated polarimetric sensor configuration N87-13279
PRESSURE SUITS
Rapid acting electro-pneumatic anti-G suit control valve
[AD-D012377] N87-13170
Improved anti-G suit
[AD-D012378] N87-13171
PRESSURE VESSELS
Welding procedure specification. Manual gas tungsten arc and semiautomatic gas metal arc welding of chromium-nickel steel. Supplement 1: Records of procedure qualification tests
[DE86-012521] N87-12886

Welding procedure specification. Semiautomatic gas metal arc welding of carbon steels. Supplement 1: Records of procedure qualification tests
[DE86-012531] N87-12888
Welding procedure specification. Manual gas tungsten arc and semiautomatic gas metal arc welding of carbon steel. Supplement 1: Records of procedure qualification tests
[DE86-012532] N87-12889
Welding procedure specification. Gas tungsten arc welding of chromium-nickel steel to chromium-molybdenum steel. Supplement 1: Records of procedure qualification tests
[DE86-012536] N87-12892
Buttered explosions in steel pressure vessels
[DE86-006763] N87-12898

PRIMARY BATTERIES
Lithium Ambient-Temperature Battery Reliability Program, May 1983-April 1985
[DE86-012247] N87-12789

PRIMATES
Radiographic determination of mass and inertial tensor of anatomical segments
[AD-A169122] N87-13126

PRINTED CIRCUITS
Review of robotic component insertion system for printed wiring assemblies
[DE86-013510] N87-12907

PRINTERS
High resolution optical fiber print head
[AD-D012384] N87-12833

PRINTERS (DATA PROCESSING)
Utilization of impact dot matrix printers
[INPE-3991-RPE/518] N87-13173

PRINTING
High resolution optical fiber print head
[AD-D012384] N87-12833

PROBABILITY DENSITY FUNCTIONS
Characteristics of atmospheric turbulence near the ground. Part 3: Variations in space and time for strong winds (neutral atmosphere)
[ESDU-86010-PT-3] N87-13042

PROBABILITY DISTRIBUTION FUNCTIONS
A reversal argument for storage models defined on semi-Markov processes
[AD-A169262] N87-13232
Pattern recognition based on scale invariant discriminant functions
[AD-A170809] N87-13241

PROBABILITY THEORY
Inequalities for probability contents of convex sets via geometric average
[AD-A169938] N87-13219
Extremal processes, record times and strong approximation
[AD-A169972] N87-13237
A Bayesian approach to quantile and response probability estimation with applications in reliability
[AD-A170455] N87-13240

PROBLEM SOLVING
SSME main injector 4000 Hertz phenomenon
[NASA-CR-178934] N87-12608
A finite element method for localized failure analysis
[AD-A169117] N87-12930
An implicit enumeration algorithm with binary-valued constraints
[AD-A169258] N87-13182
SOAR user's manual
[AD-A169005] N87-13204
Performance analysis of some numerical algorithms in the resolution of ODEs artificial satellite problems
[INPE-3996-PRE/995] N87-13206
Federal information systems management: Problems, solutions and more problems
[AD-A171366] N87-13353

PROCEDURES
Collection of ions in the stratosphere
[AD-A169905] N87-13032

PROCESS CONTROL (INDUSTRY)
NDE reliability and process control for structural ceramics
[NASA-TM-88870] N87-12910
System-ergonomic workload analysis for highly automated process control tasks N87-13152

PRODUCTION ENGINEERING
Welding research in Scandinavia: An assessment
[AD-A169036] N87-12871

PRODUCTIVITY
Quality management: An annotated bibliography
[AD-A169816] N87-12912

PROFILOMETERS
An analysis of the acoustic characteristics of ABSS (acoustic backscatter system) and its deployments
[AD-A170487] N87-13037

PROGRAM VERIFICATION (COMPUTERS)
Proceedings of the IDA Workshop on Formal Specification and Verification of Ada (trade name) (1st) held in Alexandria, Virginia on 18-20 March 1985
[AD-A171507] N87-13192

PROGRAMMING LANGUAGES
Interpretive model for a concurrency method
[DE86-012743] N87-13197
Survey of the characteristics of very high level languages
[DE86-012240] N87-13196

PROJECT MANAGEMENT
Department of Housing and Urban Development-Independent agencies appropriations for 1987, part 7
[GPO-61-970] N87-13357

PROJECTILES
Stability of liquid-filled projectiles with unusual coning frequencies
[AD-A171460] N87-12584
Circuit considerations for repetitive railguns
[DE86-012369] N87-12752
Duel between an ASAT (anti-satellite) with multiple kill vehicles and a space-based weapons platform with kinetic energy weapons
[AD-A168946] N87-13245

PROMINENCES
Magnetic field re-arrangement after prominence eruption
[DE86-012393] N87-13362

PROPELLER EFFICIENCY
Propellor/body interaction for thrust and drag
[ESDU-86017] N87-12537

PROPELLERS
Propellor/body interaction for thrust and drag
[ESDU-86017] N87-12537

PROPORTIONAL COUNTERS
Development of an inexpensive, high resolution positron multiwire proportional counter
[DE86-011576] N87-12841

PROPRIOCEPTION
Mechanical transduction: Unification
[AD-A171191] N87-13123

PROTECTIVE COATINGS
Semiconductor/insulator films for corrosion protection
[AD-A169119] N87-12652
Plasma assisted surface coating/modification processes: An emerging technology
[NASA-TM-88885] N87-12706

PROTON BEAMS
Radiation-induced segregation to grain boundaries in a Ni-Si alloy
[DE86-010027] N87-12664

PROTON FLUX DENSITY
The secondary production of gamma rays in the Jovian magnetosphere N87-13391

PROTOSTARS
The stellar upper mass limit in an OB association and implications for cosmic rays and cosmic abundances N87-13392

PROTOTYPES
A VLSI-based high-performance raster image system
[AD-A169068] N87-12761
The evaluation of a number of prototypes for the free-tip rotor constant-moment controller
[NASA-TM-88864] N87-12869
Development of a sensitive superconducting gravity gradiometer for geological and navigational applications
[NASA-CR-4011] N87-13021

PSYCHOPHYSIOLOGY
Limits of pattern discrimination in human vision
[AD-A170756] N87-13135

PULSE CODE MODULATION
Pulse Code Modulation (PCM) data storage and analysis using a microcomputer
[NASA-TP-2629] N87-12718

PULSE COMMUNICATION
Foreground effects on troposcatter digital communication systems
[AD-A169380] N87-12734

PULSE GENERATORS
Coordinated research program in pulsed power physics
[AD-A169113] N87-12762
Nanosecond spark gap switching measurements
[DE86-012279] N87-12790
Transformers for explosive pulsed power coupling to various loads
[DE86-012425] N87-12796

PULSED LASERS
Picosecond nonlinear resonant interactions in semiconductors
[AD-A170813] N87-13330

PULSED RADIATION
Kinetic and thermodynamic studies of pulsed laser irradiation
[DE86-012175] N87-12860
Repetition rates of fast pulses in MM-waves/X-ray solar bursts
[INPE-3974-PRE/966] N87-13378
Rapid fluctuations in solar flares
[NASA-CR-179694] N87-13387

PURIFICATION
Importance of interfacial phenomena in separation science and technology
[DE86-011063] N87-12837

PURITY
Effect of hydrogen on the mechanical properties and fracture behavior of high purity aluminum
[AD-A171214] N87-12658

PYRANOMETERS
Studies of humid continental haze during SPACE N87-13088

PYROLYSIS
Production of a clean carbon fuel derived from coal for use in stationary and mobile heat engines
[DE86-011203] N87-12706

PYROMETALLURGY
The influence of welding flux on the pyrometallurgical, physical and mechanical behavior of weld metal
[AD-A169067] N87-12650

PYROTECHNICS
Effects of variables upon pyrotechnically induced shock response spectra
[NASA-TP-2603] N87-12921

Q

Q FACTORS
Low Q spin-up from rest
[AD-A169106] N87-12813
Lg wave excitation and propagation in presence of one-, two-, and three-dimensional heterogeneities
[AD-A169325] N87-13030

QUADRATIC PROGRAMMING
User's guide for NPSOL (version 4.0): A Fortran package for nonlinear programming
[AD-A169115] N87-13180
An implicit enumeration procedure for the general linear complementarity problem
[AD-A170397] N87-13189
Single-phase method for quadratic programming
[DE86-012156] N87-13194

QUALIFICATIONS
Machine gas metal arc welding of carbon steel. Welding procedure specification. Supplement 1: Records of procedure qualification tests
[DE86-012530] N87-12887
Welding procedure specification. Semiautomatic gas metal arc welding of carbon steels. Supplement 1: Records of procedure qualification tests
[DE86-012531] N87-12888
Welding procedure specification. Manual gas tungsten arc and semiautomatic gas metal arc welding of carbon steel. Supplement 1: Records of procedure qualification tests
[DE86-012532] N87-12889
Gas tungsten arc and shielded metal arc welding of carbon steel. Welding procedure specification. Supplement 1: Records of procedure qualification tests
[DE86-012533] N87-12890
Welding procedure specification. Supplement 1: Records of procedure qualification tests. Shielded metal arc welding of carbon steel
[DE86-012535] N87-12891
Welding procedure specification. Gas tungsten arc welding of chromium-nickel steel to chromium-molybdenum steel. Supplement 1: Records of procedure qualification tests
[DE86-012536] N87-12892

QUALITY CONTROL
NASA's quality assurance program
[GPO-83-142] N87-12909
Photovoltaic Concentrator Technology Project, Fourteenth Project Integration Meeting, June 10-11, 1986
[DE86-012051] N87-13006
Quality assessment and control of finite element solutions
[NASA-TM-89208] N87-13227

QUANTILES
A Bayesian approach to quantile and response probability estimation with applications in reliability
[AD-A170455] N87-13240

QUANTUM CHEMISTRY
Heterogeneous catalysis with lasers
[AD-A169601] N87-12851

Quantum chemical investigations of the mechanism of cationic polymerization and theoretical prediction of crystal densities and decomposition pathways of energetic molecules
[AD-A169805] N87-13324

QUANTUM CHROMODYNAMICS
Theoretical high energy physics
[DE86-012669] N87-13259

QUANTUM ELECTRODYNAMICS
Quantum 1/F noise in solid state doubin devices, in particular Hg(1-x)CdxTe diodes
[AD-A171436] N87-13332

QUANTUM THEORY
Metrics of closed world of Friedmann, agitated by electric charge (towards a theory electromagnetic Friedmann's)
[AD-A168981] N87-12723
Heterogeneous catalysis with lasers
[AD-A169601] N87-12851
Induced quantum torsion
[DE86-702616] N87-13348
Canonical quantization of gravity
[DE86-702615] N87-13372

QUARTZ
Double-ended tuning fork quartz accelerometer
[DE86-012277] N87-12842
Quartz growth on X-seeds
[AD-D012269] N87-13315

QUASARS
Continuum radiation from active galactic nuclei: A statistical study
[NASA-CR-179925] N87-13368

QUENCHING (COOLING)
Shower and high-pressure oil temperature control
[DE86-009398] N87-12699

QUEUEING THEORY
Advanced teleprocessing systems
[AD-A170007] N87-12741
Heredity of stationary and reversible stochastic processes
[AD-A169926] N87-13234
Extreme values of birth and death processes and queues
[AD-A169932] N87-13235

R

RABBITS
Hypothermic effects on vascular contractility and reactivity
[AD-A169142] N87-13127

RADAR
Surface correlation relationships in rough surface scattering
[AD-A169327] N87-12733

RADAR CROSS SECTIONS
Radar cross-section of damped cylinders and dielectric strips
[AD-A169027] N87-12726
Surface correlation relationships in rough surface scattering
[AD-A169327] N87-12733

RADAR DETECTION
Improving foF2 prediction for the sunrise transition period
[AD-A170457] N87-13036
Obstacle-warning radar for helicopters N87-13149

RADAR ECHOES
Deep convection in mesoscale convective systems N87-13055

RADAR EQUIPMENT
Tracking servo compensator with rate aiding
[AD-D012388] N87-12735

RADAR IMAGERY
A new method of synthetic aperture radar image reconstruction using modified convolution back-projection algorithm
[AD-A170652] N87-12747
A computational method to model radar return range in a polygonally based, computer-generated-imagery simulation
[NASA-TM-88324] N87-12967

RADAR MAPS
A computational method to model radar return range in a polygonally based, computer-generated-imagery simulation
[NASA-TM-88324] N87-12967

RADAR MEASUREMENT
Proceedings of the Workshop on Atmospheric Tides, Prague, Czechoslovakia, August 14, 1985 N87-13017
Coordinated radar and satellite studies of ionospheric currents in the auroral zone and polar cap
[AD-A169466] N87-13031

RADAR RANGE
A computational method to model radar return range in a polygonally based, computer-generated-imagery simulation
[NASA-TM-88324] N87-12967
Three dimensional optical receiver having programmable gain sensor stages
[AD-D012369] N87-13267

RADAR SCATTERING
Surface correlation relationships in rough surface scattering
[AD-A169327] N87-12733

RADAR TRACKING
Tracking servo compensator with rate aiding
[AD-D012388] N87-12735
A rule-based pattern matching system for the recognition of three-dimensional line drawn objects: A foundation for video tracking
[AD-A170701] N87-13190

RADAR TRANSMISSION
Method of ray intensity calculation as applied to anomalous propagation
[AD-A169553] N87-12737

RADIANT FLUX DENSITY
Radiation flux tables for ICRCCM using the GLA GCM radiation codes
[NASA-TM-89270] N87-13098

RADIATION ABSORPTION
High energy neutrino absorption and its effects on stars in close X-ray binaries
[NASA-TM-89269] N87-13366

RADIATION BELTS
Characterization of the gamma radiation in space and in the atmosphere
[DE86-013445] N87-13397

RADIATION DAMAGE
Kinetics and mechanisms on the molecular beam etching of semiconductors
[AD-A171360] N87-13331

RADIATION DETECTORS
X-ray data booklet, revision
[DE86-012650] N87-13272

RADIATION DOSAGE
Biological and clinical dosimetry, July 1, 1984 to December 31, 1984
[DE86-006947] N87-13138

RADIATION EFFECTS
Densification of graphites by irradiation
[DE86-010026] N87-12698
Metals and Ceramics Division Materials Sciences Program
[DE86-013512] N87-12699
A simple solar, spectral model for studying the effects of cloud cover and surface albedo on the incoming solar radiation
[AD-A171284] N87-13038
Physical interaction of 1-Hz to 100 kHz electric and magnetic fields with living organisms
[DE86-012323] N87-13139
Fiber optics: A survivable and cost-effective transmission medium for terrestrial networks N87-13302

RADIATION MEASUREMENT
Measurement and calculation of the Stokes or Mueller matrix for the scattering of electromagnetic radiation from irregular particles
[AD-A171502] N87-12749

RADIATION PROTECTION
Space nuclear safety program
[DE86-012767] N87-13261

RADIATION SHIELDING
Extraterrestrial forcing, atmospheric electricity and the occurrence of thunderstorms
[AD-A170463] N87-13111

RADIATION SOURCES
Efficient, monochromatic, high-power microwave generator
[DE86-012385] N87-12792

RADIATIVE HEAT TRANSFER
Relationship of in-cylinder gaseous and particulate concentration to radiative heat transfer in direct injection-type diesel combustion
[AD-A168979] N87-12628

RADIATIVE TRANSFER
A simple solar, spectral model for studying the effects of cloud cover and surface albedo on the incoming solar radiation
[AD-A171284] N87-13038

RADIO ASTRONOMY
The space station millimeter facility
[AD-A168983] N87-12604

RADIO BEACONS
Medium-frequency data link for differential NAVSTAR/GPS broadcasts
[AD-A169788] N87-12554
SARSAT (Search and Rescue Satellite) operational data categorization and accuracy studies
[AD-A169748] N87-12589

RADIO FREQUENCIES
Stabilizing effects of finite-amplitude RF waves on the interchange instability
[DE86-013042] N87-12751
Unique mechanization to fault isolate failures of an electron tube Radio Frequency (RF) amplifier and its high voltage power supply
[AD-D012376] N87-12770
Theory and simulation of high-brightness electron beam production from laser-irradiated photocathodes in the presence of dc and RF electric fields
[DE86-012384] N87-12864

RADIO FREQUENCY INTERFERENCE
Rusty bolt intermodulation interference reducer
[AD-D012417] N87-12691

RADIO INTERFEROMETERS
Observation model and parameter partials for the JPL VLBI parameter estimation software MASTERFIT-1986
[NASA-CR-179919] N87-13178

RADIO SIGNALS
Effect of pulsating auroras on frequency-time characteristics of radio signals reflected from auroral ionosphere N87-12954
Phase fluctuations of ionosphere radio signals N87-12955

RADIO SOURCES (ASTRONOMY)
Continuum radiation from active galactic nuclei: A statistical study
[NASA-CR-179925] N87-13368

RADIO WAVES
Spatial radio wave attenuation during vertical sounding of ionosphere N87-12958

RADIOACTIVE DECAY
Low Q spin-up from rest
[AD-A169106] N87-12813

RADIOACTIVE WASTES
Meteorological tower data, Yucca Ridge (YR) site, January-June 1983. Nevada Nuclear Waste Storage Investigations Project
[DE86-012732] N87-13113

RADIOGRAPHY
Metal thickness measurements using radiography
[AD-D012373] N87-12832
NDE reliability and process control for structural ceramics
[NASA-TM-88870] N87-12910

RADIOMETERS
Studies of humid continental haze during SPACE N87-13086

RADIOMETRIC CORRECTION
Radiometric calibration of the airborne imaging spectrometer N87-12989

RAILGUN ACCELERATORS
Circuit considerations for repetitive railguns
[DE86-012369] N87-12752
Models and radiation of railgun plasma armatures with non-ideal plasma properties
[AD-A169349] N87-13258

RAIN
Estimation of precipitation from GOES IR imagery during FGGE: Application to diagnostic studies N87-13048
Satellite passive microwave rain measurement technique for land and ocean N87-13074
Remote sensing of severe convective storms N87-13075
First meeting of the Working Group on the Shuttle Microwave Precipitation Radiometer (SMPR) N87-13096

RAIN FORESTS
Energy receipt partitioning over the Amazon forest
[INPE-3980-PRE/990] N87-12962
Comparison of tropical forest surveys
[DE86-011699] N87-12969
A partition of sensible and latent heat fluxes above the terra firma area in the Amazon forest
[INPE-3949-PRE/970] N87-13008

RAIN GAGES
Estimation of precipitation from GOES IR imagery during FGGE: Application to diagnostic studies N87-13048

RAMAN SPECTRA
Raman spectroscopic investigation of molecular hydrogen
[DE86-012836] N87-12646
Raman spectroscopy of carboranes and polycarboranesiloxanes
[DE86-009030] N87-12694
Photoemission from oblate silver spheroids with polarized vacuum UV excitation
[DE86-006896] N87-13256

RAMAN SPECTROSCOPY
Optical diagnostics for diesel engine applications
[DE86-010747] N87-12641

Double-resonance techniques for high-resolution Raman-spectroscopy
[DE86-009840] N87-12645
Raman spectroscopy of carboranes and polycarboranesiloxanes
[DE86-009030] N87-12694

RANDOM ACCESS MEMORY
Reliability study of retention and memory gate integrity in a 1K MNOS RAM
[DE86-010483] N87-13175

RANDOM VARIABLES
Note on a characterization of exponential distributions
[AD-A169896] N87-13215
Inequalities for probability contents of convex sets via geometric average
[AD-A169938] N87-13219
A multivariate extension of Hoeffding's lemma
[AD-A170170] N87-13239

RANGES (FACILITIES)
Directory of range data conversion and processing system, revision
[AD-A169629] N87-12578
Joint operating procedure for interrange scheduling
[AD-A169636] N87-12579

RANK TESTS
A unified approach to constructing nonparametric rank tests
[AD-A169615] N87-13233

RANKINE CYCLE
Compact reactor/ORC power source
[DE86-011252] N87-13260
Neutronic design studies for an unattended, low power reactor
[DE86-011228] N87-13262

RARE EARTH COMPOUNDS
Neutron diffraction studies of some rare earth-transition metal deuterides
[AD-A168995] N87-12648

RAWINSONDES
Variation objective analyses for cyclone studies N87-13050

RAY TRACING
Method of ray intensity calculation as applied to anomalous propagation
[AD-A169553] N87-12737

RAYLEIGH NUMBER
Application of flux-corrected transport (FCT) to high Rayleigh number natural convection in a porous medium
[DE86-004603] N87-12618

RAYLEIGH SCATTERING
Development of ultrasonic modelling techniques for the study of seismic wave scattering due to crustal inhomogeneities
[AD-A170017] N87-13034

RAYLEIGH WAVES
Development of ultrasonic modelling techniques for the study of seismic wave scattering due to crustal inhomogeneities
[AD-A170017] N87-13034

REACTION KINETICS
New results on low temperature thermal oxidation of silicon
[AD-A169603] N87-12634
Investigation of deviations from ideality in the two liquid phase region of systems of medium molecular weight hydrocarbon mixtures and water
[AD-A169752] N87-12635
On the interplay between chemical reactions and phase transitions for molecules adsorbed on solid surfaces
[AD-A169818] N87-12636
Heterogeneous catalysis with lasers
[AD-A169601] N87-12851

REACTION TIME
Sleepability and wakeability following sleep deprivation
[AD-A169578] N87-13130
Rapid acting electro-pneumatic anti-G suit control valve
[AD-D012377] N87-13170

REACTIVITY
Hypothermic effects on vascular contractility and reactivity
[AD-A169142] N87-13127

REACTOR CORES
Neutronic design studies for an unattended, low power reactor
[DE86-011228] N87-13262

REACTOR DESIGN
Simulation of disturbances on the nuclear power plant simulator. The problem of the interpretation of operator actions and their cognitive backgrounds as a basis for design recommendations N87-13157
Compact reactor studies
[DE86-013247] N87-13263

REACTOR MATERIALS
Application of hydrogen embrittlement models to the crack growth behavior of fusion reactor materials
[DE86-011614] N87-12671
Crack propagation in high strain regions of a steel containment
[DE86-011437] N87-12943

REACTOR SAFETY
Simulation of disturbances on the nuclear power plant simulator. The problem of the interpretation of operator actions and their cognitive backgrounds as a basis for design recommendations N87-13157
Space nuclear safety program
[DE86-012767] N87-13261

REACTOR TECHNOLOGY
Japan report: Science and Technology
[JPRS-JST-86-023] N87-12715

REAL TIME OPERATION
A VLSI-based high-performance raster image system
[AD-A169068] N87-12761
ERS-1 SAR data processing
[NASA-CR-179913] N87-12965
Coordinated radar and satellite studies of ionospheric currents in the auroral zone and polar cap
[AD-A169466] N87-13031
Tool to develop real time simulation systems
[INPE-3979-TDL/233] N87-13179

RECEIVERS
Three dimensional optical receiver having programmable gain sensor stages
[AD-D012389] N87-13267

RECEPTORS (PHYSIOLOGY)
Mechanical transduction: Unification
[AD-A171191] N87-13123

RECOMBINATION REACTIONS
Study in molecular lasers
[AD-A169933] N87-12655
Comparison of 2D memory SEU transport simulation with experiments
[ATR-86(8139)-2] N87-13314
Quantum 1/F noise in solid state double devices, in particular Hg(1-x)CdxTe diodes
[AD-A171438] N87-13332

RECONSTRUCTION
Reconstruction of undersampled periodic signals
[AD-A168897] N87-12722

RECORDS
Machine gas metal arc welding of carbon steel. Welding procedure specification. Supplement 1: Records of procedure qualification tests
[DE86-012530] N87-12887
Gas tungsten arc and shielded metal arc welding of carbon steel. Welding procedure specification. Supplement 1: Records of procedure qualification tests
[DE86-012533] N87-12890
Welding procedure specification. Supplement 1: Records of procedure qualification tests. Shielded metal arc welding of carbon steel
[DE86-012535] N87-12891

RECRYSTALLIZATION
Recrystallization behavior of ion beam modified Alpha-Al sub 2 O sub 3
[DE86-009353] N87-13335

RECTANGULAR WINGS
Numerical simulation of tip vortices of wings in subsonic and transonic flows
[AD-A169116] N87-12544

RECURSIVE FUNCTIONS
Adaptive grid techniques for elliptic fluid-flow problems
[AD-A169471] N87-12814
Recursive moment formulas for semi-Markov processes
[AD-A169253] N87-13231
A reversal argument for storage models defined on semi-Markov processes
[AD-A169262] N87-13232

REDUCTION
Effects of reduced spatial resolution on the NEXRAD storm sequence algorithms
[PB86-221728] N87-13117

REDUNDANCY ENCODING
Yield and performance enhancement through redundancy in VLSI and WSI multi-processor systems
[AD-A169930] N87-13174

REENTRY GUIDANCE
Optimal descending, hypersonic turn to heading
[DE86-010989] N87-12577

REENTRY VEHICLES
Simple defense conservative model for mass requirements of hypervelocity projectile impact shields for reentry vehicles
[DE86-012407] N87-12603

REFLECTANCE
Theory for computing the field scattered from a smooth inflected surface
[NASA-TP-2632] N87-13264

REFLECTOMETERS
Progress with multiplexed sensor arrays based on reflection at spliced joints between sensors N87-13278

REFRACTIVITY
New results on low temperature thermal oxidation of silicon
[AD-A169603] N87-12634
Nonlinear ellipse rotation in a low-birefringence optical fiber N87-13282

REFRACTORY MATERIALS
Carbon fibers
[AD-A171370] N87-12622

REFRIGERATING
Analysis of magnetic refrigeration systems with staged regenerators based on an idealized magnetic material entropy model: 1
[DE86-013638] N87-12714

REGENERATORS
Analysis of magnetic refrigeration systems with staged regenerators based on an idealized magnetic material entropy model: 1
[DE86-013638] N87-12714

REGRESSION ANALYSIS
Determination of the coefficient of thermal expansion of JP-4 fuels
[AD-A171495] N87-12705
Crop yield modeling for climate impact studies. Part 1: Reasoning and results
[INPE-3967-PRE/982-PT-1] N87-12961
Comparison of various techniques for calibration of AIS data N87-12970
Atmospheric Tides Middle Atmosphere Program (ATMAP): Report of the workshop, Kyoto, Japan, December 5-8, 1984 N87-13016
Validity of Edgeworth expansions of minimum contrast estimators for Gaussian ARMA processes
[AD-A169931] N87-13217
Asymptotic theory for sieve estimators in semimartingale regression models
[AD-A169207] N87-13220
Regression models of quarterly overhead costs for six government aerospace contractors
[AD-A169165] N87-13350

RELATIVISTIC THEORY
Metrics of closed world of Friedmann, agitated by electric charge (towards a theory electromagnetic Friedmann's)
[AD-A168981] N87-12723

RELATIVITY
Induced quantum torsion
[DE86-702616] N87-13348

RELAXATION (MECHANICS)
Energetics of dislocation relaxation associated with cleavage in Cd-doped zinc crystals as probed by sychrotron topography
[DE86-002968] N87-13334

RELAXATION METHOD (MATHEMATICS)
SOR (Successive Over-Relaxation) MGR (multigrid algorithm)(nu) experiments on the crystal multicomputer
[AD-A169929] N87-13187

RELIABILITY
In-line determination of presence of liquid phase moisture in sealed IC packages
[AD-D012408] N87-12775
NDE reliability and process control for structural ceramics
[NASA-TM-88870] N87-12910
A Bayesian approach to quantile and response probability estimation with applications in reliability
[AD-A170455] N87-13240
Compact reactor/ORC power source
[DE86-011252] N87-13260

RELIABILITY ANALYSIS
Lithium Ambient-Temperature Battery Reliability Program, May 1983-April 1985
[DE86-012247] N87-12789
Reliability prediction models for mechanical equipment
[AD-A169775] N87-12911
Application of the task taxonomy method to the simulation of human service reliability in the manual control of aircraft
[MBB/LKE-301/S/PUB/216] N87-13151

RELIEF VALVES
Shock absorbing device with integral pressure relief valve
[AD-D012379] N87-12877

REMOTE CONTROL
Simulation of CIFF (Centralized IFF) remote control displays
[AD-A170367] N87-12742

REMOTE SENSING
Geologic remote sensing at INPE: An overview
[INPE-3975-PRE/967] N87-12959

Evaluation of remote sensing techniques to the detection of changes in a fluvial system due to human influence: The example of Canas River Basin (Sao Paulo State, Brazil)
[INPE-3970-PRE/983] N87-12960
Report of the Ad-Hoc Commission on remote sensing
[INPE-3981-NTE/259] N87-12963
Photographic sensors: Basic concepts
[INPE-3990-MD/031] N87-12966
In retrospect: The impact of research production in the area of remote sensing
[INPE-3987-NTE/261] N87-12968
Report on the activities of the irrigated crop survey in Sao Paulo State from remote sensing products, phase 2
[INPE-3950-RPE/513] N87-12989
Remote sensing to detect ecological impacts associated with acid deposition
[DE86-011649] N87-12992
Remote sensing of severe convective storms N87-13075
Preliminary planning for the Satellite Precipitation And Cloud Experiment (SPACE) Field Program N87-13089
Interactive information processing for NASA's mesoscale analysis and space sensor program N87-13093
Fiber optic device for temperature remote sensing N87-13280

REMOTE SENSORS
Intercomparison of DMSP OLS, NOAA AVHRR, GOES VISSR (Defense Meteorological Satellite Program Operational Linescan System, National Oceanographic and Atmospheric Administration Advanced Very High Resolution Radiometer, GOES Visible Infrared Spin-Scan Radiometer) and Landsat MSS imagery for cloud pr operty determination: Recommendations for digital data analysis
[AD-A169285] N87-12991
Guided Optical Structures in the Military Environment
[AGARD-CP-383] N87-13273
Progress in optical fiber sensors N87-13274
Optical fiber sensors for the measurement of pulsed electric currents N87-13281

REMOVAL
Light socket removal tool
[AD-D012368] N87-12710

REPORTS
Middle Atmosphere Program. Handbook for MAP, volume 21
[NASA-CR-179693] N87-13015

REQUIREMENTS
Advanced solar dynamic space power systems perspectives, requirements and technology needs
[NASA-TM-88884] N87-12606
Evaluation of the bearing and knowledge requirements of man machine systems N87-13164
Advanced EVA system design requirements study
[NASA-CR-171942] N87-13167

RESCUE OPERATIONS
SARSAT (Search and Rescue Satellite) operational data categorization and accuracy studies
[AD-A169748] N87-12599

RESEARCH AND DEVELOPMENT
Status of laser enrichment technology updated N87-12717
Welding science and technology in Europe: A survey and assessment
[AD-A169279] N87-12873
Proceedings of the conference on the design of experiments in army research development and testing (31st) held at the Madison, Wisconsin on 23-25 October 1986
[AD-A169473] N87-13246

RESEARCH MANAGEMENT
Welding science and technology in Europe: A survey and assessment
[AD-A169279] N87-12873
Quality management: An annotated bibliography
[AD-A169616] N87-12912
In retrospect: The impact of research production in the area of remote sensing
[INPE-3987-NTE/261] N87-12968
Southern California Air Quality Study (SCAQS) suggested program plan
[PB86-223427] N87-13013
Instrumentation research and support services
[AD-A169278] N87-13029

RESERVOIRS
Multiple rate shock isolator damping valve
[AD-D012394] N87-12879

RESIDUAL STRESS
Computation of residual stresses due to phase transformations during quenching of hollow cylinders
[AD-A170493] N87-12937

RESONANCE
Resonant photon pumping mechanisms for a plasma X-ray laser
[AD-D012416] N87-12857

RESONATORS
Double-ended tuning fork quartz accelerometer
[DE86-012277] N87-12842

RESOURCES MANAGEMENT
Joint operating procedure for interrange scheduling
[AD-A169636] N87-12579

RESPIRATORY SYSTEM
Quantification of respiratory muscle performance
[AD-A169208] N87-13128

RESPONSES
Evaluating ecosystem response to toxicant stress: a state space approach
[DE86-011777] N87-13009

RETINA
Limits of pattern discrimination in human vision
[AD-A170756] N87-13135

REYNOLDS NUMBER
In-line and transverse forces on smooth and rough cylinders in oscillatory flow at high Reynolds numbers
[AD-A169562] N87-12815

RIDING QUALITY
Development of a research method to determine the quality of task mastering by navigators in ship guidance N87-13154

RING LASERS
Optical rotation sensors
[AD-A169357] N87-12848
Comparison of ring laser and fiber-optic gyro technology N87-13276

RING STRUCTURES
Turbine air seal with full backside cooling
[AD-D012405] N87-12564

RIVER BASINS
Evaluation of remote sensing techniques to the detection of changes in a fluvial system due to human influence: The example of Canas River Basin (Sao Paulo State, Brazil)
[INPE-3970-PRE/983] N87-12960

ROBOTICS
On the dexterity of robotic manipulators N87-12867
Sensor controlled robotic welding for nuclear applications
[DE86-013110] N87-12905
Review of robotic component insertion system for printed wiring assemblies
[DE86-013510] N87-12907
Evaluation of automated decisionmaking methodologies and development of an integrated robotic system simulation. Appendix B: ROBSIM programmer's guide
[NASA-CR-178052] N87-13203

ROBOTS
On the dexterity of robotic manipulators N87-12867
Multi use gripper for industrial robot
[AD-D012371] N87-12876
Integrating computer vision with a robot arm system
[AD-A171278] N87-12884
Sensor controlled robotic welding for nuclear applications
[DE86-013110] N87-12905
Review of robotic component insertion system for printed wiring assemblies
[DE86-013510] N87-12907

ROCKET ENGINES
Advanced electric propulsion MPD (magnetoplasmadynamic)
[AD-A169792] N87-12610

ROCKET OXIDIZERS
Preparation of energetic compounds
[AD-A170022] N87-12704

ROCKS
Comparison of the 1984 and 1985 AIS data over the Singatse Range (Yerington), Nevada N87-12976

ROLLER BEARINGS
Analysis of mixed-mode crack propagation using the boundary integral method
[NASA-CR-179518] N87-12915

ROLLING CONTACT LOADS
Frictional and retarding forces on aircraft tyres. Part 4: Estimation of effects of yaw
[ESDU-86016-PT-4] N87-12868

ROOTS OF EQUATIONS
Zero-crossings analysis
[AD-A169937] N87-13218

ROTARY GYROSCOPES
Optical rotation sensors
[AD-A169357] N87-12848

ROTARY WING AIRCRAFT
An experimental investigation of free-tip response to a jet
[NASA-TM-88250] N87-12539

ROTARY WINGS
A summary of the development of integral aerodynamic methods for the computation of rotor wake interactions
[AD-A169254] N87-12545
An analysis of blade vortex interaction aerodynamics and acoustics N87-12547
The evaluation of a number of prototypes for the free-tip rotor constant-moment controller
[NASA-TM-86684] N87-12869

ROTATING BODIES
Effect of port corner geometry on the internal performance of a rotating-vane-type thrust reverser
[NASA-TP-2624] N87-12541
MAGINA (Materially And Geometrically Nonlinear Analysis). Addendum 1, parts 1-4
[AD-A169383] N87-12933

ROTATING FLUIDS
Theoretical and experimental studies in support of the geophysical fluid flow experiment N87-13045

ROTATING SPHERES
Theoretical and experimental studies in support of the geophysical fluid flow experiment N87-13045

ROTATION
Comparison of ring laser and fiber-optic gyro technology N87-13276
Nonlinear ellipse rotation in a low-birefringence optical fiber N87-13282
The upper atmosphere of Venus: A tentative explanation of its rotation
[NASA-TM-88505] N87-13375

ROTOR AERODYNAMICS
An analysis of blade vortex interaction aerodynamics and acoustics N87-12547

ROTOR BLADES
The evaluation of a number of prototypes for the free-tip rotor constant-moment controller
[NASA-TM-86684] N87-12869

ROTOR BLADES (TURBOMACHINERY)
A summary of the development of integral aerodynamic methods for the computation of rotor wake interactions
[AD-A169254] N87-12545
Visualisation of axial turbine tip clearance flow using a linear cascade
[CUED/A-TURBO/TR-122] N87-12560

ROTOR BODY INTERACTIONS
Propellar/body interaction for thrust and drag
[ESDU-86017] N87-12537

ROTOR SYSTEMS RESEARCH AIRCRAFT
NASA rotor systems research aircraft: Fixed-wing configuration flight-test results
[NASA-TM-86789] N87-12557

ROTORS
An experimental investigation of free-tip response to a jet
[NASA-TM-88250] N87-12539
Cryogenic wound rotor for lightweight, high voltage generators
[AD-D012370] N87-12768

ROUGHNESS
Mechanical interactions of rough surfaces
[DE86-010866] N87-12901

RUNGE-KUTTA METHOD
Performance analysis of some numerical algorithms in the resolution of ODEs artificial satellite problems
[INPE-3998-PRE/995] N87-13206

RUPTURING
Influence of experimental scatter on the analysis and extrapolation of stress-rupture data
[DE86-009510] N87-12940

S

S WAVES
Influence of shear modulus on the behavior of acoustically transparent materials
[AD-A169289] N87-12931

SAFETY FACTORS
High voltage characteristics of the electrodynamic tether and the generation of power and propulsion
[NASA-CR-178949] N87-12609
NASA's quality assurance program
[GPO-63-142] N87-12909

SAGE SATELLITE
SAGE 2 satellite data set validation
[NASA-CR-178189] N87-13024

SAMPLES
Transmission through ferrite samples at submillimeter frequencies
[AD-A169178] N87-12731

SAMPLING
Collection of ions in the stratosphere
[AD-A169905] N87-13032
Design and analysis of experiments and more realistic techniques for data analysis
[AD-A168921] N87-13228

SANDWICH STRUCTURES
Feasibility study of test problems for finite element/finite difference programs for structural dynamics
[AD-A169058] N87-12928

SATELLITE IMAGERY
Intercomparison of DMSP OLS, NOAA AVHRR, GOES VISSR (Defense Meteorological Satellite Program Operational Linescan System, National Oceanographic and Atmospheric Administration Advanced Very High Resolution Radiometer, GOES Visible Infrared Spin-Scan Radiometer) and Landsat MSS imagery for cloud pr operty determination: Recommendations for digital data analysis
[AD-A169285] N87-12991
NASA/MSFC FY-85 Atmospheric Processes Research Review
[NASA-CP-2402] N87-13043
Estimation of precipitation from GOES IR imagery during FGGE: Application to diagnostic studies N87-13048
The use of satellite data in understanding and predicting convective and large-scale dynamical processes N87-13049
Variation objective analyses for cyclone studies N87-13050
Dynamics and energetics of the South Pacific Convergence Zone during FGGE SOP-1 N87-13052
Application of satellite data to tropic/subtropic moisture coupling N87-13053
Remote observations of severe storms N87-13065
Investigations of severe/tornadic thunderstorm development and evolution based on satellite and AVE/SESAME/VAS data N87-13084

SATELLITE OBSERVATION
Study of satellite systems to monitor Earth's radiation budget
[CAP-420-071] N87-12994

SATELLITE ORBITS
Solar flux and geomagnetic activity prediction
[INPE-3884-PRE/934] N87-13377

SATELLITE ORIENTATION
Relative motion of the Sun on an artificial satellite
[INPE-3985-NTE/260] N87-12591

SATELLITE TRACKING
Meter-level orbit determination of geosynchronous satellites by an economical tracking system N87-12575

SATELLITE-BORNE INSTRUMENTS
Millimeter wave compónents — spaceborne microwave radiometers
[FTL-118521] N87-12605
A versatile Data Processing Unit (DPU) for satellite-borne composition instrumentation N87-13393

SATELLITE-BORNE PHOTOGRAPHY
The space station millimeter facility
[AD-A168983] N87-12604
Intercomparison of DMSP OLS, NOAA AVHRR, GOES VISSR (Defense Meteorological Satellite Program Operational Linescan System, National Oceanographic and Atmospheric Administration Advanced Very High Resolution Radiometer, GOES Visible Infrared Spin-Scan Radiometer) and Landsat MSS imagery for cloud pr operty determination: Recommendations for digital data analysis
[AD-A169285] N87-12991

SCALING LAWS
Analysis and verification of the icing scaling equations. Volume 1: Revision
[AD-A167976] N87-12551
Development of ultrasonic modelling techniques for the study of seismic wave scattering due to crustal inhomogeneities
[AD-A170017] N87-13034

SCATTERING
Severe storm detection with passive 37 GHz observations N87-13072
X-ray data booklet, revision
[DE86-012650] N87-13272

SCATTERING CROSS SECTIONS
Surface correlation relationships in rough surface scattering
[AD-A169327] N87-12733

SCENE ANALYSIS
Generation of images with recorded auxiliary data for the LANDSAT Thematic Mapper (TM) imagery
[INPE-3982-TDL/234] N87-12990
Application of a network associative scene analysis model
[INPE-3945-PRE/967] N87-13244

SCHEDULING
Joint operating procedure for interrange scheduling
[AD-A169536] N87-12579
Introduction to the theory of nested transactions
[AD-A171428] N87-13191

SCIENTIFIC SATELLITES
Solar flares and magnetospheric particles: Investigations based upon the ONR-60 experiments and ONR-604 experiments
[AD-A170820] N87-13381
A versatile Data Processing Unit (DPU) for satellite-borne composition instrumentation N87-13393

SCIENTISTS
In retrospect: The impact of research production in the area of remote sensing
[INPE-3987-NTE/261] N87-12988

SCINTILLATION
Digest: Proceedings of the International Conference on Optical and Millimeter Wave Propagation and Scattering in the Atmosphere
[AD-A170393] N87-12743

SCINTILLATION COUNTERS
Observations on the Stanford 4800 KG gravity wave detector with a cosmic ray monitor N87-13399

SEA BREEZE
Airborne Doppler measurements of the central California extended sea breeze N87-13066

SEA WATER
Influence of shear modulus on the behavior of acoustically transparent materials
[AD-A169289] N87-12931

SEALING
In-line determination of presence of liquid phase moisture in sealed IC packages
[AD-D012408] N87-12775

SEALS (STOPPERS)
Turbine air seal with full backside cooling
[AD-D012405] N87-12564
Sliding duct seal
[AD-D012369] N87-12875
Self-locking outer air seal with full backside cooling
[AD-D012406] N87-12880
Improved vane platform sealing and retention means
[AD-D012407] N87-12881

SEAMS (JOINTS)
Resistance seam welding
[DE86-013288] N87-12906

SEARCHING
Further results on interpolation searching of databases
[DE86-012622] N87-13356

SEASONS
Satellite passive microwave rain measurement techniques for land and ocean N87-13074

SEATS
Radiographic determination of mass and inertial tensor of anatomical segments
[AD-A169122] N87-13126
Anthropometric handicaps in the construction of a helicopter cockpit — seats N87-13148

SECONDARY EMISSION
The secondary production of gamma rays in the Jovian magnetosphere N87-13391

SEDIMENTS
An analysis of the acoustic characteristics of ABSS (acoustic backscatter system) and its deployments
[AD-A170487] N87-13037

SEGMENTS
Fracture and viscoelastic characteristics of the human cervical spine
[AD-A170002] N87-13133
Statistical models and methods for cluster analysis and image segmentation
[AD-A169145] N87-13229

SEISMIC WAVES
Lg wave excitation and propagation in presence of one-, two-, and three-dimensional heterogeneities
[AD-A169325] N87-13030
Development of ultrasonic modelling techniques for the study of seismic wave scattering due to crustal inhomogeneities
[AD-A170017] N87-13034

SEISMOLOGY
Lg wave excitation and propagation in presence of one-, two- and three-dimensional heterogeneities
[AD-A169004] N87-12724
Development of ultrasonic modelling techniques for the study of seismic wave scattering due to crustal inhomogeneities
[AD-A170017] N87-13034

SELENIUM
Possibility of using dc conductivity for investigating phase transition in amorphous semiconductors
[DE86-702646] N87-13340

SEMICONDUCTOR DEVICES
Synthesis of conjugated polymers with alternating aromatic and quinonoid sequences via elimination on precursors
[AD-A171331] N87-12693
Proceedings of the Topical Meeting on the Microphysics of Surfaces, Beams and Adsorbates held in Santa Fe, New Mexico on 4-6 February 1985
[AD-A170797] N87-13329
Picosecond nonlinear resonant interactions in semiconductors
[AD-A170813] N87-13330

SEMICONDUCTOR DIODES
Effects of optical feedback on the performance of high data rate single-mode fiber systems N87-13268
Quantum 1/F noise in solid state double devices, in particular Hg(1-x)CdxTe diodes
[AD-A171438] N87-13332

SEMICONDUCTOR LASERS
High power semiconductor laser sources
[AD-A169900] N87-12644
A study of methods of phase noise reduction of semiconductor lasers for sensor applications N87-13266

SEMICONDUCTORS (MATERIALS)
Potential applications of artificially structured materials for X-ray microanalysis
[DE86-010459] N87-12612
Solid State Photovoltaic Research Branch annual report, FY 1985
[DE86-010708] N87-13004
Degeneracy in the ensemble Monte Carlo method for high field transport in semiconductors
[AD-A169456] N87-13321
Rapid synthesis of indium phosphide
[AD-D012362] N87-13322
Thermophysical properties measurements of gallium arsenide and cadmium telluride
[AD-A169901] N87-13326
Picosecond nonlinear resonant interactions in semiconductors
[AD-A169992] N87-13327
Kinetics and mechanisms on the molecular beam etching of semiconductors
[AD-A171360] N87-13331
In-situ interdiffusion measurements in HgTe-CdTe superlattices
[DE86-011429] N87-13337

SENSITIVITY
Development of a sensitive superconducting gravity gradiometer for geological and navigational applications
[NASA-CR-4011] N87-13021

SENSORY STIMULATION
High-resolution analysis of eye movements
[AD-A170779] N87-13136

SEPARATED FLOW
Viscous-inviscid interaction in transonic separated flow over solid and porous airfoils and cascades N87-12535
A summary of the development of integral aerodynamic methods for the computation of rotor wake interactions
[AD-A169254] N87-12545
Visualisation of axial turbine tip clearance flow using a linear cascade
[CUED/A-TURBO/TR-122] N87-12560
The calculation of separated flows of low-viscosity liquids using the Batchelor Model
[BR-100272] N87-12810

SEPARATORS
Importance of interfacial phenomena in separation science and technology
[DE86-011063] N87-12637
Zinc/air cell cathode
[AD-D012425] N87-12760
Zinc/nickel oxide battery membrane separator studies
[DE86-012824] N87-12793

SEQUENTIAL ANALYSIS
User's guide for NPSOL (version 4.0): A Fortran package for nonlinear programming
[AD-A169115] N87-13180

SERVICE LIFE
Reliability study of retention and memory gate integrity in a 1K MNOS RAM
[DE86-010483] N87-13175

SERVOMECHANISMS
Tracking servo compensator with rate aiding
[AD-D012388] N87-12735

SET THEORY
Inequalities for probability contents of convex sets via geometric average
[AD-A169938] N87-13219
A unified approach to constructing nonparametric rank tests
[AD-A169815] N87-13233

SHAPES
A finite element method for localized failure analysis
[AD-A169117] N87-12990
An intuitive approach to geometric continuity for parametric curves and surfaces
[AD-A169654] N87-13211

SHEAR FLOW
An analysis of shear band development incorporating heat conduction
[AD-A169972] N87-12926
SHEAR PROPERTIES
Dynamic analysis of a Timoshenko beam using a finite element approach
[EPM/RT-86-34] N87-12919
SHEAR STRESS
Micromechanisms and toughness for cleavage fracture of steel
[AD-A169906] N87-12655
Development of buried wire gages for measurement of wall shear stress in Blastane experiments
[NASA-TM-89212] N87-12831
SHIELDING
Simple defense conservative model for mass requirements of hypervelocity projectile impact shields for reentry vehicles
[DE86-012407] N87-12603
SHIFT REGISTERS
Interrupt control switch interface system
[AD-D012414] N87-12776
SHIPS
Simulator design features for helicopter landing on small ships. 1: A performance study
[AD-A169514] N87-12572
Development of a research method to determine the quality of task mastering by navigators in ship guidance N87-13154
Nonlinear waves
[AD-A168934] N87-13207
SHOCK ABSORBERS
Shock absorbing device with integral pressure relief valve
[AD-D012379] N87-12877
Multiple rate shock isolator damping valve
[AD-D012394] N87-12879
SHOCK LOADS
Effects of variables upon pyrotechnically induced shock response spectra
[NASA-TP-2603] N87-12921
SHOCK SPECTRA
Effects of variables upon pyrotechnically induced shock response spectra
[NASA-TP-2603] N87-12921
SHOCK TESTS
Blast gust loading on a 35 degree swept-back wing
[AD-A169415] N87-12570
SHOCK TUNNELS
Further shock tunnel studies of scramjet phenomena
[NASA-CR-179937] N87-12542
SHOCK WAVE PROPAGATION
Shock-induced solid state chemistry: Theoretical background
[DE86-012741] N87-12941
SHOCK WAVES
Effect of residual strain on twinning in shock-loaded copper
[DE86-007362] N87-12660
Plane-parallel and bow shock models of Herbig-Haro objects N87-13374
SHORT CRACKS
Fatigue behavior of long and short cracks in wrought and powder aluminum alloys
[AD-A169960] N87-12656
SHORT TAKEOFF AIRCRAFT
The handling qualities and flight characteristics of the Grumman design 698 simulated twin-engine tilt Nacelle V/STOL aircraft
[NASA-TM-86785] N87-12558
SHROUDS
Journal of engineering thermophysics (selected articles)
[AD-A169452] N87-13347
SIDELOBE REDUCTION
Temperature and frequency compensated array beam steering unit
[AD-D012365] N87-12767
SIDELOBES
A brief review of adaptive null steering techniques
[AD-A169548] N87-12736
SIEVES
Asymptotic theory for sieve estimators in semimartingale regression models
[AD-A169207] N87-13230
SIGNAL ANALYSIS
Zero-crossings analysis
[AD-A169937] N87-13218
SIGNAL DETECTION
Tone calibration technique: A digital signaling scheme for mobile applications
[NASA-CR-179915] N87-12719
Rapid acting electro-pneumatic anti-G suit control valve
[AD-D012377] N87-13170
SIGNAL DETECTORS
Three dimensional optical receiver having programmable gain sensor stages
[AD-D012369] N87-13267
SIGNAL FADING
Tone calibration technique: A digital signaling scheme for mobile applications
[NASA-CR-179915] N87-12719
SIGNAL PROCESSING
Reconstruction of undersampled periodic signals
[AD-A168897] N87-12722
Knowledge-based pitch detection
[AD-A169069] N87-12730
A new method of synthetic aperture radar image reconstruction using modified convolution back-projection algorithm
[AD-A170652] N87-12747
Signal estimation, scattering theory and interpolation problems in one and two dimensions
[AD-A168969] N87-12750
Guided Optical Structures in the Military Environment
[AGARD-CP-383] N87-13273
Progress in optical fiber gyroscopes using integrated optics N87-13283
Nonlinear planar guided wave interactions and devices N87-13290
Optoelectronic broadband switching for communications and signal processing N87-13294
SIGNAL REFLECTION
Foreground effects on troposcatter digital communication systems
[AD-A169360] N87-12734
Phase fluctuations of ionosphere radio signals N87-12955
SIGNAL TO NOISE RATIOS
Multichannel phase noise measurement system
[AD-D012372] N87-13253
SILANES
Further shock tunnel studies of scramjet phenomena
[NASA-CR-179937] N87-12542
SILICON
Kinetic and thermodynamic studies of pulsed laser irradiation
[DE86-012175] N87-12660
Use of Wannier function in the calculations of band structure of covalent crystals
[DE86-702668] N87-13344
SILICON ALLOYS
Radiation-induced segregation to grain boundaries in a Ni-Si alloy
[DE86-010027] N87-12664
Kinetic and thermodynamic studies of pulsed laser irradiation
[DE86-012175] N87-12660
SILICON CARBIDES
Plasma joining of metal matrix composites
[AD-A169056] N87-12615
Mechanical testing of a coated carbon-carbon composite at elevated temperatures in air
[AD-A169355] N87-12618
SILICON DIOXIDE
Comparative thermal conductivity measurements at Sandia National Laboratories
[DE86-012926] N87-12647
Intrinsic SiO2 film stress measurements on thermally oxidized Si
[AD-A169602] N87-12935
Feasibility of making coherent fiber-optic arrays from fused silica
[AD-A170873] N87-13271
SILICON FILMS
New results on low temperature thermal oxidation of silicon
[AD-A169603] N87-12634
New ultra low permittivity composites for use in ceramic packaging of Ga:As integrated circuits
[AD-A168877] N87-12758
SILOXANES
Ionic conductivity in solid, crosslinked dimethylsiloxane-ethylene oxide copolymer networks containing sodium
[AD-A169038] N87-12683
Raman spectroscopy of carboranes and polycarboranesiloxanes
[DE86-009030] N87-12694
SILVER
Photoemission from oblate silver spheroids with polarized vacuum UV excitation
[DE86-006898] N87-13256
SIMULATION
Heat transfer characteristics of simulated microelectronic chips under normal and enhanced conditions
[PB86-224425] N87-12804
Comparison of Rayleigh-Taylor growth with 1.0 m and 0.25 m lasers
[DE86-012217] N87-12662
NOSL experiment support
[NASA-CR-178947] N87-13140
The optimal linear combination of control variates in the presence of bias
[AD-A169111] N87-13210
TSAR (Theater Simulation of Airbase Resources) database dictionary F-4E
[AD-A169575] N87-13352
SIMULATORS
Fabrication and testing of lightweight hydraulic system simulator hardware
[AD-A169664] N87-12711
Simulation of CIFF (Centralized IFF) remote control displays
[AD-A170387] N87-12742
Simulation of disturbances on the nuclear power plant simulator. The problem of the interpretation of operator actions and their cognitive backgrounds as a basis for design recommendations N87-13157
SINGLE CRYSTALS
New results on low temperature thermal oxidation of silicon
[AD-A169603] N87-12634
Single crystal fibers N87-13298
Quartz growth on X-seeds
[AD-D012269] N87-13315
Study to determine the feasibility of utilizing skull-melting techniques for the growth of single crystals of yttrium vanadate
[AD-A169249] N87-13320
SINGLE EVENT UPSETS
Comparison of 2D memory SEU transport simulation with experiments
[ATR-86(8139)-2] N87-13314
SITE SELECTION
The siting, installation and operational suitability of the Automated Weather Observing System (AWOS) at heliports
[DOT/FAA/PM-86/30] N87-13099
Meteorological tower data, Yucca Ridge (YR) site, January-June 1983. Nevada Nuclear Waste Storage Investigations Project
[DE86-012732] N87-13113
SITES
Site occupations in Li sub 2 ordered alloys by axial electron channeling microanalysis
[DE86-009421] N87-12669
Meteorological tower data, Yucca Ridge (YR) site, January-June 1983. Nevada Nuclear Waste Storage Investigations Project
[DE86-012732] N87-13113
SKIN TEMPERATURE (BIOLOGY)
Human thermoregulatory model for immersion in cold water
[AD-A169779] N87-13131
SLEEP
Pharmacological resetting of the circadian sleep-wake cycle
[AD-A170804] N87-13137
SLEEP DEPRIVATION
Sleepability and wakeability following sleep deprivation
[AD-A169578] N87-13130
SLENDER BODIES
The effect of a winglet on the spatial vortex of a slender body at high angle of attack
[AD-A169925] N87-12533
SLEWING
Tracking servo compensator with rate aiding
[AD-D012388] N87-12735
SLIDING
Study of high temperature failure mechanisms in ceramics
[AD-A170001] N87-12689
Sliding duct seal
[AD-D012369] N87-12875
SLIDING FRICTION
Mechanical interactions of rough surfaces
[DE86-010686] N87-12901
SLOTS
Super gripper variable vane arm
[AD-D012364] N87-12874
SMOKE
Advanced optical smoke meters for jet engine exhaust measurement
[NASA-CR-179459] N87-12629
SOCIAL FACTORS
Desertification: Global ecological problem N87-12950
SOCIOLOGY
Maximization of the capacity of the most survivable connections in a network
[AD-A169065] N87-12728

SODIUM SULFUR BATTERIES
Sodium-sulfur battery systems development
[DE86-011424] N87-12788
SOFTENING
An analysis of shear band development incorporating heat conduction
[AD-A168972] N87-12926
SOFTWARE ENGINEERING
Catalog of Resources for Education in Ada (Trade name) and Software Engineering (CREASE), version 4.0
[AD-A169692] N87-13186
Space plasma research
[NASA-CR-178965] N87-13307
SOFTWARE TOOLS
Tool to develop real time simulation systems
[INPE-3979-TDL/233] N87-13179
A software implementation of an interactive graphics system for three dimensional modeling and layout
[AD-A169264] N87-13183
SOIL MECHANICS
The application of boundary-element techniques for some soil-structure interaction problems
[AD-A168999] N87-12709
SOILS
Satellite passive microwave rain measurement techniques for land and ocean N87-13074
SOLAR ACTIVITY
Extraterrestrial forcing, atmospheric electricity and the occurrence of thunderstorms
[AD-A170463] N87-13111
A study of the relationship between solar activity and interplanetary field variations
[AD-A169983] N87-13380
SOLAR ACTIVITY EFFECTS
Solar flux and geomagnetic activity prediction
[INPE-3884-PRE/934] N87-13377
SOLAR ARRAYS
Solar array flight dynamic experiment
[NASA-TP-2598] N87-12581
SOLAR ATMOSPHERE
MAX '91: An advanced payload for the exploration of high energy processes on the active sun
[NASA-TM-89271] N87-13379
SOLAR CELLS
Status and future of government-supported amorphous silicon research in the US
[DE86-010702] N87-12997
Stable, high-efficiency, CuInSe2-based polycrystalline thin-film tandem solar cells
[DE86-010705] N87-13003
Solid State Photovoltaic Research Branch annual report, FY 1985
[DE86-010706] N87-13004
Photovoltaic Concentrator Technology Project, Fourteenth Project Integration Meeting, June 10-11, 1986
[DE86-012051] N87-13006
SOLAR COLLECTORS
Apparatus for downward transport of heat
[DE86-013700] N87-12824
Integrated heat pipe-thermal storage design for a solar receiver
[DE86-011235] N87-12999
SOLAR CORONA
Magnetic field re-arrangement after prominence eruption
[DE86-012393] N87-13382
Large-scale electric fields resulting from magnetic reconnection in the corona
[DE86-012391] N87-13383
SOLAR COSMIC RAYS
Solar flares and magnetospheric particles: Investigations based upon the ONR-60 experiments and ONR-604 experiments
[AD-A170620] N87-13381
SOLAR DYNAMIC POWER SYSTEMS
Advanced solar dynamic space power systems perspectives, requirements and technology needs
[NASA-TM-88864] N87-12606
SOLAR ENERGY CONVERSION
A study of energy conversion devices using photoactive organometallic electrocatalysts
[AD-A169096] N87-12996
Proof of feasibility of a novel inverter for photovoltaic power conditioning
[DE86-012729] N87-13001
Experimental investigation of thermochemical transport for solar applications using sulfur trioxide
[DE86-011762] N87-13005
SOLAR FLARES
MAX '91: An advanced payload for the exploration of high energy processes on the active sun
[NASA-TM-89271] N87-13379
Solar flares and magnetospheric particles: Investigations based upon the ONR-60 experiments and ONR-604 experiments
[AD-A170620] N87-13381
Magnetic field re-arrangement after prominence eruption
[DE86-012393] N87-13382
Large-scale electric fields resulting from magnetic reconnection in the corona
[DE86-012391] N87-13383
Rapid fluctuations in solar flares
[NASA-CR-179894] N87-13387
The gamma-ray spectrometer experiment on the solar maximum mission satellite
[NASA-CR-177877] N87-13394
Characterization of the gamma radiation in space and in the atmosphere
[DE86-013445] N87-13397
SOLAR GENERATORS
Experimental investigation of thermochemical transport for solar applications using sulfur trioxide
[DE86-011762] N87-13005
SOLAR HEATING
Studies of humid continental haze during SPACE N87-13088
SOLAR MAGNETIC FIELD
Magnetic field re-arrangement after prominence eruption
[DE86-012393] N87-13382
SOLAR MAXIMUM MISSION
MAX '91: An advanced payload for the exploration of high energy processes on the active sun
[NASA-TM-89271] N87-13379
SOLAR PHYSICS
MAX '91: An advanced payload for the exploration of high energy processes on the active sun
[NASA-TM-89271] N87-13379
Equilibrium configuration of coronal loops
[DE86-702711] N87-13384
SOLAR RADIATION
A simple solar, spectral model for studying the effects of cloud cover and surface albedo on the incoming solar radiation
[AD-A171284] N87-13038
Model studies of solar spectral irradiance at the bottom and top of a cloudy atmosphere N87-13385
SOLAR RADIO BURSTS
Repetition rates of fast pulses in MM-waves/X-ray solar bursts
[INPE-3974-PRE/986] N87-13378
SOLAR SYSTEM
The space station millimeter facility
[AD-A168983] N87-12604
The stellar upper mass limit in an OB association and implications for cosmic rays and cosmic abundances N87-13392
SOLAR TERRESTRIAL INTERACTIONS
Solar control of geophysical phenomena N87-12953
SOLAR THERMAL ELECTRIC POWER PLANTS
Proceedings of the Solar Thermal Technology Conference
[DE86-011703] N87-13002
SOLAR WIND
A study of the relationship between solar activity and interplanetary field variations
[AD-A169983] N87-13380
Characterization of the gamma radiation in space and in the atmosphere
[DE86-013445] N87-13397
SOLAR X-RAYS
Repetition rates of fast pulses in MM-waves/X-ray solar bursts
[INPE-3974-PRE/986] N87-13378
SOLENOIDS
Polarized H(-) source development at BNL
[DE86-012704] N87-13257
SOLID PROPELLANT ROCKET ENGINES
Shifts in shuttle SRM performance because of ammonium perchlorate crystal shape on missions 51-I/J and 61-A/B
[NASA-TM-86561] N87-12607
SOLID ROCKET PROPELLANTS
Pulsed-laser, high speed photography of rocket propellant surface deflagration
[AD-A169308] N87-12703
SOLID STATE
Direct writing of microstructures for solid-state electronics
[AD-A170637] N87-12783
Shock-induced solid state chemistry: Theoretical background
[DE86-012741] N87-12941
Solid State Photovoltaic Research Branch annual report, FY 1985
[DE86-010706] N87-13004
SOLIDIFICATION
Cellular solidification of transparent monotectics
[NASA-CR-177039] N87-12626
APFIM study of antiphase and grain boundaries in Ni Al
[DE86-008494] N87-12662
Kinetic and thermodynamic studies of pulsed laser irradiation
[DE86-012175] N87-12660
Stefan-type problem with void formation and its explicit solution
[DE86-013521] N87-13007
SOLIDS
Finite element analyses of shear localization in rate and temperature dependent solids
[AD-A169057] N87-12927
Shock-induced solid state chemistry: Theoretical background
[DE86-012741] N87-12941
SOLITARY WAVES
Evaluating nonlinear effects in propagation of acoustic pulse in atmospheric surface layer in inversions N87-12951
SOLUBILITY
Investigation of deviations from ideality in the two liquid phase region of systems of medium molecular weight hydrocarbon mixtures and water
[AD-A169752] N87-12635
SOLUTES
Generalization of one-dimensional solute transport: A stochastic-convective flow conceptualization
[DE86-011117] N87-12820
SOUND TRANSMISSION
MIZEX: A program for mesoscale air-ice-ocean interaction experiments in arctic marginal ice zones. 8: A science plan for a winter marginal ice zone experiment in the Fram Strait/Greenland Sea, 1987/89
[AD-A169070] N87-13119
SOUND WAVES
Liquid metal thermoacoustic engine
[DE86-011264] N87-12902
Influence of shear modulus on the behavior of acoustically transparent materials
[AD-A169289] N87-12931
Evaluating nonlinear effects in propagation of acoustic pulse in atmospheric surface layer in inversions N87-12951
SOUTH CAROLINA
Micrometeorological transitions in the morning boundary layer over rolling terrain
[AD-A169237] N87-13103
SOUTHERN HEMISPHERE
A survey of hard-X-rays at balloon altitudes of the Earth's atmosphere
[INPE-3954-PRE/972] N87-13388
SPACE CHARGE
Flight model discharge system
[AD-A169423] N87-12571
Theory and simulation of high-brightness electron beam production from laser-irradiated photocathodes in the presence of dc and RF electric fields
[DE86-012384] N87-12664
Two-dimensional dynamics of the plasma Wakefield accelerator
[DE86-012382] N87-13312
SPACE COMMERCIALIZATION
National Commission on Space report
[GPO-63-143] N87-12574
SPACE EXPLORATION
Upper stage selected for planetary missions
[NASA-NEWS-RELEASE-86-161] N87-12593
SPACE FLIGHT
Space flight operations communications phraseology and techniques
[NASA-TM-86562] N87-12721
SPACE HEATING (BUILDINGS)
Empirical determination among superintendents of the acceptable user surface in digitally automated heating-ventilation air conditioning systems N87-13165
SPACE PLASMAS
Magnetospheric plasma studies using data from the dynamics explorer high and low altitude plasma instruments
[AD-A169010] N87-13027
Space plasma research
[NASA-CR-178965] N87-13307
Neutron and antineutron production in accretion onto compact objects
[NASA-TM-89264] N87-13395
SPACE PROGRAMS
National Commission on Space report
[GPO-63-143] N87-12574
Space nuclear safety program
[DE86-012767] N87-13261

SPACE SHUTTLE MAIN ENGINE
SSME main injector 4000 Hertz phenomenon
[NASA-CR-178934] N87-12608
SPACE SHUTTLE PAYLOADS
Solar array flight dynamic experiment
[NASA-TP-2596] N87-12581
General purpose aft cargo carrier study, volume 1
[NASA-CR-178905] N87-12587
Upper stage selected for planetary missions
[NASA-NEWS-RELEASE-86-161] N87-12593
High voltage characteristics of the electrodynamic tether and the generation of power and propulsion
[NASA-CR-178949] N87-12609
NOSL experiment support
[NASA-CR-178947] N87-13140
SPACE SHUTTLES
Evaluation of a nonlinear parameter extraction mathematical model including the term C(subm(sub delta e squared))
[NASA-TM-87731] N87-12566
Lunar laboratory
[NASA-TM-89209] N87-12580
Development testing of large volume water sprays for warm fog dispersal
[NASA-TP-2607] N87-12585
A mathematical formulation of a large space structure control problem
[AD-A169950] N87-12602
NASA's quality assurance program
[GPO-63-142] N87-12909
The meteorological interactive data display system N87-13091
Ionization phenomena about the space shuttle
[AD-A170542] N87-13310
SPACE STATIONS
Lunar laboratory
[NASA-TM-89209] N87-12580
Viewport concept for space station modules
[NASA-TM-86559] N87-12592
An approach to design knowledge capture for the space station
[NASA-TM-89272] N87-12597
The ecology of microorganisms in a small closed system: Potential benefits and problems for space station
[NASA-TM-86563] N87-13166
SPACE TECHNOLOGY EXPERIMENTS
Metallurgical characterization of the interfaces and the damping mechanisms in metal matrix composites
[AD-A169186] N87-12616
SPACE TRANSPORTATION SYSTEM
General purpose aft cargo carrier study, volume 1
[NASA-CR-178905] N87-12587
SPACE WEAPONS
Development of regenerable energy storage for space multimegawatt applications
[DE86-011070] N87-12998
Duel between an ASAT (anti-satellite) with multiple kill vehicles and a space-based weapons platform with kinetic energy weapons
[AD-A168946] N87-13245
SPACE-TIME FUNCTIONS
Some investigations into variable meshes for numerical solution of partial differential equations
[AD-A168977] N87-13208
SPACEBORNE EXPERIMENTS
Theoretical and experimental studies in support of the geophysical fluid flow experiment N87-13045
Space shuttle/mesoscale lightning experiment N87-13060
SPACEBORNE PHOTOGRAPHY
Photographic sensors: Basic concepts
[INPE-3990-MD/031] N87-12966
SPACECRAFT CHARGING
Density and electrostatic potential distribution around a cylindrical satellite
[INPE-3953-NTE/258] N87-12595
Space plasma research
[NASA-CR-178965] N87-13307
SPACECRAFT COMMUNICATION
Space flight operations communications phraseology and techniques
[NASA-TM-86562] N87-12721
SPACECRAFT COMPONENTS
Investigation of the Challenger accident, volume 2
[GPO-64-548] N87-12586
Modeling the fundamental characteristics and processes of the spacecraft functioning
[NASA-TM-87999] N87-12598
New materials for spacecraft stability and damping: A feasibility study
[AD-A169826] N87-12601
SPACECRAFT CONSTRUCTION MATERIALS
New materials for spacecraft stability and damping: A feasibility study
[AD-A169826] N87-12601
SPACECRAFT DEFENSE
Duel between an ASAT (anti-satellite) with multiple kill vehicles and a space-based weapons platform with kinetic energy weapons
[AD-A168946] N87-13245
SPACECRAFT DESIGN
Modeling the fundamental characteristics and processes of the spacecraft functioning
[NASA-TM-87999] N87-12598
SPACECRAFT ENVIRONMENTS
The ecology of microorganisms in a small closed system: Potential benefits and problems for space station
[NASA-TM-86563] N87-13166
SPACECRAFT LAUNCHING
Development testing of large volume water sprays for warm fog dispersal
[NASA-TP-2607] N87-12585
Upper stage selected for planetary missions
[NASA-NEWS-RELEASE-86-161] N87-12593
SPACECRAFT MODELS
Flight model discharge system
[AD-A169423] N87-12571
SPACECRAFT MODULES
Viewport concept for space station modules
[NASA-TM-86559] N87-12592
SPACECRAFT POWER SUPPLIES
Advanced solar dynamic space power systems perspectives, requirements and technology needs
[NASA-TM-88884] N87-12606
Development of regenerable energy storage for space multimegawatt applications
[DE86-011070] N87-12998
Space nuclear safety program
[DE86-012767] N87-13261
SPACECRAFT STABILITY
New materials for spacecraft stability and damping: A feasibility study
[AD-A169826] N87-12601
SPACECRAFT STRUCTURES
A mathematical formulation of a large space structure control problem
[AD-A169950] N87-12602
SPARK GAPS
Nanosecond spark gap switching measurements
[DE86-012279] N87-12790
SPATIAL DISTRIBUTION
Periodic heat transfer through an inhomogeneous medium
[DE86-702988] N87-12825
SPATIAL RESOLUTION
Effects of reduced spatial resolution on the NEXRAD storm sequence algorithms
[PB86-221728] N87-13117
SPECIFICATIONS
Gas tungsten arc welding of aluminum alloys 6XXX. Welding procedure specification. Supplement 1: Records of procedure qualification tests
[DE86-012548] N87-12893
Gas tungsten arc welding of carbon steel to nickel-chromium-iron. Welding procedure specification. Supplement 1: Records of procedure qualification tests
[DE86-012549] N87-12894
Gas tungsten arc welding of chromium-nickel steel to nickel-molybdenum-chromium-iron. Welding procedure specification. Supplement 1: Records of procedure qualification tests
[DE86-012550] N87-12895
SPECIMENS
Localized ion milling of metallic and ceramic TEM specimens
[DE86-009538] N87-12900
SPECTRAL BANDS
Multispectral atmospheric mapping sensor of mesoscale water vapor features N87-13095
SPECTRAL RESOLUTION
Comparison of various techniques for calibration of AIS data N87-12970
Airborne spectroradiometry: The application of AIS data to detecting subtle mineral absorption features N87-12972
Atmospheric-water absorption features near 2.2 micrometers and their importance in high spectral resolution remote sensing N87-12973
SPECTRAL SIGNATURES
Patterns of vegetation in the Owens Valley, California N87-12988
SPECTRAL THEORY
A simple solar, spectral model for studying the effects of cloud cover and surface albedo on the incoming solar radiation
[AD-A171284] N87-13038
SPECTROMETERS
Slitless, intensified readout, gated spectrometer: Wavelength and efficiency calibration, time response characterization
[DE86-012349] N87-12839
Time Projection Compton Spectrometer (TPCS)
[DE86-012950] N87-12840
FET charge sensor and voltage probe
[NASA-CASE-NPO-16045-1] N87-13313
SPECTROSCOPY
Electron microprobe analysis: The upper limit of submicron spectroscopy
[DE86-009540] N87-12640
Raman spectroscopic investigation of molecular hydrogen
[DE86-012836] N87-12646
SPECTRUM ANALYSIS
Fiber-optic magnetic gradiometer with variable magnetic biasing fields
[AD-D012423] N87-12836
Acoustooptic spectrum analyzer using a planar Bragg-cell N87-13295
SPEECH
The effects of high sustained acceleration on the acoustic phonetic structure of speech: A preliminary investigation
[AD-A170563] N87-12748
SPEECH RECOGNITION
A test on the reliability and performance of the verbex series 4000 voice recognizer
[AD-A169066] N87-12729
Knowledge-based pitch detection
[AD-A169069] N87-12730
SPHERICAL COORDINATES
Relative motion of the Sun on an artificial satellite
[INPE-3985-NTE/260] N87-12591
SPIN DYNAMICS
Stability of liquid-filled projectiles with unusual coning frequencies
[AD-A171460] N87-12584
Magnetospheric plasma studies using data from the dynamics explorer high and low altitude plasma instruments
[AD-A169010] N87-13027
SPIN REDUCTION
Analysis of the nonlinear stability of circular Couette flow
[AD-A168951] N87-12811
SPIN STABILIZATION
Stability of liquid-filled projectiles with unusual coning frequencies
[AD-A171460] N87-12584
Analysis of the nonlinear stability of circular Couette flow
[AD-A168951] N87-12811
Low Q spin-up from rest
[AD-A169106] N87-12813
SPIN TESTS
An experimental investigation of free-tip response to a jet
[NASA-TM-88250] N87-12539
SPIN-SPIN COUPLING
Structural features at the Si-SiO2 interface
[DE86-012947] N87-13339
SPINE
Fracture and viscoelastic characteristics of the human cervical spine
[AD-A170002] N87-13133
Investigation of vibrations of the spinal column of healthy subjects N87-13155
SPLINE FUNCTIONS
An intuitive approach to geometric continuity for parametric curves and surfaces
[AD-A169654] N87-13211
SPRAY NOZZLES
Development testing of large volume water sprays for warm fog dispersal
[NASA-TP-2607] N87-12585
SPUTTERING
Plasma assisted surface coating/modification processes: An emerging technology
[NASA-TM-88885] N87-12708
STABILITY
Stability of multilayers at high temperatures
[DE86-010526] N87-12623
Transition metal. 2: Complexes of dithiacycloph anes
[AD-A169107] N87-12651
Use of analytical electron microscopy in evaluating ferrite stability in austenitic stainless steel welds
[DE86-008537] N87-12657
STABILITY TESTS
Mach 6 experimental and theoretical stability and performance of a finned cylindrical body at angles of attack up to 65 deg
[NASA-TM-89050] N87-12538
STABILIZATION
Stabilizing effects of finite-amplitude RF waves on the interchange instability
[DE86-013042] N87-12751

Stabilization of voltage-controlled oscillators through resonant cavities
[INPE-3941-RPE/512] N87-12757

STAGNATION FLOW
Visualisation of axial turbine tip clearance flow using a linear cascade
[CUED/A-TURBO/TR-122] N87-12560

STAINLESS STEELS
Comparative thermal conductivity measurements at Sandia National Laboratories
[DE86-012926] N87-12647
Use of analytical electron microscopy in evaluating ferrite stability in austenitic stainless steel welds
[DE86-006537] N87-12667
Welding procedure specification. Gas tungsten arc welding of chromium-nickel steel to chromium-molybdenum steel. Supplement 1: Records of procedure qualification tests
[DE86-012536] N87-12892
Unloading-compliance and load-drop analysis of J(Ic) test of irradiated 348 stainless steel
[AD-A170494] N87-12936

STANDARDS
Department of Defense gateway architecture and functional requirements
[AD-A169066] N87-13200

STAR FORMATION
The stellar upper mass limit in an OB association and implications for cosmic rays and cosmic abundances
N87-13392

STARTERS
Component improvement program task 83-01, 36E133 air turbine starter
[AD-A169483] N87-12562

STATIC FIRING
SSME main injector 4000 Hertz phenomenon
[NASA-CR-178934] N87-12808

STATIC PRESSURE
Pressure calculation for two-dimensional flow inside hydraulic structures
[AD-A169039] N87-12812

STATIC STABILITY
A procedure for attitude determination of artificial satellites utilizing techniques of static and dynamic optimal estimation
[INPE-3968-PRE/981] N87-12589

STATICS
A finite element method for localized failure analysis
[AD-A169117] N87-12930
MAGNA (Materially And Geometrically Nonlinear Analysis). Addendum 1, parts 1-4
[AD-A169383] N87-12933

STATISTICAL ANALYSIS
Determination of the coefficient of thermal expansion of JP-4 fuels
[AD-A171495] N87-12705
NDE reliability and process control for structural ceramics
[NASA-TM-88870] N87-12910
Influence of experimental scatter on the analysis and extrapolation of stress-rupture data
[DE86-009510] N87-12940
Statistical analysis and use of VAS radiance data
N87-13086
Design and analysis of experiments and more realistic techniques for data analysis
[AD-A168921] N87-13228
Statistical models and methods for cluster analysis and image segmentation
[AD-A169145] N87-13229
Two issues concerning the analysis of grouped data
[DE86-008401] N87-13242
Continuum radiation from active galactic nuclei: A statistical study
[NASA-CR-179925] N87-13368

STATISTICAL DISTRIBUTIONS
Surface correlation relationships in rough surface scattering
[AD-A169327] N87-12733
Extreme values of birth and death processes and queues
[AD-A169932] N87-13235
Two issues concerning the analysis of grouped data
[DE86-008401] N87-13242

STATISTICAL TESTS
A unified approach to constructing nonparametric rank tests
[AD-A169815] N87-13233

STATISTICAL WEATHER FORECASTING
Application of satellite data to tropic/subtropic moisture coupling N87-13053

STEADY FLOW
Time-dependent solution for axisymmetric flow over a blunt body with ideal gas, CF4, or equilibrium air chemistry
[NASA-TM-87675] N87-12806

STEADY STATE
The optimal linear combination of control variates in the presence of bias
[AD-A169111] N87-13210
Equilibrium configuration of coronal loops
[DE86-702711] N87-13384

STEAM FLOW
Fluid transients in pipes. Estimation of maximum pressures and forces in steam lines
[ESDU-86015] N87-12805

STEEL STRUCTURES
Guide to the use of data items on the fatigue strength of welded joints in steels
[ESDU-86013] N87-12914

STEELS
Bainite in chromium-molybdenum steels
[DE86-011781] N87-12668
Welding research in Scandinavia: An assessment
[AD-A169036] N87-12871
Heat measurements in inertia welding of aluminum to steel
[DE86-012463] N87-12885
Buffered explosions in steel pressure vessels
[DE86-006763] N87-12898
Effects of inertia weld parameters and contamination on weld flash shape and on joint strength: An improved study
[DE86-013074] N87-12904
Linear elastic fracture testing: Current status within ASTM committee E-24 on fracture
[AD-A169442] N87-12934
Crack propagation in high strain regions of a steel containment
[DE86-011437] N87-12943

STEERABLE ANTENNAS
Temperature and frequency compensated array beam steering unit
[AD-D012365] N87-12767

STEERING
Tracking servo compensator with rate aiding
[AD-D012368] N87-12735
A brief review of adaptive null steering techniques
[AD-A169548] N87-12736
Beam steering mirror construction
[AD-D012399] N87-13268

STELLAR ATMOSPHERES
Classification of N-type carbon stars
[AD-A171399] N87-13369

STELLAR CORONAS
Observational study of ion-electron equilibration and of cloud evaporation in supernova remnants under the HEAO-2 guest investigator program
[NASA-CR-179922] N87-13365

STELLAR EVOLUTION
Classification of N-type carbon stars
[AD-A171399] N87-13369

STELLAR MASS ACCRETION
Neutron and antineutron production in accretion onto compact objects
[NASA-TM-89264] N87-13395

STELLAR MODELS
Plane-parallel and bow shock models of Herbig-Haro objects N87-13374

STELLAR OCCULTATION
Classification of N-type carbon stars
[AD-A171399] N87-13369

STELLAR PHYSICS
Los Alamos Science, number 13, spring 1986
[DE86-012864] N87-13371

STELLAR RADIATION
Investigations of long-period DQ Herculis star
N87-13364

STELLAR ROTATION
Investigations of long-period DQ Herculis star
N87-13364

STELLAR SPECTRA
Plane-parallel and bow shock models of Herbig-Haro objects N87-13374

STIFFENING
Improved anti-G suit
[AD-D012378] N87-13171

STIRLING ENGINES
Linear harmonic analysis of free-piston Stirling engines
[DE86-012451] N87-12903
Progress of Stirling cycle analysis and loss mechanism characterization
[NASA-TM-88891] N87-13359

STOCHASTIC PROCESSES
Signal estimation, scattering theory and interpolation problems in one and two dimensions
[AD-A168969] N87-12759
Generalization of one-dimensional solute transport: A stochastic-convective flow conceptualization
[DE86-011117] N87-12820
Validity of Edgeworth expansions of minimum contrast estimators for Gaussian ARMA processes
[AD-A169931] N87-13217
Semigroups and Poisson-approximation
[AD-A170944] N87-13224
Heredity of stationary and reversible stochastic processes
[AD-A169926] N87-13234

STOICHIOMETRY
Low temperature formation of mullite
[AD-D012404] N87-12687

STOPPING
Frictional and retarding forces on aircraft tyres. Part 4: Estimation of effects of yaw
[ESDU-86016-PT-4] N87-12868

STOPPING POWER
Influence of a strong laser field on the stopping power for charged test particles in fusion plasmas
[INPE-3977-PRE/988] N87-12843

STORAGE
Holographic storage in ion-implanted, ferroelectric-phase PLZT ceramics
[DE86-010475] N87-12837

STORAGE RINGS (PARTICLE ACCELERATORS)
High-gain free electron lasers as generators of short wavelength coherent radiation
[DE86-012500] N87-12865

STORM ENHANCEMENT
Third International Symposium on Tropical Meteorology N87-12948

STORMS
Mesoscale ageostrophic circulations associated with baroclinic jet streaks N87-13070
Automated mesoscale winds derived from GOES multispectral imagery N87-13073
LAMPS software and mesoscale prediction studies N87-13076
Effects of reduced spatial resolution on the NEXRAD storm sequence algorithms
[PB86-221728] N87-13117

STORMS (METEOROLOGY)
Statistical analysis and use of VAS radiance data N87-13086
Studies of humid continental haze during SPACE N87-13088
A design study for a three-dimensional display computer terminal for meteorological information N87-13092

STRAIN ENERGY METHODS
Dynamic analysis of a Timoshenko beam using a finite element approach
[EPM/RT-86-34] N87-12919
Computation of the amplitude of stress singular terms for cracks and reentrant corners
[AD-A169796] N87-12936

STRAIN HARDENING
Finite element analyses of shear localization in rate and temperature dependent solids
[AD-A169057] N87-12927

STRAIN MEASUREMENT
A new and efficient formulation for finite element analysis of thin shell structures undergoing small and large deflection N87-12913

STRAIN RATE
Effect of strain and strain rate on residual microstructures in copper
[DE86-007361] N87-12859
Finite element analyses of shear localization in rate and temperature dependent solids
[AD-A169057] N87-12927
A finite element method for localized failure analysis
[AD-A169117] N87-12930

STRAPDOWN INERTIAL GUIDANCE
Fibre optic gyroscopes in inertial navigation
N87-13275

STRAPS
Improved anti-G suit
[AD-D012378] N87-13171

STRATEGY
Report of the Ad-Hoc Commission on remote sensing
[INPE-3961-NTE/259] N87-12963

STRATOSPHERE
Possible military applications of stratospheric airship discussed N87-12716
Description of data on the Nimbus 7 LIMS map archive tape: Ozone and nitric acid
[NASA-TP-2625] N87-13022
SAGE 2 satellite data set validation
[NASA-CR-178189] N87-13024
Collection of ions in the stratosphere
[AD-A169905] N87-13032
Parameterized numerical fit to total column ozone changes calculated by the LLNL 1-D model of the troposphere and stratosphere
[DE86-011008] N87-13040

Extraterrestrial forcing, atmospheric electricity and the occurrence of thunderstorms
[AD-A170463] N87-13111

STRESS (PHYSIOLOGY)
The effects of high sustained acceleration on the acoustic phonetic structure of speech: A preliminary investigation
[AD-A170563] N87-12746

STRESS (PSYCHOLOGY)
Determination of the load and stress of a cockpit crew during aircraft piloting using task networks and the simulation language SAINT N87-13150
Inquiry techniques for the evaluation of man machine systems N87-13162

STRESS ANALYSIS
Nuclear reaction analysis of hydrogen in metals
[AD-A169032] N87-12649
Factors influencing elastic stresses in double cantilever beam specimens
[NASA-TM-89033] N87-12922

STRESS CORROSION CRACKING
Crack-tip chemistry and fracture mechanics-based model of the crack growth rate/stress intensity relationship for Ni + P
[DE86-011106] N87-12676

STRESS INTENSITY FACTORS
Crack-tip chemistry and fracture mechanics-based model of the crack growth rate/stress intensity relationship for Ni + P
[DE86-011106] N87-12676
The control of polymer mechanical behavior by surface modification
[AD-A169252] N87-12686
Analysis of mixed-mode crack propagation using the boundary integral method
[NASA-CR-179518] N87-12915

STRESS MEASUREMENT
Intrinsic SiO2 film stress measurements on thermally oxidized Si
[AD-A169602] N87-12935

STRESS PROPAGATION
Stress assisted diffusion in elastic and viscoelastic materials
[AD-A169296] N87-12932

STRESSES
Stress effects on moisture transport in an epoxy resin and its composite
[AD-A169306] N87-12617
Influence of experimental scatter on the analysis and extrapolation of stress-rupture data
[DE86-009510] N87-12940
Crack propagation in high strain regions of a steel containment
[DE86-011437] N87-12943
Surface green function matching for a three-dimensional non-local continuum
[DE86-702647] N87-13341

STRUCTURAL ANALYSIS
Constructive and operational characteristics of a synchronous induction motor
[INPE-3976-RPE/517] N87-12755
Non-linear analysis of cylindrical shells
[EPM/RT-86-37] N87-12917
Analysis of anisotropic thin conical shells
[EPM/RT-86-36] N87-12918
MAGNA (Materially And Geometrically Nonlinear Analysis). Addendum 1, parts 1-4
[AD-A169383] N87-12933
An expert-system-like feedback approach in the hp-version of the finite element method
[AD-A169655] N87-13214
Experimental thin film deposition and surface analysis techniques
[DE86-011222] N87-13338

STRUCTURAL DESIGN
High voltage characteristics of the electrodynamic tether and the generation of power and propulsion
[NASA-CR-178949] N87-12609
Literature review on the design of composite mechanically fastened joints
[AD-A169112] N87-12872
Progress of Stirling cycle analysis and loss mechanism characterization
[NASA-TM-88801] N87-13359

STRUCTURAL DESIGN CRITERIA
General purpose aft cargo carrier study, volume 1
[NASA-CR-178905] N87-12587
Modeling the fundamental characteristics and processes of the spacecraft functioning
[NASA-TM-87999] N87-12598
Proceedings of the Solar Thermal Technology Conference
[DE86-011703] N87-13002

STRUCTURAL ENGINEERING
The application of boundary-element techniques for some soil-structure interaction problems
[AD-A168999] N87-12709

STRUCTURAL MEMBERS
New materials for spacecraft stability and damping: A feasibility study
[AD-A169626] N87-12601
Multiple rate shock isolator damping valve
[AD-D012394] N87-12679

STRUCTURAL PROPERTIES (GEOLOGY)
Theoretical study on the correlation between wideband electromagnetic spectra and geological structures
[AD-A168971] N87-13026

STRUCTURAL RELIABILITY
The 1984 IR and D (Independent Research and Development) advanced packaging study
[AD-A169388] N87-12765

STRUTS
Length adjustable strut link with low aerodynamic drag
[AD-D012279] N87-12543

SUBHARMONIC GENERATORS
Millimeter wave components — spaceborne microwave radiometers
[FTL-118521] N87-12605

SUBMERGING
Human thermoregulatory model for immersion in cold water
[AD-A169779] N87-13131

SUBMILLIMETER WAVES
Transmission through ferrite samples at submillimeter frequencies
[AD-A169178] N87-12731

SUBSTRATES
SAW transduction in electrostrictive substrates
[DE86-011651] N87-12794

SUN
Relative motion of the Sun on an artificial satellite
[INPE-3985-NTE/260] N87-12591
The stellar upper mass limit in an OB association and implications for cosmic rays and cosmic abundances N87-13392

SUNLIGHT
Solid-state electrochromic switchable window glazings
[DE86-004455] N87-12700

SUNRISE
Improving foF2 prediction for the sunrise transition period
[AD-A170457] N87-13036

SUNSET
Improving foF2 prediction for the sunrise transition period
[AD-A170457] N87-13036

SUPERCOMPUTERS
Solving scientific problems on hypercube parallel computers
[DE86-012622] N87-13199

SUPERCONDUCTORS
Development of a sensitive superconducting gravity gradiometer for geological and navigational applications
[NASA-CR-4011] N87-13021
Tunneling effect in superconductors with magnetic impurities
[DE86-702723] N87-13345
Flux spiral instability in a transport current carrying type 2 superconductor
[DE86-702724] N87-13346

SUPERCRITICAL FLUIDS
Electrochemistry in near-critical and supercritical fluids. 3: Studies of Br(-), I(-) and hydroquinone in aqueous solutions
[AD-A169138] N87-12633
Transport and relaxation processes in supercritical fluids
[DE86-007847] N87-12638

SUPERGRAVITY
Superconformal tensor calculus and matter couplings in six dimensions
[DE86-702617] N87-13349
Supergravity
[DE86-701481] N87-13370

SUPERHIGH FREQUENCIES
Microwave loss properties of hexagonal ferrites for millimeter wave applications
[AD-A168982] N87-13318

SUPERLATTICES
Potential applications of artificially structured materials for X-ray microanalysis
[DE86-010459] N87-12612
Propagation of electromagnetic waves in superlattices
[DE86-702660] N87-12753
Moessbauer-Borrmann superradiance
[DE86-012373] N87-12866
In-situ interdiffusion measurements in HgTe-CdTe superlattices
[DE86-011429] N87-13337

SUPERNOVA REMNANTS
Observational study of ion-electron equilibration and of cloud evaporation in supernova remnants under the HEAO-2 guest investigator program
[NASA-CR-179922] N87-13365
X-ray emission from supernova remnants N87-13398

SUPERSONIC COMBUSTION RAMJET ENGINES
Further shock tunnel studies of scramjet phenomena
[NASA-CR-179937] N87-12542

SUPERSONIC FLOW
An approximate method of estimating the aerodynamic interference between two parallel bodies in a supersonic flow (axial force)
[BR-100271] N87-12540

SUPERSYMMETRY
Superconformal tensor calculus and matter couplings in six dimensions
[DE86-702617] N87-13349
Supergravity
[DE86-701481] N87-13370

SURFACE ACOUSTIC WAVE DEVICES
SAW transduction in electrostrictive substrates
[DE86-011651] N87-12794

SURFACE CRACKS
Crack propagation in high strain regions of a steel containment
[DE86-011437] N87-12943

SURFACE FINISHING
Plasma assisted surface coating/modification processes: An emerging technology
[NASA-TM-88885] N87-12708

SURFACE LAYERS
Available potential energy in upper layer of world ocean N87-12949

SURFACE NAVIGATION
Medium-frequency data link for differential NAVSTAR/GPS broadcasts
[AD-A169788] N87-12554

SURFACE PROPERTIES
Comparison of methods for the calculation of thermal contact resistance of the first Brazilian satellite
[INPE-3984-TDL/217] N87-12596
Electron spectroscopy in fundamental catalytic studies
[DE86-008781] N87-12639
Digest: Proceedings of the International Conference on Optical and Millimeter Wave Propagation and Scattering in the Atmosphere
[AD-A170393] N87-12743
A constitutive law for finite element contact problems with unclassical friction
[NASA-TM-88838] N87-12924
Analysis of AIS radiometry with emphasis on determination of atmospheric properties and surface reflectance N87-12971
Near-infrared detection of ammonium minerals at Ivanhoe Hot Springs, Nevada N87-12981
Theory for computing the field scattered from a smooth inflected surface
[NASA-TP-2632] N87-13264
Experimental thin film deposition and surface analysis techniques
[DE86-011222] N87-13338

SURFACE REACTIONS
Carbon monoxide adsorption on a platinum electrode studied by polarization modulated FT-IR reflection-absorption spectroscopy. 2: CO adsorbed at a potential in the hydrogen region and its oxidation in acids
[AD-A169082] N87-12632
On the interplay between chemical reactions and phase transitions for molecules adsorbed on solid surfaces
[AD-A169818] N87-12636
Diamond-machined aluminum alloy 5083 surfaces: Controlled exposure evaluation
[DE86-012572] N87-12674
Proceedings of the Topical Meeting on the Microphysics of Surfaces, Beams and Adsorbates held in Santa Fe, New Mexico on 4-6 February 1985
[AD-A170797] N87-13329

SURFACE ROUGHNESS
Surface correlation relationships in rough surface scattering
[AD-A169327] N87-12733
In-line and transverse forces on smooth and rough cylinders in oscillatory flow at high Reynolds numbers
[AD-A169582] N87-12815
Natural convection in an enclosure with discrete roughness elements on a vertical heated wall
[DE86-004424] N87-12817

SURFACE WAVES
Lg wave excitation and propagation in presence of one-, two-, and three-dimensional heterogeneities
[AD-A169325] N87-13030
Nonlinear interactions in the microwave sensing of oceanic internal waves
[AD-A169776] N87-13120

SURFACES
An intuitive approach to geometric continuity for parametric curves and surfaces
[AD-A169654] N87-13211
SURFACTANTS
Investigation of deviations from ideality in the two liquid phase region of systems of medium molecular weight hydrocarbon mixtures and water
[AD-A169752] N87-12635
Theory of developed hydrodynamical turbulence
[DE86-012796] N87-12823
SURGES
Fluid transients in pipes. Estimation of maximum pressures and forces in steam lines
[ESDU-86015] N87-12805
SURVEILLANCE
Very low bandwidth, unattended imager for surveillance applications
[DE86-013570] N87-12799
SURVEYS
Report on the activities of the irrigated crop survey in Sao Paulo State from remote sensing products, phase 2
[INPE-3950-RPE/513] N87-12989
Comparison of tropical forest surveys
[DE86-011699] N87-12993
SURVIVAL
Duel between an ASAT (anti-satellite) with multiple kill vehicles and a space-based weapons platform with kinetic energy weapons
[AD-A168946] N87-13245
SWEPTBACK WINGS
Blast gust loading on a 35 degree swept-back wing
[AD-A169415] N87-12570
SWITCHES
Modeling of high-explosive driven plasma compression opening switches
[DE86-012421] N87-12795
SWITCHING
Nanosecond spark gap switching measurements
[DE86-012279] N87-12790
SWITCHING CIRCUITS
Component improvement program task 83-01, 36E133 air turbine starter
[AD-A169483] N87-12562
Optoelectronic broadband switching for communications and signal processing N87-13294
SYNCHRONOUS MOTORS
Constructive and operational characteristics of a synchronous induction motor
[INPE-3976-RPE/517] N87-12755
SYNCHRONOUS SATELLITES
Meter-level orbit determination of geosynchronous satellites by an economical tracking system N87-12575
Studies of lightning data in conjunction with geostationary satellite data N87-13058
SYNCHROTRON RADIATION
X-ray fluorescence with synchrotron radiation
[DE86-010543] N87-13124
X-ray data booklet, revision
[DE86-012650] N87-13272
SYNOPTIC METEOROLOGY
Application of satellite data to tropic/subtropic moisture coupling N87-13053
Mesoscale-cloud scale simulation of convective response N87-13077
A summary of research on mesoscale energetics of severe storm environments N87-13082
SYNTHESIS (CHEMISTRY)
Investigation of the effects of short chain processing additives on polymers
[NASA-TM-89023] N87-12614
Transition metal. 2: Complexes of dithiacycloph anes
[AD-A169107] N87-12651
Electrokinetic properties of polymer colloids
[NASA-CR-178938] N87-12681
Low temperature formation of mullite
[AD-D012404] N87-12687
Synthesis of conjugated polymers with alternating aromatic and quinonoid sequences via elimination on precursors
[AD-A171331] N87-12693
Methods for the syntheses of mono-, di-, tri- and tetranitro derivatives of diphenylamine
[WSRL-0436-TR] N87-12702
Rapid synthesis of indium phosphide
[AD-D012362] N87-13322
SYNTHETIC APERTURE RADAR
A new method of synthetic aperture radar image reconstruction using modified convolution back-projection algorithm
[AD-A170652] N87-12747
ERS-1 SAR data processing
[NASA-CR-179913] N87-12965
Lightwave technology in future radar equipment designs N87-13304
SYNTHETIC ARRAYS
Lightwave technology in future radar equipment designs N87-13304
SYNTHETIC FUELS
Production of a clean carbon fuel derived from coal for use in stationary and mobile heat engines
[DE86-011203] N87-12706
SYSTEM FAILURES
An application of a LISP based expert system for failure diagnosis of the CH-47 flight control hydraulic system
[AD-A168970] N87-12567
SYSTEM IDENTIFICATION
Signal estimation, scattering theory and interpolation problems in one and two dimensions
[AD-A168969] N87-12759
SYSTEMS ANALYSIS
Procedure for one axis satellites attitude control with magnetic actuation
[INPE-3895-PRE/937] N87-12590
An approach to design knowledge capture for the space station
[NASA-TM-89272] N87-12597
Advanced solar dynamic space power systems perspectives, requirements and technology needs
[NASA-TM-88884] N87-12606
Constructive and operational characteristics of a synchronous induction motor
[INPE-3976-RPE/517] N87-12755
System-ergonomic workload analysis for highly automated process control tasks N87-13152
SYSTEMS ENGINEERING
Sodium-sulfur battery systems development
[DE86-011424] N87-12788
Tool to develop real time simulation systems
[INPE-3979-TDL/233] N87-13179
SYSTEMS INTEGRATION
Problems in integrated digital networks
[AD-A170442] N87-12744
Evaluation of automated decisionmaking methodologies and development of an integrated robotic system simulation. Appendix B: ROBSIM programmer's guide
[NASA-CR-178052] N87-13203
SYSTEMS MANAGEMENT
Federal information systems management: Problems, solutions and more problems
[AD-A171366] N87-13353
SYSTEMS STABILITY
Computational and experimental study of flow-induced vibration of the SSME main injector post
[DE86-012119] N87-12611

T

TAIL ASSEMBLIES
Length adjustable strut link with low aerodynamic drag
[AD-D012279] N87-12543
TARGET ACQUISITION
The eye-mark investigation as an anthropotechnical method to study man machine systems N87-13160
TARGET RECOGNITION
Improving foF2 prediction for the sunrise transition period
[AD-A170457] N87-13036
TASKS
The measurement of the psychological workload during task-related activities, including car driving, by competing time interval estimation N87-13153
Development of a research method to determine the quality of task mastering by navigators in ship guidance N87-13154
TAXONOMY
Application of the task taxonomy method to the simulation of human service reliability in the manual control of aircraft
[MBB/LKE-301/S/PUB/216] N87-13151
TAYLOR INSTABILITY
Analysis of the nonlinear stability of circular Couette flow
[AD-A168951] N87-12811
TECHNOLOGICAL FORECASTING
The portfolio model of technological development in the aircraft industry
[AD-A170832] N87-12534
TECHNOLOGIES
Welding science and technology in Europe: A survey and assessment
[AD-A169279] N87-12873
TECHNOLOGY ASSESSMENT
The portfolio model of technological development in the aircraft industry
[AD-A170832] N87-12534
Advanced solar dynamic space power systems perspectives, requirements and technology needs
[NASA-TM-88884] N87-12606
Assessment of damage tolerance requirements and analyses: A user's manual for crack growth and crack initiation analysis: DAMGRO
[AD-A171209] N87-12939
TECHNOLOGY TRANSFER
The uncounted benefits: Federal efforts in domestic technology transfer
[NASA-CR-177044] N87-13358
An examination of technology transfer as a tool for management
[AD-A169184] N87-13360
Technology transfer at Pacific Northwest Laboratory
[DE86-012333] N87-13361
TECHNOLOGY UTILIZATION
Technology transfer at Pacific Northwest Laboratory
[DE86-012333] N87-13361
TELECOMMUNICATION
SARSAT (Search and Rescue Satellite) operational data categorization and accuracy studies
[AD-A169748] N87-12599
Maximization of the capacity of the most survivable connections in a network
[AD-A169065] N87-12728
TELEMETRY
Instrumentation research and support services
[AD-A169278] N87-13029
TELEVISION SYSTEMS
Integrating computer vision with a robot arm system
[AD-A171278] N87-12884
TEMPERATURE COMPENSATION
Temperature compensation in the 2:17 type magnet a
[AD-A169487] N87-13250
TEMPERATURE CONTROL
Shower and high-pressure oil temperature control
[DE86-009398] N87-12899
TEMPERATURE DEPENDENCE
Finite element analyses of shear localization in rate and temperature dependent solids
[AD-A169057] N87-12927
Data requirements to model creep in 9Cr-1Mo-V steel
[DE86-011754] N87-12944
TEMPERATURE EFFECTS
Vapour pressures and critical points of liquids. Part 2C: Alkadienes and alkynes
[ESDU-86001-PT-2C] N87-12624
Optical spectroscopy of dynamically compressed liquids
[AD-A169013] N87-12629
Fracture toughness of CIP-HIP beryllium at elevated temperatures
[AD-A169769] N87-12654
Temperature and frequency compensated array beam steering unit
[AD-D012365] N87-12767
TEMPERATURE GRADIENTS
Process for carbon-carbon composite fabrication
[AD-D012413] N87-12621
TEMPERATURE MEASUREMENT
Evaluation of the Collins/Rockwell two axis gyro/accelerometer sensor cluster (phase 3 unit)
[AD-A169810] N87-12834
Coordinated study of the behavior of the middle atmosphere in winter: Monthly mean comparisons of satellite and radiosonde data and derived quantities N87-13019
TEMPERATURE PROFILES
Sensor controlled robotic welding for nuclear applications
[DE86-013110] N87-12905
TEMPERATURE SENSORS
Fiber optic device for temperature remote sensing N87-13280
TENSOR ANALYSIS
Solving systems of nonlinear equations by tensor methods
[AD-A169927] N87-13216
TENSORS
Solving systems of nonlinear equations by tensor methods
[AD-A169927] N87-13216
Induced quantum torsion
[DE86-702616] N87-13348
Superconformal tensor calculus and matter couplings in six dimensions
[DE86-702617] N87-13349
TERMINAL GUIDANCE
Guidance law simulation studies for complex approaches using the Microwave Landing System (MLS)
[NASA-CR-178182] N87-12552
TERMINOLOGY
Space flight operations communications phraseology and techniques
[NASA-TM-86562] N87-12721

TERRAIN
Surface correlation relationships in rough surface scattering
[AD-A169327] N87-12733
Sensitivity tests of a surface-layer windflow model to effects of stability and vegetation
[AD-A169136] N87-13101
TERRESTRIAL RADIATION
Stratospheric balloon experiments
[INPE-3995-RPE/519] N87-13020
The use of satellite data in understanding and predicting convective and large-scale dynamical processes N87-13049
TEST FACILITIES
Joint operating procedure for interrange scheduling
[AD-A169636] N87-12579
TETHERED SATELLITES
High voltage characteristics of the electrodynamic tether and the generation of power and propulsion
[NASA-CR-178949] N87-12609
TEXAS
Revised Uniform Summary of Surface Weather Observations (RUSSWO). Parts A-F Ellington ANGB, Texas
[AD-A169389] N87-13105
THEMATIC MAPPING
The Multispectral Atmospheric Mapping Sensor (MAMS): Instrument description, calibration and data quality
[NASA-TM-86565] N87-12828
Soil types and forest canopy structures in southern Missouri: A first look with AIS data N87-12963
Generation of images with recorded auxiliary data for the LANDSAT Thematic Mapper (TM) imagery
[INPE-3982-TDL/234] N87-12990
THEORETICAL PHYSICS
Theoretical high energy physics
[DE86-012669] N87-13259
THERMAL ABSORPTION
Phase change thermal energy storage methods for combat vehicles, phase 1
[AD-A170492] N87-12713
THERMAL ANALYSIS
The 1984 IR and D (Independent Research and Development) advanced packaging study
[AD-A169388] N87-12765
THERMAL CONDUCTIVITY
Comparative thermal conductivity measurements at Sandia National Laboratories
[DE86-012926] N87-12647
Periodic heat transfer through an inhomogeneous medium
[DE86-702988] N87-12825
Finite element analyses of shear localization in rate and temperature dependent solids
[AD-A169057] N87-12927
THERMAL EXPANSION
New materials for spacecraft stability and damping: A feasibility study
[AD-A169626] N87-12601
Determination of the coefficient of thermal expansion of JP-4 fuels
[AD-A171495] N87-12705
Computation of residual stresses due to phase transformations during quenching of hollow cylinders
[AD-A170493] N87-12937
Thermophysical properties measurements of gallium arsenide and cadmium telluride
[AD-A169901] N87-13326
THERMAL INSTABILITY
Cryogenic wound rotor for lightweight, high voltage generators
[AD-D012370] N87-12768
THERMAL STABILITY
Temperature compensation in the 2:17 type magnet s
[AD-A169487] N87-13250
THERMAL STRESSES
Intrinsic SiO2 film stress measurements on thermally oxidized Si
[AD-A169602] N87-12935
THERMOCHEMISTRY
Plasma joining of metal matrix composites
[AD-A169056] N87-12615
New results on low temperature thermal oxidation of silicon
[AD-A169603] N87-12834
Plasma assisted surface coating/modification processes: An emerging technology
[NASA-TM-88885] N87-12708
Intrinsic SiO2 film stress measurements on thermally oxidized Si
[AD-A169602] N87-12935
Experimental investigation of thermochemical transport for solar applications using sulfur trioxide
[DE86-011762] N87-13005
THERMOCLINES
The Gulf Stream dynamics experiment. Inverted echo sounder data report for the June 1984 to May 1985 deployment period
[AD-A170758] N87-13121
THERMODYNAMIC PROPERTIES
Analysis and verification of the icing scaling equations. Volume 1: Revision
[AD-A167976] N87-12551
Comparison of methods for the calculation of thermal contact resistance of the first Brazilian satellite
[INPE-3864-TDL/217] N87-12596
Relationship of in-cylinder gaseous and particulate concentration to radiative heat transfer in direct injection-type diesel combustion
[AD-A168979] N87-12628
The 1984 IR and D (Independent Research and Development) advanced packaging study
[AD-A169388] N87-12765
Progress of Stirling cycle analysis and loss mechanism characterization
[NASA-TM-88891] N87-13359
THERMODYNAMICS
Phase equilibrium predictions for polar and hydrogen bonding mixtures
[DE86-011612] N87-12642
The influence of welding flux on the pyrometallurgical, physical and mechanical behavior of weld metal
[AD-A169067] N87-12650
Characterization and dynamical studies of polymers in dipolar (aprotic) liquids
[AD-A169243] N87-12685
Shock-induced solid state chemistry: Theoretical background
[DE86-012741] N87-12941
THERMOELECTRIC GENERATORS
Space nuclear safety program
[DE86-012767] N87-13261
THERMOPHYSICAL PROPERTIES
Thermophysical properties measurements of gallium arsenide and cadmium telluride
[AD-A169901] N87-13326
THERMOPLASTICITY
An analysis of shear band development incorporating heat conduction
[AD-A168972] N87-12926
THERMOREGULATION
Human thermoregulatory model for immersion in cold water
[AD-A169779] N87-13131
THICK PLATES
Influence of shear modulus on the behavior of acoustically transparent materials
[AD-A169289] N87-12931
THIN FILMS
Intrinsic SiO2 film stress measurements on thermally oxidized Si
[AD-A169602] N87-12935
Stable, high-efficiency, CuInSe2-based polycrystalline thin-film tandem solar cells
[DE86-010705] N87-13003
Solid State Photovoltaic Research Branch annual report, FY 1985
[DE86-010708] N87-13004
Growth of ferro-electric tungsten bronze epitaxial thin films for electro-optic device applications
[AD-A170783] N87-13328
Experimental thin film deposition and surface analysis techniques
[DE86-011222] N87-13338
THIN WALLED SHELLS
A new and efficient formulation for finite element analysis of thin shell structures undergoing small and large deflection N87-12913
Non-linear analysis of cylindrical shells
[EPM/RT-86-37] N87-12917
Analysis of anisotropic thin conical shells
[EPM/RT-86-38] N87-12918
THREE AXIS STABILIZATION
A procedure for attitude determination of artificial satellites utilizing techniques of static and dynamic optimal estimation
[INPE-3966-PRE/961] N87-12589
THREE DIMENSIONAL BODIES
A software implementation of an interactive graphics system for three dimensional modeling and layout
[AD-A169264] N87-13183
THREE DIMENSIONAL FLOW
On 3-D inelastic analysis methods for hot section components (base program)
[NASA-CR-175060] N87-12923
THRUST
Propellar/body interaction for thrust and drag
[ESDU-86017] N87-12537
Electronic Engineering Department Thrust Area report, FY 1985
[DE86-013172] N87-12797
THRUST CONTROL
Thrust reverser-exhaust nozzle assembly for a gas turbine engine
[AD-D012390] N87-12561
THRUST REVERSAL
Effect of port corner geometry on the internal performance of a rotating-vane-type thrust reverser
[NASA-TP-2624] N87-12541
Thrust reverser-exhaust nozzle assembly for a gas turbine engine
[AD-D012390] N87-12561
THRUST VECTOR CONTROL
Brief analysis of normal attitude accuracies of satellites with wheels or gas jets
[INPE-3993-NTE/262] N87-12594
THUNDERSTORMS
Regular noise background in VLF-radiation and world thunderstorm centers N87-12857
NASA/MSFC FY-85 Atmospheric Processes Research Review
[NASA-CP-2402] N87-13043
Severe storm electricity N87-13056
Optical characteristics of lightning and thunderstorm currents N87-13061
Optical characteristics of lightning N87-13062
Airborne atmospheric electricity experiments N87-13063
Mobile intercept of storms N87-13064
Remote observations of severe storms N87-13065
Analysis of satellite data for sensor improvement (detection of severe storms from space N87-13071
Severe storm detection with passive 37 GHz observations N87-13072
Remote sensing of severe convective storms N87-13075
A summary of research on mesoscale energetics of severe storm environments N87-13082
Investigations of severe/tornadic thunderstorm development and evolution based on satellite and AVE/SESAME/VAS data N87-13084
Extraterrestrial forcing, atmospheric electricity and the occurrence of thunderstorms
[AD-A170463] N87-13111
NOSL experiment support
[NASA-CR-178947] N87-13140
TIME DEPENDENCE
Measurement of time-dependent electric current with Rogowski coil
[INPE-3875-RPE/506] N87-12754
Time-dependent solution for axisymmetric flow over a blunt body with ideal gas, CF4, or equilibrium air chemistry
[NASA-TM-87675] N87-12806
Free-Lagrangian hydrodynamics using massless tracer points
[DE86-012406] N87-12822
Data requirements to model creep in 9Cr-1Mo-V steel
[DE86-011754] N87-12944
A sensitivity study of a one-dimensional time-dependent warm cumulus cloud model
[AD-A170141] N87-13109
TIME DIVISION MULTIPLEXING
Progress with multiplexed sensor arrays based on reflection at spliced joints between sensors N87-13278
TIME OF FLIGHT SPECTROMETERS
A versatile Data Processing Unit (DPU) for satellite-borne composition instrumentation N87-13393
TIME SERIES ANALYSIS
Vector analysis and satellite footprints
[AD-A169632] N87-12576
The Gulf Stream dynamics experiment. Inverted echo sounder data report for the June 1984 to May 1985 deployment period
[AD-A170758] N87-13121
Statistical models and methods for cluster analysis and image segmentation
[AD-A169145] N87-13229
TIMOSHENKO BEAMS
Dynamic analysis of a Timoshenko beam using a finite element approach
[EPM/RT-86-34] N87-12919
TIN
Use of Wannier function in the calculations of band structure of covalent crystals
[DE86-702668] N87-13344
TIPS
An experimental investigation of free-tip response to a jet
[NASA-TM-88250] N87-12539
Supplementary calibration test of the tip-aerodynamics-and acoustics-test pressure transducers
[NASA-TM-88312] N87-12830

TIROS SATELLITES
Application of satellite data to tropic/subtropic moisture coupling N87-13053
TISSUES (BIOLOGY)
Trace element-induced stress in freshwater wetland vegetation: Preliminary results N87-12985
TITANIUM ALLOYS
An interdisciplinary approach to predictive modeling of structural adhesive bonding. Characterization of Ti-6Al-4V oxides and the adhesive/oxide interphase [AD-A170484] N87-12690
TITANIUM OXIDES
An interdisciplinary approach to predictive modeling of structural adhesive bonding. Characterization of Ti-6Al-4V oxides and the adhesive/oxide interphase [AD-A170484] N87-12690
TOKAMAK DEVICES
Compact reactor studies [DE86-013247] N87-13263
TOLERANCES (MECHANICS)
Fatigue behavior of long and short cracks in wrought and powder aluminum alloys [AD-A169960] N87-12656
Assessment of damage tolerance requirements and analyses: A user's manual for crack growth and crack initiation analysis: DAMGRO [AD-A171209] N87-12939
TOLERANCES (PHYSIOLOGY)
Self-paced heat acclimation procedures [AD-A170533] N87-13134
Guidelines for safe human experimental exposure to impact acceleration [AD-A169347] N87-13169
TOOLS
Light socket removal tool [AD-D012368] N87-12710
TOPOGRAPHY
Development of ultrasonic modelling techniques for the study of seismic wave scattering due to crustal inhomogeneities [AD-A170017] N87-13034
Sensitivity tests of a surface-layer windflow model to effects of stability and vegetation [AD-A169136] N87-13101
TOPOLOGY
HOMPACK: A suite of codes for globally convergent homotopy algorithms [DE86-011644] N87-13196
TORNADOES
Detection of rotating thunderstorms using satellite imagery N87-13085
TORSION
Induced quantum torsion [DE86-702616] N87-13348
TOUGHNESS
Micromechanisms of crack growth and fracture toughness in metal matrix composites [AD-A169839] N87-12620
TOXICITY
Evaluating ecosystem response to toxicant stress: a state space approach [DE86-011777] N87-13009
TRACKING (POSITION)
Solar array flight dynamic experiment [NASA-TP-2596] N87-12581
Balloon-borne, high altitude gravimetry: The flight of DUCKY 1a (11 October 1983) [AD-A169942] N87-13033
Investigations of severe/tornadic thunderstorm development and evolution based on satellite and AVE/SESAME/VAS data N87-13084
TRAJECTORIES
Some tactical algorithms for spherical geometry [AD-A170615] N87-12555
Electron microprobe analysis: The upper limit of submicron spectroscopy [DE86-009540] N87-12640
Study in molecular lasers [AD-A169933] N87-12855
TRANSFER FUNCTIONS
Theoretical study on the correlation between wideband electromagnetic spectra and geological structures [AD-A168971] N87-13026
TRANSFER OF TRAINING
Simulator design features for helicopter landing on small ships. 1: A performance study [AD-A169514] N87-12572
Simulator design and instructional features for carrier landing: A field transfer study [AD-A169962] N87-12573
TRANSFERRED ELECTRON DEVICES
Investigation of a new concept in semiconductor microwave oscillators [AD-A170772] N87-12781
Investigation of a new concept in semiconductor microwave oscillators [AD-A170631] N87-12782
TRANSFORMATIONS (MATHEMATICS)
Heredity of stationary and reversible stochastic processes [AD-A169926] N87-13234
TRANSFORMERS
Transformers for explosive pulsed power coupling to various loads [DE86-012425] N87-12796
TRANSISTORS
The analysis of a transistor cap as a heat dissipator [AD-A171398] N87-12786
Comparison of 2D memory SEU transport simulation with experiments [ATR-86(8139)-2] N87-13314
TRANSITION FLOW
Transition and mixing in axisymmetric jets and vortex rings [NASA-CR-3893] N87-12808
TRANSITION METALS
Transition metal. 2: Complexes of dithiacycloph anes [AD-A169107] N87-12651
Plasma-enhanced deposition and processing of transition metals and transition metal silicides for VLSI [AD-A168963] N87-13316
TRANSITION POINTS
Micromechanisms and toughness for cleavage fracture of steel [AD-A169906] N87-12655
TRANSMISSION
Transmission through ferrite samples at submillimeter frequencies [AD-A169178] N87-12731
TRANSMISSION EFFICIENCY
Effects of optical feedback on the performance of high data rate single-mode fiber systems N87-13288
Wide bandwidth, long distance fibre-optic communication systems N87-13300
Performance of RF fiber optic links N87-13301
TRANSMITTANCE
Solid-state electrochromic switchable window glazings [DE86-004455] N87-12700
TRANSMITTER RECEIVERS
Twin aperture phased array lens antenna [AD-D012415] N87-12745
Tactical fiber optic assembly requirements N87-13305
TRANSONIC FLOW
Viscous-inviscid interaction in transonic separated flow over solid and porous airfoils and cascades N87-12535
TRANSPARENCE
Influence of shear modulus on the behavior of acoustically transparent materials [AD-A169289] N87-12931
TRANSPORT PROPERTIES
Stress effects on moisture transport in an epoxy resin and its composite [AD-A169306] N87-12617
Transport and relaxation processes in supercritical fluids [DE86-007847] N87-12638
Models and radiation of railgun plasma armatures with non-ideal plasma properties [AD-A169349] N87-13258
Degeneracy in the ensemble Monte Carlo method for high field transport in semiconductors [AD-A169456] N87-13321
TRANSVERSE OSCILLATION
In-line and transverse forces on smooth and rough cylinders in oscillatory flow at high Reynolds numbers [AD-A169562] N87-12815
TRIBOLOGY
Fundamental research on tribology [AD-A169974] N87-12682
TRIGGER CIRCUITS
Coordinated research program in pulsed power physics [AD-A169113] N87-12762
TROPICAL METEOROLOGY
USSR report: Earth sciences [JPRS-UES-86-007] N87-12946
Third International Symposium on Tropical Meteorology N87-12948
Dynamics and energetics of the South Pacific Convergence Zone during FGGE SOP-1 N87-13052
Application of satellite data to tropic/subtropic moisture coupling N87-13053
TROPICAL REGIONS
Comparison of tropical forest surveys [DE86-011699] N87-12993
TROPOSPHERE
Experimental research on turbulence in upper-level tropospheric clouds N87-12952
Parameterized numerical fit to total column ozone changes calculated by the LLNL 1-D model of the troposphere and stratosphere [DE86-011008] N87-13040
Variation objective analyses for cyclone studies N87-13050
Extraterrestrial forcing, atmospheric electricity and the occurrence of thunderstorms [AD-A170463] N87-13111
TROPOSPHERIC SCATTERING
Foreground effects on troposcatter digital communication systems [AD-A169380] N87-12734
TRUSSES
A mathematical formulation of a large space structure control problem [AD-A169950] N87-12602
TUNGSTEN ALLOYS
Growth of ferro-electric tungsten bronze epitaxial thin films for electro-optic device applications [AD-A170783] N87-13328
TUNING
Double-ended tuning fork quartz accelerometer [DE86-012277] N87-12842
TUNNEL DIODES
Millimeter-wave heterojunction two-terminal devices [AD-A168985] N87-12760
TURBINE BLADES
Journal of engineering thermophysics (selected articles) [AD-A169452] N87-13347
TURBINE ENGINES
Component improvement program task 83-01, 36E133 air turbine starter [AD-A169483] N87-12562
Turbine air seal with full backside cooling [AD-D012405] N87-12564
Improved vane platform sealing and retention means [AD-D012407] N87-12681
TURBINES
Turbine air seal with full backside cooling [AD-D012405] N87-12564
TURBOCOMPRESSORS
Journal of engineering thermophysics (selected articles) [AD-A169452] N87-13347
TURBOFAN ENGINES
Length adjustable strut link with low aerodynamic drag [AD-D012279] N87-12543
Simplified forms of performance equations. Addendum A: Effect on aeroplane level speed of small changes in thrust, drag, weight, power [ESDU-86004-ADD-A] N87-12556
Effects of test cell recirculation on high-bypass turbofan engines during simulated altitude tests [AD-A171418] N87-12565
TURBOJET ENGINES
Computational fluid dynamic studies of certain ducted bluff-body flowfields relevant to turbojet combustors. Volume 1: Time-dependent calculations with the k-epsilon turbulence model for an existing centerbody combustor [AD-A171434] N87-12816
TURBULENCE
Theory of developed hydrodynamical turbulence [DE86-012796] N87-12823
Convective surface layers: Influence of the boundary layer depth N87-13041
TURBULENT BOUNDARY LAYER
A detailed analysis of the influence of eddy exchange processes upon the development of radiation fog [AD-A169233] N87-13102
TURBULENT DIFFUSION
Middle atmosphere modeling [NASA-CR-179934] N87-13023
TURBULENT FLOW
Computational and experimental study of flow-induced vibration of the SSME main injector post [DE86-012119] N87-12611
Computational fluid dynamic studies of certain ducted bluff-body flowfields relevant to turbojet combustors. Volume 1: Time-dependent calculations with the k-epsilon turbulence model for an existing centerbody combustor [AD-A171434] N87-12816
TURNING FLIGHT
Optimal descending, hypersonic turn to heading [DE86-010989] N87-12577
TWINNING
Effect of residual strain on twinning in shock-loaded copper [DE86-007362] N87-12660
TWO DIMENSIONAL FLOW
Forced oscillation of a two-dimensional airfoil with nonlinear aerodynamic loads' [AD-A169350] N87-12546
A numerical model for two-dimensional unsteady flow calculations with a surface panel method N87-12548

Pressure calculation for two-dimensional flow inside hydraulic structures
[AD-A169039] N87-12812

TWO PHASE FLOW
Study of numerical solution methods for two-phase flows
[DE86-012265] N87-12321

U

ULTRASONIC SPECTROSCOPY
Quantitative non-destructive evaluation of composite materials based on ultrasonic wave propagation
[NASA-CR-179831] N87-12613

ULTRASONICS
Concurrent ultrasonic weld evaluation system
[DE86-013772] N87-12908
Development of ultrasonic modelling techniques for the study of seismic wave scattering due to crustal inhomogeneities
[AD-A170017] N87-13034

ULTRAVIOLET LASERS
Direct writing of microstructures for solid-state electronics
[AD-A170837] N87-12783

ULTRAVIOLET SPECTRA
Optical spectroscopy of dynamically compressed liquids
[AD-A169013] N87-12629

UNDERWATER ACOUSTICS
MIZEX: A program for mesoscale air-ice-ocean interaction experiments in arctic marginal ice zones. 8: A science plan for a winter marginal ice zone experiment in the Fram Strait/Greenland Sea, 1987/89
[AD-A169070] N87-13119

UNITED STATES
Maximization of the capacity of the most survivable connections in a network
[AD-A169065] N87-12728
The Department of Defense Very High Speed Integrated Circuit (VHSIC) Technology Availability Program plan for the Committees on Armed Services, United States Congress
[AD-A169250] N87-12763

UNIVERSE
Los Alamos Science, number 13, spring 1986
[DE86-012664] N87-13371

UNIVERSITIES
Technology transfer at Pacific Northwest Laboratory
[DE86-012333] N87-13361

UNSTEADY FLOW
A numerical model for two-dimensional unsteady flow calculations with a surface panel method N87-12548
In-line and transverse forces on smooth and rough cylinders in oscillatory flow at high Reynolds numbers
[AD-A169562] N87-12515
Computational fluid dynamic studies of certain ducted bluff-body flowfields relevant to turbojet combustors. Volume 1: Time-dependent calculations with the k-epsilon turbulence model for an existing centerbody combustor
[AD-A171434] N87-12516

UPPER ATMOSPHERE
The upper atmosphere of Venus: A tentative explanation of its rotation
[NASA-TM-86505] N87-13375

URANIUM
Status of laser enrichment technology updated N87-12717

USER MANUALS (COMPUTER PROGRAMS)
Assessment of damage tolerance requirements and analyses: A user's manual for crack growth and crack initiation analysis: DAMGRO
[AD-A171209] N87-12939
User's guide for NPSOL (version 4.0): A Fortran package for nonlinear programming
[AD-A169115] N87-13180
Evaluation of automated decisionmaking methodologies and development of an integrated robotic system simulation. Appendix B: ROBSIM programmer's guide
[NASA-CR-178052] N87-13203

USER REQUIREMENTS
General purpose aft cargo carrier study, volume 1
[NASA-CR-178905] N87-12587
SARSAT (Search and Rescue Satellite) operational data categorization and accuracy studies
[AD-A169748] N87-12599
A measure of usability — man machine systems N87-13163
Empirical determination among superintendents of the acceptable user surface in digitally automated heating-ventilation air conditioning systems N87-13165

UTAH
Abundance and distribution of mineral components associated with Moses Rock (kimberlite) diatreme N87-12975

V

VACUUM
Population inversions in laser-initiated vacuum arcs
[AD-A170811] N87-12859

VACUUM SYSTEMS
Tara vacuum system
[DE86-011873] N87-13311

VANADATES
Study to determine the feasibility of utilizing skull-melting techniques for the growth of single crystals of yttrium vanadate
[AD-A169249] N87-13320

VANES
Effect of port corner geometry on the internal performance of a rotating-vane-type thrust reverser
[NASA-TP-2624] N87-12541
Super gripper variable vane arm
[AD-D012364] N87-12874
Improved vane platform sealing and retention means
[AD-D012407] N87-12681

VAPOR DEPOSITION
Fabrication of gate array interconnect structures using direct-write deposition processes
[DE86-010785] N87-12787
Experimental thin film deposition and surface analysis techniques
[DE86-011222] N87-13338

VAPOR PRESSURE
Vapour pressures and critical points of liquids. Part 2C: Alkadienes and alkynes
[ESDU-86001-PT-2C] N87-12624
Vapour pressures and critical points of liquids. Part 3A: C6 to C10 alkylbenzenes
[ESDU-86012-PT-3A] N87-12625

VAPORIZING
Apparatus for downward transport of heat
[DE86-013700] N87-12824

VARIABILITY
Super gripper variable vane arm
[AD-D012364] N87-12874
Effects of variables upon pyrotechnically induced shock response spectra
[NASA-TP-2603] N87-12921

VARIABLE STARS
Los Alamos Science, number 13, spring 1986
[DE86-012664] N87-13371

VARIATIONAL PRINCIPLES
A variational principle for the plasma centrifuge
[INPE-3989-PRE/992] N87-12827

VARIATIONS
The optimal linear combination of control variates in the presence of bias
[AD-A169111] N87-13210
Parametric linear variation of a leakage free permanent magnet field source
[AD-D012359] N87-13249
Rapid fluctuations in solar flares
[NASA-CR-179894] N87-13387

VASOCONSTRICTION
Hypothermic effects on vascular contractility and reactivity
[AD-A169142] N87-13127

VECTOR ANALYSIS
Vector analysis and satellite footprints
[AD-A169632] N87-12576
Quantum chemical investigations of the mechanism of cationic polymerization and theoretical prediction of crystal densities and decomposition pathways of energetic molecules
[AD-A169805] N87-13324

VECTOR SPACES
Some tactical algorithms for spherical geometry
[AD-A170615] N87-12555

VECTORS (MATHEMATICS)
Induced quantum torsion
[DE86-702616] N87-13348

VEGETATION
Detection of hydrothermal alteration at Virginia City, Nevada using Airborne Imaging Spectrometry (AIS) N87-12978
Preliminary geological investigation of AIS data at Mary Kathleen, Queensland, Australia N87-12979

VELOCITY MEASUREMENT
Doppler effect laser velocity measuring system
[AD-D012401] N87-12654

VENTILATION
Empirical determination among superintendents of the acceptable user surface in digitally automated heating-ventilation air conditioning systems N87-13165

VENUS ATMOSPHERE
The upper atmosphere of Venus: A tentative explanation of its rotation
[NASA-TM-86505] N87-13375

VENUS SURFACE
Relief and geology of the north polar region of the planet Venus
[NASA-TM-86491] N87-13376

VERTEBRAL COLUMN
Fracture and viscoelastic characteristics of the human cervical spine
[AD-A170002] N87-13133

VERTICAL AIR CURRENTS
Study of the formation and transport of acidic species by non-precipitating cumulus clouds during VENTEX-84
[PB86-220357] N87-13014
Mesoscale-cloud scale simulation of convective response N87-13077

VERTICAL TAKEOFF AIRCRAFT
The handling qualities and flight characteristics of the Grumman design 698 simulated twin-engine tilt Nacelle V/STOL aircraft
[NASA-TM-86785] N87-12558

VERY LARGE SCALE INTEGRATION
Signal estimation, scattering theory and interpolation problems in one and two dimensions
[AD-A168969] N87-12759
Compaction with automatic jog introduction
[AD-A169679] N87-12772
Declarative descriptions for VLSI generators
[AD-A169952] N87-12777
Yield and performance enhancement through redundancy in VLSI and WSI multi-processor systems
[AD-A169930] N87-13174
Plasma-enhanced deposition and processing of transition metals and transition metal silicides for VLSI
[AD-A168963] N87-13316

VERY LONG BASE INTERFEROMETRY
Meter-level orbit determination of geosynchronous satellites by an economical tracking system N87-12575
Observation model and parameter partials for the JPL VLBI parameter estimation software MASTERFIT-1986
[NASA-CR-179919] N87-13178

VERY LOW FREQUENCIES
Regular noise background in VLF-radiation and world thunderstorm centers N87-12957

VHSIC (CIRCUITS)
The Department of Defense Very High Speed Integrated Circuit (VHSIC) Technology Availability Program plan for the Committees on Armed Services, United States Congress
[AD-A169250] N87-12763

VIBRATION EFFECTS
Computational and experimental study of flow-induced vibration of the SSME main injector post
[DE86-012119] N87-12611

VIBRATION TESTS
Investigation of vibrations of the spinal column of healthy subjects N87-13155

VIBRATIONAL SPECTRA
Carbon monoxide adsorption on a platinum electrode studied by polarization modulated FT-IR reflection-absorption spectroscopy. 2: CO adsorbed at a potential in the hydrogen region and its oxidation in acids
[AD-A169082] N87-12832

VIDEO DATA
Quality management: An annotated bibliography
[AD-A169616] N87-12912

VIDEO SIGNALS
Single-mode-fibers for fiberoptic-guided missiles: A comparison with graded-index multimode fibers N87-13303

VIEWING
Viewport concept for space station modules
[NASA-TM-86559] N87-12592

VISCOELASTICITY
Characterization and dynamical studies of polymers in dipolar (aprotic) liquids
[AD-A169243] N87-12685
Stress assisted diffusion in elastic and viscoelastic materials
[AD-A169296] N87-12932
Fracture and viscoelastic characteristics of the human cervical spine
[AD-A170002] N87-13133

VISCOPLASTICITY
Finite element analyses of shear localization in rate and temperature dependent solids
[AD-A169057] N87-12927

VISCOUS FLOW
Viscous-inviscid interaction in transonic separated flow over solid and porous airfoils and cascades N87-12535

VISION
The eye-mark investigation as an anthropotechnical method to study man machine systems N87-13160

VISUAL DISCRIMINATION
The event related brain potential as an index of information processing and cognitive activity. A program of basic research. Supplement A: Neuromagnetic studies
[AD-A169978] N87-13144
VISUAL PERCEPTION
Limits of pattern discrimination in human vision
[AD-A170756] N87-13135
VISUAL STIMULI
High-resolution analysis of eye movements
[AD-A170779] N87-13136
VOICE COMMUNICATION
Space flight operations communications phraseology and techniques
[NASA-TM-86562] N87-12721
A test on the reliability and performance of the verbex series 4000 voice recognizer
[AD-A169066] N87-12729
VOIDS
A study of the mechanism of dynamic ductile fracture of two-phase materials
[AD-A168966] N87-12925
Stefan-type problem with void formation and its explicit solution
[DE86-013521] N87-13007
VOLT-AMPERE CHARACTERISTICS
The current-voltage relationship in auroral current sheets
[AD-A169074] N87-13028
VOLTAGE AMPLIFIERS
High frequency, high voltage MOSFET isolation amplifier
[AD-D012403] N87-12774
VOLTAGE CONTROLLED OSCILLATORS
Stabilization of voltage-controlled oscillators through resonant cavities
[INPE-3941-RPE/512] N87-12757
VOLTAGE GENERATORS
Cryogenic wound rotor for lightweight, high voltage generators
[AD-D012370] N87-12768
VORTEX RINGS
Transition and mixing in axisymmetric jets and vortex rings
[NASA-CR-3883] N87-12808
VORTEX SHEDDING
Computational fluid dynamic studies of certain ducted bluff-body flowfields relevant to turbojet combustors. Volume 1: Time-dependent calculations with the k-epsilon turbulence model for an existing centerbody combustor
[AD-A171434] N87-12816
VORTICES
The effect of a winglet on the spatial vortex of a slender body at high angle of attack
[AD-A169925] N87-12533
A summary of the development of integral aerodynamic methods for the computation of rotor wake interactions
[AD-A168254] N87-12545
An analysis of blade vortex interaction aerodynamics and acoustics N87-12547
Visualisation of axial turbine tip clearance flow using a linear cascade
[CUED/A-TURBO/TR-122] N87-12560
Pressure calculation for two-dimensional flow inside hydraulic structures
[AD-A169039] N87-12812
VOWELS
The effects of high sustained acceleration on the acoustic phonetic structure of speech: A preliminary investigation
[AD-A170563] N87-12746
VULNERABILITY
Maximization of the capacity of the most survivable connections in a network
[AD-A169065] N87-12728

W

WAKEFULNESS
Pharmacological resetting of the circadian sleep-wake cycle
[AD-A170804] N87-13137
WALL FLOW
The calculation of separated flows of low-viscosity liquids using the Batchelor Model
[BR-100272] N87-12810
Natural convection in an enclosure with discrete roughness elements on a vertical heated wall
[DE86-004424] N87-12817
Development of buried wire gages for measurement of wall shear stress in Blastane experiments
[NASA-TM-88212] N87-12831
WALL TEMPERATURE
Analysis of laminar flow heat transfer in uniform temperature circular tubes with tape inserts
[PB86-224763] N87-12826
WALLS
Natural convection in an enclosure with discrete roughness elements on a vertical heated wall
[DE86-004424] N87-12817
Fluids in contact with a hard surface: University of the bridge functions for the density profile
[AD-A168945] N87-13308
WARNING SYSTEMS
FEL (Free Electron Laser) optics coating test program (design phase of sample introduction chamber)
[AD-A169474] N87-12849
Obstacle-warning radar for helicopters N87-13149
WASTE DISPOSAL
Meteorological tower data, Yucca Ridge (YR) site, January-June 1983. Nevada Nuclear Waste Storage Investigations Project
[DE86-012732] N87-13113
Concept study - vehicle waste disposal system
[AD-A169045] N87-13168
WATER
Development testing of large volume water sprays for warm fog dispersal
[NASA-TP-2607] N87-12585
WATER RESOURCES
Characterization of information requirements for studies of CO2 effects: Water resources, agriculture, fisheries, forests and human health
[DE86-012477] N87-13010
WATER VAPOR
Diamond-machined aluminum alloy 5083 surfaces: Controlled exposure evaluation
[DE86-012572] N87-12674
Atmospheric-water absorption features near 2.2 micrometers and their importance in high spectral resolution remote sensing N87-12973
Multispectral atmospheric mapping sensor of mesoscale water vapor features N87-13095
Radiation flux tables for ICRCCM using the GLA GCM radiation codes
[NASA-TM-89270] N87-13098
WATERSHEDS
Evaluation of remote sensing techniques to the detection of changes in a fluvial system due to human influence: The example of Canas River Basin (Sao Paulo State, Brazil)
[INPE-3970-PRE/963] N87-12960
WAVE ATTENUATION
Spatial radio wave attenuation during vertical sounding of ionosphere N87-12958
WAVE DISPERSION
Propagation of electromagnetic waves in superlattices
[DE86-702660] N87-12753
WAVE EQUATIONS
Nonlinear interactions in the microwave sensing of oceanic internal waves
[AD-A169776] N87-13120
Nonlinear waves
[AD-A168934] N87-13207
WAVE EXCITATION
Lg wave excitation and propagation in presence of one-, two- and three-dimensional heterogeneities
[AD-A169004] N87-12724
Lg wave excitation and propagation in presence of one-, two-, and three-dimensional heterogeneities
[AD-A169325] N87-13030
WAVE FRONTS
Phase conjugate optics and picosecond optoelectronics
[AD-A169180] N87-13265
WAVE FUNCTIONS
Theory of Fractional Quantum Hall Effect
[DE86-702652] N87-13343
WAVE GENERATION
High repetition rate electron beam RF-Acceleration and sub-millimeter wave generation via a free electron laser
[AD-A169846] N87-12853
WAVE INTERACTION
Nonlinear interactions in the microwave sensing of oceanic internal waves
[AD-A169776] N87-13120
Nonlinear planar guided wave interactions and devices N87-13290
WAVE PROPAGATION
Quantitative non-destructive evaluation of composite materials based on ultrasonic wave propagation
[NASA-CR-179831] N87-12613
Lg wave excitation and propagation in presence of one-, two- and three-dimensional heterogeneities
[AD-A169004] N87-12724
Method of ray intensity calculation as applied to anomalous progagation
[AD-A169553] N87-12737
Stabilizing effects of finite-amplitude RF waves on the interchange instability
[DE86-013042] N87-12751
Propagation of electromagnetic waves in superlattices
[DE86-702660] N87-12753
Influence of shear modulus on the behavior of acoustically transparent materials
[AD-A169289] N87-12931
Phase fluctuations of ionosphere radio signals N87-12955
Nonlinear waves
[AD-A168934] N87-13207
Bistability in nonlinear wavegludes N87-13291
WAVE REFLECTION
Effect of pulsating auroras on frequency-time characteristics of radio signals reflected from auroral ionosphere N87-12954
Phase fluctuations of ionosphere radio signals N87-12955
WAVE SCATTERING
Theory for computing the field scattered from a smooth inflected surface
[NASA-TP-2632] N87-13264
WAVEFORMS
Reconstruction of undersampled periodic signals
[AD-A168897] N87-12722
WAVEGUIDE LASERS
Basic and applied research in the field of electronics and communications
[AD-A169029] N87-12727
WAVEGUIDES
Dielectric antennas for millimeter-wave applications
[AD-A169885] N87-12739
Input impedance of an infinite linear scanned array of flat rectangular strips inside a dielectric loaded parallel plate waveguide
[AD-A171275] N87-12784
A 60 GHz gyrotron development program
[DE86-012488] N87-12791
WAVELENGTH DIVISION MULTIPLEXING
Wavelength division multiplexing at 1.5 microns for high capacity optical transmission N87-13284
A spherical waveguide multiplexer-demultiplexer N87-13265
WAVELENGTHS
Medium- and long-wavelength infrared emission from a laser-produced oxygen plasma
[AD-A169475] N87-13309
WEAPON SYSTEMS
The Department of Defense Very High Speed Integrated Circuit (VHSIC) Technology Availability Program plan for the Committees on Armed Services, United States Congress
[AD-A169250] N87-12763
WEAR
Fundamental research on tribology
[AD-A169974] N87-12882
WEATHER
Aircraft accident/incident summary reports: Erie, Pennsylvania, October 14, 1984; Albuquerque, New Mexico, February 11, 1985
[PB86-910407] N87-12549
Aircraft accident report: Bar Harbor Airlines Flight 1808, Beech BE-99, N300WP, Auburn-Lewiston Municipal Airport, Auburn, Maine, August 25, 1985
[PB86-910408] N87-12550
Observational and theoretical studies of the evolving structure of baroclinic waves: Attractor dynamics of global weather systems N87-13054
The meteorological interactive data display system N87-13091
Wheeler AFB, Hawaii Limited Surface Observations Climatic Summary (LISOCS), parts 1-5
[AD-A169391] N87-13107
WEATHER DATA RECORDERS
The siting, installation and operational suitability of the Automated Weather Observing System (AWOS) at heliports
[DOT/FAA/PM-86/30] N87-13099
WEATHER FORECASTING
The use of satellite data in understanding and predicting convective and large-scale dynamical processes N87-13049
Utilization of satellite cloud information to diagnose the energy state and transformations in extratropical cyclones N87-13051
LAMPS software and mesoscale prediction studies N87-13076
The assimilation of satellite soundings, winds and satellite products in a mesoscale analysis/forecast system N87-13060
A design study for a three-dimensional display computer terminal for meteorological information N87-13092
Summary of 1986 Atlantic tropical cyclone activity and verification of author's seasonal forecast N87-13097

Some proposals for modifying the Probability of Precipitation Program of the National Weather Service
[PB86-226636] N87-13115

WEATHER STATIONS
Station climatic summaries, Europe
[AD-A167888] N87-13100
Revised Uniform Summary of Surface Weather Observations (RUSSWO). Parts A-F Ellington ANGB, Texas
[AD-A169389] N87-13105
Revised Uniform Summary of Surface Weather Observations (RUSSWO). Parts A-F, Fort Richardson, Alaska
[AD-A169390] N87-13106

WEIGHT REDUCTION
Fabrication and testing of lightweight hydraulic system simulator hardware
[AD-A169884] N87-12711

WELD STRENGTH
Guide to the use of data items on the fatigue strength of welded joints in steels
[ESDU-86013] N87-12914

WELDED JOINTS
Use of analytical electron microscopy in evaluating ferrite stability in austenitic stainless steel welds
[DE86-006537] N87-12667
Microstructural study of high energy density dissimilar metal welds
[DE86-009284] N87-12668
Cleaning of aluminum alloy 5083
[DE86-012573] N87-12575
Effect of convection on weld pool shape and microstructure
[AD-A170488] N87-12883
Welding procedure specification. Manual gas tungsten arc and semiautomatic gas metal arc welding of chromium-nickel steel. Supplement 1: Records of procedure qualification tests
[DE86-012521] N87-12886
Machine gas metal arc welding of carbon steel. Welding procedure specification. Supplement 1: Records of procedure qualification tests
[DE86-012530] N87-12887
Welding procedure specification. Semiautomatic gas metal arc welding of carbon steels. Supplement 1: Records of procedure qualification tests
[DE86-012531] N87-12888
Welding procedure specification. Manual gas tungsten arc and semiautomatic gas metal arc welding of carbon steel. Supplement 1: Records of procedure qualification tests
[DE86-012532] N87-12889
Gas tungsten arc and shielded metal arc welding of carbon steel. Welding procedure specification. Supplement 1: Records of procedure qualification tests
[DE86-012533] N87-12890
Welding procedure specification. Supplement 1: Records of procedure qualification tests. Shielded metal arc welding of carbon steel
[DE86-012535] N87-12891
Welding procedure specification. Gas tungsten arc welding of chromium-nickel steel to chromium-molybdenum steel. Supplement 1: Records of procedure qualification tests
[DE86-012536] N87-12892
Gas tungsten arc welding of aluminum alloys 6XXX. Welding procedure specification. Supplement 1: Records of procedure qualification tests
[DE86-012548] N87-12893
Gas tungsten arc welding of carbon steel to nickel-chromium-iron. Welding procedure specification. Supplement 1: Records of procedure qualification tests
[DE86-012549] N87-12894
Welding procedure specification: Gas tungsten arc welding of nickel to nickel-chromium-iron. Supplement 1: Records of procedure qualification tests
[DE86-012557] N87-12896
Gas tungsten arc welding of aluminum alloys 3004, 5052 and 5x54 to 6xxx. Welding procedure specification. Supplement 1: Records of procedure qualification tests
[DE86-012561] N87-12897
Effects of inertia weld parameters and contamination on weld flash shape and on joint strength: An improved study
[DE86-013074] N87-12904
Concurrent ultrasonic weld evaluation system
[DE86-013772] N87-12908
Guide to the use of data items on the fatigue strength of welded joints in steels
[ESDU-86013] N87-12914

WELDING
Mechanics of metal forming
[DE86-012414] N87-12673
Welding research in Scandinavia: An assessment
[AD-A169036] N87-12871
Welding science and technology in Europe: A survey and assessment
[AD-A169279] N87-12873
Heat measurements in inertia welding of aluminum to steel
[DE86-012463] N87-12885
Effects of inertia weld parameters and contamination on weld flash shape and on joint strength: An improved study
[DE86-013074] N87-12904
Sensor controlled robotic welding for nuclear applications
[DE86-013110] N87-12905
Resistance seam welding
[DE86-013288] N87-12906
Concurrent ultrasonic weld evaluation system
[DE86-013772] N87-12908

WEST GERMANY
Review of the methods applied in the Federal Republic of Germany to investigate human factors in nuclear power plant control N87-13156

WETLANDS
Trace element-induced stress in freshwater wetland vegetation: Preliminary results N87-12985

WHISKERS (CRYSTALS)
Carbon fibers
[AD-A171370] N87-12622

WIDE ANGLE LENSES
Space infrared telescope facility wide field and diffraction limited array camera (IRAC)
[NASA-CR-177041] N87-13362

WIND (METEOROLOGY)
NASA/MSFC FY-85 Atmospheric Processes Research Review
[NASA-CP-2402] N87-13043
Multiscale modeling to evaluate proposed space-based Doppler lidar sampling strategies N87-13047
The use of satellite data in understanding and predicting convective and large-scale dynamical processes N87-13049
Variation objective analyses for cyclone studies N87-13050
Airborne Doppler measurements of the central California extended sea breeze N87-13066
Airborne Doppler lidar activities N87-13068
Response of the mesoscale atmosphere to diabatic heating N87-13069
Automated mesoscale winds derived from GOES multispectral imagery N87-13073
The assimilation of satellite soundings, winds and satellite products in a mesoscale analysis/forecast system N87-13080
Micrometeorological transitions in the morning boundary layer over rolling terrain
[AD-A169237] N87-13103
A review of microbursts and their analysis and detection with Doppler radar
[AD-A170458] N87-13110

WIND DIRECTION
Characteristics of atmospheric turbulence near the ground. Part 3: Variations in space and time for strong winds (neutral atmosphere)
[ESDU-86010-PT-3] N87-13042

WIND MEASUREMENT
Multiscale modeling to evaluate proposed space-based Doppler lidar sampling strategies N87-13047
Airborne Doppler measurements of the central California extended sea breeze N87-13066
Doppler wind profile experiment N87-13094
Calibration and accuracy of the NOAA/ERL gust probe system and intercomparison with other systems
[PB86-221736] N87-13116

WIND PROFILES
Atmospheric Tides Middle Atmosphere Program (ATMAP): Report of the workshop, Kyoto, Japan, December 5-6, 1984 N87-13016
Airborne Doppler lidar activities N87-13068
Automated mesoscale winds derived from GOES multispectral imagery N87-13073
Doppler wind profile experiment N87-13094

WIND TUNNEL TESTS
The effect of a winglet on the spatial vortex of a slender body at high angle of attack
[AD-A169925] N87-12533
Mach 6 experimental and theoretical stability and performance of a finned cylindrical body at angles of attack up to 65 deg
[NASA-TM-89050] N87-12538
Effect of port corner geometry on the internal performance of a rotating-vane-type thrust reverser
[NASA-TP-2624] N87-12541
Cruise noise of counterrotation propeller at angle of attack in wind tunnel
[NASA-TM-88869] N87-13252

WIND VELOCITY
Balloon-borne, high altitude gravimetry: The flight of DUCKY 1a (11 October 1983)
[AD-A169942] N87-13033

WINDING
Cryogenic wound rotor for lightweight, high voltage generators
[AD-D012370] N87-12768

WINDOWS (APERTURES)
Solid-state electrochromic switchable window glazings
[DE86-004455] N87-12700

WING LOADING
Blast gust loading on a 35 degree swept-back wing
[AD-A169415] N87-12570

WING TIP VORTICES
Numerical simulation of tip vortices of wings in subsonic and transonic flows
[AD-A169116] N87-12544

WINGLETS
The effect of a winglet on the spatial vortex of a slender body at high angle of attack
[AD-A169925] N87-12533

WINTER
Minutes of MAP/WINE experimenters meeting, Prague, Czechoslovakia, August 13, 1985 N87-13018

WIRE
Development of a numerical procedure to treat wires attached to arbitrarily shaped conducting bodies
[AD-A169384] N87-12764
Development of buried wire gages for measurement of soil shear stress in Blastane experiments
[NASA-TM-89212] N87-12831

WOOD
Preliminary material testing of ceramic and wood
[AD-A169557] N87-12771

WORDS (LANGUAGE)
The effects of high sustained acceleration on the acoustic phonetic structure of speech: A preliminary investigation
[AD-A170563] N87-12746

WORK-REST CYCLE
Self-paced heat acclimation procedures
[AD-A170533] N87-13134

WORKING FLUIDS
Apparatus for downward transport of heat
[DE86-013700] N87-12824

WORKLOADS (PSYCHOPHYSIOLOGY)
Application of heart rate measurements to maritime research simulator
[AD-A169988] N87-13132
Perceptual factors in workload: A neuromagnetic study
[AD-A169934] N87-13142
Eye movements as an index of mental workload
[AD-A169941] N87-13143
Determination of the load and stress of a cockpit crew during aircraft piloting using task networks and the simulation language SAINT N87-13150
System-ergonomic workload analysis for highly automated process control tasks N87-13152
The measurement of the psychological workload during task-related activities, including car driving, by competing time interval estimation N87-13153
Review of the methods applied in the Federal Republic of Germany to investigate human factors in nuclear power plant control N87-13156
Inquiry techniques for the evaluation of man machine systems N87-13162

WROUGHT ALLOYS
Fatigue behavior of long and short cracks in wrought and powder aluminum alloys
[AD-A169980] N87-12656

X

X RAY ANALYSIS
Potential applications of artificially structured materials for X-ray microanalysis
[DE86-010459] N87-12612

X RAY APPARATUS
Potential applications of artificially structured materials for X-ray microanalysis
[DE86-010459] N87-12612

X RAY BINARIES
High energy neutrino absorption and its effects on stars in close X-ray binaries
[NASA-TM-89269] N87-13366
On the two states of CYG X-1 and related sources
[NASA-TM-89265] N87-13367

X RAY DIFFRACTION
Identification of hydrothermal alteration assemblages using airborne imaging spectrometer data N87-12977

X RAY FLUORESCENCE
X-ray fluorescence with synchrotron radiation
[DE86-010543] N87-13124

X RAY INSPECTION
NDE reliability and process control for structural ceramics
[NASA-TM-88870] N87-12910
X RAY LASERS
Slitless, intensified readout, gated spectrometer: Wavelength and efficiency calibration, time response characterization
[DE86-012349] N87-12839
Resonant photon pumping mechanisms for a plasma X-ray laser
[AD-D012416] N87-12857
Laser produced X-ray for high resolution lithography and a photoionization laser
[AD-A170782] N87-12858
X RAY SOURCES
Time Projection Compton Spectrometer (TPCS)
[DE86-012950] N87-12840
X-ray data booklet, revision
[DE86-012650] N87-13272
X RAY SPECTRA
Electron microprobe analysis: The upper limit of submicron spectroscopy
[DE86-009540] N87-12840
Time Projection Compton Spectrometer (TPCS)
[DE86-012950] N87-12840
Stratospheric balloon experiments
[INPE-3995-RPE/519] N87-13020
Observational study of ion-electron equilibration and of cloud evaporation in supernova remnants under the HEAO-2 guest investigator program
[NASA-CR-179922] N87-13365
X-ray emission from supernova remnants N87-13398
X RAY SPECTROSCOPY
MAX '91: An advanced payload for the exploration of high energy processes on the active sun
[NASA-TM-89271] N87-13379
X RAYS
A survey of hard-X-rays at balloon altitudes of the Earth's atmosphere
[INPE-3954-PRE/972] N87-13388

Y

YAW
Frictional and retarding forces on aircraft tyres. Part 4: Estimation of effects of yaw
[ESDU-86016-PT-4] N87-12866
YIELD
Crop yield modeling for climate impact studies. Part 1: Reasoning and results
[INPE-3997-PRE/982-PT-1] N87-12961
YTTRIUM COMPOUNDS
Study to determine the feasibility of utilizing skull-melting techniques for the growth of single crystals of yttrium vanadate
[AD-A169249] N87-13320

Z

ZEEMAN EFFECT
Structural features at the Si-SiO2 interface
[DE86-012947] N87-13339
ZINC
Energetics of dislocation relaxation associated with cleavage in Cd-doped zinc crystals as probed by synchrotron topography
[DE86-002988] N87-13334
ZINC OXIDES
Zinc/nickel oxide battery membrane separator studies
[DE86-012624] N87-12793

Typical Personal Author Index Listing

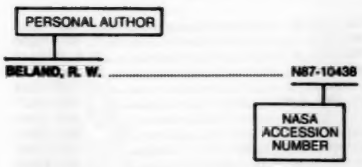

Listings in this index are arranged alphabetically by personal author. The NASA accession number denotes the number by which the citation is identified.

A

ABLOWITZ, M. J. N87-13207
ABRAHAO, A. N87-13173
ACHREKAR, P. M. N87-12832
ACHTEMEIER, G. L. N87-13050
ACOMB, D. B. N87-13122
ACREE, C. W. N87-12557
ADAMS, S. N87-12971
ADAMSKI, J. A. N87-13322
ADAMSKI, J. L. N87-12849
AFANASYEV, G. N87-12847
AHMED, M. N87-13345
AKASOFU, S. I. N87-13380
AL-KHAYYAL, F. A. N87-13189
ALDISSI, M. N87-12695
N87-12696
ALDRIDGE, K. D. N87-12813
ALESSI, J. G. N87-13257
ALFINO, N. L. N87-12712
ALKEZWEENY, A. J. N87-13014
ALLEN, G. A., JR. N87-12808
ALLEN, J. N87-12727
ALLEY, R. E. N87-12971
ALMAND, B. J. N87-13203
ALTSHULER, E. E. N87-12734
ANAYA, J. A. N87-12647
ANDERSON, B. J. N87-12585
ANDERSON, C. E. N87-13085
ANDERSON, D. N. N87-13025
ANDERSON, T. R. N87-12748
ANDONOVIC, I. N87-13289
ANNAMALAI, N. K. N87-12775
ANSELMI, I. N87-13291
APPLEBAUM, D. N87-12858
ARAKAWA, E. T. N87-13256
ARCH, D. K. N87-13337
ARCHULETA, F. A. N87-12863
ARDANUY, P. N87-13108
ARISTA, N. R. N87-12843
ARMINGTON, A. F. N87-13315
ARMSTRONG, L. E. N87-13134
ARNOLD, J. E. N87-13094
ARNOLD, R. T. N87-13064
ARSENYEV, V. S. N87-12949
ARTZ, R. S. N87-13114
ARVESEN, J. N87-12828
ARVIDSON, R. E. N87-12963
ARYKOV, A. A. N87-12954
ASHBAUGH, N. E. N87-12563
ASLAM, M. N87-13302
ASO, T. N87-13016
ATHANS, M. N87-13243
ATKINSON, R. N87-12828
N87-13095
ATKINSON, R. J. N87-13073
AULD, B. A. N87-12794
AUVINE, B. N87-13058
AVERY, S. N87-13016

B

BAAKLINI, G. Y. N87-12910
BABUSKA, I. N87-12936
N87-13212
N87-13213
N87-13214
N87-13222
N87-13227
BACIAK, M. G. N87-13270
BAEDER, J. D. N87-12544
BAER, M. R. N87-12818
N87-12821
BAERISWYL, D. N87-12697
BAETGE, M. M. N87-13122
BAILEY, W. C. N87-12767
BAIRD, J. C. N87-13309
BAK, M. J. N87-12923
BALAKRISHNAN, A. V. N87-12802
BALDWIN, G. C. N87-12866
BALDWIN, G. T. N87-12840
BALLA, M. Y. N87-12825
BANDICK, N. R. N87-13127
BANERJEE, P. K. N87-12923
BARD, A. J. N87-12833
BARDEYEV, I. N. N87-12954
BARFIELD, J. N. N87-13027
BARGER, R. L. N87-13264
BARKER, L. M. N87-12654
BARNES, I. L. N87-13011
BARNES, J. C. N87-12991
BARSKY, B. A. N87-13211
BATCHELLOR, C. R. N87-13279
BAZHENOV, V. I. N87-12598
BEARD, K. V. N87-12585
BEAUMONT, S. N87-13289
BECK, L. H. N87-12985
BECKER, G. N87-13157
BECKER, R. J. N87-12703
BEDFORD, K. W. N87-13037
BEDNARZ, B. N87-13277
BEHRENDT, V. N87-13159
BENCIVENGA, B. J. N87-12731
BENINGA, K. J. N87-12788
BENNION, D. N. N87-12793
BENSON, D. K. N87-12700
N87-12701
BENTLEY, J. N87-12669
N87-12900
BERGLES, A. E. N87-12804
N87-12826
BERGMAN, M. Y. N87-13376
BERGSHOEFF, E. N87-13349
BERNARD, R. S. N87-12812
BERNHARDT, A. F. N87-12787
BERRIER, B. L. N87-12541
BERTOLOTTI, M. N87-13291
BERTRAM, L. A. N87-12672
BETTINI, J. P. N87-13283
BEVILACQUA, R. M. N87-12604
BIBBY, M. C. N87-13181
BICKEL, W. N. N87-12711
BICKERS, L. N87-13300
BICKNELL, T. N87-12965
BIER, R. E. N87-12791
BILBRO, J. W. N87-13068
BILELLO, J. C. N87-13334
BILLUPS, S. C. N87-13196
BINDON, J. P. N87-12580
BIRKMIRE, R. W. N87-13003
BIRNBAUM, H. K. N87-12658
BLACKWELL, D. L. N87-12607
BLAKE, J. B. N87-13389
N87-13390
N87-13391
N87-13392
N87-13393
BLAKESLEE, R. J. N87-13061
N87-13063
BLANCO, F. S. N87-13020
BLANK, L. C. N87-13300
BLOCK, H. W. N87-13239
BLUM, L. N87-13308
BLUMENTHAL, D. N87-13013
BLUZER, N. N87-13267
BO-HAO, D. N87-12553
BODNER, S. E. N87-12862
BOESSER, T. N87-13164
BOGER, D. C. N87-13353
BOGOMOLOV, A. F. N87-13376
BOHN, M. S. N87-12817
BOISNAUD, P. N87-12918
BOLLWERK, W. V. N87-13369
BOND, Z. S. N87-12746
BONNER, G. A. N87-12861
BOOKER, M. K. N87-12940
BORMAN, G. L. N87-12870
BORO, K. N87-13113
BOSIO, A. C. N87-13129
BOSTICK, W. H. N87-12796
BOVARD, F. S. N87-12681
BOWDLE, D. A. N87-13088
BOWHILL, S. N87-13016
BOWMAN, B. M. N87-13129
BOYER, C. N87-13375
BRADSHAW, J. S. N87-12793
BRAGA, J. N87-13020
BRANNAN, J. R. N87-13143
BRAUSER, K. N87-13151
BRENCI, M. N87-13280
BRENNER, S. S. N87-12677
BRILMYER, G. H. N87-12801
BRINDZA, P. N87-13311
BROCKMAN, R. A. N87-12933
BROKENSHIRE, T. E. N87-12710
BROOK, M. N87-13060
N87-13140
BROUTMAN, L. J. N87-12686
BROWER, K. L. N87-13339
BROWNE, J. C. N87-13188
BRYAN, J. B. N87-12899
BRYANT, K. C. N87-12786
BUCHAU, J. N87-13036
BUCK, R. F. N87-13029
BULLINGTON, J. A. N87-12837
BULLOCK, K. R. N87-12801
BURBA, G. A. N87-13376
BURCH, J. L. N87-13028
BURKETT, B. E. N87-12735
BURKOV, V. A. N87-12949
BURNS, G. N87-12855
BURNS, R. A. N87-12585
BURRIS, D. R. N87-12635
BUTLER, B. L. N87-12788
BUTTRAM, M. T. N87-12790

C

CAHILL, R. F. N87-13276
CALDWELL, S. P. N87-13253
CALEDONIA, G. E. N87-13310
CAMP, F. E. N87-13250
CAMPBELL, A. N. N87-13336
CAMPBELL, B. N87-12858
CAMPBELL, D. K. N87-12697
CAMPBELL, J. G. N87-12994
CANADA, J. N87-12797
CANTWELL, B. J. N87-12808
CAPLAN, M. N87-12791
CAPOBIANCO, J. N87-12748
CAPONE, F. J. N87-12541
CAPPS, R. N87-13363
CARBONELL, J. G. N87-13184
CARLEN, E. A. N87-13221
CARR, M. J. N87-13336
CARRARA, V. N87-13377
CARROLL, J. J. N87-13066
CARTER, C. L. N87-13197
CARTER, L. N. N87-13033
CARTER, R. N87-12837
CARUSO, S. C. N87-12814
CERNOSEK, R. W. N87-13281
CHALLENGER, K. D. N87-12671
N87-12573
CHAMBERS, W. F. N87-12640
CHAN, C. L. N87-12883

CHAN, F. N87-12785
CHANDLER, G. I. N87-13281
CHANG, S. L. N87-12628
CHAPMAN, R. L. N87-13358
CHARKEY, A. N87-12766
CHARLES, H. C., JR. N87-12765
CHARRETTE, E. E., III N87-13034
CHARWAT, H. J. N87-13165
CHEN, M. M. N87-12883
CHEN, N. C. J. N87-12903
CHEN, S. C. N87-12989
CHEN, S. S. N87-12611
CHENG, M. K. N87-12791
CHENG, S. S. N87-13306
CHERNYSHENKO, S. I. N87-12810
CHESTON, T. C. N87-12745
CHIEN, C. H. N87-13231
CHIN, B. A. N87-12905
CHO, K. S. N87-12726
CHOI, E. N87-12791
CHRISS, D. N87-12651
CHRISTENSEN, E. L. N87-13134
CHRISTIAN, H. J. N87-13059
CHRISTODOULAKIS, T. N87-13372
CHU, B. N87-12685
CHUNCHUZOV, I. P. N87-12951
CHUPP, E. L. N87-13394
CHURCH, H. W. N87-13113
CIESLAK, M. J. N87-12668
CIESLAK, W. R. N87-12661
CLABORN, K. D. N87-12767
CLARK, J. H. E. N87-13049
CLARK, R. A. N87-12822
CLARK, R. N. N87-12973
N87-12980
CLARKE, J. N87-13249
CLATTERBAUGH, G. V. N87-12765
CLEMENS, P. N87-13295
CLEMENT, M. N87-13361
COCKS, T. D. N87-12972
N87-12979
COFFEE, M. S. N87-13133
COLES, C. E. N87-12606
COLLINS, W. E. N87-13328
COLOMBO, L. N87-13317
COMFORT, R. H. N87-13307
CONEL, J. E. N87-12971
CONFORTI, G. N87-13280
CONNELL, P. S. N87-13040
CONNELLY, D. J. N87-13326
CONNER, C. C. N87-12791
CONVEY, J. J. N87-13145
COOPER, D. E. N87-12779
COOPER, J. A., JR. N87-12761
N87-12762
COOPER, J. C. N87-12691
COOPER, N. G. N87-13371
CORDARO, J. T. N87-12569
CORREA, R. V. N87-13020
CORREIA, E. N87-13378
COSI, F. N87-13260
COWIE, R. J. N87-13033
COY, L. N87-13016
CRAIG, L. J. N87-12791
CRAIG, M. D. N87-12979
CREMERS, D. A. N87-12663
CREWS, J. H., JR. N87-12922
CRITCHLOW, D. E. N87-13233
CRONIN, M. N87-13121
CROSIGNANI, B. N87-13282
CROSIGNANI, P. N87-13273
CROSS, J. B. N87-12663
CROSS, J. L. N87-12557
CROSS, L. E. N87-12758
CROUSE, K. R. N87-12597
CROWLEY, J. A. N87-12543
CULSHAW, B. N87-13275
CUNNINGHAM, M. A. N87-12704
CURE, J. D. N87-13012
CURTIS, N. J. N87-12702
CUTCHIS, P. N87-13245
CUTLER, R. P. N87-12838

D

DACOSTA, J. M. N87-13388
DAHMEN, U. N87-12670
DAINTY, A. M. N87-13034
DAKIN, J. P. N87-13278
N87-13279
N87-13286
DALLAQUA, R. S. N87-12754
DAMICO, A. N87-13154
DANDEKAR, B. S. N87-13036
DANIELSON, M. J. N87-12676
DANKOWYCH, J. A. N87-13277
DAULTRY, S. N87-12994
DAVARIAN, F. N87-12719
DAVER, F. N87-12676
DAVID, S. A. N87-12667
DAVIDSON, D. L. N87-12620
DAVIDSON, K. N87-13119
DAVIS, J. M. N87-13103
DAWSON, P. R. N87-12673
DAY, G. W. N87-13261
DAYAN, U. N87-13114
DEABREU, A. A. N87-12960
DEACON, D. A. G. N87-12849
DEALMEIDA, F. C. N87-12961
DEANEDEABREUSA, L. N87-12962
N87-12964
N87-13008
DEARBORN, D. S. P. N87-13389
N87-13392
DEBRA, D. B. N87-12899
DECHER, R. N87-12756
DEFREITASPINTO, R. L. U. N87-13205
DEHEUVELS, P. N87-13224
DELBOSCO, E. N87-12754
DELONG, M. L. N87-13271
DELUCA, J. P. N87-13134
DEMEDEIROS, V. M. N87-12591
DENARDO, G. N87-13348
DENISENKO, P. F. N87-12958
DENNIS, J. E. N87-13209
DENNISON, B. K. N87-12604
DEOLIVEIRARIVELLES, V. N87-13370
DEPKOVICH, T. M. N87-13203
DERMER, C. D. N87-13395
DEROSE, T. D. N87-13211
DESAI, M. D. N87-12747
DESOUZA, L. C. G. N87-12588
N87-12591
DIAK, G. R. N87-13080
DICKERSON, A. N87-13001
DICKERSON, M. N87-13093
DIENES, G. J. N87-12942
DILLEHAY, M. E. N87-12559
DINEGAR, R. H. N87-12707
DION, D. N87-12737
DIPORTO, P. N87-13282
DITTMAR, J. H. N87-13252
DIVER, R. B. N87-13002
DMITRIYEV, V. K. N87-12952
DOBBS, G. M. N87-12641
DOERING, B. N87-13152
DOGAN, N. S. N87-12760
DOMINEK, A. K. N87-13264
DONCHIN, E. N87-13144
DONG, B. N87-13347
DONOHUE, M. D. N87-12642
DOOMES, E. N87-12651
DOSANJOSEFERREIRAPINTO, S. N87-12989
DOUGLAS, F., III N87-12592
DOVE, W. P. N87-12730
DRUMHELLER, K. N87-13361
DRUZHIN, G. I. N87-12957
DUAN, L. N87-13347
DUBBELDAY, P. S. N87-12931
DUGAS, R. M. N87-12565
DUKE, M. B. N87-12580
DULLECK, G. R. N87-12638
DUNLAP, W. P. N87-13143
DUPONT, T. F. N87-13208
DURKEE, J. W., JR. N87-13262
DUSTIN, M. O. N87-12608
DUTTON, J. A. N87-13049
DUVALL, D. S. N87-12705
DUVALL, G. E. N87-12629
DYER, I. N87-13119

E

EAST, J. R. N87-12760
ECKHARDT, R. J. N87-13109
EDLER, S. K. N87-13361
EDLIN, G. R. N87-12854
EDWARDS, T. A. N87-12544
EDWARDS, W. T. N87-13133
EGAMI, R. T. N87-13113
EGGERT, G. M. N87-12673
EICHEL, P. H. N87-12799
EISLER, G. R. N87-12577
EITEL, F. G. N87-13268
EKKEBUS, A. E. N87-13355
EL-MOUSLY, M. K. N87-13340
EL-SAYED, M. A. N87-13325
ELKINS, J. W. N87-13011
ELLIOTT, R. A. N87-12743
ELTA, M. E. N87-12760
ELTON, R. C. N87-12857
EMERY, M. H. N87-12862
EMMITT, G. D. N87-13047
ENGE, P. K. N87-12554
EPSTEIN, H. N87-12558
ERICKSON, R. E. N87-12557
ESCADA, J. B., JR. N87-12990
ESHERICK, P. N87-12645
ESKEY, M. A. N87-12558
EVANS, J. F. N87-12986
EVANS, S. J. N87-12791
EVERS, S. J. N87-12791

F

FALCIAI, R. N87-13260
FANG, Z. N87-13239
FANOUS, F. N87-12943
FANSELOW, J. L. N87-13178
FARRELL, J. N87-12695
FAURIE, J. P. N87-13337
FAZIO, G. G. N87-13362
FEATHER, J. B. N87-12552
FEDOROVICH, G. V. N87-12953
FEIGELSON, E. D. N87-13368
FEIGELSON, R. S. N87-13298
FELCH, K. L. N87-12791
FELD, M. S. N87-12668
FELDMAN, S. C. N87-12977
FENNELL, J. F. N87-13369
N87-13393
FERREIRA, L. D. D. N87-12590
FERRY, D. K. N87-13321
FERZIGER, J. H. N87-12814
FILDEY, J. A. N87-12690
FILHO, M. V. N87-12989
FINKEN, K. R. N87-12740
FISHER, A. T. N87-12900
FISHER, C. L. N87-12570
FITZJARRALD, D. N87-13044
FITZJARRALD, D. R. N87-13068
FLARSHEIM, W. M. N87-12833
FLOHRER, W. N87-13163
FOKAS, A. S. N87-13207
FOLLANSBEE, P. S. N87-12859
FOLTZ, G. W. N87-12844
FONG, Y. S. N87-13190
FONTANELLA, J. J. N87-12683
FORBES, J. N87-13018
FORBES, J. M. N87-13016
N87-13017
FORBES, R. A. N87-12830
FOSTER, R. M. N87-12879
FOUSHEE, H. C. N87-13122
FOWLER, M. C. N87-12839
FOWLIS, W. W. N87-13048
FRANK, P. D. N87-13216
FRANKEL, M. B. N87-12704
FRANZEN, R. L. N87-12877
FRASER, G. N87-13016
FREEMAN, B. L. N87-12796
FREEMAN, D. L. N87-13113
FREEMAN, G. L. N87-13110
FREIDAH, J. T. N87-13287
FREISER, B. S. N87-12830
FRICKE, M. N87-13150
FRIZZELL, D. R. N87-12886
N87-12887
N87-12888
N87-12889
N87-12890
N87-12891
N87-12892
N87-12893
N87-12894
N87-12895
N87-12896
N87-12897
FROEBE, J. N87-13154
FROLOV, V. P. N87-12723
FROST, L. S. N87-13258
FRY, E. S. N87-12749
FUCHS, H. N87-12761
FUELBERG, H. E. N87-13082
N87-13086
FUENMAYOR, D. Y. N87-12681
FUJIMATSU, Y. N87-12716
FUJITA, T. T. N87-13071
FUKAO, S. N87-13016

G

GAERTNER, K. P. N87-13147
GAIER, J. R. N87-12679

GAISSER, T. K. N87-13366
GALVAO, R. M. O. N87-12843
GAO, Y. N87-13347
GARDNER, J. H. N87-12862
GAUDREAU, M. P. N87-13311
GEE, C. M. N87-13304
GEIST, G. A. N87-13193
GENIN, M. N87-12797
GENXING, W. N87-12533
GEORGE, T. F. N87-12851
GEORGE, T. G. N87-13261
GERACI, D. J. N87-13271
GERASSIMENKO, M. N87-12839
GHOSN, L. J. N87-12915
GIALLORENZI, T. G. N87-13274
GILL, P. E. N87-13180
N87-13248
GILLIS, H. P. N87-13331
GILMER, R. O. N87-13116
GINN, J. W. N87-12790
GLASS, I. I. N87-12807
GLEASON, K. N87-12797
GLENN, L. A. N87-12868
GLYNN, P. W. N87-13210
GODOY, M., JR. N87-13173
GOERTZ, C. K. N87-13026
GOETZ, A. F. H. N87-12968
GOFORTH, J. H. N87-12795
GOGUEN, J. N87-13141
GOLDBERG, E. L. N87-12912
GOLDEN, W. G. N87-12631
N87-12632
GOLDMAN, A. N87-13035
GONZALEZ, R. R. N87-13131
GONZALEZ, W. D. N87-13388
GOODLING, J. S. N87-12905
GOODMAN, D. W. N87-12639
GOODMAN, S. J. N87-13055
N87-13057
N87-13062
GOODRICH, P. N87-13311
GORDLEY, L. L. N87-13022
GORDON, B. M. N87-13124
GORDON, J. G., II N87-12631
N87-12632
GORINTO, C. N87-13352
GOUDONNET, J. P. N87-13256
GRANT, E. R. N87-12682
GRANT, L. R. N87-12704
GRAY, G. T., III N87-12660
GRAY, W. M. N87-13097
GREEN, A. A. N87-12972
N87-12979
GREEN, G. M. N87-12983
GREENE, A. E. N87-12795
GREENE, W. A. N87-13088
GREENHUT, G. G. N87-13116
GREIMANN, L. N87-12943
GREIMAN, K. D. N87-13203
GRIFFIN, F. P. N87-12903
GROOT, K. J. N87-12907
GROSE, W. L. N87-13019
GROSS, R. J. N87-12818
N87-12821
GROTCH, S. L. N87-13195
GUO, B. N87-13212
GURNETT, D. A. N87-13026
GUSEV, V. D. N87-12955
GUSTAFSON, S. C. N87-13269
GUTOWSKI, W. J. N87-13104

H

HADDAD, G. I. N87-12760
HAGENA, F. W. N87-13155
HAGGAG, F. M. N87-12938
HAGGARD, K. V. N87-13022
HALE, M. D. N87-12705
HALEY, D. C. N87-13203
HALL, C. A. N87-12903
HALL, I. W. N87-12925
HALL, N. H. N87-12789
HALLER, G. L. N87-12859
HAMILTON, H. H., II N87-12806
HANING, R. K. N87-12711
HANNON, J. P. N87-12866
HANSEN, A. R. N87-13054
HANSON, A. L. N87-13124
HARELAND, W. A. N87-12672
HARRINGTON, R. F. N87-12725
HARRIS, J. O., JR. N87-12838
HARSHVARDHAN N87-13096
HART, J. N87-13045
HARTFIEL, H. D. N87-13159
HARTMAN, E. R. N87-12538
HARTMAN, G. A. N87-12563
HASEMAN, G. M. N87-12647
HASTINGS, D. N87-13310
HATHAWAY, D. H. N87-13046
HAWKINS, I. N87-13366
HAYDEN, C. N87-13063
HAYES, W. C. N87-13133
HAYS, G. N. N87-12861
HAYS, I. D. N87-13361
HEADLEY, T. J. N87-12668
HEATH, M. T. N87-13193
HEDSTROM, J. C. N87-12824
HEGARTY, J. N87-13284
HEIDENREICH, G. N87-12999
HEIMLICH, R. N87-12837
HELLSTROM, E. E. N87-12802
HENDRICKS, D. N. N87-12790
HENSON, M. N87-12617
HERBERT, T. N87-12811
HERNITER, B. N87-13025
HERRMANN, R. B. N87-12724
N87-13030
HERSHCOVITCH, A. N87-13257
HESS, D. W. N87-13316
HIBBARD, B. N87-13092
HICKEY, J. S. N87-13093
HICKOX, C. E. N87-12818
HILLS, C. R. N87-12668
HINDS, F. T. N87-12678
HINZ, W. N87-13158
HIRSCH, J. N87-13135
HIRST, K. N87-13358
HLAVA, P. F. N87-12640
HLAVKA, C. N87-12974
HODARA, H. N87-13273
HODGE, R. W. N87-12557
HOERMANN, E. N87-13298
HOFFBAUER, M. A. N87-12863
HOFFMAN, R. N. N87-13104
HOLLAND, R. N87-12726
HOLMES, B. L. N87-12776
HOLMES, S. A. N87-13287
HONEYCUTT, T. E. N87-12850
HONIH, E. M. N87-12752
HOOD, D. W. N87-12908
HOOVER, G. N87-12971
HORI, Y. N87-12941
HORN, D. N87-13119
HORNING, R. D. N87-13337
HORTON, J. A. N87-12662
HORWITZ, J. L. N87-13307
HOU, M. N87-12695
HOUGHTON, D. D. N87-13079
HOUSTON, J. E. N87-12639
HOWLAND, M. R. N87-13072
HOYLE, S. C. N87-13194
HU, C. R. N87-12749
HU, H. N87-13225
HUANG, J. C. N87-12870
HUBBARD, R. W. N87-13134
HUETTIG, F. N87-13155
HUGHES, E. E. N87-13011
HULL, D. G. N87-12577
N87-12583
HUNG, C. C. N87-12559
HUNG, R. J. N87-13075
HUNTINGTON, J. F. N87-12979
HUTSINPILLER, A. N87-12978
HUTTON, J. T. N87-12666
HYMER, J. N87-12797

I

IDIODI, J. O. A. N87-13341
IGLEHART, D. L. N87-13210
IKONOMOU, G. D. N87-12642
IM, B. J. N87-12548
INAGAKI, T. N87-13256
INGRAFFEA, A. R. N87-12945
IRENE, E. A. N87-12634
N87-12935
ISAACS, R. G. N87-12991
N87-13104
ISAACSON, D. L. N87-12987
ISOBE, T. N87-13368
IVANOV, V. N. N87-12948

J

JAEGER, C. D. N87-12769
JAHN, R. G. N87-12610
JAIN, F. C. N87-12652
JAKOWATZ, C. V., JR. N87-12799
JAMES, W. J. N87-12648
JAYANTHI, U. B. N87-13020
JEDLOVEC, G. N87-13096
JEDLOVEC, G. J. N87-12828
N87-13087
JENDRZEJCZYK, J. A. N87-12611
JENEKHE, S. A. N87-12693
JENNINGS, T. J. N87-13171
JERABEK, D. J. N87-13350
JEW, K. N87-13277
JHA, N. K. N87-12773
JOHANNESSEN, O. N87-13119
JOHNSON, A. R. N87-13009
JOHNSON, D. R. N87-13070
JOHNSON, J. A. N87-12908
JOHNSON, J. O. N87-12707
JOHNSON, K. P. N87-12693
JOHNSON, P. D. N87-12909
JOHNSON, R. L. N87-13057
JOHNSTON, G. D. N87-12606
JOHNSTON, K. J. N87-12804
JOHNSTON, P. J. N87-12538
JOHNSTONE, W. N87-13269
JONAS, J. N87-12838
JONES N87-12774
JONES, A. H. N87-12654
JONES, C. R. N87-13353
JONES, K. W. ..... N87- .3124
JONES, M. E. N87-12864
N87-13312
JONES, R. H. N87-12671
N87-12676
JONES, S. P. N87-12876
JONIDES, J. N87-13136
JOSEPH, A. A. N87-13287
JOSEPH, T. R. N87-13301
JOSLIN, G. N87-13277
JUHASZ, A. J. N87-12606
JURCZYSZYN, L. N87-13342

K

KAILATH, T. N87-12759
KALB, M. W. N87-13078
N87-13081
KALOMIRIS, V. E. N87-13305
KAMDAR, M. H. N87-12653
KAMOWITZ, D. N87-13187
KAPITANOVA, T. P. N87-12952
KAPLAN, L. D. N87-13104
KARITANI, S. N87-13093
KASS, W. J. N87-12842
KATO, S. N87-13010
KATO, T. N87-12716
KATTAWAR, G. W. N87-12749
KATZ, N. N87-13389
N87-13393
KAUFMAN, J. J. N87-13324
KAUFMAN, L. N87-13142
N87-13144
KAUFMANN, P. N87-13378
KAULKER, W. F. N87-12626
KAUNE, W. T. N87-13139
KAYANO, M. T. N87-13118
KAZANAS, D. N87-13367
KEATON, P. W. N87-12580
KEDDY, E. S. N87-12999
KEDEM, B. N87-13218
KEIL, R. N87-13288
KEINIGS, R. N87-13312
KELLER, D. N87-13093
KELLER, V. W. N87-12585
KELLEY, A. J. N87-12610
KELLY, J. D. N87-13031
KELLY, J. H. N87-13203
KELLY, W. M. N87-12605
KEMBHAVI, A. N87-13398
KENNEDY, C. R. N87-12698
KENNEDY, R. S. N87-13143
KENT, G. S. N87-13024
KESTERNICH, W. N87-12664
KHAJIL, T. M. A. N87-12678
KHOBAIB, M. N87-12563
KIDDER, S. Q. N87-13050
KIM, K. J. N87-12865
KIM, K. K. N87-12658
KIMURA, J. N87-12718
KIRCHNER, J. H. N87-13161
KIRCHNER, W. L. N87-13260
KLEIN, W. N87-12684
KLEINROCK, L. N87-12741
KLUEH, R. L. N87-12666
KNEPPER, D. H., JR. N87-12980
KNOX, R. D. N87-13337
KOBEDA, E. N87-12935
KOCZAK, M. J. N87-12657

KOELLING, D. D. N87-13255
KOGA, R. N87-13314
N87-13389
N87-13393
KOGER, J. W. N87-12674
N87-12675
KOLASINSKI, W. A. N87-13314
KOLSKY, H. N87-12928
KONDO, H. N87-12540
KONKIN, A. A. N87-12822
KONNOVA, N. F. N87-12822
KOO, K. P. N87-12836
KOPECKY, K. J. N87-13046
KOPP, F. J. N87-13077
N87-13081
KOPP, R. A. N87-13382
N87-13383
KOPP, U. N87-13150
KOREN, I. N87-13174
KOROTKOV, V. G. N87-12954
KOSTADINOV, I. Z. N87-13343
KOTA, S. N87-13215
KOU, Y. F. N87-13133
KPONOU, A. N87-13257
KRAUSS, R. J. N87-13092
KRAUZE, L. D. N87-13203
KRIDER, E. P. N87-13061
KRISHAN, V. N87-13364
KRISHNAIAH, P. R. N87-13236
KRISHNAMURTHY, L. N87-12816
KRISHNAN, M. N87-12859
KRISTIANSEN, M. N87-12762
KROH, G. N87-13148
KROHN, M. D. N87-12981
KROMPHOLZ, H. N87-12762
KRONCKE, G. T. N87-12848
KRUSE, F. A. N87-12973
N87-12960
KUDRIN, L. V. N87-13376
KUFELD, R. M. N87-12557
KUGA, H. K. N87-13377
KUNIMATSU, K. N87-12631
N87-12632
KUO, A. N87-12939
KURSHNER, D. N87-13016
KURZEJA, R. J. N87-13022
KUSUOKA, S. N87-13220
N87-13221
KUZMIN, R. O. N87-13376
KWAN, T. J. T. N87-12792
KWONG, S. K. N87-13265

L

LACY, D. E. N87-12606
LAGUNA, G. R. N87-12794
LAI, Z. J. N87-12667
LAIRD, J. E. N87-13204
LAIOS, A. A. N87-12916
N87-12917
N87-12918
N87-12919
N87-12920
LALA, G. G. N87-12585
LAM, D. K. W. N87-13294
LAMB, R. C. N87-13396
LAND, C. E. N87-12837
LANDER, J. J. N87-12769
LANDO, J. B. N87-13333
LANFORD, W. A. N87-12649
LANG, R. N87-12844
LANGLEY, P. N87-13184
LANICCI, J. M. N87-13101
LANKFORD, J. N87-12620
N87-12689
N87-12929
LARKIN, J. J. N87-13315
LAUBER, J. K. N87-13122
LAUGHLIN, J. S. N87-13138
LAVIE, P. N87-13130
LAW, C. K. N87-12627
LAWLEY, A. N87-12557
LAWSON, D. N87-13013
LAZAR, A. N87-12744
LAZAREWICZ, A. R. N87-13033
LEAODEMORAESNOVO, E. M. N87-12988
N87-12989
LEBLANC, P. N87-12546
LEE, B. H. N87-12546
LEE, D. J. N87-12547
LEE, J. R. N87-12840
LEE, L. C. N87-13380
LEE, M. A. N87-13397
LEE, T. D. N87-13259
LEFEVRE, H. C. N87-13283
LEIBOWITZ, L. M. N87-12742
LEMONDS, J. N87-12926
N87-12927
LENNON, J. F. N87-12733
LEPETRE, Y. N87-12823
LEROY, Y. N87-12930
LESLIE, F. N87-13044
LESTER, D. N87-13363
LEUNG, K. N87-12965
LEUPOLD, H. N87-13249
LEVERANT, G. R. N87-12820
LEVICH, B. N87-12823
LEVY, M. N87-12939
LEWIS, A. J. N87-12967
LEWIS, D. A. N87-13396
LEWIS, D. H. N87-13277
LEWIS, D. J. N87-12705
LI, K. N87-13347
LI, Z. J. N87-13358
LIANG, G. N87-12584
N87-12860
LIBICKI, C. M. N87-13037
LIDHOLM, S. U. N87-12605
LIEM, M. C. Y. N87-12777
LINDE, C. N87-13141
LINDEMUTH, I. R. N87-12795
LING, F. F. N87-12862
LINTERN, G. N87-12572
N87-12573
LIPOVSKI, G. J. N87-13188
LITVINOVA, V. D. N87-12952
LIU, C. C. N87-12959
N87-12966
LOEHRKE, R. I. N87-12817
LOFFMAN, R. S. N87-13196
LOGAN, R. A. N87-13284
LOGINOV, V. F. N87-12953
LOH, C. J. N87-12587
N87-12568
LONG, S. A. N87-12764
LOPES, R. V. D. N87-12589
LOPESDEOLIVEIRAESOUZA, M. N87-12594
LORD, C. K. N87-13168
LOUIS, J. F. N87-13104
LOVELAND, K. T. N87-13041
LU, D. N87-13344
LUCAS, J. N87-13299
LUDWICK, G. E. N87-12874
LUDWIG, G. O. N87-12827
LUGLI, P. N87-13321
LUHMANN, N. C., JR. N87-12853
LURIE, J. B. N87-13309
LUSTICK, L. S. N87-13169
LYNCH, F. E. N87-12713
LYNCH, N. N87-13191
LYON, R. J. P. N87-12970
N87-12976
LYONS, B. N87-12605
LYONS, N. R. N87-13353
LYZENGA, D. R. N87-13120

M

MA, B. M. N87-13250
MACDONALD, R. I. N87-13294
MACDONALD, S. B. N87-12748
MACFADYEN, D. H. N87-13289
MACGEE, A. N87-12875
MACGORMAN, D. R. N87-13058
MACINTYRE, W. G. N87-12635
MACKENZIE, J. D. N87-12601
MACLEAN, L. N87-13093
MADSEN, N. H. N87-12905
MAHATO, B. K. N87-12801
MAJUMDAR, B. S. N87-12655
MALEY, F. M. N87-12772
MANCHA, S. N87-12837
MANGLIK, R. M. N87-12826
MANKER, M. D. N87-13115
MANN, K. R. N87-12996
MANNHAUPT, H. R. N87-13159
MANNINEN, M. N87-13323
MANSI, A. O. N87-13008
MANTELLI, M. B. H. N87-12596
MANZI, A. O. N87-12962
N87-12964
MARABLE, W. P. N87-12846
MARGOLIS, S. H. N87-13389
N87-13390
N87-13391
MARKOV, M. A. N87-12723
MARKWORTH, A. J. N87-12686
MARSHALL, P. M. N87-12757
MARTIN, D. N87-13058
MARTIN, D. W. N87-13072
MARTIN, J. F. N87-13000
MARTINEZ, J. I. N87-13005
MARTINI, P. R. N87-12959
MASSEY, D. E. N87-12718
MATHUR, K. K. N87-12673
MATHYSSEK, K. N87-13288
MATONICK, J. N87-12828
MATOS, R. A. N87-13099
MAUK, R. N87-12573
MAUTZ, J. R. N87-12725
MAX, N. L. N87-13039
MAY, J. G. N87-13143
MAZUMDAR, S. N87-12697
MAZUMDER, J. N87-12863
MCADIE, C. N87-13117
MCARTHUR, D. A. N87-12861
MCCOOL, J. I. N87-12901
MCCORKENDALE, D. B. N87-13360
MCCORMICK, G. P. N87-13185
MCCOY, J. K. N87-12688
MCCRARY, G. E. N87-13005
MCCRARY, J. H. N87-13005
MCCROSKEY, W. J. N87-12544
MCDERMOTT, D. B. N87-12853
MCDONACH, A. N87-13289
MCEVOY, J. J. N87-12780
MCFADDEN, J. D. O. N87-13281
MCGUIRK, J. P. N87-13053
MCKEAGUE, I. W. N87-13230
MCNIDER, R. T. N87-13077
N87-13081
N87-13089
MCPHERSON, W. R. N87-12599
MCWHIRTER, J. G. N87-12736
MCWILLIAMS, B. M. N87-12787
MDEMORAES, I. N87-12595
MEAKIN, J. D. N87-13003
MEIER, K. L. N87-13260
MEIER, M. J. N87-12833
MELIUS, C. F. N87-12644
MENASHI, W. P. N87-13320
MENDELSON, A. N87-12915
MENDERS, J. N87-12845
MENDILLO, M. N87-13025
MENIETTI, J. D. N87-13028
MENZEL, P. N87-13095
MENZEL, W. P. N87-12828
MERAKOS, L. N87-12738
MERRIGAN, M. A. N87-12999
MERRITT, M. N87-13191
METIU, H. N87-12636
METZGER, D. W. N87-12771
MEYER, M. B. N87-12585
MICALE, F. J. N87-12681
MIGLIORI, A. N87-12902
MIGNANI, A. G. N87-13260
MIGRA, R. P. N87-12606
MIKHALEVSKY, P. N87-13119
MILICH, D. N87-13243
MILLER, D. G. N87-12770
MILLER, J. G. N87-12613
MILLER, L. L., JR. N87-13351
MILLER, M. K. N87-12662
N87-12663
MILLER, T. N87-13044
MILLER, T. L. N87-13046
MILLER, W. M. N87-13175
MILTON, N. M. N87-12984
MINA, N. K. N87-13340
MINC, H. K. N87-13247
MINDERMANN, D. N87-12998
MIRANDA, L. C. M. N87-12843
MISRA, M. S. N87-12616
MITCHELL, J. H. N87-12891
MITLITSKY, F. N87-12787
MITTRA, R. N87-12739
MOLOFSKY, J. N87-12993
MONDA, M. N87-12912
MOORE-EDE, M. C. N87-13137
MOORE, D. G. N87-12600
MOORE, T. J. N87-12746
MORAN, F. J. N87-12967
MORGAN, A. P. N87-13196
MORGAN, R. G. N87-12542
MORRIS, N. A. N87-12542
MORRISON, C. A. N87-12731
MOSKOWITZ, B. E. N87-13399
MOSS, M. N87-12647
MOSS, P. N87-13033
MOSS, S. C. N87-12779
MOTE, M. W. N87-12904
MOURA, A. D. N87-13118
MU, Y. N87-12582
MUNGSING, S. N87-13183
MURCRAY, D. G. N87-13035
MURCRAY, F. H. N87-13035

MURCRAY, F. J. N87-13035
MURPHY, C. H. N87-12584
MURPHY, M. N87-13141
MURRAY, R. N87-12987
MURRAY, W. N87-13180
N87-13248
MURTHY, S. V. N87-12831
MUSTARD, J. F. N87-12975
MUZA, S. R. N87-13128
MYERS, N. N87-12993

N

NAGLE, R. N. N87-13054
NAKAZAWA, S. N87-12923
NARASIMHAN, K. S. N87-13250
NASBY, R. D. N87-13175
NASH, D. O. N87-12543
NEAL, D. R. N87-12861
NEEDLEMAN, A. N87-12926
N87-12927
N87-12930
NEEPER, D. A. N87-12824
NEIL, G. N87-12845
NELSON, C. N87-12670
NER, M. S. N87-13289
NETHERS, R. W. N87-12771
NETO, A. R. N87-12590
N87-13177
N87-13205
NEURGAONKAR, R. R. N87-13328
NGUYEN, D. N87-12557
NGUYEN, T. N87-13203
NIEDERHOFER, K. H. N87-13303
NIEMEYER, D. N87-13150
NIINIKOSKI, T. N87-13257
NONEMAN, S. R. N87-12721
NOOR, A. K. N87-13227
NOVO, E. M. L. M. N87-12960
NURMIKKO, A. V. N87-13327
N87-13330
NUTTALL, J. D. N87-13275
NUZZO, A. M. N87-13111

O

OBERLY, C. E. N87-12768
OCH, G. M. N87-13149
OCHS, H. T. N87-13050
OLIGER, J. N87-12814
OLIVER, J. R. N87-13328
OLLING, C. R. N87-12535
OLSON, D. L. N87-12650
OLSSON, N. A. N87-13284
OLSZEWSKI, M. N87-12998
OMONGAIN, E. N87-12994
ORLANDO, V. N87-12589
N87-12590
N87-13177
ORLOVSKIY, N. S. N87-12950
ORTIZ, M. N87-12930
ORVILLE, R. E. N87-13065
OSGOOD, R. M., JR. N87-12783
OSIN, M. I. N87-12598
OSTAPENKO, A. A. N87-12956
OSTER, C. A. N87-12578
OTANI, N. F. N87-12751
OTT, R. H. N87-12576
OURICHE, H. N87-12916
OVERTON, W. C., JR. N87-12714
OWYOUNG, A. N87-12645

P

PACKAN, N. H. N87-12664
PADGETT, W. J. N87-13236
PAGE, R. A. N87-12689
PAIK, H. J. N87-13021
PAIVA, J. A. D. N87-13173
PALMER, R. G. N87-13262
PANAYAPPAN, R. N87-12691
PANDOLF, K. B. N87-13131
PAPA, R. J. N87-12733
PAPUCHON, M. N87-13283
PARIS, M. V. N87-13385
PARK, K. A. N87-12804
PARK, S. W. N87-12569
PARKER, K. G. N87-13090
N87-13093
PASLASKI, J. N87-13265
PATTON, C. E. N87-13318
PAULL, A. N87-12542
PEDERSEN, U. N87-13154
PEEBLES, H. C. N87-12672
PEEBLES, L. H., JR. N87-12692
PEERCY, P. S. N87-12660
PELLEGRINI, C. N87-12665
PENDLETON, Y. N87-13363
PENNING, W. R. N87-13364
PERKEY, D. J. N87-13078
PERONE, S. P. N87-12630
PERSON, J. C. N87-13310
PETER, W. N87-12664
PETERS, P. N87-12756
PETERSON, D. L. N87-12982
PETRO, L. D. N87-12991
PEURON, P. M. N87-13326
PFEIFER, D. N87-13224
N87-13237
PHILLIPS, J. D. N87-12967
PHILLIPS, J. E. N87-13003
PHILPOTT, M. R. N87-12631
N87-12632
PICKARD, P. S. N87-12961
PIEHLER, J. N87-13155
PIETERS, C. M. N87-12975
PILCHOWSKI, H. U. N87-12596
PINDOR, A. J. N87-13254
PINTO, O., JR. N87-13368
PINUS, N. Z. N87-12952
PITT, N. J. N87-13297
PITZ, R. W. N87-12829
PLESHA, M. E. N87-12924
PLOTZKER N87-12621
PLUNKETT, W. A. N87-12686
N87-12688
N87-12689
N87-12690
N87-12692
N87-12693
N87-12695
N87-12696
N87-12697
POLETTO, G. N87-13362
N87-13363
POLK, J. N87-12610
POON, C. N87-12672
POPA, A. E. N87-13304
POPPENDIEK, H. F. N87-13326
PORTER, F. N87-13043
POST, R. S. N87-13311
POTENZIANI, E., II N87-13349
POTERTIKOVA, G. A. N87-12662
POULTON, J. N87-12761
POUNDS, J. G. N87-13124
POWELL, A. M., JR. N87-13098
POWERS, D. L. N87-13223
PRADHAN, D. K. N87-13174
PRATT, J. R. N87-12614
PREUSS, W. N87-13159
PRITSOPOULO, C. D. N87-13020
PRITT, A. T. N87-12652
PROEYEN, A. V. N87-13349
PUKKILA, T. M. N87-13241
PURDOM, J. F. W. N87-13084
PURDY, T. L. N87-12984

Q

QUINN, G. D. N87-12618
QUINN, J. W. N87-13329

R

RAGA, A. C. N87-13374
RAJENDRAN, A. M. N87-12583
RAJU, I. S. N87-12922
RAJU, M. S. N87-12616
RAKULJIC, G. N87-13265
RAMAMOORTHY, C. V. N87-13202
RAMATY, R. N87-13395
RAMBABU, B. N87-13338
RANK, E. N87-13214
RAO, C. R. N87-13241
RAO, K. R. N87-13206
RAO, V. B. N87-13118
RATHBUN, J. S. N87-13176
RAZE, J. D. N87-12911
REAGAN, R. J. N87-12665
REAVIS, N. N87-13093
REDNER, S. N87-12684
REK, Z. N87-13334
REMSBERG, E. E. N87-13022
RENO, J. N87-13337
REUTER, W. G. N87-12936
REX, J. A. N87-13279
REYNOLDS, G. H. N87-12615
REYNOLDS, N. N87-13044
RHEE, K. T. N87-12628
RHIU, J. J. N87-12913
RHODES, T. N87-12651
RICCI, M. C. N87-12755
RICE, C. L. N87-13033
RICE, J. K. N87-12661
RICHARD, J. P. N87-13021
RICKERT, S. E. N87-13333
RIGHINI, G. C. N87-13285
RIORDAN, A. J. N87-13103
RIPPLE, W. J. N87-12987
RITCHIE, R. O. N87-12656
N87-12929
ROBERTS, C. N87-12634
N87-12635
ROBERTS, D. A. N87-12970
ROBERTS, D. E. N87-13127
ROBERTS, G. O. N87-13046
ROBERTS, H. A. N87-12748
ROBERTS, T. G. N87-12650
ROBERTSON, F. R. N87-13048
N87-13069
ROBINSON, D. N87-13352
ROBINSON, P. A., JR. N87-13313
ROBINSON, R. M. N87-13031
ROBSON, R. R. N87-12571
ROBY, C. G. N87-13192
ROCK, B. N. N87-12986
ROCKENFELLER, U. N87-13000
RODGERS, A. N87-12634
N87-12635
RODGERS, C. D. N87-13019
RODGERS, E. B. N87-13166
RODRIGUES, J. E. N87-12959
N87-12966
RONIG, A. D., JR. N87-12612
ROOK, H. L. N87-13011
ROSA, R. N87-12980
ROSENFELD, Y. N87-13306
ROSENFIELD, A. R. N87-12655
ROSS, P. N., JR. N87-12798
ROTGE, J. R. N87-12848
ROTH, E. P. N87-12647
ROTHERMEL, J. N87-13087
ROURKE, J. E. N87-13271
ROYZEN, A. M. N87-12964
RUANE, M. F. N87-12554
RUFF, G. A. N87-12551
RUMYANTSEV, S. A. N87-12954
RUSIN, J. M. N87-13361
RUSSELL, J. M., III N87-13022
RUSSO, V. N87-13285
RUST, W. D. N87-13056
RUTH, M. R. N87-12700
RUYBALDOSSANTOS, C. L. N87-13179
RZHIGA, O. N. N87-13376

S

SABIN, C. M. N87-13328
SABISKY, E. S. N87-12997
SABLOWSKI, N. N87-13154
SACHS, F. N87-13123
SACKETT, J. R. N87-13099
SACKVILLEHAMILTON, A. J. N87-13398
SAIF, A. G. N87-13346
SAKABE, Y. N87-12717
SALAM, A. N87-13373
SALGADO, A. E. M. N87-12720
SALTZMAN, B. N87-13064
SALZMAN, J. N87-12844
SAMADDAR, S. N. N87-12784
SANBORN, J. C. N87-13203
SANGIOVANNI, J. J. N87-12641
SANGSTER, W. E. N87-13115
SANTANA, C. E. N87-12757
SANTORU, J. N87-12571
SAPONE, D. N87-12797
SARIPKAYA, T. N87-12815
SAUER, K. N87-13155
SAUNDERS, M. A. N87-13180
N87-13248
SAVINO, J. M. N87-12606
SCHAEFER, G. N87-12762
SCHEGGI, A. M. N87-13260
SCHIDLOVSKY, G. N87-13124
SCHILINSKI, B. J. N87-13033
SCHLESINGER, R. N87-13085
SCHMID, L. C. N87-13361
SCHMITZ, H. A. N87-13334
SCHNABEL, R. B. N87-13216
SCHOCK, R. W. N87-12581
SCHOENBACH, K. N87-12762
SCHOFIELD, J. R., JR. N87-13354
SCHROEDER, H. N87-12664

SCHRUMPF, B. J. N87-12987
SCHUCK, W. D. N87-13303
SCHUETTE, M. N87-13182
SCHULLER, I. K. N87-12623
SCHULTZ, S. N87-12971
SCHWADERER, B. N87-13293
SCHWARTZ, M. N87-12744
SCLOVE, S. L. N87-13229
SCOTT, C. D. N87-12637
SCOTT, M. G. N87-13297
SEATON, C. T. N87-13290
N87-13292
SECHRIST, C. F., JR. N87-13015
SEKI, H. N87-12631
N87-12632
SELVIN, S. N87-13242
SEMARGE, R. E. N87-12661
SENA, J. T. N87-12999
SERFOZO, R. F. N87-13234
N87-13235
SEZGIN, E. N87-13349
SHAKED, M. N87-13219
N87-13240
SHAKERIN, S. N87-12817
SHANNON, R. L. N87-13172
SHAPAYEV, V. I. N87-12957
SHASHKINA, V. P. N87-13376
SHEFT, C. N87-12628
SHEHATA, L. N. N87-13346
SHELNUTT, J. A. N87-12694
SHEPHERD, J. E. N87-12619
SHEPPARD, D. J. N87-12573
SHERIDAN, S. G. N87-13114
SHERMAN, C. N87-13032
SHEYNBLATT, L. N87-12554
SHI, H. N87-12753
SHIH, C. N87-12845
SHIRER, H. N. N87-13049
SHIVAKUMAR, K. N. N87-12922
SHIVELY, J. F. N87-12791
SHPOCK, S. W. N87-12778
SHUDDE, R. H. N87-12555
SHUR, G. N. N87-12952
SHUSTER, P. M. N87-13099
SIBILIA, C. N87-13291
SIDORENKO, A. I. N87-13376
SIEVERS, A. J. N87-13319
SIGEL, G. H., JR. N87-12636
SILVA, A. J. N87-12722
SIMMONS, B. J. N87-12848
SIMMONS, C. S. N87-12820
SIMONI, P. O. N87-13244
SIMONIS, G. J. N87-12731
SINGH, J. J. N87-12614
N87-12660
SINGH, K. P. N87-13368
SINGPURWALLA, N. D. N87-13240
SINNO, M. N87-12920
SIVAKUMAR, J. N87-12709
SKLAD, P. S. N87-13335
SKRYPNIK, G. I. N87-13376
SLABE, M. E. N87-12679
SLINN, S. Y. N87-12599
SLUYTERS, T. N87-13257
SMARTT, H. B. N87-12908
SMIRNOV, V. S. N87-12956
SMITH, A. G. N87-13031
SMITH, J. L. N87-12921
SMITH, P. J. N87-13051
SMITH, R. E. N87-13075
SMITH, W. N87-13095
SMITH, W. L. N87-13060
SNELL, C. M. N87-12792
SNOW, G. S. N87-12842
SNYDER, A. D. N87-12705
SNYDER, D. M. N87-12534
SOLOMON, A. D. N87-13007
SOTTINI, S. N87-13285
SOU, I. K. N87-13337
SOUZA, C. D. R. E. N87-13244
SOUZA, M. L. D. E. N87-12586
SOVERS, O. J. N87-13178
SPALL, J. R. N87-12806
SPALLUCCI, E. N87-13348
SPALVINS, T. N87-12706
SPANGLER, L. H. N87-12863
SPANNER, M. A. N87-12982
SPELLER, L. C. N87-12847
SPENCER, J. H. N87-12604
SPENCER, R. W. N87-13072
N87-13074
SPEYER, J. L. N87-12583
SPILLER, E. N87-12623
SPILLMAN, G. R. N87-12603
SPRANGLE, P. N87-12846
SRINIVASAN, G. R. N87-12544
STAHL, M. N87-12559
STALKER, R. J. N87-12542
STANLEY, H. E. N87-12684
STAUDENMANN, J. L. N87-13337
STCLAIR, T. L. N87-12614
STECH, D. J. N87-12848
STECKER, F. W. N87-13368
STEGEMAN, G. I. N87-13290
N87-13292
STEIN, W. N87-13147
STEINBERG, D. J. N87-12643
STEINBERG, M. N87-12706
STEINER, D. N87-13263
STEINETZ, B. M. N87-12924
STEINLE, F. W. N87-12831
STEPHENS, W. E. N87-13301
STERN, T. N87-12744
STEUTEL, F. W. N87-13215
STEVENS, M. F. N87-12659
STEWART, L. J. N87-13172
STEYSKAL, H. P. N87-12732
STIEGLER, J. O. N87-12699
STIGLICH, J. J., JR. N87-12618
STILES, M. N87-12636
STOAKLEY, D. M. N87-12680
STOCKMANN, M. N87-13295
STOCKTON, R. V. N87-12728
STRAIN, B. R. N87-13012
STROBEL, D. F. N87-13023
STROOCK, D. N87-13220
STROOCK, D. W. N87-13221
STURROCK, P. A. N87-13387
SU, J. J. N87-13312
SUIT, W. T. N87-12566
SUMMA, J. M. N87-12545
SUNTHARALINGAM, P. N87-12729
SUOMI, V. E. N87-13091
N87-13092
SURI, M. N87-13222
SWEET, J. N. N87-12647
SWENSON, D. V. N87-12945
SWIFT, G. W. N87-12902
SWINDEMAN, R. W. N87-12944
SYLLAIOS, A. J. N87-13317
SYMONDS, P. S. N87-12928
SZABO, B. A. N87-12936

T

TAFT, S. N87-12797
TAKEDA, R. N87-12716
TANG, C. M. N87-12846
N87-13054
TANIGUCHI, M. N87-13217
TARANIK, J. V. N87-12977
N87-12978
TAYA, M. N87-12925
TAYLOR, R. L. N87-12733
TELESCO, C. M. N87-12756
TERRY, D. B. N87-13201
TESKE, R. G. N87-13365
TEW, R. C., JR. N87-13359
TEWS, E. C. N87-12630
THATCHER, R. G. N87-12906
THAYER, E. B. N87-12561
THIO, Y. C. N87-13258
THOMAS, D. B. N87-13156
N87-13159
THOMAS, E. V. N87-12789
THOMAS, G. N87-12665
THOMAS, M. M. N87-13203
THOMBS, L. A. N87-13236
THOMLEY, K. E. N87-12573
THOMPSON, A. H. N87-13053
THOMPSON, M. O. N87-12860
THOMPSON, S. N87-13226
THORPE, A. N. N87-12847
THRAPP, P. J. N87-12912
TIESZEN, S. R. N87-12819
TIKUISIS, P. N87-13131
TOKSOZ, M. N. N87-13034
TOLEDANO, A. N87-12917
TOLLAR, E. S. N87-13232
TOMAK, M. N87-12678
TONG, Y. L. N87-13219
TOOMRE, J. N87-13045
TOROPCHINOVA, T. V. N87-12957
TRACEY, K. L. N87-13121
TRACHTENBERG, I. N87-12633
TRACY, C. E. N87-12700
N87-12701
TRAMMELL, G. T. N87-12866
TRAN, D. C. N87-13296
TRIGARI, S. N87-13285
TRILLO, S. N87-13282
TRINH, N. D. N87-12919
TSAI, C. H. N87-12753
TSOU, Y. M. N87-12633
TSUNODA, R. T. N87-13031
TUCKER, D. N87-12969
TUCKER, D. L. N87-12742
TUKEY, J. W. N87-13228
TURNER, H. B. N87-13287

U

UCKERMANN, R. N87-13160
UDD, E. N87-13276
UNDERWOOD, J. H. N87-12934
N87-12938
UNRIGAR, C. J. N87-13254
USTIN, S. L. N87-12966

V

VALAVANI, L. N87-13243
VALERA, J. D. N87-13292
VALLABHAN, C. V. N87-12709
VANDERSANDE, J. B. N87-13336
VANDERZIEL, A. N87-13332
VANE, G. N87-12968
N87-12969
VANPATTEN, R. E. N87-13170
VANVORIS, P. N87-12992
VAROTTO, S. E. C. N87-12589
VASILAKIS, J. D. N87-12937
VASILYEV, A. N. N87-12954
VATOUX, S. N87-13283
VAUGHAN, D. N87-13272
VAUGHAN, O. H., JR. N87-13060
VAUGHAN, W. W. N87-13043
VEESER, L. R. N87-13281
VEIRS, K. N87-12646
VELDKAMP, W. N87-13266
VERTOGRADOV, G. G. N87-12958
VICTOR, R. A. N87-12899
VIERIRADAFONSECALOPEZ, R. N87-13377
VIMALCHAND, P. N87-12642
VINCENT, D. G. N87-13052
VINES, K. N87-12965
VINOGRADOVA, M. B. N87-12955
VISWANADHAM, Y. N87-12962
N87-12964
N87-13008
VISWANATHAN, S. N87-12766
VITEK, J. M. N87-12667
VODOLAZKIN, V. I. N87-12958
VONDERHAAR, T. H. N87-13084
VONJASKOWSKY, W. N87-12610
VONNEGUT, B. N87-13060
VONZAHN, U. N87-13018
VOSKO, S. H. N87-13254

W

WABNITZ, S. N87-13282
WADE, C. A. N87-13278
WADE, J. P. N87-12643
WALD, E. N87-13132
WALKER, S. D. N87-13300
WALLACE, W. L. N87-12997
WALSH, P. A. N87-12984
WAMBSGANSS, M. W. N87-12611
WAN, Y. H. N87-13182
WANG, B. Y. N87-12807
WANG, P. H. N87-13024
WANG, T. N87-12575
WANG, Z. N87-13347
WARD, R. C. N87-13199
WATANABE, S. F. N87-13276
N87-13287
WATKINS, R. D. N87-12802
WATSON, J. N87-13013
WATSON, L. T. N87-13196
WATTS, D. R. N87-13121
WATTS, M. E. N87-12830
WEBER, J. F. N87-12704
WECHSLER, D. B. N87-12597
WEERASOORIYA, T. N87-12563
WEFEL, J. P. N87-13381
WEILER, K. W. N87-12604
WEIMER, D. R. N87-13028
WEISS, M. S. N87-13169
WEISS, R. M. N87-13099
WEITSMAN, Y. N87-12617
N87-12619
N87-12932
WELCH, R. M. N87-13102
WENCKUS, J. F. N87-13320

WERNER, M. W. N87-13363
WEST, G. S. N87-13075
WESTMACOTT, K. H. N87-12670
WESTRA, D. P. N87-12572
N87-12573
WHALEY, R. J. N87-13326
WHEATLEY, J. C. N87-12902
WHITE, A. A., III N87-13133
WHITE, M. R. N87-13010
WHITE, R. L. N87-13175
WHITEHEAD, J. C. N87-12787
WIEGAND, D. N87-13159
WIGHTMAN, J. P. N87-12690
WILKINS, G. M. N87-12739
WILLCUTT, G. J. N87-13260
WILLIAMS, L. N87-12562
WILLIAMS, M. C. N87-13143
WILLIAMS, S. F. N87-13089
WILLIAMSON, P. R. N87-12609
WILLIAMSON, R. L. N87-12672
WILLIAMSON, S. J. N87-13142
WILLIAMSON, W. S. N87-12571
WILLMAN, C. J. N87-13250
WILSON, D. G. N87-13007
WILSON, G. N87-13093
N87-13095
WILSON, G. S. N87-12828
N87-13073
WILSON, G., S. N87-13081
WILSON, R. B. N87-12923
WILSON, S. B., III N87-12558
WILTON, D. R. N87-12764
WINFUL, H. G. N87-13290
WINGATE, J. E. N87-12884
WINTERSGILL, M. C. N87-12683
WIRTH, C. J. N87-13155
WISE, M. B. N87-12630
WITHERS, P. B. N87-13278
N87-13286
WODTKE, C. H. N87-12886
N87-12887
N87-12888
N87-12889
N87-12890
N87-12891
N87-12892
N87-12893
N87-12894
N87-12895
N87-12896
N87-12897
WOLFE, W. J. N87-13203
WOLOSHUN, K. N87-12999
WON, I. J. N87-13026
WONG, H. K. N87-13356
WOOD, B. L. N87-12985
WOODWARD, R. A. N87-12986
WORSHAM, R. D. N87-12991
WRIGHT, M. H. N87-13180
N87-13248
WRIXON, G. T. N87-12605
WUKELIC, G. E. N87-12992

Y

YAMAGUCHI, Y. N87-12970
YANG, C. L. N87-13325
YANG, G. N87-13344
YANG, L. N87-12615
YANG, T. N87-12845
YARIV, A. N87-12844
N87-13265
YEN, H. W. N87-13304
YOLDAS, B. E. N87-12687
YOON, H. S. N87-12925
YOSHIOKA, H. N87-12809
YOUNG, J. T. N87-13091
N87-13092
YOUNG, L. A. N87-12539
N87-12869
YOUNG, W. A. N87-13277
YU, D. N87-13213
YU, W. N87-12656

Z

ZAKHAROV, Y. V. N87-12598
ZANELLI, J. N87-13372
ZANNER, F. J. N87-12672
ZEHR, R. N87-12883
ZEIDES, F. N87-12658
ZEITZ, L. N87-13138
ZHANGNUO, H. N87-12582
ZHERIKHIN, N. V. N87-13376
ZIEGLER, E. N87-12623
ZIELINSKI, W. L., JR. N87-13011
ZIOLKOWSKI, R. W. N87-12750
ZIXING, W. N87-12533

Typical Corporate Source Index Listing

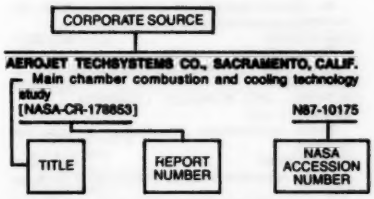

Listings in this index are arranged alphabetically by corporate source. The title of the document provides the user with a brief description of the subject matter. The report number helps to indicate the type of document cited (e.g., NASA report, translation, NASA contractor report). The NASA accession number denotes the number by which the citation is identified. The titles are arranged under each corporate source in ascending accession number order.

A

ADVISORY GROUP FOR AEROSPACE RESEARCH AND DEVELOPMENT, NEUILLY-SUR-SEINE (FRANCE).
Guided Optical Structures in the Military Environment
[AGARD-CP-383] N87-13273

AEG-TELEFUNKEN, ULM (WEST GERMANY).
Obstacle-warning radar for helicopters N87-13149

AEROSPACE CORP., EL SEGUNDO, CALIF.
Vector analysis and satellite footprints
[AD-A169832] N87-12576
Picosecond optoelectronic diagnostics of field effect transistors
[AD-A170503] N87-12779
Comparison of 2D memory SEU transport simulation with experiments
[ATR-86(8139)-2] N87-13314
Contributions to the 18th International Cosmic Ray Conference
[ATR-86(9558)-11] N87-13389
The secondary production of gamma rays in the Jovian magnetosphere N87-13391
The stellar upper mass limit in an OB association and implications for cosmic rays and cosmic abundances N87-13392
A versatile Data Processing Unit (DPU) for satellite-borne composition instrumentation N87-13393

AEROSPACE MEDICAL RESEARCH LABS., WRIGHT-PATTERSON AFB, OHIO.
The effects of high sustained acceleration on the acoustic phonetic structure of speech: A preliminary investigation
[AD-A170563] N87-12746

AIN SHAMS UNIV., CAIRO (EGYPT).
Possibility of using dc conductivity for investigating phase transition in amorphous semiconductors
[DE86-702646] N87-13340

AIR FORCE ACADEMY, COLO.
Optical rotation sensors
[AD-A169357] N87-12848

AIR FORCE ENVIRONMENTAL TECHNICAL APPLICATIONS CENTER, SCOTT AFB, ILL.
Station climatic summaries, Europe
[AD-A167888] N87-13100
Revised Uniform Summary of Surface Weather Observations (RUSSWO). Parts A-F Ellington ANGB, Texas
[AD-A169389] N87-13105
Revised Uniform Summary of Surface Weather Observations (RUSSWO). Parts A-F, Fort Richardson, Alaska
[AD-A169390] N87-13106
Wheeler AFB, Hawaii Limited Surface Observations Climatic Summary (LISOCS), parts 1-5
[AD-A169391] N87-13107

AIR FORCE GEOPHYSICS LAB., HANSCOM AFB, MASS.
A semi-empirical low-latitude ionospheric model
[AD-A168899] N87-13025
Collection of ions in the stratosphere
[AD-A169905] N87-13032
Balloon-borne, high altitude gravimetry: The flight of DUCKY 1a (11 October 1983)
[AD-A169942] N87-13033
Improving foF2 prediction for the sunrise transition period
[AD-A170457] N87-13036
Sensitivity tests of a surface-layer windflow model to effects of stability and vegetation
[AD-A169136] N87-13101
Medium- and long-wavelength infrared emission from a laser-produced oxygen plasma
[AD-A169475] N87-13309

AIR FORCE INST. OF TECH., WRIGHT-PATTERSON AFB, OHIO.
The portfolio model of technological development in the aircraft industry
[AD-A170832] N87-12534
Integrating computer vision with a robot arm system
[AD-A171278] N87-12884
A simple solar, spectral model for studying the effects of cloud cover and surface albedo on the incoming solar radiation
[AD-A171284] N87-13038
A review of microbursts and their analysis and detection with Doppler radar
[AD-A170458] N87-13110
Extraterrestrial forcing, atmospheric electricity and the occurrence of thunderstorms
[AD-A170463] N87-13111

AIR FORCE SYSTEMS COMMAND, WRIGHT-PATTERSON AFB, OHIO.
The effect of a winglet on the spatial vortex of a slender body at high angle of attack
[AD-A169925] N87-12533
The effect of coupling in an inertial navigation platform stabilized system made up of three single-degree-of-freedom gyroscopes
[AD-A169110] N87-12553
The Chinese guided missiles stride toward modernization
[AD-A169017] N87-12582
Carbon fibers
[AD-A171370] N87-12622
Metrics of closed world of Friedmann, agitated by electric charge (towards a theory electromagnetic Friedmann's)
[AD-A169981] N87-12723
Journal of engineering thermophysics (selected articles)
[AD-A169452] N87-13347

AIR FORCE WEAPONS LAB., KIRTLAND AFB, N. MEX.
Preliminary material testing of ceramic and wood
[AD-A169557] N87-12771
Holographic storage in ion-implanted, ferroelectric-phase PLZT ceramics
[DE86-010475] N87-12837

ALABAMA UNIV., HUNTSVILLE.
Cellular solidification of transparent monotectics
[NASA-CR-177039] N87-12626
Preliminary planning for the Satellite Precipitation And Cloud Experiment (SPACE) Field Program N87-13089
Space plasma research
[NASA-CR-178965] N87-13307

ALASKA UNIV., FAIRBANKS.
A study of the relationship between solar activity and interplanetary field variations
[AD-A169963] N87-13380

ALLIED BENDIX AEROSPACE, UTICA, N.Y.
Component improvement program task 83-01, 36E133 air turbine starter
[AD-A169483] N87-12582

ALLIED BENDIX CORP., KANSAS CITY, MO.
Image enhancement equipment capabilities
[DE86-013615] N87-12800
Resistance seam welding
[DE86-013288] N87-12906
Review of robotic component insertion system for printed wiring assemblies
[DE86-013510] N87-12907

AMES LAB., IOWA.
Crack propagation in high strain regions of a steel containment
[DE86-011437] N87-12943
In-situ interdiffusion measurements in HgTe-CdTe superlattices
[DE86-011429] N87-13337
Very high energy gamma ray astrophysics
[DE86-013319] N87-13396

ANALYTICAL METHODS, INC., REDMOND, WASH.
A summary of the development of integral aerodynamic methods for the computation of rotor wake interactions
[AD-A169254] N87-12545

ANCO ENGINEERS, INC., CULVER CITY, CALIF.
Radiographic determination of mass and inertial tenaor of anatomical segments
[AD-A169122] N87-13126

ANT NACHRICHTENTECHNIK, BACKNANG (WEST GERMANY).
PIN-FET preamplifier for high-speed optical transmission systems N87-13293

APPLIED PHYSICS, INC., ALBUQUERQUE, N. MEX.
Radar cross-section of damped cylinders and dielectric strips
[AD-A169027] N87-12726

ARGONNE NATIONAL LAB., ILL.
Computational and experimental study of flow-induced vibration of the SSME main injector post
[DE86-012119] N87-12611
Stability of multilayers at high temperatures
[DE86-010526] N87-12623
Band description of materials with localizing orbitals
[DE86-010529] N87-13255

ARIZONA STATE UNIV., TEMPE.
Degeneracy in the ensemble Monte Carlo method for high field transport in semiconductors
[AD-A169456] N87-13321

ARIZONA UNIV., TUCSON.
Inequalities for probability contents of convex sets via geometric average
[AD-A169938] N87-13219
A Bayesian approach to quantile and response probability estimation with applications in reliability
[AD-A170455] N87-13240
Nonlinear planar guided wave interactions and devices N87-13290
Integrated optics optical limiters N87-13292
Investigations of long-period DQ Herculis star N87-13364

ARMY BELVOIR RESEARCH AND DEVELOPMENT CENTER, FORT BELVOIR, VA.
Reliability prediction models for mechanical equipment
[AD-A169775] N87-12911

ARMY CLOSE COMBAT ARMAMENTS CENTER, WATERVLIET, N.Y.
Embrittlement of a high and a low strength steel in liquid lead environment
[AD-A169443] N87-12653
Linear elastic fracture testing: Current status within ASTM committee E-24 on fracture
[AD-A169442] N87-12934
Computation of residual stresses due to phase transformations during quenching of hollow cylinders
[AD-A170493] N87-12937
Unloading-compliance and load-drop analysis of J(Ic) test of irradiated 348 stainless steel
[AD-A170494] N87-12938

ARMY COLD REGIONS RESEARCH AND ENGINEERING LAB., HANOVER, N. H.
MIZEX: A program for mesoscale air-ice-ocean interaction experiments in arctic marginal ice zones. 8: A science plan for a winter marginal ice zone experiment in the Fram Strait/Greenland Sea, 1987/89
[AD-A169070] N87-13119

ARMY COMMUNICATIONS-ELECTRONICS COMMAND, FORT MONMOUTH, N.J.
Tactical fiber optic assembly requirements N87-13305

SOURCE

ARMY ENGINEER WATERWAYS EXPERIMENT STATION, VICKSBURG, MISS.
Pressure calculation for two-dimensional flow inside hydraulic structures
[AD-A169039] N87-12812
ARMY FIELD ARTILLERY SCHOOL, FORT SILL, OKLA.
Government libraries. A periodicals bibliography, together with list of bibliographies and indexes
[AD-A169422] N87-13351
ARMY MATERIALS AND MECHANICS RESEARCH CENTER, WATERTOWN, MASS.
Mechanical testing of a coated carbon-carbon composite at elevated temperatures in air
[AD-A169355] N87-12618
ARMY MILITARY PERSONNEL CENTER, ALEXANDRIA, VA.
Special associative preprocessing structures for qualitative feature extraction
[AD-A169147] N87-13181
ARMY MISSILE COMMAND, REDSTONE ARSENAL, ALA.
Evaluation of the Collins/Rockwell two axis gyro/accelerometer sensor cluster (phase 3 unit)
[AD-A169810] N87-12834
Evaluation of the multifunction sensor acceleration sensitive terms MU sub A and MU sub B
[AD-A169811] N87-12835
ARMY RESEARCH INST. OF ENVIRONMENTAL MEDICINE, NATICK, MASS.
Hypothermic effects on vascular contractility and reactivity
[AD-A169142] N87-13127
Quantification of respiratory muscle performance
[AD-A169208] N87-13128
Human thermoregulatory model for immersion in cold water
[AD-A169779] N87-13131
Self-paced heat acclimation procedures
[AD-A170533] N87-13134
ARMY RESEARCH OFFICE, RESEARCH TRIANGLE PARK, N. C.
Proceedings of the conference on the design of experiments in army research development and testing (31st) held at the Madison, Wisconsin on 23-25 October 1986
[AD-A169473] N87-13246
ARNOLD ENGINEERING DEVELOPMENT CENTER, ARNOLD AIR FORCE STATION, TENN.
Analysis and verification of the icing scaling equations. Volume 1: Revision
[AD-A167976] N87-12551
Effects of test cell recirculation on high-bypass turbofan engines during simulated altitude tests
[AD-A171418] N87-12565
ATMOSPHERIC AND ENVIRONMENTAL RESEARCH, INC., CAMBRIDGE, MASS.
Intercomparison of DMSP OLS, NOAA AVHRR, GOES VISSR (Defense Meteorological Satellite Program Operational Linescan System, National Oceanographic and Atmospheric Administration Advanced Very High Resolution Radiometer, GOES Visible Infrared Spin-Scan Radiometer) and Landsat MSS imagery for cloud property determination: Recommendations for digital data analysis
[AD-A169265] N87-12991
Improving numerical weather prediction by maximizing the use of assimilated satellite data
[AD-A169295] N87-13104
AUBURN UNIV., ALA.
Sensor controlled robotic welding for nuclear applications
[DE86-013110] N87-12905

B

BALLISTIC RESEARCH LABS., ABERDEEN PROVING GROUND, MD.
Blast gust loading on a 35 degree swept-back wing
[AD-A169415] N87-12570
Stability of liquid-filled projectiles with unusual coning frequencies
[AD-A171460] N87-12584
BARR AND STROUD LTD., GLASGOW (SCOTLAND).
Performance of integrated optical frequency shifters pigtailed to high birefringence fibres using ion-milled grooves N87-13289
BATTELLE COLUMBUS LABS., OHIO.
Hot isostatic pressing of ceramic powder compacts
[AD-A169971] N87-12688
Laser produced X-ray for high resolution lithography and a photoionization laser
[AD-A170782] N87-12858
BATTELLE MEMORIAL INST., COLUMBUS, OHIO.
Micromechanisms and toughness for cleavage fracture of steel
[AD-A169906] N87-12655
BATTELLE PACIFIC NORTHWEST LABS., RICHLAND, WASH.
Study of the formation and transport of acidic species by non-precipitating cumulus clouds during VENTEX-84
[PB86-220357] N87-13014
BELL COMMUNICATIONS RESEARCH, INC., MORRISTOWN, N.J.
A hybrid transmission scheme on single mode fibers for tactical communications N87-13306
BELL TELEPHONE LABS., INC., MURRAY HILL, N. J.
Introduction to the theory of nested transactions
[AD-A171428] N87-13191
Wavelength division multiplexing at 1.5 microns for high capacity optical transmission N87-13264
BETH ISRAEL HOSPITAL, BOSTON, MASS.
Fracture and viscoelastic characteristics of the human cervical spine
[AD-A170002] N87-13133
BOEING AEROSPACE CO., SEATTLE, WASH.
FEL (Free Electron Laser) optics coating test program (design phase of sample introduction chamber)
[AD-A169474] N87-12849
BOSTON UNIV., MASS.
Medium-frequency data link for differential NAVSTAR/GPS broadcasts
[AD-A169788] N87-12554
Percolation and low density materials: Theory and applications
[AD-A169204] N87-12684
Proceedings of the Workshop on Atmospheric Tides, Prague, Czechoslovakia, August 14, 1985 N87-13017
BRITISH TELECOM RESEARCH LABS., IPSWICH (ENGLAND).
Wide bandwidth, long distance fibre-optic communication systems N87-13300
BROOKHAVEN NATIONAL LAB., UPTON, N. Y.
Production of a clean carbon fuel derived from coal for use in stationary and mobile heat engines
[DE86-011203] N87-12706
Molecular dynamic studies of crack propagation. The role of the interatomic potential
[DE86-009942] N87-12942
X-ray fluorescence with synchrotron radiation
[DE86-010543] N87-13124
Polarized H(-) source development at BNL
[DE86-012704] N87-13257
BROWN UNIV., PROVIDENCE, R. I.
An analysis of shear band development incorporating heat conduction
[AD-A168972] N87-12926
Finite element analyses of shear localization in rate and temperature dependent solids
[AD-A169057] N87-12927
Feasibility study of test problems for finite element/finite difference programs for structural dynamics
[AD-A169058] N87-12928
A finite element method for localized failure analysis
[AD-A169117] N87-12930
Abundance and distribution of mineral components associated with Moses Rock (kimberlite) diatreme N87-12975
Picosecond nonlinear resonant interactions in semiconductors
[AD-A169992] N87-13327
Picosecond nonlinear resonant interactions in semiconductors
[AD-A170813] N87-13330
BUTLER UNIV., INDIANAPOLIS, IND.
Comparison of tropical forest surveys
[DE86-011699] N87-12993

C

CALIFORNIA INST. OF TECH., PASADENA.
High power semiconductor laser sources
[AD-A168900] N87-12644
Phase conjugate optics and picosecond optoelectronics
[AD-A169180] N87-13265
CALIFORNIA POLYTECHNIC STATE UNIV., SAN LUIS OBISPO.
Proof of feasibility of a novel inverter for photovoltaic power conditioning
[DE86-012729] N87-13001
CALIFORNIA UNIV., BERKELEY.
Fatigue behavior of long and short cracks in wrought and powder aluminum alloys
[AD-A169980] N87-12656
Stabilizing effects of finite-amplitude RF waves on the interchange instability
[DE86-013042] N87-12751
International Conference/Workshop on Small Fatigue Cracks (2nd) held in Santa Barbara, California on 5-10 January 1986
[AD-A169060] N87-12929
Distributed name servers: Naming and caching in large distributed computing environments
[AD-A169225] N87-13201
Availability and consistency of global information in computer networks
[AD-A169247] N87-13202
An intuitive approach to geometric continuity for parametric curves and surfaces
[AD-A169654] N87-13211
Plasma-enhanced deposition and processing of transition metals and transition metal silicides for VLSI
[AD-A168963] N87-13316
CALIFORNIA UNIV., BERKELEY. LAWRENCE BERKELEY LAB.
Raman spectroscopic investigation of molecular hydrogen
[DE86-012836] N87-12846
Atomic resolution study of precipitates in an Al-Ge alloy
[DE86-011308] N87-12870
Zinc/nickel oxide battery membrane separator studies
[DE86-012824] N87-12793
Feasibility study of a new zinc-air battery concept using flowing alkaline electrolyte
[DE86-013461] N87-12796
Very high efficacy electrodeless high intensity discharge lamps
[DE86-013760] N87-12803
High-gain free electron lasers as generators of short wavelength coherent radiation
[DE86-012500] N87-12865
Characterization of information requirements for studies of CO2 effects: Water resources, agriculture, fisheries, forests and human health
[DE86-012477] N87-13010
Two issues concerning the analysis of grouped data
[DE86-006401] N87-13242
X-ray data booklet, revision
[DE86-012650] N87-13272
Further results on interpolation searching of databases
[DE86-012822] N87-13356
CALIFORNIA UNIV., DAVIS.
Combustion and micro-explosion of water/oil emulsions in high pressure environments
[AD-A169976] N87-12627
Airborne Doppler measurements of the central California extended sea breeze N87-13066
CALIFORNIA UNIV., IRVINE.
Language acquisition and machine learning
[AD-A169581] N87-13184
CALIFORNIA UNIV., LOS ANGELES.
New materials for spacecraft stability and damping: A feasibility study
[AD-A169826] N87-12601
A mathematical formulation of a large space structure control problem
[AD-A169950] N87-12602
Advanced teleprocessing systems
[AD-A170007] N87-12741
High repetition rate electron beam RF-Acceleration and sub-millimeter wave generation via a free electron laser
[AD-A169846] N87-12853
On the dexterity of robotic manipulators N87-12867
Donor-acceptor one step energy transfer via exchange coupling on a fractal lattice
[AD-A169843] N87-13325
The carbon twelve to carbon thirteen isotope ratio of the interstellar medium in the neighborhood of the sun N87-13366
CALIFORNIA UNIV., SANTA BARBARA.
On the interplay between chemical reactions and phase transitions for molecules adsorbed on solid surfaces
[AD-A169618] N87-12636
Matrix theory
[AD-A169139] N87-13247
CAMBRIDGE UNIV. (ENGLAND).
Visualisation of axial turbine tip clearance flow using a linear cascade
[CUED/A-TURBO/TR-122] N87-12560
CASE WESTERN RESERVE UNIV., CLEVELAND, OHIO.
Analysis of mixed-mode crack propagation using the boundary integral method
[NASA-CR-179518] N87-12915
Epitaxial crystallization and epitaxial polymerization as tools for molecular engineering
[AD-A171506] N87-13333
CERES CORP., WALTHAM, MASS.
Study to determine the feasibility of utilizing skull-melting techniques for the growth of single crystals of yttrium vanadate
[AD-A169249] N87-13320

CHICAGO UNIV., ILL.
Analysis of satellite data for sensor improvement (detection of severe storms from space N87-13071
Some investigations into variable meshes for numerical solution of partial differential equations
[AD-A168977] N87-13206
CHILE UNIV., SANTIAGO.
Canonical quantization of gravity
[DE86-702615] N87-13372
CITY COLL. OF THE CITY UNIV. OF NEW YORK.
Theory of developed hydrodynamical turbulence
[DE86-012795] N87-12823
CLARKSON UNIV., POTSDAM, N.Y.
A rule-based pattern matching system for the recognition of three-dimensional line drawn objects: A foundation for video tracking
[AD-A170701] N87-13190
Nonlinear waves
[AD-A168934] N87-13207
Eigenvectors of graphs
[AD-A170562] N87-13223
COLORADO SCHOOL OF MINES, GOLDEN.
The influence of welding flux on the pyrometallurgical, physical and mechanical behavior of weld metal
[AD-A169067] N87-12650
COLORADO STATE UNIV., FORT COLLINS.
Natural convection in an enclosure with discrete roughness elements on a vertical heated wall
[DE86-004424] N87-12817
Investigations of severe/tornadic thunderstorm development and evolution based on satellite and AVE/SESAME/VAS data N87-13084
Summary of 1986 Atlantic tropical cyclone activity and verification of author's seasonal forecast N87-13097
Microwave loss properties of hexagonal ferrites for millimeter wave applications
[AD-A168862] N87-13318
COLORADO UNIV., BOULDER.
Meter-level orbit determination of geosynchronous satellites by an economical tracking system N87-12575
Theoretical and experimental studies in support of the geophysical fluid flow experiment N87-13045
Solving systems of nonlinear equations by tensor methods
[AD-A169827] N87-13216
COLUMBIA UNIV., NEW YORK.
Problems in integrated digital networks
[AD-A170442] N87-12744
Direct writing of microstructures for solid-state electronics
[AD-A170837] N87-12783
Theoretical high energy physics
[DE86-012669] N87-13259
COMMITTEE ON APPROPRIATIONS (U. S. HOUSE).
Department of Housing and Urban Development-independent agencies appropriations for 1987, part 7
[GPO-61-970] N87-13357
COMMITTEE ON SCIENCE AND TECHNOLOGY (U. S. HOUSE).
National Commission on Space report
[GPO-63-143] N87-12574
NASA's quality assurance program
[GPO-63-142] N87-12909
COMMITTEE ON SCIENCE AND TECHNOLOGY (U. S. SENATE).
Investigation of the Challenger accident, volume 2
[GPO-64-548] N87-12586
COMMONWEALTH SCIENTIFIC AND INDUSTRIAL RESEARCH ORGANIZATION, RYDE (AUSTRALIA).
Airborne spectroradiometry: The application of AIS data to detecting subtle mineral absorption features N87-12972
Preliminary geological investigation of AIS data at Mary Kathleen, Queensland, Australia N87-12979
COMMUNICATIONS RESEARCH CENTRE, OTTAWA (ONTARIO).
Optoelectronic broadband switching for communications and signal processing N87-13294
COMPUTER APPLIED TECHNIQUES LTD., MALAHIDE (IRELAND).
Study of satellite systems to monitor Earth's radiation budget
[CAP-420-071] N87-12994
COMPUTER TECHNOLOGY ASSOCIATES, INC., MCLEAN, VA.
Human performance aspects of small screen displays: A literature review revealing the lack of specific research
[AD-A170660] N87-13172
CONNECTICUT UNIV., STORRS.
Semiconductor/insulator films for corrosion protection
[AD-A169119] N87-12652
Carrier-sense stack algorithms for multiple access communication channels
[AD-A169774] N87-12738
CONSIGLIO NAZIONALE DELLE RICERCHE, FLORENCE (ITALY).
Fiber optic device for temperature remote sensing N87-13280
A spherical waveguide multiplexer-demultiplexer N87-13285
CORNELL UNIV., ITHACA, N.Y.
On the interplay between chemical reactions and phase transitions for molecules adsorbed on solid surfaces
[AD-A169818] N87-12836
Mechanics of metal forming
[DE86-012414] N87-12673
Fragmentation dynamics of energetic materials
[AD-A168925] N87-12682
Kinetic and thermodynamic studies of pulsed laser irradiation
[DE86-012175] N87-12860
Using combined experiment/analysis to generate dynamic critical stress intensity data
[DE86-013578] N87-12945
Calculated versus experimental charge density distribution of Be metal
[AD-A168924] N87-13254
Search for far infrared radiation from optically and acoustically pumped defect modes
[AD-A169159] N87-13319
Spherical clusters of simple metals: Madelung energies and structure
[AD-A169560] N87-13323
CRUCIBLE MATERIALS CORP., PITTSBURGH, PA.
Temperature compensation in the 2:17 type magnet s
[AD-A169487] N87-13250

D

DAYTON UNIV., OHIO.
Research on mechanical properties for engine life prediction
[AD-A169570] N87-12563
Pulsed-laser, high speed photography of rocket propellant surface deflagration
[AD-A169308] N87-12703
Computational fluid dynamic studies of certain ducted bluff-body flowfields relevant to turbojet combustors. Volume 1: Time-dependent calculations with the k-epsilon turbulence model for an existing centerbody combustor
[AD-A171434] N87-12816
MAGNA (Materially And Geometrically Nonlinear Analysis). Addendum 1, parts 1-4
[AD-A169383] N87-12933
Optical processing
[AD-A169882] N87-13269
DEFENCE RESEARCH ESTABLISHMENT, OTTAWA. (ONTARIO).
SARSAT (Search and Rescue Satellite) operational data categorization and accuracy studies
[AD-A169748] N87-12599
DEFENCE RESEARCH ESTABLISHMENT VALCARTIER (QUEBEC).
Method of ray intensity calculation as applied to anomalous propagation
[AD-A169553] N87-12737
DELAWARE UNIV., NEWARK.
Stable, high-efficiency, CuInSe2-based polycrystalline thin-film tandem solar cells
[DE86-010705] N87-13003
DENVER UNIV., COLO.
Measurement of atmospheric emission spectra at high altitudes
[AD-A170143] N87-13035
The uncounted benefits: Federal efforts in domestic technology transfer
[NASA-CR-177044] N87-13358
DEPARTMENT OF ENERGY, WASHINGTON, D. C.
Very high efficacy electrodeless high intensity discharge lamps
[DE86-013760] N87-12803
DEPARTMENT OF THE AIR FORCE, WASHINGTON, D.C.
Length adjustable strut link with low aerodynamic drag
[AD-D012279] N87-12543
Thrust reverser-exhaust nozzle assembly for a gas turbine engine
[AD-D012390] N87-12561
Turbine air seal with full backside cooling
[AD-D012405] N87-12564
Process for carbon-carbon composite fabrication
[AD-D012413] N87-12621
Low temperature formation of mullite
[AD-D012404] N87-12687
Light socket removal tool
[AD-D012368] N87-12710
TDD antenna: Foil formed, substrate loaded laser welded assembly
[AD-D012411] N87-12712
Tracking servo compensator with rate aiding
[AD-D012388] N87-12735
Multi-element adaptive antenna array
[AD-D012410] N87-12740
The Department of Defense Very High Speed Integrated Circuit (VHSIC) Technology Availability Program plan for the Committees on Armed Services, United States Congress
[AD-A169250] N87-12763
Cryogenic wound rotor for lightweight, high voltage generators
[AD-D012370] N87-12768
Ni-Co alloy plaque for cathode of Ni-Cd battery
[AD-D012375] N87-12769
Unique mechanization to fault isolate failures of an electron tube Radio Frequency (RF) amplifier and its high voltage power supply
[AD-D012376] N87-12770
High frequency, high voltage MOSFET isolation amplifier
[AD-D012403] N87-12774
In-line determination of presence of liquid phase moisture in sealed IC packages
[AD-D012406] N87-12775
Interrupt control switch interface system
[AD-D012414] N87-12776
Metal thickness measurements using radiography
[AD-D012373] N87-12832
High resolution optical fiber print head
[AD-D012384] N87-12833
Super gripper variable vane arm
[AD-D012364] N87-12874
Sliding duct seal
[AD-D012369] N87-12875
Multi use gripper for industrial robot
[AD-D012371] N87-12876
Shock absorbing device with integral pressure relief valve
[AD-D012379] N87-12877
Over-center toggle latch
[AD-D012393] N87-12878
Multiple rate shock isolator damping valve
[AD-D012394] N87-12879
Self-locking outer air seal with full backside cooling
[AD-D012406] N87-12880
Improved vane platform sealing and retention means
[AD-D012407] N87-12881
Rapid acting electro-pneumatic anti-G suit control valve
[AD-D012377] N87-13170
Improved anti-G suit
[AD-D012378] N87-13171
Multichannel phase noise measurement system
[AD-D012372] N87-13253
Method of fabricating high efficiency binary planar optical elements
[AD-D012374] N87-13256
Three dimensional optical receiver having programmable gain sensor stages
[AD-D012389] N87-13257
Method and apparatus for rapid optical phasing
[AD-D012412] N87-13270
Quartz growth on X-seeds
[AD-D012269] N87-13315
Rapid synthesis of indium phosphide
[AD-D012362] N87-13322
DEPARTMENT OF THE ARMY, WASHINGTON, D. C.
Temperature and frequency compensated array beam steering unit
[AD-D012365] N87-12767
Cylindrical laser welder
[AD-D012398] N87-12850
Doppler effect laser velocity measuring system
[AD-D012401] N87-12854
Parametric linear variation of a leakage free permanent magnet field source
[AD-D012359] N87-13249
Beam steering mirror construction
[AD-D012399] N87-13268
DEPARTMENT OF THE NAVY, WASHINGTON, D. C.
Rusty bolt intermodulation interference reducer
[AD-D012417] N87-12691
Adhesive repair patch
[AD-D012422] N87-12692
Twin aperture phased array lens antenna
[AD-D012415] N87-12745
Zinc/air cell cathode
[AD-D012425] N87-12780
Fiber-optic magnetic gradiometer with variable magnetic biasing fields
[AD-D012423] N87-12836
Resonant photon pumping mechanisms for a plasma X-ray laser
[AD-D012416] N87-12857

DEUTSCHE FORSCHUNGS- UND VERSUCHSANSTALT FUER LUFT- UND RAUMFAHRT, BRUNSWICK (WEST GERMANY).
The eye-mark investigation as an anthropotechnical method to study man machine systems N87-13160
DEUTSCHE GESELLSCHAFT FUER LUFT- UND RAUMFAHRT, BONN (WEST GERMANY).
Proceedings of a Symposium on the Evaluation of Man-Machine Systems: Methods and Problems [DGLR-86-04] N87-13146
The measurement of the psychological workload during task-related activities, including car driving, by competing time interval estimation N87-13153
DISTRICT OF COLUMBIA UNIV., WASHINGTON, D. C.
Feasibility of investigating Smith-Purcell free-electron laser configurations by electron energy loss studies [AD-A169059] N87-12647
DORNIER-WERKE G.M.B.H., FRIEDRICHSHAFEN (WEST GERMANY).
A method for the optimum design of the man machine interface N87-13159
DORTMUND UNIV. (WEST GERMANY).
Inquiry techniques for the evaluation of man machine systems N87-13162
DOUGLAS AIRCRAFT CO., INC., LONG BEACH, CALIF.
Guidance law simulation studies for complex approaches using the Microwave Landing System (MLS) [NASA-CR-178182] N87-12552
DREXEL UNIV., PHILADELPHIA, PA.
A fundamental study of P/M processed elevated temperature aluminum alloys [AD-A170897] N87-12657
Convective surface layers: Influence of the boundary layer depth N87-13041
LAMPS software and mesoscale prediction studies N87-13076

E

ECOLE POLYTECHNIQUE, MONTREAL (QUEBEC).
Dynamic analysis of anisotropic conical shells [EPM/RT-86-36] N87-12916
Non-linear analysis of cylindrical shells [EPM/RT-86-37] N87-12917
Analysis of anisotropic thin conical shells [EPM/RT-86-38] N87-12918
Dynamic analysis of a Timoshenko beam using a finite element approach [EPM/RT-86-34] N87-12919
Free vibration of axisymmetric and beam-like cylindrical shells, partially filled with liquid [EPM/RT-86-35] N87-12920
EDGERTON, GERMESHAUSEN AND GRIER, INC., IDAHO FALLS, IDAHO.
Concurrent ultrasonic weld evaluation system [DE86-013772] N87-12908
Characterization of the gamma radiation in space and in the atmosphere [DE86-013445] N87-13397
EIDGENOESSISCHE TECHNISCHE HOCHSCHULE, ZURICH (SWITZERLAND).
Electron-electron interaction effects in quasi-one-dimensional conducting polymers and related systems [DE86-012434] N87-12697
ENERGY RESEARCH CORP., DANBURY, CONN.
Aircraft battery state of charge and charge control system [AD-A169411] N87-12766
ENVIRONMENTAL RESEARCH INST. OF MICHIGAN, ANN ARBOR.
Nonlinear interactions in the microwave sensing of oceanic internal waves [AD-A169776] N87-13120
ESDU INTERNATIONAL LTD., LONDON (ENGLAND).
Introduction to aerodynamics derivatives, equations of motion and stability [ESDU-86021] N87-12536
Propeller/body interaction for thrust and drag [ESDU-86017] N87-12537
Simplified forms of performance equations. Addendum A: Effect on aeroplane level speed of small changes in thrust, drag, weight, power [ESDU-86004-ADD-A] N87-12556
Vapour pressures and critical points of liquids. Part 2C: Alkadienes and alkynes [ESDU-86001-PT-2C] N87-12624
Vapour pressures and critical points of liquids. Part 3A: C6 to C10 alkylbenzenes [ESDU-86012-PT-3A] N87-12625
Fluid transients in pipes. Estimation of maximum pressures and forces in steam lines [ESDU-86015] N87-12605
Frictional and retarding forces on aircraft tyres. Part 4: Estimation of effects of yaw [ESDU-86016-PT-4] N87-12666
Guide to the use of data items on the fatigue strength of welded joints in steels [ESDU-86013] N87-12914
Characteristics of atmospheric turbulence near the ground. Part 3: Variations in space and time for strong winds (neutral atmosphere) [ESDU-86010-PT-3] N87-13042
Computer-based estimation procedure for coaxial jet noise. Including far-field subsonic jet mixing noise database for stationary, coplanar conical nozzles [ESDU-86019] N87-13251
ESSEX CORP., ORLANDO, FLA.
Simulator design features for helicopter landing on small ships. 1: A performance study [AD-A169514] N87-12572
Simulator design and instructional features for carrier landing: A field transfer study [AD-A169962] N87-12573
Eye movements as an index of mental workload [AD-A169941] N87-13143
EXECUTIVE OFFICE OF THE PRESIDENT, WASHINGTON, D. C.
Earth sciences research in the Civil Space Program [PB86-232014] N87-12995

F

FACHHOCHSCHULE, HAMBURG (WEST GERMANY).
Development of a research method to determine the quality of task mastering by navigators in ship guidance N87-13154
FAIRCHILD REPUBLIC CO., FARMINGDALE, N.Y.
Assessment of damage tolerance requirements and analyses: A user's manual for crack growth and crack initiation analysis: DAMGRO [AD-A171209] N87-12939
FARRAN TECHNOLOGY LTD., BALLINCOLLIG (IRELAND).
Millimeter wave components [FTL-116521] N87-12605
FEDERAL AVIATION ADMINISTRATION, ATLANTIC CITY, N.J.
The siting, installation and operational suitability of the Automated Weather Observing System (AWOS) at heliports [DOT/FAA/PM-86/30] N87-13099
FEDERAL AVIATION ADMINISTRATION, WASHINGTON, D.C.
The Flight Service Station Training Program: 1981-1985 [AD-A171485] N87-13145
FLORIDA STATE UNIV., TALLAHASSEE.
Asymptotic theory for sieve estimators in semimartingale regression models [AD-A169207] N87-13230
A reversal argument for storage models defined on semi-Markov processes [AD-A169262] N87-13232
FONDAZIONE UGO BORDONI, ROME (ITALY).
Nonlinear ellipse rotation in a low-birefringence optical fiber N87-13282
FORSCHUNGSINSTITUT FUER ANTHROPOTECHNIK, WACHTBERG (WEST GERMANY).
Evaluation of man machine systems: Introduction and overview N87-13147
System-ergonomic workload analysis for highly automated process control tasks N87-13152
FUDAN UNIV., SHANGHAI (CHINA).
Use of Wannier function in the calculations of band structure of covalent crystals [DE86-702668] N87-13344

G

GALILEO ELECTRO-OPTICS CORP., STURBRIDGE, MASS.
Feasibility of making coherent fiber-optic arrays from fused silica [AD-A170673] N87-13271
GENERAL ELECTRIC CO., SCHENECTADY, N. Y.
Advanced optical smoke meters for jet engine exhaust measurement [NASA-CR-179459] N87-12829
GEOLOGICAL SURVEY, DENVER, COLO.
Use of digital Munsell color space to assist interpretation of imaging spectrometer data: Geologic examples from the northern Grapevine Mountains, California and Nevada N87-12980
GEOLOGICAL SURVEY, LAKEWOOD, COLO.
Atmospheric-water absorption features near 2.2 micrometers and their importance in high spectral resolution remote sensing N87-12973
GEOLOGICAL SURVEY, RESTON, VA.
Near-infrared detection of ammonium minerals at Ivanhoe Hot Springs, Nevada N87-12981
Geobotanical studies at Pilot Mountain, North Carolina using the airborne imaging spectrometer N87-12984
GEORGE WASHINGTON UNIV., WASHINGTON, D.C.
The continuous projective sumt method for convex programming [AD-A169547] N87-13185
GEORGIA INST. OF TECH., ATLANTA.
An implicit enumeration procedure for the general linear complementarity problem [AD-A170397] N87-13189
Inequalities for probability contents of convex sets via geometric average [AD-A169936] N87-13219
Heredity of stationary and reversible stochastic processes [AD-A169926] N87-13234
Extreme values of birth and death processes and queues [AD-A169932] N87-13235
Model studies of solar spectral irradiance at the bottom and top of a cloudy atmosphere N87-13365
GEOSCIENCE, LTD., SOLANA BEACH, CALIF.
Thermophysical properties measurements of gallium arsenide and cadmium telluride [AD-A169901] N87-13326
GLASGOW UNIV. (SCOTLAND).
Performance of integrated optical frequency shifters pigtailed to high birefringence fibres using ion-milled grooves N87-13269
GTE LABS., INC., WALTHAM, MASS.
Electron-electron interaction effects in quasi-one-dimensional conducting polymers and related systems [DE86-012434] N87-12697

H

HARRY DIAMOND LABS., ADELPHI, MD.
Transmission through ferrite samples at submillimeter frequencies [AD-A169178] N87-12731
Electric and magnetic field coupling through a braided-shield cable: Transfer admittance and transfer impedance [AD-A171490] N87-12748
HARVARD MEDICAL SCHOOL, BOSTON, MASS.
Pharmacological resetting of the circadian sleep-wake cycle [AD-A170804] N87-13137
HONEYWELL, INC., BLOOMINGTON, MINN.
Synthesis of conjugated polymers with alternating aromatic and quinonoid sequences via elimination on precursors [AD-A171331] N87-12693
HOUSTON UNIV., TEX.
Development of a numerical procedure to treat wires attached to arbitrarily shaped conducting bodies [AD-A169384] N87-12764
HUGHES RESEARCH LABS., MALIBU, CALIF.
Flight model discharge system [AD-A169423] N87-12571
Lightwave technology in future radar equipment designs N87-13304
Kinetics and mechanisms on the molecular beam etching of semiconductors [AD-A171360] N87-13331
HYDROGEN CONSULTANTS, INC., DENVER, COLO.
Phase change thermal energy storage methods for combat vehicles, phase 1 [AD-A170492] N87-12713

I

IIT RESEARCH INST., ROME, N.Y.
Catalog of Resources for Education in Ada (Trade name) and Software Engineering (CREASE), version 4.0 [AD-A169692] N87-13186
ILLINOIS INST. OF TECH., CHICAGO.
The control of polymer mechanical behavior by surface modification [AD-A169252] N87-12686
ILLINOIS STATE WATER SURVEY, CHAMPAIGN.
Variation objective analyses for cyclone studies N87-13050

ILLINOIS UNIV., CHAMPAIGN.
The event related brain potential as an index of information processing and cognitive activity. A program of basic research. Supplement A: Neuromagnetic studies
[AD-A169978] N87-13144
ILLINOIS UNIV., CHICAGO.
Statistical models and methods for cluster analysis and image segmentation
[AD-A169145] N87-13229
ILLINOIS UNIV., URBANA.
Transport and relaxation processes in supercritical fluids
[DE86-007847] N87-12838
Effect of hydrogen on the mechanical properties and fracture behavior of high purity aluminum
[AD-A171214] N87-12858
Dielectric antennas for millimeter-wave applications
[AD-A169685] N87-12739
A new method of synthetic aperture radar image reconstruction using modified convolution back-projection algorithm
[AD-A170652] N87-12747
Totally self-checking circuits and testable CMOS circuits
[AD-A169756] N87-12773
Optical pumping of high power lasers with an array of plasma pinches
[AD-A169960] N87-12856
Effect of convection on weld pool shape and microstructure
[AD-A170488] N87-12883
INSTITUTE FOR DEFENSE ANALYSES, ALEXANDRIA, VA.
Proceedings of the IDA Workshop on Formal Specification and Verification of Ada (trade name) (1st) held in Alexandria, Virginia on 18-20 March 1985
[AD-A171507] N87-13192
Duel between an ASAT (anti-satellite) with multiple kill vehicles and a space-based weapons platform with kinetic energy weapons
[AD-A169946] N87-13245
INSTITUTE OF AVIATION MEDICINE, MANCHING (WEST GERMANY).
Anthropometric handicaps in the construction of a helicopter cockpit N87-13148
INSTITUTO DE PESQUISAS ESPACIAIS, SAO JOSE DOS CAMPOS (BRAZIL).
Attitude control of an artificial satellite by extending the linear quadratic regulator theory
[INPE-3969-PRE/977] N87-12588
A procedure for attitude determination of artificial satellites utilizing techniques of static and dynamic optimal estimation
[INPE-3966-PRE/981] N87-12589
Procedure for one axis satellites attitude control with magnetic actuation
[INPE-3895-PRE/937] N87-12590
Relative motion of the Sun on an artificial satellite
[INPE-3965-NTE/260] N87-12591
Brief analysis of normal attitude accuracies of satellites with wheels or gas jets
[INPE-3993-NTE/262] N87-12594
Density and electrostatic potential distribution around a cylindrical satellite
[INPE-3953-NTE/258] N87-12595
Comparison of methods for the calculation of thermal contact resistance of the first Brazilian satellite
[INPE-3964-TDL/217] N87-12596
Fault tolerance mechanisms for a network communication multiprocessor
[INPE-3958-PRE/876] N87-12720
Measurement of time-dependent electric current with Rogowski coil
[INPE-3975-RPE/508] N87-12754
Constructive and operational characteristics of a synchronous induction motor
[INPE-3976-RPE/517] N87-12755
Stabilization of voltage-controlled oscillators through resonant cavities
[INPE-3941-RPE/512] N87-12757
Modulation Transfer Function (MTF) of the geometrical image resolution of the thermal infrared band
[INPE-3964-TDL/231] N87-12809
A variational principle for the plasma centrifuge
[INPE-3969-PRE/992] N87-12827
Influence of a strong laser field on the stopping power for charged test particles in fusion plasmas
[INPE-3977-PRE/988] N87-12843
Geologic remote sensing at INPE: An overview
[INPE-3975-PRE/987] N87-12959
Evaluation of remote sensing techniques to the detection of changes in a fluvial system due to human influence: The example of Canas River Basin (Sao Paulo State, Brazil)
[INPE-3970-PRE/983] N87-12960
Crop yield modeling for climate impact studies. Part 1: Reasoning and results
[INPE-3967-PRE/982-PT-1] N87-12961
Energy receipt partitioning over the Amazon forest
[INPE-3980-PRE/990] N87-12962
Report of the Ad-Hoc Commission on remote sensing
[INPE-3981-NTE/259] N87-12963
A partition of sensible and latent heat fluxes above the terra firma area in the Amazon Forest (gradient method)
[INPE-3972-PRE/986] N87-12964
Photographic sensors: Basic concepts
[INPE-3990-MD/031] N87-12966
In retrospect: The impact of research production in the area of remote sensing
[INPE-3987-NTE/261] N87-12968
Report on the activities of the irrigated crop survey in Sao Paulo State from remote sensing products, phase 2
[INPE-3950-RPE/513] N87-12969
Generation of images with recorded auxiliary data for the LANDSAT Thematic Mapper (TM) imagery
[INPE-3982-TDL/234] N87-12990
A partition of sensible and latent heat fluxes above the terra firma area in the Amazon forest
[INPE-3949-PRE/970] N87-13008
Stratospheric balloon experiments
[INPE-3995-RPE/519] N87-13020
On the Walker circulation of 1983-84
[INPE-3952-PRE/971] N87-13118
Utilization of impact dot matrix printers
[INPE-3991-RPE/518] N87-13173
A procedure for automatic treatment of dynamic systems state observation bias errors
[INPE-3908-PRE/918] N87-13177
Tool to develop real time simulation systems
[INPE-3979-TDL/233] N87-13179
A generalized projection method for the solution of algebraic linear systems
[INPE-3874-PRE/930] N87-13205
Performance analysis of some numerical algorithms in the resolution of ODEs artificial satellite problems
[INPE-3996-PRE/995] N87-13206
Application of a network associative scene analysis model
[INPE-3945-PRE/967] N87-13244
Solar flux and geomagnetic activity prediction
[INPE-3884-PRE/934] N87-13377
Repetition rates of fast pulses in MM-waves/X-ray solar bursts
[INPE-3974-PRE/985] N87-13378
A survey of hard-X-rays at balloon altitudes of the Earth's atmosphere
[INPE-3954-PRE/972] N87-13386
INTERNATIONAL BUSINESS MACHINES CORP., SAN JOSE, CALIF.
Electrode/electrolyte interphase study using polarization modulated FT-IR reflection absorption spectroscopy
[AD-A169081] N87-12631
Carbon monoxide adsorption on a platinum electrode studied by polarization modulated FT-IR reflection-absorption spectroscopy. 2: CO adsorbed at a potential in the hydrogen region and its oxidation in acids
[AD-A169082] N87-12632
INTERNATIONAL CENTRE FOR THEORETICAL PHYSICS, TRIESTE (ITALY).
Finite mean-free-paths and the electrical resistivity of liquid simple metals and binary alloys
[DE86-702662] N87-12678
Propagation of electromagnetic waves in superlattices
[DE86-702660] N87-12753
Periodic heat transfer through an inhomogeneous medium
[DE86-702988] N87-12825
Possibility of using dc conductivity for investigating phase transition in amorphous semiconductors
[DE86-702646] N87-13340
Surface green function matching for a three-dimensional non-local continuum
[DE86-702647] N87-13341
Surface and adsorption-like states within the nearly free electron approximation
[DE86-702651] N87-13342
Theory of Fractional Quantum Hall Effect
[DE86-702652] N87-13343
Use of Wannier function in the calculations of band structure of covalent crystals
[DE86-702668] N87-13344
Tunneling effect in superconductors with magnetic impurities
[DE86-702723] N87-13345
Flux spiral instability in a transport current carrying type 2 superconductor
[DE86-702724] N87-13346
Induced quantum torsion
[DE86-702616] N87-13348
Superconformal tensor calculus and matter couplings in six dimensions
[DE86-702617] N87-13349
Canonical quantization of gravity
[DE86-702615] N87-13372
Astro-particle-physics
[DE86-702948] N87-13373
Equilibrium configuration of coronal loops
[DE86-702711] N87-13384
INTERNATIONAL COUNCIL OF SCIENTIFIC UNIONS, URBANA, ILL.
Middle Atmosphere Program. Handbook for MAP, volume 21
[NASA-CR-179693] N87-13015
Atmospheric Tides Middle Atmosphere Program (ATMAP): Report of the workshop, Kyoto, Japan, December 5-8, 1984 N87-13016
Minutes of MAP/WINE experimenters meeting, Prague, Czechoslovakia, August 13, 1985 N87-13018
IOWA STATE UNIV. OF SCIENCE AND TECHNOLOGY, AMES.
Heat transfer characteristics of simulated microelectronic chips under normal and enhanced conditions
[PB86-224425] N87-12804
Analysis of laminar flow heat transfer in uniform temperature circular tubes with tape inserts
[PB86-224763] N87-12826
IOWA UNIV., IOWA CITY.
The current-voltage relationship in auroral current sheets
[AD-A169074] N87-13028
ISTITUTO NAZIONALE DI FISICA NUCLEARE, TRIESTE (ITALY).
Induced quantum torsion
[DE86-702616] N87-13348

J

JAI ASSOCIATES, MOUNTAIN VIEW, CALIF.
Numerical simulation of tip vortices of wings in subsonic and transonic flows
[AD-A169116] N87-12544
JET PROPULSION LAB., CALIFORN[illegible]IST. OF TECH., PASADENA.
Tone calibration technique: A digital signaling scheme for mobile applications
[NASA-CR-179915] N87-12719
ERS-1 SAR data processing
[NASA-CR-179913] N87-12965
Proceedings of the Second Airborne Imaging Spectrometer Data Analysis Workshop
[NASA-CR-179924] N87-12968
Radiometric calibration of the airborne imaging spectrometer N87-12969
Analysis of AIS radiometry with emphasis on determination of atmospheric properties and surface reflectance N87-12971
Patterns of vegetation in the Owens Valley, California N87-12966
Observation model and parameter partials for the JPL VLBI parameter estimation software MASTERFIT-1986
[NASA-CR-179915] N87-13178
JOHNS HOPKINS UNIV., BALTIMORE, MD.
Phase equilibrium predictions for polar and hydrogen bonding mixtures
[DE86-011812] N87-12642
Middle atmosphere modeling
[NASA-CR-179934] N87-13023
Quantum chemical investigations of the mechanism of cationic polymerization and theoretical prediction of crystal densities and decomposition pathways of energetic molecules
[AD-A169605] N87-13324
JOHNS HOPKINS UNIV., SILVER SPRING, MD.
The 1984 IR and D (Independent Research and Development) advanced packaging study
[AD-A169368] N87-12785
JOHNSON CONTROLS, INC., MILWAUKEE, WIS.
Performance of advanced lead acid batteries for electric vehicles
[DE85-011476] N87-12901
JOINT PUBLICATIONS RESEARCH SERVICE, ARLINGTON, VA.
Japan report: Science and Technology
[JPRS-JST-86-023] N87-12715
Possible military applications of stratospheric airship discussed N87-12716
Status of laser enrichment technology updated N87-12717
USSR report: Earth sciences
[JPRS-UES-86-007] N87-12946
Meteorological effects of geotectonic phenomena hypothesized N87-12947

Third International Symposium on Tropical Meteorology N87-12948
Available potential energy in upper layer of world ocean N87-12949
Desertification: Global ecological problem N87-12950
Evaluating nonlinear effects in propagation of acoustic pulse in atmospheric surface layer in inversions N87-12951
Experimental research on turbulence in upper-level tropospheric clouds N87-12952
Solar control of geophysical phenomena N87-12953
Effect of pulsating auroras on frequency-time characteristics of radio signals reflected from auroral ionosphere N87-12954
Phase fluctuations of ionosphere radio signals N87-12955
Transverse resonances of Earth-ionosphere wave guide in auroral region N87-12956
Regular noise background in VLF-radiation and world thunderstorm centers N87-12957
Spatial radio wave attenuation during vertical sounding of ionosphere N87-12958

K

KERNFORSCHUNGSANLAGE, JUELICH (WEST GERMANY).
Radiation-induced segregation to grain boundaries in a Ni-Si alloy
[DE86-010027] N87-12664
KRAFTWERK UNION A.G. REAKTORTECHNIK, ERLANGEN (WEST GERMANY).
Ergonomic requirements for the design of control rooms. Evaluation method N87-13158

L

LAWRENCE LIVERMORE NATIONAL LAB., CALIF.
Application of pattern recognition to metal ion chemical ionization mass spectra
[AD-A169061] N87-12830
Axial detonator for simultaneous ignition of multiple HE points
[DE86-011878] N87-12643
Design of strong, ductile, HSLA and dual phase steels
[DE88-011313] N87-12665
New electromagnetic effects associated with cavity-backed apertures
[DE86-008768] N87-12750
Fabrication of gate array interconnect structures using direct-write deposition processes
[DE86-010785] N87-12787
Electronic Engineering Department Thrust Area report, FY 1985
[DE86-013172] N87-12797
Slitless, intensified readout, gated spectrometer: Wavelength and efficiency calibration, time response characterization
[DE86-012349] N87-12839
Buffered explosions in steel pressure vessels
[DE86-008763] N87-12898
Shower and high-pressure oil temperature control
[DE86-009398] N87-12899
Atmospheric illumination and shadows, revision 1
[DE86-010971] N87-13039
Parameterized numerical fit to total column ozone changes calculated by the LLNL 1-D model of the troposphere and stratosphere
[DE86-011008] N87-13040
Using 3-dimensional graphics to visualize multivariate scientific data
[DE86-010788] N87-13195
LEHIGH UNIV., BETHLEHEM, PA.
Electrokinetic properties of polymer colloids
[NASA-CR-178938] N87-12681
LITTON SYSTEMS (CANADA) LTD., REXDALE, (ONTARIO).
Closed loop fiber optic gyro N87-13277
LOS ALAMOS NATIONAL LAB., N. MEX.
Simple defense conservative model for mass requirements of hypervelocity projectile impact shields for reentry vehicles
[DE86-012407] N87-12603
Effect of strain and strain rate on residual microstructures in copper
[DE86-007361] N87-12659
Effect of residual strain on twinning in shock-loaded copper
[DE86-007362] N87-12660
Initiation of pitting corrosion in martensitic stainless steels
[DE86-007627] N87-12661
Mechanics of metal forming
[DE86-012414] N87-12673
Physical characteristics of diblock polyacetylene copolymers: Processability-conductivity correlation
[DE86-011218] N87-12695
Effect of chain rigidity on conductivity of conjugated polymers
[DE86-011283] N87-12696
Electron-electron interaction effects in quasi-one-dimensional conducting polymers and related systems
[DE86-012434] N87-12697
Anvil detonator: A 300EC-stable, hot-wire-ignited, nonprimary-explosive device
[DE86-013635] N87-12707
Analysis of magnetic refrigeration systems with staged regenerators based on an idealized magnetic material entropy model: 1
[DE86-013636] N87-12714
Circuit considerations for repetitive railguns
[DE86-012389] N87-12752
Efficient, monochromatic, high-power microwave generator
[DE86-012385] N87-12792
Modeling of high-explosive driven plasma compression opening switches
[DE86-012421] N87-12795
Transformers for explosive pulsed power coupling to various loads
[DE86-012425] N87-12796
Free-Lagrangian hydrodynamics using massless tracer points
[DE86-012406] N87-12822
Apparatus for downward transport of heat
[DE86-013700] N87-12824
CO sub 2 laser sustained CW discharge atomic beam source
[DE86-012383] N87-12863
Theory and simulation of high-brightness electron beam production from laser-irradiated photocathodes in the presence of dc and RF electric fields
[DE86-012384] N87-12864
Mossebauer-Borrmann superradiance
[DE86-012373] N87-12866
Liquid metal thermoacoustic engine
[DE86-011264] N87-12902
Integrated heat pipe-thermal storage design for a solar receiver
[DE86-011235] N87-12999
Compact reactor/ORC power source
[DE86-011252] N87-13260
Space nuclear safety program
[DE86-012767] N87-13261
Neutronic design studies for an unattended, low power reactor
[DE86-011228] N87-13262
Two-dimensional dynamics of the plasma Wakefield accelerator
[DE86-012382] N87-13312
Los Alamos Science, number 13, spring 1986
[DE86-012864] N87-13371
Magnetic field re-arrangement after prominence eruption
[DE86-012393] N87-13382
Large-scale electric fields resulting from magnetic reconnection in the corona
[DE86-012391] N87-13383
LOUISIANA STATE UNIV., BATON ROUGE.
Solar flares and magnetospheric particles: Investigations based upon the ONR-60 experiments and ONR-604 experiments
[AD-A170620] N87-13381
LOUVAIN UNIV. (BELGIUM).
Superconformal tensor calculus and matter couplings in six dimensions
[DE86-702617] N87-13349
LUDWIG-MAXIMILIANS-UNIVERSITAET, MUNICH (WEST GERMANY).
Investigation of vibrations of the spinal column of healthy subjects N87-13155

M

M/A-COM, INC., VIENNA, VA.
MILSTAR modeling survey
[AD-A169789] N87-12600
MARTIN MARIETTA AEROSPACE, DENVER, COLO.
Metallurgical characterization of the interfaces and the damping mechanisms in metal matrix composites
[AD-A169186] N87-12616
Evaluation of automated decisionmaking methodologies and development of an integrated robotic system simulation. Appendix B: ROBSIM programmer's guide
[NASA-CR-178052] N87-13203
MARTIN MARIETTA AEROSPACE, NEW ORLEANS, LA.
General purpose aft cargo carrier study, volume 1
[NASA-CR-178905] N87-12587
MARTIN MARIETTA ENERGY SYSTEMS, INC., OAK RIDGE, TENN.
Data tagging in the Energy Data Base
[DE86-010821] N87-13355
MARYLAND UNIV., BALTIMORE.
The h-p version of the finite element method with quasiuniform meshes
[AD-A170144] N87-13222
MARYLAND UNIV., COLLEGE PARK.
A new and efficient formulation for finite element analysis of thin shell structures undergoing small and large deflection N87-12913
Development of a sensitive superconducting gravity gradiometer for geological and navigational applications
[NASA-CR-4011] N87-13021
Regularity of the solution of elliptic problems with piecewise analytic data. Part 1: Boundary value problems for linear elliptic equation of second order
[AD-A169771] N87-13212
Asymptotically exact a-posteriori error estimator for biquadratic elements
[AD-A169798] N87-13213
An expert-system-like feedback approach in the hp-version of the finite element method
[AD-A169855] N87-13214
Note on a characterization of exponential distributions
[AD-A169896] N87-13215
Zero-crossings analysis
[AD-A169937] N87-13218
MASSACHUSETTS INST. OF TECH., CAMBRIDGE.
Reconstruction of undersampled periodic signals
[AD-A168897] N87-12722
Basic and applied research in the field of electronics and communications
[AD-A169029] N87-12727
Knowledge-based pitch detection
[AD-A169069] N87-12730
Compaction with automatic jog introduction
[AD-A169679] N87-12772
Development of an inexpensive, high resolution positron multiwire proportional counter
[DE86-011576] N87-12841
Moessbauer-Borrmann superradiance
[DE86-012373] N87-12866
Development of ultrasonic modelling techniques for the study of seismic wave scattering due to crustal inhomogeneities
[AD-A170017] N87-13034
Introduction to the theory of nested transactions
[AD-A171428] N87-13191
Long time estimates for the heat kernel associated with a uniformly subelliptic symmetric second order operator
[AD-A169949] N87-13220
Upper bounds for symmetric Markov transition functions
[AD-A170010] N87-13221
Feedback system design with an uncertain plant
[NASA-CR-176887] N87-13243
Tara vacuum system
[DE86-011873] N87-13311
MASSACHUSETTS UNIV., AMHERST.
Yield and performance enhancement through redundancy in VLSI and WSI multi-processor systems
[AD-A169930] N87-13174
MCDONNELL-DOUGLAS ASTRONAUTICS CO., HOUSTON, TEX.
Advanced EVA system design requirements study
[NASA-CR-171942] N87-13167
MCDONNELL-DOUGLAS ASTRONAUTICS CO., HUNTINGTON BEACH, CALIF.
Comparison of ring laser and fiber-optic gyro technology N87-13276
Optical quadrature demodulator for coherent detection and sensor applications N87-13287
MESSERSCHMITT-BOELKOW-BLOHM G.M.B.H., MUNICH (WEST GERMANY).
Single-mode-fibers for fiberoptic-guided missiles: A comparison with graded-index multimode fibers N87-13303
MESSERSCHMITT-BOELKOW-BLOHM G.M.B.H., OTTOBRUNN (WEST GERMANY).
Application of the task taxonomy method to the simulation of human service reliability in the manual control of aircraft
[MBB/LKE-301/S/PUB/216] N87-13151
MICHIGAN UNIV., ANN ARBOR.
Millimeter-wave heterojunction two-terminal devices
[AD-A168985] N87-12760
Analysis of head and neck dynamic response of the US adult military population
[AD-A169563] N87-13129
High-resolution analysis of eye movements
[AD-A170779] N87-13136

Observational study of ion-electron equilibration and of cloud evaporation in supernova remnants under the HEAO-2 guest investigator program
[NASA-CR-179922] N87-13365

MIDDLE EAST TECHNICAL UNIV., ANKARA (TURKEY).
Finite mean-free-paths and the electrical resistivity of liquid simple metals and binary alloys
[DE86-702662] N87-12678

MIDWEST RESEARCH INST., GOLDEN, COLO.
Solid-state electrochromic switchable window glazings
[DE86-004455] N87-12700
Laser sealed vacuum insulating window
[DE86-013678] N87-12701
Status and future of government-supported amorphous silicon research in the US
[DE86-010702] N87-12997
Solid State Photovoltaic Research Branch annual report, FY 1985
[DE86-010708] N87-13004

MINNESOTA UNIV., MINNEAPOLIS.
A study of energy conversion devices using photoactive organometallic electrocatalysts
[AD-A169095] N87-12996
Quantum 1/F noise in solid state double devices, in particular Hg(1-x)CdxTe diodes
[AD-A171438] N87-13332

MISSISSIPPI UNIV., UNIVERSITY.
Mobile intercept of storms N87-13064

MISSOURI UNIV., ROLLA.
Neutron diffraction studies of some rare earth-transition metal deuterides
[AD-A169995] N87-12648

MONSANTO CO., DAYTON, OHIO.
Determination of the coefficient of thermal expansion of JP-4 fuels
[AD-A171495] N87-12705

MSNW, INC., SAN MARCOS, CALIF.
Plasma joining of metal matrix composites
[AD-A169056] N87-12615

MUENSTER UNIV. (WEST GERMANY).
Evaluation of the bearing and knowledge requirements of man machine systems N87-13164

N

NATIONAL AERONAUTICAL ESTABLISHMENT, OTTAWA (ONTARIO).
Forced oscillation of a two-dimensional airfoil with nonlinear aerodynamic loads
[AD-A169350] N87-12546
Literature review on the design of composite mechanically fastened joints
[AD-A169112] N87-12872

NATIONAL AERONAUTICS AND SPACE ADMINISTRATION, WASHINGTON, D.C.
Aeronautical Engineering: A continuing bibliography with indexes
[NASA-SP-7037(205)] N87-12532
Upper stage selected for planetary missions
[NASA-NEWS-RELEASE-86-161] N87-12593
Modeling the fundamental characteristics and processes of the spacecraft functioning
[NASA-TM-87999] N87-12598
Aerospace Medicine and Biology: A continuing bibliography with indexes
[NASA-SP-7011(290)] N87-13125
The upper atmosphere of Venus: A tentative explanation of its rotation
[NASA-TM-88505] N87-13375
Relief and geology of the north polar region of the planet Venus
[NASA-TM-88498] N87-13376

NATIONAL AERONAUTICS AND SPACE ADMINISTRATION. AMES RESEARCH CENTER, MOFFETT FIELD, CALIF.
An experimental investigation of free-tip response to a jet
[NASA-TM-88250] N87-12539
NASA rotor systems research aircraft: Fixed-wing configuration flight-test results
[NASA-TM-86789] N87-12557
The handling qualities and flight characteristics of the Grumman design 698 simulated twin-engine tilt Nacelle V/STOL aircraft
[NASA-TM-86785] N87-12558
Supplementary calibration test of the tip-aerodynamics-and acoustics-test pressure transducers
[NASA-TM-88312] N87-12830
Development of buried wire gages for measurement of wall shear stress in Blastane experiments
[NASA-TM-89212] N87-12831
The evaluation of a number of prototypes for the free-tip rotor constant-moment controller
[NASA-TM-86664] N87-12869
A computational method to model radar return range in a polygonally based, computer-generated-imagery simulation
[NASA-TM-88324] N87-12967
Destriping AIS data using Fourier filtering techniques N87-12974
Analysis of AIS data of the Bonanza Creek Experimental Forest, Alaska N87-12982
Trace element-induced stress in freshwater wetland vegetation: Preliminary results N87-12985
Crew factors in flight operations. Part 3: The operational significance of exposure to short-haul air transport operations
[NASA-TM-88322] N87-13122
Crew communication as a factor in aviation accidents
[NASA-TM-88254] N87-13141
Infrared reflection nebulae in Orion molecular cloud 2
[NASA-TM-88259] N87-13363

NATIONAL AERONAUTICS AND SPACE ADMINISTRATION. GODDARD SPACE FLIGHT CENTER, GREENBELT, MD.
Radiation flux tables for ICRCCM using the GLA GCM radiation codes
[NASA-TM-89270] N87-13098
High energy neutrino absorption and its effects on stars in close X-ray binaries
[NASA-TM-89269] N87-13366
On the two states of CYG X-1 and related sources
[NASA-TM-89265] N87-13367
MAX '91: An advanced payload for the exploration of high energy processes on the active sun
[NASA-TM-89271] N87-13379
Neutron and antineutron production in accretion onto compact objects
[NASA-TM-89264] N87-13395

NATIONAL AERONAUTICS AND SPACE ADMINISTRATION. LYNDON B. JOHNSON SPACE CENTER, HOUSTON, TEX.
Lunar laboratory
[NASA-TM-89209] N87-12580
An approach to design knowledge capture for the space station
[NASA-TM-89272] N87-12597

NATIONAL AERONAUTICS AND SPACE ADMINISTRATION. LANGLEY RESEARCH CENTER, HAMPTON, VA.
Mach 6 experimental and theoretical stability and performance of a finned cylindrical body at angles of attack up to 65 deg
[NASA-TM-89050] N87-12538
Effect of port corner geometry on the internal performance of a rotating-vane-type thrust reverser
[NASA-TP-2624] N87-12541
Evaluation of a nonlinear parameter extraction mathematical model including the term C(subm(sub delta e squared))
[NASA-TM-87731] N87-12566
Investigation of the effects of short chain processing additives on polymers
[NASA-TM-89023] N87-12614
Investigation of the effects of cobalt ions on epoxy properties
[NASA-TP-2639] N87-12680
Time-dependent solution for axisymmetric flow over a blunt body with ideal gas, CF4, or equilibrium air chemistry
[NASA-TM-87675] N87-12806
Factors influencing elastic stresses in double cantilever beam specimens
[NASA-TM-89033] N87-12922
Coordinated study of the behavior of the middle atmosphere in winter: Monthly mean comparisons of satellite and radiosonde data and derived quantities N87-13019
Description of data on the Nimbus 7 LIMS map archive tape: Ozone and nitric acid
[NASA-TP-2625] N87-13022
Quality assessment and control of finite element solutions
[NASA-TM-89208] N87-13227
Theory for computing the field scattered from a smooth inflected surface
[NASA-TP-2632] N87-13264

NATIONAL AERONAUTICS AND SPACE ADMINISTRATION. LEWIS RESEARCH CENTER, CLEVELAND, OHIO.
A heater made from graphite composite material for potential deicing application
[NASA-TM-88888] N87-12559
Advanced solar dynamic space power systems perspectives, requirements and technology needs
[NASA-TM-88884] N87-12606
Effects of graphitization on the environmental stability of brominated pitch-based fibers
[NASA-TM-88899] N87-12679
Plasma assisted surface coating/modification processes: An emerging technology
[NASA-TM-88885] N87-12708
NDE reliability and process control for structural ceramics
[NASA-TM-88870] N87-12910
A constitutive law for finite element contact problems with unclassical friction
[NASA-TM-88838] N87-12924
Cruise noise of counterrotation propeller at angle of attack in wind tunnel
[NASA-TM-88869] N87-13252
Progress of Stirling cycle analysis and loss mechanism characterization
[NASA-TM-88891] N87-13359

NATIONAL AERONAUTICS AND SPACE ADMINISTRATION. MARSHALL SPACE FLIGHT CENTER, HUNTSVILLE, ALA.
Solar array flight dynamic experiment
[NASA-TP-2598] N87-12581
Development testing of large volume water sprays for warm fog dispersal
[NASA-TP-2607] N87-12585
Viewport concept for space station modules
[NASA-TM-86559] N87-12592
Shifts in shuttle SRM performance because of ammonium perchlorate crystal shape on missions 51-I/J and 61-A/B
[NASA-TM-86561] N87-12607
Space flight operations communications phraseology and techniques
[NASA-TM-86562] N87-12721
Development of low-temperature transistor modules to improve the MSFC mid-infrared array
[NASA-TM-86566] N87-12756
The Multispectral Atmospheric Mapping Sensor (MAMS): Instrument description, calibration and data quality
[NASA-TM-86565] N87-12828
Effects of variables upon pyrotechnically induced shock response spectra
[NASA-TP-2603] N87-12921
NASA/MSFC FY-85 Atmospheric Processes Research Review
[NASA-CP-2402] N87-13043
Theoretical and experimental studies of baroclinic processes N87-13044
Theoretical and experimental design studies for the Atmospheric General Circulation Experiment N87-13046
Estimation of precipitation from GOES IR imagery during FGGE: Application to diagnostic studies N87-13048
Observational and theoretical studies of the evolving structure of baroclinic waves: Attractor dynamics of global weather systems N87-13054
Deep convection in mesoscale convective systems N87-13055
Storm severity detection (RF) N87-13057
Lightning mapper and the future N87-13059
Space shuttle/mesoscale lightning experiment N87-13060
Optical characteristics of lightning and thunderstorm currents N87-13061
Optical characteristics of lightning N87-13062
Airborne atmospheric electricity experiments N87-13063
Analysis of Doppler lidar data N87-13067
Airborne Doppler lidar activities N87-13068
Response of the mesoscale atmosphere to diabatic heating N87-13069
Severe storm detection with passive 37 GHz observations N87-13072
Automated mesoscale winds derived from GOES multispectral imagery N87-13073
Satellite passive microwave rain measurement techniques for land and ocean N87-13074
Remote sensing of severe convective storms N87-13075
Numerical simulation of convective response to mesoscale forcing N87-13081
Improved satellite retrievals and mesoscale moisture variability N87-13087
Studies of humid continental haze during SPACE N87-13088
Interactive information processing for NASA's mesoscale analysis and space sensor program N87-13093
Doppler wind profile experiment N87-13094
Multispectral atmospheric mapping sensor of mesoscale water vapor features N87-13095
First meeting of the Working Group on the Shuttle Microwave Precipitation Radiometer (SMPR) N87-13096
The ecology of microorganisms in a small closed system: Potential benefits and problems for space station
[NASA-TM-86563] N87-13166

NATIONAL AERONAUTICS AND SPACE ADMINISTRATION. PASADENA OFFICE, CALIF.
FET charge sensor and voltage probe
[NASA-CASE-NPO-16045-1] N87-13313
NATIONAL AERONAUTICS AND SPACE ADMINISTRATION. WALLOPS FLIGHT CENTER, WALLOPS ISLAND, VA.
Pulse Code Modulation (PCM) data storage and analysis using a microcomputer
[NASA-TP-2629] N87-12718
NATIONAL BUREAU OF STANDARDS, BOULDER, COLO.
Optical fiber sensors for the measurement of pulsed electric currents N87-13281
NATIONAL BUREAU OF STANDARDS, WASHINGTON, D.C.
High accuracy standards and reference methodology for carbon dioxide in air
[DE86-012643] N87-13011
NATIONAL MARITIME RESEARCH CENTER, KINGS POINT, N. Y.
Application of heart rate measurements to maritime research simulator
[AD-A169668] N87-13132
NATIONAL OCEANIC AND ATMOSPHERIC ADMINISTRATION, BOULDER, COLO.
Calibration and accuracy of the NOAA/ERL gust probe system and intercomparison with other systems
[PB86-221736] N87-13116
Effects of reduced spatial resolution on the NEXRAD storm sequence algorithms
[PB86-221728] N87-13117
NATIONAL OCEANIC AND ATMOSPHERIC ADMINISTRATION, NORMAN, OKLA.
Severe storm electricity N87-13056
NATIONAL OCEANIC AND ATMOSPHERIC ADMINISTRATION, SILVER SPRING, MD.
Meteorological summary of WATOX (western Atlantic Ocean experiment) 1985 research intensive, February-April
[PB86-225792] N87-13114
NATIONAL TRANSPORTATION SAFETY BOARD, WASHINGTON, D. C.
Aircraft accident/incident summary reports: Erie, Pennsylvania, October 14, 1984; Albuquerque, New Mexico, February 11, 1985
[PB86-910407] N87-12549
Aircraft accident report: Bar Harbor Airlines Flight 1808, Beech BE-99, N300WP, Auburn-Lewiston Municipal Airport, Auburn, Maine, August 25, 1985
[PB86-910408] N87-12550
NATIONAL WEATHER SERVICE, KANSAS CITY, MO.
Some proposals for modifying the Probability of Precipitation Program of the National Weather Service
[PB86-226836] N87-13115
NAVAL ACADEMY, ANNAPOLIS, MD.
Ionic conductivity in solid, crosslinked dimethylsiloxane-ethylene oxide copolymer networks containing sodium
[AD-A169038] N87-12883
NAVAL AIR SYSTEMS COMMAND, WASHINGTON, D. C.
US Navy climatic study of the Caribbean Sea and Gulf of Mexico. Volume 2: East Caribbean Sea
[AD-A171487] N87-13112
NAVAL BIODYNAMICS LAB., NEW ORLEANS, LA.
Guidelines for safe human experimental exposure to impact acceleration
[AD-A169347] N87-13169
NAVAL PERSONNEL RESEARCH AND DEVELOPMENT CENTER, SAN DIEGO, CALIF.
Quality management: An annotated bibliography
[AD-A169616] N87-12912
NAVAL POSTGRADUATE SCHOOL, MONTEREY, CALIF.
Some tactical algorithms for spherical geometry
[AD-A170615] N87-12555
Maximization of the capacity of the most survivable connections in a network
[AD-A169065] N87-12728
Two-dimensional beamforming using a frequency domain complex Least Mean-Squares (LMS) adaptive filter
[AD-A171396] N87-12785
The analysis of a transistor cap as a heat dissipator
[AD-A171398] N87-12786
In-line and transverse forces on smooth and rough cylinders in oscillatory flow at high Reynolds numbers
[AD-A169562] N87-12815
A software implementation of an interactive graphics system for three dimensional modeling and layout
[AD-A169264] N87-13183
Regression models of quarterly overhead costs for six government aerospace contractors
[AD-A169185] N87-13350
Federal information systems management: Problems, solutions and more problems
[AD-A171368] N87-13353
An examination of technology transfer as a tool for management
[AD-A169184] N87-13360
Classification of N-type carbon stars
[AD-A171399] N87-13369
NAVAL RESEARCH LAB., WASHINGTON, D. C.
The space station millimeter facility
[AD-A169983] N87-12604
Simulation of CIFF (Centralized IFF) remote control displays
[AD-A170387] N87-12742
Input impedance of an infinite linear scanned array of flat rectangular strips inside a dielectric loaded parallel plate waveguide
[AD-A171275] N87-12784
High gain free electron laser oscillators
[AD-A169002] N87-12846
Comparison of Rayleigh-Taylor growth with 1.0 m and 0.25 m lasers
[DE86-012217] N87-12862
Influence of shear modulus on the behavior of acoustically transparent materials
[AD-A169289] N87-12931
Progress in optical fiber sensors N87-13274
Preparation and properties of infrared transmitting heavy metal fluoride glass optical fibers N87-13296
NEVADA UNIV., BOULDER CITY.
Dual temperature thermal storage with complex compounds
[DE86-011511] N87-13000
NEVADA UNIV., RENO.
Identification of hydrothermal alteration assemblages using airborne imaging spectrometer data N87-12977
Detection of hydrothermal alteration at Virginia City, Nevada using Airborne Imaging Spectrometry (AIS) N87-12978
Meteorological tower data, Yucca Ridge (YR) site, January-June 1983. Nevada Nuclear Waste Storage Investigations Project
[DE86-012732] N87-13113
NEW HAMPSHIRE UNIV., DURHAM.
The gamma-ray spectrometer experiment on the solar maximum mission satellite
[NASA-CR-177877] N87-13394
NEW MEXICO INST. OF MINING AND TECHNOLOGY, SOCORRO.
NOSL experiment support
[NASA-CR-178947] N87-13140
NEW MEXICO STATE UNIV., LAS CRUCES.
Experimental investigation of thermochemical transport for solar applications using sulfur trioxide
[DE86-011762] N87-13005
NEW MEXICO UNIV., ALBUQUERQUE.
Application of the AIPA (Approximate Iterative Preprocessing Algorithm) to F-106 data
[AD-A169084] N87-12569
NEW TECHNOLOGY, INC., HUNTSVILLE, ALA.
Atmospheric Modeling And Sensor Simulation (AMASS) study N87-13090
NEW YORK UNIV., NEW YORK.
Perceptual factors in workload: A neuromagnetic study
[AD-A169934] N87-13142
NORTH CAROLINA STATE UNIV., RALEIGH.
Theoretical study on the correlation between wideband electromagnetic spectra and geological structures
[AD-A168971] N87-13026
NORTH CAROLINA UNIV., CHAPEL HILL.
New results on low temperature thermal oxidation of silicon
[AD-A169603] N87-12634
A VLSI-based high-performance raster image system
[AD-A169068] N87-12761
Intrinsic SiO2 film stress measurements on thermally oxidized Si
[AD-A169602] N87-12935
Semigroups and Poisson-approximation
[AD-A170944] N87-13224
Extremal processes, record times and strong approximation
[AD-A169972] N87-13237
NORTH CAROLINA UNIV., RALEIGH.
Micrometeorological transitions in the morning boundary layer over rolling terrain
[AD-A169237] N87-13103

O

OAK RIDGE NATIONAL LAB., TENN.
Importance of interfacial phenomena in separation science and technology
[DE86-011063] N87-12637
APFIM study of antiphase and grain boundaries in Ni Al
[DE86-006494] N87-12662
APFIM studies of phase transformations
[DE86-006533] N87-12663
Bainite in chromium-molybdenum steels
[DE86-011781] N87-12666
Use of analytical electron microscopy in evaluating ferrite stability in austenitic stainless steel welds
[DE86-006537] N87-12667
Site occupations in Li sub 2 ordered alloys by axial electron channeling microanalysis
[DE86-009421] N87-12669
Densification of graphites by irradiation
[DE86-010026] N87-12686
Metals and Ceramics Division Materials Sciences Program
[DE86-013512] N87-12689
Welding procedure specification. Manual gas tungsten arc and semiautomatic gas metal arc welding of chromium-nickel steel. Supplement 1: Records of procedure qualification tests
[DE86-012521] N87-12886
Machine gas metal arc welding of carbon steel. Welding procedure specification. Supplement 1: Records of procedure qualification tests
[DE86-012530] N87-12887
Welding procedure specification. Semiautomatic gas metal arc welding of carbon steels. Supplement 1: Records of procedure qualification tests
[DE86-012531] N87-12888
Welding procedure specification. Manual gas tungsten arc and semiautomatic gas metal arc welding of carbon steel. Supplement 1: Records of procedure qualification tests
[DE86-012532] N87-12889
Gas tungsten arc and shielded metal arc welding of carbon steel. Welding procedure specification. Supplement 1: Records of procedure qualification tests
[DE86-012533] N87-12890
Welding procedure specification. Supplement 1: Records of procedure qualification tests. Shielded metal arc welding of carbon steel
[DE86-012535] N87-12891
Welding procedure specification. Gas tungsten arc welding of chromium-nickel steel to chromium-molybdenum steel. Supplement 1: Records of procedure qualification tests
[DE86-012536] N87-12892
Gas tungsten arc welding of aluminum alloys 6XXX. Welding procedure specification. Supplement 1: Records of procedure qualification tests
[DE86-012548] N87-12893
Gas tungsten arc welding of carbon steel to nickel-chromium-iron. Welding procedure specification. Supplement 1: Records of procedure qualification tests
[DE86-012549] N87-12894
Gas tungsten arc welding of chromium-nickel steel to nickel-molybdenum-chromium-iron. Welding procedure specification. Supplement 1: Records of procedure qualification tests
[DE86-012550] N87-12895
Welding procedure specification: Gas tungsten arc welding of nickel to nickel-chromium-iron. Supplement 1: Records of procedure qualification tests
[DE86-012557] N87-12896
Gas tungsten arc welding of aluminum alloys 3004, 5052 and 5x54 to 6xxx. Welding procedure specification. Supplement 1: Records of procedure qualification tests
[DE86-012561] N87-12897
Localized ion milling of metallic and ceramic TEM specimens
[DE86-009538] N87-12900
Linear harmonic analysis of free-piston Stirling engines
[DE86-012451] N87-12903
Influence of experimental scatter on the analysis and extrapolation of stress-rupture data
[DE86-009510] N87-12940
Data requirements to model creep in 9Cr-1Mo-V steel
[DE86-011754] N87-12944
Development of regenerable energy storage for space multimegawatt applications
[DE86-011070] N87-12998
Stefan-type problem with void formation and its explicit solution
[DE86-013521] N87-13007
Evaluating ecosystem response to toxicant stress: a state space approach
[DE86-011777] N87-13009
Direct effects of atmospheric CO2 enrichment on plants and ecosystems: A bibliography with abstracts
[DE86-013525] N87-13012
Matrix factorization on a hypercube multiprocessor
[DE86-011775] N87-13193

Survey of the characteristics of very high level languages
[DE86-012240] N87-13196
Solving scientific problems on hypercube parallel computers
[DE86-012622] N87-13199
Quantitative assessment of the effect of partial pivoting in sparse ordinary differential equation solvers
[DE86-012592] N87-13226
Photoemission from oblate silver spheroids with polarized vacuum UV excitation
[DE86-006896] N87-13256
Recrystallization behavior of ion beam modified Alpha-Al sub 2 O sub 3
[DE86-009353] N87-13335

OAK RIDGE Y-12 PLANT, TENN.
Diamond-machined aluminum alloy 5083 surfaces: Controlled exposure evaluation
[DE86-012572] N87-12674
Cleaning of aluminum alloy 5083
[DE86-012573] N87-12675
Heat measurements in inertia welding of aluminum to steel
[DE86-012463] N87-12685

OFFICE OF NAVAL RESEARCH, LONDON (ENGLAND).
Welding research in Scandinavia: An assessment
[AD-A169036] N87-12671
Welding science and technology in Europe: A survey and assessment
[AD-A169279] N87-12673

OHIO STATE UNIV., COLUMBUS.
An analysis of the acoustic characteristics of ABSS (accoustic backscatter system) and its deployments
[AD-A170487] N87-13037

OKLAHOMA STATE UNIV., STILLWATER.
Instrumentation research and support services
[AD-A169278] N87-13029

OLIS ENGINEERING, SEDALIA, COLO.
Concept study - vehicle waste disposal system
[AD-A169045] N87-13168

OPHIR CORP., LAKEWOOD, COLO.
A sensitivity study of a one-dimensional time-dependent warm cumulus cloud model
[AD-A170141] N87-13109

OPTICAL SOCIETY OF AMERICA, WASHINGTON, D. C.
Proceedings of the Topical Meeting on the Microphysics of Surfaces, Beams and Adsorbates held in Santa Fe, New Mexico on 4-6 February 1985
[AD-A170797] N87-13329

OREGON GRADUATE CENTER FOR STUDY AND RESEARCH, BEAVERTON.
Digest: Proceedings of the International Conference on Optical and Millimeter Wave Propagation and Scattering in the Atmosphere
[AD-A170393] N87-12743

OREGON STATE UNIV., CORVALLIS.
AIS spectra of desert shrub canopies N87-12987

ORLANDO TECHNOLOGY, INC., SHALIMAR, FLA.
TSAR (Theater Simulation of Airbase Resources) database dictionary F-4E
[AD-A169575] N87-13352

OSSERVATORIO ASTROFISICO DI ARCETRI, FLORENCE (ITALY).
Magnetic field re-arrangement after prominence eruption
[DE86-012393] N87-13382
Large-scale electric fields resulting from magnetic reconnection in the corona
[DE86-012391] N87-13383

P

PACIFIC NORTHWEST LABS., RICHLAND, WASH.
Application of hydrogen embrittlement models to the crack growth behavior of fusion reactor materials
[DE86-011614] N87-12671
Crack-tip chemistry and fracture mechanics-based model of the crack growth rate/stress intensity relationship for Ni + P
[DE86-011106] N87-12676
Generalization of one-dimensional solute transport: A stochastic-convective flow conceptualization
[DE86-011117] N87-12820
Remote sensing to detect ecological impacts associated with acid deposition
[DE86-011649] N87-12992
Physical interaction of 1-Hz to 100 kHz electric and magnetic fields with living organisms
[DE86-012323] N87-13139
Technology transfer at Pacific Northwest Laboratory
[DE86-012333] N87-13361

PARAIBA UNIV., JOAO PESSOA (BRAZIL).
Supergravity
[DE86-701481] N87-13370

PENNSYLVANIA STATE UNIV., UNIVERSITY PARK.
New ultra low permittivity composites for use in ceramic packaging of GaAs integrated circuits
[AD-A168877] N87-12758
The use of satellite data in understanding and predicting convective and large-scale dynamical processes N87-13049
Continuum radiation from active galactic nuclei: A statistical study
[NASA-CR-179925] N87-13368

PHYSICAL SCIENCES, INC., ANDOVER, MASS.
Ionization phenomena about the space shuttle
[AD-A170542] N87-13310

PITTSBURGH UNIV., PA.
Microchemical analysis of polycrystalline Ni3Al and other ordered alloys using the field-ion microscope atom probe
[DE86-013157] N87-12677
Validity of Edgeworth expansions of minimum contrast estimators for Gaussian ARMA processes
[AD-A169931] N87-13217
On reduction of dimensionality under multivariate regression and canonical correlation models
[AD-A170025] N87-13238
A multivariate extension of Hoeffding's lemma
[AD-A170170] N87-13239
Pattern recognition based on scale invariant discriminant functions
[AD-A170600] N87-13241

PLESSEY CO. LTD., ROMSEY (ENGLAND).
Progress with multiplexed sensor arrays based on reflection at spliced joints between sensors N87-13278
Magnetic and pressure sensors using the compensated polarimetric sensor configuration N87-13279
A study of methods of phase noise reduction of semiconductor lasers for sensor applications N87-13286

PRATT AND WHITNEY AIRCRAFT, EAST HARTFORD, CONN.
On 3-D inelastic analysis methods for hot section components (base program)
[NASA-CR-175060] N87-12923

PRINCETON UNIV., N. J.
An application of a LISP based expert system for failure diagnosis of the CH-47 flight control hydraulic system
[AD-A168970] N87-12567
A prototype maintenance expert system for the CH-47 flight control hydraulic system
[AD-A169019] N87-12568
Advanced electric propulsion MPD (magnetoplasmadynamic)
[AD-A169792] N87-12610
A test on the reliability and performance of the verbex series 4000 voice recognizer
[AD-A169066] N87-12729
Design and analysis of experiments and more realistic techniques for data analysis
[AD-A169921] N87-13228

PUERTO RICO UNIV., RIO PIEDRAS.
Fluids in contact with a hard surface: University of the bridge functions for the density profile
[AD-A168945] N87-13308

PURDUE UNIV., WEST LAFAYETTE, IND.
Investigation of a new concept in semiconductor microwave oscillators
[AD-A170772] N87-12781
Investigation of a new concept in semiconductor microwave oscillators
[AD-A170831] N87-12782
Utilization of satellite cloud information to diagnose the energy state and transformations in extratropical cyclones N87-13051
Dynamics and energetics of the South Pacific Convergence Zone during FGGE SOP-1 N87-13052

Q

QUEENSLAND UNIV., ST. LUCIA (AUSTRALIA).
Further shock tunnel studies of scramjet phenomena
[NASA-CR-179937] N87-12542

R

RANGE COMMANDERS COUNCIL, WHITE SANDS MISSILE RANGE, N. MEX.
Directory of range data conversion and processing system, revision
[AD-A169629] N87-12578
Joint operating procedure for interrange scheduling
[AD-A169636] N87-12579

RENNES UNIV. (FRANCE).
Fluoride glasses for infrared waveguides N87-13299

RENSSELAER POLYTECHNIC INST., TROY, N.Y.
Fundamental research on tribology
[AD-A169974] N87-12682
Compact reactor studies
[DE86-013247] N87-13363

RESEARCH AND DATA SYSTEMS, INC., LANHAM, MD.
Conversion of the NOLAPS (Navy Operational Local Atmospheric Prediction System) model to the HP9845
[AD-A169538] N87-13106

RHODE ISLAND UNIV., KINGSTON.
The Gulf Stream dynamics experiment. Inverted echo sounder data report for the June 1984 to May 1985 deployment period
[AD-A170758] N87-13121

RICE UNIV., HOUSTON, TEX.
Moessbauer-Borrmann superradiance
[DE86-012373] N87-12866
Iterative methods for large linear and nonlinear least squares problems
[AD-A169028] N87-13209

ROCHESTER UNIV., N. Y.
Heterogeneous catalysis with lasers
[AD-A169601] N87-12851

ROCKWELL INTERNATIONAL CORP., CANOGA PARK, CALIF.
Preparation of energetic compounds
[AD-A170022] N87-12704

ROCKWELL INTERNATIONAL CORP., COLUMBUS, OHIO.
Fabrication and testing of lightweight hydraulic system simulator hardware
[AD-A169884] N87-12711

ROCKWELL INTERNATIONAL CORP., THOUSAND OAKS, CALIF.
Growth of ferro-electric tungsten bronze epitaxial thin films for electro-optic device applications
[AD-A170763] N87-13328

ROCKWELL INTERNATIONAL SCIENCE CENTER, THOUSAND OAKS, CALIF.
Iodine monofluoride energy transfer studies
[AD-A169781] N87-12852

ROME AIR DEVELOPMENT CENTER, GRIFFISS AFB, N.Y.
Phased arrays 1985 symposium: Proceedings
[AD-A169316] N87-12732
Surface correlation relationships in rough surface scattering
[AD-A169327] N87-12733
Foreground effects on troposcatter digital communication systems
[AD-A169380] N87-12734

ROME UNIV. (ITALY).
Nonlinear ellipse rotation in a low-birefringence optical fiber N87-13282
Bistability in nonlinear waveguides N87-13291

ROYAL AIRCRAFT ESTABLISHMENT, FARNBOROUGH (ENGLAND).
An approximate method of estimating the aerodynamic interference between two parallel bodies in a supersonic flow (axial force)
[BR-100271] N87-12540
The calculation of separated flows of low-viscosity liquids using the Batchelor Model
[BR-100272] N87-12810

ROYAL SIGNALS AND RADAR ESTABLISHMENT, MALVERN (ENGLAND).
A brief review of adaptive null steering techniques
[AD-A169548] N87-12736

RUTGERS - THE STATE UNIV., NEW BRUNSWICK, N. J.
Relationship of in-cylinder gaseous and particulate concentration to radiative heat transfer in direct injection-type diesel combustion
[AD-A168979] N87-12628

S

SAINT LOUIS UNIV., MO.
Lg wave excitation and propagation in presence of one-, two- and three-dimensional heterogeneities
[AD-A169004] N87-12724
Lg wave excitation and propagation in presence of one-, two-, and three-dimensional heterogeneities
[AD-A169325] N87-13030
A summary of research on mesoscale energetics of severe storm environments N87-13082
Statistical analysis and use of VAS radiance data N87-13086

SANDIA NATIONAL LABS., ALBUQUERQUE, N. MEX.
Potential applications of artificially structured materials for X-ray microanalysis
[DE86-010459] N87-12612
Electron spectroscopy in fundamental catalytic studies
[DE86-008781] N87-12939
Electron microprobe analysis: The upper limit of submicron spectroscopy
[DE86-009540] N87-12640

Real-time experimental measurements of isotopic exchange between gaseous hydrogen and palladium hydride powder
[DE86-012610] N87-12644
Double-resonance techniques for high-resolution Raman-spectroscopy
[DE86-009640] N87-12645
Comparative thermal conductivity measurements at Sandia National Laboratories
[DE86-012926] N87-12647
Microstructural study of high energy density dissimilar metal welds
[DE86-009284] N87-12668
Characterization of the atomic emission in Inconel 718 alloy metal vapor arcs
[DE86-012178] N87-12672
Raman spectroscopy of carboranes and polycarboranesiloxanes
[DE86-009030] N87-12694
Lithium Ambient-Temperature Battery Reliability Program, May 1983-April 1985
[DE86-012247] N87-12789
Nanosecond spark gap switching measurements
[DE86-012279] N87-12790
SAW transduction in electrostrictive substrates
[DE86-011651] N87-12794
Very low bandwidth, unattended imager for surveillance applications
[DE86-013570] N87-12799
Li corrosion resistant glasses for headers in ambient temperature Li batteries
[DE86-013754] N87-12802
Application of flux-corrected transport (FCT) to high Rayleigh number natural convection in a porous medium
[DE86-004603] N87-12818
Detonation cellular structure and image proces
[DE86-006467] N87-12819
Study of numerical solution methods for two-phase flows
[DE86-012265] N87-12821
Development of a large-aperture PLZT shutter with enhanced operational/environmental capabilities
[DE86-011643] N87-12836
Time Projection Compton Spectrometer (TPCS)
[DE86-012950] N87-12840
Double-ended tuning fork quartz accelerometer
[DE86-012277] N87-12842
Kinetic and thermodynamic studies of pulsed laser irradiation
[DE86-012175] N87-12860
Reactor-pumped laser experiments in the Sandia SPR-3 Facility
[DE86-012163] N87-12861
Effects of inertia weld parameters and contamination on weld flash shape and on joint strength: An improved study
[DE86-013074] N87-12904
Shock-induced solid state chemistry: Theoretical background
[DE86-012741] N87-12941
Using combined experiment/analysis to generate dynamic critical stress intensity data
[DE86-013578] N87-12945
Proceedings of the Solar Thermal Technology Conference
[DE86-011703] N87-13002
Experimental investigation of thermochemical transport for solar applications using sulfur trioxide
[DE86-011762] N87-13005
Photovoltaic Concentrator Technology Project, Fourteenth Project Integration Meeting, June 10-11, 1986
[DE86-012051] N87-13006
Meteorological tower data, Yucca Ridge (YR) site, January-June 1983. Nevada Nuclear Waste Storage Investigations Project
[DE86-012732] N87-13113
Reliability study of retention and memory gate integrity in a 1K MNOS RAM
[DE86-010483] N87-13175
SPRINT 3: Serial-Parallel Remote Interface System development report
[DE86-010590] N87-13176
Interpretive model for a concurrency method
[DE86-012743] N87-13197
Electron diffraction analysis of the pentagonal arrangement of grains found in CVD pure Ni films
[DE86-009023] N87-13336
Structural features at the Si-SiO2 interface
[DE86-012947] N87-13339
Electronic forms. How close to value-added processing
[DE86-010484] N87-13354

SCIENCE AND TECHNOLOGY CORP., HAMPTON, VA.
SAGE 2 satellite data set validation
[NASA-CR-178189] N87-13024

SCIENCE APPLICATIONS INTERNATIONAL CORP., SAN DIEGO, CALIF.
Sodium-sulfur battery systems development
[DE86-011424] N87-12788

SHAPE TECHNICAL CENTER, THE HAGUE (NETHERLANDS).
Fiber optics: A survivable and cost-effective transmission medium for terrestrial networks N87-13302

SIEMENS A.G., KARLSRUHE (WEST GERMANY).
Empirical determination among superintendents of the acceptable user surface in digitally automated heating-ventilation air conditioning systems N87-13165

SIEMENS A.G., MUNICH (WEST GERMANY).
Effects of optical feedback on the performance of high data rate single-mode fiber systems N87-13288
Acoustooptic spectrum analyzer using a planar Bragg-cell N87-13295

SIMPSON WEATHER ASSOCIATES, INC., CHARLOTTESVILLE, VA.
Multiscale modeling to evaluate proposed space-based Doppler lidar sampling strategies N87-13047

SKF INDUSTRIES, INC., KING OF PRUSSIA, PA.
Mechanical interactions of rough surfaces
[DE86-010886] N87-12901

SLOAN-KETTERING INST. FOR CANCER RESEARCH, NEW YORK.
Biological and clinical dosimetry, July 1, 1964 to December 31, 1964
[DE86-006947] N87-13138

SMITHSONIAN ASTROPHYSICAL OBSERVATORY, CAMBRIDGE, MASS.
Space infrared telescope facility wide field and diffraction limited array camera (IRAC)
[NASA-CR-177041] N87-13362

SONOMA TECHNOLOGY, INC., SANTA ROSA, CALIF.
Southern California Air Quality Study (SCAQS) suggested program plan
[PB86-223427] N87-13013

SOUTH CAROLINA UNIV., COLUMBIA.
Smooth nonparametric quantile estimation under censoring: Simulations and bootstrap methods
[AD-A169935] N87-13236

SOUTH DAKOTA SCHOOL OF MINES AND TECHNOLOGY, RAPID CITY.
Mesoscale-cloud scale simulation of convective response N87-13077
A detailed analysis of the influence of eddy exchange processes upon the development of radiation fog
[AD-A169233] N87-13102

SOUTHERN UNIV., BATON ROUGE, LA.
Transition metal. 2: Complexes of dithiacycloph anes
[AD-A169107] N87-12651
Experimental thin film deposition and surface analysis techniques
[DE86-011222] N87-13336

SOUTHWEST RESEARCH INST., SAN ANTONIO, TEX.
Micromechanisms of crack growth and fracture toughness in metal matrix composites
[AD-A169839] N87-12620
Study of high temperature failure mechanisms in ceramics
[AD-A170001] N87-12689
Magnetospheric plasma studies using data from the dynamics explorer high and low altitude plasma instruments
[AD-A169010] N87-13027

SPARTA, INC., MCLEAN, VA.
Department of Defense gateway architecture and functional requirements
[AD-A169086] N87-13200

SRI INTERNATIONAL CORP., MENLO PARK, CALIF.
Coordinated radar and satellite studies of ionospheric currents in the auroral zone and polar cap
[AD-A169466] N87-13031

STANDARD ELEKTRIK LORENZ A.G., STUTTGART (WEST GERMANY).
A measure of usability N87-13163

STANDARD TELECOMMUNICATION LABS. LTD., HARLOW (ENGLAND).
Glass fibres for transmission in the 8-12 micrometers waveband N87-13297

STANFORD TELECOMMUNICATIONS, INC., SUNNYVALE, CALIF.
Comparison of various techniques for calibration of AIS data N87-12970
Comparison of the 1984 and 1985 AIS data over the Singatse Range (Yerington), Nevada N87-12976

STANFORD UNIV., CALIF.
An analysis of blade vortex interaction aerodynamics and acoustics N87-12547
High voltage characteristics of the electrodynamic tether and the generation of power and propulsion
[NASA-CR-178949] N87-12609
Signal estimation, scattering theory and interpolation problems in one and two dimensions
[AD-A168969] N87-12759
SAW transduction in electrostrictive substrates
[DE86-011651] N87-12794
Transition and mixing in axisymmetric jets and vortex rings
[NASA-CR-3893] N87-12906
Adaptive grid techniques for elliptic fluid-flow problems
[AD-A169471] N87-12814
User's guide for NPSOL (version 4.0): A Fortran package for nonlinear programming
[AD-A169115] N87-13180
An implicit enumeration algorithm with binary-valued constraints
[AD-A169256] N87-13182
Single-phase method for quadratic programming
[DE86-012156] N87-13194
The optimal linear combination of control variates in the presence of bias
[AD-A169111] N87-13210
Algorithm for positive definite least square estimation of parameters
[DE86-012159] N87-13225
Recursive moment formulas for semi-Markov processes
[AD-A169253] N87-13231
A unified approach to constructing nonparametric rank tests
[AD-A169815] N87-13233
Maintaining LU factors of a general sparse matrix
[AD-A169255] N87-13248
Single crystal fibers N87-13296
Rapid fluctuations in solar flares
[NASA-CR-179894] N87-13387
Observations on the Stanford 4800 KG gravity wave detector with a cosmic ray monitor N87-13399

STATE UNIV. OF NEW YORK, ALBANY.
Nuclear reaction analysis of hydrogen in metals
[AD-A169032] N87-12649
Remote observations of severe storms N87-13065

STATE UNIV. OF NEW YORK, BUFFALO.
Mechanical transduction: Unification
[AD-A171191] N87-13123

STATE UNIV. OF NEW YORK, STONY BROOK.
Characterization and dynamical studies of polymers in dipolar (aprotic) liquids
[AD-A169243] N87-12685
Energetics of dislocation relaxation associated with cleavage in Cd-doped zinc crystals as probed by sychrotron topography
[DE86-002966] N87-13334

STRATHCLYDE UNIV., GLASGOW (SCOTLAND).
Fibre optic gyroscopes in inertial navigation N87-13275

SVERDRUP TECHNOLOGY, INC., ARNOLD AIR FORCE STATION, TENN.
Analysis and verification of the icing scaling equations. Volume 1: Revision
[AD-A167976] N87-12551
Effects of test cell recirculation on high-bypass turbofan engines during simulated altitude tests
[AD-A171418] N87-12565

SYRACUSE UNIV., N. Y.
Computer programs for electromagnetic scattering from a slotted TM cylindrical conductor by the pseudo-image method
[AD-A169016] N87-12725

T

TECHNION - ISRAEL INST. OF TECH., HAIFA.
Sleepability and wakeability following sleep deprivation
[AD-A169578] N87-13130

TECHNISCHE UNIV., BERLIN (WEST GERMANY).
Determination of the load and stress of a cockpit crew during aircraft piloting using task networks and the simulation language SAINT N87-13150

TECHNISCHE UNIV., BRUNSWICK (WEST GERMANY).
Basic conceptions for the evaluation of man machine systems N87-13161

TECHNISCHER UEBERWACHUNGS-VEREIN RHEINLAND, E.V., COLOGNE (WEST GERMANY).
Review of the methods applied in the Federal Republic of Germany to investigate human factors in nuclear power plant control N87-13156
Simulation of disturbances on the nuclear power plant simulator. The problem of the interpretation of operator actions and their cognitive backgrounds as a basis for design recommendations N87-13157

TERRA TEK, INC., SALT LAKE CITY, UTAH.
Fracture toughness of CIP-HIP beryllium at elevated temperatures
[AD-A169769] N87-12654

TEXAS A&M UNIV., COLLEGE STATION.
Stress effects on moisture transport in an epoxy resin and its composite
[AD-A169306] N87-12617

Coupled damage and moisture-transport in fiber-reinforced polymeric composites
[AD-A169379] N87-12619
Measurement and calculation of the Stokes or Mueller matrix for the scattering of electromagnetic radiation from irregular particles
[AD-A171502] N87-12749
Stress assisted diffusion in elastic and viscoelastic materials
[AD-A169296] N87-12932
Application of satellite data to tropic/subtropic moisture coupling N87-13053

TEXAS INSTRUMENTS, INC., DALLAS.
Incremental quench research
[AD-A169980] N87-13317

TEXAS TECHNOLOGICAL UNIV., LUBBOCK.
A numerical model for two-dimensional unsteady flow calculations with a surface panel method N87-12548
The application of boundary-element techniques for some soil-structure interaction problems
[AD-A169999] N87-12709
Coordinated research program in pulsed power physics
[AD-A169113] N87-12762

TEXAS UNIV., AUSTIN.
Viscous-inviscid interaction in transonic separated flow over solid and porous airfoils and cascades N87-12535
Optimal descending, hypersonic turn to heading
[DE86-010969] N87-12577
Advanced guidance algorithms for homing missiles with bearing-only measurements
[AD-A170633] N87-12583
Electrochemistry in near-critical and supercritical fluids. 3: Studies of Br(-), I(-) and hydroquinone in aqueous solutions
[AD-A169136] N87-12633
High performance parallel computing
[AD-A169981] N87-13186

THOMSON-CSF, ORSAY (FRANCE).
Progress in optical fiber gyroscopes using integrated optics N87-13283

TORONTO UNIV. (ONTARIO).
Finite-difference solutions for compressible laminar boundary-layer flows of a dusty gas over a semi-infinite flat plate
[UTIAS-311] N87-12807
Study in molecular lasers
[AD-A169933] N87-12855

TRW ELECTRONICS AND DEFENSE SECTOR, REDONDO BEACH, CALIF.
Application of nonlinear optics to free electron laser systems
[AD-A169950] N87-12845

TRW, INC., REDONDO BEACH, CALIF.
Performance of RF fiber optic links N87-13301

U

UNITED TECHNOLOGIES RESEARCH CENTER, EAST HARTFORD, CONN.
Optical diagnostics for diesel engine applications
[DE86-010747] N87-12641

UNIVERSITIES SPACE RESEARCH ASSOCIATION, HUNTSVILLE, ALA.
Mesoscale research activities with the LAMPS model N87-13078

UTAH UNIV., SALT LAKE CITY.
Experimental verification of soliton theory using a microwave crossed-field amplifier
[AD-A170011] N87-12778

V

VARIAN ASSOCIATES, SALT LAKE CITY, UTAH.
A 60 GHz gyrotron development program
[DE86-012466] N87-12791

VIBRATION AND ACOUSTICS, INC., HUNTSVILLE, ALA.
SSME main injector 4000 Hertz phenomenon
[NASA-CR-178934] N87-12606

VIRGINIA INST. OF MARINE SCIENCE, GLOUCESTER POINT.
Investigation of deviations from ideality in the two liquid phase region of systems of medium molecular weight hydrocarbon mixtures and water
[AD-A169752] N87-12635

VIRGINIA POLYTECHNIC INST. AND STATE UNIV., BLACKSBURG.
An interdisciplinary approach to predictive modeling of structural adhesive bonding. Characterization of Ti-6Al-4V oxides and the adhesive/oxide interphase
[AD-A170484] N87-12690
Analysis of the nonlinear stability of circular Couette flow
[AD-A169951] N87-12811
HOMPACK: A suite of codes for globally convergent homotopy algorithms
[DE86-011644] N87-13196

VIRGINIA UNIV., CHARLOTTESVILLE.
X-ray emission from supernova remnants N87-13398

W

WASHINGTON STATE UNIV., PULLMAN.
Optical spectroscopy of dynamically compressed liquids
[AD-A169013] N87-12629

WASHINGTON UNIV., SEATTLE.
Declarative descriptions for VLSI generators
[AD-A169952] N87-12777
A study of the mechanism of dynamic ductile fracture of two-phase materials
[AD-A169966] N87-12925
Plane-parallel and bow shock models of Herbig-Haro objects N87-13374

WASHINGTON UNIV., ST. LOUIS, MO.
Quantitative non-destructive evaluation of composite materials based on ultrasonic wave propagation
[NASA-CR-179831] N87-12613
Computation of the amplitude of stress singular terms for cracks and reentrant corners
[AD-A169798] N87-12936
Soil types and forest canopy structures in southern Missouri: A first look with AIS data N87-12983
The ultraheavy cosmic rays: Propagation and selective acceleration N87-13390

WEAPONS SYSTEMS RESEARCH LAB., SALISBURY (AUSTRALIA).
Methods for the syntheses of mono-, di-, tri- and tetranitro derivatives of diphenylamine
[WSRL-0436-TR] N87-12702

WESTINGHOUSE RESEARCH AND DEVELOPMENT CENTER, PITTSBURGH, PA.
Models and radiation of railgun plasma armatures with non-ideal plasma properties
[AD-A169349] N87-13258

WISCONSIN UNIV., MADISON.
Diesel cylinder gas-side heat flux to a ceramic surface
[AD-A169948] N87-12870
Studies of lightning data in conjunction with geostationary satellite data N87-13058
Mesoscale ageostrophic circulations associated with baroclinic jet streaks N87-13070
Cooperative VAS program with NASA Marshall Space Flight Center N87-13079
The assimilation of satellite soundings, winds and satellite products in a mesoscale analysis/forecast system N87-13080
Time composite sounding N87-13083
Detection of rotating thunderstorms using satellite imagery N87-13085
The meteorological interactive data display system N87-13091
A design study for a three-dimensional display computer terminal for meteorological information N87-13092
SOR (Successive Over-Relaxation) MGR (multigrid algorithm)(nu) experiments on the crystal multicomputer
[AD-A169929] N87-13187

X

XEROX CORP., PALO ALTO, CALIF.
SOAR user's manual
[AD-A169005] N87-13204

Y

YALE UNIV., NEW HAVEN, CONN.
Population inversions in laser-initiated vacuum arcs
[AD-A170811] N87-12859
Limits of pattern discrimination in human vision
[AD-A170756] N87-13135

YORK UNIV. (ONTARIO).
Low Q spin-up from rest
[AD-A169106] N87-12813

Typical Contract Number Index Listing

Listings in this index are arranged alphanumerically by contract number. Under each contract number the NASA accession numbers denoting documents that have been produced as a result of research done under that contract are arranged in ascending order. The NASA accession number denotes the number by which the citation is identified.

AF PROJ. 2301 ..... N87-12783
AF PROJ. 7600 ..... N87-13033
AF-AFOSR-0010-82 ..... N87-12657
AF-AFOSR-0017-82 ..... N87-12856
AF-AFOSR-0018-85 ..... N87-13329
AF-AFOSR-0032-84 ..... N87-12762
AF-AFOSR-0036-83 ..... N87-12635
AF-AFOSR-0052-84 ..... N87-13174
AF-AFOSR-0066-82 ..... N87-12858
AF-AFOSR-0077-81 ..... N87-12859
AF-AFOSR-0113-84 ..... N87-13239
AF-AFOSR-0127-84 ..... N87-12855
AF-AFOSR-0156-84 ..... N87-13236
AF-AFOSR-0161-82 ..... N87-12856
AF-AFOSR-0187-82 ..... N87-13218
AF-AFOSR-0193-85 ..... N87-12781
N87-12782
AF-AFOSR-0194-83 ..... N87-13137
AF-AFOSR-0205-84 ..... N87-13219
N87-13240
AF-AFOSR-0221-83 ..... N87-12801
AF-AFOSR-0236-82 ..... N87-12868
AF-AFOSR-0269-83 ..... N87-13136
AF-AFOSR-0275-82 ..... N87-13187
AF-AFOSR-0315-82 ..... N87-12936
AF-AFOSR-0318-83 ..... N87-12802
AF-AFOSR-0322-85 ..... N87-13222
AF-AFOSR-0367-84 ..... N87-13234
N87-13235
AF-AFOSR-0371-84 ..... N87-12583
ARB-A4-114-32 ..... N87-13013
ARPA ORDER 4487 ..... N87-12783
ARPA ORDER 4583 ..... N87-12777
ARPA ORDER 4871 ..... N87-13201
N87-13211
ARPA ORDER 9031 ..... N87-12849
DA PROJ. 2Q1-61102-B-74-D N87-13130
DAAA15-85-C-0111 ..... N87-13271
DAAE07-85-C-R089 ..... N87-13166
DAAG29-76-G-0298 ..... N87-13228
DAAG29-79-C-0094 ..... N87-12686
DAAG29-79-C-0205 ..... N87-13226
DAAG29-80-G-0013 ..... N87-12847
DAAG29-81-C-0032 ..... N87-12545
DAAG29-81-C-0035 ..... N87-13320
DAAG29-81-K-0082 ..... N87-12870
DAAG29-82-C-0020 ..... N87-13331
DAAG29-82-G-0013 ..... N87-12851
DAAG29-82-K-0003 ..... N87-12884
DAAG29-82-K-0036 ..... N87-12849
DAAG29-82-K-0063 ..... N87-12996
DAAG29-82-K-0113 ..... N87-12813
DAAG29-82-K-0129 ..... N87-12811
DAAG29-82-K-0143 ..... N87-12885
DAAG29-82-K-0144 ..... N87-12925
DAAG29-82-K-0155 ..... N87-13229
DAAG29-82-K-0157 ..... N87-13208
DAAG29-82-K-0168 ..... N87-13230
N87-13232
DAAG29-82-K-0183 ..... N87-13103
DAAG29-83-C-0007 ..... N87-13250
DAAG29-83-C-0020 ..... N87-12682
DAAG29-83-C-0030 ..... N87-13258
DAAG29-83-K-0003 ..... N87-12727
DAAG29-83-K-0028 ..... N87-12759
DAAG29-83-K-0035 ..... N87-13209
DAAG29-83-K-0039 ..... N87-13316
DAAG29-83-K-0042 ..... N87-12628
DAAG29-83-K-0044 ..... N87-13319
DAAG29-83-K-0046 ..... N87-12650
DAAG29-83-K-0048 ..... N87-13265
DAAG29-83-K-0058 ..... N87-12882
DAAG29-83-K-0074 ..... N87-12749
DAAG29-83-K-0086 ..... N87-13202
DAAG29-83-K-0127 ..... N87-12764
DAAG29-83-K-0130 ..... N87-13333
DAAG29-83-K-0148 ..... N87-12761
DAAG29-83-K-0152 ..... N87-13026
DAAG29-83-K-0159 ..... N87-12648
DAAG29-83-K-0165 ..... N87-13102
DAAG29-84-K-0005 ..... N87-13220
N87-13221
DAAG29-84-K-0030 ..... N87-13210
N87-13231
DAAG29-84-K-0048 ..... N87-12567
N87-12568
N87-12729
DAAG29-84-K-0058 ..... N87-13191
DAAG29-84-K-0078 ..... N87-12725
DAAG29-84-K-0140 ..... N87-13216
DAAG29-84-K-0156 ..... N87-13180
N87-13248
DAAG29-84-K-0172 ..... N87-13318
DAAG29-85-C-0002 ..... N87-12544
DAAG29-85-C-0003 ..... N87-13326
DAAG29-85-C-0005 ..... N87-13317
DAAG29-85-C-0027 ..... N87-12615
DAAG29-85-G-0110 ..... N87-12929
DAAG29-85-K-0003 ..... N87-12926
N87-12927
DAAG29-85-K-0010 ..... N87-12627
DAAG29-85-K-0035 ..... N87-12655
DAAG29-85-K-0135 ..... N87-13123
DAAG29-85-K-0183 ..... N87-12739
DAAG29-85-K-0201 ..... N87-12928
DAAG29-85-K-0235 ..... N87-13332
DAAG46-80-C-0038 ..... N87-12654
DAAK11-84-D-0008 ..... N87-13172
DAAK70-85-C-0077 ..... N87-12713
DAAL03-86-G-0088 ..... N87-12743
DACW39-83-M-1805 ..... N87-12709
DAJA37-81-C-0237 ..... N87-13130
DARPA ORDER 2496 ..... N87-12741
DARPA ORDER 4540 ..... N87-13328
DCA100-84-C-0009 ..... N87-12600
DCA100-84-C-0085 ..... N87-13200
DE-AA03-76SF-00326 ..... N87-13248
DE-AC02-76CH-00016 ..... N87-12706
N87-12942
N87-13124
N87-13257
DE-AC02-76ER-02271 ..... N87-13259
DE-AC02-76EV-03522 ..... N87-13138
DE-AC02-76ET-51013 ..... N87-13311
DE-AC02-76EV-04969 ..... N87-12841
DE-AC02-80ER-10559 ..... N87-12823
DE-AC02-80ER-10774 ..... N87-13396
DE-AC02-81ER-10982 ..... N87-12642
DE-AC02-83CH-10093 ..... N87-12700
N87-12701
N87-12817
N87-12997
N87-13003
N87-13004
DE-AC02-84ER-13163 ..... N87-12901
DE-AC03-76SF-00098 ..... N87-12646
N87-12665
N87-12670
N87-12793
N87-12798
N87-12803
N87-12885
N87-13010
N87-13242
N87-13272
N87-13356
DE-AC04-76DP-00613 ..... N87-12800
N87-12906
N87-12907
DE-AC04-76DP-00789 ..... N87-12577
N87-12612
N87-12639
N87-12640
N87-12644
N87-12645
N87-12647
N87-12661
N87-12668
N87-12672
N87-12694
N87-12788
N87-12789
N87-12790
N87-12794
N87-12799
N87-12802
N87-12818
N87-12819
N87-12821
N87-12837
N87-12838
N87-12840
N87-12842
N87-12860
N87-12861
N87-12904
N87-12911
N87-12945
N87-13001
N87-13002
N87-13005
N87-13006
N87-13113
N87-13175
N87-13176
N87-13196
N87-13197
N87-13336
N87-13339
N87-13354
DE-AC04-83AL-23523 ..... N87-12641
DE-AC05-84OR-21400 ..... N87-12637
N87-12662
N87-12663
N87-12664
N87-12666
N87-12667
N87-12689
N87-12698
N87-12699
N87-12791
N87-12885
N87-12886
N87-12887
N87-12888
N87-12889
N87-12890
N87-12891
N87-12892
N87-12893
N87-12894
N87-12895
N87-12896
N87-12897
N87-12900
N87-12903
N87-12940
N87-12944
N87-12993
N87-12998
N87-13000
N87-13007
N87-13009
N87-13012
N87-13193
N87-13198
N87-13199

DE-AC05-84OS-21400 ..... N87-13226
N87-13256
N87-13335
N87-13355
N87-12674
N87-12675
DE-AC06-76RL-01830 ..... N87-12671
N87-12676
N87-12820
N87-12992
N87-13139
N87-13361
DE-AC06-76RL01857 ..... N87-12698
DE-AC07-76ID-01570 ..... N87-12908
N87-13397
DE-AI01-76PR-06010 ..... N87-13011
DE-AS03-76ER-72018 ..... N87-13194
N87-13225
N87-13248
DE-AS03-76ET-53064 ..... N87-12751
DE-FG02-84ER-45096 ..... N87-13934
DE-FG02-85ER-45213 ..... N87-12677
DE-FG02-85ER-52118 ..... N87-13263
DE-FG05-85NE-37949 ..... N87-12905
DE-FG22-85PC-80503 ..... N87-12638
DNA001-85-0368 ..... N87-12807
DTRS57-85-C-00091 ..... N87-12554
ESA-5716/83-NL-MS N87-12994
ESTEC-5353/83-NL-GM(SC) N87-12605
F-AFOSR-82-0096 ..... N87-12807
F59-551 ..... N87-13108
F04611-79-C-0039 ..... N87-12610
F04611-83-K-0023 ..... N87-12703
F04701-85-C-0086 ..... N87-12576
N87-12779
F19628-81-C-0079 ..... N87-13029
F19628-82-K-0024 ..... N87-13027
F19628-82-K-0045 ..... N87-13031
F19628-83-C-0027 ..... N87-13104
F19628-83-C-0130 ..... N87-13109
F19628-83-C-0143 ..... N87-12571
F19628-83-K-0006 ..... N87-13035
F19628-83-K-0027 ..... N87-13034
F19628-85-C-0098 ..... N87-13310
F19628-85-C-0102 ..... N87-12991
F19628-85-K-0029 ..... N87-12724
N87-13030
F19628-85-K-0045 ..... N87-13380
F22915-84-C-2411 ..... N87-12816
F29601-83-C-0048 ..... N87-12852
F29601-84-K-0045 ..... N87-12569
F30602-82-C-0161 ..... N87-12778
F33615-81-C-2035 ..... N87-12705
F33615-81-K-1539 ..... N87-13204
F33615-82-C-3215 ..... N87-12939
F33615-82-K-3402 ..... N87-12633
F33615-83-C-2435 ..... N87-12766
F33615-84-C-5051 ..... N87-12563
F49620-81-K-0010 ..... N87-13133
F49620-82-C-0044 ..... N87-13327
N87-13330
F49620-83-C-0026 ..... N87-13135
F49620-84-C-0020 ..... N87-13188
F49620-84-C-0022 ..... N87-12783
F49620-85-C-0008 ..... N87-13217
N87-13238
N87-13241
F49620-85-C-0041 ..... N87-13144
F49620-85-C-0073 ..... N87-12689
F49620-85-C-0121 ..... N87-13143
F49620-85-C-0144 ..... N87-13224
N87-13237
F49620-85-K-0004 ..... N87-13142
MDA903-82-C-0064 ..... N87-12741
MDA903-83-C-0306 ..... N87-13186
MDA903-84-C-0031 ..... N87-13192
N87-13245
MDA903-85-K-0072 ..... N87-12777
MIPR-ARO-139-85 ..... N87-13236
NAGW-674 ..... N87-12542
NAG2-21 ..... N87-12808
NAG2-297 ..... N87-13243
NAG2-316 ..... N87-13362
NAG3-396 ..... N87-12915
NAG5-489 ..... N87-13023
NAG8-069 ..... N87-12626
NAG8-535 ..... N87-13365
NAG8-555 ..... N87-13368
NASA ORDER W-85081B N87-12608
NASW-3466 ..... N87-13358
NASW-4005 ..... N87-12598
N87-13375
N87-13376
NAS1-16759 ..... N87-13203
NAS1-17969 ..... N87-13024
NAS1-18028 ..... N87-12552
NAS3-23697 ..... N87-12923
NAS3-24084 ..... N87-12829
NAS5-23761 ..... N87-13394
NAS5-28609 ..... N87-13394
NAS8-33817 ..... N87-13140
NAS8-33822 ..... N87-13021
NAS8-33982 ..... N87-13307
NAS8-35502 ..... N87-12609
NAS8-35564 ..... N87-12587
NAS8-35989 ..... N87-12681
NAS9-17299 ..... N87-13167
NCC2-357 ..... N87-12831
NGL-05-020-272 ..... N87-13387
NGR-09-010-078 ..... N87-13227
NOOO14-82-K-0582 ..... N87-13243
NOOO14-83-K-0466 ..... N87-12658
NR PROJ. 606-003 ..... N87-13243
NR PROJ. 619003 ..... N87-13321
NSF CEE-82-10264 ..... N87-12815
NSF DCR-83-02391 ..... N87-13191
NSF DCR-84-03483 ..... N87-13216
NSF DCR-84-13211 ..... N87-13248
NSF DMS-83-15216 ..... N87-13213
N87-13222
NSF DMS-84-15211 ..... N87-13220
N87-13221
NSF ECS-82-10960 ..... N87-13243
NSF ECS-83-00970 ..... N87-12761
NSF ECS-83-12142 ..... N87-13248
NSF ECS-84-04809 ..... N87-13210
NSF ECS-84-07285 ..... N87-12722
N87-12730
NSF MCS-81-05904 ..... N87-13187
NSF MCS-82-00096 ..... N87-13219
NSF MCS-82-03483 ..... N87-13231
NSF NSM-84-19336 ..... N87-12930
NSF OCE-82-01222 ..... N87-13121
NSG-1601 ..... N87-12613
NSG2-392 ..... N87-12808
N0014-84-K-0053 ..... N87-13321
N00014-76-C-0867 ..... N87-13207
N00014-77-C-0232 ..... N87-12629
N00014-80-C-0003 ..... N87-13324
N00014-80-C-0472 ..... N87-12851
N00014-80-C-0622 ..... N87-12772
N00014-81-C-0062 ..... N87-13121
N00014-81-C-0776 ..... N87-13308
N00014-81-K-0603 ..... N87-13129
N00014-81-K-0742 ..... N87-12722
N87-12730
N00014-82-C-0067 ..... N87-13204
N00014-82-C-0583 ..... N87-12631
N87-12632
N00014-82-C-2466 ..... N87-13328
N00014-82-K-0185 ..... N87-12690
N00014-82-K-0335 ..... N87-12814
N00014-82-K-0562 ..... N87-12617
N87-12619
N87-12932
N00014-82-K-0576 ..... N87-12636
N87-13254
N87-13323
N00014-82-K-2040 ..... N87-12760
N00014-83-K-0003 ..... N87-13037
N00014-83-K-0125 ..... N87-13191
N00014-83-K-0341 ..... N87-13325
N00014-83-K-0365 ..... N87-13381
N00014-83-K-0571 ..... N87-12634
N87-12935
N00014-84-C-0149 ..... N87-12739
N87-12747
N00014-84-C-0234 ..... N87-12704
N00014-84-C-0413 ..... N87-12616
N00014-84-C-0668 ..... N87-12845
N00014-84-C-0699 ..... N87-12693
N00014-84-K-0084 ..... N87-13239
N00014-84-K-0301 ..... N87-13215
N00014-84-K-0315 ..... N87-12883
N00014-84-K-0345 ..... N87-13184
N00014-84-K-0428 ..... N87-12633
N00014-84-K-0569 ..... N87-12853
N00014-84-K-0721 ..... N87-12758
N00014-85-C-0039 ..... N87-12849
N00014-85-C-0206 ..... N87-12820
N00014-85-C-0594 ..... N87-13126
N00014-85-C-0852 ..... N87-12726
N00014-85-C-2421 ..... N87-13190
N00014-85-K-0111 ..... N87-13387
N00014-85-K-0168 ..... N87-13191
N00014-85-K-0169 ..... N87-12936
N87-13212
N87-13213
N87-13214
N87-13227
N00014-85-K-0211 ..... N87-12844
N00014-85-K-0343 ..... N87-13180
N87-13182
N87-13246
N00014-85-K-0371 ..... N87-12744
N00014-85-K-0404 ..... N87-13028
N00014-85-K-0479 ..... N87-13269
N00014-85-K-0489 ..... N87-13247
N00014-85-K-0497 ..... N87-13223
N00014-85-K-0547 ..... N87-12738
N00014-85-K-0720 ..... N87-12930
N00014-86-F-0001 ..... N87-12683
N00014-86-F-0033 ..... N87-12630
N00014-86-K-0156 ..... N87-13233
N00014-86-K-0173 ..... N87-13189
N00019-80-G-0607 ..... N87-12562
N00024-85-C-5301 ..... N87-12765
N00039-80-C-0556 ..... N87-12773
N00039-84-C-0089 ..... N87-13201
N87-13211
N00228-84-D-3155 ..... N87-13108
N61339-81-C-0105 ..... N87-12572
N61339-85-C-0044 ..... N87-12573
N62269-80-C-0261 ..... N87-12711
N62269-83-M-3295 ..... N87-12652
RRO210301 ..... N87-13321
W-31-109-ENG-38 ..... N87-12611
N87-12623
N87-12801
N87-13255
W-7405-ENG-36 ..... N87-12580
N87-12603
N87-12646
N87-12659
N87-12660
N87-12673
N87-12695
N87-12696
N87-12697
N87-12707
N87-12714
N87-12752
N87-12792
N87-12795
N87-12796
N87-12822
N87-12824
N87-12863
N87-12864
N87-12866
N87-12902
N87-12999
N87-13260
N87-13261
N87-13262
N87-13312
N87-13336
N87-13371
N87-13382
N87-13383
W-7405-ENG-48 ..... N87-12643
N87-12750
N87-12787
N87-12797
N87-12839
N87-12898
N87-12899
N87-13039
N87-13040
N87-13195
W-7405-ENG-82 ..... N87-12943
N87-13337
175-50-58 ..... N87-12828
352-02-03 ..... N87-13363
485-10-00 ..... N87-12592
505-35-21 ..... N87-13141
505-42-11 ..... N87-12869
505-42-51 ..... N87-12557
505-43-01 ..... N87-12558
505-45-35-56 ..... N87-12552
505-61-51 ..... N87-12539
N87-12830
505-62-01 ..... N87-12829
505-62-81-07 ..... N87-12538
505-63-11 ..... N87-12924
505-63-91-01 ..... N87-12614
N87-12680
505-66 ..... N87-12967
505-67-41 ..... N87-13122
505-68-11 ..... N87-12559
505-68-91-09 ..... N87-13264
505-83-11 ..... N87-12915
505-90-28 ..... N87-12679
506-40-11-02 ..... N87-12808
506-41-31 ..... N87-12606
506-43-11 ..... N87-12708
506-43-11-04 ..... N87-12922
506-45-21-01 ..... N87-13203

506-46-21-01 ..... N87-12566
533-05-11 ..... N87-12910
535-03-01 ..... N87-13252
673-41-10-70 ..... N87-13022
676-59-33 ..... N87-13021
778-35-13 ..... N87-13359

Typical Report Number Index Listing

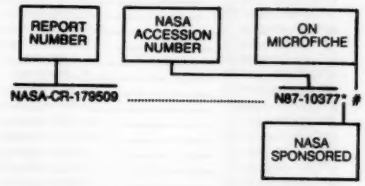

Listings in this index are arranged alphanumerically by report number. The NASA accession number denotes the number by which the citation is identified. An asterisk (*) indicates that the item is a NASA report. A pound sign (#) indicates that the item is available on microfiche.

A-85059 ..... N87-12869* #
A-85361 ..... N87-12558* #
A-85363 ..... N87-12557* #
A-86234 ..... N87-12539* #
A-86254 ..... N87-13141* #
A-86273 ..... N87-12830* #
A-86276 ..... N87-13363* #
A-86313 ..... N87-12967* #
A-86336 ..... N87-13122* #

AAMRL-TR-86-011 ..... N87-12746 #

AD-A167888 ..... N87-13100 #
AD-A167976 ..... N87-12551 #
AD-A168877 ..... N87-12758 #
AD-A168897 ..... N87-12722 #
AD-A168899 ..... N87-13025 #
AD-A168900 ..... N87-12844 #
AD-A168921 ..... N87-13228 #
AD-A168924 ..... N87-13254 #
AD-A168925 ..... N87-12682 #
AD-A168934 ..... N87-13207 #
AD-A168945 ..... N87-13308 #
AD-A168948 ..... N87-13245 #
AD-A168948 ..... N87-12870 #
AD-A168950 ..... N87-12845 #
AD-A168951 ..... N87-12811 #
AD-A168963 ..... N87-13316 #
AD-A168966 ..... N87-12925 #
AD-A168969 ..... N87-12759 #
AD-A168970 ..... N87-12567 #
AD-A168971 ..... N87-13026 #
AD-A168972 ..... N87-12926 #
AD-A168976 ..... N87-12627 #
AD-A168977 ..... N87-13208 #
AD-A168979 ..... N87-12628 #
AD-A168980 ..... N87-13317 #
AD-A168981 ..... N87-12723 #
AD-A168982 ..... N87-13318 #
AD-A168983 ..... N87-12604 #
AD-A168985 ..... N87-12760 #
AD-A168995 ..... N87-12648 #
AD-A168999 ..... N87-12709 #
AD-A169002 ..... N87-12846 #
AD-A169004 ..... N87-12724 #
AD-A169005 ..... N87-13204 #
AD-A169010 ..... N87-13027 #
AD-A169013 ..... N87-12629 #
AD-A169016 ..... N87-12725 #
AD-A169017 ..... N87-12582 #
AD-A169019 ..... N87-12568 #
AD-A169027 ..... N87-12726 #
AD-A169028 ..... N87-13209 #
AD-A169029 ..... N87-12727 #
AD-A169032 ..... N87-12649 #
AD-A169036 ..... N87-12871 #
AD-A169038 ..... N87-12683 #
AD-A169039 ..... N87-12812 #
AD-A169045 ..... N87-13168 #
AD-A169056 ..... N87-12615 #
AD-A169057 ..... N87-12927 #
AD-A169058 ..... N87-12928 #
AD-A169059 ..... N87-12847 #
AD-A169060 ..... N87-12929 #
AD-A169061 ..... N87-12630 #
AD-A169065 ..... N87-12728 #
AD-A169066 ..... N87-12729 #
AD-A169067 ..... N87-12650 #
AD-A169068 ..... N87-12761 #
AD-A169069 ..... N87-12730 #
AD-A169070 ..... N87-13119 #
AD-A169074 ..... N87-13028 #
AD-A169081 ..... N87-12631 #
AD-A169082 ..... N87-12632 #
AD-A169084 ..... N87-12569 #
AD-A169086 ..... N87-13200 #
AD-A169096 ..... N87-12996 #
AD-A169106 ..... N87-12813 #
AD-A169107 ..... N87-12651 #
AD-A169110 ..... N87-12553 #
AD-A169111 ..... N87-13210 #
AD-A169112 ..... N87-12872 #
AD-A169113 ..... N87-12762 #
AD-A169115 ..... N87-13180 #
AD-A169116 ..... N87-12544 #
AD-A169117 ..... N87-12930 #
AD-A169119 ..... N87-12652 #
AD-A169122 ..... N87-13126 #
AD-A169136 ..... N87-13101 #
AD-A169138 ..... N87-12633 #
AD-A169139 ..... N87-13247 #
AD-A169142 ..... N87-13127 #
AD-A169145 ..... N87-13229 #
AD-A169147 ..... N87-13181 #
AD-A169159 ..... N87-13319 #
AD-A169178 ..... N87-12731 #
AD-A169180 ..... N87-13265 #
AD-A169184 ..... N87-13360 #
AD-A169185 ..... N87-13350 #
AD-A169186 ..... N87-12616 #
AD-A169204 ..... N87-12684 #
AD-A169207 ..... N87-13230 #
AD-A169208 ..... N87-13128 #
AD-A169225 ..... N87-13201 #
AD-A169233 ..... N87-13102 #
AD-A169237 ..... N87-13103 #
AD-A169243 ..... N87-12685 #
AD-A169247 ..... N87-13202 #
AD-A169249 ..... N87-13320 #
AD-A169250 ..... N87-12763 #
AD-A169252 ..... N87-12686 #
AD-A169253 ..... N87-13231 #
AD-A169254 ..... N87-12545 #
AD-A169255 ..... N87-13248 #
AD-A169256 ..... N87-13182 #
AD-A169262 ..... N87-13232 #
AD-A169264 ..... N87-13183 #
AD-A169278 ..... N87-13029 #
AD-A169279 ..... N87-12873 #
AD-A169285 ..... N87-12991 #
AD-A169289 ..... N87-12931 #
AD-A169295 ..... N87-13104 #
AD-A169296 ..... N87-12932 #
AD-A169306 ..... N87-12617 #
AD-A169308 ..... N87-12703 #
AD-A169316 ..... N87-12732 #
AD-A169325 ..... N87-13030 #
AD-A169327 ..... N87-12733 #
AD-A169347 ..... N87-13169 #
AD-A169349 ..... N87-13258 #
AD-A169350 ..... N87-12546 #
AD-A169355 ..... N87-12618 #
AD-A169357 ..... N87-12848 #
AD-A169379 ..... N87-12619 #
AD-A169380 ..... N87-12734 #
AD-A169383 ..... N87-12933 #
AD-A169384 ..... N87-12764 #
AD-A169388 ..... N87-12765 #
AD-A169389 ..... N87-13105 #
AD-A169390 ..... N87-13106 #
AD-A169391 ..... N87-13107 #
AD-A169411 ..... N87-12766 #
AD-A169415 ..... N87-12570 #
AD-A169422 ..... N87-13351 #
AD-A169423 ..... N87-12571 #
AD-A169442 ..... N87-12934 #
AD-A169443 ..... N87-12853 #
AD-A169452 ..... N87-13347 #
AD-A169456 ..... N87-13321 #
AD-A169466 ..... N87-13031 #
AD-A169471 ..... N87-12814 #
AD-A169473 ..... N87-13246 #
AD-A169474 ..... N87-12849 #
AD-A169475 ..... N87-13309 #
AD-A169483 ..... N87-12562 #
AD-A169487 ..... N87-13250 #
AD-A169514 ..... N87-12572 #
AD-A169538 ..... N87-13108 #
AD-A169548 ..... N87-12736 #
AD-A169553 ..... N87-12737 #
AD-A169557 ..... N87-12771 #
AD-A169560 ..... N87-13323 #
AD-A169562 ..... N87-12815 #
AD-A169563 ..... N87-13129 #
AD-A169570 ..... N87-12563 #
AD-A169575 ..... N87-13352 #
AD-A169578 ..... N87-13130 #
AD-A169581 ..... N87-13184 #
AD-A169586 ..... N87-13387* #
AD-A169601 ..... N87-12851 #
AD-A169602 ..... N87-12935 #
AD-A169603 ..... N87-12634 #
AD-A169629 ..... N87-12578 #
AD-A169636 ..... N87-12579 #
AD-A169654 ..... N87-13211 #
AD-A169679 ..... N87-12772 #
AD-A169748 ..... N87-12599 #
AD-A169752 ..... N87-12635 #
AD-A169756 ..... N87-12773 #
AD-A169769 ..... N87-12654 #
AD-A169771 ..... N87-13212 #
AD-A169773 ..... N87-13227* #
AD-A169774 ..... N87-12738 #
AD-A169775 ..... N87-12911 #
AD-A169776 ..... N87-13120 #
AD-A169779 ..... N87-13131 #
AD-A169781 ..... N87-12852 #
AD-A169788 ..... N87-12554 #
AD-A169789 ..... N87-12600 #
AD-A169792 ..... N87-12610 #
AD-A169796 ..... N87-12936 #
AD-A169796 ..... N87-13213 #
AD-A169805 ..... N87-13324 #
AD-A169810 ..... N87-12834 #
AD-A169811 ..... N87-12835 #
AD-A169815 ..... N87-13233 #
AD-A169818 ..... N87-12912 #
AD-A169818 ..... N87-12636 #
AD-A169826 ..... N87-12601 #
AD-A169832 ..... N87-12576 #
AD-A169839 ..... N87-12620 #
AD-A169843 ..... N87-13325 #
AD-A169846 ..... N87-12853 #
AD-A169847 ..... N87-13185 #
AD-A169855 ..... N87-13214 #
AD-A169882 ..... N87-13269 #
AD-A169884 ..... N87-12711 #
AD-A169885 ..... N87-12739 #
AD-A169892 ..... N87-13186 #
AD-A169896 ..... N87-13215 #
AD-A169901 ..... N87-13326 #
AD-A169905 ..... N87-13032 #
AD-A169906 ..... N87-12855 #
AD-A169925 ..... N87-12533 #
AD-A169926 ..... N87-13234 #
AD-A169927 ..... N87-13216 #
AD-A169929 ..... N87-13187 #
AD-A169930 ..... N87-13174 #
AD-A169931 ..... N87-13217 #
AD-A169932 ..... N87-13235 #
AD-A169933 ..... N87-12855 #
AD-A169934 ..... N87-13142 #
AD-A169935 ..... N87-13236 #
AD-A169937 ..... N87-13218 #
AD-A169938 ..... N87-13219 #
AD-A169941 ..... N87-13143 #
AD-A169942 ..... N87-13033 #

AD-A169949 N87-13220 #
AD-A169950 N87-12602 #
AD-A169952 N87-12777 #
AD-A169960 N87-12856 #
AD-A169962 N87-12573 #
AD-A169971 N87-12688 #
AD-A169972 N87-13237 #
AD-A169974 N87-12682 #
AD-A169978 N87-13144 #
AD-A169980 N87-12656 #
AD-A169981 N87-13166 #
AD-A169983 N87-13380 #
AD-A169986 N87-13132 #
AD-A169992 N87-13327 #
AD-A170001 N87-12689 #
AD-A170002 N87-13133 #
AD-A170007 N87-12741 #
AD-A170010 N87-13221 #
AD-A170011 N87-12776 #
AD-A170017 N87-13034 #
AD-A170022 N87-12704 #
AD-A170025 N87-13236 #
AD-A170141 N87-13109 #
AD-A170143 N87-13035 #
AD-A170144 N87-13222 #
AD-A170170 N87-13239 #
AD-A170387 N87-12742 #
AD-A170393 N87-12743 #
AD-A170397 N87-13189 #
AD-A170442 N87-12744 #
AD-A170455 N87-13240 #
AD-A170457 N87-13036 #
AD-A170458 N87-13110 #
AD-A170463 N87-13111 #
AD-A170484 N87-12690 #
AD-A170487 N87-13037 #
AD-A170488 N87-12683 #
AD-A170492 N87-12713 #
AD-A170493 N87-12937 #
AD-A170494 N87-12938 #
AD-A170503 N87-12779 #
AD-A170533 N87-13134 #
AD-A170542 N87-13310 #
AD-A170582 N87-13223 #
AD-A170583 N87-12746 #
AD-A170615 N87-12555 #
AD-A170620 N87-13361 #
AD-A170652 N87-12747 #
AD-A170680 N87-13172 #
AD-A170697 N87-12657 #
AD-A170701 N87-13190 #
AD-A170756 N87-13135 #
AD-A170758 N87-13121 #
AD-A170772 N87-12781 #
AD-A170779 N87-13136 #
AD-A170782 N87-12858 #
AD-A170783 N87-13328 #
AD-A170797 N87-13329 #
AD-A170804 N87-13137 #
AD-A170809 N87-13241 #
AD-A170811 N87-12659 #
AD-A170813 N87-13330 #
AD-A170831 N87-12782 #
AD-A170832 N87-12534 #
AD-A170833 N87-12583 #
AD-A170837 N87-12783 #
AD-A170873 N87-13271 #
AD-A170944 N87-13224 #
AD-A171191 N87-13123 #
AD-A171209 N87-12939 #
AD-A171214 N87-12658 #
AD-A171275 N87-12784 #
AD-A171278 N87-12684 #
AD-A171284 N87-13038 #
AD-A171331 N87-12693 #
AD-A171360 N87-13331 #
AD-A171366 N87-13353 #
AD-A171370 N87-12622 #
AD-A171396 N87-12785 #
AD-A171398 N87-12786 #
AD-A171399 N87-13369 #
AD-A171418 N87-12565 #
AD-A171428 N87-13191 #
AD-A171434 N87-12616 #
AD-A171438 N87-13332 #
AD-A171460 N87-12584 #
AD-A171485 N87-13145 #
AD-A171487 N87-13112 #
AD-A171490 N87-12748 #
AD-A171495 N87-12705 #
AD-A171502 N87-12749 #
AD-A171506 N87-13333 #
AD-A171507 N87-13192 #

AD-D012269 N87-13315 #
AD-D012279 N87-12543 #
AD-D012359 N87-13249 #
AD-D012362 N87-13322 #
AD-D012364 N87-12874 #
AD-D012365 N87-12767 #
AD-D012368 N87-12710 #
AD-D012369 N87-12875 #
AD-D012370 N87-12766 #
AD-D012371 N87-12876 #
AD-D012372 N87-13253 #
AD-D012373 N87-12832 #
AD-D012374 N87-13266 #
AD-D012375 N87-12769 #
AD-D012376 N87-12770 #
AD-D012377 N87-13170 #
AD-D012378 N87-13171 #
AD-D012379 N87-12877 #
AD-D012384 N87-12833 #
AD-D012386 N87-12735 #
AD-D012389 N87-13267 #
AD-D012390 N87-12561 #
AD-D012393 N87-12878 #
AD-D012394 N87-12879 #
AD-D012396 N87-12850 #
AD-D012399 N87-13268 #
AD-D012401 N87-12854 #
AD-D012403 N87-12774 #
AD-D012404 N87-12687 #
AD-D012405 N87-12564 #
AD-D012406 N87-12880 #
AD-D012407 N87-12881 #
AD-D012408 N87-12775 #
AD-D012410 N87-12740 #
AD-D012411 N87-12712 #
AD-D012412 N87-13270 #
AD-D012413 N87-12621 #
AD-D012414 N87-12776 #
AD-D012415 N87-12745
AD-D012416 N87-12857
AD-D012417 N87-12691
AD-D012422 N87-12692
AD-D012423 N87-12636
AD-D012425 N87-12780

AD-E500768 N87-13245 #
AD-E500768 N87-13308 #
AD-E500769 N87-13387* #
AD-E500793 N87-13192 #
AD-E750914 N87-12853 #
AD-E750914 N87-13185 #
AD-E750914 N87-13214 #
AD-E900585 N87-12936 #
AD-E900585 N87-13213 #
AD-E900585 N87-13324 #
AD-E950849 N87-12834 #
AD-E950850 N87-12835 #

AD-F250645 N87-12622 #
AD-F250645 N87-13353 #
AD-F300802 N87-12584 #

AEDC-TR-85-30-VOL-1-REV N87-12551 #
AEDC-TR-85-55 N87-12565 #

AFGL-ERP-933 N87-13025 #
AFGL-ERP-934 N87-13101 #
AFGL-ERP-942 N87-13309 #
AFGL-ERP-943 N87-13033 #
AFGL-ERP-944 N87-13032 #
AFGL-ERP-946 N87-13036 #

AFGL-TR-85-0254 N87-13025 #
AFGL-TR-85-0255 N87-13029 #
AFGL-TR-85-0285 N87-13101 #
AFGL-TR-85-0298 N87-13104 #
AFGL-TR-85-0317 N87-13032 #
AFGL-TR-85-0331 N87-13109 #
AFGL-TR-85-0342 N87-13033 #
AFGL-TR-86-0012 N87-12991 #
AFGL-TR-86-0022 N87-13031 #
AFGL-TR-86-0025 N87-12724 #
AFGL-TR-86-0026 N87-13030 #
AFGL-TR-86-0028 N87-13036 #
AFGL-TR-86-0032 N87-13380 #
AFGL-TR-86-0034 N87-13027 #
AFGL-TR-86-0036 N87-12571 #
AFGL-TR-86-0045 N87-13310 #
AFGL-TR-86-0061 N87-13035 #
AFGL-TR-86-0087 N87-13034 #
AFGL-TR-0341 N87-13309 #

AFIT/CI/NR-86-84T N87-12534 #
AFIT/CI/NR-86-98T N87-13110 #
AFIT/CI/NR-86-99T N87-13111 #
AFIT/CI/NR-86-123D N87-13038 #
AFIT/CI/NR-86-127T N87-12684 #
AFOSR-86-0305TR N87-12782 #
AFOSR-86-0306TR N87-12601 #
AFOSR-86-0339TR N87-13224 #
AFOSR-86-0340TR N87-13237 #
AFOSR-86-0343TR N87-13238 #
AFOSR-86-0348TR N87-12688 #
AFOSR-86-0352TR N87-13240 #
AFOSR-86-0362TR N87-13222 #
AFOSR-86-0381TR N87-13234 #
AFOSR-86-0384TR N87-13235 #
AFOSR-86-0389TR N87-13174 #
AFOSR-86-0397TR N87-12635 #
AFOSR-86-0398TR N87-13217 #
AFOSR-86-0399TR N87-13219 #
AFOSR-86-0410TR N87-13239 #
AFOSR-86-0411TR N87-13187 #
AFOSR-86-0413TR N87-13218 #
AFOSR-86-0416TR N87-13143 #
AFOSR-86-0417TR N87-13142 #
AFOSR-86-0422TR N87-12855 #
AFOSR-86-0431TR N87-13236 #
AFOSR-86-0444TR N87-12602 #
AFOSR-86-0447TR N87-12656 #
AFOSR-86-0448TR N87-13327 #
AFOSR-86-0451TR-SUPPL-A N87-13144 #
AFOSR-86-0453TR N87-13133 #
AFOSR-86-0457TR N87-13188 #
AFOSR-86-0469TR N87-13329 #
AFOSR-86-0479TR N87-12856 #
AFOSR-86-0485TR N87-12689 #
AFOSR-86-0512TR N87-13136 #
AFOSR-86-0522TR N87-12859 #
AFOSR-86-0525TR N87-13330 #
AFOSR-86-0527TR N87-12781 #
AFOSR-86-0545TR N87-13137 #
AFOSR-86-0553TR N87-12858 #
AFOSR-86-0555TR N87-12783 #
AFOSR-86-0567TR N87-12657 #
AFOSR-86-0569TR N87-13135 #
AFOSR-86-0575TR N87-13241 #
AFOSR-86-0595TR N87-12583 #
AFOSR-86-0597TR N87-12782 #

AFRPL-TR-86-039 N87-12703 #
AFRPL-TR-86-044 N87-12610 #

AFWAL-TR-82-3098-ADD-1 N87-12933 #
AFWAL-TR-85-2093 N87-12705 #
AFWAL-TR-85-2104 N87-12786 #
AFWAL-TR-85-4154 N87-12563 #
AFWAL-TR-86-2004-VOL-1 N87-12816 #
AFWAL-TR-86-3028 N87-12939 #

AFWL-TN-85-47 N87-12771 #
AFWL-TN-85-52 N87-12569 #

AFWL-TR-85-04 N87-12852 #

AGARD-CP-383 N87-13273 #

AMI-8605 N87-12545 #

AMSMI/TR-RD-GC-86-1 N87-12635 #
AMSMI/TR-RD-GC-86-2 N87-12634 #

ANCO-1663.15 N87-13126 #

API-TR-127 N87-12726 #

AR-1 N87-13142 #
AR-3 N87-13330 #
AR-86 N87-12690 #
AR-004-307 N87-12702 #

ARB-R-86/278 N87-13013 #

ARCCB-TR-86014 N87-12653 #
ARCCB-TR-86015 N87-12934 #
ARCCB-TR-86021 N87-12938 #
ARCCB-TR-86024 N87-12937 #

ARI-RN-86-64 N87-13130 #

ARO-86-2 N87-13246 #
ARO-14244.15-MA N87-13228 #
ARO-16425.3-MS N87-12686 #
ARO-16869.28-MA N87-13228 #
ARO-17852.1-PH-H N87-12847 #
ARO-18166.3-EG N87-12870 #
ARO-18263.30-PH N87-12684 #
ARO-18265.20-MS N87-12649 #
ARO-18325.7-EG N87-12925 #
ARO-18391.3-EG-S N87-12545 #
ARO-18492.1-PH-S N87-13320 #
ARO-18744.15-MA N87-12811 #
ARO-18767.9-CH N87-12996 #

ARO-18784.3-EG ..... N87-12613 #
ARO-19026.1-MS ..... N87-12686 #
ARO-19068.1-EL ..... N87-13331 #
ARO-19085.12-MA ..... N87-13229 #
ARO-19159.3-EL ..... N87-13202 #
ARO-19251.5-CH ..... N87-12685 #
ARO-19367.35-MA ..... N87-13230 #
ARO-19367.36-MA ..... N87-13232 #
ARO-19426.4-MA ..... N87-13209 #
ARO-19442.26-MA ..... N87-13226 #
ARO-19511.3-MS ..... N87-13250 #
ARO-19524.1-MA ..... N87-13206 #
ARO-19649.3-GS ..... N87-13103 #
ARO-19740.1-CH-H ..... N87-12651 #
ARO-19783.4-MS ..... N87-12648 #
ARO-19793.4-PH ..... N87-13319 #
ARO-19838.94-EL ..... N87-12727 #
ARO-19869.13-EG ..... N87-12628 #
ARO-19876.47-MA ..... N87-12759 #
ARO-19879.25-EG ..... N87-12882 #
ARO-19881.26-PH ..... N87-13265 #
ARO-19938.7-GS ..... N87-12749 #
ARO-19998.9-MS ..... N87-13316 #
ARO-20065.2-GS ..... N87-13026 #
ARO-20115.2-EG ..... N87-13258 #
ARO-20155.5-MA ..... N87-12567 #
ARO-20155.6-MA ..... N87-12729 #
ARO-20155.8-MA ..... N87-12568 #
ARO-20174.12-MS ..... N87-12650 #
ARO-20280.1-CH ..... N87-13333 #
ARO-20576.3-GS ..... N87-13102 #
ARO-20927.12-MA ..... N87-13210 #
ARO-20927.13-MA ..... N87-13231 #
ARO-20980.53-MA ..... N87-13221 #
ARO-20980.54-MA ..... N87-13220 #
ARO-21098.1-EL ..... N87-12764 #
ARO-21107.3-EL-A ..... N87-12761 #
ARO-21210.2-MS ..... N87-13318 #
ARO-21378.5-EL ..... N87-12725 #
ARO-21453.3-MA ..... N87-13216 #
ARO-21592.8-MA ..... N87-13180 #
ARO-21673.2-MS ..... N87-12655 #
ARO-21731.1-EG ..... N87-12544 #
ARO-22306.5-EG ..... N87-12926 #
ARO-22306.6-EG ..... N87-12927 #
ARO-22486.2-EG ..... N87-12627 #
ARO-22560.1-LS ..... N87-13123 #
ARO-22600.1-MS-A ..... N87-13326 #
ARO-22602.1-MS-A ..... N87-13317 #
ARO-22634.3-EL ..... N87-12739 #
ARO-22817.2-MS-S ..... N87-12615 #
ARO-22874.1-EL ..... N87-13332 #
ARO-23038.1-MS-CF ..... N87-12929 #
ARO-23225.1-EG ..... N87-12928 #
ARO-23498.1-EL-CF ..... N87-12743 #

ASR-2 ..... N87-12923* #

ATC-86-2 ..... N87-12709 #

ATR-86(8139)-2 ..... N87-13314 #
ATR-86(9558)-11 ..... N87-13389 #

BDX-613-3511 ..... N87-12800 #
BDX-613-3512 ..... N87-12907 #
BDX-613-3557 ..... N87-12906 #

BN-1047-PT-1 ..... N87-13212 #
BN-1048 ..... N87-13214 #
BN-1049 ..... N87-13227* #
BN-1050 ..... N87-13213 #

BNL-37960 ..... N87-12942 #
BNL-38006 ..... N87-13124 #
BNL-38086 ..... N87-12706 #
BNL-38233 ..... N87-13257 #

BR-100271 ..... N87-12540 #
BR-100272 ..... N87-12810 #

BRL-CR-558 ..... N87-13271 #

BRL-MR-3519 ..... N87-12570 #
BRL-MR-3530 ..... N87-12584 #

CAORF-80-7805-01 ..... N87-13132 #

CAP-420-071 ..... N87-12994 #

CAS/CHEM-4-86 ..... N87-12690 #

CLASSIC-85-10 ..... N87-12814 #

CONF-851174-42 ..... N87-13311 #
CONF-860174-1 ..... N87-12665 #
CONF-860366-7 ..... N87-12623 #
CONF-860420-4 ..... N87-12861 #
CONF-860421-51 ..... N87-12671 #
CONF-860426-2 ..... N87-13195 #
CONF-860451-1 ..... N87-13139 #
CONF-860507-8 ..... N87-12943 #
CONF-860548-2 ..... N87-12706 #
CONF-860619 ..... N87-13002 #
CONF-860620-8 ..... N87-12860 #
CONF-860629-16 ..... N87-13257 #
CONF-860636-3 ..... N87-12863 #
CONF-860665-6 ..... N87-13312 #
CONF-860665-7 ..... N87-12864 #
CONF-860665-8 ..... N87-12792 #
CONF-860674-7 ..... N87-12790 #
CONF-860674-9 ..... N87-12752 #
CONF-860675-3 ..... N87-12945 #
CONF-860694-1 ..... N87-13242 #
CONF-860703-1 ..... N87-12843 #
CONF-860703-7 ..... N87-12796 #
CONF-860703-8 ..... N87-12795 #
CONF-860706-13 ..... N87-12840 #
CONF-860722-10 ..... N87-12940 #
CONF-860727-3 ..... N87-12940 #
CONF-860744-1 ..... N87-13196 #
CONF-860748-1 ..... N87-13339 #
CONF-860804-8 ..... N87-12819 #
CONF-860805-4 ..... N87-12818 #
CONF-860805-7 ..... N87-12817 #
CONF-860809-1 ..... N87-13334 #
CONF-860810-5 ..... N87-12999 #
CONF-860810-6 ..... N87-12902 #
CONF-860810-7 ..... N87-13260 #
CONF-860810-9 ..... N87-12998 #
CONF-860810-11 ..... N87-13000 #
CONF-860810-12 ..... N87-12788 #
CONF-860810-18 ..... N87-12798 #
CONF-860829-1 ..... N87-12660 #
CONF-860829-2 ..... N87-12659 #
CONF-860829-3 ..... N87-12661 #
CONF-860829-4 ..... N87-12662 #
CONF-860829-6 ..... N87-12667 #
CONF-860829-8 ..... N87-12663 #
CONF-860829-11 ..... N87-12639 #
CONF-860829-15 ..... N87-12694 #
CONF-860829-16 ..... N87-13336 #
CONF-860829-17 ..... N87-12668 #
CONF-860829-18 ..... N87-12640 #
CONF-860829-21 ..... N87-13335 #
CONF-860829-22 ..... N87-12669 #
CONF-860829-23 ..... N87-12900 #
CONF-860829-25 ..... N87-12612 #
CONF-860829-26 ..... N87-13124 #
CONF-860829-27 ..... N87-12670 #
CONF-860839-2 ..... N87-12899 #
CONF-860844-1 ..... N87-12898 #
CONF-860845-1 ..... N87-13256 #
CONF-860849-1 ..... N87-12750 #
CONF-860852-1 ..... N87-12942 #
CONF-860853-1 ..... N87-12645 #
CONF-860854-1 ..... N87-12669 #
CONF-860854-3 ..... N87-12664 #
CONF-860872-1 ..... N87-13175 #
CONF-860874-2 ..... N87-12997 #
CONF-860875-1-REV-1 ..... N87-13039 #
CONF-860879-1 ..... N87-12666 #
CONF-860880-10 ..... N87-12639 #
CONF-860880-14 ..... N87-12799 #
CONF-860882-2 ..... N87-12577 #
CONF-860906-13 ..... N87-13262 #
CONF-860913-1 ..... N87-12801 #
CONF-861091-1 ..... N87-12803 #
CONF-8508178-1 ..... N87-13193 #
CONF-8510160-18 ..... N87-12676 #
CONF-8603121-2 ..... N87-13255 #
CONF-8603122-1 ..... N87-12787 #
CONF-8604214-1 ..... N87-12820 #
CONF-8604219-1 ..... N87-13382 #
CONF-8604219-2 ..... N87-13383 #
CONF-8604220-1 ..... N87-12885 #
CONF-8604224-2 ..... N87-12866 #
CONF-8605111-2 ..... N87-13337 #
CONF-8605119-1 ..... N87-12637 #
CONF-8605125-1 ..... N87-13355 #
CONF-8605126-1 ..... N87-13354 #
CONF-8605137-3 ..... N87-13009 #
CONF-8605142-1 ..... N87-12611 #
CONF-8605156-1 ..... N87-12842 #
CONF-8605160-1 ..... N87-13199 #
CONF-8606113-2 ..... N87-12698 #
CONF-8606121-1 ..... N87-12837 #
CONF-8606121-2 ..... N87-12838 #
CONF-8606121-3 ..... N87-12794 #
CONF-8606123-PT-1-SUMM ..... N87-13006 #
CONF-8606132-1 ..... N87-12673 #
CONF-8606133-2 ..... N87-12696 #
CONF-8606133-3 ..... N87-12695 #
CONF-8606133-5 ..... N87-12697 #
CONF-8606136-1 ..... N87-12822 #
CONF-8606138-2 ..... N87-12944 #
CONF-8606145-1 ..... N87-12580* #
CONF-8606148-1 ..... N87-12672 #
CONF-8606152-1 ..... N87-13196 #
CONF-8606159-1 ..... N87-13338 #

COO-2271-109 ..... N87-13259 #

CPL-86-1A ..... N87-13144 #

CRREL-SR-86-9 ..... N87-13119 #

CSG-51 ..... N87-12773 #

CSSA-ASTRO-86-29 ..... N87-13387* #

CU-CS-334-86 ..... N87-13216 #

CUED/A-TURBO/TR-122 ..... N87-12560 #

DE85-011476 ..... N87-12601 #
DE86-002968 ..... N87-13334 #
DE86-004424 ..... N87-12617 #
DE86-004455 ..... N87-12700 #
DE86-004603 ..... N87-12618 #
DE86-006467 ..... N87-12619 #
DE86-006947 ..... N87-13138 #
DE86-007361 ..... N87-12659 #
DE86-007362 ..... N87-12660 #
DE86-007627 ..... N87-12661 #
DE86-007847 ..... N87-12636 #
DE86-008401 ..... N87-13242 #
DE86-008494 ..... N87-12662 #
DE86-008533 ..... N87-12663 #
DE86-008537 ..... N87-12667 #
DE86-008763 ..... N87-12898 #
DE86-008768 ..... N87-12750 #
DE86-008781 ..... N87-12639 #
DE86-008898 ..... N87-13258 #
DE86-009023 ..... N87-13336 #
DE86-009030 ..... N87-12694 #
DE86-009284 ..... N87-12668 #
DE86-009353 ..... N87-13335 #
DE86-009396 ..... N87-12899 #
DE86-009421 ..... N87-12669 #
DE86-009510 ..... N87-12940 #
DE86-009538 ..... N87-12900 #
DE86-009540 ..... N87-12640 #
DE86-009640 ..... N87-12645 #
DE86-009942 ..... N87-12942 #
DE86-010026 ..... N87-12698 #
DE86-010027 ..... N87-12664 #
DE86-010459 ..... N87-12612 #
DE86-010475 ..... N87-12837 #
DE86-010483 ..... N87-13175 #
DE86-010484 ..... N87-13354 #
DE86-010526 ..... N87-12623 #
DE86-010529 ..... N87-13255 #
DE86-010543 ..... N87-13124 #
DE86-010590 ..... N87-13176 #
DE86-010621 ..... N87-13355 #
DE86-010702 ..... N87-12997 #
DE86-010705 ..... N87-13003 #
DE86-010708 ..... N87-13004 #
DE86-010747 ..... N87-12641 #
DE86-010785 ..... N87-12787 #
DE86-010788 ..... N87-13195 #
DE86-010886 ..... N87-12901 #
DE86-010971 ..... N87-13039 #
DE86-010989 ..... N87-12577 #
DE86-011006 ..... N87-13040 #
DE86-011063 ..... N87-12637 #
DE86-011070 ..... N87-12998 #
DE86-011106 ..... N87-12676 #
DE86-011117 ..... N87-12820 #
DE86-011203 ..... N87-12706 #
DE86-011218 ..... N87-12695 #
DE86-011222 ..... N87-13338 #
DE86-011226 ..... N87-13262 #
DE86-011235 ..... N87-12999 #
DE86-011252 ..... N87-13260 #
DE86-011263 ..... N87-12696 #
DE86-011264 ..... N87-12902 #
DE86-011308 ..... N87-12670 #
DE86-011313 ..... N87-12665 #
DE86-011424 ..... N87-12788 #
DE86-011429 ..... N87-13337 #
DE86-011437 ..... N87-12943 #
DE86-011511 ..... N87-13000 #
DE86-011576 ..... N87-12941 #
DE86-011614 ..... N87-12671 #
DE86-011643 ..... N87-12838 #
DE86-011644 ..... N87-13196 #
DE86-011649 ..... N87-12992 #

DE86-011651 ..... N87-12794 #
DE86-011669 ..... N87-12993 #
DE86-011703 ..... N87-13002 #
DE86-011754 ..... N87-12944 #
DE86-011762 ..... N87-13005 #
DE86-011775 ..... N87-13193 #
DE86-011777 ..... N87-13009 #
DE86-011781 ..... N87-12686 #
DE86-011812 ..... N87-12842 #
DE86-011873 ..... N87-13311 #
DE86-011878 ..... N87-12643 #
DE86-012051 ..... N87-13006 #
DE86-012119 ..... N87-12611 #
DE86-012156 ..... N87-13194 #
DE86-012159 ..... N87-13225 #
DE86-012163 ..... N87-12861 #
DE86-012175 ..... N87-12860 #
DE86-012178 ..... N87-12672 #
DE86-012217 ..... N87-12862 #
DE86-012240 ..... N87-13198 #
DE86-012247 ..... N87-12789 #
DE86-012265 ..... N87-12821 #
DE86-012277 ..... N87-12842 #
DE86-012279 ..... N87-12790 #
DE86-012323 ..... N87-13139 #
DE86-012333 ..... N87-13361 #
DE86-012349 ..... N87-12639 #
DE86-012369 ..... N87-12752 #
DE86-012373 ..... N87-12866 #
DE86-012382 ..... N87-13312 #
DE86-012383 ..... N87-12863 #
DE86-012384 ..... N87-12864 #
DE86-012385 ..... N87-12792 #
DE86-012391 ..... N87-13383 #
DE86-012393 ..... N87-13382 #
DE86-012406 ..... N87-12822 #
DE86-012407 ..... N87-12803 #
DE86-012414 ..... N87-12673 #
DE86-012421 ..... N87-12795 #
DE86-012425 ..... N87-12796 #
DE86-012434 ..... N87-12697 #
DE86-012451 ..... N87-12903 #
DE86-012463 ..... N87-12885 #
DE86-012477 ..... N87-13010 #
DE86-012488 ..... N87-12791 #
DE86-012500 ..... N87-12865 #
DE86-012521 ..... N87-12886 #
DE86-012530 ..... N87-12887 #
DE86-012531 ..... N87-12888 #
DE86-012532 ..... N87-12889 #
DE86-012533 ..... N87-12890 #
DE86-012535 ..... N87-12891 #
DE86-012536 ..... N87-12892 #
DE86-012548 ..... N87-12893 #
DE86-012549 ..... N87-12894 #
DE86-012550 ..... N87-12895 #
DE86-012557 ..... N87-12896 #
DE86-012561 ..... N87-12897 #
DE86-012572 ..... N87-12674 #
DE86-012573 ..... N87-12675 #
DE86-012592 ..... N87-13226 #
DE86-012610 ..... N87-12644 #
DE86-012622 ..... N87-13199 #
DE86-012643 ..... N87-13011 #
DE86-012650 ..... N87-13272 #
DE86-012669 ..... N87-13259 #
DE86-012704 ..... N87-13257 #
DE86-012729 ..... N87-13001 #
DE86-012732 ..... N87-13113 #
DE86-012741 ..... N87-12941 #
DE86-012743 ..... N87-13197 #
DE86-012767 ..... N87-13261 #
DE86-012796 ..... N87-12823 #
DE86-012822 ..... N87-13356 #
DE86-012824 ..... N87-12793 #
DE86-012836 ..... N87-12646 #
DE86-012864 ..... N87-13371 #
DE86-012926 ..... N87-12647 #
DE86-012947 ..... N87-13339 #
DE86-012950 ..... N87-12840 #
DE86-013042 ..... N87-12751 #
DE86-013074 ..... N87-12904 #
DE86-013110 ..... N87-12905 #
DE86-013157 ..... N87-12677 #
DE86-013172 ..... N87-12797 #
DE86-013247 ..... N87-13263 #
DE86-013288 ..... N87-12906 #
DE86-013319 ..... N87-13396 #
DE86-013445 ..... N87-13397 #
DE86-013461 ..... N87-12798 #
DE86-013510 ..... N87-12907 #
DE86-013512 ..... N87-12699 #
DE86-013521 ..... N87-13007 #
DE86-013525 ..... N87-13012 #
DE86-013570 ..... N87-12799 #
DE86-013578 ..... N87-12945 #
DE86-013615 ..... N87-12800 #
DE86-013635 ..... N87-12707 #
DE86-013638 ..... N87-12714 #
DE86-013678 ..... N87-12701 #
DE86-013700 ..... N87-12824 #
DE86-013754 ..... N87-12802 #
DE86-013760 ..... N87-12803 #
DE86-013772 ..... N87-12908 #
DE86-701481 ..... N87-13370 #
DE86-702615 ..... N87-13372 #
DE86-702616 ..... N87-13348 #
DE86-702617 ..... N87-13349 #
DE86-702646 ..... N87-13340 #
DE86-702647 ..... N87-13341 #
DE86-702651 ..... N87-13342 #
DE86-702652 ..... N87-13343 #
DE86-702660 ..... N87-12753 #
DE86-702662 ..... N87-12678 #
DE86-702668 ..... N87-13344 #
DE86-702711 ..... N87-13384 #
DE86-702723 ..... N87-13345 #
DE86-702724 ..... N87-13346 #
DE86-702946 ..... N87-13373 #
DE86-702988 ..... N87-12825 #
DE86-0123433 ..... N87-12580* #

DGLR-85-04 ..... N87-13146 #

DOE/AL-23523/T1 ..... N87-12641 #

DOE/ER-0236 ..... N87-13010 #
DOE/ER-02271/109 ..... N87-13259 #
DOE/ER-10559/T2 ..... N87-12823 #
DOE/ER-10774/6 ..... N87-13396 #
DOE/ER-10982/T1 ..... N87-12642 #
DOE/ER-13163/11 ..... N87-12901 #
DOE/ER-45096/11 ..... N87-13334 #
DOE/ER-45213/2 ..... N87-12677 #
DOE/ER-52118/T2 ..... N87-13263 #

DOE/ET-51013/171 ..... N87-13311 #

DOE/EV-03522/T4 ..... N87-13138 #
DOE/EV-04969/T5 ..... N87-12841 #

DOE/NASA-50112/67 ..... N87-13359* #

DOE/NBB-0078 ..... N87-12993 #

DOE/NE-37949/1 ..... N87-12905 #

DOE/PC-80503/T1 ..... N87-12638 #

DOE/PR-06010/31 ..... N87-13011 #

DOT-CG-N-02-86 ..... N87-12554 #

DOT-TSC-CG-86-1 ..... N87-12554 #

DOT/FAA/AM/86-6 ..... N87-13145 #

DOT/FAA/CT-85/9 ..... N87-13099 #

DOT/FAA/PM-86/30 ..... N87-13099 #

DR/CG-157-84-REV ..... N87-12578 #

DREO-TN-85-26 ..... N87-12599 #

DREV-4407/86 ..... N87-12737 #

DRIC-BR-99244 ..... N87-12736 #

E-3181 ..... N87-12924* #
E-3274 ..... N87-12708* #
E-3275 ..... N87-13252* #
E-3276 ..... N87-12910* #
E-3292 ..... N87-12606* #
E-3298 ..... N87-12559* #
E-3302 ..... N87-13359* #
E-3323 ..... N87-12679* #

EGG-PHY-7272 ..... N87-13397 #

EPA/600/3-86/039 ..... N87-13014 #

EPM/RT-86-34 ..... N87-12919 #
EPM/RT-86-35 ..... N87-12920 #
EPM/RT-86-36 ..... N87-12916 #
EPM/RT-86-37 ..... N87-12917 #
EPM/RT-86-38 ..... N87-12918 #

EPRI-EA-4607 ..... N87-12992 #

ERIM-155900-37-R ..... N87-13120 #
ESA-CR(P)-2224 ..... N87-12605 #
ESA-CR(P)-2230 ..... N87-12994 #

ESDU-86001-PT-2C N87-12824
ESDU-86004-ADD-A N87-12558
ESDU-86010-PT-3 ..... N87-13042
ESDU-86012-PT-3A N87-12825
ESDU-86013 ..... N87-12914
ESDU-86015 ..... N87-12805
ESDU-86016-PT-4 ..... N87-12866
ESDU-86017 ..... N87-12537
ESDU-86019 ..... N87-13251
ESDU-86021 ..... N87-12536

ETN-86-98060 ..... N87-13146 #
ETN-86-98103 ..... N87-12605 #
ETN-86-98111 ..... N87-12994 #

FATR-3 ..... N87-13129 #

FJSRL-TR-86-0002 ..... N87-12848 #

FSU-STATISTICS-M722 ..... N87-13230 #

FSU-TR-M721 ..... N87-13232 #

FTD-ID(RS)T-0237-86 ..... N87-12582 #
FTD-ID(RS)T-0267-86 ..... N87-12533 #
FTD-ID(RS)T-0283-86 ..... N87-12553 #
FTD-ID(RS)T-0312-86 ..... N87-13347 #
FTD-ID(RS)T-0475-86 ..... N87-12723 #
FTD-ID(RS)T-0761-86 ..... N87-12622 #

FTL-118521 ..... N87-12605 #

GLR-254 ..... N87-13326 #

GPO-61-970 ..... N87-13357 #
GPO-63-142 ..... N87-12909 #
GPO-63-143 ..... N87-12574 #
GPO-64-548 ..... N87-12586 #

GWU/IMSE/SERIAL-T-507/86 ..... N87-13185 #

HDL-TR-2079 ..... N87-12731 #
HDL-TR-2090 ..... N87-12748 #

HEL-TN-5-86 ..... N87-13172 #

HFOSL-TN-72-86-07 ..... N87-12912 #

HTL-35 ..... N87-12804 #
HTL-39 ..... N87-12826 #

IC-85/96 ..... N87-13384 #
IC-85/102 ..... N87-13372 #
IC-85/109 ..... N87-13345 #
IC-85/111 ..... N87-13348 #
IC-85/112 ..... N87-13349 #
IC-85/119 ..... N87-13340 #
IC-85/125 ..... N87-13341 #
IC-85/136 ..... N87-13342 #
IC-85/141 ..... N87-13343 #
IC-85/153 ..... N87-13346 #
IC-85/163 ..... N87-12753 #
IC-85/165 ..... N87-12678 #
IC-85/191 ..... N87-13344 #
IC-85/220 ..... N87-12825 #
IC-85/227 ..... N87-13373 #

ICOMP-86-1 ..... N87-12924* #

IDA-M-144 ..... N87-13245 #
IDA-M-146 ..... N87-13192 #

IDA/HQ-85-30658 ..... N87-13192 #
IDA/HQ-86-30858 ..... N87-13245 #

INIS-BR-426 ..... N87-13370 #

INPE-3864-TDL/217 ..... N87-12596 #
INPE-3874-PRE/930 ..... N87-13205 #
INPE-3875-RPE/506 ..... N87-12754 #
INPE-3884-PRE/934 ..... N87-13377 #
INPE-3895-PRE/937 ..... N87-12590 #
INPE-3906-PRE/918 ..... N87-13177 #
INPE-3941-RPE/512 ..... N87-12757 #
INPE-3945-PRE/967 ..... N87-13244 #
INPE-3949-PRE/970 ..... N87-13006 #
INPE-3950-RPE/513 ..... N87-12969 #
INPE-3952-PRE/971 ..... N87-13118 #
INPE-3953-NTE/258 ..... N87-12595 #
INPE-3954-PRE/972 ..... N87-13368 #
INPE-3958-PRE/676 ..... N87-12720 #
INPE-3959-PRE/977 ..... N87-12588 #
INPE-3964-TDL/231 ..... N87-12809 #

INPE-3966-PRE/961 ..... N87-12589 #
INPE-3967-PRE/962-PT-1 ..... N87-12961 #
INPE-3970-PRE/963 ..... N87-12960 #
INPE-3972-PRE/965 ..... N87-12964 #
INPE-3974-PRE/966 ..... N87-13378 #
INPE-3975-PRE/967 ..... N87-12959 #
INPE-3976-RPE/517 ..... N87-12755 #
INPE-3977-PRE/968 ..... N87-12843 #
INPE-3979-TDL/233 ..... N87-13179 #
INPE-3980-PRE/990 ..... N87-12962 #
INPE-3981-NTE/259 ..... N87-12963 #
INPE-3982-TDL/234 ..... N87-12990 #
INPE-3985-NTE/260 ..... N87-12591 #
INPE-3987-NTE/261 ..... N87-12966 #
INPE-3989-PRE/992 ..... N87-12827 #
INPE-3990-MD/031 ..... N87-12966 #
INPE-3991-RPE/518 ..... N87-13173 #
INPE-3993-NTE/262 ..... N87-12594 #
INPE-3995-RPE/519 ..... N87-13020 #
INPE-3996-PRE/995 ..... N87-13206 #

IS-M-576 ..... N87-13337 #
IS-M-578 ..... N87-12943 #

ISBN-0-85679-553-4 ..... N87-12624
ISBN-0-85679-556-9 ..... N87-12556
ISBN-0-85679-562-3 ..... N87-13042
ISBN-0-85679-564-X N87-12625
ISBN-0-85679-565-8 ..... N87-12914
ISBN-0-85679-567-4 ..... N87-12905
ISBN-0-85679-568-2 ..... N87-12868
ISBN-0-85679-569-0 ..... N87-12537
ISBN-0-85679-571-2 ..... N87-13251
ISBN-0-85679-573-9 ..... N87-12536
ISBN-3-922010-30-X ..... N87-13146 #
ISBN-92-835-0391-0 ..... N87-13273 #

ISL-15 ..... N87-13204 #

ISSN-0082-5255 ..... N87-12907 #
ISSN-0141-397X N87-12536
ISSN-0141-397X N87-12537
ISSN-0141-4011 ..... N87-12805
ISSN-0141-4054 ..... N87-12556
ISSN-0141-4054 ..... N87-12868
ISSN-0141-4062 ..... N87-12624
ISSN-0141-4062 ..... N87-12625
ISSN-0141-4089 ..... N87-12914
ISSN-0149-2702 ..... N87-13042
ISSN-0144-2805 ..... N87-12914
ISSN-0307-0115 ..... N87-13251
ISSN-0309-6521 ..... N87-12560 #

ISU-ERI-AMES-86211 ..... N87-12804 #
ISU-ERI-AMES-86290 ..... N87-12826 #

JHU/APL/TG-1359 ..... N87-12765 #

JPL-PUB-83-39-REV-2 ..... N87-13178* #
JPL-PUB-86-33 ..... N87-12965* #
JPL-PUB-86-35 ..... N87-12966* #
JPL-PUB-86-40 ..... N87-12719* #

JPRS-JST-86-023 ..... N87-12715 #

JPRS-UES-86-007 ..... N87-12946 #

L-16135 ..... N87-12541* #
L-16136 ..... N87-13022* #
L-16157 ..... N87-13264* #
L-16196 ..... N87-12560* #

LA-UR-86-276 ..... N87-12846 #
LA-UR-86-730 ..... N87-13371 #
LA-UR-86-796 ..... N87-12560 #
LA-UR-86-797 ..... N87-12559 #
LA-UR-86-1548 ..... N87-12902 #
LA-UR-86-1585 ..... N87-12696 #
LA-UR-86-1643 ..... N87-13260 #
LA-UR-86-1744 ..... N87-12695 #
LA-UR-86-1781 ..... N87-13336 #
LA-UR-86-1840 ..... N87-12999 #
LA-UR-86-1879 ..... N87-13262 #
LA-UR-86-1906 ..... N87-13382 #
LA-UR-86-1907 ..... N87-13383 #
LA-UR-86-1937 ..... N87-12792 #
LA-UR-86-1941 ..... N87-12864 #
LA-UR-86-1943 ..... N87-12863 #
LA-UR-86-1952 ..... N87-13312 #
LA-UR-86-2010 ..... N87-12866 #
LA-UR-86-2043 ..... N87-12752 #
LA-UR-86-2085 ..... N87-12673 #
LA-UR-86-2112 ..... N87-12803 #
LA-UR-86-2118 ..... N87-12822 #
LA-UR-86-2200 ..... N87-12795 #
LA-UR-86-2207 ..... N87-12697 #

LA-UR-86-2213 ..... N87-12560* #
LA-UR-86-2259 ..... N87-12796 #

LA-10673-PR ..... N87-13261 #
LA-10676-MS ..... N87-12714 #
LA-10749-MS ..... N87-12707 #

LBL-PUB-490-REV. ..... N87-13272 #

LBL-20565 ..... N87-12646 #
LBL-20706 ..... N87-13356 #
LBL-20983 ..... N87-13242 #
LBL-21281 ..... N87-12793 #
LBL-21287 ..... N87-12670 #
LBL-21303 ..... N87-12665 #
LBL-21437 ..... N87-12798 #
LBL-21562 ..... N87-12665 #

LIDS-P-1568 ..... N87-13220 #
LIDS-P-1569 ..... N87-13221 #
LIDS-P-1614 ..... N87-13243* #

M-503 ..... N87-13043* #

MAE-1748 ..... N87-12729 #
MAE-1751 ..... N87-12566 #

MAP-HANDBOOK-21 ..... N87-13015* #

MBB/LKE-301/S/PUB/216 ..... N87-13151 #

MCR-85-605-ISSUE-3 ..... N87-12816 #
MCR-85-665-APP-B ..... N87-13203* #

MDC-W0072 ..... N87-13167* #

MIT/LCS/TR-367 ..... N87-13191 #

MM-4762-85-19 ..... N87-12932 #
MM-4762-86-2 ..... N87-12819 #
MM-4762-86-15 ..... N87-12817 #

MRR-86-1 ..... N87-13222 #

MSAT-X-136 ..... N87-12719* #

MT-CWR-086-017 ..... N87-12560 #

MTL-TR-86-10 ..... N87-12554 #
MTL-TR-86-15 ..... N87-12818 #

NA-85-0134 ..... N87-12711 #

NADC-79024-60 ..... N87-12711 #
NADC-86028-60 ..... N87-12552 #

NAE-AN-37 ..... N87-12872 #

NAE-LR-617 ..... N87-12548 #

NAS 1.15:86559 ..... N87-12592* #
NAS 1.15:86561 ..... N87-12607* #
NAS 1.15:86562 ..... N87-12721* #
NAS 1.15:86563 ..... N87-13166* #
NAS 1.15:86565 ..... N87-12829* #
NAS 1.15:86566 ..... N87-12756* #
NAS 1.15:86664 ..... N87-12569* #
NAS 1.15:86785 ..... N87-12558* #
NAS 1.15:86789 ..... N87-12557* #
NAS 1.15:87675 ..... N87-12606* #
NAS 1.15:87731 ..... N87-12566* #
NAS 1.15:87999 ..... N87-12598* #
NAS 1.15:88250 ..... N87-12539* #
NAS 1.15:88254 ..... N87-13141* #
NAS 1.15:88259 ..... N87-13363* #
NAS 1.15:88312 ..... N87-12830* #
NAS 1.15:88322 ..... N87-13122* #
NAS 1.15:88324 ..... N87-12967* #
NAS 1.15:88498 ..... N87-13376* #
NAS 1.15:88505 ..... N87-13375* #
NAS 1.15:88836 ..... N87-12924* #
NAS 1.15:88869 ..... N87-13252* #
NAS 1.15:88870 ..... N87-12910* #
NAS 1.15:88884 ..... N87-12606* #
NAS 1.15:88885 ..... N87-12706* #
NAS 1.15:88888 ..... N87-12559* #
NAS 1.15:88891 ..... N87-13359* #
NAS 1.15:88899 ..... N87-12679* #
NAS 1.15:89023 ..... N87-12614* #
NAS 1.15:89033 ..... N87-12922* #
NAS 1.15:89050 ..... N87-12538* #
NAS 1.15:89208 ..... N87-13227* #
NAS 1.15:89209 ..... N87-12580* #
NAS 1.15:89212 ..... N87-12631* #
NAS 1.15:89264 ..... N87-13395* #
NAS 1.15:89265 ..... N87-13367* #
NAS 1.15:89269 ..... N87-13366* #
NAS 1.15:89270 ..... N87-13096* #
NAS 1.15:89271 ..... N87-13379* #
NAS 1.15:89272 ..... N87-12567* #
NAS 1.21:7011(290) N87-13125*
NAS 1.21:7037(205) N87-12532*
NAS 1.26:3693 ..... N87-12908* #
NAS 1.26:4011 ..... N87-13021* #
NAS 1.26:171942 ..... N87-13167* #
NAS 1.26:175080 ..... N87-12923* #
NAS 1.26:176887 ..... N87-13243* #
NAS 1.26:177039 ..... N87-12626* #
NAS 1.26:177041 ..... N87-13362* #
NAS 1.26:177044 ..... N87-13358* #
NAS 1.26:177877 ..... N87-13394* #
NAS 1.26:178052 ..... N87-13203* #
NAS 1.26:178182 ..... N87-12552* #
NAS 1.26:178189 ..... N87-13024* #
NAS 1.26:178905 ..... N87-12587* #
NAS 1.26:178934 ..... N87-12608* #
NAS 1.26:178938 ..... N87-12681* #
NAS 1.26:178947 ..... N87-13140* #
NAS 1.26:178949 ..... N87-12609* #
NAS 1.26:178965 ..... N87-13307* #
NAS 1.26:179459 ..... N87-12829* #
NAS 1.26:179518 ..... N87-12915* #
NAS 1.26:179831 ..... N87-12613* #
NAS 1.26:179893 ..... N87-13015* #
NAS 1.26:179894 ..... N87-13387* #
NAS 1.26:179913 ..... N87-12965* #
NAS 1.26:179915 ..... N87-12719* #
NAS 1.26:179919 ..... N87-13178* #
NAS 1.26:179922 ..... N87-13365* #
NAS 1.26:179924 ..... N87-12968* #
NAS 1.26:179925 ..... N87-13368* #
NAS 1.26:179934 ..... N87-13023* #
NAS 1.26:179937 ..... N87-12542* #
NAS 1.55:2402 ..... N87-13043* #
NAS 1.60:2598 ..... N87-12561* #
NAS 1.60:2603 ..... N87-12921* #
NAS 1.60:2607 ..... N87-12585* #
NAS 1.60:2624 ..... N87-12541* #
NAS 1.60:2625 ..... N87-13022* #
NAS 1.60:2629 ..... N87-12718* #
NAS 1.60:2632 ..... N87-13264* #
NAS 1.60:2639 ..... N87-12560* #

NASA-CASE-NPO-16045-1 ..... N87-13313* #

NASA-CP-2402 ..... N87-13043* #

NASA-CR-3693 ..... N87-12908* #
NASA-CR-4011 ..... N87-13021* #
NASA-CR-171942 ..... N87-13167* #
NASA-CR-175080 ..... N87-12923* #
NASA-CR-176887 ..... N87-13243* #
NASA-CR-177039 ..... N87-12626* #
NASA-CR-177041 ..... N87-13362* #
NASA-CR-177044 ..... N87-13358* #
NASA-CR-177877 ..... N87-13394* #
NASA-CR-178052 ..... N87-13203* #
NASA-CR-178182 ..... N87-12552* #
NASA-CR-178189 ..... N87-13024* #
NASA-CR-178905 ..... N87-12587* #
NASA-CR-178934 ..... N87-12608* #
NASA-CR-178938 ..... N87-12681* #
NASA-CR-178947 ..... N87-13140* #
NASA-CR-178949 ..... N87-12609* #
NASA-CR-178965 ..... N87-13307* #
NASA-CR-179459 ..... N87-12829* #
NASA-CR-179518 ..... N87-12915* #
NASA-CR-179831 ..... N87-12613* #
NASA-CR-179893 ..... N87-13015* #
NASA-CR-179894 ..... N87-13387* #
NASA-CR-179913 ..... N87-12965* #
NASA-CR-179915 ..... N87-12719* #
NASA-CR-179919 ..... N87-13178* #
NASA-CR-179922 ..... N87-13365* #
NASA-CR-179924 ..... N87-12968* #
NASA-CR-179925 ..... N87-13368* #
NASA-CR-179934 ..... N87-13023* #
NASA-CR-179937 ..... N87-12542* #

NASA-NEWS-RELEASE-86-161 ..... N87-12593* #

NASA-SP-7011(290) N87-13125*
NASA-SP-7037(205) N87-12532*

NASA-TM-86559 ..... N87-12592* #
NASA-TM-86561 ..... N87-12607* #
NASA-TM-86562 ..... N87-12721* #
NASA-TM-86563 ..... N87-13166* #
NASA-TM-86565 ..... N87-12829* #
NASA-TM-86566 ..... N87-12756* #
NASA-TM-86664 ..... N87-12569* #
NASA-TM-86785 ..... N87-12558* #

NASA-TM-86789 ..... N87-12557* #
NASA-TM-87675 ..... N87-12806* #
NASA-TM-87731 ..... N87-12586* #
NASA-TM-87999 ..... N87-12598* #
NASA-TM-88250 ..... N87-12539* #
NASA-TM-88254 ..... N87-13141* #
NASA-TM-88259 ..... N87-13363* #
NASA-TM-88312 ..... N87-12830* #
NASA-TM-88322 ..... N87-13122* #
NASA-TM-88324 ..... N87-12967* #
NASA-TM-88498 ..... N87-13376* #
NASA-TM-88505 ..... N87-13375* #
NASA-TM-88638 ..... N87-12924* #
NASA-TM-88669 ..... N87-13252* #
NASA-TM-88670 ..... N87-12910* #
NASA-TM-88684 ..... N87-12606* #
NASA-TM-88685 ..... N87-12708* #
NASA-TM-88688 ..... N87-12559* #
NASA-TM-88691 ..... N87-13359* #
NASA-TM-88699 ..... N87-12679* #
NASA-TM-89023 ..... N87-12614* #
NASA-TM-89033 ..... N87-12922* #
NASA-TM-89050 ..... N87-12538* #
NASA-TM-89206 ..... N87-13227* #
NASA-TM-89209 ..... N87-12580* #
NASA-TM-89212 ..... N87-12831* #
NASA-TM-89264 ..... N87-13395* #
NASA-TM-89265 ..... N87-13367* #
NASA-TM-89269 ..... N87-13366* #
NASA-TM-89270 ..... N87-13098* #
NASA-TM-89271 ..... N87-13379* #
NASA-TM-89272 ..... N87-12597* #

NASA-TP-2598 ..... N87-12581* #
NASA-TP-2603 ..... N87-12921* #
NASA-TP-2607 ..... N87-12585* #
NASA-TP-2624 ..... N87-12541* #
NASA-TP-2625 ..... N87-13022* #
NASA-TP-2629 ..... N87-12718* #
NASA-TP-2632 ..... N87-13264* #
NASA-TP-2639 ..... N87-12660* #

NAVAIR-50-1C-544-VOL-2 ..... N87-13112 #

NAVTRASYSCEN-81-C-0105-13 ..... N87-12572 #
NAVTRASYSCEN-85-C-0044-2 ..... N87-12573 #

NBDL-86R008 ..... N87-13169 #

NEPRF-CR-86-03 ..... N87-13108 #

NOAA-TM-ERL-ARL-143 ..... N87-13114 #

NOAA-TM-ERL-ESG-21 ..... N87-13117 #
NOAA-TM-ERL-ESG-22 ..... N87-13116 #

NOAA-TM-NWS-CR-82 ..... N87-13115 #

NPS-54-86-006 ..... N87-13353 #

NPS55-86-006 ..... N87-12555 #
NPS69-86-003 ..... N87-12815 #

NRC-25411 ..... N87-12546 #
NRC-25442 ..... N87-12872 #

NRL-MP-5794 ..... N87-12604 #

NRL-MR-5679 ..... N87-12846 #
NRL-MR-5745 ..... N87-12931 #
NRL-MR-5796 ..... N87-12662 #
NRL-MR-5806 ..... N87-12742 #
NRL-MR-5830 ..... N87-12784 #

NTSB-AAR-86-02-SUM ..... N87-12549 #
NTSB-AAR-86-06 ..... N87-12550 #

N86.3 ..... N87-13321 #

ONRL-R-2-86 ..... N87-12671 #
ONRL-R-3-86 ..... N87-12673 #

ORNL-6207 ..... N87-13226 #
ORNL-6277 ..... N87-13007 #

ORNL/CDIC-13 ..... N87-13012 #

ORNL/CON-172 ..... N87-12903 #

ORNL/M-1/S1 ..... N87-12891 #
ORNL/M-3/S1 ..... N87-12890 #
ORNL/M-4/S1 ..... N87-12889 #
ORNL/M-5/S1 ..... N87-12888 #
ORNL/M-6/S1 ..... N87-12887 #
ORNL/M-15/S1 ..... N87-12886 #
ORNL/M-24/S1 ..... N87-12893 #
ORNL/M-36/S1 ..... N87-12892 #
ORNL/M-39/S1 ..... N87-12897 #
ORNL/M-43/S1 ..... N87-12896 #
ORNL/M-50/S1 ..... N87-12895 #
ORNL/M-51/S1 ..... N87-12894 #

ORNL/SUB-79-21453/21 ..... N87-12791 #

ORNL/TM-10033 ..... N87-12699 #

PB86-220357 ..... N87-13014 #
PB86-221728 ..... N87-13117 #
PB86-221736 ..... N87-13116 #
PB86-223427 ..... N87-13013 #
PB86-224425 ..... N87-12904 #
PB86-224763 ..... N87-12826 #
PB86-226636 ..... N87-13115 #
PB86-226792 ..... N87-13114 #
PB86-232014 ..... N87-12995 #
PB86-910407 ..... N87-12549 #
PB86-910408 ..... N87-12550 #

PDRC-86-05 ..... N87-13189 #

PFC/CP-86-4 ..... N87-13311 #

PNL-SA-13447 ..... N87-12676 #
PNL-SA-13478 ..... N87-12671 #
PNL-SA-13717 ..... N87-13361 #
PNL-SA-13861 ..... N87-12920 #
PNL-SA-13962 ..... N87-13139 #

PSI-008/TR-555 ..... N87-13310 #

PWA-5940-36 ..... N87-12923* #

P79-FINAL ..... N87-13104 #
P86-10229 ..... N87-12593* #
P142F ..... N87-12991 #

RADC-TR-85-171 ..... N87-12732 #
RADC-TR-85-232 ..... N87-12734 #
RADC-TR-85-271 ..... N87-12778 #
RADC-TR-86-21 ..... N87-12733 #

RAE-TRANS-2131 ..... N87-12540 #
RAE-TRANS-2133 ..... N87-12810 #

RCC/IOG-550-86 ..... N87-12579 #

REPT-1 ..... N87-12744 #
REPT-82N05-17 ..... N87-13236 #
REPT-822.3 ..... N87-12718* #
REPT-2425 ..... N87-12911 #
REPT-6340A ..... N87-12685 #
REPT-8720-3173U ..... N87-12562 #
REPT-020046-F ..... N87-12760 #

RI/RD86-216 ..... N87-12704 #

RR-10-86 ..... N87-12542* #

RSRE-MEMO-3939 ..... N87-12736 #

SAND-84-1633 ..... N87-12821 #
SAND-84-2273 ..... N87-13176 #
SAND-85-1063 ..... N87-13113 #
SAND-85-1518 ..... N87-12789 #
SAND-85-1552C ..... N87-12818 #
SAND-85-2748C ..... N87-12838 #
SAND-85-2830C ..... N87-12860 #
SAND-85-8239 ..... N87-12904 #
SAND-86-0033 ..... N87-12819 #
SAND-86-0058/1 ..... N87-13006 #
SAND-86-0219C ..... N87-12842 #
SAND-86-0251C ..... N87-12661 #
SAND-86-0357C ..... N87-12840 #
SAND-86-0512C ..... N87-12790 #
SAND-86-0536 ..... N87-13002 #
SAND-86-0567C ..... N87-13336 #
SAND-86-0586 ..... N87-13197 #
SAND-86-0599C ..... N87-12799 #
SAND-86-0779C ..... N87-12639 #
SAND-86-0787C ..... N87-13339 #
SAND-86-0806C ..... N87-12694 #
SAND-86-0812C ..... N87-12666 #
SAND-86-0840 ..... N87-12647 #
SAND-86-0921C ..... N87-12840 #
SAND-86-0922 ..... N87-12941 #
SAND-86-0959C ..... N87-12645 #
SAND-86-0990C ..... N87-12837 #
SAND-86-1011C ..... N87-12661 #
SAND-86-1032C ..... N87-12612 #
SAND-86-1072C ..... N87-13354 #
SAND-86-1326C ..... N87-13196 #
SAND-86-1337C ..... N87-12945 #
SAND-86-1347C ..... N87-12794 #
SAND-86-1356C ..... N87-12672 #
SAND-86-2061C ..... N87-12577 #
SAND-86-2079C ..... N87-13175 #
SAND-86-7028 ..... N87-13005 #
SAND-86-7031 ..... N87-13001 #
SAND-86-7102C ..... N87-12788 #
SAND-86-8225 ..... N87-12644 #

SASR-4 ..... N87-13362* #

SC5340.13FR ..... N87-13328 #
SC5366.51FR ..... N87-12852 #

SD-TR-86-31 ..... N87-12576 #
SD-TR-86-42 ..... N87-12779 #

SDL-0058-FTR ..... N87-12629 #

SDSMT/IAS/R-86/03 ..... N87-13102 #

SERI/PR-212-2877 ..... N87-13004 #
SERI/PR-255-2627 ..... N87-12700 #

SERI/STR-211-2951 ..... N87-13003 #

SERI/TP-211-2960 ..... N87-12997 #
SERI/TP-252-2812 ..... N87-12617 #

SOL-86-2 ..... N87-13180 #
SOL-86-9 ..... N87-13194 #
SOL-86-12 ..... N87-13225 #

SR-1 ..... N87-12724 #
SR-2 ..... N87-12571 #
SR-2 ..... N87-13030 #

STC-TR-2106 ..... N87-13024* #

SU-SOL-86-5 ..... N87-13182 #
SU-SOL-86-6 ..... N87-13248 #

SU-TR-13 ..... N87-13231 #

SWRI-06-8602 ..... N87-12620 #
SWRI-8578/2 ..... N87-12689 #

SYRU/DECE/TR-85/5 ..... N87-12725 #

TACOM-TR-13155 ..... N87-13168 #

TI-U1-134375-F ..... N87-13317 #

TR-D-85-ARO ..... N87-13232 #
TR-D-86-ARO ..... N87-13230 #

TR-3 ..... N87-12633 #
TR-3 ..... N87-12693 #
TR-4 ..... N87-12630 #
TR-4 ..... N87-12725 #
TR-4 ..... N87-13184 #
TR-5 ..... N87-12634 #
TR-6 ..... N87-13324 #
TR-7 ..... N87-12935 #
TR-9 ..... N87-12631 #
TR-10-PT-2 ..... N87-12632 #
TR-12 ..... N87-13210 #
TR-21 ..... N87-12683 #
TR-22 ..... N87-13308 #
TR-23 ..... N87-13254 #
TR-24 ..... N87-13323 #
TR-25 ..... N87-12636 #
TR-48 ..... N87-13325 #
TR-81-50 ..... N87-12654 #
TR-85-10 ..... N87-13239 #
TR-85-34 ..... N87-13196 #
TR-85-49 ..... N87-13217 #
TR-86-06-06-03 ..... N87-12777 #
TR-86-09 ..... N87-13241 #
TR-86-10 ..... N87-13238 #
TR-116 ..... N87-13236 #
TR-131 ..... N87-13237 #
TR-132 ..... N87-13224 #
TR-376 ..... N87-13233 #
TR-514 ..... N87-12722 #
TR-518 ..... N87-12730 #
TR-0086(6749)-1 ..... N87-12576 #
TR-0086(6945-06)-3 ..... N87-12779 #

U-OF-IOWA-86-21 ..... N87-13028 #

UCB/ERL-M-86/18 ..... N87-12751 #

UCB/RP/86/A1040 ..... N87-12656 #

UCI-ICS-TR-86-12 ..... N87-13184 #

UCID-20762 ..... N87-13040 #

UCRL-53700-85 ..... N87-12797 #
UCRL-93482 ..... N87-12750 #
UCRL-93658 ..... N87-13195 #
UCRL-93826 ..... N87-12643 #
UCRL-93965-REV-1 ..... N87-13039 #
UCRL-94096 ..... N87-12639 #
UCRL-94255 ..... N87-12898 #
UCRL-94273 ..... N87-12899 #
UCRL-94494 ..... N87-12787 #

UCT/DEECS/TR-86-3 ..... N87-12738 #

UD-TR-85-147 ..... N87-12703 #

UDR-TR-85-82-VOL-1 ..... N87-12816 #
UDR-TR-85-132 ..... N87-12563 #
UDR-TR-85-148 ..... N87-13269 #

UIEMC-86-5 ..... N87-12739 #

UILU-ENG-86-2217 ..... N87-12773 #
UILU-ENG-86-2225 ..... N87-12747 #
UILU-ENG-86-2547 ..... N87-12739 #

UM/MSS-86/4 ..... N87-13215 #

UMTRI-86-14 ..... N87-13129 #

URI/GSO-TR-85-3 ..... N87-13121 #

UROCHESTER/DC/85/TR-72 ..... N87-12851 #

URW-5-DCA-043 ..... N87-13200 #

US-PATENT-APPL-SN-502028 ..... N87-12833 #
US-PATENT-APPL-SN-505570 ..... N87-12745
US-PATENT-APPL-SN-566130 ..... N87-13315 #
US-PATENT-APPL-SN-569639 ..... N87-13267 #
US-PATENT-APPL-SN-569686 ..... N87-12857
US-PATENT-APPL-SN-571766 ..... N87-12854 #
US-PATENT-APPL-SN-611041 ..... N87-12561 #
US-PATENT-APPL-SN-635866 ..... N87-12692
US-PATENT-APPL-SN-640623 ..... N87-12878 #
US-PATENT-APPL-SN-640902 ..... N87-12735 #
US-PATENT-APPL-SN-641146 ..... N87-13313* #
US-PATENT-APPL-SN-641656 ..... N87-12836
US-PATENT-APPL-SN-651961 ..... N87-12879 #
US-PATENT-APPL-SN-722579 ..... N87-12691
US-PATENT-APPL-SN-726443 ..... N87-12780
US-PATENT-APPL-SN-753462 ..... N87-12543 #
US-PATENT-APPL-SN-762367 ..... N87-12824 #
US-PATENT-APPL-SN-767218 ..... N87-12701 #
US-PATENT-APPL-SN-772527 ..... N87-12908 #
US-PATENT-APPL-SN-783730 ..... N87-12803 #
US-PATENT-APPL-SN-786561 ..... N87-12802 #
US-PATENT-APPL-SN-801341 ..... N87-12877 #
US-PATENT-APPL-SN-801348 ..... N87-13322 #
US-PATENT-APPL-SN-824994 ..... N87-12740 #
US-PATENT-APPL-SN-831886 ..... N87-13171 #
US-PATENT-APPL-SN-831901 ..... N87-13170 #
US-PATENT-APPL-SN-835923 ..... N87-12770 #
US-PATENT-APPL-SN-844636 ..... N87-12874 #
US-PATENT-APPL-SN-844637 ..... N87-12769 #
US-PATENT-APPL-SN-849991 ..... N87-12776 #
US-PATENT-APPL-SN-852587 ..... N87-13266 #
US-PATENT-APPL-SN-852597 ..... N87-12621 #
US-PATENT-APPL-SN-852683 ..... N87-12832 #
US-PATENT-APPL-SN-853827 ..... N87-13253 #
US-PATENT-APPL-SN-854234 ..... N87-12876 #
US-PATENT-APPL-SN-855047 ..... N87-12768 #
US-PATENT-APPL-SN-855243 ..... N87-12875 #
US-PATENT-APPL-SN-856248 ..... N87-12710 #
US-PATENT-APPL-SN-856283 ..... N87-13268 #
US-PATENT-APPL-SN-857621 ..... N87-13270 #
US-PATENT-APPL-SN-859283 ..... N87-12767 #
US-PATENT-APPL-SN-861905 ..... N87-12881 #
US-PATENT-APPL-SN-861906 ..... N87-12880 #
US-PATENT-APPL-SN-861909 ..... N87-12564 #
US-PATENT-APPL-SN-864221 ..... N87-12712 #
US-PATENT-APPL-SN-864222 ..... N87-12775 #
US-PATENT-APPL-SN-864638 ..... N87-12850 #
US-PATENT-APPL-SN-867727 ..... N87-12687 #
US-PATENT-APPL-SN-870045 ..... N87-12774 #

US-PATENT-CLASS-60-39.31 ..... N87-12543 #
US-PATENT-CLASS-188-275 ..... N87-12879 #
US-PATENT-CLASS-239-265.29 ..... N87-12561 #
US-PATENT-CLASS-250-338 ..... N87-13313* #
US-PATENT-CLASS-250-370 ..... N87-13313* #
US-PATENT-CLASS-292-113 ..... N87-12878 #
US-PATENT-CLASS-324-244 ..... N87-12836
US-PATENT-CLASS-337-24 ..... N87-13267 #
US-PATENT-CLASS-343-7.4 ..... N87-12735 #
US-PATENT-CLASS-343-372 ..... N87-12745
US-PATENT-CLASS-346-107R ..... N87-12833 #
US-PATENT-CLASS-356-28.5 ..... N87-12854 #
US-PATENT-CLASS-357-23.1 ..... N87-13313* #
US-PATENT-CLASS-357-23.12 ..... N87-13313* #
US-PATENT-CLASS-357-29 ..... N87-13313* #
US-PATENT-CLASS-357-30 ..... N87-13313* #
US-PATENT-CLASS-357-52 ..... N87-13313* #
US-PATENT-CLASS-372-5 ..... N87-12857
US-PATENT-CLASS-423-335 ..... N87-13315 #
US-PATENT-CLASS-427-125 ..... N87-12691
US-PATENT-CLASS-427-142 ..... N87-12692
US-PATENT-CLASS-429-27 ..... N87-12780

US-PATENT-4,571,936 ..... N87-12543 #
US-PATENT-4,576,808 ..... N87-13315 #
US-PATENT-4,580,140 ..... N87-12745
US-PATENT-4,585,710 ..... N87-12780
US-PATENT-4,588,053 ..... N87-12879 #
US-PATENT-4,588,216 ..... N87-12878 #
US-PATENT-4,590,476 ..... N87-12735 #
US-PATENT-4,590,492 ..... N87-12833 #
US-PATENT-4,590,505 ..... N87-13267 #
US-PATENT-4,591,097 ..... N87-12561 #
US-PATENT-4,591,510 ..... N87-12691
US-PATENT-4,591,511 ..... N87-12692
US-PATENT-4,591,786 ..... N87-12836
US-PATENT-4,592,056 ..... N87-12857
US-PATENT-4,595,287 ..... N87-12854 #
US-PATENT-4,605,946 ..... N87-13313* #

USAFAS/MSTLD/SB116 ..... N87-13351 #

USAFETAC/DS-84/019 ..... N87-13100 #
USAFETAC/DS-86/024 ..... N87-13105 #
USAFETAC/DS-86/025 ..... N87-13106 #
USAFETAC/DS-86/026 ..... N87-13107 #
USAFETAC/DS-86/033 ..... N87-13100 #

USARIEM-M-39/86 ..... N87-13131 #

USARIEM-M38/86 ..... N87-13128 #

USARIEM-T-8/86 ..... N87-13134 #

UTIAS-311 ..... N87-12807 #

U1C/DQM/ARO-85-2 ..... N87-13229 #

VLSI-MEMO-86-316 ..... N87-12772 #

WES/MP/HL-86-2 ..... N87-12812 #

WSRL-0436-TR ..... N87-12702 #

WU/CCM-86/1 ..... N87-12936 #

Y/DV-524 ..... N87-12675 #
Y/DV-525 ..... N87-12674 #

Y/DW-627 ..... N87-12885 #

U.S. GOVERNMENT PRINTING OFFICE:1987-181-546/60002

FEDERAL DEPOSITORY LIBRARIES

ALABAMA

AUBURN UNIV. AT MONTGOMERY LIBRARY
Documents Department
Montgomery, AL 36193
(205) 279-9110, ext. 253

UNIV. OF ALABAMA LIBRARY
Documents Dept.-Box S
University, AL 35486
(205) 348-7369

ARIZONA

DEPT. OF LIBRARY, ARCHIVES AND PUBLIC RECORDS
Third Floor—State Cap.
1700 West Washington
Phoenix, AZ 85007
(602) 255-4121

UNIVERSITY OF ARIZONA LIB.
Government Documents Dept.
Tucson, AZ 85721
(602) 626-5233

ARKANSAS

ARKANSAS STATE LIBRARY
One Capitol Mall
Little Rock, AR 72201
(501) 371-2326

CALIFORNIA

CALIFORNIA STATE LIBRARY
Govt. Publications Section
P.O. Box 2037
Sacramento, CA 95809
(916) 322-4572

COLORADO

UNIV OF COLORADO LIB.
Government Pub. Division
Campus Box 184
Boulder, CO 80309
(303) 492-8834

DENVER PUBLIC LIBRARY
Govt. Pub. Department
1357 Broadway
Denver, CO 80203
(303) 571-2131

CONNECTICUT

CONNECTICUT STATE LIBRARY
Government Documents Unit
231 Capitol Avenue
Hartford, CT 06106
(203) 566-4971

FLORIDA

UNIV. OF FLORIDA LIBRARIES
Library West
Documents Department
Gainesville, FL 32611
(904) 392-0367

GEORGIA

UNIV. OF GEORGIA LIBRARIES
Government Reference Dept.
Athens, GA 30602
(404) 542-8951

HAWAII

UNIV. OF HAWAII LIBRARY
Govt. Documents Collection
2550 The Mall
Honolulu, HI 96822
(808) 948-8230

IDAHO

UNIV. OF IDAHO LIBRARY
Documents Section
Moscow, ID 83843
(208) 885-6344

ILLINOIS

ILLINOIS STATE LIBRARY
Information Services Branch
Centennial Building
Springfield, IL 62706
(217) 782-5185

INDIANA

INDIANA STATE LIBRARY
Serials Documents Section
140 North Senate Avenue
Indianapolis, IN 46204
(317) 232-3686

IOWA

UNIV. OF IOWA LIBRARIES
Govt. Documents Department
Iowa City, IA 52242
(319) 353-3318

KANSAS

UNIVERSITY OF KANSAS
Doc. Collect—Spencer Lib.
Lawrence, KS 66045
(913) 864-4662

KENTUCKY

UNIV. OF KENTUCKY LIBRARIES
Govt. Pub. Department
Lexington, KY 40506
(606) 257-3139

LOUISIANA

LOUISIANA STATE UNIVERSITY
Middleton Library
Govt. Docs. Dept.
Baton Rouge, LA 70803
(504) 388-2570

LOUISIANA TECHNICAL UNIV. LIBRARY
Documents Department
Ruston, LA 71272
(318) 257-4962

MAINE

UNIVERSITY OF MAINE
Raymond H. Fogler Library
Tri-State Regional Documents Depository
Orono, ME 04469
(207) 581-1680

MARYLAND

UNIVERSITY OF MARYLAND
McKeldin Lib.—Doc. Div.
College Park, MD 20742
(301) 454-3034

MASSACHUSETTS

BOSTON PUBLIC LIBRARY
Government Docs. Dept.
Boston, MA 02117
(617) 536-5400 ext.226

MICHIGAN

DETROIT PUBLIC LIBRARY
Sociology Department
5201 Woodard Avenue
Detroit, MI 48202
(313) 833-1409

MICHIGAN STATE LIBRARY
P.O. Box 30007
Lansing, MI 48909
(517) 373-0640

MINNESOTA

UNIVERSITY OF MINNESOTA
Government Pubs. Division
409 Wilson Library
309 19th Avenue South
Minneapolis, MN 55455
(612) 373-7813

MISSISSIPPI

UNIV. OF MISSISSIPPI LIB.
Documents Department
University, MS 38677
(601) 232-5857

MONTANA

UNIV. OF MONTANA
Mansfield Library
Documents Division
Missoula, MT 59812
(406) 243-6700

NEBRASKA

NEBRASKA LIBRARY COMM.
Federal Documents
1420 P Street
Lincoln, NE 68508
(402) 471-2045
In cooperation with University of Nebraska-Lincoln

NEVADA

UNIVERSITY OF NEVADA LIB.
Govt. Pub. Department
Reno, NV 89557
(702) 784-6579

NEW JERSEY

NEWARK PUBLIC LIBRARY
5 Washington Street
Newark, NJ 07101
(201) 733-7812

NEW MEXICO

UNIVERSITY OF NEW MEXICO
Zimmerman Library
Government Pub. Dept.
Albuquerque, NM 87131
(505) 277-5441

NEW MEXICO STATE LIBRARY
Reference Department
325 Don Gaspar Avenue
Santa Fe, NM 87501
(505) 827-2033, ext. 22

NEW YORK

NEW YORK STATE LIBRARY
Empire State Plaza
Albany, NY 12230
(518) 474-5563

NORTH CAROLINA

UNIVERSITY OF NORTH CAROLINA AT CHAPEL HILL
Wilson Library
BA/SS Documents Division
Chapel Hill, NC 27515
(919) 962-1321

NORTH DAKOTA

UNIVERSITY OF NORTH DAKOTA
Chester Fritz Library
Documents Department
Grand Forks, ND 58202
(701) 777-2617, ext. 27
In cooperation with North Dakota State Univ. Library

OHIO

STATE LIBRARY OF OHIO
Documents Department
65 South Front Street
Columbus, OH 43215
(614) 462-7051

OKLAHOMA

OKLAHOMA DEPT. OF LIB.
Government Documents
200 NE 18th Street
Oklahoma City, OK 73105
(405) 521-2502

OKLAHOMA STATE UNIV. LIB.
Documents Department
Stillwater, OK 74078
(405) 624-6546

OREGON

PORTLAND STATE UNIV. LIB.
Documents Department
P.O. Box 1151
Portland, OR 97207
(503) 229-3673

PENNSYLVANIA

STATE LIBRARY OF PENN.
Government Pub. Section
P.O. Box 1601
Harrisburg, PA 17105
(717) 787-3752

TEXAS

TEXAS STATE LIBRARY
Public Services Department
P.O. Box 12927—Cap. Sta.
Austin, TX 78753
(512) 471-2996

TEXAS TECH. UNIV. LIBRARY
Govt. Documents Department
Lubbock, TX 79409
(806) 742-2268

UTAH

UTAH STATE UNIVERSITY
Merrill Library, U.M.C. 30
Logan, UT 84322
(801) 750-2682

VIRGINIA

UNIVERSITY OF VIRGINIA
Alderman Lib.—Public Doc.
Charlottesville, VA 22901
(804) 924-3133

WASHINGTON

WASHINGTON STATE LIBRARY
Documents Section
Olympia, WA 98504
(206) 753-4027

WEST VIRGINIA

WEST VIRGINIA UNIV. LIB.
Documents Department
Morgantown, WV 26506
(304) 293-3640

WISCONSIN

MILWAUKEE PUBLIC LIBRARY
814 West Wisconsin Avenue
Milwaukee, WI 53233
(414) 278-3000

ST. HIST LIB. OF WISCONSIN
Government Pub. Section
816 State Street
Madison, WI 53706
(608) 262-4347

WYOMING

WYOMING STATE LIBRARY
Supreme Ct. & Library Bld.
Cheyenne, WY 82002
(307) 777-6344

National Aeronautics and
Space Administration
Code NTT-4
Washington, D.C.
20546

Official Business
Penalty for Private Use, $300

SPECIAL FOURTH-CLASS RATE
POSTAGE & FEES PAID
NASA
PERMIT No. G 27

NASA

POSTMASTER: If Undeliverable (Section 158
Postal Manual) Do Not Return